Daniel M. Trifiletti
Samuel T. Chao
Arjun Sahgal
Jason P. Sheehan
Editors

Stereotactic Radiosurgery and Stereotactic Body Radiation Therapy

A Comprehensive Guide

Springer

Stereotactic Radiosurgery and Stereotactic Body Radiation Therapy

Daniel M. Trifiletti • Samuel T. Chao
Arjun Sahgal • Jason P. Sheehan
Editors

Stereotactic Radiosurgery and Stereotactic Body Radiation Therapy

A Comprehensive Guide

Springer

Editors
Daniel M. Trifiletti, MD
Mayo Clinic, Radiation Oncology
Mayo Clinic School of Medicine
Radiation Oncology
Jacksonville, FL
USA

Arjun Sahgal, MD, FRCPC
Sunnybrook Odette Cancer Centre
Department of Radiation Oncology
University of Toronto
Toronto, ON
Canada

Samuel T. Chao, MD
Department of Radiation Oncology
Rose Ella Burkhardt Brain Tumor
and Neuro-Oncology Center
Cleveland Clinic
Cleveland, OH
USA

Jason P. Sheehan, MD, PhD
University of Virginia
Departments of Neurological Surgery and
Radiation Oncology
Charlottesville, VA
USA

ISBN 978-3-030-16923-7 ISBN 978-3-030-16924-4 (eBook)
https://doi.org/10.1007/978-3-030-16924-4

This Springer imprint is published by the registered company Springer Nature Switzerland AG.
The registered company address is: Gewerbestrasse 11, 6330 Cham, Switzerland

Foreword

There are a large number of books on stereotactic radiotherapy. Some focus on specific techniques, and others on specific indications. Some books try to provide an overview of all available literature, often leaving the reader with many questions on how to do what in their specific situation for an individual patient. Well, this book is different!

After the successful implementation of stereotactic techniques for intracranial lesions in the past century, stereotactic techniques have also become an important treatment option for extracranial tumors, and the role of stereotactic body radiotherapy (SBRT) for lung, liver, and spine lesions is now well established. Moreover, SBRT is being explored and advocated for tumors and functional indications at various other locations.

In this book, the editors have done an excellent job in bringing together the information on all relevant topics in stereotactic radiosurgery (SRS) and SBRT. An impressive line-up of world-renowned experts provides an outstanding and comprehensive review of the biological aspects, radiation physics principles, clinical indications, and the available evidence. Instead of summing up all available literature, the chapters provide clearly written reviews with information which is scientific, but at the same time very practical and immediately applicable to daily clinic.

In the chapters on biology, the rationale for SRS and SBRT and the mechanisms of action of the high-dose hypofractionated treatments are discussed. Latest insights on the interaction of radiotherapy with the immune systems are addressed as well.

The chapters on SRS are partly technique-based, which enables the readers to have easy access to information on the techniques used at their centers. In a separate section, SRS is discussed in detail for the most frequent indications as well.

For SBRT, the general physics aspects including immobilization and motion management are described in detail. A separate chapter focuses on the use SBRT using charged particles. Apart from the important mainstream indications such as lung and spine tumors, newer indications—such as SBRT for head and neck cancer, gastro-intestinal tumors, kidney tumors, and prostate cancer—are addressed in various chapters.

The final chapters of this book provide an excellent overview of some general aspects, such as complication management and integration with other therapies, as well as of future directions of the rapidly emerging fields of SRS and SBRT.

This book is written with the reader in mind who is looking for an up-to-date and state-of-the-art overview of stereotactic radiotherapy for intra- and extracranial indications.

Ben J. Slotman, MD, PhD, h.FACR
Department of Radiation Oncology
VU University Medical Center,
Amsterdam, The Netherlands

Preface

Advancements in technology over the past several decades have created an atmosphere of multidisciplinary collaborative care that is very unlike medicine in the early twentieth century. Today, team-based approaches allow us to leverage techniques and modalities for the benefit of the patient. Radiosurgery is a perfect example of multidisciplinary collaboration and the benefit that specialization affords the patient, by blurring the lines between traditional medical specialities. Today, centers across the world have developed skills, techniques, and expertise in use of stereotactic radiosurgery (SRS) and stereotactic body radiation therapy (SBRT) for treatment of many diseases. Perhaps stereotactic radiosurgery can be seen as a budding discipline of its own as it continues to gain distinction that differentiates it from the arenas of conventional surgery and radiation therapy. Unfortunately, the sharing of this practical knowledge has been limited to specialty-specific annual meetings, frequently with conflicting recommendations between medical disciplines.

As a result, it is currently very difficult for a clinician (either in training or in practice) to gain experience and expertise in SRS and SBRT. *Stereotactic Radiosurgery and Stereotactic Body Radiation Therapy: A Comprehensive Guide* was created for the purpose of centralizing the knowledge and experience of experts across a variety of disciplines.

Our vision is that this book be used to serve as a basis for the current state of the art of SRS and SBRT. There is no doubt that advancements are made almost daily and refinements will be made as technology advances. However, for providers seeking to expand their knowledge and grow their radiosurgical skill set, this text will serve as a resource to allow for their development.

We thank our gracious contributors for lending their expertise toward the further advancement of our field and toward the improved care of our patients. Their efforts to improve the care of patients cannot be overstated.

Jacksonville, FL, USA — Daniel M. Trifiletti
Cleveland, OH, USA — Samuel T. Chao
Toronto, Ontario, Canada — Arjun Sahgal
Charlottesville, VA, USA — Jason P. Sheehan

Contents

Contributors

Manmeet S. Ahluwalia, MD Cleveland Clinic, Burkhardt Brain Tumor and Neuro-Oncology Center, Cleveland, OH, USA

Clayton Alonso, MD University of Virginia, Radiation Oncology, Charlottesville, VA, USA

Sanjay Aneja, MD Yale New Haven Hospital, Department of Therapeutic Radiology, New Haven, CT, USA

Yale School of Medicine, Department of Therapeutic Radiology, New Haven, CT, USA

Geoffrey Appelboom, MD, PhD Department of Neurosurgery, Stanford University School of Medicine, Stanford, CA, USA

Tracy A. Balboni, MD Dana-Farber/Brigham and Women's Cancer Center, Boston, MA, USA

Harvard University, Department of Radiation Oncology, Boston, MA, USA

Aisling S. Barry, MD, MRCPI, FFR, RCSI Princess Margaret Cancer Center, Radiation Medicine Program, Toronto, ON, Canada

University of Toronto, Department of Radiation Oncology, Toronto, ON, Canada

Stanley H. Benedict, PhD, FAAPM, FACMP University of California Davis Comprehensive Cancer Center, Department of Radiation Oncology, University of California at Davis, Sacramento, CA, USA

Frank J. Bova, PhD Department of Neurosurgery, University of Florida, Gainesville, FL, USA

Juliana Bueno, MD University of Virginia Health System, Department of Radiology and Medical Imaging, Charlottesville, VA, USA

Daniel N. Cagney, MB, BAO, Bch, MSC Dana-Farber/Brigham and Women's Cancer Center, Boston, MA, USA

Harvard University, Department of Radiation Oncology, Boston, MA, USA

Eric L. Chang, MD, FASTRO University of Southern California Comprehensive Cancer Center, Department of Radiation Oncology, Los Angeles, CA, USA

Keck School of Medicine of the University of Southern California, Department of Radiation Oncology, Los Angeles, CA, USA

Steven D. Chang, MD Department of Neurosurgery, Stanford University School of Medicine, Stanford, CA, USA

Samuel T. Chao, MD Department of Radiation Oncology, Cleveland Clinic, Cleveland, OH, USA

Rose Ella Burkhardt Brain Tumor and Neuro-Oncology Center, Cleveland Clinic, Cleveland, OH, USA

Arpit M. Chhabra, MD Central Connecticut Radiation Oncology, PC, Department of Radiation Oncology, Middletown, CT, USA

Lee Chin, PhD, MCCM Sunnybrook Health Sciences Centre, Medical Physics, Toronto, ON, Canada

L. Chinsoo Cho, MD, MS University of Minnesota, Department of Radiation Oncology, Minneapolis, MN, USA

Srinivas Chivukula, MD Department of Neurosurgery, David Geffen School of Medicine at UCLA, Los Angeles, CA, USA

Mudit Chowdhary, MD Rush University Medical Center, Department of Radiation Oncology, Chicago, IL, USA

Benjamin J. Cooper, BSc, MSc Medical Physics and Radiation Engineering, Canberra Hospital, Garran, ACT, Australia

ACRF Image X Institute, Camperdown, NSW, Australia

Diogo P. Cordeiro, MD University of Virginia, Departments of Radiation Oncology and Neurological Surgery, Charlottesville, VA, USA

Leodante da Costa, MD, FRCSC Sunnybrook Health Sciences Centre, Department of Neurosurgery, Toronto, ON, Canada

University of Toronto, Department of Surgery, Toronto, ON, Canada

Gregory J. Czarnota, PhD, MD, FRCPC Physical Sciences, Sunnybrook Research Institute, Toronto, ON, Canada

Department of Medical Biophysics, University of Toronto, Toronto, ON, Canada

Odette Cancer Centre, Sunnybrook Health Sciences Centre, Toronto, ON, Canada

Department of Radiation Oncology, University of Toronto, Toronto, ON, Canada

Laura A. Dawson, MD, FRCPC, FASTRO Princess Margaret Cancer Center, Radiation Medicine Program, Toronto, ON, Canada

University of Toronto, Department of Radiation Oncology, Toronto, ON, Canada

Neil B. Desai, MD University of Texas Southwestern Medical Center, Department of Radiation Oncology, Dallas, TX, USA

Tejan Diwanji, MD University of Miami Sylvester Comprehensive Cancer Center, Department of Radiation Oncology, Miami, FL, USA

Joseph H. Donahue, MD University of Virginia Health System, Department of Radiology and Medical Imaging, Charlottesville, VA, USA

Golnaz Farhat, MSc, PhD Physical Sciences, Sunnybrook Research Institute, Toronto, ON, Canada

Salman Faruqi, MD, FRCPC Sunnybrook Odette Cancer Centre, Department of Radiation Oncology, Toronto, ON, Canada

University of Toronto, Toronto, ON, Canada

Michael R. Folkert, MD, PhD University of Texas Southwestern Medical Center, Department of Radiation Oncology, Dallas, TX, USA

Melissa A. Frick, MD Stanford University Medical Center, Department of Radiation Oncology, Stanford, CA, USA

William A. Friedman, MD Department of Neurosurgery, University of Florida, Gainesville, FL, USA

Fabio Frisoli, MD New York University Langone Medical Center, New York University, Department of Neurosurgery, New York, NY, USA

Iris C. Gibbs, MD Stanford Cancer Institute, Stanford, CA, USA

Stanford University, Department of Radiation Oncology, Stanford, CA, USA

Steven J. Goetsch, PhD San Diego Gamma Knife Center, La Jolla, CA, USA

Matthias Guckenberger, MD University Hospital Zurich, Department of Radiation Oncology, Zurich, Switzerland

Chandan Guha, MBBS, PhD Departments of Radiation Oncology, Pathology and Urology and Institute for Onco-Physics, Albert Einstein College of Medicine, Montefiore Medical Center, New York, NY, USA

Raquibul Hannan, MD, PhD University of Texas Southwestern Medical Center, Departments of Radiation Oncology and Immunology, Dallas, TX, USA

Jana Heitmann, MD University Hospital Zurich, Department of Radiation Oncology, Zurich, Switzerland

Travis C. Hill, MD, PhD New York University Medical Center, Department of Neurosurgery, New York, NY, USA

Zain Husain, MD Smilow Cancer Hospital, Department of Radiation Oncology, New Haven, CT, USA

Yale University, Department of Radiation Oncology, New Haven, CT, USA

Jason N. Itri, MD, PhD University of Virginia Health System, Department of Radiology and Medical Imaging, Charlottesville, VA, USA

Matiar Jafari, BS Department of Neurosurgery, David Geffen School of Medicine at UCLA, Los Angeles, CA, USA

Aditya Juloori, MD Department of Radiation Oncology, Cleveland Clinic, Cleveland, OH, USA

Irene Karam, MD, FRCPC Sunnybrook Health Sciences Centre, Radiation Oncology, Toronto, ON, Canada

Paul J. Keall, PhD ACRF Image X Institute, Camperdown, NSW, Australia

University of Sydney, Camperdown, NSW, Australia

John P. Kirkpatrick, MD, PhD Department of Radiation Oncology, Duke University, Durham, NC, USA

Duke Cancer Insitute, Durham, NC, USA

Department of Neurosurgery, Duke University, Durham, NC, USA

Douglas Kondziolka, MD New York University Langone Health, New York, NY, USA

Rahul J. Kumar, MD California Pacific Medical Center, Department of Radiation Oncology, San Francisco, CA, USA

Pencilla Lang, MD, PhD Sunnybrook Health Sciences Centre, Radiation Oncology, Toronto, ON, Canada

Jeremie Stephane Larouche, MD, FRCSC Sunnybrook Health Sciences Centre, Department of Orthopedic Surgery, Toronto, ON, Canada

University of Toronto, Department of Surgery, Toronto, ON, Canada

Cheng-chia Lee, MD Department of Neurosurgery, Neurological Institute, Taipei Veterans General Hospital, Taipei, Taiwan

National Yang-Ming University, Taipei, Taiwan

Yongsook C. Lee, PhD University of Arizona, Department of Radiation Oncology, Tucson, AZ, USA

Young Lee, PhD Sunnybrook Health Sciences Centre, Department of Radiation Oncology, Toronto, ON, Canada

University of Toronto, Department of Radiation Oncology, Toronto, ON, Canada

Simon S. Lo, MB, ChB, FACR, FASTRO University of Washington Medical Center, Department of Radiation Oncology, Seattle, WA, USA

University of Washington School of Medicine, Department of Radiation Oncology, Seattle, WA, USA

L. Dade Lunsford, MD Department of Neurological Surgery, University of Pittsburgh Medical Center, Pittsburgh, PA, USA

Department of Neurological Surgery, University of Pittsburgh, Pittsburgh, PA, USA

Pejman Maralani, MD, FRCPC Sunnybrook Health Sciences Centre, Department of Radiology, Toronto, ON, Canada

University of Toronto, Department of Medical Imaging, Toronto, ON, Canada

Giuseppina Laura Masucci, MD Centre Hospitalier de l'Université de Montréal (CHUM), Department of Radiation Oncology, Montréal, QC, Canada

Université de Montréal, Department of Radiology, Radiation Oncology, and Nuclear Medicine, Montréal, QC, Canada

Minesh P. Mehta, MD, FASTRO Miami Cancer Institute—Baptist Health South Florida, Department of Radiation Oncology, Miami, FL, USA

Giuseppe Minniti, MD Radiation Oncology Unit, UPMC Hillman Cancer Center, San Pietro Hospital, Rome, Italy

IRCSS Neuromed, Pozzilli, Italy

Osama Mohamad, MD, PhD University of Texas Southwestern Medical Center, Radiation Oncology, Dallas, TX, USA

Jason K. Molitoris, MD, PhD University of Maryland School of Medicine, Department of Radiation Oncology, Baltimore, MD, USA

Justin Moore, MD, PhD Beth Israel Deaconess Medical Center, Boston, MA, USA

Harvard Medical School, Boston, MA, USA

Pablo Munoz-Schuffenegger, MD Princess Margaret Cancer Center, Radiation Medicine Program, Toronto, ON, Canada

University of Toronto, Department of Radiation Oncology, Toronto, ON, Canada

Erin S. Murphy, MD Department of Radiation Oncology, Cleveland Clinic, Cleveland, OH, USA

Cleveland Clinic Lerner College of Medicine, Cleveland, OH, USA

Rose Ella Burkhardt Brain Tumor and Neuro-Oncology Center, Cleveland Clinic, Cleveland, OH, USA

Sten Myrehaug, MD, FRCPC Sunnybrook Health Sciences Centre, Odette Cancer Center, Department of Radiation Oncology, Toronto, ON, Canada

University of Toronto, Department of Radiation Oncology, Toronto, ON, Canada

Sameer K. Nath, MD Department of Radiation Oncology, University of Colorado School of Medicine, Aurora, CO, USA

Ajay Niranjan, MD, MBA Department of Neurological Surgery, University of Pittsburgh Medical Center, Pittsburgh, PA, USA

Department of Neurological Surgery, University of Pittsburgh, Pittsburgh, PA, USA

Erqi Pollom, MD, MS Stanford Cancer Institute, Stanford, CA, USA

Stanford University, Department of Radiation Oncology, Stanford, CA, USA

Ian Poon, MD, FRCPC Sunnybrook Health Sciences Centre, Radiation Oncology, Toronto, ON, Canada

Nader Pouratian, MD, PhD Department of Neurosurgery, David Geffen School of Medicine at UCLA, Los Angeles, CA, USA

Arrvind Raghunath, MBBS Cleveland Clinic Akron General, Akron, OH, USA

Cleveland Clinic Lerner School of Medicine, Department of Internal Medicine, Cleveland, OH, USA

David R. Raleigh, MD, PhD University of California at San Francisco, Departments of Radiation Oncology and Neurological Surgery, San Francisco, CA, USA

Tyler P. Robin, MD, PhD Department of Radiation Oncology, University of Colorado Cancer Center, Aurora, CO, USA

Yi Rong, PhD University of California at Davis, Radiation Oncology, Sacramento, CA, USA

Mark Ruschin, PhD Sunnybrook Health Sciences Centre, Department of Radiation Oncology, Toronto, ON, Canada

University of Toronto, Department of Radiation Oncology, Toronto, ON, Canada

Chad G. Rusthoven, MD Department of Radiation Oncology, University of Colorado School of Medicine, Aurora, CO, USA

Arjun Sahgal, MD, FRCPC Sunnybrook Odette Cancer Centre, Department of Radiation Oncology, University of Toronto, Toronto, ON, Canada

Joseph K. Salama, MD, PhD Department of Radiation Oncology, Duke University, Durham, NC, USA

Duke Cancer Insitute, Durham, NC, USA

Arman Sarfehnia, PhD Sunnybrook Health Sciences Centre, Department of Radiation Oncology, Toronto, ON, Canada

University of Toronto, Department of Radiation Oncology, Toronto, ON, Canada

Talicia Savage, MD, PhD Albert Einstein College of Medicine, Pathology Department, New York, NY, USA

Claudia Scaringi, MD Radiation Oncology Unit, UPMC Hillman Cancer Center, San Pietro Hospital, Rome, Italy

Radiation Oncology Unit, Sant' Andrea Hospital, University Sapienza, Rome, Italy

David J. Schlesinger, PhD University of Virginia Gamma Knife Center, Charlottesville, VA, USA

University of Virginia, Departments of Radiation Oncology and Neurological Surgery, Charlottesville, VA, USA

Jugal Shah, MD New York University Langone Health, Department of Neurosurgery, New York, NY, USA

Deepa Sharma, PhD Physical Sciences, Sunnybrook Research Institute, Toronto, ON, Canada

Department of Medical Biophysics, University of Toronto, Toronto, ON, Canada

Jason P. Sheehan, MD, PhD University of Virginia Medical Center, Neurological Surgery, Charlottesville, VA, USA

University of Virginia School of Medicine, Neurological Surgery, Charlottesville, VA, USA

Charles B. Simone II, MD New York Proton Center, Department of Radiation Oncology, New York, NY, USA

Penny K. Sneed, MD University of California at San Francisco, Department of Radiation Oncology, San Francisco, CA, USA

Hany Soliman, MD, FRCPC Sunnybrook Odette Cancer Centre, Department of Radiation Oncology, Toronto, ON, Canada

University of Toronto, Toronto, ON, Canada

Scott G. Soltys, MD Stanford Cancer Institute, Stanford, CA, USA

Stanford University, Department of Radiation Oncology, Stanford, CA, USA

Paul W. Sperduto, MD, MPP, FASTRO Gamma Knife Center, University of Minnesota Medical Center, Department of Radiation Oncology, Minneapolis, MN, USA

Minneapolis Radiation Oncology, Waconia, MN, USA

William A. Stokes, MD Department of Radiation Oncology, University of Colorado School of Medicine, Aurora, CO, USA

John H. Suh, MD, FASTRO Department of Radiation Oncology, Cleveland Clinic, Cleveland, OH, USA

Rose Ella Burkhardt Brain Tumor and Neuro-Oncology Center, Cleveland Clinic, Cleveland, OH, USA

Jarred Tanksley, MD, PhD Department of Radiation Oncology, Duke University, Durham, NC, USA

Duke Cancer Insitute, Durham, NC, USA

Jacqueline J. Tao, BS Stanford University School of Medicine, Stanford, CA, USA

Robert D. Timmerman, MD University of Texas Southwestern Medical Center, Departments of Radiation Oncology and Neurological Surgery, Dallas, TX, USA

University of Texas Southwestern Medical Center, Radiation Oncology and Neurological Surgery, Dallas, TX, USA

Daniel M. Trifiletti, MD Mayo Clinic, Radiation Oncology, Mayo Clinic School of Medicine, Radiation Oncology, Jacksonville, FL, USA

Chia-Lin Tseng, MD Sunnybrook Health Sciences Centre, Department of Radiation Oncology, Toronto, ON, Canada

University of Toronto, Department of Radiation Oncology, Toronto, ON, Canada

Vyshak Alva Venur, MD Dana-Farber Cancer Institute, Division of Neuro-Oncology, Boston, MA, USA

Gregory M. M. Videtic, MD, CM, FCRPC, FACR Cleveland Clinic, Department of Radiation Oncology, Cleveland, OH, USA

Cleveland Clinic Lerner College of Medicine, Cleveland, OH, USA

Lei Wang, PhD Stanford Cancer Institute, Stanford, CA, USA

Stanford University, Department of Radiation Oncology, Stanford, CA, USA

Christopher Wilke, MD, PhD University of Minnesota, Department of Radiation Oncology, Minneapolis, MN, USA

Victor Yang, MD, PhD, FRCSC Sunnybrook Health Sciences Centre, Department of Neurosurgery, Toronto, ON, Canada

University of Toronto, Department of Neurosurgery, Toronto, ON, Canada

Nicholas Au Yong, MD, PhD Department of Neurosurgery, David Geffen School of Medicine at UCLA, Los Angeles, CA, USA

James B. Yu, MD, MHS Yale New Haven Hospital, Department of Therapeutic Radiology, New Haven, CT, USA

Yale School of Medicine, Department of Therapeutic Radiology, New Haven, CT, USA

Part I

Radiobiology of Radiosurgery and Stereotactic Body Radiation Therapy

Vascular-Mediated Mechanisms and SRS/SBRT

Golnaz Farhat, Deepa Sharma, and Gregory J. Czarnota

Abbreviations

ASMase	Acid sphingomyelinase
bFGF	Basic fibroblast growth factors
CSC	Cancer stem cells
Gy	Gray
HIF	Hypoxia-inducible factors
LQ	Linear quadratic
O_2	Oxygen
ROS	Reactive oxygen species
S1P	Sphingosine-1-phosphate
SBRT	Stereotactic body radiotherapy
SM	Sphingomyelin
SRS	Stereotactic radiosurgery
USMB	Ultrasound-stimulated microbubbles
VEGF	Vascular endothelial growth factor
VEGFR	Vascular endothelial growth factor receptor

G. Farhat
Physical Sciences, Sunnybrook Research Institute, Toronto, ON, Canada

D. Sharma
Physical Sciences, Sunnybrook Research Institute, Toronto, ON, Canada

Department of Medical Biophysics, University of Toronto, Toronto, ON, Canada

G. J. Czarnota (✉)
Physical Sciences, Sunnybrook Research Institute, Toronto, ON, Canada

Department of Medical Biophysics, University of Toronto, Toronto, ON, Canada

Odette Cancer Centre, Sunnybrook Health Sciences Centre, Toronto, ON, Canada

Department of Radiation Oncology, University of Toronto, Toronto, ON, Canada
e-mail: Gregory.czarnota@sunnybrook.ca

Introduction

Tumor vasculature plays a significant role in the proliferation and survival of tumor cells. The state of the vascular component determines tumor microenvironmental conditions and the overall tumor response to radiation therapy. Until recently, our understanding of tumor radiobiology was based on conventional fractionated radiotherapy. The role of tumor vasculature was viewed as a modulating factor of the tumor response to radiation through the reoxygenation of hypoxic cells after each fraction of radiation. The engagement of the vascular component with a high dose of radiation per fraction, as seen with stereotactic radiosurgery (SRS) and stereotactic body radiotherapy (SBRT), however, is different. High single doses of radiation cause a severe vascular response, resulting in rapid vascular deterioration. The underlying cellular and molecular mechanisms leading to vascular damage and disruption involve the activation of a cell death pathway mediated by ceramide in vascular endothelial cells. Tumor cells in this response predominantly die as a secondary effect to vascular damage, as opposed to dying by apoptosis resulting from direct radiation damage. Given the significance of the vascular response with high doses of radiation, understanding the effects and underlying mechanisms will play a key role in treatment planning for SRS and SBRT.

This chapter begins with a brief review of tumor vasculature characteristics and their role in determining the radiosensitivity of tumor cells. An overview of recent studies observing the effects of high-dose-per fraction radiation on the vascular component, as well as the cellular and molecular mechanisms of vascular disruption and secondary tumor cell death will follow. Finally, novel methods currently under development for enhancing the vascular response to high doses of radiation will be reviewed.

D. M. Trifiletti et al. (eds.), *Stereotactic Radiosurgery and Stereotactic Body Radiation Therapy*,
https://doi.org/10.1007/978-3-030-16924-4_1

Background and History

Tumor Angiogenesis

Angiogenesis, the growth of new capillary blood vessels, is necessary for tumor growth and metastasis. Judah Folkman first suggested, in 1971, that a strong interdependence exists between tumor parenchymal cells and the endothelial cells within the tumor vasculature, which he described as being a "highly integrated ecosystem" [1, 2]. Angiogenesis is a highly controlled process, predominantly regulated by the availability of oxygen. In tumors, the rapid proliferation of cells results in a surge of metabolic activity, increasing the demand for oxygen (O_2). An inability to provide sufficient O_2 to tumor cells results in localized regions of tumor hypoxia [3]. In response to hypoxia, tumors release diffusible angiogenic factors [4], the expression of which are regulated by transcription factors called hypoxia-inducible factors (HIF). It is well established that the HIF pathway is the master regulator of angiogenesis. HIF-regulated proangiogenic factors increase vascular permeability, endothelial cell proliferation, sprouting, migration, adhesion, and tube formation [3, 5].

A tumor may start as an avascular mass obtaining its blood supply through vessel co-option by growing alongside existing, well-established blood vessels. However, it can also grow and develop a new vascular network through various mechanisms. Sprouting angiogenesis is the growth of new capillary vessels from pre-existing ones [6] and occurs because of endothelial cell activation by basic fibroblast growth factors (bFGF) and vascular endothelial growth factors (VEGF). Degradation of the extracellular matrix and basement membrane of the existing vessels allows the proliferation and invasion of endothelial cells into the surrounding matrix. The development of tumor vasculature also occurs through intussusceptive angiogenesis, a rapid process that results in the division of a pre-existing blood vessel into two new vessels through the formation of transvascular tissue pillars [7]. More recently, it has been discovered that entirely new vessels may be formed by the recruitment of endothelial progenitor cells and in situ differentiation of endothelial cells from these precursor cells. These are subsequently organized into a vascular structure. Endothelial progenitor cells have been found in adult peripheral blood [8]. Finally, vasculogenic mimicry – the formation of new blood vessels by tumor cells themselves – has been reported to be a precursor to sprouting angiogenesis and is present in highly aggressive tumors [9].

Characteristics of Tumor Vasculature and Blood Flow

The vascular network and branching patterns in tumors are far from the organized hierarchical branching pattern seen throughout the human body. Normal vasculature is a weblike and well-organized network of capillaries. On a smaller scale, the capillary walls in normal tissue consist of a well-constructed tube composed of endothelial cells, surrounded by a basement membrane and sparsely placed pericytes between the two layers [10]. To meet the needs of highly metabolically active and rapidly proliferating tumor cells, the tumor endothelium is also rapidly proliferating [11]. The resulting vascular network is composed of vessels that are defective and structurally abnormal, tortuous, and often dilated, elongated, and saccular [12]. The vessels are leaky due to the defective vessel lining composed of areas in which the endothelial cells are stacked atop one another and others in which the cells are sparsely distributed. These vessels have uneven diameters due to compression of the poorly formed vessel walls by neighboring tumor cells [10]. The resulting perfusion is poor, intermittent, and often stationary due to the collapse of smaller blood vessels under the high interstitial pressure of tumors caused by poor lymphatic drainage [13]. The tumor vessel network does not follow a regular branching pattern. Instead, it is highly chaotic with poor three-dimensional coverage of the tumor volume. This results in large avascular tumor regions [10] suffering from hypoxia and a highly acidic, nutrient-deprived tumor microenvironment.

Tumor Vasculature and Radiosensitivity

Tumor vasculature has a direct effect on the tumor microenvironment – in particular affecting oxygenation status and acidity. The tumor microenvironment, in turn, affects the viability and proliferative ability of tumor cells. It is well known that oxygenation status has a large influence on the radiosensitivity of tumor cells with the response to radiation therapy being very poor in hypoxic regions [14]. The availability of molecular O_2 is necessary for the cytotoxic effects of radiation, mediated through the formation of reactive oxygen species (ROS) [15]. Radiosensitivity is, therefore, closely related to the state of tumor perfusion and the structure of tumor vasculature.

In 1936, Mottram [16] observed that the well perfused, and thus well oxygenated, tumor rim was more radiosensitive than the hypoxic core. Studies conducted in France in the 1920s and 1930s by Regaud, Ferroux, and Coutard also demonstrated that the therapeutic ratio in radiotherapy could be increased by delivering treatment through multiple small fractions [17]. This was because of reoxygenation that occurred after each radiation fraction. As cells in well-perfused tumor regions were killed, oxygen-deprived cells gained access to previously inaccessible capillaries, in effect reoxygenating them and increasing their sensitivity to the next fraction of radiation [18]. The role played by the vascular effects of radiation was seen, through the lens of fractionated radiotherapy, as an indirect modulator of radiosensitization [15, 19–22]. However, in 2003, Garcia Barros demonstrated that tumor microvascular damage also regulates tumor cell responses to radiation, painting a more

complex picture of radiation-induced tumor cell death. Their work indicated that the vascular endothelial cell, rather than the tumor cell, may be the primary target for radiation therapy [23].

Recent Advances: Vascular-Mediated Mechanisms of Tumor Response

Observed Vascular Effects of High-Dose Radiation

A limited number of human studies have investigated vascular effects of radiotherapy, the majority of which are concerned with conventional fractionated radiotherapy. These studies generally observed that blood flow increased slightly, or remained the same as pre-irradiation levels, early during a course of fractionated therapy and decreased thereafter [24–26]. Recently, Kumar and colleagues reported the results of a pilot study in which 30 patients suffering from spinal metastases received either single-fractionated SRS (24 Gy) or hypo-fractionated stereotactic radiosurgery (3–5 fractions, 27–30 Gy total). Dynamic contrast-enhanced magnetic resonance imaging (DCE-MRI) scans were acquired before and after radiotherapy to assess perfusion. The plasma volume, V_p, which is related to tumor vascularity, was significantly reduced in patients who were determined to have local tumor control at their 20-month follow-up (−76%) compared to patients with local recurrence (+28%) [27]. The reduction in vascularity following SRS preceded and was predictive of local tumor control with a sensitivity of 100% and a specificity of 98%. An earlier study by the same group reported similar results in a cohort of 12 patients with metastatic sarcoma lesions in the spine [28].

Despite the limited number of published human studies investigating the vascular effects of high doses of radiation from SRS and SBRT, there are several animal studies that can provide insight into the types of effects that can be expected. While these studies, reviewed by Park and colleagues [12], span many different tumor models and have results with some level of heterogeneity, some general trends have been observed. In tumors receiving single, moderately high doses of radiation (5–10 Gy) an initial increase in blood flow is followed by a return to pre-irradiation levels, or slightly below, within a few days. At higher single doses (10–15 Gy), an immediate decrease in blood flow persists for several days, with a return to control levels in some cases. Finally, at very high single doses (15–20 Gy), tumor blood flow decreases rapidly and is accompanied by vascular disruption and, eventually, tumor cell death. Radiation-induced microvascular effects observed in clinical and preclinical studies at various doses are listed in Table 1.

High single-dose radiation effects on tumor vascular permeability have been reported by multiple groups. A large body of work contributing to our understanding of these effects was produced in the 1970s with the investigation of vascular effects in Walker 256 rat mammary carcinoma tumors treated with radiation doses ranging from 2.5 Gy up to 60 Gy in a single dose [29–31]. Vascular permeability was assessed by measuring extravasation of plasma protein via iodine-125-labeled albumin. An increase in vascular permeability peaked at 24 h after irradiation for doses ranging from 2–20 Gy. The changes were dependent on the dose and the number of fractions, with 20 Gy delivered in a single dose causing a more substantial effect than the same dose delivered in four or eight fractions. In all cases, the increase in vascular permeability was transient, returning to pre-irradiation levels within a few days. Dose-dependent decreases in vascular volume were also observed. These were transient, lasting hours, at doses below 2.5 Gy, persisting for several days at doses in the 5–10 Gy range, and were significant and lasting at higher doses. More recent studies have observed similar increases in vascular permeability with single high doses of radiation [32, 33].

Mechanisms of Vascular Damage and Vascular Collapse

Vascular effects of radiation are directly related to the death of vascular endothelial cells. Tumor endothelial cells are significantly more radiosensitive than those in normal tissue vasculature [34]. Endothelial cell death widens the junctures between cells in the vessel lining, which, in tumors, is already compromised due to poor structure and uneven distribution of endothelial cells. Eventually, the affected microvessels will rupture or collapse [31]. Erythrocyte concentration in the capillaries will increase due to extravasation of plasma, leading to slow or static blood perfusion [35] and elevation of interstitial fluid pressure in the tumor, causing further vascular collapse [29].

In recent years, the notion that the tumor cell is the primary target of ionizing radiation is being replaced by the notion that tumor microvascular endothelial cell death is required for tumor cure. The interaction between tumor microvascular endothelial cells and tumor parenchymal cells is complex and dose-dependent (Fig. 1). At low doses (1–3 Gy/fraction), tumor cell death is dependent on the presence of reactive oxygen species made newly available after each cycle of hypoxia, reperfusion, and ionization during fractionated radiotherapy [15]. Work by Moeller and colleagues has indicated that the repeated surges of reoxygenation and the presence of ROS may lead to increased HIF-1 activity and the secretion of proangiogenic cytokines, including VEGF and bFGF. These cytokines exert a protective effect on endothelial cells and have the effect of attenuating the apoptotic response of endothelial cells to radiation [36]. Moeller and colleagues further demonstrated that HIF-1 regulates pathways that promote radiosensitization and apoptosis of tumor cells through increased tumor cell proliferation and p-53 activation. The complexity of these interactions makes the net effect of HIF-1 induction difficult to predict [37].

Table 1 Radiation-induced vascular effects observed in clinical and preclinical studies

Dose per fraction	Tumor model	Observed vascular effect	Source
1.9 Gy (fractionated)	Human (advanced cervical carcinoma)	Decrease in tumor vascularity during treatment, which was associated with better treatment outcome	Pirhonen et al. [70]
2 Gy (fractioned daily for 4–5 weeks)	Human (advanced cervical cancer)	Decreased blood perfusion in 50% of patients midtherapy with further decrease in 80% of patients after completion of treatment	Mayr et al. [26]
2.5 Gy (fractionated)	Rat (Walker carcinoma 256)	Transient decrease in vascular volume and increase in vessel permeability	Wong et al. [31]
2.5 Gy	Mouse (neuroblastoma)	Initial increase in functional intravascular volume and extravasation of plasma protein and decrease thereafter	Song et al. [35]
4 Gy/fraction (daily for 5 days)	Rat (BT4C malignant glioma)	Reduction in tumor microvascular density	Johansson et al. [71]
5 Gy	Mouse (mammary carcinoma)	Slight transient decrease in vascular volume with recovery within 4 days	Hilmas et al. [72]
5 Gy	Rat (mammary adenocarcinoma, in a window chamber)	Increase in vascular density and perfusion observed 24 and 72 h after treatment	Dewhirst et al. [73]
5 Gy (once weekly for 4 weeks)	Mouse (MA148 human ovarian carcinoma)	Reduction of 50% in microvessel density	Dings et al. [74]
4.5 Gy/fraction (six fractions over 3 weeks)	Human (advanced non-small cell lung cancer)	Increase in tumor vascular blood volume and permeability, with greater changes observed in tumor periphery compared to the center	Ng et al. [75]
5 Gy/fraction, five consecutive days	Human (nonlocally advanced rectal cancer)	Early increase in tumor perfusion	Janssen et al. [76]
10 Gy and 20 Gy (single doses)	Mouse (neuroblastoma)	Early decrease in vascular blood volume with further gradual decrease thereafter	Song et al. [35]
10 Gy	Mouse (human laryngeal squamous cell carcinoma)	Slight early increase in perfused blood vessels, subsequent significant decrease at 26 h and eventual return to control level by day 11	Bussink et al. [77]
10 Gy	Mouse (human melanoma)	Reduction in tumor blood perfusion of 60% at 72 h after irradiation	Brurberg et al. [78]
10–15 Gy	Mouse (human melanoma)	Loss of function in 35–45% of 5–15 μm diameter vessels within 1 week	Solesvik et al. [79]
12 Gy	Rat (A549 human lung cancer)	Significantly decreased vascular oxygenation within 24 h	Zhou et al. [80]
15 Gy	Mouse (MCF/129 fibrosarcoma)	Significant endothelial cell apoptosis leading to microvascular damage in $ASMase^{+/+}$ mice	Garcia-Barros et al. [23]
15 Gy	Mouse (FSC-1 and T43 tumors)	Significant reduction in functional vascularity leading to tumor growth delay	Ogawa et al. [81]
15 Gy	Mouse (human glioblastoma multiforme)	Decrease in blood perfusion to 10–30% of control within 2 weeks, with restoration of damaged vasculature thereafter	Kioi et al. [82]
15 Gy	Mouse (mammary carcinoma)	Decrease in vascular volume with no recovery	Hilmas et al. [72]
16.5 Gy	Rat (transplanted rhabdomyosarcoma)	Early 35% reduction in blood flow followed by complete recovery within 24 h	Emami et al. [83]
20 Gy	Mouse (adenocarcinoma)	Disruption in blood flow induces indirect cell death in 2/3 of tumor cells beginning 2 days after irradiation	Lasnitzki et al. [84]
20 Gy	Rat (Walker carcinoma 256)	Marked increase in plasma protein extravasation soon after irradiation with abrupt decline thereafter; significant decrease in functional intravascular volume for up to 11 days post irradiation	Song et al. [30]
20 Gy	Mouse (neuroblastoma)	Progressive, significant decrease in vascular volume, transient increase in extravasation of plasma protein, tumor regression accompanied by disorganization, aggregation and condensation of vascular network	Song et al. [35]
20 Gy	Mouse (Lewis lung carcinoma)	Marked decrease in tumor blood flow within 2 days followed by substantial recovery by day 4 after irradiation. Sustained blood flow achieved with second 20 Gy dose delivered 2 days after initial dose	Kim et al. [85]
25 Gy	Mouse (murine prostate TRAMP-C1 tumors)	Progressive, significant decrease in tumor microvascular density, over 3 weeks after irradiation, to 25% of that in unirradiated tumors	Chen et al. [86]
24 Gy	Human (spinal metastases)	Significant decrease in MRI perfusion parameters measured at 20-month follow-up in patients without local recurrence	Kumar et al. [27]
45 Gy	Mouse (mammary carcinoma)	Extensive microvascular damage	Hilmas et al. [72]
60.5 Gy	Rat (transplanted rhabdomyosarcoma)	Early 50% reduction in blood flow reduction that remained decreased at 72 h postirradiation	Emami et al. [83]

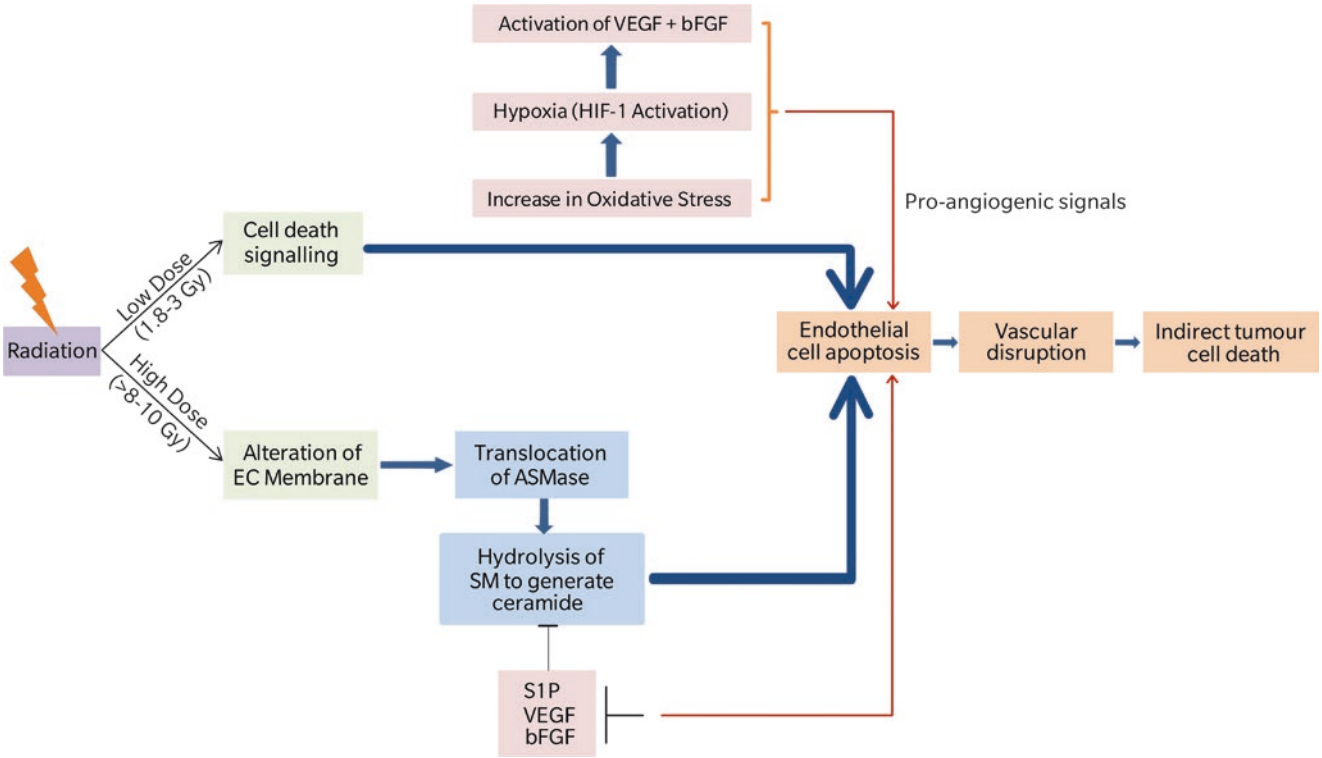

Fig. 1 Model of the dose-dependent microvascular endothelial cell response to irradiation. The vascular response to both low and high doses of radiation is illustrated in this schematic. Low-dose (1.8–3 Gy) fractionated radiation therapy initiates the activation of cell signaling pathways that result in apoptotic endothelial cell death. The generation of oxidative stress through repeated cycles of hypoxia and reoxygenation induces the release of hypoxia-inducible factor 1 (HIF-1), vascular endothelial growth factor (VEGF), and basic fibroblast growth factor (bFGF). These factors promote endothelial cell survival and have a significant quenching effect on the cell death signals. In response to high doses per fraction of irradiation (>8–10 Gy), endothelial cell ASMase is translocated to the outer leaflet of the cell membrane where it hydrolyzes sphingomyelin (SM) to generate ceramide. Ceramide acts as a second proapoptotic messenger and activates the apoptotic cascade. Proangiogenic factors such as sphingosine-1-phosphate (S1P), VEGF, and bFGF elicit a protective antiapoptotic effect if present in sufficient quantities

In the single, high-dose fraction scenario (>8–10 Gy), endothelial cell death is mediated through an acid sphingomyelinase (ASMase) pathway. Upon stimulation of cell surface receptors, ASMase, a lysosomal enzyme, translocates to the plasma membrane and hydrolyzes sphingomyelin, a phospholipid located on the outer layer of the membrane, to generate ceramide. Ceramide acts as a second messenger, activating downstream signaling pathways that initiate the cell death process [38–41]. Haimovitz-Friedman and colleagues demonstrated that ionizing radiation can interact with the cell membrane to generate an apoptotic signal through this pathway [39, 42]. This contrasts with the classic theory of ionizing radiation-induced cell death occurring through a p53-mediated pathway resulting from damage to cellular DNA. Endothelial cells are particularly vulnerable to radiation-induced apoptosis through the ASMase pathway because they have a 20-fold higher level of secretory ASMase compared to other cell types [38, 43, 44]. The mechanism of endothelial cell apoptosis through the ASMase pathway has been extensively investigated and reported by Kolesnik and Fuks. The window of radiation doses for which ceramide-mediated endothelial cell death occurs starts at 8–10 Gy in a single exposure and peaks at 20–25 Gy [38].

Endothelial Cell Damage Leads to Indirect Tumor Cell Death

Garcia-Barros and colleagues demonstrated that endothelial cell apoptosis regulates tumor cell response to radiation. Fibrosarcoma (MCA/129) and melanoma (B16F1) tumor xenografts were completely resistant to a single 15 Gy exposure when grown in ASMase-deficient mice, whereas the same condition in wild-type mice produced 50% tumor control. Their work further showed that initial rapid endothelial cell apoptosis occurred in these tumors, beginning at 1 hour and peaking at 4–6 hours post-irradiation. Tumor cell death detected during this window was minimal but increased significantly over a period of several days later. Ceramide-mediated endothelial cell apoptosis lead to secondary tumor

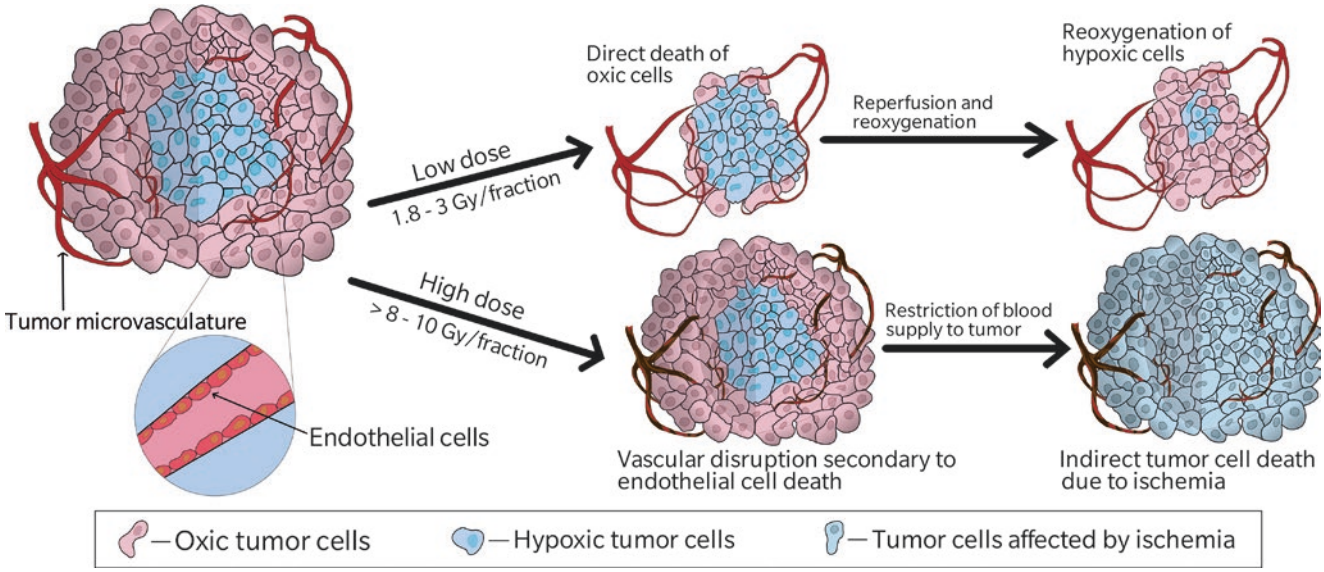

Fig. 2 Tumor cell death in response to single-high-dose or fractionated radiotherapy. Tumor response to low-dose fractionated radiotherapy is dominated by cell death resulting from radiation-induced DNA damage. Radiosensitive, oxygenated cells are preferentially killed, allowing the reperfusion and reoxygenation of hypoxic cells with each fraction of radiation. In contrast, the high-dose response is dominated by secondary tumor cell death resulting primarily from ischemia. Endothelial cell death leads to severe microvascular damage and causes starvation of tumor cells throughout the entire tumor volume

cell death and was proven to be mandatory for tumor cure. Tumors grown in ASMase-deficient mice were resistant to the curative effects of single-dose radiotherapy [23, 45]. Clinical evidence has also demonstrated that patients treated with a single high dose of spatially fractionated radiation of 15 Gy to treat large bulky tumors exhibited elevated serum levels of secretory sphingomyelinase (S-SMase), a protein product of ASMase and ceramide, and that this correlated with the level of tumor response to the treatment.

In clinical studies of cranial and extra-cranial tumors treated with SRS and SBRT, respectively, 80–90% tumor control was achieved with single radiation exposures in the range of 18–24 Gy [46–49]. Brown and colleagues conducted mathematical calculations of the expected level of cell kill using the standard linear quadratic (LQ) model and assuming 20% of cells are hypoxic. Their results concluded that the level of tumor control achieved by Yamada and colleagues at the given doses could not be explained by direct tumor cell death alone [50, 51]. Kocher and colleagues reached a similar conclusion when using a Monte Carlo simulation to fit clinical response data from 90 patients receiving single-dose irradiation (median marginal dose of 20 Gy) to treat brain metastases. The dose-response relationship observed clinically could not be reproduced using the LQ model without introducing significant vascular effects into the model [52]. Given the LQ model implicitly assumes that the underlying mechanism causing tumor cell kill is DNA damage, its inability to predict high-dose-per- fraction effects of radiation points to additional biological mechanisms at play [53]. The evidence suggests that two mechanisms contribute to tumor response to high-dose-per-fraction ionizing radiation. The first mechanism is direct cytotoxic damage to tumor cells caused by DNA damage, which occurs with both low and high doses per fraction. The second mechanism is indirect tumor cell death, preceded by vascular damage and endothelial cell death, which occurs preferentially at higher doses per fraction (Fig. 2).

The fraction of tumor cells succumbing to direct versus indirect death is dose-dependent, with indirect death becoming significant when the radiation dose per fraction reaches levels high enough to cause vascular damage. Park and colleagues, based on the conclusions from numerous clinical and preclinical studies, have estimated the threshold dose for indirect tumor cell death, resulting from a single exposure to ionizing radiation, to be in the range of 10–15 Gy for most human tumors [12]. A hypothetical illustration of the dose-dependence of cell death mechanisms in tumors has been illustrated by Song and colleagues [13]. Assuming 10% of clonogenic cells are hypoxic, direct tumor cell death of oxic cells dominates in the 0–5 Gy range, direct tumor cell death of hypoxic cells dominates in the 5–12 Gy range, and indirect tumor cell death of both oxic and hypoxic cells due to vascular damage dominates at doses greater than 10–12 Gy. The doses quoted are per fraction of ionizing radiation, implying that the relative importance of direct versus indirect cell death in SRS and SBRT is dependent on the size of the fraction rather than the overall dose.

The exact mechanisms leading to indirect tumor cell death are not fully understood. Ischemic cell death, caused by transient local hypoxia and nutrient deprivation resulting from vascular disruption, likely contributes significantly. Each endothelial cell is estimated to subtend a segment of tumor containing approximately 2000 tumor cells [54]. Disruption or collapse of even a small segment of microvasculature can lead to an avalanche of tumor cell death. A second contributing factor is thought to be a bystander effect, secondary to endothelial damage and leakage of circulating factors. Gaugler and colleagues have studied the bystander effect in unirradiated human intestinal epithelial T84 cells in a noncontact co-culture with irradiated endothelial cells [55]. They observed a 29% decrease in cell numbers and a 1.5-fold increase in apoptosis in the T84 cells. When both types of cells were irradiated together, the effects were further amplified, indicating that the bystander effect adds to the direct radiation damage. The bystander effect was specific to endothelial cells as the same effect could not be reproduced when the experiment was repeated with human colon fibroblasts. Finally, the interaction between self-renewing cancer stem cells (CSC) and microvascular endothelial cells is a potential third contributing factor. Recently it has been discovered that a small subpopulation of tumor cells, known as self-renewing cancer stem cells are responsible for tumor recurrence after radiotherapy. These CSC exhibit a higher level of radioresistance than non-stem cells [56]. This fact implies that tumor cure can only be achieved if all cancer stem cells are killed. Stem cells reside within niches composed of microenvironmental cells that regulate their proliferation and self-renewal properties through secreted factors [57–59]. Evidence suggests that the perivascular niche and the interaction of endothelial cells with brain tumor stem cells is critical for their survival [60]. Endothelial cell apoptosis and vascular disruption, resulting in disruption of the perivascular niche due to high single doses of radiation, could, therefore, have a direct effect on tumor control through the eradication of tumor stem cells.

Future Directions: Enhancing the Vascular Response with Combination Therapies

With recent advances in our understanding of the vascular component in tumor responses to high single fractions of radiation, it would be reasonable for future directions to take advantage of this interaction by combining radiotherapy with other treatment modalities that enhance the vascular response and increase the possibility of tumor cure, while de-escalating the overall delivered radiation dose. Czarnota and colleagues [61] have induced an enhancement of the vascular response to radiation using biophysical means to selectively target tumor vascular endothelial cells. This approach consists of using acoustic stimulation of microbubbles to mechanically injure the plasma membrane of endothelial cells. Microbubble solutions are currently in clinical use as ultrasound contrast agents and are comprised of gas spheres stabilized by a biocompatible lipid or protein shell. Their 3–4 micron diameter allows them to circulate freely within the microvasculature when injected intravenously. When placed within an ultrasound field at or near their resonant frequency, microbubbles may oscillate, cavitate, and even collapse, generating shear stresses on the membranes of nearby cells. This physical perturbation can have effects ranging from transient membrane permeabilization to complete destruction of the cell. In vitro and in vivo studies have demonstrated that ultrasound-stimulated, and microbubble-mediated endothelial cell perturbation can significantly enhance radiation therapy. In experiments with bladder, breast, and prostate tumor xenografts, mice were treated with ultrasound-stimulated microbubbles (USMB), followed by a single dose of 2–8 Gy of radiation. Significant tumor cell death (40–70%) was detected within 24 hours of treatment and demonstrated a whole tumor effect resulting in tumor regression [62–64]. The increase in cell death in tumors receiving a combination of USMB and radiation was significant and synergistic. A 2 Gy radiation treatment delivered to prostate tumor (PC-3) xenografts resulting in 4 ± 2% tumor cell death was converted to 40 ± 8% cell death when the treatment was combined with USMB [63]. Similar results were achieved in breast and bladder cancer xenografts [64–66]. Immunohistochemistry of tumor specimens identified endothelial cells as the primary target of the microbubble perturbation. Vascular leakage (detected using Factor VIII staining) and vascular collapse (detected using cluster of differentiation 31 (CD-31) staining) appeared to occur secondary to endothelial cell apoptosis resulting from the treatment. Significant differences in high-frequency power Doppler signals (drop in vascular index of 65% versus 20%), detected in tumors receiving the combined therapy versus radiation therapy alone, further confirmed the vascular effects. When delivered as multiple treatments, there was no evidence of a viable rim within the tumors, as seen with conventional fractionated radiotherapy. Instead, vascular disruption and cell death were observed across the whole tumor. Areas left with partially functioning vasculature responded after multiple treatments. Most importantly, survival studies demonstrated that mice receiving a 24 Gy dose (BED10 = 28.8) combined with USMB had better survival than mice receiving a much higher dose of radiation (BED10 = 58.5) alone. This method, thus, has the potential to convert a noncurative radiation dose into a curative one [63]. In vitro experiments with human umbilical vein endothelial cells, acute myeloid leukemia cells, murine fibrosarcoma (KHT) as well as breast (MDA-MB-231) and prostate (PC-3) cancer cells demonstrated that the synergy between USMB treatment and radiation is caused by mechanical damage to the endothelial cell

membrane, which activates the same cell death pathways activated by high-dose fractions of radiation. When combined with USMB, the activation of the ceramide apoptosis pathway was achieved with radiation doses as low as 2 Gy [67]. Manipulation of the ASMase pathway, either chemically or genetically, suppressed the radiation enhancement effect of USMB. A schematic of the treatment method and representative in vivo results are presented in Fig. 3.

Antiangiogenic approaches may be a viable avenue for further enhancing the vascular response to high-dose irradia-

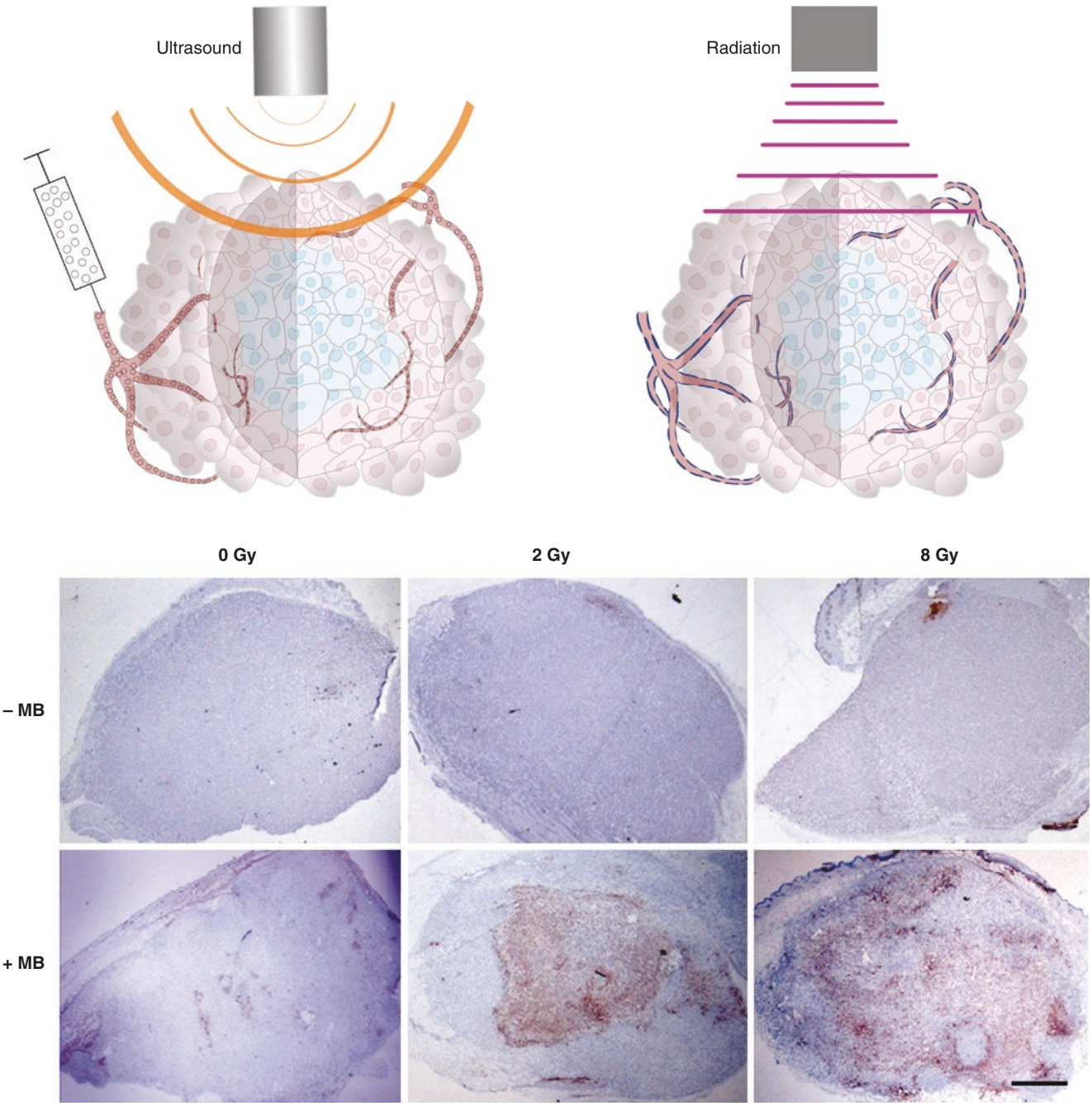

Fig. 3 Treatment schematic and representative in vivo results of ultrasound-stimulated microbubble radiation enhancement. Microbubbles are injected intravenously and circulate freely throughout the tumor microvasculature (top left). The tumor volume is subsequently targeted with ultrasound to stimulate microbubble cavitation. Endothelial cell membranes are perturbed (dark blue dashed outline, top right) by the microbubble therapy. The tumor microvasculature is radiosensitized and responds to radiation doses that are not normally sufficient to cause significant tumor cell death. The bottom panel shows representative images from in situ end labeling (ISEL)-stained sections of prostate cancer (PC3) tumors treated with radiation and/or ultrasound-activated microbubbles. Columns represent 0, 2, and 8 Gy of radiation exposure from left to right. Rows indicate the absence (–MB) or presence of microbubbles (+MB). Exposure to radiation alone (top row) resulted in no appreciable cell death as detected by ISEL-staining. Exposure to microbubbles alone resulted in minor cell death. The combination of ultrasound-stimulated microbubbles and radiation led to significant detectable cell death

tion. Antiangiogenic agents have been used in the context of radiosensitization by normalizing dysfunctional tumor vasculature, improving perfusion and, thus, the response to fractionated radiotherapy [68]. In contrast, Truman and colleagues have proposed the use of antiangiogenic therapy to enhance ceramide signaling. Their work has demonstrated that local ceramide levels within the outer leaflet of the plasma membrane dictate whether endothelial cells are in an antiapoptotic (proangiogenic) or proapoptotic (antiangiogenic) state [44]. Restoration of ceramide levels exogenously in cells where the ASMase pathway was previously inhibited by VEGF/bFGF reestablished apoptosis, even in the continued presence of VGEF/bFGF. An acute, yet transient inhibition of the vascular endothelial growth factor receptor (VEGFR) proved sufficient to evoke synergy with SBRT, indicating that the timing of antiangiogenic drug delivery is important – these agents should be delivered immediately prior to irradiation. In a preclinical study with fibrosarcoma tumors in mice, the delivery of axitinib (Pfizer), a VEGFR-selective small molecule inhibitor, enhanced tumor endothelial cell death and tumor cure when delivered immediately prior to single-dose radiosurgery [69]. The type of synergistic enhancement of the vascular response to radiation seen with USMB endothelial membrane perturbation or VEGFR inhibition using antiangiogenic therapy has the potential to allow for dose de-escalation in SRS and SBRT. Their implementation could reduce normal tissue toxicity while significantly improving treatment outcomes.

Conclusions

Studies have indicated that radiation delivered in high doses per fraction or in high single doses leads to severe vascular damage, vascular permeability, disruption, and deterioration. These effects result from vascular endothelial cell apoptosis caused by activation of the ASMase pathway through the interaction of radiation with the endothelial cell membrane. Endothelial cells are particularly sensitive to apoptosis via this pathway due to their 20-fold higher amount of secretory ASMase compared to other cells. The severe and rapid vascular deterioration leads to an ischemic event, causing secondary tumor cell death. This effect is observed across the whole tumor and is not limited to the viable tumor rim, as with conventional fractionated radiotherapy. Recent studies have investigated methods to synergistically increase tumor response to radiation by manipulating the ASMase activated apoptosis pathway in endothelial cells. Ultrasound-stimulated microbubbles can mechanically perturb the endothelial cell membrane, and antiangiogenic agents, such as axitinib can enhance ceramide signaling to achieve a similar effect. However, the presence of proangiogenic molecules, such as VEGF and bFGF, can dampen the effects of such therapies. Further investigation to determine optimal sequencing and timing of combination therapies is key to their successful clinical implementation. If implemented correctly, combination therapies may allow de-escalation of doses required to achieve tumor control or cure, thus, minimizing normal tissue toxicity.

Acknowledgments The authors would like to thank Mr. Shreyas Shankar for creating Figs. 2 and 3.

References

1. Folkman J, Judah F. Tumor angiogenesis: therapeutic implications. N Engl J Med. 1971;285(21):1182–6.
2. Folkman J. Tumor angiogenesis. Adv Cancer Res. 1985;43:175–203.
3. Krock BL, Skuli N, Simon MC. Hypoxia-induced angiogenesis: good and evil. Genes Cancer. 2011;2(12):1117–33.
4. Hanahan D, Folkman J. Patterns and emerging mechanisms review of the angiogenic switchduring tumorigenesis. Cell. 1996;86:353–64.
5. Pugh CW, Ratcliffe PJ. Regulation of angiogenesis by hypoxia: role of the HIF system. Nat Med. 2003;9(6):677–84.
6. Hillen F, Griffioen AW. Tumour vascularization: sprouting angiogenesis and beyond. Cancer Metastasis Rev. 2007;26(3–4):489–502.
7. Kurz H, Burri PH, Djonov VG. Angiogenesis and vascular remodeling by intussusception: from form to function. News Physiol Sci. 2003;18(12):65–70.
8. Asahara T, Murohara T, Sullivan A, Silver M, Van Der Zee R, Li T, et al. Isolation of putative progenitor endothelial cells for angiogenesis. Science. 1997;275(5302):964–7.
9. Zhang S, Zhang D, Sun B. Vasculogenic mimicry: current status and future prospects. Cancer Lett. 2007;254(2):157–64.
10. Jain RK. Molecular regulation of vessel maturation. Nat Med. 2003;9(6):685–93.
11. Vaupel P. Tumor microenvironmental physiology and its implications for radiation oncology. Semin Radiat Oncol. 2004;14(3):198–206.
12. Park HJ, Griffin RJ, Hui S, Levitt SH, Song CW. Radiation-induced vascular damage in tumors: implications of vascular damage in Ablative Hypofractionated Radiotherapy (SBRT and SRS). Radiat Res. 2012;177(3):311–27.
13. Song CW, Park HJ, Griffin RJ, Levitt SH. Radiobiology of stereotactic radiosurgery and stereotactic body radiation therapy. In: Levitt SH, Purdy JA, Perez CA, Poortmans P, editors. Technical basis of radiation therapy: practical clinical applications. 5th ed. Heidelberg: Springer; 2012. p. 51–61.
14. Moeller BJ, Richardson RA, Dewhirst MW. Hypoxia and radiotherapy: opportunities for improved outcomes in cancer treatment. Cancer Metastasis Rev. 2007;26(2):241–8.
15. Hall E. Radiobiology for the radiologist. 5th ed. Philadelphia: Lippincott Williams & Wilkins; 2000. p. 12–3.
16. Mottram JC. A factor of importance in the radio sensitivity of tumours. Br J Radiol. 1936;9(105):606–14.
17. Thames H. Early fractionation methods and the origins of the NSD concept. Acta Oncol (Madr). 1988;27(2):89–103.
18. Bristow RG, Hill RP. Hypoxia and metabolism: hypoxia, DNA repair and genetic instability. Nat Rev Cancer. 2008;8(3):180–92.
19. van Putten LM, Kallman RF. Oxygenation status of a transplantable tumor during fractionated radiation therapy. J Natl Cancer Inst. 1968;40(3):441–51.
20. Howes AE, Page A, Fowler JF. The effect of single and fractionated doses of x rays on the effective proportion of hypoxic cells in C 3 H mouse mammary tumours. Br J Radiol. 1972;45(532):250–6.
21. Kallman RF, DeNardo GL, Stasch MJ. Blood flow in irradiated mouse sarcoma as determined by the clearance of xenon-133. Cancer Res. 1972;32(3):483–90.

22. Clement JJ, Tanaka N, Song CW. Tumor reoxygenation and postirradiation vascular changes. Radiology. 1978;127(3):799–803.
23. Garcia-Barros M, Paris F, Cordon-Cardo C, Lyden D, Rafii S, Haimovitz-Friedman A, et al. Tumor response to radiotherapy regulated by endothelial cell apoptosis. Science. 2003;300(5622):1155–9.
24. Bergsjo P. Radiation-induced early changes in size and vascularity of cervical carcinoma. A colpophotographic and clinical study. Acta Radiol Diagn (Stockh). 1967;Suppl 274:7+.
25. Mäntylä MJ, Toivanen JT, Pitkänen MA, Rekonen AH. Radiation-induced changes in regional blood flow in human tumors. Int J Radiat Oncol. 1982;8(10):1711–7.
26. Mayr NA, Yuh WTC, Magnotta VA, Ehrhardt JC, Wheeler JA, Sorosky JI, et al. Tumor perfusion studies using fast magnetic resonance imaging technique in advanced cervical cancer: a new noninvasive predictive assay. Int J Radiat Oncol Biol Phys. 1996;36(3):623–33.
27. Kumar KA, Peck KK, Karimi S, Lis E, Holodny AI, Bilsky MH, et al. A pilot study evaluating the use of dynamic contrast-enhanced perfusion MRI to predict local recurrence after radiosurgery on spinal metastases. Technol Cancer Res Treat. 2017;16(6):857–65.
28. Spratt DE, Arevalo-Perez J, Leeman JE, Gerber NK, Folkert M, Taunk NK, et al. Early magnetic resonance imaging biomarkers to predict local control after high dose stereotactic body radiotherapy for patients with sarcoma spine metastases. Spine J. 2016;16(3):291–8.
29. Song CW, Levitt SH. Vascular changes in Walker 256 carcinoma of rats following X irradiation. Radiology. 1971;100(2):397–407.
30. Song CW, Payne JT, Levitt SH. Vascularity and blood flow in x-irradiated Walker carcinoma 256 of rats. Radiology. 1972;104(3):693–7.
31. Wong HH, Song CW, Levitt SH, Wong HH, Levitt SH. Early changes in the functional vasculature of Walker carcinoma 256 following irradiation. Radiology. 1973;108(2):429–34.
32. Kalofonos H, Rowlinson G, Epenetos AA. Enhancement of monoclonal antibody uptake in human colon tumor xenografts following irradiation. Cancer Res. 1990;50(1):159–63.
33. Kobayashi H, Reijnders K, English S, Yordanov AT, Milenic DE, Sowers AL, et al. Application of a macromolecular contrast agent for detection of alterations of tumor vessel permeability induced by radiation. Clin Cancer Res. 2004;10(22):7712–20.
34. Park M-T, Oh E-T, Song M-J, Kim W-J, Cho YU, Kim SJ, et al. The radiosensitivity of endothelial cells isolated from human breast cancer and normal tissue in vitro. Microvasc Res. 2012;84(2):140–8.
35. Song CW, Sung JH, Clement JJ, Levitt SH. Vascular changes in neuroblastoma of mice following x-irradiation. Cancer Res. 1974;34(9):2344–50.
36. Moeller BJ, Cao Y, Li CY, Dewhirst MW. Radiation activates HIF-1 to regulate vascular radiosensitivity in tumors: role of reoxygenation, free radicals, and stress granules. Cancer Cell. 2004;5(5):429–41.
37. Moeller BJ, Dreher MR, Rabbani ZN, Schroeder T, Cao Y, Li CY, et al. Pleiotropic effects of HIF-1 blockade on tumor radiosensitivity. Cancer Cell. 2005;8(August):99–110.
38. Fuks Z, Kolesnick R. Engaging the vascular component of the tumor response. Cancer Cell. 2005;8(2):89–91.
39. Kolesnick R, Fuks Z. Radiation and ceramide-induced apoptosis. Oncogene. 2003;22(37 REV. ISS. 3):5897–906.
40. Paris F, Fuks Z, Kang A, Capodieci P, Juan G, Ehleiter D, et al. Endothelial apoptosis as the primary lesion initiating intestinal radiation damage in mice. Science. 2001;293(5528):293.
41. Hua G, Kolesnick R. Using asmase knockout mice to model human diseases. Handb Exp Pharmacol. 2013;216:29–54.
42. Haimovitz-Friedman A, Kan CC, Ehleiter D, Persaud RS, McLoughlin M, Fuks Z, et al. Ionizing radiation acts on cellular membranes to generate ceramide and initiate apoptosis. J Exp Med. 1994;180(2):525–35.
43. Tabas I. Secretory sphingomyelinase. Chem Phys Lipids. 1999;102(1–2):123–30.
44. Truman JP, García-Barros M, Kaag M, Hambardzumyan D, Stancevic B, Chan M, et al. Endothelial membrane remodeling is obligate for anti-angiogenic radiosensitization during tumor radiosurgery. PLoS One. 2010;5(8):e12310.
45. García-Barros M, Thin TH, Maj J, Cordon-Cardo C, Haimovitz-Friedman A, Fuks Z, et al. Impact of stromal sensitivity on radiation response of tumors implanted in SCID hosts revisited. Cancer Res. 2010;70(20):8179–86.
46. Shiau CY, Sneed PK, Shu HK, Lamborn KR, McDermott MW, Chang S, et al. Radiosurgery for brain metastases: relationship of dose and pattern of enhancement to local control. Int J Radiat Oncol Biol Phys. 1997;37(2):375–83.
47. Vogelbaum MA, Angelov L, Lee S-Y, Li L, Barnett GH, Suh JH. Local control of brain metastases by stereotactic radiosurgery in relation to dose to the tumor margin. J Neurosurg. 2006;104(6):907–12.
48. Kim Y-J, Cho KH, Kim J-Y, Lim YK, Min HS, Lee SH, et al. Single-dose versus fractionated stereotactic radiotherapy for brain metastases. Int J Radiat Oncol Biol Phys. 2011;81(2):483–9.
49. Yamada Y, Bilsky MH, Lovelock DM, Venkatraman ES, Toner S, Johnson J, et al. High-dose, single-fraction image-guided intensity-modulated radiotherapy for metastatic spinal lesions. Int J Radiat Oncol Biol Phys. 2008;71(2):484–90.
50. Brown JM, Diehn M, Loo BW. Stereotactic ablative radiotherapy should be combined with a hypoxic cell radiosensitizer. Int J Radiat Oncol Biol Phys. 2010;78(2):323–7.
51. Brown JM, Koong AC. High-dose single-fraction radiotherapy: exploiting a new biology? Int J Radiat Oncol Biol Phys. 2008;71(2):324–5.
52. Kocher M, Treuer H, Voges J, Hoevels M, Sturm V, Müller RP. Computer simulation of cytotoxic and vascular effects of radiosurgery in solid and necrotic brain metastases. Radiother Oncol. 2000;54(2):149–56.
53. Kirkpatrick JP, Meyer JJ, Marks LB. The linear-quadratic model is inappropriate to model high dose per fraction effects in radiosurgery. Semin Radiat Oncol. 2008;18(4):240–3.
54. Denekamp J. Vascular endothelium as the vulnerable element in tumours. Acta Radiol Oncol. 1984;23(January):217–25.
55. Gaugler M-H, Neunlist M, Bonnaud S, Aubert P, Benderitter M, Paris F. Intestinal epithelial cell dysfunction is mediated by an endothelial-specific radiation-induced bystander effect. Radiat Res. 2007;167(March 2007):185–93.
56. Baumann M, Krause M, Hill R. Exploring the role of cancer stem cells in radioresistance. Nat Rev Cancer. 2008;8(7):545–54.
57. Moore KA. Stem cells and their niches. Science. 2006;311(5769):1880–5.
58. Ramirez-Castillejo C, Sanchez-Sanchez F, Andreu-Agullo C, Ferron SR, Aroca-Aguilar JD, Sanchez P, et al. Pigment epithelium-derived factor is a niche signal for neural stem cell renewal. Nat Neurosci. 2006;9(3):331–9.
59. Palmer TD, Willhoite AR, Gage FH. Vascular niche for adult hippocampal neurogenesis. J Comp Neurol. 2000;425(4):479–94.
60. Calabrese C, Poppleton H, Kocak M, Hogg TL, Fuller C, Hamner B, et al. A perivascular niche for brain tumor stem cells. Cancer Cell. 2007;11(1):69–82.
61. Czarnota GJ. Ultrasound-stimulated microbubble enhancement of radiation response. Biol Chem. 2015;396(6–7):645–57.
62. Al-Mahrouki AA, Iradji S, Tran WT, Czarnota GJ. Cellular characterization of ultrasound-stimulated microbubble radiation enhancement in a prostate cancer xenograft model. Dis Model Mech. 2014;7(3):363–72.

63. Czarnota GJ, Karshafian R, Burns PN, Wong S, Al Mahrouki A, Lee JW, et al. Tumor radiation response enhancement by acoustical stimulation of the vasculature. Proc Natl Acad Sci U S A. 2012;109(30):E2033–41.
64. Tran WT, Iradji S, Sofroni E, Giles A, Eddy D, Czarnota GJ. Microbubble and ultrasound radioenhancement of bladder cancer. Br J Cancer. 2012;107(3):469–76.
65. Lai P, Tarapacki C, Tran WT, El KA, Hupple C, Iradji S, et al. Breast tumor response to ultrasound mediated excitation of microbubbles and radiation therapy in vivo. Oncoscience. 2016;3:98–108.
66. Kwok SJJ, El Kaffas A, Lai P, Al Mahrouki A, Lee J, Iradji S, et al. Ultrasound-mediated microbubble enhancement of radiation therapy studied using three-dimensional high-frequency power doppler ultrasound. Ultrasound Med Biol. 2013;39(11):1983–90.
67. Nofiele JT, Karshafian R, Furukawa M, Al Mahrouki A, Giles A, Wong S, et al. Ultrasound-activated microbubble cancer therapy: ceramide production leading to enhanced radiation effect in vitro. Technol Cancer Res Treat. 2013;12(1):53–60.
68. Kleibeuker EA, Griffioen AW, Verheul HM, Slotman BJ, Thijssen VL. Combining angiogenesis inhibition and radiotherapy: a double-edged sword. Drug Resist Updat. 2012;15(3):173–82.
69. Rao SS, Thompson C, Cheng J, Haimovitz-Friedman A, Powell SN, Fuks Z, et al. Axitinib sensitization of high single dose radiotherapy. Radiother Oncol. 2014;111(1):88–93.
70. Pirhonen JP, Grenman SA, Bredbacka ÅB, Bahado-Singh RO, Salmi TA. Effects of external radiotherapy on uterine blood flow in patients with advanced cervical carcinoma assessed by Color Doppler ultrasonography. Cancer. 1995;76(1):67–71.
71. Johansson M, Bergenheim T, Widmark A, Henriksson R. Effects of radiotherapy and estramustine on the microvasculature in malignant glioma. Br J Cancer. 1999;80(1–2):142–8.
72. Hilmas DE, Gillette EL. Microvasculature of C3H/Bi mouse mammary tumors after x-irradiation. Radiat Res. 1975;61(1):128–43.
73. Dewhirst MW, Oliver R, Tso CY, Gustafson C, Secomb T, Gross JF. Heterogeneity in tumor microvascular response to radiation. Int J Radiat Oncol. 1990;18(3):559–68.
74. Dings RPM, Williams BW, Song CW, Griffioen AW, Mayo KH, Griffin RJ. Anginex synergizes with radiation therapy to inhibit tumor growth by radiosensitizing endothelial cells. Int J Cancer. 2005;115(2):312–9.
75. Ng Q-S, Goh V, Milner J, Padhani AR, Saunders MI, Hoskin PJ. Acute tumor vascular effects following fractionated radiotherapy in human lung cancer: in vivo whole tumor assessment using volumetric perfusion computed tomography. Int J Radiat Oncol Biol Phys. 2007;67(2):417–24.
76. Janssen MHM, Aerts HJWL, Kierkels RGJ, Backes WH, Ollers MC, Buijsen J, et al. Tumor perfusion increases during hypofractionated short-course radiotherapy in rectal cancer: sequential perfusion-CT findings. Radiother Oncol. 2010;94(2):156–60.
77. Bussink J, Kaanders JH, Rijken PF, Raleigh JA, Van der Kogel AJ. Changes in blood perfusion and hypoxia after irradiation of a human squamous cell carcinoma xenograft tumor line. Radiat Res. 2000;153(4):398–404.
78. Brurberg KG, Thuen M, Ruud E-BM, Rofstad EK. Fluctuations in pO2 in irradiated human melanoma xenografts. Radiat Res. 2006;165(1):16–25.
79. Solesvik OV, Rofstad EK, Brustad T. Vascular changes in a human malignant melanoma xenograft following single-dose irradiation. Radiat Res. 1984;98(1):115–28.
80. Zhou H, Zhang Z, Denney R, Williams JS, Gerberich J, Stojadinovic S, et al. Tumor physiological changes during hypofractionated stereotactic body radiation therapy assessed using multi-parametric magnetic resonance imaging. Oncotarget. 2017;8(23):37464–77.
81. Ogawa K, Boucher Y, Kashiwagi S, Fukumura D, Chen D, Gerweck LE. Influence of tumor cell and stroma sensitivity on tumor response to radiation. Cancer Res. 2007;67(9):4016–21.
82. Kioi M, Vogel H, Schultz G, Hoffman RM, Harsh GR, Brown JM. Inhibition of vasculogenesis, but not angiogenesis, prevents the recurrence of glioblastoma after irradiation in mice. J Clin Invest. 2010;120(3):694–705.
83. Emami B, Ten Haken RK, Nussbaum GH, Hughes WL. Effects of single-dose irradiation in tumor blood flow studied by 15O decay after proton activation in situ. Radiology. 1981;141(1):207–9.
84. Lasnitzki I. A quantitative analysis of the direct and indirect action of X radiation on malignant cells. Br J Radiol. 1947;20(234):240–7.
85. Kim DWN, Huamani J, Niermann KJ, Lee H, Geng L, Leavitt LL, et al. Noninvasive assessment of tumor vasculature response to radiation-mediated, vasculature-targeted therapy using quantified power Doppler sonography: implications for improvement of therapy schedules. J Ultrasound Med. 2006;25(12):1507–17.
86. Chen FH, Chiang CS, Wang CC, Tsai CS, Jung SM, Lee CC, et al. Radiotherapy decreases vascular density and causes hypoxia with macrophage aggregation in TRAMP-C1 prostate tumors. Clin Cancer Res. 2009;15(5):1721–9.

Radio-Immunology of Ablative Radiation

Talicia Savage and Chandan Guha

Tumor Immunity Is Critical for Local Control of Tumors After Ablative Radiation

There were significant advancements in radiation technology over the last few decades, including the advent of image guided radiation therapy. With the introduction of stereotactic radiosurgery (SRS) stereotactic body radiation therapy (SBRT) or stereotactic ablative radiotherapy (SABR), high ablative doses of radiation can be safely delivered to a small, well-defined target with high accuracy and steep dose gradients, with local control rates similar to surgery. The use of computed tomography (CT) and multiple coplanar and noncoplanar radiation fields allows for the treatment of targeted tissue with minimal toxicity to surrounding normal tissue. Although conventional fractionation schedules in radiotherapy were considered beneficial in terms of reoxygenation and redistribution of cancer cells to more radiosensitive points of the cell cycle, fractionation with lower dose per fraction also allows for the survival of cancer stem cells, enabling repopulation and tumor regrowth. Several clinical studies have recently demonstrated >90% local control of the irradiated tumor with a short course (1–5 fractions) of ablative fractionation of RT. For example, SBRT with three 18 Gy fractions had a 3-year primary tumor local control rate of 97.6% and 3-year overall survival of 55% in inoperable lung cancer [1]. In another study, a single fraction of 24 Gy to metastatic spinal lesions led to a 90% local control rate [2]. Subsequent studies by these investigators showed that single-dose SBRT can effectively control extracranial metastases, irrespective of the histologic type and target organ, provided sufficiently high doses (>22 Gy) of radiation are delivered [3, 4].

T. Savage
Albert Einstein College of Medicine, Pathology Department, New York, NY, USA
e-mail: talicia.savage@med.einstein.yu.edu

C. Guha (✉)
Departments of Radiation Oncology, Pathology and Urology and Institute for Onco-Physics, Albert Einstein College of Medicine, Montefiore Medical Center, New York, NY, USA

Tumoricidal effects of ionizing radiation is primarily attributed to dose-dependent DNA damage that results in growth arrest and senescence, as well as cell death via mitotic catastrophe, apoptosis, and necrosis of irradiated tumor cells. The lethal effects of irradiation on the tumor stroma have also contributed to tumor control. The high local control rates of single fraction SBRT have been attributed to the ablation of the tumor endothelium due to acid sphingomyelinase-mediated generation of ceramide in cell surface lipid rafts that signals the induction of apoptosis in the microvascular endothelium of the irradiated stromal tissues [5]. Although lethal effects of radiation were directly linked with the radiation-induced DNA damage in irradiated cells, numerous preclinical [6, 7] and clinical studies [8–10] have shown that an intact immune system, including cytotoxic T cells and antigen presenting dendritic cells, is not only necessary for immune surveillance but also required for efficient tumor control. In a multi-institutional report, chronically immunosuppressed patients had higher rates of cutaneous squamous cell carcinoma of the head and neck, and despite being treated with surgery and postoperative RT, these patients had poor outcomes, compared to immunocompetent patients with similar disease [9]. In a matched pair analysis of patients with prostate cancer who were treated with external beam RT, there was an increase in 3- and 5-year biochemical failure in immunocompromised patients. In another retrospective review of 244 consecutive patients with early stage non-small cell lung cancer (NSCLC) who were treated with SBRT, patients on chronic immunosuppressive therapy had poor local control and progression-free survival, compared to historic controls [10]. Although these clinical reports were all retrospective studies with small number of patients, the poor clinical outcome seen in immunocompromised patients support the hypothesis that immune response plays a critical role in tumor control after RT. Ablative radiation promotes the release of tumor antigens and damage-associated molecular pattern (DAMP) molecules from irradiated tumor cells for activation of dendritic cells (DCs). DCs engulf, process, and cross-

D. M. Trifiletti et al. (eds.), *Stereotactic Radiosurgery and Stereotactic Body Radiation Therapy*,
https://doi.org/10.1007/978-3-030-16924-4_2

present tumor antigens on class I major histocompatibility complex (MHC) for activating CD8+ cytotoxic T cells (CTLs) that are responsible for eradicating surviving clonogens in the irradiated tumor. In murine models of melanoma [6], colorectal cancer [7], and hepatocellular cancer [11, 12], ablation of immune effector cells, especially CD8+ T cells, abrogated control of both local and systemic disease and cure. These studies suggest that RT can generate an autologous in situ tumor vaccine and induce antitumoral immunity that contributes to the high rates of local tumor control, usually seen after SABR or SRS. However, despite evidence of the induction of antitumoral immunity after local tumor irradiation, RT usually fails to control systemic metastases. This suggests that therapeutic strategies to enhance antigen presentation from irradiated tumor cells, targeting the immunosuppressive features of the irradiated tumor microenvironment (TME) and reversing T cell anergy and exhaustion will be critical to realize the potential of RT-enhanced in situ tumor vaccines. This review focuses on the immunological consequences of ablative radiation and proposes a road-map for combination of RT with immunotherapy to induce a strong antitumoral immunity for both local and systemic tumor control.

Radiation-Enhanced Antigen Presentation (REAP)

The radiation-enhanced antigen presentation (REAP) would be an integral component of the proposed tumor vaccination strategy for solid tumors. Since cancer is a chronic disease, induction of the body's own immune system to fight distant microscopic metastatic disease would be highly beneficial in prolonging patient survival and eventual eradication of distant micrometastatic disease in liver cancer patients. Cancer cells express unique tumor antigens that include viral proteins, mutated oncoproteins, such as, p53 and ras, unique hybrid proteins expressed from translocated oncogenes, such as, BCR-ABL and proteins that are expressed during embryogenesis, but are not expressed by normal adult tissues [13]. Some of these "oncofetal" proteins serve as epitopes for host humoral and cellular immune response, which could potentially eradicate cancer cells. The immune system has the potential to recognize and eliminate cells with mutated proteins that are precursors to tumor. During the evolution of tumors, mutated cells lose the expression of proteins that participate in the antigen processing and presentation machinery, such as the antigen transporter gene product, TAP-2, and class I MHC molecules [14, 15]. This adaptive evasion of immune surveillance involves the selection of less immunogenic clones of tumor cells and is frequently mediated by acquisition of loss-of-function mutations and epigenetic regulation of the transcription of genes that are involved in the immune recognition and effector pathways of the adaptive tumor immunity.

Although, vaccination with defined tumor antigens and peptides has obvious appeal, natural immuno-variation, MHC polymorphism, and expected emergence of antigen-loss variants would require an ever-changing mixture of potential tumor antigens in vaccine formulations. Instead of individualized vaccines, a radiation-mediated, autologous in situ vaccination approach (Fig. 1) has been designed, whereby circulating DCs can be stimulated to infiltrate irradiated tumors and harvest tumor antigens released from dying tumor cells after RT treatment [16]. Modulation of the professional antigen presenting cells (APCs) such as DC may determine the efficacy of tumor immunity following primary tumor RT. DCs have been shown to acquire antigen from both apoptotic and necrotic cells. Localized RT by inducing tumor cell death would conceivably increase the tumor antigen available for presentation by DC. However, DCs are rare cells (<1%) in normal peripheral blood. The number of circulating DCs can be increased by administration of Flt3L (fms-like tyrosine kinase 3 ligand), which is a naturally occurring glycoprotein that stimulates the proliferation and differentiation of DCs [17, 18]. Thus, it was hypothesized that following local tumor irradiation, systemic administration of Flt3L would induce DC proliferation and infiltration of irradiated tumors by naïve circulating DCs that will readily endocytose tumor antigens released from dying tumor cells. Irradiated tumor cells could also provide "danger" signals that are necessary for DC activation. In murine models of lung cancer and hepatocellular carcinoma, it has been demonstrated that systemic administration of Flt3L, following ablative fractionation of primary tumor RT, generates effective tumor immunity that eradicates systemic metastases and cures mice with metastatic lung [16, 19] and liver cancer [11, 12].

Irradiated tumors can potentially serve as a source of tumor antigens *in vivo*, where dying tumor cells would release various tumor antigens slowly over time. Upon exposure, radiation initially increases the degradation of cellular proteins and eventually stimulates translation of novel proteins due to activation of the mammalian target of rapamycin pathway [20]. Radiation also increases the cell surface expression of Class I MHC molecules and cell death receptors, such as Fas in a dose-dependent fashion, thereby increasing peptide production, antigen presentation, and susceptibility to T cell-mediated cytotoxicity [20, 21]. Irradiation induces transcription and variant splicing of human endogenous retrovirus K (HERV-K) transcripts in human prostate and breast cancer cells, thereby raising the possibility that aberrant HERV-K peptides could also contribute to enhanced immunogenicity after RT [22]. In fact, HERV-K triggers a T cell response in breast cancer patients and chimeric antigen receptor-expressing T cells targeting HERV-K peptides have been designed that can inhibit tumor growth and metastases [23, 24]. Another source of

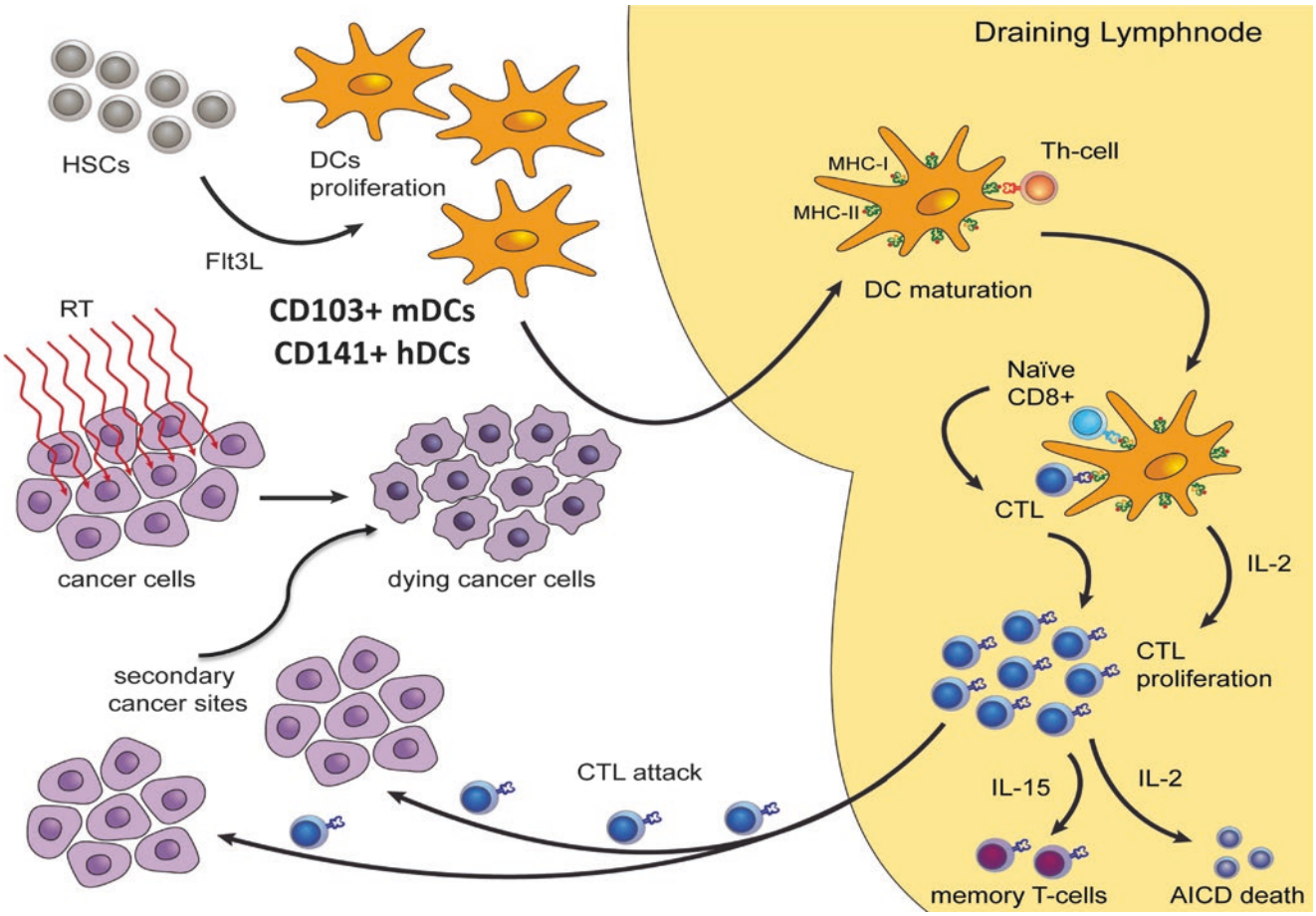

Fig. 1 **Radiation-immunity cycle for *in situ* tumor vaccines**. Ablative radiation induces cell death and secretion and presentation of DAMPs. Administration of Flt3L stimulates the proliferation and number of circulating DCs, including Batf3-dependent CD131+ and CD141+ DCs, which are able to engulf dying irradiated tumor cells for antigen presentation to T cells in draining lymph nodes. Tis results in the proliferation of cytotoxic T cells that circulate in the blood to help eradicate distant unirradiated tumor cells

neoantigens in irradiated tumor cells could be peptides encoded by alternate or cryptic translational reading frames seen in cells undergoing integrated stress response [25, 26]. While most of the peptides, presented in class I MHC, are generated from newly translated polypeptides encoded in open reading frames within mRNAs, Shastri and colleagues discovered that MHC I also present peptides encoded in alternate or cryptic translational reading frames [27]. The importance of cryptic translation for immune surveillance has become increasingly evident from independent discoveries of CD8+ T cells elicited by peptides encoded in alternate translational reading frames in tumors and viral mRNAs and human B cells [26, 28–32]. Because these "cryptic" antigens are absent in the thymus, CD8+ T cells are not tolerant and respond vigorously to these antigens. Given the immunogenicity of cryptic peptides for eliciting CD8+ T cell responses, they provide unique targets for vaccines and immunotherapy [33, 34]. Therefore, it is possible that enhanced immunogenicity of irradiated cells is due to expression of neoantigens [35].

Radiation-Induced DAMP Signals

Lack of a systemic antitumor immunity after RT is primarily due to inadequate antigen presentation by tumor cells and tolerogenic APCs in the TME and impaired host recognition of tumor cells. The innate immune system maintains homeostasis within the host by recognizing "strangers" (foreign pathogens) and sensing "dangers" (cellular stress) through binding of pathogen-associated molecular pattern (PAMP) and damage-associated molecular pattern (DAMP) ligands, respectively, to the pattern recognition receptors (PRRs), such as toll-like receptors (TLRs), retinoic acid-inducible gene (RIG-1)-like receptors (RLRs), AIM2-like receptors (ALRs), and nucleotide-binding oligomerization domain (NOD)-like receptors (NLRs) [36–38]. PAMPs, characterized in Table 1, are molecules associated with pathogenic organisms other than the host capable of providing exogenous signals for dendritic cell (DC) activation [36, 39, 40] and have been used as adjuvants for vaccines. DAMPs, characterized in Table 2, are host cell molecules that are upregu-

Table 1 Pathogen-associated molecular pattern (PAMP) molecules and their receptors

PAMP	Expression	Receptor	Downstream effect
Microbial DNA (unmethylated CpG motifs)	In cytosol	TLR9	MyD88 association and immune induction
Double-stranded RNA (dsRNA)	In cytosol, in endosomes	TLR3	TRIF association and immune induction
Single-stranded RNA (ssRNA)	In cytosol	TLR7	MyD88 association and immune induction
Lipoteichoic acid	Cell wall, gram-positive bacteria	TLR4	MyD88 association and immune induction
Peptidoglycan	Cell wall, gram-positive bacteria	TLR2	MyD88 association and immune induction
LPS	Membrane components, gram-negative bacteria	TLR4	MyD88 association and immune induction

Table 2 Danger-associated molecular pattern (DAMP) molecules and their receptors

DAMP	Expression	Receptor	Downstream effect
Calreticulin(CRT) "eat me"	Translocation to cell surface in early stage cell death	CD91 and SRF-1	Phagocytosis by macrophages
Heat shock protein 70 (HSP70)	Translocation to cell surface	NK cells CD94	NK activation
HSPs (HSP60, HSP70, and HSP72)	Released extracellularly	CD14, CD91, TLR4, and TLR2	DC activation and immune induction
HMGB1	Released extracellularly	TLR4 and TLR2	DC activation and immune induction
ATP	Released extracellularly	P2X7	DC activation and T cell priming
Uric acid		CD14, TLR2 and TLR4	
N-formyl peptides		FPR and FPRL1	
Thioredoxin		ND	
S-100 Proteins		RAGE	

lated in response to cellular stress, especially in cells undergoing immunogenic cell death (ICD) [41–43]. Irradiation induces ICD and express DAMP signals in tumor cells in a dose-dependent manner [44].

The clearance of dying tumor cells and the secretome by the phagocytic cells of the innate immune system determines the immunological outcome by recruiting immune effector cells in the TME to either induce active T cell tolerance or trigger antitumor immunity [45, 46]. In order to induce an immune response, dying cells need to provide two signals for DCs. First, a specific "eat me" signal is presented by the translocation of cytoplasmic calreticulin to the cell membrane, which allows DCs to engulf dying tumor cells [42]. Second, a specific "danger" signal is released by the dying cell that activates DCs and stimulates antigen processing and presentation to T cells. Cells undergoing ICD release nuclear nonhistone protein, high mobility group box 1 protein (HMGB1), that binds to Toll receptor 4 (TLR 4) in DCs, thereby providing a "danger" signal for TLR4-dependent antigen presentation and activation of T cells [41]. Danger signals were first postulated as endogenous and exogenous signals that induce the immune system to respond to agents that cause damage to the body, rather than to those that are simply foreign [47]. DCs are the sentinels of the immune system and sample antigens released from dying cells. In the absence of "danger" signals, DCs induce tolerance, while in the presence of these signals, DCs mature and get activated with the induction of T cell costimulatory molecules, such as CD80 and CD86. Besides HMGB1, endogenous "danger" signals are provided by stress proteins, heat shock proteins (HSPs), which are released from dying necrotic tumor cells and are actively taken up by DCs for cross-presentation via HSP receptors (CD91 for gp96, calreticulin, HSP70 and HSP90; CD14 for HSP70) [48–52]. HSPs are highly conserved, most abundant of intracellular proteins and function as molecular chaperones that guide several steps during synthesis, transportation, and degradation of proteins. HSPs have been implicated in chaperoning antigenic peptides intracellularly in order to present them on cell surface MHC molecules [53]. HSPs are not merely carriers of tumor antigens but can also induce maturation of DCs, resulting in a more efficient antigen presentation [54–57]. Besides HSPs and HMGB1s, there are several "danger" signals released in the irradiated tissues, such as ATP, oxidized lipids [58], formylated peptides, uric acid [59], etc., that can trigger an immune response. Although "danger" signals are necessary for inducing an immune response, CD8+ T cells are tolerant to "self" antigens from normal tissues and only react to mutated peptides from tumor cells.

Radiation-Induced Viral Mimicry

Although the tumoricidal effects of ionizing radiation (IR) has been attributed to double strand DNA (dsDNA) breaks in irradiated cells, the innate and adaptive antitumoral immunity plays a critical role in tumor ablation. Radiation-induced genotoxic stress results in the accumulation of dsDNA, consisting of mitochondrial DNA (mtDNA) and genomic DNA

(gDNA), in the cytosol of tumor cells [60]. The accumulation of dsDNA and RNA mimics a viral infection in irradiated cells. In addition, IR can induce the expression of epigenetically "silenced" viral genes in the tumor and induce an immune response. Upon engulfment of irradiated tumors cells by tumor-infiltrating DCs, the cytosolic DNA sensor, cyclic GMP-AMP (cGAMP) synthase (cGAS), binds to the dsDNA and produces cGAMP that activates the stimulator of interferon genes (STING), an endoplasmic reticulum (ER)-associated protein. STING then activates TANK-binding kinase 1 (TBK1) and inhibitor of nuclear factor-kappaB (NF-kB) kinase epsilon (IKKe) which in turn phosphorylates interferon regulatory factor 3 (IRF3), causing its translocation to the nucleus to induce transcription of type I interferon (IFN) genes. Multiple investigators have shown that type I IFN responses, specifically from Batf3-dependent DCs, is imperative to effective tumor control, and when type I IFNs were blocked in DCs, tumor ablation was lost [61–63]. Since the DNA sensors are intracellular, how does the extracellular self-DNA released by dying cells get recognized? It is postulated that extracellular genomic and mitochondrial dsDNA binds to the antimicrobial peptide LL37 and is endocytosed into endosomal compartments of plasmacytoid dendritic cells, leading to activation of TLR-9 and induction of type I IFNs [64]. LL37 binding confers resistance to DNase II breakdown of dsDNA and escape from autophagic recognition [64, 65], thereby allowing the activation of DNA sensors in the DCs. Oxidized dsDNA is a potent stimulator of inflammatory cytokines. Neutrophils take advantage of this response by expelling gDNA at inflammatory sites after an oxidative burst, generating neutrophil extracellular traps (NETs) that enhance cytosolic DNA delivery [66]. Another beneficial aspect of oxidized DNA is its resistance to degradation by three prime repair exonuclease 1 (TREX1), a cytosolic exonuclease important in protection against autoimmunity. Recent reports show that TREX1 was induced in some tumor cells after exposure to high dose fractions (>12–18 Gy) of IR and attenuated their immunogenicity by degrading cytosolic DNA [67].

Besides tumor-infiltrating DCs, the irradiated tumor cells can also express type I IFN genes, especially from cells with micronuclei that contains chromosomal fragments that were not incorporated into daughter cells during cell division. After radiation exposure, dsDNA repair mostly occurs during cell cycle arrest. If irradiated cells with dsDNA continue to progress through mitosis, micronuclei are formed over the course of several cell cycles and is correlated with signal transducer and activator of transcription 1 (STAT1) activation in these cells [68]. Interestingly, cGAS was found to colocalize primarily with micronuclei of treated and daughter cells, linking micronuclei with innate immunity, STING signaling, STAT1 activation, and secretion of cytokines, including interferon beta 1 (INFB1), interferon gamma (IFNG), and C-C motif chemokine ligand 5 (CCL5) [68, 69]. This explains the delayed onset of several days in the induction of inflammatory signaling after genotoxic stress. Inhibiting cell cycle progression through mitosis or suppressing the cGAS-STING pathway abrogated the inflammatory response and the regression of unirradiated abscopal tumors in the context of RT and immune checkpoint therapy [68]. The DNA damage response involves the rapid recruitment of DNA repair enzymes and a family of phosphatidylinositol 3 kinase (PI3K)-related kinases, ataxia-telangiectasia mutated (ATM) and Rad3 related (ATR), and the DNA-dependent protein kinase (DNA-PK) that acts as signal transducers of dsDNA breaks and regulate cell cycle checkpoints and cell survival. The PI3K-related kinase activation leads to Chk1 and Chk2 activation followed by NF-kB activation, leading to cell cycle arrest and apoptosis or signaling through IRFs, mainly IRF7, and interferon stimulator gene (ISG) activation with release of IFNα and IFNλ [70]. ATM acts as the primary transducer for IFN signaling and also plays a role in upregulation of cell surface NKG2DL which increases the susceptibility of DNA damaged cells to natural killer cell (NK) mediated killing [71].

Along with DNA, cytosolic RNA sensed by PRRs and TLRs is also an inducer of ISGs, typically in response to viral infection and detection [72]. Two RNA helicase enzymes that detect cytosolic dsRNA and are primarily involved in ISG signal transduction include retinoic acid -inducible gene I (RIG-I) and melanoma differentiation-associated gene 5 (MDA5). These enzymes associate with IFNB-promoter stimulator 1 (IPS-1 or MAVS) to activate TKB1 and IKKe, similar to STING activation of ISGs. Cytosolic ssRNA binds to TLRs 7 and 9 and produce type I IFN response in a STING independent manner signaling through myeloid differentiation primary response 88 (MyD88) and TIR-domain-containing adapter-inducing interferon-β (TRIF) [40]. Recent work into exosomes have observed that they are capable of carrying RNA (exoRNA) from tumor stromal cells and activating RIG-1 on neighboring cancer cells [73].

Immunosuppressive Properties of RT

IR has been classically used to ablate the lymphoid and myeloid cells of the blood and hematopoietic system as a preparative regimen for bone marrow transplantation. A systematic review of patients undergoing RT for solid tumors noted the impact of radiation-induced lymphopenia on survival [74]. Circulating peripheral blood cells are at risk of death after radiation exposure highlighting the significance of blood as an organ-at-risk during RT. For example, a conventional treatment plan for glioblastoma of 60 Gy in 30 fractions delivers a dose of ≥0.5 Gy to 99% of the circulating

blood cells during the complete course of cranial RT [75]. Treatment-related lymphopenia becomes more significant in the treatment of GBM because of myelo-suppressive effects of steroids and temozolomide during the course of treatment, thereby impacting patient outcome. Limiting the field size reduces the magnitude of lymphopenia without significantly impacting the survival parameters of these patients [76]. Similarly, bystander splenic irradiation during a course of abdominal RT contributes to lymphopenia and treatment outcome of pancreatic [77] and liver [77] cancer patients. Compared to conventional fractionated RT, SBRT is associated with significantly less radiation-induced lymphopenia during RT for patients with locally advanced pancreatic cancer [78]. High absolute lymphocyte count during neoadjuvant chemoradiation therapy is associated with higher pathological response in patients with esophageal cancer [79]. In thoracic RT of lower esophageal cancer, radiation exposure to bystander organs, such as heart and great vessels, significantly contributes to lymphopenia. The risk of radiation-induced lymphopenia can be reduced with proton beam therapy [80] and perhaps contributes to the normal tissue sparing effects of ultrahigh dose rate FLASH RT [81]. In a preclinical study in mice, conventionally fractionated thoracic RT significantly reduced the circulating levels of T and B lymphocytes and hematopoietic stem cells, which was restored by infusion of unirradiated hematopoietic stem cells after RT [82]. Interestingly, *ex vivo* irradiation of blood cells followed by autotransfusion of these cells resulted in significant lymphopenia in mice, suggesting that blood is an organ at risk both from direct cytocidal effects of RT and indirect myelosuppressive effects of irradiated blood cells.

Multiple mechanisms of RT-mediated immunosuppression are discussed in other recent reviews [83]. RT can induce tranforming growth factor beta (TGFß), which is a central regulator of the immunosuppressive network that inhibits RT-mediated in situ tumor immunity [84]. Systemic administration of blocking antibodies to TGFß induced a robust CD8+ T cell response that eliminated both primary and metastatic poorly immunogenic murine tumors. RT also promotes the accumulation of tumor-infiltrating regulatory T cells (Tregs) [85]. Single large dose fractions of RT induce the infiltration of CD8+ T cells within a week of RT, followed by an increase in CD4+CD25+ Treg to blunt the inflammatory response induced by ablative RT. In contrast, hypofractionated RT (7.5 Gy/fraction) induced CD8+ T cells without an increase in Tregs in a murine model of melanoma [86]. Interestingly, Langerhans cells, epidermal DCs, are resistant to cell death after RT and display cell cycle arrest with p21-mediated increase in expression of Cdkn1a [87]. Furthermore, irradiated Langerhans cells upregulated class II MHC molecules, migrated to draining lymph nodes, and primed the proliferation of Tregs after RT. Sub-ablative RT increases the recruitment of bone marrow-derived CD11b+ myeloid cells that promote vasculogenesis and tumor regrowth [88, 89]. Tumor regrowth after radiation failures is mediated by the CXCL12-CXCR4/CXCR7 pathway, which increases the survival of cancer stem cells, recruits bone marrow-derived stromal cells, and induces angiogenesis – all promoting the regrowth of surviving tumor clonogens [90, 91]. Targeting this pathway with CXCR4 inhibitors such as plerixafor could be helpful in limiting recurrence after RT.

Immune Evasion by Tumors and Radioresistance

Evolution of tumor progression starts with elimination of mutated cells by immune surveillance, followed by an equilibrium and dormancy stage where the tumor progression is kept at bay with an eventual escape and growth of mutated clones that evade immune recognition and suppress and co-opt the immune system to promote tumor progression. While the goal of cancer therapy has been focused on tumor ablation, ablation without restoration of the tumor immune surveillance is not curative. Immune evasion is associated with tumor progression and contributes to resistance to chemotherapy and RT. All host cells express MHC class I on their cell surface, displaying a sample of endogenous peptides to allow for immune recognition of "self" versus "non-self." Under healthy conditions, displayed peptides are derived from a combination of newly translated proteins and degraded self-proteins that are loaded on the MHC in the endoplasmic reticulum (ER). Foreign proteins, such as viral antigens from an infected cell, or peptides from mutated oncogenes in cancer cells [92], can also be loaded on the MHC allowing for recognition as nonself [13]. As the first step of immune escape, tumor cells often downregulate the expression of Class I MHC [20] and other proteins of the antigen processing, loading, and presenting machinery due to epigenetic suppression of gene expression [93]. Thus during tumor evolution, *adaptive evasion* by tumors involves the outgrowth of antigen-loss variants and nonimmunogenic clones of tumor cells due to strong immune selective pressure [94, 95]. Adaptive evasion by immune editing plays a role in developing resistance to immunotherapy in the clinic [96]. In patients undergoing checkpoint therapy with anti-PD1, about 20% develop immune resistance after initial response [97]. Molecular analysis of biopsies from recurrent melanoma lesions identified loss of ß2-microglobulin resulting in decrease in cell surface class I MHC expression and loss-of-function truncating mutation in Jak1 and Jak2 resulting in blunting of the IFNγ signaling and increased survival of tumor cells. These results have been confirmed by another study of patients developing resistance to anti-PD1 therapy [98]. Similarly, in patients failing anti-CTLA4 therapy, loss of type I IFN genes (IFN-α and IFN-ß) and loss-of-function

mutations in both type I IFN and IFNγ signaling were seen [99]. Finally, chronic interferon signaling can also develop immune resistance by epigenetic upregulation of STAT1 and induction of several redundant immune checkpoint proteins, such as lymphocyte-activation gene 3 (LAG3) and T-cell immunoglobulin and mucin-domain containing-3 (Tim3) in tumor cells [100, 101]. Type I IFNs promote antigen presentation by tumor cells, sensitizing them to immune cells killing, increase NK function, and increase the adaptive T cells response. However, chronic exposure can lead to immunosuppression with increased IL-10 secretion and upregulation of programmed death ligand 1 (PD-L1) [102, 103]. Type I IFN signaling through the interferon alpha and beta receptor 1 (INFAR) is often downregulated in tumor cells as an immune escape mechanism. Downstream signaling includes phosphorylation of STAT1 and STAT2, formation of the ISGF3 complex with interferon regulatory factor 9 (IRF9) and translocation to the nucleus to activate ISGs [102].

In contrast to adaptive resistance to cancer immunotherapy, certain solid tumors behave as an immune-privileged site that excludes immune effector cells from infiltrating the TME resulting in poor responses to immune checkpoint therapies and exhibit resistance to chemotherapy and radiation therapy. Several tumor cell-intrinsic mechanisms of immune evasion have been described [104]. This *innate evasion* by tumors depends upon aberrant signaling pathways that are activated as part of tumorigenesis. For example, melanoma-specific activation of the Wnt-ß-catenin pathway excludes T cells from the TME [105]. Vaccination and adoptive transfer of cytotoxic T cells failed to reject these tumors, but intratumoral injection of CD103+, Batf3+ DCs restored T cell infiltration and the response to immune checkpoint therapy [106]. These reports demonstrated that infiltration of effector T cells in the TME depends upon the chemokine CXCL10 that is secreted by CD103+ Batf3+ DCs. Loss-of-function mutations of PTEN also contributes to T cell excluding "cold" immunotype of tumors [105, 107], possibly due to inefficient activation of APCs and antigen presentation, thereby, failing to recruit T cells in the TME. Tumors can often attempt to evade immune recognition and phagocytosis by APCs via expression of the "don't eat me" marker, CD47 [108]. Both CD47 and PDL1 are under the transcriptional control of Myc, thereby, conferring c-Myc as a global immune regulator [109, 110]. Recent reports have shown that blockade of this CD47-signal regulatory protein alpha (SIRPalpha) axis is capable of increasing type I IFN responses in DCs over macrophages through activation of NADPH oxidase (NOX2) attenuating the acidification of the phagosome delaying DNA degradation [60].

Multiple factors contribute to the immune-privileged TME including lack of infiltration of immune effector cells, disorganized tumor vasculature, the desmoplastic reaction, infiltration of tumor-promoting immune cells, such as Treg and myeloid-derived suppressor cells (MDSCs) and immunosuppressive cytokine milieu [111–114]. Disorganized and inefficient tumor vasculature also plays a large role in perpetrating the immunosuppressive TME and is created in part by the unregulated growth of the tumor. As the tumor progresses, angiogenesis is unable to match the rate of growth and therefore a structured vessel network is unable to effectively form. The tumor vasculature is also characterized by immature and leaky vessels and contributes to the increased interstitial pressure seen in many solid tumors, that can lead to reduced accessibility of drugs and decreased immune cell extravasation [112]. There is a large population of immunosuppressive stromal cells present in tumors, such as MDSCs, cancer-associated fibroblasts (CAFs), and tumor-associated macrophages (TAMs). TAMs and CAFs are key players in the creation of excessive extracellular matrix (ECM) by collaborating to induce a desmoplastic reaction or fibrotic reaction, similar to "wound healing" response after injury [115], which further hinders accessibility of cytotoxic immune cells and separates tumor cells and blood vessels, while also decreasing permeability. TAMs constitute a large portion of the resident immune cells in solid tumors, influencing the inhibition of infiltrating cytotoxic T cells [114] and generally can be characterized as M1, antitumorigenic, and M2, pro-tumorigenic [116]. DCs are a very small population of immune cells, but those residing in the tumor are consistently tolerogenic and lead to the induction of immunosuppressive Tregs and inhibition of cytotoxic T cells [117]. These tumor-promoting immune cells secrete many cytokines and growth factors, such as TGFß, IL-10, and VEGF, that contribute to the overall immunosuppressive TME. Another immunosuppressive molecule prevalent in tumor is indoleamine 2,3-dioxygenase (IDO) and has tolerogenic activity on T cells and DCs as well as participates in the recruitment of MDSCs. IDO can protect the tumor from IFN induced apoptosis and a downstream effect is the conversion of CD4+ cells to Tregs [118, 119]. Many tumor cells also express the AXL receptor tyrosine kinase, which plays a central role in tumor progression, epithelial-mesenchymal transition, and has been implicated in radio- and immunotherapeutic resistance. It is involved in anti-inflammatory immune response through multiple mechanisms, including decreasing DC and NK activation and promoting M2 macrophage polarization and T and B cell tolerance [120, 121]. The presence of immunosuppressive Tregs in unirradiated distant tumors can inhibit the radiation-induced immunity in irradiated primary tumors in a process termed as *concomitant immune tolerance* [122]. The tumor-specific inhibition of radiation-mediated in situ vaccination by distant untreated tumors can be circumvented by a transient depletion of Tregs with systemic anti-CTLA4 or by irradiating all tumors that reduces the tumor-specific Treg infiltration [122]. Therefore, as tumors progress and adapt to immune selection and exhibit immune escape, the goal of clinical therapy is to effectively combine ablative tumor debulking therapies, such as RT with immuno-

therapy to overcome immune evasion and shift the balance in favor of immune elimination.

Radiation as an Immunomodulatory Drug: Effect of Dose and Fractionation of RT

Not all radiation fractionation is equal with respect to its immunomodulatory effects. The scheduling, dosing, and the total time of treatment of radiation on tumors have been shown to have differing immunomodulatory effects. Conventional fractionation used in the clinic consists of many low-dose fractions delivered over longer periods of time (more than 7 days). This method of delivery utilizes redistribution of cells in the cell cycle to more sensitive states and reoxygenation to increase overall cell death. However, this also allows for repair of sublethal cellular damage and repopulation of tumor cells between treatments and can decrease efficacy. When viewed from an immunologic perspective, this treatment scheme is typically considered immunosuppressive, repeatedly killing any radiosensitive infiltrating immune cells [123]. Thus, fractionated radiation over weeks have the potential to be tolerogenic by depleting infiltrating activated T cells in the primary tumor. In a model of murine colon cancer, CT26, addition of 10 daily fractions of 3 Gy over a single fraction of 30 Gy to a total tumor dose of 60Gy reduced tumor control and cure, when compared with a single fraction of 30 Gy alone [7]. In this study, 3 Gy × 10 fractions increased the tumor infiltration of MDSCs, in contrast to infiltration of CD8+ CTLs after a single fraction of 30 Gy. Therefore, conventional fractionation schedules over weeks may be detrimental to radiation-induced antitumoral immunity, while accelerated fractionation and hyperfractionated RT may be beneficial, as long as the total treatment time is within a week.

We have classified hypofractionated RT into three categories, based upon their immunomodulatory properties (Fig. 2, Table 3), and these are discussed in the next sections.

Immuno-ablative RT (IART)

Immuno-ablative radiation is typically given in 1–5 fractions of >10Gy per fraction with local control rates of >90%.

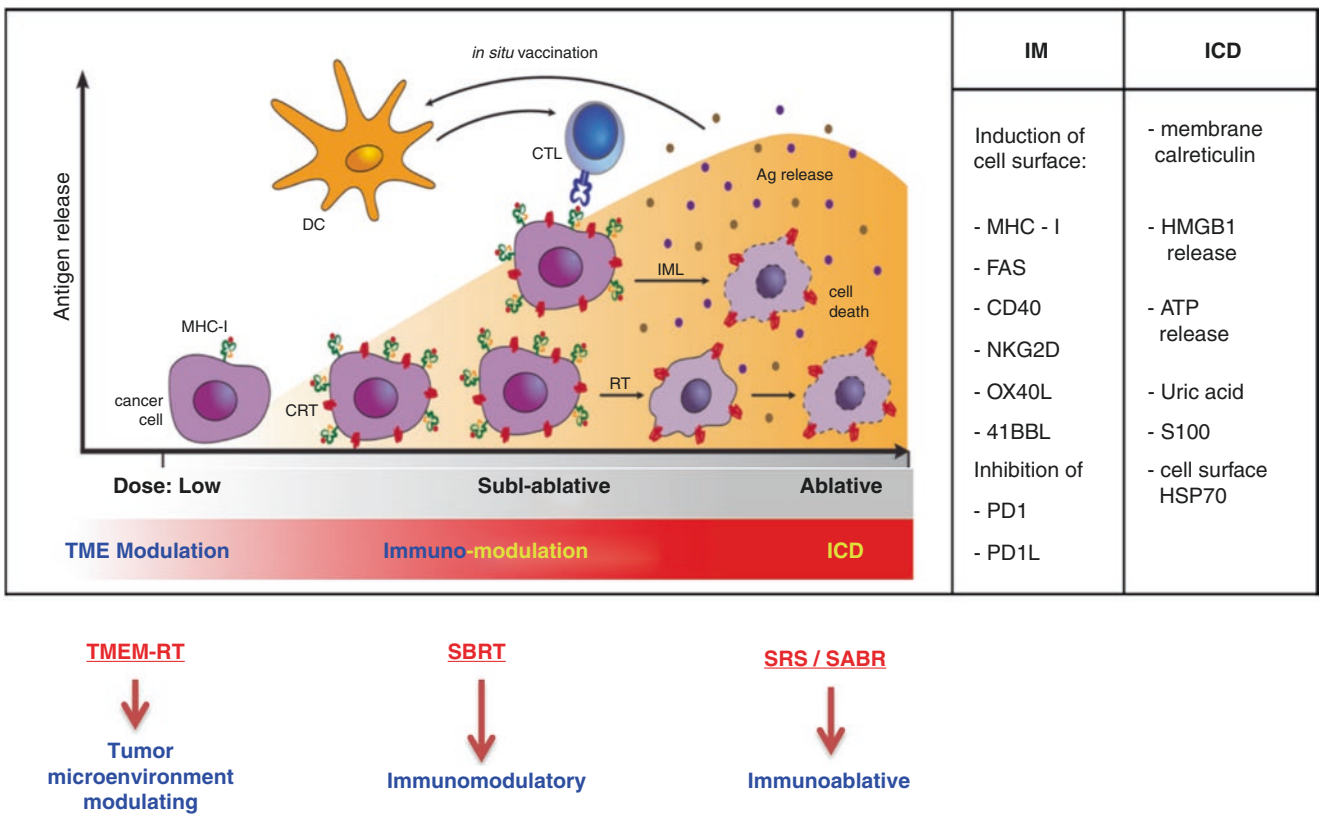

Fig. 2 **Radiation as an immunomodulatory drug**. Different fractionation of RT can be considered as distinct immunomodulatory drugs. Ablative fractionation causes immunogenic cell death with >90% local control of the irradiated tumors. Sub-ablative fractionation increases the expression of immunomodulatory molecules on the tumor cell surface, thereby increasing the susceptibility of the surviving tumor cells to CTL attack. Tumor microenvironment modulating RT is usually administered with low-dose per fraction (0.5–2 Gy) and is shown to increase the tumor perfusion and modulate tumor-infiltrating macrophages and Tregs. In this schedule, conventional RT fractionation with treatment time >7–10 days are considered to be tolerogenic and immunosuppressive for concomitant treatment with immunotherapeutics

Table 3 Examples of radiation fractionation schemes

	Clinical treatment	Hypothesized effect
Conventional fractionation	1.8Gy × 28 = 50.4Gy administered over more than 2 weeks	Immunosuppressive, poor tumor, and T cell response – treatment time greater than 7 days kills infiltrating T cells
Sub-ablative hypofractionation	8Gy × 3 = 24Gy	Immunomodulatory, but inefficient tumor control
Ablative hypofractionation	24Gy × 1 = 24Gy 18-20Gy × 3 = ~60Gy	Induces secondary wound healing fibrotic response and resistance

Ablative single or hypo- fraction RT, clinically known as SABR or SRS, causes direct cell death, releasing large amounts of antigen and DAMP signals, and can control local tumor growth. Effective antigen release and presentation are imperative to induce an effective antitumor immune response. Ablative radiation at the same time is also capable of promoting an immunomodulatory function by causing a dose-dependent increase in DAMP expression and an upregulation of MHC Class I on surviving tumor cells, reversing immune escape [20]. The disadvantage of a single ablative fraction is the upregulation of the immunoinhibitory molecule PDL1 and induction of a pro-tumor fibrotic response, orchestrated in part by TAMs in a M2 phenotype [124]-secreting TGFβ, and the attraction of immunosuppressive cells to the TME [85], which can diminish the antitumor response.

Immunomodulatory RT (IMRT)

In clinical practice, SBRT is usually administered in 3–5 fractions of 5–10 Gy per fraction, over 5–10 days for local tumor control, while respecting normal tissue tolerance. To avoid adverse late effects, sub-ablative fractions have been used in the clinical setting for treating tumors adjacent to sensitive organs, such as spinal cord, duodenum, brain stem, and others. The Hodge group at National Cancer Institute (NCI) has studied the immunomodulatory properties of sub-ablative RT and noted that radiation induces the cell surface expression of class I MHC, death receptors, and calreticulin that makes irradiated tumor cells more susceptible to CTL attack [21, 125–127]. Typically, the effects seen are dose-dependent and include upregulation of DAMPs and MHC Class I [20, 44]. There is also a dose-dependent increase in Fas/CD95, a member of the TNF receptor family that further augments CTL mediated killing. It also causes an increase in the expression of adhesion markers, such as intercellular adhesion molecule 1 (ICAM-1/CD54) and lymphocyte function-associated antigen 3 (LFA-3/CD58), and release of chemokines, including CXCL10 and CXCL16, attracting effector T cells to the tumor, and at the same time reducing the influx of immunosuppressive regulatory T cells [86, 128–130]. The Demaria group demonstrated the ability of sub-ablative, hypofractionated radiation (8 Gy × 3 fractions) to synergistically combine with CTLA-4 checkpoint blockade immunotherapy and induce an abscopal effect of unirradiated tumors due to radiation-induced, systemic antitumor effector response [128]. Mechanistically, this effect was linked with the induction of the cytosolic exonuclease, Trex1, by higher dose fractions of radiation (>12–18 Gy) in irradiated tumor cells [67]. These results have supported the design of a number of clinical trials with 8 Gy × 3 fractions of SBRT to be combined with immune checkpoint therapy with one phase II randomized trial, the PEMBRO-RT study (NCT02492568) showing a clinical benefit of combination of SBRT + anti-PD1 over anti-PD1 alone for patients with advanced lung cancer. While we await the final results of this study, the debate over selecting the optimal dose fractionation of SBRT for combination with immunotherapy is far from over. Ideally, a dose response of SBRT should be done in clinical trials in combination with immunotherapy, as was reported earlier [131, 132]. For an in situ vaccine approach, sub-ablative doses of RT could fail to provide an immune-activating TME, in part because of the post-ablation recruitment of myeloid cells and vasculogenesis, mediated by HIF-1-dependent stromal cell-derived factor-1 (SDF-1) and its receptor, CXCR4 [88, 90].

Tumor Microenvironment Modulating RT (TMEM-RT)

Tumor microenvironment modulating radiation is low-dose radiation typically under 2 Gy. Tumor vasculature is immature and tortuous, low-dose radiation has been shown to normalize the vascular network which could allow for more efficient perfusion and increase accessibility [130, 133]. Klug and colleagues demonstrated that low-dose irradiation can actually reprogram macrophages to a more proinflammatory M1 phenotype [134]. Several trials are underway to study the immunomodulatory properties of low-dose radiation [135, 136].

Roadmap for Combination of Immunotherapy with SBRT

Designing clinical trials for combination of immunotherapy with RT should consider two questions – (i) Is immunotherapy needed to overcome the ineffectiveness of sub-ablative RT because of normal tissue tolerance? (ii) Is RT needed to amplify the diversity and effectiveness of antitumoral immunity? Although abscopal effects can be very suggestive of

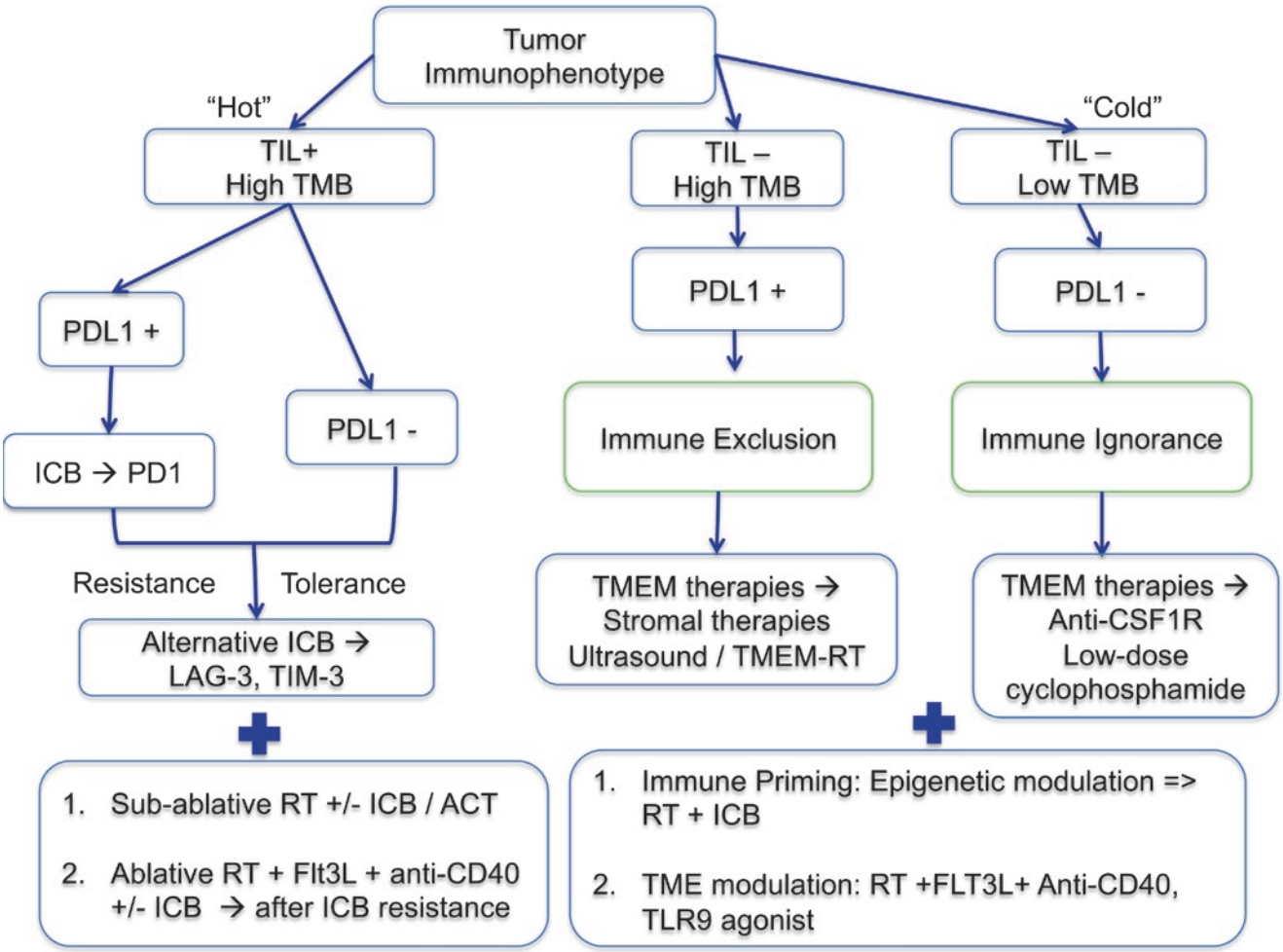

Fig. 3 **A roadmap to combination trials of SBRT and immunotherapy**

clinical effectiveness, it is not a proven surrogate of improved survival and therefore, clinical endpoints of overall survival should be considered for designing combination trials. A radiation-immunity cycle could generate protective antitumoral immunity that might be essential for effective local and systemic tumor control (Fig. 1). For in situ tumor vaccination to be effective, an intact cancer immunity cycle with each step working in cohort with the next is required [137]. The steps include the release and engulfment of tumor-associated antigens by antigen-presenting cells, especially DCs, DC activation and maturation, cross-presentation of antigen to T cells, and T cell activation and accessibility into the tumor. Combination treatments that target these various steps to augment the radiation-immunity cycle improve the likelihood of robust effector cell response within the tumor and thus, favorable clinical outcome after RT. Classifying tumor microenvironments by their immunogenic potential would allow for personalization of the most efficacious combination treatments. A roadmap has been suggested for designing combination trials of immunotherapy with SBRT, based upon the radiation-immunity cycle and the immune landscape of the tumors (Fig. 3).

A classification of the immune landscape of the TME based upon the presence or absence of tumor-infiltrating lymphocytes (TIL) and PD-L1 expression has been proposed [138]: Type I - TIL+ / PD-L1+ have adaptive immune resistance; Type II - TIL- / PD-L1- have immunological ignorance; Type III - TIL- / PD-L1+ have intrinsic induction; and Type IV - TIL+/PD-L1- have immunological tolerance. Immunologically, "hot" inflamed tumors favor infiltration of lymphocytes and typically have high mutagenic loads. These tumors have all components needed for effective immune responses; however, the immune machinery is suppressed due to adaptive immune resistance from the expression of immune checkpoint molecules, and/or tumor infiltration of Treg and TAM. Targetable candidates for immune checkpoints, such as PD-L1, PD-L2, TIM3, and LAG3 are ever increasing, as new pathways of adaptive resistance are being discovered. Tumors, expressing high levels of PD-L1 may respond well to anti-PD1/PD-L1 immune checkpoint blockade (ICB), but may

lose efficacy through compensatory mechanisms [100, 101]. Blocking alternative targets for ICB therapy should then be considered for PDL-1 negative tumors. If ablative fractionation with SABR or SRS is possible, IART followed by Flt3L can be combined with concomitant ICB in these patients for adequate in situ vaccination. When dose constraints for organs at risk preclude the use of ablative fractionation, sub-ablative immunomodulatory RT can be combined with ICB along with other therapies, such as activating anti-CD40 antibodies. Since RT induces the expression of cell death receptors on tumor cell surface, adoptive cell transfer with cytokine-activated T cells or chimeric antigen receptor expressing T (CAR-T) cells can be added after RT to increase the efficiency of immunotherapy for these tumors. Alternatively, TAMs can be targeted with blocking antibodies to CSF-1 receptor or IDO inhibitors.

Immunologically, "cold" tumors have low lymphocyte infiltration and can be then further classified into those with high mutational burden and low mutational burden. Tumors with low infiltration and high mutational load are considered to be participating in immune exclusion or immune escape, limiting accessibility or limiting visibility to immune responses, respectively. The best therapies for this tumor immunophenotype would be antiangiogenics, anti-stromal therapies, non-ablative-focused ultrasound, and TMEM-RT to increase tumor prefusion and accessibility of T cells in the tumor. Such treatments can be combined with ablative RT to induce a tumor targeted response, synergistically. Along those same lines, tumors with low lymphocyte infiltration and low mutational burden, with or without PD-L1 expression are considered to be immune ignorant and should be treated with TMEM therapies to reprogram the TME to favor effector infiltration and function. Combinations of RT, Flt3L, and anti-CD40 or a TLR9 agonist could mature and activate APCs sufficiently to induce antigen presentation and T cell activation. The goal of combination therapies is to enhance the beneficial aspects of each therapy for synergistic effects. In summary, we could augment tumor-specific immune responses for each individual patient using this roadmap with careful consideration of dose and fractionation of RT, types of immunotherapeutic agents, and the baseline immunophenotype of the tumor.

References

1. Timmerman R, Paulus R, Galvin J, Michalski J, Straube W, Bradley J, et al. Stereotactic body radiation therapy for inoperable early stage lung cancer. JAMA. 2010;303(11):1070–6.
2. Yamada Y, Bilsky MH, Lovelock DM, Venkatraman ES, Toner S, Johnson J, et al. High-dose, single-fraction image-guided intensity-modulated radiotherapy for metastatic spinal lesions. Int J Radiat Oncol Biol Phys. 2008;71(2):484–90.
3. Greco C, Zelefsky MJ, Lovelock M, Fuks Z, Hunt M, Rosenzweig K, et al. Predictors of local control after single-dose stereotactic image-guided intensity-modulated radiotherapy for extracranial metastases. Int J Radiat Oncol Biol Phys. 2011;79(4):1151–7.
4. Zelefsky MJ, Greco C, Motzer R, Magsanoc JM, Pei X, Lovelock M, et al. Tumor control outcomes after hypofractionated and single-dose stereotactic image-guided intensity-modulated radiotherapy for extracranial metastases from renal cell carcinoma. Int J Radiat Oncol Biol Phys. 2012;82(5):1744–8.
5. Garcia-Barros M, Paris F, Cordon-Cardo C, Lyden D, Rafii S, Haimovitz-Friedman A, et al. Tumor response to radiotherapy regulated by endothelial cell apoptosis. Science. 2003;300(5622):1155–9.
6. Lee Y, Auh SL, Wang Y, Burnette B, Meng Y, Beckett M, et al. Therapeutic effects of ablative radiation on local tumor require CD8+ T cells: changing strategies for cancer treatment. Blood. 2009;114(3):589–95.
7. Filatenkov A, Baker J, Mueller AM, Kenkel J, Ahn GO, Dutt S, et al. Ablative tumor radiation can change the tumor immune cell microenvironment to induce durable complete remissions. Clin Cancer Res. 2015;21(16):3727–39.
8. Ramey S, Balise R, Ritch C, Punnen S, Ishkanian A, Pollack A, et al. Immunocompromised patients with prostate cancer treated with external beam radiation: a matched pair analysis. Int J Radiat Oncol Biol Phys. 2015;93(3):E206.
9. Manyam BV, Garsa AA, Chin RI, Reddy CA, Gastman B, Thorstad W, et al. A multi-institutional comparison of outcomes of immunosuppressed and immunocompetent patients treated with surgery and radiation therapy for cutaneous squamous cell carcinoma of the head and neck. Cancer. 2017;123(11):2054–60.
10. Edwards JM, Wooten CE, Smith AJT, McGarry RC. Stereotactic body radiation therapy in patients with immune suppression. Int J Radiat Oncol Biol Phys. 2014;90(1 Supplement 1):S650.
11. Kawashita Y, Deb NJ, Garg M, Kabarriti R, Alfieri A, Takahashi M, et al. An autologous in situ tumor vaccination approach for hepatocellular carcinoma. 1. Flt3 ligand gene transfer increases antitumor effects of a radio-inducible suicide gene therapy in an ectopic tumor model. Radiat Res. 2014;182(2):191–200.
12. Kawashita Y, Deb NJ, Garg MK, Kabarriti R, Fan Z, Alfieri AA, et al. An autologous in situ tumor vaccination approach for hepatocellular carcinoma. 2. Tumor-specific immunity and cure after radio-inducible suicide gene therapy and systemic CD40-ligand and Flt3-ligand gene therapy in an orthotopic tumor model. Radiat Res. 2014;182(2):201–10.
13. Urban JL, Schreiber H. Tumor antigens. Annu Rev Immunol. 1992;10:617–44.
14. Blades RA, Keating PJ, McWilliam LJ, George NJ, Stern PL. Loss of HLA class I expression in prostate cancer: implications for immunotherapy. Urology. 1995;46(5):681–6; discussion 6-7.
15. Sanda MG, Restifo NP, Walsh JC, Kawakami Y, Nelson WG, Pardoll DM, et al. Molecular characterization of defective antigen processing in human prostate cancer [see comments]. J Natl Cancer Inst. 1995;87(4):280–5.
16. Chakravarty PK, Alfieri A, Thomas EK, Beri V, Tanaka KE, Vikram B, et al. Flt3-ligand administration after radiation therapy prolongs survival in a murine model of metastatic lung cancer. Cancer Res. 1999;59(24):6028–32.
17. Maraskovsky E, Brasel K, Teepe M, Roux ER, Lyman SD, Shortman K, et al. Dramatic increase in the numbers of functionally mature dendritic cells in Flt3 ligand-treated mice: multiple dendritic cell subpopulations identified. J Exp Med. 1996;184(5):1953–62.
18. McKenna HJ, de Vries P, Brasel K, Lyman SD, Williams DE. Effect of flt3 ligand on the ex vivo expansion of human CD34+ hematopoietic progenitor cells. Blood. 1995;86(9):3413–20.
19. Chakravarty PK, Guha C, Alfieri A, Beri V, Niazova Z, Deb NJ, et al. Flt3L therapy following localized tumor irradiation gener-

ates long-term protective immune response in metastatic lung cancer: its implication in designing a vaccination strategy. Oncology. 2006;70(4):245–54.
20. Reits EA, Hodge JW, Herberts CA, Groothuis TA, Chakraborty M, Wansley EK, et al. Radiation modulates the peptide repertoire, enhances MHC class I expression, and induces successful antitumor immunotherapy. J Exp Med. 2006;203(5):1259–71.
21. Chakraborty M, Abrams SI, Camphausen K, Liu K, Scott T, Coleman CN, et al. Irradiation of tumor cells up-regulates Fas and enhances CTL lytic activity and CTL adoptive immunotherapy. J Immunol. 2003;170(12):6338–47.
22. Agoni L, Lenz J, Guha C. Variant splicing and influence of ionizing radiation on human endogenous retrovirus K (HERV-K) transcripts in cancer cell lines. PLoS One. 2013;8(10):e76472.
23. Zhou F, Krishnamurthy J, Wei Y, Li M, Hunt K, Johanning GL, et al. Chimeric antigen receptor T cells targeting HERV-K inhibit breast cancer and its metastasis through downregulation of Ras. Oncoimmunology. 2015;4(11):e1047582.
24. Wang-Johanning F, Radvanyi L, Rycaj K, Plummer JB, Yan P, Sastry KJ, et al. Human endogenous retrovirus K triggers an antigen-specific immune response in breast cancer patients. Cancer Res. 2008;68(14):5869–77.
25. Andreev DE, O'Connor PB, Fahey C, Kenny EM, Terenin IM, Dmitriev SE, et al. Translation of 5′ leaders is pervasive in genes resistant to eIF2 repression. elife. 2015;4:e03971.
26. Starck SR, Tsai JC, Chen K, Shodiya M, Wang L, Yahiro K, et al. Translation from the 5′ untranslated region shapes the integrated stress response. Science. 2016;351(6272):aad3867.
27. Malarkannan S, Afkarian M, Shastri N. A rare cryptic translation product is presented by Kb major histocompatibility complex class I molecule to alloreactive T cells. J Exp Med. 1995;182(6):1739–50.
28. Starck SR, Ow Y, Jiang V, Tokuyama M, Rivera M, Qi X, et al. A distinct translation initiation mechanism generates cryptic peptides for immune surveillance. PLoS One. 2008;3(10):e3460.
29. Starck SR, Shastri N. Nowhere to hide: unconventional translation yields cryptic peptides for immune surveillance. Immunol Rev. 2016;272(1):8–16.
30. Starck SR, Shastri N. Non-conventional sources of peptides presented by MHC class I. Cell Mol Life Sci. 2011;68:1471–9.
31. Ho O, Green WR. Alternative translational products and cryptic T cell epitopes: expecting the unexpected. J Immunol. 2006;177(12):8283–9.
32. Laumont CM, Daouda T, Laverdure JP, Bonneil E, Caron-Lizotte O, Hardy MP, et al. Global proteogenomic analysis of human MHC class I-associated peptides derived from non-canonical reading frames. Nat Commun. 2016;7:10238.
33. Van Allen EM, Miao D, Schilling B, Shukla SA, Blank C, Zimmer L, et al. Genomic correlates of response to CTLA-4 blockade in metastatic melanoma. Science. 2015;350(6257):207–11.
34. Gubin MM, Schreiber RD. Cancer. The odds of immunotherapy success. Science. 2015;350(6257):158–9.
35. Frey B, Ruckert M, Deloch L, Ruhle PF, Derer A, Fietkau R, et al. Immunomodulation by ionizing radiation-impact for design of radio-immunotherapies and for treatment of inflammatory diseases. Immunol Rev. 2017;280(1):231–48.
36. Tang H, Wang Y, Chlewicki LK, Zhang Y, Guo J, Liang W, et al. Facilitating T cell infiltration in tumor microenvironment overcomes resistance to PD-L1 blockade. Cancer Cell. 2016;29(3):285–96.
37. Janeway CA Jr, Medzhitov R. Innate immune recognition. Annu Rev Immunol. 2002;20(1):197–216.
38. Creagh EM, O'Neill LA. TLRs, NLRs and RLRs: a trinity of pathogen sensors that co-operate in innate immunity. Trends Immunol. 2006;27(8):352–7.
39. Janeway CA Jr, Medzhitov R. Innate immunity: Lipoproteins take their Toll on the host. Curr Biol. 1999;9(23):R879–R82.
40. Savitsky D, Tamura T, Yanai H, Taniguchi T. Regulation of immunity and oncogenesis by the IRF transcription factor family. Cancer Immunol Immunother. 2010;59(4):489–510.
41. Apetoh L, Ghiringhelli F, Tesniere A, Obeid M, Ortiz C, Criollo A, et al. Toll-like receptor 4-dependent contribution of the immune system to anticancer chemotherapy and radiotherapy. Nat Med. 2007;13(9):1050–9.
42. Obeid M, Tesniere A, Ghiringhelli F, Fimia GM, Apetoh L, Perfettini JL, et al. Calreticulin exposure dictates the immunogenicity of cancer cell death. Nat Med. 2007;13(1):54–61.
43. Tesniere A, Panaretakis T, Kepp O, Apetoh L, Ghiringhelli F, Zitvogel L, et al. Molecular characteristics of immunogenic cancer cell death. Cell Death Differ. 2008;15(1):3–12.
44. Golden EB, Frances D, Pellicciotta I, Demaria S, Helen Barcellos-Hoff M, Formenti SC. Radiation fosters dose-dependent and chemotherapy-induced immunogenic cell death. Oncoimmunology. 2014;3:e28518.
45. Kono H, Rock KL. How dying cells alert the immune system to danger. Nat Rev Immunol. 2008;8(4):279–89.
46. Lauber K, Ernst A, Orth M, Herrmann M, Belka C. Dying cell clearance and its impact on the outcome of tumor radiotherapy. Front Oncol. 2012;2:116.
47. Matzinger P. Tolerance, danger, and the extended family. Annu Rev Immunol. 1994;12:991–1045.
48. Melcher A, Todryk S, Hardwick N, Ford M, Jacobson M, Vile RG. Tumor immunogenicity is determined by the mechanism of cell death via induction of heat shock protein expression. Nat Med. 1998;4(5):581–7.
49. Basu S, Binder RJ, Ramalingam T, Srivastava PK. CD91 is a common receptor for heat shock proteins gp96, hsp90, hsp70, and calreticulin. Immunity. 2001;14(3):303–13.
50. Basu S, Binder RJ, Suto R, Anderson KM, Srivastava PK. Necrotic but not apoptotic cell death releases heat shock proteins, which deliver a partial maturation signal to dendritic cells and activate the NF-kappa B pathway. Int Immunol. 2000;12(11):1539–46.
51. Basu S, Srivastava PK. Calreticulin, a peptide-binding chaperone of the endoplasmic reticulum, elicits tumor- and peptide-specific immunity. J Exp Med. 1999;189(5):797–802.
52. Todryk S, Melcher AA, Hardwick N, Linardakis E, Bateman A, Colombo MP, et al. Heat shock protein 70 induced during tumor cell killing induces Th1 cytokines and targets immature dendritic cell precursors to enhance antigen uptake. J Immunol. 1999;163(3):1398–408.
53. Srivastava PK, Menoret A, Basu S, Binder RJ, McQuade KL. Heat shock proteins come of age: primitive functions acquire new roles in an adaptive world. Immunity. 1998;8(6):657–65.
54. Manjili MH, Wang XY, Park J, Facciponte JG, Repasky EA, Subjeck JR. Immunotherapy of cancer using heat shock proteins. Front Biosci. 2002;7:d43–52.
55. Srivastava P. Interaction of heat shock proteins with peptiedes and antigen presenting cells: chaperoning of the innate and adaptive immune responses. Annu Rev Immunol. 2002;20:395–425.
56. Srivastava PK, Udono H, Blachere NE, Li Z. Heat shock proteins transfer peptides during antigen processing and CTL priming. Immunogenetics. 1994;39(2):93–8.
57. Udono H, Srivastava PK. Heat shock protein 70-associated peptides elicit specific cancer immunity. J Exp Med. 1993;178(4):1391–6.
58. Binder CJ, Papac-Milicevic N, Witztum JL. Innate sensing of oxidation-specific epitopes in health and disease. Nat Rev Immunol. 2016;16(8):485–97.
59. Kono H, Chen CJ, Ontiveros F, Rock KL. Uric acid promotes an acute inflammatory response to sterile cell death in mice. J Clin Invest. 2010;120(6):1939–49.

60. Xu MM, Pu Y, Han D, Shi Y, Cao X, Liang H, et al. Dendritic cells but not macrophages sense tumor mitochondrial DNA for cross-priming through signal regulatory protein alpha signaling. Immunity. 2017;47(2):363–73 e5.
61. Burnette BC, Liang H, Lee Y, Chlewicki L, Khodarev NN, Weichselbaum RR, et al. The efficacy of radiotherapy relies upon induction of type I interferon-dependent innate and adaptive immunity. Cancer Res. 2011;71(7):2488–96.
62. Deng L, Liang H, Xu M, Yang X, Burnette B, Arina A, et al. STING-dependent cytosolic DNA sensing promotes radiation-induced Type I interferon-dependent antitumor immunity in immunogenic tumors. Immunity. 2014;41(5):843–52.
63. Corrales L, McWhirter SM, Dubensky TW Jr, Gajewski TF. The host STING pathway at the interface of cancer and immunity. J Clin Invest. 2016;126(7):2404–11.
64. Chamilos G, Gregorio J, Meller S, Lande R, Kontoyiannis DP, Modlin RL, et al. Cytosolic sensing of extracellular self-DNA transported into monocytes by the antimicrobial peptide LL37. Blood. 2012;120(18):3699–707.
65. Zhang Z, Meng P, Han Y, Shen C, Li B, Hakim MA, et al. Mitochondrial DNA-LL-37 complex promotes atherosclerosis by escaping from autophagic recognition. Immunity. 2015;43(6):1137–47.
66. Gehrke N, Mertens C, Zillinger T, Wenzel J, Bald T, Zahn S, et al. Oxidative damage of DNA confers resistance to cytosolic nuclease TREX1 degradation and potentiates STING-dependent immune sensing. Immunity. 2013;39(3):482–95.
67. Vanpouille-Box C, Alard A, Aryankalayil MJ, Sarfraz Y, Diamond JM, Schneider RJ, et al. DNA exonuclease Trex1 regulates radiotherapy-induced tumour immunogenicity. Nat Commun. 2017;8:15618.
68. Harding SM, Benci JL, Irianto J, Discher DE, Minn AJ, Greenberg RA. Mitotic progression following DNA damage enables pattern recognition within micronuclei. Nature. 2017;548(7668):466–70.
69. Mackenzie KJ, Carroll P, Martin CA, Murina O, Fluteau A, Simpson DJ, et al. cGAS surveillance of micronuclei links genome instability to innate immunity. Nature. 2017;548(7668):461–5.
70. Brzostek-Racine S, Gordon C, Van Scoy S, Reich NC. The DNA damage response induces IFN. J Immunol. 2011;187(10):5336–45.
71. Gasser S, Orsulic S, Brown EJ, Raulet DH. The DNA damage pathway regulates innate immune system ligands of the NKG2D receptor. Nature. 2005;436(7054):1186–90.
72. Minn AJ. Interferons and the immunogenic effects of cancer therapy. Trends Immunol. 2015;36(11):725–37.
73. Nabet BY, Qiu Y, Shabason JE, Wu TJ, Yoon T, Kim BC, et al. Exosome RNA unshielding couples stromal activation to pattern recognition receptor signaling in cancer. Cell. 2017;170(2):352–66 e13.
74. Venkatesulu BP, Mallick S, Lin SH, Krishnan S. A systematic review of the influence of radiation-induced lymphopenia on survival outcomes in solid tumors. Crit Rev Oncol Hematol. 2018;123:42–51.
75. Yovino S, Kleinberg L, Grossman SA, Narayanan M, Ford E. The etiology of treatment-related lymphopenia in patients with malignant gliomas: modeling radiation dose to circulating lymphocytes explains clinical observations and suggests methods of modifying the impact of radiation on immune cells. Cancer Investig. 2013;31(2):140–4.
76. Rudra S, Hui C, Rao YJ, Samson P, Lin AJ, Chang X, et al. Effect of radiation treatment volume reduction on lymphopenia in patients receiving chemoradiotherapy for glioblastoma. Int J Radiat Oncol Biol Phys. 2018;101(1):217–25.
77. Chadha AS, Liu G, Chen HC, Das P, Minsky BD, Mahmood U, et al. Does unintentional splenic radiation predict outcomes after pancreatic cancer radiation therapy? Int J Radiat Oncol Biol Phys. 2017;97(2):323–32.
78. Wild AT, Herman JM, Dholakia AS, Moningi S, Lu Y, Rosati LM, et al. Lymphocyte-sparing effect of stereotactic body radiation therapy in patients with unresectable pancreatic cancer. Int J Radiat Oncol Biol Phys. 2016;94(3):571–9.
79. Fang P, Jiang W, Davuluri R, Xu C, Krishnan S, Mohan R, et al. High lymphocyte count during neoadjuvant chemoradiotherapy is associated with improved pathologic complete response in esophageal cancer. Radiother Oncol. 2018;128:584.
80. Fang P, Shiraishi Y, Verma V, Jiang W, Song J, Hobbs BP, et al. Lymphocyte-sparing effect of proton therapy in patients with esophageal cancer treated with definitive chemoradiation. Int J Part Ther. 2018;4(3):23–32.
81. Favaudon V, Caplier L, Monceau V, Pouzoulet F, Sayarath M, Fouillade C, et al. Ultrahigh dose-rate FLASH irradiation increases the differential response between normal and tumor tissue in mice. Sci Transl Med. 2014;6(245):245ra93.
82. Kapoor V, Khudanyan A, de la Puente P, Campian J, Hallahan DE, Azab AK, et al. Stem cell transfusion restores immune function in radiation-induced lymphopenic C57BL/6 mice. Cancer Res. 2015;75(17):3442–5.
83. Wennerberg E, Lhuillier C, Vanpouille-Box C, Pilones KA, Garcia-Martinez E, Rudqvist NP, et al. Barriers to radiation-induced in situ tumor vaccination. Front Immunol. 2017;8:229.
84. Vanpouille-Box C, Diamond JM, Pilones KA, Zavadil J, Babb JS, Formenti SC, et al. TGFbeta Is a master regulator of radiation therapy-induced antitumor immunity. Cancer Res. 2015;75(11):2232–42.
85. Schaue D, Xie MW, Ratikan JA, McBride WH. Regulatory T cells in radiotherapeutic responses. Front Oncol. 2012;2:90.
86. Schaue D, Ratikan JA, Iwamoto KS, McBride WH. Maximizing tumor immunity with fractionated radiation. Int J Radiat Oncol Biol Phys. 2012;83(4):1306–10.
87. Price JG, Idoyaga J, Salmon H, Hogstad B, Bigarella CL, Ghaffari S, et al. CDKN1A regulates Langerhans cell survival and promotes Treg cell generation upon exposure to ionizing irradiation. Nat Immunol. 2015;16(10):1060–8.
88. Kioi M, Vogel H, Schultz G, Hoffman RM, Harsh GR, Brown JM. Inhibition of vasculogenesis, but not angiogenesis, prevents the recurrence of glioblastoma after irradiation in mice. J Clin Invest. 2010;120(3):694–705.
89. Brown JM. Vasculogenesis: a crucial player in the resistance of solid tumours to radiotherapy. Br J Radiol. 2014;87(1035):20130686.
90. Kozin SV, Kamoun WS, Huang Y, Dawson MR, Jain RK, Duda DG. Recruitment of myeloid but not endothelial precursor cells facilitates tumor regrowth after local irradiation. Cancer Res. 2010;70(14):5679–85.
91. Duda DG, Kozin SV, Kirkpatrick ND, Xu L, Fukumura D, Jain RK. CXCL12 (SDF1alpha)-CXCR4/CXCR7 pathway inhibition: an emerging sensitizer for anticancer therapies? Clin Cancer Res. 2011;17(8):2074–80.
92. Schumacher TN, Schreiber RD. Neoantigens in cancer immunotherapy. Science. 2015;348(6230):69–74.
93. Heninger E, Krueger TE, Lang JM. Augmenting antitumor immune responses with epigenetic modifying agents. Front Immunol. 2015;6:29.
94. DuPage M, Mazumdar C, Schmidt LM, Cheung AF, Jacks T. Expression of tumour-specific antigens underlies cancer immunoediting. Nature. 2012;482(7385):405–9.
95. Matsushita H, Vesely MD, Koboldt DC, Rickert CG, Uppaluri R, Magrini VJ, et al. Cancer exome analysis reveals a T-cell-dependent mechanism of cancer immunoediting. Nature. 2012;482(7385):400–4.
96. Coulie PG, Van den Eynde BJ, van der Bruggen P, Boon T. Tumour antigens recognized by T lymphocytes: at the core of cancer immunotherapy. Nat Rev Cancer. 2014;14(2):135–46.
97. Zaretsky JM, Garcia-Diaz A, Shin DS, Escuin-Ordinas H, Hugo W, Hu-Lieskovan S, et al. Mutations associated with acquired

resistance to PD-1 blockade in melanoma. N Engl J Med. 2016;375(9):819–29.
98. Shin DS, Zaretsky JM, Escuin-Ordinas H, Garcia-Diaz A, Hu-Lieskovan S, Kalbasi A, et al. Primary resistance to PD-1 blockade mediated by JAK1/2 mutations. Cancer Discov. 2017;7(2):188–201.
99. Gao J, Shi LZ, Zhao H, Chen J, Xiong L, He Q, et al. Loss of IFN-gamma pathway genes in tumor cells as a mechanism of resistance to Anti-CTLA-4 therapy. Cell. 2016;167(2):397–404 e9.
100. Benci JL, Xu B, Qiu Y, Wu TJ, Dada H, Twyman-Saint Victor C, et al. Tumor interferon signaling regulates a multigenic resistance program to immune checkpoint blockade. Cell. 2016;167(6):1540–54 e12.
101. Minn AJ, Wherry EJ. Combination cancer therapies with immune checkpoint blockade: convergence on interferon signaling. Cell. 2016;165(2):272–5.
102. Ivashkiv LB, Donlin LT. Regulation of type I interferon responses. Nat Rev Immunol. 2014;14(1):36–49.
103. Reading JL, Quezada SA. Too much of a good thing? Chronic IFN fuels resistance to cancer immunotherapy. Immunity. 2016;45(6):1181–3.
104. Spranger S, Gajewski TF. Impact of oncogenic pathways on evasion of antitumour immune responses. Nat Rev Cancer. 2018;18(3):139–47.
105. Spranger S, Bao R, Gajewski TF. Melanoma-intrinsic beta-catenin signalling prevents anti-tumour immunity. Nature. 2015;523(7559):231–5.
106. Spranger S, Dai D, Horton B, Gajewski TF. Tumor-residing Batf3 dendritic cells are required for effector T Cell trafficking and adoptive T Cell therapy. Cancer Cell. 2017;31(5):711–23 e4.
107. Peng W, Chen JQ, Liu C, Malu S, Creasy C, Tetzlaff MT, et al. Loss of PTEN Promotes Resistance to T Cell-Mediated Immunotherapy. Cancer Discov. 2016;6(2):202–16.
108. Jaiswal S, Jamieson CH, Pang WW, Park CY, Chao MP, Majeti R, et al. CD47 is upregulated on circulating hematopoietic stem cells and leukemia cells to avoid phagocytosis. Cell. 2009;138(2):271–85.
109. Casey SC, Baylot V, Felsher DW. The MYC oncogene is a global regulator of the immune response. Blood. 2018;131(18):2007–15.
110. Casey SC, Tong L, Li Y, Do R, Walz S, Fitzgerald KN, et al. MYC regulates the antitumor immune response through CD47 and PD-L1. Science. 2016;352(6282):227–31.
111. Martin JD, Fukumura D, Duda DG, Boucher Y, Jain RK. Reengineering the tumor microenvironment to alleviate hypoxia and overcome cancer heterogeneity. Cold Spring Harb Perspect Med. 2016;6(12):a027094.
112. Reitan NK, Thuen M, Goa PE, de Lange Davies C. Characterization of tumor microvascular structure and permeability: comparison between magnetic resonance imaging and intravital confocal imaging. J Biomed Opt. 2010;15(3):036004--11.
113. Apte M, Park S, Phillips P, Santucci N, Goldstein D, Kumar R, et al. Desmoplastic reaction in pancreatic cancer: role of pancreatic stellate cells. Pancreas. 2004;29(3):179–87.
114. Joyce JA, Fearon DT. T cell exclusion, immune privilege, and the tumor microenvironment. Science. 2015;348(6230):74–80.
115. Crittenden MR, Savage T, Cottam B, Baird J, Rodriguez PC, Newell P, et al. Expression of arginase I in myeloid cells limits control of residual disease after radiation therapy of tumors in mice. Radiat Res. 2014;182(2):182–90.
116. Hu W, Li X, Zhang C, Yang Y, Jiang J, Wu C. Tumor-associated macrophages in cancers. Clin Transl Oncol. 2016;18(3):251–8.
117. Dudek AM, Martin S, Garg AD, Agostinis P. Immature, semi-mature, and fully mature dendritic cells: toward a DC-cancer cells interface that augments anticancer immunity. Front Immunol. 2013;4:438.
118. Munn DH, Mellor AL. IDO in the tumor microenvironment: inflammation, counter-regulation, and tolerance. Trends Immunol. 2016;37(3):193–207.
119. Zhai L, Ladomersky E, Lenzen A, Nguyen B, Patel R, Lauing KL, et al. IDO1 in cancer: a Gemini of immune checkpoints. Cell Mol Immunol. 2018;15(5):447–57.
120. Rankin EB, Giaccia AJ. The receptor tyrosine kinase AXL in cancer progression. Cancers. 2016;8(11):103.
121. Aguilera TA, Rafat M, Castellini L, Shehade H, Kariolis MS, Hui AB-Y, et al. Reprogramming the immunological microenvironment through radiation and targeting Axl. Nat Commun. 2016;7:13898.
122. Morris ZS, Guy EI, Werner LR, Carlson PM, Heinze CM, Kler JS, et al. Tumor-specific inhibition of in situ vaccination by distant untreated tumor sites. Cancer Immunol Res. 2018;6(7):825–34.
123. MacLennan I, Kay H. Analysis of treatment in childhood leukemia. IV. The critical association between dose fractionation and immunosuppression induced by cranial irradiation. Cancer. 1978;41(1):108–11.
124. Gorchs L, Hellevik T, Bruun J-A, Camilio K-A, Al-Saad S, Stuge T-B, et al. Cancer-associated fibroblasts from lung tumors maintain their immunosuppressive abilities after high-dose irradiation. Front Oncol. 2015;5:87.
125. Chakraborty M, Abrams SI, Coleman CN, Camphausen K, Schlom J, Hodge JW. External beam radiation of tumors alters phenotype of tumor cells to render them susceptible to vaccine-mediated T-cell killing. Cancer Res. 2004;64(12):4328–37.
126. Gameiro SR, Jammeh ML, Wattenberg MM, Tsang KY, Ferrone S, Hodge JW. Radiation-induced immunogenic modulation of tumor enhances antigen processing and calreticulin exposure, resulting in enhanced T-cell killing. Oncotarget. 2014;5(2):403–16.
127. Garnett CT, Palena C, Chakraborty M, Tsang KY, Schlom J, Hodge JW. Sublethal irradiation of human tumor cells modulates phenotype resulting in enhanced killing by cytotoxic T lymphocytes. Cancer Res. 2004;64(21):7985–94.
128. Dewan MZ, Galloway AE, Kawashima N, Dewyngaert JK, Babb JS, Formenti SC, et al. Fractionated but not single-dose radiotherapy induces an immune-mediated abscopal effect when combined with anti–CTLA-4 antibody. Clin Cancer Res. 2009;15(17):5379–88.
129. Matsumura S, Wang B, Kawashima N, Braunstein S, Badura M, Cameron TO, et al. Radiation-induced CXCL16 release by breast cancer cells attracts effector T cells. J Immunol. 2008;181(5):3099–107.
130. Potiron VA, Abderrahmani R, Clément-Colmou K, Marionneau-Lambot S, Oullier T, Paris F, et al. Improved functionality of the vasculature during conventionally fractionated radiation therapy of prostate cancer. PLoS One. 2013;8(12):e84076.
131. Gough MJ, Crittenden MR, Young KH. Comparing equals when evaluating immunotherapy with different doses and fractions of radiation therapy. Immunotherapy. 2015;7(8):847–9.
132. Seung SK, Curti BD, Crittenden M, Walker E, Coffey T, Siebert JC, et al. Phase 1 study of stereotactic body radiotherapy and interleukin-2--tumor and immunological responses. Sci Transl Med. 2012;4(137):137ra74.
133. Ministro A, de Oliveira P, Nunes RJ, dos Santos Rocha A, Correia A, Carvalho T, et al. Low-dose ionizing radiation induces therapeutic neovascularization in a pre-clinical model of hindlimb ischemia. Cardiovasc Res. 2017;113(7):783–94.
134. Klug F, Prakash H, Huber PE, Seibel T, Bender N, Halama N, et al. Low-dose irradiation programs macrophage differentiation to an iNOS(+)/M1 phenotype that orchestrates effective T cell immunotherapy. Cancer Cell. 2013;24(5):589–602.
135. Reissfelder C, Timke C, Schmitz-Winnenthal H, Rahbari NN, Koch M, Klug F, et al. A randomized controlled trial to investigate the influence of low dose radiotherapy on immune stimula-

tory effects in liver metastases of colorectal cancer. BMC Cancer. 2011;11:419.
136. Timke C, Winnenthal HS, Klug F, Roeder FF, Bonertz A, Reissfelder C, et al. Randomized controlled phase I/II study to investigate immune stimulatory effects by low dose radiotherapy in primarily operable pancreatic cancer. BMC Cancer. 2011;11:134.
137. Chen DS, Mellman I. Oncology meets immunology: the cancer-immunity cycle. Immunity. 2013;39(1):1–10.
138. Teng MW, Ngiow SF, Ribas A, Smyth MJ. Classifying cancers based on T-cell infiltration and PD-L1. Cancer Res. 2015;75(11):2139–45.

Rationale for Fractionated SRS and Single SRS Session Approaches

Jarred Tanksley, Joseph K. Salama, and John P. Kirkpatrick

Introduction

As ionizing radiation began to be recognized as a therapeutic option for cancer in the late nineteenth and early twentieth century, the concept of a therapeutic ratio began to emerge. The therapeutic ratio relates the likelihood of a beneficial outcome, like tumor control, to the likelihood of an adverse outcome or toxicity with a given treatment regimen. Maximizing the therapeutic ratio is a central consideration in any radiation plan. The "standard" or "conventional" fraction size is around 2 Gy (+/− 0.2 Gy), which has been found to offer the greatest therapeutic ratio when large fields, often encompassing large volumes of normal tissue, must be treated to a high total dose. More recently, stereotactic radiosurgery (SRS) has emerged as a modality to treat a variety of intracranial disease processes with a single-fraction of high-dose radiotherapy (12–24 Gy) while minimizing, although not eliminating irradiation of the surrounding normal tissue. Thus, SRS is often constrained by concern over normal tissue toxicity given the large and ablative doses.

The radiobiologic basis for the standard fraction size is the differential ability of normal healthy cells to recover intra-fractionally from the molecular and metabolic damage caused by ionizing radiation, as compared to the ability of cancer cells to do the same. This differential sensitivity is a product of both cell-specific factors like the functionality of DNA repair mechanisms, and environment-specific factors like local oxygen content and vascular integrity. With larger fraction sizes, in which the resultant damage to individual cells and the microenvironment is substantially greater, both normal and cancer cells are more equally likely to experience a lethal hit. Hence, the therapeutic window narrows as the field size increases.

Standard SRS is given in a single fraction of up to 24 Gy with minimal expansion from gross tumor volume (GTV) to the clinical and planning tumor volumes (CTV and PTV). In the initial systems, immobilization and precise accurate localization were assured by the use of rigid head frames secured to the patient's skull at four points by screws. Obviously, these head frames did not lend themselves to treatment of the same patient on successive days, but the need for reliable, secure immobilization and positioning dictated their use in SRS over the inherently less stable and precise first generation of "relocatable" masks. With the introduction of more reliable relocatable immobilization devices and the implementation of high-fidelity on-machine imaging guidance systems over the past ten years, it is now possible to achieve a daily setup variation of less than 1 mm [1, 2]. In addition, with the advances in treatment planning algorithms and beam-shaping capabilities, there can be exquisite conformality and rapid dose fall-off at the target boundaries, even with irregularly shaped targets. This, in turn, should increase the therapeutic ratio by targeting and treating, essentially, only tumor. However, even with the present capabilities, some volume of normal tissue around and within the PTV will receive an ablative dose, which increases proportionally with PTV. Consequently, for larger lesions or resection cavities, or for those located next to a critical structure like the optic chiasm or brainstem, there can be difficulty in attaining an acceptable balance of tumor control and normal tissue damage. In these scenarios, opting for a two- to five-fraction SRS regimen, termed hypofractionated-SRS (HF-SRS), offers a means of treating intracranial targets in a manner that increases the therapeutic ratio by maintaining

J. Tanksley · J. K. Salama
Duke University, Department of Radiation Oncology, Durham, NC, USA

Duke Cancer Insitute, Durham, NC, USA
e-mail: Jarred.tanksley@duke.edu; Joseph.salama@duke.edu

J. P. Kirkpatrick (✉)
Duke University, Department of Radiation Oncology, Durham, NC, USA

Duke Cancer Insitute, Durham, NC, USA

Duke University, Department of Neurosurgery, Durham, NC, USA
e-mail: John.kirkpatrick@duke.edu

D. M. Trifiletti et al. (eds.), *Stereotactic Radiosurgery and Stereotactic Body Radiation Therapy*,
https://doi.org/10.1007/978-3-030-16924-4_3

a tumor control probability equivalent to single-fraction SRS, but with an improved toxicity profile.

This chapter will focus on the rationale for choosing HF-SRS over single-fraction SRS, herein also called more simply SRS, in the treatment of metastatic, malignant, and benign primary brain tumors. However, the principles discussed can be applied to the treatment of other intracranial and extracranial targets. Deciding on the appropriate dose/fraction regimen requires an understanding of tumor control and normal tissue toxicity as a function of dose, volume, and time (particularly the volume of normal tissue receiving a certain dose), and for certain structures the maximum dose received can be of critical importance (e.g., optic chiasm). We will begin this chapter with a presentation on basic radiobiologic principles specific to fractionation, before proceeding on to discuss the known toxicities of SRS. It will close with a review of the evidence suggesting that in many cases HF-SRS is an equally efficacious and better tolerated approach compared to SRS.

The Radiobiology of Fractionation

In order to compare the efficacy and toxicity of different fractionation schemes it is essential to understand the concept of biologically equivalent dose (BED) and therapeutic ratio. These concepts are ultimately based on preclinical experiments where in vitro survival curves were generated by irradiating different cell types (more malignant versus less malignant versus "benign"), with contributions from experiments assessing the response to radiation of various murine cell populations in vivo, in addition to orthotopic tumor implantation experiments.

The model that is most widely employed to fit the resultant survival curves, both mathematically and mechanistically, is the linear-quadratic (LQ) model. Specifically, the LQ model is a mathematical explanation of how, for a given cell population, the "surviving cell fraction" (SCF) is related to radiation dose. In the LQ model, the SCF at a given dose is dependent upon two cell-specific variables. At lower doses, the SCF decreases linearly with dose, and the slope in this range can be represented as $-\alpha$. As the dose increases beyond a certain point, the SCF begins to decrease more rapidly, depending on both dose and dose squared, which is the quadratic portion of the model. This final portion of the curve has the slope of $-\beta$, and the overall relationship of SCF to total dose is: $\mathrm{SCF} = \exp[-\alpha D - \beta D^2]$. In addition to fitting the data, this formula makes sense from a molecular point-of-view, in that the α parameter can be thought to represent a cell's susceptibility to single radiation tracks while the β parameter represents susceptibility to two tracks in close proximity, consistent with the known, lethal molecular aberrations caused by ionizing radiation [3]. Simplistically, α and β are specific to a particular cell-type, though these can also change in different environmental contexts.

In the LQ model, this response curve must "bend" from a lesser to greater downward slope as the dose increases, and it is in this bend that we get the α/β ratio or the dose at which the contribution of each component (the linear and quadratic) is equal. For cell-types that respond early, or are more sensitive to smaller doses of radiation, the α/β ratio is relatively larger than for those cells that are less sensitive to lower doses. Given the dysfunction of the DNA repair machinery in cancer, a cancer cell is more likely to be killed than a normal cell in the range of conventional doses, though this is an admittedly gross over-simplification. With this in mind, the α/β ratio of cancer is generally considered to be around 10, it is thought to be lower for more indolent cancers like prostate and benign CNS tumors, and the α/β ratio of normal cells is thought to be 2–3.

In order to attempt to equate variable dose-fractionation schemes and how they will impact a given cell-type with a given α/β ratio, the concept of biologically equivalent dose (BED) was created. To calculate BED, the α/β ratio, total dose (D), and dose per fraction (d) are needed. The formula is as follows: $\mathrm{BED}_{\alpha/\beta} = D[1 + d/(\alpha/\beta)]$. Thus, as dose per fraction increases, there is a relatively greater increase in BED for cell- and tissue-types with a lower α/β ratio, suggesting that single-fraction courses will be more toxic to normal tissue than fractionated regimens at the same total dose (representative isoeffect curves are presented in Fig. 1a, b). On the other hand, the potential exists to exploit these α/β ratio differences such that we maintain tumor BED while reducing normal tissue BED. For example, consider the resultant BEDs of the following regimens: 15 Gy in a single fraction, 21 Gy in three fractions, and 25 Gy in five fractions. The BED_{10} for cancer cells with these three regimens, using the above BED formula and $\alpha/\beta = 10$, is 35.7–37.5 Gy. On the other hand, the BED_2 for normal tissue ($\alpha/\beta = 2$) is 127.5 Gy for the single-fraction regimen, 94.5 Gy for the three-fraction course, and 87.5 Gy for the five-fraction course. Thus, a comparison of the three fractionation schemes suggests in theory a similar likelihood of tumor control for each, but with an approximately 30% reduction in normal tissue BED in the fractionated courses (Fig. 2). Importantly, the five-fraction course has a superior normal tissue BED if the α/β ratio is 2, while the three-fraction course is superior if the α/β ratio is 3.

The LQ model has been relatively accurate in predicting toxicity and efficacy in conventionally fractionated radiotherapy. There is ongoing controversy about the shape of the survival curve beyond a single fraction of 10 Gy and how well it conforms to reality. It is thought that clinical observations noted at these higher doses, which seem to be inconsistent with the LQ model, suggest a "new radiobiology" [4–6]. Factors like profound vascular damage that can compromise

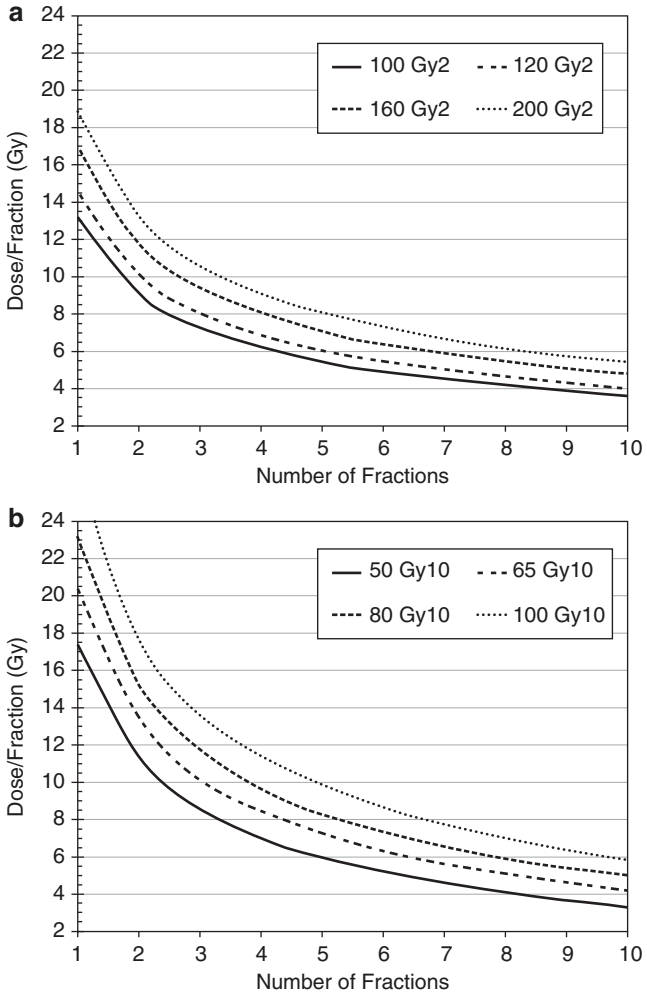

Fig. 1 (**a**, **b**) Biologically equivalent dose (BED) isoeffect plots for dose-fractionation schemes for tissues with (**a**) $\alpha/\beta = 2$ and (**b**) $\alpha/\beta = 10$. These were calculated using the linear-quadratic (LQ) model. (**a**, **b**: Used with permission of Oxford University Press from Kirkpatrick et al. [77])

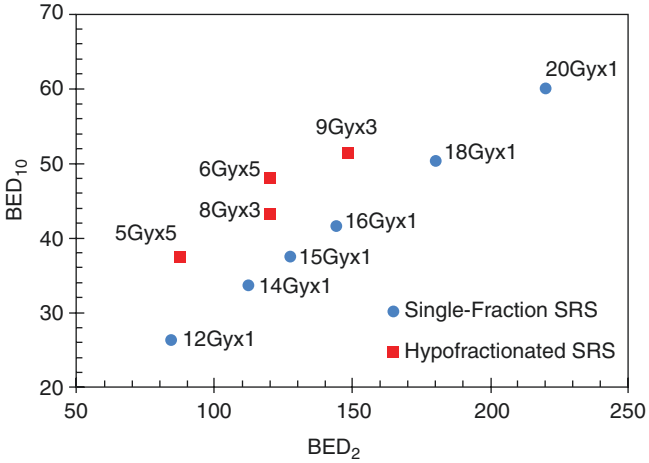

Fig. 2 BED_2 and BED_{10} for various SRS and HF-SRS fractionation schemes. BED_2 is associated with the response of normal tissue to radiation, with increases in BED_2 representing greater toxicity risk. BED_{10} is associated with the response of tumor tissue, with increases representing higher tumor control probability, as described in the test. (Used with permission of Oxford University Press from Kirkpatrick et al. [77])

tumor blood supply over time and changes in antigen presentation that can generate clinically important immune responses, both contributing to tumor eradication in the context of large single fractions, are more complex radiobiologic mechanisms of tumor control unaccounted for in the LQ model. Nevertheless, though the cell-survival curves from which the LQ model are derived are based on more simplified models that generally lack the nuances of the microenvironment, there are substantial clinical and preclinical data suggesting that at doses in the relevant range, dose per fraction up to 8 Gy, the LQ model still accurately models outcomes [7–9].

The ability to place disparate dose-fractionation schemes on somewhat equal ground with respect to a biological outcome, i.e., SCF and toxicity, allows for quick consideration of the therapeutic ratio. Though there are innumerable nuances that make a clinically relevant therapeutic ratio dependent on variables more complex than the SCFs of the tumor and normal tissues, it logically holds true that when comparing two schemes with an equivalent tumor BED, the one with a lower normal tissue BED will be associated with less side effects in the patient. To that end, the rationale for choosing HF-SRS over SRS is built on knowledge of what is an unacceptable normal tissue BED (too much), an unacceptable tumor BED (too little), and how to dose-fractionate so that things are just right. It is also important to remember that one must treat the entirety of the tumor, and findings regarding the efficacy of various dose-fractionation schemes with respect to tumor control will be discussed later in this chapter. The question that must be answered first, for any model, is what volume of normal tissue are we "allowed" to treat to a given dose before we have an unacceptable toxicity risk? Finally, while the linear-quadratic model may be to convert different dose/fraction schemes to some uniform basis, the most relevant method for doing so remains unclear. Recognizing these limitations, the fundamental principles of SRS, which include highly conformal plans, minimal margin, accurate and precise target localization, minimization of position deviation, and robust quality assurance, will aid in minimizing the irradiated volume of normal tissue and *should always be employed*.

A potential caveat to the experimentally derived survival curves is the aforementioned "new radiobiology," which considers the indirect ways in which radiotherapy can eradicate tumor, i.e., immunomodulation and alteration of the blood supply. Emerging evidence suggests that radiotherapy can cause stimulation of the immune system through the exposure of new antigens, which may lead to both improved local and distant control, and that this phenomenon may be

somewhat dependent upon the fraction size [10, 11]. Further, the single-fraction doses employed with SRS may enhance locally within the tumor by damaging the vasculature [12–14]. However, this may be disadvantageous inasmuch as it alters perfusion by limiting the ability of immune cells to reach the tumor and develop a response. In this regard, HF-SRS might stimulate antigen exposure and better allow the immune system to "see" the tumor, allowing for a more robust response [15, 16]. Much is unknown in this vein, and it is unclear how the receipt of concurrent immunomodulatory therapy will alter the therapeutic ratio, but it is clear that practitioners should remain thoughtful in their approach to patients receiving this type of therapy.

Factors Predicting Toxicity with SRS

The acute side effects of SRS are minimal and, depending on location, include headache, nausea and vomiting, and less frequently vertigo and seizures. These symptoms are generally temporary and responsive to medications. Of more concern are the chronic side effects, many of which can be severe and have a substantial impact on patient quality of life. SRS is much less likely to result in cognitive deterioration than WBRT in both the short- and long-run, which is attributed to the global versus focal nature of the two treatments. The ablative doses used in SRS, however, can cause different types of toxicities. The most common toxicity is radionecrosis (RN), which can cause significant symptoms through edema and mass effect. Other subacute to chronic side effects that can be caused by SRS are the product of ablating a structure that is not redundant or that functions in series. The tolerance of the optic chiasm, for instance, is above that of common WBRT regimens, but well below the doses commonly used in SRS. The following is a brief discussion of what is currently known, or presumed, about the dosimetric parameters that correlate with toxicity risk in single-fraction treatment of the brain.

The risk for developing RN typically peaks around 6–12 months following SRS, and though occurring in a minority of patients, the sequelae can be severe. On imaging, it can appear similar to disease progression and commonly progresses if unaddressed. New medical and surgical interventions are being employed in its treatment, including the anti-VEGF antibody bevacizumab (Avastin) [17] or Laser Interstitial Thermal Therapy (LITT) [18], in addition to previously used treatments like steroids and surgical resection. The Quantitative Estimates of Normal Tissue Effects in the Clinic project (QUANTEC) has emphasized the importance of the volume of brain receiving 10 and 12 Gy (V_{10} and V_{12}) in predicting RN, with the likelihood rising rapidly when the volume receiving these doses exceeded 5–10 mL [19, 20]. This corresponds roughly to a sphere with a diameter of 2.5 cm. A recent retrospective analysis did note that keeping the V_{10} under 10 mL and V_{12} under 8.5 mL would keep the risk of RN under 10% at 1 year [21]. It is not known whether these parameters pertain to the total volume treated to either dose or to the volume of normal tissue receiving the dose (i.e., GTV subtracted from the total volume receiving said dose). Importantly, this trial also found that only 20% of those patients with RN were symptomatic. This is not to say that the risk of symptomatic RN is equal throughout the brain, as analysis of patients with arteriovenous malformations treated with SRS noted substantially greater susceptibility to symptomatic RN if the target involved the basal ganglia, somewhat less if involving the medulla, and even less for the corpus callosum, temporal, and parietal lobes [22].

There are a number of structures in the brain subject to maximum dose constraints given the serial nature of their function: the optic nerves, chiasm, and brainstem. As well, given functional nonredundancy, the cochlea is also subject to a maximum dose. Some of these parameters are also a product of the QUANTEC project. It was noted that the risk of radiation-induced optic neuropathy became unacceptable when a maximum dose of 10 Gy was exceeded, and that it is perhaps more reasonable to limit the maximum to 8 Gy [23]. The recommended maximum dose to the brainstem is 12.5 Gy, with a > 5% risk of symptomatic sequelae [24]. In an analysis of hearing preservation following the use of SRS in the treatment of acoustic neuromas, it was found that there is better preservation if the central cochlear point dose is kept to <4.2 Gy [25].

These are the basic dosimetric parameters that are typically paid heed in the evaluation of an SRS plan. Many questions remain [26]. Some of these data were, for instance, derived from patients with arteriovenous malformations, which may impart an entirely different level of risk than in the treatment of brain metastases. Further, as we are able to treat multiple lesions throughout the brain during a single session, the import of proximity of the volumes of normal tissue receiving a certain dose in predicting RN is unclear. Nonetheless, these parameters, while perhaps overly conservative, are a reasonable approach until further data are accumulated, not least of which is the need to understand how immunotherapy might increase the likelihood of developing RN, and if bevacizumab might decrease that risk.

Clinical Outcomes of HF-SRS

The preceding discussion has laid out the theoretical basis for opting for HF-SRS over SRS and the dosimetric parameters that when exceeded in the single-fraction scenario present a risk for unacceptable toxicity and support the need for an alternative approach. If the probability of tumor control and the therapeutic ratio are equivalent for a single- versus multi-fraction course, the single-fraction course should be chosen for the sake of patient convenience. Otherwise, it

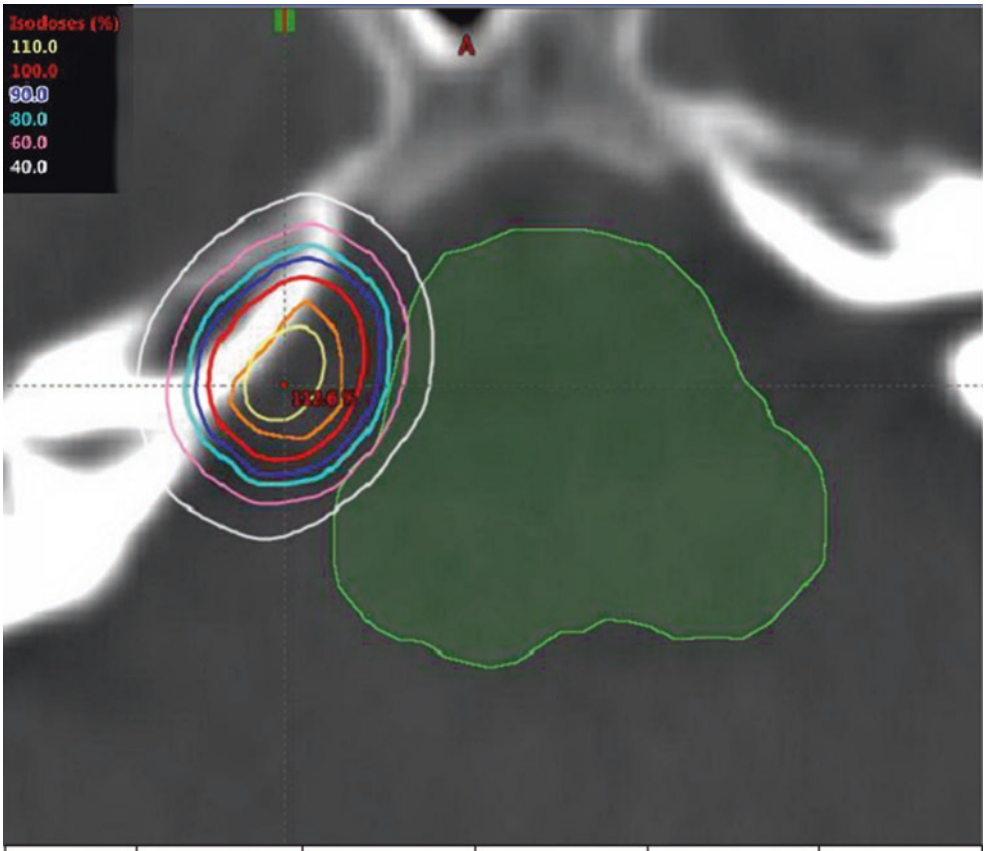

Number of Fractions	Dose/Fraction (Gy)	Total Prescribed Dose (Gy)	**BED**10Gy for Prescribed Dose to Lesion	Maximum Dose to Brainstem (Gy)	**BED**2Gy for Max Dose to Brainstem
1	15	20	37.5	12.0	84.0
5	5	25	37.5	20.0	60.0
1	12	12	26.4	9.6	60.0

Fig. 3 Illustration of the concept of the potential advantages of hypofractionation for radiosurgery of a lesion (orange contour above) adjacent to the brainstem. In this plan, the 100% isodose line just encompasses the target lesion and the 80% isodose line impinges on the brainstem. Treating in a single fraction with a marginal dose of 15 Gy or in five 5 Gy fractions yields a BED_{10} of 37.5 Gy_2 for both plans, suggesting equivalent tumor control. However, the BED_2 is far higher for the single-fraction treatment than for the HF-SRS plan (84 Gy_2 versus 60 Gy_2), substantially increasing the risk of normal tissue toxicity. Decreasing the single-fraction dose to 12 Gy yields an equivalent risk normal tissue toxicity to the HF-SRS plan, at the risk of reduced tumor control

becomes a question of balancing efficacy and toxicity, as illustrated in Fig. 3. The following section focuses on patient outcomes when SRS and HF-SRS are used in the treatment of benign and malignant intracranial tumors, with many findings supporting the notion that the radiobiologic concepts discussed earlier translate into clinical practice.

Brain metastases occur in 20–40% of cancer patients, or nearly 200,000 patients yearly in the United States, and are most commonly found in patients with melanoma, and lung, breast, and kidney cancer, but are seen in any systemic malignancy [27]. SRS is commonly used in the treatment of brain metastases, and this usage is accelerating as we become more capable of addressing disease outside of the brain with more efficacious systemic therapies. SRS is also conceptually ideal in this context given the lack of invasiveness relative to surgical intervention in a patient population that may be debilitated or with a limited prognosis. The two Patchell studies addressing the roles of surgery and whole brain radiation therapy (WBRT) in patients with a single metastasis, emphasized the import of local control [28, 29]. SRS has been found to offer local control rates similar to surgery, and in the RTOG 95-08 trial, addressing the addition of an SRS boost to WBRT, it was found that an SRS boost did appear to offer a survival advantage in a subset of patients [30, 31]. In postoperative patients, SRS reduces local recurrence when compared to observation [32]. Compared to SRS, WBRT is more debilitating neurocognitively. In a recent trial comparing postoperative SRS to WBRT in patients with brain metastases, the rate of cognitive deterioration was significantly less in patients treated with SRS (52% vs. 85%). Though not compared statistically, the crude rates of many grade 1–3 toxicities including alopecia, fatigue, and hearing impairment were higher with WBRT in that trial [33].

The above trials – and many more – have established SRS as an alternative to surgery or WBRT in the treatment of asymptomatic metastases, as a better-tolerated approach than WBRT, and data are accumulating suggesting that SRS can be used in select patients with ten or more brain metastases. As the likelihood of toxicity increases with the volume of normal tissue receiving some dose of radiation, and as we are able to treat a greater number of metastases during a single session, margin size (the expansion from GTV to PTV) is an

important variable. In the treatment of brain metastases, two different scenarios must be considered: the treatment of unresected lesions and the treatment of postoperative resection cavities. An autopsy study has shown that microscopic extension beyond the capsule occurs in the majority of lung cancer metastases in the brain, though this extension is generally less than 1 mm [34]. To that end, a 1 mm expansion appears to offer superior local control, with a 3 mm expansion being no better and potentially more toxic [35]. A slightly larger expansion is necessary when treating postoperative resection cavities as a 2 mm expansion to CTV offers superior local control compared to no expansion, with no significant difference in toxicity [36].

The question of regarding the maximum dose that could be safely delivered in a single fraction was addressed in the RTOG 90-05 dose escalation study. It is important to recognize that this study was performed in a population of patients who received prior brain irradiation, whether WBRT for metastatic disease, or partial brain irradiation for malignant gliomas [37]. Dose limits of 24 Gy, 18, Gy, and 15 Gy were established for lesions measuring <2 cm, 2.1–3 cm, and 3.1–4 cm respectively, by escalating at 3 Gy increments, and considering a greater than 20% risk of toxicity as unacceptable. The rate of chronic neurotoxicity for each of the chosen dose levels was greater than 10%, was 20% for 18 Gy to a 2.1–3 cm lesion, and greater than 30% at the next highest dose level used for each group. Nonetheless, this is the approach employed in clinic, with some latitude in prescribing doses near the transition points (i.e., treating a 2.1 cm lesion to 20–22 Gy).

The findings of RTOG 90-05 have shown us the maximum tolerable dose in the treatment of brain lesions of a given maximum diameter, albeit in the setting of reirradiation. Paradoxically, larger lesions, which would require greater doses for equivalent proportional cell kill, are instead treated to a lower dose. This would be expected to result in worse local control for larger lesions, which has borne out in practice. A retrospective study from the Cleveland Clinic noted 1-year local control of 85% for lesions treated with 24 Gy and less than 50% for those treated with 18 and 15 Gy [38]. These findings would suggest that 24 Gy to a smaller lesion has a high likelihood of tumor control and an acceptable toxicity profile. Therefore, it is in the treatment of larger lesions, which must be treated to a lower dose in the single-fraction setting, where HF-SRS may prove superior.

To date, the relative efficacy and toxicity of SRS and HF-SRS in the treatment of brain metastases has been evaluated only in retrospect, and as such, data are subject to the various biases inherent in any retrospective analysis [39–53]. Nonetheless, they have supported the principles discussed above. This is best exemplified in two retrospective studies from Italy, addressing the use of HF-SRS in the intact and postoperative setting. In the first study, patients with intact tumors >2 cm in size were treated according to the aforementioned RTOG 90-05 dosing schema or else received 27 Gy in three fractions [50]. Despite having larger GTVs and PTVs, those patients receiving the fractionated course had better local control at 1 year (90% vs. 77%). Furthermore, the risk of RN was significantly lower in the fractionated group (8% vs. 20% overall and 14% vs. 33% for lesions >3 cm). Notably, in the fractionated course, the V_{18} tended to predict for RN, and was 14% when >30.2 mL. In the setting of postoperative treatment, the same fractionation scheme was analyzed (though not compared to single-fraction SRS) noting a 1- and 2-year local control rate of 93% and 84%, respectively [49]. There are a number of prospective, single-arm trials underway to address the efficacy of HF-SRS in the treatment of brain metastases, some of which are also including concurrent systemic therapy.

Single-fraction SRS as a component of the primary treatment of GBM has not proven efficacious. RTOG 93-05 addressed this question by randomizing patients to receive conventionally fractionated radiation with BCNU chemotherapy, which in the treatment arm was preceded by an SRS boost [54]. There were no differences in either survival outcomes or patterns of failure. A hypofractionated course of partial brain irradiation (25 Gy in five fractions) has also proven reasonable in patients with a poor performance status [55]. Nonetheless, SRS and HF-SRS are presently not felt to have a role in the primary treatment of GBM. However, none of these trials were performed in the temozolomide era, and there is presently a nearly completed study concerning the safety and efficacy of five-fraction HF-SRS courses with concurrent temozolomide.

There is evidence to support the use of SRS and HF-SRS in the treatment of recurrent GBM. A number of small prospective trials and retrospective analyses in both contexts have suggested a median survival of 6–18 months in patients treated with these modalities at recurrence, which compares favorably with historic controls [56–60]. As GBM typically recurs within the prior treatment field, in the majority of cases SRS for recurrent GBM will involve reirradiation, putting the patient at increased risk for the development of RN. Whether this is seen in practice is not entirely clear based on retrospective analyses where rates of RN range from 0–44%. Nonetheless, it is reasonable to think that this patient population is more susceptible to developing symptomatic RN, and given the very limited prognosis, the development of symptomatic necrosis may compromise a patient's quality of life. With this in mind, the addition of concurrent bevacizumab to SRS in recurrent GBM has been found on retrospective analyses to reduce the rate of necrosis to 5–9% as compared to 19–43% in those who received SRS alone [17, 61, 62]. The RTOG 12-05 trial is a randomized phase II comparing bevacizumab with or without a course of 35 Gy in ten fractions.

SRS can also be used in the treatment of benign brain tumors, and is not uncommonly preferred to surgery given the high rates of observed efficacy and often lower morbid-

ity. The use of SRS in two of the most common benign brain tumors, vestibular schwannomas and meningiomas, has been well-studied. As these lesions are extra-axial and are typically non-infiltrative with sharp margins of demarcation on contrast imaging, they are readily amenable to SRS. Unfortunately, they are also commonly located adjacent to, or involve, critical structures necessitating a more fractionated and even fully conventionally fractionated approach.

Vestibular schwannomas can be well-controlled with a more modest dose of single-fraction SRS as compared to brain metastases. A 98% rate of local control was noted in an early trial in which a marginal dose of 16 Gy was employed [63]. However, this trial also found that hearing was preserved in only 51%, and injuries to the trigeminal and facial nerves were reported in more than 20% of patients. This prompted investigation of a lower dose of 12–13 Gy, which has proven essentially equally efficacious [64]. The use of HF-SRS in larger lesions has been investigated, with dose-fractionation schemes of 18–21 Gy in three fractions and 25 Gy in five fractions, with similar rates of local control and toxicity, although the HF-SRS literature is typically associated with shorter follow-up as compared to the single-fraction SRS literature [65–70]. Thus, both the rates of local control and toxicity may change with further follow-up. Nonetheless, in the case of a vestibular schwannoma that abuts or compresses the brainstem, where the brainstem tolerance would be exceeded with a single-fraction regimen, it may be more reasonable to use a HF-SRS regimen.

Meningiomas are also well-controlled with a single fraction of 12–13 Gy, with rates above 90% commonly reported at intermediate times post radiosurgery [71, 72]. The toxicity risk is generally less than 10%, though the rate is higher when the lesion is not located in the skull base [73]. For example, it has been noted in an institutional study concerning parafalcine and parasaggital meningiomas that 38.2% of patients developed progressive peritumoral edema [74]. Just as with vestibular schwannomas, location can necessitate the decision to use HF-SRS. In a study from Stanford, which included patients with meningiomas within 2 mm of the optic apparatus, local control and vision preservation were found to be 94% when a hypofractionated course was used [75]. This high-level of local control was corroborated by a study from UPMC, in which local control of 95% with HF-SRS was seen [76].

There are a number of clinical trials presently underway addressing the use of HF-SRS in all of the above contexts (Table 1) [77]. For example, a study at Stanford is seeking to determine the maximum tolerated doses (MTD) for a three-

Table 1 Clinical trials presently underway addressing the use of HF-SRS

Trial	Disease site	Primary outcome	Clinicaltrials.gov identifier
Phase I/II Study of Fractionated Stereotactic Radiosurgery to Treat Large Brain Metastases	Brain metastases	Determine MTD of SRS given in 3 fractions for brain metastases 4.2–14.1 cm^3 and 14.2–33.5 cm^3	NCT00928226
Fractionated Stereotactic Radiotherapy (FSRT) in Treatment of Brain Metastases		Determine MTD of TPI 287 given concurrently with FSRT to treat brain metastases	NCT02187822
Hypofractionated Stereotactic Radiosurgery in Treating Patients With Large Brain Metastasis		Determine MTD of 5-fraction SRS for brain metastases, 3–6 cm diameter	NCT01705548
Perfexion Brain Metastasis (HF-SRT)		Determine MTD of HF-SRS for recurrent brain metastases (at least 1 > 2 cm diameter) post WBRT	NCT00805103
Fractionated Stereotactic Radiosurgery with Concurrent Bevacizumab for Brain Metastases: A Phase I Dose- escalation Trial		Determine MTD of 3-fraction SRS + bevacizumab for brain metastases, 1.5–3.5 cm diameter	NCT02672995
Frameless Fractionated Stereotactic Radiation Therapy (FSRT) for Brain Mets Study		Incidence of failure based on imaging for each lesion (up to 5 cm diameter) after 3–5 fraction SRS	NCT02798029
Fractionated Stereotactic Radiosurgery for Large Brain Metastases		MTD for 3-fraction SRS for brain metastases, 3–5 cm diameter	NCT02054689
Hypofractionated Stereotactic Radiation Therapy of Brain Metastases: Evaluation of WBRT		Overall survival of patients with 1–3 brain metastases treated with HF-FSRT	NCT02913534
Phase I/II Study of Temozolomide and Hypofractionated Radiotherapy for Newly Diagnosed Supratentorial GBM	GBM	Determine MTD of 5-fraction SRS with 5 mm margins with temozolomide for newly diagnosed GBM	NCT01120639
Multisession SRS for Optic Nerve Sheath Meningiomas (ONSMsmSRS)	Meningioma	Visual function outcome in ONSM treated with 5-fraction SRS	NCT02594709
1 versus 3 fraction SRS for Patients with Neurinomas (ACOUNEU)	Acoustic neuroma	Hearing preservation in patients with acoustic neuromas randomized to 1- versus 3-fraction SRS	NCT02055859

Adapted with permission of Oxford University Press from Kirkpatrick et al. [77]

fraction regimen in the setting of brain metastases measuring up to 33.5 mL (NCT00928226), while a study at Emory is searching for the MTD for five-fraction HF-SRS in the setting of 3–6 cm brain metastases (NCT017055480). A separate study is seeking the MTD of a five-fraction regimen with concurrent temozolomide for newly diagnosed GBM (NCT01120639). Two exciting studies in Italy concern benign diseases. One is assessing visual outcomes following treatment of optic nerve sheath meningiomas with five-fraction HF-SRS, which should give insight into the toxicity risk for this regimen (NCT02594709). A separate study is comparing SRS against three-fraction HF-SRS in the treatment of vestibular schwannomas (NCT02055859).

Conclusion

While conventionally fractionated radiation therapy can provide an acceptable balance of tumor control and toxicity when treating large fields, single-fraction SRS can offer an optimal balance of tumor control, minimal toxicity and favorable logistics, when treating small fields. For intermediate target volumes or those that are intimately associated with critical structures, HF-SRS appears to potentially offer a superior balance of the desired outcomes as compared to single-fraction SRS. In this chapter, we discussed the radiobiological basis for improved therapeutic ratio with HF-SRS, and pertinent clinical data, focusing on the rationale for choosing one dose/fraction regimen over the other in the treatment of intracranial lesions. However, the principles discussed can be more widely applied to targets in different body sites. In using SBRT to treat lung cancer, for example, it is important to consider the size and location of the target, as central airway necrosis and chronic chest wall pain are less likely with more fractionated schemes. This also applies to liver SBRT, where both liver and bowel toxicity must be considered. As more clinical data accumulates, the variables that factor into the therapeutic ratio, however incalculable that truly is, will continue to emerge and be modified, and, in turn, inform our fractionation schemes.

References

1. Ahmad SS, Duke S, Jena R, Williams MV, Burnet NG. Advances in radiotherapy. BMJ. 2012;345:e7765.
2. Sahgal A. Technological advances in brain and spine radiosurgery. Technol Cancer Res Treat. 2012;11(1):1–2.
3. Chadwick KH, Leenhouts HP. A molecular theory of cell survival. Phys Med Biol. 1973;18(1):78–87.
4. Guerrero M, Li XA. Extending the linear-quadratic model for large fraction doses pertinent to stereotactic radiotherapy. Phys Med Biol. 2004;49(20):4825–35.
5. Hanin LG, Zaider M. Cell-survival probability at large doses: an alternative to the linear-quadratic model. Phys Med Biol. 2010;55(16):4687–702.
6. Park C, Papiez L, Zhang S, Story M, Timmerman RD. Universal survival curve and single fraction equivalent dose: useful tools in understanding potency of ablative radiotherapy. Int J Radiat Oncol Biol Phys. 2008;70(3):847–52.
7. Brown JM, Carlson DJ, Brenner DJ. The tumor radiobiology of SRS and SBRT: are more than the 5 Rs involved? Int J Radiat Oncol Biol Phys. 2014;88(2):254–62.
8. Brown JM, Carlson DJ, Brenner DJ. Dose escalation, not "new biology," can account for the efficacy of stereotactic body radiation therapy with non-small cell lung cancer. In reply to Rao et al. Int J Radiat Oncol Biol Phys. 2014;89(3):693–4.
9. Kirkpatrick JP, Brenner DJ, Orton CG. Point/Counterpoint. The linear-quadratic model is inappropriate to model high dose per fraction effects in radiosurgery. Med Phys. 2009;36(8):3381–4.
10. Fuks Z, Kolesnick R. Engaging the vascular component of the tumor response. Cancer Cell. 2005;8(2):89–91.
11. Garcia-Barros M, Paris F, Cordon-Cardo C, Lyden D, Rafii S, Haimovitz-Friedman A, et al. Tumor response to radiotherapy regulated by endothelial cell apoptosis. Science. 2003;300(5622):1155–9.
12. Kirkpatrick JP, Meyer JJ, Marks LB. The linear-quadratic model is inappropriate to model high dose per fraction effects in radiosurgery. Semin Radiat Oncol. 2008;18(4):240–3.
13. Song CW, Lee YJ, Griffin RJ, Park I, Koonce NA, Hui S, et al. Indirect tumor cell death after high-dose hypofractionated irradiation: implications for stereotactic body radiation therapy and stereotactic radiation surgery. Int J Radiat Oncol Biol Phys. 2015;93(1):166–72.
14. Sperduto PW, Song CW, Kirkpatrick JP, Glatstein E. A hypothesis: indirect cell death in the radiosurgery era. Int J Radiat Oncol Biol Phys. 2015;91(1):11–3.
15. Demaria S, Formenti SC. Radiation as an immunological adjuvant: current evidence on dose and fractionation. Front Oncol. 2012;2:153.
16. Demaria S, Golden EB, Formenti SC. Role of local radiation therapy in cancer immunotherapy. JAMA Oncol. 2015;1(9):1325–32.
17. Levin VA, Bidaut L, Hou P, Kumar AJ, Wefel JS, Bekele BN, et al. Randomized double-blind placebo-controlled trial of bevacizumab therapy for radiation necrosis of the central nervous system. Int J Radiat Oncol Biol Phys. 2011;79(5):1487–95.
18. Buttrick S, Komotar RJ. Introduction for Laser Interstitial Thermal Therapy (LITT) in neurosurgery supplement. Neurosurgery. 2016;79(Suppl 1):S1–2.
19. Lawrence YR, Li XA, el Naqa I, Hahn CA, Marks LB, Merchant TE, et al. Radiation dose-volume effects in the brain. Int J Radiat Oncol Biol Phys. 2010;76(3. Suppl):S20–7.
20. Marks LB, Yorke ED, Jackson A, Ten Haken RK, Constine LS, Eisbruch A, et al. Use of normal tissue complication probability models in the clinic. Int J Radiat Oncol Biol Phys. 2010;76(3. Suppl):S10–9.
21. Minniti G, Clarke E, Lanzetta G, Osti MF, Trasimeni G, Bozzao A, et al. Stereotactic radiosurgery for brain metastases: analysis of outcome and risk of brain radionecrosis. Radiat Oncol. 2011;6:48.
22. Flickinger JC, Kondziolka D, Lunsford LD, Kassam A, Phuong LK, Liscak R, et al. Development of a model to predict permanent symptomatic postradiosurgery injury for arteriovenous malformation patients. Arteriovenous Malformation Radiosurgery Study Group. Int J Radiat Oncol Biol Phys. 2000;46(5):1143–8.
23. Mayo C, Martel MK, Marks LB, Flickinger J, Nam J, Kirkpatrick J. Radiation dose-volume effects of optic nerves and chiasm. Int J Radiat Oncol Biol Phys. 2010;76(3. Suppl):S28–35.
24. Mayo C, Yorke E, Merchant TE. Radiation associated brainstem injury. Int J Radiat Oncol Biol Phys. 2010;76(3. Suppl):S36–41.
25. Kano H, Kondziolka D, Khan A, Flickinger JC, Lunsford LD. Predictors of hearing preservation after stereotactic radiosurgery for acoustic neuroma. J Neurosurg. 2009;111(4):863–73.

26. Kirkpatrick JP, Marks LB, Mayo CS, Lawrence YR, Bhandare N, Ryu S. Estimating normal tissue toxicity in radiosurgery of the CNS: application and limitations of QUANTEC. J Radiosurg SBRT. 2011;1:95–102.
27. Sperduto PW, Chao ST, Sneed PK, Luo X, Suh J, Roberge D, et al. Diagnosis-specific prognostic factors, indexes, and treatment outcomes for patients with newly diagnosed brain metastases: a multi-institutional analysis of 4,259 patients. Int J Radiat Oncol Biol Phys. 2010;77(3):655–61.
28. Patchell RA, Tibbs PA, Regine WF, Dempsey RJ, Mohiuddin M, Kryscio RJ, et al. Postoperative radiotherapy in the treatment of single metastases to the brain: a randomized trial. JAMA. 1998;280(17):1485–9.
29. Patchell RA, Tibbs PA, Walsh JW, Dempsey RJ, Maruyama Y, Kryscio RJ, et al. A randomized trial of surgery in the treatment of single metastases to the brain. N Engl J Med. 1990;322(8):494–500.
30. Andrews DW, Scott CB, Sperduto PW, Flanders AE, Gaspar LE, Schell MC, et al. Whole brain radiation therapy with or without stereotactic radiosurgery boost for patients with one to three brain metastases: phase III results of the RTOG 9508 randomised trial. Lancet. 2004;363(9422):1665–72.
31. Sperduto PW, Shanley R, Luo X, Andrews D, Werner-Wasik M, Valicenti R, et al. Secondary analysis of RTOG 9508, a phase 3 randomized trial of whole-brain radiation therapy versus WBRT plus stereotactic radiosurgery in patients with 1-3 brain metastases; poststratified by the graded prognostic assessment (GPA). Int J Radiat Oncol Biol Phys. 2014;90(3):526–31.
32. Mahajan A, Ahmed S, McAleer MF, Weinberg JS, Li J, Brown P, et al. Post-operative stereotactic radiosurgery versus observation for completely resected brain metastases: a single-centre, randomised, controlled, phase 3 trial. Lancet Oncol. 2017;18(8):1040–8.
33. Brown PD, Ballman KV, Cerhan JH, Anderson SK, Carrero XW, Whitton AC, et al. Postoperative stereotactic radiosurgery compared with whole brain radiotherapy for resected metastatic brain disease (NCCTG N107C/CEC.3): a multicentre, randomised, controlled, phase 3 trial. Lancet Oncol. 2017;18(8):1049–60.
34. Baumert BG, Rutten I, Dehing-Oberije C, Twijnstra A, Dirx MJ, Debougnoux-Huppertz RM, et al. A pathology-based substrate for target definition in radiosurgery of brain metastases. Int J Radiat Oncol Biol Phys. 2006;66(1):187–94.
35. Kirkpatrick JP, Wang Z, Sampson JH, McSherry F, Herndon JE 2nd, Allen KJ, et al. Defining the optimal planning target volume in image-guided stereotactic radiosurgery of brain metastases: results of a randomized trial. Int J Radiat Oncol Biol Phys. 2015;91(1):100–8.
36. Choi CY, Chang SD, Gibbs IC, Adler JR, GRt H, Lieberson RE, et al. Stereotactic radiosurgery of the postoperative resection cavity for brain metastases: prospective evaluation of target margin on tumor control. Int J Radiat Oncol Biol Phys. 2012;84(2):336–42.
37. Shaw E, Scott C, Souhami L, Dinapoli R, Kline R, Loeffler J, et al. Single dose radiosurgical treatment of recurrent previously irradiated primary brain tumors and brain metastases: final report of RTOG protocol 90-05. Int J Radiat Oncol Biol Phys. 2000;47(2):291–8.
38. Vogelbaum MA, Angelov L, Lee SY, Li L, Barnett GH, Suh JH. Local control of brain metastases by stereotactic radiosurgery in relation to dose to the tumor margin. J Neurosurg. 2006;104(6):907–12.
39. Eaton BR, Gebhardt B, Prabhu R, Shu HK, Curran WJ Jr, Crocker I. Hypofractionated radiosurgery for intact or resected brain metastases: defining the optimal dose and fractionation. Radiat Oncol. 2013;8:135.
40. Ernst-Stecken A, Ganslandt O, Lambrecht U, Sauer R, Grabenbauer G. Phase II trial of hypofractionated stereotactic radiotherapy for brain metastases: results and toxicity. Radiother Oncol. 2006;81(1):18–24.
41. Fahrig A, Ganslandt O, Lambrecht U, Grabenbauer G, Kleinert G, Sauer R, et al. Hypofractionated stereotactic radiotherapy for brain metastases--results from three different dose concepts. Strahlenther Onkol. 2007;183(11):625–30.
42. Fokas E, Henzel M, Surber G, Kleinert G, Hamm K, Engenhart-Cabillic R. Stereotactic radiosurgery and fractionated stereotactic radiotherapy: comparison of efficacy and toxicity in 260 patients with brain metastases. J Neuro-Oncol. 2012;109(1):91–8.
43. Follwell MJ, Khu KJ, Cheng L, Xu W, Mikulis DJ, Millar BA, et al. Volume specific response criteria for brain metastases following salvage stereotactic radiosurgery and associated predictors of response. Acta Oncol. 2012;51(5):629–35.
44. Kim YJ, Cho KH, Kim JY, Lim YK, Min HS, Lee SH, et al. Single-dose versus fractionated stereotactic radiotherapy for brain metastases. Int J Radiat Oncol Biol Phys. 2011;81(2):483–9.
45. Kwon AK, Dibiase SJ, Wang B, Hughes SL, Milcarek B, Zhu Y. Hypofractionated stereotactic radiotherapy for the treatment of brain metastases. Cancer. 2009;115(4):890–8.
46. Ling DC, Vargo JA, Wegner RE, Flickinger JC, Burton SA, Engh J, et al. Postoperative stereotactic radiosurgery to the resection cavity for large brain metastases: clinical outcomes, predictors of intracranial failure, and implications for optimal patient selection. Neurosurgery. 2015;76(2):150–6. discussion 6-7; quiz 7
47. Manning MA, Cardinale RM, Benedict SH, Kavanagh BD, Zwicker RD, Amir C, et al. Hypofractionated stereotactic radiotherapy as an alternative to radiosurgery for the treatment of patients with brain metastases. Int J Radiat Oncol Biol Phys. 2000;47(3):603–8.
48. Minniti G, Esposito V, Clarke E, Scaringi C, Bozzao A, Falco T, et al. Fractionated stereotactic radiosurgery for patients with skull base metastases from systemic cancer involving the anterior visual pathway. Radiat Oncol. 2014;9:110.
49. Minniti G, Esposito V, Clarke E, Scaringi C, Lanzetta G, Salvati M, et al. Multidose stereotactic radiosurgery (9 Gy x 3) of the postoperative resection cavity for treatment of large brain metastases. Int J Radiat Oncol Biol Phys. 2013;86(4):623–9.
50. Minniti G, Scaringi C, Paolini S, Lanzetta G, Romano A, Cicone F, et al. Single-fraction versus multifraction (3 x 9 Gy) stereotactic radiosurgery for large (>2 cm) brain metastases: a comparative analysis of local control and risk of radiation-induced brain necrosis. Int J Radiat Oncol Biol Phys. 2016;95(4):1142–8.
51. Rajakesari S, Arvold ND, Jimenez RB, Christianson LW, Horvath MC, Claus EB, et al. Local control after fractionated stereotactic radiation therapy for brain metastases. J Neuro-Oncol. 2014;120(2):339–46.
52. Wang CC, Floyd SR, Chang CH, Warnke PC, Chio CC, Kasper EM, et al. Cyberknife hypofractionated stereotactic radiosurgery (HSRS) of resection cavity after excision of large cerebral metastasis: efficacy and safety of an 800 cGy x 3 daily fractions regimen. J Neuro-Oncol. 2012;106(3):601–10.
53. Wegner RE, Leeman JE, Kabolizadeh P, Rwigema JC, Mintz AH, Burton SA, et al. Fractionated stereotactic radiosurgery for large brain metastases. Am J Clin Oncol. 2015;38(2):135–9.
54. Souhami L, Seiferheld W, Brachman D, Podgorsak EB, Werner-Wasik M, Lustig R, et al. Randomized comparison of stereotactic radiosurgery followed by conventional radiotherapy with carmustine to conventional radiotherapy with carmustine for patients with glioblastoma multiforme: report of Radiation Therapy Oncology Group 93-05 protocol. Int J Radiat Oncol Biol Phys. 2004;60(3):853–60.
55. Roa W, Kepka L, Kumar N, Sinaika V, Matiello J, Lomidze D, et al. International Atomic Energy Agency randomized phase III study of radiation therapy in elderly and/or frail patients with newly diagnosed glioblastoma multiforme. J Clin Oncol Off J Am Soc Clin Oncol. 2015;33(35):4145–50.
56. Gutin PH, Iwamoto FM, Beal K, Mohile NA, Karimi S, Hou BL, et al. Safety and efficacy of bevacizumab with hypofractionated ste-

reotactic irradiation for recurrent malignant gliomas. Int J Radiat Oncol Biol Phys. 2009;75(1):156–63.
57. Hall WA, Djalilian HR, Sperduto PW, Cho KH, Gerbi BJ, Gibbons JP, et al. Stereotactic radiosurgery for recurrent malignant gliomas. J Clin Oncol Off J Am Soc Clin Oncol. 1995;13(7):1642–8.
58. Hudes RS, Corn BW, Werner-Wasik M, Andrews D, Rosenstock J, Thoron L, et al. A phase I dose escalation study of hypofractionated stereotactic radiotherapy as salvage therapy for persistent or recurrent malignant glioma. Int J Radiat Oncol Biol Phys. 1999;43(2):293–8.
59. Koga T, Maruyama K, Tanaka M, Ino Y, Saito N, Nakagawa K, et al. Extended field stereotactic radiosurgery for recurrent glioblastoma. Cancer. 2012;118(17):4193–200.
60. Minniti G, Scaringi C, Paolini S, Clarke E, Cicone F, Esposito V, et al. Repeated stereotactic radiosurgery for patients with progressive brain metastases. J Neuro-Oncol. 2016;126(1):91–7.
61. Cuneo KC, Vredenburgh JJ, Sampson JH, Reardon DA, Desjardins A, Peters KB, et al. Safety and efficacy of stereotactic radiosurgery and adjuvant bevacizumab in patients with recurrent malignant gliomas. Int J Radiat Oncol Biol Phys. 2012;82(5):2018–24.
62. Park KJ, Kano H, Iyer A, Liu X, Niranjan A, Flickinger JC, et al. Salvage gamma knife stereotactic radiosurgery followed by bevacizumab for recurrent glioblastoma multiforme: a case-control study. J Neuro-Oncol. 2012;107(2):323–33.
63. Kondziolka D, Lunsford LD, McLaughlin MR, Flickinger JC. Long-term outcomes after radiosurgery for acoustic neuromas. N Engl J Med. 1998;339(20):1426–33.
64. Murphy ES, Suh JH. Radiotherapy for vestibular schwannomas: a critical review. Int J Radiat Oncol Biol Phys. 2011;79(4):985–97.
65. Karam SD, Tai A, Strohl A, Steehler MK, Rashid A, Gagnon G, et al. Frameless fractionated stereotactic radiosurgery for vestibular schwannomas: a single-institution experience. Front Oncol. 2013;3:121.
66. Meijer OW, Vandertop WP, Baayen JC, Slotman BJ. Single-fraction vs. fractionated linac-based stereotactic radiosurgery for vestibular schwannoma: a single-institution study. Int J Radiat Oncol Biol Phys. 2003;56(5):1390–6.
67. Morimoto M, Yoshioka Y, Kotsuma T, Adachi K, Shiomi H, Suzuki O, et al. Hypofractionated stereotactic radiation therapy in three to five fractions for vestibular schwannoma. Jpn J Clin Oncol. 2013;43(8):805–12.
68. Song DY, Williams JA. Fractionated stereotactic radiosurgery for treatment of acoustic neuromas. Stereotact Funct Neurosurg. 1999;73(1–4):45–9.
69. Tsai JT, Lin JW, Lin CM, Chen YH, Ma HI, Jen YM, et al. Clinical evaluation of CyberKnife in the treatment of vestibular schwannomas. Biomed Res Int. 2013;2013:297093.
70. Vivas EX, Wegner R, Conley G, Torok J, Heron DE, Kabolizadeh P, et al. Treatment outcomes in patients treated with CyberKnife radiosurgery for vestibular schwannoma. Otol Neurotol. 2014;35(1):162–70.
71. Flannery TJ, Kano H, Lunsford LD, Sirin S, Tormenti M, Niranjan A, et al. Long-term control of petroclival meningiomas through radiosurgery. J Neurosurg. 2010;112(5):957–64.
72. Lee JY, Niranjan A, McInerney J, Kondziolka D, Flickinger JC, Lunsford LD. Stereotactic radiosurgery providing long-term tumor control of cavernous sinus meningiomas. J Neurosurg. 2002;97(1):65–72.
73. Mansouri A, Guha D, Klironomos G, Larjani S, Zadeh G, Kondziolka D. Stereotactic radiosurgery for intracranial meningiomas: current concepts and future perspectives. Neurosurgery. 2015;76(4):362–71.
74. Sheehan JP, Cohen-Inbar O, Ruangkanchanasetr R, Bulent Omay S, Hess J, Chiang V, et al. Post-radiosurgical edema associated with parasagittal and parafalcine meningiomas: a multicenter study. J Neuro-Oncol. 2015;125(2):317–24.
75. Adler JR Jr, Gibbs IC, Puataweepong P, Chang SD. Visual field preservation after multisession cyberknife radiosurgery for perioptic lesions. Neurosurgery. 2008;62(Suppl 2):733–43.
76. Bria C, Wegner RE, Clump DA, Vargo JA, Mintz AH, Heron DE, et al. Fractionated stereotactic radiosurgery for the treatment of meningiomas. J Cancer Res Ther. 2011;7(1):52–7.
77. Kirkpatrick JP, Soltys SG, Lo SS, Beal K, Shrieve DC, Brown PD. The radiosurgery fractionation quandary: single fraction or hypofractionation? Neuro-Oncology. 2017;19(suppl_2):ii38–49.

Part II

Intracranial Radiosurgery Technique

Physics of Radiosurgery

Yongsook C. Lee, Steven J. Goetsch, David J. Schlesinger, and Stanley H. Benedict

Introduction

The methods for treating disease using ionizing radiation originated contemporaneously with some of the earliest methods of noninvasively imaging interior anatomy. At this early stage, there was no way for a physician to directly visualize the location and extent of disease inside the body. There was no way to apply the new technique of radiotherapy selectively to the diseased tissue without including normal healthy tissue in the treatment as well. The providential discovery of time-dose fractionation made it possible to use differences in the radiobiological response to accumulate dose in diseased tissue without fatally damaging normal tissue. Thus, for much of its history radiotherapy using external beam sources evolved in the direction of treating using broad fields with a uniform dose distribution. The uniform dose distribution allowed the differential responses of normal and disease tissues, quantified in a variety of in vitro experiments, to be directly applied to clinical dose-fractionation prescriptions. The use of flattening filters in linear accelerators and the emphasis placed on flat, symmetric, large fields in linear accelerator quality assurance is a testament to this evolutionary direction.

Radiosurgery turned this traditional method of radiotherapy on its head. Developments toward less-invasive neurosurgery and improved medical imaging converged in a way which allowed Lars Leksell, an innovative Swedish neurosurgeon, to conceive of a revolutionary approach. Instead of treating broad areas of normal and diseased tissue to a uniform dose in a highly fractionated treatment schedule, he would attempt to deliver an ablative dose to only the diseased tissue in a single treatment while largely sparing the surrounding healthy tissue. This chapter will describe the historical developments which made the idea of radiosurgery possible, the physics and engineering solutions which allow radiosurgery to meet its requirements, and recent and future developments which will see radiosurgery evolve to encompass further advances in imaging technology and our understanding of the underlying biology.

History of Radiosurgery

Discovery and Initial Advances in Radiotherapy

If a visitor from the Middle Ages somehow travelled through time to the year 1895, they would likely find the state of medicine (and of neurosurgery in particular) to be quite familiar. Little progress had been made over those hundreds of years in our understanding of neuroanatomy, the germ theory of disease, surgical technology, or antiseptic surgical techniques. Few methods existed to investigate the internal anatomy of a patient other than exploratory surgery. Morbidity and mortality were very high, with death from infection a common occurrence following any surgical procedure. However, in December 1895, Professor Wilhelm C Röntgen discovered his "New Kind of Rays," demonstrating his discovery with

Y. C. Lee
University of Arizona, Department of Radiation Oncology, Tucson, AZ, USA
e-mail: yclee@email.arizona.edu

S. J. Goetsch
San Diego Gamma Knife Center, La Jolla, CA, USA
e-mail: sgoetsch@sdgkc.com

D. J. Schlesinger
University of Virginia, Departments of Radiation Oncology and Neurological Surgery, Charlottesville, VA, USA
e-mail: Djs9c@virginia.edu

S. H. Benedict (✉)
University of California Davis Comprehensive Cancer Center, Department of Radiation Oncology, University of California at Davis, Sacramento, CA, USA
e-mail: shbenedict@ucdavis.edu

D. M. Trifiletti et al. (eds.), *Stereotactic Radiosurgery and Stereotactic Body Radiation Therapy*,
https://doi.org/10.1007/978-3-030-16924-4_4

Fig. 1 X-ray and Radium Martyrs Memorial, Hamburg, Germany

the first radiograph in history of his own hand. The state of medicine was about to undergo a revolution.

Six months after Röntgen's discovery and only 350 miles away, Professor Antoine Henri Becquerel of the University of Paris discovered natural radioactivity. His brilliant graduate student Marie Sklodowska Curie (assisted by her husband Pierre Curie) purified the radioactive elements polonium and radium in 1898. By 1903, Röntgen, Becquerel, and Marie and Pierre Curie had all been honored with the Nobel Prize in Physics [1]. Ionizing radiation was well established medically for both diagnostic imaging and therapy by that time. In 1896 the American neurosurgeon Harvey Cushing used a radiographic device to uncover the location of a bullet lodged in a patient's cervical spine [2]. That same year at least 23 cases of radiation dermatitis were reported in the literature [3]. Perhaps the first purposeful therapeutic use of X-rays to treat cancer also occurred in 1896 when a Chicago medical student, Emil Herman Grubbe, built an X-ray apparatus and used it to treat a recurrent carcinoma of the breast [4]. In parallel, the discoveries of the Curies were exploited by using the newly discovered element radium for therapy and the search for radioactive elements that could be used in medical practice was ignited [5].

Radiation injuries were quite common in those early days of experimenting with radiation. Grubbe's opportunity to use X-rays therapeutically came about in part because of radiation burns which he experienced and which were noted by a physician colleague who suggested they may be also capable of treating diseased tissue [4]. Thomas Edison's unfortunate assistant Clarence Dally may have been the first person to die of cancer (in 1904) induced by radiation after his extensive work with X-rays. A monument to the "X-ray and Radium Martyrs of All Nations" was dedicated in Hamburg in 1936 (Fig. 1). Originally it had 169 names but by 1959 there were 359 names including Marie Curie and her daughter Irene. Fortunately for the early development of radiotherapy, experiments performed in the 1920s and 1930s by Claudius Regaud in France demonstrated that a ram could be sterilized via exposure to ionizing radiation while avoiding excessive skin damage if the dose was spread out over a period of weeks [6]. This discovery of the effects of time/dose fractionation was critical at a time when there were very limited methods for visualizing disease in situ in a living person. A uniform dose could be delivered to a large volume of tissue, and the differential radiobiological effects of the radiation on healthy and diseased tissue would do most of the work. For much of the history of external-beam radiotherapy, the importance of a uniform dose distribution and fractionated dose schedules was considered as dogma.

Advances in Neurosurgery and the Invention of Stereotaxy

Contemporaneous with the discovery and initial development of X-rays were important advances that were beginning to change the practice of neurosurgery. One advance directly relevant to the future of radiosurgery was the development of the first stereotactic frame in 1905 by Robert Henry Clarke, a neurophysiologist, and Sir Victor Horsley, neurosurgeon and inventor. The Horsley-Clarke frame, as it was known, could be fixed to a live animal and permitted selective elec-

trode stimulation and ablation of deep cerebellar nuclei [7]. At almost the same time, another neurosurgeon, Walter Dandy, realized that soft tumors in the paranasal sinuses stood out in radiographs because they were silhouetted against a background of air and that more of the brain could be treated this way if the fluid in the cerebral ventricles could be similarly displaced with a different density medium. After several experiments with different materials, Dandy found success using room air, creating the technique of ventriculography, a first attempt to visualize lesions throughout the brain, followed closely by pneumoencephalography [8]. This advance in turn helped to inspire Ernest Spiegel and Henry Wycis to adapt the Horsley-Clarke stereotactic frame for image guidance and the technique of stereoencephalotomy [9]. However, while it was a start, imaging quality was still quite poor. This problem motivated the development of stereotactic coordinate systems and stereotactic atlases such as the piecewise linear atlas developed by Jean Talairach which used the anterior and posterior commissure (AC-PC) line as the basis for a navigational neurosurgical atlas and coordinate system [10].

Higher-Energy Radiotherapy

The early developments of external beam radiotherapy were primary low-energy X-ray systems. In the 1920s and 1930s advances in the understanding of the underlying physics and improved engineering allowed for the creation of higher-energy devices that could attain accelerating potentials of 150–300 kVp. These higher penetrating X-rays made possible the successful treatment of deeper tumors using fractionated treatment techniques. The beginnings of basic multiple field techniques such as two-field parallel-opposed techniques and four-field box techniques appeared during this time; an early attempt at using cross-firing beams to improve dose homogeneity for what were still poorly visualized tumors [11].

The dawn of the nuclear age at the end of World War II and the development of nuclear reactors for research led to the creation of by-product material such as cobalt-60, which has a long half-life of 5.26 years, much higher energy (1.17 MeV and 1.33 MeV), and a high-specific activity. Cobalt-60 was packaged into a therapy device by a team led by Harold Johns and termed teletherapy. The high-specific activity allowed for small sources with sharp geometric penumbras. The higher-energy photons allowed for even deeper lesions to be reached and created a skin-sparing effect as the electrons freed in tissue at this energy tend to deposit energy at depth rather than scattering to the surface and the long half-life made for relatively stable dose rates [12]. A second technological development that resulted directly from World War II was the creation of radiofrequency devices such as magnetrons, klystrons, and waveguides. These led to the development of the first linear accelerators, capable of creating megavoltage energy X-rays. The related development of the cyclotron allowed for the acceleration of protons.

Lars Leksell and the Invention of Radiosurgery

Lars Leksell, a Swedish neurosurgeon, was frustrated by the morbidity and mortality of open neurosurgical procedures and was interested in finding minimally invasive techniques. Leksell further developed the ideas of Spiegel and Wycis to create an arc-centered stereotactic frame that improved image-guided neurosurgery (Fig. 2). But he found the requirement of physically opening the skull of the patient to be less than satisfactory. Leksell's innovation was to synthesize the developments in minimally invasive neurosurgery with the recent developments in radiotherapy to create a method for performing "surgery" on a deep-seated part of the brain without any need for opening the skull. He married the targeting capability of the stereotactic frame, the imaging capability of ventriculography and pneumoencephalography, the stereo-

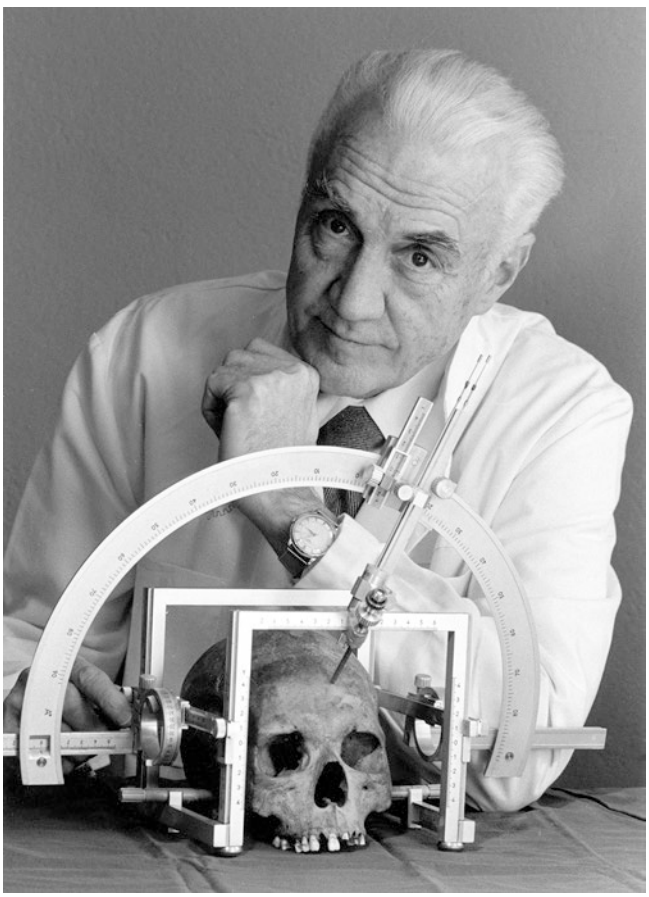

Fig. 2 Swedish neurosurgeon Lars Leksell with his stereotactic frame. (Used with permission of Elekta Instrument, Stockholm, Sweden)

tactic navigation techniques of Talairach, and the therapy capability of X-rays in a technique he termed "stereotactic radiosurgery." However, as he was a neurosurgeon, he viewed his objective from a surgical point of view. Rather than attempting to treat a broad volume of tissue with a uniform dose distributed over multiple treatment sessions, he instead was interested in treating a focal area of tissue to a high, cytotoxic dose in a single fraction. Similar to how a surgeon would resect tissue, Leksell wanted to destroy it in place.

Leksell initially attempted his technique using orthovoltage X-rays to treat two patients with trigeminal neuralgia. While successful, Leksell decided higher-energy photons and particles might be more effective, so he began treatment using a 185 MeV cyclotron in Uppsala, Sweden. The distance and complexity of a cyclotron had its own disadvantages, however. So Leksell, along with his physics collaborator Borge Larsson, created a device utilizing cobalt-60, which had a photon energy high enough to be effective for deep brain lesions but also a half-life long enough to be practical in a medical facility. Leksell and Larsson extended the idea of cross-firing beams to an extreme, realizing that by maximizing the number and directions of the beams (by using numerous cobalt-60 sources) they could maximize the dose falloff in a manner that approximated the beam characteristics of the proton cyclotron they tried earlier. The first design of what would eventually be coined the "Gamma Knife" contained 179 cobalt-60 sources collimated with elliptical collimators to form a precise focal spot (Fig. 3a, b). The use of cobalt-60 was critical, as there was no practical way to create such a large number of beams with electrically driven X-rays. Leksell had the first "Gamma unit" constructed by the Swedish shipbuilding firm Mottola and treated his first patients for functional disorders in 1967. Two other prototype units were created, and the field of radiosurgery began its slow climb to clinical acceptance. Leksell and his sons commercialized their inventions with the formation of Elekta Instrument, AB in 1972. A commercial version of the Leksell Gamma Unit was created (later referred to as the Model U) with 201 cobalt-60 sources, followed a few years later by two other designs (Model B and Model C) which were much easier to reload with new sources and (in the case of the Model C) included a robotic positioning system (termed the "Automatic Positioning System"). The fully roboticized Leksell Gamma Knife® Perfexion™ (Elekta, Stockholm, Sweden) was introduced in 2006.

Teletherapy and Linear Accelerator-Based Radiosurgery

The design of the Gamma Knife was not the only method to reduce unwanted radiation dose outside the target volume and achieve the steep dose gradients required for SRS. As the idea of delivering large hypofractionated doses slowly gained traction, attempts began to adapt teletherapy and linear accelerator systems to emulate SRS dose distributions as the Gamma Knife would make. By mounting tertiary collimators on the treatment heads of the units and special adaptors to mount stereotactic frames, very small fields with sharp penumbras could be created and targeted in stereotactic coordinate space. Juan Luis Barcia-Saloro first attempted this method on a cobalt-60 teletherapy device at the University of Valencia in 1982. During the same year, Osvaldo Betti and Victor Derechinsky adapted a Varian linear accelerator to perform a similar experiment and included

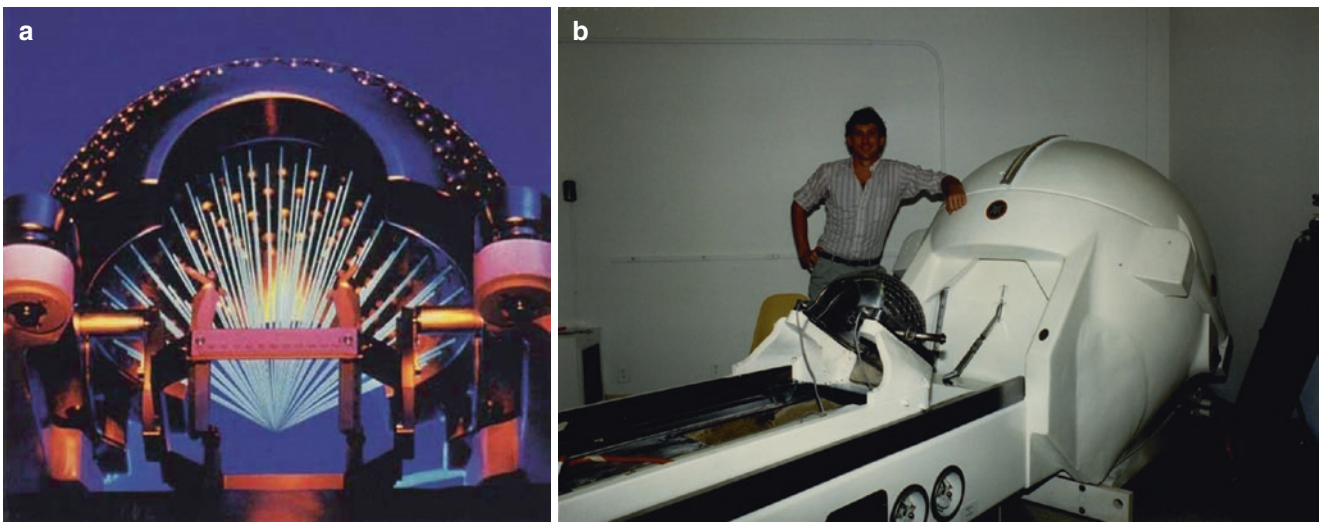

Fig. 3 (**a**) Elekta Gamma Knife converging beams in original Model U helmet. (**b**) Original Leksell Gamma Unit after relocation to UCLA Medical Center in 1982. (**a**: Used with permission of Elekta Instrument, Stockholm, Sweden)

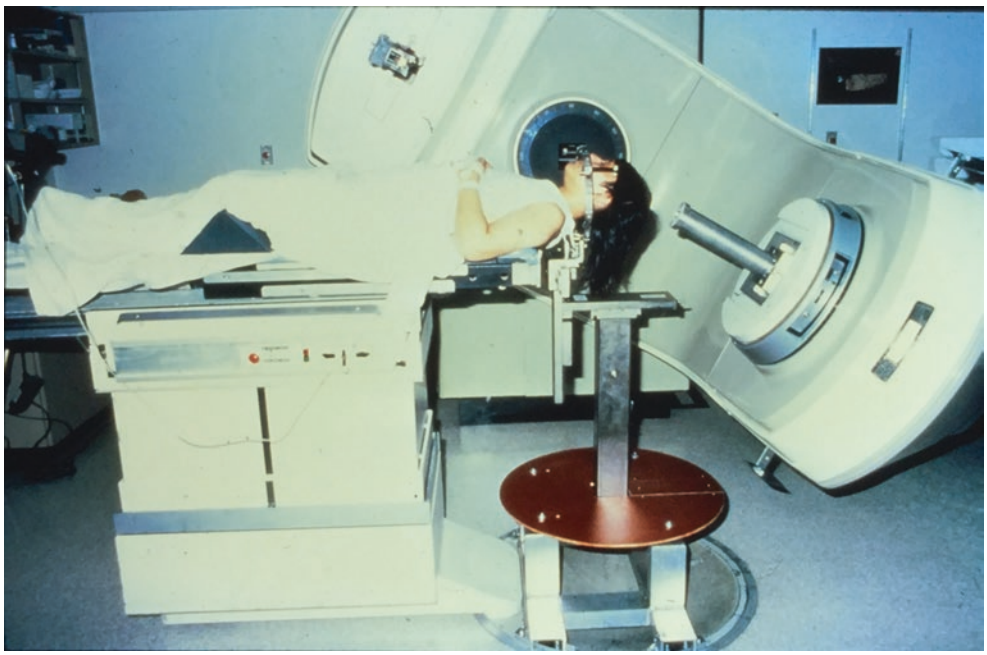

Fig. 4 The first SRS patient treated at the JCRT. (Courtesy of Dr. Wendell Lutz, Tucson, AZ, USA)

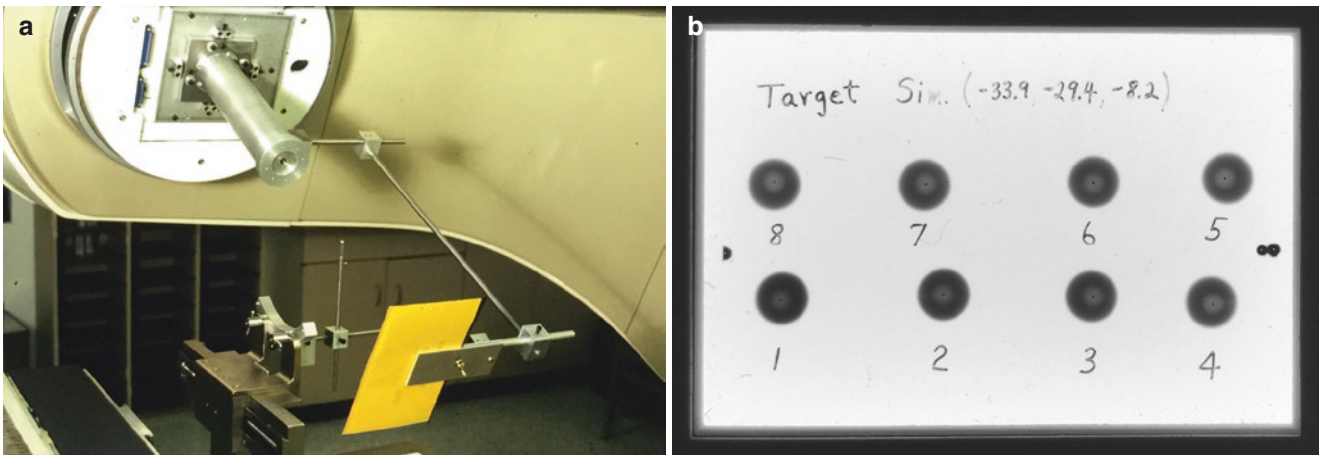

Fig. 5 (**a**) A setup for the Winston-Lutz test at JCRT (steel ball bearing represents patient's specific target). (**b**) Film results. (Courtesy of Dr. Wendell Lutz, Tucson, AZ, USA)

a rocking chair mechanism to allow noncoplanar arcs to be delivered to better approximate the multiple beams of a Gamma Knife. However, perhaps the best-known developments in linear accelerator-based SRS were created at the Joint Center for Radiation Therapy (JCRT, Harvard Medical School) in the mid-to-late 1980s. The team at JCRT created a series of circular, tertiary collimators (called "stereotactic cones") which could be mounted on the accessory tray of the linear accelerator to create different size narrow beams (Fig. 4). A floor stand was created that could precisely position a stereotactic frame with respect to the linac isocenter. Quality assurance methods (today known as the Winston-Lutz test) were developed which used film and a steel ball to verify the center of rotation of the linac gantry and collimator (Fig. 5a, b). These developments formed the basis for further advances in linac SRS and SBRT to come.

Recent Advances

The clinical acceptance of radiosurgery was initially quite limited. Much radiation treatment planning in the 1970s and 1980s was based on invasive pneumoencephalography with biplane radiographs and X-ray simulators, which were diagnostic X-ray units mounted on a rotating gantry in a similar geometry as the treatment devices. Broad radiation fields were used to target anatomy with both diseased and normal tissue. Treatment fields were designed and aligned using the

X-ray simulators. Patient positioning was verified pretreatment and on a weekly basis using port films on the therapy devices. Dosimetric calculations were performed using dose ratio tables created by the medical physicist for the device at different fields sizes. The limited ability to visualize diseased tissue created an incentive to maintain the technique of treating broad fields using fractionated dose schedules.

Neurosurgeons tended to be more interested in the idea of SRS due to their established experience with stereotactic neurosurgery techniques such as pallidotomy and thalamotomy. They were relatively comfortable with the principle of a device such as the Gamma Knife where the objective was to place a focal spot of radiation at a particular point in three-dimensional stereotactic space. However, even for neurosurgeons, limitations on imaging capability restricted the adoption of SRS to only a few specialized academic medical centers.

The confluence of new imaging techniques and advances in computing power allowed SRS to mature into the field that we know it today. The invention of tomographic imaging techniques in the form of computed tomography in the 1970s and magnetic resonance imaging (MRI) in the 1980s provided clinicians with new, fully three-dimensional images of internal anatomy. MRI is particularly effective in allowing neurosurgeons to visualize internal brain anatomy and tumors in exquisite detail. Radiation treatment planning systems were developed to implement this three-dimensional imaging, and advances borrowed from computer graphics allowed more advanced dose computation and dose visualization. As more targets became radiologically visible, the field expanded rapidly. With these advances it became more practical to attempt to deliver focal doses to small areas of well-visualized disease, sparing dose to normal tissue as much as possible. More recent advances in imaging and beam delivery technology have worked to further reduce treatment uncertainty and increase treatment flexibility in SRS.

Relocatable Stereotactic Frames

SRS was conceived as a technique delivering a single, large dose of radiation to a focal target. However, it can be viewed as one extreme along a continuum of dose fractionation strategies, with traditional 2 Gy/fraction schedules over 30–40 days on the other extreme. In certain clinical situations (larger targets, very close organs at risk, etc.) there may be dosimetric and radiobiological advantage to treating in a hypofractionated, but not single-fraction dose schedule. Traditional stereotactic frames become impractical in these scenarios, as the frame (and its invasive fixation pins) would have to be re-applied for each treatment, or the patient would have to live with the frame in place over several treatment days. A more practical solution was a frame that could be repositioned. Several relocatable frame strategies have been developed including the Gill-Thomas-Cosman frame, the Boston Children's frame, the Laitinen Stereoadapter frame, the Solstice™ SRS immobilization, and the trUpoint ARCH™ SRS/SRT Immobilization System (CIVCO Radiotherapy, Coralville, IA, USA) (Fig. 6).

One important factor to note is that relocatable frame systems may not immobilize as well as more rigid SRS frames (Fig. 7). To achieve the similar minimal levels of uncertainty as stationary frames, some kind of intrafraction motion management system is required (see below).

Fig. 6 trUpoint ARCH™ SRS/SRT Immobilization System. (Courtesy of CIVCO Radiotherapy, Coralville, IA, USA)

Fig. 7 Radionics BRW CT guided biopsy system adopted for SRS frames later. (Courtesy of Dr. Wendell Lutz, Tucson, AZ, USA)

Integration of On-Board Imaging

One of the most significant developments in treatment delivery technology has been the integration of imaging devices directly with the treatment machines in the form of portal imagers, orthogonal X-ray systems, and more recently on-board cone-beam CT (CBCT) systems. The latter two techniques in particular continue to have an important impact on SRS as they allow setup localization of the patient in three dimensions. CBCT systems create a three-dimensional image of the patient in treatment position and can be directly compared to the simulation imaging used for treatment planning. The system can automatically adjust the patient's position to eliminate any discrepancies, greatly reducing setup uncertainty. As the CBCT has a known calibration to the linac isocenter, the resulting images partially eliminate the need for a stereotactic frame with and an implicit SRS coordinate system. CBCT imaging makes SRS using mask-based immobilization practical. Orthogonal X-ray systems use two stationary X-ray systems that can operate even during beam delivery. Several devices use this technique for intrafraction monitoring of the patient's position.

On-board imaging has also reached the Gamma Knife community with the release of the Gamma Knife Icon™ (2015), which includes an on-board CBCT calibrated to the Gamma Knife isocenter. The system can be used for mask-based SRS as well as for a QA step immediately before treatment for frame-based SRS (Fig. 8).

Fig. 8 Leksell Gamma Knife Perfexion with Icon conebeam CT system. (Used with permission of Elekta Instrument, Stockholm, Sweden)

Multileaf Collimators and IMRT

Another major development in treatment delivery technology was the invention of the multileaf collimator (MLC) and intensity-modulated radiation therapy (IMRT). MLCs allowed individual beams to be arbitrarily shaped (within the design limits of the MLC). Initially this led to "conformal" treatments where the individual beams were shaped to match the beams-eye-view (BEV) of the target. But with the invention of inverse-planning optimization algorithms treatment planning systems were able to devise more complicated schemes where individual beams may only partially irradiate the tumor, but the sum total of several beams could make a highly conformal dose distribution (Fig. 9).

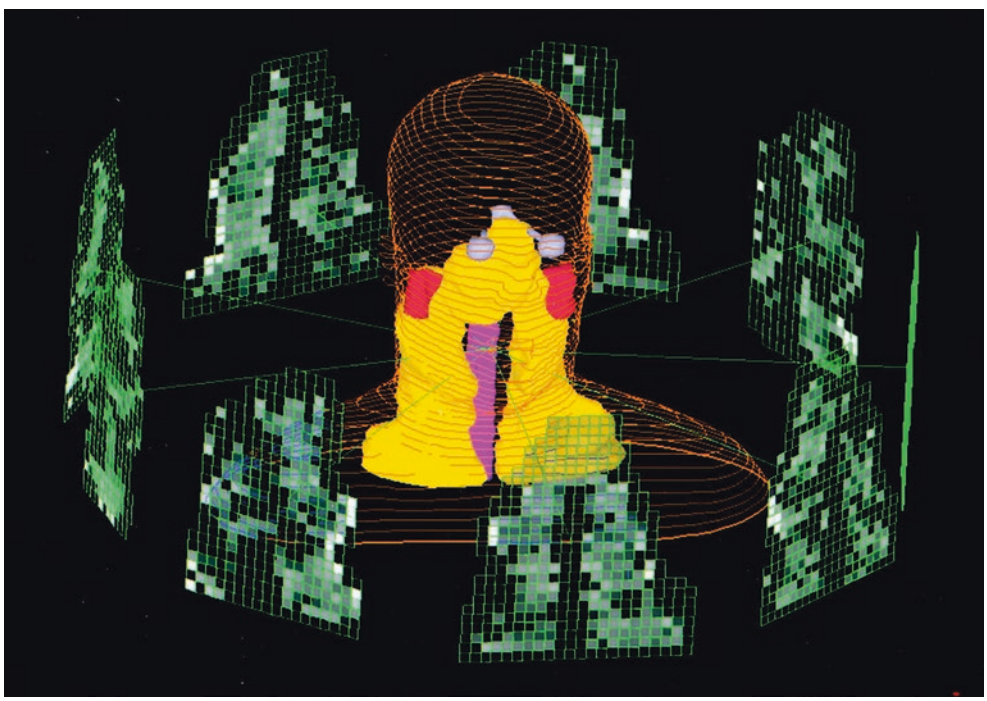

Fig. 9 IMRT beam pattern. (Used with permission of Elsevier from Intensity Modulated Radiation Therapy Collaborative Working Group [13])

Conformal Arcs and VMAT

Recent improvements in computational power and manufacturing control systems have extended the IMRT concept and combined it with the idea of stereotactic arcs to create conformal arcs and VMAT. Conformal arcs modulate the MLCs as the linac gantry is rotating so that the beam shape closely matches the BEV of the tumor over the course of the arc (normally divided in 5–10 degree segments) (Fig. 10). Volumetric modulated arc therapy (VMAT) synchronizes the MLCs, gantry motion, and dose rate to conformally irradiate the target(s) (Fig. 11a–f). In both cases, the intent is to spread out energy over a large volume of tissue, concentrating the high-dose portion of the dose distribution within the intended target(s). The most recent iteration of this technique is the single-isocenter, multiple target VMAT technique. This uses recent advances in MLC technology to create "islands" of beams off of the central axis during the arc rotation. This then allows multiple targets to be treated simultaneously, with the isocenter generally placed at the centroid of all of the targets to be treated.

Limitations

Of course, stereotactic radiosurgery is not the "magic bullet" suggested by Paul Ehrlich in 1900 that can cure any intracranial disease without causing any harm. It is critical for clinicians practicing radiosurgery to be acutely aware of the limitations of the technique, including limits on total volume of lesions treated, the sorts of indications where SRS is contraindicated, uncertainty in determining response versus radiation necrosis, and the need for additional therapies to control systemic disease.

SRS Is a Local Therapy

Perhaps the most significant limitation of SRS is that it is by definition a local therapy. SRS can be curative for benign conditions such as meningiomas, vascular malformations, functional disorders, and in situations of limited metastatic disease. However, for most metastatic indications the primary objective of SRS is local tumor control, which can be

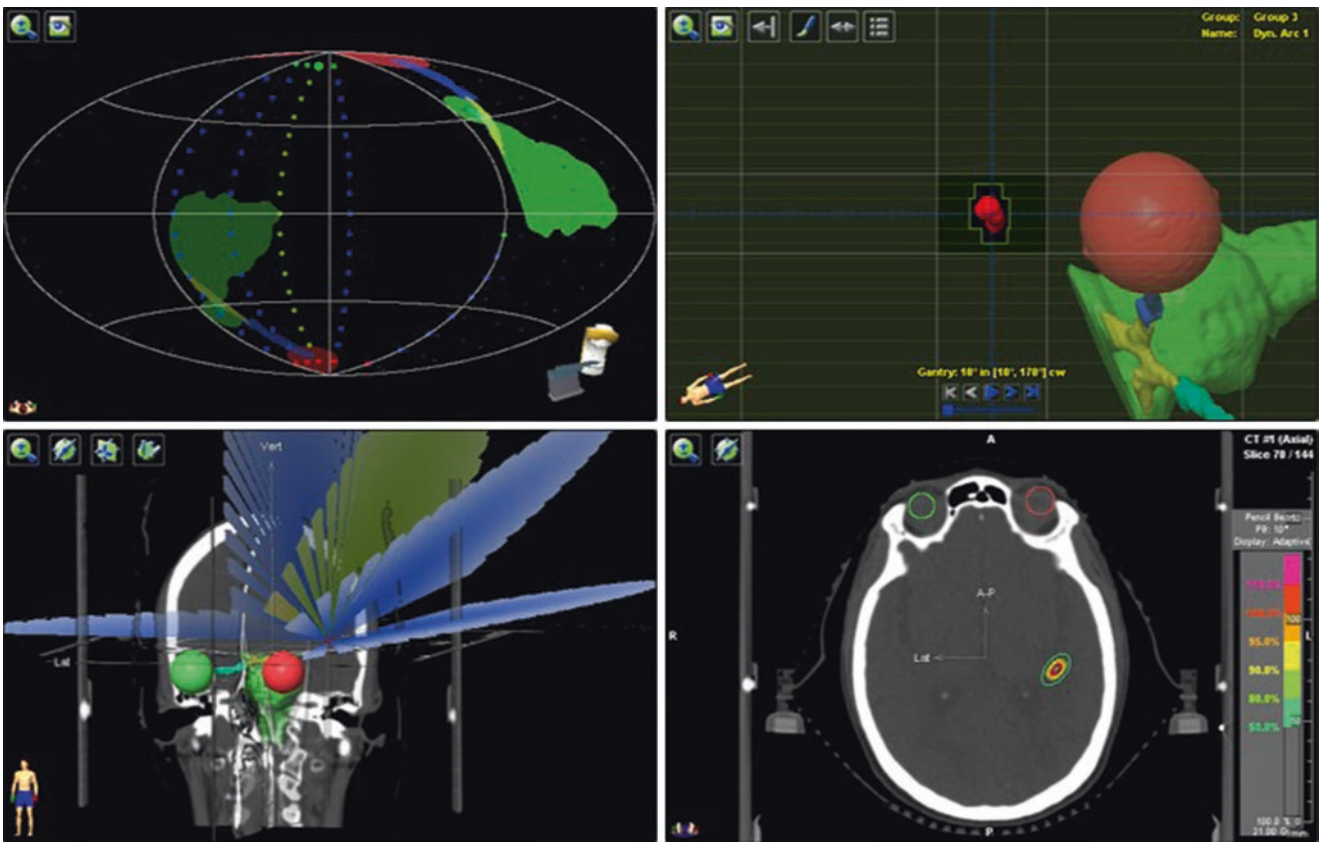

Fig. 10 An SRS plan using dynamic conformal arcs in iPlan RT TPS (BrainLab, Munich, Germany)

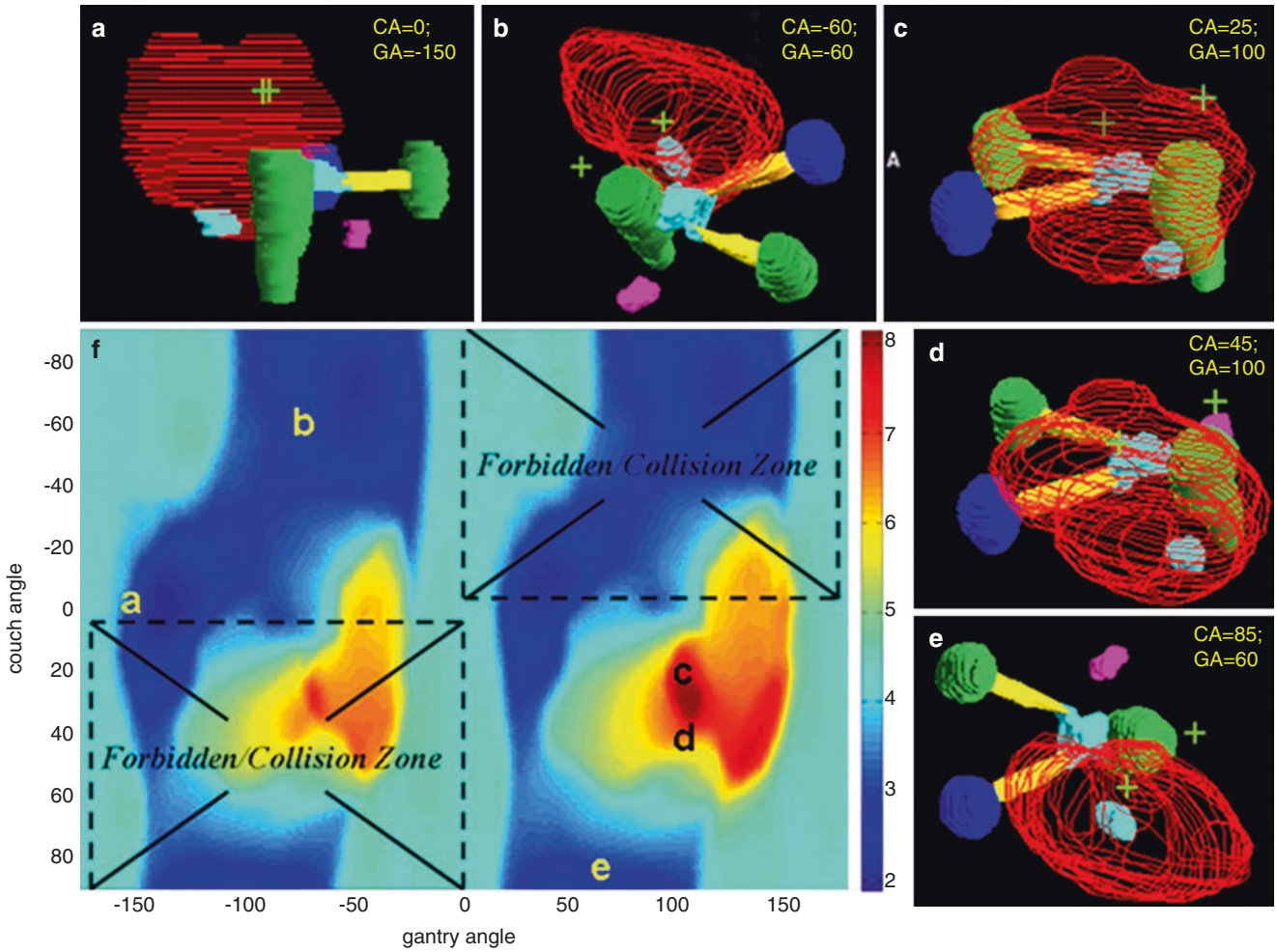

Fig. 11 (**a**–**f**) Illustration of VMAT therapy. (Used with permission of Elsevier from Yang et al. [14])

quite effective with local control rates in the range of 90%. Despite the high probability of local control, patients with metastatic disease often acquire subsequent metastases that must be managed with some combination of surgery, repeat SRS, or whole-brain radiotherapy.

Total Number/Volume of Lesions Treated

There is a limit on the volume of tissue in the brain which can safely be treated with ablative, hypofractionated doses of radiation. Kjellberg at the Harvard Proton Therapy Center published a paper linking the risk of permanent radiation necrosis with tumor volume and prescribed dose. Sadly, the risk of permanent radiation injury rises logarithmically with the total volume irradiated, requiring prudent clinicians to decrease prescribed doses for large intracranial tumors. Kondziolka (University of Pittsburgh) published a retrospective paper debunking the belief that the total number of metastatic tumors is a valid risk factor [15]. He proposed instead that the total volume of tumor burden is a better indicator of negative outcome. This has been confirmed by several subsequent studies.

Level of Evidence for Dose/Fractionation

As a field, doses for various SRS indications have developed empirically, with a minimum of well-controlled level 1 evidence. Most clinical reports on SRS, especially historically, have been single-institution retrospective experiences that gained traction as they were repeated among various institutions.

Future Directions

Much of the technology required to accurately and precisely deliver ablative doses of radiation as required for radiosurgery have matured to the point where future advances are

likely to be small. On the beam delivery side, advances may come from applying lessons learned in the manufacturing world to the delivery of radiosurgery. However, much work is likely to improve the ability to visualize disease, tailor radiosurgery treatments to better match the biology of the underlying disease, and assist the body's own immune system in recognizing that fighting disease. Also, the same technologies that underpin radiosurgery with ionizing radiation may be applied to new, nonionizing methods for delivering ablative levels of energy which may be able to achieve similar results without the drawbacks of ionizing radiation.

Increased Automation

As computing power and control systems continue to improve, so will the level of automation in the SRS procedure. Moore's law (1965) postulated that the speed of computing would double every 18 months, a prediction which has so far been very accurate. This incredibly enhanced computing speed (and memory) has made formidable calculations almost trivially easy.

Functional Biological Imaging

Improvements in imaging will continue to improve, permitting visualization of not only structural, but also functional and biological information about patients. A variety of researchers [16] have reported on the use of functional imaging techniques such as diffusion-tensor imaging and fiber-tracking to help inform treatment planning in order to spare critical fibers from high doses of radiation. Biological imaging techniques such as MR diffusion, MR perfusion, PET, [list others] will help identify active areas of tumor growth and areas of oxygen-starved tissue which may benefit from a higher radiation dose via dose-painting techniques.

Biological Optimization

Current treatment planning systems optimize dose based on physical dose metrics such as dose/volume metrics for tumor coverage or OAR sparing. In the near future, these optimization algorithms will be able to include information on biological response, including tumor control probability and normal tissue complication probabilities. Optimization may also better include treatment uncertainties, including contouring uncertainties, and treatment planning systems may be better equipped to communicate treatment planning uncertainties to the treatment team. A manuscript has been published defining the Radiosensitivity Index (RSI), based on analysis of genomic data. This could be implemented as the Genomic-Adjusted Radiation Dose (GARD) [17].

Immunotherapy

One of the most important current advances in cancer therapy are improvements in the ability to utilize the patient's own immune system to fight their disease. Many researchers have reported on the abscopal effect in radiosurgery; that is the occurrence of tumor regression for lesions distant to the SRS treatment site in the absence of concurrent therapy. A variety of strategies currently under investigation aims to enhance this effect through the complementary use of radiosurgery and one of a number of immune system-enhancing drugs that target specific receptors in different cancer subtypes.

Further Improvements in Spreading Out Energy

As treatment machines become more automated, it becomes more practical to create treatment schemes using many beams or arcs that can better spread out energy and therefore create sharp dose gradients. Advances in on-board imaging make placing the focus of these sharp dose gradients accurately at the intended targets. Perhaps the logical endpoints of this development are proposed 4-Pi geometry treatments, which use numerous beams with fully automated gantry collimator, and couch to treat the patient [18].

Nonionizing Techniques

Ionizing has many advantages such as a proven track-record, ability to treat deeply within the body, and a favorable radiobiological response. However, especially for ablative treatments, it has several disadvantages as well; treatment response is often delayed by weeks or months, there is a limit on the number of times a treatment may be repeated due to the risk to surrounding normal anatomy, and the risk of radiation necrosis. However, a variety of nonionizing techniques are quickly developing that make use of many of the lessons learned in the development of radiosurgery. Laser-interstitial thermal therapy (LITT) uses insertable laser probes to ablate tumors by heating them to a lethal level. High-intensity focused ultrasound (HIFU) uses arrays of ultrasound elements to heat up targeted tissue to a similar lethal level. Some variants of HIFU use MR imaging as a way of providing temperature feedback about the procedure via a technique called MR thermometry. HIFU may also find applications in opening the blood-brain-barrier (BBB) to better permit the passage of chemotherapy and immunotherapy agents and may be an effective complementary treatment with ionizing radiation as it may work in the setting of hypoxic tumors.

MR-LINAC

A new wave of linear accelerators with built-in MRI imaging capability is now entering the marketplace. The Viewray MRIdian® (Oakwood, Village, OH < USA) system was first installed at Washington University (St. Louis) in 2014 utilizing three very large rotating cobalt-60 radiation sources [19]. Two other early sites implemented this technology, which has since replaced the radioisotope sources with a compact 6MV linear accelerator. The device utilizes a 0.345 T MRI field for patient alignment and adaptive radiotherapy. Elekta, Inc. (Stockholm, Sweden) is in premarket testing at seven cancer centers worldwide with a 6MV linear accelerator matched with a 1.5 T MRI imaging system. Several other companies are also preparing MRI-linac combination devices.

Practical Considerations

Large single-fraction doses, extremely sharp dose falloff, and small field sizes characteristic of SRS create a requirement for extreme accuracy and precision in beam delivery and a critical need for practitioners to understand the nuances of the techniques. For more information on establishing a stereotactic program, please see the ASTRO/ACR recommendations published by Benedict and colleagues and Solberg and colleagues [20, 21].

Small Field Dosimetry

Fields sizes used in SRS are often smaller than fields regularly encountered in radiotherapy physics. Small fields have dosimetric behavior that significantly departs from large fields, including a partial occlusion of the radiation source by the collimation system (as viewed from the isocenter) and a loss of lateral electronic equilibrium as the field diameters are smaller than the range of secondary electrons. These characteristics make small fields difficult to measure and require specialized detectors that are specifically designed for small field measurements. A variety of references are available that thoroughly discuss the issue of small fields, how to measure them, and how to relate them to standard, calibration-size fields [19].

Differences in Radiation Biology

As discussed earlier, the radiobiological response to SRS may involve more than damage to DNA, including microvascular and immune effects. Radiobiological models widely used in traditional radiotherapy, such as the linear quadratic model, have been found to not perform well under large, hypofractionated conditions. There is also a paucity of clinical evidence regarding the dose response to organs at risk under these conditions. An extreme amount of care should be exercised when prescribing doses. As suggested in ICRU Report 91, doses should be based on well-established literature, and any departure from accepted (community standard) prescriptions should only be attempted in the setting of a supervised clinical trial.

Considerations for SRS Treatment Planning

Dose falloff in SRS is very sharp, but it is not infinitely sharp. The large doses prescribed for SRS mean that it is critical for a dosimetrist to examine the dose not only at the tumor margin but also at lower dose levels. It is quite easy to develop an SRS plan where if the energy is not distributed among enough beams, a finger of dose large enough to damage tissue and skin can be generated.

Understanding of the Total Uncertainty Chain

As discussed earlier in the chapter, regardless of the technology platform used to deliver treatment, SRS is a complex, multistep procedure. Each step in the end-to-end clinical procedure has its own uncertainty components that must be considered. A failure to respect the overall procedural uncertainty greatly increases the risk of a misadventure, and at the doses used in SRS those misadventures can be quite serious. The New York Times published a 15-part series in 2010 and 2011 highlighting extremely unfortunate radiotherapy incidents and accidents, some of which were fatal to the patients involved [22]. Especially troublesome was a series of three patients treated at a highly respected Midwestern hospital for trigeminal neuralgia, a painful but not fatal syndrome. Due to systematic error three consecutive patients received a fatal nearly whole brain radiotherapy dose and died horrible deaths.

Proper Training and Credentialing

The strict requirements for accuracy and precision, the large number of potential sources of procedural uncertainty, and the resulting possibility of harm to the patient (or even the treatment team) means that a thorough understanding of the SRS procedure is critical for all practitioners. Proper training and credentialing is one of the primary methods for mitigating risk in delivering SRS. ASTRO and the AANS have issued specific guidance on minimum standards for training and credentialing in SRS and SBRT.

References

1. Riesenfeld G. Rutherford and the Curies. Lancet. 1971;1(7690):132.
2. Cushing H. Haematomyelia from gunshot wound of the cervical spine: a report of two cases, with recovery following symptoms of hemilesion of the cord. Am J Med Sci. 1898;115:654–83.
3. Goetsch SJ. Historic development of stereotactic radiosurgery and stereotactic body radiation therapy. In: Benedict S, Schlesinger D, Goetsch S, Kavanagh B, editors. Stereotactic radiosurgery and stereotactic body radiation therapy. Boca Raton: CRC Press; 2014.
4. Obituary: E. H. Grubbe, M.D., F.A.C.P. Br Med J. 1960;2(5198):609.
5. Hall EJ, Giaccia AJ. Radiobiology for the radiologist. Philadelphia: Lippincott William & Wilkins; 2006.
6. Del Regato JA. Claudius Regaud. Int J Radiat Oncol Biol Phys. 1976;1:993–1001.
7. Tan TC, Black PM. Sir Victor Horsley (1857-1916): pioneer of neurological surgery. Neurosurgery. 2002;50(3):607–11. discussion 11-2
8. Kilgore EJ, Elster AD. Walter Dandy and the history of ventriculography. Radiology. 1995;194(3):657–60.
9. Spiegel EA, Wycis HT, Marks M, Lee AJ. Stereotaxic apparatus for operations on the human brain. Science. 1947;106(2754):349–50.
10. Talairach J, Tournoux P. Stereotaxic localization of central gray nuclei. Neurochirurgia. 1958;1(1):88–93. A propos du reperage stereotaxique des noyaux gris centraux.
11. Orton CG. Uses of therapeutic X-rays in medicine. Health Phys. 1995;69(5):662–76.
12. Washington CM, Leaver D. Principles and practice of radiation therapy. 4th ed. Philadelphia: Elsevier, Mosby; 2016.
13. Intensity Modulated Radiation Therapy Collaborative Working Group. Intensity-modulated radiotherapy: current status and issues of interest. Int J Radiat Oncol Biol Phys. 2001;51(4):880–914.
14. Yang Y, Zhang P, Happersett L, Xiong J, Yang J, Chan M, et al. Choreographing couch and collimator in volumetric modulated arc therapy. Int J Radiat Oncol Biol Phys. 2011;80(4):1238–47.
15. Grandhi R, Kondziolka D, Panczykowski D, Monaco EA 3rd, Kano H, Niranjan A, et al. Stereotactic radiosurgery using the Leksell Gamma Knife Perfexion unit in the management of patients with 10 or more brain metastases. J Neurosurg. 2012;117:237–45.
16. Duma CM, Kim BS, Chen PV, Plunkett ME, Mackintosh R, Mathews MS, et al. Upfront Gamma Knife "leading-edge" radiosurgery to FLAIR MRI-defined tumor migration pathways. 2016. J Neurosurg. 125(1):40–9.
17. Hall WA, Bergon C, Thompson RF, Baschnagel AM, Vijayakumar S, Willers H, et al. Precision oncology and genomically guided radiation therapy. Int J Radiat Oncol Biol Phys. 2018;101(2):274–84.
18. Nguyen D, Ruan D, O'Connor D, Woods K, Low DA, Boucher S, et al. A novel software and conceptual design of the hardware platform for intensity modulated radiation therapy. Med Phys. 2016;43(2):917–29.
19. International Commission on Radiation Units and Measurements. Report 91: prescribing, reporting and recording of stereotactic treatments with small photon beams. Oxford: Oxford University Press; 2014.
20. Solberg TD, Balter JM, Benedict SH, Fraass BA, Kavanagh BD, Miyamoto C, et al. Quality and safety considerations in stereotactic radiosurgery and stereotactic body radiation therapy: executive summary (Supplemental Material On-Line: Full Text). Pract Radiat Oncol. 2012;2:2–9.
21. Benedict SH, Yenice KM, Followill D, Galvin J, Hinson W, Kavanagh B, et al. Stereotactic body radiation therapy (SBRT), the Report from the AAPM Task Group No. 101. Med Phys. 2010;37(8):4078–101.
22. Bogdanich W, Rebelo R. A pinpoint beam strays invisibly, harming instead of healing. December 26, 2010. New York Times.

Leksell Gamma Knife Radiosurgery

Diogo P. Cordeiro and David J. Schlesinger

Introduction

Since Lars Leksell's conceptual invention of radiosurgery in 1951 [1], the fundamental principle of radiosurgery has always been to focus energy within a targeted lesion while minimizing injury to surrounding tissue. Leksell and his collaborators were able to create practical connections among several different lines of thinking in order to eliminate the barriers to actualizing this vision: stereotaxy to solve the problem of navigating to a precise point in space; a rigid frame system to solve the problem of a consistent targeting; ionizing radiation to eliminate the problem of an invasive burr-hole and probe; multiple cross-firing radiation beams to create a method for concentrating energy on the target location, and the use of cobalt-60 practically generate a large number of small radiation beams.

Today, Gamma Knife® (Elekta, Stockholm, Sweden) radiosurgery (GKSRS) continues to be an outstanding example of the foundational principles of radiosurgery. The purposeful design of the Gamma Knife has survived decades of technological development in a form that would be easily recognized by Leksell, yet remains the reference standard against which competing technologies are judged. It has also heavily influenced the entire field of radiotherapy, inspiring the application of radiosurgical principles to indications outside of the head and continuing today in an escalating trend of dose hypofractionation and dose conformity.

D. P. Cordeiro
University of Virginia, Departments of Neurological Surgery, Charlottesville, VA, USA

D. J. Schlesinger (✉)
University of Virginia, Departments of Radiation Oncology and Neurological Surgery, Charlottesville, VA, USA
e-mail: Djs9c@virginia.edu

History

Much has been written of the history of Gamma Knife radiosurgery. The interested reader is especially directed to a detailed recounting by Ganz [2]. In this section, we will summarize some important aspects of this history as it relates to creating integrated solutions to practical problems critical to the acceptance of radiosurgery as a discipline.

Early Vision and Initial System Designs

Leksell first attempted to realize the vision of his famous paper from 1951 [1] which introduced the concept of radiosurgery by treating two patients with trigeminal neuralgia, using the Gasserian ganglion as a target and a tightly collimated 280 kV X-ray beam as the energy source. While these cases were not published for many years [3], in 1954 Leksell reported the case of a patient treated for schizophrenia [4]. The report addressed his observations of the strengths and weaknesses of the technique, noting that higher-energy X-rays might have been advantageous and that perhaps particles such as protons should be considered.

After experimenting with proton beams at Uppsala starting in the 1960s [5] and finding them impractical, Leksell and his colleagues (Börje Larsson, Bert Sarby, and Kurt Lidén) investigated alternative radiation sources, settling on cobalt-60 due to its availability, relatively high photon energy (average 1.25 MeV), long half-life (5.26 years), and high specific activity, making it possible to use many small sources to make many small beams [6, 7]. They settled on a machine design that would use 179 stationary beams, elliptically collimated and arranged to have a precision of beam focus of 0.1 mm and a penumbra at the focus of 0.5 mm. This first gamma unit was constructed by the Mottola Company, and the first patients were treated in 1967 in Studsvik, the location of a Swedish nuclear research center and a convenient place to acquire and load cobalt-60 sources. Later that

D. M. Trifiletti et al. (eds.), *Stereotactic Radiosurgery and Stereotactic Body Radiation Therapy*,
https://doi.org/10.1007/978-3-030-16924-4_5

year the device was moved to the Sophiahemmet Hospital in Stockholm. A second device was created for Leksell when he moved to Karolinska Hospital in 1975 [2].

From 1968 to 1983 Leksell and his colleagues treated 762 patients with Gamma Knife: 177 functional, 209 vascular, 342 tumor, and 32 diverse cases [8]. However, during this period, the entire worldwide reach of Gamma Knife radiosurgery was limited to Stockholm.

Revisiting the Design: The Gamma Knife Model U and Commercialization

The early experience of Leksell and colleagues demonstrated that Gamma Knife radiosurgery was useful for more than the originally planned functional indications [9–11], and word slowly began to spread. Lars Leksell, along with his sons Daniel and Laurent, founded Elekta Instrument, AB, in 1972 with the intention of commercializing Dr. Leksell's various neurosurgical innovations. The first Gamma Knife units outside of Sweden were in Buenos Aires in 1983 and Sheffield in 1985, both the result of personal inquiries by neurosurgeons who had visited Leksell in Stockholm. These units differed from the original prototypes by making use of 201 cobalt-60 sources and circular collimators which were better equipped to treat vascular malformations and solid tumors rather than only functional indications. As Elekta as of yet had no manufacturing capability, these two units were built by Nucletec SA, a subsidiary of Scanditronix Medical AB of Sweden [2, 12].

The first Elekta produced Gamma Knife was brought to the United States by Dr. Dade Lunsford at the University of Pittsburgh in 1987 [13]. This new model, termed the Model U, retained a design similar to the Buenos Aires and Sheffield units (as well as the original prototypes). This simplified regulatory approval in the United States as the original prototype had by this time been relocated to UCLA and was being used for research, so the model U was not considered a radical departure. The model U used 201 cobalt-60 sources of approximately 30 curies each. The patient was positioned in the unit in a supported supine, semi-upright position with the help of a hydraulic system, and a nearly hemispheric tertiary collimator "helmet" with either 4 mm, 8 mm, 14 mm, or 18 mm beams could be used to size each isocenter, or "shot." The unit was manually controlled; the neurosurgeon and the treatment team would manually set sliders on the patient's frame for the Y and Z coordinates and a trunnion system for the X coordinate. Individual beam channels could be replaced with solid "plugs" in order to block beams to protect critical structures. Elaborate protocols were required to ensure that no mistakes were made when setting coordinates and plug patterns, and treatments could often take hours to complete. As the unit opened like a clamshell in order to expose the sources, reloading the unit required removing it from the treatment vault and constructing a hot cell around it, using remote manipulating arms to remove and replace each source. Reloading was expensive and could require 4–6 weeks of downtime to complete (Fig. 1) [14].

Fig. 1 Gamma Knife® Model U (Elekta, Stockholm, Sweden) at the University of Virginia being prepared for source reloading. The clamshell design of the unit required it be removed from the treatment vault and placed in a temporary bunker

To address the problem of reloading and create a more commercially acceptable machine, in 1988, Elekta introduced a "model B" unit. The model B was a significant redesign of the system to permit a streamlined reloading procedure using an in-room "loading machine" which significantly simplified the time and expense of the process. The hydraulic system of the model U was replaced with a more robust electric system. The collimator retained the same beam sizes as the model U, but the patient was placed in a more supine position and the sources were arranged in five concentric rings in an annular hemispheric design. Because of regulatory complexities in the United States the model B was sold primarily in Europe and Asia [2, 12].

The manual nature of the model U and model B systems could make them cumbersome to use by a treatment team, prone to human error in setting the patient position, and quite slow in terms of total procedure time. Recognizing these problems required a solution, in 2000, Elekta introduced the "model C" unit. This unit introduced an "automatic positioning system," or APS, which could automatically position the patient's head at the correct stereotactic coordinate [15]. It also included GammaPlan® (Elekta, Stockholm, Sweden), an interfaced treatment planning system. The improved treatment planning capability made practical the use of multiple shots in a treatment and thus the ability to better conform to more irregularly shaped targets [16, 17]. A slightly upgraded "model 4C" followed a few years later.

By the mid-2000s, radiosurgery had gained significant traction as an efficacious treatment paradigm for a large

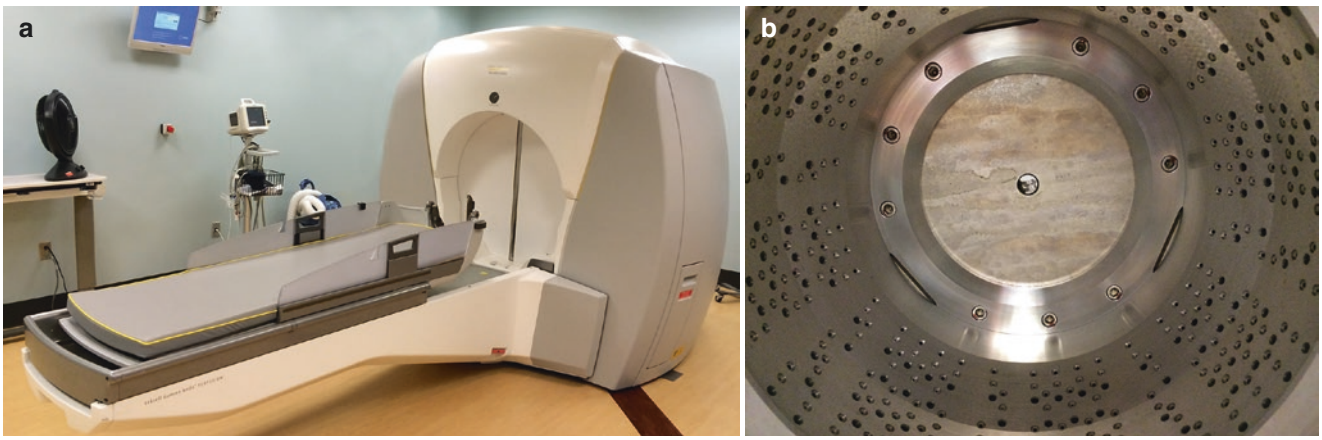

Fig. 2 (**a**, **b**) The Gamma Knife® model Perfexion™ (Elekta, Stockholm, Sweden) at the University of Virginia. (**a**). The Perfexion unit. (**b**) Closeup of the built-in collimator system of the Gamma Knife Perfexion. The beam channel pattern repeats eight times around the circumference of the collimator, matching up to eight source sectors

range of vascular, solid tumor, and functional indications, including for patients with more than a single tumor. Elekta completed work on a major paradigm change in 2006 with the release of the Gamma Knife Perfexion™ (Fig. 2a) with the aim of optimizing the unit for treating multiple lesions in a single setting and by greatly increasing the volume of a patient's head reachable by the system. The Perfexion also automates many treatment and quality assurance tasks, significantly increasing patient safety as well as decreasing beam-delivery uncertainties [18]. The resulting design included significant changes to the radiation unit, collimator, mechanics, patient positioning system, quality assurance tools, and treatment planning system.

The radiation unit of the Perfexion uses 192 cobalt-60 sources arranged in a cylindrical rather than the previous hemispherical geometry. The new geometry means the system has a variable source to focus distance. The previous external "helmet"-base tertiary collimator system is replaced with a single, integral tungsten collimator (Fig. 2b). Beam channels are machined into the collimator arranged in five concentric rings, with each ring containing 4 mm, 8 mm, and 16 mm beam channels as well as a blocked position. The beam channels are arranged in a way that the pattern repeats eight times over the circumference of the collimator, creating eight sectors. Matched to these sectors are the sources, which are no longer fixed in place, but instead are mounted on eight sliding carriages holding 24 sources each (one carriage per sector) that are driven by linear motors from the rear of the unit. The beam configuration of a given isocenter is set automatically by the system by moving each sector independently to any of the three beam sizes (or blocked) per the instructions in the treatment plan. Rather than manually plugging individual ports, an entire sector of sources may be blocked at one time. The system permits new isocenter configurations, as it is now possible to include mixed size isocenters (i.e., where different sectors have different beam sizes) [19].

Comparing to the older models, the treatable volume within the radiation cavity of the Perfexion is increased by 300%. The increase in the potential treatment volume enhances the ability of the system to treat patients with multiple lesions distributed throughout the brain in a single frame placement [20].

The automatic positioning system included with the model C is replaced by the Patient Position System (PPS) that instead of moving only the patient's head moves the whole bed to the desired treatment coordinates. The patient's head is fixed to PPS at one of three possible head angles (70°, 90°,110°) using an adapter which attaches to the stereotactic frame, and once attached the relative position of the patient's head and neck remains fixed throughout that part of the treatment, significantly increasing patient comfort. The PPS is controlled by a dual-encoder system that ensures the bed is at the correct stereotactic coordinates [18, 19].

Much of the quality assurance for the Perfexion has been similarly automated. Most significantly, a diode tool is included with the unit which through an automated routine determines the location of the radiation isocenter and compares this to a stored calibration value, with a difference that cannot exceed 0.4 mm. An installation diode tool ensures that all Gamma Knife Perfexion installations worldwide have absolute calibrations within 0.15 mm [21].

Evolution of Imaging and Treatment Planning for Gamma Knife Radiosurgery

As imaging techniques evolved and computing power improved, so did the technology and techniques for radiosurgery treatment planning. At the time the Gamma Knife was

first invented, planar X-rays were the state-of-the-art method for visualizing internal anatomy. In the brain, work on ventriculography and pneumoencephalography provided a rudimentary capability to resolve gross brain anatomy and in some cases solid tumors [22, 23]. In these early years of GKRS dose-planning programs did not exist. Treatment calculations were performed manually by the neurosurgeon and physicist. Precomputed isodose plots showing single-isocenter dose distributions in each plane could be overlaid on AP and lateral X-rays to identify the desired position of the isocenter. The required duration of the treatment was then calculated using a nomogram by the physicist via a combination of prescribed dose and location, using the average depth of the isocenter in the skull in the calculation [2]. The isodose distribution was assumed to be invariant to position, so absolute dose profiles could be understood by simply scaling according to the desired prescription dose. A bit later, depth calculations were refined to use distance measurements from ten preselected collimators in the collimator helmet to the skull surface. Treatment using multiple isocenters was extremely rare [24].

The introduction of tomographic imaging with the installation of a computed tomography (CT) system in Stockholm in 1973 changed the situation. In 1978 Elekta developed an attachment to fix the stereotactic frame to the CT scanner, permitting registration of the images to stereotactic space and usable for radiosurgery [25]. The three-dimensional imaging information led to a desire for a computerized treatment planning system that could make better use of the new imaging information. One such system was designed in the department of Radiophysics at the Karolinska, and another at A. B. Chinela Centro de Radiocirugia Neurologica in Buenos Aires [26] (Fig. 3a).

The first commercially available treatment planning system for the Gamma Knife was the KULA program (Elekta Instrument, AB) [24]. This program used as an input the shape and size of the skull, calculated from a plastic measuring helmet (termed the "bubble" helmet) which permitted radial measurements taken along predefined measurement vectors rather than through beam channels in the collimator helmet. The system was limited in that manipulating images in real time was not yet possible; treatment planning remained a lengthy procedure. The results of the plan were plotted graphically using a pen and ink plotter on transparency sheet, which could be overlaid on printed films to verify isocenter and isodose distribution locations (Fig. 3b).

Meanwhile, in the 1980s the first MRI units were being introduced into the clinic [27, 28]. MR imaging provided vastly improved soft tissue resolution, greatly reducing the visualization uncertainty of targeted disease and surrounding normal tissue structures. As MR pulse sequence design progressed and MR installations became widely adopted, MR became the imaging standard for Gamma Knife cases. Over time, a variety of pulse sequences were incorporated that could be used to highlight different aspects of brain anatomy including sequences to highlight detailed anatomical structures within the cerebrospinal fluid space [29], parasellar region [30], and sequences useful for visualizing subcortical gray matter structures [31]. More recently, perfusion [32] and diffusion [33, 34] sequences have been adopted which can provide physiological as well as anatomical information to help inform a treatment plan.

In part to harness the rapid improvements in imaging technology, in 1991 a major upgrade to the treatment planning system was released in the form of GammaPlan® (Elekta Instrument, AB). GammaPlan introduced several major advancements, including the ability to load and manipulate DICOM-based images of a variety of modalities including CT, MR, and angiography; networking to allow these images to be sent directly to the workstation from the imaging suites; contouring and measurement tools such as dose-volume histograms to make it possible to more carefully evaluate dose-volume coverage and constraints to targets and organs at risk; and a direct serial interface to the treatment unit to allow plans to be transferred without risk of human error. Multiple isocenter plans were directly supported, and

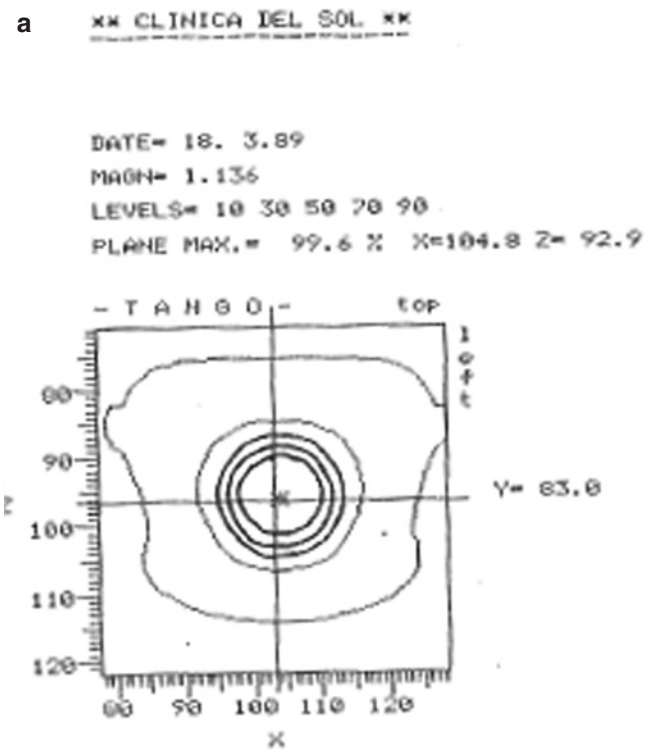

Fig. 3 (**a**–**c**) The evolution of Gamma Knife® (Elekta, Stockholm, Sweden) treatment planning. (**a**) The Tango treatment planning system used at the Centro de Radiocirugia Neurologica in Buenos Aires. (**b**). The output of the KULA treatment planning system drawn on a transparency by a computer plotter. (**c**). A screenshot of the dose comparison workflow in Leksell GammaPlan®

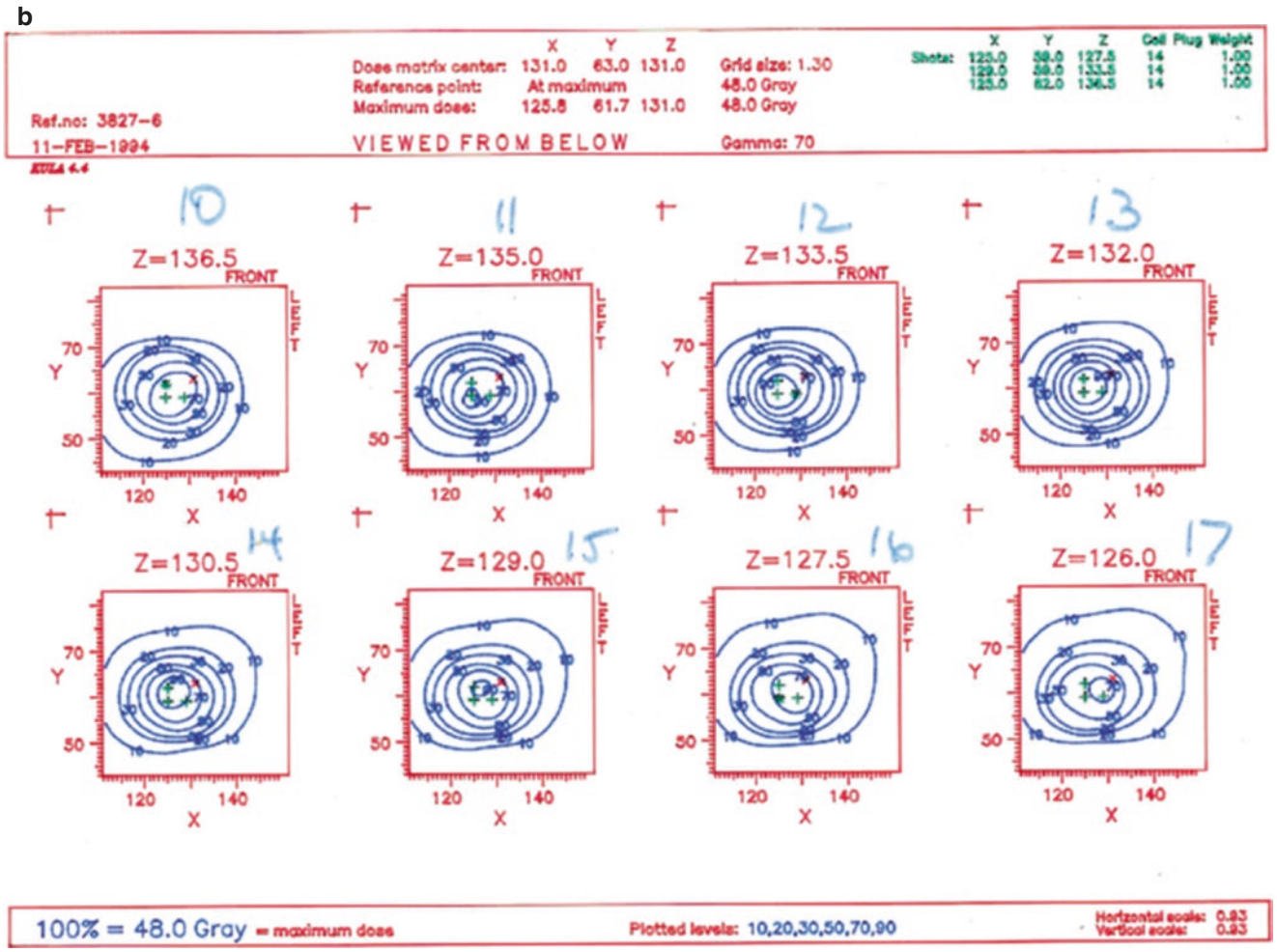

Fig. 3 (continued)

differential doses could be prescribed to different targets by "scaling" the dose to different dose calculation "matrices." GammaPlan continues to evolve today; the current version (Fig. 3c) and runs on personal computer hardware platforms with high-end graphics processors and networking solutions that allow the treatment planning system to communicate with multiple imaging providers and multiple Gamma Knife treatment units.

Recent Developments: Hypofractionation and Onboard Image Guidance

Certain clinical situations are not amenable to single-fraction radiosurgery, including large tumors or tumors situated very close to radiosensitive normal anatomy [35, 36]. There are also patients who are not ideal choices for a stereotactic frame placement. Recent developments in GKSRS were motivated by a desire to provide options for multi-session radiosurgery using alternative immobilization techniques to replace the traditional stereotactic frame. These developments include the Extend System, built on top of the Gamma Knife Perfexion platform, and the recently introduced Gamma Knife Icon system.

Extend™ System for Gamma Knife Perfexion

The Gamma Knife Extend System (Elekta, Stockholm, Sweden) represents a first attempt at replacing the absolute need for a fixed stereotactic frame system with a less-invasive, relocatable frame system that would be practical in a multi-fraction/multi-session setting. The Extend System consists of several components; a patient-specific immobilization device comprised of a carbon-fiber, dental-impression assisted frame and vacuum cushion; a monitored vacuum system interlocked to the Gamma Knife control system; and a measurement template and associated digital measurement probes. Each patient is fitted for a dental impression of the upper palate which is attached to the front plate of the frame system. A rigid head-pillow is created by removing air from the vacuum cushion. The front plate of the frame system is then attached to the body of the frame system and the position of the dental impression remains locked for the duration of the treatment course. The front plate can be attached and removed from the back of the frame system to permit multiple treatment fractions and imaging sessions. Planning CT images of the patient are acquired with the frame and an associated imaging box after taking a reference set of measurements with the digital measurement probes. These images are co-registered to other volumetric (CT/MR/PET) imaging and used for treatment planning. Prior to a treatment session, the patient is set back up on the treatment bed with the frame attached. The treatment team works with the patient to adjust position until the digital measurement probes agree to within a small tolerance (on the order of 1 mm) of the planned position. During treatment, the vacuum system monitors the vacuum level to the mouthpiece of the system as a proxy for motion. If the vacuum level drops, the treatment pauses automatically and new measurements/adjustments of position are completed [37]. Treatment uncertainties and the use of the vacuum surveillance system as a proxy for patient motion were both found to be satisfactory for use in a multi-session radiosurgery setting [38, 39].

Gamma Knife Icon™

The Extend System for the Gamma Knife succeeded in its goal of providing a practical, albeit sometimes cumbersome, option for multiple fraction treatments. The latest release of the Gamma Knife, the Icon model (Elekta, Stockholm, Sweden), rethinks the solution entirely and introduces onboard image guidance and intrafraction motion management capabilities to allow patients to be treated without a frame at all, instead of using thermoplastic mask immobilization for multisession treatments [40].

The overall Gamma Knife Icon design is similar to the Perfexion model. The primary modification is the addition of a cone-beam computed tomography (CBCT) system and an infrared motion tracking system known as the intrafraction motion management (IFMM) system (Fig. 4). The CBCT system is designed in a novel, double-hinged form-factor. The imaging gantry lowers into scanning position at the same time as the PPS moves the patient to the end-scanning position. The imaging gantry then rotates again to reach the starting scan position. During imaging, the scanning arm rotates 200 degrees in approximately 30 seconds, with a 1000 mm source to detector distance. The scanner uses 90 kVp X-rays and two preset imaging modes. In both cases, the resulting images are reconstructed from 332 projections, and a voxel size of 0.5 mm, and an image volume of 448 mm^3 voxels [41, 42]. The imaging isocenter of the CBCT system has a known calibrated relationship to the radiation isocenter of the system, meaning that the resulting CBCT images can be used as the basis for stereotactic targeting [43]. The IFMM system is a stereoscopic infrared camera system that tracks the position of a small reflective sticker that can be placed on a patient's nose relative to reference markers placed on posts attached to the back-plate of the immobilization system [44].

The Icon system provides several new potential treatment workflows [45]. Patients may be treated in a thermoplastic mask using a CBCT as reference stereotactic coordinates. Prior to each treatment, the patient is set up on the machine in the thermoplastic mask, a new CBCT is acquired, and the treatment plan is shifted to match the current stereotactic

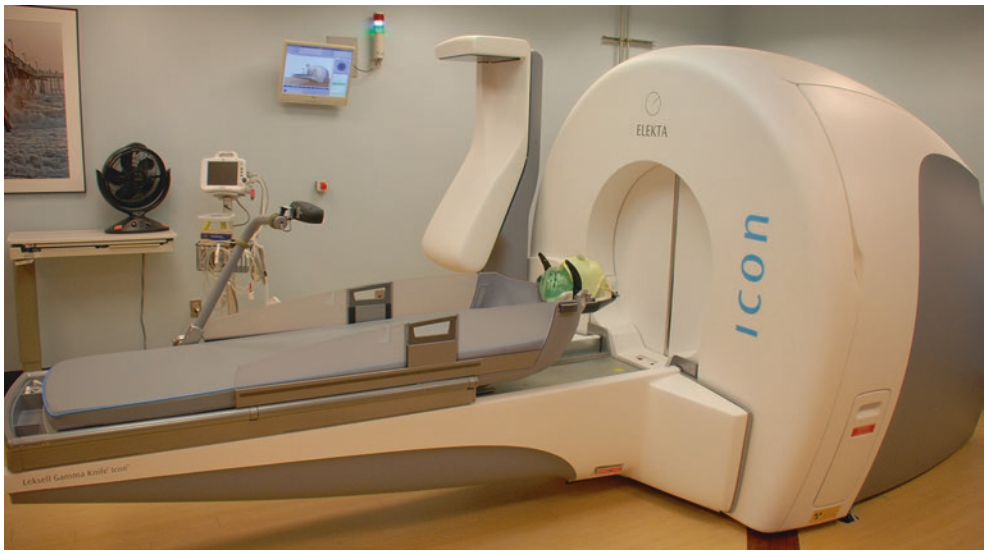

Fig. 4 The Gamma Knife model Icon™ (Elekta, Stockholm, Sweden) at the University of Virginia. This unit was upgraded in-place from the Perfexion™ model of Fig. 2. Notice the cone-beam CT scanning gantry and the intrafraction motion management camera that make possible GKSRS treatments with a thermoplastic mask

position of the patient. During treatment, the IFMM tracks the patient's nose marker. If it drifts out of position beyond some tolerance, the beams will gate to a blocked position. Beams will resume if the patient returns to the planned position within a short time interval; if not the patient will pause, a new CBCT can be acquired. The ICON system may also be used with a traditional stereotactic frame. In this workflow, the CBCT can be used as a valuable last-minute quality assurance check of the patient's frame and stereotactic position.

Limitations of Gamma Knife Stereotactic Radiosurgery

The design of the Gamma Knife is well-matched to the task of intracranial radiosurgery. The use of radioactive sources as a source of radiation and a radiation body and collimator system with an essentially fixed geometry specifically designed to receive a patient's head make it an elegant, extremely reliable intracranial radiosurgery solution. However, these design choices also drive the primary limitations of the technique.

Restriction to Intracranial Indications

Perhaps the most prominent limitation of Gamma Knife radiosurgery is that it is restricted to treating the head and at most the upper cervical spine indications. Targets inferior to the C2 vertebrae are difficult or impossible to treat, partly limited by the available space to correctly position the target at isocenter without colliding with the top of the cranium, but more importantly because it is practically difficult to immobilize the spine inferior than the C2 level [46].

Long Beam-Delivery Duration

A newly loaded Gamma Knife has a dose rate (as measured at the center of a 8 cm diameter spherical plastic phantom using a 16 mm collimator) of between 3.0 and 4.0 Gy/min (compared to ~14Gy - 24Gy/min for a linear accelerator equipped with a flattening-filter-free (FFF) treatment mode.). This base dose rate is further reduced by radioactive decay and during a given treatment the output factors for the different collimator sizes used. Beam-on time for the Gamma Knife can thus be long and the beam time scales linearly with the number of lesions treated [47]. This would seem to compare negatively against recent developments in linac radiosurgery, especially single-isocenter VMAT techniques which have an approximately constant beam time regardless of the number of lesions treated [48]. However, if one compares the total procedure time, including simulation, treatment planning, and patient-specific quality assurance then the total procedure time of the Gamma Knife compares favorably [49]. Dosimetric studies also show a tradeoff between the speed of VMAT treatment delivery and the magnitude of low dose spill to normal brain [47, 50, 51], as well as the potential for targeting errors due to rotational setup uncertainties [52]. However, both techniques achieve similar dosimetric metrics such as tumor coverage and conformity index and image guidance can potentially minimize any setup uncertainty [53].

Dose Rate Decay and Potential Implications for Radiobiological Effectiveness

The radioactive decay and commensurate decrease in the dose rate could potentially reduce the biological effectiveness of the procedure as the lower dose rate affords cells' time for repair of sublethal DNA damage. Several studies have examined this hypothesis with mixed results. Niranjan and colleagues examined 9 L rat gliosarcoma cells and found no statistical difference in cell survival over a range of dose rates representing greater than two half-lives of 60Co [54]. Balamucki and colleagues retrospectively analyzed data for 239 patients treated for trigeminal neuralgia and when controlling for other variables found no correlation between the dose rate and pain control [55]. In contrast, Lee and coauthors investigated 133 trigeminal neuralgia patients who were treated over the duration of slightly more than one half-life of source decay. Patients were administered a standardized pain scoring test before GKRS and at first follow-up (mean 1.3 months). Serial follow-up phone calls were used to obtain information on pain recurrence. Both short and long term results correlated with dose rate; with patients treated with higher dose rates experience greater decreases in pain and fewer recurrences [56].

Requirement for Source Reloading

The use of radioactive material-based sources allows the Gamma Knife to create extremely stable beams of radiation quite reliably. As there are few electronic or moving parts, Gamma Knife units tend to have extremely infrequent downtime [57]. However, the radioactive sources are also a limitation. The sources require replacing to prevent the dose rate of the machine from become so low that radiobiology is affected or that patients will not accept the duration of the procedure. Source reloading remains an extensive procedure that requires several weeks of downtime and a significant amount of coordination.

Future Directions

The history of Gamma Knife radiosurgery has always involved the integration of new technologies as they have reached the clinic. After many decades of development, treatment delivery with the Gamma Knife has matured. The next phase of the evolution of Gamma Knife radiosurgery (and radiosurgery in general) will likely focus on methods for stimulating the body's own immune system to help fight disease, complementary therapies that may help trigger these immune system effects, and harnessing the vast amounts of imaging and dosimetric data created during the radiosurgery process which can better inform patient selection, evaluation of treatment efficacy, and clinical decision-making.

Perhaps the most significant near-term future development may be the recruitment of the body's own immune system to help control and even cure malignant disease. Radiosurgery is by definition a local treatment. Although progression-free survival is an often-reported endpoint for clinical radiosurgery outcome studies, in reality the degree and duration of local tumor control has always been the most logical outcome for SRS. Patients with metastatic disease are often managed with systemic treatments such as chemotherapy or whole-brain radiotherapy for overall disease control. However, hints published in the literature of the so-called abscopal effect [58], combined with a much more nuanced understanding of the local tumor immune environment [59] have inspired efforts to try to use focal treatment such as radiosurgery to create cellular "debris" which can be detected by the immune system and used as the basis for a systemic response [60].

Help in this regard may come from alternative treatment modalities that can complement the strengths and weaknesses of radiosurgery. Several emerging technologies use heating as opposed to high-dose ionizing radiation to achieve ablative levels of cell death within small volume targets. Two examples are high-intensity focused ultrasound (HIFU) [61, 62] and laser interstitial thermal therapy (LITT) [63]. HIFU and LITT can be combined with near-real time MR-thermometry [64] for image guidance. Energy deposited as heat from lasers or ultrasound has several attractive characteristics; it is nonionizing; it can be repeated; the biological effect is much faster than for ionizing radiation; it is effective under conditions of hypoxia where ionizing radiation can be less effective; and the effect is deterministic. The technologies can be used to deliver therapeutic payloads in microbubbles, selectively open the blood-brain barrier, and potentially create heat-shock proteins and other cellular debris which be used to prime the immune system [65, 66].

The widespread deployment of parallel computing technologies such as graphics processing units (GPUs) and especially cloud computing infrastructures has created significant opportunities to apply large increases in computing power to the clinic [67, 68], including radiosurgery. Dose calculations and image processing pipelines are well-suited to parallelizable hardware architectures such as those offered by onboard GPU chips. These can create order-of-magnitude increases in dose calculation speed, helping to make techniques such as inverse treatment planning fast enough to be clinically practical in a single-fraction environment where patients are waiting for treatment with headframe fixation. GPU-enabled algorithms have made tremendous impacts in a variety of radiotherapy scenarios, and could have an equally important impact on Gamma Knife radiosurgery.

Cloud computing infrastructures make possible the storage and computation of large datasets that would be impractical to analyze on one or a few computers. This in turn has led to the rise of a series of techniques termed "Radiomics," where large numbers of image features are extracted from large numbers of image sets and then analyzed for patterns that correlate with various clinical features [69–71]. Radiosurgery commonly involves imaging from several MR pulse sequences and frequently also includes CT, PET, and X-ray imagery at the time of treatment planning. Patients often have pretreatment and serial posttreatment imaging as well. Radiomics analysis of these data may help to enhance our ability to evaluate treatment efficacy and make informed clinical conclusions about local failure vs. adverse treatment effect.

The potential for Radiomics to make a difference will itself be enhanced by steady improvements in imaging. Newer MR pulse sequence techniques such as diffusion imaging, perfusion imaging, and MR spectrography will help bring functional information into the treatment planning process as well as to posttreatment evaluation. Advances in PET imaging, and in new combined modalities such as PET-MR [72] will complement these new MR pulse sequences. Emerging imaging modalities may also play a role, perhaps 1 day including photoacoustic tomography [73, 74], which can image to extremely high-resolution in near real time, and can use a variety of molecules as intrinsic contrast agents to make possible the visualization of entire vascular trees, oxygen transfer, and even individual circulating tumor cells.

However, perhaps the most important development of the next 10 years may be the continuing rapid advance of machine learning. Machine learning technologies such as deep convolutional neural networks [75] have been revolutionizing a wide range of industries, and radiotherapy is no exception [76]. Machine learning techniques may 1 day make it possible to fully automate the treatment planning process and may create important new opportunities to evaluate treatment efficacy and predict the future course of disease on a per-patient basis. This in turn may help make radiosurgery a much more personalized treatment experience.

Practical Considerations

The workflow and indications for GKSRS have been refined and matured over many years of experience and many generations of technological advancement. However, SRS remains a treatment technique requiring extreme care and attention to detail. The authors believe the practical considerations summarize in Table 1 can help when beginning a new GKSRS program.

Table 1 Practical considerations when considering a GKSRS program

Key consideration	Description/rationale
Credentialing and training	GKSRS is a specialized procedure requiring specialized training. The planning process and patient workflow differ significantly from other radiation therapy techniques. Formal institutional criteria for credentialing and training can help to prevent mistake [77]
Care during commissioning and QA	The precision and accuracy required for GKSRS is demanding. Careful commissioning and quality assurance maximize the probability of detecting any problems before they reach the patient during treatment
Patient selection	Understanding of the indications and contraindications for GKSRS is a critical part of practice
Proper understanding of dose/dose limitations	Prescription dose and dose/fractionation schemes should be well supported by published evidence. Deviations should occur only under in the settings of multi-institutional or single-instruction trials under the supervision of an institutional review board
Balance between time of treatment and the "perfect" plan	Conformity of the prescription isodose to the target is one measure of a plan's fitness. However, the best plan is often a balance between many factors, including dose falloff, beam-on time, and dose to nearby normal anatomy
Icon – new flexibility in workflow requires careful attention to process	The Gamma Knife Icon provides several new possible treatment workflows. This flexibility requires extra vigilance to prevent mistakes
Consider total workflow when thinking of time differences between Gamma Knife and other modalities	One potential shortcoming of GKSRS is the longer beam-on time as compared to a high-dose rate linear accelerator. However, the required treatment time should be considered as one part of a longer treatment process. If one factors in the relative simplicity and speed of treatment planning and quality assurance, as well as overall plan quality, the beam-on time differences may not be as significant

References

1. Leksell L. The stereotaxic method and radiosurgery of the brain. Acta Chir Scand. 1951;102(4):316–9.
2. Ganz JC. Chapter 13 – Changing the gamma knife. In: Ganz JC, editor. Progress in Brain Research, vol. 215. Amsterdam: Elsevier; 2014. p. 117–25.
3. Leksell L. Cerebral radiosurgery. I. Gammathalanotomy in two cases of intractable pain. Acta Chir Scand. 1968;134(8):585–95.
4. Leksell L. [Clinical research; a comment]. Svenska lakartidningen. 1954;51(48):3078–83. Klinisk forskning: ett diskussionsinlagg.
5. Leksell L, Larsson B, Andersson B, Rexed B, Sourander P, Mair W. Research on "localized radio-lesions". VI. Restricted radio-lesions in the depth of the brain produced by a beam of high energy protons. AFOSR TN United States Air Force Off Sci Res. 1960;60–1406:1–13.

6. Larsson B, Liden K, Sarby B. Irradiation of small structures through the intact skull. Acta Radiol Ther Phys Biol. 1974;13(6):512–34.
7. Sarby B. Cerebral radiation surgery with narrow gamma beams; physical experiments. Acta Radiol Ther Phys Biol. 1974;13(5):425–45.
8. Leksell L. Stereotactic radiosurgery. J Neurol Neurosurg Psychiatry. 1983;46(9):797–803.
9. Leksell L. Stereotaxic radiosurgery in trigeminal neuralgia. Acta Chir Scand. 1971;137(4):311–4.
10. Leksell L. A note on the treatment of acoustic tumours. Acta Chir Scand. 1971;137(8):763–5.
11. Steiner L, Leksell L, Greitz T, Forster DM, Backlund EO. Stereotaxic radiosurgery for cerebral arteriovenous malformations. Report of a case. Acta Chir Scand. 1972;138(5):459–64.
12. Goetsch SJ. Gamma Knife. In: Benedict SH, Schlesinger DJ, Goetsch SJ, Kavanagh BD, editors. Stereotactic radiosurgery and stereotactic body radiation therapy. Boca Raton, FL: CRC Press; 2014. p. 39–53.
13. Lunsford LD, Flickinger J, Lindner G, Maitz A. Stereotactic radiosurgery of the brain using the first United States 201 cobalt-60 source gamma knife. Neurosurgery. 1989;24(2):151–9.
14. Wu A, Lindner G, Maitz A, Kalend A, Lunsford L, Flickinger J, et al. Physics of gamma knife approach on convergent beams in stereotactic radiosurgery. Int J Radiat Oncol Biol Phys. 1990;18(4):941–9.
15. Soanes T, Hampshire A, Vaughan P, Brownett C, Rowe J, Radatz M, et al. The commissioning and quality assurance of the Automatic Positioning System on the Leksell gamma knife. J Neurosurg. 2002;97(5 Suppl):574–8.
16. Kondziolka D, Maitz AH, Niranjan A, Flickinger JC. An evaluation of the Model C gamma knife with automatic patient positioning. Neurosurgery. 2002;50(2):429–32.
17. Kuo JS, Yu C, Giannotta SL, Petrovich Z, Apuzzo ML. The Leksell gamma knife Model U versus Model C: a quantitative comparison of radiosurgical treatment parameters. Neurosurgery. 2004;55(1):168–73.
18. Lindquist C, Paddick I. The Leksell Gamma Knife Perfexion and comparisons with its predecessors. Oper Neurosurg. 2007;61(suppl_3):ONS-130–ONS-41.
19. Novotny J Jr, Bhatnagar JP, Niranjan A, Quader MA, Huq MS, Bednarz G, et al. Dosimetric comparison of the Leksell Gamma Knife perfexion and 4C. J Neurosurg. 2008;109(Suppl):8–14.
20. Régis J, Tamura M, Guillot C, Yomo S, Muraciolle X, Nagaje M, et al. Radiosurgery with the world's first fully robotized Leksell Gamma Knife PerfeXion in clinical use: a 200-patient prospective, randomized, controlled comparison with the Gamma Knife 4C. Neurosurgery. 2009;64(2):346–56.
21. Elekta Instrument A. Leksell Gamma Knife® Perfexion™ installation manual. Stockholm: Elekta Instrument, AB; 2013. Contract No: 1022537 Rev. 02.
22. Campbell E, Walter E. Dandy-surgeon, 1886-1946. J Neurosurg. 1951;8(3):249–62.
23. Kilgore EJ, Elster AD. Walter Dandy and the history of ventriculography. Radiology. 1995;194(3):657–60.
24. Arndt J. Early Gamma Knife Development: A Physicist's personal memories. http://www.calameo.com/books/000768098b32993dd76b5.
25. Lewander R, Bergström M, Boethius J, Collins V, Edner G, Greitz T, et al. Stereotactic computer tomography for biopsy of gliomas. Acta Radiol Diagn. 1978;19(6):867–88.
26. Larner JM, Berk HW, Agarwal SK, Steiner L. The dosimetric consequences of weighted fields using the same isocenter in radiosurgery. Stereotact Funct Neurosurg. 1993;61(Suppl. 1):142–50.
27. Leksell L, Leksell D, Schwebel J. Stereotaxis and nuclear magnetic resonance. J Neurol Neurosurg Psychiatry. 1985;48(1):14–8.
28. Sampath S. The history of MRI. IEEE Eng Med Biol Mag. 2000;19(1):26. PubMed
29. Stuckey SL, Harris AJ, Mannolini SM. Detection of acoustic schwannoma: use of constructive interference in the steady state three-dimensional MR. AJNR Am J Neuroradiol. 1996;17(7):1219–25.
30. Wetzel SG, Johnson G, Tan AG, Cha S, Knopp EA, Lee VS, et al. Three-dimensional, T1-weighted gradient-echo imaging of the brain with a volumetric interpolated examination. AJNR Am J Neuroradiol. 2002;23(6):995–1002.
31. Sudhyadhom A, Haq IU, Foote KD, Okun MS, Bova FJ. A high resolution and high contrast MRI for differentiation of subcortical structures for DBS targeting: the Fast Gray Matter Acquisition T1 Inversion Recovery (FGATIR). NeuroImage. 2009;47(Suppl 2):T44–52.
32. Barajas RF, Chang JS, Sneed PK, Segal MR, McDermott MW, Cha S. Distinguishing recurrent intra-axial metastatic tumor from radiation necrosis following gamma knife radiosurgery using dynamic susceptibility-weighted contrast-enhanced perfusion MR imaging. AJNR Am J Neuroradiol. 2009;30(2):367–72.
33. Chang Z, Kirkpatrick JP, Wang Z, Cai J, Adamson J, Yin FF. Evaluating radiation-induced white matter changes in patients treated with stereotactic radiosurgery using diffusion tensor imaging: a pilot study. Technol Cancer Res Treat. 2014;13(1):21–8.
34. Lee CC, Wintermark M, Xu Z, Yen CP, Schlesinger D, Sheehan JP. Application of diffusion-weighted magnetic resonance imaging to predict the intracranial metastatic tumor response to gamma knife radiosurgery. J Neuro-Oncol. 2014;118(2):351–61.
35. Kirkpatrick JP, Soltys SG, Lo SS, Beal K, Shrieve DC, Brown PD. The radiosurgery fractionation quandary: single fraction or hypofractionation? Neuro Oncol. 2017;19(suppl_2):ii38–49.
36. Rosenthal DI, Glatstein E. We've got a treatment, but what's the disease? Or a brief history of hypofractionation and its relationship to stereotactic radiosurgery. Oncologist. 1996;1(1 & 2):1–7.
37. Sayer FT, Sherman JH, Yen CP, Schlesinger DJ, Kersh R, Sheehan JP. Initial experience with the eXtend System: a relocatable frame system for multiple-session gamma knife radiosurgery. World Neurosurg. 2011;75(5–6):665–72.
38. Reiner B, Bownes P, Buckley DL, Thwaites DI. Quantifying the trigger level of the vacuum surveillance system of the Gamma-Knife eXtend™ positioning system and evaluating the potential impact on dose delivery. J Radiosurg SBRT. 2016;4(1):31.
39. Schlesinger D, Xu Z, Taylor F, Yen CP, Sheehan J. Interfraction and intrafraction performance of the Gamma Knife Extend system for patient positioning and immobilization. J Neurosurg. 2012;117(Suppl):217–24.
40. Zeverino M, Jaccard M, Patin D, Ryckx N, Marguet M, Tuleasca C, et al. Commissioning of the Leksell Gamma Knife® Icon™. Med Phys. 2017;44(2):355–63.
41. AlDahlawi I, Prasad D, Podgorsak MB. Evaluation of stability of stereotactic space defined by cone-beam CT for the Leksell Gamma Knife Icon. J Appl Clin Med Phys. 2017;18(3):67–72.
42. Elekta Instrument A. Design and performance characteristics of a Cone Beam CT system for Leksell Gamma Knife® Icon™. Stockholm: Elekta Instrument, AB; 2015. Contract No: 1509394.
43. Elekta Instrument A. Geometric quality assurance for Leksell Gamma Knife® Icon™. Stockholm: Elekta Instrument, AB; 2015. Contract No: 1518146.
44. Wright G, Harrold N, Hatfield P, Bownes P. Validity of the use of nose tip motion as a surrogate for intracranial motion in mask-fixated frameless Gamma Knife® Icon™ therapy. J Radiosurg SBRT. 2017;4(4):289.
45. Elekta Instrument A. Leksell Gamma Knife Icon instructions for use. Stockholm: Elekta Instrument, AB; 2015. Contract No: 1505194.
46. Tonetti D, Bhatnagar J, Lunsford LD. Quantitative analysis of movement of a cervical target during stereotactic radiosur-

gery using the Leksell Gamma Knife Perfexion. J Neurosurg. 2012;117(Suppl):211–6.
47. Ma L, Nichol A, Hossain S, Wang B, Petti P, Vellani R, et al. Variable dose interplay effects across radiosurgical apparatus in treating multiple brain metastases. Int J Comput Assist Radiol Surg. 2014;9(6):1079–86.
48. Thomas EM, Popple RA, Wu X, Clark GM, Markert JM, Guthrie BL, et al. Comparison of plan quality and delivery time between volumetric arc therapy (RapidArc) and Gamma Knife radiosurgery for multiple cranial metastases. Neurosurgery. 2014;75(4):409–17. discussion 17-8
49. Klein EE, Hanley J, Bayouth J, Yin FF, Simon W, Dresser S, et al. Task Group 142 report: quality assurance of medical accelerators. Med Phys. 2009;36(9):4197–212.
50. Liu H, Andrews DW, Evans JJ, Werner-Wasik M, Yu Y, Dicker AP, et al. Plan quality and treatment efficiency for radiosurgery to multiple brain metastases: non-coplanar RapidArc vs. Gamma Knife. Front Oncol. 2016;6:26.
51. McDonald D, Schuler J, Takacs I, Peng J, Jenrette J, Vanek K. Comparison of radiation dose spillage from the Gamma Knife Perfexion with that from volumetric modulated arc radiosurgery during treatment of multiple brain metastases in a single fraction. J Neurosurg. 2014;121(Suppl):51–9.
52. Roper J, Chanyavanich V, Betzel G, Switchenko J, Dhabaan A. Single-Isocenter multiple-target stereotactic radiosurgery: risk of compromised coverage. Int J Radiat Oncol Biol Phys. 2015;93(3):540–6.
53. Fiorentino A, Levra N, Mazzola R, Fersino S, Ricchetti F, Alongi F. Correspondence: Volumetric Arc Therapy (RapidArc) vs Gamma Knife Radiosurgery for Multiple Brain Metastases: Not Only a Dosimetric Issue. Neurosurgery. 2015;77(2):310.
54. Niranjan A, Gobbel G, Novotny J Jr, Bhatnagar J, Fellows W, Lunsford LD. Impact of decaying dose rate in gamma knife radiosurgery: in vitro study on 9L rat gliosarcoma cells. J Radiosurg SBRT. 2012;1(4):257–64.
55. Balamucki CJ, Stieber VW, Ellis TL, Tatter SB, Deguzman AF, McMullen KP, et al. Does dose rate affect efficacy? The outcomes of 256 gamma knife surgery procedures for trigeminal neuralgia and other types of facial pain as they relate to the half-life of cobalt. J Neurosurg. 2006;105(5):730–5.
56. Lee JY, Sandhu S, Miller D, Solberg T, Dorsey JF, Alonso-Basanta M. Higher dose rate Gamma Knife radiosurgery may provide earlier and longer-lasting pain relief for patients with trigeminal neuralgia. J Neurosurg. 2015;123(4):961–8.
57. Stieber VW, Bourland JD, Tome WA, Mehta MP. Gentlemen (and ladies), choose your weapons: Gamma knife vs. linear accelerator radiosurgery. Technol Cancer Res Treat. 2003;2(2):79–86.
58. Ishiyama H, Teh BS, Ren H, Chiang S, Tann A, Blanco AI, et al. Spontaneous regression of thoracic metastases while progression of brain metastases after stereotactic radiosurgery and stereotactic body radiotherapy for metastatic renal cell carcinoma: abscopal effect prevented by the blood-brain barrier? Clin Genitourin Cancer. 2012;10(3):196–8.
59. Vaupel P. Tumor microenvironmental physiology and its implications for radiation oncology. Semin Radiat Oncol. 2004;14(3):198–206.
60. Szeifert GT, Salmon I, Rorive S, Massager N, Devriendt D, Simon S, et al. Does gamma knife surgery stimulate cellular immune response to metastatic brain tumors? A histopathological and immunohistochemical study. Journal of neurosurgery. 2005;102(s_supplement):180–4.
61. Hynynen K, Clement G. Clinical applications of focused ultrasound-the brain. Int J Hypertens. 2007;23(2):193–202.
62. Schlesinger D, Benedict S, Diederich C, Gedroyc W, Klibanov A, Larner J. MR-guided focused ultrasound surgery, present and future. Med Phys. 2013;40(8):080901.
63. Rahmathulla G, Recinos PF, Kamian K, Mohammadi AM, Ahluwalia MS, Barnett GH. MRI-guided laser interstitial thermal therapy in neuro-oncology: a review of its current clinical applications. Oncology. 2014;87(2):67–82.
64. Rieke V, Butts PK. MR thermometry. J Magn Reson Imaging. 2008;27(2):376–90.
65. Burke CW, Klibanov AL, Sheehan JP, Price RJ. Inhibition of glioma growth by microbubble activation in a subcutaneous model using low duty cycle ultrasound without significant heating. J Neurosurg. 2011;114(6):1654–61.
66. Timbie KF, Mead BP, Price RJ. Drug and gene delivery across the blood-brain barrier with focused ultrasound. J Control Release. 2015;219:61–75.
67. de Greef M, Crezee J, van Eijk JC, Pool R, Bel A. Accelerated ray tracing for radiotherapy dose calculations on a GPU. Med Phys. 2009;36(9):4095–102.
68. Poole CM, Cornelius I, Trapp JV, Langton CM. Radiotherapy Monte Carlo simulation using cloud computing technology. Australas Phys Eng Sci Med. 2012;35(4):497–502.
69. Kotrotsou A, Zinn PO, Colen RR. Radiomics in brain tumors: an emerging technique for characterization of tumor environment. Magn Reson Imaging Clin N Am. 2016;24(4):719–29.
70. Ortiz-Ramon R, Larroza A, Arana E, Moratal D. A radiomics evaluation of 2D and 3D MRI texture features to classify brain metastases from lung cancer and melanoma. Conf Proc IEEE Eng Med Biol Soc. 2017;2017:493–6.
71. Zhou M, Scott J, Chaudhury B, Hall L, Goldgof D, Yeom KW, et al. Radiomics in brain tumor: image assessment, quantitative feature descriptors, and machine-learning approaches. AJNR Am J Neuroradiol. 2018;39(2):208–16.
72. Ng TS, Bading JR, Park R, Sohi H, Procissi D, Colcher D, et al. Quantitative, simultaneous PET/MRI for intratumoral imaging with an MRI-compatible PET scanner. J Nucl Med. 2012;53(7):1102–9.
73. Wang LV, Yao J. A practical guide to photoacoustic tomography in the life sciences. Nat Methods. 2016;13(8):627–38.
74. Zhang P, Li L, Lin L, Hu P, Shi J, He Y, et al. High-resolution deep functional imaging of the whole mouse brain by photoacoustic computed tomography in vivo. J Biophotonics. 2018;11(1):e201700024.
75. Krizhevsky A, Sutskever I, Hinton GE. ImageNet classification with deep convolutional neural networks. Commun ACM. 2017;60(6):84–90.
76. Oermann EK, Rubinsteyn A, Ding D, Mascitelli J, Starke RM, Bederson JB, et al. Using a machine learning approach to predict outcomes after radiosurgery for cerebral arteriovenous malformations. Sci Rep. 2016;6:21161.
77. Solberg TD, Balter JM, Benedict SH, Fraass BA, Kavanagh B, Miyamoto C, et al. Quality and safety considerations in stereotactic radiosurgery and stereotactic body radiation therapy: executive summary. Practical radiation oncology. 2012;2(1):2–9.

CyberKnife Robotic Stereotactic Radiosurgery

Erqi Pollom, Lei Wang, Iris C. Gibbs, and Scott G. Soltys

Introduction

The CyberKnife® (Accuray, Sunnyvale, CA, USA), conceived and developed by Dr. John Adler, a neurosurgeon at Stanford, treated its first patient in 1994. This pioneering radiosurgical system, the first that did not require a stereotactic frame, consists of a linear accelerator mounted on a robotic treatment delivery system that allows for six degrees of freedom, coupled to an image-guided targeting system. Intrafraction image guidance allows for submillimeter accuracy for both intracranial and extracranial body treatments.

As the first dedicated radiosurgical system capable of extracranial radiosurgery or stereotactic body radiotherapy, early trials explored the use of stereotactic principles, developed for intracranial radiosurgery, for treatment in the body. Among the earliest reports of body radiosurgery are series of patients treated with the CyberKnife for tumors of the spine, lung, pancreas, prostate, and liver. The early pioneering studies continue with recent reports of CyberKnife treatment for cardiac arrhythmia, ocular melanoma, and functional disorders.

We review the early history of the development of the CyberKnife, describe the components of the system that allow for stereotactic accuracy, highlight how advances in the technology over the years have contributed to clinical outcomes, and look to where the CyberKnife, and the field of radiosurgery, may be headed in the future.

History

Stereotactic radiosurgery (SRS) was conceived by Swedish neurosurgeon Dr. Lars Leksell in 1951 [1] and initially relied on rigid fixation of the skull by a stereotactic head frame used as reference in order to precisely target radiation beams to intracranial lesions. A frame-based approach had limitations which included patient discomfort and inability to deliver multi-session treatments. American neurosurgeon Dr. John Adler was inspired to develop a frameless radiosurgical device after a neurosurgical fellowship with Dr. Leksell at the Karolinska Institute in Stockholm in 1985 [2]. He believed that frameless targeting could be achieved through X-ray image-to-image correlation and that this type of image-guided radiosurgery would obviate the need for an invasive stereotactic frame. In addition to greater patient comfort, a frameless system would allow for fractionated treatment over several days while maintaining stereotactic accuracy, as well as extracranial radiosurgery.

When Dr. Adler accepted a position at Stanford in 1987, he set out to build the first frameless radiosurgical system with collaborators, former Varian and Stanford linear accelerator engineers, from Schomberg Engineering. His original concept, as described in a series of technical papers in the 1990s, described a linear accelerator mounted on a robotic arm to precisely deliver multiple non-isocentric and noncoplanar treatment beams with near real-time X-ray image guidance [3–7]. He founded Accuray, Inc. (Sunnyvale, Calif., USA) in 1990 to develop and manufacture the CyberKnife system.

The first CyberKnife prototype, initially called the Neurotron 1000, was installed and treated patients at Stanford University Medical Center between 1994 and 2000. On June 8, 1994, the first patient was treated, an elderly woman with a solitary brain metastasis. CyberKnife was approved by the United States Food and Drug Administration for intracranial applications in 1999, and then received clearance in 2001 for radiosurgical treatment of lesions anywhere in the body where radiation is indicated.

E. Pollom · L. Wang · I. C. Gibbs · S. G. Soltys (✉)
Stanford Cancer Institute, Stanford, CA, USA

Stanford University, Department of Radiation Oncology, Stanford, CA, USA
e-mail: sgsoltys@stanford.edu

D. M. Trifiletti et al. (eds.), *Stereotactic Radiosurgery and Stereotactic Body Radiation Therapy*,
https://doi.org/10.1007/978-3-030-16924-4_6

Since the initial CyberKnife prototype, there have been five subsequent models through 2017. The second generation CyberKnife in 2001 introduced a new robot system (Kuka Roboter GmbH, Augsburg, Germany) and replaced the fluoroscopic screen/charge-coupled device camera with high resolution flat-panel amorphous silicon detectors. In 2002, the G3 model was introduced with more advanced image-tracking algorithms: six-degree skull tracking (6D Skull Tracking), fiducial-free spine tracking (XSight® Spine Tracking, Accuray, Sunnyvale, CA, USA), and Synchrony® (Accuray, Sunnyvale, CA, USA) for dynamic tracking on moving targets. Advances in imaging tracking techniques significantly improved delivery accuracy [8]. The G4 model was introduced in 2005 with an automated exchange table for the beam collimators. With the VSI model in 2009, improvements included a 6D Robot Couch, floor mounted high resolution (1024 × 1024) amorphous silicon detectors, higher dose rate (1000 monitor unite/minutes), the IRIS™ (Accuray, Sunnyvale, CA, USA) variable aperture collimator system, and fiducial-less lung tracking with Synchrony. The combination of high dose rate delivery and IRIS™ collimator significantly improved the delivery efficiency with the VSI system.

Improvements have led to the M6 model in 2012 with a new robot and a new room layout for a better robot working space. One significant advance of the M6 is multi-leaf colli-

Fig. 1 Representative models of the CyberKnife® (Accuray, Sunnyvale, CA, USA) system. (**a**) CyberKnife G3 system (2002). (**b**) CyberKnife G4 system (2005). (**c**) CyberKnife VSI system (2009). (**d**) CyberKnife M6 system (2012). (All images courtesy of Accuray Incorporated. © 2019 Accuray Incorporated. All rights reserved)

mator (MLC) capabilities which can improve treatment efficiency and expand the capability for larger treatment targets (Fig. 1a–d). In addition to hardware, advances in software optimization, segmentation, dose calculation, and beam/time reduction techniques have also been made over the years to the treatment planning system from the original On Target system to MultiPlan® system in 2005 to the most recent Precision™ system in 2017. Monte Carlo calculation was implemented in both MultiPlan and Precision planning system for more accurate dose calculations.

Given that the CyberKnife was frameless, radiosurgical treatment outside of the brain was soon explored. Some of the earliest reports of spine and body radiosurgery, also termed stereotactic body radiotherapy (SBRT), were performed with the CyberKnife. For lung cancer, among the first prospective trials was a phase I dose escalation trial of single-fraction SBRT using the CyberKnife, with doses up to 30 Gy in one fraction [9, 10]. A recent analysis of a national CyberKnife registry reported excellent outcomes on 723 patients with early-stage lung cancer treated with SRS/SBRT [11].

The CyberKnife was involved in the earliest reports of SBRT for treatment of primary and metastatic tumors of the liver. After a case report in 2006 on one patient treated to 36 Gy in three fractions [12], subsequent series of patients treated to higher doses of 30 Gy in one fraction or 46 Gy in five fractions noted good tumor control outcomes; reports in 2016 found 2-year local control of 82% in 115 patients [13] and 91% in 132 patients [14].

Similarly, prospective trials of CyberKnife pancreas SBRT noted early promise of the technique. First reported in 15 patients in a phase I dose escalation trial in 2004 [15], these early treatments often consisted of a breath-hold technique to manage intrafraction respiratory motion, with treatment up to 3 hours not uncommon. Subsequent phase II data reported local control of 94% in 19 patients treated with 45 Gy conventionally fractionated treatment followed by a 25 Gy SBRT boost [16]. Based on these experiences, a prospective, multi-institutional trial was conducted of SBRT to 33 Gy in five fractions with concurrent gemcitabine and reported slightly lower local control of 78% but acceptable rates of late gastrointestinal toxicities [17].

Prostate SBRT has become a standard of care for treatment of prostate cancer. Early pioneering studies investigated a homogeneous dose distribution [18] comparable to standard fractionated radiotherapy. Many large, single-institution series of nearly 500 patients with prostate cancer [19] treated with CyberKnife SBRT have subsequently been reported using the fractionation scheme of 35–40 Gy in five fractions and show promising tumor control and quality of life outcomes [20], similar to a later pooled, multi-institutional registry analysis of 2000 patients [21]. An alternative five-fraction protocol to emulate the heterogeneous dosimetry of high-dose rate (HDR) brachytherapy has also reported excellent prospective outcomes, suggesting that "Virtual HDR" CyberKnife SBRT may be a noninvasive alternative to brachytherapy for treating prostate cancer [22].

For head and neck malignancies, early data explored a CyberKnife radiosurgical boost to improve local control of nasopharyngeal carcinoma [23]. A prospective trial determined the maximum tolerated dose of five-fraction radiosurgery for recurrent head and neck carcinoma [24]; another prospective trial analyzed results of a six-fraction regimen [25]. Despite the precise dose delivery and highly conformal dose distribution CyberKnife allows in the re-irradiation setting, a large series of 381 patients reported the risks of carotid body blow-out with repeat CyberKnife irradiation for recurrent head and neck tumors [26], highlighting the importance of patient selection.

Although the basic concept that Dr. Adler created has remained unchanged over time, significant developments of the CyberKnife system have led to improvements in treatment planning, treatment delivery accuracy, treatment time, and range of body regions and indications that can technically be treated.

Recent Advances

The CyberKnife is a robotic treatment delivery system coupled to an image-guided targeting system. The treatment delivery system is composed of a lightweight, compact 6 MV X-band linear accelerator mounted to a robotic manipulator with six degrees of freedom. The image-guided targeting system consists of paired X-ray imaging sources and amorphous silicon flat panel detectors mounted on either side of the patient. Orthogonal images are obtained repeatedly throughout treatment and compared to digitally reconstructed radiographs (DRRs) derived from the pretreatment CT by aligning to bony anatomy or implanted fiducials. The treatment couch and robotic manipulator are then adjusted to resolve translational and rotational offsets between the orthogonal images and DRRs, allowing precise targeting of the LINAC. The overall system accuracy for intracranial targets of this frameless system with intrafraction motion management is less than 1 mm, similar to frame-based systems. A study on anthropomorphic head phantoms found targeting accuracy of approximately 0.5 mm [27].

While intracranial accuracy relies on skull tracking, early CyberKnife software did not allow for bone tracking of extracranial sites. The initial CyberKnife spinal radiosurgery procedures required placement of metal fiducial markers within the adjacent vertebral body, an open surgical procedure prior to spinal SRS [28]. While 6D skull tracking allows for treatment delivery to intracranial targets, XSight™ (Accuray, Sunnyvale, CA, USA) is a modification of the CyberKnife system that allows accurate tracking anywhere within or adjacent to spine. As with skull tracking, image registration with the XSight spine tracking system is based on high contrast bone data. A 9

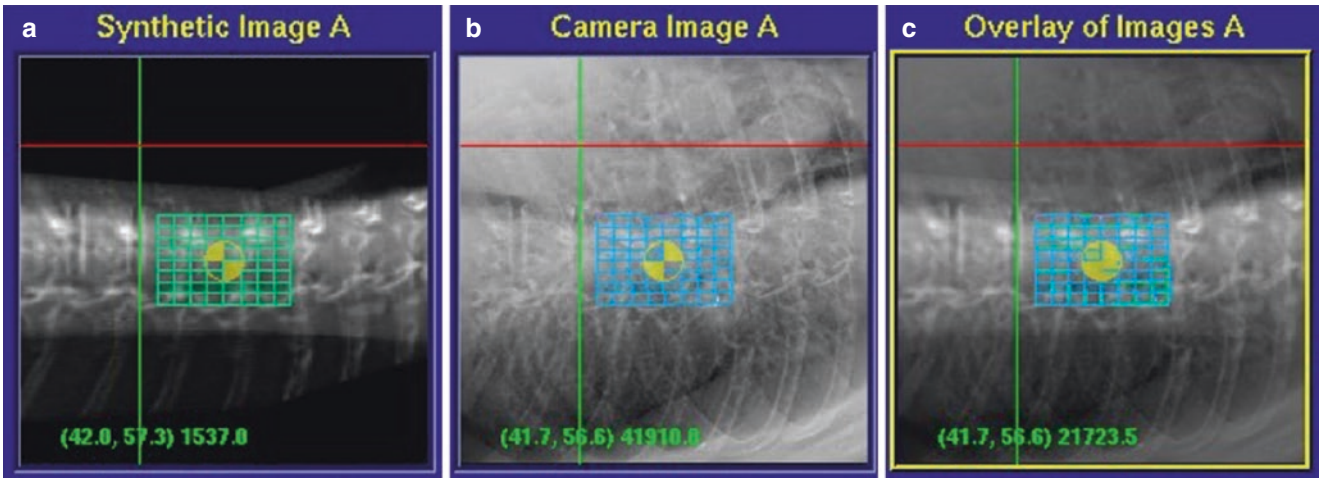

Fig. 2 Fiducial-less tracking of the spine by the XSight® (Accuray, Sunnyvale, CA, USA) spine software for intrafraction motion management. In (**a**), a 9 × 9 deformable grid, each intersecting point acting as a fiducial, is overlaid onto the digitally reconstructed radiograph (DRR). In (**b**), the patient's live radiograph is shown; notice the deformation of the tracking grid to match the patient's position. (**c**) is a fused image of (**a**) and (**b**) as a summary view. (All images courtesy of Accuray Incorporated. © 2019 Accuray Incorporated. All rights reserved)

by 9 grid of 81 nodes, each of which fulfills the role of a virtual fiducial, is displayed over each of the two orthogonal DRRs (Fig. 2a–c). The grid size can be adjusted to maximize the number of nodes containing bony anatomy. A matching algorithm then computes local displacement vectors for each node between images acquired during treatment and the original DRR and computes a final translation and rotation vector used to register the patient. This system can accurately target spinal lesions with submillimeter accuracy without spine-implanted fiducials [29].

With frameless image guidance technology came the ability to perform body radiosurgery. Similar to the early experience of spinal radiosurgery, the treatment of body sites required implantation of fiducials. To account for intrafraction motion management due to respiratory motion, these pioneering early treatments utilized deep-inspiration breath-hold techniques, stopping treatment delivery between breaths, and often would take up to 3 hours. Innovations in motion tracking and treatment delivery led to the Synchrony™ (Accuray, Sunnyvale, CA, USA) system. This image-guided system allows targeting of tumors that move with respiration in the thorax or abdomen. Unlike respiratory gating, where the beam position is fixed, turning on for a fraction of the respiratory cycle to deliver dose when the tumor is within position, Synchrony utilizes respiratory tracking, where the entire beam position moves with the tumor, treating it during the entire respiratory cycle. This system separately images light-emitting diodes (LEDs) placed on the chest wall to track respiratory movement as well as radiopaque fiducial markers placed within or near the tumor. The movement of the LEDs on the chest wall is correlated with internal movement of the fiducials [30]. Based on both data sets, a predictive model is generated and updated throughout the treatment based on changes in the patient's breathing pattern (Fig. 3a, b). The accuracy of Synchrony has been demonstrated even for irregular motion patterns and phase shifts between external chest and internal tumor motion [31, 32]. Software advances led to Xsight™ Lung which, in conjunction with Synchrony respiratory tracking system, allows for some lung tumors to be tracked directly, without implanted fiducials [33]. This approach uses direct soft tissue tracking rather than invasive fiducial insertion and requires sufficient tumor size and contrast against surrounding lung tissue in X-ray images, typically peripheral or apical lung regions, larger than 15 mm, and distant from the spine.

In 2012, the CyberKnife M6 series was released followed by the addition of a micro-multileaf collimator (InCise™ MLC, Accuray, Sunnyvale, CA, USA) in 2014 [34]. The InCise™ MLC allowed delivery of irregularly shaped fields, thus using fewer beams and lower total monitor units compared with non-isocentric fixed or IRIS™ variable aperture collimated fields. The major advantage of MLC is treatment time reduction. Compared to cone-based plan, an average of 30–35% time and MU reduction are reported. MLC plans have the potential of achieving a better dose gradient at the low-dose region [35, 36] as investigated in liver [37], intra-

cranial, and prostate targets [38]. The second version of InCise™ MLC has leaf width of 3.8 mm at 80 cm source to target distance with maximum field size of 100 mm by 115 mm at 80 cm from source.

Furthermore, the robotic mounting of the CyberKnife linac allows for non-isocentric treatment planning, a significant departure from most other radiosurgical systems that utilize isocentric sphere packing techniques, isocentric coplanar volumetric modulated arcs, or isocentric noncoplanar arcs. While high-dose regions of the treatment plans are similar among different techniques, a noncoplanar, non-isocentric plan may allow for a steeper gradient of low dose, particularly for body and spinal SRS plans [39].

a

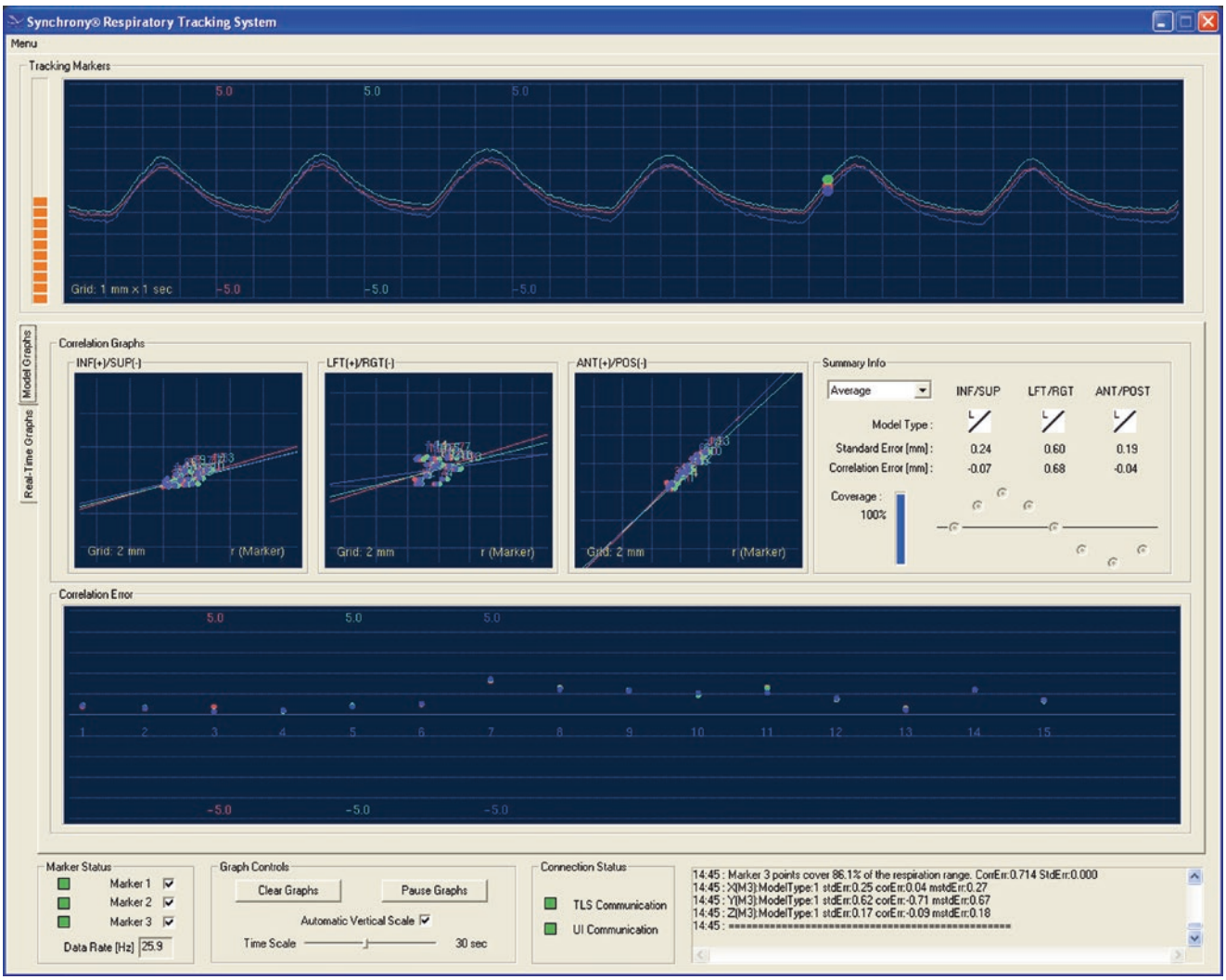

Fig. 3 A Synchrony® (Accuray, Sunnyvale, CA, USA) tracking screen for management of respiratory motion. The respiratory cycle trace from externally placed light-emitting diode (LED) (**a**) is correlated with the position of fiducials internally implanted into the tumor (the correlation model of the external LED and internal fiducial is shown in the middle panel). The total treatment correlation error accounted for in the treatment is shown in (**b**). (All images courtesy of Accuray Incorporated. © 2019 Accuray Incorporated. All rights reserved)

b

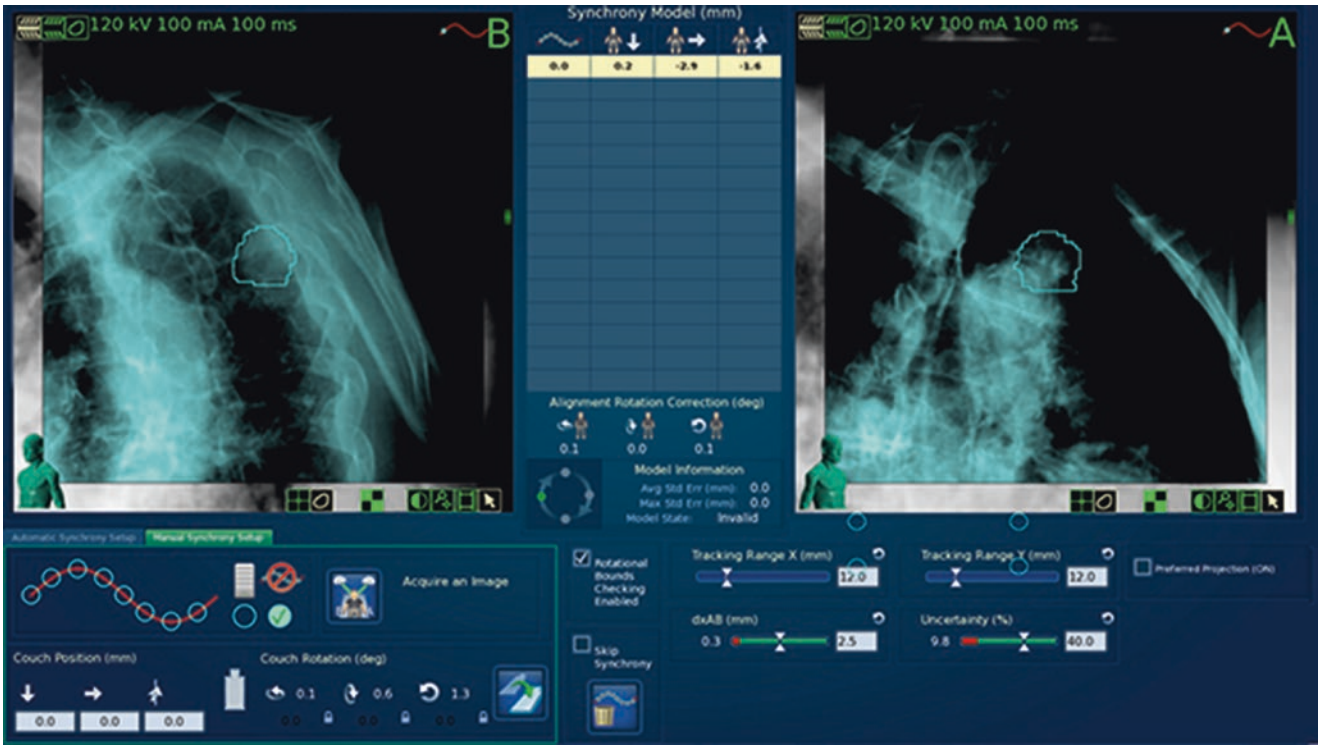

Fig. 3 (continued)

Limitations

The dose rate of earlier CyberKnife models was 300 MU/minute. It has been increased to 600–1000 MU/minute for the G4 and VSI models, and 1000MU/minute for the M6. In addition to increased dose rate, the treatment times of the newer models are improved over older models due to a time reduction function during treatment planning, the IRIS™ variable collimator and MLC capabilities. The treatment time for a typical intracranial plan with current CyberKnife technology (VSI and M6) is about 25–30 minutes compared to 45–60 minutes on earlier models. However, due to the step and shoot method used with CyberKnife and the significant robot travel time between delivery nodes, treatment efficiency is still the major drawback compared to the continuous arc delivery on linac-based systems, where a plan can be delivered within 5 minutes. Better optimization techniques and continuous delivery method are required to further reduce treatment times.

The CyberKnife delivers dose at predesignated node positions with most of the beams coming from an anterior oblique direction. Posterior beams are restricted to avoid collision of linac head with the ground. Compared to VSI and earlier models, the M6 model has the robot aligned at the head of the treatment couch instead of to the right or left superior corner of the couch. The M6 treatment space is now symmetric laterally and allows many more posterior oblique beams, up to 20 degrees below horizontal. Despite this improvement, the limited posterior beams is a weakness of the system and introduces more dose anteriorly, the clinical relevance of this relatively low dose spill is uncertain [40].

The current CyberKnife imaging guidance system provides great speed and low imaging dose [41–43], but the lack of volumetric imaging is a potential drawback compared with cone beam CT imaging guidance on other linac systems. Additionally, although the smaller beamlets used in CyberKnife provide steep gradients, they also result in higher MUs compared to linac arc plans, which introduces higher peripheral dose and leakage dose to the patients. This higher body dose is of unknown clinical significance.

For the functional disorder trigeminal neuralgia, the non-isocentric treatment of a length of the trigeminal nerve is a standard of care [44], distinct from the isocentric approach of GammaKnife. However, the treatment of functional targets other than trigeminal neuralgia with the CyberKnife system can be challenging. Past and current versions of SRS treatment planning software have not allowed multi-planar rotation of the native CT and MR images. Although case series of functional treatments exist [45, 46], this lack of image rotation makes targeting of cranial targets for ablation (e.g., thalamotomy for movement disorders, capsulotomies for obsessive compulsive disorders) difficult, as the coordi-

nates are based on a coplanar view of the anterior commissure-posterior commissure (AC-PC) line. Targeting via brain atlas coordinates often requires target identification with external software, then importation of that target into the CyberKnife system for SRS planning. Furthermore, the greater lateral penumbra from the higher energy 6MV photons of the CyberKnife leads to a less steep low-dose gradient than for lower energy photons such as the average 1.25 MV photons from cobalt sources. Whether this inherently greater low dose region has clinical implications is unknown.

Overall, further studies are required to compare not only effectiveness of competing technologies but also costs and impact on patient quality of life.

Future Directions

CyberKnife radiosurgery has been increasingly used as a noninvasive method to treat malignant and benign conditions, both intracranially as well as extracranially. This technology has also shown promise in a number of diseases not previously treated with radiotherapy. Conditions traditionally treated with thermal ablation, which causes injury through heating and coagulation, can be targeted for ablation through radioablation with high dose radiotherapy. For example, the first-in-human radiosurgical ablation of the heart to treat a cardiac arrhythmia [47] was performed with the CyberKnife. A later series of patients treated with noninvasive stereotactic radioablation which targeted the arrhythmogenic area of the heart found a reduction in the burden of refractory ventricular tachycardia [48]. CyberKnife treatment has shown potential in treating other cardiovascular condition such as nephrogenic hypertension, where a reduction in norepinephrine was seen following radiosurgical injury of the renal nerve in porcine models [49].

Lars Leksell first described Gamma Knife to create highly focused lesions in the brain to treat a variety of pain syndromes and movement disorders. The most common functional disorder for CyberKnife radiosurgery has been trigeminal neuralgia [44]. Radiosurgery for trigeminal neuralgia appears to work through partial axonal injury and degeneration at doses of 80 Gy [50]. The remaining intact axon population is usually sufficient to maintain facial sensation. Interest has naturally extended to explore these principles of decreasing pain conductibility while maintaining sensation and function for extracranial pain syndromes. Specifically, spinal SRS could potentially be used to treat chronic pain syndromes, as shown in a proof-of-principle experiment using Yucatan minipigs treated with a 90 Gy single dose of radiation targeting a small volume of spinal nerve [51]. The authors found that targeted nerves had a 65% loss of both large and small myelinated fibers and unmyelinated fibers associated with focal collagen deposition. The sections of the dorsal root ganglia demonstrated intact ganglia, satellite cells, and myelinated and unmyelinated nerve fibers leading into and out of the ganglia. The authors concluded that it is possible to irradiate spinal nerves, causing partial nerve fiber degeneration and possibly decreasing conductibility through the nerve but not completely abolishing function. Such treatment requires high levels of imaging and targeting accuracy, which have been made possible with improvements in spinal radiosurgery with the CyberKnife treatment system.

CyberKnife radiosurgery has also been used to perform a rhizotomy of the nerves innervating the spinal facet joint in five patients with facetogenic back pain [52]. Three of the five patients experienced pain improvement within one month of radiation treatment with a median follow-up of 10 months. No patient experienced acute or late-onset toxicity.

Although CyberKnife radiosurgery for uveal melanoma is a standard treatment in the Herzog Carl Theodor Eye Hospital in Munich, Germany, its use elsewhere in the world has not been widely reported and is a potential area of growth for any radiosurgery program. The initial paper of this approach described 20 patients treated with the process of retrobulbar anesthesia followed by SRS planning and delivery of a median dose of 20 Gy in one fraction, all within 3 hours while the eye is immobilized [53]. Localization during treatment delivery can be achieved by either retrobulbar anesthesia for eye immobilization [54–56] or a camera system to monitor eye motion [57]. The latest report note good outcomes for this high risk population, with 5 year local control of 71% in 217 patients [56] with similar quality of life compared to those treated with enucleation [58].

Although SBRT is a standard of care in the spine, lung, liver, pancreas, and prostate, less data are noted for renal radiosurgery, another indication for potential growth in the field of stereotactic body radiotherapy. The first CyberKnife renal SBRT report consisted of a single patient treated to 25 Gy in one fraction in 2010 [59]. The latest reports show local tumor control rate of 93% with doses up to 48 Gy in three fractions [60].

Looking forward, the future of CyberKnife and the field of radiosurgery and stereotactic body radiotherapy as a whole relies on identifying new conditions where radiation is not currently an indication. For example, the recent high-profile report on cardiac radiosurgery for ablation of arrhythmia [48] will likely lead to further research to optimize and expand this indication. Similarly, our field should look to areas where thermal ablation is a current treatment and explore comparative outcomes of noninvasive ablation with irradiation. These areas may include SRS for facetogenic back pain [52], thalamotomy for movement disorder or capsulotomy for obsessive compulsive disease rather than thermal ablation [61, 62], and renal artery hypertension [49] and

neuromodulation (rather than neuro-ablation) for psychiatric disorders [63]. Additionally, as reported above, the overall trend in radiation oncology is to pursue hypofractionated treatment as opposed to traditional fractionation to shorten treatment times, improve toxicity and quality of life, and potentially improve outcomes. The goal of hypofractionation is slowly being explored in neuro-oncology [64] but is still not the standard of care. We await expansion and maturation of early reports showing promising outcomes of primary radiosurgery for chordoma [65] as opposed to 8 weeks of traditionally fractionated radiotherapy, for newly diagnosed glioblastoma [66, 67], shorter than the standard 6 weeks of radiotherapy, and eagerly await future reports of new indications for radiosurgery.

Practical Considerations

Patient Setup

- Ensure comfortable patient position as treatment times can take up to an hour
- For brain lesions, a thermoplastic head mask with head rest is used
- For cervical spine lesions, a longer mask is used to stabilize head and neck
- For thoracic/lumbar spine and thoracic/abdominal/pelvic lesions, a vacuum bag is used for immobilization
- CT scan is performed using 1–1.5 mm slices (for higher-resolution DRRs and better tracking accuracy), centered on target extending 10–15 cm above and below the target, and encompassing organs at risk
- The primary CT used for treatment planning should be non-contrasted as contrast may distort DRR quality and impact tracking accuracy

Target Definition and Treatment Planning

- CT image acquired at simulation is used for dose calculation during treatment planning and for generating DRRs used for setup and tracking during treatment delivery.
- Can import MRI, PET, and additional CT scans into the Treatment Planning System (TPS) to register with primary CT image to aid in target delineation.
- Treatment plans are generated using one of three optimization methods: isocentric, conformal, or sequential optimization. Treatment plans should be optimized on critical structure constraints, plan conformity, and dose gradient.
- Given the multiple non-isocentric, noncoplanar beams of irradiation, one may pay attention to dose delivered outside of the axial plane of the target for extracranial targets.

Treatment Delivery

- A pair of orthogonal KV X-ray sources and detectors allow for accurate target localization and near real-time tracking using bony landmarks (for intracranial or spine lesions) or fiducial markers (usually for prostate, lung, liver)
- On initial setup, visual examination of the alignment between the live images and the DRRs is essential. The alignment is approved by a physician before treatment starts. Standard radiosurgery safety procedures should be followed
- During the treatment, images should be taken every 15–150 seconds, depending on treatment site and patient motion stability

References

1. Leksell L. The stereotaxic method and radiosurgery of the brain. Acta Chir Scand. 1951;102:316–9.
2. Adler JR. Accruray, incorporated: a neurosurgical business case study. Clin Neurosurg. 2005;52:87.
3. Adler JR Jr, Chang SD, Murphy MJ, Doty J, Geis P, Hancock SL. The Cyberknife: a frameless robotic system for radiosurgery. Stereotact Funct Neurosurg. 1997;69(1–4 Pt 2):124–8.
4. Adler JR Jr, Murphy MJ, Chang SD, Hancock SL. Image-guided robotic radiosurgery. Neurosurgery. 1999;44(6):1299–306; discussion 1306–7
5. Murphy MJ, Cox RS. The accuracy of dose localization for an image-guided frameless radiosurgery system. Med Phys. 1996;23(12):2043–9.
6. Murphy MJ. An automatic six-degree-of-freedom image registration algorithm for image-guided frameless stereotaxic radiosurgery. Med Phys. 1997;24(6):857–66.
7. Schweikard A, Bodduluri M, Adler JR. Planning for camera-guided robotic radiosurgery. IEEE Trans Rob Autom. 1998;14(6):951–62.
8. Fu D, Kuduvalli G. A fast, accurate, and automatic 2D-3D image registration for image-guided cranial radiosurgery. Med Phys. 2008;35(5):2180–94.
9. Whyte RI, Crownover R, Murphy MJ, Martin DP, Rice TW, DeCamp MM Jr, et al. Stereotactic radiosurgery for lung tumors: preliminary report of a phase I trial. Ann Thorac Surg. 2003;75(4):1097–101.
10. Le Q-T, Loo BW, Ho A, Cotrutz C, Koong AC, Wakelee H, et al. Results of a phase I dose-escalation study using single-fraction stereotactic radiotherapy for lung tumors. J Thorac Oncol. 2006;1(8):802–9.
11. Davis JN, Medbery C 3rd, Sharma S, Perry D, Pablo J, D'Ambrosio DJ, et al. Stereotactic body radiotherapy for early-stage non-small cell lung cancer: clinical outcomes from a National Patient Registry. J Radiat Oncol. 2015;4(1):55–63.
12. Chung YW, Han DS, Paik CH, Kim JP, Choi JH, Sohn JH, et al. Localized esophageal ulcerations after CyberKnife treatment for metastatic hepatic tumor of colon cancer. Korean J Gastroenterol. 2006;47(6):449–53.
13. Que J, Kuo H-T, Lin L-C, Lin K-L, Lin C-H, Lin Y-W, et al. Clinical outcomes and prognostic factors of cyberknife stereotactic body radiation therapy for unresectable hepatocellular carcinoma. BMC Cancer. 2016;16:451.
14. Su T-S, Liang P, Lu H-Z, Liang J, Gao Y-C, Zhou Y, et al. Stereotactic body radiation therapy for small primary or recurrent

hepatocellular carcinoma in 132 Chinese patients. J Surg Oncol. 2016;113(2):181–7.
15. Koong AC, Le QT, Ho A, Fong B, Fisher G, Cho C, et al. Phase I study of stereotactic radiosurgery in patients with locally advanced pancreatic cancer. Int J Radiat Oncol Biol Phys. 2004;58(4):1017–21.
16. Koong AC, Christofferson E, Le QT, Goodman KA, Ho A, Kuo T, et al. Phase II study to assess the efficacy of conventionally fractionated radiotherapy followed by a stereotactic radiosurgery boost in patients with locally advanced pancreatic cancer. Int J Radiat Oncol Biol Phys. 2005;63(2):320–3.
17. Herman JM, Chang DT, Goodman KA, Dholakia AS, Raman SP, Hacker-Prietz A, et al. Phase 2 multi-institutional trial evaluating gemcitabine and stereotactic body radiotherapy for patients with locally advanced unresectable pancreatic adenocarcinoma. Cancer. 2015;121(7):1128–37.
18. King CR, Brooks JD, Gill H, Pawlicki T, Cotrutz C, Presti JC Jr. Stereotactic body radiotherapy for localized prostate cancer: interim results of a prospective phase II clinical trial. Int J Radiat Oncol Biol Phys. 2009;73(4):1043–8.
19. Katz AJ, Kang J. Stereotactic body radiotherapy as treatment for organ confined low- and intermediate-risk prostate carcinoma, a 7-year study. Front Oncol. 2014;4:240.
20. Katz AJ, Kang J. Quality of life and toxicity after SBRT for organ-confined prostate cancer, a 7-year study. Front Oncol. 2014;4:301.
21. Freeman D, Dickerson G, Perman M. Multi-institutional registry for prostate cancer radiosurgery: a prospective observational clinical trial. Front Oncol. 2014;4:369.
22. Fuller DB, Naitoh J, Mardirossian G. Virtual HDR CyberKnife SBRT for localized prostatic carcinoma: 5-year disease-free survival and toxicity observations. Front Oncol. 2014;24(4):321.
23. Le Q-T, Tate D, Koong A, Gibbs IC, Chang SD, Adler JR, et al. Improved local control with stereotactic radiosurgical boost in patients with nasopharyngeal carcinoma. Int J Radiat Oncol Biol Phys. 2003;56(4):1046–54.
24. Heron DE, Ferris RL, Karamouzis M, Andrade RS, Deeb EL, Burton S, et al. Stereotactic body radiotherapy for recurrent squamous cell carcinoma of the head and neck: results of a phase I dose-escalation trial. Int J Radiat Oncol Biol Phys. 2009;75(5):1493–500.
25. Lartigau EF, Tresch E, Thariat J, Graff P, Coche-Dequeant B, Benezery K, et al. Multi institutional phase II study of concomitant stereotactic reirradiation and cetuximab for recurrent head and neck cancer. Radiother Oncol. 2013;109(2):281–5.
26. Yamazaki H, Ogita M, Kodani N, Nakamura S, Inoue H, Himei K, et al. Frequency, outcome and prognostic factors of carotid blowout syndrome after hypofractionated re-irradiation of head and neck cancer using CyberKnife: a multi-institutional study. Radiother Oncol. 2013;107(3):305–9.
27. Antypas C, Pantelis E. Performance evaluation of a CyberKnife G4 image-guided robotic stereotactic radiosurgery system. Phys Med Biol. 2008;53(17):4697–718.
28. Ryu SI, Chang SD, Kim DH, Murphy MJ, Le QT, Martin DP, et al. Image-guided hypo-fractionated stereotactic radiosurgery to spinal lesions. Neurosurgery. 2001;49(4):838–46.
29. Ho AK, Fu D, Cotrutz C, Hancock SL, Chang SD, Gibbs IC, et al. A study of the accuracy of cyberknife spinal radiosurgery using skeletal structure tracking. Neurosurgery. 2007;60(2 Suppl 1):ONS147–56; discussion ONS156.
30. Schweikard A, Shiomi H, Adler J. Respiration tracking in radiosurgery. Med Phys. 2004;31(10):2738–41.
31. Pepin EW, Wu H, Zhang Y, Lord B. Correlation and prediction uncertainties in the cyberknife synchrony respiratory tracking system. Med Phys. 2011;38(7):4036–44.
32. Nioutsikou E, Seppenwoolde Y, Symonds-Tayler JRN, Heijmen B, Evans P, Webb S. Dosimetric investigation of lung tumor motion compensation with a robotic respiratory tracking system: an experimental study. Med Phys. 2008;35(4):1232–40.
33. Urschel HC. Robotic radiosurgery. Treating tumors that move with respiration. Springer-Verlag Berlin Heidelberg: Springer Science & Business Media; 2007. 317 p.
34. Fürweger C, Prins P, Coskan H, Heijmen BJM. Characteristics and performance of the first commercial multileaf collimator for a robotic radiosurgery system. Med Phys. 2016;43(5):2063.
35. van de Water S, Hoogeman MS, Breedveld S, Nuyttens JJME, Schaart DR, Heijmen BJM. Variable circular collimator in robotic radiosurgery: a time-efficient alternative to a mini-multileaf collimator? Int J Radiat Oncol Biol Phys. 2011;81(3):863–70.
36. McGuinness CM, Gottschalk AR, Lessard E, Nakamura JL, Pinnaduwage D, Pouliot J, et al. Investigating the clinical advantages of a robotic linac equipped with a multileaf collimator in the treatment of brain and prostate cancer patients. J Appl Clin Med Phys. 2015;16(5):284–95.
37. Jin L, Price RA, Wang L, Meyer J, Fan JJ, Ma C, et al. Dosimetric and delivery efficiency investigation for treating hepatic lesions with a MLC-equipped robotic radiosurgery--radiotherapy combined system. Med Phys. 2016;43(2):727–33.
38. Kathriarachchi V, Shang C, Evans G, Leventouri T, Kalantzis G. Dosimetric and radiobiological comparison of CyberKnife M6™ InCise multileaf collimator over IRIS™ variable collimator in prostate stereotactic body radiation therapy. J Med Phys. 2016;41(2):135–43.
39. Nalichowski A, Kaufman I, Gallo J, Bossenberger T, Solberg T, Ramirez E, et al. Single fraction radiosurgery/stereotactic body radiation therapy (SBRT) for spine metastasis: a dosimetric comparison of multiple delivery platforms. J Appl Clin Med Phys. 2017;18(1):164–9.
40. Fürweger C, Drexler C, Muacevic A, Wowra B, de Klerck EC, Hoogeman MS. CyberKnife robotic spinal radiosurgery in prone position: dosimetric advantage due to posterior radiation access? J Appl Clin Med Phys. 2014;15(4):4427.
41. Chuang CF, Larson DA, Zytkovicz A, Smith V, Petti PL. Peripheral dose measurement for CyberKnife radiosurgery with upgraded linac shielding. Med Phys. 2008;35(4):1494–6.
42. Murphy MJ, Balter J, Balter S, BenComo JA Jr, Das IJ, Jiang SB, et al. The management of imaging dose during image-guided radiotherapy: report of the AAPM Task Group 75. Med Phys. 2007;34(10):4041–63.
43. Petti PL, Chuang CF, Smith V, Larson DA. Peripheral doses in CyberKnife radiosurgery. Med Phys. 2006;33(6):1770–9.
44. Adler JR Jr, Bower R, Gupta G, Lim M, Efron A, Gibbs IC, et al. Nonisocentric radiosurgical rhizotomy for trigeminal neuralgia. Neurosurgery. 2009;64(2 Suppl):A84–90.
45. Stancanello J, Romanelli P, Pantelis E, Sebastiano F, Modugno N. Atlas-based functional radiosurgery: early results. Med Phys. 2009;36(2):457–63.
46. Franzini A, Marchetti M, Brait L, Milanesi I, Messina G, Forapani E, et al. Deep brain stimulation and frameless stereotactic radiosurgery in the treatment of bilateral parkinsonian tremor: target selection and case report of two patients. Acta Neurochir. 2011;153(5):1069–75.
47. Loo BW Jr, Soltys SG, Wang L, Lo A, Fahimian BP, Iagaru A, et al. Stereotactic ablative radiotherapy for the treatment of refractory cardiac ventricular arrhythmia. Circ Arrhythm Electrophysiol. 2015;8(3):748–50.
48. Cuculich PS, Schill MR, Kashani R, Mutic S, Lang A, Cooper D, et al. Noninvasive cardiac radiation for ablation of ventricular tachycardia. N Engl J Med. 2017;377(24):2325–36.
49. Bhatt N, Long SA, Gardner EA, Tay J, Ladich E, Chamberlain D, et al. Radiosurgical ablation of the renal nerve in a porcine model: a minimally invasive therapeutic approach to treat refractory hypertension. Cureus. 2017;9(2):e1055.
50. Kondziolka D, Lacomis D, Niranjan A, Mori Y, Maesawa S, Fellows W, et al. Histological effects of trigeminal nerve radiosurgery in a

primate model: implications for trigeminal neuralgia radiosurgery. Neurosurgery. 2000;46(4):971–6. discussion 976–7.
51. De Salles AAF, Medin P. Functional spine radiosurgery. Spine Radiosurgery. 2009;1:176.
52. Li G, Patil C, Adler JR, Lad SP, Soltys SG, Gibbs IC, et al. CyberKnife rhizotomy for facetogenic back pain: a pilot study. Neurosurg Focus. 2007;23(6):E2.
53. Muacevic A, Nentwich M, Wowra B, Staerk S, Kampik A, Schaller U. Development of a streamlined, non-invasive robotic radiosurgery method for treatment of uveal melanoma. Technol Cancer Res Treat. 2008;7(5):369–74.
54. Klingenstein A, Fürweger C, Nentwich MM, Schaller UC, Foerster PI, Wowra B, et al. Quality of life in the follow-up of uveal melanoma patients after CyberKnife treatment. Melanoma Res. 2013;23(6):481–8.
55. Zorlu F, Selek U, Kiratli H. Initial results of fractionated CyberKnife radiosurgery for uveal melanoma. J Neuro-Oncol. 2009;94(1):111–7.
56. Eibl-Lindner K, Fürweger C, Nentwich M, Foerster P, Wowra B, Schaller U, et al. Robotic radiosurgery for the treatment of medium and large uveal melanoma. Melanoma Res. 2016;26(1):51–7.
57. Béliveau-Nadeau D, Callejo S, Roberge D. Technique for robotic stereotactic irradiation of choroidal melanoma. Cureus. 2016;8(4):e582.
58. Klingenstein A, Fürweger C, Mühlhofer AK, Leicht SF, Schaller UC, Muacevic A, et al. Quality of life in the follow-up of uveal melanoma patients after enucleation in comparison to CyberKnife treatment. Graefes Arch Clin Exp Ophthalmol. 2016;254(5):1005–12.
59. Staehler M, Fürweger C, Kufeld M, Karl A, Roosen A, Stief C, et al. Cyberknife radiosurgery of a renal pelvis tumor to avoid renal dialysis. Cureus [Internet]. 2010;Cureus 2(11):e17. https://doi.org/10.7759/cureus.17.
60. Sun MRM, Brook A, Powell MF, Kaliannan K, Wagner AA, Kaplan ID, et al. Effect of stereotactic body radiotherapy on the growth kinetics and enhancement pattern of primary renal tumors. AJR Am J Roentgenol. 2016;206(3):544–53.
61. Witjas T, Carron R, Krack P, Eusebio A, Vaugoyeau M, Hariz M, et al. A prospective single-blind study of gamma knife thalamotomy for tremor. Neurology. 2015;85(18):1562–8.
62. Kondziolka D, Flickinger JC, Hudak R. Results following gamma knife radiosurgical anterior capsulotomies for obsessive compulsive disorder. Neurosurgery. 2011;68(1):28–32; discussion 23–3
63. Borchers DJ, Litchfield CP, Schaal DW, Adler JR. Stereotactic Radiosurgical Neuromodulation for chemical dependency: a theoretical approach to addiction therapy. Cureus. 2009;Cureus 1(12):e6. https://doi.org/10.7759/cureus.6.
64. Shah JL, Li G, Shaffer JL, Azoulay MI, Gibbs IC, Nagpal S, et al. Stereotactic radiosurgery and hypofractionated radiotherapy for glioblastoma. Neurosurgery. 2018;82(1):24–34.
65. Yamada Y, Laufer I, Cox BW, Lovelock DM, Maki RG, Zatcky JM, et al. Preliminary results of high-dose single-fraction radiotherapy for the management of chordomas of the spine and sacrum. Neurosurgery. 2013;73(4):673–80; discussion 680
66. Pollom EL, Fujimoto D, Wynne J, Seiger K, Modlin LA, Jacobs LR, et al. Phase 1/2 trial of 5-fraction stereotactic radiosurgery with 5-mm margins with concurrent and adjuvant Temozolomide in newly diagnosed Supratentorial glioblastoma: health-related quality of life results. Int J Radiat Oncol Biol Phys. 2017;98(1):123–30.
67. Ney DE, Carlson JA, Damek DM, Gaspar LE, Kavanagh BD, Kleinschmidt-DeMasters BK, et al. Phase II trial of hypofractionated intensity-modulated radiation therapy combined with temozolomide and bevacizumab for patients with newly diagnosed glioblastoma. J Neuro-Oncol. 2015;122(1):135–43.

Linear Accelerator-Based Radiosurgery: Technique

William A. Friedman and Frank J. Bova

Introduction

Stereotactic radiosurgery (SRS) is a minimally invasive treatment modality that delivers a large and typically single dose of radiation to a specific intracranial target while sparing surrounding tissue. Unlike conventional fractionated radiotherapy, SRS does not rely on, or exploit, the higher radiosensitivity of neoplastic lesions relative to normal brain (therapeutic ratio). Its selective destruction is dependent mainly on sharply focused high-dose radiation and a steep dose gradient away from the defined target. The biological effect is irreparable cellular damage and delayed vascular occlusion within the high-dose target volume. Because a therapeutic ratio is not required, traditionally radioresistant lesions can be treated. Since destructive doses are used, however, any normal structure included in the target volume is subject to damage.

The basis for SRS was conceived over 40 years ago by Lars Leksell. He proposed the technique of focusing multiple nonparallel beams of external radiation on a stereotactically defined intracranial target. The averaging of these intersecting beams results in very high doses of radiation to the target volume but innocuously low doses to nontarget tissues along the path of any given beam. His team's implementation of this concept culminated in the development of the Gamma Knife. The patient is stereotactically positioned in the Gamma Knife so that the intracranial target coincides with the isocenter of radiation. Using variable collimation, beam blocking, and multiple isocenters, the radiation target volume is shaped to conform to the intracranial target.

W. A. Friedman (✉) · F. J. Bova
Department of Neurosurgery, University of Florida, Gainesville, FL, USA
e-mail: friedman@neurosurgery.ufl.edu

An alternate radiosurgical solution using a linear accelerator (LINAC) was first described in 1984 by Betti and colleagues [1]. Colombo and coauthors described such a system in 1985 [2], and LINACs have subsequently been modified in various ways to achieve the precision and accuracy required for radiosurgical applications. In 1986, a team composed of neurosurgeons, radiation physicists and computer programmers began development of the University of Florida LINAC-based radiosurgery system [3]. This system has been used to treat over 4500 patients at the University of Florida since May 1988, and it is in use at multiple sites worldwide.

Most LINAC radiosurgical systems rely on the same basic paradigm: A collimated X-ray beam is focused on a stereotactically identified intracranial target. The gantry of the LINAC rotates around the patient, producing an arc of radiation focused on the target (Fig. 1). The patient couch is then rotated in the horizontal plane and another arc performed. In this manner, multiple noncoplanar arcs of radiation intersect at the target volume and produce a high target dose, with minimal radiation to the surrounding brain. This dose concentration method is exactly analogous to the multiple intersecting beams of cobalt radiation in the Gamma Knife.

The target dose distribution can be tailored by varying collimator sizes, eliminating undesirable arcs, manipulating arc angles, using multiple isocenters, and differentially weighting the isocenters. In recent years, a number of LINAC systems have employed alternative beam shaping techniques involving "intensity modulation" and micromultileaf collimators (discussed under dose planning). Achievable dose distributions are similar for LINAC-based and Gamma Knife systems. With both systems, it is possible to achieve dose distributions that conform closely to the shape of the intracranial target, thus sparing the maximum amount of normal brain. Recent advances in stereotactic imaging and computer technology for dose planning, as well as refinements in radiation delivery systems have led to improved efficacy, fewer complications and a remarkable amount of interest in the various applications of SRS. Perhaps of equal importance is

D. M. Trifiletti et al. (eds.), *Stereotactic Radiosurgery and Stereotactic Body Radiation Therapy*,
https://doi.org/10.1007/978-3-030-16924-4_7

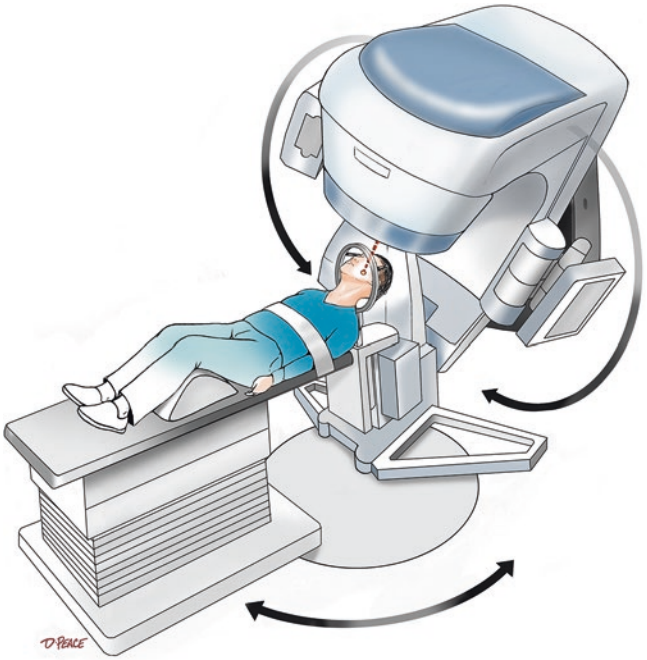

Fig. 1 The linear accelerator produces a high energy photon beam electronically. The beam is shaped by a circular collimator and focused on the stereotactic target point as the LINAC rotates. The patient couch is then moved to a new horizontal position, and the LINAC arcs again. Typically, five 100-degree, noncoplanar arcs are used for each target isocenter. Physically this produces exactly the same radiation concentration as is accomplished by the multiple hundreds of cobalt target sources in the older "Gamma Knife"

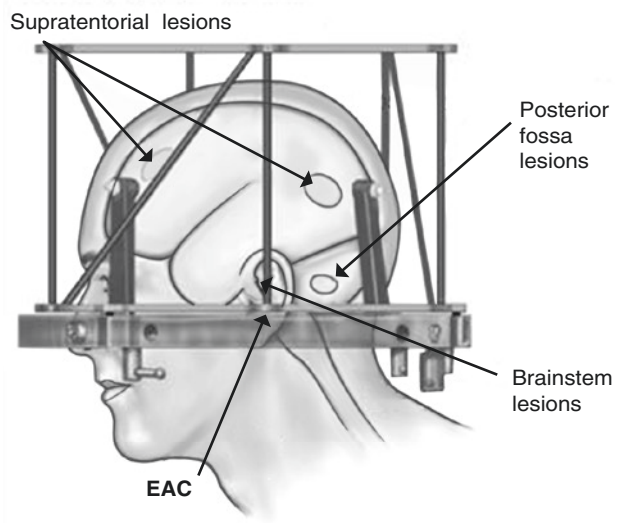

Fig. 2 A modified stereotactic head ring is used for frame-based radiosurgery. The patient is premedicated with diazepam. The head ring's four posts are positioned as shown. If the top of the base ring is located below the external auditory canal, the entire cranial volume will be reliably imaged in follow-up CT scanning, allowing supratentorial, brainstem, and all posterior fossa lesions to be treated. Local anesthetic is injected prior to the placement of stereotactic pins which penetrate the scalp and rest against the skull. No prepping is required

the fact that increasing amounts of scientific evidence have persuaded the majority of the international neurosurgical community that radiosurgery is a viable treatment option for selected patients suffering from a variety of challenging neurosurgical disorders.

This chapter will present a brief description of LINAC radiosurgical technique. We will emphasize the specific technique used at the University of Florida, but will also reference alternative methods used elsewhere.

Head Ring Application

Most stereotactic radiosurgical (single fraction) methodology requires attachment of a stereotactic head ring. The rigidly attached ring allows us to acquire spatially accurate information from angiography, CT, and MRI. The images obtained with this ring establish fixed relationships between the ring and the target lesion that are later translated during treatment planning so that the treatment target is accurately placed at the precise isocenter of the radiation delivery device. Because the stereotactic head ring is bolted to the treatment delivery device, it also immobilizes the patient during treatment. At the University of Florida, a modified stereotactic head ring (Fig. 2) is used. Most LINAC radiosurgical centers use some variation of this equipment.

In general, patients are premedicated with 10 mg of oral diazepam given approximately one-half hour before ring application. Premedication is optional. No skin shaving or preparation is required. After the ring is assembled, with post drives and posts approximately positioned for application, the surgeon places the ring roughly in position. The post drives are moved in or out until the post tips rest loosely against the patient's skin. As a rule, the front pin holes are positioned about an inch above the supraorbital ridges and in the midpupillary planes. The back pins are positioned just above the external occipital protuberance and approximately 2 inches from the midline. Having the patient slightly flex the head usually facilitates ring placement. In this position, the pins are usually perpendicular to the skull surface and, therefore, very unlikely to become dislodged.

As soon as the head ring is in final position for attachment, an assistant firmly stabilizes the ring from behind the patient while local anesthetic is injected through each of the post tip holes into the underlying skin. A wheal is raised with a solution containing equal parts of 0.5% lidocaine and 0.25% bupivacaine. This solution provides a quick onset of anesthetic action as well as long duration.

Approximately 1 minute after anesthetic injection, the pins are inserted into the post holes and screwed through the skin until they rest against the skull. Using the pin wrench,

we tighten the pins until the wrench cannot easily be turned using the thumb and first finger only. Care should be taken to avoid accidentally placing the pins into a burr hole, shunt, or onto a bone flap from a prior craniotomy. Occasionally, it is necessary to obtain skull fixation with three pins as opposed to the normal four because a large bone flap interferes.

At the conclusion of this procedure, the patient is transferred to a wheelchair and transported to the diagnostic radiology department for the next step (imaging) in the radiosurgery process.

Note well, that a number of papers describe radiosurgery using an external mask immobilizer instead of a head ring, along with infrared light emitting diode or fluoroscopic tracking of head movement [4]. Most of these treatments are multi-fraction, not single fraction.

Stereotactic Angiography

Angiography is the prime imaging modality for diagnosis and anatomic characterization of cerebral AVMs. It is also the time-honored means of judging the result of their treatment. For planning microsurgical or endovascular treatment of an AVM, angiography is clearly the gold standard. Because of its inherent limitations as a two-dimensional database representing a three-dimensional structure, however, stereotactic angiography alone frequently fails to indicate the true size and shape of the AVM, leading to errors in dose planning. For radiosurgery, the two most critical features of AVM anatomy are the tridimensional size and shape of the nidus. Underestimation of the target size may result in treatment failure. Overestimation of size results in the inclusion of normal brain within the treatment volume. Misrepresentation of an irregular target shape may lead to radiation damage of normal brain tissue. This, when affecting an eloquent area, may result in a neurologic deficit. In order to avoid these errors, we recommend a combination of CT angiography and/or MR imaging instead of angiography. It has been many years since we have used stereotactic angiography alone to guide radiosurgical treatment.

Stereotactic MR Imaging and Image Fusion

Stereotactic magnetic resonance images for use in radiosurgical treatment planning can be obtained in one of two ways: (1) By using a customized, MRI compatible, head ring and localizer coupled to a specially tuned MRI coil to minimize the spatial inaccuracies that result from perturbation of the magnetic field; or (2) Through the use of computer generated image annealing software programs, commonly termed *image fusion*.

Image fusion techniques allow MRI images acquired without the stereotactic head ring to be used for treatment planning. The MRI scan used for image fusion is routinely obtained the day before treatment. Images acquired for image fusion use the standard diagnostic MRI head coil and the scan is not limited to the area of interest, but includes the entire head. The scan technique uses volumetric image acquisition with a modified T_1-weighted sequence. This technique allows rapid image acquisition so that movement during the MRI is minimized. Image fusion eliminates many of the hardware incompatibility problems involved with using MRI for treatment planning. The volumetric scan technique also allows submillimetric slices, similar to the CT technique. Image resolution is identical to that used for diagnostic MRI scanning.

Stereotactic CT Scan

After ring application the patient is transported to the CT scanner. A special bracket is attached to the head of the CT table, replacing the usual CT head holder. Bolts on the undersurface of the head ring attach it to this bracket, holding the head ring (and the patient's head) stationary and in a fixed, nonrotated position in relation to the CT couch. After securing the head ring to the CT table, the CT localizer is attached to the ring. A volumetric, helical CT sequence is then rapidly acquired. Software can be used to adjust for any gantry tilt or rotation.

Image Processing

CT images are next transferred to the dosimetry planning computer. A program in the dosimetry computer automatically identifies the nine fiducial rods surrounding each axial image. Using geometric equations, the computer determines the AP, lateral, and vertical position of each point (pixel) in each CT slice. This information is then replotted in the computer's memory and all CT images are mathematically referenced to the head ring, which remains fixed to the patient's head. Hence, any point seen on the CT scan image is co-identified as a Cartesian coordinate related to the head ring. Furthermore, because the entire head is scanned and is represented as a conglomeration of unique pixels in the computer, the distance from the scalp to any target point can be mathematically determined from any point along the image. This information is vital for dose calculations, because attenuation of each entering radiation beam is proportional to the target depth for that beam. Rapid calculation of dose distribution for hundreds of beams represented by arcs of radiation requires a defined

three-dimensional image within the computer. This image is defined during image processing before treatment planning. The MRI images obtained the day before treatment are "fused" with software, thus registering the MRI to the stereotactic head ring. Treatment planning then proceeds based on the MRI images.

Radiosurgery Treatment Planning

Once the necessary stereotactic images have been acquired and transferred to the treatment-planning computer, the next step is to plan the precise delivery of radiation. This is accomplished through the use of a computer workstation and specialized treatment planning software "tools."

Goals of Radiosurgery Treatment Planning

An ideal radiation treatment plan would deliver 100% of the desired dose to the treatment target and none to the normal brain. This is not possible in reality, but the primary goal of radiosurgery treatment planning is to achieve a plan that conforms to the target as closely as possible, as defined by radiation *isodose shells*. Isodose shells are volumes bounded by surfaces that receive the same radiation dose – expressed as a specified percentage of the maximum radiation dose. A number of treatment planning tools are available for adjusting the shape of treatment isodose shells so that they fit even highly irregular target shapes. Regardless of its shape, the entire target must be treated within the prescription isodose shell (most commonly the 70% or 80% line), with as little normal brain included as possible (Fig. 3).

Another goal of dose planning is to adjust the dose gradient such that critical brain structures near the target receive the lowest possible dose of radiation. In addition, most LINAC radiosurgeons strive to produce a treatment dose distribution that maximizes uniformity (homogeneity) of dose throughout the entire target volume.

Dose Concentration Through the Use of Intersecting Beams

Radiation dose can be concentrated on a given deep target by focusing multiple radiation beams so they intersect at the target. The relative dose delivered to the (nontarget) tissue along the entry and exit paths of a given beam is very low compared to the dose at the intersection (target/isocenter) of multiple beams. The concept of using multiple beams is extended by the radiosurgery treatment paradigm used for LINAC and Gamma Knife systems. Gamma Knife units use 192 to 201 separate cobalt sources, all aimed at one target.

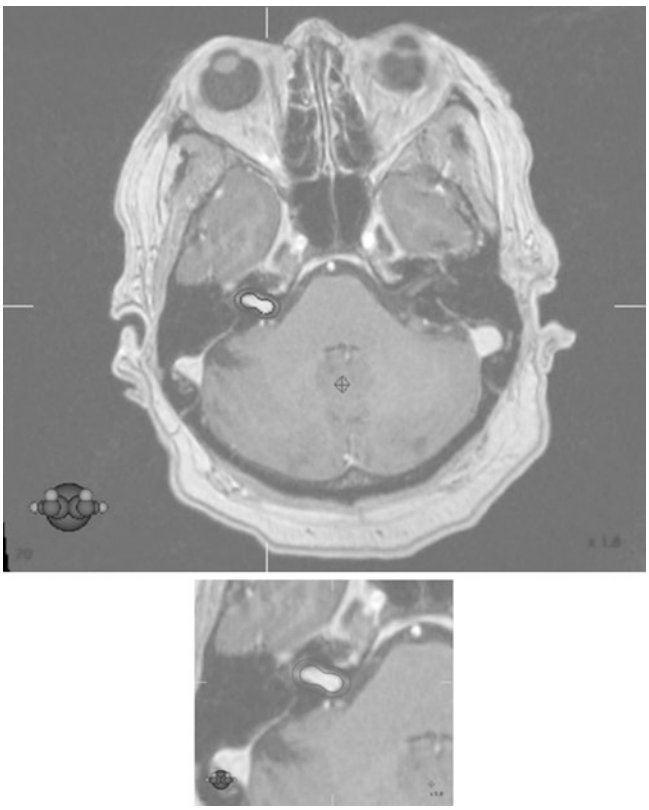

Fig. 3 These images show a small vestibular schwannoma treatment plan, utilizing two isocenters. The "sum" of the two circular dose distributions produces a highly conformal "isodose line" around the periphery of the tumor. This is the "70% isodose line." That means that 70% of the maximum radiation dose is being applied to the periphery of the tumor. The second, outer isodose line is the 35% line. This demonstrates the very steep dose gradient from treatment dose to half treatment dose in just a few millimeters

LINACs use multiple, noncoplanar arcs of radiation, all focused on one target. In the stereotactic paradigm, the equivalent of hundreds of radiation beams is focused on a selected target.

Treatment Planning Tools

In practice, a set of beam attenuation curves is determined for each size of collimator (beam-shaping device) used in radiosurgery. In this way, the dose contributed by each radiation beam to a target at a given depth is defined. Typically, beam diameters of 5–40 mm are available for standard LINAC radiosurgery. The distance each beam will travel through tissue before it reaches the target is readily computed during treatment planning from the reconstructed CT scans. Using the predetermined, collimator-specific attenuation data and the known depths to target, dosimetry software programs can rapidly compute and display the isodose information for any proposed combination of radiation beams and target dose desired [5].

Arc Elimination

In general, we begin treatment planning by directing five equally spaced arcs of radiation at the center of the target. Each arc span is 100°, and each arc is spaced 30° from its neighboring arcs. This results in a spherical dose distribution, with the dose falling off equally in all directions.

Many radiosurgical targets are not perfectly spherical; rather, they are shaped more like an elongated sphere (ellipsoidal). It is relatively easy to change the spherical dose distribution into an ellipsoidal distribution with LINAC radiosurgery systems. All that is required is to eliminate the arcs (reduce their weight to zero) that are most perpendicular to the long axis of the ellipsoid. For any target that is approximately ellipsoidal and has its principal axis anywhere in the coronal plane, treatment can be planned by eliminating the arcs that are most perpendicular to its principal axis. In addition, arc elimination maximizes the dose gradient in the direction of the eliminated arc.

Differential Collimator Sizes

The overall weight of an arc can be changed (increased or reduced), rather than completely eliminated, by increasing or reducing the size of the beam (i.e., collimator size) used for the arc. If the most horizontal collimators are reduced in size, the distribution becomes less elongated in the superior-inferior direction because the height is most controlled by the horizontal beams. Conversely, decreasing the size of the more vertically oriented arcs will diminish the lateral spread of the overlapping tubes of radiation and will create a distribution of the same height that is slightly narrower. Hence, as an alternative to arc elimination, different collimator sizes can be used on different arcs. This strategy results in slightly more or less severe elongation (i.e., ratio of principal to non-principal axis) of the treatment isodose configuration, with much less change in elongation of the lower isodose lines into surrounding tissue.

As a practical matter, differential collimator sizes and arc elimination are often used in combination to fine-tune the shape of the treatment isodose curve. This is especially useful when arc elimination is used primarily to reduce irradiation to surrounding structures.

Multiple Isocenters

Arc weighting is used in treatment planning for lesions that are ellipsoidal in the coronal plane. If, however, the lesion is non-spherical and non-ellipsoidal, multiple isocenters must be used.

Once the 3D shape of the lesion and the number of isocenters needed are determined, the isocenters must be positioned. This is accomplished by first filling in the largest spherical volume which can be contained by the lesion. Then small spherical volumes are added around the periphery, with appropriate spacing, until a conformal plan is obtained.

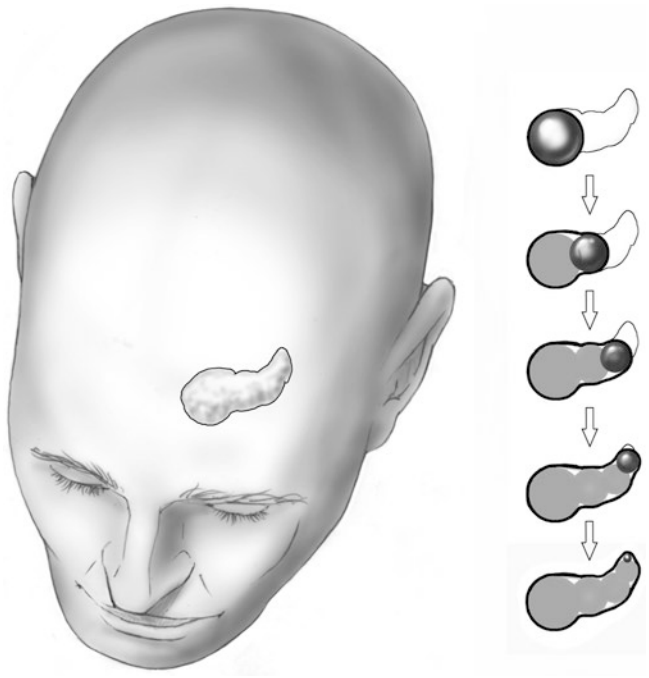

Fig. 4 This illustration demonstrates the "sphere packing algorithm" by which multiple spherical radiation shapes can be positioned and spaced to produce a highly conformal, non-spherical plan, again usually at the 70% isodose line. The planner (which can be the computer) sequentially positions the largest possible spherical volume, then the next largest, etc.) until the desired conformality is achieved

With this strategy, multiple isocenter plans can be rapidly constructed (Fig. 4). This interactive process is tremendously aided by fast computation times, as many adjustments are often necessary. Multiple isocenter planning requires training, practice, and real expertise to be applied optimally. Alternatively, most modern dose planning systems allow "inverse planning." That is, the user can simply outline the tumor shape on consecutive MRI slices from the top to the bottom of the tumor. The computer will then use a complex mathematical algorithm to select the appropriately sized and spaced isocenters to produce a highly conformal plan.

Multileaf Collimators

Multileaf collimators were originally designed as beam-shaping devices for conventional LINAC fractionated radiotherapy. MLCs are made up of many thin tungsten blades that can be individually controlled during radiation beam delivery (Fig. 5). By varying the position and speed of blade movement during arcing therapy, "intensity modulation" is achieved. Like radiosurgery with circular beams (the Gamma Knife-like approach), a steep dose gradient from target to normal brain cannot be achieved without enough noncoplanar beam (usually arcs but sometimes individual beams). MLC treatments generally result is slightly less conformal radiation shapes but have the advantage of treatment speed versus a traditional multiple isocenter approach when the number of isocenters is large [6].

Fig. 5 These images show a modern linear accelerator. Attached to the head of the machine is the micromultileaf collimator, seen in cross section below (follow arrow). The leaves are computer driven to match the shape of the target as the gantry rotates

Dose Selection

After a treatment plan is optimized, the radiation dose (expressed in gray (Gy)) is selected. In general, the dose is prescribed to the isodose line (or shell, in reality) that conforms to the periphery of the target lesion. For example, a typical dose prescription would be "12.5 Gy to the 80% isodose line." When the 80% isodose line corresponds to the periphery of the lesion, the maximum delivered dose, or 100% of the dose (which lies near the center of the lesion), is 25% higher than the prescribed dose at the 80% isodose line (12.5/0.8 = 15.6 Gy in this example). The lower the isodose line to which the treatment dose is prescribed, the greater the difference between the prescribed treatment dose and the maximum dose; in other words, the greater the dose inhomogeneity across the target.

Dose selection requires a detailed understanding of the radiosurgical literature; many papers provide historical dose guidelines for different radiosurgical situations. In practice, the selection of a safe and effective radiosurgical dose prescription requires experience and a close interaction between the neurosurgeon, radiation oncologist, and radiation physicist. In general, we strive for the following peripheral doses: 12.5 Gy for schwannomas and meningiomas; 20 Gy for arteriovenous malformations and metastatic tumors. Doses need to be adjusted downward as lesion size increases or for proximity to radiation-sensitive neural structures.

References

1. Betti OO, Derechinsky VE. Hyperselective encephalic irradiation with a linear accelerator. Acta Neurochir Suppl. 1984;33:385–90.
2. Colombo F, Benedetti A, Pozza F, Avanzo RC, Marchetti C, Chierego G, et al. External stereotactic irradiation by linear accelerator. Neurosurgery. 1985;16:154–60.
3. Friedman WA, Bova FJ. The University of Florida radiosurgery system. Surg Neurol. 1989;32:334–42.
4. Ryken TC, Meeks SL, Pennington EC, Hitchon P, Traynelis V, Mayr NA, et al. Initial clinical experience with frameless stereotactic radiosurgery: analysis of accuracy and feasibility. Int J Radiat Oncol Biol Phys. 2001;51(4):1152–8.
5. Friedman WA. LINAC radiosurgery. In: Friedman WA, editor. Neurosurgical Clinics of North America: stereotactic neurosurgery. Philadelphia: WB Saunders; 1990. p. 991–1008.
6. Lawson JD, Wang JZ, Nath SK, Rice R, Pawlicki T, Mundt AJ, et al. Intracranial application of IMRT based radiosurgery to treat multiple or large irregular lesions and verification of infra-red frameless localization system. J Neuro-Oncol. 2010;97(1):59–66.

Fractionated Radiosurgery

Giuseppe Minniti and Claudia Scaringi

Introduction

Stereotactic radiosurgery (SRS) is a well-established technique to deliver highly conformal irradiation with a steeper dose gradient between the tumor and the surrounding normal tissue [1]. Traditionally, a stereotactic head frame is fixed to the patient's skull, and high single-radiation doses are precisely delivered to the target while reducing the amount of surrounding normal brain receiving high doses of radiation and minimizing the potentially acute and long-term toxicity of treatment.

Single-fraction SRS is a safe and effective treatment for several benign and malignant intracranial tumors of limited size below 2–3 cm, including acoustic neuromas, meningiomas, pituitary tumors, and primary and secondary malignant tumors. However, as the tumor size becomes larger, the volume of normal brain that receives high doses of radiation significantly increases, resulting in a greater risk of severe acute and long-term neurotoxicity [2, 3].

More recently, fractionated SRS has been employed as an alternative to single-fraction SRS, with the aim of maintaining the precision and accuracy of treatment delivery while exploiting the potential radiobiological advantage of fractionation in terms of efficacy and reduced toxicity [4, 5]. Fractionated SRS, also called hypofractionated SRS, multifraction SRS, multidose SRS, multisession SRS, or hypofractionated stereotactic radiotherapy, usually involves delivering higher fraction doses to the target for up to five fractions. The use of fractionated SRS may improve the balance between tumor control and normal tissue toxicity over single-fraction SRS, particularly for large lesions or for those located in close proximity to critical anatomic structures, such as the optic apparatus or the brainstem.

Recent Advances

The objective of fractionated SRS is to obtain an improved therapeutic ratio for treatments in which high-dose single-fraction SRS would result in unacceptable risk of severe toxicity. The linear-quadratic (LQ) model has been generally used to evaluate the effect of a radiation dose to neoplastic and normal cells [6, 7]. According to the LQ formula, the fraction of cells surviving at a dose D ($S(D)$) curve is characterized by a linear component α, describing the initial slope of the cell survival curve, and a quadratic component β, representing the terminal slope of the survival curve ($S(D) = e-^{\alpha D-\beta D2}$). The α/β ratio, which represents the dose at which the linear and quadratic components of cell killing are equal, is commonly used to determine the optimal dose of irradiation to achieve high tumor control while minimizing toxicity to normal tissues. According to the α/β ratio, normal tissues can be classified in early responding tissues, characterized by a high α/β ratio, and in late responding tissues, which have a low α/β ratio [8]. Based on preclinical and clinical data, the α/β ratio of normal brain tissue is estimated to be in the order of 2, while the average α/β ratio of malignant brain tumors is 10, similar to that of early responding tissues, and the average α/β ratio of benign brain tumors is 3, similarly to late responding tissues [9, 10]. The linear-quadratic model is also used to calculate a biologically effective dose (BED) when using different radiation schedules, according to the formula BED = $D[1 + d/(\alpha/\beta)]$ [11] for a specific α/β ratio, total dose (D), and dose per fraction (d).

Although the LQ formula is widely used to model the effect of total dose and dose per fraction in conventionally fraction-

G. Minniti (✉)
Radiation Oncology Unit, UPMC Hillman Cancer Center, San Pietro Hospital, Rome, Italy

IRCSS Neuromed, Pozzilli, Italy

C. Scaringi
Radiation Oncology Unit, UPMC Hillman Cancer Center, San Pietro Hospital, Rome, Italy

Radiation Oncology Unit, Sant'Andrea Hospital, University Sapienza, Rome, Italy

D. M. Trifiletti et al. (eds.), *Stereotactic Radiosurgery and Stereotactic Body Radiation Therapy*,
https://doi.org/10.1007/978-3-030-16924-4_8

Table 1 Unvalidated normal tissue dose constraints for multifraction SRS

Organ	Fractionation	Dose (Gy) or dose/volume parameters	Toxicity rate (%)	Type of toxicity	References
Brain	3-fraction SRS	18 (6 Gy/fx) to <26 ml	<3%	Symptomatic necrosis	[27]
Brainstem	3-fraction SRS 5-fraction SRS	18 (6 Gy/fx) to <1 ml, maxPD 23 (7.67 Gy/fx) 26 (5.2 Gy/fx) to <1 ml, maxPD 31 (6.2 Gy/fx)	<3%	Permanent cranial deficit or necrosis	[21, 24]
Optic nerve/ chiasm	3-fraction SRS 5-fraction SRS	15 (5 Gy/fx) to <0.2 ml, maxPD 19.5 (6.5 Gy/fx) 20 (4 Gy/fx) to <0.2 ml, maxPD 25 (5 Gy/fx)	<3%	Optic neuropathy	[21, 24, 26]
Cochlea	3-fraction SRS 5-fraction SRS	maxPD 20 (6.67 Gy/fx) maxPD 27.5 (5 Gy/fx)	NA	Hearing loss	[21]
Medulla oblongata	3-fraction SRS 5-fraction SRS	18 (6 Gy/fx) to <0.25 ml, maxPD 22.5 (6.67 Gy/fx) 22.5 (4.5 Gy/fx) to <0.25 ml, maxPD 30 (6 Gy/fx)	1%	Myelopathy	[21, 23]

SRS stereotactic radiosurgery; *maxPD* maximum point dose

ated radiation therapy (RT), its application is generally considered inappropriate to model high dose per fraction effects as used in SRS. Clinical results have generally validated its application for fractions up to about 8–10 Gy, whereas the effect for doses above 10 Gy remains controversial [12]. Potential mechanisms of damage produced by high radiation doses, i.e., vascular and stromal damage, as well the impact on radioresistant subpopulations of cells may, at least in part, explain limitations of LQ model to describe the response of the linear component of cell sensitivity to killing at high radiation doses. As an alternative to LQ model, Joiner and colleagues [13] have proposed the linear-quadratic-cubic model, in which BEDs are calculated by adding an additional term proportional to the cube of dose to the LQ formula; accordingly, three fractions of 9 Gy correspond to a single dose of approximately 22 Gy, suggesting that fractionated SRS may represent a valid option for controlling lesions larger than 3 cm in size, for whom single-fraction doses >15–16 Gy are associated with a significant risk of radiation-induced brain necrosis.

Advances in RT technology for performing frameless SRS have enabled the treatment of large lesions using 2–5 fractions. Commonly used techniques to deliver fractionated SRS include the CyberKnife (Accuray, Sunnyvale, CA), the Gamma Knife (Gamma Knife™; Elekta Inc., Stockholm, Sweden), or a modified linear accelerator (LINAC). Patients are usually immobilized in a high precision frameless stereotactic mask fixation system with a repositioning accuracy during the course of a fractionated treatment of 1–2 mm [14]. Dose is delivered throughout multiple fixed fields or arcs shaped with a micromultileaf collimator (2.5–3.0 mm leaf); for LINAC SRS, conformity can be improved by the use of intensity modulation of the beams (IMRS) or volumetric modulated arc radiotherapy (VMAT). Further improvements of techniques include improved accuracy of patient repositioning with the use of either orthogonal x-rays (ExacTrac®, Brainlab, Munich, Germany) or cone beam computed tomography (CBCT) in-room imaging systems that are able to correct positioning errors by translating and rotating the treatment table in six directions with a reported accuracy <0.5 mm [15–17], similar to that observed for invasive frame-based SRS. Despite technical differences in treatment planning and dose delivery, the reported degree of dose conformity and accuracy of patient repositioning for tumors planned with Gamma Knife, CyberKnife, and LINAC-based SRS are similar [18, 19].

The risk of radiation-induced toxicity following SRS is influenced by different factors, including the total dose, dose per fraction, and the volume of normal tissue irradiated at high doses. In this regard, current clinical recommendations for SRS are based on a combination of clinical studies and reviews [20–29]; however, data on tolerance doses of central nervous system (CNS) organs at risk (OARs) to fractionated SRS are relatively limited, and dose constraints remain not validated. For three-fraction and five-fraction treatments, a summary of dose/volume data and clinical risk estimates for CNS structures is presented in Table 1.

In clinical practice, fractionated SRS is generally used as an alternative to single-fraction SRS for lesions >3 cm diameter or in close proximity to critical structures, such as the optic pathway or the brainstem, since high single doses are perceived to carry a higher risk of neurological complications. Results of selected studies of fractionated SRS for brain tumors are summarized in Table 2 [27, 29–44]. Several retrospective studies have reported the outcome of intact and resected brain metastases following fractionated SRS [27, 30, 33, 34, 45–48]. Minniti and colleagues [29] have reported clinical outcomes in 289 patients with 343 brain metastases >2 cm in size treated with LINAC-based single-fraction SRS or fractionated SRS (3 × 9 Gy) at the University of Rome Sapienza. Fractionated SRS was associated with a significantly better local control and to less radiation-induced brain necrosis: 1-year cumulative local control rates were 77% and 91% in the single-fraction SRS group and fractionated SRS group ($p = 0.01$), respectively, and 1-year cumulative incidence rates of brain necrosis were 18% and 9% ($p = 0.01$), respectively. A local control up to 90% at 1 year has been observed in other studies using schedules of 5 × 6–7 Gy or 3 × 8–9 Gy, with a low risk of radiation-induced toxicity [27, 31–33]. A similar approach has been suggested for the treatment of tumor cavity following gross-total resection of a brain metastasis, with a reported 12-month local control in

Table 2 Selected published studies on fractionated SRS in patients with brain tumors

Authors	Type of tumor	Patients/ lesions (*n*)	Tumor size	SRS technique	SRS dose (Gy/ fractions)	Median follow-up (months)	Median local control	Median OS (months)	Toxicity (any grade)
Aoyama et al. [30]	Brain mets	87/159	3.3 cc	LINAC	35 Gy in 4 fractions	6.3	81% at 1 year	8.7	2.7% brain necrosis
Ernst Stecken et al. [31]	Brain mets	51/72	13 cc	LINAC	30-35 Gy in 5 fractions	7	76% at 1 year	11	50% brain necrosis
Minniti et al. [29]	Brain mets	135/171	16.4 cc	LINAC	27 Gy in 3 fractions 36 Gy in 3 fractions	11.4	88% at 1 year	14.8	9% brain necrosis
Murai et al. [32]	Brain mets	54/61	> 2.5 cm	CyberKnife	31–35 Gy in 5 fractions	NA	69% at 1 year	6	no grade 3 toxicity
Minniti et al. [27]	Brain mets	138/164	>2 cm	LINAC	27 Gy in 3 fractions	29	90% at 1 year	13.4	8% brain necrosis
Kim et al. [33]	Brain mets	36/40	21.2 cc	Gamma Knife	5–11 Gy in 2-4 fractions	13.4	90%	16.2	2.7% brain necrosis
Minniti et al. [34]	Resected brain mets	101/101	17.5 cc	LINAC	27 Gy in 3 fractions	16	93% at 1 year	17	9% brain necrosis
Ahmed et al. [35]	Resected brain mets	65	16.8 cc	LINAC	20-30 Gy in 5 fractions	8.5	87% at 1 year	10.1	1.5% brain necrosis
Ling et al. [36]	Resected brain mets	99/100	>3 cm	CyberKnife	22 Gy in 1-5 fractions	12.2	71.8% at 1 year	12.7	9% brain necrosis
Gutin et al. [37]	Recurrent gliomas[a]	25	≤3.5 cm	LINAC	30 Gy in 5 fractions plus Bevacizumab	6.6[b]	7.3 months (grade IV)[c] 7.5 months (grade III)[c]	12.5 Grade IV 16.5 Grade III	12% grade 3 toxicity
McKenzie et al. [38]	Recurrent gliomas[a]	35	8.54 cc	LINAC	30 Gy in 5 fractions	NA	62% at 6 months	8.6	9% brain necrosis
Minniti et al. [39]	Recurrent gliomas[a]	54	30.3 cc	LINAC	30 Gy in 5 fractions plusTMZ	NA	6 months[c]	11.4 Grade IV 16.1 Grade III	7% brain necrosis
Colombo et al. [40]	Grade I meningiomas	150	> 8 cc	CyberKnife	14-25 Gy in 2-5 fractions	30	97.3%	NA	0.5%
Bria et al. [41]	Grade I meningiomas	60	5.54 cc	CyberKnife	6-27 Gy in 1-5 fractions	16.1	95% at 1 year	NA	1%
Iwata et al. [42]	Pituitary adenomas	100	5.1 cc	CyberKnife	21 Gy in 3 fractions 25 Gy in 5 fractions	33	98% at 3 years	NA	4% hypopituitarism
Hansasuta et al. [43]	Acoustic neuromas	383	1.1 cc	CyberKnife	18 Gy in 3 fractions	42	96% at 5 years	NA	5%
Patel et al. [44]	Acoustic neuromas	383	1.58 cc	LINAC	25 Gy in 5 fractions	72	78.3%	NA	9%, new CNVII deficit 9.4% CNVIII deficit 1.3% hydrocephalus

SRS stereotactic radiosurgery, *OS* overall survival, *PTV* planning target volume, *NA* not assessed, *TMZ* temozolomide, *CN* cranial nerve
[a]Series including either grade III or grade IV recurrent gliomas; [b]for surviving patients; [c]*PFS* progression-free survival

the range of 70–90% using doses of 24–35 Gy in 3–5 fractions [34–36, 49].

Several studies have evaluated the efficacy of re-irradiation in patients with recurrent primary brain tumors [37–39, 50, 51]. In a series of 54 patients with recurrent malignant gliomas who received fractionated SRS (30 Gy in 5 fractions) combined with continuous temozolomide (50 mg/m^2 everyday up to one year) at the University of Rome Sapienza, 1-year and 2-year survival rates were 53% and 16%, respectively, and progression-free survival rates were 24% and 10%, respectively [39]. Grade 3 neurological deficits attributable to radiation-induced toxicity occurred in 7% of patients. Similar survival benefits have been observed in patients re-irradiated for recurrent high-grade gliomas using doses of 25–30 Gy delivered in 3–5 fractions [37–39]. The combination of fractionated SRS and bevacizumab has been recently evaluated in a few prospective studies [37, 50, 51]. In a series of 25 patients with progressive high-grade gliomas after standard RT, Gutin and colleagues [37] reported a 1-year survival of 54% after fractionated SRS using a total dose of 30 Gy delivered in five fractions in combination with bevacizumab. In another small phase-1 study exploring the combination of fractionated SRS plus bevacizumab in patients with recurrent glioblastoma, Clarke and coauthors [51] concluded that 30 Gy given in three fractions delivered every other day plus bevacizumab was a feasible and well-tolerated treatment, achieving an overall survival of 13 months.

SRS is a well-established treatment for benign brain tumors, including meningiomas, pituitary adenomas, and acoustic neuromas, resulting in excellent local control and acceptable toxicity rate [52–54]. In general, SRS is recommended for brain lesions <3 cm diameter not in close proximity to critical structures, whereas fractionated stereotactic RT, typically delivered in 1.8–2 Gy daily to a total dose of 45–54 Gy, is employed for larger tumors. More recently, several studies have evaluated the feasibility of fractionated SRS for complex skull base tumors.

In a series of 199 benign intracranial meningiomas (157 skull base meningiomas) treated with CyberKnife SRS, Colombo and colleagues [40] reported a 5-year control of 93.5%. Local control for tumors larger than 8 ml and/or situated close to critical structures treated with 2–5 daily fractions was similar to that obtained in smaller lesions after single-fraction SRS. Neurological deterioration was observed in 4% of patients, mainly visual deficits. In another series of 60 patients treated at the University of Pittsburgh with CyberKnife with a median dose of 17.5 Gy (range 6–27 Gy) in three fractions (range 1–5), Bria and coauthors [41] observed a local control of 96% at a median follow-up of 16.1 months. A subjective improvement in the existing, tumor-related symptoms was noted in 60% of the patients, with grade 3 toxicity observed in only one patient. In a small series of 26 patients with meningioma treated with LINAC-based fractionated SRS (30 Gy in 5 fractions), Navarria and coauthors [55] reported a local control of 100% at a median follow-up of 24.5 months, with no significant late toxicity, and similar clinical outcomes have been reported by other authors [56–58]. Larger series with appropriate follow-up should confirm the excellent local control and low risk of neurological toxicity in patients treated with fractionated SRS, as well as its superiority over other radiation techniques.

With the same rationale, fractionated SRS has been employed for relatively large pituitary tumors that are generally not suitable for SRS [42, 59–61]. Iwata and coauthors [42] reported the clinical outcomes in 100 patients with non-functioning pituitary adenoma who received fractionated SRS with CyberKnife using doses of 21 in 3 fractions or 25 Gy in 5 fractions. At a median follow-up of 33 months, the reported local control rate was 98% at 3 years; complications were represented by grade 2 visual deficits and new onset of hypopituitarism in 1% and 4% of patients, respectively. Using the same doses, the authors reported a biochemical remission of acromegaly in 17% of 52 patients with a GH-secreting pituitary adenoma at a median follow-up of 66 months [61]. In another series of 46 patients with a pituitary adenoma or a meningioma within 2 mm from the optic apparatus treated with CyberKnife at doses of 18–25 Gy delivered in 2–5 sessions, Adler and coauthors [56] observed a tumor control of 94% with no visual impairments at a median follow-up of 49 months. Similar tumor control and low toxicity have been reported in other few series [59, 60]. While these initial results are promising, the optimal fractionated regimen in terms of tumor control, biochemical control, and risk of radiation-related adverse effects needs to be better elucidated in larger studies with appropriate number of patients and longer follow-up.

A few recent studies on fractionated SRS for vestibular schwannoma report local control rates of 92–100% using doses of 18 Gy in three fractions or 25 Gy in five fractions, with the majority of patients who maintain serviceable hearing and present low rates of trigeminal and facial nerve injury [43, 44, 62–64]. In a large study of 383 patients treated from 1999 to 2007 with fractionated SRS (18 Gy in 3 sessions) for an acoustic neuroma at the Stanford University Medical Centre, Hansasuta and coauthors [43] reported local control rates of 99% and 96% at 3 and 5 years, respectively. On 200 evaluable patients with serviceable hearing, the crude rate of hearing preservation was 76%, being significantly better for smaller acoustic neuromas. In another large multicenter retrospective series of 383 patients treated with fractionated SRS (25 Gy, five fractions) between 1995 and 2007, Patel and coauthors [44] observed a local control rate of 78.3% at a median follow-up of 72 months; however, only 2.3% of patients with an increase of tumor volume at MRI of greater than 20% required additional salvage therapy. After fractionated SRS, 51% of patients had serviceable hearing at the last follow-up; 9.4% of patients experienced new VII nerve defi-

cits, which was persistent in 3.9%. Similar local control, high preservation of serviceable hearing, and low rate of permanent trigeminal nerve or facial nerve toxicity have been reported by other authors [62–64].

Limitations

There have been numerous retrospective published studies suggesting that fractionated SRS may offer a better balance of efficacy and toxicity as compared with single-fraction SRS in patients with large brain tumors or tumors located in close proximity to critical brain structures. Moreover, the improved efficacy and less toxicity of hypofractionated schedules would also be expected by applying the LQ model, especially for malignant tumors. Although data indicate that fractionated SRS may represent an appropriate treatment for larger lesions, results should be interpreted with caution and understanding limitations; no prospective randomized studies have provided evidence to support the superiority of hypofractionation in terms of control and toxicity over other technical modalities, including single-fraction SRS or conventionally fractionated stereotactic RT. In addition, data reporting clinical outcomes of fractionated SRS are generally extracted from relatively small retrospective series with relatively short follow-up.

Another limitation is that dose constraints and recommendations for intracranial organs at risk when fractionated SRS is used are poorly known. Relationships between volume of normal tissue receiving different doses and complications are in fact extracted from small retrospective studies and need to be validated in larger prospective studies with appropriate follow-up. In addition, the applicability of *BED* based on the LQ model to estimate the effects of different SRS regimens remains a controversial issue. Nevertheless, published data indicate that relatively large lesions can be effectively treated by fractionated SRS respecting current dose-volume constraints, whereas single-fraction SRS is likely to exceed dose constraints. Of course, conventionally fractionated stereotactic radiotherapy remains the recommended treatment for very large lesions and/or involving critical brain structures.

Finally, a robust quality assurance program is mandatory to ensure the accuracy and safety of fractionated cranial SRS. Regardless of the technology used, all the technical aspects of cranial SRS, including accurate target delineation, highly conformal dose distribution to the target, minimal margin, submillimeter accuracy of patient positioning, and position monitoring, should always be employed.

Future Research

Recent published data have clearly suggested that fractionated SRS may offer a superior balance between efficacy and safety for large brain tumors or tumors in close proximity to sensitive structures as compared with single-fraction SRS. The rationale of fractionated SRS given in 3–5 fractions is to combine the high precision of SRS with the radiobiological advantages of fractionation. Future research is needed to identify the optimal application for dose and fractionation according to tumors size and location. Robust and prospective data will evaluate the dose/volume constraints for all organs at risk, including the optic pathway, cranial nerves, brainstem, cochlea, pituitary gland, and pituitary stalk to limit the long-term neurological, neurocognitive, and hormonal consequences of fractionated SRS. Specifically, randomized trials need to assess the superiority of fractionated SRS versus single-fraction SRS and fractionated stereotactic RT with regard to local control, radiation-induced toxicity, and quality of life in the setting of newly diagnosed and recurrent brain tumors.

Other research fields include the combination of fractionated SRS with new targeted agents and immunotherapy for the treatment of brain metastases [65–67]. Recent advances in the knowledge of the immunostimulatory effects of irradiation have provided evidence that radiation can induce direct antitumor immune response through the release of cancer cell antigens to the immune system, thus resulting in improved local and distant control [68]. When RT is used alone, these effects are generally insufficient at subverting the tumor-specific immunosuppression that is present in cancer patients. However, when combined with immunotherapy, such as immune checkpoint blockade, localized RT can effectively immunize the patient against the irradiated tumor, converting the tumor into an individualized in situ vaccine. Regression of metastatic cancer at distant sites that are not irradiated was described and defined as the abscopal effect (from "ab scopus," i.e., away from the target). Interestingly, evidence from murine systems has shown that fractionated irradiation (3 × 8 Gy vs 20 Gy given in single fraction), when combined with anti-CTLA-4 therapy, is more likely to generate abscopal reactions in distant nonirradiated tumors than single high doses [69, 70]. Future trials are required to evaluate the optimal dose/fractionation and timing of SRS given in combination with immunotherapy and new targeted agents with regard to local and distant control and toxicity.

Practical Considerations

- In clinical practice, fractionated SRS is employed as an alternative to single-fraction SRS for relatively large tumors or tumors located in proximity to critical brain structures, since single doses may carry a higher risk of neurological complications.
- For intact or resected brain metastases, fractionated SRS, using total doses of 24–27 Gy given in three fractions or 30–35 Gy given in five fractions, results in local control rates of 70–90% with an acceptable risk of radiation-

induced neurological toxicity. Similar regimens are employed for patients with small- and moderate-sized recurrent tumors, such as gliomas, atypical or malignant meningiomas, and ependymomas, who have already received a full course of RT. For brainstem metastases, doses of 18 Gy given in three fractions are usually recommended.

- Fractionated SRS, usually 25 Gy in five fractions, may represent a safer treatment option than single-fraction SRS for large complex benign skull base tumors larger than 3 cm or in close proximity to the optic chiasm, when single doses to the optic apparatus exceed 8–10 Gy.
- Currently, no data support the use of fractionated SRS for patients with very large lesions or lesions involving the optic apparatus; in such cases, conventionally fractionated stereotactic RT would be the recommended radiation treatment.

References

1. Leksell L. Stereotactic radiosurgery. J Neurol Neurosurg Psychiatry. 1983;46:797–803.
2. Shaw E, Scott C, Souhami L, Dinapoli R, Kline R, Loeffler J, et al. Single dose radiosurgical treatment of recurrent previously irradiated primary brain tumors and brain metastases: final report of RTOG protocol 90-05. Int J Radiat Oncol Biol Phys. 2000;47:291–8.
3. Kirkpatrick JP, Soltys SG, Lo SS, Beal K, Shrieve DC, Brown PD. The radiosurgery fractionation quandary: single fraction or hypofractionation? Neuro-Oncology. 2017;19:ii38–49.
4. Chang SD, Adler JR Jr. Current status and optimal use of radiosurgery. Oncology (Williston Park). 2001;15:209–16; discussion 219–21
5. Shrieve DC. Basic principles of radiobiology applied to radiotherapy of benign intracranial tumors. Neurosurg Clin N Am. 2006;17:67–78.
6. Fowler JF. The linear-quadratic formula and progress in fractionated radiotherapy. Br J Radiol. 1989;62:679–94.
7. Song CW, Cho LC, Yuan J, Dusenbery KE, Griffin RJ, Levitt SH. Radiobiology of stereotactic body radiation therapy/stereotactic radiosurgery and the linear-quadratic model. Int J Radiat Oncol Biol Phys. 2013;87:18–9.
8. Williams MV, Denekamp J, Fowler JF. A review of alpha/beta ratios for experimental tumors: implications for clinical studies of altered fractionation. Int J Radiat Oncol Biol Phys. 1985;11:87–96.
9. Hall EJ, Brenner DJ. The radiobiology of radiosurgery: rationale for different treatment regimes for AVMs and malignancies. Int J Radiat Oncol Biol Phys. 1993;25:381–5.
10. Santacroce A, Kamp MA, Budach W, Hänggi D. Radiobiology of radiosurgery for the central nervous system. Biomed Res Int. 2013;2013:362761.
11. Fowler JF. 21 years of biologically effective dose. Br J Radiol. 2010;83:554–68.
12. Kirkpatrick JP, Meyer JJ, Marks LB. The linear-quadratic model is inappropriate to model high dose per fraction effects in radiosurgery. Semin Radiat Oncol. 2008;18:240–3.
13. Joiner M. Quantifying cell kill and survival. In: Joiner M, Van der Kogel A, editors. Basic clinical radiobiology. 4th ed. London: Hodder Arnold; 2009. p. 102–19.
14. Minniti G, Scaringi C, Clarke E, Valeriani M, Osti M, Enrici RM. Frameless linac-based stereotactic radiosurgery (SRS) for brain metastases: analysis of patient repositioning using a mask fixation system and clinical outcomes. Radiat Oncol. 2011;6:158.
15. Rahimian J, Chen JC, Rao AA, Girvigian MR, Miller MJ, Greathouse HE. Geometrical accuracy of the Novalis stereotactic radiosurgery system for trigeminal neuralgia. J Neurosurg. 2004;101(Suppl 3):351–5.
16. Wurm RE, Erbel S, Schwenkert I, Gum F, Agaoglu D, Schild R, et al. Novalis frameless image-guided noninvasive radiosurgery: initial experience. Neurosurgery. 2008;62(Suppl):A11–7.
17. Lamba M, Breneman JC, Warnick RE. Evaluation of image-guided positioning for frameless intracranial radiosurgery. Int J Radiat Oncol Biol Phys. 2009;74:913–9.
18. Ramakrishna N, Rosca F, Friesen S, Tezcanli E, Zygmanszki P, Hacker F. A clinical comparison of patient setup and intra-fraction motion using frame based radiosurgery versus a frameless image-guided radiosurgery system for intracranial lesions. Radiother Oncol. 2010;95:109–15.
19. Gevaert T, Verellen D, Tournel K, Linthout N, Bral S, Engels B, et al. Setup accuracy of the Novalis ExacTrac 6DOF system for frameless radiosurgery. Int J Radiat Oncol Biol Phys. 2012;82:1627–35.
20. Clark BG, Souhami L, Pla C, Al-Amro AS, Bahary JP, Villemure JG, et al. The integral biologically effective dose to predict brain stem toxicity of hypofractionated stereotactic radiotherapy. Int J Radiat Oncol Biol Phys. 1998;40:667–75.
21. Timmerman RD. An overview of hypofractionation and introduction to this issue of seminars in radiation oncology. Semin Radiat Oncol. 2008;18:215–22.
22. Kirkpatrick JP, van der Kogel AJ, Schultheiss TE. Radiation dose-volume effects in the spinal cord. Int J Radiat Oncol Biol Phys. 2010;76(3 Suppl):S42–9.
23. Marks LB, Yorke ED, Jackson A, Ten Haken RK, Constine LS, Eisbruch A, et al. Use of normal tissue complication probability models in the clinic. Int J Radiat Oncol Biol Phys. 2010;76(3 Suppl):S10–9.
24. Mayo C, Martel MK, Marks LB, Flickinger J, Nam J, Kirkpatrick J. Radiation dose-volume effects of optic nerves and chiasm. Int J Radiat Oncol Biol Phys. 2010;76(3 Suppl):S28–35.
25. Kirkpatrick JP, Marks LB, Mayo CS, Lawrence YR, Bhandare N, Ryu S. Estimating normal tissue toxicity in radiosurgery of the CNS: application and limitations of QUANTEC. J Radiosurg SBRT. 2011;1:95–107.
26. Minniti G, Esposito V, Clarke E, Scaringi C, Bozzao A, Falco T, et al. Fractionated stereotactic radiosurgery for patients with skull base metastases from systemic cancer involving the anterior visual pathway. Radiat Oncol. 2014;9:110.
27. Hiniker SM, Modlin LA, Choi CY, Atalar B, Seiger K, Binkley MS, et al. Dose-Response Modeling of the Visual Pathway Tolerance to Single-Fraction and Hypofractionated Stereotactic Radiosurgery. Semin Radiat Oncol. 2016;26:97–104.
28. Minniti G, Scaringi C, Paolini S, Lanzetta G, Romano A, Cicone F, et al. Single-Fraction Versus Multifraction (3 × 9 Gy) Stereotactic Radiosurgery for Large (>2 cm) Brain Metastases: A Comparative Analysis of Local Control and Risk of Radiation-Induced Brain Necrosis. Int J Radiat Oncol Biol Phys. 2016;95:1142–8.
29. Minniti G, D'Angelillo RM, Scaringi C, Trodella LE, Clarke E, Matteucci P, et al. Fractionated stereotactic radiosurgery for patients with brain metastases. J Neuro-Oncol. 2014;117:295–301.
30. Aoyama H, Shirato H, Onimaru R, Kagei K, Ikeda J, Ishii N, et al. Hypofractionated stereotactic radiotherapy alone without whole brain irradiation for patients with solitary and oligo brain metastasis using noninvasive fixation of the skull. Int J Radiat Oncol Biol Phys. 2003;56:793–800.
31. Ernst-Stecken A, Ganslandt O, Lambrecht U, Sauer R, Grabenbauer G. Phase II trial of hypofractionated stereotactic radiotherapy

for brain metastases: results and toxicity. Radiother Oncol. 2006;8:18–24.
32. Murai T, Ogino H, Manabe Y, Iwabuchi M, Okumura T, Matsushita Y, et al. Fractionated stereotactic radiotherapy using CyberKnife for the treatment of large brain metastases: a dose escalation study. Clin Oncol (R Coll Radiol). 2014;26:151–8.
33. Kim JW, Park HR, Lee JM, Kim JW, Chung HT, Kim DG, et al. Fractionated stereotactic gamma knife radiosurgery for large brain metastases: a retrospective, single center study. PLoS One. 2016;11:e0163304.
34. Minniti G, Esposito V, Clarke E, Scaringi C, Lanzetta G, Salvati M, et al. Multidose stereotactic radiosurgery (9 Gy × 3) of the postoperative resection cavity for treatment of large brain metastases. Int J Radiat Oncol Biol Phys. 2013;86:623–9.
35. Ahmed KA, Freilich JM, Abuodeh Y, Figura N, Patel N, Sarangkasiri S, et al. Fractionated stereotactic radiotherapy to the post-operative cavity for radioresistant and radiosensitive brain metastases. J Neuro-Oncol. 2014;118:179–86.
36. Ling DC, Vargo JA, Wegner RE, Flickinger JC, Burton SA, Engh J, et al. Postoperative stereotactic radiosurgery to the resection cavity for large brain metastases: clinical outcomes, predictors of intracranial failure, and implications for optimal patient selection. Neurosurgery. 2015;76:150–6; discussion 156–7.
37. Gutin PH, Iwamoto FM, Beal K, Mohile NA, Karimi S, Hou BL, et al. Safety and efficacy of bevacizumab with hypofractionated stereotactic irradiation for recurrent malignant gliomas. Int J Radiat Oncol Biol Phys. 2009;75:156–63.
38. McKenzie JT, Guarnaschelli JN, Vagal AS, Warnick RE, Breneman JC. Hypofractionated stereotactic radiotherapy for unifocal and multifocal recurrence of malignant gliomas. J Neuro-Oncol. 2013;113:403–9.
39. Minniti G, Scaringi C, De Sanctis V, Lanzetta G, Falco T, Di Stefano D, et al. Hypofractionated stereotactic radiotherapy and continuous low-dose temozolomide in patients with recurrent or progressive malignant gliomas. J Neuro-Oncol. 2013;111:187–94.
40. Colombo F, Casentini L, Cavedon C, Scalchi P, Cora S, Francescon P. Cyberknife radiosurgery for benign meningiomas: short-term results in 199 patients. Neurosurgery. 2009;64(2 Suppl):A7–13.
41. Bria C, Wegner RE, Clump DA, Vargo JA, Mintz AH, Heron DE, et al. Fractionated stereotactic radiosurgery for the treatment of meningiomas. J Cancer Res Ther. 2011;7:52–7.
42. Iwata H, Sato K, Tatewaki K, Yokota N, Inoue M, Baba Y, et al. Hypofractionated stereotactic radiotherapy with CyberKnife for nonfunctioning pituitary adenoma: high local control with low toxicity. Neuro-Oncology. 2011;13:916–22.
43. Hansasuta A, Choi CYH, Gibbs IC. Multisession stereotactic radiosurgery for vestibular schwannomas: single-institution experience with 383 cases. Neurosurgery. 2011;69:1200–9.
44. Patel MA, Marciscano AE, Hu C, Jusué-Torres I, Garg R, Rashid A, et al. Long-term treatment response and patient outcomes for vestibular Schwannoma patients treated with hypofractionated stereotactic radiotherapy. Front Oncol. 2017;7:200.
45. Fahrig A, Ganslandt O, Lambrecht U, Grabenbauer G, Kleinert G, Sauer R, et al. Hypofractionated stereotactic radiotherapy for brain metastases--results from three different dose concepts. Strahlenther Onkol. 2007;183:625–30.
46. Narayana A, Chang J, Yenice K, Chan K, Lymberis S, Brennan C, et al. Hypofractionated stereotactic radiotherapy using intensity-modulated radiotherapy in patients with one or two brain metastases. Stereotact Funct Neurosurg. 2007;85:82–7.
47. Wegner RE, Leeman JE, Kabolizadeh P, Rwigema JC, Mintz AH, Burton SA, et al. Fractionated stereotactic radiosurgery for large brain metastases. Am J Clin Oncol. 2015;38:135–9.
48. Eaton BR, LaRiviere MJ, Kim S, Prabhu RS, Patel K, Kandula S, et al. Hypofractionated radiosurgery has a better safety profile than single fraction radiosurgery for large resected brain metastases. J Neuro-Oncol. 2015;123:103–11.
49. Wang CC, Floyd SR, Chang CH, Warnke PC, Chio CC, Kasper EM, et al. Cyberknife hypofractionated stereotactic radiosurgery (HSRS) of resection cavity after excision of large cerebral metastasis: efficacy and safety of an 800 cGy × 3 daily fractions regimen. J Neuro-Oncol. 2012;106:601–10.
50. Minniti G, Agolli L, Falco T, Scaringi C, Lanzetta G, Caporello P, et al. Hypofractionated stereotactic radiotherapy in combination with bevacizumab or fotemustine for patients with progressive malignant gliomas. J Neuro-Oncol. 2015;122:559–66.
51. Clarke J, Neil E, Terziev R, Gutin P, Barani I, Kaley T, et al. Multicenter, phase 1, dose escalation study of hypofractionated stereotactic radiation therapy with bevacizumab for recurrent glioblastoma and anaplastic astrocytoma. Int J Radiat Oncol Biol Phys. 2017;99:797–804.
52. Minniti G, Amichetti M, Enrici RM. Radiotherapy and radiosurgery for benign skull base meningiomas. Radiat Oncol. 2009;4:42.
53. Régis J, Carron R, Delsanti C, Porcheron D, Thomassin JM, Murracciole X, et al. Radiosurgery for vestibular schwannomas. Neurosurg Clin N Am. 2013;24:521–30.
54. Minniti G, Osti MF, Niyazi M. Target delineation and optimal radiosurgical dose for pituitary tumors. Radiat Oncol. 2016;11:135.
55. Navarria P, Pessina F, Cozzi L, Clerici E, Villa E, Ascolese AM, et al. Hypofractionated stereotactic radiation therapy in skull base meningiomas. J Neuro-Oncol. 2015;124:283–9.
56. Adler JR Jr, Gibbs IC, Puataweepong P, Chang SD. Visual field preservation after multisession cyberknife radiosurgery for perioptic lesions. Neurosurgery. 2008;62(Suppl 2):733–43.
57. Tuniz F, Soltys SG, Choi CY, Chang SD, Gibbs IC, Fischbein NJ, et al. Multisession cyberknife stereotactic radiosurgery of large, benign cranial base tumors: preliminary study. Neurosurgery. 2009;65:898–907.
58. Han J, Girvigian MR, Chen JC, Miller MJ, Lodin K, Rahimian J, et al. A comparative study of stereotactic radiosurgery, hypofractionated, and fractionated stereotactic radiotherapy in the treatment of skull base meningioma. Am J Clin Oncol. 2014;37:255–60.
59. Killory BD, Kresl JJ, Wait SD, Ponce FA, Porter R, White WL. Hypofractionated CyberKnife radiosurgery for perichiasmatic pituitary adenomas: early results. Neurosurgery. 2009;64(2 Suppl):A19–25.
60. Liao HI, Wang CC, Wei KC, Chang CN, Hsu YH, Lee ST, et al. Fractionated stereotactic radiosurgery using the Novalis system for the management of pituitary adenomas close to the optic apparatus. J Clin Neurosci. 2014;21:111–5.
61. Iwata H, Sato K, Nomura R, Tabei Y, Suzuki I, Yokota N, et al. Long-term results of hypofractionated stereotactic radiotherapy with CyberKnife for growth hormone-secreting pituitary adenoma: evaluation by the Cortina consensus. J Neuro-Oncol. 2016;128:267–75.
62. Kapoor S, Batra S, Carson K, Shuck J, Kharkar S, Gandhi R, et al. Long-term outcomes of vestibular schwannomas treated with fractionated stereotactic radiotherapy: an institutional experience. Int J Radiat Oncol Biol Phys. 2011;81:647–53.
63. Tsai JT, Lin JW, Lin CM. Clinical evaluation of cyberknife in the treatment of vestibular schwannomas. Biomed Res Int. 2013;2013:297093.
64. Vivas EX, Wegner R, Conley G. Treatment outcomes in patients treated with CyberKnife radiosurgery for vestibular schwannoma. Otol Neurotol. 2014;35:162–70.
65. Rudà R, Franchino F, Soffietti R. Treatment of brain metastasis: current status and future directions. Curr Opin Oncol. 2016;28:502–10.
66. Trino E, Mantovani C, Badellino S, Ricardi U, Filippi AR. Radiosurgery/stereotactic radiotherapy in combination with immunotherapy and targeted agents for melanoma brain metastases. Expert Rev Anticancer Ther. 2017;17:347–56.

67. Di Lorenzo R, Ahluwalia MS. Targeted therapy of brain metastases: latest evidence and clinical implications. Ther Adv Med Oncol. 2017;9:781–96.
68. Demaria S, Golden EB, Formenti SC. Role of Local Radiation Therapy in Cancer Immunotherapy. JAMA Oncol. 2015;1:1325–32.
69. Dewan MZ, Galloway AE, Kawashima N, Dewyngaert JK, Babb JS, Formenti SC, et al. Fractionated but not single-dose radiotherapy induces an immune-mediated abscopal effect when combined with anti-CTLA-4 antibody. Clin Cancer Res. 2009;15:5379–88.
70. Habets TH, Oth T, Houben AW, Huijskens MJ, Senden-Gijsbers BL, Schnijderberg MC, et al. Fractionated radiotherapy with 3 × 8 Gy induces systemic anti-tumour responses and abscopal tumour inhibition without modulating the humoral anti-tumour response. PLoS One. 2016;11:e0159515.

Charged-Particle Proton Radiosurgery

Arpit M. Chhabra, Mudit Chowdhary,
and Minesh P. Mehta

Introduction/History

The origins of intracranial SRS date back to 1951 when Dr. Lars Leksell first proposed the concept. The underlying basis of SRS is to utilize multiple, noncoplanar beam angles that isocentrically converge on the target volume; limiting the dose along each beam path ensures low-dose exposure of tissues in the path of the beam, whereas the central convergence ensures a high target dose. This methodology therefore allows for the delivery of hypofractionated regimens of high doses per fraction in one or a small number of treatments. Over the years, there has been a rapid increase in the adoption of intracranial SRS for a wide range of benign and malignant intracranial conditions, including, but not limited to, arteriovenous malformation (AVM), acoustic neuroma, pituitary adenoma, meningioma, trigeminal neuralgia, and metastatic tumors [1]. There has been rapid development of systems that allow for SRS delivery, primarily utilizing photon-based approaches. The utilization of proton beam therapy for SRS and/or fractionated stereotactic radiotherapy (FSRT) has to date been limited, in large measure due to the rapid proliferation of excellent photon SRS technologies and lack of rapid technology development in the proton sphere. However, given the superior dose distribution of proton radiation, and the burgeoning number of proton centers, as well as a spurt in technological development, there is a renaissance in evaluating the merits of proton-based SRS and/or FSRT.

Proton-based SRS was first pioneered by Dr. Raymond Kjellberg in 1960 at the Harvard Cyclotron Laboratory [2]. The initial phases of the program utilized a fixed beam with a couch that had to be manually maneuvered, thereby resulting in lengthy treatment sessions with limited availability of beam angles. However, under the guidance of Dr. Paul Chapman, the program progressed in developing the STAR device, in which the patient's head frame was attached to a couch apparatus that could be rotated relative to the fixed beam, thereby allowing increased degrees of freedom (Fig. 1a, b). With the ultimate advent of the mounted mobile beam nozzle on a gantry, analogous to modern-day proton units, full degrees of freedom were achievable (Fig. 2). Since the 1960s, multiple outcomes and toxicity data have been published evaluating the use of proton-based SRS/FSRT treatments for many indications. Herein, we provide a comprehensive review of the available dosimetric and clinical data.

A. M. Chhabra
Central Connecticut Radiation Oncology, PC, Department of Radiation Oncology, Middletown, CT, USA

M. Chowdhary
Rush University Medical Center, Department of Radiation Oncology, Chicago, IL, USA

M. P. Mehta (✉)
Miami Cancer Institute—Baptist Health South Florida, Department of Radiation Oncology, Miami, FL, USA
e-mail: mineshm@baptisthealth.net

D. M. Trifiletti et al. (eds.), *Stereotactic Radiosurgery and Stereotactic Body Radiation Therapy*,
https://doi.org/10.1007/978-3-030-16924-4_9

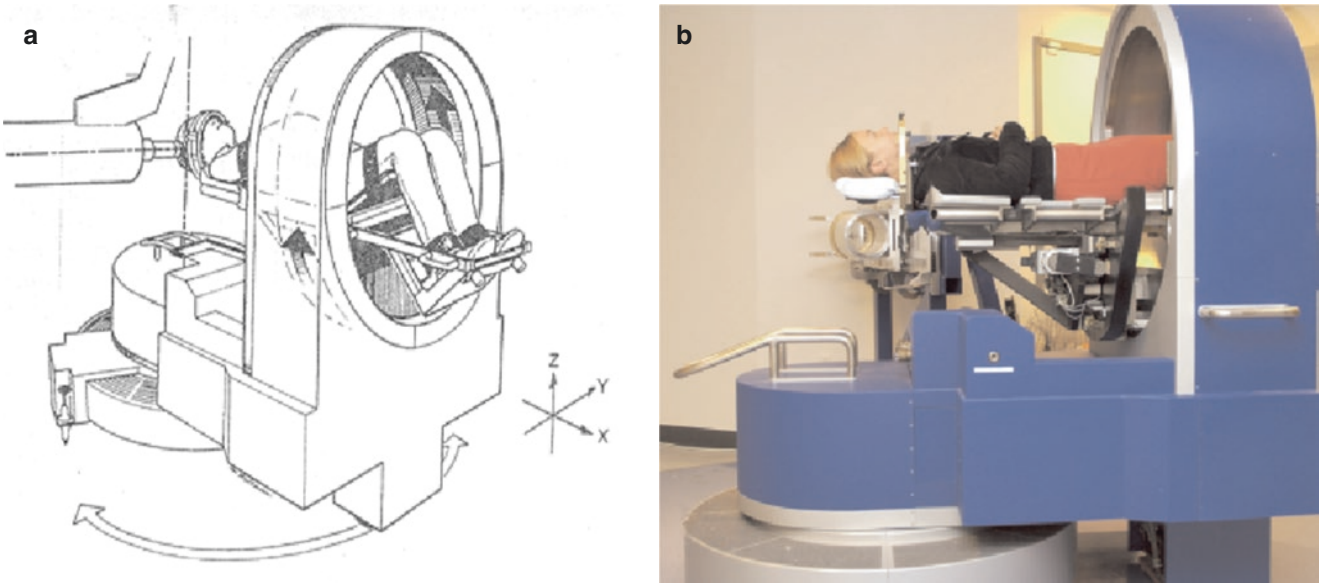

Fig. 1 (**a**, **b**) STAR Device as developed at the MGH-Northeast Proton Therapy Center. The patient's head frame is mounted to a rotating couch, with a directed fixed proton beam line thereby allowing five degrees of freedom (three linear motions and two rotational). (Used with permission from Chen et al. [2])

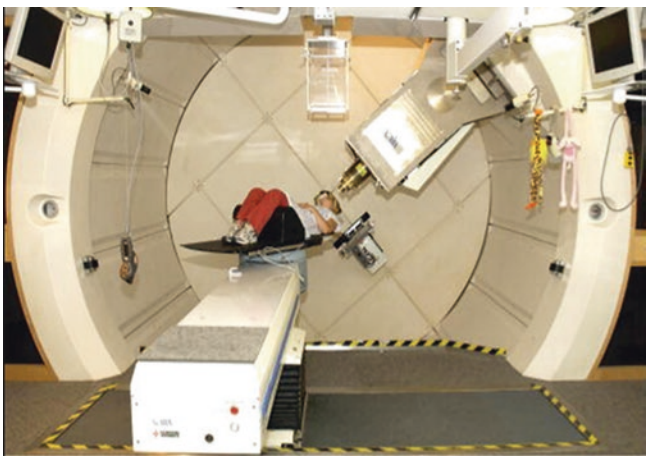

Fig. 2 Modern-day proton therapy unit utilizing a mounted proton beam line on a rotatable gantry with six degrees of freedom on a robotic patient positioning couch. (Used with permission from Chen et al. [2])

Dosimetric Data

Verhey and coauthors conducted one of the earliest dosimetric comparisons between photon and proton radiation therapy techniques for stereotactic radiosurgery of intracranial lesions [3]. In their analysis, they compared the dose-volume histograms for target and nontarget brain tissue for five patients with intracranial lesions treated with the following plans: Gamma Knife (GK), a five-field passively scattered proton plan, or a linear accelerator (linac) arc-based technique. The authors reported that the choice of optimal modality, as judged by the ability to reduce nontarget dose, was a function of size of the lesion, shape of the lesion, and location. For small regular target volumes, the proton plan was actually found to deliver more doses to the normal brain tissue, as a result of needing larger treatment planning margins to account for proton uncertainty, whereas for large regular targets, proton plans produced the greatest dosimetric benefit. For irregularly shaped lesions, both proton and GK plans were dosimetrically superior with respect to higher conformality than achievable with the arc-based treatments due to the restricted number of isocenters utilized for the linac plans. With regard to location, the more peripheral a tumor, the larger the dosimetric sparing achieved with protons, given the stopping ability relative to GK and linac photon beams.

In a companion paper, this group analyzed the tumor control probability (TCP) and normal tissue complication probability (NTCP) based on the DVH information from the abovementioned study. By comparing the various plans (linac vs. GK vs. protons) using biological assumptions, the authors concluded the superiority of proton beam therapy in reducing complication probabilities primarily for large target volumes and for those situated peripherally, whereas the advantage diminished with smaller centrally located tumors [4].

Baumert and colleagues conducted a dosimetric comparison of six intracranial lesions receiving stereotactic radiation therapy with IMRT, single-field optimized proton plans (SFO-PT), or multi-field optimized proton plans (MFO-PT/IMPT) to doses that ranged from ultra-hypofractionation to conventional fractionation [5, 6]. Their analysis revealed similar plan conformality with RTOG conformality indices of 1.03, 1.04, and 1.03 for IMRT, SFO-PT, and MFO-PT/

IMPT plans, respectively. However, similar levels of conformality were achieved with proton planning, albeit with fewer fields (~three fields) than with photon planning which generally needed a median of five fields. In comparing the amount of the normal tissue outside the PTV that received 20 to 90% of the prescription dose, IMPT had the greatest volume sparing effect for tissue receiving 20 to 50% of prescription dose. Minimal difference was seen among techniques when evaluating the volume of normal tissue receiving >50% of prescription dose.

Serago and colleagues compared target coverage of four hypothetical intracranial target volumes planned using the following techniques: (a) four, noncoplanar, multiple-arc, circular X-ray beams with single or multiple isocenters; (b) noncoplanar, irregular X-ray beam shaping with a single isocenter using either static IMRT or arc therapy; and (c) noncoplanar, irregular passively scattered proton plan with a single isocenter using 5 or 13 fields [7]. The target volumes selected were meant to represent a sampling of different shapes, sizes, and locations of lesions including nearly spherical and also irregularly shaped targets. The proton plans consistently yielded equal or superior results compared to X-ray techniques in reducing the integral dose to normal brain outside the target, with the greatest benefit present in the less than the 50% isodose region. Only minimal differences were observed between the 5 and 13 field proton plans. This normal tissue sparing effect reported by Serago and colleagues is analogous with the results of Baumert and colleagues.

Clinical Data

Meningioma

In contrast to the abundance of outcomes data for conventionally fractionated proton beam therapy in the management of meningiomas [8–12], studies utilizing radiosurgery or fractionated stereotactic proton therapy remain limited to a small set of institutions. Nevertheless, these data consistently reveal the ability to achieve excellent local control rates as will be highlighted in this section [13]. Vernimmen and colleagues reported one of the earliest experiences of 23 patients receiving proton beam therapy for the management of skull base meningiomas. Seventy-eight percent ($n = 18$) of the patients received a hypofractionated stereotactic regimen (HSRT) of 20.3 CGyE in 3 fractions, whereas 22% of the patients received fractionated stereotactic regimens (SRT) of 54.1–61.6 CGyE in 16–28 fractions [14]. With a mean follow-up of 40 months, the HSRT group achieved a 5-year local control rate of 88%, whereas the SRT group achieved a control rate of 100%. With respect to toxicity, in the HSRT group, 11% ($n = 2$) of the patients developed a transient new cranial neuropathy after treatment, whereas 11% ($n = 2$) developed a late side effect. In the SRT group, no acute toxicity was observed, whereas one patient suffered short-term memory disturbance. Overall, the control rates compared favorably to previously reported series utilizing photon-based SRS techniques. For instance, Morita and colleagues achieved a 5-year progression-free survival rate of 95% for skull base meningiomas after GK radiosurgery to a median tumor margin dose of 16 Gy [15]. Similarly, Chang and colleagues achieved 2-year control rate of 100% for cavernous sinus meningiomas treated with multiple noncoplanar linac arc SRS to a median dose of 17.7 Gy [16]. In summary, the results of this series demonstrated that proton irradiation was both safe and effective in the management of skull base meningiomas, especially for large irregularly shaped lesions.

The group from Uppsala, Sweden, compared their outcomes and toxicity data in a pilot study using hypofractionated passively scattered proton beam therapy for the treatment of skull base meningiomas [17]. Nineteen patients were analyzed, of which 79% ($n = 15$) had undergone prior surgical resection for a WHO Grade I meningioma, whereas the remaining 21% had either refused surgery or were deemed unresectable. All patients received a dose of 24 Gy in four 6-Gy fractions. With a minimum follow-up of 36 months, no patient was noted to have tumor progression. Two patients developed delayed edema 6 months after treatment, which responded to corticosteroids. None of the 19 patients developed any late cranial nerve dysfunction during follow-up.

In 2017, this group updated their series with a total of 170 patients receiving hypofractionated proton beam therapy as adjuvant or primary treatment for WHO Grade I benign meningiomas [18]. Of note, 91% of tumors were situated at the skull base. Passively scattered proton beam therapy was utilized for all patients with the majority of the patients (91%) receiving either a dose of 24 Gy in 4 fractions or 20 Gy in 4 fractions. The 5-year and 10-year PFS rates were 93% and 85%, respectively. With respect to toxicity, 2.9% of the patients suffered from radiation necrosis, whereas 4.4% of the patients displayed either visual deterioration or visual field deficits during follow-up. Additionally, 7.4% of the patients developed pituitary insufficiency during follow-up requiring medical supplementation.

In 2011, the group from Harvard reported their retrospective results using passively scattered proton SRS in 50 patients with 51 benign meningiomas [19]. In contrast to the prior studies which treated larger lesions, patients in this series were eligible for treatment with proton SRS only if the tumors were $\leq$4 cm in maximum diameter and were located $\geq$2 mm from the optic nerves and chiasm. Seventy-five percent ($n = 38$) of the lesions were at the skull base. Sixty-four percent of meningiomas were diagnosed radiographically, whereas 36% of tumors were diagnosed histologically. Median prescribed dose was 13 Gy with the goal

of having the 90% isodose encompass the PTV. With a median follow-up of 32 months, 3-year local control was 94%. Thirty-four patients with symptoms prior to treatment had adequate follow-up with 47% displaying improvement of symptoms, 44% showing unchanged symptoms, and 9% having symptom worsening. With regard to treatment-related toxicity, acute and late toxicity was only seen in 5.9% and 5.9% of the patients, respectively. No patients were noted to develop additional cranial nerve deficits following treatment. These control rates are analogous to those achieved by comparable published photon SRS series [20]. Additionally, the authors of this series provided a pictorial comparison of proton and photon SRS dose distribution for a left cavernous sinus meningioma showing the lower integral dose with proton therapy and potential for a lower risk of late sequelae (Fig. 3).

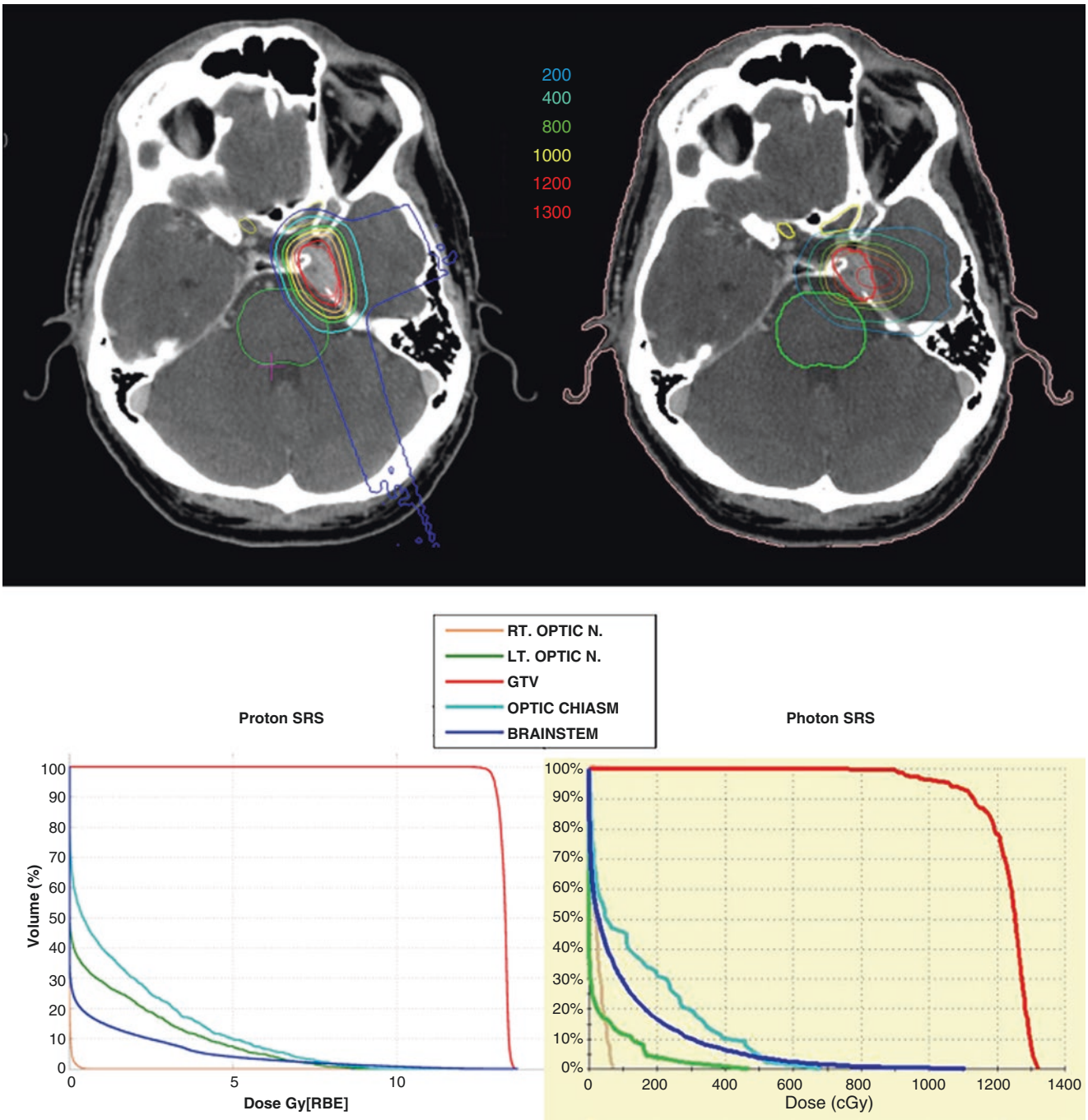

Fig. 3 Dose distribution comparison for a proton and photon SRS treatment for a left cavernous sinus meningioma. (Used with permission of Elsevier from Halasz et al. [19])

While the aforementioned series display that passively scattered proton beam therapy can serve an excellent modality, especially for skull base lesions, there is a paucity of data on the use of spot-scanning/intensity-modulated proton therapy fractionated stereotactic or radiosurgery techniques.

Practical Considerations When Utilizing PBT for Meningiomas

- Consider the volume of disease as well as its shape and location, especially its proximity to critical organs. Protons provide an enhanced dosimetric benefit over photon approaches for tumors that are larger and/or irregularly shaped; however, if the critical organ-at-risk (OAR) is immediately adjacent to the tumor, considerations of the end-of-range falling within the OAR could result in a degraded plan, and the possibility of an inferior lateral penumbra from protons, relative to photon radiosurgery techniques, could actually result in inferior OAR dosimetry from proton therapy.
- For small-sized lesions, consider single-session proton SRS as this approach excellent outcomes and enhanced dosimetric benefits over photon-based SRS approaches in certain select situations; however, photon SRS for small lesions, and especially geometrically symmetric lesions, can provide excellent dosimetric coverage which often will clinically not be surpassed by a proton plan; it must also be remembered that for very small targets, the lower spot size limit of pencil-beam scanning could provide another challenge [19].
- For large-sized lesions, including those arising from the cavernous sinus or skull base, consider that hypofractionated proton beam therapy achieves excellent outcomes with lower toxicity rates [14, 18].
- Consider referral to endocrinology for patients receiving proton beam therapy for centrally situated meningiomas, given the risk of late pituitary insufficiency.
- For lesions in and around the optic pathway, always involve a neuro-ophthalmologist in the care team.

Arteriovenous Malformations

An arteriovenous malformation (AVM) is an abnormal communication between arterioles and venules, without an intervening capillary bed, which creates a high-flow, turbulent flow situation through thin-walled vessels, highly susceptible to rupture and hemorrhage. The point of abnormal connection is termed the nidus and represents the radiation therapy target to achieve obliteration [2]. Given the occurrence of these lesions in younger patients, proton beam therapy presents a unique opportunity to limiting the overall integral dose while delivering the high doses necessary for obliteration [13].

In 1983, the group from the Massachusetts General Hospital (MGH), led by Kjellberg and colleagues, published the first series on the use of proton SRS for the management of AVMs [21]. They reviewed the results of the first 75 patients treated who had ≥2 years of follow-up, as well as the course of all 205 patients treated up to 1980, irrespective of follow-up time. The 90% isodose line was prescribed to the margin of the lesion, as determined by angiograms. The marginal dose was determined based on the size of the malformation, utilizing prior published data on isoeffective doses that correlate with the risk of brain necrosis. Median marginal doses were 16.5 Gy (range, 7.2–33 Gy) [22]. Follow-up arteriogram findings were available for 62 patients and revealed total obliteration greater than 50% reduction and no change in 20%, 56%, and 13% of cases, respectively. No lesion displayed any worsening on follow-up arteriograms. Four of the initial 27 patients incurred a complication. As a result, the group revised their planning and prescription technique and subsequently had no procedure-induced new persistent deficit in any patient. Additionally, no patient died of proton-related hemorrhage, thromboembolic events, or infection. Given these results, they subsequently continued utilizing proton beam therapy for AVMs not manageable by other means.

This supported the continued use of single-fraction proton beam stereotactic radiosurgery for AVMs at MGH, and in 2014, they reported additional results reviewing their modern experience of 254 lesions treated from 1991 to 2010 [23]. Of note, lesions with an AVM nidus generally >10–14 cc, nidus in a central/eloquent location (brainstem, basal ganglia, motor strip), or both were generally treated with a 2-fraction proton SRS approach, which will be discussed separately below. In this series, 9% of lesions had previously received radiation before 1991 with single-fraction SRS to a median dose of 12 Gy, with a median of 10 years to the second treatment. Median AVM nidus size in this report was 3.5 cc. All patients received SRS single treatment using 2–4 beams using passively scattered proton therapy to a median prescription dose of 15 Gy (range, 10–20 Gy (RBE)) targeting the entire nidus. Patients underwent yearly MRI, angiography, or both, with primary outcome being AVM obliteration with results defined as total (entire obliteration), partial (<100% obliteration), or stable disease (no change in nidus size). With a median follow-up of 35 months, total and partial obliterations rates were 64.6% and 35.4%, respectively, with a median time to obliteration of 31 months. The 5- and 10-year cumulative incidences of obliteration were 70 and 91%, respectively. On multivariate analysis, critical/deep location and target volume/nidus size were associated with lower rates of obliteration. Of note, after receiving proton SRS, 5.1% of lesions hemorrhaged with a 5-year cumulative incidence of 7%. With regard to acute and long-term complications, the majority of the patients (88%) experienced no

acute side effects. About 7.9% of the patients experienced mild seizures acutely, which were self-limiting. Additionally, the most common long-term side effect was also seizures, in 9.1% of the patients, controlled with antiepileptics. Apart from this, one patient developed memory disturbances at 1-year post-treatment, whereas another patient developed partial right hemiplegia 1-year post-treatment despite total obliteration of a left frontal AVM. These rates of obliteration with proton SRS compare favorably to those reported using Gamma Knife or linac-based approaches for similarly sized AVMs [24, 25].

For larger lesions, and those situated in critical areas such as the thalamus or brainstem, the group from MGH completed a retrospective review of 1250 patients treated with single-fraction proton SRS [26]. In this analysis published in 2003, they evaluated 1250 patients with median treatment volume of 33.7 cc with 77% of lesions being larger than 10 cc. The median treatment dose was 10.5 Gy, dose selection being based on the Kjellberg isoeffective doses for brain necrosis. With a median follow-up of 6.5 years, 4.1% of the patients suffered permanent neurological complications with a median time to complication of 1.1 years. Of note, the rate of complications correlated with treatment dose, with only 0.5% of the patients suffering a complication below 12 Gy. On the contrary, the median dose for a patient with a complication was 17 Gy. Additionally, a thalamic or brainstem location predicted a higher rate of complications.

As a result of these increased toxicities, the group at MGH transitioned to a 2-fraction proton SRS approach for high-risk lesions. In 2011, they reported the outcomes and toxicity data of 59 patients with lesions that were large (nidus size >10 cc) or if the AVM was in an eloquent location (brainstem, basal ganglia, motor strip). Of note, 12% of the patients had prior proton SRS to a median dose of 10.5 Gy. Median nidus volume was 22.9 cc. The 90% isodose line encompassed the volume with a median prescription dose (includes both fractions) of 16 Gy (RBE) (range, 12–28 Gy). The median number of days between fractions was 7 (range, 1–56 days). At a median of 56.1 months, complete and partial obliteration rates were 15.3%, and 33.9%, respectively. The 5-year rates of total or partial obliteration rates were 8%, and the 5-year actuarial rate of hemorrhage was 21.9%. With regard to acute complications, 67.8% had no acute complications, with the most common side effect within the first 3 months post-treatment being Grade 1 headaches. Additionally, 12% of the patients experienced partial seizures within 48 hours of proton SRS. Eighty percent of the patients did not experience a late complication. Grade 1 headaches were the most common late side effect. Despite the low rates of toxicity, given the high-risk AVM lesions included in this series, the authors concluded that their 2-fraction approach did not achieve the intended rates of obliteration. Irrespective of radiation modality used (photon or proton), larger lesions and those in critical locations remain a challenge to treat and require alternative strategies.

The group from Uppsala, Sweden, has similarly reported on this challenge [27, 28]. In 2016, they published their updated results of outcomes and toxicity in 67 AVM lesions receiving proton-fractionated stereotactic radiotherapy. Median nidus volume in this series was 3 cc. Prescription doses were 18–25 Gy delivered in 2 equal fractions (separated by 24 hours) to 64 lesions, whereas the remaining 3 lesions received 35 Gy in 5 equal fractions. Their results revealed complete obliteration, partial obliteration, and lesion stability rates of 68%, 18%, and 14%, respectively. Of note, there was a statistically significant difference in the median target volume between the lesions that totally regressed and those with partial regression/stability (3 cc vs. 10.5 cc, $p < 0.03$). When dividing lesion volumes into cohorts, occlusion rates for target volume 0–2 cc, 3–10 cc, 11–15 cc, and 16–51 cc were 77%, 80%, 50%, and 20%, respectively. Twenty-two patients had seizures at diagnosis, of whom 68% reported an improvement in seizure symptoms after proton radiation therapy. Sixty-two percent of the patients developed edema after proton treatment, with most cases being mild and transient. Two patients developed late permanent neurological deficits with otherwise low rates of toxicity. These results confirmed the efficacy of proton beam SRS/fractionated stereotactic approach in smaller AVM lesions, with comparably low obliteration rates (15–20%) for larger sizes.

The group from South Africa led by Vernimmen and coauthors similarly reported their results of hypofractionated stereotactic proton approaches for large AVMs, primarily >14 cc [29]. Overall 64 patients were included in their analysis with 41% ($n = 26$) having lesions <14 cc, whereas the remaining 59% ($n = 38$) had lesions >14 cc. Radiation dose was administered as per AVM volume cohorts of <10 cc, 10–13.9 cc, and >14 cc. Median total dose and median number of fractions was 27.24 Gy in 2 fractions, 23.2 Gy in 2 fractions, and 27 Gy in 3 fractions for lesions <10 cc, 10–13.9 cc, and >14 cc, respectively. With a median follow-up of 62 months, complete and partial obliteration rates for lesions <14 cc were 67% and 17%, respectively. In the group with lesions >14 cc, complete and partial obliteration rates were 43% and 21%, respectively. About 15.6% of the patients developed acute complications, ranging from transient cranial nerve palsy, nausea, vomiting, and status epilepticus. While 23% of the patients experienced transient late side effects, 80% had complete recovery with no late permanent side effects. In all, only 4% of the patients developed a permanent late Grade III or IV side effect. These results utilizing a longer hypofractionated approach with a median of 3 fractions for larger AVMs (>14 cc) seem to provide superior control probabilities in comparison to the low obliteration rates achieved in the aforementioned Uppsala and MGH series.

In 1994, the group from Keil, Germany, also reported their outcomes data on 63 lesions treated over a 10-year period [30]. AVM diameters were <3 cm, 3–6 cm, and >6 cm in 26.9%, 58.7%, and 14.2% of lesions, respectively. In 88.3% of the patients ($n = 60$), stereotactic proton beam therapy was used alone, whereas in the remaining patients, embolization or ligation preceded proton beam therapy. One of the major limitations of this series was the lack of reporting regarding the dosimetry or target volumes. Results revealed a strong correlation between obliteration rates and initial diameter of the AVM. Of the AVMs <3 cm in size, 58.8% were completely obliterated, 0% were partially obliterated, and 41.2% were unchanged on angiography. Whereas for AVMs between 3–6 cm and >6 cm, none were partially or completely obliterated. Of all the 63 lesions treated, only 15.3% were completely obliterated, whereas 84.1% showed no change. Unfortunately, while these results display a lack of benefit for proton beam therapy in medium- to large-sized lesions, this is in stark contrast to the higher rates of obliteration observed by Vernimmen and coauthors [29]. As such, it appears that there may be an inherent limitation in methodology or in patient selection that resulted in poorer outcomes seen in this series than would be expected.

Approximately around this time, in the late 1990s, Russia and the Soviet Union experienced a renaissance in proton therapy [31]. This increased the utilization of proton radiosurgery for the treatment of benign lesions such as AVMs. In 1991, the group from Russia reported on the use of proton radiosurgery in 46 lesions with a mean volume of 14.22 ± 2.14 cc. Of note, all AVM lesions were prospectively assigned to size-based cohorts for stratification: <4.9 cc, 5–9.9 cc, 10–24.9 cc, and >25–82 cc. Dose prescription was defined at the isocenter and corresponded to the 100% isodose point. For small (up to 5 cc)- and medium-sized (up to 25 cc) lesions away from critical areas, the dose was 25 GyE. For small and medium lesions near critical structures, the dose prescription was 24 GyE, whereas for larger AVMs (>25 cc), the dose was 20–23 GyE. With a minimum of 2 years of follow-up, complete obliteration, partial obliteration, and no change occurred in 50%, 47%, and 3%, respectively. Complete obliteration rates for AVM lesions <4.9 cc, 5–9.9 cc, 10–24.9 cc, and >25 cc were 89%, 43.8%, 46.6%, and 16.6%, respectively. Acute radiation reactions were mild to moderate. Eleven percent of the patients developed a late reaction, most commonly 12 months after radiosurgery. This group reports some of the best obliteration rates achieved with proton beam therapy for large (>10 cc) AVMs, possibly as a result of their higher doses, in comparison to the obliteration achieved by the MGH and Uppsala groups (15–20%).

Practical Considerations When Utilizing PBT for AVMs

- Consider the size and location of the AVM and associated nidus in deciding between hypofractionated regimens.
- For small (about 3–3.5 cc) peripherally situated AVMs, either single- or 2-fraction proton regimens yield high obliteration with low rates of toxicity [23, 27, 28].
- Large (usually >10 cc) peripherally situated lesions treated with single proton SRS fractions should be considered for dose-escalated approaches or treated with hypofractionated [2, 3] proton beam therapy [29, 31].
- Appreciate that centrally/eloquently situated AVMs present significant risks of late toxicities with single-fraction proton beam regimens [22].
- Appreciate that achieving obliteration for centrally/eloquently situated AVMs with proton beam therapy suffers the same challenges as with photon-based therapies. As such, consider multidisciplinary or staged approaches.

Pituitary Adenomas

In the early era of proton therapy, proton SRS was limited by the relatively inadequate neuroradiological techniques, limited imaging options, rudimentary treatment planning systems, and lack of onboard volumetric imaging [32]. Nevertheless, treatment of pituitary tumors remained feasible even at this time given the visibility of the sella turcica on radiographs. As such, the utilization of proton SRS for the management of pituitary tumors has one of the longest histories. The group from the Lawrence Radiation Laboratory at the University of California-Berkeley described one of the earliest reports of managing Cushing's disease with charged particle therapy in 1963. This group highlighted that the increased depth-dose penetration and biological effectiveness of particles such as protons provided a significant advancement at the time when orthovoltage X-rays and gamma rays limited the ability of delivering ablative doses to the depth of pituitary gland [33]. The early experience of the group from the Lawrence Laboratory successfully utilized proton irradiation with conventional fractionation of 20,000–30,000 rads in patients with either metastatic breast cancer to the pituitary, diabetes mellitus with retinopathy, or acromegaly with resultant hormonal dysfunction [34].

Additionally, in 1991, this group reported their results treating 840 patients with the aforementioned pathologies using either proton radiosurgery or helium ion beams. Dose prescriptions included 30–50 Gy in 4 fractions, 30–150 Gy in 3–4 fractions, and 50–150 Gy in 4 fractions for acromegaly, Cushing's disease, and prolactinomas, respectively. Overall, the majority of patients achieved control of neoplastic growth and/or reduction of hormonal hypersecretion states. While hypopituitarism occurred in a subset of patients, this was corrected with supplemental therapy [35].

Around the 1960s, while the proton SRS program at the Lawrence Laboratory was burgeoning, the group at MGH was also utilizing proton radiosurgery for the management of pituitary hypersecretion. In 2014, the group from MGH published their updated results of proton therapy for func-

tional pituitary adenomas treated between 1992 and 2012 [36]. Ninety-two percent of the patients were treated with three-dimensional conformal passively scattered proton therapy using 2 to 5 beams to a median dose of 20 Gy(RBE) (range, 15–25 Gy) encompassing the visible tumor and entire sella with a superior margin defined to limit the undersurface of the chiasm to 8 Gy (RBE) maximum dose. Eight percent of the patients received fractionated stereotactic treatments to a median dose of 50.4 Gy due to proximity of critical structures. With a median follow-up of 52 months, the 5-year rate of biochemical complete response, defined as at least 3 months of sustained normalized hormonal levels, was 59%. With a median of 43 months, 98% of the patients had local radiographic control, defined as absence of disease or stable residual disease. Overall late toxicity was limited, with the most common adverse event being hypopituitarism. The 5-year rate of developing a new hormonal deficiency was 62%. Four patients developed temporal lobe seizures. Otherwise, no documented cerebrovascular events or radiation induced tumors occurred in this cohort. In summary, the hormonal control rate achieved in this series is superior to rates (44.7–54%) reported by various photon SRS publications [37, 38] with overall an excellent tumor control rate.

Practical Considerations When Utilizing PBT for Pituitary Adenomas

Proton radiosurgery approaches provide effect local control and biochemical response rate, comparable to rates achieved with photon SRS treatments [36].

- In utilizing proton radiosurgery, consider the proximity of normal organs at risk such as the optic nerves and chiasm to reduce long-term risks.
- Appreciate the lower integral dose with proton-based SRS and the resultant potential to reduce long-term side effects such as cerebrovascular events or radiation-induced tumors.
- Consider referral to endocrinology for patients receiving proton beam therapy of the pituitary given the high rate of developing additional hormonal deficiency [36].

Vestibular Schwannoma/Acoustic Neuroma

Proton therapy, with varying fractionation schema ranging from conventional to hypofractionation to single-session SRS, has been utilized for the treatment of vestibular schwannomas with overall progression-free survival rates of 85–100% [39].

One of the earliest series evaluating single-session proton SRS for vestibular schwannomas was published in 2002 [40]. Sixty-eight patients received passively scattered proton beam therapy using 3–5 fields, to a prescription dose of 12 Gy to the 70% isodose line at the tumor margin while constraining the maximum brainstem dose to 12 Gy. The 5-year tumor control rate was 84%, with an overwhelming majority (95.3%) of the patients reporting satisfaction with the procedure and outcomes. Acute toxicities were minimal, with new cranial nerve (CN) neuropathies being infrequent. Severe permanent V and VII nerve injury occurred in each of the 4.7% patients. Mild transient V and VII nerve injury occurred in 9.4% and 18.8% of the patients, respectively.

In 2003, the same group updated their results, now reporting on 87 patients. The median tumor diameter was 1.6 cm; the median prescribed dose was 12 Gy CGE (range, 10–18) to a median isodose line of 70% (range, 70–108%) [41]. With a median follow-up of 38.7 months, the 5-year local control rate was 93.6%. The 5-year rate of hearing preservation rate in the 21 patients (24%) who had pre-SRS functional hearing was 22%. After proton SRS, the 5-year V and VII normalcy rates were 89.4% and 91.1%. No radiation therapy-induced secondary malignancies were noted.

In 2009 the group from South Africa initiated a proton hypofractionated stereotactic radiation therapy program using passively scattered proton beam radiosurgery for acoustic neuromas treating 21.4 CGyE in 3 fractions to a median isodose line of 85%. [42] With a median follow-up time of 72 months, they achieved a 5-year local control of 98%. Of patients with pre-RT serviceable hearing, the 5-year rate of hearing preservation was 43%. New VII nerve dysfunction was seen in 8.3% of the patients, of which two cases were mild and two were complete paralysis, with an overall 5-year rate of normal CN VII function of 90.5%. New cranial nerve V nerve dysfunction was also seen in 8.3% of the patients, all of which were mild, with an overall 5-year rate of normal CN VII function of 93%.

Considerations for VS/AN

- Appreciate the size of the lesion and its proximity to the brainstem, especially compression and effect on CSF flow, when considering a proton SRS/hypofractionated treatment approach.
- Consider limiting the maximum brainstem surface dose to 12 Gy, in an effort to minimize the risk of long-term side effect [41].
- Both proton SRS and hypofractionated (3-fraction) approaches provide excellent local control rates, comparable to rates achieved with photon-based therapy [41, 42]. Both fractionation schedules provide comparable rates of CN V and VII toxicity.
- Consider a protracted hypofractionated (3-fraction) proton therapy course for patients with functional hearing as it may better preserve hearing, although the data supporting this are sparse and weak [42].

Limitations

The published clinical data for proton SRS and hypofractionated stereotactic regimens reveal excellent local control rates of benign conditions such as meningiomas, schwannomas, pituitary adenomas, and AVMs. However, several limitations in these series exist. For example, in the modern era, proton therapy delivery techniques have undergone an evolution from a passively scattered approach to a spot scanning intensity-modulated ability. The generalization and applicability of results achieved with passive scattering to spot-scanning remain a question, strongly necessitating publication of modern clinical results.

Additionally, while the studies presented herein display excellent overall results comparable to those achieved with photon SRS approaches, the retrospective nature of these studies presents an inherent limitation. As highlighted by Wattson and coauthors, the predominant benefit of proton SRS is in optimally reducing integral dose to normal tissue [36]. Given the reported occurrence of radiation necrosis [43], secondary malignancies [44], and cerebrovascular accidents [45] after photon radiation for benign pathologies, proton SRS has significant potential to reduce these risks, especially in long-term survivors. Since the event rate for these sequelae is low, it would require rather large-sized sample studies with extremely long follow-up periods to statistically prove this.

A common limitation to the use of proton therapy for any disease site is the lack of an absolutely precise estimate of the relative biological effectiveness (RBE) of protons to photon therapy. While a general RBE of 1.1 is currently utilized, many studies reveal significant RBE variability [46]. Greater understanding of this will be critical in ensuring that appropriate tumor control doses are being utilized with proton approaches, as well as to ensure that proton-specific normal tissue dose constraints are adhered to.

Decision Criteria When Deciding Between Proton and Photon Treatments

As mentioned above, there are no significant publications prospectively comparing photon and proton outcomes using SRS/hypofractionated regimens for the pathologies discussed in this chapter. Given the understanding that proton regimens will likely achieve their greatest benefit in reducing the risk of long-term side effects, a patient's age, performance status, as well as associated co-morbidities must be taken into account when considering the treatment modality of choice. For patients who are judged to have a relatively poor prognosis or estimated to have a shortened life span, the utilization of protons may not provide the greatest magnitude of benefit relative to cost. An exception for stronger consideration of proton beam therapy would be for patients with intracranial comorbidities such as multiple sclerosis, severe end-arteriolar disease processes, or neurofibromatosis for which a reduction in the integral dose would reduce the risk of potential acute as well as late toxicities. Additionally, for patients who are otherwise young, and/or those patients with excellent performance status, proton therapy should be strongly considered given the benign nature of the disease processes resulting in decades of longevity and hence a higher likelihood of delayed radiation toxicities.

Pencil-beam scanning intensity modulated proton therapy (IMPT) is rapidly replacing older techniques, especially because of its ability to better sculpt dose around OARs that lie proximal to target volumes, and data for this modality are rapidly emerging but not yet adequately published [47].

When comparing photon to proton-based plans, one must consider not only set up uncertainties but also range uncertainties. This is generally completed with the creation of a beam-specific PTV with margins created to prevent geometric and range miss and in addition to analyze these plans robustly. When deciding on field directionality for proton-based plans, it is important to appreciate the potential for enhanced RBE at the distal end of the beam, which therefore should provide caution about ranging into a critical OAR, especially when only one or one very heavily weighted beam is used. Multiple fields [2, 3] should be utilized when treating and angles chosen so as to limit the number of beams ranging on critical OARs. Additional risk reduction can be achieved by ensuring that heavily weighted spots are not in close proximity to OARs.

Conclusion

Proton SRS has a longstanding history and has proven itself to be an effective treatment strategy to achieve excellent control for benign intracranial conditions. The dosimetric benefit of proton therapy in reducing dose to normal tissues has been associated with low acute and late toxicities, at least in retrospective series. Modern-day proton series, including prospective evaluations against photon approaches, remain warranted.

References

1. Davis JN, Medbery C 3rd, Sharma S, Danish A, Mahadevan A. The RSSearch Registry: patterns of care and outcomes research on patients treated with stereotactic radiosurgery and stereotactic body radiotherapy. Radiat Oncol. 2013;8:275.
2. Chen CC, Chapman P, Petit J, Loeffler J. Proton radiosurgery in neurosurgery. Neurosurg Focus. 2007;23(6):E5.
3. Verhey LJ, Smith V, Serago CF. Comparison of radiosurgery treatment modalities based on physical dose distributions. Int J Radiat Oncol Biol Phys. 1998;40(2):497–505.

4. Smith V, Verhey L, Serago CF. Comparison of radiosurgery treatment modalities based on complication and control probabilities. Int J Radiat Oncol Biol Phys. 1998;40(2):507–13.
5. Baumert BG, Norton IA, Lomax AJ, Davis JB. Dose conformation of intensity-modulated stereotactic photon beams, proton beams, and intensity-modulated proton beams for intracranial lesions. Int J Radiat Oncol Biol Phys. 2004;60(4):1314–24.
6. Baumert BG, Lomax AJ, Miltchev V, Davis JB. A comparison of dose distributions of proton and photon beams in stereotactic conformal radiotherapy of brain lesions. Int J Radiat Oncol Biol Phys. 2001;49(5):1439–49.
7. Serago CF, Thornton AF, Urie MM, Chapman P, Verhey L, Rosenthal SJ. and coauthors. Comparison of proton and x-ray conformal dose distributions for radiosurgery applications. Med Phys. 1995;22(12):2111–6.
8. Weber DC, Lomax AJ, Rutz HP, Stadelmann O, Egger E, Timmermann B, et al. Spot-scanning proton radiation therapy for recurrent, residual or untreated intracranial meningiomas. Radiother Oncol. 2004;71(3):251–8.
9. Slater JD, Loredo LN, Chung A, Bush DA, Patyal B, Johnson WD, et al. Fractionated proton radiotherapy for benign cavernous sinus meningiomas. Int J Radiat Oncol Biol Phys. 2012;83(5):e633–7.
10. Wenkel E, Thornton AF, Finkelstein D, Adams J, Lyons S, De La Monte S, et al. Benign meningioma: partially resected, biopsied, and recurrent intracranial tumors treated with combined proton and photon radiotherapy. Int J Radiat Oncol Biol Phys. 2000;48(5):1363–70.
11. Noel G, Habrand JL, Mammar H, Haie-Meder C, Pontvert D, Dederke S, et al. Highly conformal therapy using proton component in the management of meningiomas. Preliminary experience of the Centre de Protontherapie d'Orsay. Strahlenther Onkol. 2002;178(9):480–5.
12. Noel G, Bollet MA, Calugaru V, Feuvret L, Haie-Meder C, Dhermain F, et al. Functional outcome of patients with benign meningioma treated by 3D conformal irradiation with a combination of photons and protons. Int J Radiat Oncol Biol Phys. 2005;62(5):1412–22.
13. Vernimmen F. Intracranial stereotactic radiation therapy with charged particle beams: an opportunity to regain the momentum. Int J Radiat Oncol Biol Phys. 2016;95(1):52–5.
14. Vernimmen FJ, Harris JK, Wilson JA, Melvill R, Smit BJ, Slabbert JP. Stereotactic proton beam therapy of skull base meningiomas. Int J Radiat Oncol Biol Phys. 2001;49(1):99–105.
15. Morita A, Coffey RJ, Foote RL, Schiff D, Gorman D. Risk of injury to cranial nerves after gamma knife radiosurgery for skull base meningiomas: experience in 88 patients. J Neurosurg. 1999;90(1):42–9.
16. Chang SD, Adler JR Jr, Martin DP. LINAC radiosurgery for cavernous sinus meningiomas. Stereotact Funct Neurosurg. 1998;71(1):43–50.
17. Gudjonsson O, Blomquist E, Nyberg G, Pellettieri L, Montelius A, Grusell E, et al. Stereotactic irradiation of skull base meningiomas with high energy protons. Acta Neurochir. 1999;141(9):933–40.
18. Vlachogiannis P, Gudjonsson O, Montelius A, Grusell E, Isacsson U, Nilsson K, et al. Hypofractionated high-energy proton-beam irradiation is an alternative treatment for WHO grade I meningiomas. Acta Neurochir. 2017;159(12):2391–400.
19. Halasz LM, Bussiere MR, Dennis ER, Niemierko A, Chapman PH, Loeffler JS, et al. Proton stereotactic radiosurgery for the treatment of benign meningiomas. Int J Radiat Oncol Biol Phys. 2011;81(5):1428–35.
20. Lee JY, Niranjan A, McInerney J, Kondziolka D, Flickinger JC, Lunsford LD. Stereotactic radiosurgery providing long-term tumor control of cavernous sinus meningiomas. J Neurosurg. 2002;97(1):65–72.
21. Kjellberg RN, Hanamura T, Davis KR, Lyons SL, Adams RD. Bragg-peak proton-beam therapy for arteriovenous malformations of the brain. N Engl J Med. 1983;309(5):269–74.
22. Amin-Hanjani S, Ogilvy CS, Candia GJ, Lyons S, Chapman PH. Stereotactic radiosurgery for cavernous malformations: Kjellberg's experience with proton beam therapy in 98 cases at the Harvard Cyclotron. Neurosurgery. 1998;42(6):1229–36; discussion 1236–1228
23. Hattangadi-Gluth JA, Chapman PH, Kim D, Kim D, Niemierko A, Bussière MR, et al. Single-fraction proton beam stereotactic radiosurgery for cerebral arteriovenous malformations. Int J Radiat Oncol Biol Phys. 2014;89(2):338–46.
24. Karlsson B, Lindquist C, Steiner L. Prediction of obliteration after gamma knife surgery for cerebral arteriovenous malformations. Neurosurgery. 1997;40(3):425–30; discussion 430–421
25. Starke RM, Yen CP, Ding D, Sheehan JP. A practical grading scale for predicting outcome after radiosurgery for arteriovenous malformations: analysis of 1012 treated patients. J Neurosurg. 2013;119(4):981–7.
26. Barker FG 2nd, Butler WE, Lyons S, Cascio E, Ogilvy CS, Loeffler JS, et al. Dose-volume prediction of radiation-related complications after proton beam radiosurgery for cerebral arteriovenous malformations. J Neurosurg. 2003;99(2):254–63.
27. Blomquist E, Engstrom ER, Borota L, Gál G, Nilsson K, Lewén A, et al. Positive correlation between occlusion rate and nidus size of proton beam treated brain arteriovenous malformations (AVMs). Acta Oncol. 2016;55(1):105–12.
28. Silander H, Pellettieri L, Enblad P, Montelius A, Grusell E, Vallhagen-Dahlgren C, et al. Fractionated, stereotactic proton beam treatment of cerebral arteriovenous malformations. Acta Neurol Scand. 2004;109(2):85–90.
29. Vernimmen FJ, Slabbert JP, Wilson JA, Fredericks S, Melvill R. Stereotactic proton beam therapy for intracranial arteriovenous malformations. Int J Radiat Oncol Biol Phys. 2005;62(1):44–52.
30. Seifert V, Stolke D, Mehdorn HM, Hoffmann B. Clinical and radiological evaluation of long-term results of stereotactic proton beam radiosurgery in patients with cerebral arteriovenous malformations. J Neurosurg. 1994;81(5):683–9.
31. Tseitlina MA, Kizhaev EV, Luchin EI, et al. Proton three-dimensional conformal radiosurgery of arteriovenous malformation of the brain. Zh Vopr Neirokhir Im N N Burdenko. 2013;77(4):43–50; discussion 50.
32. Levy RP, Schulte RW, Slater JD, Miller DW, Slater JM. Stereotactic radiosurgery--the role of charged particles. Acta Oncol. 1999;38(2):165–9.
33. Lawrence JH. Proton irradiation of the pituitary. Cancer. 1957;10(4):795–8.
34. Lawrence JH, Tobias CA, Born JL, Wangcc LJH. Heavy-particle irradiation in neoplastic and neurologic disease. J Neurosurg. 1962;19:717–22.
35. Levy RP, Fabrikant JI, Frankel KA, Phillips MH, Lyman JT, Lawrence JH, et al. Heavy-charged-particle radiosurgery of the pituitary gland: clinical results of 840 patients. Stereotact Funct Neurosurg. 1991;57(1–2):22–35.
36. Wattson DA, Tanguturi SK, Spiegel DY, Niemierko A, Biller BM, Nachtigall LB, et al. Outcomes of proton therapy for patients with functional pituitary adenomas. Int J Radiat Oncol Biol Phys. 2014;90(3):532–9.
37. Castinetti F, Nagai M, Morange I, Dufour H, Caron P, Chanson P, et al. Long-term results of stereotactic radiosurgery in secretory pituitary adenomas. J Clin Endocrinol Metab. 2009;94(9):3400–7.
38. Sheehan JP, Pouratian N, Steiner L, Laws ER, Vance ML. Gamma Knife surgery for pituitary adenomas: factors related to radiological and endocrine outcomes. J Neurosurg. 2011;114(2):303–9.
39. Murphy ES, Suh JH. Radiotherapy for vestibular schwannomas: a critical review. Int J Radiat Oncol Biol Phys. 2011;79(4):985–97.

40. Harsh GR, Thornton AF, Chapman PH, Bussiere MR, Rabinov JD, Loeffler JS. Proton beam stereotactic radiosurgery of vestibular schwannomas. Int J Radiat Oncol Biol Phys. 2002;54(1):35–44.
41. Weber DC, Chan AW, Bussiere MR, Harsh GR 4th, Ancukiewicz M, Barker FG 2nd, et al. Proton beam radiosurgery for vestibular schwannoma: tumor control and cranial nerve toxicity. Neurosurgery. 2003;53(3):577–86; discussion 586–578
42. Vernimmen FJ, Mohamed Z, Slabbert JP, Wilson J. Long-term results of stereotactic proton beam radiotherapy for acoustic neuromas. Radiother Oncol. 2009;90(2):208–12.
43. Mitsumori M, Shrieve DC, Alexander E 3rd, Kaiser UB, Richardson GE, Black PM, et al. Initial clinical results of LINAC-based stereotactic radiosurgery and stereotactic radiotherapy for pituitary adenomas. Int J Radiat Oncol Biol Phys. 1998;42(3):573–80.
44. Minniti G, Traish D, Ashley S, Gonsalves A, Brada M. Risk of second brain tumor after conservative surgery and radiotherapy for pituitary adenoma: update after an additional 10 years. J Clin Endocrinol Metab. 2005;90(2):800–4.
45. Erridge SC, Conkey DS, Stockton D, Strachan MW, Statham PF, Whittle IR, et al. Radiotherapy for pituitary adenomas: long-term efficacy and toxicity. Radiother Oncol. 2009;93(3):597–601.
46. Paganetti H, Niemierko A, Ancukiewicz M, Gerweck LE, Goitein M, Loeffler JS, et al. Relative biological effectiveness (RBE) values for proton beam therapy. Int J Radiat Oncol Biol Phys. 2002;53(2):407–21.
47. Dinh J, Stoker J, Georges RH, Sahoo N, Zhu XR, Rath S, et al. Comparison of proton therapy techniques for treatment of the whole brain as a component of craniospinal radiation. Radiat Oncol. 2013;8:289.

Part III

Intracranial Radiosurgery by Indication

Stereotactic Radiosurgery for Brain Metastases

Clayton Alonso, Jason P. Sheehan, and Daniel M. Trifiletti

Introduction

Brain metastases are common among patients with systemic cancer. Twenty-four to forty-five percent of patients with cancer will develop brain metastases every year [1]. Brain metastases are the most common intracranial malignancy among adults [2], and median survival after diagnosis with brain metastases has been poor at approximately 4.5 months [1]. Several models exist to aid in predicting survival [1]. Older age, poorly controlled primary disease, additional sites of metastatic disease, histology, increased number of brain metastases, and lower Karnofsky performance status (KPS) score are all associated with worse survival among patients with brain metastases [1].

Treatment Options

Multiple treatment options are available in the treatment of brain metastases including supportive care, systemic therapy, surgical resection, whole brain radiation therapy (WBRT), stereotactic radiosurgery (SRS), or some combination thereof. Treatment decisions are stratified largely on the extent of intracranial involvement including tumor number, size and location, histology, and overall patient prognosis. Generally speaking, patients with fewer lesions and better prognosis are considered favorable candidates for more aggressive local therapy. Tumor histologies which are highly sensitive to radiation therapy or systemic therapies, such as lymphoma and small cell lung cancer, tend to favor treatment with WBRT and/or chemotherapy. Specific tumor locations, especially near the optic chiasm and brainstem, also impact treatment decision making. It is clear that there is considerable heterogeneity among patients with brain metastases, and any therapy should be tailored to patient-specific factors.

Several studies have been impactful in shaping current treatment standards. Patchell and colleagues showed improvements in local control, quality of life, and overall survival (OS) for patients with single brain metastases treated with WBRT and resection compared to WBRT alone [3]. This was followed by a randomized study of surgical resection with either observation or adjuvant WBRT. It showed improved intracranial recurrence rates, 18 vs. 70%; improved treatment site recurrence, 10 vs. 46%; and decreased neurologic death, 14 vs. 44%, with the addition of WBRT [4]. These studies have led to surgical management followed by adjuvant radiation therapy being the preferred treatment strategy for patients with limited brain metastases ($\leq$3 metastases) and good prognosis [5].

For patients with poor KPS and prognosis, who are not candidates for resection or SRS, it may be reasonable to consider omitting radiation therapy entirely in favor of palliative therapy using corticosteroids. The QUARTZ trial randomized patients with non-small cell lung cancer metastatic to the brain, with KPS < 70, who were not eligible for resection or SRS to dexamethasone with or without WBRT. Systemic therapy was allowed at the treating physician's preference. No difference in the quality of life, KPS, or OS was seen between the two groups. Subgroup analysis did show a survival benefit for patients less than 60 years old with the addition of WBRT. The median survival was 8.5 weeks for patients treated without WBRT and 9.2 weeks for patients

C. Alonso
University of Virginia, Radiation Oncology, Charlottesville, VA, USA

J. P. Sheehan
University of Virginia Medical Center, Neurological Surgery, Charlottesville, VA, USA

University of Virginia School of Medicine, Neurological Surgery, Charlottesville, VA, USA

D. M. Trifiletti (✉)
Mayo Clinic, Radiation Oncology, Mayo Clinic School of Medicine, Radiation Oncology, Jacksonville, FL, USA
e-mail: trifiletti.daniel@mayo.edu

D. M. Trifiletti et al. (eds.), *Stereotactic Radiosurgery and Stereotactic Body Radiation Therapy*,
https://doi.org/10.1007/978-3-030-16924-4_10

Table 1 Randomized SRS trials for brain metastases

References	Randomization	Number of patients	SRS dose range (Gy)	Median survival (mo)	Outcome (%)
Andrews et al. [34]	WBRT +/−SRS	333	15–24	4.9 vs. 6.5	1 year LC 71 vs. 82
Aoyama et al. [35]	SRS +/−WBRT	132	18–25	7.5 vs. 8.0	1 year LC 72.5 vs. 88.7
Brown et al. [8]	SRS +/−WBRT	213	18–24	10.4 vs. 7.4	3 mo intracranial control 93.7 vs. 75.3 Less cognitive decline with SRS alone
Mahajan et al. [9]	Resection +/−SRS	132	12–16	18 vs. 17	1 year LC 43 vs. 72
Brown et al. [10]	Resection + SRS or WBRT	194	12–20	11.6 vs. 12.2	Cognitive deterioration-free survival 3.7 vs. 3.0 mo
Kirkpatrick et al. [30]	SRS with 1 or 3 mm margins	49	15–24	10.6 overall	1 year LC 91 vs. 95

treated with WBRT [6]. Based on this data, it is reasonable to omit WBRT in older patients with poor performance status and poor prognosis.

SRS Alone

More recently, SRS has been used as an alternative to whole brain adjuvant therapy in the setting of limited brain metastases, primarily as a means of minimizing cognitive decline (Table 1) [7]. A prior study showed increased rates of cognitive decline in patients treated with SRS and WBRT (92%) compared to SRS alone (64%) [8]. A recent study of patients with ≤3 brain metastases and KPS ≥ 70 randomized to either resection alone or resection followed by SRS showed improved freedom from local recurrence rates with the addition of SRS (43 vs. 72%) [9]. A similar study was conducted, randomizing patients to adjuvant SRS or WBRT. This trial allowed for only one resected brain metastasis, but did allow for up to three additional unresected lesions. It showed improved median cognitive-deterioration-free survival and quality of life in the SRS group, and no difference in overall survival, with worse tumor bed control (80.4% vs. 87%) and time to intracranial progression in the SRS group [10]. Given the improved quality of life outcomes and unchanged OS between the groups, the authors of the study concluded that SRS is an effective adjuvant treatment for brain metastases [10]. This is consistent with current practice standards suggesting the use of SRS as the preferred adjuvant treatment option for patients with a good prognosis and limited intracranial disease [5].

There is also interest in the use of SRS alone as a primary treatment for patients with limited brain metastases (Fig. 1). A meta-analysis in 1999 of over 1700 patients treated for brain metastases with SRS alone showed a local control of 83% and a median survival of 9.6 months, both of which were comparable to contemporaneous surgical outcomes [11]. There are also comparative retrospective data supporting the use of SRS as a primary treatment with improved local control when compared to surgery alone (0/21 local recurrences with SRS vs. 11/64 in the resection group). Despite having a lower number of patients with a good performance score in the SRS group, survival was no different between patients treated with SRS or resection; this equipoise was maintained on multivariate analysis and propensity-matched analysis [12]. To our knowledge, there is no phase III evidence comparing radiosurgery with resection alone. Two randomized trials have been previously established: one was withdrawn prior to enrollment and a second accrued 64 patients but has no published results [13, 14]. As previously discussed, there is evidence that adding SRS to resection is associated with improved local control [9]. Conducting a randomized trial with a surgery-only arm could be considered unethical at this time, given its demonstrated inferiority to a combined modality approach.

The maximum number of brain metastases which should be treated with SRS varies institutionally. Current national consensus guidelines in the United States state that SRS is preferred for three or more brain metastases but includes it as an option of patients with a good prognosis and more than three lesions. An upper limit to the number of lesions which should be treated is not specified [5]. In an exciting recent paper, Yamamoto and colleagues performed a retrospective propensity-matched analysis of patients treated with SRS with two to nine brain metastases and ten or more metastases. No difference in median survival, neurologic death-free survival times, repeat STS for new lesions, and neurologic deterioration nor SRS related complications were found [15]. This suggests that treating more than three lesions or even more than ten lesions with SRS may be appropriate; however, further investigation is needed to better define the risks and benefits of this approach in this patient population.

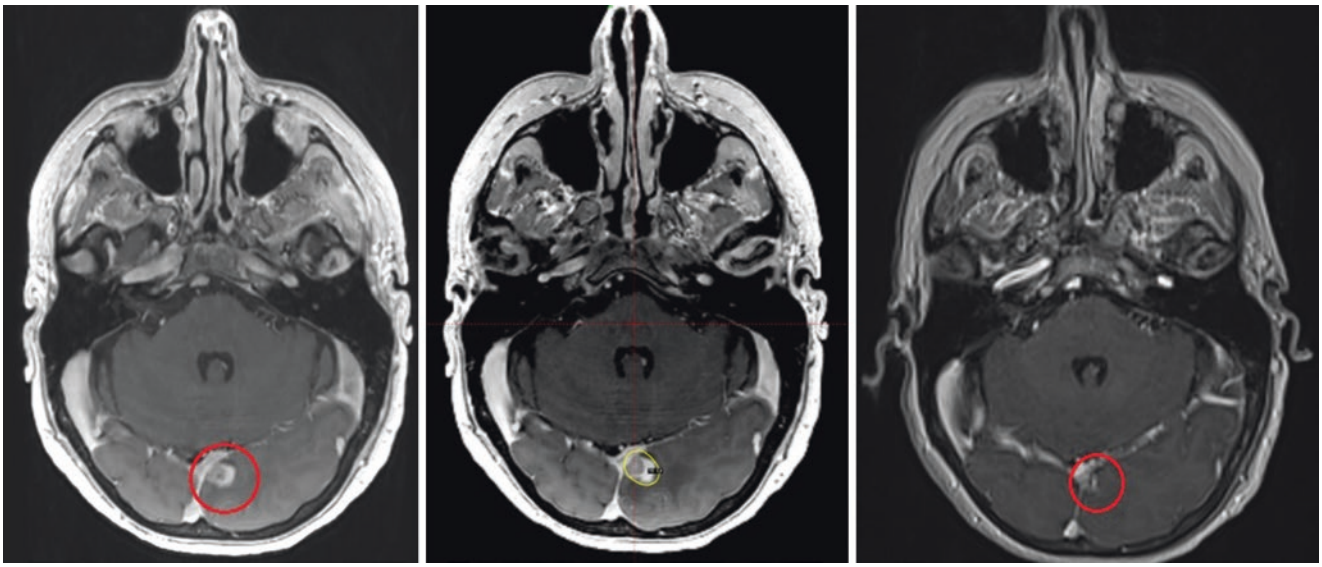

Fig. 1 Axial MRI showing a left occipital lobe uterine carcinoma metastasis (left, circled). The tumor margin was treated with Gamma Knife radiosurgery to 16 Gy to the 50% isodose line (center), and 3-month post-radiosurgery scan demonstrated near-complete resolution of the treated metastasis without evidence of toxicity (right)

SRS and Targeted Therapy

Data regarding the combination of SRS and targeted therapies or immunotherapy are beginning to emerge, with the majority being retrospective in nature. Recent publications have supported the safety and efficacy of SRS in combination with immunotherapy and BRAF inhibitors [16, 17]. Kotecha and colleagues reported local failure rates among patients treated with SRS with BRAF inhibitors or immunotherapy of 1%, compared to 7% for patients treated with SRS alone. No increase in radionecrosis was found among patients treated with combined therapy with none identified in the combined BRAF inhibitor arm and 2% found in the combination immunotherapy arm [16]. Additionally, distant intracranial failure has been retrospectively shown to be improved by combining SRS and immunotherapy or BRAF/MEK inhibitors compared to SRS alone (11.5%, 10%, 60%, respectively, $p < 0.001$) [18].

The ideal timing of immunotherapy in relationship to SRS has not been established in a randomized setting; however, retrospective data show a benefit with concurrent usage compared to sequential therapy. Median volumetric response at 6 months in this study was found to be 94.9% with concurrent therapy compared to 66.2% with nonconcurrent therapy [19]. There is also interest in the use of immunotherapy alone in the treatment of intracranial metastases; CheckMate 204 is an ongoing phase II clinical trial investigating the use of immunotherapy alone for the treatment of melanoma brain metastases, with preliminary data showing a 56% intracranial response rate at 6.3 months [20]. The authors conclude that these results suggest using immunotherapy alone as a new treatment paradigm; however, no level 1 evidence exists to support such a conclusion. Furthermore, the 56% response rate seen in this study does not compare favorably with historical local control with SRS alone, as discussed earlier.

Dose, Fractionation, and Isodose Line Selection

For patients who are eligible for treatment with SRS, dose is largely determined by the size of the target (Fig. 2). Recommended doses for single fraction SRS were, at least initially, primarily driven by the results of the SRS dose escalation trial RTOG 9005. This study included patients with previously irradiated primary or metastatic brain tumors, who were stratified by tumor size. Radiation doses were escalated as long as grade 3 or greater toxicity remained under 20%. The highest marginal doses tolerated were 24 Gy, 18 Gy, and 15 Gy for tumors ≤20 mm, 21–30 mm, and 31–40 mm, respectively [21]. Of note, unacceptable toxicities were never reached in the ≤20 mm tumor group, but additional dose escalation to 27 Gy was considered unwarranted. It should also be noted that this study was performed in patients who had received prior radiation therapy to these sites; it is plausible that radiation-naïve patients could toler-

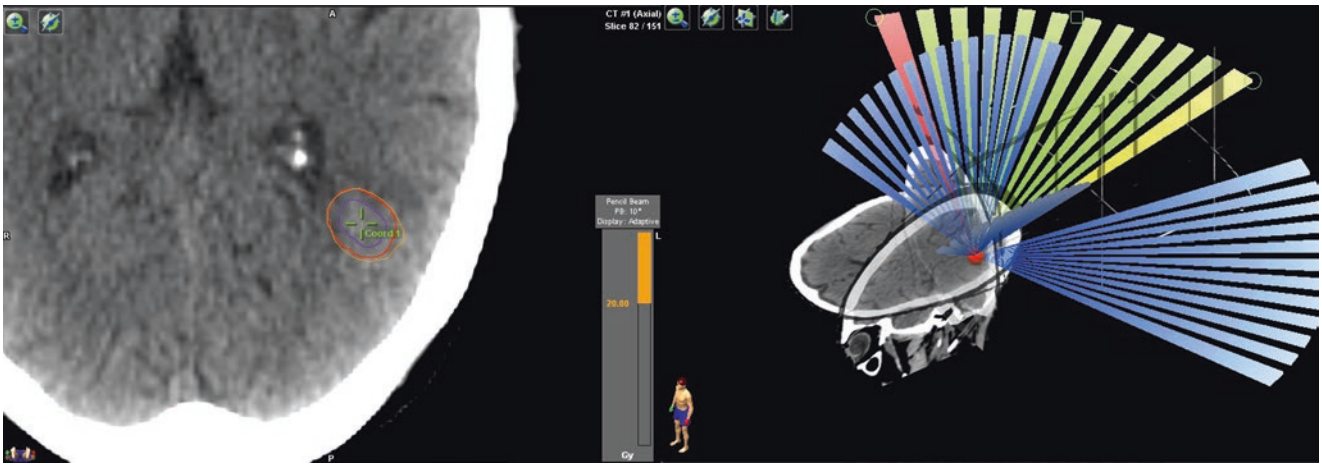

Fig. 2 LINAC-based SRS utilizing noncoplanar beam arrangements to achieve a highly conformal dose distribution for a patient with a brain metastasis

ate even higher doses, although the benefits of such a dose escalation are unknown. There is an ongoing phase I dose escalation trial seeking to address this question in patients who have not had prior radiation therapy [22].

SRS dose escalation must always be weighed against the risk to adjacent organs at risk (OARs). The primary dose-limiting OARs in the setting of intracranial SRS are the brainstem, optic nerves, and optic chiasm. The authors of Task Group (TG) 101 recognize that their dose constraints are to some degree educated guesses but list single fraction maximum point dose constraints for the brainstem of 15 Gy and the optic pathways as 10 Gy [23]. Retrospective analysis of brainstem SRS has shown it to be well tolerated, with grade 3 or greater toxicity reported in 2 out of 189 patients treated to a median marginal dose of 18 Gy [24]. The largest retrospective review on single fraction dose tolerance of optic structures showed a 1.9% risk of radiation optic neuropathy with a median maximum dose of 10 Gy. All patients who developed radiation optic neuropathy had prior surgery and 75% had received prior radiation therapy. Clinically significant optic toxicity was found in 1.1% of patients receiving less than 12 Gy to the optic nerves [25].

One strategy for treating patients who would otherwise have been limited by surrounding normal tissue tolerance is through the use of hypofractionated SRS. Hypofractionated SRS is generally defined as treatment with 2–5 fractions of SRS [26]. It has been made feasible by the advent of noninvasive motion management systems, i.e., deformable mask rather than frame-based systems [26]. Fractionated radiation therapy doses are not as well established, but several groups have demonstrated relatively safe and effective options (Fig. 3). One study, including large tumors with a median diameter of 3.9 cm, used 21 Gy in 3 fractions, 24 Gy in 4 fractions, and 30 Gy in 5 fractions, with local control rates of 61% reported [27]. Another retrospective study compared single fraction SRS with 35 Gy in 5 fractions and 40 Gy in 4 fractions; no difference in local control was found between treatment arms, with decreased grade I–III toxicity in the fractionated arms despite having larger tumors in less favorable location in the fractionated arms [28].

Gamma Knife-based SRS doses are typically prescribed to a low isodose line but LINAC-based ones to a higher isodose line [23]. At our institution, we typically prescribe to the 50–70% isodose line using the Gamma Knife, as the dose gradient is steepest at this point (depending on the SRS technique used), minimizing the dose to surrounding OARs. By definition, this will result in a "hot spot" that is much higher than the prescribed dose. It is hypothesized that such a hot spot improves outcomes in radioresistant cell populations, like hypoxic cells [29]. Prescribing to additional margin around the gross disease is a topic of controversy [30]. Prior autopsy studies have shown microscopic disease spread beyond the capsule in 45 of 76 metastases, with a mean maximum extension of 0.63 mm [31]. Retrospective studies evaluating the benefit of no margin vs. 1–2 mm margins have found conflicting results on the impact of the margin on local control [32, 33]. A randomized trial has been completed comparing 1 mm margins with 3 mm margins. No difference was found in local recurrence between the groups, but there was a trend toward increased radionecrosis in the 3 mm margin cohort [30].

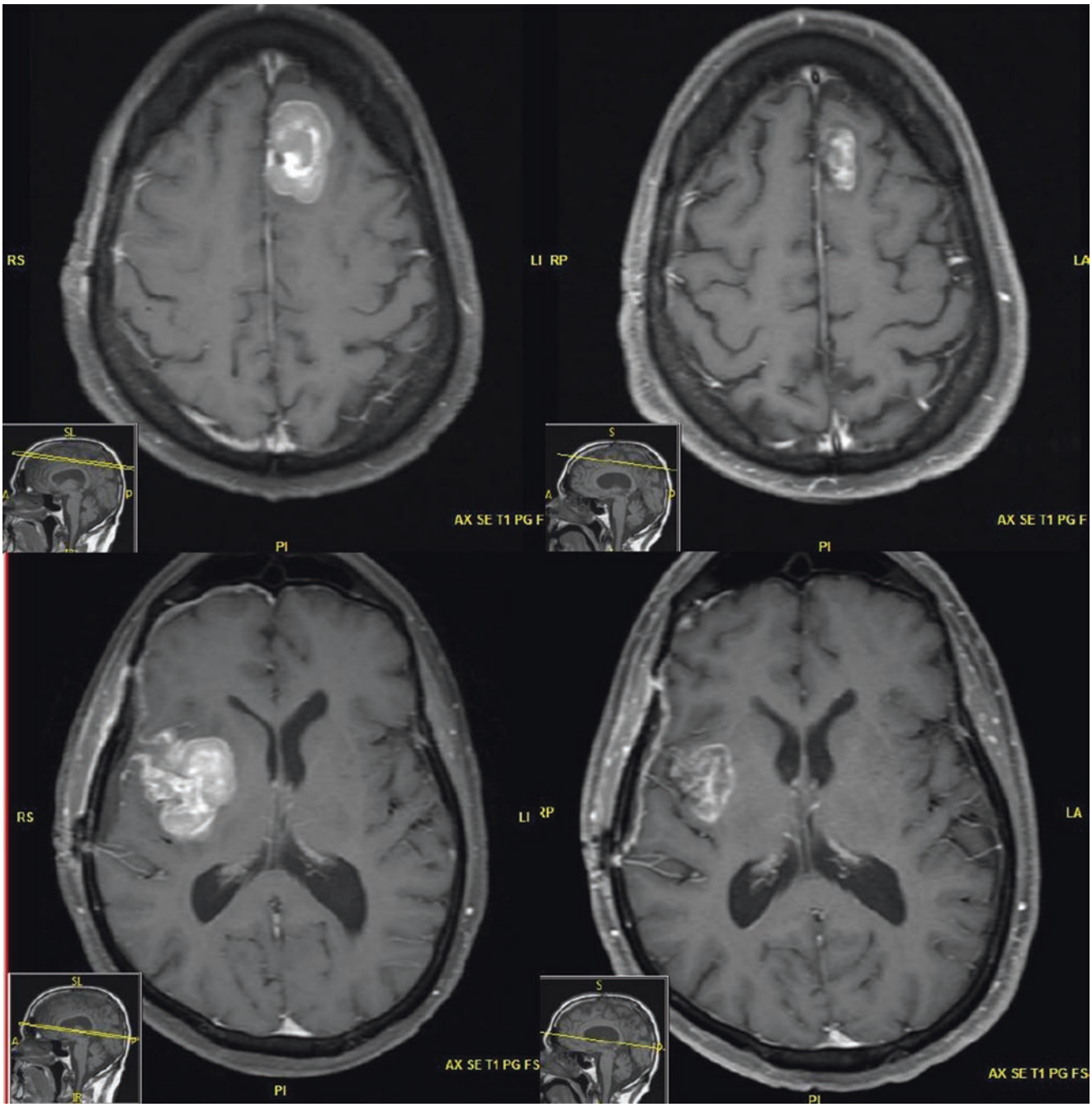

Fig. 3 A man with metastatic undifferentiated sarcoma presented with two large brain metastases (left panels). These were treated with fractionated stereotactic radiosurgery to 25 Gy in 5 fractions and demonstrated favorable radiographic response at 2 months (right panels) without evidence of clinical toxicity

Practical Considerations

- Patient selection is critical and should be determined based on prognosis, performance status, and extent of intracranial disease.
- SRS is favored in patients with good prognoses and less intracranial disease burden. There is no well-established upper limit to the number of brain metastases which should be treated with SRS.
- Workflow and technical details of radiosurgery will depend on SRS platforms. Several SRS platforms allow for intracranial use with demonstrated safety and efficacy.
- MRI with gadolinium contrast should be performed in the treatment position and co-registered to the treatment plan-

ning system for accurate target delineation. CT with contrast can be utilized when MRI is contraindicated.

- SRS doses should be based on tumor size: 20–24 Gy, 18 Gy, and 15 Gy for tumors ≤20 mm, 21–30 mm, and 31–40 mm, respectively.
- SRS margins are controversial and should be dictated based on site-specific physics recommendations and immobilization techniques (i.e., framed vs. frameless). There is evidence to support 0–1 mm margins.
- There is a low risk of injury to the brainstem and optic structures if maximum doses are kept below 15 and 10 Gy, respectively.
- There is evidence supporting the use of SRS in combination with targeted agents and immunotherapy, and future research will better define potential synergy between therapies.
- Large tumors and tumors in close proximity to dose-limiting structures may be candidates for hypofractionated radiation therapy. Common doses range between 21 and 40 Gy in 3–5 fractions.
- Patients should be followed with surveillance MRI every 2–3 months following SRS, or sooner, if symptoms warrant.

References

1. Barnholtz-Sloan JS, Yu C, Sloan AE, Vengoechea J, Wang M, Dignam JJ, et al. A nomogram for individualized estimation of survival among patients with brain metastasis. Neuro-Oncology. 2012;14(7):910–8.
2. Eichler AF, Loeffler JS. Multidisciplinary management of brain metastases. Oncologist. 2007;12(7):884–98.
3. Patchell RA, Tibbs PA, Walsh JW, Dempsey RJ, Maruyama Y, Kryscio RJ, et al. A randomized trial of surgery in the treatment of single metastases to the brain. N Engl J Med. 1990;322(8):494–500.
4. Patchell RA, Tibbs PA, Regine WF, Dempsey RJ, Mohiuddin M, Kryscio RJ, et al. Postoperative radiotherapy in the treatment of single metastases to the brain: a randomized trial. JAMA. 1998;280(17):1485–9.
5. Network NCC. NCCN clinical practice guidelines in Oncology: Central Nervous System Cancers Version 1.2017. 2017. Available from: https://www.nccn.org/professionals/physician_gls/pdf/cns.pdf.
6. Mulvenna P, Nankivell M, Barton R, Faivre-Finn C, Wilson P, McColl E, et al. Dexamethasone and supportive care with or without whole brain radiotherapy in treating patients with non-small cell lung cancer with brain metastases unsuitable for resection or stereotactic radiotherapy (QUARTZ): results from a phase 3, non-inferiority, randomised trial. Lancet. 2016;388(10055):2004–14.
7. Soltys SG, Adler JR, Lipani JD, Jackson PS, Choi CY, Puataweepong P, et al. Stereotactic radiosurgery of the postoperative resection cavity for brain metastases. Int J Radiat Oncol Biol Phys. 2008;70(1):187–93.
8. Brown PD, Jaeckle K, Ballman KV, Farace E, Cerhan JH, Anderson SK, et al. Effect of Radiosurgery Alone vs Radiosurgery With Whole Brain Radiation Therapy on Cognitive Function in Patients With 1 to 3 Brain Metastases: A Randomized Clinical Trial. JAMA. 2016;316(4):401–9.
9. Mahajan A, Ahmed S, McAleer MF, Weinberg JS, Li J, Brown P, et al. Post-operative stereotactic radiosurgery versus observation for completely resected brain metastases: a single-centre, randomised, controlled, phase 3 trial. Lancet Oncol. 2017;18(8):1040–8.
10. Brown PD, Ballman KV, Cerhan JH, Anderson SK, Carrero XW, Whitton AC, et al. Postoperative stereotactic radiosurgery compared with whole brain radiotherapy for resected metastatic brain disease (NCCTG N107C/CEC.3): a multicentre, randomised, controlled, phase 3 trial. Lancet Oncol. 2017;18(8):1049–60.
11. Boyd TS, Mehta MP. Stereotactic radiosurgery for brain metastases. Oncology (Williston Park). 1999;13(10):1397–409; discussion, 409–10, 413
12. O'Neill BP, Iturria NJ, Link MJ, Pollock BE, Ballman KV, O'Fallon JR. A comparison of surgical resection and stereotactic radiosurgery in the treatment of solitary brain metastases. Int J Radiat Oncol Biol Phys. 2003;55(5):1169–76.
13. Zadeh G. Surgery versus radiosurgery for the treatment of single brain metastases 2013. Available from: https://clinicaltrials.gov/ct2/show/NCT01295970.
14. Lang FF. Surgery versus stereotactic radiosurgery in the treatment of single brain metastasis: a randomized trial 2012. Available from: https://clinicaltrials.gov/ct2/show/NCT00460395.
15. Yamamoto M, Kawabe T, Sato Y, Higuchi Y, Nariai T, Watanabe S, et al. Stereotactic radiosurgery for patients with multiple brain metastases: a case-matched study comparing treatment results for patients with 2-9 versus 10 or more tumors. J Neurosurg. 2014;121. Suppl:16–25.
16. Kotecha R, Miller JA, Venur VA, Mohammadi AM, Chao ST, Suh JH, et al. Melanoma brain metastasis: the impact of stereotactic radiosurgery, BRAF mutational status, and targeted and/or immune-based therapies on treatment outcome. J Neurosurg. 2018;129(1):50–9.
17. Anderson ES, Postow MA, Wolchok JD, Young RJ, Ballangrud A, Chan TA, et al. Melanoma brain metastases treated with stereotactic radiosurgery and concurrent pembrolizumab display marked regression; efficacy and safety of combined treatment. J Immunother Cancer. 2017;5(1):76.
18. Acharya S, Mahmood M, Mullen D, Yang D, Tsien CI, Huang J, et al. Distant intracranial failure in melanoma brain metastases treated with stereotactic radiosurgery in the era of immunotherapy and targeted agents. Adv Radiat Oncol. 2017;2(4):572–80.
19. Qian JM, Yu JB, Kluger HM, Chiang VL. Timing and type of immune checkpoint therapy affect the early radiographic response of melanoma brain metastases to stereotactic radiosurgery. Cancer. 2016;122(19):3051–8.
20. Tawbi HA-H, Forsyth PAJ, Algazi AP, Hamid O, Hodi FS, Moschos SJ, et al. Efficacy and safety of nivolumab (NIVO) plus ipilimumab (IPI) in patients with melanoma (MEL) metastatic to the brain: Results of the phase II study CheckMate 204. J Clin Oncol. 2017;35(15 suppl):9507.
21. Shaw E, Scott C, Souhami L, Dinapoli R, Kline R, Loeffler J, et al. Single dose radiosurgical treatment of recurrent previously irradiated primary brain tumors and brain metastases: final report of RTOG protocol 90-05. Int J Radiat Oncol Biol Phys. 2000;47(2):291–8.
22. Timmerman R. A phase I dose-escalation study of stereotactic radiosurgery (SRS) for brain metastasis without whole brain radiation (WBRT) 2017. Available from: http://www.utsouthwestern.edu/research/fact/detail.html?studyId=STU%20022015-106.
23. Benedict SH, Yenice KM, Followill D, Galvin JM, Hinson W, Kavanagh B, et al. Stereotactic body radiation therapy: the report of AAPM Task Group 101. Med Phys. 2010;37(8):4078–101.
24. Trifiletti DM, Lee CC, Winardi W, Patel NV, Yen CP, Larner JM, et al. Brainstem metastases treated with stereotactic radiosurgery: safety, efficacy, and dose response. J Neuro-Oncol. 2015;125(2):385–92.

25. Stafford SL, Pollock BE, Leavitt JA, Foote RL, Brown PD, Link MJ, et al. A study on the radiation tolerance of the optic nerves and chiasm after stereotactic radiosurgery. Int J Radiat Oncol Biol Phys. 2003;55(5):1177–81.
26. Kirkpatrick JP, Soltys SG, Lo SS, Beal K, Shrieve DC, Brown PD. The radiosurgery fractionation quandary: single fraction or hypofractionation? Neuro-Oncology. 2017;19(suppl 2):ii38–49.
27. Eaton BR, Gebhardt B, Prabhu R, Shu HK, Curran WJ Jr, Crocker I. Hypofractionated radiosurgery for intact or resected brain metastases: defining the optimal dose and fractionation. Radiat Oncol. 2013;8:135.
28. Fokas E, Henzel M, Surber G, Kleinert G, Hamm K, Engenhart-Cabillic R. Stereotactic radiosurgery and fractionated stereotactic radiotherapy: comparison of efficacy and toxicity in 260 patients with brain metastases. J Neuro-Oncol. 2012;109(1):91–8.
29. Fowler JF, Tome WA, Fenwick JD, Mehta MP. A challenge to traditional radiation oncology. Int J Radiat Oncol Biol Phys. 2004;60(4):1241–56.
30. Kirkpatrick JP, Wang Z, Sampson JH, McSherry F, Herndon JE 2nd, Allen KJ, et al. Defining the optimal planning target volume in image-guided stereotactic radiosurgery of brain metastases: results of a randomized trial. Int J Radiat Oncol Biol Phys. 2015;91(1):100–8.
31. Baumert BG, Rutten I, Dehing-Oberije C, Twijnstra A, Dirx MJ, Debougnoux-Huppertz RM, et al. A pathology-based substrate for target definition in radiosurgery of brain metastases. Int J Radiat Oncol Biol Phys. 2006;66(1):187–94.
32. Noel G, Simon JM, Valery CA, Cornu P, Boisserie G, Hasboun D, et al. Radiosurgery for brain metastasis: impact of CTV on local control. Radiother Oncol. 2003;68(1):15–21.
33. Nataf F, Schlienger M, Liu Z, Foulquier JN, Gres B, Orthuon A, et al. Radiosurgery with or without A 2-mm margin for 93 single brain metastases. Int J Radiat Oncol Biol Phys. 2008;70(3):766–72.
34. Andrews DW, Scott CB, Sperduto PW, Flanders AE, Gaspar LE, Schell MC, et al. Whole brain radiation therapy with or without stereotactic radiosurgery boost for patients with one to three brain metastases: phase III results of the RTOG 9508 randomised trial. Lancet. 2004;363(9422):1665–72.
35. Aoyama H, Shirato H, Tago M, Nakagawa K, Toyoda T, Hatano K, et al. Stereotactic radiosurgery plus whole-brain radiation therapy vs stereotactic radiosurgery alone for treatment of brain metastases: a randomized controlled trial. JAMA. 2006;295(21):2483–91.

Stereotactic Radiosurgery for Pituitary Adenoma

Cheng-chia Lee, Daniel M. Trifiletti, and Jason P. Sheehan

Introduction

Pituitary adenomas account for 10–20% of all intracranial tumors [1]. They are classified according to hormonal secretory status and size. Despite homogeneity in appearance and anatomical location, pituitary tumors generate a wide variety of clinical sequelae. Enlargement of nonfunctioning pituitary adenomas can result in compression of the optic apparatus, which can cause visual field deficits, and compression of the normal pituitary gland, which can cause hypopituitarism. In contrast, functioning pituitary adenomas can cause a variety of syndromes. Prolactinomas can lead to amenorrhea-galactorrhea syndrome; growth hormone (GH)-secreting adenomas cause acromegaly in adults and gigantism in children; and adrenocorticotropic hormone (ACTH)-secreting adenomas cause Cushing's disease.

Pituitary tumors can be treated using medical therapy, microscopic or endoscopic transsphenoidal surgery, radiosurgery, radiation therapy, or observation. Stereotactic radiosurgery (SRS) is usually indicated for [1] incomplete surgical resections that leave residual tumor, [2] tumor recurrence, or [3] cases in which medical therapy provides inadequate hormone control. In this chapter, we discuss the principles and methods associated with SRS for the treatment of pituitary tumors, primarily focusing on nonfunctioning adenomas, GH-secreting adenomas, and ACTH-secreting adenomas. The post-radiosurgery radiographic tumor control rate for nonfunctioning/functioning adenomas is close to 90%; however, the incidence rate of biochemical remission for functioning adenomas is lower. Among patients with pituitary tumors, those with Cushing's disease enjoy the highest endocrine remission rates, while patients with prolactinomas have the lowest remission rates (ranging from 30% to 80%). Due to the high risk of late recurrence after endocrine remission, rigorous long-term clinical and radiographic follow-up should be implemented in all cases of pituitary adenoma treated with SRS.

Site-Specific Considerations

All suspected pituitary tumors should be subjected to a complete neuroimaging study, an endocrine evaluation, and an ophthalmologic examination prior to treatment with SRS. Endocrine examinations should consider all aspects of the hypothalamic-pituitary-end organ axis, including the levels of GH, insulin-like growth factor-1 (IGF-1), ACTH, serum cortisol, prolactin, T4 or free T4, thyroxin-stimulating hormone (TSH), luteinizing hormone (LH), follicle-stimulating hormone (FSH), and testosterone (in men). Imaging studies should include magnetic resonance imaging (MRI) with thin slices and volume acquisition through the region of the sella turcica. Ophthalmological evaluation should include visual acuity and testing of the visual field.

An initial diagnosis of pituitary adenoma can generally be made based on the radiographic characteristics of the tumor in conjunction with a biochemical assessment. In cases other than prolactinoma, initial craniotomy or surgical resection via transsphenoidal surgery is recommended. In cases of prolactinoma, medical treatment with bromocriptine and cabergoline is preferred, with surgical resection or

C.-c. Lee
Department of Neurosurgery, Neurological Institute, Taipei Veterans General Hospital, Taipei, Taiwan

National Yang-Ming University, Taipei, Taiwan

D. M. Trifiletti
Mayo Clinic, Radiation Oncology, Mayo Clinic School of Medicine, Radiation Oncology, Jacksonville, FL, USA

J. P. Sheehan (✉)
University of Virginia Medical Center, Neurological Surgery, Charlottesville, VA, USA

University of Virginia School of Medicine, Neurological Surgery, Charlottesville, VA, USA
e-mail: jsheehan@virginia.edu

D. M. Trifiletti et al. (eds.), *Stereotactic Radiosurgery and Stereotactic Body Radiation Therapy*,
https://doi.org/10.1007/978-3-030-16924-4_11

radiosurgery used only when prolactinomas show biochemical resistance to dopamine agonists.

SRS is generally recommended for residual or recurrent functioning and nonfunctioning pituitary adenomas. In cases of neurological deficit due to adenoma, surgical resection is the preferred treatment modality unless the tumor is a prolactinoma. In cases of Cushing's disease and acromegaly, endoscopic and microscopic transsphenoidal surgery can provide rapid relief of mass effect and control over hormone levels. Finally, for all cases that involve a functioning adenoma, initial surgical resection can also be performed to facilitate a smaller target, further away from critical structures in radiosurgery (like the optic chiasm), and during radiosurgery, higher doses of radiation can more safely be applied.

Stereotactic frame surgeries, such as the Leksell frame for Gamma Knife, can be performed under sedation or local anesthesia [2]. For this type of surgery, the angle of the optic apparatus can be adopted as the axis of the frame, as it approximates a line between the lateral canthus and the top of the pinna. This alignment allows the optic nerves, chiasm, and tracts to be identified within a single MRI slice [3].

Clinical Evidence

Outcomes of Radiosurgery for Nonfunctioning Pituitary Adenomas

The fact that endocrine presentation is frequently silent means that radiologic tumor control is the primary goal of radiosurgery in cases of nonfunctioning adenoma. Multiple studies have reported that SRS achieves tumor control rates of 94–97% at 5 years and 76–87% at 10 years. Furthermore, new-onset hypopituitarism was only observed in 2–30% of all cases (with a median occurrence rate of 21%) [4–8]. Table 1 lists the major radiosurgical series for nonfunctioning adenoma. One trial that investigated the role of SRS among 512 patients with nonfunctioning pituitary adenomas reported an overall tumor control rate of 93% (median follow-up of 36 months; range, 1–223 months) [7]. Tumor control and neurological preservation including visual function and other cranial nerves for eyeball movements were more common among [1] older patients (>50 years), [2] patients with a tumor volume <5 cc, and [3] patients who had not previously undergone fractionated radiation therapy [7]. Figure 1 presents an illustrative case involving a nonfunctioning pituitary adenoma.

Outcomes of Radiosurgery for Functioning Pituitary Adenomas

When applied to functioning adenomas, the primary objectives of radiosurgery are endocrine remission and tumor control. However, in some cases tumor control is not accompanied by endocrine remission. Radiosurgery also plays an important role in treating Cushing's disease, acromegaly, and prolactinomas that are resistant to medical management.

Between 28% and 70% of Cushing's disease patients undergo endocrine remission within 12 months of radiosurgery [9–14]. Endocrine remission is typically defined by normal levels of 24-hour urinary free cortisol (UFC) and serum cortisol while off of antisecretory medications. For Cushing's disease, higher radiosurgical doses are generally required to achieve endocrine remission than to control the growth of nonfunctioning adenomas, and delays in endocrine recurrence following radiosurgery-induced remission are common. In one radiosurgical series involving 90 patients with Cushing's disease (mean follow-up of 45 months), ten patients suffered disease recurrence within a mean duration of 27 months after initial remission [11]. Table 2 lists a number of major radiosurgical series for Cushing's disease.

Studies on acromegaly have reported a great deal of variation in endocrine remission rates (range, 0–82%), likely due to different remission criteria adopted by different researchers. When remission is defined as the normalization of IGF-1

Table 1 Major radiosurgical series for nonfunctioning adenoma

Study	Year	*n*	FU period (mo)	Margin dose (Gy)	Tumor control (%)	Hypopituitarism (%)	New-onset CN deficits (%)
Liscak et al. [5]	2007	140	60	20	100% at 5 years	2%	0%
Iwata et al.[a] [4]	2011	100	33	21Gy/3Fr, 25Gy/5Fr	98% at 3 years	4%	1%
Park et al. [6]	2011	125	62	13	99%, 94%, and 76% at 1, 5, and 10 years	24%	0.8% from CN2, 1.6% from other CN
Starke et al. [8]	2012	140	50	18	98%, 97%, 91%, and 87% at 2, 5, 8, and 10 years	30.3%	12.8% from CN2, 0.9% from other CN
Sheehan et al.[b] [13]	2013	512	36	16	98%, 95%, 91%, and 85% at 3, 5, 8, and 10 years	21%	6.6% from CN2, 2.7% from other CN

Abbreviation: *CN* cranial nerve, *Fr* fraction, *FU* follow-up, *Gy* gray, *mo* month, *NA* not available
[a]CyberKnife series, others were Gamma Knife
[b]From a multicenter study

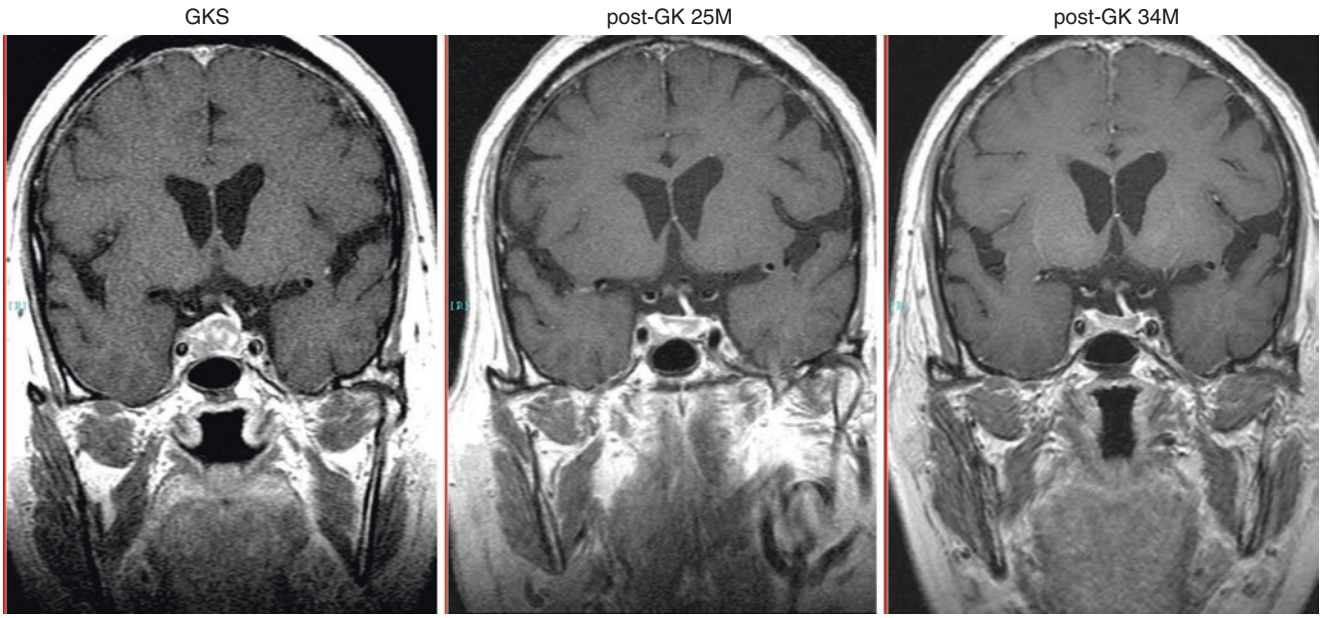

Fig. 1 An illustrative case with a nonfunctioning pituitary adenoma. The adenoma was apart from the optic nerve after transsphenoidal surgery and suitable for GK radiosurgery. The post-GK MRI showed the continuously tumor regression within 3 years

Table 2 Major radiosurgical series for Cushing's disease

Study	Year	*n*	FU period (mo)	Margin dose (Gy)	Endocrine remission (%)	Hypopituitarism (%)	New-onset CN deficits (%)
Devin et al.[a] [10]	2004	35	42	15	49	40%	0%
Castinetti et al. [9]	2007	40	55	30	43	15%	5%
Kobayashi et al. [12]	2009	30	64	29	35	N/A	N/A
Wan et al. [14]	2009	68	67	23	28	N/A	N/A
Sheehan et al. [13]	2013	96	48	22	70	36%	5.2%

Abbreviation: *CN* cranial nerve, *Fr* fraction, *FU* follow-up, *Gy* gray, *mo* month, *NA* not available
[a]From LINAC series

Table 3 Major radiosurgical series for acromegaly

Study	Year	*n*	FU period (mo)	Margin dose (Gy)	Endocrine remission (%)	Hypopituitarism (%)	New-onset CN deficits (%)
Castinetti et al. [16]	2005	82	50	25	17%	17%	1.2%
Jezkova et al. [18]	2006	96	54	35	54% at 54 months f/u	14–41% in various axis	0%
Losa et al. [19]	2008	83	69	22	53% at 5 years	8.5%	0%
Wan et al. [14]	2009	103	67	21	37%	N/A	N/A
Franzin et al. [17]	2012	103	71	23	58% at 5 years	7.8%	0%
Lee et al. [15]	2014	136	62	25	32, 65, 73, and 83% at 2, 4, 6, and 8 years	31.6%	1.5%

Abbreviation: *CN* cranial nerve, *Fr* fraction, *FU* follow-up, *Gy* gray, *mo* month, *NA* not available

or nadir serum GH <2.5 ug/dL [15], the remission rate for acromegaly patients is 53–60% 5 years after radiosurgery [14–19]. A number of studies have also used the oral glucose tolerance test (OGTT) to define endocrine remission for acromegaly (Table 3). Acromegaly patients are more likely to achieve endocrine remission if they [1] underwent surgical resection prior to radiosurgery or [2] had a functioning adenoma with a volume measuring <3 cc at the time of radiosurgery [20]. In one study that was conducted at the University of Virginia, the median time to endocrine remission after

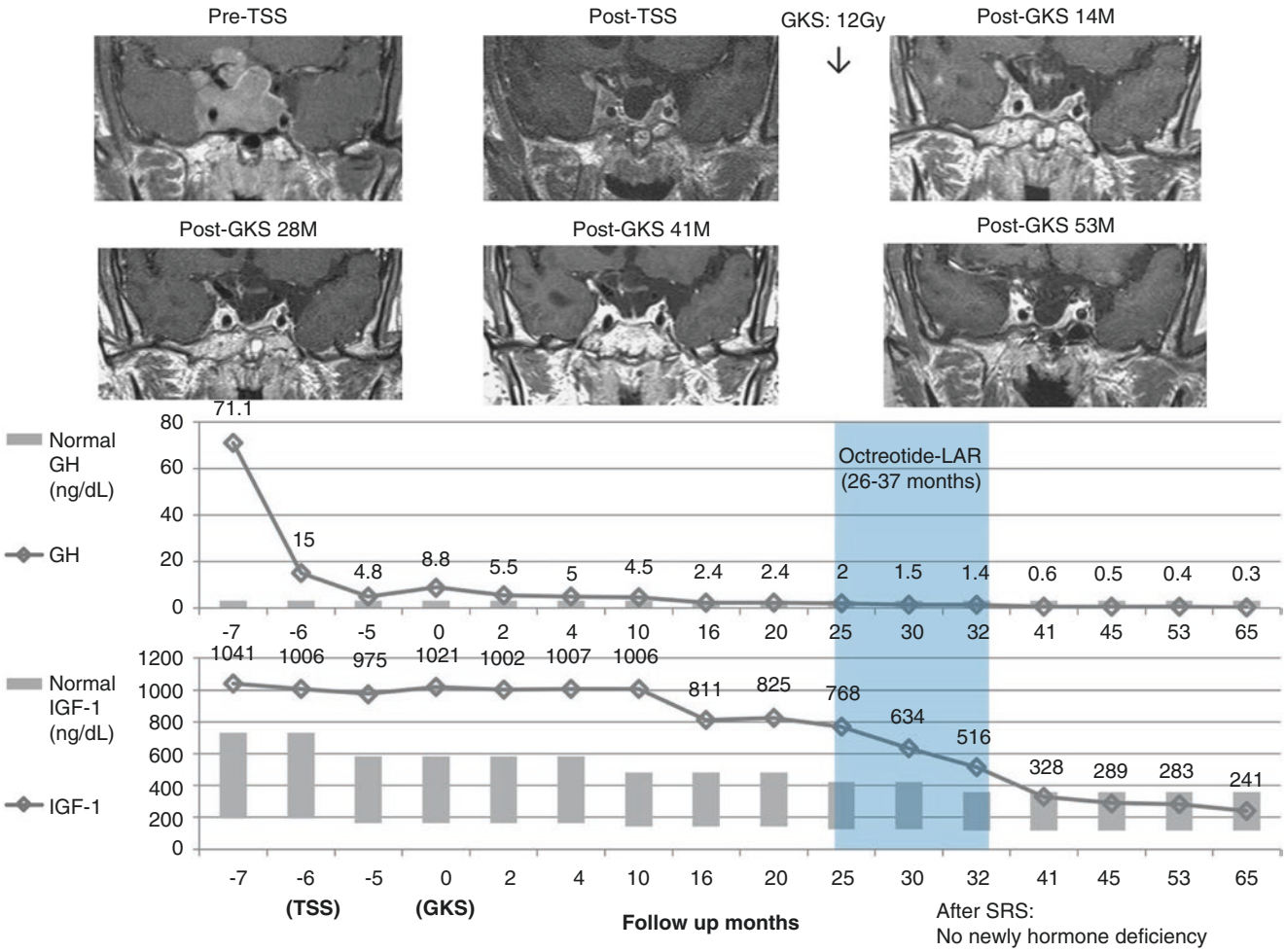

Fig. 2 An illustrative case with acromegaly. The adenoma can be controlled after GK radiosurgery; furthermore, the hormone remission was achieved 32 months after GK radiosurgery. During the period of latency, before hormone remission, octreotide can be prescribed for preventing the risks of growth hormone hypersecretion

radiosurgery for acromegaly was 24 months, which is longer than that of patients with Cushing's disease [20]. Evidence from retrospective studies further indicated that temporarily halting pituitary suppressive medications at the time of radiosurgery increases the likelihood of endocrine remission in acromegaly patients [21]. Figure 2 presents an illustrative case with acromegaly.

Treating prolactinoma with a margin dose of 13–30 Gy radiation has led to remission rates that range between 0% and 84% [22–28], whereby higher radiation doses were significantly associated with higher remission rates [24–26, 29]. Witt and colleagues reported no remission among prolactinoma patients treated with margin doses below 19 Gy [29]. Conversely, Pan and colleagues reported that, when SRS was used as an upfront treatment for prolactinoma, margin doses exceeding 30 Gy resulted in a remission rate of 52% [30]. Furthermore, a study conducted at the University of Virginia reported that only 26% of patients with medical-refractory prolactinomas achieved prolactin normalization within 24.5 months of SRS. Individuals who were not taking antisecretory medication at the time of SRS were more likely to achieve endocrine remission [26]. These results are consistent with the findings of Landolt and Lomax [23]. Nonetheless, despite evidence to support its efficacy, SRS is not typically used as the primary treatment for prolactinoma in most medical centers [30]. Indeed, most prolactinomas respond well to medical therapy. Therefore, SRS is generally reserved as a salvage therapy for patients who demonstrate medical refractory prolactinomas (i.e., a more aggressive adenoma phenotype).

Toxicity

The side effects of ionizing radiation are classified as resulting from acute toxicity (i.e., they occur within days), early delayed toxicity (i.e., they occur within weeks), or late delayed toxicity (they occur within months to years). Acute

toxicity is far less common in frequency with stereotactic radiosurgery than with conventional radiotherapy. Most injuries associated with acute radiation poisoning, such as hair loss and skin changes, are rarely encountered in clinical settings. Early delayed radiation injuries include hypopituitarism and hypothalamic dysfunction, radiation necrosis, new-onset visual deterioration, and other cranial nerve dysfunctions. The risk of late delayed radiation injuries is low when radiosurgery is used in the treatment of sellar tumors. Complications resulting from stereotactic radiosurgery vary according to the target volume, proximity of the tumor near critical structures, and radiation dose delivered.

Hypopituitarism and Hypothalamic Dysfunction

The most common intermediate to late SRS complication related to pituitary adenoma is hypothalamic-pituitary dysfunction. Approximately 30–50% of patients develop a new hormone deficiency within 5–10 years of radiosurgery [7, 11, 20, 31, 32]. In a University of Virginia study that investigated the use of SRS in treating pituitary adenoma, 30% patients developed delayed onset hypopituitarism within 3 years. Thyroid hormones were most affected, followed by gonadotrophic hormone, ACTH, and GH [33]. Two independent variables appear to be strong predictors of hormone deficiency: margin dose to the tumor and suprasellar extension [33]. An ideal radiosurgical plan applies a steep gradient index to minimize the amount of radiation that is received by normal pituitary tissue, thereby reducing the risk of treatment-induced hypopituitarism. Nonetheless, there is no completely "safe dose" below which the patient will not experience any hypopituitarism, and the radiosurgical dose that is determined to be optimal for a target lesion should not be compromised in order to avoid hypopituitarism. The clinical consequences of macroscopic tumor progression, tumor recurrence, or persistent hormone hypersecretion far outweigh those of radiosurgery-induced hypopituitarism, which can generally be managed by neuroendocrinologists.

On the other hand, very few patients present new-onset diabetes insipidus following SRS, and the incidence of the disorder following radiosurgery is generally related to changes in the tumor complex, which can have a mechanical impact on the pituitary gland. Other forms of hypothalamic dysfunction, such as poor control of body temperature and changes in sleep or appetite, are exceedingly rare post-SRS.

Cranial Neuropathy

Cranial neuropathies are another common complication related to radiosurgical treatment of pituitary adenomas. By virtue of their location in the parasellar and suprasellar regions, multiple cranial nerves, including II, III, IV, V, and VI, are at risk of inadvertent injury from radiosurgery. Nonetheless, most radiosurgical series have reported neurological deficits in fewer than 5% of all cases. Optic neuropathy is the most common deficit, due to the CN II's high sensitivity to radiation-induced damage [7]. In a recent study of 217 pituitary adenoma patients who underwent radiosurgery, nine (4%) developed new or worsened cranial nerve dysfunction. Among patients with radiosurgery-induced cranial neuropathies, six (67%) achieved complete resolution during a median follow-up period of 32 months. The maximum single session radiosurgical dose to the optic apparatus is typically kept below 8–12 Gy in order to minimize the risk of damage to the optic nerve. Careful dose planning with contouring and shielding of critical structures should allow optimal doses to be delivered to the target area while also safeguarding critical structures.

Late Delayed RE

During the era of conventional radiotherapy, radiation complications related to late toxicity following treatment of sellar tumors included radiation-induced secondary brain tumors and cerebrovascular disturbances [34–37]. Now that radiosurgery is used to treat sellar tumors, the risk of a radiation-induced secondary tumor has been substantially reduced. This may be due to a longer latency period; however, it may also be explained by the sharp dose gradient that is applied to facilitate stereotactic radiosurgery, which greatly lowers the number of cells that are at risk for malignant transformation compared to broad-field radiation therapy [38]. This hypothesis is supported by a long-term follow-up study published by Rowe [39], in which only one new primary intracranial tumor was reported among 4877 patients that had been treated using SRS. In addition, no cases of radiation-induced neoplasm have been reported following the use of radiosurgery to treat pituitary tumors, and few cases of cerebrovascular complications have been reported following SRS of pituitary tumors. Such cerebrovascular complications albeit rare can cause cerebral infarction from internal carotid artery (ICA) occlusion [40].

Plan Quality

The treatment regimes used for pituitary adenoma include Gamma Knife (GK) radiosurgery, CyberKnife, linear accelerator (LINAC)-based radiosurgery, 3D conformal radiotherapy (CRT), stereotactic radiotherapy (SRT), intensity-modulated radiotherapy (IMRT), volumetric arc therapy (VMAT), and proton beam therapy. Stereotactic radiosurgery (SRS) is

generally the preferred treatment approach due to the benign tumor nature and clear radiographic tumor margins that characterize most pituitary adenomas.

In conventional, single fraction Gamma Knife radiosurgery, a Leksell frame is used to immobilize the head. Other forms of radiosurgery and radiation therapy rely on CT simulation in conjunction with a thermoplast mask for immobilization. In the latest Gamma Knife (Icon®) model, CT simulation and infrared tracking may be used in conjunction with a thermoplast mask to achieve immobilization.

It is preferable to obtain a volumetric thin-slice MRI with T2 and T1 pre- and post-gadolinium (for postoperative adenomas, sometimes thin-section dynamic contrast-enhanced imaging or fat suppression imaging is used) for target delineation. Pre-contrast sequences include coronal and sagittal T1-weighted images (1 mm sections), fast spin echo (FSE) axial images, and coronal T2-weighted images (1 mm sections). Post-contrast sequences include coronal T1-weighted images (1 mm sections), sagittal FSE T1-weighted images (1 mm sections), and coronal spoiled gradient echo (SPGR) T1-weighted images. The use of CT with and without contrast for target delineation can be valuable for dose correction calculations and distortion correction for various systems.

In cases of partially removed or recurrent adenomas, the border between the remaining tumor and normal pituitary tissue should be clearly defined. In cases where dural invasion is detected intraoperatively, the dural edge along the cavernous sinus may need to be included in the gross target volume (GTV). Radiation can generally be delivered to the dural edge when treating functioning adenomas, such as acromegaly and Cushing's disease, due to the frequency of dural invasion of these subtypes.

Whenever possible, care should be taken to avoid high doses of radiation or "hot spots" in critical neurovascular structures, such as the optic apparatus around the tumor, cranial nerves, or the carotid artery within the cavernous sinus region. Ideally, the optic apparatus can be clearly delineated to obtain a precise estimate of radiation exposure and thereby mitigate radiation-induced optic neuropathy. The cavernous portion of the internal carotid artery (ICA) can be included in the GTV if the adenoma encases the ICA and invades the dura within the cavernous sinus.

Dose Prescriptions

Single session radiosurgical margin doses are generally 12–18 Gy for nonfunctioning adenomas and 15–30 Gy for functioning adenomas. The systemic effects of radiation can be highly effective against functioning adenomas; therefore, the intuitive approach would be to deliver a sufficiently high dose (≥20 Gy to the margin) to allow for effective control of tumor growth and rapid normalization of hormone levels.

Table 4 Suggested target volumes

Target volumes	Definition and description
GTV (gross target volume)	Tumor extent observed in postoperative T1 pre- and post-gadolinium images and in 3-month postoperative MRIs are helpful in identifying residual/recurrent tumors; thin-section dynamic contrast-enhanced images can be used to identify microadenomas
CTV (clinical target volume)	Generally equal to GTV in cases of pituitary adenoma; however, a margin may be extended to account for dural and/or cavernous sinus invasion
PTV (planned target volume)	Generally equal to CTV in cases of single fraction SRS. When performing hypofractionated SRS or fully fractionated RT, a margin may be added to account for targeting uncertainties

Table 5 Recommended normal tissue constraints

Structure at risk	Suggested dose constraints
Optic nerves and chiasm	<8–12 Gy to Dmax (maximal dose)
Hippocampi and hypothalamus	Beam angles and techniques (e.g., GK, CyberKnife, LINAC-based radiosurgery, IMRT, and proton therapy) should be selected to minimize the dose received by the hippocampi and hypothalamus
Normal pituitary tissue	Beam angles and techniques (e.g., GK, CyberKnife, LINAC-based radiosurgery, IMRT, and proton therapy) should be selected to minimize the dose received by the normal pituitary gland and stalk

Unfortunately, it is not known to what degree a higher margin dose (e.g., 20 Gy vs. 30 Gy) results in delayed hypopituitarism. In cases of functioning adenomas that have radiologically identifiable targets in the cavernous sinus, radiosurgical plans can be based on higher margin doses, as much of the normal stalk, gland, and optic apparatus can be shielded. Nonfunctioning pituitary adenomas appear to require lower radiosurgery margin doses than functioning adenomas. The minimum dose required to effectively treat a nonfunctioning tumor is currently unknown; however, many medical centers apply 12–15 Gy to the margin of nonfunctioning adenomas when radiation is delivered in a single fraction.

Hypofractionated and fractionated dose regimens vary according to target volume, location, tumor type (functioning vs. nonfunctioning), prior radiation treatments, and proximity to critical structures.

Tables 4 and 5 showed the suggested target volumes and normal tissue constraints.

Future Directions

Role of Upfront Radiosurgery

In managing pituitary adenomas, radiosurgery should generally be reserved for [1] recurrent or residual lesions and [2]

patients with a functioning adenoma that shows persistent hormone hypersecretion despite surgical intervention. Use of upfront radiosurgery for functioning pituitary adenomas should be considered in selected cases where there is a clear diagnosis of an adenoma, no need to decompress critical structures or reduce the adenoma volume, and/or for patients who are not fit or unwilling to undergo a resection. In one multicenter study [41], patients with nonfunctioning adenoma underwent GK radiosurgery as the primary management strategy due to advanced age, multiple comorbidities, or psychiatric disorders. The overall tumor control rate was 92.7%, and the actuarial tumor control rates were 94% and 85% at 5 and 10 years post-radiosurgery, respectively. Radiosurgery can also be considered for upfront treatment in cases where the adenoma resides largely in the cavernous sinus or in cases where resection is unlikely to substantially reduce tumor size.

Efficacy of SRS in Treating Various Histological Entities of Nonfunctioning Adenomas

Silent corticotroph pituitary adenoma is a rare form of nonfunctioning adenoma, which tends to be particularly aggressive and has a high recurrence rate after SRS. One study at the University of Virginia identified 27 patients with silent corticotroph pituitary adenoma, based on a histopathological analysis. At 3, 5, and 8 years, actuarial progression-free survival rates were 97%, 95%, and 89% in the nonfunctioning group and 84%, 52%, and 52% in the silent corticotroph pituitary adenoma group, respectively [42]. In such cases, doses higher than those generally used to treat nonfunctioning adenomas (13–18 Gy) may be considered reasonable. Further studies will be required to confirm these findings.

The Treatment Strategy for Functioning Adenomas Depends on Their Histological Characteristics

Various subtypes of somatotroph-cell pituitary adenomas are correlated with a range of clinical and histopathological variables. In most cases, densely granulated (DG) somatotroph-cell adenomas are more responsive to somatostatin analog drugs than are sparsely granulated (SG) somatotroph-cell adenomas. Nonetheless, the patients with SG adenoma show a similar response to SRS as do patients with DG adenoma. Thus, early SRS intervention may be considered reasonable for patients with SG adenoma for whom medical therapy is less effective [43].

In a study conducted at the University of Virginia [43], patients with SG adenoma were more likely to be younger and female, and SG adenomas tended to be highly invasive into the cavernous sinus. The actuarial remission rates in the DG adenoma group at 2, 4, and 6 years post-radiosurgery were 35.1%, 71.4%, and 79.3%, respectively, whereas those in the SG adenoma group were 35.4%, 73.1%, and 82.1%, respectively.

Radioresistant Effects of Antisecreting Medications

Somatostatin analogs have been shown to negatively affect the outcomes of SRS for acromegaly [23, 44]. Landolt and colleagues observed that patients treated with octreotide in conjunction with SRS reached normal growth hormone and IGF-1 levels more slowly than patients who did not receive the drug [23]. The Mayo group reported similar results in 2002 [44]. A similar situation was encountered among patients with prolactinomas who received antisecretory medication at the time of radiosurgery [30]. Based on these findings, we generally advise patients to discontinue antisecretory medications for 6 weeks prior to SRS and resume them 2–6 weeks after SRS. Researchers have observed similar deleterious effects in Cushing's disease patients when ketoconazole was administered after SRS [13]. Nonetheless, larger, randomized clinical trials will be required to confirm the negative relationship between hormone suppression medications and radiosurgery outcomes.

Whole-Sellar SRS for MR Indeterminate Functioning Adenomas

Whole-sellar SRS is based on hypophysectomies for MRI-negative, but hormone-active, Cushing's disease. Although MRI is the most effective imaging modality used to define pituitary adenomas, detection fails in 36–64% of patients with ACTH-secreting pituitary adenomas [45]. Residual tumors that present microscopic infiltration of the venous sinuses or adjacent dura tend to resist detection in neuroimaging studies and are not surgically accessible. Moreover, the recurrence rates for Cushing's disease have been found to range from 5% to 27%, over a mean follow-up of 6.7–9.6 years [46–49]. Therefore, whole-sellar SRS appears to be a reasonable approach in some cases. Specifically, this procedure attempts to treat recurrent or persistent tumors by delivering focused, high-dose radiation to the entire sellar and parasellar contents. At the University of Virginia, radiosurgery was applied to the entire sella of symptomatic patients with medically refractory, invasive, or imaging-negative functioning pituitary adenomas [50]. Endocrine remission rates of 54%, 78%, and 87% were achieved within 2, 4, and 6 years after SRS, respectively. Hypopituitarism was observed in 42.2% of the patients, and 3.1% eventually developed panhypopituitarism. Hypopituitarism in patients with whole-sellar radiosurgery is likely greater than for those

in which a well-demarcated adenoma is targeted alone. The fact that patients with post-radiosurgery hypopituitarism can be treated using hormone replacements means that whole-sellar SRS may be an effective treatment for patients with a functioning adenoma that does not appear as a discrete entity in MRI [50].

Practical Considerations

- Gamma Knife radiosurgery, CyberKnife, LINAC-based radiosurgery, 3D CRT, IMRT, VMAT, and proton therapy can all be used for the treatment of pituitary adenomas. Techniques and tools have advanced tremendously in recent decades.
- The popularity of radiosurgery in the treatment of pituitary adenomas has been growing. Typically, pituitary adenomas tend to be discrete, small-volume tumors comprised of late responding tissue. These adenomas often occur in proximity to critical structures.
- Radiosurgery (e.g., Gamma Knife Icon or Extend, CyberKnife, LINAC-based and radiosurgery) can be hypofractionated into 2–5 sessions in order to tailor a dose plan to the specifics of a particular case, typically the dose to the optic apparatus.
- In some cases, standard fractionation schemes (>5 fractions), 3D CRT, IMRT, VMAT, or proton therapy can be used to treat tumors of larger volume, tumors with less distinct margins, and tumors which are so close to critical structures that single or hypofractionated approaches are not feasible.
- Computer-based dose planning software (e.g., Gamma Plan®, Elekta, Stockholm, Sweden) is generally used to formulate treatment plans for pituitary adenoma. Initially, the target lesion and surrounding structures are contoured. A dose plan, which aims to deliver an ideal dose to the target and a safe dose to adjacent critical structures, is then developed. Lastly, conformality, dose uniformity, and gradient index are assessed in order to further refine the dose plan.
- Visual deterioration following SRS is rare and can usually be avoided by restricting the dose to the optic apparatus to <8 Gy. Nonetheless, some researchers have reported cases where the optic apparatus was exposed to 10–12 Gy without complications.
- It is generally preferable to maintain a distance of 3 mm or more between the rostral extent of the adenoma and the optic apparatus. The absolute distance between the adenoma and optic apparatus defines how steeply the radiation gradient must be to ensure that the delivered radiation dose is tolerable to the optic apparatus but is still effective in treating the adenoma. If an acceptable gradient cannot be achieved, then an alternative treatment should be considered. State-of-the-art radiosurgical devices may allow a distance of as little as 1–2 mm between the target volume and the optic apparatus.
- The tolerable absolute dose permitted to critical structures ultimately varies from patient to patient and can be affected by a variety of factors, such as previous damage to the optic apparatus caused by pituitary adenoma compression, ischemic changes, type and timing of previous interventions (e.g., fractionated radiation therapy and surgery), patient age, and the presence or absence of other comorbidities (e.g., diabetes or hypertension).
- Most of the cranial nerves in the cavernous sinus are more resistant to the effects of radiation than the optic nerve. However, reports of cranial neuropathy, particularly after repeated radiosurgeries, have been documented. The tolerable limit to the cavernous sinus nerve is not precisely known; however, reports have detailed effective single session radiosurgical doses that range from 19 to 30 Gy and have a low risk of appreciable side effects. Injuries to the cavernous segment of the carotid artery after SRS are very rare.

References

1. Vance ML. Treatment of patients with a pituitary adenoma: one clinician's experience. Neurosurg Focus. 2004;16:E1.
2. Walton L, Hampshire A, Roper A, Mitchell P, Vaughan P, Forster DM, et al. Development of a relocatable frame technique for Gamma Knife radiosurgery. Technical note. J Neurosurg. 2000;93(Suppl 3):198–202.
3. Hayashi M, Taira T, Chernov M, Fukuoka S, Liscak R, Yu CP, et al. Gamma Knife surgery for cancer pain-pituitary gland-stalk ablation: a multicenter prospective protocol since 2002. J Neurosurg. 2002;97:433–7.
4. Iwata H, Sato K, Tatewaki K, Yokota N, Inoue M, Baba Y, et al. Hypofractionated stereotactic radiotherapy with CyberKnife for nonfunctioning pituitary adenoma: high local control with low toxicity. Neuro-Oncology. 2011;13:916–22.
5. Liscak R, Vladyka V, Marek J, Simonova G, Vymazal J. Gamma Knife radiosurgery for endocrine-inactive pituitary adenomas. Acta Neurochir. 2007;149:999–1006. discussion 1006.
6. Park KJ, Kano H, Parry PV, Niranjan A, Flickinger JC, Lunsford LD, et al. Long-term outcomes after Gamma Knife stereotactic radiosurgery for nonfunctional pituitary adenomas. Neurosurgery. 2011;69:1188–99.
7. Sheehan JP, Starke RM, Mathieu D, Young B, Sneed PK, Chiang VL, et al. Gamma Knife radiosurgery for the management of nonfunctioning pituitary adenomas: a multicenter study. J Neurosurg. 2013;119:446–56.
8. Starke RM, Williams BJ, Jane JA Jr, Sheehan JP. Gamma Knife surgery for patients with nonfunctioning pituitary macroadenomas: predictors of tumor control, neurological deficits, and hypopituitarism. J Neurosurg. 2012;117:129–35.
9. Castinetti F, Nagai M, Dufour H, Kuhn JM, Morange I, Jaquet P, et al. Gamma Knife radiosurgery is a successful adjunctive treatment in Cushing's disease. Eur J Endocrinol. 2007;156:91–8.
10. Devin JK, Allen GS, Cmelak AJ, Duggan DM, Blevins LS. The efficacy of linear accelerator radiosurgery in the management of patients with Cushing's disease. Stereotact Funct Neurosurg. 2004;82:254–62.

11. Jagannathan J, Sheehan JP, Pouratian N, Laws ER, Steiner L, Vance ML. Gamma Knife surgery for Cushing's disease. J Neurosurg. 2007;106:980–7.
12. Kobayashi T. Long-term results of stereotactic Gamma Knife radiosurgery for pituitary adenomas. Specific strategies for different types of adenoma. Prog Neurol Surg. 2009;22:77–95.
13. Sheehan JP, Xu Z, Salvetti DJ, Schmitt PJ, Vance ML. Results of Gamma Knife surgery for Cushing's disease. J Neurosurg. 2013;119(6):1486–92.
14. Wan H, Chihiro O, Yuan S. MASEP Gamma Knife radiosurgery for secretory pituitary adenomas: experience in 347 consecutive cases. J Exp Clin Cancer Res. 2009;28:36.
15. Lee CC, Vance ML, Xu Z, Yen CP, Schlesinger D, Dodson B, et al. Stereotactic radiosurgery for acromegaly. J Clin Endocrinol Metab. 2014;99:1273–81.
16. Castinetti F, Taieb D, Kuhn JM, Chanson P, Tamura M, Jaquet P, et al. Outcome of Gamma Knife radiosurgery in 82 patients with acromegaly: correlation with initial hypersecretion. J Clin Endocrinol Metab. 2005;90:4483–8.
17. Franzin A, Spatola G, Losa M, Picozzi P, Mortini P. Results of Gamma Knife radiosurgery in acromegaly. Int J Endocrinol. 2012;2012:342034.
18. Jezkova J, Marek J, Hana V, Krsek M, Weiss V, Vladyka V, et al. Gamma Knife radiosurgery for acromegaly – long-term experience. Clin Endocrinol. 2006;64:588–95.
19. Losa M, Gioia L, Picozzi P, Franzin A, Valle M, Giovanelli M, et al. The role of stereotactic radiotherapy in patients with growth hormone-secreting pituitary adenoma. J Clin Endocrinol Metab. 2008;93:2546–52.
20. Sheehan JP, Pouratian N, Steiner L, Laws ER, Vance ML. Gamma Knife surgery for pituitary adenomas: factors related to radiological and endocrine outcomes. J Neurosurg. 2011;114:303–9.
21. Loeffler JS, Shih HA. Radiation therapy in the management of pituitary adenomas. J Clin Endocrinol Metab. 2011;96:1992–2003.
22. Jezkova J, Hana V, Krsek M, Weiss V, Vladyka V, Liscak R, et al. Use of the Leksell Gamma Knife in the treatment of prolactinoma patients. Clin Endocrinol. 2009;70:732–41.
23. Landolt AM, Haller D, Lomax N, Scheib S, Schubiger O, Siegfried J, et al. Octreotide may act as a radioprotective agent in acromegaly. J Clin Endocrinol Metab. 2000;85:1287–9.
24. Liu X, Kano H, Kondziolka D, Park KJ, Iyer A, Shin S, et al. Gamma Knife stereotactic radiosurgery for drug resistant or intolerant invasive prolactinomas. Pituitary. 2013;16:68–75.
25. Pan L, Zhang N, Wang EM, Wang BJ, Dai JZ, Cai PW. Gamma Knife radiosurgery as a primary treatment for prolactinomas. J Neurosurg. 2000;93(Suppl 3):10–3.
26. Pouratian N, Sheehan J, Jagannathan J, Laws ER Jr, Steiner L, Vance ML. Gamma Knife radiosurgery for medically and surgically refractory prolactinomas. Neurosurgery. 2006;59:255–66. discussion 255–266.
27. Tanaka S, Link MJ, Brown PD, Stafford SL, Young WF Jr, Pollock BE. Gamma Knife radiosurgery for patients with prolactin-secreting pituitary adenomas. World Neurosurg. 2010;74:147–52.
28. Zhang N, Pan L, Wang EM, Dai JZ, Wang BJ, Cai PW. Radiosurgery for growth hormone-producing pituitary adenomas. J Neurosurg. 2000;93(Suppl 3):6–9.
29. Witt TC. Stereotactic radiosurgery for pituitary tumors. Neurosurg Focus. 2003;14:e10.
30. Landolt AM, Lomax N. Gamma Knife radiosurgery for prolactinomas. J Neurosurg. 2000;93(Suppl 3):14–8.
31. Gutt B, Wowra B, Alexandrov R, Uhl E, Schaaf L, Stalla GK, et al. Gamma-knife surgery is effective in normalising plasma insulin-like growth factor I in patients with acromegaly. Exp Clin Endocrinol Diabetes. 2005;113:219–24.
32. Jagannathan J, Sheehan JP, Pouratian N, Laws ER Jr, Steiner L, Vance ML. Gamma Knife radiosurgery for acromegaly: outcomes after failed transsphenoidal surgery. Neurosurgery. 2008;62:1262–9. discussion 1269–1270.
33. Xu Z, Lee Vance M, Schlesinger D, Sheehan JP. Hypopituitarism after stereotactic radiosurgery for pituitary adenomas. Neurosurgery. 2013;72:630–7.
34. Brada M, Ashley S, Ford D, Traish D, Burchell L, Rajan B. Cerebrovascular mortality in patients with pituitary adenoma. Clin Endocrinol. 2002;57:713–7.
35. Brada M, Burchell L, Ashley S, Traish D. The incidence of cerebrovascular accidents in patients with pituitary adenoma. Int J Radiat Oncol Biol Phys. 1999;45:693–8.
36. Brada M, Ford D, Ashley S, Bliss JM, Crowley S, Mason M, et al. Risk of second brain tumour after conservative surgery and radiotherapy for pituitary adenoma. BMJ. 1992;304:1343–6.
37. Minniti G, Osti M, Jaffrain-Rea ML, Esposito V, Cantore G, Maurizi Enrici R. Long-term follow-up results of postoperative radiation therapy for Cushing's disease. J Neuro-Oncol. 2007;84:79–84.
38. Buatti JM, Friedman WA, Meeks SL, Bova FJ. The radiobiology of radiosurgery and stereotactic radiotherapy. Med Dosim. 1998;23:201–7.
39. Rowe J, Grainger A, Walton L, Silcocks P, Radatz M, Kemeny A. Risk of malignancy after Gamma Knife stereotactic radiosurgery. Neurosurgery. 2007;60:60–5. discussion 65–66.
40. Lim YJ, Leem W, Park JT, Kim TS, Rhee BA, Kim GK. Cerebral infarction with ICA occlusion after Gamma Knife radiosurgery for pituitary adenoma: a case report. Stereotact Funct Neurosurg. 1999;72(Suppl 1):132–9.
41. Lee CC, Kano H, Yang HC, Xu Z, Yen CP, Chung WY, et al. Initial Gamma Knife radiosurgery for nonfunctioning pituitary adenomas. J Neurosurg. 2014;120:647–54.
42. Xu Z, Ellis S, Lee CC, Starke RM, Schlesinger D, Lee Vance M, et al. Silent corticotroph adenomas following Gamma Knife radiosurgery. International journal of radiation oncology biology and physics. Int J Radiat Oncol Biol Phys. 2014;90(4):903–10.
43. Lee CC, Vance ML, Lopes MB, Xu Z, Chen CJ, Sheehan J. Stereotactic radiosurgery for acromegaly: outcomes by adenoma subtype. Pituitary. 2015;18:326–34.
44. Pollock BE, Nippoldt TB, Stafford SL, Foote RL, Abboud CF. Results of stereotactic radiosurgery in patients with hormone-producing pituitary adenomas: factors associated with endocrine normalization. J Neurosurg. 2002;97:525–30.
45. Ludecke DK, Flitsch J, Knappe UJ, Saeger W. Cushing's disease: a surgical view. J Neuro-Oncol. 2001;54:151–66.
46. Chee GH, Mathias DB, James RA, Kendall-Taylor P. Transsphenoidal pituitary surgery in Cushing's disease: can we predict outcome? Clin Endocrinol. 2001;54:617–26.
47. Invitti C, Pecori Giraldi F, de Martin M, Cavagnini F. Diagnosis and management of Cushing's syndrome: results of an Italian multicentre study. Study Group of the Italian Society of endocrinology on the pathophysiology of the hypothalamic-pituitary-adrenal axis. J Clin Endocrinol Metab. 1999;84:440–8.
48. Sonino N, Zielezny M, Fava GA, Fallo F, Boscaro M. Risk factors and long-term outcome in pituitary-dependent Cushing's disease. J Clin Endocrinol Metab. 1996;81:2647–52.
49. Yap LB, Turner HE, Adams CB, Wass JA. Undetectable postoperative cortisol does not always predict long-term remission in Cushing's disease: a single centre audit. Clin Endocrinol. 2002;56:25–31.
50. Lee CC, Chen CJ, Yen CP, Xu Z, Schlesinger D, Fezeu F, et al. Whole-sellar stereotactic radiosurgery for functioning pituitary adenomas. Neurosurgery. 2014;75:227–37. discussion 237.

Stereotactic Radiosurgery for Meningioma

David R. Raleigh and Penny K. Sneed

Introduction

Meningioma is the most common primary intracranial tumor, accounting for 36.1% of all primary brain tumors and 53.7% of all primary nonmalignant brain tumors [1]. In 2015, there were 25,190 new diagnoses of meningioma in the United States, and it is estimated that more than 170,000 patients are alive with meningioma. Although meningioma can occur in pediatric patients, the median age of diagnosis is 65 years, and the incidence of meningioma increases dramatically with age [1]. Beyond advanced age, other risk factors for meningioma include clinical neurofibromatosis type II, which is associated with germline mutation of the *NF2* gene, a past medical history of ionizing radiation to the head or neck, African-American ethnicity, and female sex, which more than doubles the risk of meningioma. Incidental findings on brain magnetic resonance imaging (MRI) in the general population suggest that meningiomas are present in approximately 1% of asymptomatic adults [2]. Perhaps related to regional imaging practice patterns, there is significant geographic variation of meningioma diagnosis in the United States [1].

The term "meningioma" was popularized by the famed neurosurgeon Harvey Cushing, who first used it in 1922 to describe a collection of "dural endotheliomas" that occurred throughout the neural axis [3, 4]. Although associated with tremendous histopathologic and clinical diversity, the tumors Cushing described were unified by their shared origin from the meningeal coverings of the brain and spinal cord. Over the intervening years, the World Health Organization (WHO) has repeatedly refined a histopathologic classification system for meningiomas that provides accurate prognostic information [5]. That system, which is based on mitotic activity and a variety of histopathologic features, such as brain invasion, segregates meningiomas into grade I, grade II (atypical), and grade III (anaplastic) categories. The majority of meningiomas are grade I (70%), associated with 5-year overall survival rates often exceeding 90% (Fig. 1a, b) [6]. Grade II and grade III meningiomas, which account for approximately 20% and 5% of meningiomas, respectively, follow an aggressive clinical course characterized by serial local recurrence and, in rare cases, distant hematogenous metastases to the liver or lungs. Thus, local control is paramount for meningioma treatment. Yet, even with the most advanced surgical and radiosurgical techniques, up to 60% of grade II and more than 80% of grade III meningiomas recur within 5 years of treatment [6] (Fig. 1a, b). Compounding the clinical challenges of treating high-grade tumors, there are currently no effective systemic therapies for meningioma [7].

For decades, fully fractionated radiotherapy to ~50.4–57.6 Gy at 1.8 Gy per day has played an important role in the management of meningiomas, with very good results. As an example, in a series of 507 skull base meningioma patients treated to a median dose of 57.6 Gy with or without prior biopsy or subtotal resection, local control was 91% at 10 years for benign meningiomas and 81% at 5 years and 53% at 10 years for high-risk meningiomas, with unchanged quality of life in 47.7% of patients and improved quality of life in 37.5% of patients [8]. Despite these good results, there has been interest in using single-fraction and hypofractionated stereotactic radiosurgery (SRS) as alternatives to fully fractionated radiotherapy for selected small- to medium-sized meningiomas to shorten the length of treatment and allow for much more focal radiation, lessening dose to surrounding normal tissue.

Various groups began reporting on early experience with SRS for meningioma around 1990, and now a large number of series have evaluated the use of single-session SRS and, to a lesser extent, fractionated SRS for meningioma. Largely retrospective or single arm in design, these reports suggest

D. R. Raleigh (✉)
University of California at San Francisco, Departments of Radiation Oncology and Neurological Surgery, San Francisco, CA, USA
e-mail: David.raleigh@ucsf.edu

P. K. Sneed
University of California at San Francisco, Departments of Radiation Oncology, San Francisco, CA, USA

D. M. Trifiletti et al. (eds.), *Stereotactic Radiosurgery and Stereotactic Body Radiation Therapy*,
https://doi.org/10.1007/978-3-030-16924-4_12

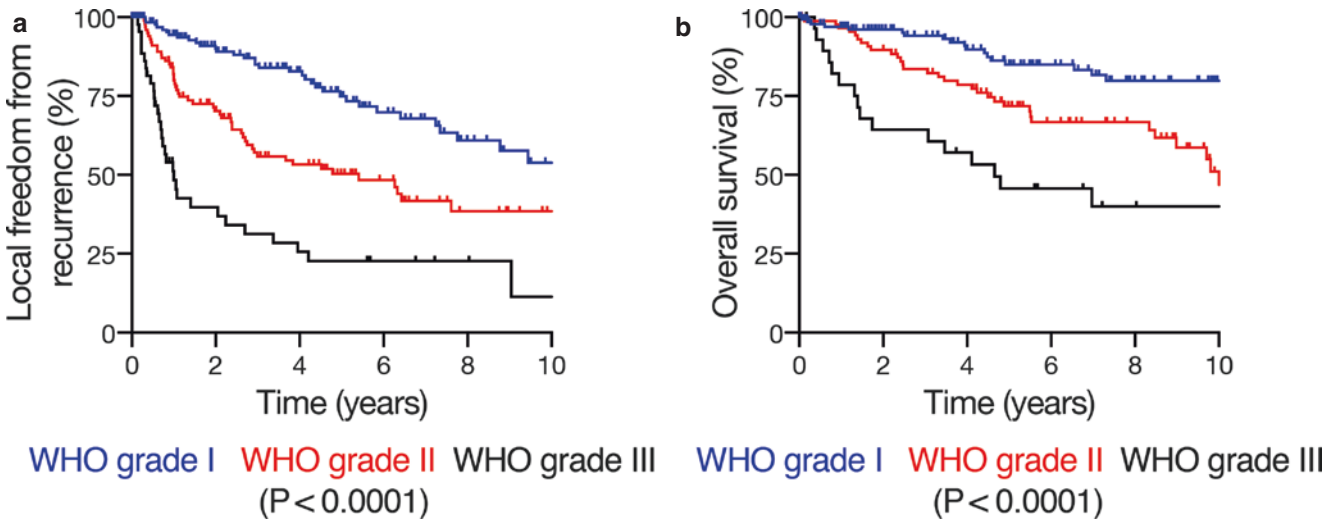

Fig. 1 Long-term meningioma outcomes. Ten-year local freedom from progression (**a**) and overall survival (**b**) from 157 patients with grade I, 93 patients with grade II, and 30 patients with grade III meningioma treated at the University of California, San Francisco, from 1990 to 2015 with a median follow-up of 4.6 years

that in properly selected cases, meningioma control after SRS is comparable to complete resection or fully fractionated radiotherapy, with a good toxicity profile. Indeed, more than 95% of patients report that radiosurgery provides a satisfactory outcome for their meningioma [9]. However, given the absence of prospective trials, the most appropriate patients, target volumes, radiation doses, and fractionation schemes for meningioma SRS remain undefined. Here, we review the highest quality clinical data for the use of SRS for meningioma and provide practical day-to-day considerations, guidelines, and applications for clinicians. Clinician judgment, ideally in the setting of multidisciplinary consensus recommendations from a tumor board specialized in central nervous system radiosurgery, is paramount.

Site-Specific Considerations

Meningiomas can arise from dural surfaces throughout the brain and spinal cord. Immobilization devices may consist of a stereotactic frame or mask for intracranial or skull base meningiomas, head and shoulder mask for tumors with significant infratemporal extent or for cervical or very high thoracic tumors, and vacuum bag or other body fixation for other thoracic or lumbosacral meningiomas, generally with daily image guidance to minimize setup uncertainty.

Clinical Evidence

Importantly, not all meningiomas require treatment, especially in asymptomatic patients and in patients with medical comorbidities and limited life expectancy. In that regard, observation with imaging surveillance is an acceptable early course of treatment for small asymptomatic meningiomas, especially those with an initial diameter <2 cm [10]. For meningiomas that do require treatment, abundant data demonstrate that, in appropriately selected cases, SRS is a feasible, safe, and effective option for both definitive and adjuvant treatments (Table 1).

The largest report of SRS for meningiomas encompasses 4565 consecutive patients with 5300 grade I and imaging-defined tumors from 15 European centers treated with Gamma Knife SRS [11]. The median tumor volume in this series was 4.8 cm^3, and the median dose to tumor margin was 14 Gy. Restricting the analysis to the 3768 meningiomas with at least 24 months of imaging follow-up after SRS, the volume of the treated lesion decreased in 58% of cases, remained unchanged in 34.5%, and increased in 7.5%, yielding 5- and 10-year rates of local control of 95.2% and 88.6%, respectively. Local control was superior for imaging defined versus grade I meningiomas, which may suggest that surgical resection induces cell proliferative gene expression in the residual tumor, or alternatively, may be an artifact of selection bias from the retrospective study. Regardless, SRS was well tolerated with permanent morbidity in only 6.6% of patients (1.8% mild, 3.6% non-disabling, 1.2% disabling).

Many other retrospective reports are available to corroborate the efficacy and safety of SRS for meningioma. Some of these also demonstrate that SRS can be used for high-grade meningioma, albeit with less durable long-term control [12, 13]. In sum, these reports indicate that SRS is most effective for small meningiomas in patients with solitary tumors who have not undergone prior therapy. For larger meningiomas, or those that are very close to the optic chiasm, fractionated SRS appears to be an effective and safe alternative to SRS, although data are much more limited for single-session Gamma Knife treatments [14, 15]. Fully fractionated radiotherapy using

Table 1 Select SRS series for meningioma publications

Publication	Patients	Meningiomas	Years	Location	Tumor size (median)	Margin dose (median)	Grade	Radiographic follow-up (median)	Outcomes	Toxicity	Notes
Santacroce et al. [11]	4565	5300	1987–2003	15 European centers	4.8 cm^3	14 Gy	Imaging defined, 2976; grade I, 2324	63 months	5- and 10-year PFS: overall 95.2% and 88.6%, imaging defined 96.8% and 92.7%, grade I 92.7% and 83.2%	6.6% permanent morbidity (1.8% mild, 3.6% non-disabling, 1.2% disabling)	Local control significantly worse for grade I vs. imaging-defined meningioma, male vs. female patients, patients with multiple vs. solitary meningiomas, and convexity vs. skull base tumors
Kondziolka et al. [12]	972	1045	Unspecified 18-year period	University of Pittsburgh	7.4 cm^3	14 Gy	Imaging defined, 534; grade I, 424; grade II, 56; grade III, 31	48 months	Overall 5- and 10-year PFS: 97% and 87% (grade II 50% at 24 months, grade III 17% at 15 months)	7.7% rate of any complication (35% completely resolved)	Local control significantly worse for large meningiomas and multiple vs. solitary meningiomas
Kaprealian et al. [13]	280	438	1991–2007	University of California, San Francisco	2.4 cm maximum diameter	15 Gy	Imaging defined, 37%; grade I, 32%; grade II, 12%; grade III, 19%	76 months	5-year FFP: imaging defined 97%, grade I 87%, grade II 56%, and grade III 47%	One- and two-year probabilities of adverse radiation effect after SRS: 8% and 5% for recurrence after surgery, 15% and 30% for recurrence after radiotherapy	Local control significantly worse for large meningiomas and after prior radiotherapy

~54 Gy at ~1.8 Gy per daily fraction is preferred for very large meningiomas or those intimately associated with or extensively involving the optic chiasm, limiting optic chiasm dose to ~54 Gy.

Toxicity

The adverse radiation effects of SRS for meningioma are similar to the anticipated sequelae of radiosurgery for other intracranial targets. Toxicities are related not only to radiation dose but also to target location, prior treatment, and in rare cases, radiation sensitivity syndromes. For larger superficial targets, temporary hair loss may be observed ~3 weeks after treatment with regrowth ~3 months after treatment. Delayed adverse radiation effects months after treatment may include central nervous system edema or radionecrosis, symptomatic with headaches, seizures, and/or neurological symptoms depending on brain location. In the long term (years post-treatment), it is possible to have cyst formation or development of vascular malformations. In rare cases, surgical intervention is required to correct persistent symptomatic adverse radiation effect, cysts, or vascular malformations.

The majority of toxicities from meningioma SRS, either single- or multisession, are self-limited and mild and may not require intervention. Corticosteroids may be given prophylactically on the day of SRS to reduce the risk of acute central nervous system edema, and a course of steroids may be required to ameliorate later symptoms from edema or radionecrosis. Care should be taken with treatment of meningiomas that are associated with significant central nervous system edema from mass effect at presentation, as even minor amounts of radiosurgery-induced swelling could have disastrous consequences for the patient. Both meningioma size and location, such as parasagittal location, are risk factors for edema [16, 17], and anecdotal clinical experience suggests that several weeks of corticosteroid pretreatment before SRS for meningioma may reduce the risk of exacerbating central nervous system edema.

Dose to optic apparatus is often an important consideration in selecting appropriate cases for SRS to limit risk of vision loss to a very low level. Recommended optic apparatus dose constraints are provided in Table 2. Low risk of cranial neuropathy has been reported in SRS series for tumors involving or adjacent to other cranial nerves.

In general, fractionated SRS may provide a more favorable toxicity profile than single-session SRS for larger meningiomas and/or those too close to critical structures, but as described above, the long-term efficacy and toxicity of fractionated SRS for meningioma are less well established than single-session SRS.

Table 2 Normal tissue dose constraints for meningioma SRS

Tissue	One fraction	Three fractions	Five fractions
Optic pathway	Max point dose: 10 Gy	Max point dose: 17.4 Gy	Max point dose: 25 Gy
Cochlea	Max point dose: 9 Gy Mean: 4.5 Gy	Max point dose: 17.1 Gy	Max point dose: 25 Gy
Brainstem	Max point dose: 15 Gy	Max point dose: 23.1 Gy	Max point dose: 31 Gy
Spinal cord and medulla	Threshold dose: 7 Gy	Threshold dose: 12.3 Gy	Threshold dose: 14.5 Gy
Brachial plexus	Max point dose: 17.5 Gy	Max point dose: 24 Gy	Max point dose: 30.5 Gy
Cauda equine and sacral plexus	Max point dose: 16 Gy	Max point dose: 24 Gy	Max point dose: 32 Gy

Data from Reference [20]

For cavernous sinus and other central skull base meningiomas, radiation-induced hypopituitarism may be an irreversible and progressive adverse effect of either single-session or fractioned SRS [18]. Radiation-induced hypopituitarism is most common within 3 years of radiation, and the total dose, fraction size, and duration between fractions may influence the nature and extent of hormone deficiency. Growth hormone deficiency is most common and occurs in 50–100% of patients who receive biologic equivalent doses of radiation as low as 30–50 Gy at standard fractionation [18]. Within the same dose range, luteinizing hormone and follicle-stimulating hormone deficiency, hyperprolactinemia, and thyroid-stimulating hormone and adrenocorticotropic hormone deficiency are also common, occurring in 20–50%, 5–20%, and 3–6% of patients, respectively [18]. Thus, long-term neuroendocrinology follow-up is recommended for all patients undergoing single-session or fractionated SRS with significant dose to the pituitary gland or infundibulum. Patients who receive SRS for skull base meningiomas are also at risk for developing cranial nerve deficits, such as optic neuropathy, although these late sequelae are relatively rare complications.

Plan Quality

Single-session and multisession SRS plan evaluation for meningioma involves assessment of target coverage and dose to surrounding normal structures (Fig. 2). Most Gamma Knife SRS plans are prescribed to the 50% isodose contour. In contrast, fractionated SRS plan prescriptions are more variable. Single-institution data suggest that SRS dose escalation may improve local control of meningiomas [19], but given the lack of clear benefit, care should be taken not to violate normal tissue tolerance when performing SRS for meningioma (Table 2) [20]. Although the optimal dose and fractionation for meningioma SRS remain to be established

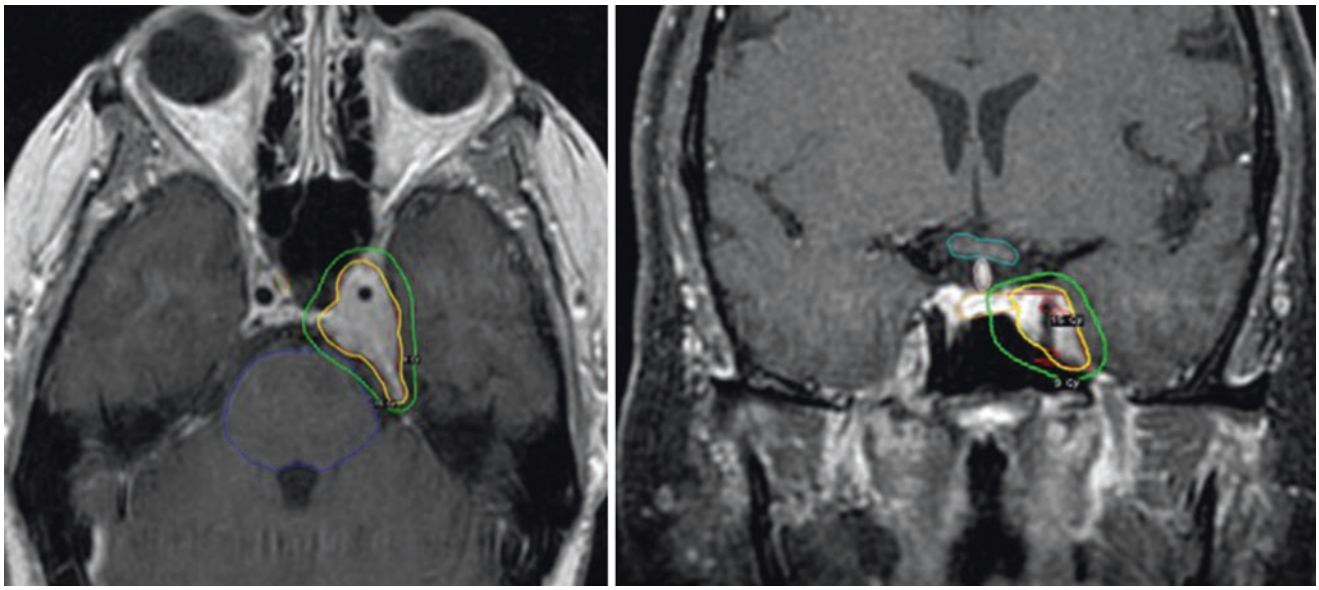

Fig. 2 Plan evaluation for meningioma SRS. Axial and coronal images of a Gamma Knife SRS plan for a meningioma involving the left cavernous sinus (red) abutting the pituitary gland (orange). The 15 Gy isodose contour is shown in yellow, and the 9 Gy isodose contour, which avoids the optic apparatus (light blue), is shown in green

by prospective trials, a dose of 13–15 Gy is likely sufficient for most imaging defined and grade I tumors, and doses below 12 Gy are associated with worse local control [12, 21]. Local control of high-grade meningiomas may be improved by slight SRS dose escalation to 16–20 Gy, but a clear relationship for a dose-response in meningioma is lacking. Thus, SRS dose escalation for meningioma remains investigational.

Future Directions

SRS, single- and multisession, are feasible and effective options for both definitive and adjuvant treatments of selected meningiomas. SRS are highly evolved techniques from the standpoints of accuracy, precision, and dose conformity; thus it is unlikely that advances in planning or treatment delivery will significantly improve outcomes for meningioma patients' future. Moreover, it is unlikely that single- or multifraction SRS will replace resection for meningioma. Many meningiomas are too large for even multisession SRS to be safely delivered or are intimately associated with critical nervous structures that preclude adequate doses of SRS to be administered. Further, some meningioma patients present with important or even life-threatening symptoms that necessitate surgical resection for central nervous system decompression. In contrast, many meningiomas treated with SRS do not change in size over time, and some may even show mild, transient enlargement after SRS before relapsing into a quiescent state [11, 21]. Despite these limitations, it is notable that multiple series suggest outcomes are superior with SRS monotherapy as compared to resection followed by SRS for meningioma [11, 13]. Prospective, randomized trials are required to establish if these data are influenced by selection or other biases, but in the absence of such data, SRS remain feasible and effective treatment options for meningioma.

It is tempting to speculate that improved understanding of meningioma biology might reveal novel molecular targets to improve outcomes, especially for high-grade tumors [22]. Whether as monotherapy or in conjunction with stereotactic radiation, molecular therapy remains the final frontier of meningiomas. Next-generation sequencing analyses of meningioma genomes and exomes reveal mutations in canonical cancer drivers that are associated with tumor location and histopathologic characteristics, but not necessarily with clinical outcomes [23–27]. In contrast, DNA hypermethylation appears to correlate with poor meningioma outcomes, but it is unclear if epigenomic alterations can be targeted to improve survival in these tumors [28, 29]. Finally, immunotherapy has revolutionized the ways scientists conceptualize cancer growth and clinicians treat patients, and increased expression of the immune modulatory molecule PD-L1 appears to correlate with aggressive meningioma behavior [30, 31]. Further investigation is required to validate these and other biomarkers in meningioma, but molecular therapy based on improved understanding of meningioma biology, as is being explored in the Alliance A071401 prospective clinical trial, is likely to transform meningioma therapy in the coming years.

Practical Considerations

- No prospective data are available to guide patient selection, treatment planning, dose selection, treatment delivery, or follow-up; thus, recommendations are based on extensive retrospective and largely single-institution reports.
- Patient selection:
  - SRS may be used as definitive treatment for small meningiomas in patients who are unable or unwilling to undergo definitive safe surgical resection or in patients with asymptomatic or minimally symptomatic tumors not requiring surgical debulking in whom curative resection would not be possible or in whom risks of surgery may outweigh benefits.
  - SRS may also be used as adjuvant treatment of high-grade or gross residual meningiomas after resection.
  - Patients should have sufficient life expectancy, be able to undergo stereotactic frame placement or mask fitting, and tolerate treatment.
- Treatment planning:
  - Treatment planning imaging: Thin-cut MRI (T1 post-contrast, T2, and fat-suppressed sequences) for primary treatment planning or fusion with treatment planning CT, depending on the SRS platform; CT may also be useful in selected cases to evaluate bone involvement.
  - Immobilization: Stereotactic frame or stereotactic mask with daily image guidance, with or without intrafraction motion monitoring.
  - Target volume: For SRS using a stereotactic frame, the target is the gross tumor volume (GTV) with no planning target volume (PTV) expansion. For mask-based SRS, the target is the GTV with 1–2 mm PTV expansion.
- Dose selection:
  - Single-session SRS: 13–15 Gy in 1 fraction is likely sufficient for most grade I meningiomas, but high-grade tumors may benefit from dose escalation to 16–20 Gy.
  - Fractionated SRS: 25 Gy in 5 fractions versus 30 Gy in 3 fractions depending on tumor size and dose tolerance of adjacent critical structures.
- Follow-up: Gadolinium-enhanced T1- and T2- weighted MRI surveillance with fat suppression:
  - Grade I: Surveillance imaging every 6 months for ~2 years, followed by yearly surveillance imaging for another 2–3 years, and then every other year surveillance.
  - Grade II and grade III: Surveillance imaging every 3 months for 2–3 years, followed by imaging every 6–12 months.

References

1. Ostrom QT, Gittleman H, Fulop J, Liu M, Blanda R, Kromer C, et al. CBTRUS statistical report: primary brain and central nervous system tumors diagnosed in the United States in 2008–2012. Neuro-oncology. Oxford University Press. 2015;17(Suppl 4):iv1–iv62.
2. Vernooij MW, Ikram MA, Tanghe HL, Vincent AJPE, Hofman A, Krestin GP, et al. Incidental findings on brain MRI in the general population. N Engl J Med. 2007;357(18):1821–8.
3. Barthélemy EJ, Sarkiss CA, Lee J, Shrivastava RK. The historical origin of the term "meningioma" and the rise of nationalistic neurosurgery. J Neurosurg. 2016;125(5):1283–90.
4. Cushing H. The meningiomas (dural endotheliomas): their source, and favoured seats of origin. Brain. 1922;45(2):282–316.
5. Louis DN, Perry A, Reifenberger G, von Deimling A, Figarella-Branger D, Cavenee WK, et al. The 2016 World Health Organization classification of tumors of the central nervous system: a summary. Acta Neuropathol. Springer Berlin Heidelberg. 2016;131(6):803–20.
6. Rogers L, Barani I, Chamberlain M, Kaley TJ, McDermott M, Raizer J, et al. Meningiomas: knowledge base, treatment outcomes, and uncertainties. A RANO review. J Neurosurg. 2015;122(1):4–23.
7. Wen PY, Quant E, Drappatz J, Beroukhim R, Norden AD. Medical therapies for meningiomas. J Neurooncol. Springer US. 2010;99(3):365–78.
8. Combs SE, Thilmann C, Edler L, Debus J, Schulz-Ertner D. Efficacy of fractionated stereotactic reirradiation in recurrent gliomas: long-term results in 172 patients treated in a single institution. J Clin Oncol. 2005;23(34):8863–9.
9. Kondziolka D, Levy EI, Niranjan A, Flickinger JC, Lunsford LD. Long-term outcomes after meningioma radiosurgery: physician and patient perspectives. J Neurosurg. 1999;91(1):44–50.
10. Sughrue ME, Rutkowski MJ, Aranda D, Barani IJ, McDermott MW, Parsa AT. Treatment decision making based on the published natural history and growth rate of small meningiomas. J Neurosurg. 2010;113(5):1036–42.
11. Santacroce A, Walier M, Régis J, Liščák R, Motti E, Lindquist C, et al. Long-term tumor control of benign intracranial meningiomas after radiosurgery in a series of 4565 patients. Neurosurgery. 2012;70(1):32–9. –discussion 39.
12. Kondziolka D, Mathieu D, Lunsford LD, Martin JJ, Madhok R, Niranjan A, et al. Radiosurgery as definitive management of intracranial meningiomas. Neurosurgery. 2008;62(1):53–8. –discussion 58–60.
13. Kaprealian T, Raleigh DR, Sneed PK, Nabavizadeh N, Nakamura JL, McDermott MW. Parameters influencing local control of meningiomas treated with radiosurgery. J Neurooncol. Springer US. 2016;128(2):357–64.
14. Bria C, Wegner RE, Clump DA, Vargo JA, Mintz AH, Heron DE, et al. Fractionated stereotactic radiosurgery for the treatment of meningiomas. J Cancer Res Ther. Medknow Publications. 2011;7(1):52–7.
15. Han M-S, Jang W-Y, Moon K-S, Lim S-H, Kim I-Y, Jung T-Y, et al. Is fractionated gamma knife radiosurgery a safe and effective treatment approach for large-volume (>10 cm3) intracranial meningiomas? World Neurosurg. 2017;99:477–83.
16. Sheehan JP, Cohen-Inbar O, Ruangkanchanasetr R, Bulent Omay S, Hess J, Chiang V, et al. Post-radiosurgical edema associated with parasagittal and parafalcine meningiomas: a multicenter study. J Neuro-Oncol. 2015;125(2):317–24.
17. Cai R, Barnett GH, Novak E, Chao ST, Suh JH. Principal risk of peritumoral edema after stereotactic radiosurgery for intracranial meningioma is tumor-brain contact interface area. Neurosurgery. 2010;66(3):513–22.
18. Darzy KH, Shalet SM. Hypopituitarism following radiotherapy. Pituitary. Springer US. 2009;12(1):40–50.

19. Sethi RA, Rush SC, Liu S, Sethi SA, Parker E, Donahue B, et al. Dose-response relationships for meningioma radiosurgery. Am J Clin Oncol. 2015;38(6):600–4.
20. Benedict SH, Yenice KM, Followill D, Galvin JM, Hinson W, Kavanagh B, et al. Stereotactic body radiation therapy: the report of AAPM Task Group 101. Med Phys. 2010;37(8):4078–101.
21. Kollová A, Liščák R, Novotný J Jr, Vladyka V, Šimonová G, Janoušková L. Gamma Knife surgery for benign meningioma. J Neurosurg. 2007;107(2):325–36.
22. Bi WL, Abedalthagafi M, Horowitz P, Agarwalla PK, Mei Y, Aizer AA, et al. Genomic landscape of intracranial meningiomas. J Neurosurg. 2016;125(3):1–11.
23. Clark VE, Erson-Omay EZ, Serin A, Yin J, Cotney J, Ozduman K, et al. Genomic analysis of non-NF2 meningiomas reveals mutations in TRAF7, KLF4, AKT1, and SMO. Science. 2013;339(6123):1077–80.
24. Sahm F, Bissel J, Koelsche C, Schweizer L, Capper D, Reuss D, et al. AKT1E17K mutations cluster with meningothelial and transitional meningiomas and can be detected by SFRP1 immunohistochemistry. Acta Neuropathol. 2013;126(5):757–62.
25. Clark VE, Harmancı AS, Bai H, Youngblood MW, Lee TI, Baranoski JF, et al. Recurrent somatic mutations in POLR2A define a distinct subset of meningiomas. Nat Genet. 2016;48(10):1253–9.
26. Bi WL, Greenwald NF, Abedalthagafi M, Wala J, Gibson WJ, Agarwalla PK, et al. Genomic landscape of high-grade meningiomas. NPJ Genom Med. 2017;2(1):iv1.
27. Reuss DE, Piro RM, Jones DTW, Simon M, Ketter R, Kool M, et al. Secretory meningiomas are defined by combined KLF4 K409Q and TRAF7 mutations. Acta Neuropathol. 2013;125(3):351–8.
28. Sahm F, Schrimpf D, Stichel D, Jones DTW, Hielscher T, Schefzyk S, et al. DNA methylation-based classification and grading system for meningioma: a multicentre, retrospective analysis. Lancet Oncol. 2017;18(5):682–94.
29. Harmanci AS, Youngblood MW, Clark VE, Coşkun S, Henegariu O, Duran D, et al. Integrated genomic analyses of de novo pathways underlying atypical meningiomas. Nat Commun. 2017;8:14433.
30. Du Z, Abedalthagafi M, Aizer AA, McHenry AR, Sun HH, Bray M-A, et al. Increased expression of the immune modulatory molecule PD-L1 (CD274) in anaplastic meningioma. Oncotarget. Impact Journals. 2015;6(7):4704–16.
31. Han SJ, Reis G, Kohanbash G, Shrivastav S, Magill ST, Molinaro AM, et al. Expression and prognostic impact of immune modulatory molecule PD-L1 in meningioma. J Neurooncol. Springer US. 2016;130(3):543–52.

Stereotactic Radiosurgery for Intracranial Arteriovenous Malformations

Jacqueline J. Tao, Justin Moore, Geoffrey Appelboom, and Steven D. Chang

Introduction

Arteriovenous malformations (AVMs) are vascular deformities involving direct connections between arteries and veins without an intervening capillary network. The vascular mass consisting of this direct connection, referred to as the nidus, is composed of a complex tangle of abnormal and dilated vessels (Fig. 1). Direct shunting of blood from the high-pressure arterial system into the venous outflow tract disrupts the venous vasculature and leads to vessel wall arterialization, venous dilation, and vasogenic edema (Fig. 2). AVMs occur throughout the body but are particularly significant when located intracranially, due to the associated neurologic morbidity and mortality. Intracranial AVMs are typically located in the superficial cerebral cortex, but an estimated one-third occur in deep structures including the brainstem, basal ganglia, thalamus, and cerebellum [1].

AVMs occur in the population with an incidence of 1.12–1.42 cases per 100,000 and are diagnosed with equal frequency in men and women, typically by the fourth decade of life [2, 3]. Acute intracranial hemorrhage is the most common presenting manifestation, accounting for approximately half of all AVM presentations, while the remainder of cases present as headache, seizure, and focal neurologic deficits or as incidental findings on imaging for other conditions [1]. Thus, AVMs represent a significant source of hemorrhagic stroke and associated neurologic morbidity in young adults.

The genetics and pathogenesis of AVMs remain poorly understood, and classically they were considered congenital malformations that arise from disrupted embryologic vascular development [4]. However, challenging this congenital theory are reports in the literature of de novo AVM formation associated with both sporadic and inherited syndromes, as well as dynamic expansion and regression of AVMs on imaging studies. Syndromic AVMs are most commonly associated with hereditary hemorrhagic telangiectasia, which involves mutations in regulators of the transforming growth factor β-SMAD pathway. Several additional mechanisms have been proposed as drivers of sporadic AVM formation, including single-nucleotide polymorphisms (SNPs) in inflammatory factors such as TGF-β and IL-6, as well as overexpression of angiogenesis-related genes including VEGF and angiopoietin-2 [2]. A recent analysis by Nikolaev and colleagues identified frequent activating KRAS mutations in AVM specimens and proposed activation of the MAPK-ERK pathway in endothelial cells as a driver for sporadic AVM pathogenesis [5].

The mainstays of interventional treatment for AVMs are microsurgical resection (Fig. 3), stereotactic radiosurgery (SRS), and endovascular embolization (Fig. 4), utilized as standalone therapies or in combination. The goal of any treatment regimen for AVMs is to obliterate the nidus, which abolishes the risk of subsequent hemorrhage. SRS is a valuable noninvasive treatment modality with particular benefit for AVMs less amenable to surgery, but also has a unique complication profile that includes latency hemorrhage and adverse radiation effects. Given the evolving data on the natural history of AVMs as well as the efficacy of SRS, an evaluation of the current indications, outcomes, and complications of SRS is critical to its appropriate application in individual AVM cases.

J. J. Tao
Stanford University School of Medicine, Stanford, CA, USA

J. Moore
Beth Israel Deaconess Medical Center, Boston, MA, USA

Harvard Medical School, Boston, MA, USA

G. Appelboom · S. D. Chang (✉)
Department of Neurosurgery, Stanford University School of Medicine, Stanford, CA, USA
e-mail: sdchang@stanford.edu

D. M. Trifiletti et al. (eds.), *Stereotactic Radiosurgery and Stereotactic Body Radiation Therapy*,
https://doi.org/10.1007/978-3-030-16924-4_13

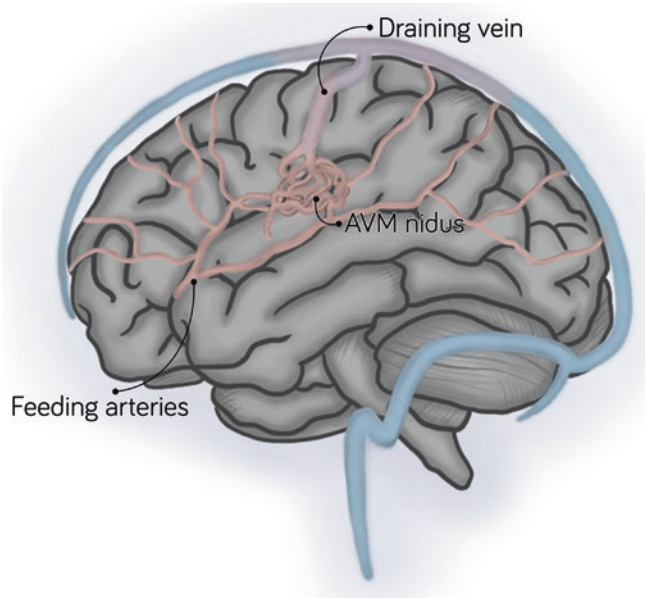

Fig. 1 Arteriovenous malformations (AVMs) are vascular deformities involving direct connections between the arteries and veins without an intervening capillary network. The vascular mass consisting of this direct connection is referred to as the nidus and is composed of a complex tangle of abnormal and dilated vessels

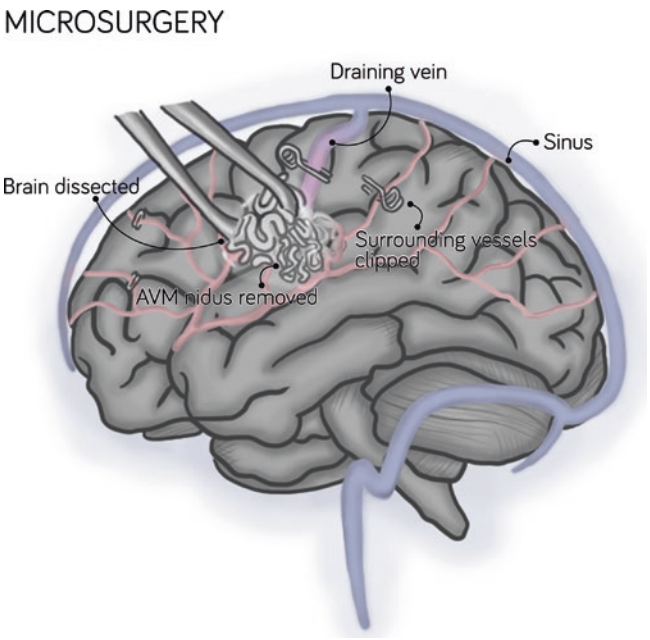

Fig. 3 Microsurgical resection of an arteriovenous malformations (AVMs). As can be seen, the arteries feeding the AVM are initially clipped and divided. Once the AVM has been devascularized from the arterial side, the venous outflow can be divided. The devascularized AVM nidus is then resected completely from the underlying brain

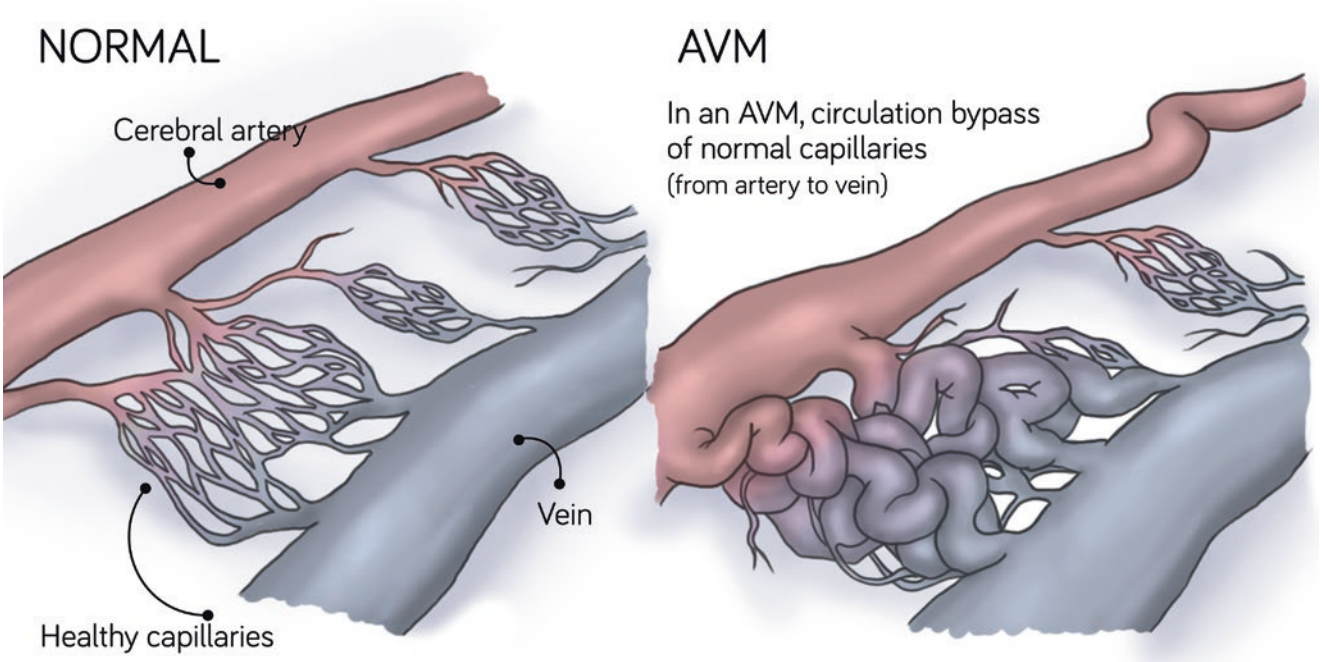

Fig. 2 Left panel: A diagram of a typical cerebrovascular anatomy, where blood flows from the arteries through the capillaries and is eventually collected within the venous circulation. Right panel: The abnormal direct connection between the arteries and veins, without intervening capillary network which from the nidus of the arteriovenous malformation

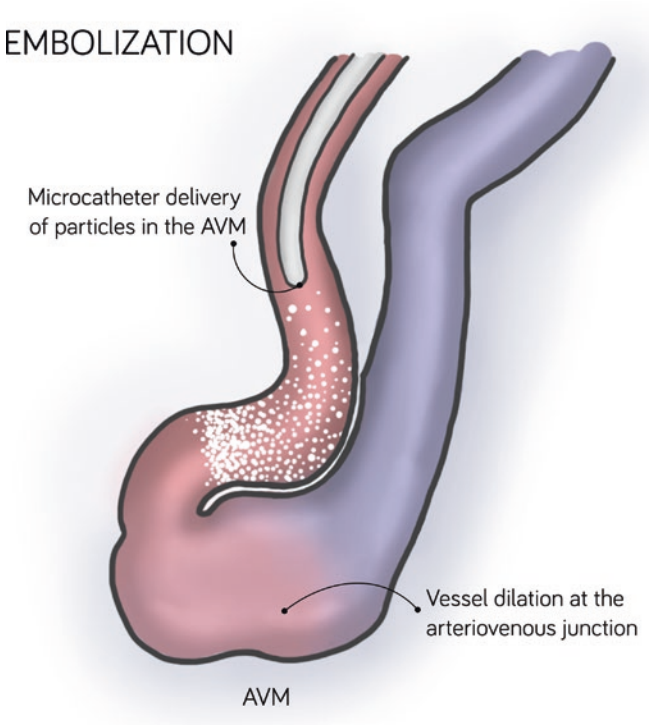

Fig. 4 Endovascular embolization of the AVM. Large particles or onyx (as well as a variety of other material) is used to obstruct the arterial inflow of the AVM. Ideally, while obliterating the arterial feeders, the embolizing agent passes through the nidus into the early draining veins completing the obliteration

Natural History

Hemorrhage is generally regarded as the most common cause of AVM-related mortality and morbidity, and thus hemorrhage rates and risk factors have been the primary focus of AVM natural history studies. The estimated morbidity and mortality rates from AVM hemorrhage range from 10–30% and 20–30%, respectively [4], and the general consensus for annual risk of hemorrhage from AVMs is 2–4%. A meta-analysis of nine natural history studies found an overall hemorrhage rate of 3.0%, with unruptured AVMs bearing a lower hemorrhage rate (2.2%) than ruptured AVMs (4.5%). Among ruptured AVMs, the risk of re-rupture within the first year was notably elevated at 6–15% [1]. Similar figures were reported by a 2014 meta-analysis, which identified an overall annual hemorrhage rate of 2.3%, stratified as 1.3% for unruptured AVMs and 4.8% for ruptured AVMs [6]. These results are also corroborated by data from the ARUBA randomized trial, which found spontaneous rupture rates of 2.2% per year among previously unruptured and untreated AVMs [7].

Significant risk factors for hemorrhage identified in the meta-analysis include prior hemorrhage, deep AVM location, exclusively deep venous drainage, presence of associated aneurysms, and possible pregnancy. Female sex showed some increased risk, but was not statistically significant, and contrary to prior data, small AVM size and older patient age were not significant risk factors for rupture [1].

Following hemorrhage, seizure is the second most common initial symptom of AVMs, accounting for around one-fourth of presentations [1, 8]. A subset of AVM patients, including those who do and do not initially present with seizure, will develop de novo epilepsy over their disease course. A natural history study of 217 patients found that 18% of all patients developed seizures over a 20-year follow-up, among which the subset of patients who presented with hemorrhage had the greatest risk (22%). Risk of seizure was also elevated for AVMs in the temporal lobe (37%) compared to other lobes (16%) [9]. A prospective cohort study found a comparable 26% 5-year risk of first unprovoked seizure in patients who presented with hemorrhage. In patients who first presented with seizures, the 5-year risk of recurrent seizure was significantly elevated at 72% [8]. Thus, AVM-related seizures occur in approximately one-fifth of patients overall, with major risk factors including seizure presentation, prior hemorrhage, and temporal location.

History and Pathophysiology of AVM Radiosurgery

Brief History

Stereotactic radiosurgery has been used to treat AVMs for over four decades. Since the initial use of Gamma Knife® (GK) (Elekta, Stockholm, Sweden) to treat an AVM in Stockholm in 1970, developments in adjunct technologies such as digital subtraction angiography and MRI imaging have greatly improved SRS targeting and dose planning. Additional radiosurgical devices followed GK as treatment options for AVM, including the linear accelerator (LINAC), which was first used to treat an AVM in 1983, and more recently CyberKnife® (Accuray, Sunnyvale, CA, USA), a frameless system. By 2011, over 60,000 patients worldwide had undergone radiosurgery for AVMs [10].

Evaluations of the different radiosurgical platforms have shown comparable obliteration and complication rates. A retrospective analysis of outcomes in patients treated with GK versus LINAC found obliteration rates of 72% and 60%, respectively, but the difference was not statistically significant. Chronic toxicity occurred at equal rates in both groups [11]. A study of CyberKnife outcomes in 80 patients who underwent angiographic evaluation after at least 3 years of follow-up revealed complete obliteration in 81.2%, which falls within the general range of obliteration rates observed following SRS of any type [12]. Thus, each of the radiosurgical platforms delivers effective outcomes and low complication rates, though GK and LINAC have been in use for a longer period of time and thus used in the majority of radiosurgical AVM cases to date.

Grading Scales

Several classification and grading systems for AVMs have been developed and validated as tools for predicting the risk of intervention to a given lesion (Table 1). The most widely used system is the Spetzler-Martin (SM) grade, which predicts the risk of morbidity and mortality following microsurgery. Scores are calculated as the sum of points given to each of three criteria – lesion size, presence of venous drainage, and eloquence of the brain region – with a higher score reflecting higher operative risk [13]. Though designed to predict microsurgical outcomes, the SM grade has good predictive value for radiosurgery outcomes as well, as studies have found that increasing SM grade appropriately correlates with decreasing obliteration rates and increasing complication rates following SRS [14].

Nevertheless, radiosurgery-specific scoring systems have also been developed with the goal of consolidating the variables that influence the risk of radiosurgery. The RBAS (radiosurgery-based AVM score) was developed to predict the likelihood of excellent outcome following radiosurgery, defined as complete obliteration with no new neurologic deficits. The original score was a weighted sum of AVM location and volume, patient age, number of draining veins, and embolization status; the system was subsequently simplified to incorporate only AVM location, AVM volume and patient age [15, 16]. Studies have validated use of the RBAS grade in predicting outcomes for lesions located in various intracranial regions and treated with different radiosurgery platforms [17].

Pathophysiologic Changes Post-SRS

Characterizations of the pathophysiologic changes that occur in AVMs treated with radiosurgery have helped to elucidate the mechanisms underlying their obliteration. In vitro studies and pathologic reviews of resected AVMs have identified endothelial cell damage as a prominent response to irradiation. At the cellular level, significant phosphatidylserine internalization with accompanying cell cycle block and growth arrest were observed in endothelial cells subject to ionizing radiation of 15 Gy or higher [18]. At the tissue level, a pathologic review of 33 AVMs found endothelial proliferation to be the most commonly observed change, followed by hyalinization of vessel walls, thrombosis of irradiated vessels, and local vascular and tissue necrosis [19]. Similarly, endothelial cell damage was the earliest change noted in a study of 9 AVMs observed at different intervals (10 months to >5 years) following GK radiosurgery. The progressive changes that followed endothelial injury and culminated in vessel obliteration included smooth muscle cell proliferation and ECM deposition, intimal thickening, and finally hyalinization and cell degeneration [20].

Table 1 Comparison of AVM classification systems

	Spetzler-Martin (SM) grade	Modified radiosurgery-based AVM score (RBAS)
Size	Maximum diameter: <3 cm = 1 point 3–6 cm = 2 points >6 cm = 3 points	0.1 * volume (cm^3)
Location	Noneloquent = 0 points Eloquent (sensorimotor/language/visual cortex, hypothalamus, thalamus, internal capsule, brainstem, cerebellar peduncles, deep cerebellar nuclei) = 1 point	0.3 * location (hemispheric, corpus callosum, cerebellar = 0; basal ganglia, thalamus, brainstem = 1)
Venous drainage	Superficial only = 0 points Deep = 1 point	–
Age	–	0.02 * (patient age, years)

Indications for Use of SRS

Treatment of Unruptured Versus Ruptured AVMs

Results to date from short-term prospective studies comparing outcomes of conservative versus interventional treatment for unruptured AVMs have cautiously favored the use of medical management over intervention. The ARUBA study (A Randomized Trial of Unruptured Brain AVMs) randomized 233 patients with previously unruptured and untreated AVMs into two groups – medical management alone versus medical management with interventional therapy. The primary endpoint was defined as death from any cause or symptomatic stroke with evidence of hemorrhage or infarction on imaging. After a mean follow-up of 33 months, 30.7% of patients in the interventional group reached the primary outcome compared with 10.7% of patients in the medical management group. The risk of death or stroke was substantially lower in the latter group (HR 0.27) [7]. A prospective, population-based study conducted in Scotland similarly analyzed 204 patients in conservative versus interventional treatment groups, and reported lower rates of functional impairment in the conservative management cohort during the first 4 years of follow up (HR 0.59). Furthermore, an extended follow up to 12 years revealed lower rates of symptomatic stroke or death in the conservative management group (HR 0.37) [21].

Enrollment in the ARUBA trial was halted prematurely by the Data Safety Monitoring Board due to evidence of superior outcomes in the medical management group. Enrolled patients will continue to be followed to determine whether these outcome disparities will persist. However, a major criticism of both studies is the short follow-up time, which is particularly important in AVM treatment, as the risks of

interventional procedures manifest within the first few years, while the risks associated with the natural history of AVM accumulate over decades. A recent retrospective cohort study of ARUBA-eligible, low-grade (SM I-II) AVMs showed that long-term outcomes assessed at 5 years and 10 years from treatment were favorable compared to commonly cited natural history outcomes [22], which argues that SRS is warranted for low-grade, unruptured lesions. Overall, consensus on the management of unruptured AVMs remains to be established through longer term follow up. To this end, the Treatment Of Brain Aneurysm Study (TOBAS) has begun recruiting patients in both randomized and registry arms [23].

In contrast to unruptured AVMs, ruptured AVMs carry a high risk of annual hemorrhage which, in some estimates, can exceed that of unruptured AVMs by greater than threefold. Thus, treatment is generally warranted for ruptured AVMs. A cohort study of 639 patients with prior AVM rupture found a cumulative obliteration rate of 76% with an annual latency period hemorrhage risk of 2.0%, which represents an improvement over natural history estimates of hemorrhage risk in ruptured AVMs and speaks to benefit of SRS in this population [24].

Indications for the Use of SRS in AVMs

Surgical resection has traditionally been the first-line therapy for low-grade AVMs in superficial brain regions due to its highly effective and immediate AVM obliteration [25]. However, resection can be challenging to accomplish in deep locations, where it carries a higher risk of morbidity and mortality. Furthermore, some patients may not be suitable candidates for surgery due to comorbidities and age, or have a strong preference for non-invasive treatment. SRS is a widely used alternative recommended for small- to medium-sized AVMs less than 3–3.5 cm in diameter and is first-line treatment for AVMs located in deep or eloquent brain regions [26, 27]. A meta-analysis of 69 cohorts of SRS-treated patients found that small nidus size, low AVM grade (SM I-III), and increasing margin dose were associated with lower case fatality and hemorrhage rate [25]. A multivariate analysis of 220 patients similarly identified small AVM volume as a predictor for successful SRS, defined as nidus obliteration without new neurologic deficit [27]. Thus, the ideal candidate for SRS treatment would be a patient with an AVM that is less than 3.5 cm in diameter, either symptomatic or previously ruptured, and located in deep regions.

Endovascular Embolization

For AVMs exceeding a size and volume appropriate for SRS (diameter > 3–3.5 cm or volume > 10–15 mL), endovascular embolization can be performed prior to radiation to achieve the necessary size reduction. Additional roles for endovascular treatment include optimal treatment planning by identification of the AVMs angioarchitectural and detection of associated abnormalities including arteriovenous fistulas (AVFs) or perinidal and intranidal aneurysms. However, multiple studies have found that prior embolization decreases the probability of obliteration after radiosurgery [27–29]. Several mechanisms have been proposed to explain this phenomenon – embolic agents may decrease effective radiation dose to the nidal vessels via absorption or scattering, embolization-induced neoangiogenesis may occur around the AVM site, or obscuration of the nidus borders resulting from embolization may impede SRS targeting of the AVM [30]. Compared with unruptured AVMs, ruptured AVMs are less likely to achieve complete obliteration in the context of prior embolization [24, 31]. Ding and colleagues conducted a matched, prospective study of SRS for unruptured and ruptured AVMs and found that complete obliteration at 10 years following SRS with embolization was significantly lower in ruptured lesions (42% vs. 54%) [31].

Studies have generally found posttreatment hemorrhage risk to be unaffected or slightly increased by embolization, though there is no consensus on this controversy. A matched study of 244 patients undergoing SRS alone versus SRS with embolization found that the SRS alone group had lower rates of hemorrhage and higher rates of excellent outcome (obliteration plus no deficit) overall, but these differences were not statistically significant [28]. A similarly matched case control study confirmed a significantly lower rate of total obliteration follow embolization, but also found the overall annual hemorrhage risk (2.7%) to be unaffected by embolization [29].

Volume-Staged and Dose-Staged SRS

In addition to prior embolization for size reduction, other treatment strategies for large AVMs include volume-staged or dose-staged radiosurgery, which differ from conventional radiosurgery in that they do not deliver radiation during a single session and as a single dose. Volume-staged SRS partitions the AVM nidus into smaller volume targets and treats each one in an independent SRS session, with successive treatments spaced apart by 3–6 months. Dose-staged or hypofractionated SRS treats the entire nidus in fractions of lower doses, which are delivered over a period of a few weeks. Analyses of the outcomes and complications associated with each technique have consistently found that volume-staged SRS achieves higher obliteration rates, but is associated with slightly elevated complication rates. A systematic review of 11 volume-staged and 10 dose-staged SRS studies found that the former achieved

higher obliteration rates (40.3% vs. 32.7%). However, volume-staged SRS also had a less favorable complication profile, with elevated rates of symptomatic RICs (13.7% vs. 12.2%), posttreatment hemorrhage (19.5% vs. 10.6%), and death (7.4% vs. 4.6%) [32]. An earlier systematic review found a more substantial difference in obliteration rates between volume-staged and dose-staged SRS (47.5% vs. 22.8%). Volume-staged SRS also exceeded dose-staged SRS in post-SRS hemorrhage and mortality rates, but the two techniques had nearly identical rates of symptomatic RIC [33]. Thus, the choice of either form of staged radiosurgery would be a reasonable approach for a large AVM, though volume-staged SRS may be preferred for its higher obliteration rates.

Outcomes of SRS for AVMs

Obliteration Rates

The proportion of SRS-treated AVMs that eventually achieve complete obliteration is the primary outcome by which success of SRS is assessed. Obliteration rates depend on a multitude of factors relating to AVM characteristics and treatment parameters, and they vary widely from 50% to 90% in reported studies. Generally, post-SRS obliteration rates fall in the range of 70–80% [14, 34]. Compared with microsurgery and embolization, both the outcomes and complications of SRS manifest over a substantially longer time period. AVMs typically do not achieve complete obliteration until 1–3 years after SRS treatment, and those that remain patent at 3–4 years are considered for retreatment [25].

Ionizing radiation dose is strongly and positively correlated with obliteration rates following SRS. A dose response analysis of 197 AVM patients found that margin doses of 13 Gy, 16 Gy, 20 Gy, and 25 Gy were associated with obliteration rates of 50%, 70%, 90%, and 98%, respectively [35]. Margin dose normally varies from 16 to 25 Gy, and obliteration rates tend to improve at doses greater than 17 Gy [30]. However, higher radiation doses also have higher propensity to cause adverse radiation effects – thus, dose planning is necessary to optimize obliteration rates while minimizing the risk of radiologic complications. A commonly referenced guideline states that radiation dose should be low enough to cause <3% risk of permanent injury to adjacent tissue [35]. In addition to radiation dose, other predictors of successful radiosurgical outcome include small AVM volume, fewer draining veins, younger patient age, and hemispheric location [27]. Prior hemorrhage status was not found to affect obliteration rates in one matched case-control study of ruptured versus unruptured AVMs (73% vs. 76% at 10-year follow up) [31].

Latency-Period Hemorrhage

During the latency period of typically 1–3 years between SRS treatment and complete obliteration, the patent nidus remains at risk of hemorrhage. This risk persists until obliteration is confirmed, at which point future hemorrhage risk falls to less than 1% [30]. Hemorrhage risk during the latency period is a key component of the outcome and complication profile of SRS. Whether annual hemorrhage rate during the latency period is reduced compared with that of an AVM's natural history is debated. An observational study comparing hemorrhage rates before and after radiosurgery for 315 patients found a 2.4% annual hemorrhage rate pre-surgery, consistent with natural history estimates of 2–4%. The actuarial hemorrhage rate following radiosurgery was 4.8% per year (95% CI 2.4–7.0%) in the first 2 years of follow-up and 5.0% (95% CI 2.3–7.3%) for the third to fifth year of follow-up. The authors concluded that there was no statistically significant change in hemorrhage rate during the latency period versus prior to treatment [36]. Multivariate analysis of the data set demonstrated that the presence of an unsecured proximal aneurysm was a significant risk factor for post-SRS hemorrhage (RR 4.56). Another study of 1204 patients treated with Gamma Knife found latency period hemorrhage to be reduced compared with hemorrhage rate from diagnosis to treatment. Overall preradiosurgical annual hemorrhage rate was 2.0% from birth or 6.6% from AVM diagnosis, and corresponding rates were higher in the subset of patients who initially presented with hemorrhage (3.7% from birth and 10.4% from diagnosis). Annual hemorrhage rates following radiosurgery were 2.5% overall and 2.8% in patients who had initially presented with hemorrhage, which remain comparable to annual hemorrhage rates since birth, but are reduced compared with annual hemorrhage rate from diagnosis to treatment [37].

Deep AVMs of the brainstem, basal ganglia, and thalamus have shown more consistent reductions in latency-period hemorrhage compared to their superficial counterparts, potentially reflecting their more hemorrhage-prone natural history. While around half all AVMs initially present with hemorrhage, 72–91% of basal ganglia and thalamic AVMs present in this manner. Their annual hemorrhage risk approaches 10%, compared with 2–4% among AVMs in all locations [3, 38]. A review of six studies of SRS for thalamus and basal ganglia AVMs found a median annual hemorrhage rate of 3.3% (range 0.36–9.5%) in the first year after SRS [38], which is reduced compared with the natural hemorrhage rates of deep AVMs. Thus, improvements in annual hemorrhage risk following radiosurgery further support the role of SRS as a first line treatment for deep AVMs.

Seizure Outcomes

While the primary treatment objective for AVMs is to abolish hemorrhage risk via obliteration, SRS has also been found to reduce AVM-associated seizures. A meta-analysis of seizure outcome data for 1157 patients found that those who received SRS and had complete AVM obliteration had the highest rate of seizure control (85.2%) compared to patients receiving surgery or embolization. In overall rates of seizure control, microsurgery was most effective (78.3%), followed by SRS (62.8%) and embolization (49.3%). Furthermore, the rate of development of new onset seizures following treatment occurred least frequently in SRS (5.4%) and was comparatively elevated in microsurgery (9.1%) and embolization (39.4%) [39]. A retrospective study of 65 AVM patients with a history of seizures found that at 3-year follow-up after SRS, 51% of all patients were seizure-free and 61% of patients with medically intractable partial epilepsy had excellent outcomes [40].

Complications and Follow-Up

Adverse Radiation Effects

The most commonly observed complications in patients receiving treatment are radiation-induced changes (RIC), or adverse radiation effects (ARE). They typically develop 6–18 months following treatment and appear as increased perinidal T2 hyperintensity on imaging [41]. The pathophysiology of RIC development is not well understood, but cerebral edema secondary to blood brain disruption may account for the classic radiologic appearance of RIC. A prospective study also found the presence of radiologic RICs to be a statistically significant predictor of eventual obliteration [26], which suggests a potential overlap in the pathophysiologic changes underlying the two processes. Indeed, vascular endothelial injury has been suggested as a mechanism for both RIC and obliteration [41].

As outlined by Ding and colleagues, the occurrence of RIC can be estimated by a rule of thirds – approximately one-third (30–40%) of patients undergoing SRS develop radiologic RIC appreciable on imaging, one-third of those patients develop neurologic symptoms secondary to RIC (10% of all cases), and one-third of symptomatic patients develop permanent neurologic morbidity (2–3% of all cases) [14]. A meta-analysis by Ilyas and colleagues looked at 51 studies of patients undergoing GK or LINAC treatment and found RIC rates that corroborated the aforementioned estimates [41]. Overall rates of radiologic, symptomatic, and permanent RIC were 35.5%, 9.2%, and 3.8%, respectively. Hemiparesis was the most commonly documented neurologic symptom. Observed neurologic symptoms lasting any duration included hemiparesis (48.9% of all symptomatic patients), headache (16.3%), seizures (12.1%), sensory dysfunction (7.1%), and ataxia (3.5%). Of patients who had permanent neurologic deficits, approximately half had hemiparesis, more than a quarter had visual field deficits, and the remaining fraction had diplopia, seizures, ataxia, and other sensory dysfunction.

Among individual studies, RIC risk consistently correlated with higher margin dose and larger AVM volume. In the meta-analysis as a whole, lack of prior AVM hemorrhage and repeat SRS were two factors significantly associated with radiologic RIC. An independent case-control study also found a significantly increased rate of RIC in unruptured AVMs (48.9%) versus ruptured AVMs (30.4%) [31]. One hypothesis to account for this association is that perinidal gliosis resulting from prior rupture may be protective against RIC. Deep AVM location was significantly associated with symptomatic RIC, reflecting the eloquence of deep brain regions.

Cyst Formation

Cyst formation is a late and rare complication of SRS that occurs in approximately 2–5% of patients [14]. Pan and colleagues found that in a population of 1203 patients undergoing gamma knife radiosurgery, 20 patients developed cysts (1.6%); among them, 1 patient developed a cyst within 5 years, 9 developed cysts between 5 and 10 years, and 10 developed cysts between 10 and 23 years [42]. A systematic review of 22 studies found that overall post-SRS cyst formation rate was 3.0%, and mean latency period to cyst formation was 6.5 years [44]. A pathologic characterization of post-SRS cysts on 17 patient samples revealed dilated capillary vessels with hyalinization and fibrinoid necrosis, massive protein exudation from damaged vessels, and hemorrhage. Grossly, cysts were associated with nodular lesions and chronic encapsulated expanding hematomas [43]. The pathogenesis of cyst formation may relate to the presence of prior RIC, which can prime the brain parenchyma surrounding the original nidus to downstream events that culminate in cyst formation. In the Ilyas and colleagues 2017 review, approximately one-third of cysts were either symptomatic or enlarging, and were treated with surgical intervention; the remaining majority were asymptomatic and managed conservatively [44].

Follow-Up and Retreatment

Post-SRS follow-up protocols vary between individual practitioners and institutions, but a typical long-term protocol may consist of an MRI at 6 months, 1, 2, and 3 years following the

procedure. If an MRI within 3 years suggests complete obliteration, angiography is performed to confirm the result. In cases of confirmed obliteration, patients are recommended to have follow-up MRIs at 2, 4, and 8 years to monitor for long-term outcomes and complications. Patients whose AVMs remain patent 3–4 years after initial treatment are evaluated by angiography for the option of salvage management, which could include microsurgery, repeat SRS, or embolization [10].

A retrospective study of 996 patients receiving Gamma Knife identified 105 (10.5%) who underwent repeat SRS due to incomplete obliteration. Median latency between first and repeat SRS was 40.9 months. The actuarial rates of total obliteration following repeat SRS were 35%, 68%, 77%, and 80% at 3, 4, 5, and 10 years, respectively. Smaller residual target volume and volume reduction exceeding 50% on initial SRS were associated with improved obliteration rates after repeat SRS. Factors associated with hemorrhage after repeat SRS were similar to those associated with hemorrhage after original SRS, namely prior hemorrhages, larger AVM volume, and higher Pollock-Flickinger score [34]. Stahl and colleagues likewise demonstrated the efficacy and safety of repeat SRS as salvage treatment, identifying a 69% relative decrease in median nidus volume following repeat SRS as well as low rates of RICs (4.9%) and posttreatment hemorrhage (5.8%) [45].

Conclusion

Stereotactic radiosurgery has become an established noninvasive treatment modality for intracranial arteriovenous malformations and is most effective for small AVMs in deep and eloquent locations. The results of prospective studies on whether unruptured AVMs should be treated have generated controversy, and further follow-up and independent studies will continue to clarify this important decision point. In contrast, ruptured AVMs warrant treatment in the majority of cases due to the elevated hemorrhage risk associated with their natural history. Overall, SRS has been shown to achieve high obliteration rates of 70–80% and carry a low complication profile that most commonly includes symptomatic radiation-induced changes in approximately 10% of treated patients.

Guidelines

- General considerations
  - Latency period from radiosurgery treatment to complete obliteration is typically 1–3 years, and overall obliteration rates post-radiosurgery are estimated at 70–80%.
  - It remains unclear whether latency period hemorrhage risk is altered following treatment, but it certainly remains and should be discussed with patients.
  - Radiation-induced changes are the most common complication arising from radiosurgery, and are radiographically appreciable in 30–40% of patients, symptomatic in 10% of patients, and cause permanent neurologic morbidity in 2–3% of patients.
  - AVMs should be followed by periodic MRIs for the first 2–3 years following treatment. If obliteration is observed on MRI, it can be confirmed by angiography. AVMs not obliterated by 3–4 years following radiosurgery should be considered for salvage management, commonly accomplished via repeat radiosurgery.
- Asymptomatic/unruptured AVMs
  - Results to date from the ARUBA trial on interventional versus conservative treatment for previously unruptured and untreated AVMs have shown better *short-term* outcomes in the conservative treatment group (10.7% versus 30.7% of patients reached the primary outcome of death or stroke).
  - A major criticism of the trial is that the short-term complications following treatment cannot be adequately compared with longer-term risks of AVM natural history within the short follow-up time of the trial.
  - Longer-term data are required to clarify whether interventional treatments including radiosurgery lead to better outcomes than conservative management.
- Symptomatic/unruptured AVMs
  - Radiosurgery would be appropriate, particularly for small lesions (<3.5 cm diameter), deep lesions, and elderly patients, specifically with improvements in seizure control.
- Symptomatic/ruptured AVMs
  - Radiosurgery is generally indicated, as the latency period hemorrhage risk following treatment is lower than risk of re-rupture in the natural course of the disease.
  - Radiosurgery would be appropriate for lesions less amenable to surgery, such as those in deep locations, and achieves higher obliteration rates when the lesion is small.
- Large AVMs
  - Typically defined as lesions exceeding 3–3.5 cm in diameter or 10–15 mL in volume.
  - Endovascular embolization can be used preceding radiosurgery to reduce nidus size but is associated with lower eventual obliteration rates compared with no embolization.
  - Volume-staged radiosurgery achieves good obliteration rates (40–50%) and has an acceptable complication profile.
  - Dose-staged radiosurgery achieves lower obliteration rates (20–35%) compared with volume-staged radiosurgery but has a marginally improved complication profile.

References

1. Gross BA, Du R. Natural history of cerebral arteriovenous malformations: a meta-analysis. J Neurosurgery. 2013;118(2):437–43.
2. Ozpinar A, Mendez G, Abla AA. Epidemiology, genetics, pathophysiology, and prognostic classifications of cerebral arteriovenous malformations. Handb Clin Neurol. 2017;143:5–13.
3. Cohen-Inbar O, Ding D, Chen C-J, Sheehan JP. Stereotactic radiosurgery for deep intracranial arteriovenous malformations, part 1: brainstem arteriovenous malformations. J Clin Neurosci. 2016;24:30–6.
4. Can A, Gross BA, Du R. The natural history of cerebral arteriovenous malformations. Handb Clin Neurol. 2017;143:15–24.
5. Nikolaev SI, Vetiska S, Bonilla X, Boudreau E, Jauhiainen S, Rezai Jahromi B, et al. Somatic activating KRAS mutations in arteriovenous malformations of the brain. N Engl J Med. 2018;378(3):250–61.
6. Kim H, Al-Shahi Salman R, McCulloch CE, Stapf C, Young WL. Untreated brain arteriovenous malformation: patient-level meta-analysis of hemorrhage predictors. Neurology. 2014;83(7):590–7.
7. Mohr JP, Parides MK, Stapf C, Moquete E, Moy CS, Overbey JR, et al. Medical management with or without interventional therapy for unruptured brain arteriovenous malformations (ARUBA): a multicenter, non-blinded, randomised trial. Lancet. 2014;383(9917):614–21.
8. Josephson CB, Bhattacharya JJ, Counsell CE, Papanastassiou V, Ritchie V, Roberts R, et al. Seizure risk with AVM treatment or conservative management: prospective, population-based study. Neurology. 2012;79(6):500–7.
9. Crawford PM, West CR, Chadwick DW, Shaw MD. Arteriovenous malformations of the brain: natural history in unoperated patients. J Neurol Neurosurg Psychiatry. 1986;49(1):1–10.
10. Lunsford LD, Niranjan A, Kano H, Kondziolka D. The technical evolution of Gamma Knife radiosurgery for arteriovenous malformations. Prog Neurol Surg. 2013;27:22–34.
11. Orio P, Stelzer KJ, Goodkin R, Douglas JG. Treatment of arteriovenous malformations with linear accelerator-based surgery compared with Gamma Knife surgery. J Neurosurg. 2006;105(Suppl):58–63.
12. Colombo F, Cavedon C, Casentini L, Francescon P, Causin F, Pinna V. Early results of CyberKnife radiosurgery for arteriovenous malformations. J Neurosurg. 2009;111(4):807–19.
13. Spetzler RF, Martin NA. A proposed grading system for arteriovenous malformations. J Neurosurg. 1986;65(4):476–83.
14. Ding D, Starke RM, Sheehan JP. Radiosurgery for the management of cerebral arteriovenous malformations. Handb Clin Neurol. 2017;143:69–83.
15. Pollock BE, Flickinger JC. A proposed radiosurgery-based grading system for arteriovenous malformations. J Neurosurg. 2002;96(1):79–85.
16. Pollock BE, Flickinger JC. Modification of the radiosurgery-based arteriovenous malformation grading system. Neurosurgery. 2008;63(2):239–43.
17. Pollock BE. Development and testing of a radiosurgery-based arteriovenous malformation grading system. Prog Neurol Surg. 2013;27:58–66.
18. Zhao Z, Johnson MS, Chen B, Grace M, Ukath J, Lee VS, et al. Live-cell imaging to detect phosphatidylserine externalization in brain endothelial cells exposed to ionizing radiation: implications for the treatment of brain arteriovenous malformations. J Neurosurg. 2016;124(6):1780–7.
19. Chang SD, Shuster DL, Steinberg GK, Levy RP, Frankel K. Stereotactic radiosurgery of arteriovenous malformations: pathologic changes in resected tissue. Clin Neuropathol. 1997;16(2):111–6.
20. Schneider BF, Eberhard DA, Steiner LE. Histopathology of arteriovenous malformations after gamma knife radiosurgery. J Neurosurg. 1997;87(3):352–7.
21. Al-Shahi Salman R, White PM, Counsell CE, du Plessis J, van Beijnum J, Josephson CB, et al. Outcome after conservative management or intervention for unruptured brain arteriovenous malformations. JAMA. 2014;311(16):1661–9.
22. Ding D, Starke RM, Kano H, Mathieu D, Huang PP, Kondziolka D, et al. Stereotactic radiosurgery for ARUBA (A Randomized Trial of Unruptured Brain Arteriovenous Malformations)-Eligible Spetzler-Martin grade I and II arteriovenous malformations: a multicenter study. World Neurosurg. 2017;102:507–17.
23. Darsaut TE, Magro E, Gentric J-C, Batista AL, Chaalala C, Roberge D, et al. Treatment of brain AVMs (TOBAS): study protocol for a pragmatic randomized controlled trial. Trials. 2015;16:497.
24. Ding D, Yen CP, Starke RM, Xu Z, Sheehan JP. Radiosurgery for ruptured intracranial arteriovenous malformations. J Neurosurg. 2014;121(2):470–81.
25. Van Beijnum J, van der Worp HB, Buis DR, Al-Shahi Salman R, Kappelle LJ, Rinkel GJ, et al. Treatment of brain arteriovenous malformations: a systematic review and meta-analysis. JAMA. 2011;306(18):2011–9.
26. Ding D, Yen CP, Xu Z, Starke RM, Sheehan JP. Radiosurgery for patients with unruptured intracranial arteriovenous malformations. J Neurosurg. 2013;118(5):958–66.
27. Pollock BE, Flickinger JC, Lunsford LD, Maitz A, Kondziolka D. Factors associated with successful arteriovenous malformation radiosurgery. Neurosurgery. 1998;42(6):1239–47.
28. Andrade-Souza YM, Ramani M, Scora D, Tsao MN, terBrugge K, Schwartz ML. Embolization before radiosurgery reduces the obliteration rate of arteriovenous malformations. Neurosurgery. 2007;60(3):443–52.
29. Kano H, Kondziolka D, Flickinger JC, Park KJ, Iyer A, Yang HC, et al. Stereotactic radiosurgery for arteriovenous malformations after embolization: a case-control study. J Neurosurg. 2012;117(2):265–75.
30. Rubin BA, Brunswick A, Riina H, Kondziolka D. Advances in radiosurgery for arteriovenous malformations of the brain. Neurosurgery. 2014;74(Suppl 1):S50–9.
31. Ding D, Yen CP, Starke RM, Xu Z, Sheehan JP. Effect of prior hemorrhage on intracranial arteriovenous malformation radiosurgery outcomes. Cerebrovasc Dis. 2015;39(1):53–62.
32. Ilyas A, Chen CJ, Ding D, Taylor DG, Moosa S, Lee CC, et al. Volume-staged versus dose-staged stereotactic radiosurgery outcomes for large brain arteriovenous malformations: a systematic review. J Neurosurg. 2018;128(1):154–64.
33. Moosa S, Chen CJ, Ding D, Lee CC, Chivukula S, Starke RM, et al. Volume-staged versus dose-staged radiosurgery outcomes for large intracranial arteriovenous malformations. Neurosurg Focus. 2014;37(3):E18.
34. Kano H, Kondziolka D, Flickinger JC, Yang HC, Flannery TJ, Awan NR, et al. Stereotactic radiosurgery for arteriovenous malformations, part 3: outcome predictors and risks after repeat radiosurgery. J Neurosurg. 2012;116(1):21–32.
35. Flickinger JC, Pollock BE, Kondziolka D, Lunsford LD. A dose-response analysis of arteriovenous malformation obliteration after radiosurgery. Int J Radiat Oncol Biol Phys. 1996;36(4):873–9.
36. Pollock BE, Flickinger JC, Lunsford LD, Bissonette DJ, Kondziolka D. Hemorrhage risk after stereotactic radiosurgery of cerebral arteriovenous malformations. Neurosurgery. 1996;38(4):652–61.
37. Yen CP, Sheehan JP, Schwyzer L, Schlesinger D. Hemorrhage risk of cerebral arteriovenous malformations before and during the latency period after GAMMA knife radiosurgery. Stroke. 2011;42(6):1691–6.
38. Cohen-Inbar O, Ding D, Sheehan JP. Stereotactic radiosurgery for deep intracranial arteriovenous malformations, part 2: basal gan-

glia and thalamus arteriovenous malformations. J Clin Neurosci. 2016;24:37–42.
39. Baranoski JF, Grant RA, Hirsch LJ, Visintainer P, Gerrard JL, Gunel M, et al. Seizure control for intracranial arteriovenous malformations is directly related to treatment modality: a meta-analysis. J Neurointerv Surg. 2014;6(9):684–90.
40. Schauble B, Cascino GD, Pollock BE, Gorman DA, Weigand S, Cohen-Gadol AA, et al. Seizure outcomes after stereotactic radiosurgery for cerebral arteriovenous malformations. Neurology. 2004;63(4):683–7.
41. Ilyas A, Chen CJ, Ding D, Buell TJ, Raper DMS, Lee CC, et al. Radiation-induced changes after stereotactic radiosurgery for brain arteriovenous malformations: a systematic review and meta-analysis. Neurosurgery. 2018;83(3):365–76.
42. Pan HC, Sheehan J, Stroila M, Steiner M, Steiner L. Late cyst formation following gamma knife surgery of arteriovenous malformations. J Neurosurg. 2005;102(Suppl):124–7.
43. Ilyas A, Chen CJ, Ding D, Mastorakos P, Taylor DG, Pomeraniec IJ, et al. Cyst formation after stereotactic radiosurgery for brain arteriovenous malformations: a systematic review. J Neurosurg. 2017;26:1–10.
44. Shuto T, Yagishita S, Matsunaga S. Pathological characteristics of cyst formation following gamma knife surgery for arteriovenous malformation. Acta Neurochir. 2015;157(2):293–8.
45. Stahl JM, Chi YY, Friedman WA. Repeat radiosurgery for intracranial arteriovenous malformations. Neurosurgery. 2012;70(1):150–4.

Radiosurgical Management of Trigeminal Neuralgia

Srinivas Chivukula, Nicholas Au Yong, Matiar Jafari, and Nader Pouratian

Introduction

Trigeminal neuralgia (TN) is a disabling pain syndrome that typically manifests as paroxysmal, lancinating pain along the dermatomal distribution of one or more branches of the trigeminal nerve [1–3]. Medical management remains the mainstay of its treatment. However, for cases when medical therapy fails, several surgical techniques exist, with high rates of initial success. These include radiofrequency rhizotomy, glycerol rhizolysis, balloon compression, and microvascular decompression (MVD) [3–5]. Stereotactic radiosurgery (SRS) has gained traction as a treatment for medical refractory TN, even as first-line treatment, especially in patients with advanced age or medical comorbidities, those patients on long-term antiplatelet or anticoagulant therapy, and others in whom more invasive techniques may be contraindicated [3, 5, 6]. A wealth of literature has accumulated around the planning and treatment of patients with trigeminal neuralgia [1, 2]. We highlight generally agreed upon practice principles, complication profiles, and toxicity mitigation strategies. We also briefly discuss the use of SRS in special instances of TN, such as in the treatment of TN secondary to multiple sclerosis (MS) or to compressive mass lesions and in the treatment of recurrent TN.

Diagnosis, Etiology, and Pathophysiology

Trigeminal neuralgia is a clinical diagnosis that depends critically on a patient's description of pathognomonic pain attacks [1, 2]. Classically, these attacks are described as paroxysmal, lancinating pain confined to a distribution encompassing one or more branches of the trigeminal nerve on one side of the face with intervening pain-free periods (so-called trigeminal neuralgia, type I) [4]. Variants are recognized, including those with persistent facial pain (so-called trigeminal neuralgia, type II). While the pain most often occurs without evident pathology (classical, idiopathic, or primary TN), it may also be secondary to neurological insult (for instance, demyelinating disorders such as multiple sclerosis (MS) or compressive mass lesions) [1, 2, 4, 7, 8]. The lack of a specific, objective tool for the identification and assessment of pain has compounded the difficulty in adequately diagnosing TN over the years [2]. Numerous classification schemes and criteria have been proposed, but these remain of controversial and actively contested [2, 4, 9]. For the current discussion, we limit the distinction in TN to two forms – idiopathic (or primary) and secondary TN.

The etiology of primary TN remains unclear but empirical evidence suggests that in a majority of cases (~95%), vascular compression of the trigeminal nerve is at least partially responsible for the neuropathic pain [1, 9]. Although most frequently (85–90%) the vascular compression is noted to be arterial, compressive venous pathology is occasionally noted as well [9, 10]. It is postulated that TN results from a combination of central demyelination of the nerve root entry zone (REZ) and the subsequent, reinforced electrical excitability of the nerve [9, 11]. Recent studies suggest that the demyelination leads to an impairment of the nociceptive system, with loss of central inhibition [11–13]. The implication of vascular compression in neuropathic pain is supported by several lines of evidence. First, magnetic resonance imaging (MRI) and direct surgical observations consistently show a blood vessel in contact with the nerve root [14]. Second, elimination of the compression in most cases leads to long-term pain relief [15, 16]. Additionally, intraoperative recordings show immediate improvement in nerve conduction following decompression [16].

S. Chivukula · N. A. Yong · M. Jafari · N. Pouratian (✉)
Department of Neurosurgery, David Geffen School of Medicine at UCLA, Los Angeles, CA, USA
e-mail: schivukula@mednet.ucla.edu; npouratian@mednet.ucla.edu

D. M. Trifiletti et al. (eds.), *Stereotactic Radiosurgery and Stereotactic Body Radiation Therapy*,
https://doi.org/10.1007/978-3-030-16924-4_14

The remaining small subset of cases of secondary trigeminal neuralgia are associated with MS (with or without radiographic plaques), lacunar infarctions (often within the brainstem trigeminal system), or compressive mass lesions (often of the cerebellopontine angle, CPA) [1, 2, 8]. Multiple sclerosis is identified in approximately 2–4% of patients with TN [17]. Demyelinating MS plaques have been reported involving brainstem trigeminal nuclei [18]. In a small proportion of patients with MS, TN is the first manifestation of the disease [17, 18]. In these patients, the neuralgia is frequently bilateral [19]. Tumors are identified in another approximately 2–3% of patient with classical TN symptoms, particularly posterior fossa meningiomas or neuromas [7]. Tumors affecting the peripheral branches or the Gasserian ganglion usually give rise to sensory change and constant pain (trigeminal neuropathy, as opposed to trigeminal neuralgia) [20]. When tumors cause TN, they tend to be slow-growing tumors that distend the trigeminal root rather than invade it [7, 13].

From large-scale MRI studies, the localization of the lesion common to all patients appears to be the pontine margin of the fascicular trigeminal nerve root, especially at the REZ [14]. This lends further support to the idea that demyelination at the central nerve root if fundamental to symptom manifestation in TN [11]. The REZ represents the junction between the peripheral and the central myelin of Schwann cells and astrocytes and as such, central branches of unipolar ganglion cells enter the pons through this transition zone on their course toward the brainstem and spinal trigeminal nuclei [11]. Any process at this level could potentially alter the function of all neurons involved, frequently a branch of the trigeminal nerve. Additional support for the REZ involvement in the pathophysiology of the pain comes from close inspection of the long-term effects of several treatments for TN. Simple blocks or minimally destructive peripheral procedures lead to transient pain relief, much shorter than seen in more proximal lesions to the nerve fascicles, or decompression [21].

Stereotactic Radiosurgery (SRS) for Trigeminal Neuralgia

Microvascular decompression has historically been considered the gold standard of surgical treatment for TN, with reported rates of immediate pain relief postoperatively of approximately 87–98%, and persistent complete pain relief rates at 2 years postoperatively of between 75% and 80% [16]. Only 4–12% of patients that undergo MVD are reported to experience recurrences at 10 years postoperatively [21, 22]. Moreover, in experienced hands, the risks of MVD are considered minimal; mortality rates of 0.2–1% are described, and rates of other complications are low, including cerebellar injury (<1%), eighth cranial nerve injury (<1%), and cerebrospinal fluid (CSF) leaks (1–2%) [16]. Still, because of its less invasive nature, stereotactic radiosurgery (SRS) has become a well-established alternative surgical option with an equally low risk of complications [3–6].

The idea of SRS for TN originated in 1953 when x-rays were first used to treat two patients with TN [23]. Their long-term success (>17 years) was reported in 1971 and in the decades since the technique has undergone tremendous refinement in its various parameters including radiation source and intensity, treatment target, and treatment volume [23–25]. For most of the 1970s and 1980s, several surgeons irradiated the trigeminal ganglion [23, 24]. As our understanding of TN pathophysiology has increased, however, the root entry zone at the pontine margin has become a more frequent radiosurgical target for primary TN [24]. In a well-cited, multicenter study using SRS targeted at the REZ for the treatment of primary TN in 50 patients, 58% were free of pain at a median follow-up of 18 months, and another 36% had significant improvement (>50%) in their pain [26]. Higher radiation doses (up to 90 Gy) were found to be associated with higher chances of pain relief [24, 26].

The mechanism of pain relief following irradiation of the trigeminal nerve remains unclear. It is speculated that nerve irradiation may induce functional electrophysiologic blockade of ephaptic transmission, since most patients continue to maintain normal trigeminal function [11, 27]. With the delivery of between 60 Gy and 100 Gy, there is decreased peak sodium current through the axons of the trigeminal nerve fascicles, and consequently, a conduction block [28, 29]. The heterogeneous fiber composition (gamma, alpha, and beta fibers, among others) of the trigeminal nerve and the partial demyelination (with demyelinated areas acting as hyperexcitable pacemakers) have different densities of membrane receptors [29]. Radiation-induced electrical conduction block may depend on these differences, and moreover, these differences may explain the interindividual difference in the mean latency duration to pain relief following radiosurgical treatment, which often ranges between 4 and 6 weeks [29].

Delivery

Various forms of delivering radiation have been introduced over the years but mainly include gamma knife radiosurgery (GKRS)- and linear accelerator (LINAC)-based delivery. The gamma knife bundles up to 192 individual beams of radiation (using cobalt 60 as a radiation source) with collimator cones of variable sizes, most often 4 mm or 5 mm [25, 30]. This results in a focused beam with diameter of a few millimeters called an isocenter with a high-dose gradient (high in the center, low in the neighborhood), protecting the surrounding tissue from doses above their radiation tolerance

level [24, 25, 30]. In comparison, LINAC devices emit x-rays which are bundled by tertiary collimators such as multileaf or ring collimators and allow the precise and focused direction of radiation [31, 32]. In significant contrast to GKRS, LINAC-based delivery only has one radiation source [32]. The emitter head must be moved around the patient, otherwise the tolerance of the tissue in the pathway of the ray will quickly be exceeded and the therapeutic target dose in the target lesion may not be reached [33]. Despite these differences, most studies have reported nearly identical results in the treatment of trigeminal neuralgia [31–33].

Both GKRS- and LINAC-based delivery have historically relied on the use of skull fixation frames [34, 35]. Frame-based radiosurgery, as it is known, required skeletal fixation and the mechanical linkage between the target and the radiosurgical device [34]. Although patient movement is minimized, displacement can still occur, called "application error" [35, 36]. Despite the application error, accuracy of most Gamma Knife devices has been shown to be in the millimeter range. Similar geometric accuracy has been demonstrated with LINAC-based systems as well [36, 37]. In contrast, frameless stereotaxy is becoming increasingly widespread [33, 37]. This relies on maintaining a fixed relationship between the target and treatment device by a virtual frame of reference, established on the basis of intraprocedural CT and x-ray imaging [33, 34]. This is noninvasive, provides for pin-free radiosurgery, and eliminates the need for anesthesia and for sterile processing and greatly decreases the close patient monitoring required with frame-based approaches [33–37]. The accuracy of LINAC-based radiosurgery device has been validated and found to be comparable to frame-based methods [17, 38]. In two important evaluations with SRS for primary TN, Chen and associates reported that 91% of 44 patients experienced satisfactory outcomes (BNI grades I or II) with Novalis LINAC-based image-guided radiosurgery (IGRS), and Fariselli and associates reported that with CyberKnife LINAC-based IGRS, 94% experienced similar outcomes. The mean follow-up duration in both studies was over 15 months [33, 38].

Assessment

A number of pain assessment criteria and rubrics have been developed for trigeminal neuralgia. The rather subjective and patient specific nature of the pathology often makes the development of universal criteria difficult [1–3]. Here, we use the Barrow Neurological Institute (BNI) pain intensity criteria in grading pain and evaluating outcomes, specifically, score I (no pain, no medication), score II (occasional pain, not requiring medication), score IIIa (no pain, but continued medication), score IIIb (pain controlled with medication), score IV (pain improved, but not adequately controlled with medication), and score IV (persistent inadequately controlled pain) [39]. The initial score developed by Rogers and associates only contained a single score for category III but we utilized a modification to include two subcategories (IIIa and IIIb as described) [3, 39]. Unless otherwise specified, BNI score I is considered complete pain relief, BNI scores II–IIIb are incomplete relief, and BNI scores IV and V are no significant relief. BNI scores I–IIIb are considered adequate pain relief [3].

Radiation Planning, Toxicity, and Mitigation Strategies

In his initial experiences, Lars Leksell targeted the Gasserian ganglion [25]. At the time, x-ray imaging modalities were based on bony or surface landmarks or cisternography-based targeting [24, 25]. Radiation was delivered using an orthovoltage tube aimed with a stereotactic frame at the Gasserian ganglion in two patients (16.5 Gy and 22 Gy), resulting in long-term pain control that lasted 17 years [25–27]. Despite this successful initial demonstration, subsequent studies could not replicate these results. In 46 patients in whom Lindquist and associates targeted the Gasserian ganglion for TN, pain control was only achieved in approximately 50% of patients [40]. Moreover, a majority suffered a recurrence. It was not until much later, when MRI use became widespread in neurosurgery that the radiation target began to see a transition more proximally along the nerve's course into the brainstem, toward the REZ [24, 26, 27]. The safety and efficacy of radiosurgery for TN depends upon both treatment target and dosimetry. Typical doses have ranged from 70 Gy to 90 Gy, targeting the trigeminal REZ with the 30–40% isodose line placed tangential to the brainstem [23, 24]. There is still no universally agreed upon treatment plan. In this section, we review the relevant and available evidence in formulating TN treatment plans, with emphasis on safety and efficacy.

Dose

The widely used parameters of a 4 mm isocenter targeting the REZ at doses ranging from 60 Gy to 90 Gy were put forth by Kondziolka and colleagues at the University of Pittsburgh. In their initial report, of 51 patients evaluated, 37% were pain-free and another 41% experienced at least satisfactory relief at follow-up ranging between 2 months and 29 months (mean, 9.6 months) [24, 26]. It was found that doses ≥70 Gy were associated with a greater chance of pain relief [26]. This was re-demonstrated in a follow-up multi-institutional study of 50 patients treated with the same parameters [26]. At a median follow-up of 18 months (range, 11–36 months), 29 patients (58%) were pain-free and 18 patients (36%)

experienced good relief (50–90% relief). Pollock and associates compared treatment with low (70 Gy) doses to high (90 Gy) doses in 70 patients with idiopathic TN treated with GKRS using a 4 mm isocenter; although no significant complications occurred, 66% of patients in the high-dose group developed trigeminal sensory deficits, compared with 22% of the low-dose group [41]. Among the high-dose group, 32% of patients developed bothersome dysesthesia, and three patients developed corneal numbness. This was in contrast with the low-dose group, where a single patient developed dysesthias [41].

Similar results have also been reported with LINAC-based systems. Goss and colleagues reported on 19 patients treated with 90 Gy, with the 50% isodose volume at the brainstem surface [42]. Of these patients, 75% achieved complete pain relief, while another 24% experienced BNI score II–IIIb relief. Similar to the GKRS studies, 32% of patients developed some degree of facial hypesthesia [41, 42]. Subsequent studies such as Smith and colleagues evaluated radiation doses ranging the spectrum between 70 Gy and 90 Gy and using collimators of different sizes (5 mm and 7 mm), targeting the REZ [43, 44]. At a mean follow-up period of 23 months, Smith and colleagues reported that of 41 patients with TN, 87.8% experienced significant pain relief, although those with essential TN and typical features fared far better than those with atypical features to their facial pain [43, 44]. The conclusion from various studies to date appears to be that patients with typical features to their TN fare better, and higher doses (up to 90 Gy) delivered to the REZ appear to provide the best results. Higher treatment doses may strongly correlate with greater chances of pain relief, but come with an increased risk of trigeminal nerve dysfunction.

Target Length

What is the effect of treatment location or target length of the trigeminal nerve on safety and efficacy? Flickinger and colleagues examined this question in 87 patients whose treatment was randomized to one or two isocenters (separated by 3–5 mm), in the retrogasserian nerve segment [46]. A 4 mm diameter collimator was used, with a maximal dose of 75 Gy delivered with 50% isodose volume outside the brainstem [45]. Pain relief was found to be approximately equal between both groups, but the rate of complications was found to correlate with the length of irradiated nerve [45]. Various studies have examined radiation to different areas of the trigeminal nerve in order to identify the optimal target location [46–49]. Massager and colleagues delivered high dose (90 Gy) to the cisternal portion immediately posterior to the Gasserian ganglion (targeting the plexus triangularis) [47]. Regis and colleagues examined a more anterior target as well, in 100 patients treated with 85 Gy delivered to various portions of the retrogasserian cisternal portion [46, 48–49]. Many studies appear to recommend an optimal target of 5 mm to 8 mm from the brainstem, such that the first 1 mm^3 receives a total dose of 13–15 Gy and the first 10 mm^3 receives no more than 10–12 Gy. A shorter distance from the brainstem appears to be a statistically significant predictive factor of favorable pain outcomes [29, 43–49].

Brainstem Volume

In a report by Matsuda and colleagues, a maximal dose of 80 Gy was provided to a single isocenter, planned with the 30–40% isodose line tangential to the brainstem [50]. Of 41 patients studied, 7 patients developed facial hypesthesia and 3 developed dry eyes and diminution of the corneal reflex. Paradoxically in some sense, Brisman and colleagues reported earlier that from 126 patients treated with 75 Gy at the REZ, it was recommended that the volume of brainstem receiving 20% of the total dose be at least 20 mm^3 for optimal pain outcomes [51]. Gorgulho and colleagues examined MRI demonstrations of trigeminal nerve and brainstem changes following radiosurgery in 37 patients in whom treatment doses ranged from 70 Gy to 90 Gy [29]. MRI enhancement or T2 hyperintensity was noticed in 16 cases, mostly pontine; none of these patients suffered from trigeminal sensory dysfunction but those patients with pontine enhancement, with or without enhancement of the adjacent nerve, was correlated with pain relief [29]. In other words, enhancement of the pons but not of the nerve correlated with better outcomes. The mechanism through which this may provide therapeutic benefit remains to be clarified [14, 29].

Primary Trigeminal Neuralgia

The role for radiosurgery in the treatment of primary (or idiopathic) TN is well supported [6, 12, 17, 52–57]. Rates of initial pain relief ranging from 78% to 94% have been reported following radiosurgery, with between 32% and 81% experiencing complete pain relief [52–57]. Regis et al. reported 87% of patients initially pain-free with a treatment dose between 75 Gy and 90 Gy [56]. In a large series of 441 patients, Young and colleagues noted again 87% of patients pain-free after radiosurgery (with or without medication, BNI scores I, IIIa, or IIIb) at a median follow-up of nearly 4.8 years [5]. Brisman and colleagues reported complete pain relief in 22% of patients (BNI score I) and another 56% of patients with at least satisfactory relief that persisted to last follow-up at a median of 30 months [51]. Although these series were all of GKRS, results with LINAC-based SRS

have been identical. In 60 patients treated with central doses of 70–90 Gy in one study, for instance, 87.5% of patients with essential or primary TN experienced at least satisfactory relief that persisted in 58.3% of patients at 2 years of follow-up [42]. Moreover, the mean latency to pain relief does not appear to vary between GKRS- and LINAC-based SRS, ranging on average between 2 months and 4 months post procedurally [42].

Recurrence is a major concern after radiosurgery [3, 5]. From the collective experience of many series, the time to recurrence after the first radiosurgical procedure varies widely, ranging from 3 months to 64 months [6, 12, 17, 39, 58]. The mean time to recurrence appears to average around 18–24 months post procedurally. From Kaplan Meier survival analyses in multiple studies, rates of persistent pain relief at 1 year following radiosurgery average between 60% and 80% and between 50% and 60% at 3 years of follow-up [58]. There is evidence that not having had prior surgical treatment for radiosurgery may be associated with increased rates of achieving and maintaining complete pain relief after the first radiosurgical treatment for TN, although this point must be considered carefully, noting that those patients in whom treatment fails may be genetically or otherwise predisposed to a more resistant form of TN that presents a challenge to any modality of treatment [58]. From both GKRS- and LINAC-based SRS data available to date, the rate of recurrence following initial radiosurgery is between 3.3% and 21% at approximately 2 years following the SRS [31, 59, 60].

Various studies have analyzed factors predictive of positive outcomes following SRS for TN [52–57, 59, 60]. Some that have been identified are the absence of multiple sclerosis, higher radiation dose (up to 90 Gy), no previous surgery, typical pain features, and proximity of the isocenters to the brainstem [60]. In 54 patients, Rogers and colleagues reported that 49% of patients with typical features of TN experienced BNI grade I outcomes following radiosurgery, in comparison with only 9% of those with atypical features [39]. In another series, Brisman and colleagues reported complete pain relief in 41% of patients with typical features, compared with 17% amongst those with atypical features [51]. Similar results have been described by several other authors, as well as between GKRS- and LINAC-based SRS literature [31, 59, 60]. In fact, the presence of atypical pain has been described as the most important negative predictive factor of response to SRS for TN [58–60].

Percutaneous techniques such as RFA, glycerol rhizolysis and balloon compression seem to offer higher rates of early complete pain relief than SRS [1–5]. However, excluding facial sensory loss, approximately one quarter of patients treated with RFA or glycerol rhizolysis experience some transient or permanent complication, compared with an overall less than 10% rate with SRS [1, 2]. When doses of up to 90 Gy are used, permanent sensory loss is seen in approximately 15% of patients treated with SRS [54, 55]. Corneal numbness is reported in approximately 10% of patients, but keratitis has not been documented [6, 12]. Various quality of life studies indicate that the rates of truly cumbersome facial sensory dysfunction (including moderate to severe dysesthesias and anesthesia dolorosa) is exceedingly rare following SRS for TN, occurring only in 1–3% of patients [58–60]. In short, available data suggest that currently SRS is the safest technique for the treatment of TN, with a very high efficacy rate, although not reaching the level of MVD when considering initial and persistent relief 2 years and beyond after treatment [16, 22, 52–57].

Secondary Trigeminal Neuralgia

Compressive Mass Lesions

In a fraction of patients with TN, facial pain is not due to vascular compression of the nerve but rather to compressive mass lesions including tumors, benign or malignant, or aneurysmal dilatations along the trigeminal pathway in the middle or posterior cranial fossa [7, 12, 20, 21, 22, 61]. Radiosurgery is a noninvasive alternative for many such lesions. Outcomes following radiosurgery for TN in such patients have historically not been viewed favorably in comparison with those from surgical procedures, such as tumor resection whether alone or in combination with MVD for secondary TN [20–22, 48, 49, 56]. Regis and colleagues reported in at least one large series that although 84% of patients with secondary TN experienced initial pain improvement (not complete relief), this was transient, and at 2 years of follow-up, only 47% continued to experience partial relief [48, 49]. This contrasted with surgical series of tumor resection in which it was reported that upward of 80% of patients remained pain-free at greater than 2 years postoperatively [21, 22]. As our understanding of radiobiology has increased, evidence has accumulated that radiosurgically targeting the nerve itself rather than the mass may provide better outcomes in patients with intractable tumor-related TN, and with a low complication profile [7].

Tumors tend to cause pain by direct compression of the nerve root, or by vascular compression from displacement by the tumor, which in turn causes abnormal electrical transmission [5, 62]. Surgical resection dissects the tumor off the nerve to provide relief [7, 21, 22]. In contrast, radiation to the lesion only (rather than to the nerve root) can at best only achieve tumor volume reduction; tumor remains around the nerve and pathological electrical propagation unavoidably continues [7]. We recall that radiation to the nerve REZ provides early pain relief as a result of cessation of ephaptic electrical transmission, and a delayed, persistent relief from

demyelination injury, or injury to the nerve microvasculature [11, 12]. Targeting the nerve root, therefore and not the lesion itself, may provide the greatest pain relief in these cases [7].

A recent radiosurgical series evaluated these two treatment paradigms in twelve patients with tumor-related TN from diverse tumor pathologies (including meningioma, squamous cell carcinoma, vestibular schwannoma, and hemangiopericytoma) [7]. Of ten patients who underwent initial radiation targeted toward their tumors, only six (60%) experienced at least partial relief which lasted a mean of only 6 months. In contrast, ten of these twelve (83.3%) patients who underwent radiation of the trigeminal REZ experienced at least satisfactory pain relief, complete in 50% of patients. Pain relief continued for a mean of 41 months post-procedurally (the extent of follow-up in the study) [7]. It deserves mention that among those patients who underwent radiation to both targets, the treatment volumes did not overlap on the trigeminal nerve to any significant extent. While a small sample, the results are encouraging compared to surgical series (Barker and colleagues reported that 81% of patients experienced excellent relief following MVD in patients with tumor-related TN, maintained at 10 years postsurgically) [21, 22]. Longer follow-up and larger study samples are needed, but the available data suggest a role for radiosurgery in patients with tumor-related TN, especially when targeting the nerve or REZ itself.

Tumor-related TN poses a particular challenge [21, 22]. Radiation to the nerve REZ appears to provide pain relief, yet tumor growth can cause recurrence and require further treatment [7]. Even when surgical series are considered, a large number of recurrent cases of tumor-related TN are due to tumor growth or recurrence, rather than to treatment failure. Barker and colleagues reported a recurrence rate of 17% following surgical resection (50% of which were correlated with tumor recurrence) and Regis and colleagues noted a recurrence rate of 13% following radiosurgery (with 7% of patients experiencing pain due to tumor recurrence) [21, 22, 48, 49]. Radiated patients can be retreated with radiation but as has been described before, comes with the risk of brainstem injury with high cumulative doses (greater than approximately 110 Gy) [3, 7]. Moreover, the rate of trigeminal sensory dysfunction increases with increasing doses. Ultimately it appears that the management of trigeminal neuralgia when secondary to tumor-related compression may require a multiply targeted approach – a combination of surgical tumor debulking and radiosurgery to the nerve REZ may provide optimal results. Radiosurgery in these cases may not be failsafe, but it appears to provide a tool in the treating physician's armamentarium that should carefully be considered as a viable option in the well-chosen patient.

Multiple Sclerosis

Approximately 4% of patients with MS develop TN during their lifetime [63]. MS-related TN is thought to occur as a direct consequence of demyelination, a plaque of demyelination encompassing the REZ of the trigeminal nerve in the pons [18, 63]. It tends to present with an earlier age of onset, and with more aggressive pain symptoms than classical TN, and is often bilateral [63, 64]. Various studies have found patients with MS-related TN to be less responsive to pharmacological therapy [65]. Moreover, because the pathophysiology involves demyelination rather than compression, traditional surgical therapies such as MVD or glycerol or radiofrequency rhizotomy have lower rates of response and durability of pain relief for MS related TN than for idiopathic TN [66, 67]. SRS has been reported as a viable treatment option for medically refractory MS-related TN [68]. Although initial results have been promising, it appears that dosimetric- and patient-related variables that predict treatment success and toxicity require further clarification. Because of the putative differences in the pathophysiology between the facial pain of MS-related and idiopathic TN, the targets of radiation effect, as well as the threshold for such effects, may be different [65–69].

Several groups have recently reported the use of SRS (especially GKRS) in the treatment of MS-related TN (Table 1) [8, 69–75]. Huang and coauthors reported that seven patients (100%) experienced >90% pain relief following SRS for MS-related TN that lasted to 28 months of follow-up [70]. Rogers and coauthors reported a series of 15 patients over a mean follow-up of 17 months, and noted 12 patients (80%) experienced >90% pain relief [71]. More recently, Zorro and coauthors evaluated the outcomes for 37 patients with a median follow-up of 57 months and noted complete pain relief in 23 patients (62.1%) immediately after SRS and in 36 (97.3%) at some point in the treatment course [75]. In another radiosurgical series, 43 patients with MS-related TN were evaluated at 1 year after SRS to the cisternal trigeminal nerve immediately posterior to the Gasserian ganglion (7.5 mm to 8 mm anterior to the nerve's entrance into the brainstem), with a median maximum dose of 85 Gy [74]. The initial rate of pain cessation was 90.7%, with a low rate of facial (or corneal) numbness of 16%, never bothersome or disabling. The recurrence rate was nonetheless high at 61.5% [74]. Other series are listed in the table [8, 69–75]. Despite the promising results, the rates of trigeminal sensory dysfunction also appear to be higher in MS patients. Rates of numbness between 5% and 57% have been reported [73–75]. Moreover, unlike idiopathic TN where the development of facial numbness is correlated with treatment success, this has not borne out to be true with MS related TN [69, 70]. It may be that preexisting demyelination in MS patients may predispose to a greater incidence of post

Table 1 Radiosurgery in the treatment of multiple sclerosis-related trigeminal neuralgia

Authors	Patients, *N*	Median/mean age (years)	Delivery system	Maximum dose (Gy)	Target	Results		Median follow up (months)	Recurrence rate
						Pain-free	>90% pain control		
Conti et al. [8]	27	53.3 (36.0–62.0)	LINAC	73	Plexus triangularis	48%	85%	37.0	66%
Alvarez-Pinzon et al. [72]	124	51.0 (N/A)	GKRS	74	N/A	N/A	90%	37.6	14.3%
Weller et al. [73]	35	62.0 (39.0–86.0)	GKRS	90	Retrogasserian	35%	88%	39.0	N/A
Tuleasca et al. [74]	43	57.2 (36.5–82.6)	GKRS	80 Gy (22/43); 90 Gy (31/43)	Plexus triangularis	90.7%	90.7%	53.8	61.5%
Diwanji et al. [69]	13	N/A	GKRS	75	REZ	42%	57%	67.0	N/A
Zorro et al. [75]	37	59.0 (38.0–74.0)	GKRS	80	Plexus triangularis	62.1%	97.3%	56.7	37.8%
Rogers et al. [71]	15	N/A	GKRS	80 (12/15); >80 (3/15)	REZ	N/A	80%	17.0	33.3%
Huang et al. [70]	7	51.0 (40.0–63.0)	GKRS	80 (5/7); 90 (2/7)	REZ	100%	N/A	28.0	14.3%

Gy Gray, *LINAC* linear accelerator, *GKRS* gamma knife radiosurgery, *N/A* not applicable, *REZ* root entry zone
Note: N/A was used to designate unavailable data, either because it was not provided in the original study or could not be inferred

procedural trigeminal sensory alteration and a differential tolerance of neuronal tissue to radiation [72, 74].

Compared with idiopathic TN, high rates of recurrence have also been noted among patients with MS-related TN undergoing SRS. Recurrence rates have ranged between 14.3% and 62%, within follow-up durations that have ranged from 28 months to 54 months [70–75]. One difficulty in interpreting these data is that in the various series from which the data are pooled, treatment targets were not identical. Although in some series the REZ was targeted, varying lengths of the trigeminal nerve measured from the Gasserian ganglion were targeted in others. Despite the relative paucity of literature to date, a recent multivariate analysis of all data available regarding SRS for MS-related TN suggests that dosimetric factors with the highest odds ratios for favorable outcomes are the dose delivered to the pons (negative predictive factor) and the dose delivered to the REZ (positive predictive factor) [69–75]. While the literature supports a role of SRS for MS related TN, further studies are required to elucidate optimal treatment parameters.

Recurrent Trigeminal Neuralgia

As with all surgical procedures for TN, SRS is associated with a risk of recurrence. From several large series, recurrence rates of approximately 50% have been noted at a median of 30 months following initial radiosurgical treatment for TN [6, 12, 15]. Patients who experienced favorable results following initial SRS have frequently been considered good candidates for repeat radiosurgery, and more than 60% of patients undergoing repeat SRS appear to experience significant (>50%) pain relief [17, 76–84]. Nonetheless, even among such patients, 25–30% experience severe recurrent trigeminal neuropathic pain at a median of 17 months following SRS [77–79]. It has been hypothesized that even amongst this group of patients, there may exist a subset of patients who may benefit from a third radiosurgical procedure, predicted by their prior favorable response to SRS [3].

Data on multiply repeated SRS for TN are scant. In a large series of 119 patients who underwent a single repeat radiosurgical procedure for TN, Park and coauthors reported that 87% of patients achieved pain relief in the immediate few weeks post procedurally, of whom 88% maintained relief at 1 year and 70% of whom maintained relief at 3 years of follow-up [59]. In other analyses, between 70% and 85% of patients who underwent repeat SRS for TN remained pain-free at a median of 15–19 months following repeat SRS, whether by LINAC or GKRS [24, 85, 86]. Less is known in comparison regarding multiply repeated SRS for TN. In one series by Tempel and coauthors, 17 patients who underwent three total radiosurgical procedures for recurrent TN were studied [3]. Following initial repeat radiosurgery, severe pain requiring repeat SRS occurred at a median of 35 months. Sixteen of 17 (94%) remained pain-free at a mean 23 months following the second repeat (or third, overall) SRS for recurrent TN [3].

The greatest potential risk of repeat radiosurgery is cumulative trigeminal sensory dysfunction. After primary SRS for TN, some degree of trigeminal dysfunction occurs in between 6% and 54% of patients [6, 30, 41, 55, 59, 76, 84]. In 11%–74% of these patients, there is worsening of preexisting trigeminal sensory disturbance or new onset dysfunction following repeat radiosurgery [87]. In the series described above of triple SRS for TN, 18% of patients developed trigeminal sensory dysfunction after primary SRS, and another

12% after the second SRS (but none after the third SRS procedure) [3]. Better pain control is often correlated with trigeminal sensory dysfunction, and most patients report that the sensory dysfunction in these situations is not bothersome [23–27]. It has been reported that the maximum cumulative lateral pontine edge dose predicts the development of facial sensory dysfunction, and 44 Gy of cumulative brainstem dose has been cited as the threshold in one study, while in another, 115 Gy of cumulative maximum target dose increased the chance that patients develop new sensory symptoms [30, 59, 77, 85]. In the Tempel and coauthors series, the lack of sensory dysfunction following the third radiosurgery procedure may stem from the target selection [3]. For each subsequent procedure, the target was moved anteriorly (toward the Gasserian ganglion), limiting the cumulative dose received by the brainstem [3].

Despite the apparent efficacy of three-time SRS for recurrent TN, one may conjecture that such patients are at risk for relapse [3, 80–85]. In the Tempel and coauthors series, four patients (23.5%) relapsed (BNI score of at least IV) at a mean of 19 months following the last (third) SRS procedure [3]. The question arises then as to whether radiosurgery continues to remain a viable treatment option for such patients. Only limited evidence is available thus far but multiply repeat SRS appears safe and at least moderately efficacious in providing freedom from pain for a mean of approximately 2 years in a select subset of patients, especially those who are poor candidates for alternative therapies because they (1) are of advanced age and/or have several general medical comorbidities, (2) are on a regimen of anticoagulation medication, (3) have undergone prior surgical procedures that have failed, or (4) continue to experience intractable pain despite maximal and varied medical therapy [3, 84–87]. Even following extended follow-up periods, it does not appear associated with increased instances of trigeminal sensory dysfunction when treatment target, dose, and volume are carefully chosen.

Conclusion

In the years since Leksell performed the first radiosurgical procedure for TN, tremendous strides have been made in improving its safety, efficacy, and applicability. A growing body of literature has developed, comparing various treatment targets, dosimetric variables, and patient factors, and has enabled the treatment of various forms of trigeminal neuralgia with often very encouraging and favorable results. MVD continues to remain the reference standard for the treatment of medically refractory TN, but accruing evidence suggests that radiosurgery may efficaciously achieve identical long-term results, often with significantly lesser morbidity. As our understanding of radiobiology and the pathophysiology of pain continues to grow, we may expect further refinement in the radiosurgical technique and optimization of its application.

References

1. Elias W, Burchiel K. Trigeminal neuralgia and other neuropathic pain syndromes of the head and face. Curr Pain Headache Rep. 2002;6(2):115–24.
2. Eller J, Raslan A, Burchiel K. Trigeminal neuralgia: definition and classification. Neurosurg Focus. 2005;18(5):1–3.
3. Tempel Z, Chivukula S, Monaco E, Bowden G, Kano H, Niranjan A, et al. The results of a third Gamma Knife procedure for recurrent trigeminal neuralgia. J Neurosurg. 2015;122(1):169–79.
4. Wang D, Ouyang D, Englot D, Rolston J, Molinaro A, Ward M, et al. Trends in surgical treatment for trigeminal neuralgia in the United States of America from 1988 to 2008. J Clin Neurosci. 2013;20(11):1538–45.
5. Young B, Shivazad A, Kryscio R, St. Clair W, Bush H. Long-term outcome of high-dose Gamma Knife surgery in treatment of trigeminal neuralgia. J Neurosurg. 2013;119(5):1166–75.
6. Dhople A, Adams J, Maggio W, Naqvi S, Regine W, Kwok Y. Long-term outcomes of Gamma Knife radiosurgery for classic trigeminal neuralgia: implications of treatment and critical review of the literature. J Neurosurg. 2009;111(2):351–8.
7. Chivukula S, Kim W, Zhuo X, Tenn S, Kaprealian T, DeSalles A, et al. Radiosurgery for secondary trigeminal neuralgia: revisiting the treatment paradigm. World Neurosurg. 2017;99:288–94.
8. Conti A, Pontoriero A, Iatì G, Esposito F, Siniscalchi E, Crimi S, et al. Frameless stereotactic radiosurgery for treatment of multiple sclerosis–related trigeminal neuralgia. World Neurosurg. 2017;103:702–12.
9. Cruccu G, Finnerup N, Jensen T, Scholz J, Sindou M, Svensson P, et al. Trigeminal neuralgia. Neurology. 2016;87(2):220–8.
10. Hong W, Zheng X, Wu Z, Li X, Wang X, Li Y, et al. Clinical features and surgical treatment of trigeminal neuralgia caused solely by venous compression. Acta Neurochir. 2011;153(5):1037–42.
11. Love S, Hilton D, Coakham H. Central demyelination of the Vth nerve root in trigeminal neuralgia associated with vascular compression. Brain Pathol. 2006;8(1):1–11.
12. Chang C, Huang C, Chou H, Lin L, Huang C. Outcome of Gamma Knife radiosurgery for trigeminal neuralgia associated with neurovascular compression. J Clin Neurosci. 2018;47:174–7.
13. Cheng T, Cascino T, Onofrio B. Comprehensive study of diagnosis and treatment of trigeminal neuralgia secondary to tumors. Neurology. 1993;43(11):2298.
14. Hughes M, Frederickson A, Branstetter B, Zhu X, Sekula R. MRI of the trigeminal nerve in patients with trigeminal neuralgia secondary to vascular compression. AJR Am J Roentgenol. 2016;206(3):595–600.
15. Zacest A, Magill S, Miller J, Burchiel K. Preoperative magnetic resonance imaging in Type 2 trigeminal neuralgia. J Neurosurg. 2010;113(3):511–5.
16. Cohen-Gadol A. Microvascular decompression surgery for trigeminal neuralgia and hemifacial spasm: nuances of the technique based on experiences with 100 patients and review of the literature. Clin Neurol Neurosurg. 2011;113(10):844–53.
17. Huang CF, Tu HT, Liu WS, Chiou SY, Lin LY. Gamma Knife surgery used as primary and repeated treatment for idiopathic trigeminal neuralgia. J Neurosurg. 2008;109. Suppl:179–84.
18. Broggi G, Ferroli P, Franzini A, Nazzi V, Farina L, La Mantia L, et al. Operative findings and outcomes of microvascular decom-

pression for trigeminal neuralgia in 35 patients affected by multiple sclerosis. Neurosurgery. 2004;55(4):830–8.
19. Meaney J, Watt J, Eldridge P, Whitehouse G, Wells J, Miles J. Association between trigeminal neuralgia and multiple sclerosis: role of magnetic resonance imaging. J Neurol Neurosurg Psychiatry. 1995;59(3):253–9.
20. Bullitt E, Tew J, Boyd J. Intracranial tumors in patients with facial pain. J Neurosurg. 1986;64(6):865–71.
21. Barker F, Jannetta P, Babu R, Pomonis S, Bissonette D, Jho H. Long-term outcome after operation for trigeminal neuralgia in patients with posterior fossa tumors. J Neurosurg. 1996;84(5):818–25.
22. Barker F, Jannetta P, Bissonette D, Larkins M, Jho H. The long-term outcome of microvascular decompression for trigeminal neuralgia. N Engl J Med. 1996;334(17):1077–84.
23. Sheehan J, Pan H, Stroila M, Steiner L. Gamma knife surgery for trigeminal neuralgia: outcomes and prognostic factors. J Neurosurg. 2005;102(3):434–41.
24. Kondziolka D, Perez B, Flickinger J, Habeck M, Lunsford L. Gamma Knife radiosurgery for trigeminal neuralgia. Arch Neurol. 1998;55(12):1524.
25. Leksell L. Sterotaxic radiosurgery in trigeminal neuralgia. Acta Chir Scand. 1971;137(4):311–4.
26. Kondziolka D, Lunsford LD, Flickinger JC, Young RF, Vermeulen S, Duma CM, et al. Stereotactic radiosurgery for trigeminal neuralgia: a multiinstitutional study using the gamma unit. J Neurosurg. 1996;84:940–5.
27. Kondziolka D, Lacomis D, Niranjan A, Mori Y, Maesawa S, Fellows W, et al. Histological effects of trigeminal nerve radiosurgery in a primate model: implications for trigeminal neuralgia radiosurgery. Neurosurgery. 2000;46(4):971–7.
28. Al-Quliti KW. Update on neuropathic pain treatment for trigeminal neuralgia. The pharmacological and surgical options. Neurosciences (Riyadh). 2015;20(2):107–14.
29. Gorgulho A. Radiation mechanisms of pain control in classical trigeminal neuralgia. Surg Neurol Int. 2012;3(2):17.
30. Park H, Wang E, Rutter C, Corso C, Chiang V, Yu J. Changing practice patterns of Gamma Knife versus linear accelerator-based stereotactic radiosurgery for brain metastases in the US. J Neurosurg. 2016;124(4):1018–24.
31. Varela-lema L, Lopez-garcia M, Maceira-rozas M, Munoz-garzon V. Linear accelerator stereotactic radiosurgery for trigeminal neuralgia. Pain Physician. 2015;18(1):15–27.
32. Pokhrel D, Sood S, McClinton C, Saleh H, Badkul R, Jiang H, et al. Linac-based stereotactic radiosurgery (SRS) in the treatment of refractory trigeminal neuralgia: detailed description of SRS procedure and reported clinical outcomes. J Appl Clin Med Phys. 2017;18(2):136–43.
33. Chen JC, Rahimian J, Rahimian R, Arellano A, Miller MJ, Girvigian MR. Frameless image-guided radiosurgery for initial treatment of typical trigeminal neuralgia. World Neurosurg. 2010;74(4–5):538–43.
34. Maciunas RJ, Galloway RL Jr, Latimer JW. The application accuracy of stereotactic frames. Neurosurgery. 1994;35:682–294.
35. Rahimian J, Chen JC, Rao AA, Girvigian MR, Miller MJ, Greathouse HE. Geometrical accuracy of the Novalis stereotactic radiosurgery system for trigeminal neuralgia. J Neurosurg. 2004;101:351–5.
36. Hayashi N1, Obata Y, Uchiyama Y, Mori Y, Hashizume C, Kobayashi T. Assessment of spatial uncertainties in the radiotherapy process with the Novalis system. Int J Radiat Oncol Biol Phys. 2009;75(2):549–57.
37. Yu C, Jozsef G, Apuzzo ML, Petrovich Z. Measurements of the relative output factors for CyberKnife collimators. Neurosurgery. 2004;54:157–61.
38. Fariselli L, Marras C, De Santis M, Marchetti M, Milanesi I, Broggi G. CyberKnife radiosurgery as a first treatment for idiopathic trigeminal neuralgia. Neurosurgery. 2009;64:A96–101.
39. Rogers C, Shetter A, Fiedler J, Smith K, Han P, Speiser B. Gamma knife radiosurgery for trigeminal neuralgia: the initial experience of the Barrow Neurological Institute. Int J Radiat Oncol Biol Phys. 2000;47(4):1013–9.
40. Lindquist C, Kihlstrom L, Hellstrand E. Functional neurosurgery – a future for the gamma knife? Stereotact Funct Neurosurg. 1991;57(1–2):72–81.
41. Pollock B. High-dose trigeminal neuralgia radiosurgery associated with increased risk of trigeminal nerve dysfunction. Neurosurgery. 2002;50(6):1402–3.
42. Goss B, Frighetto L, DeSalles A, Smith Z, Solberg T, Selch M. Linear accelerator radiosurgery using 90 gray for essential trigeminal neuralgia: results and dose volume histogram analysis. Neurosurgery. 2003;53(4):823–30.
43. Smith Z, De Salles A, Frighetto L, Goss B, Lee S, Selch M, et al. Dedicated linear accelerator radiosurgery for the treatment of trigeminal neuralgia. J Neurosurg. 2003;99(3):511–6.
44. Smith Z, Gorgulho A, Bezrukiy N, McArthur D, Agazaryan N, Selch M, et al. Dedicated linear accelerator radiosurgery for trigeminal neuralgia: a single-center experience in 179 patients with varied dose prescriptions and treatment plans. Int J Radiat Oncol Biol Phys. 2011;81(1):225–31.
45. Flickinger J, Pollock B, Kondziolka D, Phuong L, Foote R, Stafford S, et al. Does increased nerve length within the treatment volume improve trigeminal neuralgia radiosurgery? A prospective double-blind, randomized study. Int J Radiat Oncol Biol Phys. 2001;51(2):449–54.
46. Régis J. High-dose trigeminal neuralgia radiosurgery associated with increased risk of trigeminal nerve dysfunction. Neurosurgery. 2002;50(6):1401–2.
47. Massager N, Lorenzoni J, Devriendt D, Desmedt F, Brotchi J, Levivier M. Gamma knife surgery for idiopathic trigeminal neuralgia performed using a far-anterior cisternal target and a high dose of radiation. J Neurosurg. 2004;100(4):597–605.
48. Régis J, Tuleasca C, Resseguier N, Carron R, Donnet A, Gaudart J, et al. Long-term safety and efficacy of Gamma Knife surgery in classical trigeminal neuralgia: a 497-patient historical cohort study. J Neurosurg. 2016;124(4):1079–87.
49. Régis J, Tuleasca C, Resseguier N, Carron R, Donnet A, Yomo S, et al. The very long-term outcome of radiosurgery for classical trigeminal neuralgia. Stereotact Funct Neurosurg. 2016;94(1):24–32.
50. Matsuda S, Nagano O, Serizawa T, Higuchi Y, Ono J. Trigeminal nerve dysfunction after Gamma Knife surgery for trigeminal neuralgia: a detailed analysis. J Neurosurg. 2010;113.(Suppl:184–90.
51. Brisman R. Gamma knife surgery with a dose of 75 to 76.8 Gray for trigeminal neuralgia. J Neurosurg. 2004;100(5):848–54.
52. Drzymala R, Malyapa R, Dowling J, Rich K, Simpson J, Mansur D. Gamma Knife radiosurgery for trigeminal neuralgia: The Washington University initial experience. Stereotact Funct Neurosurg. 2005;83(4):148–52.
53. Fountas K, Lee G, Smith J. Outcome of patients undergoing Gamma Knife stereotactic radiosurgery for medically refractory idiopathic trigeminal neuralgia: Medical College of Georgia's experience. Stereotact Funct Neurosurg. 2006;84(2–3):88–96.
54. Maesawa S, Salame C, Flickinger J, Pirris S, Kondziolka D, Lunsford L. Clinical outcomes after stereotactic radiosurgery for idiopathic trigeminal neuralgia. J Neurosurg. 2001;94(1):14–20.
55. Pollock B, Phuong L, Gorman D, Foote R, Stafford S. Stereotactic radiosurgery for idiopathic trigeminal neuralgia. J Neurosurg. 2002;97(2):347–53.
56. Régis J, Metellus P, Hayashi M, Roussel P, Donnet A, Bille-Turc F. Prospective controlled trial of Gamma Knife surgery for essential trigeminal neuralgia. J Neurosurg. 2006;104(6):913–24.
57. Riesenburger R, Hwang S, Schirmer C, Zerris V, Wu J, Mahn K, et al. Outcomes following single-treatment Gamma Knife sur-

gery for trigeminal neuralgia with a minimum 3-year follow-up. J Neurosurg. 2010;112(4):766–71.
58. Shetter AG, Rogers CL, Ponce F, Fiedler JA, Smith K, Speiser BL. Gamma knife radiosurgery for recurrent trigeminal neuralgia. J Neurosurg. 2002;97(5 Suppl):536–8.
59. Park K, Kondziolka D, Berkowitz O, Kano H, Novotny J, Niranjan A, et al. Repeat Gamma Knife radiosurgery for trigeminal neuralgia. Neurosurgery. 2012;70(2):295–305.
60. Kano H, Kondziolka D, Yang H, Zorro O, Lobato-Polo J, Flannery T, et al. Outcome predictors after Gamma Knife radiosurgery for recurrent trigeminal neuralgia. Neurosurgery. 2010;67(6):1637–45.
61. Marco JKD, Hesselink JR. Trigeminal neuropathy. Neurosurg Clin North Am. 1997;8:103–30.
62. Urgošik D, Vymazal J, Vladyka V, Liščák R. Gamma Knife treatment of trigeminal neuralgia: clinical and electrophysiological study. Stereotact Funct Neurosurg. 1998;70(1):200–9.
63. Fallata A, Salter A, Tyry T, Cutter G, Marrie R. Trigeminal neuralgia commonly precedes the diagnosis of multiple sclerosis. Int J MS Care. 2017;19(5):240–6.
64. Kondziolka D, Lunsford LD, Bissonette DJ. Long-term results after glycerol rhizotomy for multiple sclerosis-related trigeminal neuralgia. Can J Neurol Sci. 1994;21(2):137–40.
65. Kanpolat Y, Berk C, Savas A, Bekar A. Percutaneous controlled radiofrequency rhizotomy in the management of patients with trigeminal neuralgia due to multiple sclerosis. Acta Neurochir. 2000;142(6):685–9.
66. Mohammad-mohammadi A, Recinos PF, Lee JH, Elson P, Barnett GH. Surgical outcomes of trigeminal neuralgia in patients with multiple sclerosis. Neurosurgery. 2013;73(6):941–50.
67. Montano N, Papacci F, Cioni B, Di bonaventura R, Meglio M. What is the best treatment of drug-resistant trigeminal neuralgia in patients affected by multiple sclerosis? A literature analysis of surgical procedures. Clin Neurol Neurosurg. 2013;115(5): 567–72.
68. Pickett GE, Bisnaire D, Ferguson GG. Percutaneous retrogasserian glycerol rhizotomy in the treatment of tic douloureux associated with multiple sclerosis. Neurosurgery. 2005;56(3):537–45.
69. Diwanji TP, Dhople AA, Chin LS, Maggio WW, Adams JR, Regine WF, et al. Long-term outcome of Gamma Knife stereotactic radiosurgery for multiple sclerosis associated trigeminal neuralgia. Int J Radiat Oncol Biol Phys. 2010;78:S264–5.
70. Huang E, The BS, Zeck O, Woo SY, Lu HH, Chiu JK, Butler EB, et al. Gamma knife radiosurgery for treatment of trigeminal neuralgia in multiple sclerosis patients. Stereotact Funct Neurosurg. 2002;79(1):44–50.
71. Rogers CL, Shetter AG, Ponce FA, Fiedler JA, Smith KA, Speiser BL. Gamma knife radiosurgery for trigeminal neuralgia associated with multiple sclerosis. J Neurosurg. 2002;97(5 Suppl): 529–32.
72. Alvarez-Pinzon A, Wolf A, Swedberg H, Barkley K, Cucalon J, Curia L, et al. Comparison of percutaneous retrogasserian balloon compression and Gamma Knife radiosurgery for the treatment of trigeminal neuralgia in multiple sclerosis. World Neurosurg. 2017;97:590–4.
73. Weller M, Marshall K, Lovato J, Bourland J, deGuzman A, Munley M, et al. Single-institution retrospective series of Gamma Knife radiosurgery in the treatment of multiple sclerosis-related trigeminal neuralgia: factors that predict efficacy. Stereotact Funct Neurosurg. 2014;92(1):53–8.
74. Tuleasca C, Carron R, Resseguier N, Donnet A, Roussel P, Gaudart J, et al. Multiple sclerosis-related trigeminal neuralgia: a prospective series of 43 patients treated with Gamma Knife surgery with more than one year of follow-up. Stereotact Funct Neurosurg. 2014;92(4):203–10.
75. Zorro O, Lobato-Polo J, Kano H, Flickinger J, Lunsford L, Kondziolka D. Gamma knife radiosurgery for multiple sclerosis-related trigeminal neuralgia. Neurology. 2009;73(14):1149–54.
76. Han JH, Kim DG, Chung HT, Paek SH, Kim YH, Kim CY, et al. Long-term outcome of gamma knife radiosurgery for treatment of typical trigeminal neuralgia. Int J Radiat Oncol Biol Phys. 2009;75(3):822–7.
77. Aubuchon AC, Chan MD, Lovato JF, Balamucki CJ, Ellis TL, Tatter SB, et al. Repeat gamma knife radiosurgery for trigeminal neuralgia. Int J Radiat Oncol Biol Phys. 2011;81:1059–65.
78. Dvorak T, Finn A, Price LL, Mignano JE, Fitzek MM, Wu JK, et al. Retreatment of trigeminal neuralgia with Gamma Knife radiosurgery: is there an appropriate cumulative dose? Clinical article. J Neurosurg. 2009;111:359–64.
79. Herman JM, Petit JH, Amin P, Kwok Y, Dutta PR, Chin LS. Repeat gamma knife radiosurgery for refractory or recurrent trigeminal neuralgia: treatment outcomes and quality-of-life assessment. Int J Radiat Oncol Biol Phys. 2004;59:112–6.
80. Huang CF, Chuang JC, Tu HT, Lin LY. Repeated gamma knife surgery for refractory trigeminal neuralgia. J Neurosurg. 2006;105:99–102.
81. Gellner V, Kurschel S, Kreil W, Holl EM, Ofner-Kopeinig P, Unger F. Recurrent trigeminal neuralgia: long term outcome of repeat Gamma Knife radiosurgery. J Neurol Neurosurg Psychiatry. 2001;79:58–62.
82. Hasegawa T, Kondziolka D, Spiro R, Flickinger JC, Lunsford LD. Repeat radiosurgery for refractory trigeminal neuralgia. Neurosurgery. 2002;50:494–500.
83. Kimball BY, Sorenson JM, Cunningham D. Repeat gamma knife surgery for trigeminal neuralgia: long-term results. Clinical article. J Neurosurg. 2010;113:178–83.
84. Pollock BE, Foote RL, Link MJ, Stafford SL, Brown PD, Schomberg PJ. Repeat radiosurgery for recurrent trigeminal neuralgia. Int J Radiat Oncol Biol Phys. 2005;61:192–5.
85. Villavicencio AT, Lim M, Burneikiene S, Romanelli P, Adler JR, McNeely L, et al. CyberKnife radiosurgery for trigeminal neuralgia treatment: a preliminary multicenter experience. Neurosurgery. 2008;62:647–55.
86. Lim M, Villavicencio AT, Burneikiene S, Chang SD, Romanelli P, McNeely L, et al. CyberKnife radiosurgery for idiopathic trigeminal neuralgia. Neurosurg Focus. 2005;18:E9.
87. Verheul JB, Hanssens PEJ, Lie ST, Leenstra S, Piersma H, Beute GN. Gamma Knife surgery for trigeminal neuralgia: a review of 450 consecutive cases. J Neurosurg. 2010;113. Suppl:160–7.

Radiosurgery for Vestibular Schwannomas

Fabio Frisoli, Jugal Shah, Travis C. Hill, and Douglas Kondziolka

Introduction

Vestibular schwannomas (more commonly referred to as acoustic neuromas) are tumors arising from the Schwann cells of the eighth cranial nerve. These tumors are commonly slow-growing, but growth can be variable [1]. They are most commonly unilateral, but in patients who have bilateral vestibular schwannomas, the association is with neurofibromatosis 2 (NF2) [2]. The incidence may be approximately 1–1.5/100,000 people [3, 4].

Patients usually present with symptoms that can include hearing loss, tinnitus, disequilibrium, or other symptoms typically found with larger volume tumors. In one large study, 94% of patients presented with sensorineural high-frequency hearing loss [5].

Management options include definitive therapies such as microsurgical resection or stereotactic radiosurgery, or expectant approaches such as observation with serial imaging and audiometry. Typically, radiosurgery is considered for smaller volume tumors without disabling symptoms from brain compression.

Stereotactic Radiosurgery

Vestibular schwannoma stereotactic radiosurgery using the Gamma Knife® (Elekta, Stockholm, Sweden) was first performed by Leksell in 1969 [6]. It is now used with the confidence of many long-term outcomes studies. During the past decades, radiosurgery is preferred by many patients and physicians, as an alternative to a more invasive surgical tumor resection. Advanced multi-isocenter dose planning software, high-resolution MRI for targeting, dose optimization, and robotic delivery reflect the evolution of this technology. Other image-guided linear accelerator devices (Trilogy® [Varian, Palo Alto, CA, USA], Synergy S® [Elekta, Stockholm, Sweden], Novalis® [BrainLab, Munich, Germany], X-Knife® [Integra, Palinsboro, NJ, USA], TomoTherapy® [Accuray, Sunnyvale, CA, USA], and CyberKnife® [Accuray, Sunnyvale, CA, USA]) can be used to fractionate radiation delivery in 5–30 sessions. Proton beam technology is also used to deliver fractionated radiation therapy. These latter technologies have far fewer outcome reports published. The goals of vestibular schwannoma radiosurgery are to prevent further tumor growth, preserve neurologic function where possible, and avoid the risks associated with resection.

Stereotactic Radiosurgery Technique

Diagnosis, treatment, and outcomes utilize MRI (CT may be substituted in patients who cannot undergo MRI scans) and audiological tests that include pure tone average (PTA) and speech discrimination score (SDS) measurements. Hearing is graded using the Gardner-Robertson (GR) modification of the Silverstein and Norell classification and/or the American Academy of Otolaryngology-Head and Neck Surgery guidelines, and facial nerve function is assessed according to the House-Brackmann grading system. "Serviceable" hearing (Class I and II) is defined as a PTA or speech reception threshold lower than 50 dB and speech discrimination score

F. Frisoli
New York University Langone Medical Center, New York University, Department of Neurosurgery, New York, NY, USA

J. Shah
New York University Langone Health, Department of Neurosurgery, New York, NY, USA

T. C. Hill
New York University Medical Center, Department of Neurosurgery, New York, NY, USA

D. Kondziolka (✉)
New York University Langone Health, New York, NY, USA
e-mail: Douglas.kondziolka@nyumc.org

D. M. Trifiletti et al. (eds.), *Stereotactic Radiosurgery and Stereotactic Body Radiation Therapy*,
https://doi.org/10.1007/978-3-030-16924-4_15

better than 50%. "Serviceable" hearing (Class A and B) is similar to Class I and II of Gardner-Robertson hearing classes. Patients should be counseled about the options of microsurgical and radiosurgical management strategies, as well as the natural history.

Radiosurgery can be performed using the Gamma Knife®, modified linear accelerator-based systems, or a proton beam unit. Head fixation, device, hardware, and software differ significantly with these devices. In Gamma Knife® radiosurgery (GKRS), an MRI-compatible Leksell stereotactic frame (model G, Elekta, Stockholm, Sweden) is first attached to the patient's head. High-resolution images are acquired with a fiducial system attached to the stereotactic frame. For vestibular schwannoma radiosurgery, a 3-D volume acquisition MRI using a gradient pulse sequence (divided into 1 mm slice intervals) is performed in order to cover the entire lesion and surrounding critical structures. A T2-weighted 3-D volume sequence (CISS or Fiesta) is performed to better identify cranial nerves and delineate inner ear structures. Centers using LINAC or proton beam systems may use mask immobilization of the patient's head along with image guidance and typically deliver the radiation dose in five or more fractions. The Gamma Knife "ICON" unit can also allow mask-based fixation and hypofractionation, though we do not advocate this over frame fixation in our patients. CT can be used for planning if an MRI cannot be obtained or co-registered accurately with MRI.

Dose Planning

The concept of the "optimal" dose plan is one that meets the goals of the patient and their physicians. Proper coverage of the tumor with conformal and selective irradiation is the goal [7]. Regional structures to consider include the cochlea, brainstem, and other cranial nerves. Gamma Knife® radiosurgery techniques include accurate definition of the tumor volume, use of multiple small beam isocenters, isocenter weighting, and selective beam blocking to achieve conformality. A high percentage of the tumor should receive the desired minimum dose. A series of 4 mm isocenters are used to create a tapered isodose plan to conform to the intracanalicular portion of the tumor. Although most clinicians aim to restrict the cochlear dose, the long-term value of this for hearing preservation remains to be determined with further research. It may be that the quality of hearing pre-radiosurgery and the length of time the tumor has been present (often unknown) are crucial factors for the eventual outcome.

In Gamma Knife® radiosurgery, a dose of 12–13 Gy is typically prescribed to the 50% (or other) isodose line that conforms to the tumor margin. The most common dose is 12.5 Gy, used for hearing preservation in smaller tumors. Larger tumors may receive 12 Gy and in those with hearing loss or prior resection 13 Gy (Fig. 1a, b). Some centers report the use of even lower margin doses such as 11 or 11.5 Gy. We can be confident in outcomes associated with the 12–13 Gy range, which has been used for several decades, is associated with a low complication rate and yet maintains a high rate of tumor control [8]. Similar doses are also used for patients with bilateral (NF2 related) vestibular schwannomas.

After considering the tumor margin dose, the mean dose to the cochlea, trigeminal nerve, and brainstem is assessed depending on the patient condition and tumor volume. A mean cochlear dose less than 4.2 Gy may be important for hearing preservation. This finding is supported by the work from several centers, however cannot be the only factor important in hearing preservation. Other factors must include age, tumor volume, hearing status, possible nerve ischemia from atherosclerosis or other causes, prior treatments, and tumor growth rate. Some of these are impossible to measure of course. While many clinicians performing radiosurgery have evolved toward similar dose selection parameters, the doses and regimens chosen for fractionated radiotherapy continue to vary.

After radiosurgery, all patients are followed using serial MRI scans, which are generally requested at 6, 12, and 24 months and then less frequently thereafter as guided by the response. All patients who have detectable hearing are requested to obtain audiological tests (PTA and SDS) as well for follow-up.

Gamma Knife® Radiosurgery: Clinical Results

Long-term results of Gamma Knife® radiosurgery for vestibular schwannomas have been documented [8–15]. Recent reports suggest a tumor control rate of 93–100% after radiosurgery [7–12, 14–30]. In an early report, Kondziolka and colleagues studied 5- to 10-year outcomes in 162 vestibular schwannoma patients who had radiosurgery at the University of Pittsburgh [25]. In this study, a long-term 98% tumor control rate was reported. Some tumors initially enlarged 1–2 mm during the first 6–12 months after radiosurgery as they lost their central contrast enhancement [13, 18, 19]. Such tumors generally regressed in volume compared to their pre-radiosurgery size. Only 2% of patients required tumor resection after radiosurgery. Noren, in his 28-year experience with vestibular schwannoma radiosurgery, reported a 95% long-term tumor control rate [29]. Litvack and colleagues reported a 98% tumor control rate at a mean follow-up of 31 months after radiosurgery using a 12 Gy margin dose [31]. Niranjan and colleagues reported on intracanalicular tumor radiosurgery [32]. All patients (100%) had imaging-documented tumor growth control. Lunsford and colleagues reviewed their 15-year experience for radiosurgery

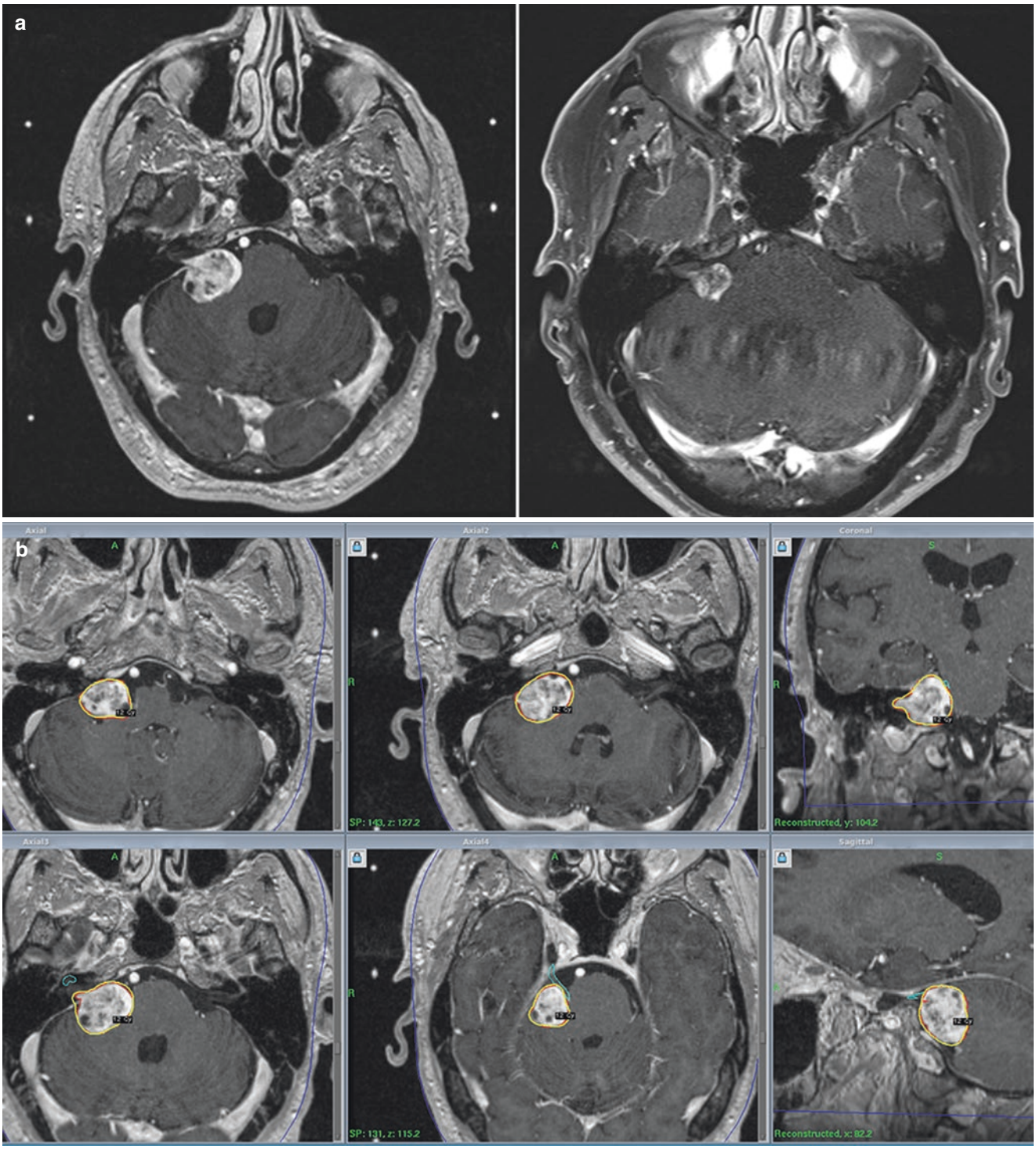

Fig. 1 Axial MRI images (**a**) in a 67-year-old man with a right vestibular schwannoma before (right) and 2 years after (left) 12 Gy Gamma Knife® radiosurgery. He presented with tinnitus and some mild dysequilibrium but still had good balance function. The radiosurgery dose plan (**b**) is shown for this 7.2 cc tumor

of 829 vestibular schwannomas and reported a 97% tumor control rate at 10 years [14]. No patient developed a radiation-associated malignant or benign tumor (defined as a histologically confirmed and distinct neoplasm arising in the initial radiation field after at least 2 years have passed). In another series that focused on younger patients (under 40 years), with minimum 4-year follow-up, all remained employed and active [33].

One controversy goes to the issue of tumor size. What is the upper limit of suitability for radiosurgery? Is this based on a maximum tumor measurement or on the clinical condition of the patient? We suggest that the latter is the most important, at least for tumors under 4 cm in maximum diameter if they do not have disabling symptoms from mass effect. Such cases must be studied individually. Yang and colleagues retrospectively reviewed 65 patients with tumors between 3 and 4 cm in one extracanalicular maximum diameter treated with Gamma Knife® surgery [34]. At 6 months follow-up, 8% of tumors expanded, 82% were stable, and 11% were smaller. Two years later, 25% of tumors had >50% volume reduction, 35% had 10–50% volume reduction, 29% were stable, and 11% had volume increase. Of 22 patients, 18 (82%) continued to have serviceable hearing after SRS more than 2 years later, and 5% of patients required VPS for hydrocephalus. Another study by Huang and colleagues found that ≥15 cm^3 was a significant factor predictive of GKRS failure in a cohort of 35 patients but concluded that satisfactory management of tumors with a single dimension >3 cm and a volume >10 cm^3 can be achieved with GKRS [35].

Hearing Preservation

Hearing preservation is desired by many patients with vestibular schwannomas, particularly those with high-level hearing at diagnosis. Pre-radiosurgery hearing can now be preserved in 60–90% of patients, with higher preservation rates found for smaller tumors [32]. In a long-term (5–10-year follow-up) study conducted at the University of Pittsburgh, 51% of patients had no change in hearing ability [17, 25]. In a prior report at median of 6 years, the same Gardner-Robertson level was preserved in 71%, serviceable hearing in 74%, and any testable hearing in 95%. For intracanalicular tumors, these rates were 84%, 92%, and 100%.

A report by Lin and coauthors reviewed 100 patients managed over 10 years with a 12–13 Gy margin dose [36]. Useful hearing preservation was noted at 1, 3, and 5 years follow-up to be 89%, 68%, and 63%, respectively, with a mean cochlear dose lower than 4 Gy as a favorable predictor of hearing outcome [36, 37].

Facial Nerve and Trigeminal Nerve Preservation

Facial nerve function is now preserved in the majority of patients. We quote a <1% chance of facial weakness (even mild) in tumors without prior resection. Trigeminal nerve dysfunction is seen in <5% of larger tumors and not in intracanalicular tumors. In a study using MR-based dose planning, a 13 Gy tumor margin dose was associated with 0% risk of new facial weakness and 3.1% risk of facial numbness (5-year actuarial rates). In earlier reports, a margin dose of >14 Gy was associated with a 2.5% risk of new-onset facial weakness and a 4% risk of facial numbness (5-year actuarial rates) [10]. Occasionally, patients will describe some periocular facial twitching without weakness that can be a sign of facial nerve irritation. It typically resolves over time.

Neurofibromatosis 2

Patients with vestibular schwannomas associated with neurofibromatosis 2 represent a special challenge. Tumors associated with NF2 tend to form nodular clusters that engulf or even infiltrate the cochlear nerve. Complete resection may not always be possible. Radiosurgery has been performed for patients with NF2 for many years, although most clinical series are relatively small. Subach and coauthors studied 40 early patients (with 45 tumors). Serviceable hearing was preserved in 6 of 14 patients (43%), and this rate improved to 67% after modifications were made to the technique in 1992. The tumor control rate was 98% [38, 39]. Only one patient showed imaging documented growth. In two recent series, serviceable hearing was preserved in only 30% and 40% of cases, respectively [40, 41]. The tumor control rates were respectively 71% and 79%. In 2007, Mathieu and coauthors updated outcomes of the Pittsburgh NF2 series [42]. The tumor control rate was 87.5%. The rate of serviceable hearing preservation using current technique was 52.6%.

In a recent report, Kruyt and coauthors described 47 patients after Gamma Knife® radiosurgery [43]. The tumor control rate was also 87% at 10 years. Facial nerve function worsened in only one patient (2.5%). They matched patients with a non-NF2 cohort and found no difference in morbidity. Patients with a tumor volume <6 cc had better outcomes.

Clinicians have had concerns with the hearing preservation rate after radiosurgery and have opted for other management approaches in some patients. These include continued observation despite tumor growth or hearing loss, partial resections, and use of medical agents such as bevacizumab which may provide temporary benefit. However, it appears that preservation of serviceable hearing in patients with NF2 is an attainable goal using Gamma Knife® radiosurgery. We believe that early radiosurgery when the hearing level is still excellent may become an appropriate strategy in the future. At present, we continue to delay radiosurgery in NF2 patients until we document hearing deterioration or tumor growth.

Proton Beam Radiosurgery

There has been only limited use of proton beam-based irradiation in the care of patients with vestibular schwannomas [20, 44, 45]. Typically tumor control rates have been adequate, but cranial nerve morbidity has been higher than with

stereotactic radiosurgery. Weber and associates evaluated 88 patients. Serviceable hearing was preserved in one-third. Actuarial 5-year normal facial and trigeminal nerve function preservation rates were 91.1% and 89.4%, respectively. Harsh and coauthors evaluated 68 patients. After mean imaging follow-up of 34 months, actuarial control rates of 94% at 2 years and 84% at 5 years were reported. Cranial neuropathies included persistent facial hypoesthesia (4.7%), intermittent facial paresthesias (9.4%), persistent facial weakness (4.7%) requiring oculoplasty, transient partial facial weakness (9.4%), and synkinesis (9.4%). Vernimmen and coauthors evaluated 51 patients at a mean of 6 years, with 98% local control, 42% hearing preservation, 91% facial nerve preservation, and 93% trigeminal nerve preservation [45].

LINAC Radiosurgery

A modified linear accelerator system can be used to deliver photon radiosurgery to a vestibular schwannoma [46]. This can be done in a single session or in a multisession manner. Spiegelman and coauthors reported their results of LINAC radiosurgery for 44 patients with vestibular schwannomas [47]. After a mean follow-up period of 32 months (range, 12–60 months), 98% of the tumors were controlled. The actuarial hearing preservation rate was 71%. New transient facial neuropathy developed in 24% of the patients and persisted to a mild degree in 8%. Friedman and coauthors published clinical outcomes from 390 patients, with a high control rate and a facial neuropathy rate of 0.7% using current techniques [19]. Rezk and coauthors reported 96% progression-free status on actuarial 5-year and 10-year follow-up [48]. Ikonomidis and coauthors treated 84 patients and found 51% functional hearing preservation at 1 year and 36% at 3 years, with 94% and 91% tumor control, respectively [49]. Currently, some clinicians use mask fixation rather than rigid-frame fixation for LINAC radiosurgery which adds additional quality control concerns that must be addressed.

Stereotactic Radiotherapy (SRT)

Limited or extended fractionation can be used in the radiation management of a vestibular schwannoma patient. At the present time, there are neither randomized controlled trials nor any compelling radiobiological principles supporting the use of SRT over radiosurgery. For those centers that cannot achieve the necessary conformal plan to permit accurate radiosurgery, SRT may be an option if they are technically uncomfortable with or have a higher complication rate using LINAC radiosurgery.

Ishihara and coauthors reported 94% tumor control rate at a median follow-up of 32 months in a small series after CyberKnife® SRT for vestibular schwannoma. One patient developed transient facial paresis (2.6%) and one developed trigeminal nerve neuropathy (2.6%) [23]. Fuss and coauthors described 51 patients with vestibular schwannomas who were treated with SRT [50]. The mean follow-up was 42 months and the actuarial 5-year tumor control rate was 95%. One patient developed a transient facial nerve paresis and two noted new trigeminal dysesthesias. Chung et al. using SRT for 25 patients with useful hearing reported 57% hearing preservation at 2 years [51].

Sawamura and coauthors treated 101 patients with vestibular schwannoma using fractionated SRT to a total dose of 40–50 Gy, administered in 20–25 fractions over a 5- to 6-week period [52]. At median follow-up of 45 months, the actuarial 5-year tumor control was 91%. The actuarial 5-year rate of useful hearing preservation (Gardner-Robertson Class I or II) was 71%. The complications of fractionated SRT included transient facial nerve palsy (4%), trigeminal neuropathy (14%), and balance disturbance (17%). Eleven patients (11%) who had progressive communicating hydrocephalus required a cerebrospinal fluid shunt.

Andrews and coauthors provided results after stereotactic radiotherapy at total dose of 50.4 or 46.8 Gy. In patients with high-grade hearing, the median follow-up was 65 weeks. Although no patient had later tumor growth, the hearing preservation rates were better at the lower dose. At 3 years, the hearing preservation rate was 55–60%, and no patient with grade 2 hearing preserved it at the 50 Gy dose [53].

Meijer and coauthors performed a single-institution trial to study whether fractionated stereotactic radiation therapy is superior to single-session LINAC-based radiosurgery in patients with vestibular schwannomas [54]. Stereotactic radiation therapy was performed on 80 patients with a relocatable device using 5 × 4 Gy and later 5 × 5 Gy at the 80% isodose. Forty-nine patients had stereotactic radiosurgery of 1 × 10 Gy and later 1 × 12.5 Gy at the 80% isodose using a stereotactic frame. There was no statistically significant difference between the single-fraction group and the fractionated group with respect to mean tumor diameter (2.6 vs. 2.5 cm) or mean follow-up time (33 months). Outcome differences between the single-session group and the fractionated treatment group with respect to 5-year local control probability (100% vs. 94%), 5-year facial nerve preservation probability (93% vs. 97%), and 5-year hearing preservation probability (75% vs. 61%) were not statistically significant. These conclusions were supported in a 2017 review by Persson and associates, who reviewed 19 case series on SRS and FSRT and found that an average of 5.0% of patients treated with SRS and 4.8% with FSRT had loss of tumor control requiring new intervention. They found deterioration in serviceable hearing was 49% for SRS and 45% for FSRT, the risk of facial nerve deterioration was 3.6% for SRS and 11.2% for FSRT, and the risk of trigeminal dysfunction was 6.0% for SRS and 8.4% for FSRT [55].

Comparing Outcomes for Radiosurgery and Surgical Resection

Both stereotactic radiosurgery and microsurgical resection can offer excellent tumor control with low complication rates when performed by experienced clinicians. There has not been a randomized comparison of these two approaches, and we do not anticipate that one will ever be conducted. Patient preference is a strong driver in the decision to choose a specific treatment. Radiosurgery nearly eliminates the short-term risk associated with surgical intervention and stops tumor growth over the ensuing months, with most procedural morbidity arising years later in terms of hearing loss or, much less often, facial and other cranial nerve palsies. Indeed, over the past few decades, radiosurgery has proven highly effective in controlling tumor growth while minimizing procedural morbidity. Microsurgery similarly controls growth in the immediate term while also relieving any mass effect, but the risk to hearing and other cranial nerves is also realized more immediately, along with inherent surgical risks such as spinal fluid leakage, infection and hemorrhage, and venous thrombosis. Useful comparison studies require long-term follow-up, on the order of 10 years or more, and it has taken time for studies with such follow-up to emerge.

A number of studies have performed cohort comparisons to directly compare outcomes between Gamma Knife® radiosurgery and microsurgery (Table 1). First, microsurgery and radiosurgery offer similar tumor control rates, though this depends on the initial goal of resection [56–58]. Second, radiosurgery is associated with better short-term preservation of hearing and facial nerve function [56–60]. This is consistently reported. Facial nerve function preservation is durable [33, 61]. However, hearing preservation rates after radiosurgery appear to decline over time, even when examining more recent cochlea-sparing dose plans [62]. Of course, there is a natural decline in hearing with age. We realize that longer term hearing outcomes data past 5 years need to be collected. After microsurgical resection, the majority of risk is realized in the immediate postoperative period, and preserved cranial nerve function is likely to be durable and long term, with some exceptions. For similar size tumors, it is unclear if resection leads to faster relief of vestibular dysfunction [63]. Most comparison studies do not support that, although in an individual patient it could be difficult to predict. Detailed balance testing, not commonly performed, might provide clues in this setting.

Tumor Control

Contemporary Gamma Knife® radiosurgery provides tumor control rates comparable to those obtained with surgical resection. Radiosurgery offers tumor control rates in the 96–97% range during the first 5 years, and this remains high over the long term [15, 56]. Tumor control rates do not appear to be adversely affected by dose planning that limits the cochlear

Table 1 Comparison studies between Gamma Knife® radiosurgery and surgical resection

References	Study characteristics	Tumor control	Hearing preservation	CN7 preservation
Pollock et al. [103]	Retrospective *N* = 87 VS < 3.0		GKS > MS	GKS > MS
Karpinos et al. [57]	Retrospective *N* = 96 14.5 Gy GKS	MS 100% GKS 91%	MS 14.4% GKS 57.5%	MS 65% GKS 94%
Myrseth et al. [58]	Retrospective *N* = 189 (MS 86, GKS 103) VS < 3 cm			MS 79.8% GKS 94.8%
Pollock et al. [104]	Prospective *N* = 82 (MS 36, GKS 46) VS < 3.0	MS 100% GKS 96%	GKS > MS at all time points	GKS > MS at all time points
Myrseth et al. [59]	Prospective *N* = 91 (MS 28, GKS 63) VS < 2.5 SOC only 2y f/u	MS 100% GKS 98%	MS 0% GKS 68%	MS 54% GKS 98%
Regis et al. [60]	Prospective *N* = 207 Koos 2–3 4y f/u		MS 37.5% GKS 70%	MS 37% GKS 100%
Golfinos et al. [56]	Retrospective matched cohort *N* = 399 VS < 2.8	MS 98% GKS 98%	MS 43% GKS 86%	MS 89% GKS 100%

dose [15] and are also unaffected by the size of the tumor [64, 65]. Having said that, some patients with larger tumors who hope to avoid a resection, may later come to a resection to improve symptoms even in the absence of tumor growth. In general, tumor control rates are lower for patients with NF2 [66], and, in particular, the Wishart phenotype [67]. However, these tumor control rates may approach 80% or more [43, 68].

Microsurgical resection can be curative when resection of the tumor is accomplished in total. Control rates exceed 90% at 10 years by most reports [69, 70]. Extent of resection is the strongest predictor of tumor progression [36, 71], and subtotal resection is associated with an approximate threefold greater risk of recurrence [72]. Intraoperative factors may limit the extent of resection including adhesion to the facial nerve or other critical structures and attempts to preserve hearing. There is current interest in performing subtotal tumor removal followed by radiosurgery several months later to the reduced volume, in order to maintain cranial nerve function [73, 74]. In most contemporary studies, the tumor control rates obtained with radiosurgery and microsurgery are similar.

Timing of Care and Hearing Preservation

Contemporary dose plans that limit tumor marginal doses to <13 Gy and cochlear dose <4 Gy offer hearing preservation rates on the order of 50–70% at 5 years [15, 36, 75, 76]. Overall, hearing preservation rates after microsurgical resection vary widely and correlate with many factors [77]. In an important comparison study, Regis and coauthors reported outcomes for intracanalicular tumors after either observation alone or proactive Gamma Knife® radiosurgery. Hearing outcomes and tumor control were better in the radiosurgery group [78]. Another recent study from Italy reported superior hearing outcomes in younger patients and those with better hearing preoperatively [79]. Of particular interest, these outcomes were assessed nearly 10 years after treatment. In patients with hearing classified as Gardner-Robertson (GR) Class I, preserved hearing was noted in 71% and reached 93% among cases of GR Class I hearing in patients younger than 55 years. They argue for performing earlier radiosurgery to preserve hearing. We agree.

Unlike the time-dependent hearing loss associated with radiosurgery, hearing preservation after resection is normally durable when it can be achieved, but certainly can deteriorate over time. Most risk to hearing is assumed at the time of surgery [80, 81]. Between 20% and 70% of patients with serviceable hearing preoperatively will have serviceable hearing after surgery, but this is dependent on tumor size, surgical experience, and technique [56, 80–82]. Tumor size and location, extent of resection, approach, baseline neurophysiologic characteristics, and goals of surgery all influence postoperative hearing preservation rates [83–86].

Facial Nerve Preservation in Decision Making

Preservation of facial nerve function is one of the most important goals in vestibular schwannoma management. Indeed, we think that the popularity of the radiosurgery option emerged largely from the twin goals of avoiding open surgery, and avoiding disabling facial weakness. As noted above, facial function is preserved after stereotactic radiosurgery in almost all patients using contemporary dose plans [14, 56, 87–91]. A large meta-analysis by Yang and colleagues [90] incorporated data from 23 studies involving 2204 patients across multiple treatment centers. They noted patients with tumor volumes less than 1.5 cc had significantly better facial nerve outcomes than those with larger tumors. Similarly, treatment plans with a margin dose greater than 13 Gy were associated with higher risk of facial nerve dysfunction than plans with lower margin doses. Finally, they reported that patients younger than 60 years of age were more likely to have good facial nerve preservation after treatment.

Facial nerve preservation rates after microsurgical resection are not as good as those after radiosurgery, though specific centers and surgeons may report comparable preservation rates. Following resection, facial nerve function is preserved in 70–90% of patients [56, 82, 92]. Early facial weakness can improve over time [93]. Multiple factors have been correlated with facial nerve outcome including tumor size, neuromonitoring characteristics, and extent of resection and surgical approach [94–97]. Bloch and colleagues [95] performed a large single-center study on prospectively collected data for 624 patients over 25 years and found that large tumors were associated with worse postoperative facial nerve function than smaller tumors. This is a consistent finding. When facial nerve preservation is the main consideration, the published data unequivocally support the choice of radiosurgery.

Quality of Life

A number of methods are available to study quality of life for patients with vestibular schwannoma. These include the Short Form Health Survey (SF-36) and the VS-specific Penn Acoustic Neuroma Quality of Life survey [98]. In addition, periodic patient surveys conducted by the Acoustic Neuroma Association have been of great value. In a recent report, 353 participants who underwent GKRS between 1997 and 2007 noted that vertigo and balance problems had the largest effect on scores, followed by reduced hearing. Overall satisfaction rates were 91% with their current overall level of functioning, and 97% noted they would recommend GKRS for their VS.

Vestibular dysfunction and headache are the strongest predictors of long-term quality of life in patients with sporadic vestibular schwannoma [99]. However, when present, facial nerve dysfunction is consistently reported to have a large negative impact on quality of life [99, 100]. Most groups report that quality of life is comparable between patients treated with radiosurgery or resection [98, 101, 102]. Radiosurgery offers superior quality of life in the short term, likely reflecting lower perioperative risk [101].

Future Directions

Future research should focus on the following: (a) long-term clinical outcomes past 10 years; (b) quantitative measures of balance function; (c) tinnitus research; (d) new concepts for pharmacological modulation of the radiosurgery response; (e) value of cochlear implants post radiosurgery for hearing augmentation; (f) cost-effectiveness; and (g) imaging tools to evaluate the tumor biologic response.

References

1. Simmermacher S, Vordermark D, Kegel T, Strauss C. Malignization of a vestibular schwannoma 13 years after radiation therapy. HNO. 2017;65(Suppl 2):153–7.
2. Lanser MJ, Sussman SA, Frazer K. Epidemiology, pathogenesis, and genetics of acoustic tumors. Otolaryngol Clin N Am. 1992;25:499–520.
3. Tos M, Stangerup SE, Caye-Thomasen P, Tos T, Thomsen J. What is the real incidence of vestibular schwannoma? Arch Otolaryngol Head Neck Surg. 2004;130:216–20.
4. Kleijwegt M, Ho V, Visser O, Godefroy W, van der Mey A. Real incidence of vestibular schwannoma? Estimations from a national registry. Otol Neurotol. 2016;37:1411–7.
5. Kentala E, Pyykko I. Clinical picture of vestibular schwannoma. Auris Nasus Larynx. 2001;28:15–22.
6. Leksell L. A note on the treatment of acoustic tumours. Acta Chir Scand. 1971;137:763–5.
7. Linskey ME. Stereotactic radiosurgery versus stereotactic radiotherapy for patients with vestibular schwannoma: a Leksell Gamma Knife Society 2000 debate. J Neurosurg. 2000;93(Suppl 3):90–5.
8. Linskey ME, Johnstone PA. Radiation tolerance of normal temporal bone structures: implications for Gamma Knife stereotactic radiosurgery. Int J Radiat Oncol Biol Phys. 2003;57:196–200.
9. Chung WY, Liu KD, Shiau CY, Wu HM, Wang LW, Guo WY, Ho DM, Pan DH. Gamma Knife surgery for vestibular schwannoma: 10-year experience of 195 cases. J Neurosurg. 2005;102(Suppl):87–96.
10. Flickinger JC, Kondziolka D, Niranjan A, Maitz A, Voynov G, Lunsford LD. Acoustic neuroma radiosurgery with marginal tumor doses of 12 to 13 Gy. Int J Radiat Oncol Biol Phys. 2004;60:225–30.
11. Hasegawa T, Kida Y, Kobayashi T, Yoshimoto M, Mori Y, Yoshida J. Long-term outcomes in patients with vestibular schwannomas treated using Gamma Knife surgery: 10-year follow up. J Neurosurg. 2005;102:10–6.
12. Kondziolka D, Lunsford LD, Flickinger JC. Acoustic neuroma radiosurgery. Origins, contemporary use and future expectations. Neuro-Chirurgie. 2004;50:427–35.
13. Kondziolka D, Nathoo N, Flickinger JC, Niranjan A, Maitz AH, Lunsford LD. Long-term results after radiosurgery for benign intracranial tumors. [See comment]. Neurosurgery. 2003;53:815–21; discussion 821–812.
14. Lunsford LD, Niranjan A, Flickinger JC, Maitz A, Kondziolka D. Radiosurgery of vestibular schwannomas: summary of experience in 829 cases. J Neurosurg. 2005;102(Suppl):195–9.
15. Watanabe S, Yamamoto M, Kawabe T, Koiso T, Yamamoto T, Matsumura A, Kasuya H. Stereotactic radiosurgery for vestibular schwannomas: average 10-year follow-up results focusing on long-term hearing preservation. J Neurosurg. 2016;125(Suppl 1):64–72.
16. Delbrouck C, Hassid S, Massager N, Choufani G, David P, Devriendt D, Levivier M. Preservation of hearing in vestibular schwannomas treated by radiosurgery using Leksell Gamma Knife: preliminary report of a prospective Belgian clinical study. Acta Otorhinolaryngol Belg. 2003;57:197–204.
17. Flickinger JC, Kondziolka D, Niranjan A, Lunsford LD. Results of acoustic neuroma radiosurgery: an analysis of 5 years' experience using current methods. [See comment]. J Neurosurg. 2001;94:1–6.
18. Flickinger JC, Kondziolka D, Pollock BE, Lunsford LD. Evolution in technique for vestibular schwannoma radiosurgery and effect on outcome. Int J Radiat Oncol Biol Phys. 1996;36:275–80.
19. Friedman WA, Bradshaw P, Myers A, Bova FJ. Linear accelerator radiosurgery for vestibular schwannomas. J Neurosurg. 2006;105:657–61.
20. Harsh GR, Thornton AF, Chapman PH, Bussiere MR, Rabinov JD, Loeffler JS. Proton beam stereotactic radiosurgery of vestibular schwannomas. Int J Radiat Oncol Biol Phys. 2002;54:35–44.
21. Horstmann GA, Van Eck AT. Gamma Knife model C with the automatic positioning system and its impact on the treatment of vestibular schwannomas. J Neurosurg. 2002;97:450–5.
22. Inoue HK. Low-dose radiosurgery for large vestibular schwannomas: long-term results of functional preservation. J Neurosurg. 2005;102(Suppl):111–3.
23. Ishihara H, Saito K, Nishizaki T, Kajiwara K, Nomura S, Yoshikawa K, Harada K, Suzuki M. CyberKnife radiosurgery for vestibular schwannoma. Minim Invasive Neurosurg. 2004;47:290–3.
24. Kondziolka D, Lunsford LD, Flickinger JC. Gamma Knife radiosurgery for vestibular schwannomas. Neurosurg Clin N Am. 2000;11:651–8.
25. Kondziolka D, Lunsford LD, McLaughlin MR, Flickinger JC. Long-term outcomes after radiosurgery for acoustic neuromas. [See comment]. N Engl J Med. 1998;339:1426–33.
26. Linskey ME, Lunsford LD, Flickinger JC. Tumor control after stereotactic radiosurgery in neurofibromatosis patients with bilateral acoustic tumors. Neurosurgery. 1992;31:829–38; discussion 838–829
27. Lunsford LD. Vestibular schwannomas. Neuro-Chirurgie. 2004;50:151–2.
28. Meijer OW, Wolbers JG, Vandertop WP, Slotman BJ. Stereotactische bestraling van het vestibulair schwannoom (acusticusneurinoom). Ned Tijdschr Geneeskd. 2000;144:2088–93.
29. Noren G. Long-term complications following Gamma Knife radiosurgery of vestibular schwannomas. Stereotact Funct Neurosurg. 1998;70(Suppl 1):65–73.
30. Petit JH, Hudes RS, Chen TT, Eisenberg HM, Simard JM, Chin LS. Reduced-dose radiosurgery for vestibular schwannomas. Neurosurgery. 2001;49:1299–306; discussion 1306–1297.
31. Litvack ZN, Noren G, Chougule PB, Zheng Z. Preservation of functional hearing after Gamma Knife surgery for vestibular schwannoma. Neurosurg Focus. 2003;14:33.

32. Niranjan A, Lunsford LD, Flickinger JC, Maitz A, Kondziolka D. Dose reduction improves hearing preservation rates after intracanalicular acoustic tumor radiosurgery. Neurosurgery. 1999;45:753–62; discussion 762–755.
33. Lobato-Polo J, Kondziolka D, Zorro O, Kano H, Flickinger JC, Lunsford LD. Gamma Knife radiosurgery in younger patients with vestibular schwannomas. Neurosurgery. 2009;65:294–301; discussion 300–291.
34. Yang HC, Kano H, Awan NR, Lunsford LD, Niranjan A, Flickinger JC, Novotny J Jr, Bhatnagar JP, Kondziolka D. Gamma Knife radiosurgery for larger-volume vestibular schwannomas: clinical article. J Neurosurg. 2013;119(Suppl):801–7.
35. Huang CW, Tu HT, Chuang CY, Chang CS, Chou HH, Lee MT, Huang CF. Gamma Knife radiosurgery for large vestibular schwannomas greater than 3 cm in diameter. J Neurosurg. 2017;14:1–8.
36. Lin RH, Wang TC, Lin CD, Lin HL, Chung HK, Wang CY, et al. Predictors of hearing outcomes following low-dose stereotactic radiosurgery in patients with vestibular schwannomas: a retrospective cohort review. Clin Neurol Neurosurg. 2017;162:16–21.
37. Kano H, Kondziolka D, Flickinger JC, Lunsford LD. Predictors of hearing preservation after stereotactic radiosurgery for acoustic neuromas. J Neurosurg. 2009;111:863–73.
38. Subach BR, Kondziolka D, Lunsford LD, Bissonette DJ, Flickinger JC, Maitz AH. Stereotactic radiosurgery in the management of acoustic neuromas associated with neurofibromatosis Type 2. [See comment]. J Neurosurg. 1999;90:815–22.
39. Subach BR, Kondziolka D, Lunsford LD, Bissonette DJ, Flickinger JC, Maitz AH. Stereotactic radiosurgery in the management of acoustic neuromas associated with neurofibromatosis Type 2. J Neurosurg. 2013;119(Suppl):815–22.
40. Roche PH, Robitail S, Thomassin JM, Pellet W, Regis J. Radiochirurgie Gamma Knife des schwannomes vestibulaires associes a une neurofibromatose de type 2. Neuro-Chirurgie. 2004;50:367–76.
41. Rowe JG, Radatz MW, Walton L, Soanes T, Rodgers J, Kemeny AA. Clinical experience with Gamma Knife stereotactic radiosurgery in the management of vestibular schwannomas secondary to type 2 neurofibromatosis. J Neurol Neurosurg Psychiatry. 2003;74:1288–93.
42. Mathieu D, Kondziolka D, Flickinger JC, Niranjan A, Williamson R, Martin JJ, Lunsford LD. Stereotactic radiosurgery for vestibular schwannomas in patients with neurofibromatosis type 2: an analysis of tumor control, complications, and hearing preservation rates. Neurosurgery. 2007;60:460–8; discussion 468–470.
43. Kruyt IJ, Verheul J, Hanssens P, Kunst HP. Gamma Knife radiosurgery for treatment of growing vestibular schwannomas in patients with neurofibromatosis type 2: a matched cohort study with sporadic vestibular schwannomas. J Neurosurg. 2018;128:49–59.
44. Weber DC, Chan AW, Bussiere MR, GRt H, Ancukiewicz M, Barker FG 2nd, Thornton AT, Martuza RL, Nadol JB Jr, Chapman PH, Loeffler JS. Proton beam radiosurgery for vestibular schwannoma: tumor control and cranial nerve toxicity. Neurosurgery. 2003;53:577–86; discussion 586–578.
45. Vernimmen FJ, Mohamed Z, Slabbert JP, Wilson J. Long-term results of stereotactic proton beam radiotherapy for acoustic neuromas. Radiother Oncol. 2009;90(2):208–12.
46. Suh JH, Barnett GH, Sohn JW, Kupelian PA, Cohen BH. Results of linear accelerator-based stereotactic radiosurgery for recurrent and newly diagnosed acoustic neuromas. Int J Cancer. 2000;90:145–51.
47. Spiegelmann R, Lidar Z, Gofman J, Alezra D, Hadani M, Pfeffer R. Linear accelerator radiosurgery for vestibular schwannoma. [See comment]. J Neurosurg. 2001;94:7–13.
48. Rezk EM, El Majdoub F, Kocher M, Treuer H, Sturm V, Maarouf M. Micro-multileaf collimator LINAC radiosurgery for vestibular schwannomas. World Neurosurg. 2017. pii:S1878-8750(17)30337-6 [E-pub ahead of print].
49. Ikonomidis C, Pica A, Bloch J, Maire R. Vestibular schwannoma. The evolution of hearing and tumor size in natural course and after treatment by LINAC stereotactic radiosurgery. Audiol Neurootol. 2015;20(6):406–15.
50. Fuss M, Debus J, Lohr F, Huber P, Rhein B, Engenhart-Cabillic R, Wannenmacher M. Conventionally fractionated stereotactic radiotherapy (FSRT) for acoustic neuromas. Int J Radiat Oncol Biol Phys. 2000;48:1381–7.
51. Chung HT, Ma R, Toyota B, Clark B, Robar J, McKenzie M. Audiologic and treatment outcomes after linear accelerator-based stereotactic irradiation for acoustic neuroma. Int J Radiat Oncol Biol Phys. 2004;59:1116–21.
52. Sawamura Y, Shirato H, Sakamoto T, Aoyama H, Suzuki K, Onimaru R, Isu T, Fukuda S, Miyasaka K. Management of vestibular schwannoma by fractionated stereotactic radiotherapy and associated cerebrospinal fluid malabsorption. J Neurosurg. 2003;99:685–92.
53. Andrews D, Werner-Wasik M, Den R, Paek S, Downes-Phillips B, Willcox T, Bednarz G, Maltenfort M, Evans J, Curran W. Toward dose optimization for fractionated stereotactic radiotherapy for acoustic neuromas: comparison of two dose cohorts. Int J Radiat Oncol Biol Phys. 2009;74:419–26.
54. Meijer OW, Vandertop WP, Baayen JC, Slotman BJ. Single-fraction vs. fractionated linac-based stereotactic radiosurgery for vestibular schwannoma: a single-institution study. [See comment]. Int J Radiat Oncol Biol Phys. 2003;56:1390–6.
55. Persson O, Bartek J Jr, Shalom NB, Wangerid T, Jakola AS, Förander P. Stereotactic radiosurgery vs. fractionated radiotherapy for tumor control in vestibular schwannoma patients: a systematic review. Acta Neurochir. 2017;159(6):1013–21.
56. Golfinos JG, Hill TC, Rokosh R, Choudhry O, Shinseki M, Mansouri A, et al. A matched cohort comparison of clinical outcomes following microsurgical resection or stereotactic radiosurgery for patients with small- and medium-sized vestibular schwannomas. J Neurosurg. 2016;125:1472–82.
57. Karpinos M, Teh BS, Zeck O, Carpenter LS, Phan C, Mai WY, et al. Treatment of acoustic neuroma: stereotactic radiosurgery vs. microsurgery. Int J Radiat Oncol Biol Phys. 2002;54:1410–21.
58. Myrseth E, Møller P, Pedersen PH, Vassbotn FS, Wentzel-Larsen T, Lund-Johansen M. Vestibular schwannomas: clinical results and quality of life after microsurgery or Gamma Knife radiosurgery. Neurosurgery. 2005;56:927–35; discussion 927–935.
59. Myrseth E, Moller P, Pedersen PH, Lund-Johansen M. Vestibular schwannoma: surgery or Gamma Knife radiosurgery? A prospective, nonrandomized study. Neurosurgery. 2009;64:654–61; discussion 661–653.
60. Regis J, Pellet W, Delsanti C, Dufour H, Roche PH, Thomassin JM, et al. Functional outcome after Gamma Knife surgery or microsurgery for vestibular schwannomas. J Neurosurg. 2013;119(Suppl):1091–100.
61. Hasegawa T, Kida Y, Kato T, Iizuka H, Kuramitsu S, Yamamoto T. Long-term safety and efficacy of stereotactic radiosurgery for vestibular schwannomas: evaluation of 440 patients more than 10 years after treatment with Gamma Knife surgery. J Neurosurg. 2013;118:557–65.
62. Carlson ML, Jacob JT, Pollock BE, Neff BA, Tombers NM, Driscoll CL, et al. Long-term hearing outcomes following stereotactic radiosurgery for vestibular schwannoma: patterns of hearing loss and variables influencing audiometric decline. J Neurosurg. 2013;118:579–87.
63. Samii M, Metwali H, Gerganov V. Efficacy of microsurgical tumor removal for treatment of patients with intracanalicular vestibular schwannoma presenting with disabling vestibular symptoms. J Neurosurg. 2017;126:1514–9.

64. Bailo M, Boari N, Franzin A, Gagliardi F, Spina A, Del Vecchio A, et al. Gamma Knife radiosurgery as primary treatment for large vestibular schwannomas: clinical results at long-term follow-up in a series of 59 patients. World Neurosurg. 2016;95:487–501.
65. Iorio-Morin C, AlSubaie F, Mathieu D. Safety and efficacy of Gamma Knife radiosurgery for the management of Koos grade 4 vestibular schwannomas. Neurosurgery. 2016;78:521–30.
66. Sun S, Liu A. Long-term follow-up studies of Gamma Knife surgery for patients with neurofibromatosis Type 2. J Neurosurg. 2014;121(Suppl):143–9.
67. Kruyt IJ, Verheul JB, Hanssens PEJ, Kunst HPM. Gamma Knife radiosurgery for treatment of growing vestibular schwannomas in patients with neurofibromatosis Type 2: a matched cohort study with sporadic vestibular schwannomas. J Neurosurg. 2017:1–11. https://doi.org/10.3171/2016.11.JNS16498.
68. Mallory GW, Pollock BE, Foote RL, Carlson ML, Driscoll CL, Link MJ. Stereotactic radiosurgery for neurofibromatosis 2-associated vestibular schwannomas: toward dose optimization for tumor control and functional outcomes. Neurosurgery. 2014;74:292–300; discussion 300–291.
69. Putz F, Müller J, Wimmer C, Goerig N, Knippen S, Iro H, et al. Stereotactic radiotherapy of vestibular schwannoma : hearing preservation, vestibular function, and local control following primary and salvage radiotherapy. Strahlenther Onkol. 2017;193:200–12.
70. Nakatomi H, Jacob JT, Carlson ML, Tanaka S, Tanaka M, Saito N, et al. Long-term risk of recurrence and regrowth after gross-total and subtotal resection of sporadic vestibular schwannoma. J Neurosurg. 2017:1–7.
71. Monfared A, Corrales CE, Theodosopoulos PV, Blevins NH, Oghalai JS, Selesnick SH, et al. Facial nerve outcome and tumor control rate as a function of degree of resection in treatment of large acoustic neuromas: preliminary report of the acoustic neuroma subtotal resection study (ANSRS). Neurosurgery. 2016;79:194–203.
72. Rosahl S, Esser D. Vestibular schwannoma – management and microsurgical results. HNO. 2017;65:381–7.
73. Daniel RT, Tuleasca C, George M, Pralong E, Schiappacasse L, Zeverino M, et al. Preserving normal facial nerve function and improving hearing outcome in large vestibular schwannomas with a combined approach: planned subtotal resection followed by Gamma Knife radiosurgery. Acta Neurochir. 2017;159:1197–211.
74. Starnoni D, Daniel RT, Tuleasca C, George M, Levivier M, Messerer M. Systematic review and meta-analysis of the technique of subtotal resection and stereotactic radiosurgery for large vestibular schwannomas: a "nerve-centered" approach. Neurosurg Focus. 2018;44:E4.
75. Yang I, Sughrue ME, Han SJ, Aranda D, Pitts LH, Cheung SW, et al. A comprehensive analysis of hearing preservation after radiosurgery for vestibular schwannoma. J Neurosurg. 2010;112:851–9.
76. Yang I, Sughrue ME, Han SJ, Aranda D, Pitts LH, Cheung SW, et al. A comprehensive analysis of hearing preservation after radiosurgery for vestibular schwannoma: clinical article. J Neurosurg. 2013;119(Suppl):851–9.
77. Carlson ML, Vivas EX, McCracken DJ, Sweeney AD, Neff BA, Shepard NT, et al. Congress of neurological surgeons systematic review and evidence-based guidelines on hearing preservation outcomes in patients with sporadic vestibular schwannomas. Neurosurgery. 2018;82:E35–9.
78. Regis J, Carron R, Park MC, Soumare O, Delsanti C, Thomassin JM, et al. Wait-and-see strategy compared with proactive Gamma Knife surgery in patients with intracanalicular vestibular schwannomas. J Neurosurg. 2010;113(Suppl):105–11.
79. Boari N, Bailo M, Gagliardi F, Franzin A, Gemma M, del Vecchio A, et al. Gamma Knife radiosurgery for vestibular schwannoma: clinical results at long-term follow-up in a series of 379 patients. J Neurosurg. 2014;121(Suppl):123–42.
80. Wang AC, Chinn SB, Than KD, Arts HA, Telian SA, El-Kashlan HK, et al. Durability of hearing preservation after microsurgical treatment of vestibular schwannoma using the middle cranial fossa approach. J Neurosurg. 2013;119:131–8.
81. Quist TS, Givens DJ, Gurgel RK, Chamoun R, Shelton C. Hearing preservation after middle fossa vestibular schwannoma removal: are the results durable? Otolaryngol Head Neck Surg. 2015;152:706–11.
82. Zhang J, Xu BN, Hou YZ, Sun GC, Jiang Y. Facial and cochlear nerve complications following microsurgical resection of vestibular schwannomas in a series of 221 cases. Med Sci Monit. 2015;21:1674–8.
83. Sughrue ME, Yang I, Aranda D, Kane AJ, Parsa AT. Hearing preservation rates after microsurgical resection of vestibular schwannoma. J Clin Neurosci. 2010;17:1126–9.
84. Sughrue ME, Kaur R, Rutkowski MJ, Kane AJ, Yang I, Pitts LH, et al. A critical evaluation of vestibular schwannoma surgery for patients younger than 40 years of age. Neurosurgery. 2010;67:1646–53; discussion 1653–1644.
85. Samii M, Matthies C. Management of 1000 vestibular schwannomas (acoustic neuromas): hearing function in 1000 tumor resections. Neurosurgery. 1997;40:248–60; discussion 260–24.
86. Cohen-Inbar O. The multidisciplinary treatment of vestibular schwannoma (acoustic neuroma). Harefuah. 2016;155:181–4, 194–5.
87. Combs SE, Thilmann C, Debus J, Schulz-Ertner D. Long-term outcome of stereotactic radiosurgery (SRS) in patients with acoustic neuromas. Int J Radiat Oncol Biol Phys. 2006;64:1341–7.
88. Zeiler FA, Bigder M, Kaufmann A, McDonald PJ, Fewer D, Butler J, et al. Gamma Knife radiosurgery for large vestibular schwannomas: a Canadian experience. Can J Neurol Sci. 2013;40:342–7.
89. Muacevic A, Jess-Hempen A, Tonn JC, Wowra B. Results of outpatient Gamma Knife radiosurgery for primary therapy of acoustic neuromas. Acta Neurochir. 2004;91(Suppl):75–8.
90. Yang I, Sughrue ME, Han SJ, Fang S, Aranda D, Cheung SW, et al. Facial nerve preservation after vestibular schwannoma Gamma Knife radiosurgery. J Neuro-Oncol. 2009;93:41–8.
91. Ogunrinde OK, Lunsford DL, Kondziolka DS, Bissonette DJ, Flickinger JC. Cranial nerve preservation after stereotactic radiosurgery of intracanalicular acoustic tumors. Stereotact Funct Neurosurg. 1995;64(Suppl 1):87–97.
92. Chen L, Chen L, Liu L, Ling F, Yuan X, Fang J, et al. Vestibular schwannoma microsurgery with special reference to facial nerve preservation. Clin Neurol Neurosurg. 2009;1:47–53.
93. Torres R, Nguyen Y, Vanier A, Smail M, Ferrary E, Sterkers O, et al. Multivariate analysis of factors influencing facial nerve outcome following microsurgical resection of vestibular schwannoma. Otolaryngol Head Neck Surg. 2017;156:525–33.
94. Liu SW, Jiang W, Zhang HQ, Li XP, Wan XY, Emmanuel B, et al. Intraoperative neuromonitoring for removal of large vestibular schwannoma: facial nerve outcome and predictive factors. Clin Neurol Neurosurg. 2015;133:83–9.
95. Bloch O, Sughrue ME, Kaur R, Kane AJ, Rutkowski MJ, Kaur G, et al. Factors associated with preservation of facial nerve function after surgical resection of vestibular schwannoma. J Neuro-Oncol. 2011;102:281–6.
96. Virk JS, Tripathi S, Randhawa PS, Kwasa EA, Mendoza ND, Harcourt J. Tumour resection volumes and facial nerve outcomes for vestibular schwannomas. Indian J Otolaryngol Head Neck Surg. 2014;66:191–5.
97. Arlt F, Trantakis C, Seifert V, Bootz F, Strauss G, Meixensberger J. Recurrence rate, time to progression and facial nerve function in microsurgery of vestibular schwannoma. Neurol Res. 2011;33:1032–7.
98. Carlson ML, Tveiten OV, Driscoll CL, Goplen FK, Neff BA, Pollock BE, et al. Long-term quality of life in patients with ves-

tibular schwannoma: an international multicenter cross-sectional study comparing microsurgery, stereotactic radiosurgery, observation, and nontumor controls. J Neurosurg. 2015;122:833–42.
99. Carlson ML, Tveiten ØV, Driscoll CL, Goplen FK, Neff BA, Pollock BE, et al. What drives quality of life in patients with sporadic vestibular schwannoma? Laryngoscope. 2015;125:1697–702.
100. Browne S, Distel E, Morton P, Petrie KJ. Patients' quality of life, reported difficulties, and benefits following surgery for acoustic neuroma. J Otolaryngol Head Neck Surg. 2008;37:417–22.
101. Robinett ZN, Walz PC, Miles-Markley B, Moberly C, Welling DB. Comparison of long-term quality-of-life outcomes in vestibular schwannoma patients. Otolaryngol Head Neck Surg. 2014;150:1024–32.
102. Brooker JE, Fletcher JM, Dally MJ, Briggs RJ, Cousins VC, Smee RI, et al. Quality of life among acoustic neuroma patients managed by microsurgery, radiation, or observation. Otol Neurotol. 2010;31:977–84.
103. Pollock BE, Lunsford LD, Kondziolka D, Flickinger JC, Bissonette DJ, Kelsey SF, et al. Outcome analysis of acoustic neuroma management: a comparison of microsurgery and stereotactic radiosurgery. Neurosurgery. 1995;36:215–24.
104. Pollock BE, Driscoll CL, Foote RL, Link MJ, Gorman DA, Bauch CD, et al. Patient outcomes after vestibular schwannoma management: a prospective comparison of microsurgical resection and stereotactic radiosurgery. Neurosurgery. 2006;59:77–85.

Stereotactic Radiosurgery for Glial Tumors

Ajay Niranjan and L. Dade Lunsford

Background

Although the management of glial tumors remains a challenge, during the past decade, modest improvements in survival have been achieved. Although surgical resection or biopsy with histological definition remains the initial treatment of choice for many gliomas, these infiltrative tumors may grow in regions of critical brain function, making gross total resection impossible. Low-grade gliomas (LGG) consist primarily of the World Health Organization grade 1–2 astrocytomas and oligodendrogliomas, as well as mixed tumors. Each individual subtype of tumor represents a distinct histological subtype of glial neoplasm with differences in prognosis. For low-grade glial neoplasms, adverse location, tumor recurrence, and progression despite surgery require the use of other treatment modalities. High-grade gliomas (HGG) are the most common primary brain tumor in adults and consist primarily of the World Health Organization grade 3–4 tumors (anaplastic glioma and glioblastoma multiforme). As of 2018, the standard of care for symptomatic patients with HGG includes maximal safe resection followed by fractionated radiotherapy (FRT), often coupled with concomitant temozolomide. FRT remains a critically important treatment option for patients with high-grade gliomas. A typical cone down dose is 60 GY at the imaging-defined tumor margin using 1.8–2 Gy fractions. While many patients with HGG are treated with systemic chemotherapy either as an initial or salvage therapy, the overall benefit of chemotherapeutic agents remains modest.

A. Niranjan (✉) · L. D. Lunsford
Department of Neurological Surgery, University of Pittsburgh Medical Center, Pittsburgh, PA, USA

Department of Neurological Surgery, University of Pittsburgh, Pittsburgh, PA, USA
e-mail: niraax@upmc.edu

The Role of Radiosurgery

Stereotactic radiosurgery (SRS) has been used as a primary option for unresectable LGG such as pilocytic astrocytoma and selected oligodendrogliomas. Its primary role is for salvage therapy in patients with recurrent or residual glial tumors. At present, most SRS series have reported outcomes using the Leksell Gamma Knife (GK). The role of GK SRS for patients with glial tumors is constantly evolving. Due to the possibility of adverse radiation effects (ARE) after repeated fractionated radiation therapy, SRS is often used to boost the tumor radiobiological effect for smaller-volume recurrent or progressive tumors. In contrast to FRT, SRS relies on highly conformal and selective delivery of radiation based on up-to-date brain imaging. It is delivered in one to three sessions using stereotactic guiding technologies [1]. This article reviews the outcome of radiosurgery in the treatment of glial tumors.

Pilocytic Astrocytoma

Pilocytic astrocytomas typically do not directly invade adjacent neural tissue and accordingly have relatively sharp borders defined by imaging. They can grow to considerable size before a diagnosis is made. These tumors generally arise from within the cerebellum, brainstem, and hypothalamus of younger patients. These can present as solid tumors, or a mixture of cystic and solid components. Complete resection is the goal of surgical management. The clinical management of pilocytic astrocytoma is challenging. If a gross total resection is achieved, then patients are followed with neuroimaging and generally have excellent long-term tumor control.

If a gross total resection cannot be achieved, adjuvant management is needed. Appropriate adjuvant options include radiosurgery, radiation therapy, or chemotherapy. This decision is typically made based on tumor size, location,

D. M. Trifiletti et al. (eds.), *Stereotactic Radiosurgery and Stereotactic Body Radiation Therapy*,
https://doi.org/10.1007/978-3-030-16924-4_16

symptoms, and patient expectations. In general, SRS is recommended for patients with unresectable smaller and deep-seated tumors adjacent to or within critical locations (i.e., brainstem and optic structures). SRS is also used as a salvage technique for tumor progression or recurrence after initial resection. FRT is appropriate for large tumors and tumors encasing critical structures such as the optic apparatus.

We evaluated the role of SRS as part of multimodality management of pilocytic astrocytoma in adult as well as pediatric patients. For adults, the median radiosurgery target volume was 4.7 cc (range, 0.6–33.7 cc), and the median margin dose was 13.3 Gy (range, 10–20 Gy) [2]. The overall survival (OS) after SRS for the entire series was 100%, 88.9%, and 88.9% at 1, 3, and 5 years, respectively. The progression-free survival (PFS) for adults after SRS (solid as well as cystic) was 84%, 32%, and 32% at 1, 3, and 5 years, respectively (Fig. 1a–d). Prior surgical resection was associated with better progression-free survival after SRS. We found that SRS was most valuable for patients after maximal safe surgical resection. Delayed cystic progression contributed to loss of tumor control. In addition, we studied 50 pediatric patients with juvenile pilocytic astrocytomas (JPA) who underwent GK SRS [3]. The median radiosurgery target volume was 2.1 cc and the median margin dose was 14.5 Gy. At a median follow-up of 56 months, 1 patient died and 49 were alive. The progression-free survival (PFS) for pediatric patients after SRS was 92%, 83%, and 71% at 1, 3, and 5 years, respectively. The best response was observed in small volume residual solid tumors.

Hallemeier and coauthors reported 18 patients with recurrent or unresectable pilocytic astrocytoma (PA) treated with GK SRS [4]. The median treatment volume was 9.1 cc and the median tumor margin dose was 15 Gy. The median follow-up was 8.0 years. OS at 1, 5, and 10 years after SRS was 94%, 71%, and 71%, respectively. PFS at 1, 5, and 10 years was 65%, 41%, and 17%, respectively. Prior FRT was associated with inferior overall survival and progression-free survival. Symptomatic edema after SRS occurred in eight patients (44%) and resolved with short-term corticosteroid therapy.

Simonova and coauthors evaluated long-term treatment outcomes in 25 patients with pilocytic astrocytoma treated with GK SRS [5]. Patients were treated with several methods (five daily fractions, ten fractions, or single fraction). Complete regression occurred in ten patients (40%) and partial regression in ten patients (40%). The 10-year OS rate was 96% and the 10-year PFS rate was 80%. Temporary adverse radiation effects (ARE) unrelated to tumor progression were noted in two patients (8%) and permanent ARE in two patients (8%). In this study, the target volume was a significant prognostic factor for PFS. Trifiletti and coauthors reported 28 patients who underwent SRS for residual or recurrent pilocytic astrocytoma [6]. At a median clinical follow-up of 5.2 years and median radiographic follow-up of 4.6 years, these authors reported a long-term tumor control rate of 93% without ARE.

Grade 2 Astrocytoma

The World Health Organization (WHO) grade 2 fibrillary astrocytoma mostly affects young adults and tends to develop in lobar locations. These tumors may have a core mass of uniformly neoplastic tissue and are usually surrounded by a

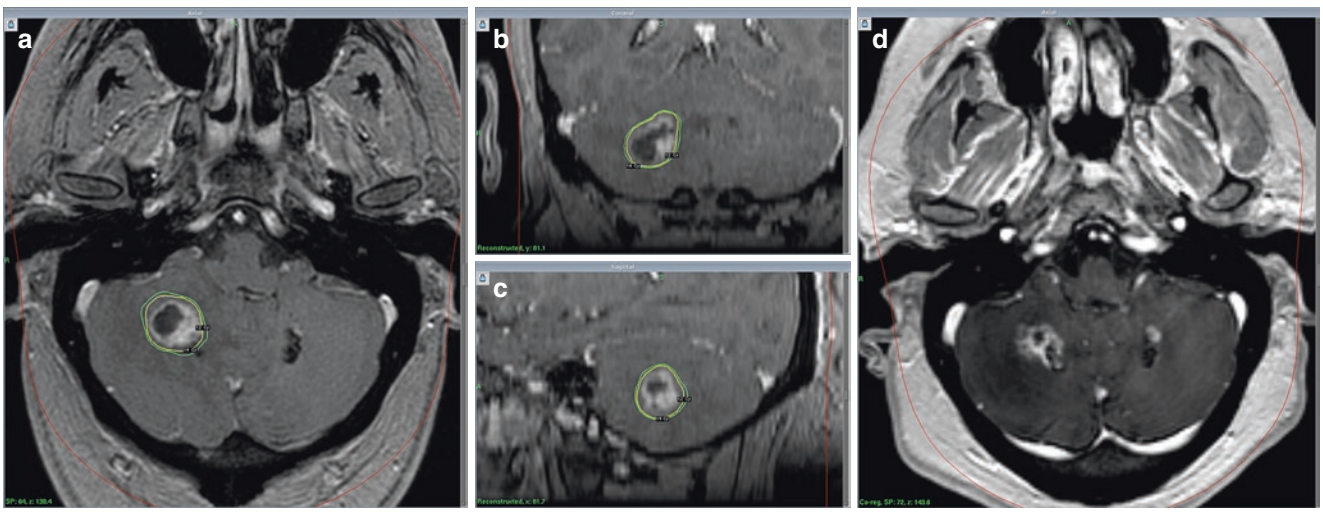

Fig. 1 A 32-year-old woman presented with imaging evidence of progressive right cerebellar pilocytic astrocytoma. She underwent Gamma Knife radiosurgery using a margin dose of 14 Gy to 50% isodose line for a 2.4 cc tumor volume. Axial contrast-enhanced images (**a**) with coronal (**b**) and sagittal reconstruction (**c**) show a conformal radiosurgery dose plan. A follow-up MRI 3 years after radiosurgery shows regressed and stable tumor (**d**)

zone of brain adjacent infiltrated with neoplastic cells. The timing and options for management of these tumors remain controversial despite more than 70 years of growing knowledge related to their progression rate and median survival. By 2018, no consensus has evolved related to the role of observation with imaging follow-up, biopsy alone, attempted aggressive resection, the use of chemotherapy, and the value of FRT as primary or adjuvant management. Complete resection is rarely achieved due to the infiltrative nature of these tumors. The median survival of patients with these tumors after aggressive resection and FRT varies from 7 to 10 years. Because grade 2 fibrillary astrocytomas tend to be infiltrative of regional brain, the role of SRS has been more difficult to define. When feasible based on tumor volume, SRS potentially provides improved radiobiological effectiveness by delivering high radiation dose most often in a single treatment session.

Kida and associates reported 39 patients with grade 2 astrocytomas [7]. Using a median margin dose of 15.7 Gy, a tumor control rate of 87.2% was reported. Radiation-related edema was noted in 41% of cases, and half of these were symptomatic and needed steroid administration. Hadjipanayis and coauthors studied 12 patients who had GK SRS using a margin dose of 16 Gy [8]. These authors reported a solid tumor growth control rate of 92%. Three patients developed cyst enlargement; thus the overall control rate of 67% was achieved. No patients developed ARE.

Wang and associates reported 24 patients who underwent SRS for low-grade astrocytomas (including grade1 and 2) [9]. The authors reported that the tumor control rate was 67% at a median of 49 months. If cyst enlargement was included in the determination of tumor control, it dropped to 59%. Szeifert and associates reported outcomes in 17 grade 2 astrocytoma patients followed for a median of 33 months [10]. A tumor control rate of 71% was shown. These authors recommended SRS as an alternative or supplementary treatment modality to surgery in small-volume low-grade astrocytomas, especially in deep-seated or critical locations.

We evaluated the role of GKRS in 25 patients with newly diagnosed (early) or progressive grade 2 astrocytomas [11]. The median tumor volume was 3.7 cm^3 and the median margin dose was 14 Gy. At a median of 65 months, the OS was 80%. Local tumor control was documented in 13 (52%) of 25 tumors at a median of 65 months after SRS. The timing of SRS (early vs. delayed) did not affect the eventual development of tumor progression. Four (67%) of six partially cystic tumors showed a decrease in size of both cystic and solid tumor components. Nine (47%) of 19 patients with solid tumors demonstrated tumor control. Eventual cystic or solid tumor progression occurred in 12 patients. The PFS rates after SRS for the entire series were 91%, 54%, and 37% at 1, 5, and 10 years, respectively. The median PFS time after SRS was 61 months. A tumor volume of less than 6.0 cm^3 and marginal dose of 15 Gy or more were significantly associated with longer PFS.

Anaplastic (Grade 3) Gliomas

Anaplastic gliomas (AG) are a diverse group of grade 3 tumors that include anaplastic astrocytoma, anaplastic oligodendroglioma, anaplastic oligoastrocytoma, and anaplastic ependymoma with the median survival in most series is 2–5 years, depending on location and response to therapy. As opposed to the standard treatment of glioblastoma, there is no accepted standard treatment for grade 3 tumors. Treatment options include surgery, radiation, temozolomide chemotherapy, novel chemotherapeutic including targeted agents, or a combination of these approaches. No prospective randomized studies have addressed the utility of repeat resection in recurrent anaplastic gliomas. Nonrandomized studies have suggested improvement in survival in select patients with reoperation, but the efficacy of resection in recurrent AG has not been clearly demonstrated. Surgery for recurrent tumors may be of value in differentiating tumor progression from ARE and in confirming possible transformation to higher grade 4 tumors. SRS has been used in the management of recurrent AG in selected cases, usually for progression after failure of more standard management.

Kondziolka and coauthors reported 43 anaplastic astrocytomas that underwent GK SRS. The median survival time after diagnosis for these patients was 32 months and the median survival time after radiosurgery was 21 months. The 2-year OS was 67%. Ten patients (23%) underwent subsequent craniotomies at a mean of 8 months after initial surgery, and two underwent repeat SRS. There was no acute neurological morbidity after radiosurgery. Histologically proven ARE occurred in two patients (4.7%). For 21 patients for whom SRS was part of the initial management plan, the median survival time after diagnosis was 56 months. This study identified improved survival benefit after SRS for patients, in comparison with historical controls. Elliott and associates [1] treated 26 patients with progressive grade 3 tumors after standard management. The 12-month actuarial survival for patients with anaplastic astrocytoma was 80%. In a prospective study, Kong and associates [12] treated 114 high-grade glioma patients with SRS (GKRS in 109 patients; linear accelerator radiosurgery in 5 patients). They reported that the median period of survival from the time of diagnosis and median progression-free survival for patients with grade 3 glioma were 37.5 months and 8.6 months, respectively.

Kohshi and associates reported the use of hyperbaric oxygen therapy before fractionated GK SRS to increase the susceptibility of hypoxic, radioresistant cells to radiosurgery [13]. They enrolled 25 patients in their study. All patients had previously undergone radiation therapy with concurrent

chemotherapy as an initial management approach. In clinical analysis, it was reported that the median survival was 19 months for patients with anaplastic astrocytoma.

Glioblastoma Multiforme

Salvage options for residual or recurrent grade 4 tumors such as glioblastoma multiforme (GBM) are limited by cumulative toxicity and limited efficacy despite advances in surgical, chemotherapeutic, and radiotherapeutic techniques. The survival of patients with glial tumors has not changed significantly. The prognosis for patients with GBM remains poor despite aggressive multimodality management that includes resection when feasible, fractionated radiation therapy (RT), and chemotherapy. Patient survivals are improved when patients are eligible for aggressive resection, radiation therapy, and temozolomide chemotherapy. However, overall medial survival data that include all patients with glioblastoma, regardless of location, have shown little improvement during the last 30 years. The expected five-year survival rate is less than 5% [14] .

The standard management of GBM includes biopsy or cytoreductive surgery followed by FRT and concomitant chemotherapy. Survival without radiation therapy is poor regardless of the extent of the initial tumor resection. The survival advantage afforded by radiation therapy has been documented in prospective trials. Postoperative FRT up to doses of 60 Gy in 30 fractions improves patient survival with limited toxicity [15, 16]. The use of concomitant temozolomide with RT prolonged survival and significantly increased median survivals, although only by an average of 1.5–2 months [17]. Additional Implantation of gliadel wafers resulted in a median improvement in survival of approximately 1.5 months in patients eligible for reoperation [18]. SRS is a minimally invasive management strategy that has been used to provide a targeted additional radiation boost to residual or recurrent tumors. While several retrospective studies have documented a modest survival advantage with the addition of SRS [19–26], other studies found no significant difference in outcomes [27–31]. Although boost SRS has shown benefit in improving survival in patients with recurrent or residual GBMs, it has remained underutilized as part of multimodality management of these patients.

Several retrospective studies have shown survival benefit for patients with recurrent GBMs [32, 33]. Mahajan and associates reported a case control series and found that recurrent GBM patients treated with radiosurgery had longer survival and required fewer surgical procedures compared to controls [34]. Other studies have also documented the potential benefit of SRS in the management of recurrent glioblastoma. Kondziolka and coauthors reported a median survival of 30 months for after GBM patients who underwent radiosurgery at the time of tumor progression [19]. In this study, the median OS after radiosurgery was 16 months. Kong and associates [12] compared the survival of 65 patients who underwent salvage radiosurgery for recurrent GBM and compared their survival to 264 historic controls. These investigators reported significantly longer median overall survival (OS) of 23 months in patients who had radiosurgery compared to 12 months in patients who did not undergo radiosurgery. In a study of 77 patients with recurrent GBM, Skeie and associates reported that patients treated with SRS had significantly longer survival compared to those who had repeat resection [35]. Pouratin and coauthors reported an overall median survival of 16.2 months for 48 glioblastoma patients who underwent SRS [36]. In this study, patients treated at the time of progression had significantly longer median survival compared to those who had SRS as part of the initial treatment paradigm (15.1 versus 7.4 months) [36].

Linear accelerator-based radiosurgery has also been used in the treatment of malignant gliomas [26, 37]. Shrieve and associates performed LINAC-based SRS for 86 GBM patients and reported median actuarial survival of 10.2 months [37]. The 1- and 2-year overall survival rates were 45% and 19%, respectively. In this study, age and tumor volume were considered prognostic factors. In a multicenter study using CyberKnife® (Accuray, Sunnyvale, CA, USA) radiosurgery, the median survival after early SRS was 11.5 months compared to 24 months for patients treated at the time of tumor recurrence or progression [38].

We retrospectively reviewed the prospectively collected data in 297 consecutive patients who underwent GKRS for histologically proven GBM [39]. The median patient age was 58 years (range, 23–89 years). Gross tumor volume (GTV) was defined as the paramagnetic contrast-enhanced tumor margin using T1-weighted MR images. The median GTV was 14 cc (0.26–84.2 cc). The entire GTV was included in the planned isodose volume. The median prescription dose delivered to the tumor margin was 15.0 Gy (9–25 Gy). Local tumor control was achieved in 34% of patients, and delayed tumor growth was documented in 65.6% patients (Fig. 2a–d). The median OS from the date of diagnosis was 18 months. Using multivariate analysis, factors associated with improved overall survival from diagnosis were younger age (<60) at diagnosis, smaller tumor volume (<than 14 cc), SRS at the time of recurrence, and use of prior chemotherapy. Median OS after SRS was 9 months. Median post-radiosurgery OS for patients with tumor volumes <14 cc was 11.2 months. For patients with tumor volumes <14 cc, 1-year, 2-year, 3-year, and 5-year survival after SRS were 47.8%, 23.6%, 11.4%, and 8.1% respectively. Median OS form SRS was significantly better for patients who underwent SRS for progressive tumors (10.2 months) compared to those who had early SRS for residual unresected tumor (8.4 months) (Fig. 3). Using multivariate analysis, factors associated

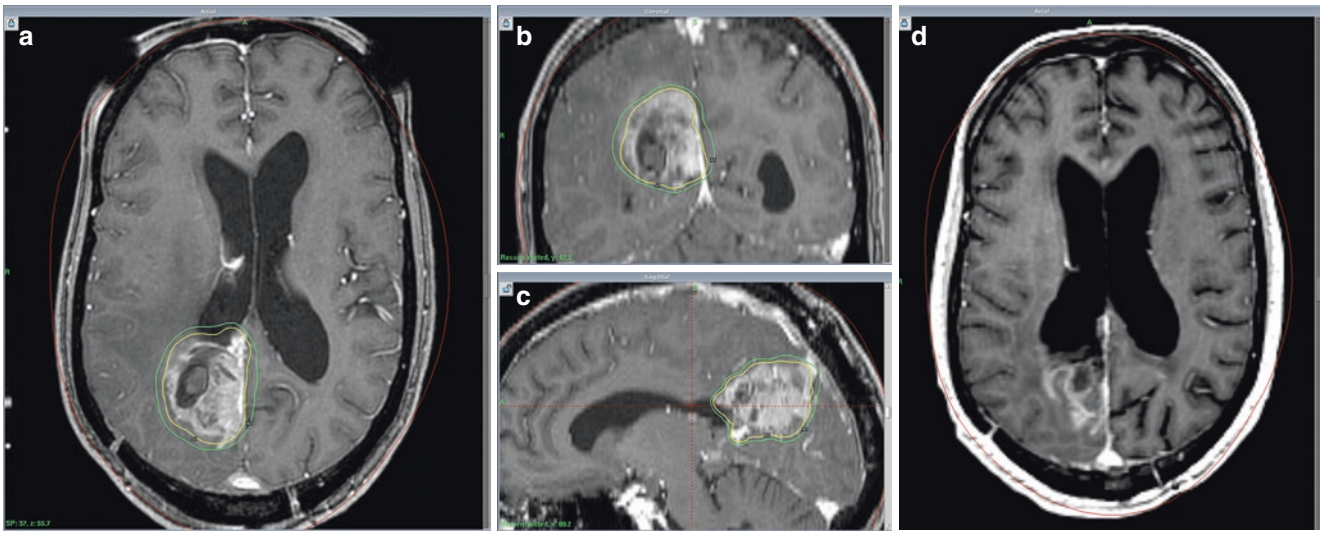

Fig. 2 A 69-year-old man who had undergone resection followed by external-beam radiation therapy along with concomitant temozolomide for management glioblastoma presented with imaging evidence of progressive right parieto-occipital glioblastoma multiforme. He underwent Gamma Knife radiosurgery using a margin dose of 12 Gy to 50% isodose line for a 28 cc tumor volume. Axial contrast-enhanced images (**a**) with coronal (**b**) and sagittal reconstruction (**c**) show a conformal radiosurgery dose plan. A follow-up MRI 4 months after radiosurgery shows regressed enhancing tumor (**d**)

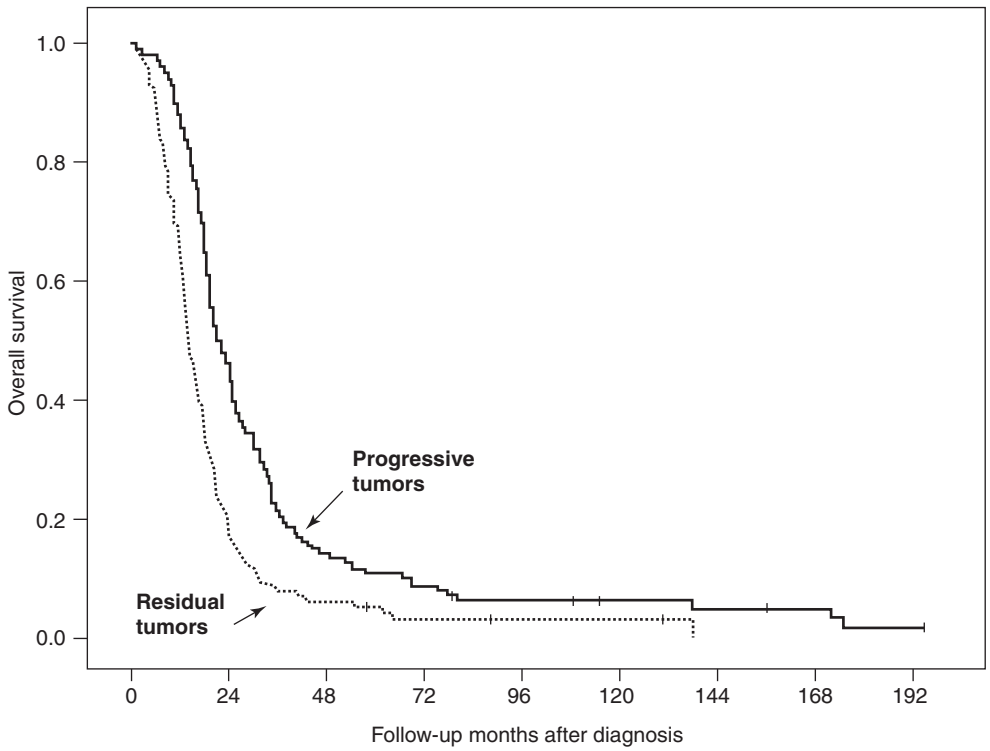

Fig. 3 Radiosurgery performed for GBM at the time of documented tumor progression is associated with improved overall patent survival. Kaplan-Meier estimate shows better overall survival for patients treated with radiosurgery at the time of tumor progression compared with those who underwent radiosurgery for residual tumors

with improved survival after SRS were age <60 years and tumor volume <14 cc. The median PFS was 4.3 months. PFS rates at 1 year, 2 years, 3 years, and 5 years were 29%, 19%, 15%, and 11%, respectively. In univariate analysis, smaller tumor volume (<14 cc) was associated with relatively better progression-free survival ($p = 0.011$). Median PFS for patients with tumors <14 cc was 4.9 months (95% Cl 3.08–6.72) compared to 4 months for patients with tumors 14 cc or larger (Fig. 4). Adverse radiation effects (ARE) were noted in 69 patients (23%) who developed new neurologic signs or symptoms associated with imaging changes.

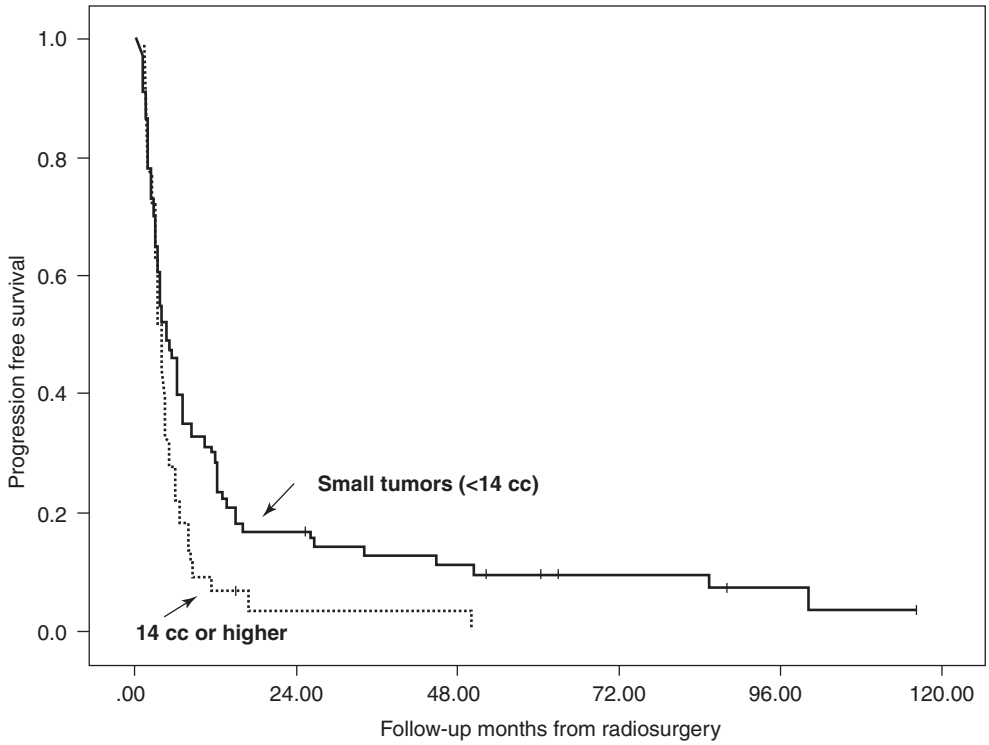

Fig. 4 GBM patients with smaller tumor volume (less than 14 cc) achieve better overall progression-free survival after radiosurgery. Kaplan-Meier estimate showing better progression-free survival for patients with tumors smaller than 14 cc compared to patients with tumors 14 CC or larger

The Controversial Role of SRS for Glioblastoma

The role of radiosurgery in the management of GBM is considered controversial by some oncologists because of their invasive nature and the fact that radiosurgery is a focused treatment. Critics note that the imaging-defined tumor (especially the contrast enhanced tumor) does not correlate with the extent of adjacent tumor cell infiltration in the brain (the same criticism being apropos of surgery). A randomized trial by the RTOG (RTOG 93-05) [40] found no improvement in overall survival (OS) when SRS was given *prior* to conventional RT [41]. This study, however, does not replicate the current standard of care which is surgery, followed by adjuvant FRT, plus temozolomide. In this study, radiosurgery was performed as upfront management even prior to fractionated RT. This study was not designed to evaluate the potential role of SRS at the time of tumor recurrence. The overall analysis of current studies suggests that SRS provides a survival benefit for glioblastoma patients, especially in comparison with alternatives such as additional resection, chemotherapy, or best supportive care [42]. Unfortunately, most studies are limited by the wide variation in technologies used to deliver SRS, target volumes, tumor locations, patient selection, and variation in the SRS doses delivered.

Radiosurgery in Combination with Bevacizumab

In recent years, bevacizumab, a humanized monoclonal antibody to VEGF, has shown promising results in combination with radiosurgery. The rationale for combining bevacizumab and radiotherapy is based on the potential radiosensitizing effect of bevacizumab. This synergistic effect has been proposed on the basis of both the ability of anti-angiogenic agents to normalize blood vessels (thereby reducing tumor hypoxia) and its ability to counteract the effects of radiation-induced VEGF secretion from tumor cells [43–45]. Gutin and associates studied the effect of combining stereotactic radiotherapy and bevacizumab in the management of patients with recurrent malignant glioma [46]. For patients with GBM, the overall tumor response rate was 50%, and median PFS and OS of the patients were 7.3 and 12.5 months, respectively. Cuneo and associates [47] analyzed the outcomes of 49 patients with recurrent GBM in this context. Thirty-three patients received bevacizumab before or after LINAC-based radiosurgery, and 16 patients underwent radiosurgery without bevacizumab. Patients who received radiosurgery followed by bevacizumab therapy had significantly longer progression-free and overall survival compared with patients who had radiosurgery without bevacizumab (median PFS 5.2 vs. 2.1 months; median OS 11.2 vs. 3.9 months).

We evaluated the outcome of 11 patients who underwent bevacizumab therapy after radiosurgery for GBMs and compared these with age- and sex-matched cohorts who had radiosurgery alone [48]. The OS after initial diagnosis was a median of 33.2 months. The median survival from the time of SRS was 17.9 months, and 1- and 2-year survival rates after SRS were 73% and 42%, respectively. The median PFS after SRS was 14.9 months. The 6-month and 1-year PFS rates were 73% and 55%, respectively. Imaging improvement was noted in seven patients (64%). In comparison with controls who underwent radiosurgery alone, patients who were treated with SRS plus bevacizumab had longer PFS and OS. The incidence of AREs in patients who received bevacizumab was significantly lower than our patients who did not receive bevacizumab (9% vs. 46%). Abbassy and coauthors conducted a prospective trial to determine the safety and benefit of higher doses of SRS administered with bevacizumab for recurrent GBM [49]. These authors treated nine patients with bevacizumab followed by SRS and noted that pre-SRS bevacizumab administration was associated with a reduction of the volume of the enhancing lesion (from 4.7 cm^3 to 2.86 cm^3) on the day of SRS. This treatment resulted in a partial response in three patients and stable disease in six patients. Median PFS and OS were 7.5 and 13 months, respectively. In this study, a single pre-SRS dose of bevacizumab allowed for safe prescription dose escalation of up to 22 Gy for recurrent GBM SRS. These findings support the potential benefit of bevacizumab as a means to reduce tumor-related edema and to reduce the incidence of ARE [50]. A phase I/II clinical trial to evaluate the safety and efficacy of border zone radiosurgery in combination with bevacizumab therapy is underway at our institution. Emerging data suggest the safety and efficacy of bevacizumab and radiosurgery either alone or in combination [47, 51, 52].

Conclusion

Despite advances in surgical and postoperative radiation therapy techniques, innovative strategies are needed to improve survival of patients with glial tumors. SRS offers a precise, local administration of radiation. Our 30-year experience with glial tumor radiosurgery suggests that SRS has a favorable survival benefit and is well tolerated. SRS is associated with a relatively low risk of ARE in glial tumor patients who otherwise have relatively few options. Data from retrospective multi-institutional studies suggest that radiosurgery may be a viable alternative for low-grade gliomas, with improved survival and a low rate of complications. Although the prognosis for malignant gliomas is poor even after radiosurgery, radiosurgical treatment allows the surgeon more flexibility in terms of operative planning and subsequently results in better quality of life for patients. Further assessment of SRS for the treatment of malignant gliomas requires prospective, randomized clinical evaluation.

References

1. Elliott RE, Parker EC, Rush SC, Kalhorn SP, Moshel YA, Narayana A, et al. Efficacy of Gamma Knife radiosurgery for small-volume recurrent malignant gliomas after initial radical resection. World Neurosurg. 2011;76:128–40; discussion 61–2.
2. Kano H, Kondziolka D, Niranjan A, Flickinger JC, Lunsford LD. Stereotactic radiosurgery for pilocytic astrocytomas part 1: outcomes in adult patients. J Neuro-Oncol. 2009;95:211–8.
3. Kano H, Niranjan A, Kondziolka D, Flickinger JC, Pollack IF, Jakacki RI, et al. Stereotactic radiosurgery for pilocytic astrocytomas part 2: outcomes in pediatric patients. J Neuro-Oncol. 2009;95:219–29.
4. Hallemeier CL, Pollock BE, Schomberg PJ, Link MJ, Brown PD, Stafford SL. Stereotactic radiosurgery for recurrent or unresectable pilocytic astrocytoma. Int J Radiat Oncol Biol Phys. 2012;83:107–12.
5. Simonova G, Kozubikova P, Liscak R, Novotny J Jr. Leksell Gamma Knife treatment for pilocytic astrocytomas: long-term results. J Neurosurg Pediatr. 2016;18:58–64.
6. Trifiletti DM, Peach MS, Xu Z, Kersh R, Showalter TN, Sheehan JP. Evaluation of outcomes after stereotactic radiosurgery for pilocytic astrocytoma. J Neuro-Oncol. 2017;134:297–302.
7. Kida Y, Kobayashi T, Mori Y. Gamma Knife radiosurgery for low-grade astrocytomas: results of long-term follow up. J Neurosurg. 2000;93(Suppl 3):42–6.
8. Hadjipanayis CG, Niranjan A, Tyler-Kabara E, Kondziolka D, Flickinger JC, Lunsford LD. Stereotactic radiosurgery for well-circumscribed fibrillary grade II astrocytomas: an initial experience. Stereotact Funct Neurosurg. 2002;79:13–24.
9. Wang LW, Shiau CY, Chung WY, Wu HM, Guo WY, Liu KD, et al. Gamma Knife surgery for low-grade astrocytomas: evaluation of long-term outcome based on a 10-year experience. J Neurosurg. 2006;105(Suppl):127–32.
10. Szeifert GT, Prasad D, Kamyrio T, Steiner M, Steiner LE. The role of the Gamma Knife in the management of cerebral astrocytomas. Prog Neurol Surg. 2007;20:150–63.
11. Park KJ, Kano H, Kondziolka D, Niranjan A, Flickinger JC, Lunsford LD. Early or delayed radiosurgery for WHO grade II astrocytomas. J Neuro-Oncol. 2011;103:523–32.
12. Kong DS, Lee JI, Park K, Kim JH, Lim DH, Nam DH. Efficacy of stereotactic radiosurgery as a salvage treatment for recurrent malignant gliomas. Cancer. 2008;112:2046–51.
13. Kohshi K, Yamamoto H, Nakahara A, Katoh T, Takagi M. Fractionated stereotactic radiotherapy using gamma unit after hyperbaric oxygenation on recurrent high-grade gliomas. J Neuro-Oncol. 2007;82:297–303.
14. Mahaley MS Jr, Mettlin C, Natarajan N, Laws ER Jr, Peace BB. National survey of patterns of care for brain-tumor patients. J Neurosurg. 1989;71:826–36.
15. Bleehen NM, Stenning SP. A Medical Research Council trial of two radiotherapy doses in the treatment of grades 3 and 4 astrocytoma. The Medical Research Council Brain Tumour Working Party. Br J Cancer. 1991;64:769–74.

16. Walker MD, Strike TA, Sheline GE. An analysis of dose-effect relationship in the radiotherapy of malignant gliomas. Int J Radiat Oncol Biol Phys. 1979;5:1725–31.
17. Stupp R, Mason WP, van den Bent MJ, Weller M, Fisher B, Taphoorn MJ, et al. Radiotherapy plus concomitant and adjuvant temozolomide for glioblastoma. N Engl J Med. 2005;352:987–96.
18. Westphal M, Hilt DC, Bortey E, Delavault P, Olivares R, Warnke PC, et al. A phase 3 trial of local chemotherapy with biodegradable carmustine (BCNU) wafers (Gliadel wafers) in patients with primary malignant glioma. Neuro-Oncology. 2003;5:79–88.
19. Kondziolka D, Flickinger JC, Bissonette DJ, Bozik M, Lunsford LD. Survival benefit of stereotactic radiosurgery for patients with malignant glial neoplasms. Neurosurgery. 1997;41:776–83; discussion 83–5.
20. Loeffler JS, Alexander E 3rd, Shea WM, Wen PY, Fine HA, Kooy HM, et al. Radiosurgery as part of the initial management of patients with malignant gliomas. J Clin Oncol. 1992;10:1379–85.
21. Loeffler JS, Alexander E 3rd, Wen PY, Shea WM, Coleman CN, Kooy HM, et al. Results of stereotactic brachytherapy used in the initial management of patients with glioblastoma. J Natl Cancer Inst. 1990;82:1918–21.
22. Mehta MP, Masciopinto J, Rozental J, Levin A, Chappell R, Bastin K, et al. Stereotactic radiosurgery for glioblastoma multiforme: report of a prospective study evaluating prognostic factors and analyzing long-term survival advantage. Int J Radiat Oncol Biol Phys. 1994;30:541–9.
23. Nwokedi EC, DiBiase SJ, Jabbour S, Herman J, Amin P, Chin LS. Gamma Knife stereotactic radiosurgery for patients with glioblastoma multiforme. Neurosurgery. 2002;50:41–6; discussion 6–7.
24. Prisco FE, Weltman E, de Hanriot RM, Brandt RA. Radiosurgical boost for primary high-grade gliomas. J Neuro-Oncol. 2002;57:151–60.
25. Sarkaria JN, Mehta MP, Loeffler JS, Buatti JM, Chappell RJ, Levin AB, et al. Radiosurgery in the initial management of malignant gliomas: survival comparison with the RTOG recursive partitioning analysis. Radiation Therapy Oncology Group. Int J Radiat Oncol Biol Phys. 1995;32:931–41.
26. Shrieve DC, Alexander E 3rd, Black PM, Wen PY, Fine HA, Kooy HM, et al. Treatment of patients with primary glioblastoma multiforme with standard postoperative radiotherapy and radiosurgical boost: prognostic factors and long-term outcome. J Neurosurg. 1999;90:72–7.
27. Cho KH, Hall WA, Lo SS, Dusenbery KE. Stereotactic radiosurgery versus fractionated stereotactic radiotherapy boost for patients with glioblastoma multiforme. Technol Cancer Res Treat. 2004;3:41–9.
28. Gannett D, Stea B, Lulu B, Adair T, Verdi C, Hamilton A. Stereotactic radiosurgery as an adjunct to surgery and external beam radiotherapy in the treatment of patients with malignant gliomas. Int J Radiat Oncol Biol Phys. 1995;33:461–8.
29. Larson DA, Gutin PH, McDermott M, Lamborn K, Sneed PK, Wara WM, et al. Gamma Knife for glioma: selection factors and survival. Int J Radiat Oncol Biol Phys. 1996;36:1045–53.
30. Selker RG, Shapiro WR, Burger P, Blackwood MS, Arena VC, Gilder JC, et al. The Brain Tumor Cooperative Group NIH Trial 87-01: a randomized comparison of surgery, external radiotherapy, and carmustine versus surgery, interstitial radiotherapy boost, external radiation therapy, and carmustine. Neurosurgery. 2002;51:343–55; discussion 55–7.
31. Shenouda G, Souhami L, Podgorsak EB, Bahary JP, Villemure JG, Caron JL, et al. Radiosurgery and accelerated radiotherapy for patients with glioblastoma. Can J Neurol Sci. 1997;24:110–5.
32. Curran WJ Jr, Scott CB, Weinstein AS, Martin LA, Nelson JS, Phillips TL, et al. Survival comparison of radiosurgery-eligible and -ineligible malignant glioma patients treated with hyperfractionated radiation therapy and carmustine: a report of Radiation Therapy Oncology Group 83-02. J Clin Oncol. 1993;11:857–62.
33. Irish WD, Macdonald DR, Cairncross JG. Measuring bias in uncontrolled brain tumor trials--to randomize or not to randomize? J Can Sci Neurol. 1997;24:307–12.
34. Mahajan A, McCutcheon IE, Suki D, Chang EL, Hassenbusch SJ, Weinberg JS, et al. Case-control study of stereotactic radiosurgery for recurrent glioblastoma multiforme. J Neurosurg. 2005;103:210–7.
35. Skeie BS, Enger PO, Brogger J, Ganz JC, Thorsen F, Heggdal JI, et al. Gamma Knife surgery versus reoperation for recurrent glioblastoma multiforme. World Neurosurg. 2012;78:658–69.
36. Pouratian N, Crowley RW, Sherman JH, Jagannathan J, Sheehan JP. Gamma Knife radiosurgery after radiation therapy as an adjunctive treatment for glioblastoma. J Neuro-Oncol. 2009;94:409–18.
37. Shrieve DC, Alexander E 3rd, Wen PY, Fine HA, Kooy HM, Black PM, et al. Comparison of stereotactic radiosurgery and brachytherapy in the treatment of recurrent glioblastoma multiforme. Neurosurgery. 1995;36:275–82; discussion 82–4.
38. Villavicencio AT, Burneikiene S, Romanelli P, Fariselli L, McNeely L, Lipani JD, et al. Survival following stereotactic radiosurgery for newly diagnosed and recurrent glioblastoma multiforme: a multicenter experience. Neurosurg Rev. 2009;32:417–24.
39. Niranjan A, Kano H, Iyer A, Kondziolka D, Flickinger JC, Lunsford LD. Role of adjuvant or salvage radiosurgery in the management of unresected residual or progressive glioblastoma multiforme in the pre-bevacizumab era. J Neurosurg. 2015;122:757–65.
40. Souhami L, Seiferheld W, Brachman D, Podgorsak EB, Werner-Wasik M, Lustig R, et al. Randomized comparison of stereotactic radiosurgery followed by conventional radiotherapy with carmustine to conventional radiotherapy with carmustine for patients with glioblastoma multiforme: report of Radiation Therapy Oncology Group 93-05 protocol. Int J Radiat Oncol Biol Phys. 2004;60:853–60.
41. Kondziolka D, Lunsford LD, Flickinger JC. In regard to Dr. Souhami et al. (Int J Radiat Oncol Biol Phys. 2004;60:853–60). Int J Radiat Oncol Biol Phys. 2005;62:614–5; author reply 5–6.
42. Tsao MN, Mehta MP, Whelan TJ, Morris DE, Hayman JA, Flickinger JC, et al. The American Society for Therapeutic Radiology and Oncology (ASTRO) evidence-based review of the role of radiosurgery for malignant glioma. Int J Radiat Oncol Biol Phys. 2005;63:47–55.
43. Hovinga KE, Stalpers LJ, van Bree C, Donker M, Verhoeff JJ, Rodermond HM, et al. Radiation-enhanced vascular endothelial growth factor (VEGF) secretion in glioblastoma multiforme cell lines--a clue to radioresistance? J Neuro-Oncol. 2005;74:99–103.
44. Nieder C, Wiedenmann N, Andratschke N, Molls M. Current status of angiogenesis inhibitors combined with radiation therapy. Cancer Treat Rev. 2006;32:348–64.
45. Wachsberger PR, Burd R, Cardi C, Thakur M, Daskalakis C, Holash J, et al. VEGF trap in combination with radiotherapy improves tumor control in u87 glioblastoma. Int J Radiat Oncol Biol Phys. 2007;67:1526–37.
46. Gutin PH, Iwamoto FM, Beal K, Mohile NA, Karimi S, Hou BL, et al. Safety and efficacy of bevacizumab with hypofractionated stereotactic irradiation for recurrent malignant gliomas. Int J Radiat Oncol Biol Phys. 2009;75:156–63.
47. Cuneo KC, Vredenburgh JJ, Sampson JH, Reardon DA, Desjardins A, Peters KB, et al. Safety and efficacy of stereotactic radiosurgery and adjuvant bevacizumab in patients with recurrent malignant gliomas. Int J Radiat Oncol Biol Phys. 2012;82:2018–24.
48. Park KJ, Kano H, Iyer A, Liu X, Niranjan A, Flickinger JC, et al. Salvage Gamma Knife stereotactic radiosurgery followed by bevacizumab for recurrent glioblastoma multiforme: a case-control study. J Neuro-Oncol. 2012;107(2):323–33.

49. Abbassy M, Missios S, Barnett GH, Brewer C, Peereboom DM, Ahluwalia M, et al. Neurosurgery. 2018;83(3):385–92.
50. Silbergeld DL, Chicoine MR. Isolation and characterization of human malignant glioma cells from histologically normal brain. J Neurosurg. 1997;86:525–31.
51. Cabrera AR, Cuneo KC, Desjardins A, Sampson JH, McSherry F, Herndon JE 2nd, et al. Concurrent stereotactic radiosurgery and bevacizumab in recurrent malignant gliomas: a prospective trial. Int J Radiat Oncol Biol Phys. 2013;86:873–9.
52. Cabrera AR, Cuneo KC, Vredenburgh JJ, Sampson JH, Kirkpatrick JP. Stereotactic radiosurgery and bevacizumab for recurrent glioblastoma multiforme. J Natl Compr Cancer Netw: JNCCN. 2012;10:695–9.

Part IV

Stereotactic Body Radiation Therapy Technique

Physics of Stereotactic Body Radiotherapy

Young Lee, Arman Sarfehnia, and Mark Ruschin

Introduction

"Stereotactic body radiotherapy" (SBRT)—also referred to as "stereotactic ablative body radiotherapy" (SABR)—is a precise radiotherapy technique in which accurate target localization combined with a high dose per fraction is used to treat certain tumors within the body in up to five fractions [1]. The term *stereotactic* in the present context refers to the target-centric nature of SBRT, in which online imaging is used to place the tumor at its intended location. SBRT targets are typically small, which minimizes dose-volume-related adverse effects in normal tissue. SBRT can be used in multiple organ sites [2]. The term *body* refers to the fact that SBRT excludes intracranial disease, which has its own dedicated technique, stereotactic radiosurgery (SRS), which is discussed in another chapter. SBRT and SRS employ similar concepts for achieving high accuracy and precision. However, SRS has historically remained distinct and uses ultra-small fields, sometimes as narrow as 4 mm, as used in Gamma Knife® (Elekta AB, Stockholm, Sweden).

The characteristics of an SBRT-like dose distribution include steep dose gradient, high conformality, and heterogeneous dose distribution within the target (Fig. 1). Whereas the radiobiological basis for SBRT is Discussed in Part I, the success of SBRT depends on solving several technical and physics-based challenges: minimization sources of uncertainty in order to minimize PTV margin; complex planning and delivery; and achieving accurate small field dosimetry [3, 4]. As outlined in the ACR-ASTRO practice parameter and in the AAPM-RSS Medical Physics Practice Guideline, the medical physicist's responsibilities in SBRT include technical aspects, acceptance testing and commissioning, managing quality assurance, developing standard operating procedures, and overseeing dosimetric treatment planning processes [3]. In this chapter, we will briefly elaborate on the physics issues of SBRT.

Uncertainties and Margins

In order to safely achieve the high doses to the target required for SBRT, accurate target localization is imperative; otherwise, the PTV margin needed to ensure target coverage is too large and prohibits satisfying organ-at-risk (OAR) tolerances. Systematic uncertainties can lead to missing all (e.g., positional errors) or part (e.g., delineation uncertainty) of the target. Random errors tend to lead a blurring of the dose distribution compared to what was planned. The following sections briefly describe sources of uncertainty that could factor into determination of PTV margin.

Localization Accuracy, Patient Stability, and Baseline Shifts

Reproducible patient positioning is essential for accurate delivery of dose to the target. Patient positioning/immobilization devices—such as masks, arm positioning devices, vacuum cushions, etc.—are used to place the patient in the same position as planned and can reduce inter-fraction and intra-fraction setup errors. Online image guidance in the form of volumetric cone-beam CT (CBCT) has allowed for quantification and mitigation of many sources of random and systematic positional uncertainty. However, the target itself typically has limited or no visibility on CBCT; therefore, assessing localization accuracy can only be done via implanted marker or using bony surrogates. Bony landmarks

Y. Lee · A. Sarfehnia · M. Ruschin (✉)
Sunnybrook Health Sciences Centre, Department of Radiation Oncology, Toronto, ON, Canada

University of Toronto, Department of Radiation Oncology, Toronto, ON, Canada
e-mail: mark.ruschin@sunnybrook.ca

D. M. Trifiletti et al. (eds.), *Stereotactic Radiosurgery and Stereotactic Body Radiation Therapy*,
https://doi.org/10.1007/978-3-030-16924-4_17

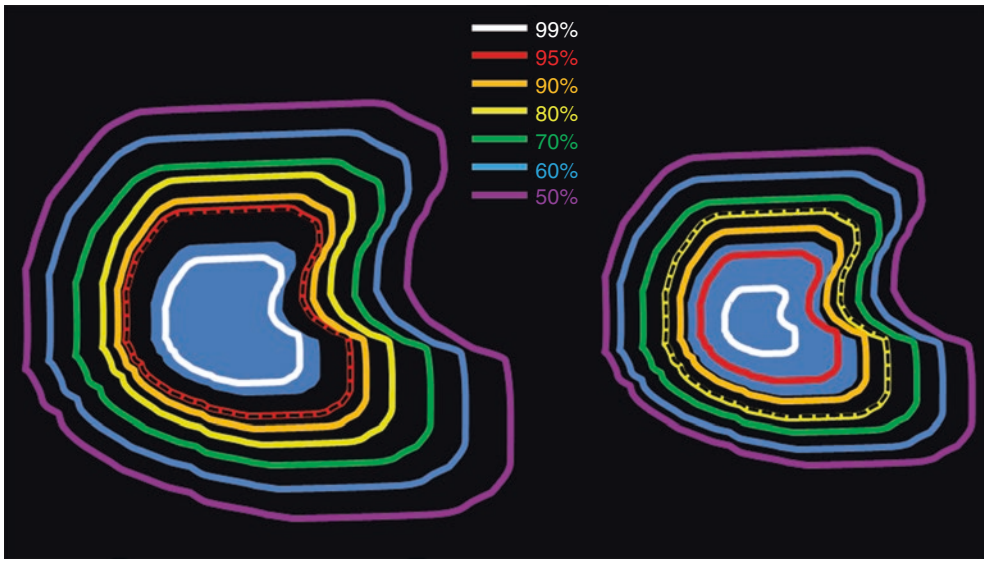

Fig. 1 Graphical illustration of a conventional (left) versus SBRT-like (right) dose distribution. The GTV in both cases is illustrated as a blue color wash. The PTV is a dashed black line. The simulated plans are normalized such that the hot spot is 100% in both cases. For the conventional case, the 95% isodose line covers the PTV and the dose profile is fairly flat within the target. In the SBRT plan, the 80% isodose line covers the PTV and the dose is fairly heterogeneous within the target

are often poor surrogates for tumor position, as baseline shifts (changes in the distance between tumor and bone) are quite common due to tumor changes, organ deformations, etc. The assessment of uncertainties and margins must be done in conjunction with the immobilization device being used for each site.

Respiratory Motion

As also discussed in the following chapters, respiratory motion is of particular concern in SBRT, as the degree of motion limits the extent to which one can precisely deliver high doses of radiation. Motion management strategies range in complexity and include internal target volume (ITV) generation, population-based approaches (e.g., mid ventilation), gating, breath hold, abdominal compression, and tracking [5–7]. For free-breathing approaches, 4D-CT is indicated for simulation, as substantial errors may result by using a conventional 3D scan during free breathing [8–10]. With 4D-CT, the ITV approach is the simplest motion management approach, in that no additional hardware or software is required. As discussed in the next chapter, the mid-ventilation approach is also gaining popularity, specifically for the lung and liver [11, 12].

Target Delineation

Although it is the role of radiation oncologist to delineate the tumor and organs-at-risk (OARs), inter- and intra-observer variation can lead to systematic errors in what dose tumor cells receive. Given that online image guidance has led to a reduction in localization uncertainties, contouring variability may now be one of the primary sources of uncertainty that faces SBRT. This has been investigated in the context of the lung, as well as spine [13–15]. As shown in Fig. 2, the variation between observers in contouring the GTV in the lung and spine can be substantial.

Machine-Related Uncertainties

With SBRT employing small field sizes and steep dose gradients, there is an increased susceptibility to machine-related uncertainties. Small-field dosimetry is a special topic demanding its own focus and is discussed in section "Small-Field Dosimetry". However, other sources of mechanically related linac-based uncertainty include isocenter variation and multi-leaf collimator (MLC) positioning accuracy [16].

Isocenter variation has been a common area of focus in the linac-based SRS field for several decades, and the principles are the same for SBRT, except that MLCs are the tertiary collimation system for linac-based SBRT rather than stereotactic cones. Non-ideality in gantry rotation caused by gravity (gantry "sag") results in a radiation field center (RFC) wobble primarily along the gun-to-target direction. Other factors such as wear on the machine and collimator misalignment can also contribute to isocenter variation. The "true" isocenter of the machine can be thought of as the averaged center of RFCs over the entire rotational space, including collimator and couch rotations. The variation can be described by a bounding sphere, which is defined by the minimum diameter needed to contain all of the RFCs. For sharp fields and accurate target positioning, international guidelines recommend submillimeter diameter isocenter variation be maintained on SBRT linacs [16, 17]. The isocenter variation can be measured using various methods adopted from the SRS literature and is often reproducible on and among linacs of the same vendor (Fig. 3) [18–22].

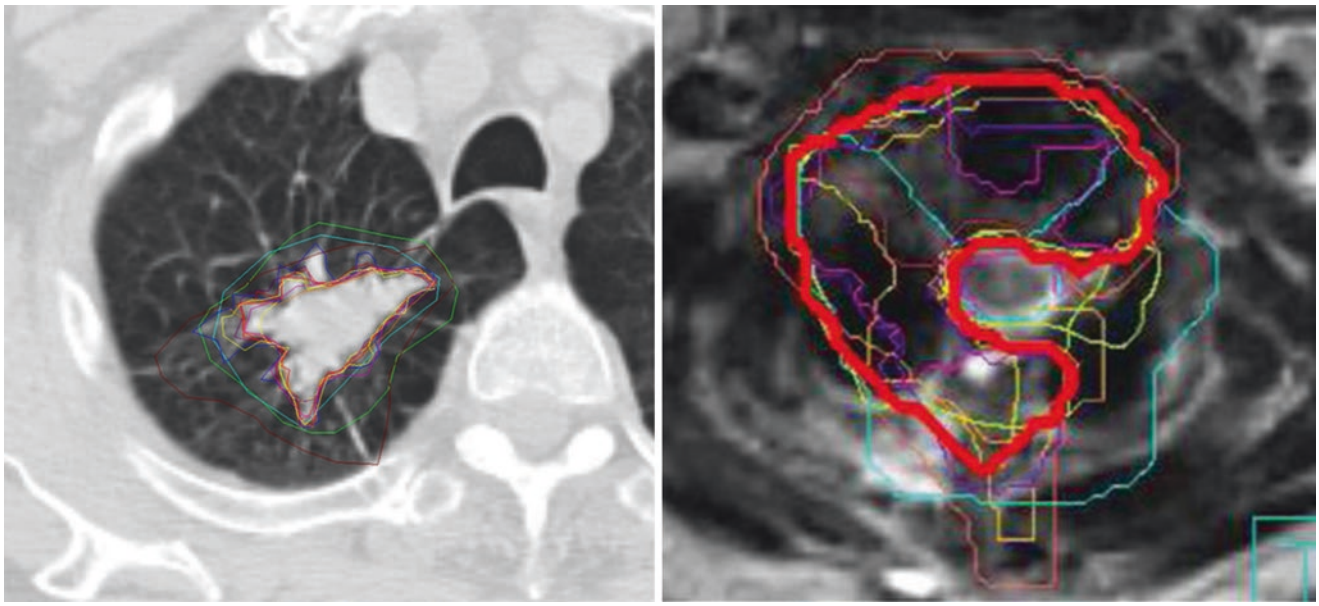

Fig. 2 Examples of target delineation uncertainty in two SBRT sites. Left panel: Lung SBRT example. Each contour represents a different observer. Right panel: Spine SBRT example. Each contour represents a different observer, and the thick red line is the consensus-generated contour. (Left panel, Used with permission of Elsevier from Peulen et al. [13]; right panel, Used with permission of Elsevier from Redmond et al. [14])

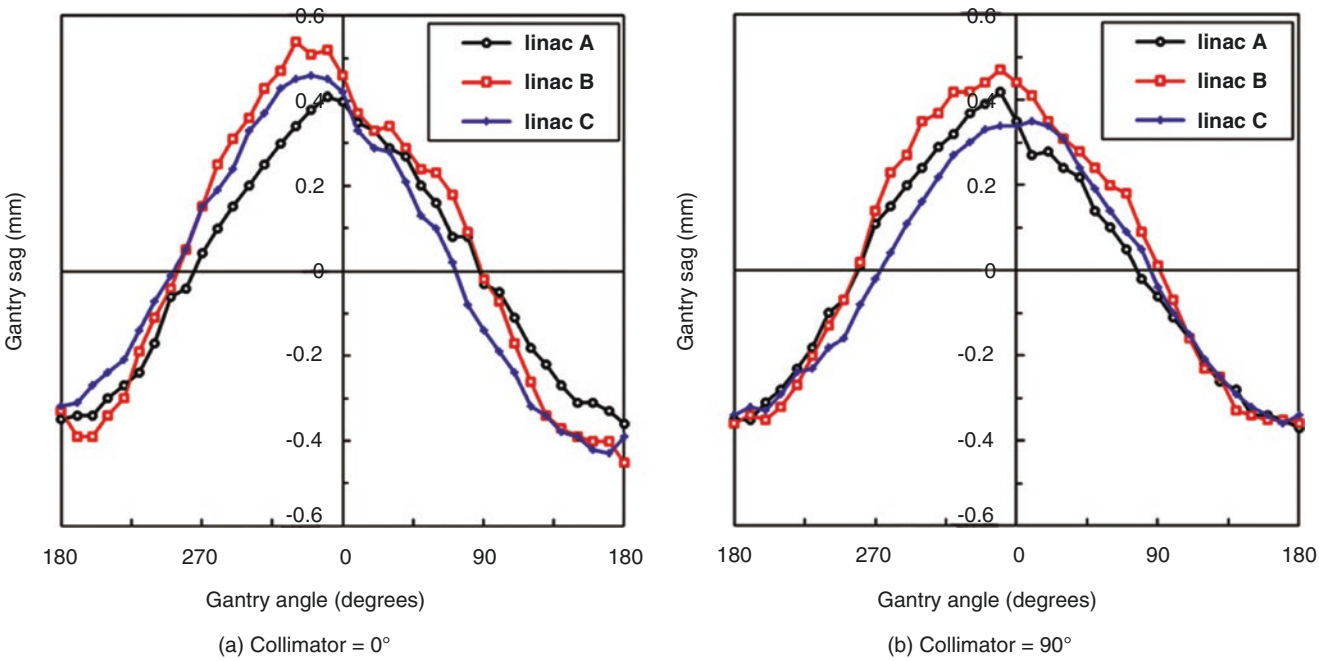

Fig. 3 Gantry sag (in mm) plotted as a function of gantry angle for three linacs exhibiting similar mechanical performance. (Used with permission of John Wiley and Sons from Du et al. [18])

Another source of mechanical uncertainty is MLC-positioning error. The MLC leaves are individually calibrated, and modern linacs have optically based feedback mechanisms to ensure each leaf is correctly positioned during treatment delivery. However, it is vital that the MLCs be checked routinely for accurate positioning, since errors of only 1 millimeter (mm) can lead to systematic increase or decrease in dose by 2–5% or cause the entire distribution to shift [23, 24]. MLC positional accuracy can be tested in a variety of ways, most commonly using a variation of the so-called

"picket fence" test [25, 26]. The tolerance for MLC positional accuracy for SBRT/SRS applications using IMRT or VMAT is 1 mm [16].

Imaging-Related Uncertainties

Image-guided radiotherapy (IGRT) has been the primary technology to minimize positional uncertainties and facilitate SBRT. The primary IGRT modality has been CBCT using an orthogonally mounted kV x-ray tube and detector system that rotates with gantry rotation [27]. Although the CBCT system calculates the shift of the patient relative to the linac isocenter, if the CBCT system is miscalibrated, the patient may be shifted to an incorrect position, which would have adverse dosimetric consequences. Therefore, the calibration of the CBCT is a systematic source of uncertainty requiring a dedicated quality assurance program [28, 29].

Another major area of imaging for SBRT concerns the increasing role of MRI in radiation oncology [30]. Although MRI enhances tumor and OAR definition compared to CT, artifacts such as those caused by geometric distortion are of primary concern in radiation oncology, where one is trying to achieve submillimeter accuracy. As emerging technologies such as integrated MRI-linacs start to become widely available, there will be a stronger emphasis on quality assurance of MRI equipment [30–32].

Treatment Planning and Delivery

Beam Geometry

In SBRT, the selection of beam geometry has been the focus of much attention in the literature. As sketched in Fig. 4, there are various techniques to optimize radiation dose conformality and achieve the steepest dose falloff. The use of non-coplanar, multiple beam, or arc geometry (both in IMRT and VMAT deliveries) with large solid angles between each beam has been demonstrated to achieve steep dose falloffs

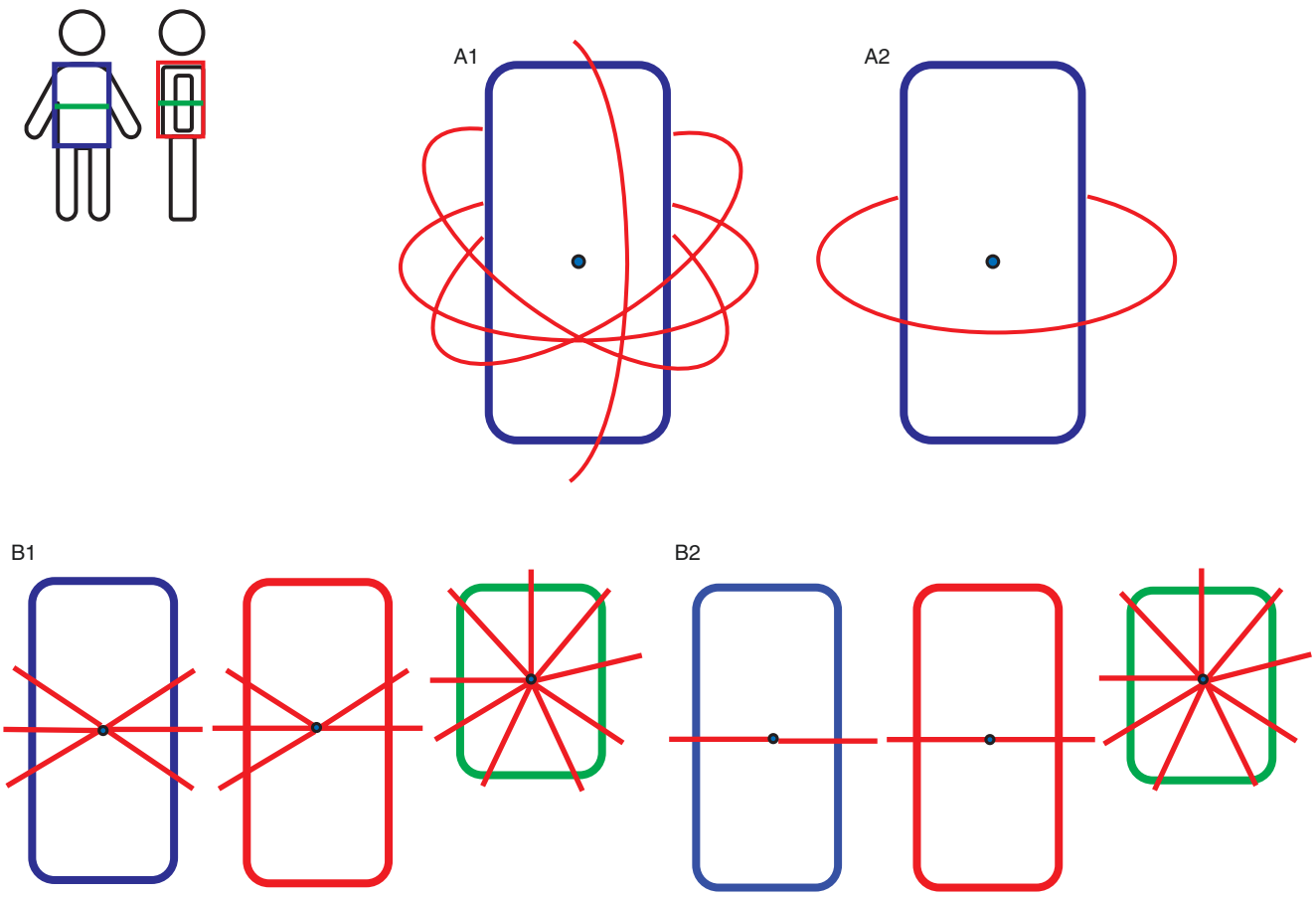

Fig. 4 The cartoon illustrations show coronal (blue), sagittal (orange), and axial (green) view of patient with the arcs and beams shown in red. This diagram assumes the patient will be lying on the couch supine with the head toward the gantry and the isocenter will be placed around the mid-section of the patient (illustrated as a blue dot). A1 and A2 views illustrate some of the allowable VMAT non-coplanar and coplanar geometries, respectively. B1 view shows the coronal, sagittal, and axial views of non-coplanar IMRT beams. B2 view shows the coronal, sagittal, and axial views of coplanar IMRT beams

[33]. However, as discussed earlier, the mechanical accuracy of the couch rotation must undergo stringent quality assurance testing, and practical issues such as collisions must be considered; see section on practical considerations.

Delivery Technology

There are multiple machines that are capable of delivering SBRT, most commonly linear accelerators (linacs), CyberKnife (linac mounted on robotic arm), and Tomotherapy units. Linacs offer flexibility in terms of delivering radiation dose across multiple anatomical sites and are also widely available in most radiation oncology clinics. The use of VMAT and FFF beams in SBRT has greatly reduced treatment times [34, 35].

Treatment Planning Systems

Treatment planning system beam models must reflect the small fields that are required for SBRT [36–39]. Most modern treatment planning systems employ dose calculation algorithms that account for lateral electron disequilibrium, and this is a basic requirement for SBRT as older systems using pencil-beam-based approaches can misrepresent lung/tumor dose distributions by as much as 30% [40]. SBRT should make use of advanced photon dose-calculation techniques that are either Monte-Carlo based or use Monte Carlo pre-calculated dose-spread kernels and employ convolution/superposition techniques. Although in the latter case, the inhomogeneity correction is still approximate, by taking into account recoil electron transport, relatively accurate results can be obtained [41, 42]. The beam model must also be accurate for off-axis dose calculation to account for lateral displacement of the isocenter from the midline of the patient by 5–8 cm, as this is not unusual.

Collimation System

The MLC leaf thickness used for SBRT is generally 5 mm or less. Although smaller leaf thicknesses provide a higher degree of dose shaping, there are limited data demonstrating benefits of using less than 5 mm for most sites [43, 44]. There are varying sizes of linac MLCs available in the market (e.g., HD120, Varian, uses 2.5 mm MLC thickness) and also external micro-MLCs that can be mounted onto the linac head (e.g., AccuLeaf). Other factors in addition to leaf thickness will ultimately effect the resulting penumbra and conformality, and these include proximity of collimation system to patient, leaf speed, and ability to interdigitate [45].

Prescription Dose: Effect of Dose Heterogeneity

For SBRT, the collimator margin is smaller than in conventional fractionated treatments, and thus a lower isodose line

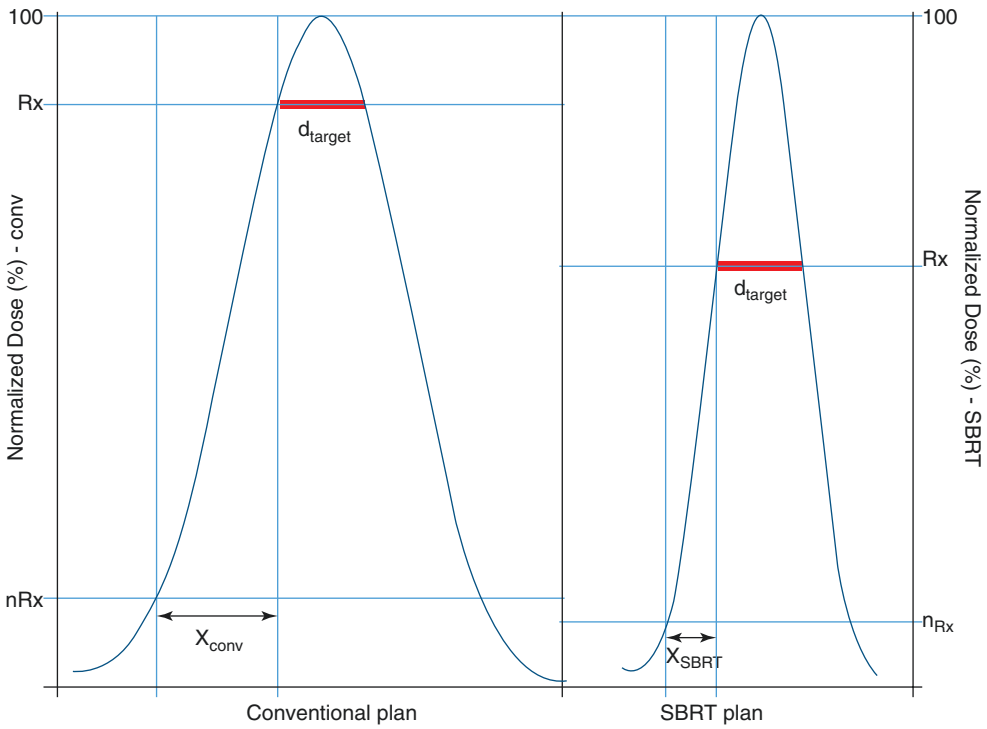

Fig. 5 The graphs illustrate a simplified version of a normalized dose profile across the patient where the diameter of the target volume (d_{target}) is illustrated in red. The left graph shows the isodose line that would be typically chosen as the prescription dose (Rx) for a conventional plan (usually >90%) and the right graph illustrates the typical prescription dose (Rx) isodose line that would be chosen for an SBRT plan. (Here, it is shown as approximately 60%)

is often used to prescribe treatments (Fig. 5). This equates to a relatively higher maximum point dose within the target volume and is different from the International Commission on Radiation Units and Measurements (ICRU) recommendation in conventional treatments of achieving >95% prescription dose and minimizing D_2% [46]. High maximum dose is of less concern in SBRT, as the volumes treated are small and achieving a higher gradient is considered of higher importance, and some guidance on reporting SBRT doses can be found in the recently published ICRU 91 [47]. As illustrated in Fig. 5, the use of a different prescribing methodology yields a narrower penumbra ($x_{SBRT} < x_{conv}$) for the same target size (d_{target}), thus lowering dose to surrounding normal tissue and achieving a steep falloff of dose.

Practical Considerations

The practice of non-coplanar beams (Fig. 4) requires attention due to the increased chance of machine-patient or machine-immobilization system collisions [48]. Furthermore, complicated beam/arc geometries usually equate to difficult treatment delivery with long treatment times. This can cause patient discomfort, which can lead to inaccurate treatment delivery, as well as requiring a more stringent intra-fractional monitoring. For both non-coplanar multiple-arc VMAT and non-coplanar IMRT, the gantry-couch rotation combinations must be carefully adopted taking into account patient anatomy, accessories, target location/laterality, and couch height. For large couch rotations (>45°) in conjunction with posterior beams/arcs, a pretreatment setup verification is useful. This can be done by setting up the immobilization system without the patient present (e.g., the formed vacloc system) using mock setup to test for collision. This is a limited test, as without the patient, patient-machine collision may be difficult to assess.

Radiation beams must avoid many parts of immobilization systems, which may be made of high-density material [47], where the modeling of the dose is not accurate and the insufficient delivery of the dose to target can occur [49]. Some common high-density materials present for SBRT occur within compression plates and metal reinforcements on couches, and avoidance of these devices further reduces the range of acceptable angles.

In conclusion, the choice of planning geometry, delivery system (including MLC size), and prescription method are factors in planning for SBRT. Practical considerations such as balancing treatment time with beam geometry and plan quality must be made to tailor the plan for each patient. Considerations can only be made if one is an expert in planning and understands all the physics that play a role in SBRT planning. A physicist is usually involved throughout the simulation-planning-treatment process and can guide staff to try and optimize the treatment procedure.

Small-Field Dosimetry

Given the routine use of complex, composite, and modulated small fields in SBRT, accurate dosimetry in small fields is very important. Challenges arise due to loss of lateral electronic equilibrium, dose-volume averaging, detector-interface artifacts, collimator effects, and detector position-orientation effects [17].

According to the recently published joint report of the International Atomic Energy Agency (IAEA) and AAPM on dosimetry of small static fields used in external beam radiotherapy, an MV external photon beam can be designated as small if one or more of the following three physical conditions are satisfied [50]:

1. Lateral charge particle equilibrium (CPE) is lost (i.e., dimensions of the field are comparable or smaller than the range of lateral secondary electrons).
2. Primary photon source is partially occluded by the collimating devices.
3. The size of the detector is similar to or larger than the beam dimensions.

Although the first two conditions are beam related and put a limit of around 10 mm on a 6 MV linac-produced photon beam [51], the third condition is detector related and can differ based on the choice of the detector. Doblado and colleagues showed in 2007 the importance of the choice of the detector in small field dosimetry [52]. They observed response differences for the various detectors for field sizes less than 3.0 cm, with deviations in excess of 50% for very small fields less than 10 mm when inappropriate detectors such as large-volume ionization chambers are used.

Over the past decade, following many thorough studies on small-field dosimetry effects, and based on the formalism proposed by Alfonso and colleagues [53], several national and international societies have begun working on small-field dosimetry guidelines. Most notably, some of these reports include the AAPM Task Group 155 report on small-field photon beam dosimetry; the aforementioned joint IAEA-AAPM TRS 483 report [50]; the International Commission on Radiation Units and Measurements (ICRU) report 91 on prescribing, recording, and reporting of stereotactic treatments with small photon beams [47]; and the report 103 of the Institute of Physics and Engineering in Medicine (IPEM) on small-field MV photon dosimetry [54].

Reference Dosimetry

Currently, AAPM Task Group 51 protocol [55] and its update [56], as well as the IAEA TRS-398 [57], form the basic formalism for clinical reference dosimetry. These protocols

require reference condition (10 × 10 cm^2 field size, 100 cm source to axis or source to surface distance, etc.) and do not encompass such delivery units as CyberKnife or Tomotherapy, which cannot produce these. In such cases, the proposed remedy is to use a so-called machine-specific reference field (MSR field) which is an intermediate stationary field deliverable by the specific unit that most closely resembles the reference conditions. The larger the difference between the MSR field and the reference field and reference conditions (i.e., calibration conditions of the detector), the larger the potential differences in the beam quality and variations in detector response. It is the physicist's responsibility first to ensure use of appropriate reference-caliber detectors for the given MSR field and, second, to make sure to apply appropriate beam quality correction factors to account for differences between the MSR and the reference field/conditions.

The reference conditions for a few common SBRT units are noted below:

- For *linear accelerator-based SBRT* programs, the reference conditions should be taken as the conventional 10 × 10 cm^2 square reference field at 100 cm from the source (or a field as close to this as possible; e.g., 9.6 × 10.4 cm^2 field if the MLC does not allow for an exact 10 × 10 cm^2 setting). All other collimator settings and field sizes are calibrated through relative dosimetry.
- For *CyberKnife*, the 60 mm diameter-fixed collimator (80 cm from the source) provides a relatively flat and uniform field that normally is recommended as the MSR field.
- If *Tomotherapy* is used for small target therapy, the 5 × 10 cm^2 field size (85 cm from the source) is the recommended MSR field.
- Although integrated MRI and linac systems are just being introduced to the community at the time of the writing, in addition to obtaining the proper MSR field in such cases, the effects of the magnetic field must be quantified. There are currently no published guidelines for dosimetry in such units, although a few groups have studied the effects [58].

Relative Dosimetry

Relative dosimetry is the measurement of the relationship between absorbed dose to water at a point in any non-reference conditions to that determined under reference conditions. Although in large fields, often the ratio of the detector reading (instead of absorbed dose) is used without any significant clinical implications, the same approximation may result in devastatingly large errors in small fields. Indeed, as pointed out earlier, the detector response can vary as a function of field size with larger effects at smaller field sizes. As a general practice, the difference between detector response in the MSR field relative to that in reference field has to be taken into account, for example, using Monte Carlo calculated corrections [59]. Proper alignment and orientation of the detector with respect to the field are also important to consider in relative small-field dosimetry. In the case of small fields, higher tolerances than 1 mm in positioning need to be exercised, while as a general rule, the detector's sensitive volume's smallest dimension should be perpendicular to the scanning direction. Care must be taken as several of the small-field detectors are not perfectly symmetrical, or they may show response differences based on the amount of stem/cable irradiation due to small volume [50].

Detector Selection

Care must be taken in selection of the appropriate measuring device to avoid such issues as volume-averaging effect and beam perturbations. For relative dosimetry, a number of dosimeters have been used in SBRT fields, including small-volume ionization chambers [60], micro-ionization chamber [61], liquid ionization chambers [62], diamond detectors [63], silicon diodes [64], plastic and organic scintillators [65], radiochromic and radiographic films [65], metal-oxide semiconductor filed effect transistors (MOSFET) [66], thermoluminescent dosimeters (TLD) [64], optically stimulated luminescence (OSL) detectors [67], alanine detectors [68], and polymer gels [69].

References

1. American College of Radiology. ACR-ASTRO practice parameter for the performance of stereotactic body radiation therapy, amended. 2014.
2. Timmerman RD, Kavanagh BD, Cho LC, Papiez L, Xing L. Stereotactic body radiation therapy in multiple organ sites. J Clin Oncol. 2007;25(8):947–52.
3. Halvorsen PH, Cirino E, Das IJ, Garrett JA, Yang J, Yin FF, et al. AAPM-RSS medical physics practice guideline 9.a. for SRS-SBRT. J Appl Clin Med Phys. 2017;18(5):10–21.
4. Das IJ, Ding GX, Ahnesjö A. Small fields: nonequilibrium radiation dosimetry. Med Phys. 2008;35(1):206–15.
5. Wulf J, Hädinger U, Oppitz U, Olshausen B, Flentje M. Stereotactic radiotherapy of extracranial targets: CT-simulation and accuracy of treatment in the stereotactic body frame. Radiother Oncol. 2000;57(2):225–36.
6. Lax I, Blomgren H, Näslund I, Svanström R. Stereotactic radiotherapy of malignancies in the abdomen. Methodological aspects. Acta Oncol. 1994;33(6):677–83.
7. Ford EC, Mageras GS, Yorke E, Ling CC. Respiration-correlated spiral CT: a method of measuring respiratory-induced anatomic motion for radiation treatment planning. Med Phys. 2003;30(1):88–97.
8. Guckenberger M, Wilbert J, Krieger T, Richter A, Baier K, Meyer J, et al. Four-dimensional treatment planning for stereotactic body radiotherapy. Int J Radiat Oncol Biol Phys. 2007;69(1):276–85.

9. Solberg TD, Balter JM, Benedict SH, Fraass BA, Kavanagh B, Miyamoto C, et al. Quality and safety considerations in stereotactic radiosurgery and stereotactic body radiation therapy: executive summary. Pract Radiat Oncol. 2012;2(1):2–9.
10. Balter JM, Ten Haken RK, Lawrence TS, Lam KL, Robertson JM. Uncertainties in CT-based radiation therapy treatment planning associated with patient breathing. Int J Radiat Oncol Biol Phys. 1996;36(1):167–74.
11. Sonke JJ, Rossi M, Wolthaus J, van Herk M, Damen E, Belderbos J. Frameless stereotactic body radiotherapy for lung cancer using four-dimensional cone beam CT guidance. Int J Radiat Oncol Biol Phys. 2009;74(2):567–74.
12. Velec M, Moseley JL, Brock KK. Simplified strategies to determine the mean respiratory position for liver radiation therapy planning. Pract Radiat Oncol. 2014;4(3):160–6.
13. Peulen H, Belderbos J, Guckenberger M, Hope A, Grills I, van Herk M, et al. Target delineation variability and corresponding margins of peripheral early stage NSCLC treated with stereotactic body radiotherapy. Radiother Oncol. 2015;114(3):361–6.
14. Redmond KJ, Robertson S, Lo SS, Soltys SG, Ryu S, McNutt T, et al. Consensus contouring guidelines for postoperative stereotactic body radiation therapy for metastatic solid tumor malignancies to the spine. Int J Radiat Oncol Biol Phys. 2017;97(1):64–74.
15. Cox BW, Spratt DE, Lovelock M, Bilsky MH, Lis E, Ryu S, et al. International Spine Radiosurgery Consortium consensus guidelines for target volume definition in spinal stereotactic radiosurgery. Int J Radiat Oncol Biol Phys. 2012;83(5):e597–605.
16. Klein EE, Hanley J, Bayouth J, Yin FF, Simon W, Dresser S, et al. Task Group 142 report: quality assurance of medical accelerators. Med Phys. 2009;36(9):4197–212.
17. Benedict SH, Yenice KM, Followill D, Galvin JM, Hinson W, Kavanagh B, et al. Stereotactic body radiation therapy: the report of AAPM Task Group 101. Med Phys. 2010;37(8):4078–101.
18. Du W, Gao S, Wang X, Kudchadker RJ. Quantifying the gantry sag on linear accelerators and introducing an MLC-based compensation strategy. Med Phys. 2012;39(4):2156–62.
19. Low DA, Li Z, Drzymala RE. Minimization of target positioning error in accelerator-based radiosurgery. Med Phys. 1995;22(4):443–8.
20. Lutz W, Winston KR, Maleki N. A system for stereotactic radiosurgery with a linear accelerator. Int J Radiat Oncol Biol Phys. 1988;14(2):373–81.
21. Rowshanfarzad P, Sabet M, O'Connor DJ, Greer PB. Isocenter verification for linac-based stereotactic radiation therapy: review of principles and techniques. J Appl Clin Med Phys. 2011;12(4):3645.
22. Hartmann GH, Bauer-Kirpes B, Serago CF, Lorenz WJ. Precision and accuracy of stereotactic convergent beam irradiations from a linear accelerator. Int J Radiat Oncol Biol Phys. 1994;28(2):481–92.
23. Moiseenko V, Lapointe V, James K, Yin L, Liu M, Pawlicki T. Biological consequences of MLC calibration errors in IMRT delivery and QA. Med Phys. 2012;39(4):1917–24.
24. Nithiyanantham K, Mani GK, Subramani V, Mueller L, Palaniappan KK, Kataria T. Analysis of direct clinical consequences of MLC positional errors in volumetric-modulated arc therapy using 3D dosimetry system. J Appl Clin Med Phys. 2015;16(5):296–305.
25. Bayouth JE, Morrill SM. MLC dosimetric characteristics for small field and IMRT applications. Med Phys. 2003;30(9):2545–52.
26. Ezzell GA, Galvin JM, Low D, Palta JR, Rosen I, Sharpe MB, et al. Guidance document on delivery, treatment planning, and clinical implementation of IMRT: report of the IMRT Subcommittee of the AAPM Radiation Therapy Committee. Med Phys. 2003;30(8):2089–115.
27. Jaffray DA, Siewerdsen JH, Wong JW, Martinez AA. Flat-panel cone-beam computed tomography for image-guided radiation therapy. Int J Radiat Oncol Biol Phys. 2002;53(5):1337–49.
28. Bissonnette JP, Moseley DJ, Jaffray DA. A quality assurance program for image quality of cone-beam CT guidance in radiation therapy. Med Phys. 2008;35(5):1807–15.
29. Bissonnette JP, Balter PA, Dong L, Langen KM, Lovelock DM, Miften M, et al. Quality assurance for image-guided radiation therapy utilizing CT-based technologies: a report of the AAPM TG-179. Med Phys. 2012;39(4):1946–63.
30. Paulson ES, Erickson B, Schultz C, Allen Li X. Comprehensive MRI simulation methodology using a dedicated MRI scanner in radiation oncology for external beam radiation treatment planning. Med Phys. 2015;42(1):28–39.
31. Ma L, Wang L, Tseng CL, Sahgal A. Emerging technologies in stereotactic body radiotherapy. Chin Clin Oncol. 2017;6(Suppl 2):S12.
32. Seibert TM, White NS, Kim GY, Moiseenko V, McDonald CR, Farid N, et al. Distortion inherent to magnetic resonance imaging can lead to geometric miss in radiosurgery planning. Pract Radiat Oncol. 2016;6(6):e319–e28.
33. Dong P, Lee P, Ruan D, Long T, Romeijn E, Yang Y, et al. 4pi noncoplanar liver SBRT: a novel delivery technique. Int J Radiat Oncol Biol Phys. 2013;85(5):1360–6.
34. Navarria P, Ascolese AM, Mancosu P, Alongi F, Clerici E, Tozzi A, et al. Volumetric modulated arc therapy with flattening filter free (FFF) beams for stereotactic body radiation therapy (SBRT) in patients with medically inoperable early stage non small cell lung cancer (NSCLC). Radiother Oncol. 2013;107(3):414–8.
35. Thomas EM, Popple RA, Prendergast BM, Clark GM, Dobelbower MC, Fiveash JB. Effects of flattening filter-free and volumetric-modulated arc therapy delivery on treatment efficiency. J Appl Clin Med Phys. 2013;14(6):4328.
36. Foster RD, Speiser MP, Solberg TD. Commissioning and verification of the collapsed cone convolution superposition algorithm for SBRT delivery using flattening filter-free beams. J Appl Clin Med Phys. 2014;15(2):4631.
37. Ishii K, Okada W, Ogino R, Kubo K, Kishimoto S, Nakahara R, et al. A treatment-planning comparison of three beam arrangement strategies for stereotactic body radiation therapy for centrally located lung tumors using volumetric-modulated arc therapy. J Radiat Res. 2016;57(3):273–9.
38. Kim J, Wen N, Jin JY, Walls N, Kim S, Li H, et al. Clinical commissioning and use of the Novalis Tx linear accelerator for SRS and SBRT. J Appl Clin Med Phys. 2012;13(3):3729.
39. Fürweger C, Prins P, Coskan H, Heijmen BJ. Characteristics and performance of the first commercial multileaf collimator for a robotic radiosurgery system. Med Phys. 2016;43(5):2063.
40. Schuring D, Hurkmans CW. Developing and evaluating stereotactic lung RT trials: what we should know about the influence of inhomogeneity corrections on dose. Radiat Oncol. 2008;3:21.
41. Martens C, Reynaert N, De Wagter C, Nilsson P, Coghe M, Palmans H, et al. Underdosage of the upper-airway mucosa for small fields as used in intensity-modulated radiation therapy: a comparison between radiochromic film measurements, Monte Carlo simulations, and collapsed cone convolution calculations. Med Phys. 2002;29(7):1528–35.
42. Woo MK, Cunningham JR. The validity of the density scaling method in primary electron transport for photon and electron beams. Med Phys. 1990;17(2):187–94.
43. Subramanian SV, Subramani V, Thirumalai Swamy S, Gandhi A, Chilukuri S, Kathirvel M. Is 5 mm MMLC suitable for VMAT-based lung SBRT? A dosimetric comparison with 2.5 mm HDMLC using RTOG-0813 treatment planning criteria for both conventional and high-dose flattening filter-free photon beams. J Appl Clin Med Phys. 2015;16(4):112–24.
44. Tanyi JA, Summers PA, McCracken CL, Chen Y, Ku LC, Fuss M. Implications of a high-definition multileaf collimator (HD-MLC)

on treatment planning techniques for stereotactic body radiation therapy (SBRT): a planning study. Radiat Oncol. 2009;4:22.
45. Ruschin M, Sahgal A, Iradji S, Soliman H, Leavens C, Lee Y. Investigation of two linac head designs for treating brain metastases with hypofractionated volumetric modulated arc radiotherapy. Br J Radiol. 2016 Jul;89(1063):20160093.
46. DeLuca P, Jones D, Gahbauer R, Whitmore G, Wambersie A. Prescribing, recording, and reporting photon-beam intensity-modulated radiation therapy (IMRT). J ICRU Rep. 2010;83
47. Menzel HG, DeLuca P, Mackie TR, Boone JM, Brandan ME, Burns DT, et al. ICRU report 91: prescribing, recording, and reporting of stereotactic treatments with small photon beams. J ICRU. 2014;14(2)
48. Hua C, Chang J, Yenice K, Chan M, Amols H. A practical approach to prevent gantry-couch collision for linac-based radiosurgery. Med Phys. 2004;31(7):2128–34.
49. Sauer OA. Calculation of dose distributions in the vicinity of high-Z interfaces for photon beams. Med Phys. 1995;22(10):1685–90.
50. Vatnisky S, Meghzifene A, Christaki K, Palmans H, Andrew P, Saiful Huq M, et al. IAEA TRS-483. Dosimetry of small fields used in external beam radiotherapy: an international code of practice for reference and relative dose determination. International Atomic Energy Agency. 2017.
51. Bjärngard BE, Tsai JS, Rice RK. Doses on the central axes of narrow 6-MV x-ray beams. Med Phys. 1990;17(5):794–9.
52. Sánchez-Doblado F, Hartmann GH, Pena J, Roselló JV, Russiello G, Gonzalez-Castaño DM. A new method for output factor determination in MLC shaped narrow beams. Phys Med. 2007;23(2):58–66.
53. Alfonso R, Andreo P, Capote R, Huq MS, Kilby W, Kjäll P, et al. A new formalism for reference dosimetry of small and nonstandard fields. Med Phys. 2008;35(11):5179–86.
54. Aspradakis MM, Byme H, Palmans S, Duane S, Conway J, Warrington AP, et al. IPEM report 103: small field MV photon dosimetry. 2010.
55. Almond PR, Biggs PJ, Coursey BM, Hanson WF, Huq MS, Nath R, et al. AAPM's TG-51 protocol for clinical reference dosimetry of high-energy photon and electron beams. Med Phys. 1999;26(9):1847–70.
56. McEwen M, DeWerd L, Ibbott G, Followill D, Rogers DW, Seltzer S, et al. Addendum to the AAPM's TG-51 protocol for clinical reference dosimetry of high-energy photon beams. Med Phys. 2014;41(4):041501.
57. Andreo P, Huq MS, Westermark M, Song H, Tilikidis A, DeWerd L, et al. Protocols for the dosimetry of high-energy photon and electron beams: a comparison of the IAEA TRS-398 and previous international codes of practice. International Atomic Energy Agency. Phys Med Biol. 2002;47(17):3033–53.
58. Smit K, van Asselen B, Kok JG, Aalbers AH, Lagendijk JJ, Raaymakers BW. Towards reference dosimetry for the MR-linac: magnetic field correction of the ionization chamber reading. Phys Med Biol. 2013;58(17):5945–57.
59. Bouchard H, Seuntjens J. Ionization chamber-based reference dosimetry of intensity modulated radiation beams. Med Phys. 2004;31(9):2454–65.
60. Agostinelli S, Garelli S, Piergentili M, Foppiano F. Response to high-energy photons of PTW31014 PinPoint ion chamber with a central aluminum electrode. Med Phys. 2008;35(7):3293–301.
61. Capote R, Sánchez-Doblado F, Leal A, Lagares JI, Arráns R, Hartmann GH. An EGSnrc Monte Carlo study of the microionization chamber for reference dosimetry of narrow irregular IMRT beamlets. Med Phys. 2004;31(9):2416–22.
62. Andersson J, Kaiser FJ, Gómez F, Jäkel O, Pardo-Montero J, Tölli H. A comparison of different experimental methods for general recombination correction for liquid ionization chambers. Phys Med Biol. 2012;57(21):7161–75.
63. Ralston A, Tyler M, Liu P, McKenzie D, Suchowerska N. Over-response of synthetic microDiamond detectors in small radiation fields. Phys Med Biol. 2014;59(19):5873–81.
64. Westermark M, Arndt J, Nilsson B, Brahme A. Comparative dosimetry in narrow high-energy photon beams. Phys Med Biol. 2000;45(3):685–702.
65. Zhu XR, Allen JJ, Shi J, Simon WE. Total scatter factors and tissue maximum ratios for small radiosurgery fields: comparison of diode detectors, a parallel-plate ion chamber, and radiographic film. Med Phys. 2000;27(3):472–7.
66. Francescon P, Cora S, Cavedon C, Scalchi P, Reccanello S, Colombo F. Use of a new type of radiochromic film, a new parallel-plate micro-chamber, MOSFETs, and TLD 800 microcubes in the dosimetry of small beams. Med Phys. 1998;25(4):503–11.
67. Aguirre JF, Alvarez P, Ibbott GG, Followwill DS, editors. Testing, commissioning, and validating an optically stimulated luminescence (OSL) dosimetry system for mailed dosimetry at the Radiological Physics Center. Standards, Applications and Quality Assurance in Medical Radiation Dosimetry (IDOS). Vienna: IAEA; 2010.
68. Mack A, Scheib SG, Major J, Gianolini S, Pazmandi G, Feist H, et al. Precision dosimetry for narrow photon beams used in radiosurgery-determination of Gamma Knife output factors. Med Phys. 2002;29(9):2080–9.
69. Pantelis E, Antypas C, Petrokokkinos L, Karaiskos P, Papagiannis P, Kozicki M, et al. Dosimetric characterization of CyberKnife radiosurgical photon beams using polymer gels. Med Phys. 2008;35(6):2312–20.

Immobilization for SBRT: A Crucial Prerequisite Toward Accurate Treatment

Jana Heitmann and Matthias Guckenberger

Abbreviations

6 DOF	Six degrees of freedom
ACROP	Advisory Committee on Radiation Oncology Practice
ASTRO	American Society for Radiation Oncology
CB-CT	Cone-beam computed tomography
EORTC	European Organisation for Research and Treatment of Cancer
ESTRO	European SocieTy for Radiotherapy and Oncology
Fx	Fraction(s)
IFV-MTP	Intrafraction variation of the mean target position
IGRT	Image-guided radiotherapy
PTV	Planning target volume
SBF	Stereotactic body frame
SBRT	Stereotactic body radiation therapy
SD	Standard deviation

Introduction

According to the ASTRO consensus, stereotactic body radiation therapy (SBRT) is defined as a high-precision radiotherapy delivered in three or more fractions to very potent doses of highly conformal radiation with steep dose gradients around the target. The word "stereotactic" contains two Greek-originating words: "stereos" for "solid" and "taxis" for "order." It is used to describe the localization of a target within a defined 3D space using correspondence to an external reference frame with coordinates. In the medical field, it was first used by neurosurgeons. In 1951, Lars Leksell developed stereotactic radiosurgery, and his first patient treated with a Gamma Knife in 1968 was immobilized with a molded plaster headpiece [1].

Irradiation can be conformal, reproducible, and of highest technical performance. However, if the patient cannot be reproducibly immobilized, the treatment is rendered ineffective and even dangerous with regard to organs at risk in close proximity. Reproducible immobilization allows for reduction of margins around the targets to minimize high doses delivered to healthy tissue. Hence, immobilization is at the heart of SBRT treatment, and this chapter is going to focus on this crucial step in treatment planning and delivery.

When radiotherapy was first used in patients, immobilization played a minor role, because margins were large and treatment times short. Simple head cups, neck rolls, and tapes were used for the head, while the rest of the body remained entirely unimmobilized. In the 1960s and 1970s, with the advent of cobalt teletherapy and megavoltage x-ray therapy, skin markers were introduced to align the patient using laser and kV images to verify the patient's position. By the 1980s, CT planning and 3D techniques improved conformity of treatment planning but likewise introduced the realization that immobilization in a 3D manner is crucial. By the mid-1990s, immobilization for a multitude of body sites was available: the Alpha Cradle® (Smithers Medical Products, Inc., North Canton, OH, USA) (abdominal tumors), thermal body casts (prostate), bead bags (breast), upper body casts (thorax), and masks with and without bite blocks (head and neck), albeit none of these were yet intended for SBRT [2].

Such hypofractionated stereotactic treatments were first applied to intracranial targets. Immobilization consecutively evolved from invasive to noninvasive and from frame-based to frameless systems. To achieve invasive immobilization and connection to a stereotactic frame, three to four steel pins are drilled into the skull of patients and attached to the

J. Heitmann · M. Guckenberger (✉)
University Hospital Zurich, Department of Radiation Oncology, Zurich, Switzerland
e-mail: Matthias.guckenberger@usz.ch

D. M. Trifiletti et al. (eds.), *Stereotactic Radiosurgery and Stereotactic Body Radiation Therapy*,
https://doi.org/10.1007/978-3-030-16924-4_18

frame. While this allows for exact immobilization permitting set-up errors of less than 1 mm, it constitutes an invasive technique [3]. Examples include the Leksell® frame (Elekta, Stockholm, Sweden) and the Cosman-Robert-Wells frame. These frames are solely suited for single fraction treatments and are prone to systematic errors stemming from MRI distortions and rare, but consequential slippage mistakes resulting in systematic errors that may not be detected without imaging [4, 5]. Noninvasive frames provide a stereotactic fiducial-based localizer system that can be attached to immobilizers while sparing the patient from an uncomfortable and painful procedure. Examples include the TALON® removable head frame system (Best NOMOS, Pittsburgh, PA, USA) [6], the Gill-Thomas-Cosman frame [7, 8], the Laitinen Stereoadapter® 5000 frame (Sandstrom Trade and Technology Inc., Welland, Ontario, Canada) [9], and the BrainLAB® mask system (Reuther, Koblenz, Germany) [10, 11].

The implementation of frameless systems was facilitated by the advent of image-guided radiotherapy (IGRT). Frameless systems include the eXtend frame for Gamma Knife (Elekta, AB, Stockholm, Sweden) [12, 13], the PinPoint® frame (Aktina Medical, Congers, NY, USA) [14], optically guided frameless systems [15–17], and BrainLAB® frameless systems [18, 19].

In summary, cranial immobilization techniques have evolved from drilling pins into patients' skulls to positioning patients on nonrigid mattresses and achieving accuracy in radiation treatment through daily image guidance. In the following section, we will discuss the transfer of the stereotactic technique from intracranial to extracranial sites focusing on the immobilization of patients.

History of Immobilization for SBRT

Lax and Blomgren developed a stereotactic body frame (SBF) in 1994 to localize target volumes within a patient's body. The patient is positioned in a vacuum pillow that extends from the head to the thighs. The walls of the frame – made out of wood and plastic to avoid artifacts in imaging and attenuation of the beam – support this pillow on each side of the patient. Contrary to head frames, this SBF uses a large contact area between the patient and the frame. Indicators inside the frame enable positioning within the frame using tomographic slices. The authors applied slight pressure with a belt on the abdomen to reduce diaphragmatic motion to 0.5–1.0 cm. They reported no systematic errors, and 93% of deviations in the transversal plane were within 5 mm and 100% within 7 mm. In the longitudinal plane, 88% of deviations were within 8 mm and 100% within 1 cm of the target lesion in relation to the first CT scan [20]. The first sites treated by radiosurgery outside the skull were malignancies of the head and neck followed by the spine [21, 22].

The first radiosurgery unit designed for extracranial treatment was described by Hamilton and colleagues 1 year thereafter. It included a skeletal fixation frame immobilizing the patient in a prone position to provide spinal stereotactic radiosurgery that limited the appeal of this technique [23]. Later, extracranial targets were treated using newer frames, such as the Elekta (AB, Stockholm, Sweden) SBF discussed below. In accordance with intracranial stereotactic treatments, these invasive methods were widely abandoned after the advent of image guidance, frameless techniques, and improvements in beam targeting.

Recent Advances in Immobilization

Frames

Before the advent and widespread implementation of IGRT, frames were used to keep targets stationary with respect to an outer coordinate system. Wulf and coauthors evaluated the abovementioned SBF by Lax and Blomgren for a variety of target lesions in 2000 and suggested that a planning target volume (PTV) margin of 5 mm was sufficient for compensation of target positioning uncertainties. The authors report alignment errors in a variety of treatment sites with a standard deviation (SD) of the SBF system of 3.9 mm, 2.2, mm and 3.5 mm along the x- (left-right), y- (anteroposterior) and z- (cranio-caudal) axis [24]. For CT-guided hypofractionated treatment of paraspinal tumors, Yenice and coauthors developed a novel rigid but noninvasive SBF in 2003. To immobilize patients, pressure is applied to the pelvis, ribs, and sternum. In addition, a three-piece vacuum body mold is used by the authors. The frame contains fiducial plates to be identified by CT imaging [25]. Lohr and colleagues modified a frame developed in Heidelberg (Leibinger, Freiburg, Germany) with a whole-body cast [26]. The body frame that subsequently gained most popularity for SBRT is the SBF by Elekta. Table 1 presents a chronologic list of developed frames along with the associated set-up errors.

Of note, the introduction of kilovoltage imaging and later cone-beam CT (CB-CT) imaging into modern linear accelerators has rendered frame systems less important and lead to the development of a multitude of immobilization devices [24, 27–32].

Mattresses

An immobilization system widely used is the Elekta BodyFIX® (Elekta, AB, Stockholm, Sweden) system. It consists of a baseplate, a vacuum cushion filled with Styrofoam, a base cushion and a foil placed on top of the patient, as well as a vacuum pump to establish a vacuum around the patient's torso (Fig. 1). A frame can be attached to

Table 1 Set-up errors for different stereotactic body frames (SBF) used for SBRT

Frame	Treatment site	Mean set-up error (mm)	Study
Invasive fixation	Spine	2	Hamilton et al. [23]
SBF (Leibinger; Freiburg, Germany) + Body cast (Scotch) + head mask	Spine	≤ 3.9	Lohr et al. [26]
SBF (Lax and Blomgren)	Lung, liver, abdomen, bone	≤ 3.9	Wulf et al. [24]
SBF (Memorial Sloan-Kettering Cancer Center (MSKCC)) + vacuum body mold	Spine	2–3	Yenice et al. [25]
SBF (Elekta) + Scotch cast and mask	Spine	≤ 0.8	Stoiber et al. [38]
SBF (Elekta) + vacuum pillow	Lung, liver, prostate, spine	≤ 2.4	Foster et al. [69]
SBF (Elekta) vs. in-house SBF	Spine	≤0.9 vs. ≤3.9	Han et al. [70]

MSKCC Memorial Sloan-Kettering Cancer Center

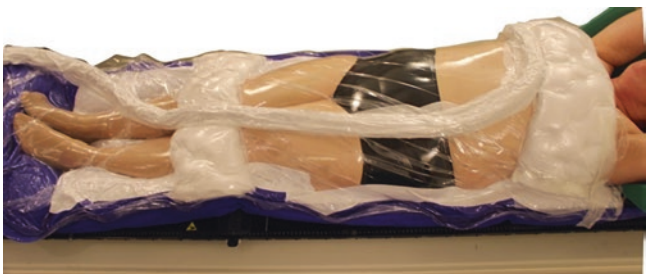

Fig. 1 A patient with spine metastases is immobilized for CT scanning using the Elekta BodyFIX® system (Stockholm, Sweden). A complete vacuum is crucial

the construction with fiducials visible in imaging. The patient is placed on the cushion that is fixed to the base plate in a supine position. After attaching the clear plastic foil to the patient's torso with sticky tape, a vacuum is created between the foil, the patient, and the vacuum cushion. The base cushion, which is not air-free, can be molded to the patient.

The first study to investigate the double-vacuum-assisted whole-body immobilization by Fuss and colleagues in 2004 analyzed the set-up repositioning accuracy of the device using control CT scans in 36 patients with lung and/or liver lesions treated with SBRT. They reported a deviation of anatomical bony landmarks of −0.4 ± 3.9 mm, −0.1 ± 1.6 mm, and 0.3 ± 3.6 mm (mean ± SD) along the *x*-, *y*-, and *z*-axis, respectively. In 29.4% of repositioning controls, a set-up error of more than 5 mm was reported prompting the authors to recommend performing pretreatment imaging and position correction routinely. Furthermore, the authors observed mean rotational errors about the *x*-, *y*-, and *z*-axis of 0.9° ± 0.7°, 0.8° ± 0.7°, and 1.8° ± 1.6°, respectively [33]. Gutfeld and colleagues likewise investigated the rotational displacements on courses for thoracic, lumbar, and sacral metastases and reported a roll error of maximally −6.64° [34].

Hyde and coauthors investigated the intrafraction error of the same Elekta BodyFIX® with wrap analyzing the treatments of 42 patients with thoracic or lumbar spinal metastases. The authors reported an average of 1 ± 0.9 mm intrafractional error along the *x*-axis and a rotational roll error of 0.8° ± 0.6° [35]. Another study investigated the mean 3D positioning error of the BodyFIX® system with foil and reported a mean value of 2.5 ± 1.1 mm [36].

Recently, Hubie and colleagues conducted a randomized comparison of three immobilization devices including the Qfix Arm Shuttle™ (Qfix, Avondale, PA, USA) and the BodyFIX® with and without wrap in 45 patients treated with either conventionally fractionated radiotherapy or SBRT. They did not find significant differences regarding the accuracy of the three devices. Of note, the BodyFIX® with wrap took significantly longer to set up and ranked last among the three immobilization systems regarding technician rating for usability [37].

Another patient immobilization device for SBRT is the scotch system (Scotch Cast™ 3M, St. Paul, MN, USA) consisting of a wrap-around body cast and a custom-made mask that can be attached to a SBF. The first group reporting on accuracy of this device was Lohr and colleagues in 1999. The authors evaluated 31 CT scans from five patients treated with SBRT for paraspinal lesions. They reported mean patient movements of 1.6 ± 1.2 mm (*x*-axis), 1.4 ± 1.0 mm (*y*-axis), and 2.3 ± 1.3 mm (transversal vectorial error). Compared to Fuss and coauthors, they found slightly smaller SD along the *x*- and *y*-axis (1.6 mm and 1.4 mm and 1.4 mm and 1.2 mm, respectively).

A decade thereafter, Stoiber and colleagues presented a larger dataset with 321 CT scans of 45 patients with spinal tumors. They reported "negligible" rotational errors, but in some cases, large translational errors, especially in lumbar tumors with error means of 0.7 ± 1.3 mm, 0.0 ± 0.9 mm, and 0.5 ± 1.6 mm in the *x*-, *y*-, and *z*-axis, respectively. The authors recommended daily imaging prior to treatment [38]. Of note, this study focused on conventionally fractionated treatment, not SBRT.

For spine SBRT, Li and coauthors compared three immobilization devices in 2012 in 84 patients, namely, an evacuated cushion, a semirigid vacuum body fixation, or a thermoplastic S-frame mask for cervical targets. The devices did not differ in residual set-up errors. The semirigid vacuum body fixation device showed least intrafraction motion justifying a 2 mm PTV margin [39].

But even without rigid immobilization, spine stability can be achieved with less than 1 mm of posttreatment errors and <1° rotational errors in 97% of patients, as reported by Dahele

and colleagues [40]. The group studied intrafractional patient motion in SBRT for lung cancer and simply used supporting devices, such as a mattress with support for the arms above the head and the knees. However, they used advanced image guidance techniques, such as 4D CT and real-time position management to compensate for the lack of immobilization.

Masks

Tumors in the head and neck region typically do not move as significantly as tumors in the thorax and abdomen. Nevertheless, immobilization was optimized in recent years especially through shoulder immobilization in addition to masks as well as mouthpieces and bite blocks. An example of the head and shoulder mask used at our department is shown in Fig. 2. In head and neck sites, masks have become more rigid as number of fractions decreased. In 2006, Georg and colleagues reported a set-up error 3D vector of 1.3 ± 0.9 mm across 202 fractions of two noninvasive masks (BrainLAB®) [41]. This very high level of set-up accuracy could not be reproduced in subsequent studies, possibly because all consecutive studies used CB-CT imaging to assess set-up errors (Table 2). Polat and coauthors, for instance, reported set-up errors of 3.2 ± 1.7 mm (mean ± SD) in 11 patients using CB-CTs [42]. In 2017, set-up errors could be further reduced by intraoral stents [43]. These stents consist of maxillar, mandibular, and plate sections. Of note, errors for normofractionated treatments were reported. In an effort to reduce skin toxicity resulting from increased surface dose underneath the masks, Velec and colleagues evaluated skin-sparing masks and found similar inter- and intrafraction errors compared to conventional masks while radiation dermatitis was reduced, albeit no significant differences were found [44]. Wang and colleagues recently showed that a Cushion-Mask-Biteblock (customized head and shoulder Klarity AccuCushion (Klarity Medical Products, Newark, OH), a thermoplastic head neck and shoulder mask (Orfit Industries America, Wijnegem, Belgium), preheated moldable bite-block (Precise Bite, Civico, Coralville, IA)) immobilization device is able to allow for 2 mm PTV margins in SBRT treatments in the head and neck [45]. Tryggestad and colleagues even suggested that a PTV margin of 1 mm is sufficient for head and neck SBRT treatments using a head and shoulder thermoplastic mask with a mouthpiece, if daily pretreatment correction is performed [46].

Fig. 2 A patient is immobilized using a Posicast® five-point head and shoulder mask by Civco® (Rotterdam, The Netherlands). It is tightly fitted and allows for accurate treatment

Table 2 Set-up errors of different head and neck masks for SBRT

Device	Reported value	Set-up error (mm)	Imaging	Study
Thermoplastic mask (BrainLab®) or Scotch-Cast mask™ (3M)	Mean ± SD	0.9 ± 0.9	CB-CT	Guckenberger et al. [71]
Head mask (BrainLab®)	3D vector	1.3	Portal images	Georg et al. [41]
Head and neck mask (BrainLab®)	3D vector	1.3	Portal images	Georg et al. [41]
Thermoplastic head mask (BrainLab®)	3D vector Mean ± SD	3.2 ± 1.7	CB-CT	Polat et al. [42]
Type-S-mask™ (Civco) + head cushion	Mean ± SD	2.3 ± 1.4	CB-CT	Tryggestad et al. [46]
Uni-frame mask® (Civco) + head cushion, BlueBag™ (Medical Intelligence, Schwabmünchen, Germany)	Mean ± SD	2.2 ± 1.1	CB-CT	Tryggestad et al. [46]
Type-S head and shoulder mask™ + head and shoulder cushion (Civco)	Mean ± SD	2.7 ± 1.5	CB-CT	Tryggestad et al. [46]
Type-S head and shoulder mask™ + head and shoulder cushion (Civco); + mouthpiece	Mean ± SD	2.1 ± 1.0	CB-CT	Tryggestad et al. [46]
Cushion-Mask-Biteblock	3D vector	2.7 ± 1.4	CB-CT	Wang et al. [45]
Thermoplastic mask™ (Aquaplast RT) Qfix™ (Avondale, PA, USA) + intraoral stent	Mean	2.42	CB-CT	Doi et al. [43]

Immobilization for Moving Target Volumes

SBRT treatments of tumors located in the thorax or the abdomen hold a higher risk of a geographical miss compared to conventional fractionation [40, 47]. In mobile tumors, baseline shifts independent of the bony anatomy result in a target position variability. These baseline shifts may result from breathing, the beating heart, peristalsis, or swallowing. Other potential movements include edema, bladder/rectal filling, and muscle tension. Especially prone to target volume variability are targets within the lung and the liver.

The impact of immobilization of moving tumors was evaluated by Navarro-Martin and colleagues, who compared the interfraction set-up accuracy for pulmonary SBRT targets of a thermoplastic mask system (Lorca Marin S.A., Spain) and whole-body vacuum cushions (Civco Medical Solutions, Rotterdam, the Netherlands) in a retrospective study. They reported mean set-up errors ranging from <6.4 mm for the mask system to <10.5 mm for the vacuum cushion ($P = 0.0002$). Siva and colleagues compared tumor volume movement in 12 patients either immobilized with the BodyFIX® system or not immobilized and reported that immobilization reduced the volume of tumor displacement by a mean of 83% ($P = 0.021$) [48].

Abdominal compression, first described by Lax and colleagues [20], remains controversial. The diaphragm movement when breathing creates a vector in the cranio-caudal direction causing large target displacements. If abdominal pressure is applied, patients are forced to use chest wall expansion, a process generating vectors in all directions that are cancelling each other out (Fig. 3). While abdominal compression has shown to reduce the movement of the target, it may be an uncomfortable device for some patients and may increase interfraction variation in tumor position requiring daily target matching [49–52]. The abdominal compression technique still was reported easier to use and even more comfortable than the BodyFIX® system, while both devices showed a similar ability to reduce tumor movement [47].

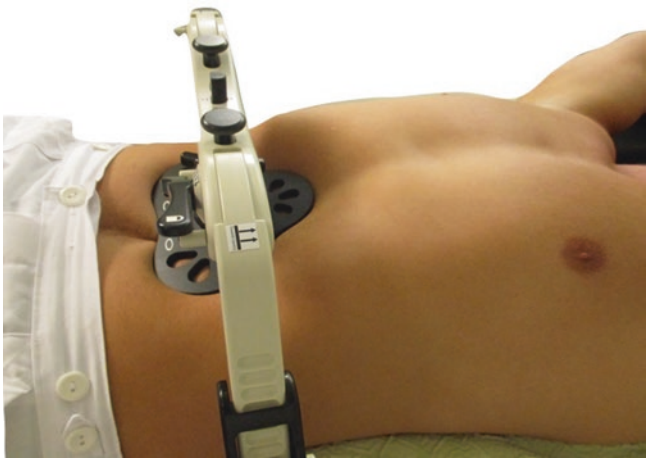

Fig. 3 Abdominal compression plate used to limit the cranio-caudal movement while breathing

For pulmonary SBRT, Bouihol and colleagues investigated the usefulness of abdominal compression performed on 27 NSCLC (non-small cell lung cancer) patients with varying target localization. The authors reported a motion suppression in lower lobe tumors (3.5 mm), whereas lesions located in the upper or middle lobe of the lung could not be motion-reduced as much (0.8 mm) [53]. For hepatic SBRT, Hu and colleagues compared treatment delivery with and without abdominal compression and found that while abdominal compression can reduce target movement, a high body mass index and male gender are predictors of less effective abdominal compression [54].

The clinical outcome using abdominal compression was investigated by Mampuya and colleagues in 47 lung tumor patients in a retrospective study evaluating overall survival, local control, and disease-free survival. While no statistically significant differences were found between patients treated with or without abdominal compression, the 3-year local control rate was 65.4% and 82.5% in patients treated with and without abdominal compression, respectively, suggesting that there might be a negative impact of abdominal compression on local control [55].

Treatment time and respiratory movement influence the intrafraction variability of tumor position. Shah and colleagues compared four immobilization devices regarding their ability to reduce the intrafraction variation of the mean target position (IFV-MTP) on 126 patients suffering from stage I/II NSCLC treated with pulmonary SBRT. The mean IFV-MTP vectors for the Elekta SBF, the Alpha Cradle®, the Elekta BodyFIX®, and a hybrid of the latter two were 1.5 ± 1.1 mm, 2.6 ± 2.1 mm, 2.7 ± 2.6 mm, and 1.9 ± 1.5 mm, respectively. The authors concluded that a 5 mm PTV margin is therefore sufficient for a body frame immobilization technique, but not necessarily for a sole BodyFIX® immobilization [56].

The new as well as the 2010 EORTC lung SBRT guidelines [57, 58] recommend stable knee and arm support above the head if possible. Rigid immobilization is not needed for SBRT treatments according to these guidelines [59]. Similarly, the guidelines by the Advisory Committee on Radiation Oncology Practice (ACROP) of the ESTRO consider immobilization with a body frame or the BodyFIX® system discussed above, as well as abdominal compression as "optional" for SBRT for early stage peripheral lung tumors [60]. Optional in this case means that the mentioned devices might improve clinical outcome, but sufficient clinical evidence is still lacking. For pulmonary SBRT, Table 3 summarizes studies that reported inter- and/or intrafractional errors of varying immobilization devices.

Table 3 Intrafraction and interfraction target motion of pulmonary SBRT targets

Immobilization Device	Reported statistical value	Patient #	Intrafractional motion (mm)	Interfractional motion (mm)	Study
No device	Mean vector	12	7.8	–	Siva et al. [48]
No device	Mean vector	30	0.8	–	Dahele et al. [40]
Alpha Cradle®	Mean ± SD	126	< 2.6 ± 2.1	–	Shah et al. [56]
Alpha Cradle®	Mean systematic error	24	< 1.3	< 5.8	Grills et al. [72]
Alpha Cradle® + BodyFIX®	Mean ± SD	126	1.9 ± 1.5	–	Shah et al. [56]
BodyFIX®	Mean ± SD	7	–	< 0.9 ± 3.6	Wang et al. [73]
BodyFIX®	Mean ± SD	126	2.7 ± 2.6	–	Shah et al. [56]
BodyFIX®	Mean ± SD	24	< 2.8 ± 1.6	< 4.3	Guckenberger et al. [74]
BodyFIX®	Mean ± SD	24	2.3 ± 1.3	–	Han et al. [47]
BodyFIX®	Tumor positioning error	19	2.1 ± 0.7	< 3.8	Worm et al. [75]
BodyFIX®	Mean vector	12	4.9	–	Siva et al. [48]
BodyFIX®	Mean	24	< 1.0	< 3.4	Grills et al. [72]
BodyFIX®	SD	36	–	< 3.2	Fuss et al. [33]
BodyFIX® + Abdominal compression	Mean ± SD	28	2.2 ± 1.2	–	Purdie et al. [76]
Abdominal compression	Mean ± SD	24	< 2.0 ± 1.2	–	Han et al. [47]
Abdominal compression	Mean		< 0.8	< 1.9	Li et al. [77]
SBF (Elekta)	Mean ± SD	126	1.5 ± 1.1	–	Shah et al. [56]
SBF (Elekta)	Mean ± SD	6	–	2.0 ± 4.3	Guckenberger et al. [71]
SBF (Elekta)	Mean	41	–	< 2.3	Ueda et al. [78]
SBF (Elekta) or Thermoplastic frame (MED-TEC Inc., Orange City, IA, USA)	Mean ± SD	30	–	< 0.7 ± 3.1	Wang et al. [73]
Vac Loc™ (Civco)	Mean	75	< 1.3	< 1.3	Li et al. [77]
Body Pro-Lok™ (Civco)	Mean ± SD	41	–	< 0.7	Ueda et al. [78]
Body Pro-Lok™ (Civco)		5			Shi et al. [29]
Chest board (Med-Tec, Inc.)	Mean	75	<1.1	< 1.7	Li et al. [77]
Thermoplastic mask (Lorca Marin, S.A., Spain)	Mean	73 Fx	–	< 6.4	Navarro-Martin et al. [79]
Vacuum cushion (Civco)	Mean	73 Fx	–	< 10.5	Navarro-Martin et al. [79]

For targets within the liver, similar techniques are used. Shimogashi and colleagues performed a retrospective study with ten patients receiving liver SBRT investigating the tumor motion with and without abdominal compression. They reported interfractional changes of a mean of 1.3 ± 1.0 mm in the cranio-caudal direction, the largest direction of movement. Intrafractional errors were <0.7 ± 0.7 mm again in the cranio-caudal direction [61]. Unlike the most frequently used small compression plate, at Memorial Sloan Kettering Cancer Center, an abdominal compression belt for abdominal SBRT was developed and later commercially available from Aktina Medical, Congers, NY, USA. It was analyzed by Lovelock and colleagues, who treated 42 patients with various abdominal tumors that had been marked with either fiducial markers or surgical clips. Pneumatic pressure was applied to an air bubble around the patient. Using this technique, cranio-caudal tumor motion could be reduced from 11.4 mm (5–20 mm range) to 4.4 mm (1–8 mm range) ($P = 0.001$). In 93% of patients, the tumor excursion could thus be limited to <5 mm [31].

Limitations of Immobilization

Each of the immobilization devices introduced above has its own sets of limitations in accuracy, feasibility, or comfort for patients. Frames hold the intrinsic threat of a systematic error and invasive frames the risk of infection and definitely discomfort and pain. Masks and bite blocks take time to mold and may also be uncomfortable. The same is true for abdominal compression. For moving targets, immobilization needs to be accompanied by motion control. Localization techniques, such as fiducial seeds, lasers, and fluoroscopic imaging, can aid in treatment planning and execution as well. In summary, risks and benefits need to be weighed against each other for all immobilization techniques.

Future of Immobilization

In the future, immobilization in SBRT will play a minor, but important, role: While the choice of device does not seem to matter much overall, the exact positioning, and in the case of moving tumors, exact tracking of the tumor are only possible through the intertwining potentials of immobilization and modern imaging and motion control. Nanotechnology, to detect tumor margins for radiation guidance, focused ultrasound technology, and real-time adaptive radiotherapy, is evolving quickly [62, 63]. Six degree of freedom (6 DOF) correction of set-up and intrafractional errors is likely to be implemented into SBRT treatments as it already has shown to reduce PTV margins for IGRT [64]. First results for using real-time tumor tracking and 6 DOF correction for prostate and spinal SBRT have recently been published [65, 66].

There is evidence that keeping treatment time short improves accuracy due to slippage or irregularity of breathing cycles calling for easy-to-implement immobilization [66–68]. Cho and colleagues recently presented a prototype robotic immobilization system that accommodates tumor motion in real time using a 6 DOF robotic arm, a mobile couch, an optical tracker, and a computational control system integrating data from all the three aforementioned components leading to real-time correction of position [68]. Although this is a system yet to be studied before entering the clinic, it does show the need to integrate immobilization, imaging, and motion control in the future to improve accuracy and alleviate potential side effects of SBRT.

References

1. Niranjan A, Lunsford LD. Radiosurgery: where we were, are, and may be in the third millennium. Neurosurgery. 2000;46(3):531–43.
2. Verhey LJ. Immobilizing and positioning patients for radiotherapy. Semin Radiat Oncol. 1995;5(2):100–14.
3. Schell MC, Bova FJ, Larson DA, Leavitt DD, Lutz WA, Podgorsak ED, et al. AAPM report no. 54. 1995.
4. Burchiel KJ, Nguyen TT, Coombs BD, Szumoski J. MRI distortion and stereotactic neurosurgery using the Cosman-Roberts-Wells and Leksell frames. Stereotact Funct Neurosurg. 1996;66(1–3):123–36.
5. Lamba M, Breneman JC, Warnick RE. Evaluation of image-guided positioning for frameless intracranial radiosurgery. Int J Radiat Oncol. 2009;74(3):913–9.
6. Salter BJ, Fuss M, Vollmer DG, Sadeghi A, Bogaev CA, Cheek DA, et al. The TALON removable head frame system for stereotactic radiosurgery/radiotherapy: measurement of the repositioning accuracy. Int J Radiat Oncol Biol Phys. 2001;51(2):555–62.
7. Kumar S, Burke K, Nalder C, Jarrett P, Mubata C, A'hern R, et al. Treatment accuracy of fractionated stereotactic radiotherapy. Radiother Oncol. 2005;74(1):53–9.
8. Das S, Isiah R, Rajesh B, Ravindran BP, Singh RR, Backianathan S, et al. Accuracy of relocation, evaluation of geometric uncertainties and clinical target volume (CTV) to planning target volume (PTV) margin in fractionated stereotactic radiotherapy for intracranial tumors using relocatable Gill-Thomas-Cosman (GTC) frame. J Appl Clin Med Phys. 2010;12(2):3260.
9. Laitinen LV, Liliequist B, Fagerlund M, Eriksson AT. An adapter for computed tomography-guided stereotaxis. Surg Neurol. 1985;23(6):559–66.
10. Alheit H, Dornfeld S, Dawel M, Alheit M, Henzel B, Steckler K, et al. Patient position reproducibility in fractionated stereotactically guided conformal radiotherapy using the BrainLab mask system. Strahlenther Onkol. 2001;177(5):264–8.
11. Bednarz G, Machtay M, Werner-Wasik M, Downes B, Bogner J, Hyslop T, et al. Report on a randomized trial comparing two forms of immobilization of the head for fractionated stereotactic radiotherapy. Med Phys. 2009;36(1):4;12–7.
12. Ruschin M, Nayebi N, Carlsson P, Brown K, Tamerou M, Li W, et al. Performance of a novel repositioning head frame for gamma knife perfexion and image-guided linac-based intracranial stereotactic radiotherapy. Int J Radiat Oncol Biol Phys. 2010;78(1):306–13.
13. Sayer FT, Sherman JH, Yen C-P, Schlesinger DJ, Kersh R, Sheehan JP, et al. Initial experience with the eXtend system: a relocatable frame system for multiple-session gamma knife radiosurgery. World Neurosurg. 2011;75(5–6):665–72.
14. Li G, Ballangrud Å, Kuo LC, Kang H, Kirov A, Lovelock M, et al. Motion monitoring for cranial frameless stereotactic radiosurgery using video-based three-dimensional optical surface imaging. Med Phys. 2011;38(7):3981–94.
15. Bova FJ, Buatti JM, Friedman WA, Mendenhall WM, Yang CC, Liu C, et al. The University of Florida frameless high-precision stereotactic radiotherapy system. Int J Radiat Oncol Biol Phys. 1997;38(4):875–82.
16. Meeks SL, Bova FJ, Wagner TH, Buatti JM, Friedman WA, Foote KD, et al. Image localization for frameless stereotactic radiotherapy. Int J Radiat Oncol Biol Phys. 2000;46(5):1291–9.
17. Wang J-Z, Rice R, Pawlicki T, Mundt AJ, Sandhu A, Lawson J, et al. Evaluation of patient setup uncertainty of optical guided frameless system for intracranial stereotactic radiosurgery. J Appl Clin Med Phys. 2010;11(2):3181.
18. Minniti G, Scaringi C, Clarke E, Valeriani M, Osti M, Enrici RM. Frameless linac-based stereotactic radiosurgery (SRS) for brain metastases: analysis of patient repositioning using a mask fixation system and clinical outcomes. Radiat Oncol. 2011;16(6):158.
19. Gevaert T, Verellen D, Engels B, Depuydt T, Heuninckx K, Tournel K, et al. Clinical evaluation of a robotic 6-degree of freedom treatment couch for frameless radiosurgery. Int J Radiat Oncol Biol Phys. 2012;83(1):467–74.
20. Lax I, Blomgren H, Näslund I, Svanström R. Stereotactic radiotherapy of malignancies in the abdomen. Methodological aspects. Acta Oncol. 1994;33(6):677–83.
21. Kondziolka D, Lunsford LD. Stereotactic radiosurgery for squamous cell carcinoma of the nasopharynx. Laryngoscope. 1991;101(5):519–22.
22. Kaplan ID, Adler JR, Hicks WL, Fee WE, Goffinet DR. Radiosurgery for palliation of base of skull recurrences from head and neck cancers. Cancer. 1992;70(7):1980–4.
23. Hamilton AJ, Lulu BA, Fosmire H, Stea B, Cassady JR. Preliminary clinical experience with linear accelerator-based spinal stereotactic radiosurgery. Neurosurgery. 1995;36(2):311–9.
24. Wulf J, Hädinger U, Oppitz U, Olshausen B, Flentje M. Stereotactic radiotherapy of extracranial targets: CT-simulation and accuracy of treatment in the stereotactic body frame. Radiother Oncol. 2000;57(2):225–36.
25. Yenice KM, Lovelock DM, Hunt MA, Lutz WR, Fournier-Bidoz N, Hua C-H, et al. CT image-guided intensity-modulated therapy for paraspinal tumors using stereotactic immobilization. Int J Radiat Oncol. 2003;55(3):583–93.
26. Lohr F, Debus J, Frank C, Herfarth K, Pastyr O, Rhein B, et al. Noninvasive patient fixation for extracranial stereotactic radiotherapy. Int J Radiat Oncol Biol Phys. 1999;45(2):521–7.
27. Andersen JB, Factor VM, Marquardt JU, Raggi C, Lee Y-H, Seo D, et al. An integrated genomic and epigenomic approach predicts

therapeutic response to zebularine in human liver cancer. Sci Transl Med. 2010;2(54):54ra77.
28. Gutiérrez AN, Stathakis S, Crownover R, Esquivel C, Shi C, Papanikolaou N. Clinical evaluation of an immobilization system for stereotactic body radiotherapy using helical tomotherapy. Med Dosim. 2011;36(2):126–9.
29. Shi C, Tazi A, Fang DX, Iannuzzi C. Implementation and evaluation of modified dynamic conformal arc (MDCA) technique for lung SBRT patients following RTOG protocols. Med Dosim. 2013;38(3):287–90.
30. Guckenberger M, Meyer J, Wilbert J, Baier K, Mueller G, Wulf J, et al. Cone-beam CT based image-guidance for extracranial stereotactic radiotherapy of intrapulmonary tumors. Acta Oncol (Madr). 2006;45(7):897–906.
31. Lovelock MD, Zatcky J, Goodman K, Yamada Y. The effectiveness of a pneumatic compression belt in reducing respiratory motion of abdominal tumors in patients undergoing stereotactic body radiotherapy. Technol Cancer Res Treat. 2014;13(3):259–67.
32. Bentel GC, Marks LB, Hendren K, Brizel DM. Comparison of two head and neck immobilization systems. Int J Radi ati Oncol Biol Phys. 1997;38(4):867–73.
33. Fuss M, Salter BJ, Rassiah P, Cheek D, Cavanaugh SX, Herman TS. Repositioning accuracy of a commercially available double-vacuum whole body immobilization system for stereotactic body radiation therapy. Technol Cancer Res Treat. 2004;3(1):59–67.
34. Gutfeld O, Kretzler AE, Kashani R, Tatro D, Balter JM. Influence of rotations on dose distributions in spinal stereotactic body radiotherapy (SBRT). Int J Radiat Oncol Biol Phys. 2009;73(5):1596–601.
35. Hyde D, Lochray F, Korol R, Davidson M, Wong CS, Ma L, et al. Spine stereotactic body radiotherapy utilizing cone-beam CT image-guidance with a robotic couch: intrafraction motion analysis accounting for all six degrees of freedom. Int J Radiat Oncol. 2012;82(3):e555–62.
36. Nevinny-Stickel M, Sweeney RA, Bale RJ, Posch A, Auberger T, Lukas P. Reproducibility of patient positioning for fractionated extracranial stereotactic radiotherapy using a double- vacuum technique. Strahlenther Onkol. 2004;180(2):117–22.
37. Hubie C, Shaw M, Bydder S, Lane J, Waters G, McNabb M, et al. A randomised comparison of three different immobilisation devices for thoracic and abdominal cancers. J Med Radiat Sci. 2017;64(2):90–6.
38. Stoiber EM, Lechsel G, Giske K, Muenter MW, Hoess A, Bendl R, et al. Quantitative assessment of image-guided radiotherapy for paraspinal tumors. Int J Radiat Oncol. 2009;75(3):933–40.
39. Li W, Sahgal A, Foote M, Millar B-A, Jaffray DA, Letourneau D. Impact of immobilization on intrafraction motion for spine stereotactic body radiotherapy using cone beam computed tomography. Int J Radiat Oncol Biol Phys. 2012;84(2):520–6.
40. Dahele M, Verbakel W, Cuijpers J, Slotman B, Senan S, Belderbos J. An analysis of patient positioning during stereotactic lung radiotherapy performed without rigid external immobilization. Radiother Oncol. 2012;104(1):28–32.
41. Georg D, Bogner J, Dieckmann K, Pötter R. Is mask-based stereotactic head-and-neck fixation as precise as stereotactic head fixation for precision radiotherapy? Int J Radiat Oncol. 2006;66(4):S61–6.
42. Polat B, Wilbert J, Baier K, Flentje M, Guckenberger M. Nonrigid patient setup errors in the head-and-neck region. Strahlentherapie Onkol. 2007;183(9):506–11.
43. Doi H, Tanooka M, Ishida T, Moridera K, Ichimiya K, Tarutani K, et al. Utility of intraoral stents in external beam radiotherapy for head and neck cancer. Reports Pract Oncol Radiother. 2017;22(4):310–8.
44. Velec M, Waldron JN, O'Sullivan B, Bayley A, Cummings B, Kim JJ, et al. Cone-beam CT assessment of interfraction and intrafraction setup error of two head-and-neck cancer thermoplastic masks. Int J Radiat Oncol. 2010;76(3):949–55.
45. Wang H, Wang C, Tung S, Dimmitt AW, Wong PF, Edson MA, et al. Improved setup and positioning accuracy using a three-point customized cushion/mask/bite-block immobilization system for stereotactic reirradiation of head and neck cancer. J Appl Clin Med Phys. 2016;17(3):180–9.
46. Tryggestad E, Christian M, Ford E, Kut C, Le Y, Sanguineti G, et al. Inter- and intrafraction patient positioning uncertainties for intracranial radiotherapy: a study of four frameless, thermoplastic mask-based immobilization strategies using daily cone-beam CT. Int J Radiat Oncol Biol Phys. 2011;80(1):281–90.
47. Han K, Cheung P, Basran PS, Poon I, Yeung L, Lochray F. A comparison of two immobilization systems for stereotactic body radiation therapy of lung tumors. Radiother Oncol. 2010;95(1):103–8.
48. Siva S, Devereux T, Kron T, Gill S, MacManus M, Bressel M, et al. Vacuum immobilisation reduces tumour excursion and minimises intrafraction error in a cohort study of stereotactic ablative body radiotherapy for pulmonary metastases. J Med Imaging Radiat Oncol. 2014;58(2):244–52.
49. Mampuya WA, Nakamura M, Matsuo Y, Ueki N, Iizuka Y, Fujimoto T, et al. Interfraction variation in lung tumor position with abdominal compression during stereotactic body radiotherapy. Med Phys. 2013;40(9):91718.
50. Richmond ND, Pilling KE, Peedell C, Shakespeare D, Walker CP. Positioning accuracy for lung stereotactic body radiotherapy patients determined by on-treatment cone-beam CT imaging. Br J Radiol. 2012;85(1014):819–23.
51. Wunderink W, Méndez Romero A, de Kruijf W, de Boer H, Levendag P, Heijmen B. Reduction of respiratory liver tumor motion by abdominal compression in stereotactic body frame, analyzed by tracking fiducial markers implanted in liver. Int J Radiat Oncol. 2008;71(3):907–15.
52. Herfarth KK, Debus J, Lohr F, Bahner ML, Fritz P, Höss A, et al. Extracranial stereotactic radiation therapy: set-up accuracy of patients treated for liver metastases. Int J Radiat Oncol Biol Phys. 2000;46(2):329–35.
53. Bouilhol G, Ayadi M, Rit S, Thengumpallil S, Schaerer J, Vandemeulebroucke J, et al. Is abdominal compression useful in lung stereotactic body radiation therapy? A 4DCT and dosimetric lobe-dependent study. Phys Med. 2013;29(4):333–40.
54. Hu Y, Zhou Y-K, Chen Y-X, Zeng Z-C. Magnitude and influencing factors of respiration-induced liver motion during abdominal compression in patients with intrahepatic tumors. Radiat Oncol. 2017; https://doi.org/10.1186/s13014-016-0762-z. [published online].
55. Mampuya WA, Matsuo Y, Ueki N, Nakamura M, Mukumoto N, Nakamura A, et al. The impact of abdominal compression on outcome in patients treated with stereotactic body radiotherapy for primary lung cancer. J Radiat Res. 2014;55(5):934–9.
56. Shah C, Grills IS, Kestin LL, McGrath S, Ye H, Martin SK, et al. Intrafraction variation of mean tumor position during image-guided hypofractionated stereotactic body radiotherapy for lung Cancer. Int J Radiat Oncol. 2012;82(5):1636–41.
57. De Ruysscher D, Faivre-Finn C, Moeller D, Nestle U, Hurkmans CW, Le Péchoux C, et al. European Organization for Research and Treatment of Cancer (EORTC) recommendations for planning and delivery of high-dose, high precision radiotherapy for lung cancer. Radiother Oncol. 2017;124(1):1–10.
58. De Ruysscher D, Faivre-Finn C, Nestle U, Hurkmans CW, Le Péchoux C, Price A, et al. European Organisation for Research and Treatment of Cancer recommendations for planning and delivery of high-dose, high-precision radiotherapy for lung cancer. J Clin Oncol. 2010;28(36):5301–10.
59. Timmerman R, Galvin J, Michalski J, Straube W, Ibbott G, Martin E, et al. Accreditation and quality assurance for Radiation Therapy Oncology Group: multicenter clinical trials using stereotactic body radiation therapy in lung cancer. Acta Oncol (Madr). 2006;45(7):779–86.

60. Guckenberger M, Andratschke N, Dieckmann K, Hoogeman MS, Hoyer M, Hurkmans C, et al. ESTRO ACROP consensus guideline on implementation and practice of stereotactic body radiotherapy for peripherally located early stage non-small cell lung cancer. Radiother Oncol. 2017;124(1):11–7.
61. Shimohigashi Y, Toya R, Saito T, Ikeda O, Maruyama M, Yonemura K, et al. Tumor motion changes in stereotactic body radiotherapy for liver tumors: an evaluation based on four-dimensional cone-beam computed tomography and fiducial markers. Radiat Oncol. 2017;12:61.
62. De Salles AAF, Sedrak M, Lemaire JJ. The future of radiosurgery and radiotherapy. In: De Salles AAF, Gorgulho A, Agarzayan N, Slotman B, Selch M, Burwick A, editors. Shaped beam radiosurgery. Berlin: Springer; 2011. p. 305–9.
63. Colvill E, Booth J, Nill S, Fast M, Bedford J, Oelfke U, et al. A dosimetric comparison of real-time adaptive and non-adaptive radiotherapy: a multi-institutional study encompassing robotic, gimbaled, multileaf collimator and couch tracking. Radiother Oncol. 2016;119(1):159–65.
64. Guckenberger M, Meyer J, Wilbert J, Baier K, Sauer O, Flentje M. Precision of image-guided radiotherapy (IGRT) in six degrees of freedom and limitations in clinical practice. Strahlentherapie und Onkol. 2007;183(6):307–13.
65. Nguyen DT, O'Brien R, Kim J-H, Huang C-Y, Wilton L, Greer P, et al. The first clinical implementation of a real-time six degree of freedom target tracking system during radiation therapy based on Kilovoltage Intrafraction Monitoring (KIM). Radiother Oncol. 2017;123(1):37–42.
66. Finnigan R, Lamprecht B, Barry T, Jones K, Boyd J, Pullar A, et al. Inter- and intra-fraction motion in stereotactic body radiotherapy for spinal and paraspinal tumours using cone-beam CT and positional correction in six degrees of freedom. J Med Imaging Radiat Oncol. 2016;60(1):112–8.
67. Hoogeman MS, Nuyttens JJ, Levendag PC, Heijmen BJM. Time dependence of intrafraction patient motion assessed by repeat stereoscopic imaging. Int J Radiat Oncol. 2008;70(2):609–18.
68. Cho B, Chung H, Cho S. Feasibility study of robotics-based patient immobilization device for real-time motion compensation. Prog Med Phys. 2016;27(3):117–24.
69. Foster R, Meyer J, Iyengar P, Pistenmaa D, Timmerman R, Choy H, et al. Localization accuracy and immobilization effectiveness of a stereotactic body frame for a variety of treatment sites. Int J Radiat Oncol. 2013;87(5):911–6.
70. Han Z, Bondeson JC, Lewis JH, Mannarino EG, Friesen SA, Wagar MM, et al. Evaluation of initial setup accuracy and intrafraction motion for spine stereotactic body radiation therapy using stereotactic body frames. Pract Radiat Oncol. 2016;6(1):e17–24.
71. Guckenberger M, Meyer J, Vordermark D, Baier K, Wilbert J, Flentje M. Magnitude and clinical relevance of translational and rotational patient setup errors: a cone-beam CT study. Int J Radiat Oncol. 2006;65(3):934–42.
72. Grills IS, Hugo G, Kestin LL, Galerani AP, Chao KK, Wloch J, et al. Image-guided radiotherapy via daily online cone-beam CT substantially reduces margin requirements for stereotactic lung radiotherapy. Int J Radiat Oncol. 2008;70(4):1045–56.
73. Wang J, Zhong R, Bai S, Lu Y, Xu Q, Zhou X, et al. Evaluation of positioning accuracy of four different immobilizations using cone-beam CT in radiotherapy of non–small-cell lung cancer. Int J Radiat Oncol. 2010;77(4):1274–81.
74. Polat B, Guenther I, Wilbert J, Goebel J, Sweeney RA, Flentje M, et al. Intra-fractional uncertainties in image-guided intensity-modulated radiotherapy (IMRT) of prostate cancer. Strahlentherapie und Onkol. 2008;184(12):668–73.
75. Worm ES, Hansen AT, Petersen JB, Muren LP, Præstegaard LH, Høyer M. Inter- and intrafractional localisation errors in cone-beam CT guided stereotactic radiation therapy of tumours in the liver and lung. Acta Oncol (Madr). 2010;49(7):1177–83.
76. Purdie TG, Bissonnette J-P, Franks K, Bezjak A, Payne D, Sie F, et al. Cone-beam computed tomography for on-line image guidance of lung stereotactic radiotherapy: localization, verification, and intrafraction tumor position. Int J Radiat Oncol. 2007;68(1):243–52.
77. Li W, Purdie TG, Taremi M, Fung S, Brade A, Cho BCJ, et al. Effect of immobilization and performance status on intrafraction motion for stereotactic lung radiotherapy: analysis of 133 patients. Int J Radiat Oncol. 2011;81(5):1568–75.
78. Ueda Y, Teshima T, Cárdenes H, Das IJ. Evaluation of initial setup errors of two immobilization devices for lung stereotactic body radiation therapy (SBRT). J Appl Clin Med Phys. 2017;18(4):62–8.
79. Navarro-Martin A, Cacicedo J, Leaman O, Sancho I, García E, Navarro V, et al. Comparative analysis of thermoplastic masks versus vacuum cushions in stereotactic body radiotherapy. Radiat Oncol. 2015;10:176.

Motion Management in Stereotactic Body Radiation Therapy

Benjamin J. Cooper, Yi Rong, and Paul J. Keall

Scope

In this chapter, we build on the physics and immobilization outlined in previous chapters. Within the context of stereotactic body radiation therapy (SBRT), we describe (1) the sources of motion, (2) concepts for motion management, and (3) systems used for monitoring and measuring motion. The main focus is on gantry-mounted linear accelerator systems and accompanying subsystems. The emerging field of integrated MRI-linear accelerators will be discussed briefly. There is overlap between motion management for photons and protons. In this chapter, we focus on photon SBRT, and the preceding chapter explains proton SBRT in more detail. Broadly speaking, sources of organ motion arise from voluntary patient movement (e.g., moving a limb) and involuntary movement (respiration, cardiovascular system, gastrointestinal system, and urinary system). The focus of this chapter will be on respiratory motion management, described as having the highest need for SBRT applications in the report of Task Group 101 from the American Association of Physicists in Medicine (AAPM TG 101) [1].

B. J. Cooper (✉)
Medical Physics and Radiation Engineering, Canberra Hospital, Garran, ACT, Australia

ACRF Image X Institute, Camperdown, NSW, Australia
e-mail: Ben.cooper@act.gov.au

Y. Rong
University of California at Davis, Radiation Oncology, Sacramento, CA, USA
e-mail: yrong@ucdavis.edu

P. J. Keall
ACRF Image X Institute, Camperdown, NSW, Australia

University of Sydney, Camperdown, NSW, Australia
e-mail: Paul.keall@sydney.edu.au

Introduction

Motion is an unavoidable part of radiation therapy. How much motion might be expected is very closely dependent on the clinical location of the treatment target. For example, cranial tumors (above the base of the skull) exhibit very little movement with respect to the bony cranium (covered in a previous chapter), whereas lung tumors may exhibit relatively large motions with respect to the surrounding bony anatomy (vertebrae, ribs, etc.). The success of stereotactic body radiation therapy critically depends on the ability to manage patient motion. Often, the treatment targets are small, and the planned dose distributions have steep gradients with potentially very high doses delivered in a small number of fractions (Fig. 1a). If the geometric error between the target and the beam is more than that allowed for in planning, there will be a geographic miss with a lower dose in the target and higher dose in normal tissues (Fig. 1b).

Therefore, a comprehensive motion management strategy is an integral part of any SBRT program.

Respiratory Motion Management

One of the simplest methods to deal with respiratory motion is to apply a treatment margin based on the range of internal motion due to respiration (e.g., lung cancer) with the goal of covering any tumor motion within the planned treatment volume (PTV). This is not an optimal solution for a number of reasons. Firstly, nontarget, healthy tissue is getting the prescribed dose of radiation which is undesirable. Secondly, a consequence of using a large enough margin in the PTV to account for any tumor excursions during respiration puts an upper limit on the prescription dose because of concerns for normal tissue complications (toxicity). A patient receiving radiation therapy must first have a planning CT acquired. This must be performed with the

D. M. Trifiletti et al. (eds.), *Stereotactic Radiosurgery and Stereotactic Body Radiation Therapy*,
https://doi.org/10.1007/978-3-030-16924-4_19

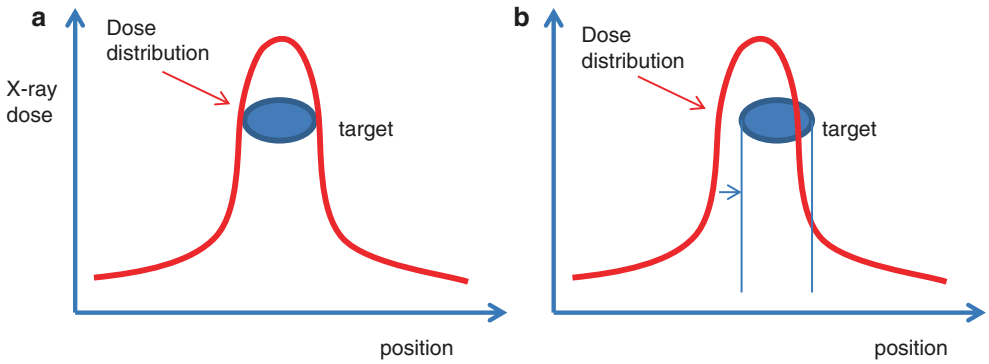

Fig. 1 (**a**, **b**) Steep dose distributions in SBRT must coincide with targets accurately: (**a**) ideal target dose and (**b**) a small deviation between the dose distribution and the target can lead to a geographical miss

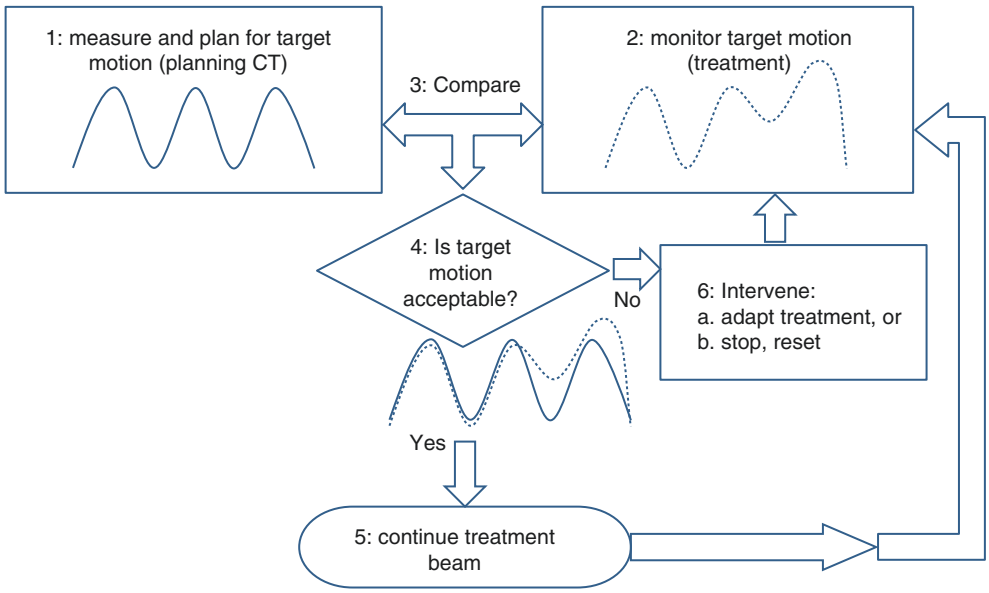

Fig. 2 Generalized motion management workflow schematic

patient set up in the same position as that in which the patient will be treated. Historically, a 3D CT scan would be used giving rise to imaging artifacts (doubling, jagged edges, and nonphysical features) due to motion from respiration [2, 3]. A four-dimensional CT (4D CT) allows respiratory motion to be elucidated; however, there are other challenges that arise from using 4D CT including irregular breathing. There are various planning techniques that incorporate the respiratory motion information from 4D CTs into planning. A fundamental problem with treatment planning is that the planning CT (either 3D or 4D) only gives information about the patient's anatomy on that day; in general, the anatomy will be in a slightly (or grossly) different position on the day of treatment, usually several days or possibly even weeks after the planning CT scan acquisition. How can we be sure that the treatment plan will still be valid on the day of treatment? This is where respiratory motion management has a central role to play. A general workflow is presented (Fig. 2):

1. Measure and plan for target motion during planning with 4D CT scan.
2. Monitor target motion at treatment.
3. Compare target motion measured at planning (1) with target motion at treatment (2).
4. Is target motion acceptable?
5. Yes – Continue treatment, loop back to (2).
6. a. No – Intervene, either by real-time treatment adaptation or loop from (2), or
   b. stop treatment and reset patient (e.g., reposition, re-establish regular breathing) and loop from (2).

Sources of Motion

Voluntary Motion

Before considering internal tumor motion sources, it is important to consider the whole patient as a source of motion,

in the sense that the patient as a whole body is moved into position prior to treatment. In general, image guidance, whereby radiological images taken during the treatment session, must be employed for SBRT. For large dose, hypofractionated treatments, it may be necessary to take intra-fraction guidance images during the treatment delivery. Details regarding immobilization can be found elsewhere within the book.

Involuntary Motion

Respiration

The most significant source of motion in thoracic and abdominal SBRT is respiration. Respiration is characterized as largely involuntary (i.e., automatic) but with some voluntary control (e.g., holding one's breath). The involuntary neural control of respiration is a complex interplay between chemoreceptors responsive to the partial pressures of oxygen, carbon dioxide, and acidity in the blood [4]. Keall and associates have tabulated lung tumor motion from 14 investigators in the report from AAPM TG 76 [5]. To give the reader a feel for the magnitude of motion reported in lung tumor motion, Table 1 depicts the mean and maximum range in millimeters based on the motion data reported in the TG 76 report [5].

The range of target motion due to respiration is very variable and patient specific. As such, each individual patient should be assessed for developing the best motion management strategy in SBRT.

Generally speaking, respiration may be characterized by several parameters: (1) "tidal volume," how deep or shallow is the respiration; (2) "regularity," how much does period and amplitude vary over the course of a treatment beam; and (3) respiratory period, time from end exhale to inhale and to end exhale again. A mathematical model that parameterizes respiratory motion z as a function of time t has been described [6]:

$$z(t) = z_0 - b\cos^{2n}\left(\pi t/\tau - \phi\right) \qquad (1)$$

where z_0 is the position at exhale, b is the amplitude of motion (thus $z_0 - b$ is the position at inhale), τ is the respiration period, n is the "fitting parameter," and ϕ is the initial phase in radians. See Fig. 3.

Table 1 Mean and maximum ranges of lung tumor motion in millimeters in three dimensions: SI is superior-inferior; AP is anterior-posterior; LR is left-right

Direction of lung tumor motion					
SI		AP		LR	
Mean	Max.	Mean	Max.	Mean	Max.
8.4	50	3.5	22	4.6	16

Data from Ref. [5]

This model is a useful starting point for respiratory motion modeling; however, it makes certain assumptions of constant respiratory periodicity and consistent amplitude which are not true in the general case for respiration because of its voluntary/involuntary nature as previously mentioned.

George and associates applied the model described by Eq. 1 to the study of 331 respiratory traces from 24 patients. Extending this model, it was reported that rather than fixed values for z_0, b, and τ, respiration may be modeled more realistically with a statistical distribution of those values [7].

Seppenwoolde and associates successfully modeled 20 patients' 3D tumor trajectories through a method of finding the best-fit parameters for Eq. 1 in all three cardinal directions (SI, AP, LR) using real-time 3D fluoroscopic positional data of implanted gold seeds [8]. Nearly half of the patients exhibited tumor trajectories with a 1–5 mm hysteresis (i.e., the tumor path during inhale and exhale was different). For a third of patients, cardiac motion affected trajectories by 1–4 mm. Both these effects highlight the complexity of respiratory-induced tumor motion and underscore the notion that Eq. 1 is a useful but limited parametric model for tumor motion and cannot be expected to model all respiratory patterns. Figure 4 summarizes the 21 tumor trajectories from the study, illustrating a variety of complex tumor motions [8].

In an effort to address these deficiencies, Ruan and associates proposed an algorithm for real-time profiling of respiratory motion where features such as baseline drift, phase variation, and fundamental pattern change can be decomposed from the signal, helping to characterize the real-time changes in respiration, potentially during treatment, which in turn can facilitate clinical decisions/response actions to mitigate treatment degradation [9].

A further complication is the consistency of patient breathing. Shah and associates investigated the use of elec-

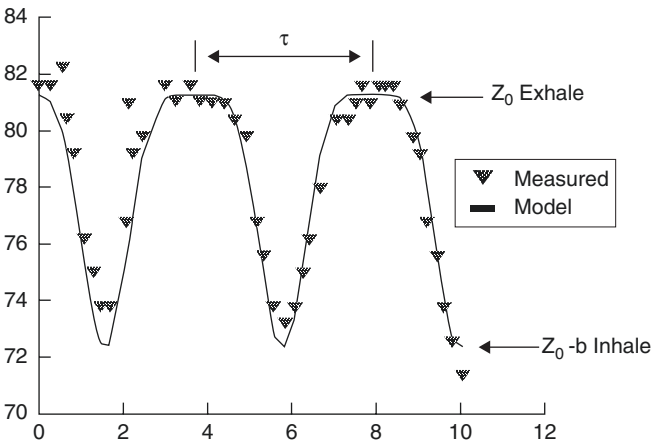

Fig. 3 Example of the mathematical motion model (solid line) fitted to diaphragm position measurements (inverted triangles). (Used with permission of John Wiley and Sons from Lujan et al. [6])

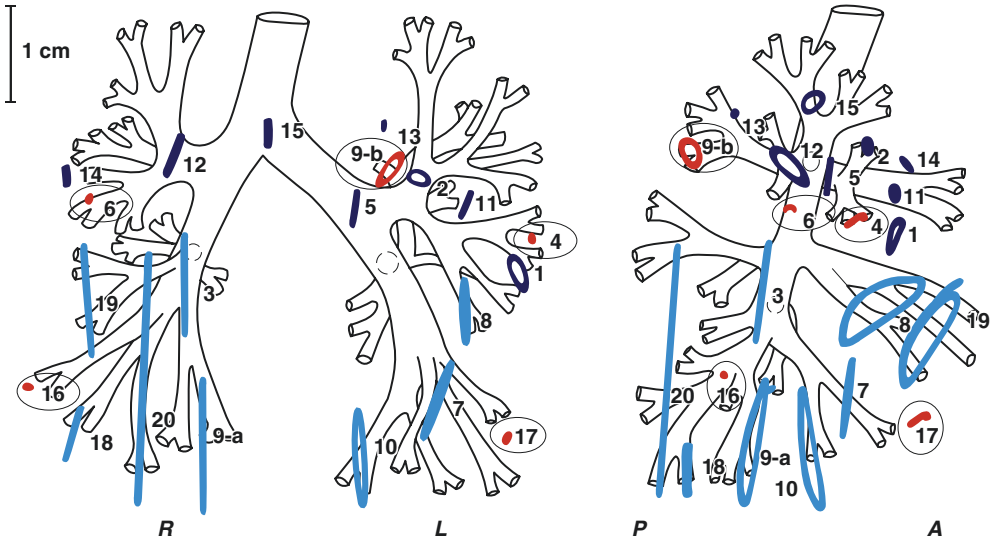

Fig. 4 Coronal (left) and sagittal (right) projections of 21 tumor trajectories (dark lines, numbered). Circled numbers represent tumor attachment to bony structures. (Used with permission of Elsevier from Seppenwoolde et al. [8])

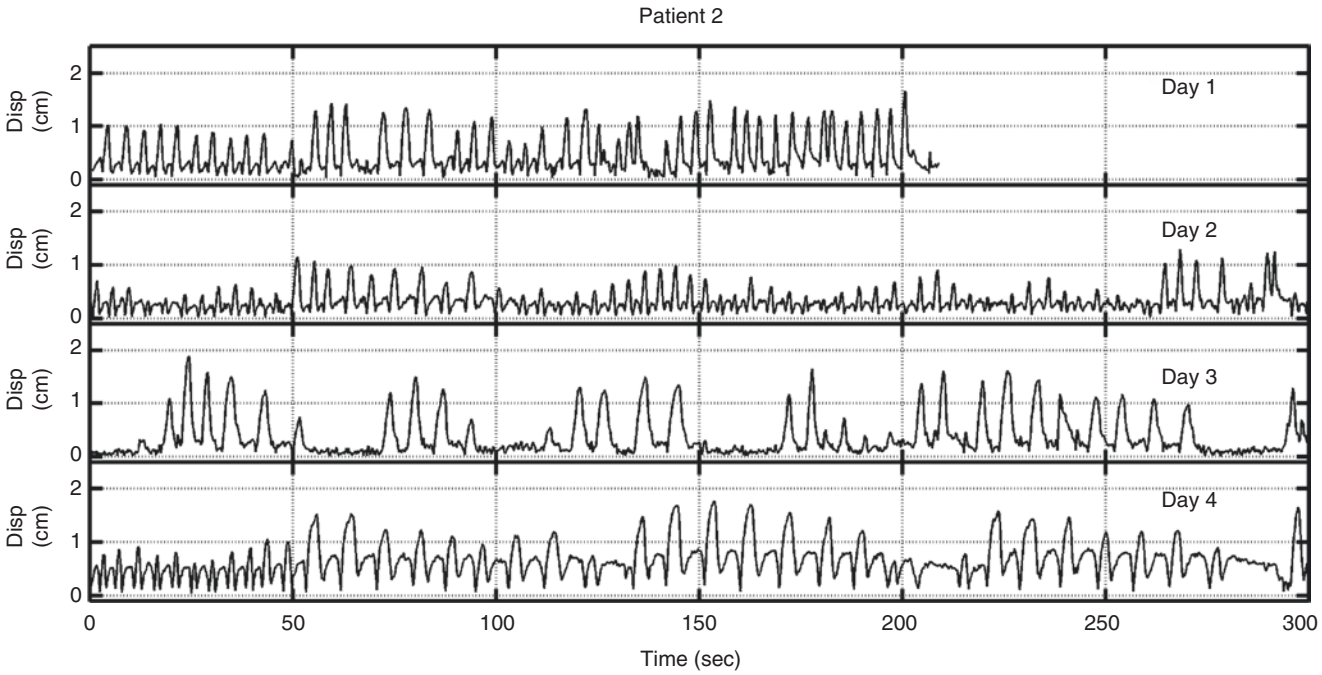

Fig. 5 Lung tumor displacement recorded over four consecutive days illustrating intra- and inter-fractional variations. (Used with permission of Elsevier from Shah et al. [10])

tromagnetic transponder implants from the commercially available Calypso® system (Varian, Palo Alto, CA, USA). The motion trace from "Patient 2" (Fig. 5) indicates the potential for both large intra- and inter-fractional variations in lung tumor motion including variation in amplitude and periodicity [10].

Bladder and Gastrointestinal Filling

Both the bladder and rectum are sources of inter- and intra-fractional motion of particular importance for stereotactic radiation therapy of the prostate. Careful adherence to bladder and bowel preparation protocols is typically required for patients. Bladder preparation protocols may include direc-

tions to drink certain volumes of liquid at defined times prior to treatment. Depending on the clinical circumstance, the protocol may involve voiding the bladder and/or bowel before treatment. The aim is to have the bladder, rectum, and prostate in a position as close to the planning scan as possible.

Concepts for Motion Management

In the context of SBRT, there exists the highest need for respiratory motion management and the maintenance of high spatial targeting accuracy throughout the entire treatment [11]. The clinician must decide on which motion management strategy is the most appropriate to achieve the clinical goals, taking into consideration all of the patient's capabilities and tolerances for undergoing motion management. In this section we discuss some of the strategies that are available. Figure 6 illustrates that motion management strategies generally become increasingly complex as the treatment margin requirements become "tighter."

Planning for Tumor Motion

There is a need to accurately identify the anatomy and trajectory of targets and surrounding tissue to enable the evaluation of the cumulative dose over the respiratory cycle in lung SBRT [12]. Four-dimensional computed tomography (4D CT) is a central imaging tool to fulfill these requirements, and its use in treatment planning is described below.

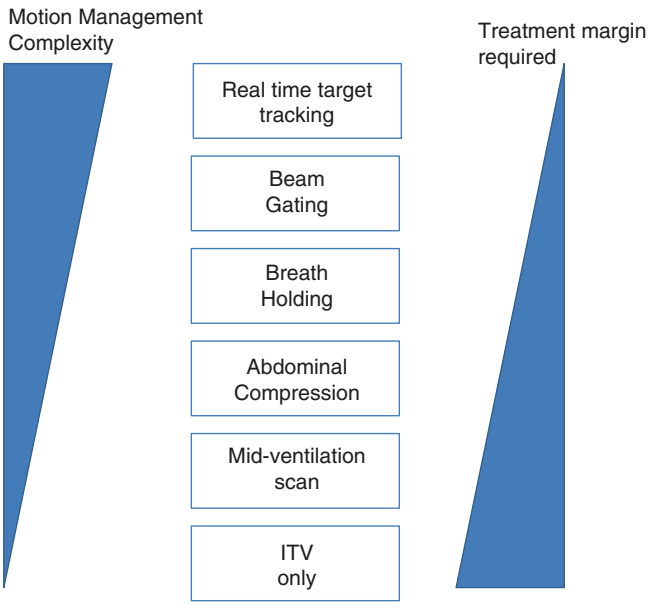

Fig. 6 A more precise and accurate treatment requires smaller treatment margins but at the cost of greater motion management complexity

Internal Motion Margin

Perhaps the simplest approach to manage respiratory-induced tumor motion is to use the patient's respiratory motion information for creating an internal motion margin (IM) in the context of creating an internal target volume (ITV) [13]. In this scenario, the IM can be derived from a 4D CT scan. This allows the clinician to visualize the extrema of tumor motion from which the IM is defined. However, it has been reported that this simple approach can lead to an overestimation of planning target volumes [14]. A common approach is to use a maximum intensity projection across all phases of a 4D CT scan in lung to generate the ITV (Fig. 7a) permitting rapid assessment of mobility of targets in lung cancer radiotherapy [15, 16]. Unfortunately, tumor motion, particularly tumors located in the vicinity of the diaphragm, can be tens of millimeters in magnitude leading to potentially large IMs and PTVs, unnecessarily irradiating healthy lung tissue. In general, margins do not account for respiratory variations (e.g., if the patient takes a deeper breath). On the other hand, if the clinician judges the tumor motion to be acceptably small in magnitude, these methods for determining ITVs might suffice.

A mid-ventilation CT scan technique proposes to use a single, "well-chosen" CT scan from a 4D CT set (Fig. 7b). The chosen scan acts as a representative reference average position of a mobile tumor target over the breathing cycle in lung, allowing for the possibility of margin reduction in planning [17, 18]. Mid-ventilation reference images can facilitate treatment of free breathing patients (without compression or breath-hold) and a potentially reduced treatment margin; however, there is an increased risk of breathing artifacts for mid-ventilation imaging because the tumor velocity is high at this phase of the breathing cycle [18].

Tumor Motion Detection: Treatment Compared to Planning

The work performed on characterizing and accounting for the motion of a tumor during the planning stage of SBRT must be followed up with careful assessment of the tumor motion detected immediately prior to, and during, treatment. It is critical to the success of the treatment that the tumor motion is assessed to be within the planning margins. Fortunately, gantry-mounted kV imaging systems (usually orthogonal to the treatment beam axis) are universally available on current release linear accelerators, making a revolutionary contribution to image guidance workflow for patient positioning accuracy and motion management in SBRT. Reference radiological images from planning (3D/4DCT and/or digitally reconstructed radiographs, DRRs) may be registered with radiological images (orthogonal planar kV pairs, 3D and 4D CBCT) from the gantry-mounted kV imaging system. Matching the "images of the

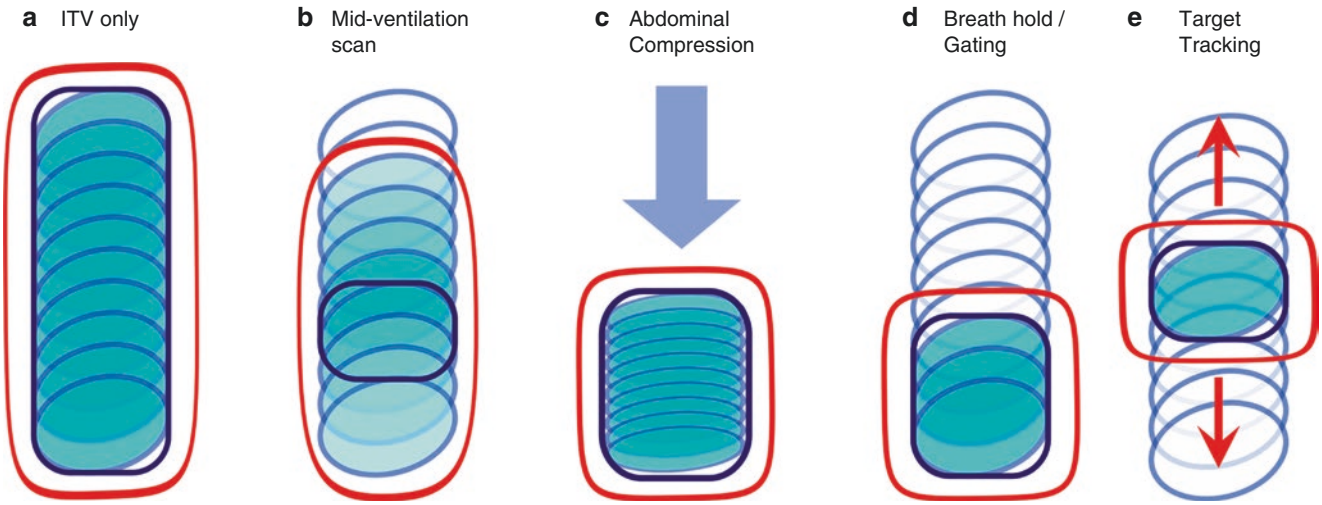

Fig. 7 (**a**–**e**) Schematic illustrating five techniques for motion management. The ellipse shape depicts tumor target motion over breathing phases; the smaller rectangles depict the ITV, and the larger rectangles depict the beam aperture. (**a**). ITV only, (**b**). mid-ventilation scan, (**c**). abdominal compression, (**d**). breath-hold/gating, (**e**). target tracking. (Based on data from Ehrbar et al. [11])

day" at the time of treatment with the reference images is designed to yield a repositioning vector: either a 3D translation (most commonly) or a 6D vector which incorporates three translational movements as well as three rotational (pitch, roll, yaw) movements (Fig. 8).

Commercial systems – such as ExacTrac® (BrainLab, Munich, Germany), PerfectPitch™ six degrees of freedom (Varian, Palo Alto, CA, USA), and HexaPOD™ Evo RT (Elekta, Stockholm, Sweden) – all follow a similar generalized workflow summarized as follows: (1) acquire "fresh" patient images immediately prior to treatment; (2) process those images to calculate a possible patient repositioning vector; and (3) execute the patient repositioning action by automatically sending motion instructions to the linac couch, either a 3D translational movement or possibly a couch capable of 6D movement, including pitch, roll, and yaw. Figure 9 schematically illustrates how a pre-treatment 4D CBCT can resolve a lung tumor trajectory into respiratory phases (numbered), and in this example, there is hysteresis in the target trajectory. The initial setup shows that the PTV would miss the target, but after the repositioning vector is applied, following Fig. 8, the PTV covers the entire respiratory cycle with no miss. This example encompasses the entire tumor trajectory (Fig. 7a), but 4D CBCT could also be used in conjunction with gated beam delivery reducing the required PTV.

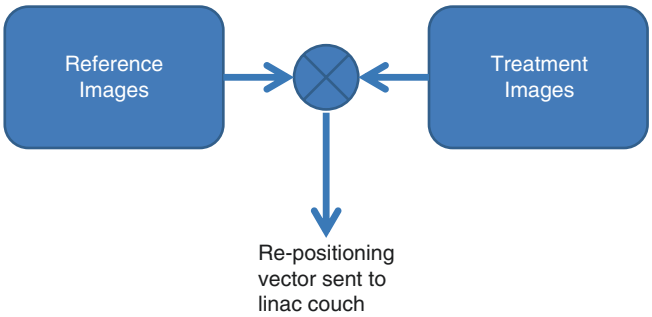

Fig. 8 Reference images from planning are compared to treatment images from imaging systems "on-board" the linac treatment machine. The difference between the images is used to calculate a repositioning vector with the goal of minimizing mismatch

Restricting Tumor Motion

Breath-Hold Approaches

The clinician, treatment, and planning teams need to decide if motion compensation is going to be used at treatment delivery or not [1] because this will have an impact on the magnitude of the ITV used in planning: if any kind of breath-hold technique is used, then this opens the possibility for a smaller internal margin and less normal tissue irradiation. This is difficult because it requires a high degree of confidence in getting the tumor into position via patient breath hold at the planned respiratory phase. Typically, breath-hold techniques require respiratory motion signals to be monitored and used in conjunction with image guidance systems, possibly using radio-opaque marker implants, to verify an acceptable correlation between phase of breath-hold and actual tumor position.

Deep Inspiration Breath-Hold

Hanley and associates investigated the potential value of deep inspiration breath-hold (DIBH) in lung radiation therapy. The idea of DIBH is that patients modify their

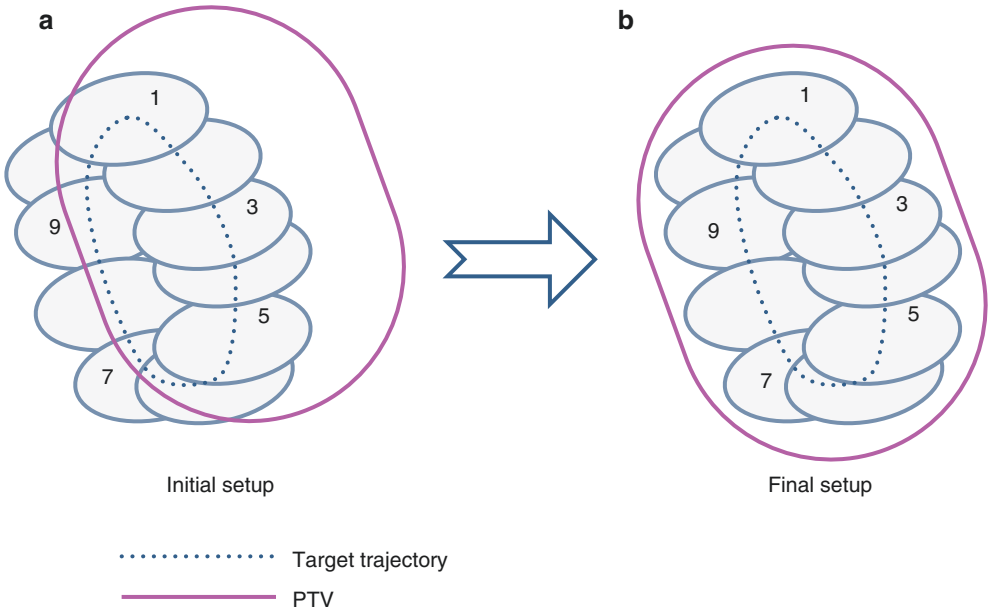

Fig. 9 (**a**) A pre-treatment 4D CBCT scan resolves a tumor target trajectory (small ellipses, odd phases numbered for clarity). The initial setup shows the planned PTV would miss; (**b**). After repositioning (see Fig. 8), a second 4D-CBCT scan confirms a good match between the planned PTV covering the tumor target trajectory

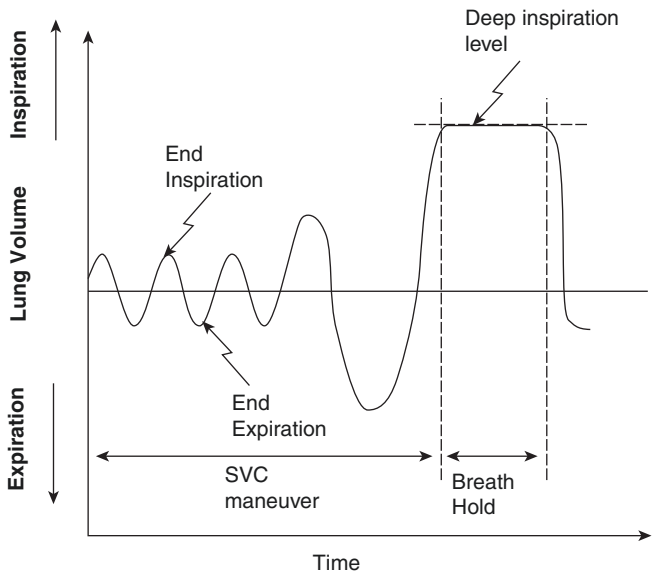

Fig. 10 Lung volume changing over time showing the slow vital capacity maneuver (SVC) and breath-hold. (Used with permission of Elsevier from Hanley et al. [19])

normal breathing pattern by forcibly expelling air in a slow vital capacity maneuver and then taking a deep breath and holding at inspiration during treatment delivery (Figs. 7d and 10).

The benefits are (1) lung volume is increased which lowers lung density overall, helping to reduce normal lung tissue irradiation, and (2) tumor target motion due to respiration is effectively arrested [19]. In a planning study, the authors report that the DIBH technique can reduce the relative volume of lung receiving 25 Gy by 30% [19]. Another DIBH study by Mah and coauthors demonstrated the use of spirometry to infer the displacement of the tumor centroid at treatment time as compared to tumor position at planning. Using a DIBH maneuver and spirometry, the authors reported a mean displacement and standard deviation of 0.02 ± 0.14 cm between the treatment time tumor position and the planned position, and this was consistent with independent tumor position measurements with port films [20]. Unfortunately, only around 50% of lung cancer patients were able to perform the DIBH breathing maneuver [20].

Active Breathing Control (ABC)

Active breathing control, or "ABC," is a treatment technique whose goal it is to minimize tumor target motion due to respiration. This is achieved by controlling the flow of air into the patient's lungs via a computer-controlled valve inside a breathing tube system. Airflow is continuously monitored by the ABC computer giving a respiratory signal. At a predetermined phase of the respiratory cycle (usually full inspiration), the ABC system stops the airflow and forces a controlled patient breath-hold during which the treatment beam is delivered (Fig. 11).

It is often the case that a treatment beam's duration is longer than the time a patient is able to hold their breath comfortably necessitating two or more consecutive breath-holds to complete the treatment beam. A study of the reproducibility of repeat ABC breath-holds of eight patients receiving treatment for intrahepatic tumors reported a mean diaphragmatic reproducibility of 2.5 mm (cranio-caudal direction). The same study reported an average absolute inter-fractional offset of 5.2 mm in the CC direction. The relatively large inter-fractional offsets can be addressed by daily imaging and are required if any substantial reduction in PTV margin is desired [21].

Abdominal Compression to Force Shallow Breathing

Normal breathing occurs when the action of the diaphragm "pulls" down into the abdominal cavity causing air to fill the lungs. Abdominal compression is a simple technique to reduce lung and liver tumor motion by restricting the normal action of the diaphragm and enforcing shallow breathing (Fig. 7c). Lax and coauthors have described tumor motion in the liver ranging from 1.5 to 2.5 cm during quiet breathing. Applying a light, constant pressure to the abdomen by tightening a belt around the patient, diaphragm motion could be reduced to 0.5–1.0 cm [22], thereby reducing the likelihood of the target moving out of the high-dose region. Utilizing 4D CT for analysis, tumor and organ motion can be significantly reduced under medium and high abdominal compression. In a small ten-patient study, the mean tumor motion was reduced from 13.6 mm (no compression) to 8.3 mm (medium compression at an average pressure of 48 N) and to 7.2 mm (high compression pressure, 91 N) [23]. Abdominal compression must be assessed on a patient-by-patient basis for suitability in SBRT given that the authors reported that three out of ten patients still exhibited tumor trajectories exceeding 1 cm, deemed to be unacceptable for SBRT [23].

Fig. 11 Active Breathing Coordinator System™. (Courtesy of Elekta, Stockholm, Sweden)

Gating the Beam During Treatment

Beam gating is where the treatment beam is switched on only when the target is in a pre-determined position during the respiratory cycle. The aim is to reduce normal tissue irradiation by trimming the radiation beam down to a smaller aperture where instantaneous target motion is at or near a minimum (Figs. 7d and 12).

There is a balance between having a small beam on duty cycle, which gives less residual motion but higher treatment times, and a larger beam on time which is faster but has higher residual motion. The gating concept is straightforward; however, the practical execution is technically difficult for numerous reasons: (1) internal/external correlation (phase shift), (2) longer treatment time (beam can be off for 50–70% of duty cycle), (3) irregular breathing, and (4) residual motion during the "beam on" phase. For these reasons, some authors have reported that the difficulty with gating may not outweigh the benefits for patients with tumor motions less than 2 cm [24–26].

Tumor Tracking and Real-Time Beam Adaptation

Tumor tracking is an advanced technique, whereby measured tumor motion signals during treatment can be used in a feed-

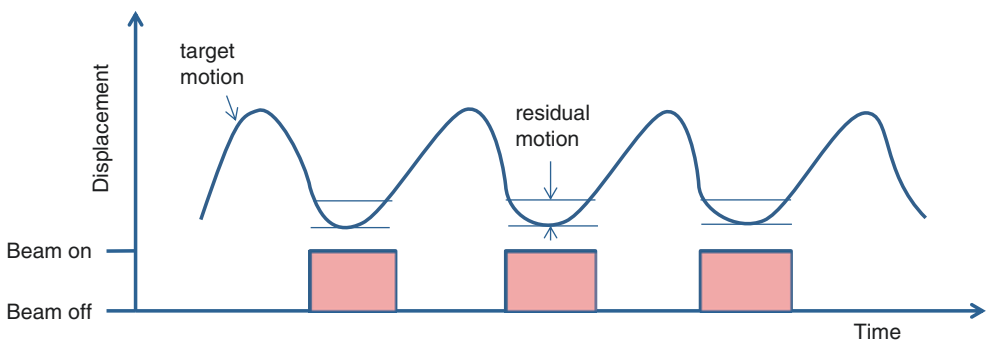

Fig. 12 Gating the treatment beam is switching the beam on at a predetermined part of the breathing cycle. The on-duty cycle of the beam (shaded rectangles) is only allowed to occur within the residual motion window that is pre-set

back loop to change the beam aperture dynamically and "adapt" the treatment to compensate for the tumor motion. The ability to detect motion and use this information to update the beam collimation and "track" the target in real time allows greater conformality to treatment targets and can reduce the need for manually repositioning the patient during treatment. The CyberKnife® system (Accuray Incorporated, Sunnyvale, CA, USA), a specialized robotic radiation therapy device, was one of the first systems capable of tracking respiratory motion [27, 28]. The Vero™ system (BrainLab, Munich, Germany) (no longer commercially available) took a different approach, whereby the radiation beamline, assembled on orthogonal gimbals, could track moving tumors [29]. A feasibility study of multi-leaf collimator (MLC) linac-based in vivo tumor tracking was first demonstrated in pigs [30]. The first human clinical implementation of linac-based dynamic MLC beam shaping to track tumor motion relied on the motion signals coming from electromagnetic transponder implants. These motion signals are processed by a computer program whose output instructs the MLC leaves to optimally align the treatment beam to the target, all during "beam on" (Fig. 13) [31].

The motion detection-to-adaptation feedback loop has been clinically demonstrated. The first human treatment using this technique was for a prostate cancer patient being treated with a dual-arc volumetric modulated arc therapy (VMAT) technique [32]. Keall and coauthors reported that without tracking, there was a 30% increase in the fractional rectal volume receiving 60 Gy compared to the original plan [32]. More recently, the same electromagnetic-guided real-time adaptive radiotherapy technique was applied to a lung cancer patient receiving 48 Gy over 4 fractions using stereotactic ablative body radiotherapy (SABR) [31]. In lung cancer radiotherapy, the target motion is generally more complex due to respiratory motion, especially for tumor sites located close to the diaphragm. At the planning stage, 4D CT was used to attain respiratory motion information. The end-of-exhale phase was used to define a "tracking" GTV ($GTV_{Tracking}$) and then expanded by 5 mm to define a PTV. A fundamental difference in adaptive radiotherapy planning is that the actual tumor trajectory on the day of treatment cannot be known exactly a priori. A novel planning technique was developed to deal with this issue, whereby an "isocenter shift method" considers each planned treatment arc as many sub arcs each with isocenter shifted in 2 mm bins to mimic target volume motion. Treatment log files, recording actual MLC leaf positions during treatment, and the EM transponder trajectories (assumed surrogates for target motion) inform the isocenter shift method to reconstruct the dose delivered utilizing the treatment planning system [31]. Booth and coauthors report that in comparison to standard ITV-based planning, the real-time adaptive radiotherapy with MLC tracking reduced the PTV from 18.7 to 11 cm^3; the mean lung dose reduced from 202 to 140 cGy with lung V20 and V5 reduced by 35% and 9% respectively [31]. Another broadly available technology yet to be clinically implemented for real-

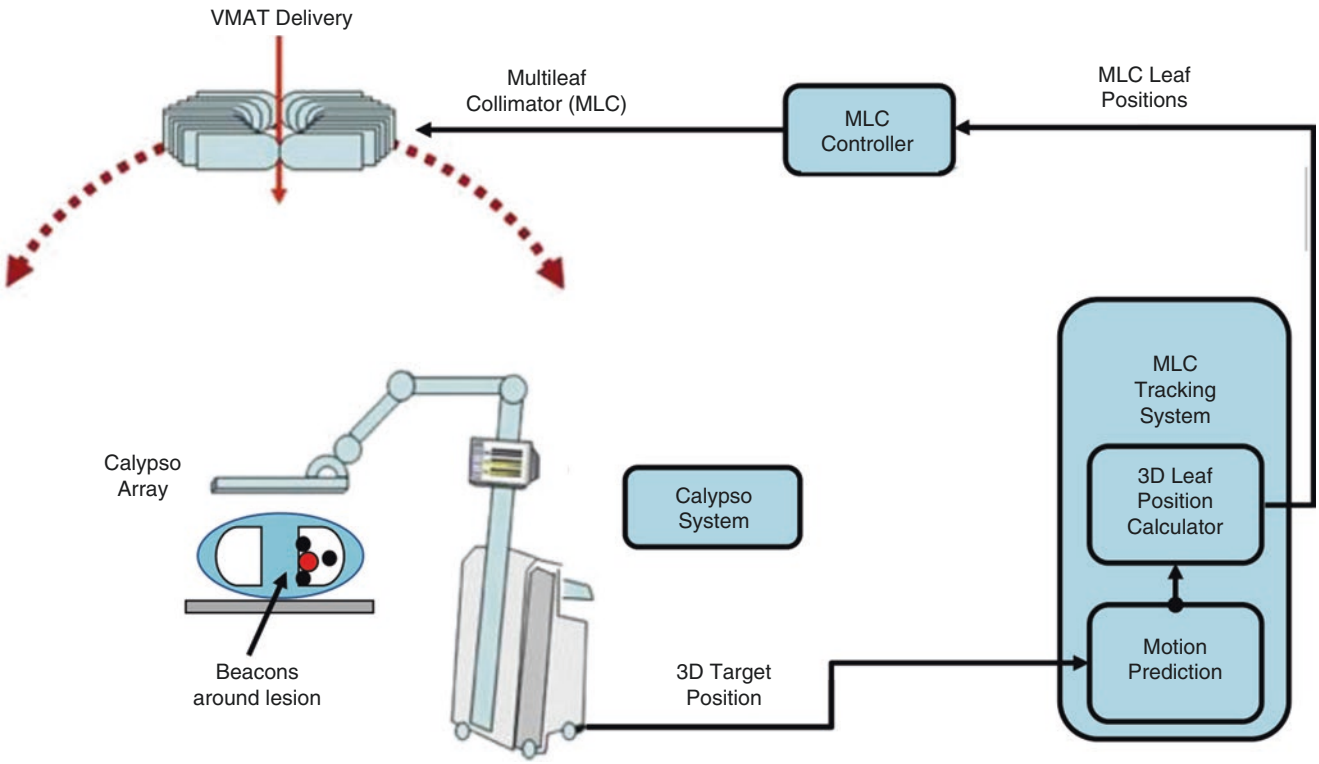

Fig. 13 Real-time tumor tracking feedback loop. Tumor motions are detected by the 3D target position system (Calypso,® Varian, Palo Alto, CA, USA) and processed by the MLC tracking software to automatically adjust the MLC leaf positions in real time. (Used with permission of Elsevier from Booth et al. [31])

time adaptation is the treatment couch, for which there has been considerable research and development, e.g., refs [33, 34] and subsequent articles. The community awaits the clinical translation of this technology which could be used as the sole adaptation method or in conjunction with MLC tracking and other degrees of freedom that could be modified on a modern linear accelerator, such as the gantry and collimator angles to improve beam-tumor targeting.

Systems for Monitoring and Measuring Motion

The motion monitoring and measuring can be performed using the in-room image guidance solutions, which can be categorized as (1) radiation-based systems and (2) non-radiation-based systems. This section elaborates on the technical details of those clinically available monitoring and measuring systems.

Radiation-Based Systems

For those radiation-based systems, motion monitoring relies on continuous imaging of the moving objects. Images are formed on imagers while detecting the attenuated x-ray photons. Important parameters that are relevant to motion monitoring are image resolution, acquisition rate, imaging dose, and accuracy. The fundamentals of image source, detectors, and imaging parameters are elaborated below.

X-Ray Sources

Radiation-based systems for in-room image guidance use x-ray sources with energy ranging from kilovoltage to megavoltage. Systems with MV x-ray sources either directly uses the 6 MV treatment beam (C-arm linac or Accuray CyberKnife) or a ramp-down 3.6 MV beam (Accuray Tomotherapy®). Systems with kV x-ray source require an independent kV x-ray generator that can be mounted directly on the linac gantry or within a ceiling/floor space. Typical kV x-ray energy is similar to conventional CT scanners, with a range of 100–140 kV.

Imaging Detectors

The most common imaging detector for both kV and MV x-ray sources is the solid-state flat panel imager (FPI). The FPI acquires images from a layer of phosphor screen made of gadolinium oxysulfide base doped with terbium (Gd_2O_2S/Tb) [35]. The imagers are mounted on a mechanical arm, 180 degrees from the imaging source. The detailed specifications of the MV and kV imaging system are listed in Table 2. Another imaging detector is xenon gas detector. Adopted from the old generation of CT scanners, Accuray Tomotherapy uses xenon-filled 640 channel CT detectors housed in an aluminum box [36]. These detector channels are separated by tungsten septa that are not in the line of divergence of beam axis. Signals are proportional to the scattering photons from Compton interactions of MV x-ray beams and the tungsten septa. This out-of-focus design allows higher scatter along the beam edge as compared to the beam center, resulting in a signal dip at the center of the detector-measured profiles [37].

Clinical Systems and Their Use in Motion Monitoring and Management

With the combination of different x-ray sources and detectors, the available imaging modes include 2D, 3D, and 4D for both kV and MV systems, as listed in Fig. 14.

Table 2 Flat panel detectors for kV and MV imaging

Flat panel detector type	MV			kV	
Linac	Varian-TrueBeam® (Varian, Palo Alto, CA, USA)	Varian-TrueBeam®/ EDGE®	Elekta-VersaHD™	Varian-TrueBeam®	Elekta-VersaHD™
Detector model	aS1000	aS1200	XRD 1642	4030CB	XRD 1642
Scintillator	Gadolinium Oxysulfide (GOS)	GOS	Various GOS	CsI	CsI
(Active) imaging area (cm^2)	40 × 30	43.0 × 43.0 (40.0 × 40.0)	41 × 41	39.7 × 29.8	41 × 41
Pixel matrix (1 × 1) (2 × 2)	1024 × 768 512 × 384	1280 × 1280 (1190 × 1190) 640 × 640	1024 × 1024	2048 × 1536 1024 × 768	1024 × 1024
Pixel pitch (mm)	0.392 or 0.784	0.336 or 0.672	0.4	0.194 or 0.388	0.4
Lag 1st frame	4%	1.5% at 7.5fps	<5% at 10fps	<5% at 7.5fps	<8%
Energy range	40 kV–15MV	40 kV–15MV	20 kV–15 MV	40–150 kV	40–150 kV
Max image acquisition rate	Up to 23fps	20fps	Up to 100 fps	Up to 30fps	Up to 100 fps
Contrast resolution	0.2% for 6MV, 0.8MU/ frame, 10 frames	0.15% for 6MV, 1.5MU/ frame, 2 frames			2.58 lp/mm at 7.5 fps (1 × 1) 1.29 lp/mm at 30 fps (2 × 2)
Modulation Transfer Function (MTF)		0.35 cycles/mm for 6MV		>45% at 1lp/mm for 80kVp	63% (0.5 cy/mm), 31% (1 cy/ mm) for RQA5 with CsI

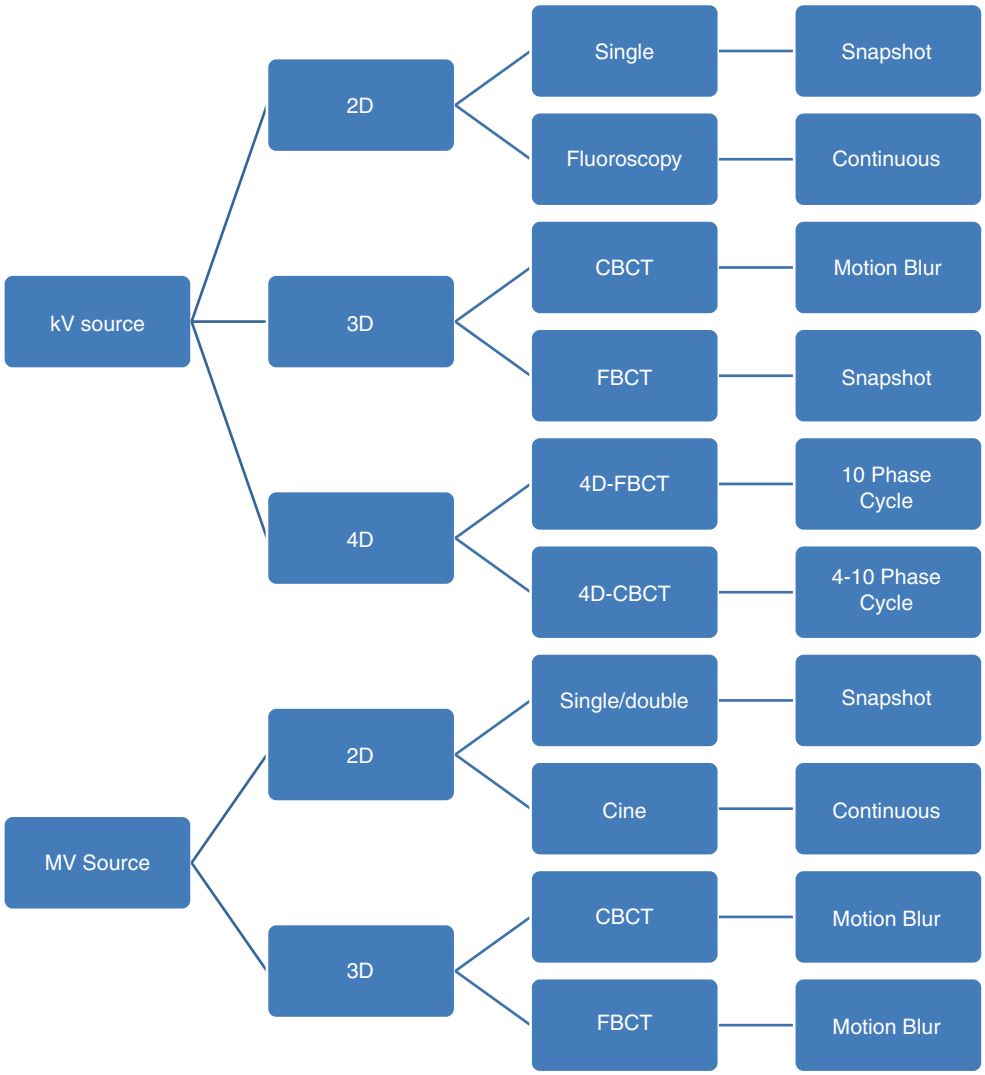

Fig. 14 Clinically available imaging modes and their applications in motion management

kV Imaging

With the combination of kV x-ray source and solid-state detectors, images can be generated in various dimensions, including 2D, 3D, and 4D. All of them can serve the purpose of patient positioning and motion management. In the initial phase of patient simulation, a 4D CT sorted through ten respiratory phases is usually acquired on the planning CT unit when the treating area is involved with significant motion. In the treatment room, various imaging modes can be utilized to manage or track motion. As shown in Fig. 15, the two commonly used systems in conjunction with a linear accelerator include gantry-mounted imaging system [38] (Fig. 15a, b) and floor-ceiling-mounted imaging system [39] (Fig. 15c, d).

For gantry-mounted systems (C-arm linacs from Varian or Elekta), kV x-ray tube and the FPI are mounted directly on the linac gantry, orthogonal to the beam axis. In this setting, the available image modes include 2D single/fluoroscopy, 3D CBCT, and 4D CBCT imaging. Motion monitoring and assessment can be achieved using 2D fluoroscopy and 4D CBCT modes. Continuous kV images can be acquired by the imager at an acquisition rate of 15 fps prior or during treatment. If used prior to treatment, the kV x-ray tube can be placed at the same gantry angle as the treatment beam, in order to assess the target motion in a beam's eye view. If used during treatment, the kV x-ray tube can be turned on at the same time as the treatment beam on, but 90 degrees from the treatment angle. This mode is mostly used for motion monitoring. In both cases, visualization of the moving target is challenging with the 2D imaging mode. There are two ways to mediate the issue: one is to use a surrogate that can be visualized on the 2D image, i.e., the diaphragm for lung cancer [40, 41], and the other is to plant fiducial markers that can be seen on kV images in or around the target [42, 43]. Typical imaging dose at skin surface ranges from 1 to 3 mGy per kV radiograph image, thus can ramp up to approximately 10 mGy/min during fluoroscopy [44]. The time-synchronized 4D CBCT image is created through sorting and binning a group (four phases and ten phases) of 3D CBCT image slices based on their correspond-

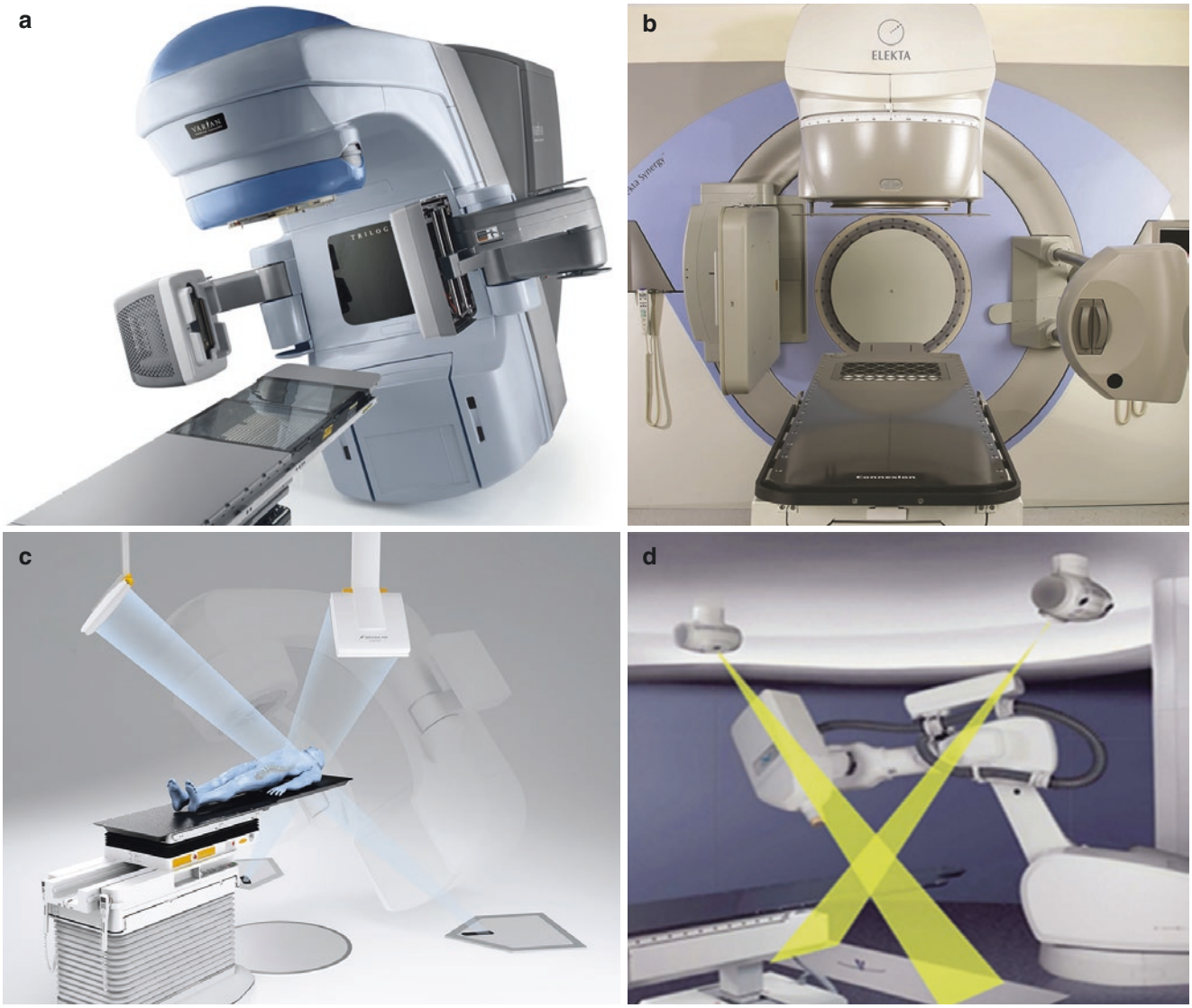

Fig. 15 (**a**–**d**) Typical gantry-mounted imaging systems (**a**: Varian Trilogy®; and **b**: Elekta Synergy®) and floor-ceiling-mounted imaging systems (**c**: BrainLab ExacTrac®; and **d**: Accuray CyberKnife®) (**a**: Courtesy of Varian, Palo Alto, CA, USA; **b**: Courtesy of Elekta, Stockholm, Sweden; **c**: Courtesy of BrainLab AG, Munich, Germany; **d**: Courtesy of Accuray Incorporated, Sunnyvale, CA, USA)

ing breathing cycles, available on the new models of Elekta [45, 46] and Varian linacs [47]. In comparison with the 4D CT acquired at the time of simulation/planning, 4D CBCT provides the most accurate way in managing and verifying the respiration-induced target motion prior to treatment delivery. The limitations include prolonged imaging time and elevated imaging dose to patients [47, 48].

Ceiling−/floor-mounted systems include BrainLab ExacTrac and CyberKnife. BrainLab ExactTrac is a stereotactic hybrid system, equipped with kV stereoscopic imaging, infrared tracking, and 6D couch [39]. The stereoscopic imaging system is composed of two kV x-ray tubes mounted on the floor and two aSi FPDs mounted on the ceiling. The infrared tracking system is composed of two infrared cameras, one video camera, and an infrared marker array. The motion tracking capability relies on the infrared system and/or x-ray with bony anatomy. This system is mostly designed for intracranial treatments, therefore not ideal for extracranial sites where large motion may occur. CyberKnife also has a stereoscopic imaging system, but with the x-ray tube mounted on the ceiling and the aSi FPDs mounted on the floor. Unlike BrainLab, the x-ray images can be acquired continuously at an interval of 5–90 s depending on the imaging mode [49]. This provides the capability of real-time tracking with the options of using bony structure, fiducial marker, or soft tissue [49]. The drawback is that each image adds an additional 0.01–0.07 cGy of imaging dose to patients.

MV Imaging

The imaging systems with the MV x-ray sources are all gantry mounted, with the options of generating 2D portal images or 3D reconstructed MV CT images. The MV

imager is mounted on the linac gantry, 180 degrees from the treatment head, as shown in Fig. 16a, b.

The 2D single−/double-exposure mode is mostly used for patient setup or field shape verification prior to treatment. Typical dose per image ranges from 2 to 3 cGy, depending on the imaging mode chosen and the MU used for imaging (1–5 MU for most users) [44]. The MV-Cine mode collects exit radiation using the MV panel during

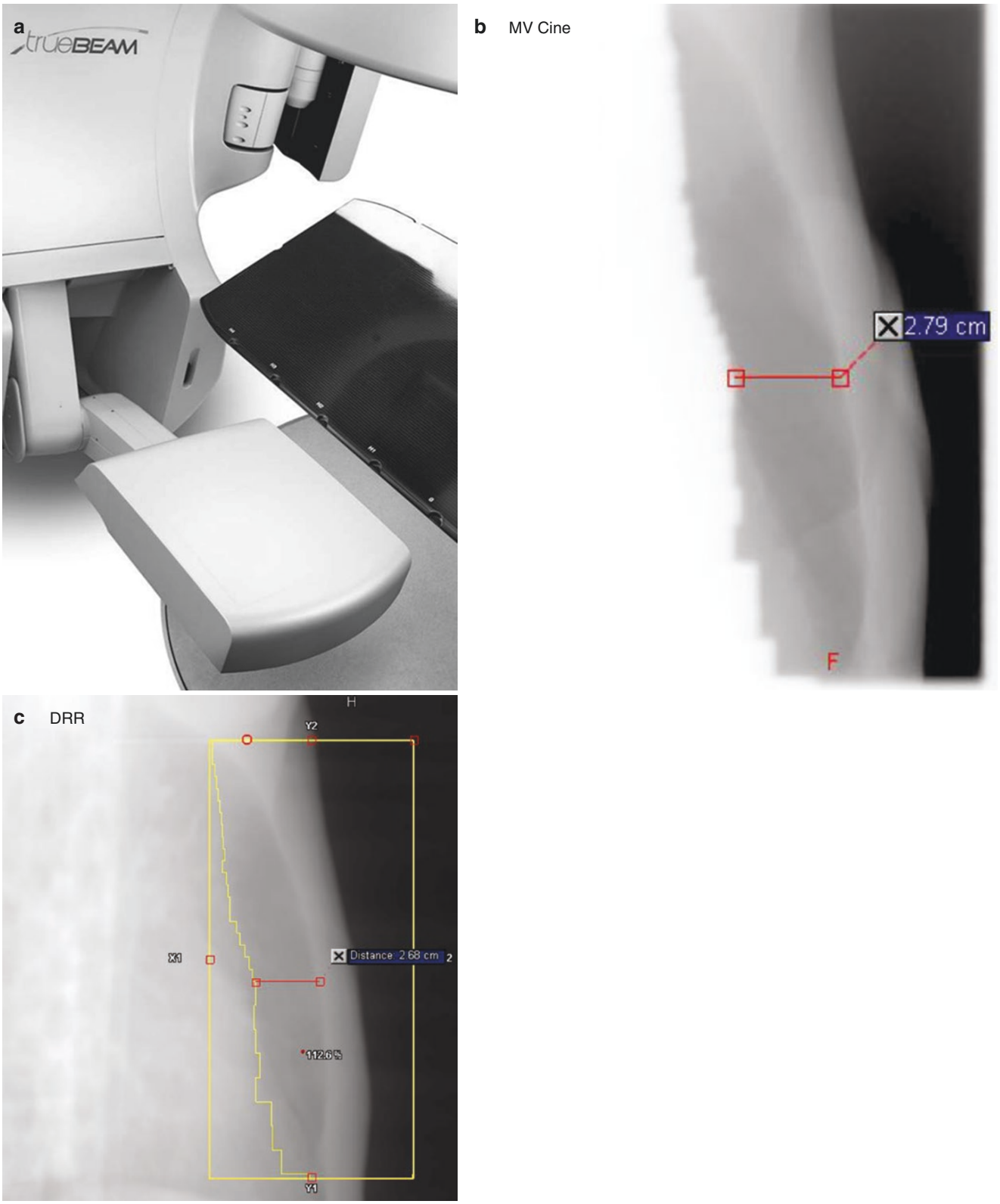

Fig. 16 (**a**) Varian robotic three-axis arm; (**b**). Elekta retractable EPID arm; (**c**). EPID MV-Cine imaging during treatment for motion tracking. (**a**: Courtesy of Varian, Palo Alto, CA, USA; **b**: Courtesy of Elekta, Stockholm, Sweden; **c**: Source: Rong et al. [51])

treatment at a certain frame rate (Fig. 16c). The benefit of this continuous imaging mode is that there is no additional dose to patients [50]. The limitation is low soft tissue contrast due to the inherent tissue interaction property with MV beams. The most use of this capability in motion monitoring is on the tangent beams when treating breast cancer, as shown in Fig. 16c [51]. It distinctively shows the boundary of the chest wall as opposed to the edge of the MLC collimation, which can be compared with DRRs from the treatment plan in order to monitor the positioning of the patient's breast or chest wall during treatment. This is especially useful for deep inspiration breath-hold (DIBH) treatment for left breast cancer [51].

The 3D MV CBCT acquisition mode is available on Siemens linacs [52] (discontinued) and the recently released Varian Halcyon™. The MV fan-beam CT (FBCT) acquisition mode is available on Accuray Tomotherapy linacs [52, 53], with the use of xenon-filled CT detectors as mentioned previously in this chapter. The use of these modes is limited for the application in motion management, since the image is acquired prior to treatment in a static CT mode with a blur trajectory of the target motion. However, due to the limited soft tissue contrast of the MV imaging, this blur trajectory can hardly be seen. Therefore, this mode is mostly used for patient positioning only.

Non-radiation-Based Systems

Non-radiation-based systems for monitoring and measuring target motion include camera-based, radiofrequency-based (RF), and ultrasound-based systems. Both camera-based systems and RF systems operate in the very-low-frequency region of the EM spectrum, using light waves or RF waves, respectively. Ultrasound-based systems rely on sound-waves for imaging but also incorporate infrared tracking technology for localization. Quality assurance for these systems has been mostly described in [54, 55].

Camera-Based Systems

Camera-based systems can be categorized into stereoscopic imaging and monoscopic imaging based on the method of 3D reconstruction [54]. The former relies on two sensors to identify the relative geometry information of a feature and derives its 3D information through triangulation. The latter derives 3D geometry information of an object through a single sensor with added geometric data. Both of these systems can only be used for surrogate or surface monitoring.

The infrared tracking system, based on stereoscopic imaging, can efficiently extract feature (infrared marker) information and detect motions. The infrared markers are usually placed on patients' surface as motion surrogates. One typical example of this system is real-time position management (RPM) (Varian Medical Systems, Palo Alto, CA, USA), which is composed of an infrared tracking camera (mounted on the ceiling or the rear end of the couch) and a reflective infrared six-dot marker box (placed on the patient's chest or abdomen where largest respiratory motion occurs). The system provides three-dimensional respiratory motion waveforms by measuring the displacement of the box with respect to the origin. The use of this RPM device has been well described by Keall and coauthors [5]. Other more complicated systems also incorporate this infrared technology to track motion, i.e., BrainLab ExacTrac, or determine spatial coordinates of a motion tracking device, i.e., Calypso system or SonArray® US system (Varian, Palo Alto, CA, USA).

Instead of using emissive or reflective fiducials as extracting features, video-based camera systems rely on the projected light pattern as known features and derive 3D information of the projecting object [56–58]. They are primarily used in surface-guided radiotherapy, which compares real-time surface imaging of regions of interests with the skin rendering from patient's planning CT scan, and provides patient positioning accuracy, as well as real-time monitoring [51, 59]. The commercially available systems can be categorized based on their imaging triangulation method: stereoscopic imaging (VisionRT and AlignRT [London, UK] and HumediQ [Varian, Palo Alto, CA, USA]) and monoscopic imaging (Catalyst [C-RAD, Uppsala, Sweden]). Stereoscopic imaging generates 3D surface through passive triangulation, which requires two video binocular cameras to acquire depth information of each structure point. Take the AlignRT system, for example. The system needs two or three pods (depending on the version) to create a complete patient's surface image, as shown in Fig. 17a. Each pod consists of two data cameras for stereovision, one projector for continuous speckle projection and one texture camera to capture a gray-scale image for visual information, as shown in Fig. 17b [57, 58]. The monoscopic imaging system, Catalyst C-RAD, only has one unit to generate a 3D surface image. This unit includes a high-speed CMOS camera and a structured light projector (Fig. 17c). The latter projects coded stripe light patterns to patients' body, which can be captured by the high-speed camera from a different angle. The depth information of the 3D surface can be calculated based on the angle-coded stripe patterns, thus the name active triangulation (Fig. 17d) [60–62]. The clinical usages of these camera-based systems include initial patient setup and intra-fractional patient motion monitoring specifically on patient's surface [51, 56, 59, 63–65].

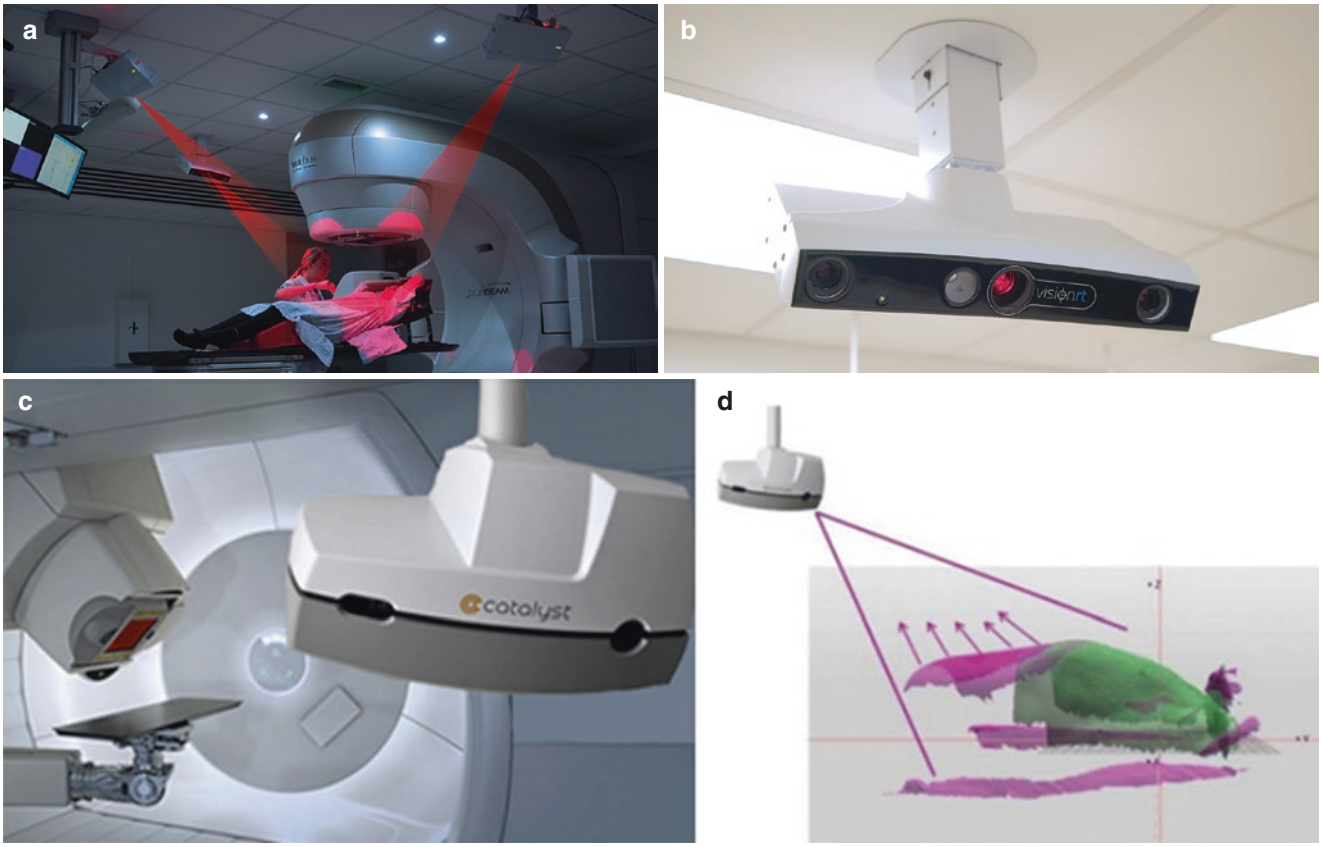

Fig. 17 (**a**–**d**) Room installation and device image for VisionRT (**a** and **b**) and Catalyst C-RAD (**c** and **d**). (**a**, **b**: Courtesy of VisionRT, London, UK; **c**, **d**: Courtesy of C-RAD, Uppsala, Sweden)

Radio-Frequency-Based System

The use of radio-frequency (RF) signals covers a variety of applications in radiology (i.e., MR imaging) and surgery (i.e., RF-guided bronchoscopy, SuperDimension, Inc., Minneapolis, MN, USA). The latter can be of assistance in placing fiducials within the lung lesion for gated thoracic SBRT treatments, as shown in Fig. 18a, b [66]. The RF system operates based on the ability to detect one or more RF-emitted coils that can be implanted in or on patients or attached to a device. A current commercial radio-frequency system used for motion management is the Calypso system (Varian Medical Systems, Palo Alto, CA, USA), as shown in Fig. 18c. The system consists of EM source coils, EM transponders (Beacon™), sensor array with infrared markers, and infrared cameras, as shown in Fig. 18d [67]. Prior to the treatment, the transponders (8 mm in length and 2 mm in diameter) are implanted inside or near the target (mostly used for prostate) by surgeons. Two or three transponders are usually used considering possible migrations in the patients' body. During the treatment, transponders are excited by the EM field from the EM source coils and send out signals that can be detected by the sensor array. The coordinates of the transponders can be determined with respect to the sensor array position. The sensor array position with respect to the linac isocenter can be determined by the infrared markers on the panel and the infrared cameras. The overall coordinates of the transponders with respect to the linac isocenter can then be determined. These coordinates are updated at a rate of 10 Hz prior and during patients' treatment, in order to monitor and manage possible target motion, with proved submillimeter accuracy [68] and clinical benefits especially for prostate target tracking [69]. Despite the advantages, the Calypso system still has fundamental limitations due to RF signal interference with other magnetic fields or metal objects, as well as signal strength [54, 70]. Therefore, it may not be an option for patients with metal implants, pacemakers/defibrillators, and/or a separation between the transponder and array larger than 27 cm for localization and 23 cm for target tracking [67, 71]. Furthermore, even with patients who met the Calypso criteria, only 91% of those were actually appropriate for the Calypso system [71]. Calypso system also requires a special kVue™ couch to replace the conventional carbon fiber couch due to possible carbon fiber interference with the signals. Other limitations include invasive surgery operation (thus, surgeons' time) for placing the markers, marker migrations, etc.

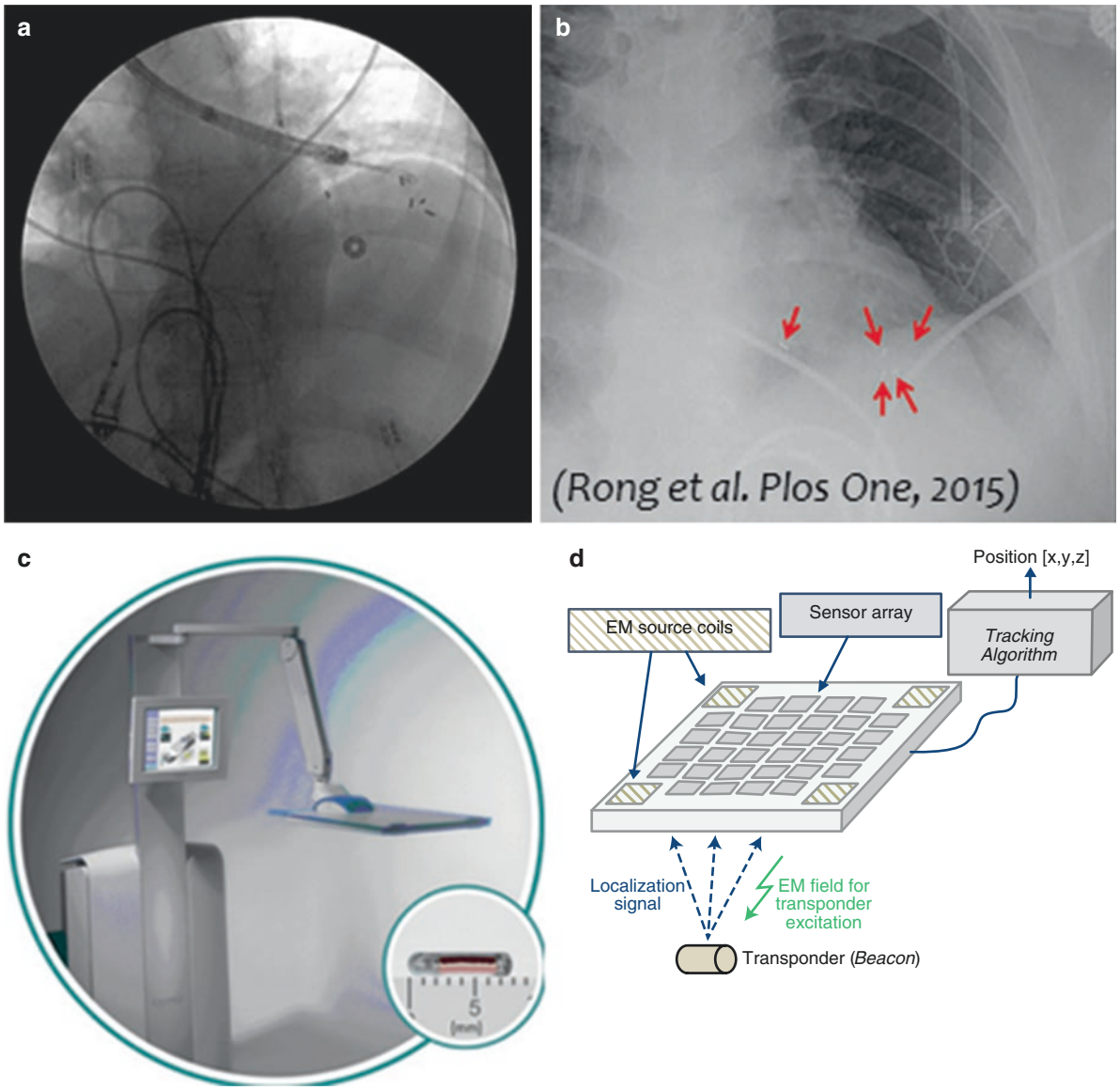

Fig. 18 (**a**, **b**) shows fiducial placements using RF-guided bronchoscopy by SuperDimension (Minneapolis, MN, USA). (**c**, **d**) shows the Calypso® system (Varian, Palo Alto, CA, USA) and its configurations. (**a**, **b**: Source: Rong et al. [66]. **c**, **d**: Used with permission of IOP Publishing from Franz et al. [70]. All Rights Reserved. © Institute of Physics and Engineering in Medicine)

Ultrasound-Based Systems The use of ultrasound (US) systems in patient setup and verification for radiotherapy began in the late 1990s, when conventional films were the only resources for daily setup and patient positioning. US offers real-time volumetric image with soft tissue contrast and no radiation to patients. Its imaging technique limits the application to the pelvic, abdominal, and breast sites. The brightness-mode acquisition and targeting (BAT) system (Best Nomos, Pittsburgh, PA, USA) provides 2D orthogonal US images of the treatment area to determine the target positional accuracy through matching the structure outlines from treatment plans. Its use has been intensively studied for prostate external beam treatment, and results have demonstrated its superiority in reducing target misalignment due to internal organ motions [72–77]. Adapted from the 2D US system, 3D US imaging was proposed [78, 79] and can be formed through mechanical scanning, freehand scanning with position sensor, or electronic scanning with 2D matrix arrays. The most common approach in RT is optical tracking, which tracks the probe position via infrared markers or reflectors and ceiling-mount optical cameras. The commercial systems include SonArray (Varian Medical Systems, Palo Alto, CA, USA), BATCAM™, and Clarity® (Elekta, Stockholm, Sweden) (Fig. 19a–c), which were found to be superior to 2DUS in detecting internal target/organ displacements [59, 80–83]. However, their limitations are also nontrivial, which include inter-modality errors between CT and US,

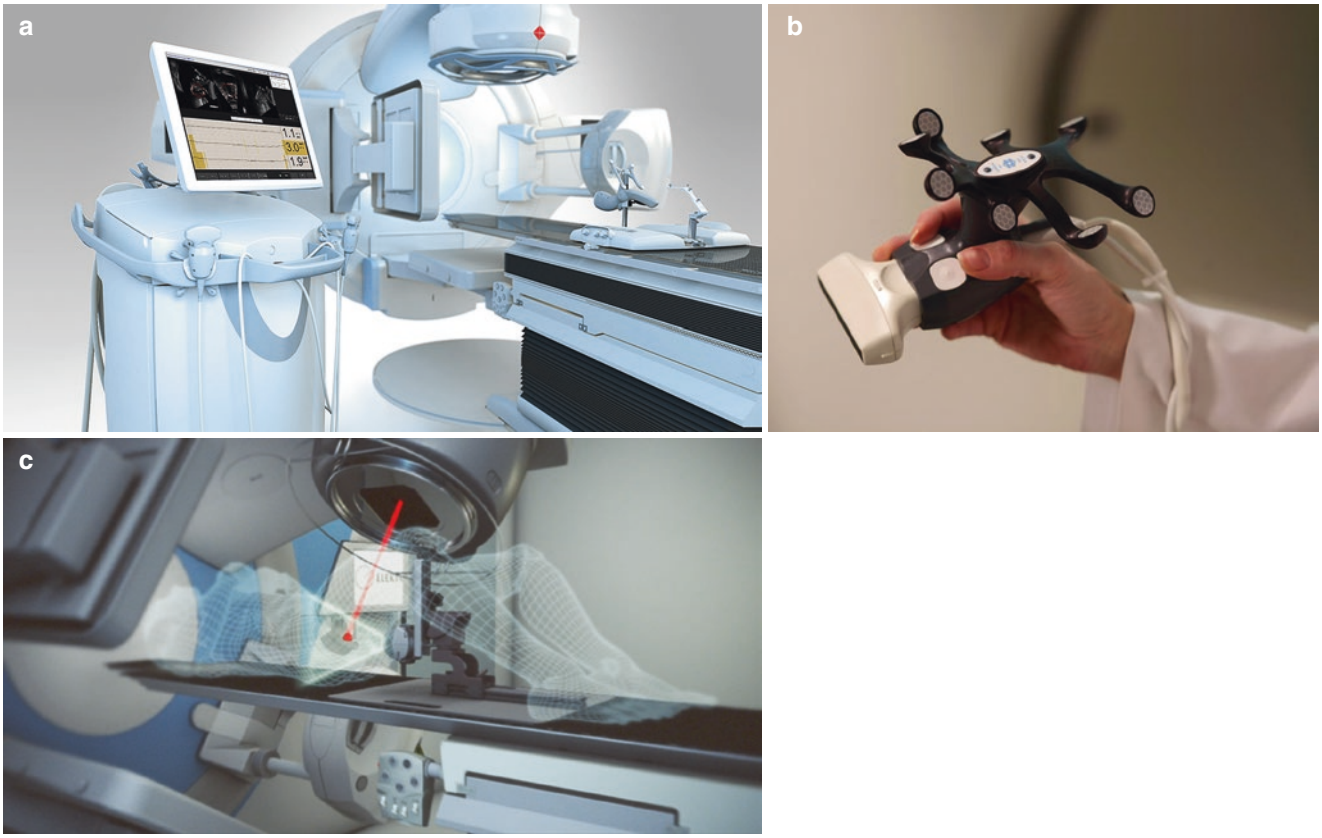

Fig. 19 (**a**–**c**) shows the Clarity® system, the Clarity® US probe, and the Autoscan kit setup during treatment for intro-fractional motion monitoring. (Courtesy of Elekta, Stockholm, Sweden)

anatomical deformation caused by abdominal pressure, inter-user inconsistency from freehand probe sweeping, incompatibility for intra-fractional motion monitoring, etc. The Clarity system provides a solution to overcome the inter-modality inconsistency, by letting users to acquire a 3D US image at the time of CT sim and register to the planning CT. This allows users to determine patient setup and positioning errors based on the daily US image in the reference frame of the CT during treatment (Fig. 19b). In addition, the concept of 4D US has been proposed with the intra-fractional real-time monitoring as the fourth dimension. Clarity Autoscan system provides hands-free intra-fractional US monitoring through a static transperineal transducer housed within an Autoscan kit (Fig. 19c), which motorizes the sweeping motion and enables a complete scan of 0.5 s, 75-degree sweep [84, 85]. Furthermore, other robotic abdominal sweeping systems for hands-free US scanning are being developed, which are used to overcome the limitation of performing inter- and intra-fractional target monitoring [86, 87]. A complete radiotherapy workflow with the use of US imaging in various steps is well summarized by Fontanarosa and coauthors [88] and O'Shea and coauthors [87]. A comparison of the available imaging modalities that can be used with SBRT is presented in Table 3.

Magnetic Resonance Imaging Linear Accelerator Systems

An emerging area of clinical radiotherapy is the introduction of integrated magnetic resonance imaging linear accelerator (MRI-linac) systems. MRI-linacs combine the exquisite soft tissue imaging offered by MRI with the linac's radiotherapy targeting capabilities. This field was clinically pioneered by the MRIdian device [89] (ViewRay, Oakwood, Village, OH, USA), a 0.35 T MRI which initially was integrated with cobalt-60 radiation sources. In 2017, new MRIdian models replaced the cobalt-60 source with a linac and started treating patients. The MRIdian workflow involves pre-treatment volumetric MRI images with intra-treatment 2D planar images which can be used for gating the treatment beam based on the MRI-measured tumor position. The superior image quality offered by MRI has also enabled the introduction of online adaptive radiotherapy into routine clinical use [90]. In 2017, a prototype 1.5 T Elekta Unity was first used to treat patients at Utrecht University [91], and it is anticipated that the use of the Unity will expand rapidly. The Alberta [92] and Sydney [93] groups have also built MRI-linacs. It is anticipated that the role of MRI-linacs in cancer radiotherapy will grow substantially over the next 10 years.

Table 3 Comparison within various imaging modalities for their physical characteristics (CT refers to devices specific for RT (such as CBCT or CT-on-rails). Two cases are distinguished: when the beam is in the kV range (standard CT and kV cone beam CT (kV CBCT)) and when it is in the MV range (MV CBCT and Tomotherapy). MRI refers to the MR for guiding RT treatment

Imaging modality	CT	US	MRI	2D kV/MV	Surface imaging	Varian Calypso®/ EM
Acquisition time (with setup/ preparation)	~2 min	~2 min	5 min	<1 min	<1 min	8 min
Spatial resolution	1–3 mm	Sub-mm	0.5–5 mm	~1 mm	Sub-mm	No
Visualization capabilities	kVCT: soft tissue in the whole body. Whole-body imaging MVCT: bone contrast only	Soft tissues: high contrast Difficult to image through air or bones (no lungs/ brain)	Soft tissues: high contrast	2D, poor contrast (only bones and fiducial markers)	Surface 3D (no internal organs)	Markers
Invasiveness	Yes with fiducial markers or contrast	Yes for some applications (intracavity) or using contrast	Yes for special application with contrast	Yes with fiducial markers or contrast	No	Yes with beacon transponders
Dose delivered	1–3 cGy (kV); 1–15 cGy (MV)	None	None	<1 cGy (kV); 6 cGy (MV)	No	No
Operator dependence	No	Yes	No	No	Yes (ROI selection)	No
Inter-fraction motion monitoring	Yes, 4D CT or 4D CBCT, kV	Yes	Yes, 2D	Yes (fluoroscopy)	Yes (surface only)	Yes (marker tracking)
Intra-fraction motion monitoring	No	Yes (with Clarity autoscan)	Yes (semi real-time)	Yes (kV fluoroscopy or MV-Cine)	Yes (surface only)	Yes (real-time marker tracking)
Image distortion and artifacts	Streaking, beam hardening, scatter	Probe pressure, aberrations	Motion, metal parts, geometrical uncertainties depending on acquisition type	Streaking, low signal-to-noise ratio, motion	Partial image based on camera view, reflection, gantry blocking	No images, but signals can be affected by metal or carbon fiber
Functional/ biological information	Yes	Yes	Yes	No	No	No
Extra time for system setup and preparation	No, unless contrast CT	Yes	No, unless contrast MRI	No	No	Yes

Adapted with modifications from O'Shea et al. [87]

Summary

Motion management in radiotherapy remains one of the most challenging technical aspects of radiation oncology, particularly for SBRT. Motion affects the imaging, treatment planning, setup, and delivery phases of the radiotherapy process. Motion adds time and complexity to the radiotherapy process. Motion varies between patients, and between tumor sites, from day to day and from breath to breath. A variety of technology has been developed to measure motion and account for motion. In this chapter, we have outlined the challenges, technology available, and clinical processes for motion management in radiotherapy. The selection and safe application of this technology require a multidisciplinary team effort supported by experience, published guidelines, ongoing education, and a strong quality assurance program. The complexity of current motion management offers opportunities for future innovations to make motion management safer, simpler, and more time efficient.

References

1. Benedict SH, Yenice KM, Followill D, Galvin JM, Hinson W, Kavanagh B, et al. Stereotactic body radiation therapy: the report of AAPM Task Group 101. Med Phys. 2010;37(8):4078–101.
2. Balter JM, Ten Haken RK, Lawrence TS, Lam KL, Robertson JM. Uncertainties in CT-based radiation therapy treatment planning associated with patient breathing. Int J Radiat Oncol Biol Phys. 1996;36(1):167–74.
3. Yamamoto T, Langner U, Loo BW, Shen J, Keall PJ. Retrospective analysis of artifacts in four-dimensional CT images of 50 abdominal and thoracic radiotherapy patients. Int J Radiat Oncol Biol Phys. 2008;72(4):1250–8.
4. Berger AJ, Mitchell RA, Severinghaus JW. Regulation of respiration. N Engl J Med. 1977;297(2):92–7.

5. Keall PJ, Mageras GS, Balter JM, Emery RS, Forster KM, Jiang SB, et al. The management of respiratory motion in radiation oncology report of AAPM Task Group 76. Med Phys. 2006;33(10):3874–900.
6. Lujan AE, Larsen EW, Balter JM, Ten Haken RK. A method for incorporating organ motion due to breathing into 3D dose calculations. Med Phys. 1999;26(5):715–20.
7. George R, Vedam S, Chung T, Ramakrishnan V, Keall P. The application of the sinusoidal model to lung cancer patient respiratory motion. Med Phys. 2005;32(9):2850–61.
8. Seppenwoolde Y, Shirato H, Kitamura K, Shimizu S, Van Herk M, Lebesque JV, et al. Precise and real-time measurement of 3D tumor motion in lung due to breathing and heartbeat, measured during radiotherapy. Int J Radiat Oncol Biol Phys. 2002;53(4):822–34.
9. Ruan D, Fessler JA, Balter J, Keall P. Real-time profiling of respiratory motion: baseline drift, frequency variation and fundamental pattern change. Phys Med Biol. 2009;54(15):4777.
10. Shah AP, Kupelian PA, Waghorn BJ, Willoughby TR, Rineer JM, Mañon RR, et al. Real-time tumor tracking in the lung using an electromagnetic tracking system. Int J Radiat Oncol Biol Phys. 2013;86(3):477–83.
11. Ehrbar S, Jöhl A, Stieb S, Riesterer O, Stark L, Guckenberger M, et al. PO-0926: Dosimetric comparison of different motion management techniques. Radiother Oncol. 2015;115:S482–S3.
12. Hugo GD, Rosu M. Advances in 4D radiation therapy for managing respiration: Part I–4D imaging. Z Med Phys. 2012;22(4):258–71.
13. Landberg T, Chavaudra J, Dobbs J, Gerard J-P, Hanks G, Horiot J-C, et al. Prescribing, recording and reporting photon beam therapy (Supplement to ICRU report 50). 1999.
14. Stevens CW, Munden RF, Forster KM, Kelly JF, Liao Z, Starkschall G, et al. Respiratory-driven lung tumor motion is independent of tumor size, tumor location, and pulmonary function. Int J Radiat Oncol Biol Phys. 2001;51(1):62–8.
15. Bradley JD, Nofal AN, El Naqa IM, Lu W, Liu J, Hubenschmidt J, et al. Comparison of helical, maximum intensity projection (MIP), and averaged intensity (AI) 4D CT imaging for stereotactic body radiation therapy (SBRT) planning in lung cancer. Radiother Oncol. 2006;81(3):264–8.
16. Underberg RW, Lagerwaard FJ, Slotman BJ, Cuijpers JP, Senan S. Use of maximum intensity projections (MIP) for target volume generation in 4DCT scans for lung cancer. Int J Radiat Oncol Biol Phys. 2005;63(1):253–60.
17. Wolthaus JW, Schneider C, Sonke J-J, van Herk M, Belderbos JS, Rossi MM, et al. Mid-ventilation CT scan construction from four-dimensional respiration-correlated CT scans for radiotherapy planning of lung cancer patients. Int J Radiat Oncol Biol Phys. 2006;65(5):1560–71.
18. Guckenberger M, Wilbert J, Krieger T, Richter A, Baier K, Flentje M. Mid-ventilation concept for mobile pulmonary tumors: internal tumor trajectory versus selective reconstruction of four-dimensional computed tomography frames based on external breathing motion. Int J Radiat Oncol Biol Phys. 2009;74(2):602–9.
19. Hanley J, Debois MM, Mah D, Mageras GS, Raben A, Rosenzweig K, et al. Deep inspiration breath-hold technique for lung tumors: the potential value of target immobilization and reduced lung density in dose escalation. Int J Radiat Oncol Biol Phys. 1999;45(3):603–11.
20. Mah D, Hanley J, Rosenzweig KE, Yorke E, Braban L, Ling CC, et al. Technical aspects of the deep inspiration breath-hold technique in the treatment of thoracic cancer. Int J Radiat Oncol Biol Phys. 2000;48(4):1175–85.
21. Dawson LA, Brock KK, Kazanjian S, Fitch D, McGinn CJ, Lawrence TS, et al. The reproducibility of organ position using active breathing control (ABC) during liver radiotherapy. Int J Radiat Oncol Biol Phys. 2001;51(5):1410–21.
22. Lax I, Blomgren H, Näslund I, Svanström R. Stereotactic radiotherapy of malignancies in the abdomen: methodological aspects. Acta Oncol. 1994;33(6):677–83.
23. Heinzerling JH, Anderson JF, Papiez L, Boike T, Chien S, Zhang G, et al. Four-dimensional computed tomography scan analysis of tumor and organ motion at varying levels of abdominal compression during stereotactic treatment of lung and liver. Int J Radiat Oncol Biol Phys. 2008;70(5):1571–8.
24. Guckenberger M, Krieger T, Richter A, Baier K, Wilbert J, Sweeney RA, et al. Potential of image-guidance, gating and real-time tracking to improve accuracy in pulmonary stereotactic body radiotherapy. Radiother Oncol. 2009;91(3):288–95.
25. Korreman SS, Juhler-Nøttrup T, Boyer AL. Respiratory gated beam delivery cannot facilitate margin reduction, unless combined with respiratory correlated image guidance. Radiother Oncol. 2008;86(1):61–8.
26. Sonke J-J, Rossi M, Wolthaus J, van Herk M, Damen E, Belderbos J. Frameless stereotactic body radiotherapy for lung cancer using four-dimensional cone beam CT guidance. Int J Radiat Oncol Biol Phys. 2009;74(2):567–74.
27. Dieterich S, Tang J, Rodgers J, Cleary K. Skin respiratory motion tracking for stereotactic radiosurgery using the CyberKnife. Int Congr Ser. 2003;1256:130–6.
28. Murphy MJ. Tracking moving organs in real time. Semin Radiat Oncol. 2004;14(1):91–100.
29. Depuydt T, Verellen D, Haas O, Gevaert T, Linthout N, Duchateau M, et al. Geometric accuracy of a novel gimbals based radiation therapy tumor tracking system. Radiother Oncol. 2011;98(3):365–72.
30. Poulsen PR, Carl J, Nielsen J, Nielsen MS, Thomsen JB, Jensen HK, et al. Megavoltage image-based dynamic multileaf collimator tracking of a NiTi stent in porcine lungs on a linear accelerator. Int J Radiat Oncol Biol Phys. 2012;82(2):e321–e7.
31. Booth JT, Caillet V, Hardcastle N, O'Brien R, Szymura K, Crasta C, et al. The first patient treatment of electromagnetic-guided real time adaptive radiotherapy using MLC tracking for lung SABR. Radiother Oncol. 2016;121(1):19–25.
32. Keall PJ, Colvill E, O'Brien R, Ng JA, Poulsen PR, Eade T, et al. The first clinical implementation of electromagnetic transponder-guided MLC tracking. Med Phys. 2014;41(2):020702.
33. D D'Souza W, Naqvi SA, Cedric XY. Real-time intra-fraction-motion tracking using the treatment couch: a feasibility study. Phys Med Biol. 2005;50(17):4021.
34. Wilbert J, Meyer J, Baier K, Guckenberger M, Herrmann C, Hess R, et al. Tumor tracking and motion compensation with an adaptive tumor tracking system (ATTS): system description and prototype testing. Med Phys. 2008;35(9):3911–21.
35. Tao S, Gu ZH, Nathan A. Fabrication of Gd2O2S:Tb based phosphor films coupled with photodetectors for x-ray imaging applications. J Vac Sci Technol A. 2002;20(3):1091–4.
36. Fenwick JD, Tome WA, Soisson ET, Mehta MP, Rock MT. Tomotherapy and other innovative IMRT delivery systems. Semin Radiat Oncol. 2006;16(4):199–208.
37. Keller H, Glass M, Hinderer R, Ruchala K, Jeraj R, Olivera G, et al. Monte Carlo study of a highly efficient gas ionization detector for megavoltage imaging and image-guided radiotherapy. Med Phys. 2002;29(2):165–75.
38. Berbeco RI, Jiang SB, Sharp GC, Chen GTY, Mostafavi H, Shirato H. Integrated radiotherapy imaging system (IRIS): design considerations of tumour tracking with linac gantry-mounted diagnostic x-ray systems with flat-panel detectors. Phys Med Biol. 2004;49:12.
39. Jin JY, Yin FF, Tenn SE, Medin PM, Solberg TD. Use of the BrainLAB ExacTrac X-Ray 6D system in image-guided radiotherapy. Med Dosim. 2008;33(2):124–34.
40. Christelle Gendrin HF, Weber C. Monitoring tumor motion by real time 2D/3D registration during radiotherapy. Radiother Oncol. 2012;102:6.
41. Lin T, Cervino LI, Tang X, Vasconcelos N, Jiang SB. Fluoroscopic tumor tracking for image-guided lung cancer radiotherapy. Phys Med Biol. 2009;54(4):981–92.

42. Shirato H, Harada T, Harabayashi T, Hida K, Endo H, Kitamura K, et al. Feasibility of insertion/implantation of 2.0-mm-diameter gold internal fiducial markers for precise setup and real-time tumor tracking in radiotherapy. Int J Radiat Oncol Biol Phys. 2003;56(1):240–7.
43. Tang X, Sharp GC, Jiang SB. Fluoroscopic tracking of multiple implanted fiducial markers using multiple object tracking. Phys Med Biol. 2007;52(14):4081–98.
44. Murphy MJ, Balter J, Balter S, BenComo JA Jr, Das IJ, Jiang SB, et al. The management of imaging dose during image-guided radiotherapy: report of the AAPM Task Group 75. Med Phys. 2007;34(10):4041–63.
45. Thengumpallil S, Smith K, Monnin P, Bourhis J, Bochud F, Moeckli R. Difference in performance between 3D and 4D CBCT for lung imaging: a dose and image quality analysis. J Appl Clin Med Phys. 2016;17(6):9.
46. Yoganathan SA, Maria Das KJ, Mohamed Ali S, Agarwal A, Mishra SP, Kumar S. Evaluating the four-dimensional cone beam computed tomography with varying gantry rotation speed. Br J Radiol. 2016;89(1060):20150870.
47. Santoso AP, Song KH, Qin Y, Gardner SJ, Liu C, Chetty IJ, et al. Evaluation of gantry speed on image quality and imaging dose for 4D cone-beam CT acquisition. Radiat Oncol. 2016;11:98.
48. Thengumpallil S, Smith K, Monnin P, Bourhis J, Bochud F, Moeckli R. Difference in performance between 3D and 4D CBCT for lung imaging: a dose and image quality analysis. J Appl Clin Med Phys. 2016;17(6):97–106.
49. Goyal S, Kataria T. Image guidance in radiation therapy: techniques and applications. Radiol Res Pract. 2014;2014:705604.
50. Warren K, Clare S. The effect of the Varian amorphous silicon electronic portal imaging device on exit skin dose. Phys Med Biol. 2003;48(19):3117.
51. Rong Y, Walston S, Welliver MX, Chakravarti A, Quick AM. Improving intra-fractional target position accuracy using a 3D surface surrogate for left breast irradiation using the respiratory-gated deep-inspiration breath-hold technique. Plos One. 2014;9(5):e97933.
52. Chan M, Yang J, Song Y, Burman C, Chan P, Li S. Evaluation of imaging performance of major image guidance systems. Biomed Imaging Interv J. 2011;7(2):e11.
53. Yunfei Hu MB, Archibald-Heeren B, Squires M, Teh A, Seiffert K, Cheers S, Wang Y. A feasibility study on the use of tomotherapy megavoltage computed tomography images for palliative patient treatment planning. J Med Phys. 2017;42:7.
54. Willoughby T, Lehmann J, Bencomo JA, Jani SK, Santanam L, Sethi A, et al. Quality assurance for nonradiographic radiotherapy localization and positioning systems: report of Task Group 147. Med Phys. 2012;39(4):1728–47.
55. Molloy JA, Chan G, Markovic A, McNeeley S, Pfeiffer D, Salter B, et al. Quality assurance of U.S.-guided external beam radiotherapy for prostate cancer: report of AAPM Task Group 154. Med Phys. 2011;38(2):857–71.
56. Djajaputra D, Li SD. Real-time 3D surface-image-guided beam setup in radiotherapy of breast cancer. Med Phys. 2005;32(1):65–75.
57. Bert C, Metheany KG, Doppke K, Chen GTY. A phantom evaluation of a stereo-vision surface imaging system for radiotherapy patient setup. Med Phys. 2005;32(9):2753–62.
58. Siebert JP, Marshall SJ. Human body 3D imaging by speckle texture projection photogrammetry. Sens Rev. 2000;20(3):218–26.
59. Robinson D, Liu DR, Steciw S, Field C, Daly H, Saibishkumar EP, et al. An evaluation of the Clarity 3D ultrasound system for prostate localization. J Appl Clin Med Phys. 2012;13(4):100–12.
60. Moore C, Lilley F, Sauret V, Lalor M, Burton D. Opto-electronic sensing of body surface topology changes during radiotherapy for rectal cancer. Int J Radiat Oncol. 2003;56(1):248–58.
61. Brahme A, Nyman P, Skatt B. 4D laser camera for accurate patient positioning, collision avoidance, image fusion and adaptive approaches during diagnostic and therapeutic procedures. Med Phys. 2008;35(5):1670–81.
62. Stieler F, Wenz F, Shi M, Lohr F. A novel surface imaging system for patient positioning and surveillance during radiotherapy A phantom study and clinical evaluation. Strahlenther Onkol. 2013;189(11):938–44.
63. Pham NL, Reddy PV, Murphy JD, Sanghvi P, Hattangadi JA, Kim GY, et al. Frameless, real time, surface imaging guided radiosurgery: clinical outcomes for brain metastases. Int J Radiat Oncol. 2015;93(3):E105-E.
64. Cervino LI, Pawlicki T, Lawson JD, Jiang SB. Frame-less and mask-less cranial stereotactic radiosurgery: a feasibility study. Phys Med Biol. 2010;55(7):1863–73.
65. Walter F, Freislederer P, Belka C, Heinz C, Sohn M, Roeder F. Evaluation of daily patient positioning for radiotherapy with a commercial 3D surface-imaging system (Catalyst (TM)). Radiat Oncol. 2016;11:154.
66. Rong Y, Bazan JG, Sekhon A, Haglund K, Xu-Welliver M, Williams T. Minimal inter-fractional fiducial migration during image-guided lung stereotactic body radiotherapy using superlock nitinol coil fiducial markers. Plos One. 2015;10(7):e0131945.
67. Balter JM, Wright JN, Newell LJ, Friemel B, Dimmer S, Cheng Y, et al. Accuracy of a wireless localization system for radiotherapy. Int J Radiat Oncol. 2005;61(3):933–7.
68. Santanam L, Malinowski K, Hubenshmidt J, Dimmer S, Mayse ML, Bradley J, et al. Fiducial-based translational localization accuracy of electromagnetic tracking system and on-board kilovoltage imaging system. Int J Radiat Oncol. 2008;70(3):892–9.
69. Litzenberg DW, Willoughby TR, Balter JM, Sandler HM, Wei J, Kupflian PA, et al. Positional stability of electromagnetic transponders used for prostate localization and continuous, real-time tracking. Int J Radiat Oncol. 2007;68(4):1199–206.
70. Franz A, Schmitt D, Seitel A, Chatrasingh M, Echner G, Oelfke U, et al. Standardized accuracy assessment of the calypso wireless transponder tracking system. Phys Med Biol. 2014;59(22):6797.
71. Kimple RJ, Wallen EM, Pruthi R, Marks LB. A simple algorithm to assess patient suitability for Calypso-seed implantation for four-dimensional prostate localization. J Appl Clin Med Phys. 2010;11(1):252–62.
72. Lattanzi J, McNeeley S, Donnelly S, Palacio E, Hanlon A, Schultheiss TE, et al. Ultrasound-based stereotactic guidance in prostate cancer--quantification of organ motion and set-up errors in external beam radiation therapy. Comput Aided Surg. 2000;5(4):289–95.
73. Trichter F, Ennis RD. Prostate localization using transabdominal ultrasound imaging. Int J Radiat Oncol. 2003;56(5):1225–33.
74. Kuban DA, Dong L, Cheung R, Strom E, De Crevoisier R. Ultrasound-based localization. Semin Radiat Oncol. 2005;15(3):180–91.
75. Fung AYC, Enke CA, Ayyangar KM, Raman NV, Zhen WN, Thompson RB, et al. Prostate motion and isocenter adjustment from ultrasound-based localization during delivery of radiation therapy. Int J Radiat Oncol. 2005;61(4):984–92.
76. Lattanzi J, McNeeley S, Pinover W, Horwitz E, Das I, Schultheiss TE, et al. A comparison of daily CT localization to a daily ultrasound-based system in prostate cancer. Int J Radiat Oncol. 1999;43(4):719–25.
77. Little DJ, Dong L, Levy LB, Chandra A, Kuban DA. Use of portal images and bat ultrasonography to measure setup error and organ motion for prostate IMRT: implications for treatment margins. Int J Radiat Oncol. 2003;56(5):1218–24.
78. Fenster A, Downey DB. Three-dimensional ultrasound imaging. Annu Rev Biomed Eng. 2000;2:457–75.

79. Fenster A, Downey DB. Three-dimensional ultrasound imaging and its use in quantifying organ and pathology volumes. Anal Bioanal Chem. 2003;377(6):982–9.
80. Chinnaiyan P, Tome W, Patel R, Chappell R, Ritter M. 3D-ultrasound guided radiation therapy in the post-prostatectomy setting. Technol Cancer Res Treat. 2003;2(5):455–8.
81. Tome WA, Meeks SL, Orton NP, Bouchet LG, Bova FJ. Commissioning and quality assurance of an optically guided three-dimensional ultrasound target localization system for radiotherapy. Med Phys. 2002;29(8):1781–8.
82. Peignaux K, Truc G, Barillot I, Ammor A, Naudy S, Crehange G, et al. Clinical assessment of the use of the Sonarray system for daily prostate localization. Radiother Oncol. 2006;81(2):176–8.
83. Chandra A, Dong L, Huang E, Kuban DA, O'Neill L, Rosen I, et al. Experience of ultrasound-based daily prostate localization. Int J Radiat Oncol. 2003;56(2):436–47.
84. Baker M, Behrens CF. Determining intrafractional prostate motion using four dimensional ultrasound system. BMC Cancer. 2016;16:484.
85. Abramowitz MC, Bossart E, Flook R, Wu X, Brooks R, Lachaine M, et al. Noninvasive real-time prostate tracking using a transperineal ultrasound approach. Int J Radiat Oncol. 2012;84(3):S133-S.
86. Western C, Hristov D, Schlosser J. Ultrasound imaging in radiation therapy: from Interfractional to intrafractional guidance. Cureus. 2015;7(6):e280.
87. O'Shea T, Bamber J, Fontanarosa D, van der Meer S, Verhaegen F, Harris E. Review of ultrasound image guidance in external beam radiotherapy part II: intra-fraction motion management and novel applications. Phys Med Biol. 2016;61(8):R90–137.
88. Fontanarosa D, van der Meer S, Bamber J, Harris E, O'Shea T, Verhaegen F. Review of ultrasound image guidance in external beam radiotherapy: I. Treatment planning and inter-fraction motion management. Phys Med Biol. 2015;60(3):R77–114.
89. Mutic S, Dempsey JF. The ViewRay system: magnetic resonance–guided and controlled radiotherapy. Semin Radiat Oncol. 2014;24(3):196–9.
90. Acharya S, Fischer-Valuck BW, Kashani R, Parikh P, Yang D, Zhao T, et al. Online magnetic resonance image guided adaptive radiation therapy: first clinical applications. Int J Radiat Oncol Biol Phys. 2016;94(2):394–403.
91. Raaymakers B, Jürgenliemk-Schulz I, Bol G, Glitzner M, Kotte A, van Asselen B, et al. First patients treated with a 1.5 T MRI-Linac: clinical proof of concept of a high-precision, high-field MRI guided radiotherapy treatment. Phys Med Biol. 2017;62(23):L41.
92. Fallone BG. The rotating biplanar linac–magnetic resonance imaging system. Semin Radiat Oncol. 2014;24(3):200–2.
93. Keall PJ, Barton M, Crozier S, et al. The Australian magnetic resonance imaging–linac program. Semin Radiat Oncol. 2014;24(3):203–6.

Charged Particle Stereotactic Body Radiation Therapy

Arpit M. Chhabra, Melissa A. Frick, Tejan Diwanji, Jason K. Molitoris, and Charles B. Simone II

Introduction

Stereotactic body radiation therapy (SBRT) has well-established roles in the treatment of a number of solid tumors, including lung, gastrointestinal, and genitourinary malignancies, and the frequency of its use for these tumors continues to increase. While local control with this technique is consistently as good as or more favorable than conventionally fractionated radiation therapy, concerns remain that such high doses per fraction can result in damage to adjacent normal tissues and lead to increases in late toxicities and potentially fatal complications from treatment [1, 2].

In efforts to reduce the toxicities associated with photon-based SBRT, recent interest has emerged in the delivery of these ultrahigh doses per fraction with proton therapy. Proton therapy allows energy to be deposited at a specific depth, termed the Bragg peak, and achieves a rapid energy falloff beyond this depth, thus allowing normal tissues on the distal side of the target volume to be spared [3]. With these unique physical properties of proton therapy, SBRT delivered with proton therapy can reduce the irradiation doses to critical structures adjacent to the target volume, thus potentially reducing the risks treatment.

There are several potential advantages of proton SBRT over photon SBRT (Box 20.1) [4]. By reducing the irradiation doses to adjacent critical structures, proton SBRT may allow for fewer treatment-related toxicities compared with photon-based SBRT. Similarly, for tumors immediately adjacent to critical organs (i.e., the esophagus or mainstem bronchus for lung tumors, the duodenum for pancreatic tumors) or particularly large primary tumors (i.e., lung tumors >5 cm), SBRT delivered with protons may be more likely to allow for definitive doses to be delivered to these difficult to treat tumors, which may improve cure rates. Protons may also allow for the safer delivery of dose-escalated SBRT beyond what is thought deliverable with photons, which may improve tumor control rates, especially for large tumors or for radioresistant tumors or metastases in an attempt to increase the biological effective dose (BED) of treatment. Additionally, as radiation oncologists are increasingly being asked to deliver SBRT to oligometastatic or oligoprogressive sites of disease, by reducing the dose to critical structures, proton SBRT may be safer when combining ultrahigh-dose irradiation with chemotherapy, targeted therapy, or immunotherapy. Furthermore, protons may more safely allow for reirradiation of tumors that are locally recurrent, which may allow for a second chance of cure [5].

This chapter reviews the rationale and current data for the use of proton SBRT across multiple disease sites, including thoracic, gastrointestinal, and genitourinary malignancies.

A. M. Chhabra
Central Connecticut Radiation Oncology, PC,
Department of Radiation Oncology, Middletown, CT, USA

M. A. Frick
Stanford University Medical Center, Department of Radiation Oncology, Stanford, CA, USA

T. Diwanji
University of Miami Sylvester Comprehensive Cancer Center, Department of Radiation Oncology, Miami, FL, USA
e-mail: tdiwanji@med.miami.edu

J. K. Molitoris
University of Maryland School of Medicine, Department of Radiation Oncology, Baltimore, MD, USA
e-mail: jmolitoris@umm.edu

C. B. Simone II (✉)
New York Proton Center, Department of Radiation Oncology, New York, NY, USA
e-mail: csimone@nyproton.com

D. M. Trifiletti et al. (eds.), *Stereotactic Radiosurgery and Stereotactic Body Radiation Therapy*,
https://doi.org/10.1007/978-3-030-16924-4_20

Box 20.1 Rationales for the Use of Proton Stereotactic Body Radiation Therapy

- Reduce irradiation doses to adjacent critical structures, which may reduce treatment toxicities.
- More safely treat tumors immediately adjacent to critical organs (i.e., the esophagus or mainstem bronchus for lung tumors, the duodenum for pancreatic tumors), which can allow for curative doses delivered to the tumor volume.
- More safely treat large tumors (i.e., lung tumors >5 cm), which can allow for curative doses delivered to the tumor volume.
- Deliver dose-escalated SBRT (i.e., for large tumors or for radioresistant tumors or metastases in an attempt to increase the biological effective dose (BED) of treatment), which may improve tumor control rates.
- More safely allow for SBRT to be combined with chemotherapy, targeted therapy, or immunotherapy for oligometastatic or oligoprogressive disease.
- More safe ability to reirradiate tumors that are locally recurrent, which may allow for a second chance of cure.

Hypofractionated/SBRT Proton Therapy for Early-Stage Primary Non-small Cell Lung Cancer (Fig. 1)

The use of SBRT has emerged as a standard management approach for the treatment of unresectable early-stage non-small cell lung cancers. While the initial use of lung SBRT was limited to the treatment of peripheral lung lesions [6], results of retrospective and prospective series have expanded the indications to the treatment of central [7], recurrent [8], and multifocal [9] lesions. Additionally, lung SBRT is increasingly being considered for resectable disease in patients who are felt to be at high operative risk, as determined in a multidisciplinary setting [10, 11]. Despite the extensive work to date evaluating the outcomes and toxicities of lung SBRT for early-stage NSCLC, much more limited data exist regarding the delivery of SBRT with a proton-based approach. This is highlighted by Daly and colleagues, who studied thoracic SBRT patterns of care in the United States and discovered a proton delivery utilization rate of only 1% [12]. As such, in this section, we address the current data highlighting the clinical and dosimetric potential of proton therapy for the treatment of early-stage NSCLC.

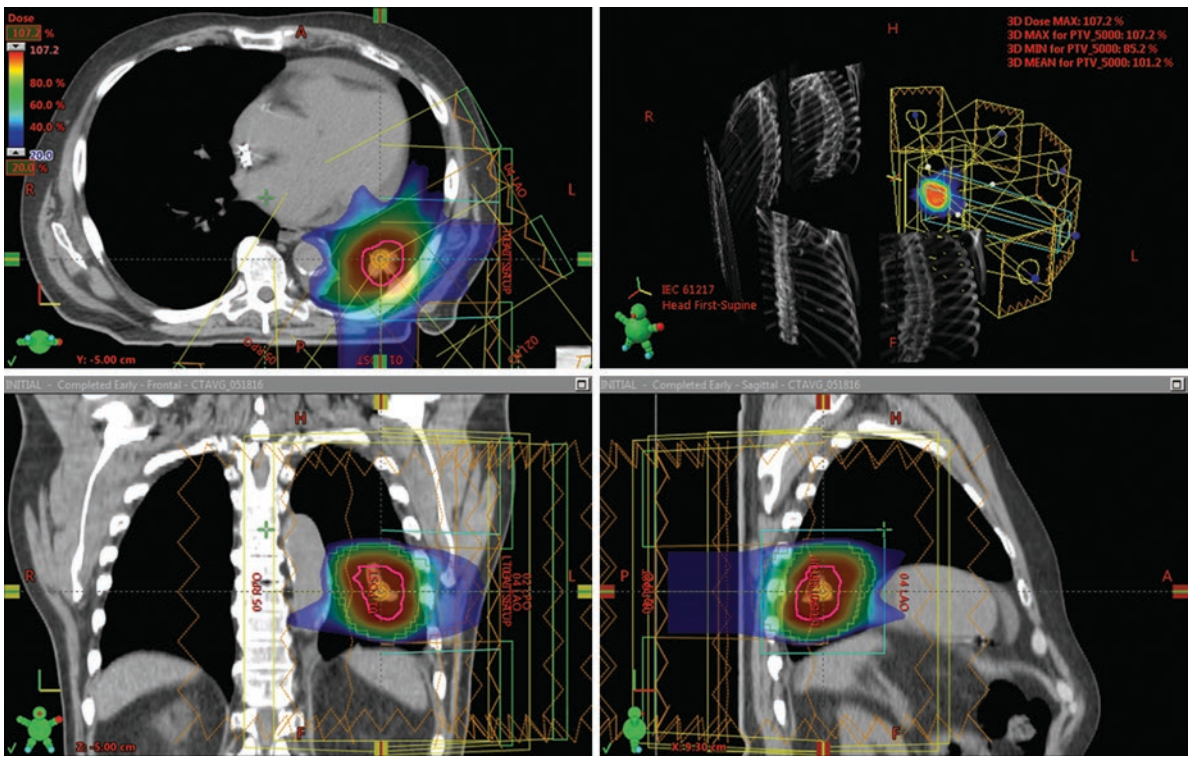

Fig. 1 Representative treatment planning images for proton stereotactic body radiation therapy for a stage I non-small cell lung cancer. This patient had a prior locally advanced lung cancer treated with chemoradiation immediately adjacent to this area 2 years earlier. In the interval, he had a cardiac pacemaker placed. Proton therapy was used in an attempt to reduce the dose to the patient's heart and also to reduce the irradiation overlap with the prior adjacent course of treatment. The treatment plan is depicted in colorwash in the axial (top left), coronal (bottom left), and sagittal (bottom right) planes. The beam orientations for this five-field treatment plan are also depicted (top right). Contours: magenta = iGTV. Dose gradient: 20% of the prescription dose (blue) to the dose maximum (red)

Clinical

One of the earliest clinical uses of hypofractionated proton beam therapy for early-stage lung cancer was initiated at the Loma Linda Medical Center [13]. This group reported the outcomes and toxicity data of 68 patients treated on a Phase II protocol utilizing passive scattered proton beam radiotherapy for clinical Stage I NSCLC who either refused surgery or were medically inoperable. Thirty-two percent of patients received a dose of 51Gy (Cobalt Gray Equivalent/CBE) in 10 fractions, whereas the remainder received 60Gy(CBE) in 10 fractions to the gross tumor volume (GTV) plus a margin for respiratory excursion. Results revealed 3-year local control (LC), metastatic relapse, and disease-specific survival rates of 74%, 31%, and 72%, respectively. The 3-year overall survival (OS) rate was 44% for all patients, with a significant improvement in overall survival for patients receiving 60Gy(CBE) as compared to 51Gy(CBE) (55% vs. 27%, respectively, $p = 0.03$). Acute toxicities were limited to fatigue and mild dermatitis, with no other major acute or late toxicities identified.

In 2013, the group from Loma Linda published their updated results of patients treated on the phase II protocol, which was amended to include a dose-escalated regimen of 70Gy in 10 fractions. In total, 115 patients were evaluable at the time of their updated analysis. Results revealed that 4-year OS rates were improved with increasing doses of proton therapy, with 70Gy achieving a 4-year OS rate of 51%. In comparing LC among patients with T1 or T2 disease receiving 60Gy vs. 70Gy, T1 lesions had similar and excellent 4-year LC rates of 86–91% with either dose regimen, whereas T2 tumors had 4-year LC rates of 74% and 45% with 70Gy and 60Gy, respectively ($p = 0.10$). Toxicity analysis revealed no occurrence of clinically significant radiation pneumonitis or central airway stricture, with pulmonary function being maintained one year after completion of treatment. Four cases of rib fractures were noted in patients with lesions adjacent to the chest wall. Otherwise, the delivery of hypofractionated passively scattered proton beam therapy was well tolerated.

Similarly, in 2011, investigators from the MD Anderson Cancer Center (MDACC) reported their initial results of a Phase I/II prospective trial using a moderate hypofractionated passively scattered proton beam regimen of 87.5Gy(RBE) at 2.5Gy(RBE) per fraction for inoperable centrally or superiorly located Stage IA (T1N0M0), any Stage IB (T2N0M0), and select Stage II (T3N0M0) NSCLC lesions [14]. Target volumes consisted of the iGTV, defined as the GTV as reconstructed on the maximum intensity projection (MIP) image, with an 8 mm margin to account for microscopic tumor extension to create the iCTV. From each beam's eye view, the iCTV was expanded 5 mm laterally to account for set up certainties, with a proximal and distal margin added to account for range uncertainties to create the planning PTV. Eighteen patients received the prescribed treatment. Preliminary results revealed LC, regional lymph node failure, and distant metastasis rates of 89%, 11% and 28%, respectively. Additionally, 2-year DFS and OS rates were 45.5% and 54.5%, respectively. No grade 4 or 5 toxicities were observed at the time of initial publication, and no patient experienced a decline in pulmonary function from pre-RT levels to 3–6 months post-proton beam therapy.

This group more recently reported their long-term results with 35 patients having been treated on trial [15]. Five-year freedom from local recurrence, freedom from regional recurrence, and freedom from distant metastasis rates were 85.0%, 89.2%, and 54.4%, respectively. Additionally, 5-year OS and progression-free survival (PFS) rates were 28.1% and 53.6%, respectively. Despite 72% of patients having either central or superiorly located tumors and 17% having tumors ≥5 cm, the reported local and regional control rates compare favorably with modern-day SBRT results utilizing photon-based approaches. Updated toxicity analysis revealed no evidence of grade 4 or 5 toxicities, as well as no change in pulmonary function before and after therapy. Rates of Grade 2 and 3 radiation pneumonitis were 11.4% and 2.9%, respectively. Otherwise, toxicities were limited to rare instances of grade 2 esophagitis (2.9%), grade 2 cardiac toxicities (5.7%), grade 2 rib fracture (2.9%), grade 1 chest wall pain (11.4%), and grade 2 chest wall pain (2.9%).

In 2017, a group from Japan led by Ono and colleagues also reported their safety and efficacy data of hypofractionated proton beam therapy for centrally located lung cancers [16]. T1-3N0M0 tumors with a median size of 3.95 cm that were centrally situated less than 2 cm from the trachea, mainstem bronchus, or lobar bronchus received passively scattered proton beam therapy to a dose of 80Gy (RBE) in 25 fractions. The two-year local control rate was 78.5%, with all local recurrences being in field, and the two-year OS rate was 73.8%. Despite all lesions being in close proximity to critical organs at risk, no grade 3–5 toxicities were observed. Grade 2 radiation pneumonitis and grade 2 rib fracture rates were 10% and 10%, respectively. As such, these results in conjunction with those of the MDACC group highlight the ability to safely deliver moderate hypofractionated proton beam therapy for centrally located lung tumors.

In addition to centrally located tumors, larger tumors (≥5 cm) also prove more difficult to treat with photon-based SBRT approaches than small, peripherally situated tumors [17, 18]. In an effort to assess the effectiveness of particle therapy for larger tumors, Iwata and colleagues analyzed the clinical outcomes of proton and carbon-ion therapy for cT2aN0M0 (67%) and cT2bN0M0 (23%) histologically confirmed inoperable NSCLC lesions [19, 20]. Overall, 86% of tumors were peripherally located. For proton beam therapy, dose-fractionation schemes varied between 80GyE in

20 fractions, 60GyE in 10 fractions, 66GyE in 10 fractions, and 70.2GyE in 26 fractions based on the time period in which patients were treated. With use of proton beam therapy, four-year OS and LC rates were 58% and 75%, respectively. In comparison to the 2-year and 3-year LC rates of 70% and 40% from Dunlap and colleagues [21] and Koto and colleagues [22], respectively, for T2 tumors receiving photon based ultra-hypofractionated SBRT treatments, the results of Iwata and colleagues using protons comparable favorably.

This group in 2013 also reported on their retrospective experience using particle therapy (proton and carbon-ion therapy) for a larger cohort of clinical Stage I patients (cT1-T2aN0M0) [23]. Proton therapy dose-fractionation regimens were 60GyE in 10 fractions ($n = 35$), 80GyE in 20 fractions ($n = 16$), 66GyE in 10 fractions ($n = 10$), 52.8GyE in 4 fractions ($n = 7$), and 70.2GyE in 26 fractions ($n = 2$). The 3-year OS, PFS, and LC rates in the proton group were 72%, 44%, and 81%, respectively. The majority of failures were regional or distant. Late grade ≥ 3 radiation pneumonitis, dermatitis, and rib fracture rates were low and occurred in 0%, 4%, and 1% of patients, respectively.

Hata and colleagues, in their prospective report of the University of Tsukuba experience of proton beam therapy for inoperable Stage I NSCLC, also observed no therapy-related Grade ≥ 3 toxicities. In this report, 21 patients with cT1-2aN0M0 unresectable peripherally situated histologically confirmed NSCLC were treated with proton beam therapy to 50–60Gy in 10 fractions. Two-year local progression-free, disease-free, and OS rates were 95%, 79%, and 74%, respectively.

While the aforementioned series help evaluate the overall safety and efficacy of hypofractionated proton beam regimens for early-stage NSCLC, these reports are limited in the evaluation of factors that correlate with clinical outcomes. In this regard, Kanemoto and coauthors [24] and Hatayama and coauthors [25] independently studied their institutional results of proton beam therapy for early-stage tumors to determine prognostic factors associated with disease recurrence. Kanemoto and coauthors evaluated 74 patients with Stage I NSCLC, with 26% of tumors being centrally situated, which were treated with two dose regimens based on location: 72.6Gy (RBE) in 22 fractions for centrally located tumors and 66Gy (RBE) in 10–12 fractions for peripheral tumors. The 5-year rates of LC, PFS, and OS were 82%, 52%, and 66%, respectively. Multivariate analysis revealed that only radiation dose ($p = 0.014$) and patient age ($p = 0.039$) were associated with recurrence. Similarly, in the evaluation of tumor and patient factors that correlated with LC, only radiation dose was significantly associated with LC. The 3-year LC was 64% for central tumors receiving 72.6Gy (RBE) and 88% for peripheral tumors receiving 66Gy (RBE) ($p = 0.026$). No significant difference in LC was observed between age, stage, tumor diameter, or histology.

Hatayama and coauthors reported results of 50 patients with 52 peripherally located Stage I NSCLC lesions treated with proton beam therapy to 66GyE in 10 fractions. The 3-years rates of LC, PFS, and OS were 95.7%, 76.3%, and 87.9%, respectively. This group subsequently analyzed prognostic factors that were associated with OS and discovered that 3-year OS rates were significantly better for patients with a ECOG performance status of 0 as compared to 1–2 (100% vs. 77.5%, respectively, $p = 0.029$). Gender, age, or tumor location significantly did not correlate with OS. Toxicity evaluation revealed a 2% incidence of Grade 2 radiation pneumonitis, and no Grade ≥ 3 acute or late toxicities were seen.

While the aforementioned series of moderately hypofractionated proton beam dose-fractionation regimens display excellent control rates with an acceptable toxicity profile, these regimens remain protracted in comparison with the ultra-hypofractionated modern photon SBRT regimens that deliver treatments in 1–5 total fractions. Therefore, the group from MGH led by Westover and coauthors retrospectively reviewed their institutional outcomes for 15 patients with 20 Stage I NSCLC lesions receiving primarily a 3-fraction proton approach [26]. The majority of patients had underlying COPD, interstitial lung disease, multiple primary tumors, and/or had received prior thoracic radiation therapy. Fractionation was chosen to achieve a biological effective dose of at least 100Gy, with a median total dose of 45GyRBE (range: 42–50GyRBE) and median fraction size of 14GyRBE (range: 10–16GyRBE). Outcomes data revealed 2-year LC, regional control, distant control and OS rates of 100%, 78%, 86%, and 64%, respectively. Treatments overall were well tolerated, with only one instance of Grade 2 chest wall pain, one instance of Grade 2 dermatitis, and one instance of Grade 2 fatigue, as well as one case of Grade 3 radiation pneumonitis. Otherwise, no other Grade ≥ 3 toxicities were observed. These results provide confirmatory preliminary data to support the use of an ultra-hypofractionated proton SBRT regimen in comparison with photon-based SBRT for early-stage tumors.

Investigators from MD Anderson Cancer Center conducted a randomized trial of photon SBRT versus proton SBPT for high-risk (centrally located or < 5 cm-T3 or isolated lung parenchymal recurrences) medically inoperable early-stage NSCLC to 50 Gy(RBE) in 4 fractions. Proton SBPT was given with passive scattering and IGRT with KVs, as opposed to CBCT that was used in the photon SBRT arm. The study closed early due to poor accrual, attributed largely due to lack of insurance coverage for proton therapy and physician concern of lack of volumetric imaging for proton SBPT. At the time of termination, 21

patients had enrolled, 19 of whom were evaluable (9 SBRT, 10 SBPT). At a median follow-up of 32 months, the median overall survival (not reached versus 28 months) and 3-year survival rate (90% vs. 27.8%) favored proton SBRT. Local control was high in both arms, with the 3-year control rate being 87.5% with SBRT and 90.0% with proton SBPT. Three-year regional control was 47.6% for photons and 90.0% for protons. Furthermore, no patient in either arm experienced a grade ≥ 3 acute toxicity, and only 1 proton SBPT patient developed a grade ≥ 3 late toxicity (grade 3 skin fibrosis) [27].

In an effort to compare the results of proton- and photon-based approaches while ongoing trial results mature, Chi and coauthors conducted a comprehensive review comparing the efficacy of hypofractionated proton beam therapy to that of photon SBRT in the treatment of early-stage (cT1-3N0M0) NSCLC [28]. The meta-analysis compared 9 studies that utilized proton beam therapy, many of which have been mentioned in this section, to 72 series using photon SBRT. No significant differences in age, gender, performance status, percentage of patients with histological confirmation, percentage of operable patients, tumor location, or percentages of patients receiving a BED of at least $100Gy_{10}$ were observed. However, patients receiving proton beam therapy were noted to have larger median tumor sizes (2.92 cm vs. 2.41 cm, $p = 0.02$) and were less likely to have T1 disease (57% vs. 71%, $p = 0.05$). Results revealed improved 5-year OS (60% vs. 41%, $p = 0.005$) and PFS (57.2% vs. 37.7%, $p = 0.01$) for proton beam therapy in comparison with photon SBRT. However, no difference in 5-year local control was observed between treatment modalities (proton: 87.2% vs. photon: 80.8%). Similarly, no difference in crude rates of regional failures or distant metastasis was observed between treatment modalities. The overall incidence of grade 3–5 toxicities was low but was noted to be significantly higher with photon SBRT (6.9% vs. 4.8%, $p = 0.05$). Rates of Grade ≥ 3 radiation pneumonitis were 0.9% with proton beam therapy and 3.4% with photon SBRT ($p = 0.001$). In contrast, the rib fracture rates were 13% for proton beam therapy vs. 3.2% for photon SBRT ($p < 0.001$). Overall, these results confirm the safety and efficacy of a hypofractionated proton SBRT approach for the management of early-stage NSCLC, especially in patients at a higher risk of developing side effects due to unfavorable tumor location, prior radiotherapy, and/or underlying comorbidities.

Dosimetric

One of the earliest dosimetric comparisons was published by the group in Vienna, Austria, in 2008 and evaluated plans for 12 patients with early-stage lung lesions using the following techniques: 3D-conformal radiation therapy (3D-CRT), passively scattered proton therapy (PSPT), and intensity-modulated proton therapy (IMPT) [29]. Plans were compared on CT datasets with shallow breathing and abdominal compression in place, as well as with patients assuming deep inspiratory breath hold (DIBH). For all patients, the clinical target volume was a margin of 2–3 mm around the gross lesion (GTV). For shallow breathing/abdominal compression conditions, a 4–10 mm PTV margin was applied depending on the location of the lesion and the degree of respiratory excursion. For the DIBH plans, an isotropic 5 mm PTV margin was applied. No significant differences were noted in maximum (D1%), minimum (D99%) and mean PTV doses between 3D-CRT, PSPT, and IMPT for either respiratory condition. For organs at risk, DIBH improved dose-volume distributions irrespective of treatment modality used. For both respiratory conditions, the ipsilateral lung V2Gy was on average 6–8% lower with both PSPT and IMPT in comparison with 3D-CRT. For the ipsilateral lung 4Gy, only the IMPT approach had a significant reduction in comparison to 3D-CRT ($p = 0.049$). In contrast, the ipsilateral lung V6Gy and V12Gy were equivalent for all three techniques. For the contralateral lung, both PSPT and IMPT had complete organ sparing in both respiratory conditions, whereas the 3D-CRT plan had a contralateral lung maximum dose of approximately 2Gy. Similarly, both PSPT and IMPT provided superior heart sparing in comparison to 3D-CRT, with significantly lower D1%, V2Gy, and V4Gy values. These results confirm the dosimetric benefits of proton-based SBRT techniques in reducing the low-dose bath on the ipsilateral and contralateral lungs and heart.

Similarly, the group from Mayo Clinic conducted their respective dosimetric comparison of eight patients with Stage I inoperable peripheral NSCLC using the following techniques: 3D-CRT, PSPT, and IMPT [30]. For all patients, the GTV was defined as the gross volume, with an internal target volumes (ITV) created to account for tumor motion. A uniform 5 mm axial and 10 mm longitudinal expansion on the ITV was added to create the PTV. The prescription dose for all patients was 60Gy in three fractions. Both proton plans exhibited lower maximum doses and higher minimum doses in the PTV compared to 3D-CRT. Additionally, the mean dose 2 cm from the PTV was significantly lower for both proton plans as compared to 3D-CRT. With respect to total lung tissue, both PSPT and IMPT achieved lower V5Gy values as compared to 3D-CRT, with only IMPT achieving a lower mean total lung dose than 3D-CRT. On the contrary, while the V20Gy was equivalent between 3D-CRT and IMPT techniques, it was significantly worse with PSPT. Median values for the spinal cord, heart, bronchial tree, esophagus, skin and ribs were all lower with PSPT and IMPT as opposed to 3D-CRT.

With the increasing utilization of IMRT-based lung SBRT treatments, the group from University of Florida (UF) dosimetrically compared plans for eight patients with peripherally located stage I lung lesions using the following techniques: 3D-CRT ($n = 2$) or IMRT ($n = 6$) in comparison to PSPT [31]. All plans were prescribed a dose of 48Gy in 4 fractions to the PTV. The target volumes consisted of an ITV with a 5 mm expansion to create the CTV, which in turn was expanded by 3 mm to create the PTV. The group found that the median PTV D95% coverage was not significantly different between PSPT, 3D-CRT, and IMRT. On the contrary, in all plans, the proton plan had a significant reduction in the ipsilateral lung mean and ipsilateral lung V5, V10, and V20 doses in comparison with photon delivery. With respect to exposure to other OARs, the PSPT was consistently better at sparing the heart, esophagus, trachea, ipsilateral bronchus, and spinal cord. In contrast to the studies from Vienna, Austria, and the Mayo Clinic that showed the ability to spare OARs with proton therapy among a few dosimetric points, the group from the UF showed the dosimetric benefits of protons among a wider array of dose-volume points and OARs. The authors from UF noted that one explanation for this increased benefit is that the PTV volumes were substantially larger as compared to those of the two prior aforementioned studies, thereby allowing PSPT the ability to better spare OARs such as the ipsilateral lung in comparison to 3D-CRT or IMRT. As such, one clinical subgroup in which the authors recommended the use of proton therapy over photons was for larger primary lung lesions. Similar findings of the ability of proton therapy to spare multiple OARs was found in the in press ROCOCO multicentric in silico study, with the authors of that report noting that the benefits of proton therapy over more advanced photon SBRT approaches may only be clinically relevant in selected patients, such as those with large, central, or recurrent tumors [32].

The group from Japan led by Kadoya and coauthors provided further results to support the enhanced dosimetric benefit of proton therapy in larger primaries [33]. In their series, they dosimetrically compared 21 patients with peripherally located Stage I NSCLC receiving 66GyE in 10 fractions using PSPT and 3D-CRT. No difference in PTV coverage between proton- and photon-based techniques was observed. However, with respect to OAR sparing, PSPT allowed significantly greater sparing of the ipsilateral and contralateral lungs at all assessed dose levels (V5, V10, V13, V15, and V20), with greater proportional sparing at the lower dose levels. Additionally, the dose-volume parameters for the lung were strongly associated with PTV volume size, with greater sparing for PSPT of the total lung V5, V10, V15, and V20 parameters as the PTV size increased. Proton therapy was also able to significantly reduce the V2, V10, and V20Gy to the heart, as well as reduce the max dose to the spinal cord and esophagus as compared to 3D-CRT plans.

In addition to a greater benefit with proton therapy for larger PTV volumes, tumor location in proximity to the mediastinum may also be more suitable to treatment with proton therapy. Therefore, the group from MDACC dosimetrically compared plans for 15 central lesions that were situated within 2 cm of trachea, bronchial tree, esophagus, heart, major vessels, and/or spinal cord with the following techniques: PSPT, IMPT, and 3D-CRT [34]. The target volume was the GTV as defined by envelope of motion on the maximum intensity projection images with an 8 mm CTV margin to account for microscopic extension. PTV margins were individualized based on photon- or proton-based planning. Plans were prescribed to a dose of 50Gy in 12.5Gy per fraction. Based on predefined maximum tolerated doses (MTD) for surrounding critical OARs, only 6 photon plans both satisfied PTV coverage and respected these MTD constraints in comparison with 12 PSPT ($p = 0.009$) plans and 14 IMPT plans ($p = 0.001$). In comparison to 3D-CRT plans, both PSPT and IMPT plans significantly reduced the mean total lung dose, as well as the total lung V5Gy, V10Gy, and V20Gy. The average maximum dose to the aorta, brachial plexus, bronchial tree, esophagus, heart, pulmonary vessels and spinal cord were all significantly reduced with both proton techniques in comparison to a 3D-CRT approach. Additionally, IMPT was better able to spare the brachial plexus, esophagus, and spinal cord in comparison to PSPT. In contrast, no increase in skin or chest wall dose was observed with proton therapy relative to photon SBRT.

In summary, the aforementioned dosimetric evaluations reveal the superior organ-sparing ability of proton SBRT/hypofractionated therapy without any compromise in target coverage. Taken together, these available dosimetric studies provide compelling evidence for the potential clinical benefits of proton therapy in treating early-stage primary lung lesions. Additional clinical trials, especially those delivering proton SBRT in 5 or fewer fractions and to central or ultra-central lesions, are eagerly awaited to appreciate the magnitude of this potential clinical benefit.

Hypofractionated/SBRT Proton Therapy for Liver Tumors

While surgical resection, orthotopic liver transplantation, transcatheter arterial chemoembolization (TACE), and radiofrequency ablation (RFA) have all been proven as effective treatment modalities for primary and metastatic liver tumors, the ability to deliver any of those modalities is often limited by high tumor burden in either size or number, preexisting impaired hepatic function, or medical comorbidities [35–42]. Historically, radiotherapy for liver tumors has not been adopted as a standard therapy because the dose constraints of critical organs have limited adequate dose delivery to achieve

acceptable rates of local control. The introduction of SBRT has challenged this traditional concept, as the precise delivery of ablative radiation doses has been shown to be safe, with high rates of local control [43–51]. PBT, especially, is optimal for tumors positioned in a critical structure with a low threshold tolerance to radiation – the liver being a principal example of such organ. Although there has been a generous amount of literature dedicated to the use of PBT in the treatment of liver tumors, there is a dearth of information regarding hypofractionated or SBRT proton-based approaches [52–55]. We herein discuss both the current clinical and dosimetric data regarding the use of hypofractionated and SBRT proton therapy for the treatment of primary and metastatic liver tumors.

Clinical

One of the earliest reports investigating the use of high-dose proton-based therapy for hepatocellular carcinoma (HCC) was a 2004 preliminary report on Loma Linda's prospective phase II trial [56]. Using a moderate hypofractionated proton beam regimen, 63.0 Gy(CGE) in 15 fractions was delivered to 34 patients over a three-week period. Notably, this procedure was restricted to plans in which no more than one-third of the normal liver was encompassed by the 50% isodose line. Additionally, this group of patients was heavily represented by advanced-stage HCC and decompensated liver disease. Despite this, 2-year LC and OS rates were 75% and 55%, respectively. Of the six patients to ultimately undergo liver transplantation, two had pathology demonstrating no evidence of residual disease, providing promising evidence that proton therapy may be effective at eradicating HCC in some patients.

In 2011, this same group updated their phase II trial results with a total of 76 patients [57]. Median PFS time was 36 months and for patients within the Milan criteria, and 3-year PFS was 60%. In the 18 patients who underwent liver transplantation, a pathologic complete response was observed in 33% and the three-year survival rate was 70% for this cohort. Acute toxicities were minimal and limited to grade 1 fatigue and radiation dermatitis. Five patients experienced grade 2 late adverse effects related to GI inflammation or ulceration, and all were successfully treated with medical management. Additionally, these late effects were noted early in the trial, and consequent modification of treatment fields mitigated subsequent bowel toxicities. MELD scores did not change significantly after treatment and no patient demonstrated clinical or laboratory evidence of radiation-induced liver disease (RILD).

Another early prospective trial to investigate use of hypofractionated proton therapy for HCC was published by a group at the University of Tsukuba [58]. In this phase II protocol, a total of 51 patients with peripheral lesions (≥2 cm from the GI tract or porta hepatis) received 66 Gy in 10 fractions. This cohort of patients had relatively good underlying liver function, with 80% having Child-Pugh's class A disease. Local control was outstanding at 94.5% and 87.8% at three and five years, respectively. Three- and 5-year OS rates were 49.2% and 38.7%, respectively. Acute toxicities were minimal and limited to decreased white blood counts. Most patients experienced no change in Child-Pugh class, with 3 patients improving from class B to A and 8 patients deteriorating from Child-Pugh class A to B. Late toxicities were minimal and limited in severity. Of the 3 patients experiencing rib fractures, all had received doses more than 90% of the isocenter dose to the ribs, and all cases were managed with conservative measures. A single patient experienced radiation pneumonitis that was successfully treated with a 4-week steroid course. No patient experienced common bile duct stenosis or GI tract bleeding, suggesting that peripherally situated tumors (defined by >2 cm from porta hepatis and digestive tract) can be safely treated with proton SBRT.

In fact, this group concurrently investigated three different radiation schedules with PBT, including the aforementioned hypofractionated regimen [59]. The assigned proton beam radiation schedule was dependent on tumor location: 66.0 GyE in 10 fractions was assigned for tumors that were not adjacent to either the GI tract or porta hepatis, 72.6 GyE in 22 fractions for tumors within 2 cm of the porta hepatis, and 77.0 GyE in 35 fractions for tumor within 2 cm of the GI tract. There was no significant difference in 5-year OS or LC among these three treatment protocols, and toxicities were minimal. The authors concluded that the choice of fractionation schedule should be dictated by the proximity of dose-limiting organs and stipulated that if more advanced planning and delivery could be accommodated, shorter courses of treatment may be possible even for tumors close to the GI tract.

Investigators at the Hyogo Ion Beam Medical Center published their retrospective experience using particle-based therapies (proton and carbon-ion therapy) to treat HCC [60]. Eight protocols for PBT were employed in 242 patients and analyzed by biologic effective dose (BED_{10}), including those with a $BED_{10} < 100$ (75 GyE in 38 fractions [$n = 11$], 56 GyE in 8 fractions [$n = 4$], and 60 GyE in 10 fractions [$n = 89$]) and $BED_{10} \geq 100$ (76 GyE in 20 fractions [$n = 70$], 66 GyE in 10 fractions [$n = 53$], 80 GyE in 20 fractions [$n = 3$], 84 GyE in 20 fractions [$n = 3$], and 52.8 GyE in 4 fractions [$n = 9$]). Five-year LC and OS for all patients receiving proton therapy was 90.2% and 38.0%. When analyzing survival outcomes by BED_{10}, 5-year LC after treatment with protocols characterized by $BED_{10} < 100$ and $BED_{10} \geq 100$ were 93.3% and 87.4%, respectively, and 5-year OS was 31.7% and 43.9%, respectively, and neither differences in outcomes were significantly different. Acute grade ≥ 3 dermatitis,

upper GI ulcer, biloma, and elevation of transaminase levels were low and occurred in 5, 1, 1, and 1 patient(s), respectively. Notably, the single patient to experience grade 4 dermatitis was treated with one portal to obtain an adequate spread-out Bragg peak; upon using two or more portals in subsequent cases, similar complications were not observed.

The CONSORT study recently reported results of a phase II multi-institutional study in 2016 detailing the safety and efficacy of high-dose hypofractionated PBT in patients with localized, unresectable HCC and intrahepatic cholangiocarcinoma (ICC) [61]. Patients were required to have relatively good liver function (i.e., only Child-Pugh class A or B and laboratory evidence of adequate hepatic synthetic function) and naïve to prior liver radiation therapy, including radioembolization. However, they were represented by a preponderance of large liver tumors with a median tumor size of 6 cm (median gross tumor volume of 133.7 cc). Total radiation dose delivered was dependent on tumor location – 67.5 GyE in 15 fractions for peripheral tumors (>2 cm from porta hepatis) and 58.0 GyE in 15 fractions for central tumors (within 2 cm of the porta hepatis) – and dose de-escalation was allowed to conserve the liver not involved by gross tumor volume (GTV) to a mean dose of ≤24 GyE. Of 92 patients enrolled, 83 patients were evaluable for analysis and included 44 cases of HCC and 39 cases of ICC. Overall, 95.5% and 92.3% of HCC and ICC patients completed their prescribed dose, with a median delivered dose of 58.0 GyE in 15 fractions (range 15.1 to 67.5 GyE).

Proton radiation was relatively well tolerated; although a majority of patients (85.5%) experienced mild to moderate toxicities, severe toxicity and worsening hepatic function were rare events. A high rate of LC was observed, with 2-year LC in HCC and ICC patients at 94.8% and 94.1%, respectively. Notably, all patients who experienced local progression had received <60 GyE. The 2-year PFS and OS for HCC patients were 39.9% and 63.2%, respectively. These survival outcomes are highly concordant with the previously discussed proton-based studies and compare favorably to other photon-based SBRT studies, even in a population that presented technical challenges due to increased median lesion size [43–51]. Survival outcomes in the ICC patients were also encouraging, with 2-year PFS and OS at 25.7% and 46.5%, respectively. These excellent survival outcomes in both HCC and ICC, despite inclusion of a technically challenging population with large tumor sizes, is demonstrative of the dose-sparing properties of PBT that allow for appropriate tumoricidal doses while limiting radiation-associated liver toxicities. On a related note, a current NRG trial (NCT02200042) is actively accruing, in which patients with localized unresectable ICC receive gemcitabine/cisplatin chemotherapy and are subsequently randomized to receive the aforementioned 15-fraction radiation schedule (protons or photons) versus continuing chemotherapy alone.

Use of high-dose ablative radiotherapy has also demonstrated promising outcomes for treatment of liver-dominant metastatic disease and has surmounted many of the same clinical challenges faced in the management of primary liver disease [62–65]. The feasibility and efficacy of proton-based SBRT for the treatment of liver metastases was recently investigated in a single-institution phase II trial [66]. SBRT dosing was determined by a previously defined radiobiologic parameter, "effective volume radiated" (Veff) [63], and was 30–50 GyE in five fractions (median dose, 40 GyE). A heterogeneous cohort of 89 patients with one to four liver metastases from solid tumors (colorectal ($n = 34$), pancreatic ($n = 13$), esophago-gastric ($n = 12$), other ($n = 30$)) with relatively good liver function and large tumor sizes (≥6 cm, 25.8% of all patients) were evaluable. One- and three-year LC rates were 71.9% and 61.2%, respectively, and good LC at 1 year of 73.9% for tumors larger than 6 cm. One- and three-year PFS rates were 24.7% and 9.2%, respectively, and OS rates were 66.3% and 20.8%, respectively. Overall, proton-based SBRT was well tolerated, and there were no cases of RILD or other serious grade ≥ 3 adverse events. Finally, the presence of a KRAS mutation was found to be the strongest predictor of local failure, as rapid progression of these irradiated tumors often occurred within 6 months of treatment.

With the increasing utilization of hypofractionated proton beam therapy for hepatic lesions, there has been a parallel increase in the analysis of toxicity risks to particular surrounding organs, most notably, the gallbladder. A secondary analysis – including data from two prospective studies discussed above – reported on gallbladder toxicities in patients with primary or metastatic liver lesions following high-dose hypofractionated RT and SBRT with protons [67]. Ninety-three patients received 45–67.5 GyE in 15 fractions over 3 weeks for primary liver neoplasms ($n = 45$) and 30–50 GyE in 5 fractions over 2 weeks for metastatic tumors ($n = 48$). Maximum gallbladder doses of >70 GyE, >80 GyE, and > 90 GyE were administered to 41%, 31%, and 13% of this cohort, respectively. Despite this, no attributable cases of gallbladder toxicities were observed. Two non-attributable cases of cholecystitis were noted, with both cases occurring in patients with a strong history of cholelithiasis before radiotherapy and history of biliary stenting.

Dosimetric

Petersen and coauthors were the first to complete a dosimetric comparison of SBRT intensity-modulated proton therapy (IMPT) and photon-based intensity-modulated radiotherapy (IMRT) plans for patients with solitary liver tumors [68]. Ten patients who had completed multi-field SBRT treatments for fairly large solitary liver metastases were retrospectively re-planned with both proton pencil beam scanning

(PBS) and IMRT techniques. All patients were immobilized in an SBRT frame with a mounted abdominal compression device to limit respiration-related motion to less than 10 mm in amplitude, an approach shown by Lin and coauthors to successfully mitigate moderate and large motion and optimally facilitate pencil beam scanning proton therapy of liver tumors [69]. The planning target volume (PTV) margin was 5 mm in the transverse plane and 10 mm in the cranio-caudal direction on the clinical target volume (CTV). Photon plans utilized five to six coplanar and noncoplanar fields, while proton-based plans used two to three coplanar fields based on the same geometrical considerations. A risk-adapted strategy was used, applying a dose prescription to the PTV surface of 12.50–16.75 Gy per fraction in three fractions. A greater volume of the liver was spared with the IMPT plans compared to IMRT plans for all planned cases. While this effect was most pronounced at the lower doses, it remained superior at the highest dose level as well such that the median liver volumes receiving less than 15 Gy were 1411 cm^3 for IMPT versus 955 cm^3 for IMRT ($p < 0.005$) and the mean liver doses were 9.1 Gy versus 20.0, respectively ($p < 0.005$). When applying the $D_{mean} \leq 15$ Gy constraint, nine of ten patients could be treated at the highest prescription dose using IMPT, whereas only two cases met this constraint under the same prescription level using IMRT. These results indicate that proton-based SBRT can be used to design more favorable treatment plans by reducing dose to normal liver tissue and, resultantly, allow for dose-escalation and improved clinical outcomes for SBRT in liver tumors.

Toramatsu and coauthors sought to investigate the impact of tumor size on the risk of RILD in a dosimetric comparison of proton versus photon radiotherapy [70]. Ten patients with HCC with tumors greater than 6 cm and portal vein tumor thrombosis (PVTT) treated with palliative photon-based radiotherapy to the PVTT were included in this study. A margin of 0.5 cm upon the GTV, minus overlap with uninvolved extra-hepatic structures, defined the CTV. A uniform expansion of 1 cm added to the CTV was used to define the PTV. Photon IMRT and spot-scanning proton therapy (SSPT) plans were generated to deliver 60 Gy in 15 fractions covering 95% of the PTV. Dose-volume constraints were applied using normal tissue tolerances estimated by Emami and coauthors such that the maximum dose delivered to one-third and two-thirds of the normal liver could not exceed the probability of 5% complications within 5 years of irradiation (otherwise defined as the tolerance dose [TD] of 5/5) [71]. Additional constraints included liver $V_{33} < 67\%$ and $V_{42} < 42\%$. For all patients with targets ≤6.3 cm, target dose optimization was achievable with IMRT; however, for patients with targets ≥7.9 cm, no IMRT plans were able to deliver the prescribed dose without exceeding the defined dose constraints. In comparison, SSPT plans achieved adequate target coverage without compromising normal liver constraints except for one plan with a 16.1 cm GTV. Mean V_{eff} for normal liver was lower for SSPT plans than IMRT plans (0.64 vs. 0.42, $p < 0.001$) and was found to plateau at ~0.5 with increasing tumor size in SSPT plans but continued to increase with tumor size for the IMRT plans. While risk of RILD – estimated using the Lyman normal-tissue complication probability model [72] with Michigan parameters [73] – was comparably low between IMRT and SSPT plans when tumor diameter was <6.3 cm (1.6% and 0.9%, respectively), the difference in risk was notable in tumors greater than 6.3 cm (94.5% and 6.2%, respectively).

To determine clinical situations in which proton-based SBRT holds a particular advantage in the treatment of liver tumors, Gandhi and coauthors developed and validated a treatment decision model following comparison of in silico dosimetry plans [74]. This group manually contoured six mock tumors ranging from 1 to 6 cm in size within four regions of the liver, including the dome, caudal, left medial, and central locations; all tumors were placed at least 1.5 cm away from visceral organs to remain consistent with standard SBRT practice. The PTV margin was defined by a uniform expansion of 0.5 cm around the gross tumor volume (GTV), and patients were assumed to be treated using the breath-hold technique to limit target motion. Photon volumetric modulated arc therapy (VMAT) and proton PBS were designed to deliver 50 Gy in 5 fractions with at least 95% of the PTV receiving 100% of the prescription dose. Notable dose constraints included the mean liver dose <14 Gy and at least 700^3 cm of normal liver receiving <15 Gy. For caudal (liver segments 5 and 6) and left medial (segments 2 and 3) tumors of any size, there was no improvement in normal liver sparing with protons versus photons; however, for larger (≥ 3 cm) dome or central tumors, protons were found to spare a higher volume of normal liver (dome,134 +/− 21 cm^3, $p = 0.03$; central, 108 +/− 4 cm^3, $p = 0.002$).

Based on these results, a treatment decision model was generated to identify the optimal modality for maximal liver sparing based on tumor size and location and was found to correctly predict the optimal SBRT modality on a validation set of 10 patients previously treated with photon SBRT. Notably, the use of protons versus photons spared a higher volume of normal liver for the 4 patients with large dome or central tumors (176 +/− 21 cm^3, $p = 0.01$), as well as a reduced mean liver dose (8.4 GyE vs. 12.2 Gy, $P = 0.01$). For the 6 patients with smaller tumors at any location, or those with caudal and left medial tumors of any size, no significant sparing of normal liver was found with proton plans over photon plans, although proton-based plans did deliver a numerically reduced mean liver dose in all six cases. These findings suggest a role of protons for tumors larger than 3 cm in the dome and in central locations, and that protons should be considered for tumors larger than 5 cm in any location,

particularly if photon-based plans do not achieve adequate target coverage or exceed constraint thresholds such as the mean liver dose.

Hypofractionated/SBRT Proton Therapy for Pancreatic Tumors

Radiotherapy is commonly utilized for the treatment of pancreatic cancer, both as definitive therapy for unresectable tumors and as neoadjuvant or adjuvant therapy for resectable disease. Its role, however, remains controversial, as randomized trials have produced mixed conclusions regarding the benefit of chemoradiation over chemotherapy [75–79]. These studies, furthermore, collectively illustrate how modern-day therapies remain limited in effectiveness and offer little chance of long-term survival. The rationale for continued investigation into the use of radiotherapy is rooted in the observation that 30% of patients die from complications related to local disease progression [80], therein suggesting that local progression is a limiting factor in long-term survival in many cases. While evidence has indicated that intensification of local therapy may lead to improved outcomes, delivery of such doses has so far been precluded by unacceptable toxicities [81, 82]. Such observations suggest a role for proton therapy, as sparing of particularly radiosensitive organs surrounding the pancreas may permit consequent delivery of tumoricidal doses to the local site. The abbreviated time course of an SBRT approach may also be especially relevant in pancreatic cancer, whose proclivity to metastasize limits the window in which local therapy can prevent regional or distant dissemination and can be leveraged in the case of borderline resectable disease. This theory has been established by previous research in rectal cancer, where short-term preoperative RT has been demonstrated to reduce the risk of pelvic failure [83–85]. Below, we highlight the few clinical experiences and dosimetric data to support further investigation of SBRT with a proton-based approach for the treatment of pancreatic cancer.

Clinical

Investigators from Massachusetts General Hospital were one of the first to publish on a prospectively enrolled trial regarding the clinical use of high-dose proton therapy for the treatment of pancreatic cancer [86]. They reported on the outcomes and safety of 15 patients treated on a phase I protocol utilizing preoperative short-course chemoradiation with PBT for treatment of localized, resectable pancreatic head adenocarcinoma. Patients were assigned to treatment regimens ranging from 10 fractions in 2 weeks through progressively shorter five-fraction schedules. Of note, elective nodal regions were included in the CTV. Patients additionally received concurrent capecitabine followed by surgery and adjuvant gemcitabine. The shortest dose schedule (Dose level 4: 25 GyE in five fractions over five days) was selected as the maximally tolerated dose with only one of six patients treated on this schedule experiencing severe, but not dose-limiting, acute events. Of the 11 patients able to undergo resection, nine (82%) had an R0 resection and no patient had to delay or decline surgery due to toxicities. Survival outcomes were favorable, as median survival had not been met at a median follow-up of 12 months, and one-year OS of 75%. Notably, of the patients who underwent resection, 10 were still alive at the time of analysis. Local control was also promising, as only one patient (7%) experienced local progression with synchronous liver metastasis following a margin-positive resection. Distant metastases were experienced in all eight (53%) cases of failure with a median relapse-free survival of 10 months.

Given the demonstrated feasibility of the above treatment schedule, the same group embarked upon a Phase II study to determine the efficacy and long-term tolerability associated with this regimen. Additional 35 patients were treated in the phase II portion for a total of 50 patients available for analysis [87]. This treatment approach continued to achieve acceptable rates of toxicity, with only 2 of the 35 patients included in the Phase II component experiencing a grade 3 acute event, including colitis and chest wall pain, and none experiencing postoperative complications within 30 days. Thirty-nine patients underwent resection; of those eligible for pathologic review, a majority (84%) achieved negative margins. For all eligible patients, the median PFS was 10.4 months, median OS was 17.3 months, and 2-year OS was 42%. Survival outcomes were notably improved in the patients who were able to undergo surgical resection, with a median PFS of 14.5 months and median OS of 27.0 months. Locoregional control remained favorable with only 6 of 37 eligible resected patients (16%) experiencing locoregional recurrence or progression, all of whom either progressed with metastatic disease or experienced synchronous metastatic disease. However, distant control was poor, with 35 or 48 patients (73%) developing distant metastases. These results suggest a potential role for short-course chemoradiation before surgery and adjuvant chemotherapy in providing a therapeutic opportunity for R0 resection and LC without delay to systemic therapy.

A group from the Rinecker Proton Therapy Center also reported on their institutional experience using hypofractionated PBT for pancreatic cancer [88]. Of 49 patients with inoperable pancreatic cancer, most had unresectable primary tumors (57%), although a notable proportion had lymph node involvement (18%) or distant metastases (25%). Dosing schedules varied: 36 patients (73%) received a total dose of 54 GyE in 18 fractions to the primary tumor site, 12 patients received 40 GyE in 4 fractions to primary tumor site due to concurrent stereotactic proton therapy to liver metastases,

and 1 patient received a reduced dose of 45 GyE in 15 fractions due to side effects of chemotherapy. Just over half of all patients (56%) received concurrent gemcitabine. PBT was well tolerated with no grade ≥ 3 toxicities observed during treatment and for up to 29 months following treatment. Local control was excellent and was achieved in 100% of patients who had reached 3 months ($n = 45$) and 6 months ($n = 22$) in follow-up. At a median follow-up of 7.5 months, 14 patients had died, with 12 deaths attributed to metastatic-related disease. These results provide evidence for further prospective studies to optimize overall dose and concurrent/adjuvant systemic therapies in the case of inoperable pancreatic cancer.

Dosimetric

In a preclinical evaluation for the abovementioned phase I/II short-course PBT trials, Kozak and associates were the first to provide a dosimetric assessment of hypofractionated PBT for pancreatic cancer [89]. Using 9 consecutive patients treated with conventional neoadjuvant chemoradiation with IMRT (50.4 Gy in 28 fractions), proton-based treatment plans delivering 25 GyE in 5 fractions were generated. In both IMRT and proton-based plans, the GTV included the GTV and enlarged regional lymph nodes, and the CTV was contoured to include at-risk nodal basins. Generation of the PTV, however, varied between modalities: a universal expansion of 5–15 mm and 10 mm was used for IMRT and proton planning, respectively, except for the posterior margin where a 5 mm expansion was used in both approaches. Despite these differences in PTV margins, the difference in PTV volume was not statistically different. While both techniques provided clinically acceptable target volume coverage, protons offered improved coverage of the PTV, CTV, and GTV receiving 100% of the prescribed dose, in addition to superior dose homogeneity. Furthermore, proton plans achieved significant irradiation dose reductions to the liver, kidney, and small bowel, particularly to the regions receiving low doses of irradiation. The clinical ramifications of these dose reductions, however, have yet to be realized, as the limited life expectancy of these patients may predate development of late toxicities. Normal tissue sparing, however, may provide the opportunity for dose escalation in clinical trials.

Hypofractionated/SBRT Proton Therapy for Prostate Cancer

External beam radiation therapy (EBRT) has long provided a comparable alternative to the surgical management of prostate cancer [90]. Traditionally, EBRT was delivered with 2-dimensional planning to doses of approximately 70 Gy [90]. With the advent of more modern treatment planning and delivery techniques including three-dimensional conformal radiation therapy, IMRT, VMAT, and even proton therapy, multiple trials have established the superiority of dose-escalated radiation therapy to doses of 75–80 Gy [91–94]. However, logistical concerns of prolonged treatment times of over eight weeks such as patient convenience, treatment cost, and treatment access, have driven the exploration of alternative hypofractionated regimens including SBRT approaches [95, 96]. Potential radiobiological advantages exploiting the intrinsic radiosensitivity differences of prostate cancer and surrounding organs at risk have further bolstered such explorations [97–105]. Despite the mounting clinical experience across a spectrum of hypofractionated and SBRT approaches [106–118], the data are considered by some to be relatively immature due to the lack of long-term follow-up [119]. Nevertheless, the relatively successful implementation of these short-course regimens with photon techniques has further stimulated explorations regarding the feasibility of hypofractionated treatments with proton therapy. Herein, we summarize some of the key clinical and dosimetric data of hypofractionated and stereotactic body proton therapy for prostate cancer.

Clinical

One of the earliest clinical experiences incorporating hypofractionated proton therapy into the treatment plan for prostate cancer was reported by the Swedish group in Uppsala in 2012 [120]. Johansson and colleagues administered a 4-fraction, proton therapy boost to a dose of 20 Gy which after a 1 week rest period was followed by a conventionally fractionated photon therapy course to 50 Gy. They delivered this regimen to 278 patients, and with a median follow-up of 57 months, they demonstrated excellent 5-year PSA progression-free survival rates of 100% and 95% in the low- and intermediate-risk patients, respectively. High-risk patients included in the study also demonstrated excellent control rates of 74%. Perhaps more importantly, they demonstrated that such a hypofractionated approach could be delivered safely with proton therapy, with 5-year Grade ≥ 2 GI toxicity of 0%. They divided their GU toxicity analysis by the presence or absence of symptoms pretreatment and noted that asymptomatic patients had a 1% rate of grade ≥ 2 GU toxicity, whereas pretreatment symptomatic patients were unsurprisingly at an increased risk with 5-year rates of grade 3 or grade 4 GU toxicities of 8% and 3%, respectively.

The Loma Linda group presented one of the earlier experiences of pure proton beam hypofractioned treatment of prostate cancer at the annual meeting for the American Society for Radiation Oncology in 2013 [121]. Preliminary data from their institutional Phase I/II study included a total of 61 low-risk prostate cancer patients treated to a dose of

60 Gy in 20 fractions over a 4-week timeframe. Outcomes were excellent, with no PSA-failures, although median follow-up was only 36 months. Toxicity profiles were also favorable, with no grade ≥ 3 GI or GU toxicities noted in the cohort. Final publication is currently eagerly awaited.

That same year, a group from South Korea also published their early results of a phase II clinical trial of hypofractionated proton therapy for prostate cancer [122]. This trial included 5 arms as follows: Arm 1, 60 Cobalt Gray Equivalent (CGE) in 20 fractions over 5 weeks; Arm 2, 54 CGE in 15 fractions over 5 weeks; Arm 3, 47 CGE in 10 fractions over 5 weeks; Arm 4, 35 CGE in 5 fractions over 2.5 weeks; and Arm 5, 35 CGE in 5 fractions over 5 weeks. Four-year biochemical failure-free survival was approximately 85%. Acute toxicity was again relatively low, with no acute grade ≥ 2 GI toxicity and only a 5% rate of GU toxicity. Grade 2+ late GI and GU toxicity rates were also deemed to be within acceptable limits at 16% and 7%, respectively. The authors further noted that acute GU toxicities were minimized in Arm 3 and that late GI toxicities were lowest in Arm 2.

Similarly, the Proton Collaborative Group (PCG) has also conducted a clinical trial on this subject (PCG GU 002). While the final results are still pending, the group reported an interim analysis in 2018 [123]. They randomized 82 patients to receive either stereotactic body proton therapy to 38 Gy relative biological effectiveness (RBE) in 5 fractions (n = 49) or conventionally fractionated proton therapy to 79.2 Gy RBE in 44 fractions (n = 33). Median follow-up was fairly limited at 18 months for the entire cohort. However, toxicity data were again quite positive with no grade ≥ 3 toxicities in either arm. Additionally, the group also evaluated the American Urological Association Symptom Index (AUASI) at multiple follow-ups and found that the only time point with a significant difference between the two arms was at 12 months (8 vs. 5). Other metrics such as the Expanded Prostate Index Composite (EPIC) urinary, bowel, and bladder scores were not statistically different between the two groups across multiple time points.

Lastly, the group from the University of Florida Health Proton Therapy Institute published their prospective data on 215 low- and intermediate-risk prostate cancer patients treated with hypofractionated proton therapy [124]. They treated low-risk patients (n = 120) to a dose of 70 Gy RBE and intermediate-risk patients to a dose of 72.5 Gy RBE, each in 2.5 Gy fractions. With the longest median follow-up of any of the proton studies, the group reported a freedom from biochemical and clinical disease progression of 98.3% and 92.7% for low- and intermediate-risk patients, respectively. Additionally, similar to the aforementioned studies, toxicity rates were very low with 5-year rates of grade ≥ 3 GI and GU toxicities of 0.5% and 1.7%, respectively. There were also no clinically significant changes in the International Prostate Symptom Scores for either risk group with this treatment.

Dosimetric

Estimating the potential benefit of hypofractionated proton beam therapy is inherently more intricate than it may seemingly appear. There are numerous challenges including accounting for the uncertainties in the relative biological effectiveness and dose delivery due to movement of the prostate due to differences in bowel or bladder filling. Currently, most treatment planning systems assign a constant relative biological effectiveness of 1.1 to proton therapy planning [125]. Newer data, however, suggest that other parameters, including linear energy transfer (LET) and intrinsic tissue properties, may affect this value [126]. Therefore, fractionation and tissue parameters can impact dosimetric studies [127]. To this end, Ödén and colleagues studied a series of proton and photon plans for prostate cancer treatment with and without the inclusion of variable RBE values in the treatment planning process [128]. They used three equivalent schedules, assuming an α/β value of 3: 78 Gy in 39 fractions, 57.2 Gy in 15 fractions, and 42.8 Gy in 7 fractions. They demonstrated that applying variable RBE models to nominal plans revealed increased rectal tissue complication probability when compared to photon plans. However, this effect was larger for conventionally fractionated plans. Of note, reoptimizing plans accounting for the variable RBE allowed a reduction in this risk. The authors cautioned that the changes in the proton dose in these scenarios are very much dependent on the variable RBE model utilized as well as the assumed α/β ratio; therefore, treatment planning should be undertaken with appropriate caution until further clinical and radiobiological validation is obtained.

Another significant uncertainty that must be considered when delivering hypofractionated proton therapy for prostate cancer is interfractional organ motion and the ensuing perturbation of dose. This effect was measured dosimetrically by Wang and associates from Massachusetts General Hospital [129]. In their study, the authors utilized serial CT scans acquired during the routine treatments of three patients. They then created 3D-CRT plans for a comparison basis. Additionally, they simulated the delivery of multiple hypofractionated proton therapy courses ranging from 5 to 28 fractions by computing the dose on each CT and then mapping it onto the simulation CT through deformable image registration. They then used the simulated fractions with the poorest target coverage to simulate a "worst-case scenario" per patient per plan. Their study revealed that tar-

get coverage V100% could decline by 1–4% and D100% by 2–6%. Furthermore, they noted that the uncertainty in dose was limited to the peripheral 5% of the target.

Finally, despite these potential pitfalls, in effort to quantify the dosimetric advantage to hypofractionation with proton therapy, the groups from University of Florida Proton Therapy Institute and Georgetown performed a comparative planning study of passively scattered proton therapy and SBRT as delivered by CyberKnife® (Accuray, Sunnyvale, CA, USA) [130]. They evaluated 10 patients with localized disease and evaluated photon versus proton planning to a dose of 36.25 Gy in 5 fractions. While both sets of plans were able to meet normal tissue dose constraints, suggesting that either platform provided a feasible modality for the delivery of ultra-hypofractionated radiation therapy, there were some dosimetric differences. Proton therapy tended to have lower doses to the urethra, rectum, and penile bulb as compared to the photon plans. Additionally, they tended to be more homogenous in the target volume with fewer hot spots. On the other hand, the photon plans tended to be more conformal and had lower doses to the bladder and femoral heads. A similar head-to-head comparison was presented at the ASTRO Annual Meeting in 2017 [131]. This time, Multi-Field Optimized (MFO) three-field (Y-shaped) plans were utilized for the proton comparison in five patients, but similar findings were seen, with photon plans being more conformal.

Conclusion

Photon-based SBRT has improved local control and even overall survival for a number of malignancies, but concerns of potential high-grade toxicities and potentially fatal complications from treatment still limit its use. With the unique physical properties of proton therapy, SBRT delivered with proton therapy can reduce the irradiation doses to critical structures adjacent to the target volume, thus potentially reducing the risks treatment. Proton SBRT can also allow for definitive treatment of select tumors not easily treatable with photon-based SBRT. Pencil beam scanning proton SBRT can further allow for the stereotactic delivery of complex tumors and toxicities reductions, but motion management and mitigation are even more critical for this treatment than for passively scattered proton SBRT or photon-based SBRT. The strongest evidence for extracranial proton SBRT currently exists for lung cancer, gastrointestinal malignancies, and genitourinary malignancies. As more proton centers emerge with pencil beam scanning and cone-beam CT capabilities, the use of proton-based SBRT is expected to increase.

References

1. Timmerman R, McGarry R, Yiannoutsos C, Papiez L, Tudor K, DeLuca J, et al. Excessive toxicity when treating central tumors in a phase II study of stereotactic body radiation therapy for medically inoperable early-stage lung cancer. J Clin Oncol. 2006;24(30):4833–9.
2. Corradetti MN, Haas AR, Rengan R. Central-airway necrosis after stereotactic body-radiation therapy. N Engl J Med. 2012;366(24):2327–9.
3. Gerweck LE, Kozin SV. Relative biological effectiveness of proton beams in clinical therapy. Radiother Oncol. 1999;50(2):135–42.
4. Simone CB 2nd, Rengan R. The use of proton therapy in the treatment of lung cancers. Cancer J. 2014;20(6):427–32.
5. Verma V, Rwigema JM, Malyapa RS, Regine WF, Simone CB 2nd. Systematic assessment of clinical outcomes and toxicities of proton radiotherapy for reirradiation. Radiother Oncol. 2017;125(1):21–30.
6. Timmerman R, Paulus R, Galvin J, Michalski J, Straube W, Bradley J, et al. Stereotactic body radiation therapy for inoperable early stage l ung cancer. JAMA. 2010;303(11):1070–6.
7. Chaudhuri AA, Tang C, Binkley MS, Jin M, Wynne JF, von Eyben R, et al. Stereotactic ablative radiotherapy (SABR) for treatment of central and ultra-central lung tumors. Lung Cancer. 2015;89(1):50–6.
8. Trovo M, Minatel E, Durofil E, Polesel J, Avanzo M, Baresic T, et al. Stereotactic body radiation therapy for re-irradiation of persistent or recurrent non-small cell lung cancer. Int J Radiat Oncol Biol Phys. 2014;88(5):1114–9.
9. Owen D, Olivier KR, Mayo CS, Miller RC, Nelson K, Bauer H, et al. Outcomes of stereotactic body radiotherapy (SBRT) treatment of multiple synchronous and recurrent lung nodules. Radiat Oncol. 2015;10:43.
10. Videtic GMM, Donington J, Giuliani M, Heinzerling J, Karas TZ, Kelsey CR, et al. Stereotactic body radiation therapy for early-stage non-small cell lung cancer: Executive Summary of an ASTRO Evidence-Based Guideline. Pract Radiat Oncol. 2017;7(5):295–301.
11. Simone CB 2nd, Dorsey JF. Additional data in the debate on stage I non-small cell lung cancer: surgery versus stereotactic ablative radiotherapy. Ann Transl Med. 2015;3(13):172.
12. Daly ME, Perks JR, Chen AM. Patterns-of-care for thoracic stereotactic body radiotherapy among practicing radiation oncologists in the United States. J Thorac Oncol. 2013;8(2):202–7.
13. Bush DA, Slater JD, Shin BB, Cheek G, Miller DW, Slater JM. Hypofractionated proton beam radiotherapy for stage I lung cancer. Chest. 2004;126(4):1198–203.
14. Chang JY, Komaki R, Wen HY, De Gracia B, Bluett JB, McAleer MF, et al. Toxicity and patterns of failure of adaptive/ablative proton therapy for early-stage, medically inoperable non-small cell lung cancer. Int J Radiat Oncol Biol Phys. 2011;80(5):1350–7.
15. Chang JY, Zhang W, Komaki R, Choi NC, Chan S, Gomez D, et al. Long-term outcome of phase I/II prospective study of dose-escalated proton therapy for early-stage non-small cell lung cancer. Radiother Oncol. 2017;122(2):274–80.
16. Ono T, Yabuuchi T, Nakamura T, Kimura K, Azami Y, Hirose K, et al. High dose hypofractionated proton beam therapy is a safe and feasible treatment for central lung cancer. Radiol Oncol. 2017;51(3):324–30.
17. Verma V, Shostrom VK, Zhen W, Zhang M, Braunstein SE, Holland J, et al. Influence of fractionation scheme and tumor location on toxicities after stereotactic body radiation therapy for large (>/=5 cm) non-small cell lung cancer: a multi-institutional analysis. Int J Radiat Oncol Biol Phys. 2017;97(4):778–85.

18. Verma V, Shostrom VK, Kumar SS, Zhen W, Hallemeier CL, Braunstein SE, et al. Multi-institutional experience of stereotactic body radiotherapy for large (>/=5 centimeters) non-small cell lung tumors. Cancer. 2017;123(4):688–96.
19. Iwata H, Demizu Y, Fujii O, Terashima K, Mima M, Niwa Y, et al. Long-term outcome of proton therapy and carbon-ion therapy for large (T2a-T2bN0M0) non-small-cell lung cancer. J Thorac Oncol. 2013;8(6):726–35.
20. Iwata H, Murakami M, Demizu Y, Miyawaki D, Terashima K, Niwa Y, et al. High-dose proton therapy and carbon-ion therapy for stage I nonsmall cell lung cancer. Cancer. 2010;116(10):2476–85.
21. Dunlap NE, Larner JM, Read PW, Kozower BD, Lau CL, Sheng K, et al. Size matters: a comparison of T1 and T2 peripheral non-small-cell lung cancers treated with stereotactic body radiation therapy (SBRT). J Thorac Cardiovasc Surg. 2010;140(3):583–9.
22. Koto M, Takai Y, Ogawa Y, Matsushita H, Takeda K, Takahashi C, et al. A phase II study on stereotactic body radiotherapy for stage I non-small cell lung cancer. Radiother Oncol. 2007;85(3):429–34.
23. Fujii O, Demizu Y, Hashimoto N, Araya M, Takagi M, Terashima K, et al. A retrospective comparison of proton therapy and carbon ion therapy for stage I non-small cell lung cancer. Radiother Oncol. 2013;109(1):32–7.
24. Kanemoto A, Okumura T, Ishikawa H, Mizumoto M, Oshiro Y, Kurishima K, et al. Outcomes and prognostic factors for recurrence after high-dose proton beam therapy for centrally and peripherally located stage I non--small-cell lung cancer. Clin Lung Cancer. 2014;15(2):e7–12.
25. Hatayama Y, Nakamura T, Suzuki M, Azami Y, Ono T, Yabuuchi T, et al. Clinical outcomes and prognostic factors of high-dose proton beam therapy for peripheral stage i non-small-cell lung cancer. Clin Lung Cancer. 2016;17(5):427–32.
26. Westover KD, Seco J, Adams JA, Lanuti M, Choi NC, Engelsman M, et al. Proton SBRT for medically inoperable stage I NSCLC. J Thorac Oncol. 2012;7(6):1021–5.
27. Nantavithya C, Gomez DR, Wei X, Komaki R, Liao Z, Lin SH, et al. Phase 2 study of stereotactic body radiation therapy and stereotactic body proton therapy for high-risk, medically inoperable, early-stage non-small cell lung Cancer. Int J Radiat Oncol Biol Phys. 2018;101(3):558–63.
28. Chi A, Chen H, Wen S, Yan H, Liao Z. Comparison of particle beam therapy and stereotactic body radiotherapy for early stage non-small cell lung cancer: A systematic review and hypothesis-generating meta-analysis. Radiother Oncol. 2017;123(3):346–54.
29. Georg D, Hillbrand M, Stock M, Dieckmann K, Potter R. Can protons improve SBRT for lung lesions? Dosimetric considerations. Radiother Oncol. 2008;88(3):368–75.
30. Macdonald OK, Kruse JJ, Miller JM, Garces YI, Brown PD, Miller RC, et al. Proton beam radiotherapy versus three-dimensional conformal stereotactic body radiotherapy in primary peripheral, early-stage non-small-cell lung carcinoma: a comparative dosimetric analysis. Int J Radiat Oncol Biol Phys. 2009;75(3):950–8.
31. Hoppe BS, Huh S, Flampouri S, Nichols RC, Oliver KR, Morris CG, et al. Double-scattered proton-based stereotactic body radiotherapy for stage I lung cancer: a dosimetric comparison with photon-based stereotactic body radiotherapy. Radiother Oncol. 2010;97(3):425–30.
32. KCJ W, Roelofs E, Simone CB 2nd, Dechambre D, Santiago A, van der Stoep J, et al. Photons, protons or carbon ions for stage I non-small cell lung cancer - Results of the multicentric ROCOCO in silico study. Radiother Oncol. 2018;128(1):139–46.
33. Kadoya N, Obata Y, Kato T, Kagiya M, Nakamura T, Tomoda T, et al. Dose-volume comparison of proton radiotherapy and stereotactic body radiotherapy for non-small-cell lung cancer. Int J Radiat Oncol Biol Phys. 2011;79(4):1225–31.
34. Register SP, Zhang X, Mohan R, Chang JY. Proton stereotactic body radiation therapy for clinically challenging cases of centrally and superiorly located stage I non-small-cell lung cancer. Int J Radiat Oncol Biol Phys. 2011;80(4):1015–22.
35. Chen MS, Li JQ, Zheng Y, Liang HH, Zhang YQ, Lin XJ, et al. A prospective randomized trial comparing percutaneous local ablative therapy and partial hepatectomy for small hepatocellular carcinoma. Ann Surg. 2006;243(3):321–8.
36. Huang GT, Lee PH, Tsang YM, Lai MY, Yang PM, Hu RH, et al. Percutaneous ethanol injection versus surgical resection for the treatment of small hepatocellular carcinoma: a prospective study. Ann Surg. 2005;242(1):36–42.
37. Lencioni RA, Allgaier HP, Cioni D, Olschewski M, Deibert P, Crocetti L, et al. Small hepatocellular carcinoma in cirrhosis: randomized comparison of radio-frequency thermal ablation versus percutaneous ethanol injection. Radiology. 2003;228(1):235–40.
38. Pacella CM, Francica G, Di Lascio FM, Arienti V, Antico E, Caspani B, et al. Long-term outcome of cirrhotic patients with early hepatocellular carcinoma treated with ultrasound-guided percutaneous laser ablation: a retrospective analysis. J Clin Oncol. 2009;27(16):2615–21.
39. Shiina S, Teratani T, Obi S, Hamamura K, Koike Y, Omata M. Nonsurgical treatment of hepatocellular carcinoma: from percutaneous ethanol injection therapy and percutaneous microwave coagulation therapy to radiofrequency ablation. Oncology. 2002;62(Suppl 1):64–8.
40. Takayasu K, Arii S, Ikai I, Omata M, Okita K, Ichida T, et al. Prospective cohort study of transarterial chemoembolization for unresectable hepatocellular carcinoma in 8510 patients. Gastroenterology. 2006;131(2):461–9.
41. Tateishi R, Shiina S, Teratani T, Obi S, Sato S, Koike Y, et al. Percutaneous radiofrequency ablation for hepatocellular carcinoma. An analysis of 1000 cases. Cancer. 2005;103(6):1201–9.
42. Yoo HY, Patt CH, Geschwind JF, Thuluvath PJ. The outcome of liver transplantation in patients with hepatocellular carcinoma in the United States between 1988 and 2001: 5-year survival has improved significantly with time. J Clin Oncol. 2003;21(23):4329–35.
43. Andolino DL, Johnson CS, Maluccio M, Kwo P, Tector AJ, Zook J, et al. Stereotactic body radiotherapy for primary hepatocellular carcinoma. Int J Radiat Oncol Biol Phys. 2011;81(4):e447–53.
44. Bujold A, Massey CA, Kim JJ, Brierley J, Cho C, Wong RK, et al. Sequential phase I and II trials of stereotactic body radiotherapy for locally advanced hepatocellular carcinoma. J Clin Oncol. 2013;31(13):1631–9.
45. Jang WI, Kim MS, Bae SH, Cho CK, Yoo HJ, Seo YS, et al. High-dose stereotactic body radiotherapy correlates increased local control and overall survival in patients with inoperable hepatocellular carcinoma. Radiat Oncol. 2013;8:250.
46. Kwon JH, Bae SH, Kim JY, Choi BO, Jang HS, Jang JW, et al. Long-term effect of stereotactic body radiation therapy for primary hepatocellular carcinoma ineligible for local ablation therapy or surgical resection. Stereotact Radiother Liver Cancer BMC Cancer. 2010;10:475.
47. Liu E, Stenmark MH, Schipper MJ, Balter JM, Kessler ML, Caoili EM, et al. Stereotactic body radiation therapy for primary and metastatic liver tumors. Transl Oncol. 2013;6(4):442–6.
48. Takeda A, Sanuki N, Eriguchi T, Kobayashi T, Iwabutchi S, Matsunaga K, et al. Stereotactic ablative body radiotherapy for previously untreated solitary hepatocellular carcinoma. J Gastroenterol Hepatol. 2014;29(2):372–9.
49. Tse RV, Hawkins M, Lockwood G, Kim JJ, Cummings B, Knox J, et al. Phase I study of individualized stereotactic body radiotherapy for hepatocellular carcinoma and intrahepatic cholangiocarcinoma. J Clin Oncol. 2008;26(4):657–64.
50. Yamashita H, Onishi H, Murakami N, Matsumoto Y, Matsuo Y, Nomiya T, et al. Survival outcomes after stereotactic body radiotherapy for 79 Japanese patients with hepatocellular carcinoma. J Radiat Res. 2015;56(3):561–7.

51. Yoon SM, Lim YS, Park MJ, Kim SY, Cho B, Shim JH, et al. Stereotactic body radiation therapy as an alternative treatment for small hepatocellular carcinoma. PLoS One. 2013;8(11):e79854.
52. Chiba T, Tokuuye K, Matsuzaki Y, Sugahara S, Chuganji Y, Kagei K, et al. Proton beam therapy for hepatocellular carcinoma: a retrospective review of 162 patients. Clin Cancer Res. 2005;11(10):3799–805.
53. Hata M, Tokuuye K, Sugahara S, Fukumitsu N, Hashimoto T, Ohnishi K, et al. Proton beam therapy for hepatocellular carcinoma with limited treatment options. Cancer. 2006;107(3):591–8.
54. Kawashima M, Furuse J, Nishio T, Konishi M, Ishii H, Kinoshita T, et al. Phase II study of radiotherapy employing proton beam for hepatocellular carcinoma. J Clin Oncol. 2005;23(9):1839–46.
55. Mizumoto M, Tokuuye K, Sugahara S, Nakayama H, Fukumitsu N, Ohara K, et al. Proton beam therapy for hepatocellular carcinoma adjacent to the porta hepatis. Int J Radiat Oncol Biol Phys. 2008;71(2):462–7.
56. Bush DA, Hillebrand DJ, Slater JM, Slater JD. High-dose proton beam radiotherapy of hepatocellular carcinoma: preliminary results of a phase II trial. Gastroenterology. 2004;127(5 Suppl 1):S189–93.
57. Bush DA, Kayali Z, Grove R, Slater JD. The safety and efficacy of high-dose proton beam radiotherapy for hepatocellular carcinoma: a phase 2 prospective trial. Cancer. 2011;117(13):3053–9.
58. Fukumitsu N, Sugahara S, Nakayama H, Fukuda K, Mizumoto M, Abei M, et al. A prospective study of hypofractionated proton beam therapy for patients with hepatocellular carcinoma. Int J Radiat Oncol Biol Phys. 2009;74(3):831–6.
59. Mizumoto M, Okumura T, Hashimoto T, Fukuda K, Oshiro Y, Fukumitsu N, et al. Proton beam therapy for hepatocellular carcinoma: a comparison of three treatment protocols. Int J Radiat Oncol Biol Phys. 2011;81(4):1039–45.
60. Komatsu S, Fukumoto T, Demizu Y, Miyawaki D, Terashima K, Sasaki R, et al. Clinical results and risk factors of proton and carbon ion therapy for hepatocellular carcinoma. Cancer. 2011;117(21):4890–904.
61. Hong TS, Wo JY, Yeap BY, Ben-Josef E, McDonnell EI, Blaszkowsky LS, et al. Multi-institutional phase II study of high-dose hypofractionated proton beam therapy in patients with localized, unresectable hepatocellular carcinoma and intrahepatic cholangiocarcinoma. J Clin Oncol. 2016;34(5):460–8.
62. Hoyer M, Roed H, Traberg Hansen A, Ohlhuis L, Petersen J, Nellemann H, et al. Phase II study on stereotactic body radiotherapy of colorectal metastases. Acta Oncol. 2006;45(7):823–30.
63. Lee MT, Kim JJ, Dinniwell R, Brierley J, Lockwood G, Wong R, et al. Phase I study of individualized stereotactic body radiotherapy of liver metastases. J Clin Oncol. 2009;27(10):1585–91.
64. Rusthoven KE, Kavanagh BD, Cardenes H, Stieber VW, Burri SH, Feigenberg SJ, et al. Multi-institutional phase I/II trial of stereotactic body radiation therapy for liver metastases. J Clin Oncol. 2009;27(10):1572–8.
65. Scorsetti M, Arcangeli S, Tozzi A, Comito T, Alongi F, Navarria P, et al. Is stereotactic body radiation therapy an attractive option for unresectable liver metastases? A preliminary report from a phase 2 trial. Int J Radiat Oncol Biol Phys. 2013;86(2):336–42.
66. Hong TS, Wo JY, Borger DR, Yeap BY, McDonnell EI, Willers H, et al. Phase II study of proton-based stereotactic body radiation therapy for liver metastases: importance of tumor genotype. J Natl Cancer Inst. 2017;109(9):djx031.
67. Tanguturi SK, Niemierko A, Wo JY, Nguyen KN, Prichard H, Zhu AX, et al. Gallbladder toxicity and high-dose ablative-intent radiation for liver tumors: Should we constrain the dose? Pract Radiat Oncol. 2017;7(5):e323–9.
68. Petersen JB, Lassen Y, Hansen AT, Muren LP, Grau C, Hoyer M. Normal liver tissue sparing by intensity-modulated proton stereotactic body radiotherapy for solitary liver tumours. Acta Oncol. 2011;50(6):823–8.
69. Lin L, Souris K, Kang M, Glick A, Lin H, Huang S, et al. Evaluation of motion mitigation using abdominal compression in the clinical implementation of pencil beam scanning proton therapy of liver tumors. Med Phys. 2017;44(2):703–12.
70. Toramatsu C, Katoh N, Shimizu S, Nihongi H, Matsuura T, Takao S, et al. What is the appropriate size criterion for proton radiotherapy for hepatocellular carcinoma? A dosimetric comparison of spot-scanning proton therapy versus intensity-modulated radiation therapy. Radiat Oncol. 2013;8:48.
71. Emami B, Lyman J, Brown A, Coia L, Goitein M, Munzenrider JE, et al. Tolerance of normal tissue to therapeutic irradiation. Int J Radiat Oncol Biol Phys. 1991;21(1):109–22.
72. Lyman JT. Complication probability as assessed from dose-volume histograms. Radiat Res Suppl. 1985;8:S13–9.
73. Dawson LA, Normolle D, Balter JM, McGinn CJ, Lawrence TS, Ten Haken RK. Analysis of radiation-induced liver disease using the Lyman NTCP model. Int J Radiat Oncol Biol Phys. 2002;53(4):810–21.
74. Gandhi SJ, Liang X, Ding X, Zhu TC, Ben-Josef E, Plastaras JP, et al. Clinical decision tool for optimal delivery of liver stereotactic body radiation therapy: Photons versus protons. Pract Radiat Oncol. 2015;5(4):209–18.
75. Gastrointestinal Tumor Study Group. Treatment of locally unresectable carcinoma of the pancreas: comparison of combined-modality therapy (chemotherapy plus radiotherapy) to chemotherapy alone. J Natl Cancer Inst. 1988;80(10):751–5.
76. Chauffert B, Mornex F, Bonnetain F, Rougier P, Mariette C, Bouché O, et al. Phase III trial comparing intensive induction chemoradiotherapy (60 Gy, infusional 5-FU and intermittent cisplatin) followed by maintenance gemcitabine with gemcitabine alone for locally advanced unresectable pancreatic cancer. Definitive results of the 2000–01 FFCD/SFRO study. Ann Oncol. 2008;19(9):1592–9.
77. Hammel P, Huguet F, van Laethem JL, Goldstein D, Glimelius B, Artru P, et al. Effect of chemoradiotherapy vs chemotherapy on survival in patients with locally advanced pancreatic cancer controlled after 4 months of gemcitabine with or without erlotinib: the lap07 randomized clinical trial. JAMA. 2016;315(17):1844–53.
78. Klaassen DJ, MacIntyre JM, Catton GE, Engstrom PF, Moertel CG. Treatment of locally unresectable cancer of the stomach and pancreas: a randomized comparison of 5-fluorouracil alone with radiation plus concurrent and maintenance 5-fluorouracil--an Eastern Cooperative Oncology Group study. J Clin Oncol. 1985;3(3):373–8.
79. Loehrer PJ Sr, Feng Y, Cardenes H, Wagner L, Brell JM, Cella D, et al. Gemcitabine alone versus gemcitabine plus radiotherapy in patients with locally advanced pancreatic cancer: an Eastern Cooperative Oncology Group trial. J Clin Oncol. 2011;29(31):4105–12.
80. Iacobuzio-Donahue CA, Fu B, Yachida S, Luo M, Abe H, Henderson CM, et al. DPC4 gene status of the primary carcinoma correlates with patterns of failure in patients with pancreatic cancer. J Clin Oncol. 2009;27(11):1806–13.
81. Ben-Josef E, Lawrence TS. Chemoradiotherapy for unresectable pancreatic cancer. Int J Clin Oncol. 2008;13(2):121–6.
82. Murphy JD, Adusumilli S, Griffith KA, Ray ME, Zalupski MM, Lawrence TS, et al. Full-dose gemcitabine and concurrent radiotherapy for unresectable pancreatic cancer. Int J Radiat Oncol Biol Phys. 2007;68(3):801–8.
83. Bujko K, Nowacki MP, Nasierowska-Guttmejer A, Michalski W, Bebenek M, Kryj M. Long-term results of a randomized trial comparing preoperative short-course radiotherapy with preoperative conventionally fractionated chemoradiation for rectal cancer. Br J Surg. 2006;93(10):1215–23.
84. Kapiteijn E, Marijnen CA, Nagtegaal ID, Putter H, Steup WH, Wiggers T, et al. Preoperative radiotherapy combined with total mesorectal excision for resectable rectal cancer. N Engl J Med. 2001;345(9):638–46.

85. Ngan SY, Burmeister B, Fisher RJ, Solomon M, Goldstein D, Joseph D, et al. Randomized trial of short-course radiotherapy versus long-course chemoradiation comparing rates of local recurrence in patients with T3 rectal cancer: Trans-Tasman Radiation Oncology Group trial 01.04. J Clin Oncol. 2012;30(31):3827–33.
86. Hong TS, Ryan DP, Blaszkowsky LS, Mamon HJ, Kwak EL, Mino-Kenudson M, et al. Phase I study of preoperative short-course chemoradiation with proton beam therapy and capecitabine for resectable pancreatic ductal adenocarcinoma of the head. Int J Radiat Oncol Biol Phys. 2011;79(1):151–7.
87. Hong TS, Ryan DP, Borger DR, Blaszkowsky LS, Yeap BY, Ancukiewicz M, et al. A phase 1/2 and biomarker study of preoperative short course chemoradiation with proton beam therapy and capecitabine followed by early surgery for resectable pancreatic ductal adenocarcinoma. Int J Radiat Oncol Biol Phys. 2014;89(4):830–8.
88. Bachtiary B, Haldenberger A, Hauffe J, Rinecker H, Walser M. First results of proton therapy for pancreatic cancer. In: Fourth annual report: the state of the art in radio oncology. Munich: ProHealth AG; 2013. p. 86–91.
89. Kozak KR, Kachnic LA, Adams J, Crowley EM, Alexander BM, Mamon HJ, et al. Dosimetric feasibility of hypofractionated proton radiotherapy for neoadjuvant pancreatic cancer treatment. Int J Radiat Oncol Biol Phys. 2007;68(5):1557–66.
90. Kupelian PA, Potters L, Khuntia D, Ciezki JP, Reddy CA, Reuther AM, et al. Radical prostatectomy, external beam radiotherapy <72 Gy, external beam radiotherapy > or =72 Gy, permanent seed implantation, or combined seeds/external beam radiotherapy for stage T1-T2 prostate cancer. Int J Radiat Oncol Biol Phys. 2004;58(1):25–33.
91. Beckendorf V, Guerif S, Le Prise E, Cosset JM, Lefloch O, Chauvet B, et al. The GETUG 70 Gy vs. 80 Gy randomized trial for localized prostate cancer: feasibility and acute toxicity. Int J Radiat Oncol Biol Phys. 2004;60(4):1056–65.
92. Peeters ST, Heemsbergen WD, van Putten WL, Slot A, Tabak H, Mens JW, et al. Acute and late complications after radiotherapy for prostate cancer: results of a multicenter randomized trial comparing 68 Gy to 78 Gy. Int J Radiat Oncol Biol Phys. 2005;61(4):1019–34.
93. Pollack A, Zagars GK, Starkschall G, Antolak JA, Lee JJ, Huang E, et al. Prostate cancer radiation dose response: results of the M. D. Anderson phase III randomized trial. Int J Radiat Oncol Biol Phys. 2002;53(5):1097–105.
94. Zietman AL, DeSilvio ML, Slater JD, Rossi CJ Jr, Miller DW, Adams JA, et al. Comparison of conventional-dose vs high-dose conformal radiation therapy in clinically localized adenocarcinoma of the prostate: a randomized controlled trial. JAMA. 2005;294(10):1233–9.
95. Halpern JA, Sedrakyan A, Hsu WC, Mao J, Daskivich TJ, Nguyen PL, et al. Use, complications, and costs of stereotactic body radiotherapy for localized prostate cancer. Cancer. 2016;122(16):2496–504.
96. Tan TJ, Siva S, Foroudi F, Gill S. Stereotactic body radiotherapy for primary prostate cancer: a systematic review. J Med Imaging Radiat Oncol. 2014;58(5):601–11.
97. Bentzen SM, Ritter MA. The alpha/beta ratio for prostate cancer: what is it, really? Radiother Oncol. 2005;76(1):1–3.
98. Brenner D, Armour E, Corry P, Hall E. Sublethal damage repair times for a late-responding tissue relevant to brachytherapy (and external-beam radiotherapy): implications for new brachytherapy protocols. Int J Radiat Oncol Biol Phys. 1998;41(1):135–8.
99. Brenner DJ. Fractionation and late rectal toxicity. Int J Radiat Oncol Biol Phys. 2004;60(4):1013–5.
100. Brenner DJ, Hall EJ. Fractionation and protraction for radiotherapy of prostate carcinoma. Int J Radiat Oncol Biol Phys. 1999;43(5):1095–101.
101. Dasu A. Is the alpha/beta value for prostate tumours low enough to be safely used in clinical trials? Clin Oncol (R Coll Radiol). 2007;19(5):289–301.
102. Dewit L, Oussoren Y, Bartelink H, Thames HD. The effect of cis-diamminedichloroplatinum(II) on radiation damage in mouse rectum after fractionated irradiation. Radiother Oncol. 1989;16(2):121–8.
103. Duchesne GM, Peters LJ. What is the alpha/beta ratio for prostate cancer? Rationale for hypofractionated high-dose-rate brachytherapy. Int J Radiat Oncol Biol Phys. 1999;44(4):747–8.
104. Fiorino C, Sanguineti G, Valdagni R. Fractionation and late rectal toxicity: no reliable estimates of alpha/beta value for rectum can be derived from studies where different volumes of rectum are irradiated at different dose levels: in regard to Brenner (Int J Radiat Oncol Biol Phys 2004;60:1013–1015.). Int J Radiat Oncol Biol Phys. 2005;62(1):289–90; author reply 290–281
105. van der Kogel AJ, Jarrett KA, Paciotti MA, Raju MR. Radiation tolerance of the rat rectum to fractionated X-rays and pi-mesons. Radiother Oncol. 1988;12(3):225–32.
106. Aluwini S, Pos F, Schimmel E, van Lin E, Krol S, van der Toorn PP, et al. Hypofractionated versus conventionally fractionated radiotherapy for patients with prostate cancer (HYPRO): acute toxicity results from a randomised non-inferiority phase 3 trial. Lancet Oncol. 2015;16(3):274–83.
107. Arcangeli G, Saracino B, Gomellini S, Petrongari MG, Arcangeli S, Sentinelli S, et al. A prospective phase III randomized trial of hypofractionation versus conventional fractionation in patients with high-risk prostate cancer. Int J Radiat Oncol Biol Phys. 2010;78(1):11–8.
108. Boike TP, Lotan Y, Cho LC, Brindle J, DeRose P, Xie XJ, et al. Phase I dose-escalation study of stereotactic body radiation therapy for low- and intermediate-risk prostate cancer. J Clin Oncol. 2011;29(15):2020–6.
109. Chen LN, Suy S, Uhm S, Oermann EK, Ju AW, Chen V, et al. Stereotactic body radiation therapy (SBRT) for clinically localized prostate cancer: the Georgetown University experience. Radiat Oncol. 2013;8:58.
110. Dearnaley D, Syndikus I, Mossop H, Khoo V, Birtle A, Bloomfield D, et al. Conventional versus hypofractionated high-dose intensity-modulated radiotherapy for prostate cancer: 5-year outcomes of the randomised, non-inferiority, phase 3 CHHiP trial. Lancet Oncol. 2016;17(8):1047–60.
111. Hoskin PJ, Motohashi K, Bownes P, Bryant L, Ostler P. High dose rate brachytherapy in combination with external beam radiotherapy in the radical treatment of prostate cancer: initial results of a randomised phase three trial. Radiother Oncol. 2007;84(2):114–20.
112. Jabbari S, Weinberg VK, Kaprealian T, Hsu IC, Ma L, Chuang C, et al. Stereotactic body radiotherapy as monotherapy or post-external beam radiotherapy boost for prostate cancer: technique, early toxicity, and PSA response. Int J Radiat Oncol Biol Phys. 2012;82(1):228–34.
113. Katz AJ, Santoro M, Diblasio F, Ashley R. Stereotactic body radiotherapy for localized prostate cancer: disease control and quality of life at 6 years. Radiat Oncol. 2013;8:118.
114. Loblaw A, Cheung P, D'Alimonte L, Deabreu A, Mamedov A, Zhang L, et al. Prostate stereotactic ablative body radiotherapy using a standard linear accelerator: toxicity, biochemical, and pathological outcomes. Radiother Oncol. 2013;107(2):153–8.
115. Lukka H, Hayter C, Julian JA, Warde P, Morris WJ, Gospodarowicz M, et al. Randomized trial comparing two fractionation schedules for patients with localized prostate cancer. J Clin Oncol. 2005;23(25):6132–8.
116. Madsen BL, Hsi RA, Pham HT, Fowler JF, Esagui L, Corman J. Stereotactic hypofractionated accurate radiotherapy of the prostate (SHARP), 33.5 Gy in five fractions for localized dis-

ease: first clinical trial results. Int J Radiat Oncol Biol Phys. 2007;67(4):1099–105.
117. Oliai C, Lanciano R, Sprandio B, Yang J, Lamond J, Arrigo S, et al. Stereotactic body radiation therapy for the primary treatment of localized prostate cancer. J Radiat Oncol. 2013;2(1):63–70.
118. Pollack A, Hanlon AL, Horwitz EM, Feigenberg SJ, Konski AA, Movsas B, et al. Dosimetry and preliminary acute toxicity in the first 100 men treated for prostate cancer on a randomized hypofractionation dose escalation trial. Int J Radiat Oncol Biol Phys. 2006;64(2):518–26.
119. Bossi A, Blanchard P. Hypofractionation for prostate cancer: a word of caution. Lancet Oncol. 2016;17(4):406–7.
120. Johansson S, Astrom L, Sandin F, Isacsson U, Montelius A, Turesson I. Hypofractionated proton boost combined with external beam radiotherapy for treatment of localized prostate cancer. Prostate Cancer. 2012;2012:654861.
121. Slater J, Schulte R, Kang J, David A, Grove RI, Slater JM, et al. Hypofractionated Proton Therapy for Low-Risk Prostate Cancer: Preliminary Results of a Phase 1/2 Study. Int J Radiat Oncol Biol Phys. 2013;87(2):S25.
122. Kim YJ, Cho KH, Pyo HR, Lee KH, Moon SH, Kim TH, et al. A phase II study of hypofractionated proton therapy for prostate cancer. Acta Oncol. 2013;52(3):477–85.
123. Vargas CE, Hartsell WF, Dunn M, Keole SR, Doh L, Eisenbeisz E, et al. Hypofractionated Versus Standard Fractionated Proton-beam Therapy for Low-risk Prostate Cancer: Interim Results of a Randomized Trial PCG GU 002. Am J Clin Oncol. 2018;41(2):115–20.
124. Henderson RH, Bryant C, Hoppe BS, Nichols RC, Mendenhall WM, Flampouri S, et al. Five-year outcomes from a prospective trial of image-guided accelerated hypofractionated proton therapy for prostate cancer. Acta Oncol. 2017;56(7):963–70.
125. Jones D, Suit H, Akine Y, et al. Prescribing, recording, and reporting proton-beam therapy. J ICRU. 2007;7(2):210.
126. Paganetti H. Relative biological effectiveness (RBE) values for proton beam therapy. Variations as a function of biological endpoint, dose, and linear energy transfer. Phys Med Biol. 2014;59(22):R419–72.
127. Dasu A, Toma-Dasu I. Impact of variable RBE on proton fractionation. Med Phys. 2013;40(1):011705.
128. Oden J, Eriksson K, Toma-Dasu I. Inclusion of a variable RBE into proton and photon plan comparison for various fractionation schedules in prostate radiation therapy. Med Phys. 2017;44(3):810–22.
129. Wang Y, Efstathiou JA, Lu HM, Sharp GC, Trofimov A. Hypofractionated proton therapy for prostate cancer: dose delivery uncertainty due to interfractional motion. Med Phys. 2013;40(7):071714.
130. Kole TP, Nichols RC, Lei S, Wu B, Huh SN, Morris CG, et al. A dosimetric comparison of ultra-hypofractionated passively scattered proton radiotherapy and stereotactic body radiotherapy (SBRT) in the definitive treatment of localized prostate cancer. Acta Oncol. 2015;54(6):825–31.
131. Goddard L, Brodin P, Garg M, Tome W, Bodner W. Comparing Photon and Proton Based Hypofractioned SBRT for Prostate Cancer Accounting for Robustness and Realistic Treatment Deliverability. Int J Radiat Oncol Biol Phys. 2017;99(2):E664–5.

Part V

Stereotactic Body Radiation Therapy by Indication

Stereotactic Body Radiation Therapy (SBRT) for Primary Lung Cancer

Gregory M. M. Videtic

Abbreviations

BED	Biologically equivalent dose
CBCT	Cone beam computed tomography
CTV	Clinical target volume
EORTC	European Organisation for Research and Treatment of Cancer
GTV	Gross tumor volume
Gy	Gray
HRQOL	Health-related quality of life
IGRT	Image-guided radiotherapy
ITV	Internal target volume
kV	Kilovolt
LC	Local control
MTD	Maximum tolerable dose
Mv	Megavolt
NSCLC	Non-small cell lung cancer
OAR	Organ at risk
OS	Overall survival
PET; FDG-PET	Positron emission tomography; fluorodeoxyglucose-PET
PTV	Planning target volume
QOL	Quality of life
ROSEL	Radiosurgery Or Surgery for operable Early stage non-small cell Lung cancer
RTOG	Radiation Therapy Oncology Group
SABR	Stereotactic ablative body radiotherapy
SBRT	Stereotactic body radiotherapy
STARS	Stereotactic Ablative Radiotherapy in Stage I Non-small Cell Lung Cancer Patients Who Can Undergo Lobectomy
SUV	Standardized uptake value
SUVmax	Maximum standardized uptake value
VEGF	Vascular endothelial growth factor

Introduction

Lung cancer is the most common malignancy worldwide, with over one million cases being diagnosed yearly [1]. The most common histologic type seen is non-small cell lung cancer (NSCLC) [2]. It is the leading cause of cancer death in the United States, with more than 158,000 estimated deaths predicted for 2016 [3]. About 10–20% of lung cancer patients will present with early-stage ($T_{1–2}$ N_0) disease [4]. Early-stage NSCLC in medically fit patients is conventionally managed by surgical resection [5]. However, many lung cancer patients are considered medically inoperable due to their concurrent cardiovascular, pulmonary, or other comorbidities and these preclude surgical management [5]. Despite these substantial patient comorbidities, observation alone of inoperable patients results in unacceptable outcomes; in a study by McGarry and coauthors [6], lung cancer was shown to be cause of death in 53% of 75 stage I medically inoperable patients not receiving definitive therapy. Historically, any treatment offered this population aimed at limiting treatment-related injury. Options often then considered included limited surgical resection such as a wedge [7] or conventional radiotherapy (RT) given over 6–7 weeks [8]; however, cancer outcomes with either of these were found generally to be inferior to anatomic resection [5]. When conventional radiotherapy was used for these vulnerable patients, the practice was often to use simple beam arrangements and/or modest doses for safety. However, this approach resulted not only in high rates of local failure because of inability to deliver effective dose, but also often unwanted lung toxicity because

G. M. M. Videtic (✉)
Cleveland Clinic, Department of Radiation Oncology, Cleveland, OH, USA

Cleveland Clinic Lerner College of Medicine, Cleveland, OH, USA
e-mail: videtig@ccf.org

D. M. Trifiletti et al. (eds.), *Stereotactic Radiosurgery and Stereotactic Body Radiation Therapy*,
https://doi.org/10.1007/978-3-030-16924-4_21

of both the underlying functional impairments of the patients and the radiation oncologist's limitations in defining and constraining the cancer target volume [9].

This clinical challenge was eventually resolved in two ways. Technologic advances occurred in the diagnostic and radiologic disciplines that better defined early-stage disease, and clinicians adapted the high RT dose delivery techniques already in use for brain tumors (SRS) to extracranial sites [5]. The publication in 1995 by Blomgren and coauthors was the first to describe an experience of stereotactic high-dose fraction radiation therapy of extracranial tumors using a linear accelerator that delivered very high doses of radiation to tumors, including those in the lung, over a few fractions using highly conformal techniques [10]. The subsequent two decades following the publication of that landmark paper have seen the evolution and refinement of the technological developments in lung stereotactic body radiotherapy (SBRT; also known as stereotactic ablative body radiotherapy or SABR), so that its utilization in the medically inoperable early-stage lung cancer population has emerged as the standard of care for these patients.

Site-Specific Considerations

From its inception, SBRT has been considered primarily appropriate for organs whose functional structures can support focal ablation of physiologic units without compromising overall functionality. Because the lung has been considered such an organ based on the concept of its functional subunits being in "parallel," it was an early site for testing the feasibility and efficacy of SBRT [5]. Nonetheless, limiting the amount of normal thoracic tissues that are exposed to any amount of radiation that is prescribed to the target remains crucial. In that regard, the thorax includes a number of normal structures which historically have always elicited particular caution when planning radiotherapy. Based on a hierarchy of severe and/or irreversible injury potential, these structures always include the spinal cord, the esophagus, the major airways, the heart and the lungs. Accurate delineation of both the tumor and its adjacent organs at risk (OARs) is therefore essential for successful and safe planning and delivery of lung SBRT. In principle, to achieve both effective delivery of very high individual doses of radiation and minimal damage to normal tissues, SBRT dose to the primary tumor must be (1) tightly conformed to the shape of the tumor, (2) rapidly dropped off in the surrounding normal tissues, and (3) administered to discrete targets without regional micrometastatic spread (i.e., without nodal involvement) [5].

Gross tumor volume (GTV) is defined as all visible tumor on images acquired during simulation with assistance from fused diagnostic images as needed. Targets in lung will generally be drawn using CT pulmonary windows; however, soft tissue windows, ideally with contrast, may be used to avoid inclusion of adjacent vessels, atelectasis, or mediastinal or chest wall structures within the GTV. As indicated by clinical presentations where the GTV is ill-defined, fusion of planning studies with positron emission tomography (PET) studies may facilitate contouring. By convention, a clinical target volume (CTV) is not designated in routine lung SBRT planning based on the characteristics of dose deposition around the target, so that the GTV is equal to the CTV [11]. In accounting for any residual respiratory motion noted on imaging after implementation of the selected motion management technique (see below), the GTV is expanded to create an internal target volume (ITV). Lastly a planning target volume (PTV) is defined to account for setup error, deformation, and any additional uncertainty during the treatment process and is typically 5 mm based on the robustness of most SBRT systems (Fig. 1).

Accurate OAR delineation is as noted necessary for accurate treatment planning. Consistency in outlining structures as well as uniformity of OAR definitions between plans helps in minimizing inter- and intra-observer variability. For example, lung SBRT plans usually include several OARs not commonly delineated or considered in standard fractionated lung treatment, such as the ribs, the proximal bronchial tree and the brachial plexus. In that regard, clinicians can access original protocols wherein detailed instructions on standardized OAR definitions and contouring are readily available, e.g., NRG Oncology's Radiation Therapy Oncology Group (RTOG) 0236 [12].

By its nature, lung SBRT requires reproducible means to achieve highly accurate treatment setups and to account for, and mitigate the effects of, respiratory motion. To provide accuracy in treatment setup for lung SBRT, a robust immobilization system is necessary to keep the patient precisely in

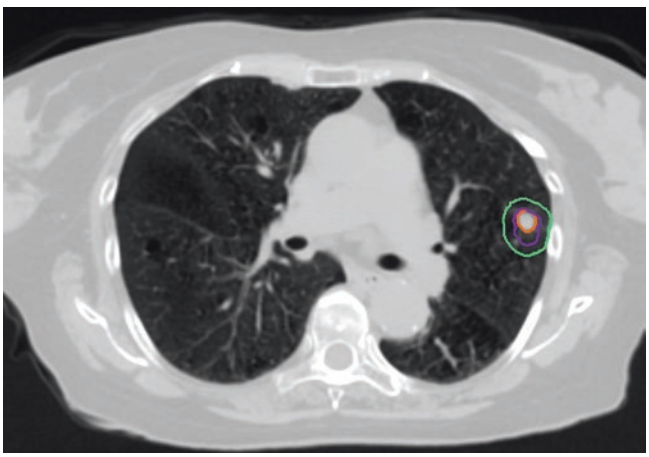

Fig. 1 Representative axial slice from the planning CT images of the chest for a $T_{1a}N_0M_0$ cancer of the left upper lobe of the lung, demonstrating the GTV (orange), ITV (purple), and PTV (green) contours used for lung SBRT planning

the same position throughout the whole treatment delivery. Devices such as body frames, vacuum pillows, and thermoplastic devices have been used for such immobilization. Regardless of the device used, by customizing it so that it is fitted snugly around the patient any potential movement of the torso is then limited. With proper usage, the type of device used will not have an impact on clinical outcomes. The next critical step in lung SBRT patient simulation is accounting for tumor and organ motion. Maneuvers to control the impact of breathing can be divided into restriction, gating, and tracking approaches, as summarized by Folkert and Timmerman [13]. Techniques used for limiting or minimizing motion include abdominal compression and breath-hold maneuvers to freeze the tumor in a specific stage of the respiratory cycle. Gating involves tracking the tumor's range of motion during respiratory cycles; the radiation beam is triggered only during a specific segment of each cycle. Tracking (or chasing) involves moving the radiation beam in real time so that the motion of the target is followed during respiration. This may require placement of radiographically identifiable markers (fiducials) in the vicinity of the tumor. Regardless of the system used to control for the effects of motion, the acquisition of planning data should incorporate the same considerations. Lastly, reproducible means of verification at the time of SBRT delivery (termed image guidance radiotherapy, or IGRT) complete the requirement for accuracy. Different treatment platforms will provide various IGRT capabilities to enable verification of the location of the tumor or target volume before treatment delivery. These methods include radiographic and tomographic imaging systems (cone beam CT, or CBCT) integrated into a linear accelerator, using photon energies in the kV range for target localization; automatic six-dimensional fusion of reference digitally reconstructed radiographs and stereoscopic X-rays taken prior to treatment which identify any setup errors or target shifts in any direction and compensate for the discrepancy for with robotic table movements; and frameless systems in which orthogonal radiographs allow for real-time tracking by imaging reliable bony landmarks or implanted fiducial markers are utilized for target tracking and treatment delivery.

Regarding dose/fractionation schedules in lung SBRT, there is no single standard regimen for all tumor presentations. Published data have generally reflected single institution experiences, and this explains to some degree variations among institutions with respect to total dose, fractionation schedules, overall treatment time, and techniques of dose delivery. These differences have made it challenging to standardize dose schedules and dosimetric specifications in the administration of SBRT. For example, in some of the earliest work in lung SBRT accomplished by investigators in Japan, Uematsu and coauthors [14] reported outcomes from 50 patients treated with SBRT to dose fractionation schedules ranging from 50 to 60 Gy in 5–10 fractions in 2001. The majority of patients (47 of 50) achieved long-term local control (LC), with 3-year overall survival (OS) of 66% and cause-specific survival of 88%. In this same era, clinicians at Indiana University were conducting prospective phase I/II trials of dose escalation starting at 8 Gy per fraction for a total of 3 fractions delivered over 2 weeks. The maximum tolerated dose (MTD) was not reached for T1 tumors and the MTD for T2 tumors greater than 5 cm was met at 24 Gy per fraction. LC was excellent with only 1 failure seen when dose per fraction was higher than 16 Gy compared to 9 failures at doses less than 16 Gy, and this was achieved without significant toxicity [15, 16]. With that Indiana experience, the phenomenon of toxicity dependency on dose delivered and tumor location in the lung was also revealed, something not previously described. It showed that treatment of "central" and perihilar tumors with greater than 60 Gy in 3 fractions, where "central" was defined as a tumor within 2 cm of the proximal tracheobronchial tree, posed a higher risk of severe toxicity than treatment of "peripheral" tumors [17]. When the RTOG initiated a prospective phase I/II trial (RTOG 0236) in medically inoperable peripheral early-stage NSCLC, they consequently assessed 60 Gy (without heterogeneity corrections) in 3 fractions over 8–14 days, with minimal interfraction intervals of 40 hours. This pioneering study showed a survival rate of 55.8% at 3 years, high rates of local tumor control with an estimated 3-year primary tumor control rate of 97.6%, and moderate treatment-related morbidity with protocol-specified treatment-related grade 3 or higher adverse events of 16.3% and with no grade 5 events [18]. Investigation of dose schedules for central tumors has included RTOG 0813, dose escalation study starting at 50 Gy in 5 fractions given every other day and achieving the MTD of 60 Gy in 5 fractions. The LungTech trial (European Organisation for Research and Treatment of Cancer (EORTC) 22113-08113) is studying 60 Gy in 8 fractions for central tumors. In the United States, Chang and coauthors at MD Anderson Cancer Center have published their experience with a regimen of 50 Gy in 4 fractions [19]. Recent studies have looked at single-fraction lung SBRT in peripheral tumors. For example, RTOG 0915 was a prospective, randomized phase II trial that compared 34 Gy in 1 fraction with 48 Gy in 4 fractions and based on a co-primary endpoint of toxicity and local control showed that the single-fraction arm had the least toxicity for equal efficacy of the two regimens [20]. As presented in abstract form, results from a randomized phase II trial that compared 30 Gy in one fraction to 60 Gy in 3 fractions showed the arms with equal efficacy and modest toxicity [21].

Clinical Evidence

Published results for lung SBRT over the past two decades consistently report on its outstanding LC in inoperable stage I NSCLC patients, with nearly all series reporting 85–95%

control rates [11, 15, 18, 22, 23]. Clinicians must be mindful, however, that the definition of local control after this form of therapy can be difficult because distinguishing true tumor failure from radiation-induced lung damage is often challenging. Many treated patients develop radiographic changes of fibrosis that may be mistaken for recurrence, and interpretation of images may require an experienced reader [24]. Positron emission tomography (PET)-based imaging may help in the interpretation of ambiguous cases on CT imaging [25] (Fig. 2a–d), though biopsy may occasionally be required. That said, lung SBRT LC rates are in keeping with those from prospective surgical series showing a locoregional failure rate of 5–7% for lobectomy and 8–17% for sublobar resection [26, 27]. A pooled meta-analysis of 40 SBRT studies totaling 4850 patients and 23 surgical studies (lobar or sublobar resection, 7071 patients in total) likewise suggested LC by this definition is similar [28]. It remains that identifying local failure after SBRT is more challenging than after lobectomy (where there is no longer any physical tumor), so that postradiation fibrosis may lead to overestimation of local failure or, on the other hand, the comparatively shorter follow-up of most published SBRT series might result in underestimation of local failure [29]. Another issue in making comparisons between surgical and radiation treatment modalities is that LC in surgical series is more often reported as locoregional control. Concerning LC after SBRT, radiation oncologists have typically defined LC as the absence of tumor progression within 1 cm of the primary tumor site. If using surgical definitions when accounting for lobar failure, LC in SBRT series drops slightly. RTOG 0236, a landmark prospective trial of SBRT utilizing 60 Gy in 3 fractions (estimated 54 Gy in 3 fractions with heterogeneity corrections) for peripheral stage I NSCLC, demonstrated 3-year LC of 97.6%, lobar control of 90.6%, locoregional control of 87.2%, and a 22.1% rate of distant recurrence [11].

When it comes to regional nodal failure after lung SBRT, its reported incidence ranging from 6% to 22% is surprisingly lower than might be expected for non-resected patients given the known rate of nodal upstaging after surgical nodal dissection for clinical stage I lung cancer [30, 31]. Increasing quality of pretreatment imaging as well as availability of nonsurgical nodal staging techniques, only modestly used in most SBRT series, may also impact the incidence of nodal failure going forward. Another theory for the low nodal recurrence rate after SBRT is that ablative doses of radiation may initiate a T-cell, immune-mediated tumor cell killing response [32]. Others suggest that radiation may scatter effective dose to the regional lymph nodes that may be harboring microscopic metastases [33].

In keeping with what is seen in surgical series of resected operable early-stage lung cancer patients, distant failure remains the predominant pattern of failure in medically inop-

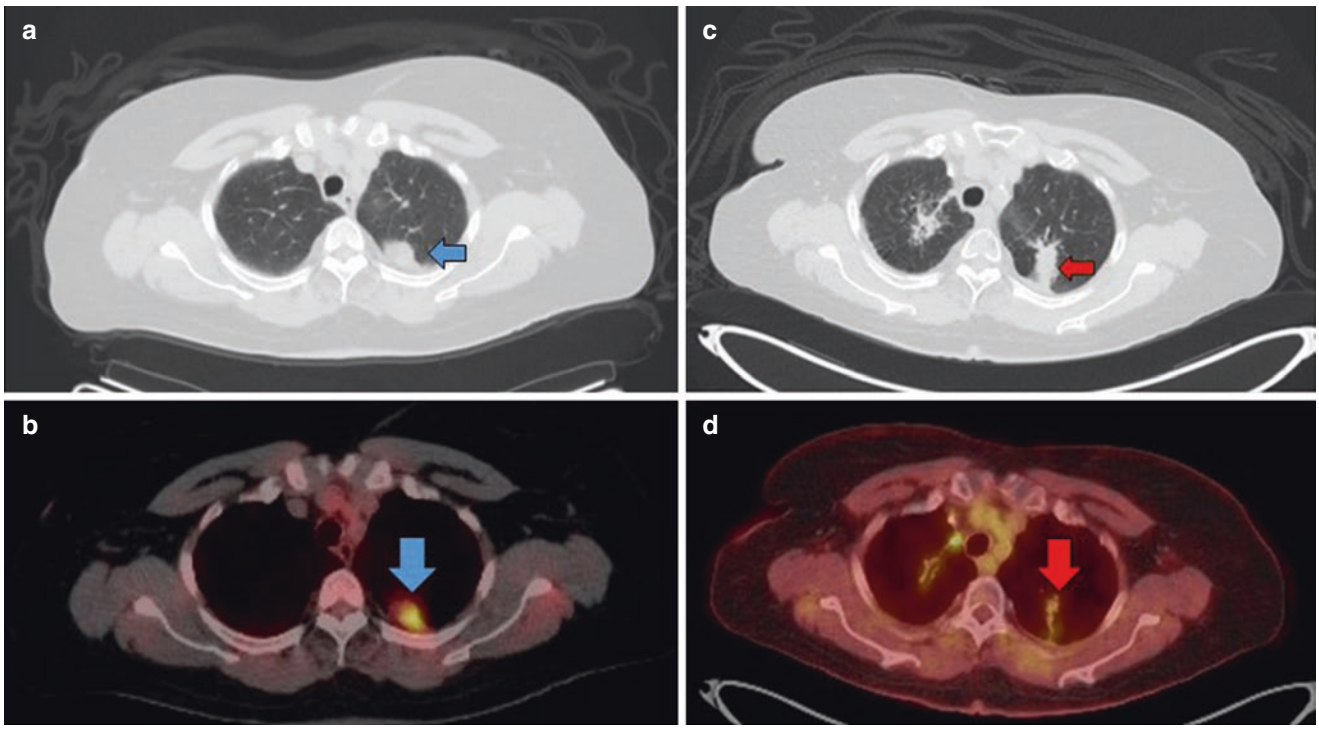

Fig. 2 (**a**–**d**) Representative axial FDG-PET CT images from a 68-year-old female with medically inoperable, early-stage squamous cell carcinoma of the left upper lobe of the lung, following lung SBRT (34 Gy/1 fraction): **a**, **b** lesion (blue arrow) pre-treatment, dated Nov 2007, 1.6 cm, SUVmax 15.3, and **c**, **d** lesion (red arrow) posttreatment dated Aug 2017, 3.4 cm, SUVmax 3.6

erable patients treated with SBRT, even though early stage. Distant metastasis is reported to occur in 15% to 30% of stage I patients treated with SBRT, mimicking the rates seen in resected patients [34–36].

In comparison to surgical series, SBRT for stage I NSCLC is typically associated with lower reported OS. This is likely in large part due to patient selection given the predominance of medically inoperable patients and high rates of death due to comorbid conditions in SBRT series [28, 31, 37]. It is supported by the observation that after performing multivariate adjustment or propensity score–based analysis SBRT OS is typical similar to surgical cohorts [28, 31, 37]. Notably small series of SBRT in medically operable patients have yielded excellent OS [34, 35]. The previously noted pooled analysis also demonstrated a relationship between OS and the percent of operable patients within individual SBRT series, which when curve-fit to surgical series also suggested the potential for similar OS in equally operable patients [28]. Ultimately, however, modeling data cannot replace clinical data, and with no long-term series of sufficient volume for SBRT in operable patients in the US population, surgery should be the standard of care for operable patients in this country.

Patient-related outcomes for lung SBRT have also been validated by prospective measurements using quality-of-life (QoL) instruments. A recent systematic review addressing QoL after SBRT for early-stage lung cancer found 9 prospective studies published between 2010 and 2015 [38]. The overall results of this review suggested few clinically significant changes in health-related quality-of-life (HRQoL) scores after lung SBRT, further indicating the appropriateness of SBRT in the medically inoperable population.

Toxicity

Considering the remarkably high radiation doses used in lung SBRT, the consistent finding from numerous clinical reports over the last decades has been the paucity of severe lung toxicity seen after treatment. For patients already with baseline pulmonary dysfunction, the rates of grade 3 or higher radiation pneumonitis have been typically less than 5% [39]. These low rates of toxicity are presumably due to both the precision of treatment delivery and the structural physiology of lung tissue. While SBRT causes inevitable focal lung parenchymal changes (as seen on CT imaging of the chest over years) in most patients [24], its functional impact (as evidenced by symptom development) is typically minimal, likely because adequate remaining functional lung tissue is preserved. In addition, it is hypothesized that the high doses may obliterate blood vessels in the treated area, thereby mitigating ventilation-perfusion mismatch felt to play a role in the symptomatic toxicity of standard RT [5]. On average there is little to no decrease in the pulmonary function of treated patients, with a report showing that post-SBRT, fluctuations in pulmonary function tests from baseline occur in both positive and negative direction, and with these results ultimately falling into a normal distribution so that no association between treatment and PFT changes can be made [40]. In a secondary analysis of RTOG 0236, Stanic and coauthors also showed no clinically significant changes in pulmonary function following lung SBRT [41]. Even patients with extremely compromised pulmonary function (e.g., diffusion capacity <20% predicted) show overall survival outcomes comparable to less compromised patients [40, 42], suggesting no lower limit to pulmonary function when selecting patients as appropriate for lung SBRT, along as they are medically stable. In noting that lung toxicity is generally low, it has become clear that tumor location does play a critical role in the risk and development of treatment-related lung morbidity. Thus, the exception to the low rates of SBRT toxicity was first reported by Timmerman and colleagues following their experience of treating "central" lung tumors in the setting of their phase I/II at Indiana University, where "central" was defined as lesions lying within 2 cm of the tracheobronchial tree [17, 43]. In that phase II experience, patients with tumors treated in the central lung had 2-year freedom from severe toxicity of only 54%. That the particular interaction between tumor location and toxicity is SBRT dose/fractionation-specific since "central" lesions have otherwise been safely treated with slightly lower total doses and doses per fraction (such as 50 Gy in five fractions) with similar local control and toxicity as seen in treatment of peripheral lesions to higher doses [23, 34].

As clinical experience with lung SBRT evolved over years and with routine follow-up of patients following treatment, non-lung toxicities began to declare themselves. Thus, chest wall pain or rib fracture developing many months to years after treatment became an increasingly reported delayed side effect. Though symptoms are typically mild to moderate, chest wall symptoms are reported in 5–15% of patients with peripheral lesions, and appear to be related to treatment dose, fractionation, and beam arrangement [23, 44, 45]. With advances in understanding of the causative factors, and improved treatment planning, rates of toxicity may be lowered for future patients. Overall the prospect of chest wall toxicity remains mild in comparison with surgical alternatives [46], is typically self-limited and can be managed medically [47]. Other less common late side-effects such as soft-tissue fibrosis [48], skin reaction [49], and brachial plexopathy [50] have been described; however, these occur in less than 1% of treatments and are likewise preventable with changes in treatment planning. Grade 5 toxicities are very rare and not predictable. For example, esophageal fistula development followed by death was seen in 2 patients as a rare complication of SBRT and only in those patients who also received adjuvant vascular endothelial growth factor

(VEGF)-modulating agents after treatment, suggesting that clinicians need to be mindful of the potential interaction of SBRT and adjuvant therapy [51]. Fatal central-airway necrosis was reported in a patient with a very centrally located lung tumor and who had received SBRT, with 50 Gy administered in 5 fractions, 8 months earlier [52].

Plan Quality

Early reports in lung SBRT often provided institution-specific approaches to planning development and review. With time, prospective trials, such as RTOG 0236, provided structured and rigorous parameters to ensure uniform approaches to planning across a range of institutions. This allowed for consistent development of high quality plans for the delivery of lung SBRT and thus provided a model for structured planning review. In addressing the treatment requirements for an early-stage lung cancer, lung SBRT has to provide an extremely conformal radiation dose distribution around the PTV generated off of the tumor, while simultaneously allowing for a very rapid falloff of the radiation dose beyond the prescribed isodose line (Fig. 3). One of the most important parameters in the evaluation of a computerized treatment plan for SBRT, therefore, has been the conformality index (i.e., dosing to tumor) and zones of high-dose and low-dose spillage (i.e., dosing to OARs). As outlined in RTOG 0236 [12] and applied to subsequent lung SBRT protocols from NRG, the conformality index is the ratio of the prescription isodose volume to the planning target volume (PTV). High-dose spillage refers to the amount of normal tissue included in the prescription isodose shell, which can be quantified using the conformality index. Low-dose spillage is defined as the maximum dose at a defined distance away from the PTV or the ratio of 50% of the prescription isodose volume to the PTV. RTOG protocol tables in that regard provide tumor size-specific reference tables to ensure compliance with these treatment requirements for safety. Likewise, organ-specific point and/or volumetric dosing limits are provided per protocol to ensure plan appropriateness so that in situations in which the PTV is particularly in close proximity to critical organs or structures, the maximum point doses as well as the dose volume histograms of those organs or structures can be evaluated to provide a hierarchy of planning constraints based on OAR-specific injury implications.

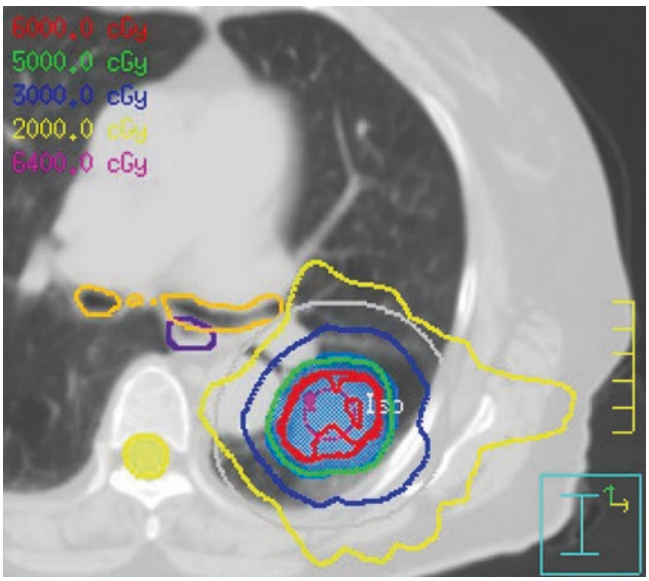

Fig. 3 Representative axial slice from the CT images of the SBRT plan for a stage I left lower lobe cancer treated with 50 Gy in 5 fractions: PTV (blue cloud), 60 Gy isodose line (red), 50 Gy isodose line (green), 30 Gy isodose line (blue), 20 Gy isodose line (yellow), 2 cm ring expansion from the PTV for planning (gray line), esophagus (purple line), and proximal bronchial tree (orange line)

Typically, to achieve the above planning goals at delivery, three-dimensional conformal radiotherapy planning with a large number of highly conformal beams, or intensity modulated radiation therapy planning is used, depending on the site of the tumor and the preference of the treating clinician and physicist. Coplanar or non-coplanar, non-overlapping, non-opposing beams or arc therapy are all valid approaches to beam arrangement, with some authors encouraging non-coplanar arcs to improve conformality and OAR sparing in complex anatomical geometries. Combination of static and arc beams can also be employed. Gantry clearance verification prior to treatment is generally recommended to ensure technical deliverability. As with the general principles regarding use of photons in the thorax, lower energies $\leq$10MV are preferred for lung, although specific clinical scenarios may require other approaches.

Future Directions

Establishing a standard SBRT schedule with uniform planning approaches for medically inoperable tumors has been considered a desirable goal by many clinicians. Thus, within the RTOG, in the formulation of RTOG 0915 there were stated plans in the protocol to utilize the optimal regimen determined by that randomized phase II trial for a randomized phase III trial comparing it to the current standard of 60 Gy in three fractions set by RTOG 0236, with a primary endpoint of overall survival. Such a proposal, however, has not been able to move forward and currently there is no single "optimal" regimen. Thus, selection of dose regimens will have to continue to, first, reflect tumor location. Second, Onishi and coauthors [34] observed that in order to achieve equivalence in local control, differing SBRT schedules require a biologically equivalent dose (BED) of at least equivalent 100 Gy_{10}, where the Gy_{10} value represents a con-

version factor for making comparison between dose and fractionation schedules using a mathematical model based on tissue responses [53].

Since distant failure remains the predominant pattern of failure for medically inoperable early-stage lung cancer patients treated with SBRT, the appropriate use of adjuvant systemic or biologic therapies has also become a question of great interest. It is nonetheless controversial since that practice is currently ill-defined in the standard surgical population and is relatively contraindicated in the medically compromised with more advanced disease. In that regard, it is important to note that the treatment of advanced NSCLC has undergone a major theory shift in the past decade, from the primary use of cytotoxic chemotherapy to the discovery of driver mutations and the subsequent discovery and use of genotype-directed targeted therapies [54]. Such agents are not only favored due to their selectivity but also due to their potentially more favorable side effect profile. Hence, many such agents are now being considered in the non-metastatic setting. In that regard, recently discovered strategies using monoclonal antibodies targeting the immune-checkpoint pathways have recently shown impressive activity in several solid tumors including NSCLC [55]. These drug features explain the rationale in developing research proposals involving immunotherapy for early-stage lung cancer patients being treated with lung SBRT.

Lastly, among the most provocative findings published in the early lung cancer SBRT literature were the results of Onishi and colleagues [34] in which the survival of a subgroup of medically operable patients treated with SBRT was equivalent to similar-stage patients treated with video-assisted thoracoscopic surgery or lobectomy. This evidence combined with the favorable treatment profile for lung SBRT eventually prompted 3 randomized trials in the medically operable population (American College of Surgeons Oncology Group Z4099/RTOG 1021; ROSEL [Radiosurgery Or Surgery for operable Early stage non-small cell Lung cancer]; and Stereotactic Ablative Radiotherapy in Stage I Non-small Cell Lung Cancer Patients Who Can Undergo Lobectomy (STARS)). Unfortunately, all were terminated early because of poor accrual, but a pooled analysis of 2 of the trials (ROSEL and STARS) was published recently and involved 58 patients. The results, which have been controversial not the least because of the small sample size, suggested a potential survival benefit to SBRT over surgery, if not equivalence with respect to local control [56]. The role of lung SBRT for operable patients therefore remains a contentious question. Currently, there are two ongoing multi-institutional trials in the United States for high-risk operable patients comparing limited surgical resection versus SBRT with a primary endpoint of overall survival [57].

Practical Considerations

(a) Patient Selection:
  (i) Patient evaluation by experienced multidisciplinary thoracic oncology team, including, at a minimum, a thoracic surgeon, a pulmonologist, and a radiation oncologist, is recommended.
  (ii) Active medical conditions likely to influence short-term patient survival need to be addressed and may preclude appropriateness of lung SBRT for early-stage inoperable cancer.
  (iii) There is no lower limit to the degree of impaired pulmonary function which acts as a contra-indication to lung SBRT.
  (iv) Pathologic confirmation of malignancy by biopsy is desirable but may not be readily achievable in many inoperable patients due to medical contraindications. For non-biopsied patients, one may consider a clinical diagnosis of malignancy based on radiographic criteria such as serial CT chest scans showing growth and/or FDG-PET scan either demonstrating high (SUV >5) metabolic activity on a single scan or progression of intermediate activity over serial scans.
  (v) Invasive mediastinal staging is not absolutely required prior to lung SBRT. On a case by case basis, clinicians can consider the appropriateness of endobronchial ultrasound-, or PET-only-, based staging to characterize and clinically define mediastinal lymph nodes.

(b) Dose Selection:
  (i) To be deemed "SBRT," any schedule requires BED of at least equivalent 100 Gy_{10}.
  (ii) Dose schedule will be selected as a function of location with reference to the airways and/or mediastinum.
  (iii) For lesions deemed "peripheral," SBRT lung schedules may include 60 Gy in 3 fractions, 50 Gy in 5 fractions, 48 Gy in 4 fractions, and 30 Gy or 34 Gy in 1 fraction.
  (iv) "Central" lesions are preferentially treated with 50 Gy in 4/5 fractions or 60 Gy in 8 fractions.
  (v) See Table 1.

(c) Treatment Delivery:
  (i) Ensure usage of a robust immobilization device integrated with a reliable system to account for motion.
  (ii) Ensure proficiency in the use of any of the range of SBRT treatment platforms available, with fiducial usage as indicated by the technical characteristics of the given platform and per clinician preference.

Table 1 Representative dose constraints for organs at risk (OARs) when planning lung SBRT based on selected common fractionation schedules

		One-fraction treatment		Three-fraction treatment		Five-fraction treatment		
Critical structure	Max critical volume above threshold (cc)	Threshold dose (Gy)	Max point dose (Gy)[a]	Threshold dose (Gy)	Max point dose (Gy)[a]	Threshold dose (Gy)	Max point dose (Gy)[a]	Toxicity endpoint
Spinal cord	Point	14 (14 Gy/fx)	(Gy/fx)	21.9 (7.3 Gy/fx)	21.9 (7.3 Gy/fx)	30 (6 Gy/fx)	30 (6 Gy/fx)	Myelitis
	<0.35	10 (10 Gy/fx)	(Gy/fx)	18 (6 Gy/fx)	(Gy/fx)	23 (4.6 Gy/fx)	(Gy/fx)	
	<0.12	7 (7 Gy/fx)	(Gy/fx)	12.3 (4.1 Gy/fx)	(Gy/fx)	14.5 (2.9 Gy/fx)	(Gy/fx)	
Esophagus[b]	<5	11.9 (11.9 Gy/fx)	15.4 (15.4 Gy/fx)	17.7 (5.9 Gy/fx)	25.2 (8.4 Gy/fx)	19.5 (3.9 Gy/fx)	35 (7 Gy/fx)	Stenosis or fistula
Brachial plexus	<3	14 (14 Gy/fx)	17.5 (17.5 Gy/fx)	20.4 (6.8 Gy/fx)	24.0 (8.0 Gy/fx)	27.0 (5.4 Gy/fx)	30.5 (6.1 Gy/fx)	Neuropathy
Heart/pericardium	<15	16 (16 Gy/fx)	22 (22 Gy/fx)	24.0 (8.0 Gy/fx)	30.0 (10.0 Gy/fx)	32.0 (6.4 Gy/fx)	38 (7.6 Gy/fx)	Pericarditis
Great vessels	<10	31 (31 Gy/fx)	37 (37 Gy/fx)	39.0 (13.0 Gy/fx)	45.0 (15.0 Gy/fx)	47.0 (9.4 Gy/fx)	53 (10.6 Gy/fx)	Aneurysm
Trachea and large bronchus[b]	<4	10.5 (10.5 Gy/fx)	20.2 (20.2 Gy/fx)	15.0 (5.0 Gy/fx)	30.0 (10.0 Gy/fx)	16.5 (3.3 Gy/fx)	40 (8 Gy/fx)	Stenosis or fistula
Rib/chest wall[c]	<1	22 (22 Gy/fx)	30 (30 Gy/fx)	28.8 (9.6 Gy/fx)	36.9 (12.3 Gy/fx)	35.0 (7.0 Gy/fx)	43 (8.6 Gy/fx)	Pain or fracture
Skin	<10	23 (23 Gy/fx)	26 (26 Gy/fx)	30.0 (10.0 Gy/fx)	33.0 (11.0 Gy/fx)	36.5 (7.3 Gy/fx)	39.5 (7.9 Gy/fx)	Ulceration
Lung (right and left)	1500	7 (7 Gy/fx)	(Gy/fx)	11.6 (2.9 Gy/fx)	–	12.5 (2.5 Gy/fx)	–	Basic lung function
	1000	7.4 (7.4 Gy/fx)	(Gy/fx)	12.4 (3.1 Gy/fx)	–	13.5 (2.7 Gy/fx)	–	Pneumonitis

Data from Refs. [58, 59]
Gy gray, *fx* fraction
[a]Max point dose corresponds to 0.035 cc of tissue or less
[b]Avoid circumferential radiation
[c]In attempting to optimize target treatment parameters, being mindful of rib dosing (as low as reasonably achievable [ALARA]) should in no way compromise target coverage or restrict potential delivery parameters for the sake of rib dosing. Rib "limits" provided in the table above may in that respect be exceeded for an otherwise excellent plan

(iii) Observe rules for overall treatment time as published; e.g., for 60 Gy in 3 fractions, overall treatment time is 8–14 days, and interfraction interval is minimum of 40 hours/maximum of 7 days.

(d) Follow-Up:
  (i) Optimal follow-up schedules and testing requirements after lung SBRT are not formalized.
  (ii) Clinicians should employ thoracic CT scans for follow-up imaging since there is limited evidence to support routine use of FDG-PET/CT.
  (iii) Consider patient visits at months 3, 6, and 12 in year 1, every 6 months in year 2, and annually in years 3–5, after completion of SBRT.
  (iv) Consider FDG-PET/CT imaging only if CT findings are suspicious for local recurrence.
  (v) Consider pathologic confirmation if suspicion of recurrence, but consider imaging findings alone if biopsy is not safe or feasible.
  (vi) Consider yearly survivorship monitoring after 5 years, using CT imaging for assessment.

References

1. Hansen H. Introduction. In: Hansen H, editor. Lung cancer therapy annual. 6th ed. London: Informa Health Care; 2009. p. 1–6.
2. Rengan R, Chetty IJ, Decker R, Langer CL, O'Meara WP, Movsas B. Lung cancer. In: Perez CA, Halperin EC, Brady LW, Wazer DE, editors. Perez & Brady's principles and practice of radiation oncology. 6th ed. Philadelphia: Wolters Kluwer - Lippincott, Wilkins & Williams; 2013.
3. Siegel RL, Miller KD, Jemal A. Cancer statistics, 2016. CA Cancer J Clin. 2016;66(1):7–30.
4. Anonymous A. Cancer of the lung and bronchus (invasive). In: Howlader N, Noone A, Krapcho M, et al., editors. SEER cancer statistics review, 1975-2014. Bethesda: National Cancer Institute; 2016.
5. Videtic GM, Stephans KL. The role of stereotactic body radiotherapy in the management of non-small cell lung cancer: an emerging standard for the medically inoperable patient? Curr Oncol Rep. 2010;12(4):235–41.
6. McGarry RC, Song G, des Rosiers P, Timmerman R. Observation-only management of early stage, medically inoperable lung cancer: poor outcome. Chest. 2002;121(4):1155–8.
7. Jensik RJ, Faber LP, Milloy FJ, Monson DO. Segmental resection for lung cancer. A fifteen-year experience. J Thorac Cardiovasc Surg. 1973;66(4):563–72.

8. Sibley GS. Radiotherapy for patients with medically inoperable stage I nonsmall cell lung carcinoma: smaller volumes and higher doses--a review. Cancer. 1998;82(3):433–8.
9. Dosoretz DE, Katin MJ, Blitzer PH, Rubenstein JH, Salenius S, Rashid M, et al. Radiation therapy in the management of medically inoperable carcinoma of the lung: results and implications for future treatment strategies. Int J Radiat Oncol Biol Phys. 1992;24(1):3–9.
10. Blomgren H, Lax I, Naslund I, Svanstrom R. Stereotactic high dose fraction radiation therapy of extracranial tumors using an accelerator. Clinical experience of the first thirty-one patients. Acta Oncol. 1995;34(6):861–70.
11. Timmerman R, Paulus R, Galvin J, Michalski J, Straube W, Bradley J, et al. Stereotactic body radiation therapy for inoperable early stage lung cancer. JAMA. 2010;303(11):1070–6.
12. RTOG 0236: a phase II trial of stereotactic body radiation therapy (SBRT) in the treatment of patients with medically inoperable stage I/II non-small cell lung cancer. http://www.rtog.org/ClinicalTrials/ProtocolTable/StudyDetails.aspx?study=0236. Updated 9 Sept 2009.
13. Folkert MR, Timmerman RD. Stereotactic ablative body radiosurgery (SABR) or stereotactic body radiation therapy (SBRT). Adv Drug Deliv Rev. 2017;109:3–14.
14. Uematsu M, Shioda A, Suda A, Fukui T, Ozeki Y, Hama Y, et al. Computed tomography-guided frameless stereotactic radiotherapy for stage I non-small cell lung cancer: a 5-year experience. Int J Radiat Oncol Biol Phys. 2001;51(3):666–70.
15. Timmerman R, Papiez L, McGarry R, Likes L, DesRosiers C, Frost S, et al. Extracranial stereotactic radioablation: results of a phase I study in medically inoperable stage I non-small cell lung cancer. Chest. 2003;124(5):1946–55.
16. McGarry RC, Papiez L, Williams M, Whitford T, Timmerman RD. Stereotactic body radiation therapy of early-stage non-small-cell lung carcinoma: phase I study. Int J Radiat Oncol Biol Phys. 2005;63(4):1010–5.
17. Timmerman R, McGarry R, Yiannoutsos C, Papiez L, Tudor K, DeLuca J, et al. Excessive toxicity when treating central tumors in a phase II study of stereotactic body radiation therapy for medically inoperable early-stage lung cancer. J Clin Oncol Off J Am Soc Clin Oncol. 2006;24(30):4833–9.
18. Zimmermann F, Wulf J, Lax I, Nagata Y, Timmerman RD, Stojkovski I, et al. Stereotactic body radiation therapy for early non-small cell lung cancer. Front Radiat Ther Oncol. 2010;42:94–9114.
19. Chang JY, Balter PA, Dong L, Yang Q, Liao Z, Jeter M, et al. Stereotactic body radiation therapy in centrally and superiorly located stage I or isolated recurrent non-small-cell lung cancer. Int J Radiat Oncol Biol Phys. 2008;72(4):967–71.
20. Videtic GM, Hu C, Singh AK, Chang JY, Parker W, Olivier KR, et al. A randomized phase 2 study comparing 2 stereotactic body radiation therapy schedules for medically inoperable patients with stage I peripheral non-small cell lung cancer: NRG oncology RTOG 0915 (NCCTG N0927). Int J Radiat Oncol Biol Phys. 2015;93(4):757–64.
21. Singh AK, Suescun JAG, Stephans KL, et al. A phase 2 randomized study of 2 stereotactic body radiation therapy regimens for medically inoperable patients with node-negative, peripheral non-small cell lung cancer. Int J Radiat Oncol Biol Phys. 2017;98(1):221–2.
22. Nagata Y, Takayama K, Matsuo Y, Norihisa Y, Mizowaki T, Sakamoto T, et al. Clinical outcomes of a phase I/II study of 48 Gy of stereotactic body radiotherapy in 4 fractions for primary lung cancer using a stereotactic body frame. Int J Radiat Oncol Biol Phys. 2005;63(5):1427–31.
23. Stephans KL, Djemil T, Reddy CA, Gajdos SM, Kolar M, Mason D, et al. A comparison of two stereotactic body radiation fractionation schedules for medically inoperable stage I non-small cell lung cancer: the Cleveland clinic experience. J Thorac Oncol. 2009;4(8):976–82.
24. Bradley J. Radiographic response and clinical toxicity following SBRT for stage I lung cancer. J Thorac Oncol. 2007;2(7 Suppl 3):S118–24.
25. Henderson MA, Hoopes DJ, Fletcher JW, Lin PF, Tann M, Yiannoutsos CT, et al. A pilot trial of serial 18F-fluorodeoxyglucose positron emission tomography in patients with medically inoperable stage I non-small-cell lung cancer treated with hypofractionated stereotactic body radiotherapy. Int J Radiat Oncol Biol Phys. 2010;76(3):789–95.
26. Ginsberg RJ, Rubinstein LV. Randomized trial of lobectomy versus limited resection for T1 N0 non-small cell lung cancer. Lung cancer study group. Ann Thorac Surg. 1995;60(3):615–22; discussion 622–3.
27. Fernando HC, Landreneau RJ, Mandrekar SJ, Nichols FC, Hillman SL, Heron DE, et al. Impact of brachytherapy on local recurrence rates after sublobar resection: results from ACOSOG Z4032 (alliance), a phase III randomized trial for high-risk operable non-small-cell lung cancer. J Clin Oncol Off J Am Soc Clin Oncol. 2014 Aug 10;32(23):2456–62.
28. Zheng X, Schipper M, Kidwell K, Lin J, Reddy R, Ren Y, et al. Survival outcome after stereotactic body radiation therapy and surgery for stage I non-small cell lung cancer: a meta-analysis. Int J Radiat Oncol Biol Phys. 2014 Nov 1;90(3):603–11.
29. Huang K, Palma DA, IASLC Advanced Radiation Technology Committee. Follow-up of patients after stereotactic radiation for lung cancer: a primer for the nonradiation oncologist. J Thorac Oncol. 2015;10(3):412–9.
30. Marwaha G, Stephans KL, Woody NM, Reddy CA, Videtic GM. Lung stereotactic body radiation therapy: regional nodal failure is not predicted by tumor size. J Thorac Oncol. 2014 Nov;9(11):1693–7.
31. van den Berg LL, Klinkenberg TJ, Groen HJ, Widder J. Patterns of recurrence and survival after surgery or stereotactic radiotherapy for early stage NSCLC. J Thorac Oncol. 2015;10(5):826–31.
32. Lee Y, Auh SL, Wang Y, Burnette B, Wang Y, Meng Y, et al. Therapeutic effects of ablative radiation on local tumor require CD8+ T cells: changing strategies for cancer treatment. Blood. 2009;114(3):589–95.
33. Grills IS, Mangona VS, Welsh R, Chmielewski G, McInerney E, Martin S, et al. Outcomes after stereotactic lung radiotherapy or wedge resection for stage I non-small-cell lung cancer. J Clin Oncol Off J Am Soc Clin Oncol. 2010;28(6):928–35.
34. Onishi H, Shirato H, Nagata Y, Hiraoka M, Fujino M, Gomi K, et al. Hypofractionated stereotactic radiotherapy (HypoFXSRT) for stage I non-small cell lung cancer: updated results of 257 patients in a japanese multi-institutional study. J Thorac Oncol. 2007;2(7 Suppl 3):S94–100.
35. Lagerwaard FJ, Haasbeek CJ, Smit EF, Slotman BJ, Senan S. Outcomes of risk-adapted fractionated stereotactic radiotherapy for stage I non-small-cell lung cancer. Int J Radiat Oncol Biol Phys. 2008;70(3):685–92.
36. Bradley JD, El Naqa I, Drzymala RE, Trovo M, Jones G, Denning MD. Stereotactic body radiation therapy for early-stage non-small-cell lung cancer: the pattern of failure is distant. Int J Radiat Oncol Biol Phys. 2010;77(4):1146–50.
37. Crabtree TD, Denlinger CE, Meyers BF, El Naqa I, Zoole J, Krupnick AS, et al. Stereotactic body radiation therapy versus surgical resection for stage I non-small cell lung cancer. J Thorac Cardiovasc Surg. 2010;140(2):377–86.
38. Louie AV, van Werkhoven E, Chen H, Smit EF, Paul MA, Widder J, et al. Patient reported outcomes following stereotactic ablative radiotherapy or surgery for stage IA non-small-cell lung cancer: results from the ROSEL multicenter randomized trial. Radiother Oncol. 2015;117(1):44–8.
39. Videtic GM, Chang JY, Chetty IJ, Ginsburg ME, Kestin LL, Kong FM, et al. ACR appropriateness criteria® early-stage non-small-cell lung cancer. Am J Clin Oncol. 2014;37(2):201–7.

40. Stephans KL, Djemil T, Reddy CA, Gajdos SM, Kolar M, Machuzak M, et al. Comprehensive analysis of pulmonary function test (PFT) changes after stereotactic body radiotherapy (SBRT) for stage I lung cancer in medically inoperable patients. J Thorac Oncol. 2009;4(7):838–44.
41. Stanic S, Paulus R, Timmerman RD, Michalski JM, Barriger RB, Bezjak A, et al. No clinically significant changes in pulmonary function following stereotactic body radiation therapy for early-stage peripheral non-small cell lung cancer: an analysis of RTOG 0236. Int J Radiat Oncol Biol Phys. 2014;88(5):1092–9.
42. Henderson M, McGarry R, Yiannoutsos C, Fakiris A, Hoopes D, Williams M, et al. Baseline pulmonary function as a predictor for survival and decline in pulmonary function over time in patients undergoing stereotactic body radiotherapy for the treatment of stage I non-small-cell lung cancer. Int J Radiat Oncol Biol Phys. 2008;72(2):404–9.
43. Fakiris AJ, McGarry RC, Yiannoutsos CT, Papiez L, Williams M, Henderson MA, et al. Stereotactic body radiation therapy for early-stage non-small-cell lung carcinoma: four-year results of a prospective phase II study. Int J Radiat Oncol Biol Phys. 2009;75(3):677–82.
44. Dunlap NE, Cai J, Biedermann GB, Yang W, Benedict SH, Sheng K, et al. Chest wall volume receiving >30 Gy predicts risk of severe pain and/or rib fracture after lung stereotactic body radiotherapy. Int J Radiat Oncol Biol Phys. 2010;76(3):796–801.
45. Woody NM, Videtic GM, Stephans KL, Djemil T, Kim Y, Xia P. Predicting chest wall pain from lung stereotactic body radiotherapy for different fractionation schemes. Int J Radiat Oncol Biol Phys. 2012;83(1):427–34.
46. McKenna RJ Jr, Mahtabifard A, Yap J, McKenna R 3rd, Fuller C, Merhadi A, et al. Wedge resection and brachytherapy for lung cancer in patients with poor pulmonary function. Ann Thorac Surg. 2008;85(2):S733–6.
47. Barriger R. Chest wall toxicities: prediction and management. In: Lo S, Mayr N, Teh B, Machtay M, editors. Stereotactic body radiotherapy: lung cancer. 1st ed. London: Future Medicine Ltd; 2013. p. 109–28.
48. Kawase T, Takeda A, Kunieda E, Kokubo M, Kamikubo Y, Ishibashi R, et al. Extrapulmonary soft-tissue fibrosis resulting from hypofractionated stereotactic body radiotherapy for pulmonary nodular lesions. Int J Radiat Oncol Biol Phys. 2009;74(2):349–54.
49. Hoppe BS, Laser B, Kowalski AV, Fontenla SC, Pena-Greenberg E, Yorke ED, et al. Acute skin toxicity following stereotactic body radiation therapy for stage I non-small-cell lung cancer: Who's at risk? Int J Radiat Oncol Biol Phys. 2008;72(5):1283–6.
50. Forquer JA, Fakiris AJ, Timmerman RD, Lo SS, Perkins SM, McGarry RC, et al. Brachial plexopathy from stereotactic body radiotherapy in early-stage NSCLC: dose-limiting toxicity in apical tumor sites. Radiother Oncol. 2009;93(3):408–13.
51. Stephans KL, Djemil T, Diaconu C, Reddy CA, Xia P, Woody NM, et al. Esophageal dose tolerance to hypofractionated stereotactic body radiation therapy: risk factors for late toxicity. Int J Radiat Oncol Biol Phys. 2014;90(1):197–202.
52. Corradetti MN, Haas AR, Rengan R. Central-airway necrosis after stereotactic body-radiation therapy. N Engl J Med. 2012;366(24):2327–9.
53. Fowler JF, Tome WA, Fenwick JD, Mehta MP. A challenge to traditional radiation oncology. Int J Radiat Oncol Biol Phys. 2004;60(4):1241–56.
54. Zeng J, Baik C, Bhatia S, Mayr N, Rengan R. Combination of stereotactic ablative body radiation with targeted therapies. Lancet Oncol. 2014;15(10):e426–34.
55. Brahmer JR, Tykodi SS, Chow LQ, Hwu WJ, Topalian SL, Hwu P, et al. Safety and activity of anti-PD-L1 antibody in patients with advanced cancer. N Engl J Med. 2012;366(26):2455–65.
56. Chang JY, Senan S, Paul MA, Mehran RJ, Louie AV, Balter P, et al. Stereotactic ablative radiotherapy versus lobectomy for operable stage I non-small-cell lung cancer: a pooled analysis of two randomised trials. Lancet Oncol. 2015;16(6):630–7.
57. Siva S, Ball D. Curing operable stage I non-small cell lung cancer with stereotactic ablative body radiotherapy: the force awakens. Oncologist. 2016;21(4):393–8.
58. Benedict SH, Yenice KM, Followill D, Galvin JM, Hinson W, Kavanagh B, et al. Stereotactic body radiation therapy: the report of AAPM task group 101. Med Phys. 2010;37(8):4078–101.
59. Timmerman RD, Park C, Kavanagh BD. The North American experience with stereotactic body radiation therapy in non-small cell lung cancer. J Thorac Oncol. 2007;2(7):101–12.

Stereotactic Body Radiation Therapy (SBRT) for Lung Metastases

William A. Stokes, Tyler P. Robin, Sameer K. Nath, and Chad G. Rusthoven

Introduction

In recent years, there has been growing interest in the role of local therapies, including surgery and radiation, for patients with limited metastatic foci, termed *oligometastases*, as a strategy to improve progression-free survival (PFS), to extend the duration of benefit from well-tolerated systemic therapies, and to hopefully prolong life. The lungs are one of the most common sites of metastatic spread, and ablation of pulmonary oligometastases is now increasingly being considered in the setting of favorable prognostic features, including young age, good performance status, indolent tumor biology, and targetable driver mutations [1]. Stereotactic body radiotherapy (SBRT) is an established, noninvasive treatment strategy for well-circumscribed lung tumors in the setting of early-stage non-small cell lung cancer (NSCLC) [2, 3]. A growing body of literature now indicates that SBRT for lung metastases is also a safe, well-tolerated intervention that has been associated with high rates of local tumor control. Herein, we review the published experience with SBRT for lung metastases, discuss the potential toxicities and strategies to mitigate them, outline the elements of patient selection and treatment planning, and describe practical considerations to guide providers.

W. A. Stokes · S. K. Nath · C. G. Rusthoven (✉)
Department of Radiation Oncology, University of Colorado School of Medicine, Aurora, CO, USA
e-mail: chad.rusthoven@ucdenver.edu

T. P. Robin
Department of Radiation Oncology, University of Colorado Cancer Center, Aurora, CO, USA

Site-Specific Considerations

The delivery of SBRT for lung metastases requires several unique considerations, including patient and tumor motion, tumor size, tumor location within the lung, baseline pulmonary function, and history of prior thoracic surgery and/or radiation. Effective delivery of lung SBRT requires a comprehensive approach accounting for each of these factors. While an assessment of risks and benefits is essential to any management discussion, in considering SBRT for metastatic disease the onus of minimizing risk is often magnified as the benefits of oligometastatic ablation with SBRT in this setting are only beginning to be defined. For instance, in the curative setting of an early-stage medically inoperable primary lung cancer, it may be reasonable to accept radiation doses in the upper limits of normal tissue constraints to obtain adequate PTV coverage. However, an identical plan for a lesion in a patient with metastatic disease may be less justifiable. Therefore, treatment decisions are often more nuanced when considering SBRT for patients with metastatic disease. Where relevant, we will highlight additional considerations specific to metastatic disease in our discussion of lung SBRT.

Immobilization of the external patient anatomy must be considered first, as stable and reproducible patient positioning is critical. This can be accomplished by multiple methods with some acceptable variation in setup practices between institutions [4, 5]. As a basic guide, the arms should be positioned overhead if tolerable for the patient (to allow for uninterrupted arcs in the case of VMAT and to provide additional beam angle choices for static IMRT), and a vacuum-type or synthetic body immobilization mold can be applied. As with other SBRT target sites, such as liver, management of internal tumor motion is paramount to safe and effective treatment. Lung tumor motion during free breathing has been reported to be greatest in the cranial-caudal dimension and on average between about 7 and 14 mm with maximum motion reported to be over 20 mm in some patients [6–10]. The AAPM Task Group report 76 recommends the use of

D. M. Trifiletti et al. (eds.), *Stereotactic Radiosurgery and Stereotactic Body Radiation Therapy*,
https://doi.org/10.1007/978-3-030-16924-4_22

motion management strategies if tumor motion exceeds 5 mm [11]. We recommend four-dimensional computed tomography (4DCT) simulation to assess target motion in the setting of lung SBRT. There are multiple strategies for motion management during the delivery of lung SBRT, the most common being motion dampening via abdominal compression, respiratory gating, breath hold techniques, and real-time tumor tracking [11, 12]. A detailed technical discussion of motion management techniques is beyond the scope of this chapter and has been thoroughly reviewed elsewhere. We recommend referring to reports of the AAPM Task Group 76 and 101 [11, 12].

Tumor size is an important consideration, and available prospective trials of lung SBRT for metastatic tumors have implemented size constraints. For example, Rusthoven and colleagues enrolled patients with one to three lung metastases with a cumulative diameter smaller than 7 cm, and patients were treated with doses ranging from 48 and 60 Gy in three fractions, without significant toxicities [13]. The median tumor volume of metastatic lesions on this trial was 4.2 cc, corresponding to a spherical diameter of 2.0 cm. US cooperative group studies in primary early-stage non-small cell lung cancer (NSCLC) have used an eligibility cutoff for a single lesion of 5 cm [14], although the original phase II trial from Indiana University included tumors up to 7 cm in diameter [15]. Timmerman and colleagues have also reported that patients with a GTV greater than 10 cc (corresponding to spherical diameter of 2.7 cm) had an eight-fold increased risk of high-grade toxicity [15]. However, other studies have shown acceptable toxicity profiles with SBRT for larger tumors. The aforementioned study by Rusthoven and colleagues included 18 (28.6%) patients with tumor volumes ≥10 cc and reported very low rates of high-grade toxicity [13]. Investigators from the Cleveland Clinic performed a dedicated analysis of SBRT for tumors >5 cm and reported excellent local control with limited high-grade toxicity (grade ≥3 toxicity in 7.5% of patients) [16]. Similarly, in a multi-institutional analysis of 92 patients with primary NSCLC tumors 5 cm or greater treated with SBRT, the toxicity was also considered acceptable with grade ≥3 radiation pneumonitis developing in only 5.4% of patients (although there was one reported event of grade 5 radiation pneumonitis in a patient with a 7.5-cm tumor and 150 pack-year smoking history) [17]. Overall, there does not appear to be a firm size cutoff for SBRT; however, in an effort to minimize the risk of toxicity, more protracted schedules with lower doses per fraction are reasonable to consider with increasing tumor size, particularly in the setting of metastatic disease.

Tumor location requires careful consideration when planning SBRT. Timmerman and colleagues showed in their prospective institutional primary NSCLC SBRT trial that pericentral/hilar tumor location was associated with a significant increase in high-grade toxicity compared with peripheral tumors ($p = 0.004$), and only 54% of patients with pericentral/hilar tumors receiving 60–66 Gy in 3 fractions were free of severe toxicity at 2 years [15]. In response to this reported toxicity, subsequent trials and guideline statements have discouraged high-dose 3-fraction SBRT regimens for central tumors (often defined as within 2 cm of the proximal bronchial tree, although varying definitions have been proposed [Fig. 1a, b]) in favor of more protracted SBRT regimens with lower doses per fraction [3, 18]. RTOG 0813 is investigating SBRT dosing for central tumors in five-fraction regimens in a dose-escalation prospective fashion. In addition to 5-fraction regimens, series have demonstrated acceptable toxicity with 8-fraction regimens for central lung tumors [19] and even more protracted hypofractionated courses in the range of 10–15 fractions, which may also be considered depending on toxicity risk assessment [3, 18, 20, 21]. However, the heterogeneity of tumor location and the retrospective nature of these studies limit their broad generalizability. Overall, in the setting of central lung tumors, the level of acceptable risk may be significantly different between curative-intent SBRT for early-stage NSCLC and ablation of a metastatic lesion. With the current state of evidence, we recommend a careful assessment of the risks and benefits of SBRT for centrally located metastases, and, in our practice, we often favor less aggressive, more protracted hypofractionated radiation regimens (e.g., 8–15 fractions depending on the scenario) with lower doses per fraction to minimize the risk of significant toxicities in the metastatic setting.

Additional clinical factors including prior lung surgery or radiation, pulmonary function, and underlying lung disease are relevant to the evaluation of any patient for lung SBRT and are particularly important when considering SBRT for metastatic disease. To assess baseline pulmonary function, pretreatment pulmonary function testing (PFT) and functional lung imaging may be helpful in some cases. Underlying interstitial lung disease has been associated with high-grade pulmonary complications after SBRT [22], suggesting that substantial caution should be exercised when considering SBRT for metastatic disease in these patients. Further, in contrast to the typical early-stage NSCLC patient, patients with metastatic disease frequently present with more than one lung tumor for potential ablation. The decision to offer SBRT to multiple lung tumors must be made carefully in the context of the overall oncologic picture as well as a patient's baseline lung function; pretreatment PFT assessment may have an increased value in this setting. Of note, the aforementioned prospective phase I/II study of SBRT for lung metastases from the University of Colorado allowed patients with multiple lung metastases as long as the cumulative tumor diameter was less than 7 cm. Twenty five of 38 patients

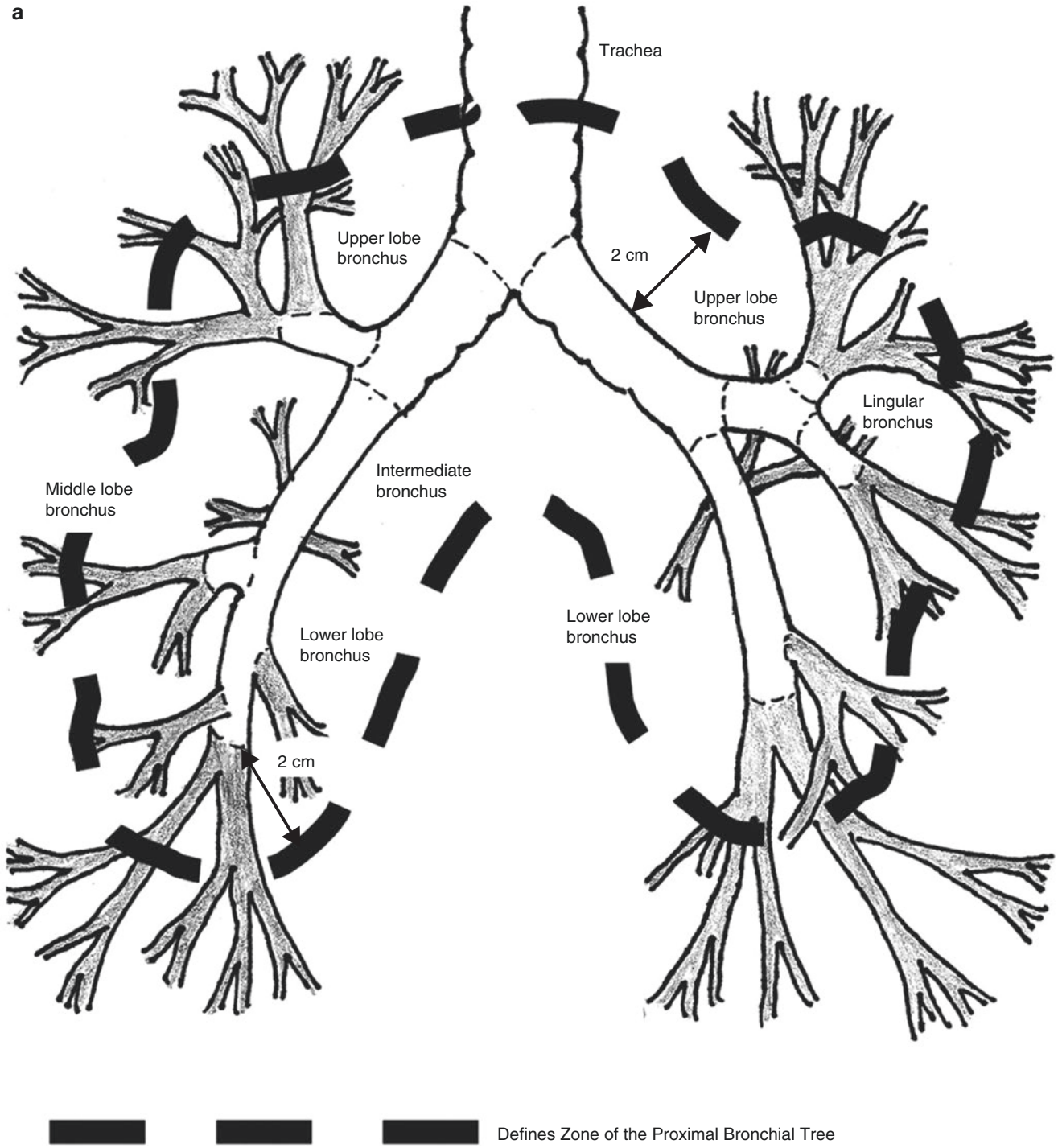

Fig. 1 Illustrative representations of the "central lung" for consideration when planning lung SBRT. Importantly, the definition of the "central lung" can vary in the literature. As depicted by Timmerman and coauthors in their article in 2006 in *J Clin Oncol* (**a**), the central lung is defined based on the proximal bronchial tree, compared with the definition used by Chang and colleagues in their article in 2015 in *J Thorac Oncol* (**b**), which, in addition to the proximal bronchial tree, specifically recommends inclusion of critical mediastinal structures, including the esophagus, heart, major vessels, spinal cord, phrenic nerve, and recurrent laryngeal nerve. (**a**: Used with permission of the American Society of Clinical Oncology from Timmerman et al. [15]. **b**: Used with permission of Elsevier from Chang et al. [94])

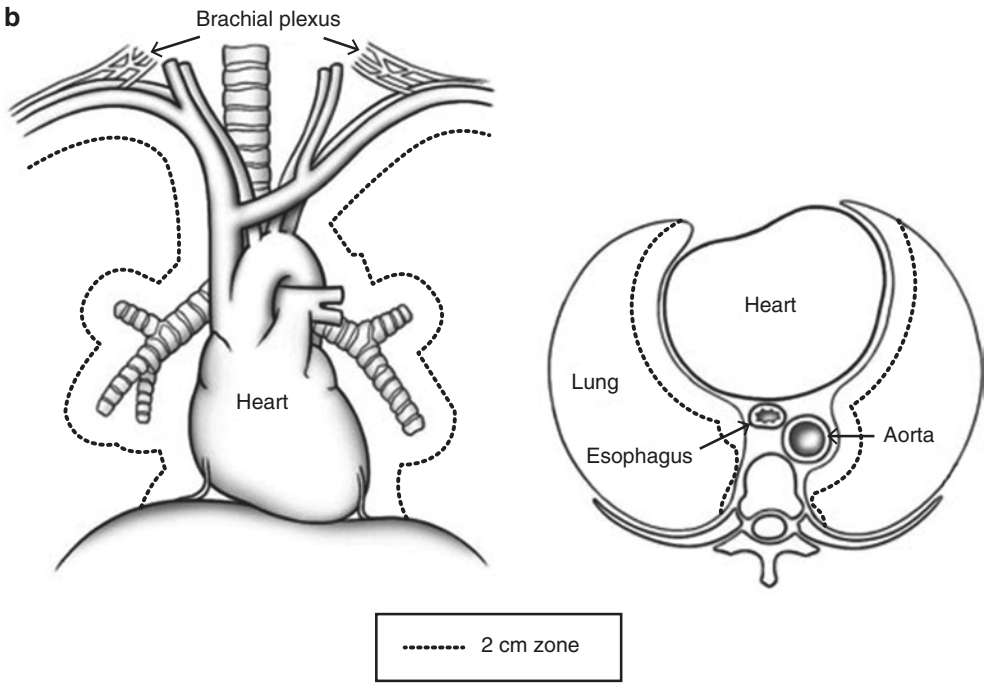

Fig. 1 (continued)

were in fact treated to more than one lung metastasis, with only 1 of 38 patients developing symptomatic radiation pneumonitis [13]. A V15 <35% was used as the lung constraint in the study [13].

For patients with metastatic disease, it is also vital to have a comprehensive understanding of past, current, and planned systemic therapy when considering SBRT to lung metastases. There are generally limited safety data to guide SBRT sequencing in the rapidly evolving landscape of new systemic therapy options, and a number of practical questions often arise: Is it acceptable to continue a systemic therapy concurrently with SBRT? If not, how long should systemic therapy be held? Should these interruptions differ between cytotoxic chemotherapy, targeted agents, and immune checkpoint inhibitors?

Several studies have explored the use of SBRT with targeted agents. In particular, a multicenter phase II trial from the University of Texas Southwestern and the University of Colorado explored the role of SBRT in patients with EGFR-mutated metastatic NSCLC with progression in limited sites. In all, 24 patients with 52 progressing metastatic sites (18 lung, 13 mediastinum/hilum, 21 other) were treated with SBRT and concurrent erlotinib. Toxicities included one grade 5 event possibly related to SBRT (acute respiratory distress syndrome/pneumonia 3 months after SBRT to three sites—parenchymal lung lesion, right scapular lesion, anterior chest wall lesion), one grade 4 event possibly related to SBRT, and two grade 3 events definitely related to SBRT [23]. This small prospective trial provides some of the highest quality evidence to date supporting the safety and efficacy if combining concurrent erlotinib with SBRT for lung metastases, but it cannot exclude the potential for increased synergistic toxicities with SBRT and other existing or emerging tyrosine kinase inhibitors (TKIs). NRG BR001, a phase I study of SBRT for patients with oligometastatic (≤4 metastases) breast cancer, prostate cancer, and NSCLC, allows erlotinib and afatinib to be continued concurrently with SBRT in the NSCLC cohort and hormone therapy to be continued concurrently with ablative therapies in the prostate and breast groups. However, this trial mandates that SBRT starts at least 2 weeks after cytotoxic chemotherapy that is delivered on 14- to 28-day cycles and at least 1 week after chemotherapy that is delivered on weekly cycles; chemotherapy cannot be resumed until 14 days after completion of SBRT. The Eastern Cooperative Oncology Group (ECOG) has issued guidelines for combining BRAF inhibitors with radiation therapy for patients with metastatic melanoma [24]. They recommend holding BRAF inhibitors at least 1 day before and 1 day after SRS and at least 3 days before and after fractionated radiation [24]. In general, we recommend delivering SBRT in between cycles of cytotoxic chemotherapy, with at least 1 week on either side of SBRT wherever possible. We typically recommend holding targeted therapies on the day of SBRT and for a few days before and after SBRT delivery, and often we recommend longer periods for newer agents for which there is less experience.

Immune checkpoint inhibitors bring about a complex discussion regarding the timing to radiotherapy, as the potential for synergy with SBRT may lead to improved responses both inside and outside of the target field [25]. At present, the optimal timing and sequencing remains to be determined, and there is a paucity of data supporting the safety or efficacy of any specific sequencing over another. Notably, the PACIFIC trial, which randomized patients with locally advanced NSCLC after thoracic chemoradiation (via conventionally fractionated radiotherapy) to maintenance anti-PD-L1 therapy (initiated within 1–42 days after chemoradiation) or placebo, demonstrated not only a large improvement in progression-free survival in the anti-PD-L1 arm but also a relatively modest increase in grade 3–4 pneumonitis or radiation pneumonitis, from 2.6% in the placebo arm to 3.4% in the anti-PD-L1 arm. These data provide prospective evidence that immune checkpoint inhibitors can be initiated in close temporal proximity to conventional radiotherapy. Further prospective data on the safety of combining SBRT and immunotherapy are needed, and numerous trials have been launched which will hopefully address these questions in the coming years.

Clinical Evidence

Prospective Trials

A number of prospective trials have investigated the use of SBRT in treating lung metastases, summarized in Table 1. These trials have generally enrolled patients irrespective of primary histology and feature a variety of fractionation schedules.

Onimaru and colleagues [26] conducted a prospective study of hypofractionated radiotherapy in 46 patients with either primary or metastatic lung cancers. Twenty patients with 32 metastases received 60 Gy in 8 fractions to small peripheral lesions and 48 Gy in 8 fractions to larger or central lesions. At a median follow-up of 18 months, two of these patients experienced local failure, both in the lower-dose group, translating to a crude local control (LC) rate of 94%. One patient developed grade 5 esophageal ulceration, leading to termination of the trial. Among metastatic patients, overall survival 2 years following SBRT (OS2) was 49%.

Subsequently, Okunieff and colleagues [27] published a prospective study of SBRT for lung metastases at the University of Rochester. Enrolled subjects were stratified into a "curative" group of 30 patients, each of whom had thoracic-only metastases and/or no more than 5 total lesions and a "palliative" group of 19 patients not meeting those criteria but for whom their thoracic disease was deemed life-limiting. Both groups typically received 50 Gy in ten fractions to no more than five lung metastases. The radiation dose was prescribed to the 100% isodose line, requiring that the 80% isodose line (i.e., 40 Gy in a 50 Gy prescription) cover the PTV. Local control was excellent, with 91% of all lesions controlled at 3 years. In the favorable group of "curative" patients, median progression-free survival (PFS) was 5.8 months and the 2-year PFS rate was only 16%. Most had disease progression elsewhere, with 12 (40%) experiencing regional failure, defined as a new lesion within the thorax but outside the high-dose field, and 7 (23%) developing distant failure. "Curative" patients experienced an OS2 of 38%. Among the group of 20 patients who were progression free at 15 months postradiation, subsequent disease recurrence events were rare. No grade 4 or 5 toxicities were noted.

A phase I trial at Stanford [28] followed a dose-escalation strategy for single-fraction SBRT for lung tumors and enrolled 20 patients with early-stage NSCLC and 12 patients with solitary lung metastases. Patients were treated by Cyberknife in sequential cohorts of 15 Gy, 25 Gy, and 30 Gy. Among patients with metastases, 3 were treated at the 15 Gy level, of whom 1 (33%) failed locally and 2 (67%) experienced nodal or distant failure, and 9 were treated at the 25 Gy level, of whom 4 (44%) failed locally and 7 (77%) experienced nodal or distant failure. One-year rates of freedom from relapse and overall survival were 25% and 56%, respectively. Among the 32 patients enrolled, the authors reported 8 late toxicity events, each occurring at the 25 or 30 Gy level, including 5 grade 2–3 events and 3 grade 5 events.

Rusthoven and colleagues [13] conducted a multi-institutional phase I/II trial dedicated to patients with 1–3

Table 1 Outcomes of prospective trials dedicated to SBRT to lung lesions

Study	Patients (lesions)	Tumor characteristics	Dose/fractions	Local control	Survival
Onimaru 2003 [26]	20 (32)	Mixed histologies	48–60/8	94% crude	49% at 2 years
Okunieff 2006 [27]	49 (125) 30 "curative"	Mixed histologies, "curative" subset with ≤5 lung metastases	50/10 preferred	91% at 2 years 91% at 3 years	38% at 2 years 25% at 3 years ("curative" intent)
Le 2006 [28]	12 (12)	Mixed histologies, solitary lung metastasis	15–25/1	25% at 1 year	56% at 1 year
Rusthoven 2009 [13]	38 (63)	Mixed histologies, ≤3 lung metastases	48–60/3	96% at 2 years	39% at 2 years
Nuyttens 2015 [29]	30 (57)	Mixed histologies, ≤5 total metastases	30–60/1–7	79% at 1 year	63% at 2 years 38% at 4 years

lung metastases. Sixty-three lesions in 38 patients were treated to 48–60 Gy in three fractions. SBRT was well-tolerated, with three patients developing grade 3 toxicity, and none experiencing grade 4–5 events. Among 50 assessable lesions at a median follow-up of 15 months, a single local failure occurred at 13 months posttreatment, translating to a LC2 of 96%. However, 24 patients (63%) experienced distant progression at a median of 4 months posttreatment, and OS2 was 39%.

Nuyttens and colleagues [29] reported the results of a phase II study of Dutch patients with lung metastases from a controlled primary tumor, 5 or fewer metastases involving 2 or fewer organs, and no plan for surgery or chemotherapy. Fifty-seven tumors in 30 patients were treated by Cyberknife in a location- and size-dependent fashion with 23 smaller (≤3 cm) peripheral lesions receiving 30 Gy in 1 fraction, 23 larger peripheral lesions receiving 60 Gy in 3 fractions, 4 central tumors receiving 60 Gy in 5 fractions, and 7 ultracentral tumors receiving 56 Gy in 7 fractions. At a median follow-up of 36 months, seven patients experienced ten local failures, mostly within the first year, leading to a 1-year local control rate of 79%. Local control appeared to be superior with more protracted SBRT fraction schedules, with seven failures occurring in the 1-fraction group, two failures in the 3-fraction group, and one failure in the 5–7-fraction group. These patients tolerated SBRT well, with five patients experiencing acute grade 3 toxicity and three patients experiencing chronic grade 3 toxicity. In this selected group of patients, OS2 was comparatively high at 63%.

In contrast to the aforementioned five trials, which focused on SBRT to lung lesions exclusively, some trials have investigated SBRT to multiple metastatic sites. They report disease control outcomes for all sites together and are reported in Table 2 and summarized below.

In a follow-up to the earlier publication of the University of Rochester trial, Milano and colleagues [30] elaborated on 121 patients with five or fewer metastases, of whom 50 had lung lesions. Patients generally received 50 Gy in 10 fractions (again prescribed to the 100% isodose line, requiring that the 80% isodose line [i.e., 40 Gy in a 50 Gy Rx] cover the PTV [31]) to extracranial lesions. Outcomes in the overall group of patients treated to multiple sites were encouraging; the LC2 among all patients was 87%, and this rate was maintained 6 years post-SBRT. Rates of freedom from widespread metastasis were 52% at 2 years and 36% at 6 years. OS2 was also encouraging at 74%, while the corresponding 6-year rate was 47%.

A dose-escalation study of patients undergoing SBRT to extracranial oligometastases was conducted by Salama and coauthors [32]. Sixty-one patients, each with five or fewer metastases, were treated with three fractions on a schedule that started at 24 Gy total and reached 48 Gy. Of the 113 lesions treated, 41 (36%) involved the lung, with most receiving 36–42 Gy. SBRT was well tolerated, with one of these patients experienced an acute grade 3 toxicity attributed to therapy and two experiencing late grade 3 events. No grade 4 or 5 events were attributed to SBRT. LC2 for all treated lesions was 53%, lower than other prospective studies but potentially a result of the lower cumulative doses studied in this protocol.

Two recent randomized trials dedicated to metastatic NSCLC have evaluated the impact of consolidative therapy to oligometastases following response to systemic therapy and warrant mentioning. First, Gomez and coauthors [33] randomized patients with three or fewer oligometastases from NSCLC after first-line systemic therapy to either local consolidative therapy to all lesions (including SBRT, more protracted RT schedules, or surgery) or maintenance treatment. Consolidation therapy dramatically prolonged progression-free survival to a median 11.9 months from the median 3.9 months observed with maintenance. Consolidative therapy was also associated with a prolongation in time to appearance of new metastatic sites, suggesting that tumor ablation altered the natural history of disease (Fig. 2a, b). However, for the purposes of this chapter, it should be noted that only a minority of enrolled patients had lung metastases. Of the 49 randomized patients, there were 9 lung metastases among 6 patients, with 6 lesions in 4 patients undergoing consolidation, and 3 lesions in 2 patients receiving maintenance therapy. Five of the six consolidated lesions were treated with SBRT, all 50 Gy in four fractions, with the final lesion managed surgically.

Table 2 Outcomes of prospective trials featuring SBRT to multiple metastatic sites including lung; local control and survival reflect all patients enrolled

Study	Patients (lesions)	Tumor characteristics	Dose/fractions	Local control	Survival
Milano 2012 [30]	50	Mixed histologies, ≤5 total metastases	50/10 preferred	87% at 2 years 87% at 6 years	74% at 2 years 47% at 6 years
Salama 2012 [32]	31 (44)	Mixed histologies, ≤5 total metastases	24–48/3	53% at 2 years	57% at 2 years
Gomez 2016 [33]	3 (5)	NSCLC, ≤3 total metastases	50/4		Median not reached
Iyengar 2017 [34]	13 (16)	NSCLC, ≤5 total metastases	20–21/1 most common	100% crude	Median not reached

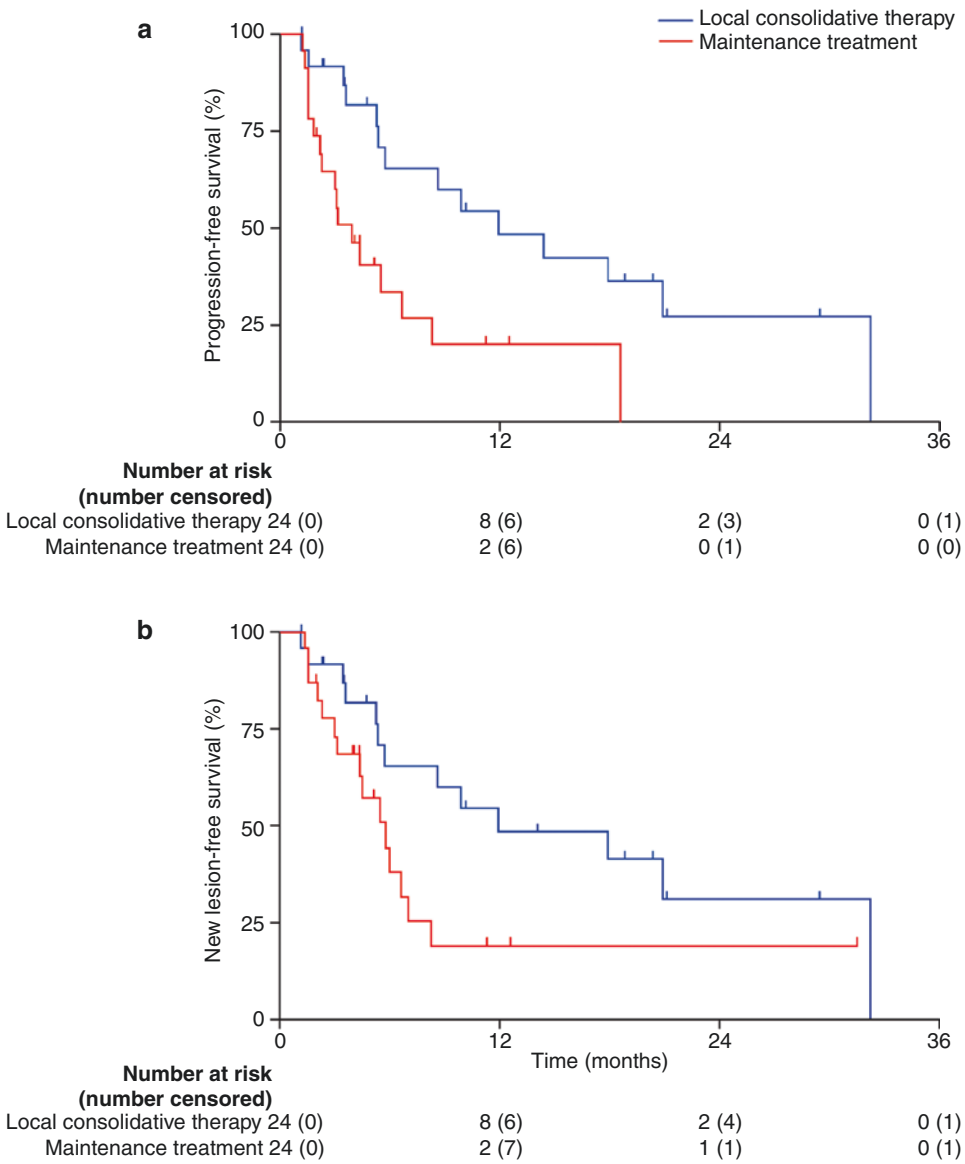

Fig. 2 Kaplan-Meier curves comparing outcomes between patients receiving local consolidative therapy (*blue*) versus maintenance alone (*red*). (**a**) Progression-free survival. (**b**) Freedom from new lesions. Both outcomes were significantly improved with local consolidative therapy. (**a** and **b**: Used with permission of Elsevier from Gomez et al. [33])

A similar randomized trial conducted by Iyengar and coauthors [34] at UT Southwestern enrolled patients with five or fewer oligometastases from NSCLC and employed a comparable design, although the consolidation arm in this trial received radiotherapy exclusively (SBRT to all metastases; hypofractionated radiotherapy was permitted for the primary lesion). Among 29 patients enrolled, 14 were randomized to consolidation and underwent radiotherapy (typically 20–21 Gy in 1 fraction) to 31 lesions, of which 16 involved lung parenchyma. Thus, compared to the Gomez and coauthors trial, the UT Southwestern trial was comparatively enriched for SBRT to lung metastases. No local failures were reported in the consolidation arm, as compared to 7 "in-field" failures among the 15 patients in the no-consolidation arm. Similar to the trial by Gomez and coauthors, patients in the consolidation arm of the UT Southwestern trial had significantly prolonged PFS (9.7 vs 2.5 months) and experienced fewer distant progression events.

Taken together, the body of prospective trials involving SBRT for lung metastases characterizes a low incidence of severe toxicity and impressive rates of local control, generally exceeding 80–90% for multifraction schedules. The randomized phase II trials reported by Gomez and coauthors and Iyengar and coauthors, in particular, suggest that oligometastatic ablation with SBRT may alter the natural history of metastatic disease and improve long-term oncologic outcomes; however, larger phase III trials powered for OS evaluating oligometastatic ablation are needed to fully evaluate this question.

Retrospective Studies

Multiple retrospective studies have reported outcomes following SBRT for lung metastases and are summarized in Table 3. Importantly, these have featured a variety of doses and fractionation schedules, included patients with varying histologies and burdens of lung metastases, and reported a variety of disease control and survival outcomes. In the interest of illustrating general trends across these studies, we have attempted to depict the most commonly reported local control and survival outcomes. Where available, we reported actuarial rates of local control at 2 and/or 3 years

Table 3 Outcomes of retrospective series of SBRT for lung metastases

Study	Patients (lesions)	Tumor characteristics	Dose/fractions	Local control	Survival
Blomgren 1995	6 (6)	Mixed histologies	26–64/1–3		
Uematsu 1998	(43)	Mixed histologies	33–76/5–13	98% crude	
Nakagawa 2000	14 (21)	Mixed histologies	15–25/1	95% crude	
Nagata 2002	9 (9)	Mixed histologies, ≤2 lung metastases	40–48/4	67% crude	
Hara 2002	11 (15)	Mixed histologies	20–30/1	73% crude	
Lee 2003	19 (26)	Mixed histologies	30–40/3–4	88% crude	88% crude
Wulf 2004	41 (51)	Mixed histologies	37.5–48/1–3	72% at 2 years	33% at 2 years
Song 2005	12 (19)	Mixed histologies, ≤3 lung metastases	24–45/3	89% crude	
Fritz 2006	25 (31)	Mixed histologies, ≤2 lung metastases	30/1	83% at 4 years	73% at 2 years 42% at 4 years
Yoon 2006	53	Mixed histologies, ≤3 lung metastases	30–48/3–4	~80% at 2 years	
Aoki 2007	8	Mixed histologies, ≤3 lung metastases	54/9	100% crude	88% at 2 years
Hof 2007	61 (71)	Mixed histologies	12–30/1	74% at 2 years 63% at 3 years	65% at 2 years 48% at 3 years
Brown 2008	35 (69)	Mixed histologies	5–60/1–4	71% crude	
Norihisa 2008	34 (43)	Mixed histologies, ≤2 lung metastases	48–60/4–5	90% at 2 years	84% at 2 years
Salazar 2008	7 (8)	Mixed histologies	40/4	86% crude	29% at 2 years 23% at 3 years
Hamamoto 2009	10 (12)	Mixed histologies, ≤3 lung metastases	48/4	25% at 2 years	86% at 2 years
Kim 2009	13 (18)	Colorectal, ≤3 lung metastases	39–51/3	53% at 2 years 53% at 3 years	76% at 2 years 65% at 3 years
Inoue 2010	16 (22)	Mixed histologies, ≤5 total metastases	35–60/4		63% at 3 years 63% at 5 years
Takeda 2011	34 (44)	Mixed histologies	50/5	82% at 2 years	
Zhang 2011	71 (172)	Mixed histologies	30–60/2–12	75% at 3 years 75% at 5 years	41% at 3 years 25% at 5 years
Ricardi 2012	61 (77)	Mixed histologies	26–45/1–3	89% at 2 years	67% at 2 years
Oh 2012	57 (67)	Mixed histologies, ≤4 lung metastases	50–60/4–5	95% at 3 years	60% at 2 years 56% at 5 years
Dhakal 2012	14 (74)	Sarcoma	50/5 preferred	88% at 2 years 82% at 3 years	
Baschnagel 2013	32 (47)	Mixed histologies, ≤3 lung metastases	48–65/4–10 Median 60/4	92% at 2 years 85% at 3 years	76% at 2 years 63% at 2 years
Inoue 2013	87 (189)	Mixed histologies		80% at 2 years 80% at 2 years	47% at 2 years 32% at 3 years
Widder 2013	42	Mixed histologies, ≤5 lung metastases	60/3–8	85% at 3 years	60% at 3 years 49% at 5 years
Mehta 2013	16 (25)	Sarcoma	36–54/3–4	94% at 3 years	72% at 4 years
Davis 2013	64 (66)	Mixed histologies, central	16–60/1–5	70% at 2 years	50% at 2 years
Osti 2013	66 (103)	Mixed histologies, ≤5 lung metastases	23–30/1	82% at 2 years	31% at 2 years

Table 3 (continued)

Study	Patients (lesions)	Tumor characteristics	Dose/fractions	Local control	Survival
Singh 2014	34 (63)	Mixed histologies, ≤5 lung metastases	40–60/5	88% at 2 years 80% at 3 years	44% at 2 years 23% at 3 years
Filippi 2014	67 (90)	Mixed histologies, ≤3 lung metastases	26/1	88% at 2 years	71% at 2 years
Navarria 2014	76 (118)	Mixed histologies, ≤5 total metastases	48–60/3–8	89% at 2 years 89% at 3 years	73% at 2 years 73% at 3 years
Comito 2014	41 (60)	Colorectal, ≤3 lung metastases	48–60/3–4	75% at 2 years 70% at 3 years	68% at 2 years 58% at 3 years
Filippi 2014	40 (59)	Colorectal, ≤5 lung metastases	26–60/1–8	92.5% crude	73% at 2 years 39% at 5 years
Wang 2014	95 (134)	Mixed histologies, ≤4 lung metastases	30–60/1–5	91% at 2 years 87% at 3 years	61% at 2 years 56% at 3 years
Ahmed 2015	9 (12)	Colorectal	60/5	100% at 2 years	89% at 2 years
Binkley 2015	77 (122)	Mixed histologies		84% at 2 years	75% at 2 years
Carvajal 2015	13	Colorectal, solitary metastasis	34–60/1–8	92% at 2 years	92% at 2 years
Siva 2015	41 (49) 24 (33)	Mixed histologies, ≤3 lung metastases	18–26/1 48–50/4–5	90% at 2 years 92% at 2 years	71% at 2 years
García-Cabezas 2015	44 (53)	Mixed histologies, ≤5 lung metastases	50–60/5–10	87% at 2 years	60% at 2 years
Jung 2015	50 (79)	Colorectal	40–60/3–4	71% at 3 years	64% at 3 years
Qiu 2015	65	Colorectal	50/5–10	31% at 2 years	43% at 2 years
Frakulli 2015	24 (68)	Sarcoma	30–60/3–8	86% at 2 years	66% at 2 years
Guckenberger 2015	397 (525)	Mixed histologies	Median 37.5/3	87% at 16 months	
Navarria 2015	28 (51)	Sarcoma, ≤4 lung metastases	30–60/1–8	96% at 2 years 96% at 5 years	85% at 2 years 54% at 5 years
Tanadini-Lang 2016	670 92 145	Mixed histologies			24% at 5 years 32% at 5 years 38% at 5 years
Janssen 2016	46	Mixed histologies, ≤3 lung metastases	36–60/3–15		56% at 2 years
Kinj 2016	53 (87)	Colorectal	25–60/1–5 Median 60/3	78% at 2 years	69% at 2 years 58% at 5 years
Lischalk 2016	20	Mixed histologies, ultracentral	35–40/5	57% at 2 years	40% at 2 years
Yamashita 2016	96	Mixed histologies		74% at 3 years	53% at 3 years
Aoki 2016	66 (76)	Mixed histologies, ≤3 lung metastases	45–60/5–9	91% at 3 years	76% at 3 years
Rieber 2016	700	Mixed histologies	Median 37.5/3	81% at 2 years	54% at 2 years
Agolli 2016	44 (69)	Colorectal, ≤4 lung metastases	23–45/1–3	60% at 2 years 54% at 3 years	68% at 2 years 51% at 3 years
Jang 2016	72 (85)	Mixed histologies	45–60/4–5	98% at 2 years	72% at 2 years
De Rose 2016	60 (90)	NSCLC, ≤4 lung metastases	48–60/3–8	89% at 2 years 45% at 3 years	75% at 2 years 64% at 3 years 22% at 5 years
Filippi 2016	28 (43)	Colorectal, ≤5 lung metastases	26–60/1–8		77% at 2 years
Baumann 2016	30 (39)	Sarcoma	24–50/4–5	86% at 2 years	43% at 2 years
Helou 2017	120 (180)	Mixed histologies	48–60/4–5	85% at 2 years	
Janvary 2017	26 (39)	Mixed histologies	40–60/3–5	59% at 2 years 53% at 3 years	
Franceschini 2017	200	Radioresistant histologies, ≤3 total metastases	30–60/1–8	85% at 2 years 82% at 3 years	65% at 2 years 55% at 3 years
Soyfer 2017	22 (53)	Sarcoma, ≤6 lung metastases	24–60/3–4	100% crude	50% at 5 years
Ricco 2017	447	Mixed histologies	8–60/1–8	59% at 3 years 46% at 5 years	33% at 2 years 22% at 5 years

and of OS at 2, 3, and/or 5 years post-SBRT. When these endpoints were not provided in the studies, we reported the most comparable reported outcome. Despite the disparate populations, treatment regimens, and outcomes among these studies, some general themes are worth noting.

First, some investigators have focused on histologies that are traditionally considered radioresistant, including colorectal adenocarcinoma (CRCa) and soft-tissue sarcoma (STS). Series depicting outcomes of SBRT for CRCa lung metastases [35–42] report a wide range of 2-year local control (LC2) rates, ranging from 31% to 100%, with most larger series reporting rates of less than 75%. Comparative series from Stanford [43] and Sunnybrook [44] stratifying by CRCa vs other histologies reported lower LC2 rates following SBRT for CRCa (58% and 76%, respectively) versus non-CRCa histologies (90% and 92%, respectively), with differences that remain significant after multivariate adjustment and suggest that dose escalation in this histology may prove useful. In contrast, series dedicated to STS [45–50], ranging from 14 to 30 patients receiving SBRT to 25–74 lesions, have reported rates of LC2 exceeding 85%. These rates appear roughly comparable to those for histologies traditionally considered to be more radiosensitive. One of the largest series of radioresistant histologies by Franceschini and coauthors [51] evaluated lung metastases in 200 oligometastatic patients, including 99 with CRCa, 41 with STS, and 24 with renal cell carcinoma, with a majority receiving 48 Gy in 4 fractions. LC2 was 85% for all histologies, although significantly lower for CRCa at 78% versus others at 92%.

Second, more contemporary series, particularly those using 3–5-fraction courses delivering 50 Gy or greater, tend to report high rates of LC2 in the 85–90% range, irrespective of histology (Table 3). These rates are comparable to those observed in prospective trials.

Third, OS outcomes vary widely across studies, which may be indicative of the broad range of patients receiving SBRT for lung metastases from one institution to the next. Two-year OS (OS2) rates range from 29% to 92% but appear to cluster around 60–80%. Both LC and OS have generally been more favorable among patients receiving at least 45–50 Gy in 3–5 fractions; however, OS rates in retrospective studies are likely to be heavily influenced by various confounders including study selection criteria and years of analysis, as OS generally improves over time as more effective systemic therapies are introduced (e.g., molecularly targeted therapies, immunotherapy, etc.).

In summary, clinical data from both prospective trials and retrospective studies demonstrate high rates of local control and a range of survival outcomes following SBRT for lung metastases. Local control has generally been superior with more aggressive SBRT regimens. The impact of SBRT for metastatic disease on OS remains to be clarified by phase III trials.

Toxicity

As previously discussed, the incidence and severity of toxicities following lung SBRT may vary between peripheral and central tumors, and therefore, in this section, we will address toxicity in the context of tumor location.

Peripheral Tumors

In general, SBRT to peripheral lung tumors represents a well-tolerated therapy for most patients when standard dose constraints are followed. In the multi-institutional phase I/II trial of SBRT for 1–3 lung metastases presented by Rusthoven and coauthors (which was amended to exclude central lesions after the 2006 publication by Timmerman and coauthors reporting increased toxicities for central lesions [15]), only three patients (7.9%) experienced grade 3 toxicity [skin (1), chest wall (1), pneumonitis (1)], and no patients experienced grade 4 or 5 toxicities [13]. Only one patient (2.6%) experienced symptomatic radiation pneumonitis [13]. Extrapolating from primary early-stage NSCLC data, the RTOG 0236 trial was a phase II study of 54 Gy in three fractions for inoperable patients with peripheral early-stage NSCLC, which demonstrated rates of grade 3, 4, and 5 toxicity of 12.7%, 3.6%, and 0%, respectively [14]. The grade 3 events included decrease in FEV1, hypoxia, pneumonitis decrease in PFT, and NOS, with the grade 4 events including hypocalcemia and decrease in PFT and NOS [14]. Although well tolerated overall, more common side effects from SBRT to peripheral tumors to discuss with patients include fatigue, cough, skin irritation, and chest wall discomfort (for very peripheral tumors), with less common side effects to include radiation pneumonitis and symptomatic decreases in pulmonary function, as well as brachial plexopathy for apical lesions. A dedicated analysis of pulmonary function tests (PFTs) in 92 patients treated with SBRT found that changes in FEV1 and DLCO followed a bell-shaped distribution at a median of 10.4 months after treatment, with most patients having no clinically meaningful changes (mean change in FEV1 and DLCO predicted were −1.9% and −2.6%, respectively), while some patients had more significant decline or improvement in lung function (the latter presumably related to a reduction in tumor) (Fig. 3a, b) [52]. Similar bell-shaped distributions for both early (0–6 months) and late (7–24 months) PFT changes were reported in an international multi-institutional analysis of 191 patients [53]. PFT analysis of 127 patients treated on a prospective trial of lung SBRT showed only mild mean decrements in FEV1 and DLCO at 12 and 24 months [54]. Overall, the literature suggests that, on average, PFT changes after lung SBRT tend to be mild, but more meaningful declines in PFTs can occur in a minority of patients.

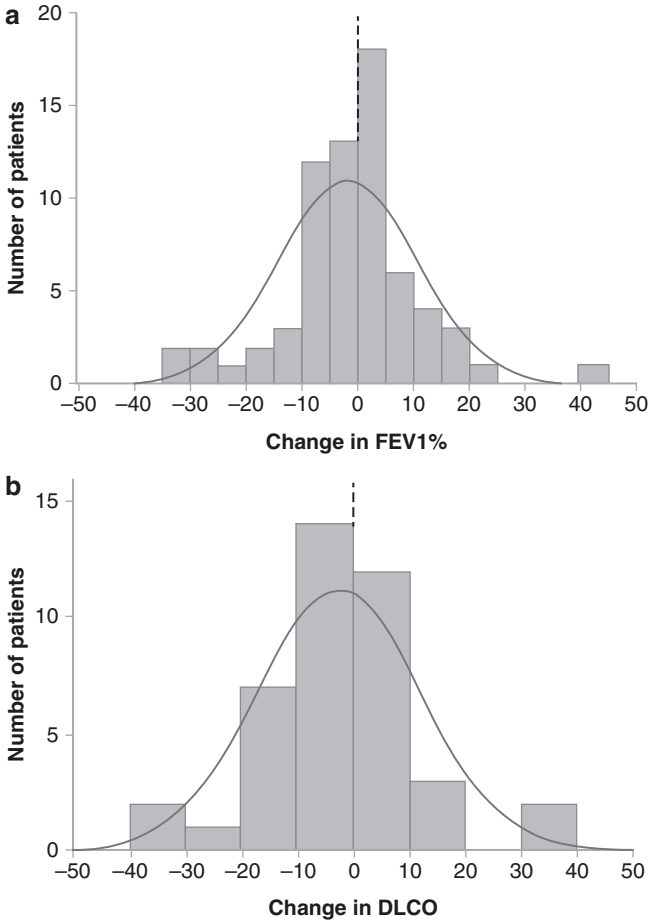

Fig. 3 Changes in pulmonary function tests (PFTs) ≥6 months after lung SBRT (median 10.4 months) in a series of 92 patients. (**a**) Changes in forced expiratory volume at 1 second (FEV1). (**b**) Changes in diffusion capacity to carbon monoxide (DLCO). Mean changes in PFTs were not significant for the group as a whole, but more meaningful changes were seen in a minority of patients. (**a** and **b**: Used with permission of Elsevier from Stephans et al. [52])

Radiation pneumonitis can occur following treatment of either peripheral or central tumors but will be expanded upon in this section on peripheral tumor treatment. As with conventionally fractionated radiotherapy, pneumonitis after SBRT has been associated with increasing mean lung dose (MLD) and V20 [55–57]. Current RTOG SBRT studies utilize the whole lung minus GTV V20 constraint of less than 10%. In our practice, we typically aim for *total* (bilateral) lung V20 minus ITV goal of less than 6% if possible, but will allow up to 10% (per current RTOG protocols), and an *ipsilateral* (single) lung minus ITV to a mean dose of less than 9 Gy [58]. Of note, one retrospective series from Barriger and associates support even lower V20 constraints, with reported rates of grade 2–4 radiation pneumonitis of 16.4% versus 4.3% for patients with V20 >4% versus V20 ≤4%, respectively, although, in practice, a V20 below 4% can often be difficult to achieve depending on tumor location and size. Total lung SBRT dose constraints, as opposed to ipsilateral lung constraints, may be particularly useful in cases where bilateral or multiple lung metastases are being treated with SBRT.

Although the treatment of central tumors carries a risk of injury to several critical organs at risk (OAR) discussed below, chest wall toxicity (rib fracture and/or pain) remains an important consideration in the treatment of peripheral tumors. Although there is no universally accepted constraint for the chest wall/ribs, our group in collaboration with the University of Virginia has shown that the volume of chest wall receiving 30 Gy predicts for a risk of severe chest wall pain and/or rib fracture. A 30% risk of severe chest wall toxicity was observed when 35 cc of chest wall received 30 Gy. In our practice, we limit the V30 to less than 30 cc [59]. RTOG 0915, which compared a single-fraction (34 Gy) regimen to 12 Gy × 4 fractions for medically inoperable peripheral NSCLC, used a 4-fraction rib constraint of <1 cc greater than 32 Gy and a max point dose of 40 Gy. The single-fraction rib constraint in RTOG 0915 recommended keeping doses exceeding 22 Gy to less than 1 cc of rib volume and a max point dose below 30 Gy [60]. The Joint Lung Cancer Trialist's Coalition is conducting a randomized phase III study comparing sublobar resection with SBRT for patients with peripheral stage I NSCLC at high risk of surgical complications. In this study, patients will receive 54 Gy in three fractions with a rib constraint of <5 cc greater than 40 Gy and a max point dose below 50 Gy.

A consideration specific to apical tumors is the proximity of the tumor to the brachial plexus. Forquer and associates reviewed rates of brachial plexopathy in 37 apical lesions treated with SBRT. The incidence of grade ≥2 brachial plexus toxicity was 18.9% (grade 2: 4, grade 3: 2, grade 4: 1). In this series, the median maximum dose to the brachial plexus was 30 Gy in patients who developed brachial plexus toxicity, and the authors suggested a maximum dose constraint to the brachial plexus of <26 Gy (in 3 or 4 fractions) based on an observation of 2-year risk of brachial plexopathy of 46% for maximum point dose >26 Gy versus 8% for a maximum point dose ≤26 Gy [61]. Additional guidance comes from the Memorial Sloan Kettering Cancer Center. They presented an abstract which differentiated between radiation-related brachial plexopathy and brachial plexopathy related to tumor recurrence and noted that the median Dmax in patients who developed radiation-related brachial plexopathy was 27.9 Gy in 3 fractions (or 35 Gy in 5 fractions) and median D05 of 24 Gy in 3 fractions (or 30 Gy in 5 fractions). Median time to radiation-related brachial plexopathy was 6.2 months [62]. Of note, RTOG 0236 required a 3-fraction ipsilateral brachial plexus max point dose constraint of 24 Gy [14], and RTOG 0813 used a 5-fraction constraint of 32 Gy.

Central Tumors

Central tumors bring about a more complex risk/benefit assessment in the setting of metastatic disease. As previously discussed, a seminal paper from Timmerman and associates described a significant increase in severe toxicities (grades 3–5) for tumors within 2 cm of the proximal bronchial tree [15]. Treatment of central tumors was associated with an 11-fold increase in risk of severe toxicity, including four grade 5 toxicities in their study [15]. With adoption of 5-fraction schema, as per RTOG 0813, or even more extended fractionation schedules, it appears that central tumors can be treated safely, but some risks of severe and even fatal toxicities remain.

SBRT to central tumors comes with a low, but important, risk of airway and esophageal stenosis, fistula, and hemorrhage. For luminal structures (such as the esophagus, airways, and vessels), our center places a conceptual emphasis on avoiding ablative doses to the full circumference of a lumen, in an effort to preserve the requisite normal tissue, blood supply, and lymphatics to allow healing of the treated luminal segment over time. In 2008, Timmerman proposed a 5-fraction airway constraint of <4 cc greater than 18 Gy with a max point dose of 38 Gy [63]. For detailed normal tissue complication probability (NTCP) modeling of the bronchus, we refer you to the excellent article by Duijm and associates [64]. Based on these data, Pollom and associates recently suggested a major airway constraint of <4 cc greater than 33.5 Gy (with attention to achieving steep dose gradient across the airway) and a max point dose <52.5 Gy [56]. Importantly, while the max point dose suggested by Pollom and associates is the same max point dose allowed on RTOG 0813, the volumetric constraint for RTOG 0813 was more conservative at <4 cc greater than 18 Gy. For the great vessels, Xue and associates presented a dose-response model based on 625 cases and demonstrated that the RTOG 0813 constraint (vessel max point dose <52.5 Gy for 50 Gy in five fractions) is associated with a 1.2% risk of grade 3–5 toxicity. RTOG 0813 specifies a great vessel volumetric constraint of <10 cc greater than 47 Gy, as initially proposed by Timmerman [63].

Several institutions have raised particular concern when treating "ultracentral" lesions with SBRT. Definitions of ultracentrality have varied across studies but generally encompass lesions whose gross tumor volume abuts proximal airways. In a multi-institutional series of 108 central tumors, 18 patients had lesions abutting the proximal bronchial tree [65]. Among these 18 patients, four experienced fatal complications; however, no other patients with central tumors developed a grade 5 complication. Of note, two of the four patients with SBRT-related death had received anti-vascular endothelial growth factor (anti-VEGF) therapy, suggesting a possible interaction with this therapy and complications with ultracentral tumors. Tekatli and associates [66] reported on 47 patients with primary or recurrent NSCLC treated with hypofractionated radiation and observed a 15% rate of fatal pulmonary hemorrhage. Finally, in a series of 20 patients treated with five-fraction SBRT for ultracentral in-field recurrences following conventionally fractionated radiotherapy, one patient developed grade 5 pulmonary hemorrhage [67]. Conversely, Stanford has also reported retrospective outcomes from a series of patients with ultracentral tumors treated with 50 Gy in 4–5 fractions but observed no additional high-grade toxicity. In summary, the risk of toxicity among all central tumors may not be the same, and lesions abutting the proximal bronchial tree may be at a higher risk for significant toxicity. In the context of metastatic disease, we recommend caution in applying aggressive dose-fractionation schemes in this location, particularly in patients who have recently received anti-VEGF therapy.

Particular attention should also be given to esophageal dosing. RTOG 0813 mandated that the esophagus receives a max point dose of <52.5 Gy and that <5 cc receive a dose greater than 27.5 Gy; however, these esophageal constraints are far more liberal than others reported in the literature. Nuyttens and associates evaluated the NTCP for the esophagus based on 58 cases and found that a max point dose of 43.4 Gy was associated with a 50% risk of moderate (grade 2) toxicity. Based on this modeling, Pollom and associates have proposed a five-fraction max point dose to the esophagus of <35 Gy to minimize the risk of grade 2 toxicity while also proposing that a max point dose of <50 Gy in five fractions can be utilized to minimize the risk of more significant grade 3 toxicity while acknowledging that grade 2 toxicity will be likely at these higher doses [56]. A 2018 UK stereotactic consensus guideline recommended maximum doses <25.2 for three fractions, <32–34 for five fractions, and <40 Gy for eight fractions. Of note, the UK consensus statement also provides general SBRT dose guidelines across multiple organ systems, including other organs-at-risk discussed above, and represents useful resources for general SBRT dose constraints [68].

Overall, the constraints above have been developed primarily in the setting of curative-intent therapy for early-stage NSCLC. It bears re-emphasizing that the thresholds for acceptable toxicity rates are generally lower in the setting of metastatic ablation, and it is often preferable to consider more stringent OAR constraints for patients with metastatic disease.

Management of Toxicities

In the acute setting, common side effects from lung SBRT may include fatigue and treatment-related cough. Cough in this setting is frequently self-limited, but pharmacologic

cough suppressants, such as dextromethorphan, codeine, and benzonatate, can be helpful in minimizing symptoms in some cases. Chest wall pain and/or rib fracture can typically be managed conservatively with anti-inflammatory and analgesic medications, and also are typically self-limited. However, more severe long-term chest wall pain syndromes, which may have a neuropathic component, can occur in rare cases and may require more complex and sometimes multidisciplinary management strategies, including neuropathic pain medications and nerve blocks.

Symptomatic radiation pneumonitis after SBRT has been reported to develop between 0.5 and 12 months after SBRT, with the greatest incidence between 3 and 6 months [55, 69]. Typical symptoms include mild to severe dyspnea, nonproductive cough, and low-grade fever. Importantly, to differentiate from infectious pneumonia, in radiation pneumonitis, the most pronounced radiographic findings should geographically correspond to the radiation treatment field. Although there is no universal standard approach to the management of radiation pneumonitis, most practitioners advocate corticosteroids. One reasonable approach is to use prednisone at 60–100 mg by mouth daily for 2 weeks followed by a gradual taper over 3–12 weeks [70, 71]. There is also limited evidence that pentoxifylline may be beneficial in reducing the incidence of radiation pneumonitis and preserving pulmonary function. In a small single-institution, double-blind randomized trial of pentoxifylline or placebo during radiation in 40 patients with lung or breast cancer, late effects normal tissue-subjective, objective, management, and analytic (LENT-SOMA) scores favored the pentoxifylline group ($p = 0.016$). The pentoxifylline group also showed improved DLCO at 3 ($p = 0.01$) and 6 ($p = 0.01$) months and improved regional perfusion scans at 3 ($p = 0.03$) and 6 ($p = 0.01$) months [72]. More data are needed, however, and routine use is not currently warranted.

For a number of rare but more serious late toxicities discussed above, such as esophageal stenosis or airway necrosis, little can be done to reverse the underlying normal tissue damage following high-dose SBRT. Multidisciplinary evaluation for serious complications is advised; surgical or endoscopic procedures, such as luminal stent placements, should be considered on an individual basis.

Plan Quality

Systematic and thorough plan evaluation of high-dose lung SBRT is essential. At the time of plan review, we recommend first taking the time to re-evaluate the delineation of the target on lung and soft tissues windows and the planning expansions and to review the beam arrangements used. Next, review the qualitative dose distribution focusing on coverage of the PTV (e.g. maximum dose within the PTV in RTOG 0236 dose was prescribed to the 60–90% isodose line [14], corresponding to 110–140% prescription dose centrally within the PTV) and hot spots outside of the PTV (hot spots should be avoided in OARs). In general, it is preferable to have ≥95% of the PTV covered by the prescription dose, which can be evaluated qualitatively on the planning images and quantitatively using the dose volume histogram (DVH). Once satisfied with the qualitative dose distribution, turn to your dose DVH and confirm quantitative coverage of the PTV. Next, carefully review dose to OARs (see the "Toxicity" section for suggested constraints). As suggested above, while these constraints are likely sufficient to minimize the risk of treatment-related toxicities, in the context of metastatic disease, the level of acceptable risk is often lower and more conservative OAR dose constraints warrant consideration. Some radiation oncologists also consider quantitative assessment of dose conformity, and multiple metrics are available. RTOG 0236 mandated a conformity index (CI) (prescription isodose volume/PTV ratio) of <1.2, as well as an R50% (ratio of 50% prescription isodose volume/PTV) of <2.9–3.9 (depending on maximum PTV dimension) [14].

Future Directions: SBRT in the Rapidly Evolving Landscape of Systemic Therapy

As systemic therapies continue to improve, the value of local therapy to foci of treatment resistance is likely to grow (Fig. 4). One of the more promising advances in metastatic disease management in recent years has been the rise of molecularly targeted agents, with notable successes in NSCLC, melanoma, and breast cancer. Taking NSCLC as an example, patients with EGFR and ALK driver mutations are now preferentially offered TKIs in the first-line and often subsequent lines of therapy due to their improved efficacy and lower toxicity profiles versus cytotoxic chemotherapy in comparable settings [2]. However, acquired treatment resistance invariably develops, with median PFS rates generally on the order of 9–24 months depending on the specific TKI [73–75]. At the time of progression, patients often present with solitary or few sites of disease (a.k.a. *oligoprogression* or *oligorecurrence*), which may represent limited foci of clonal TKI resistance occurring in advance of widespread, systemic treatment resistance. As such, there is theoretical rationale for ablative therapy to "weed the garden" of these limited foci of resistance in order to permit ongoing administration of a targeted therapy that is continuing to provide an overall clinical benefit [76]. Studies dedicated to this concept in EGFR- and ALK-driven NSCLC have demonstrated extensions in PFS by an additional 6–10 months and prolongations in TKI delivery by up to 22 months [77–79]. As a result, oligometastatic ablation and continued TKI therapy are now a recognized paradigm for oligoprogressive EGFR-

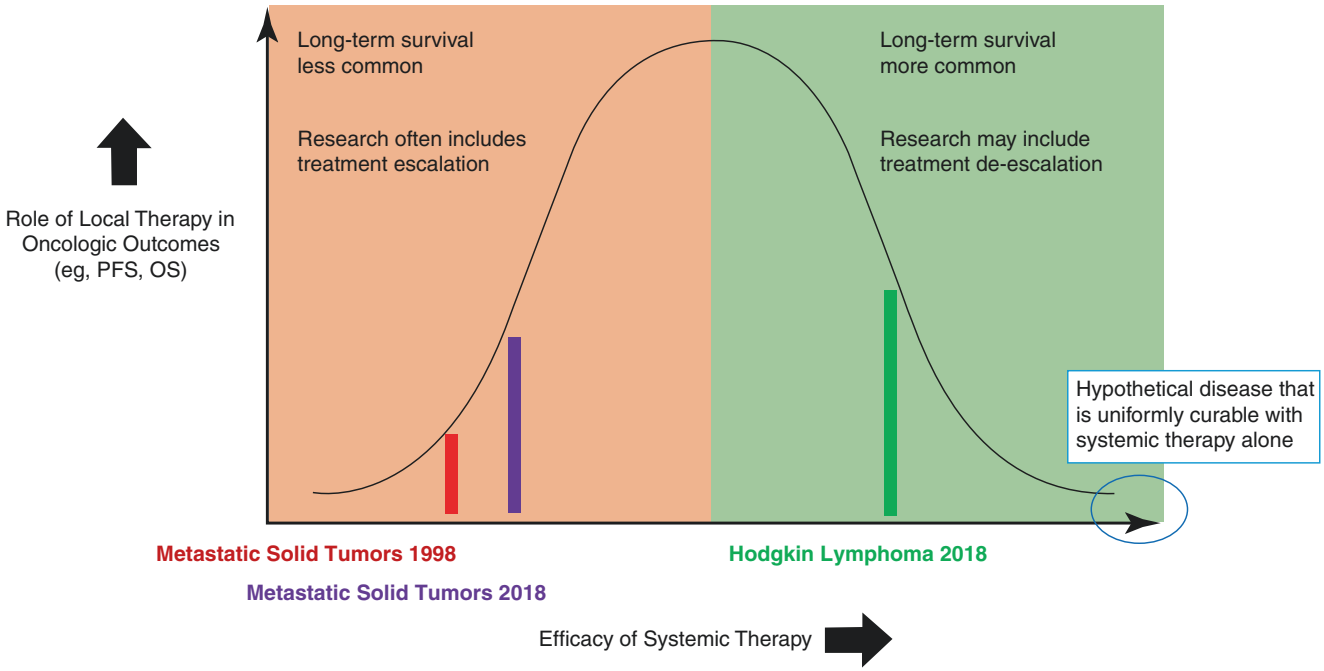

Fig. 4 Conceptual value of local therapy in relation to efficacy of systemic therapy for metastatic disease

and ALK-driven NSCLC in the contemporary national guidelines [2], and similar paradigms are likely to arise for primary tumors across the oncologic spectrum as new molecularly targeted agents emerge.

In the armamentarium of locally ablative therapies for metastatic disease, which includes metastasectomy [80] and radiofrequency ablation [81], SBRT may be unique in its ability to stimulate the immune system. The immunostimulatory mechanisms of high-dose radiotherapy are still being characterized but appear to include T-cell priming [82], antigen release [83], upregulation of PD-1 [84], and T-cell trafficking [85]. This raises the exciting possibility of combining the immunostimulatory capacity of radiation with immunotherapy [86], and emerging lines of clinical data suggest potential synergy between immunotherapy and radiation [87, 88]. With the advent of checkpoint inhibitors targeting CTLA-4 and PD-1/PD-L1, as well as other emerging immunotherapeutic agents currently in development, prospective investigation into the optimal sequencing, dose, and fractionation of SBRT with immunotherapy will represent an important area of clinical research in the coming years.

The noninvasive and repeatable nature of lung SBRT makes it a particularly attractive ablative strategy for patients who may be suboptimal candidates for surgery or other invasive local interventions. Future research is needed to elucidate the best integration of local therapy with evolving systemic regimens (including chemotherapy, targeted agents, and immunotherapy), to optimize the radiation dose and normal tissue tolerance, and to refine patient selection for aggressive local therapy.

Practical Considerations

- Patient selection:
  1. Disease state: Is this patient appropriate for aggressive management of metastatic disease? What are the goals of care (e.g., progression-free survival vs pain control, etc.)? What is the overall burden of disease? Is a conventional palliative course (e.g., 30 Gy/10 fractions, 8 Gy × 1) more appropriate, or no local therapy?
  2. Pulmonary status: Has the patient had prior thoracic radiation (SBRT after conventional thoracic radiation therapy can be considered for otherwise appropriate patients [89])? Prior surgical management? Underlying lung disease (e.g., significant COPD, interstitial lung disease)? Will PFTs and/or functional lung imaging inform decisions to treat or offer aggressive dose/fractionation schedules?
- Tumor-specific factors: Consider tumor size, location, and nearby organs at risk during initial consultation to guide informed discussion of expected risks, benefits, and duration of treatment course.
- Have plans been made to hold systemic therapy if indicated to do so?
- CT simulation: Is the setup stable and reproducible? Can the patient tolerate this setup? 4D CT to assess tumor motion.
- Selection of dose/treatment planning:
  1. For peripheral tumors under 5 cm that are amenable to 3–5-fraction SBRT, we often consider dose-fractionation schedules ranging from 45–54 Gy in

three fractions or 40–50 Gy in five fractions (prescribed to the PTV margin) depending on the clinical scenario. With very peripheral lesions including those abutting the chest wall, effort should be made to meet the chest wall constraint, but ultimately if it must be exceeded, patients should be counseled appropriately. Patients with tumors invading the chest wall have generally been underrepresented in the existing literature. Recent guidelines have been hesitant to endorse SBRT for tumors invading the chest wall [18], and in our practice, we generally defer to more prolonged hypofractionated regimens (≥5 fractions, often favoring 8- to 15-fraction regimens) in the metastatic setting.

2. For central tumors, we generally recommend more conservative fractionation schedules in the metastatic setting (≥5 fractions) such as those described above. In our practice, doses of 35–50 Gy in 10 fractions are often considered for central metastatic lesions, depending on the clinical scenario. All organs at risk should be meticulously contoured, including the esophagus, proximal bronchial tree, great vessels, heart, spinal cord, and (for apical lesions) the brachial plexus. The decision to offer SBRT or more protracted hypofractionated radiotherapy regimens should be carefully considered in the setting of metastatic disease, given the risk of severe toxicities; more conservative OAR constraints than those used for curative-intent early-stage NSCLC cases may be appropriate.

- Plan evaluation: PTV coverage, conformity, OAR DVH, hot spots.
- Treatment delivery: Plan for motion management (abdominal compression, respiratory gating, breath hold, real-time tumor tracking).
- Follow-up: Counsel patients on the possibility of radiation pneumonitis and encourage them to contact their radiation oncology team with any concerns—this can help avoid mismanagement of radiation pneumonitis as infectious pneumonia. Depending on the clinical scenario, patients with metastatic disease who receive SBRT will often have routine surveillance imaging. In general, for the specific purposes of evaluating the efficacy of SBRT, we tend to wait at least 2–3 months prior to the first axial chest imaging on order to allow adequate time for radiographic improvement. Radiographic changes are likely to continue to evolve after the initial CT, and on each follow-up exam, images should be reviewed in the axial, coronal, and sagittal planes in addition to the axial plane in order to help discern normal fibrotic changes from disease recurrence. High-risk features for local recurrence include sustained growth on serial imaging, infiltration into adjacent structures, bulging margins, mass-like growth pattern, spherical growth, craniocaudal growth, and loss of air bronchograms [90, 91]. Post-SBRT imaging can often be difficult to interpret due to evolving treatment-related changes [92]. PET/CT may be useful in some cases to help differentiate posttreatment effects from recurrence [93]; however, in general, we recommend waiting at least 6 months after SBRT to avoid confounding from posttreatment inflammation. Correlation with serum tumor markers may also be useful in some cases.

References

1. Palma DA, Louie AV, Rodrigues GB. New strategies in stereotactic radiotherapy for oligometastases. Clin Cancer Res. 2015;21(23):5198–204.
2. Ettinger DS, Wood DE, Aisner DL, Akerley W, Bauman J, Chirieac LR, et al. Non-small cell lung cancer, Version 5.2017, NCCN Clinical Practice Guidelines in Oncology. J Natl Compr Canc Netw. 2017;15(4):504–35.
3. Videtic GMM, Donington J, Giuliani M, Heinzerling J, Karas TZ, Kelsey CR, et al. Stereotactic body radiation therapy for early-stage non-small cell lung cancer: Executive Summary of an ASTRO Evidence-Based Guideline. Pract Radiat Oncol. 2017;7(5):295–301.
4. De Ruysscher D, Faivre-Finn C, Nestle U, Hurkmans CW, Le Pechoux C, Price A, et al. European Organisation for Research and Treatment of Cancer recommendations for planning and delivery of high-dose, high-precision radiotherapy for lung cancer. J Clin Oncol. 2010;28(36):5301–10.
5. De Ruysscher D, Faivre-Finn C, Moeller D, Nestle U, Hurkmans CW, Le Pechoux C, et al. European Organization for Research and Treatment of Cancer (EORTC) recommendations for planning and delivery of high-dose, high precision radiotherapy for lung cancer. Radiother Oncol. 2017;124(1):1–10.
6. Seppenwoolde Y, Shirato H, Kitamura K, Shimizu S, van Herk M, Lebesque JV, et al. Precise and real-time measurement of 3D tumor motion in lung due to breathing and heartbeat, measured during radiotherapy. Int J Radiat Oncol Biol Phys. 2002;53(4):822–34.
7. Plathow C, Ley S, Fink C, Puderbach M, Hosch W, Schmahl A, et al. Analysis of intrathoracic tumor mobility during whole breathing cycle by dynamic MRI. Int J Radiat Oncol Biol Phys. 2004;59(4):952–9.
8. Negoro Y, Nagata Y, Aoki T, Mizowaki T, Araki N, Takayama K, et al. The effectiveness of an immobilization device in conformal radiotherapy for lung tumor: reduction of respiratory tumor movement and evaluation of the daily setup accuracy. Int J Radiat Oncol Biol Phys. 2001;50(4):889–98.
9. Heinzerling JH, Anderson JF, Papiez L, Boike T, Chien S, Zhang G, et al. Four-dimensional computed tomography scan analysis of tumor and organ motion at varying levels of abdominal compression during stereotactic treatment of lung and liver. Int J Radiat Oncol Biol Phys. 2008;70(5):1571–8.
10. Harada K, Katoh N, Suzuki R, Ito YM, Shimizu S, Onimaru R, et al. Evaluation of the motion of lung tumors during stereotactic body radiation therapy (SBRT) with four-dimensional computed tomography (4DCT) using real-time tumor-tracking radiotherapy system (RTRT). Phys Med. 2016;32(2):305–11.
11. Keall PJ, Mageras GS, Balter JM, Emery RS, Forster KM, Jiang SB, et al. The management of respiratory motion in radiation oncology report of AAPM Task Group 76. Med Phys. 2006;33(10):3874–900.
12. Benedict SH, Yenice KM, Followill D, Galvin JM, Hinson W, Kavanagh B, et al. Stereotactic body radiation therapy: the report of AAPM Task Group 101. Med Phys. 2010;37(8):4078–101.

13. Rusthoven KE, Kavanagh BD, Burri SH, Chen C, Cardenes H, Chidel MA, et al. Multi-institutional phase I/II trial of stereotactic body radiation therapy for lung metastases. J Clin Oncol. 2009;27(10):1579–84.
14. Timmerman R, Paulus R, Galvin J, Michalski J, Straube W, Bradley J, et al. Stereotactic body radiation therapy for inoperable early stage lung cancer. JAMA. 2010;303(11):1070–6.
15. Timmerman R, McGarry R, Yiannoutsos C, Papiez L, Tudor K, DeLuca J, et al. Excessive toxicity when treating central tumors in a phase II study of stereotactic body radiation therapy for medically inoperable early-stage lung cancer. J Clin Oncol. 2006;24(30):4833–9.
16. Woody NM, Stephans KL, Marwaha G, Djemil T, Videtic GM. Stereotactic body radiation therapy for non-small cell lung cancer tumors greater than 5 cm: safety and efficacy. Int J Radiat Oncol Biol Phys. 2015;92(2):325–31.
17. Verma V, Shostrom VK, Kumar SS, Zhen W, Hallemeier CL, Braunstein SE, et al. Multi-institutional experience of stereotactic body radiotherapy for large (≥ 5 centimeters) non–small cell lung tumors. Cancer. 2017;123(4):688–96.
18. Schneider BJ, Daly ME, Kennedy EB, Antonoff MB, Broderick S, Feldman J, et al. Stereotactic body radiotherapy for early-stage non-small-cell lung cancer: American Society of Clinical Oncology Endorsement of the American Society for Radiation Oncology Evidence-Based Guideline. J Clin Oncol. 2018;36(7):710–9.
19. Lagerwaard FJ, Verstegen NE, Haasbeek CJ, Slotman BJ, Paul MA, Smit EF, et al. Outcomes of stereotactic ablative radiotherapy in patients with potentially operable stage I non-small cell lung cancer. Int J Radiat Oncol Biol Phys. 2012;83(1):348–53.
20. Hasselle MD, Haraf DJ, Rusthoven KE, Golden DW, Salgia R, Villaflor VM, et al. Hypofractionated image-guided radiation therapy for patients with limited volume metastatic non-small cell lung cancer. J Thorac Oncol. 2012;7(2):376–81.
21. Xia T, Li H, Sun Q, Wang Y, Fan N, Yu Y, et al. Promising clinical outcome of stereotactic body radiation therapy for patients with inoperable Stage I/II non–small-cell lung cancer. Int J Radiat Oncol Biol Phys. 2006;66(1):117–25.
22. Chen H, Senan S, Nossent EJ, Boldt RG, Warner A, Palma DA, et al. Treatment-related toxicity in patients with early-stage non-small cell lung cancer and coexisting interstitial lung disease: a systematic review. Int J Radiat Oncol Biol Phys. 2017;98(3):622–31.
23. Iyengar P, Kavanagh BD, Wardak Z, Smith I, Ahn C, Gerber DE, et al. Phase II trial of stereotactic body radiation therapy combined with erlotinib for patients with limited but progressive metastatic non–small-cell lung cancer. J Clin Oncol. 2014;32(34):3824–30.
24. Anker CJ, Grossmann KF, Atkins MB, Suneja G, Tarhini AA, Kirkwood JM. Avoiding severe toxicity from combined BRAF inhibitor and radiation treatment: consensus guidelines from the Eastern Cooperative Oncology Group (ECOG). Int J Radiat Oncol Biol Phys. 2016;95(2):632–46.
25. Young KH, Baird JR, Savage T, Cottam B, Friedman D, Bambina S, et al. Optimizing timing of immunotherapy improves control of tumors by hypofractionated radiation therapy. PLoS One. 2016;11(6):e0157164.
26. Onimaru R, Shirato H, Shimizu S, Kitamura K, Xu B, Fukumoto S, et al. Tolerance of organs at risk in small-volume, hypofractionated, image-guided radiotherapy for primary and metastatic lung cancers. Int J Radiat Oncol Biol Phys. 2003;56(1):126–35.
27. Okunieff P, Petersen AL, Philip A, Milano MT, Katz AW, Boros L, et al. Stereotactic Body Radiation Therapy (SBRT) for lung metastases. Acta Oncol. 2006;45(7):808–17.
28. Le QT, Loo BW, Ho A, Cotrutz C, Koong AC, Wakelee H, et al. Results of a phase I dose-escalation study using single-fraction stereotactic radiotherapy for lung tumors. J Thorac Oncol. 2006;1(8):802–9.
29. Nuyttens JJ, van der Voort van Zyp NC, Verhoef C, Maat A, van Klaveren RJ, van der Holt B, et al. Stereotactic body radiation therapy for oligometastases to the lung: a phase 2 study. Int J Radiat Oncol Biol Phys. 2015;91(2):337–43.
30. Milano MT, Katz AW, Zhang H, Okunieff P. Oligometastases treated with stereotactic body radiotherapy: long-term follow-up of prospective study. Int J Radiat Oncol Biol Phys. 2012;83(3):878–86.
31. Milano MT, Katz AW, Schell MC, Philip A, Okunieff P. Descriptive analysis of oligometastatic lesions treated with curative-intent stereotactic body radiotherapy. Int J Radiat Oncol Biol Phys. 2008;72(5):1516–22.
32. Salama JK, Hasselle MD, Chmura SJ, Malik R, Mehta N, Yenice KM, et al. Stereotactic body radiotherapy for multisite extracranial oligometastases: final report of a dose escalation trial in patients with 1 to 5 sites of metastatic disease. Cancer. 2012;118(11):2962–70.
33. Gomez DR, Blumenschein GR Jr, Lee JJ, Hernandez M, Ye R, Camidge DR, et al. Local consolidative therapy versus maintenance therapy or observation for patients with oligometastatic non-small-cell lung cancer without progression after first-line systemic therapy: a multicentre, randomised, controlled, phase 2 study. Lancet Oncol. 2016;17(12):1672–82.
34. Iyengar P, Wardak Z, Gerber DE, Tumati V, Ahn C, Hughes RS, et al. Consolidative radiotherapy for limited metastatic non-small-cell lung cancer: a Phase 2 Randomized Clinical Trial. JAMA Oncol. 2017;4:e173501.
35. Kim MS, Yoo SY, Cho CK, Yoo HJ, Choi CW, Seo YS, et al. Stereotactic body radiation therapy using three fractions for isolated lung recurrence from colorectal cancer. Oncology. 2009;76(3):212–9.
36. Comito T, Cozzi L, Clerici E, Campisi MC, Liardo RL, Navarria P, et al. Stereotactic Ablative Radiotherapy (SABR) in inoperable oligometastatic disease from colorectal cancer: a safe and effective approach. BMC Cancer. 2014;14:619.
37. Carvajal C, Navarro-Martin A, Cacicedo J, Ramos R, Guedea F. Stereotactic body radiotherapy for colorectal lung oligometastases: preliminary single-institution results. J BUON. 2015;20(1):158–65.
38. Ahmed KA, Fulp WJ, Berglund AE, Hoffe SE, Dilling TJ, Eschrich SA, et al. Differences between colon cancer primaries and metastases using a molecular assay for tumor radiation sensitivity suggest implications for potential oligometastatic SBRT patient selection. Int J Radiat Oncol Biol Phys. 2015;92(4):837–42.
39. Jung J, Song SY, Kim JH, Yu CS, Kim JC, Kim TW, et al. Clinical efficacy of stereotactic ablative radiotherapy for lung metastases arising from colorectal cancer. Radiat Oncol. 2015;10:238.
40. Qiu H, Katz AW, Chowdhry AK, Usuki KY, Singh DP, Metcalfe S, et al. Stereotactic body radiotherapy for lung metastases from colorectal cancer: prognostic factors for disease control and survival. Am J Clin Oncol. 2018;41(1):53–8.
41. Kinj R, Bondiau PY, Francois E, Gerard JP, Naghavi AO, Leysalle A, et al. Radiosensitivity of colon and rectal lung oligometastasis treated with stereotactic ablative radiotherapy. Clin Colorectal Cancer. 2017;16(3):e211–e20.
42. Agolli L, Bracci S, Nicosia L, Valeriani M, De Sanctis V, Osti MF. Lung metastases treated with stereotactic ablative radiation therapy in oligometastatic colorectal cancer patients: outcomes and prognostic factors after long-term follow-up. Clin Colorectal Cancer. 2017;16(1):58–64.
43. Binkley MS, Trakul N, Jacobs LR, von Eyben R, Le QT, Maxim PG, et al. Colorectal histology is associated with an increased risk of local failure in lung metastases treated with stereotactic ablative radiation therapy. Int J Radiat Oncol Biol Phys. 2015;92(5):1044–52.
44. Helou J, Thibault I, Poon I, Chiang A, Jain S, Soliman H, et al. Stereotactic ablative radiation therapy for pulmonary metastases:

histology, dose, and indication matter. Int J Radiat Oncol Biol Phys. 2017;98(2):419–27.
45. Dhakal S, Corbin KS, Milano MT, Philip A, Sahasrabudhe D, Jones C, et al. Stereotactic body radiotherapy for pulmonary metastases from soft-tissue sarcomas: excellent local lesion control and improved patient survival. Int J Radiat Oncol Biol Phys. 2012;82(2):940–5.
46. Mehta N, Selch M, Wang PC, Federman N, Lee JM, Eilber FC, et al. Safety and efficacy of stereotactic body radiation therapy in the treatment of pulmonary metastases from high grade sarcoma. Sarcoma. 2013;2013:360214.
47. Navarria P, Ascolese AM, Cozzi L, Tomatis S, D'Agostino GR, De Rose F, et al. Stereotactic body radiation therapy for lung metastases from soft tissue sarcoma. Eur J Cancer. 2015;51(5):668–74.
48. Frakulli R, Salvi F, Balestrini D, Parisi A, Palombarini M, Cammelli S, et al. Stereotactic radiotherapy in the treatment of lung metastases from bone and soft-tissue sarcomas. Anticancer Res. 2015;35(10):5581–6.
49. Baumann BC, Nagda SN, Kolker JD, Levin WP, Weber KL, Berman AT, et al. Efficacy and safety of stereotactic body radiation therapy for the treatment of pulmonary metastases from sarcoma: a potential alternative to resection. J Surg Oncol. 2016;114(1) :65–9.
50. Soyfer V, Corn BW, Shtraus N, Honig N, Meir Y, Kollender J, et al. Single-institution experience of SBRT for lung metastases in sarcoma patients. Am J Clin Oncol. 2017;40(1):83–5.
51. Franceschini D, Cozzi L, De Rose F, Navarria P, Franzese C, Comito T, et al. Role of stereotactic body radiation therapy for lung metastases from radio-resistant primary tumours. J Cancer Res Clin Oncol. 2017;143(7):1293–9.
52. Stephans KL, Djemil T, Reddy CA, Gajdos SM, Kolar M, Machuzak M, et al. Comprehensive analysis of pulmonary function Test (PFT) changes after stereotactic body radiotherapy (SBRT) for stage I lung cancer in medically inoperable patients. J Thorac Oncol. 2009;4(7):838–44.
53. Guckenberger M, Klement RJ, Kestin LL, Hope AJ, Belderbos J, Werner-Wasik M, et al. Lack of a dose-effect relationship for pulmonary function changes after stereotactic body radiation therapy for early-stage non-small cell lung cancer. Int J Radiat Oncol Biol Phys. 2013;85(4):1074–81.
54. Stone B, Mangona VS, Johnson MD, Ye H, Grills IS. Changes in pulmonary function following image-guided stereotactic lung radiotherapy: neither lower baseline nor post-SBRT pulmonary function are associated with worse overall survival. J Thorac Oncol. 2015;10(12):1762–9.
55. Barriger RB, Forquer JA, Brabham JG, Andolino DL, Shapiro RH, Henderson MA, et al. A dose–volume analysis of radiation pneumonitis in non–small cell lung cancer patients treated with stereotactic body radiation therapy. Int J Radiat Oncol Biol Phys. 2012;82(1):457–62.
56. Pollom EL, Chin A, Diehn M, Loo BW, Chang DT, editors. Normal tissue constraints for abdominal and thoracic SBRT. Semin Radiat Oncol. 2017;27(3):197–208. Elsevier.
57. Zhao J, Yorke ED, Li L, Kavanagh BD, Li XA, Das S, et al. Simple factors associated with radiation-induced lung toxicity after stereotactic body radiation therapy of the thorax: a pooled analysis of 88 studies. Int J Radiat Oncol Biol Phys. 2016;95(5):1357–66.
58. Chang JY, Liu H, Balter P, Komaki R, Liao Z, Welsh J, et al. Clinical outcome and predictors of survival and pneumonitis after stereotactic ablative radiotherapy for stage I non-small cell lung cancer. Radiat Oncol. 2012;7(1):152.
59. Dunlap NE, Cai J, Biedermann GB, Yang W, Benedict SH, Sheng K, et al. Chest wall volume receiving > 30 Gy predicts risk of severe pain and/or rib fracture after lung stereotactic body radiotherapy. Int J Radiat Oncol Biol Phys. 2010;76(3):796–801.
60. Videtic GM, Hu C, Singh AK, Chang JY, Parker W, Olivier KR, et al. A randomized phase 2 study comparing 2 stereotactic body radiation therapy schedules for medically inoperable patients with stage I peripheral non-small cell lung cancer: NRG Oncology RTOG 0915 (NCCTG N0927). Int J Radiat Oncol Biol Phys. 2015;93(4):757–64.
61. Forquer JA, Fakiris AJ, Timmerman RD, Lo SS, Perkins SM, McGarry RC, et al. Brachial plexopathy from stereotactic body radiotherapy in early-stage NSCLC: dose-limiting toxicity in apical tumor sites. Radiother Oncol. 2009;93(3):408–13.
62. Din S, Yamada J, Yorke E, Foster A, Poppens E, Thompson M, et al. Brachial plexopathy after high-dose stereotactic body radiation therapy (SBRT). Int J Radiat Oncol Biol Phys. 2013;87(2):S518–S9.
63. Timmerman RD, editor. An overview of hypofractionation and introduction to this issue of seminars in radiation oncology. Semin Radiat Oncol. 2008;18(4):215–22. Elsevier.
64. Duijm M, Schillemans W, Aerts JG, Heijmen B, Nuyttens JJ, editors. Dose and volume of the irradiated main bronchi and related side effects in the treatment of central lung tumors with stereotactic radiotherapy. Semin Radiat Oncol. 2016;26(2):140–8. Elsevier.
65. Haseltine JM, Rimner A, Gelblum DY, Modh A, Rosenzweig KE, Jackson A, et al. Fatal complications after stereotactic body radiation therapy for central lung tumors abutting the proximal bronchial tree. Pract Radiat Oncol. 2016;6(2):e27–33.
66. Tekatli H, Haasbeek N, Dahele M, De Haan P, Verbakel W, Bongers E, et al. Outcomes of hypofractionated high-dose radiotherapy in poor-risk patients with "Ultracentral" non-small cell lung cancer. J Thorac Oncol. 2016;11(7):1081–9.
67. Repka MC, Aghdam N, Kataria SK, Campbell L, Suy S, Collins SP, et al. Five-fraction SBRT for ultra-central NSCLC in-field recurrences following high-dose conventional radiation. Radiat Oncol. 2017;12(1):162.
68. Hanna GG, Murray L, Patel R, Jain S, Aitken KL, Franks KN, et al. UK consensus on normal tissue dose constraints for stereotactic radiotherapy. Clin Oncol. 2018;30(1):5–14.
69. Yamashita H, Nakagawa K, Nakamura N, Koyanagi H, Tago M, Igaki H, et al. Exceptionally high incidence of symptomatic grade 2-5 radiation pneumonitis after stereotactic radiation therapy for lung tumors. Radiat Oncol. 2007;2:21.
70. Gross NJ. Pulmonary effects of radiation therapy. Ann Intern Med. 1977;86(1):81–92.
71. Graves PR, Siddiqui F, Anscher MS, Movsas B. Radiation pulmonary toxicity: from mechanisms to management. Semin Radiat Oncol. 2010;20(3):201–7.
72. Ozturk B, Egehan I, Atavci S, Kitapci M. Pentoxifylline in prevention of radiation-induced lung toxicity in patients with breast and lung cancer: a double-blind randomized trial. Int J Radiat Oncol Biol Phys. 2004;58(1):213–9.
73. Rosell R, Carcereny E, Gervais R, Vergnenegre A, Massuti B, Felip E, et al. Erlotinib versus standard chemotherapy as first-line treatment for European patients with advanced EGFR mutation-positive non-small-cell lung cancer (EURTAC): a multicentre, open-label, randomised phase 3 trial. Lancet Oncol. 2012;13(3):239–46.
74. Solomon BJ, Mok T, Kim DW, Wu YL, Nakagawa K, Mekhail T, et al. First-line crizotinib versus chemotherapy in ALK-positive lung cancer. N Engl J Med. 2014;371(23):2167–77.
75. Peters S, Camidge DR, Shaw AT, Gadgeel S, Ahn JS, Kim DW, et al. Alectinib versus crizotinib in untreated ALK-positive non-small-cell lung cancer. N Engl J Med. 2017;377(9):829–38.
76. Rusthoven CG, Yeh N, Gaspar LE. Radiation therapy for oligometastatic non-small cell lung cancer: theory and practice. Cancer J. 2015;21(5):404–12.
77. Weickhardt AJ, Scheier B, Burke JM, Gan G, Lu X, Bunn PA Jr, et al. Local ablative therapy of oligoprogressive disease prolongs

disease control by tyrosine kinase inhibitors in oncogene-addicted non-small-cell lung cancer. J Thorac Oncol. 2012;7(12):1807–14.
78. Yu HA, Sima CS, Huang J, Solomon SB, Rimner A, Paik P, et al. Local therapy with continued EGFR tyrosine kinase inhibitor therapy as a treatment strategy in EGFR-mutant advanced lung cancers that have developed acquired resistance to EGFR tyrosine kinase inhibitors. J Thorac Oncol. 2013;8(3):346–51.
79. Gan GN, Weickhardt AJ, Scheier B, Doebele RC, Gaspar LE, Kavanagh BD, et al. Stereotactic radiation therapy can safely and durably control sites of extra-central nervous system oligoprogressive disease in anaplastic lymphoma kinase-positive lung cancer patients receiving crizotinib. Int J Radiat Oncol Biol Phys. 2014;88(4):892–8.
80. Pfannschmidt J, Dienemann H, Hoffmann H. Surgical resection of pulmonary metastases from colorectal cancer: a systematic review of published series. Ann Thorac Surg. 2007;84(1):324–38.
81. de Baere T, Auperin A, Deschamps F, Chevallier P, Gaubert Y, Boige V, et al. Radiofrequency ablation is a valid treatment option for lung metastases: experience in 566 patients with 1037 metastases. Ann Oncol. 2015;26(5):987–91.
82. Lee Y, Auh SL, Wang Y, Burnette B, Wang Y, Meng Y, et al. Therapeutic effects of ablative radiation on local tumor require CD8+ T cells: changing strategies for cancer treatment. Blood. 2009;114(3):589–95.
83. Zhang B, Bowerman NA, Salama JK, Schmidt H, Spiotto MT, Schietinger A, et al. Induced sensitization of tumor stroma leads to eradication of established cancer by T cells. J Exp Med. 2007;204(1):49–55.
84. Dovedi SJ, Adlard AL, Lipowska-Bhalla G, McKenna C, Jones S, Cheadle EJ, et al. Acquired resistance to fractionated radiotherapy can be overcome by concurrent PD-L1 blockade. Cancer Res. 2014;74(19):5458–68.
85. Lugade AA, Moran JP, Gerber SA, Rose RC, Frelinger JG, Lord EM. Local radiation therapy of B16 melanoma tumors increases the generation of tumor antigen-specific effector cells that traffic to the tumor. J Immunol (Baltimore, Md: 1950). 2005;174(12):7516–23.
86. Deng L, Liang H, Burnette B, Beckett M, Darga T, Weichselbaum RR, et al. Irradiation and anti-PD-L1 treatment synergistically promote antitumor immunity in mice. J Clin Invest. 2014;124(2):687–95.
87. Antonia SJ, Villegas A, Daniel D, Vicente D, Murakami S, Hui R, et al. Durvalumab after chemoradiotherapy in stage III non-small-cell lung cancer. N Engl J Med. 2017;377(20):1919–29.
88. Shaverdian N, Lisberg AE, Bornazyan K, Veruttipong D, Goldman JW, Formenti SC, et al. Previous radiotherapy and the clinical activity and toxicity of pembrolizumab in the treatment of non-small-cell lung cancer: a secondary analysis of the KEYNOTE-001 phase 1 trial. Lancet Oncol. 2017;18(7):895–903.
89. Amini A, Yeh N, Gaspar LE, Kavanagh B, Karam SD. Stereotactic body radiation therapy (SBRT) for lung cancer patients previously treated with conventional radiotherapy: a review. Radiat Oncol. 2014;9:210.
90. Nguyen TK, Senan S, Bradley JD, Franks K, Giuliani M, Guckenberger M, et al. Optimal imaging surveillance after stereotactic ablative radiation therapy for early-stage non-small cell lung cancer: findings of an International Delphi Consensus Study. Pract Radiat Oncol. 2018;8(2):e71–8.
91. Huang K, Senthi S, Palma DA, Spoelstra FO, Warner A, Slotman BJ, et al. High-risk CT features for detection of local recurrence after stereotactic ablative radiotherapy for lung cancer. Radiother Oncol. 2013;109(1):51–7.
92. Ronden MI, van Sornsen de Koste JR, Johnson C, Slotman BJ, Spoelstra FOB, Haasbeek CJA, et al. Incidence of high-risk radiologic features in patients without local recurrence after stereotactic ablative radiation therapy for early-stage non-small cell lung cancer. Int J Radiat Oncol Biol Phys. 2018;100(1):115–21.
93. Huang K, Dahele M, Senan S, Guckenberger M, Rodrigues GB, Ward A, et al. Radiographic changes after lung stereotactic ablative radiotherapy (SABR) – can we distinguish recurrence from fibrosis? A systematic review of the literature. Radiother Oncol. 2012;102(3):335–42.
94. Chang JY, Bezjak A, Mornex F. Stereotactic ablative radiotherapy for centrally located early stage non-small-cell lung cancer: what we have learned. J Thorac Oncol. 2015;10:577–85.

Stereotactic Body Radiation Therapy (SBRT) for Spinal Tumors

Salman Faruqi, Chia-Lin Tseng, Jeremie Stephane Larouche, Leodante da Costa, Victor Yang, Giuseppina Laura Masucci, Hany Soliman, Simon S. Lo, Eric L. Chang, Zain Husain, Pejman Maralani, Sten Myrehaug, and Arjun Sahgal

Disclosure: Dr. Arjun Sahgal has received honorarium for past educational seminars from Medtronic, Elekta AB, Accuray Inc., and Varian Medical Systems and research grants from Elekta AB. Dr. Sahgal also belongs to the Elekta MR Linac Research Consortium. Zain Husain has received research funding from Merck.

S. Faruqi · H. Soliman
Sunnybrook Odette Cancer Centre, Department of Radiation Oncology, Toronto, ON, Canada

University of Toronto, Toronto, ON, Canada
e-mail: muhammad.faruqi@albertahealthservices.ca; Hany.soliman@sunnybrook.ca

C.-L. Tseng
Sunnybrook Health Sciences Centre, Department of Radiation Oncology, Toronto, ON, Canada

University of Toronto, Department of Radiation Oncology, Toronto, ON, Canada
e-mail: Chia-lin.tseng@sunnybrook.ca

J. S. Larouche
Sunnybrook Health Sciences Centre, Department of Orthopedic Surgery, Toronto, ON, Canada

University of Toronto, Department of Surgery, Toronto, ON, Canada
e-mail: Jeremie.larouche@sunnybrook.ca

L. da Costa
University of Toronto, Department of Surgery, Toronto, ON, Canada

Sunnybrook Health Sciences Centre, Department of Neurosurgery, Toronto, ON, Canada
e-mail: Leo.dacosta@sunnybrook.ca

V. Yang
Sunnybrook Health Sciences Centre, Department of Neurosurgery, Toronto, ON, Canada

University of Toronto, Department of Neurosurgery, Toronto, ON, Canada
e-mail: Victor.yang@sunnybrook.ca

G. L. Masucci
Centre Hospitalier de l'Université de Montréal (CHUM), Department of Radiation Oncology, Montréal, QC, Canada

Université de Montréal, Department of Radiology, Radiation Oncology, and Nuclear Medicine, Montréal, QC, Canada
e-mail: g.laura.masucci.chum@ssss.qc.ca

S. S. Lo
University of Washington Medical Center, Department of Radiation Oncology, Seattle, WA, USA

University of Washington School of Medicine, Department of Radiation Oncology, Seattle, WA, USA
e-mail: simonslo@uw.edu

E. L. Chang
University of Southern California Comprehensive Cancer Center, Department of Radiation Oncology, Los Angeles, CA, USA

Keck School of Medicine of the University of Southern California, Department of Radiation Oncology, Los Angeles, CA, USA
e-mail: Eric.chang@med.usc.edu

Z. Husain
Smilow Cancer Hospital, Department of Radiation Oncology, New Haven, CT, USA

Yale University, Department of Radiation Oncology, New Haven, CT, USA
e-mail: Zain.husain@yale.edu

P. Maralani
Sunnybrook Health Sciences Centre, Department of Radiology, Toronto, ON, Canada

University of Toronto, Department of Medical Imaging, Toronto, ON, Canada
e-mail: Pejman.maralani@sunnybrook.ca

S. Myrehaug
University of Toronto, Department of Radiation Oncology, Toronto, ON, Canada

Sunnybrook Health Sciences Centre, Odette Cancer Center, Department of Radiation Oncology, Toronto, ON, Canada
e-mail: Sten.myrehaug@sunnybrook.ca

A. Sahgal (✉)
Sunnybrook Odette Cancer Centre, Department of Radiation Oncology, University of Toronto, Toronto, ON, Canada
e-mail: Arjun.sahgal@sunnybrook.ca

D. M. Trifiletti et al. (eds.), *Stereotactic Radiosurgery and Stereotactic Body Radiation Therapy*,
https://doi.org/10.1007/978-3-030-16924-4_23

Abbreviations

6DOF	6 Degrees of Freedom
BED	Biologically Effective Dose
CBCT	Cone-Beam Computed Tomography
cRT	Conventional External Beam Radiation Therapy
CT	Computed Tomography
CTV	Clinical Target Volume
DVH	Dose-volume Histogram
fx(s)	Fraction(s)
GTV	Gross Tumor Volume
MESCC	Malignant Epidural Spinal Cord Compression
mo	Month
nBED $Gy_{2/2}$	2Gy Equivalent Dose
Pmax	Point Max
PRV	Planning Organ-at-Risk Volume
PTV	Planning Target Volume
RCC	Renal Cell Carcinoma
SBRT	Stereotactic Body Radiotherapy
SINS	Spinal Instability Neoplastic Score
SRS	Stereotactic Radiosurgery
VCF	Vertebral Compression Fracture
yr	Year

Introduction

Bone metastases are a frequent occurrence upon developing metastatic disease and, when involving the spine, they can cause devastating complications including fracture, severe pain, and malignant epidural spinal cord compression (MESCC). Traditionally, spinal metastases have been treated with conventional external beam radiation therapy (cRT), with dose and fractionation regimens designed to be safe with respect to spinal cord and normal tissue tolerance, typically ranging from 20 Gy in 5 fractions (fx) to 30 Gy in 10 fractions (fxs). The intent of cRT has been short-term pain control as opposed to sustained pain relief, complete response to pain, and local tumor control.

More recently, the focus of radiation oncology for metastatic disease (in particular for patients with oligometastases) has shifted toward the delivery of biologically effective doses (BED) considered radical, with highly conformal dose distributions, steep dose gradients, and image-guided delivery. The technique is now known as stereotactic body radiotherapy (SBRT) which refers to high total dose and dose per fraction radiotherapy delivered in ≤5 fxs [1]. SBRT to the spine was a later development as compared to liver and lung SBRT, due to the requirement of steep dose gradients ranging from 10% to 20% per millimeter and a delivery precision ranging from 1 to 2 mm [2]. One of the potential advantages of SBRT in the spine, and in general as compared to cRT, is an increased rate of local control as opposed to symptom control alone [3–5]. Local control is increasingly becoming important, as patients are living longer with metastatic disease. In the spine, progression can be associated with neurologic morbidity, pain, and limited further treatment options, making it an ideal site to treat with SBRT, similar to the reason brain metastases are treated with stereotactic radiosurgery (SRS). With respect to patient-reported outcomes such as pain, the data suggest higher rates of complete response rates to pain than would otherwise be achieved with cRT [6, 7]. Randomized trials are underway to provide the much-needed level 1 evidence to demonstrate the superiority of SBRT to cRT in the local control of the treated lesions.

The most common and ideal indications for spine SBRT are in patients with no prior history of radiation, oligometastatic disease, limited or no epidural disease and no spinal instability [5]. Reirradiation is also a major indication given that spinal cord tolerance to further cRT is limiting and, with SBRT, the tumor can be dose escalated with a safe constraint maintained to the spinal cord [8]. More recently, the use of postoperative spine SBRT is also gaining prominence in practice and in the literature [9]. Patients with a mechanically unstable spine and/or frank cord compression will often undergo surgical intervention, and treatment with postoperative SBRT likely maximizes the therapeutic outcome of local control given that the tumor is likely more biologically aggressive having required up-front surgery.

Support for an increased need for local control, in a subset of patients, was provided by a study of 603 spine metastases patients from Japan. All patients received cRT ranging from 8 Gy in 1 fx to 40 Gy in 20 fxs [10]. Patients with mass-type tumors, defined as having a clear boundary outside the vertebra, were compared to patients with bone-confined disease. Predictors of local control were assessed after treatment, and a statistically significant difference was observed at 1 year (yr) in patients with mass type tumors with a 1-yr local control rate of 46%, as opposed to 86% in those with non-mass-type tumors. Therefore, patients with associated paraspinal masses may especially benefit from the inherent dose escalation associated with spine SBRT.

A second group of patients who may benefit most from SBRT are those with radioresistant histologies, which typically include melanoma, sarcoma, and renal cell carcinoma (RCC). In a study by Thibault and associates, 71 spinal segments with RCC received a median dose of 24 Gy in 2 fx, and the 1-yr local control rate was 83% [11]. Leeman and associates analyzed data from their sarcoma cohort. A 12-month local control rate of 86% was observed in 120 spinal segments treated with a median dose of 24 Gy in 1 fx [12]. In an analysis of 28 melanoma and 25 RCC spinal metastases, treated with 42 to 60 Gy in 3 to 5 fx, an 18-month actuarial local control rate of 88% was observed [13]. These high rates of local control support the efficacy and role of

SBRT in radioresistant tumor histologies, but comparative evidence is limited given the lack of imaging-based outcomes in patients treated with cRT.

Pain is the number one indication for the treatment of spine metastases and its management and relief are of the utmost importance for the palliative patient. A wealth of literature and many randomized trials exist in the setting of cRT. Partial pain response rates have ranged from 60% to 80%; however, complete pain response rates have ranged from only 0– 24% [14, 15]. Therefore, the question of whether spine SBRT can further improve on the complete pain response rate is of critical importance. However, outcomes from multiple institutions thus far indicate complete pain response rates ranging from 28% to 90% following SBRT, suggesting that patients with painful spinal metastases may be best treated with SBRT [6, 7, 16, 17]. Currently, randomized clinical trials comparing SBRT to cRT are in the process of being completed [18, 19].

Guidelines have been reported to define scope of practice, and this chapter will review key elements to spine SBRT outcomes and safe practice.

Site-Specific Considerations

Spine metastases are best managed with a multidisciplinary team evaluating multiple clinical and radiographic factors to determine surgical versus nonsurgical management and the use of cRT or SBRT. Patient, tumor, and treatment-related factors all need to be considered prior to proceeding with radiotherapy. Some important considerations when assessing the patient are listed in Box 1, and guidelines for patient selection have recently been published for patients undergoing de novo as well as reirradiation SBRT by the International Stereotactic Radiosurgery Society (Box 2) [5, 8].

One of the most important and somewhat subjective assessments is that of mechanical pain and potential instability, defined as pain with movement, upright position, loading of the spine, and/or pain relief with recumbence. There is good evidence in the literature for using the Spinal Instability Neoplastic Score (SINS) to evaluate patients for spine instability, as this tool has demonstrated reliability in studies among surgeons, radiologists, and radiation oncologists [20, 21]. It has also been incorporated in the inclusion criteria for trials specific to spine SBRT [19]. Table 1 summarizes SINS criteria. The final score categorizes patients into stable (0–6 points), potentially unstable (7–12 points), or unstable (>13 points). A spine surgery consult should be considered for any total score ≥ 7. More recently, there are also data to indicate increased risk of adverse events that include vertebral compression fracture (VCF) with a high SINS score [22]. Therefore, the understanding of SINS and stability is critical for a spine SBRT program.

Box 1 Factors to consider when assessing patients for suitability of spine SBRT treatment

Patient factors
Severity, type, and duration of pain
Neurologic status
Performance status
Patient preference
Tumor factors
Disease burden (osseous and extra-osseous)
Tumor histology
Presence of epidural disease
Number of spinal segments involved
Treatment factors
Location of tumor in the spine
Spinal instability
Prior radiotherapy
Systemic therapy (current or planned)

Box 2 International Spine Radiosurgery Consortium (ISRS) recommendations for the treatment of spine metastases with SBRT

Inclusion
Oligometastasis involving the spine
Radioresistant histology (RCC, CRC, melanoma, sarcoma)
Paraspinal extension contiguous to the spine
*Following conventional EBRT based on multidisciplinary assessment
*Following spine SBRT based on multidisciplinary assessment
Exclusion
Symptomatic high-grade spinal cord compression or cauda equina syndrome
Frank mechanically instability based on the SINS score
Patients with an expected survival time < 3 months
>3 contiguous vertebral segments to be treated in a single session

*ISRS recommendations for spine SBRT in the re-irradiation setting

Patients who present with high-grade epidural disease should also be considered for a spinal surgery consult. A classification system has been devised by Bilksy and associates to identify the severity of epidural disease, and this can be used to communicate with the surgical team concisely and accurately [3]. Patients with single-level MESCC of Bilsky 2 or 3 could be managed by surgical decompression followed by spine SBRT to maximize local control and minimize the likelihood of neurologic compromise. Although surgery has been shown to improve outcomes, including the ability to walk and improvements in quality of life measures, patient selection is critical. Typically, surgery benefits patients with single-level cord compression and a prognosis of at least

Table 1 Spinal Instability Neoplastic Score (SINS)

SINS components	Score[a]
Radiographic:	
Location	
Junctional (occiput-C2, C7-T2, T11-L1, L5-S1)	3
Mobile spine (C3-C6, L2-L4)	2
Semi rigid (T3-T10)	1
Rigid (S2-S5)	0
Bone lesion type	
Lytic	2
Mixed (lytic and blastic)	1
Blastic	0
Radiographic spinal alignment	
Subluxation/translation	4
Kyphosis/scoliosis	2
Normal alignment	0
Vertebral body collapse	
> 50% collapse	3
≤ 50% collapse	2
No collapse with >50% of body involved by tumor	1
None of the above	0
Posterolateral involvement of spinal elements	
Bilateral	3
Unilateral	1
None of the above	0
Clinical	
Pain	
Mechanical[b]	3
Occasional pain but not mechanical	1
None	0

Data from Ref. [21]

[a]Final Score: 0 to 6, stable; 7 to 12, potentially unstable; 13 to 18, unstable

[b]Pain with movement, upright position, loading of the spine and/or pain relief with recumbence

3 months [23, 24]. Furthermore, communication with the surgeon should take place to identify the goals of surgery, which includes tumor debulking to allow for at least 2 mm of separation between the remaining tumor mass and the neural elements, as well as to ensure that the construct chosen to stabilize the spine does not interfere with future imaging and treatment. Examples of this would be the addition of a cross-link over the tumor site, which obstructs the necessary imaging required to plan postsurgical SBRT.

Given the close proximity of the spinal cord to the bony boundaries of the spinal segment, the ability to generate highly conformal radiation therapy plans with steep dose gradients is paramount. Therefore, this technique requires significant technical investment to be performed safely and effectively. Patient immobilization devices resulting in near rigid body immobilization are used to minimize intrafraction motion. Linear accelerators with on-board image guidance systems and robotic repositioning devices with 6-degrees of freedom work together to ensure millimeter precision with treatment delivery. For example, the use of cone-beam computed tomography (CBCT), a robotic couch with 6 degrees-of-freedom (6DOF) and the BodyFIX (Elekta AB, Stockholm, Sweden) immobilization system has shown the reproducibility of target localization during treatment delivery to be within 1.2 mm and 0.9 degrees 95% of the time [25].

Target visualization for each patient is achieved by obtaining volumetric thin-slice axial T1 and T2 non-enhanced MRI sequences and fusing these to the computed tomography (CT) simulation scan. The scan limits should encompass the target vertebral segment(s) as well as at least one spinal segment above and below. In postoperative cases where surgical hardware can obscure visualization of the spinal cord, a treatment planning simulation CT myelogram can be performed immediately prior to immobilization and simulation. Guidelines on the ideal use of imaging modalities for both simulation and follow-up for spine SBRT were addressed in the 2015 SPINO report [26]. In summary, a treatment planning CT with <= 2 mm slice thickness fused with volumetrically acquired T1 and T2-weighted MRI sequences of <= 3 mm slice thickness are advised. Local failure was defined when there is unequivocal increase in tumor volume, new or increased disease in the epidural space/paraspinal tissues, and/or neurologic deterioration attributable to pre-existing epidural disease. It was recognized that when determining intra-osseous progression, both pseudoprogression and bone necrosis should also be considered. Follow-up imaging with MRI is recommended at a frequency of every 2–3 months post-SBRT for the first 12–18 months, followed by every 3–6 months thereafter. Image evaluation is performed ideally by a radiologist, a radiation oncologist, and the involved neurosurgeon.

Clinical Evidence

Treatment of De Novo Metastases

Much of the evidence for spine SBRT relates to treating spinal metastases that have had no prior radiotherapy exposure or surgery. In these patients with de novo metastases, excellent local control rates have been observed exceeding 80% at 1 year. In a large multi-institutional analysis reported by Guckenberger and coauthors in 2014, a total of 387 spinal metastases across 8 institutions were treated with a median dose of 24 Gy in 3 fxs. Median overall survival was noted to be 19.5 months, and 1-yr and 2-yr local control rates were 89.9% and 83.9%, respectively [27]. Selected studies that have been pivotal in establishing these data are summarized in Table 2. In addition, Husain and associates recently reported guidelines specific to this indication on behalf of the International Stereotactic Radiosurgery Society [5].

Table 2 Selected spine SBRT series in the treatment of de novo, reirradiation and postoperative metastases

Study (year)	Number of patients	Number of spinal segments treated	Median total dose (range)/ number of fractions (range)	Median follow-up in months (range)	Local control	Overall survival
De novo						
Yamada et al. (2008)	93	103	24 Gy (18–24 Gy)/1	15 (2–45)	90% (15 mo)	15 mo (median)
Sahgal et al. (2009)	14	23	24 Gy (7–40 Gy)/3 (1–5)	9 (1–26)	85% (1 yr)/ 69% (2 yr)	45% (2 yr)
Wang et al. (2012)	149	166	27–30 Gy/3	15.9 (1.0–91.6)	80.5% (1 yr)/ 72.4% (2 yr)	68.5% (1 yr)/ 46.4% (2 yr)
Guckenberger et al. (2014)	301	387	24 Gy (10–60 Gy)/3 (1–20)	11.8 (0–105)	89.9% (1 yr)/ 83.9% (2 yr)	64.9% (1 yr)/ 43.7% (2 yr)
Reirradiation						
Sahgal et al. (2009)	25	37	24 Gy (7–40 Gy)/3 (1–5)	7 (1–48)	92% (1 yr)	45% (2 yr)
Damast et al. (2011)	95	97	30 Gy (16–30 Gy)/5 (4–6)	12.1 (0.2–63.6)	66% (1 yr)	52–59% (1 yr) 13.6 mo (median)
Thibault et al. (2015)	40	56	30 Gy (20–35 Gy)/4 (2–5)	6.8 (0.9–39)	80.6% (1 yr)/ 71.5% (2 yr)	48% (1 yr)
Garg et al. (2011)	59	63	27 Gy (24–30 Gy)/3 (3–5)	13 (0.9–67.5)	76% (1 yr)	76% (1 yr)
POST-OP						
Al-Omair et al. (2013)	80	80	24 Gy (18–40 Gy)/2 (1–5)	8.3 (0.14–39.1)	84% (1 yr)	64% (1 yr)
Laufer et al. (2013)	186	186	24 Gy/1, or 24–30 Gy/3, or 18–36 Gy/5–6	7.6 (1–66.4)	83.6% (1 yr)	29% (crude)
Tao et al. (2016)	66	69	27 Gy (16–30)/3 (1–5)	30 (1–145)	85% (1 yr)	74% (1 yr)/ 60% (2 yr)

Postoperative Spine SBRT

Although radiologic data on local failures (LF) after cRT are scarce, the available evidence suggests a crude LF rate ranging from 21% to 96% [9]. Local failures in the spinal column can be catastrophic leading to cord compression, spinal nerve impingement and instability of the spine leading to VCF.

Even though high-level evidence is lacking, a review of postoperative spine SBRT series by Redmond and associates assessed 426 patients treated with various surgical techniques and postoperative SBRT. A crude local control rate of 88.6% was observed. Interestingly, this review noted that a higher number of patients in the SBRT cohort were defined as having radioresistant disease (40.5%) compared to the cRT cohort (26.6%). In addition, 92–100% of patients achieved a durable pain response after postoperative SBRT in the four studies that reported on this outcome. Although a direct comparison has not been done between cRT and SBRT, radiographic control appears to be better post-SBRT ranging from ~60 to 100% as compared to neurologic and pain control rates after cRT of ~40.7% [9].

Alongside the paradigm shift of SBRT, surgical techniques are evolving to accommodate the radiation delivery both in terms of epidural disease resection and spinal stabilization in those patients at risk for vertebral compression fracture (VCF). Minimally invasive surgical techniques are increasingly used in practice with early data suggesting good outcomes. Gerszten and associates reported on the outcomes of 26 patients with pre-SBRT VCF who received treatment with a cement augmentation procedure and a mean SBRT dose of 18 Gy [28]. Pain improvement was noted in 92% of patients with no radiation toxicity or neurologic compromise. Other techniques include minimally invasive approaches with tubular retraction systems for tumor removal, decompression and fusion, laser interstitial thermotherapy using real-time MRI guidance and video-assisted thoracotomy [3]. Although growing in popularity, these procedures have specific indications and often invasive surgery will nonetheless be the best option for the patient. Depending on the procedure, special consideration needs to be given to the hardware and its placement due to effects on imaging and dosimetry during treatment planning. As a result, new implants with carbon fiber may be optimal for patients intended to be treated postoperatively with SBRT.

Reirradiation Spine SBRT

Conventional reirradiation for painful bony metastases is performed in up to 42% of patients for further pain or recurrent disease after initial cRT [29]. Given the tolerance of the

spinal cord, re-treatment dose and fractionations tend to be more conservative than the original course of radiotherapy. In Canada, 25 Gy in 10 fxs and 20 Gy in 8 fxs are popular doses for a second treatment to the spine. A randomized trial in reirradiation with two different conventional dose fractionations, however, revealed a complete response rate of only 11–14% in the setting of painful bony metastases [14].

Multiple series on reirradiation (salvage) SBRT after cRT have been completed and report local control rates of 66–92% at one year. Pain response is similarly noted to be 65–79% in these cohorts, although high-quality data are lacking. Myrehaug and coauthors recently reported a comprehensive review on this topic and guidelines on behalf of the International Stereotactic Radiosurgery Society [8].

As spine SBRT practice grows, there will be increasing need to develop salvage regimens given that around 10–20% of patients will locally progress despite spine SBRT. Thibault and coauthors recently reported outcomes specific to salvage SBRT [30]. Fifty-six spinal segments were evaluated and a median reirradiation dose of 30 Gy in 4 fx was utilized after initial course of SBRT; 43% of these segments had initially been irradiated with cRT before the first course of SBRT and, therefore, received three courses of radiotherapy in total. The median point max cord planning organ at risk volume (PRV) and thecal sac EQD2 dose in this group of patients were 73.9 Gy and 80.4 Gy (α/β ratio of 2), respectively. Across all patients, the 1-year overall survival and local control rates were 48% and 81%, respectively. No radiation-induced myelopathy was observed with median follow-up time of 6.8 months after the second course of SBRT.

Toxicities

Pain Flare

Pain flare has been reported in up to 68% of patients receiving spine SBRT, with subsequent evidence of effective rescue with dexamethasone [31]. Prophylactic treatment with 4 mg or 8 mg of dexamethasone starting on day 1 of SBRT, prior to each daily fx, and for four days after resulted in a 19% rate of pain flare suggesting a role for prophylactic therapy. In another study by Pan and coauthors [32], a pain flare risk of 23% post-SBRT was observed. The only independent factor that predicted flare on multivariate analysis was the number of treatment fractions, with the incidence being higher with single-fraction SBRT. Of note, the Pan study did not employ a strict protocol specific to pain flare evaluation within the first 10 days post-SBRT. A randomized trial evaluating prophylactic dexamethasone following cRT has been reported by Chow and coauthors. This study suggests efficacy with a reduction in the incidence of pain flare from 35% to 26% with the use of dexamethasone; however, a similar trial in SBRT-induced pain flare has yet to be conducted [33].

Myelopathy

Treatment-related radiation myelopathy is rightly the most serious and feared complication of spine SBRT. When evaluating the data for spinal cord tolerance, one must first examine what contoured structure and technique has the spinal cord constraint been applied to. In general, there are three approaches to contouring. Contours and dose constraints can be applied to the cord itself, the cord plus a PRV margin, or the thecal sac. When the cauda equina is present, the thecal sac should be contoured; the transition from spinal cord to cauda equina is clearly visible on MRI and typically occurs at the level of T12 to L1.

Published evidence-based guidelines on spinal cord tolerance in the de novo and reirradiation setting have been reported. In the de novo setting, Sahgal and coauthors published a logistic regression model with the probability of myelopathy after collecting dosimetric data for 9 cases of radiation myelopathy and 66 cases of SBRT without myelopathy [34]. A risk of radiation myelopathy of 5% or less was reported when limiting the thecal sac point max (Pmax) dose to 12.4 Gy in a single fraction, 17.0 Gy in two fractions, 20.3 Gy in three fractions, 23 Gy in four fractions, and 25.3 Gy in five fractions. More recently, Katsoulakis and coauthors created dose-volume histogram (DVH) atlases for 228 patients, of whom 2 developed radiation myelopathy [35]. Their analysis concluded that a cord Pmax of 13.85 Gy is safe and carries a less than 1% rate of myelopathy.

Sahgal and coauthors also published guidelines for dose constraints in the reirradiation setting [36]. They found that reirradiation with SBRT is safe when it is given at least 5 months after conventional radiotherapy, the reirradiation thecal sac Pmax nBED $Gy_{2/2}$ (2-Gy equivalent dose) is kept to 20–25 Gy, the total Pmax nBED does not exceed 70 $Gy_{2/2}$, and the SBRT dose accounts for no more than 50% of the total nBED. Practical thresholds for up to 5-fraction reirradiation SBRT are reported in that publication.

Gastrointestinal Toxicity

Depending on the location of the spine undergoing treatment, the small bowel and esophagus are at risk for late toxicity. Cox and coauthors reviewed 204 spinal segments treated with a median prescription dose of 24 Gy in a single fx, and observed a rate of grade 3 esophageal toxicity of 6.8% [37]. Based on their analysis, the authors recommended maintaining the maximum point dose to the esophagus of less than 22 Gy, and the volume receiving 14 Gy to less than

2.5 ml. All seven of the grade 4 toxicities were related to recall reactions from chemotherapeutic agents or iatrogenic manipulation of the esophagus.

Vertebral Compression Fracture

VCF is the most serious common toxicity observed in clinical practice, with a rate across the literature of approximately 14%. Certain risk factors have been identified as predisposing to this event including lytic lesions, baseline VCF, higher dose per fraction, age, spinal deformity or > 40% of vertebral body involved by tumor. These factors, along with SINS score, should be used preoperatively to guide pre-SBRT surgical intervention because this has been demonstrated to reduce the risk of VCF in properly selected patients. Sahgal and colleagues were the first to describe the dose-complication relationship and VCF. The multi-institutional pooled data revealed a 39% rate of VCF when treating with 24 Gy per fx, 19% with 20 to 23 Gy per fx, and 10% with ≤19 Gy per fraction [38].

Therapeutic interventions for VCF include vertebroplasty, kyphoplasty, or surgical stabilization. A recent comprehensive review was reported on VCF by Faruqi and colleagues that summarizes the data and management approach for this complication [39].

Plan Quality

Treatment Planning

Clinical Target Volume (CTV) delineation should proceed as per the International Spine Research Consortium consensus guidelines [40]. Gross Tumor Volume (GTV) is defined as the gross imaging abnormality suspicious of tumor including any epidural or paraspinal disease extension. The CTV should include any abnormal bone marrow signal that is suspicious as well as an adjacent bony margin which then defines the target volume at risk. No epidural margin is recommended unless there is epidural disease extension. As a general rule, the entire portion of the spinal segment involved is included within the CTV as well as the adjacent normal marrow space. For example, if a lesion involved the vertebral body and left pedicle, the CTV would include the entire vertebral body, left pedicle, left transverse process, and left lamina (Fig. 1a–d). Our protocol is to also apply a 5-mm CTV for paraspinal disease into the adjacent soft tissues while respecting anatomic barriers. These guidelines are applicable to both the reirradiation and de novo setting. Importantly, limited data suggest treating GTV alone has been shown to increase the risk of local progression [33].

For the postoperative CTV, a report with detailed epidural disease failure patterns was first published by Chan and colleagues [41]. The intent was to determine the minimum CTV needed within the epidural space for postoperative cases. Several critical observations were made from that study. First, the preoperative epidural disease extension predicted where failure occurred as opposed to sectors of residual postoperative disease. Therefore, it is critical to evaluate the preoperative MRI and map out where the epidural disease was located when designing the postoperative CTV. Second, detailed sector-based anatomic analyses showed that when epidural disease is restricted to the anterior compartment, the diametrically opposed most posterior sector of the canal could safely be excluded from the CTV. This often results in a horseshoe type distribution (Fig. 2a–d). Otherwise, if circumferential epidural disease was present preoperatively, then the CTV should include the entire epidural space and create a "donut" distribution, as further detailed in the paper by Chan and colleagues. Recent consensus guidelines have been published to guide practice of postoperative spine SBRT by Redmond and colleagues [9].

Plan Evaluation

When assessing plan quality, attention should be applied to the dose gradient from the cord PRV or thecal sac to the target volume. This is especially true in the setting of epidural disease in which case, the dose immediately surrounding the cord should be as high as possible (while respecting tolerance) to maximize dose coverage in this area. Ensuring coverage of the epidural space as risk with a 5 mm superior and inferior extension is also critical while respecting anatomic boundaries. The isodose lines should also be checked to ensure target coverage and limited OAR exposure. The SC.24 Randomized Trial (NCT02512965) evaluating 24 Gy in 2 SBRT frxs to 20 Gy in 5 conventional fxs states that at least 80% of the CTV should get 100% of the prescribed 24 Gy, and a dose of heterogeneity of +50% is allowed in the Planning Target Volume (PTV) [19]. In cases of reirradiation, the coverage of CTV and PTV may be lower as ultimately target coverage is determined by OAR constraints specific to the case. The DVH of the plan in Fig. 2a–d is shown in Fig. 3.

Future Directions

No randomized trials have been published to date to guide clinical practice. However, a randomized study by the Radiation Therapy Oncology Group (RTOG) has completed accrual examining the effect of 16 to 18 Gy in 1 fx compared to 8 Gy in 1 fx for symptomatic spinal metastases [18].

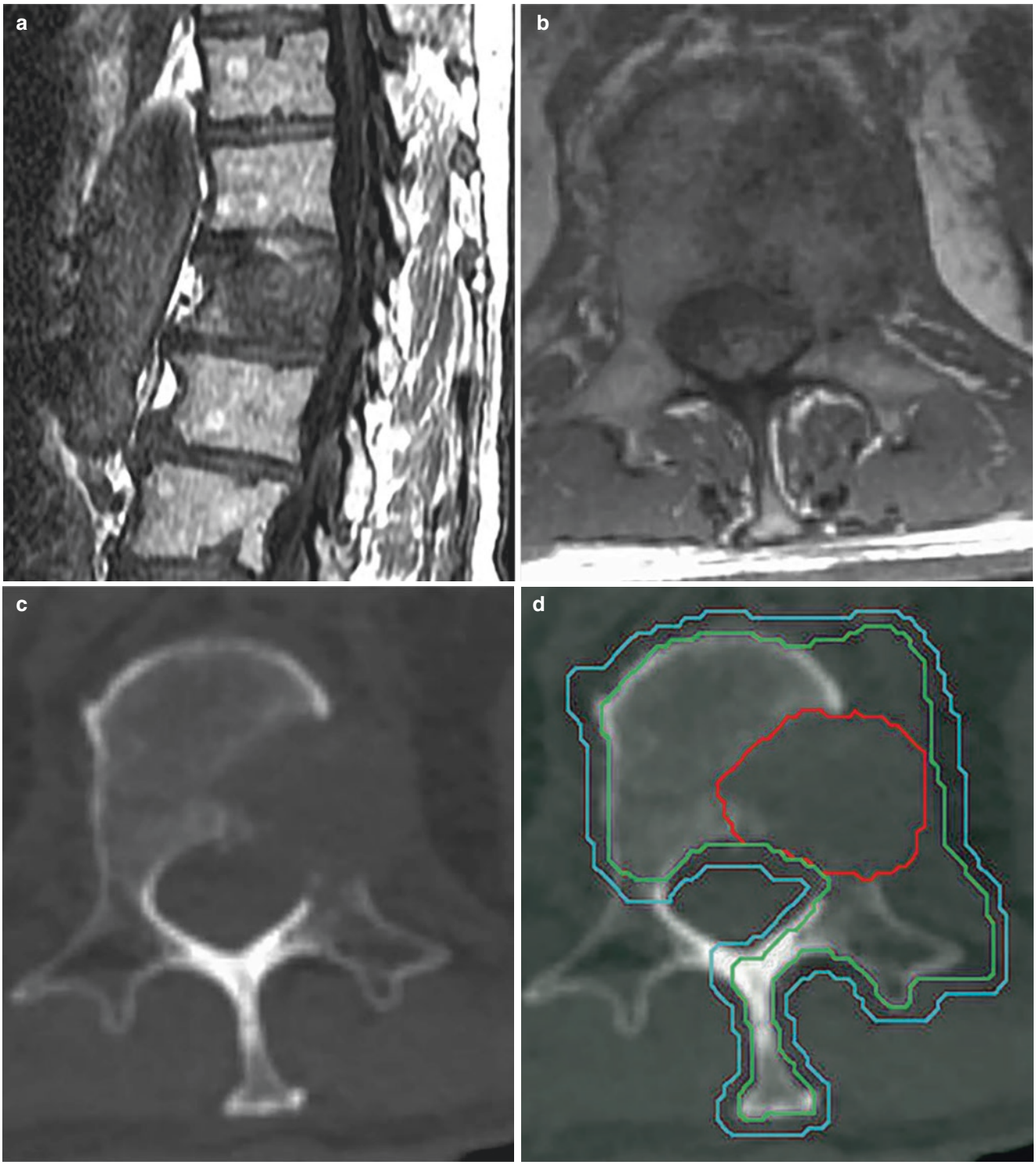

Fig. 1 (**a**–**d**) Case of a 77-year-old gentleman with renal cell carcinoma presenting with mechanical pain of his lower back. MR imaging revealed a 2.6 cm mass involving the left side of his vertebral body and extending to his pedicle. Sagittal (**a**) and axial (**b**) T1 MRI images and CT (**c**) of his L1 spinal segment are displayed above. He was treated with 24 Gy in 2 fractions. The GTV includes all gross disease (**d**), displayed in red. CTV includes the GTV, the spinal segments involved (vertebral body and pedicle) and at-risk segments which include the transverse process, the lamina, and the spinous process. Attention is paid to soft tissue extension of disease where a margin is applied (typically 5 mm). This is especially important in the spinal canal with epidural disease where a 5-mm superior and inferior margin in the canal beyond the GTV is recommended. A PTV of 2 mm is displayed in light blue

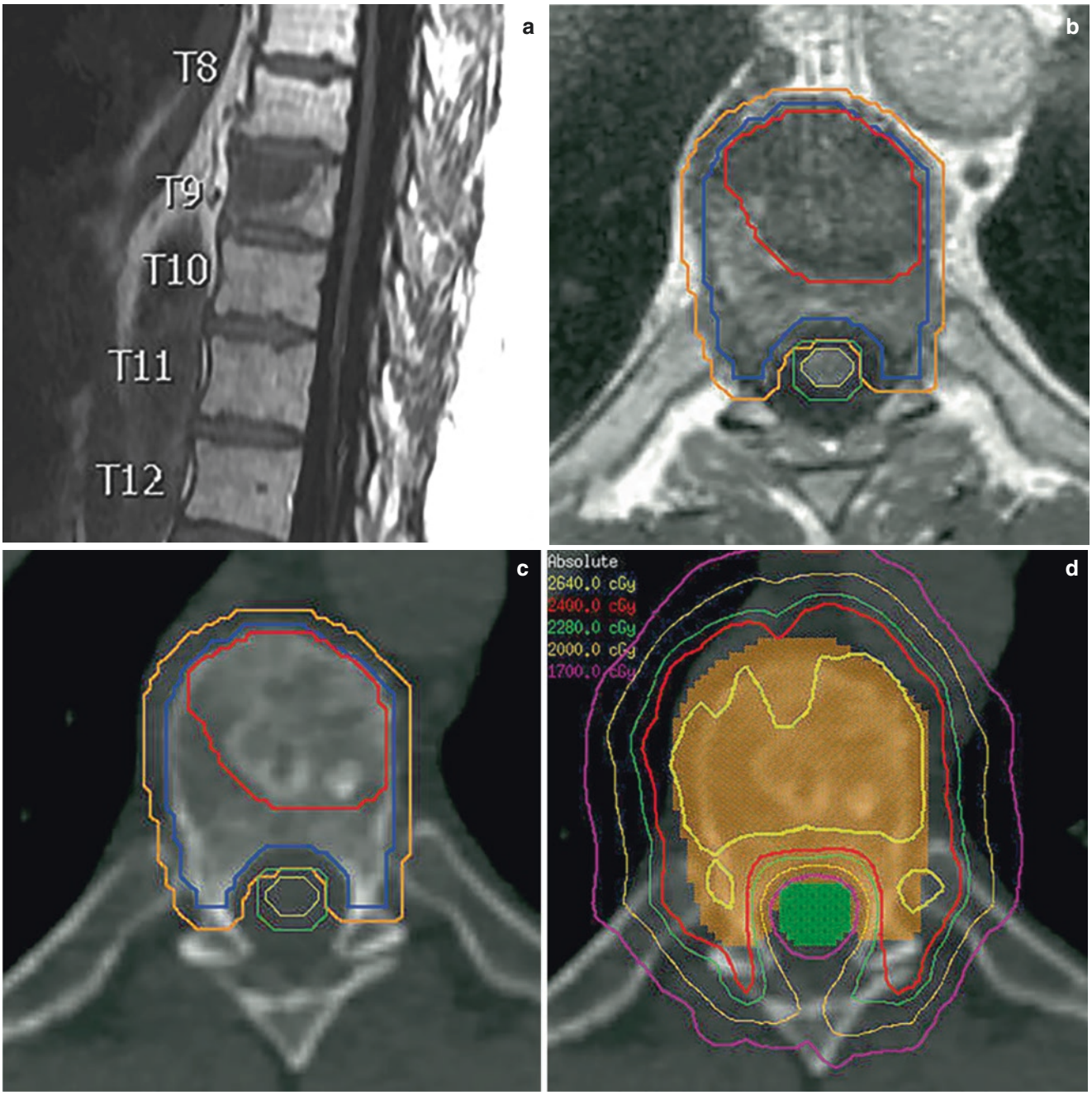

Fig. 2 (**a**–**d**) Case of a 62-year-old gentleman with metastatic castrate-resistant prostate cancer. Imaging revealed a metastatic lesion in the T9 vertebral body. Sagittal T1 MRI, axial T1 MRI and axial CT are shown in panels A, B, and C, respectively. Patient underwent 24 Gy in 2-fraction SBRT. Contours include (**b**, **c**) GTV in red, CTV in blue and PTV in orange. The cord is contoured in yellow and cord planning organ-at-risk volume (PRV) of 1.5 mm is in green. MRI T1 is helpful during planning in the delineation of cord. When assessing dose distribution (**d**), the focus should be both on coverage overall with the 95% and 100% isodose lines and also on the gradient adjacent to the cord PRV (green) and PTV (orange). The steeper the gradient, the more dose will cover the portion of the target volume closest to the cord PRV. The maximum dose prescribed in this plan to the cord PRV is 17 Gy, and the purple 17 Gy isodose line can be seen "hugging" the cord PRV color-wash contour

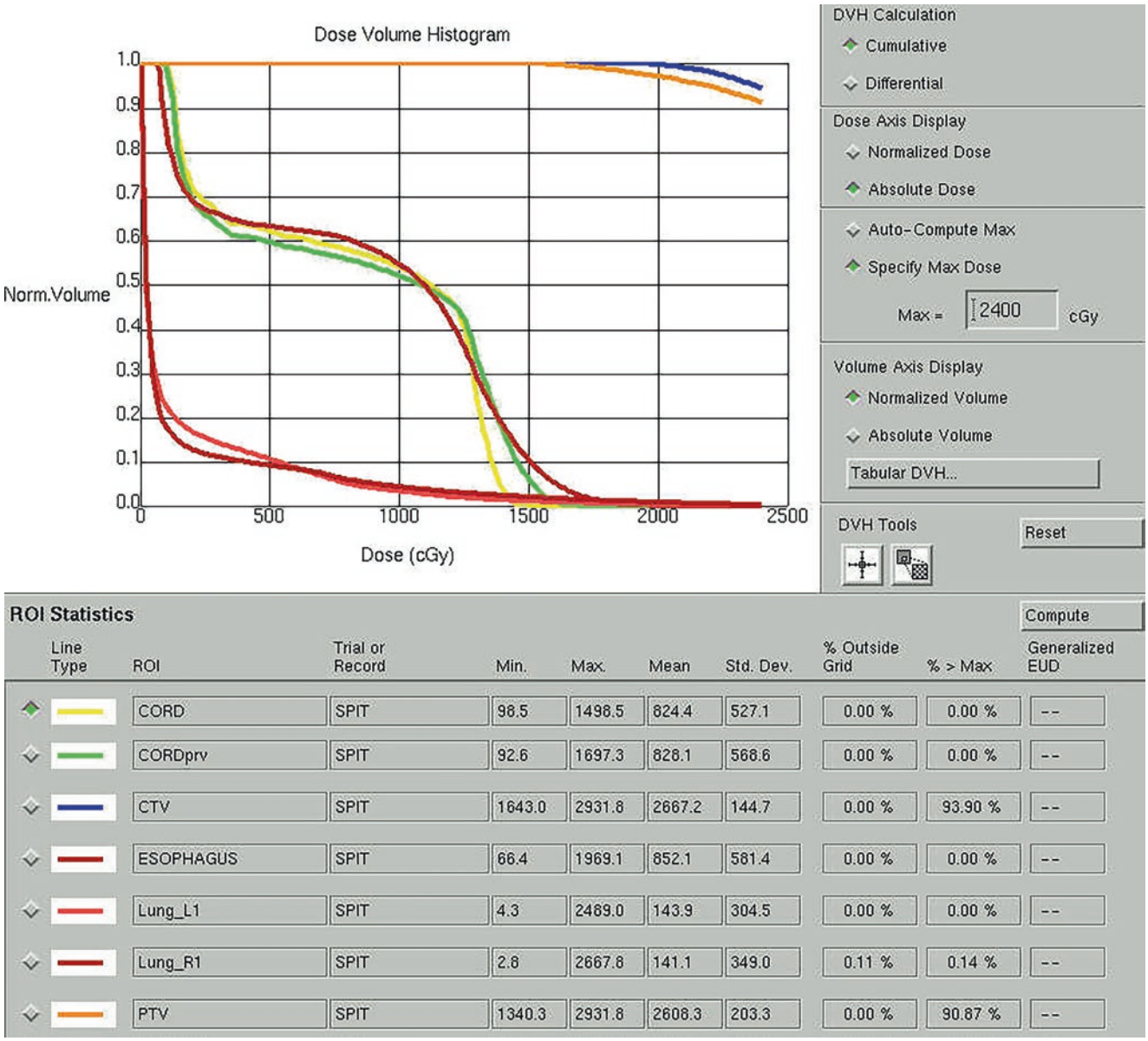

ROI Statistics Compute

Line Type	ROI	Trial or Record	Min.	Max.	Mean	Std. Dev.	% Outside Grid	% > Max	Generalized EUD
	CORD	SPIT	98.5	1498.5	824.4	527.1	0.00 %	0.00 %	--
	CORDprv	SPIT	92.6	1697.3	828.1	568.6	0.00 %	0.00 %	--
	CTV	SPIT	1643.0	2931.8	2667.2	144.7	0.00 %	93.90 %	--
	ESOPHAGUS	SPIT	66.4	1969.1	852.1	581.4	0.00 %	0.00 %	--
	Lung_L1	SPIT	4.3	2489.0	143.9	304.5	0.00 %	0.00 %	--
	Lung_R1	SPIT	2.8	2667.8	141.1	349.0	0.11 %	0.14 %	--
	PTV	SPIT	1340.3	2931.8	2608.3	203.3	0.00 %	90.87 %	--

Fig. 3 DVH for patient presented in Fig. 2. As per SC 24 protocol, max point dose constraints of 17 Gy to the cord PRV and 20 Gy to the esophagus were met. More than 90% of the PTV received the prescription dose of 24 Gy

Another Canadian phase III trial is currently accruing patients comparing 24 Gy in 2 fxs with 20 Gy in 5 fxs in the treatment of spinal metastases. Table 3 outlines the organ at risk dose constraints used in the SC.24 Canadian randomized controlled trial (NCT02512965) [19]. Both have complete pain response as their primary endpoint. The final results of each of these trials may dictate the extent of adoption of this practice worldwide when treating painful spinal metastases. Studies in the oligometastatic setting are also underway, and this paradigm shift in oncology toward an ablative approach in the oligometastatic setting is also leading to increased use of spine SBRT.

Extending SBRT dosimetry planning to further inform surgical planning, in the context of separation surgery for patients with spinal metastases, may be another avenue for multidisciplinary care. Further work on software algorithms to model decompression and reconstitution of the thecal sac based on the preoperative MRI, and linked to the decompression as it is being performed in real-time, may help to guide separation surgery for the optimal extent of epidural resection. While preliminary work has been done, additional clinical tools need to be developed to incorporate radiation dose planning software with surgical planning and spinal navigation software [42].

Table 3 Organs at Risk (OAR) Tolerance Guidelines for 24 Gy in 2-fraction SBRT specific to de novo metastases as per the SC24 randomized trial protocol

Organ	Dose constraints
CORD PRV (1.5 mm beyond true cord contour) and/or thecal sac	17 Gy maximum point dose
Esophagus, stomach, rectum, and bowel	20 Gy maximum point dose
Kidneys	26 Gy maximum point dose
	Mean dose to each <= 6 Gy
Liver	26 Gy maximum point dose
	Mean dose <= 8 to 9 Gy
Lungs	V5 < 35%, V10 < 10%, V20 < 3%[a]
	Mean dose to each <= 5 Gy
Parotids	Mean dose to each <= 7 Gy
Pharynx and larynx	20Gy maximum point dose
	Mean dose <= 9 Gy
Sacral nerve roots (for S1–S5 tumors)	<=26 Gy maximum point dose
Trachea	<=20 Gy maximum point dose

Data from Ref. [19]
[a]Dose to each lung considered separate

Going forward, predicting which patients require surgical intervention, or are at risk of toxicity, is of the utmost importance. Evidence-based algorithms guiding surgical intervention both before SBRT and in the setting of developing a VCF are sorely needed. For example, computational segmentation processes to determine the volume of lytic disease in the vertebral body has been shown to predict the risk of VCF. Thibault and colleagues observed that when the volumetric lytic disease threshold exceeds 11.6%, the odds ratio was 37.4 with respect to predicting subsequent VCF [43]. The future lies in these types of studies that are based on semi-automated computational processes to provide objective and quantitative measures of the spinal segment characteristics to guide risk analyses for VCF, thereby, minimizing subjectivity in the SINS when determining risk of VCF.

Practical Considerations

- Patients with oligometastatic disease and a limited number of spinal metastases are eligible for spine SBRT.
- SINS score and Bilsky grade should be evaluated at presentation with appropriate referral to a spine surgeon if high risk for instability and/or cord compression.
- A rigorous evaluation of the simulation procedure, immobilization devices, and imaging modalities should be performed to ensure ability to accurately delineate the target and to minimize the PTV.
- CTV delineation should follow International Spine Research Consortium consensus guidelines [40].
- Plan evaluation includes ensuring slice by slice that the dose gradient adjacent to the spinal cord and thecal sac is maximized especially in the case of epidural disease.
- Follow-up with an MRI whole spine every 3 months for the first year is critical as VCF also occurs most often within the first 6 months post-SBRT.
- Worsening, or incidence, of mechanical pain should prompt x-ray and further imaging as indicated to rule out spine fracture which has an incidence of 10–15% but can be as high as 40% with 24 Gy in a single fraction.

References

1. Sahgal A, Roberge D, Schellenberg D, Purdie TG, Swaminath A, Pantarotto J, et al. The Canadian Association of Radiation Oncology scope of practice guidelines for lung, liver and spine stereotactic body radiotherapy. Clin Oncol. 2012;24:629–39.
2. Foote M, Letourneau D, Hyde D, Massicotte E, Rampersaud R, Fehlings M, et al. Technique for stereotactic body radiotherapy for spinal metastases. J Clin Neurosci. 2011;18:276–9.
3. Tseng C-L, Eppinga W, Charest-Morin R, Soliman H, Myrehaug S, Maralani PJ, et al. Spine stereotactic body radiotherapy: indications, outcomes, and points of caution. Glob spine J. 2017;7:179–97.
4. Jabbari S, Gerszten PC, Ruschin M, Larson DA, Lo SS, Sahgal A. Stereotactic body radiotherapy for spinal metastases. Cancer J. 2016;22:280–9.
5. Husain ZA, Sahgal A, De SA, Funaro M, Glover J, Hayashi M, et al. Stereotactic body radiotherapy for de novo spinal metastases: systematic review. J Neurosurg Spine. 2017 Sep;27(3):295–302.
6. Ryu S, Jin R, Jin J-Y, Chen Q, Rock J, Anderson J, Movsas B. Pain control by image-guided radiosurgery for solitary spinal metastasis. J Pain Symptom Manag. 2008;35:292–8.
7. Wang XS, Rhines LD, Shiu AS, ,Yang JN, Selek U, Gning I, et al. Stereotactic body radiation therapy for management of spinal metastases in patients without spinal cord compression: a phase 1-2 trial. Lancet Oncol 2012;13:395–402.
8. Myrehaug S, Sahgal A, Hayashi M, Levivier M, Ma L, Martinez R, Paddick I, Régis J, Ryu S. Reirradiation spine stereotactic body radiation therapy for spinal metastases: systematic review. J Neurosurg Spine. 2017;27(4):428–35.
9. Redmond KJ, Lo SS, Fisher C, Sahgal A. Postoperative stereotactic body radiation therapy (SBRT) for spine metastases: a critical review to guide practice. Int J Radiat Oncol Biol Phys. 2016;95:1414–28.
10. Mizumoto M, Harada H, Asakura H, Hashimoto T, Furutani K, Hashii H, et al. Radiotherapy for patients with metastases to the spinal column: a review of 603 patients at shizuoka cancer center hospital. Int J Radiat Oncol Biol Phys. 2011;79:208–13.
11. Thibault I, Al-Omair A, Masucci GL, Masson-Côté L, Lochray F, Korol R, et al. Spine stereotactic body radiotherapy for renal cell cancer spinal metastases: analysis of outcomes and risk of vertebral compression fracture. J Neurosurg Spine. 2014;21:711–8.
12. Leeman JE, Bilsky M, Laufer I, Folkert MR, Taunk NK, Osborne JR, et al. Stereotactic body radiotherapy for metastatic spinal sarcoma: a detailed patterns-of-failure study. J Neurosurg Spine. 2016;25:52–8.
13. Stinauer MA, Kavanagh BD, Schefter TE, Gonzalez R, Flaig T, Lewis K, Robinson W, Chidel M, Glode M, Raben D. Stereotactic body radiation therapy for melanoma and renal cell carcinoma: impact of single fraction equivalent dose on local control. Radiat Oncol. 2011;6:34.

14. Chow E, van der Linden YM, Roos D, Hartsell WF, Hoskin P, Wu JS, et al. Single versus multiple fractions of repeat radiation for painful bone metastases: a randomised, controlled, non-inferiority trial. Lancet Oncol. 2014;15:164–71.
15. Chow E, Harris K, Fan G, Tsao M, Sze WM. Palliative radiotherapy trials for bone metastases: a systematic review. J Clin Oncol. 2007;25:1423–36.
16. Nguyen Q-N, Shiu AS, Rhines LD, Wang H, Allen PK, Wang XS, Chang EL. Management of spinal metastases from renal cell carcinoma using stereotactic body radiotherapy. Int J Radiat Oncol. 2010;76:1185–92.
17. Anand AK, Venkadamanickam G, Punnakal AU, Walia BS, Kumar A, Bansal AK, Singh HM. Hypofractionated stereotactic body radiotherapy in spinal metastasis – with or without epidural extension. Clin Oncol. 2015;27:345–52.
18. Ryu S, Pugh SL, Gerszten PC, Yin FF, Timmerman RD, Hitchcock YJ, et al. RTOG 0631 phase 2/3 study of image guided stereotactic radiosurgery for localized (1-3) spine metastases: phase 2 results. Pract Radiat Oncol. 2014;4:76–81.
19. Sahgal A, Myrehaug S, Dennis K, Liu M, Chow E, Wong R, et al. A randomized phase II/III study comparing stereotactic body radiotherapy (SBRT) versus conventional palliative radiotherapy (CRT) for patients with spinal metastases (NCT02512965). J Clin Oncol. 2017;35:TPS10129-TPS10129.
20. Versteeg AL, Verlaan J-J, Sahgal A, Mendel E, Quraishi NA, Fourney DR, Fisher CG. The spinal instability neoplastic score: impact on oncologic decision-making. Spine (Phila Pa 1976). 2016;41:S231–7.
21. Fisher CG, DiPaola CP, Ryken TC, Bilsky MH, Shaffrey CI, Berven SH, et al. A novel classification system for spinal instability in neoplastic disease: an evidence-based approach and expert consensus from the Spine Oncology Study Group. Spine (Phila Pa 1976). 2010;35:E1221–9.
22. Lee S-HH, Tatsui CE, Ghia AJ, Amini B, Li J, Zavarella SM, Tannir NM, Brown PD, Rhines LD. Can the spinal instability neoplastic score prior to spinal radiosurgery predict compression fractures following stereotactic spinal radiosurgery for metastatic spinal tumor?: a post hoc analysis of prospective phase II single-institution trials. J Neuro-Oncol. 2016;126:509–17.
23. Patchell RA, Tibbs PA, Regine WF, Payne R, Saris S, Kryscio RJ, Mohiuddin M, Young B. Direct decompressive surgical resection in the treatment of spinal cord compression caused by metastatic cancer: a randomised trial. Lancet. 2005;366:643–8.
24. Fehlings MG, Nater A, Tetreault L, Kopjar B, Arnold P, Dekutoski M, et al. Survival and clinical outcomes in surgically treated patients with metastatic epidural spinal cord compression: results of the prospective multicenter AOSpine study. J Clin Oncol. 2016;34:268–76.
25. Hyde D, Lochray F, Korol R, Davidson M, Wong CS, Ma L, Sahgal A. Spine stereotactic body radiotherapy utilizing cone-beam CT image-guidance with a robotic couch: Intrafraction motion analysis accounting for all six degrees of freedom. Int J Radiat Oncol Biol Phys. 2012;82:e555–62.
26. Thibault I, Chang EL, Sheehan J, Ahluwalia MS, Guckenberger M, Sohn MJ, et al. Response assessment after stereotactic body radiotherapy for spinal metastasis: a report from the SPIne response assessment in Neuro-Oncology (SPINO) group. Lancet Oncol. 2015;16:e595–603.
27. Guckenberger M, Mantel F, Gerszten PC, Flickinger JC, Sahgal A, Létourneau D, et al. Safety and efficacy of stereotactic body radiotherapy as primary treatment for vertebral metastases: a multi-institutional analysis. Radiat Oncol. 2014;9:226.
28. Gerszten PC, Germanwala A, Burton SA, Welch WC, Ozhasoglu C, Vogel WJ. Combination kyphoplasty and spinal radiosurgery: a new treatment paradigm for pathological fractures. J Neurosurg Spine. 2005;3:296–301.
29. Huisman M, van den Bosch MAAJ, Wijlemans JW, van Vulpen M, van der Linden YM, Verkooijen HM. Effectiveness of reirradiation for painful bone metastases: a systematic review and meta-analysis. Int J Radiat Oncol. 2012;84:8–14.
30. Thibault I, Campbell M, Tseng CL, Atenafu EG, Letourneau D, Yu E, Cho BCJ, Lee YK, Fehlings MG, Sahgal A. Salvage stereotactic body radiotherapy (SBRT) following in-field failure of initial SBRT for spinal metastases. Int J Radiat Oncol Biol Phys. 2015;93:353–60.
31. Chiang A, Zeng L, Zhang L, Lochray F, Korol R, Loblaw A, Chow E, Sahgal A. Pain flare is a common adverse event in steroid-naïve patients after spine stereotactic body radiation therapy: a prospective clinical trial. Int J Radiat Oncol Biol Phys. 2013;86:638–42.
32. Pan HY, Allen PK, Wang XS, Chang EL, Rhines LD, Tatsui CE, et al. Incidence and predictive factors of pain flare after spine stereotactic body radiation therapy: secondary analysis of phase 1/2 trials. Int J Radiat Oncol. 2014;90:870–6.
33. Chow E, Meyer RM, Ding K, Nabid A, Chabot P, Wong P, et al. Dexamethasone in the prophylaxis of radiation-induced pain flare after palliative radiotherapy for bone metastases: a double-blind, randomised placebo-controlled, phase 3 trial. Lancet Oncol. 2015;16:1463–72.
34. Sahgal A, Weinberg V, Ma L, Chao S, Muacevic A, Gorgulho A, et al. Probabilities of radiation myelopathy specific to stereotactic body radiation therapy to guide safe practice. Int J Radiat Oncol Biol Phys. 2013;85:341–7.
35. Katsoulakis E, Jackson A, Cox B, Lovelock M, Yamada Y. A detailed dosimetric analysis of spinal cord tolerance in high-dose spine radiosurgery. Int J Radiat Oncol Biol Phys. 2017;99:598–607.
36. Sahgal A, Ma L, Weinberg V, Gibbs IC, Chao S, Chang UK, et al. Reirradiation human spinal cord tolerance for stereotactic body radiotherapy. Int J Radiat Oncol Biol Phys. 2012;82:107–16.
37. Cox BW, Jackson A, Hunt M, Bilsky M, Yamada Y. Esophageal toxicity from high-dose, single-fraction paraspinal stereotactic radiosurgery. Radiat Oncol Biol. 2012;83:e661–7.
38. Sahgal A, Atenafu EG, Chao S, Al-Omair A, Boehling N, Balagamwala EH, et al. Vertebral compression fracture after spine stereotactic body radiotherapy: a multi-institutional analysis with a focus on radiation dose and the spinal instability neoplastic score. J Clin Oncol. 2013;31:3426–31.
39. Faruqi S, Tseng C-L, Whyne C, Alghamdi M, Wilson J, Myrehaug S, et al. Vertebral compression fracture after spine stereotactic body radiation therapy: a review of the pathophysiology and risk factors. Neurosurgery. 2018 Sep 1;83(3):314–22.
40. Cox BW, Spratt DE, Lovelock M, Bilsky MH, Lis E, Ryu S, et al. International spine radiosurgery consortium consensus guidelines for target volume definition in spinal stereotactic radiosurgery. Int J Radiat Oncol Biol Phys. 2012 Aug 1;83(5):e597–605.
41. Chan MW, Thibault I, Atenafu EG, Yu E, John Cho BC, Letourneau D, et al. Patterns of epidural progression following postoperative spine stereotactic body radiotherapy: implications for clinical target volume delineation. J Neurosurg Spine. 2016;24:652–9.
42. Jakubovic R, Ruschin M, Tseng CL, Pejovic-Milic A, Sahgal A, Yang VXD. Surgical resection with radiation treatment planning of spinal tumours. Neurosurgery. 2018; https://doi.org/10.1093/neuros/nyy176. [Epub ahead of print]
43. Thibault I, Whyne CM, Zhou S, Campbell M, Atenafu EG, Myrehaug S, et al. Volume of lytic vertebral body metastatic disease quantified using computed tomography based image-segmentation predicts fracture risk following spine stereotactic body radiotherapy. Int J Radiat Oncol. 2016;97:75–81.

Stereotactic Body Radiation Therapy for Gastrointestinal Cancers

Pablo Munoz-Schuffenegger, Aisling S. Barry, and Laura A. Dawson

Introduction

Two-thirds of patients diagnosed with hepatocellular carcinoma (HCC) are unsuitable for liver transplant or surgical resection due to poor liver function, poor performance status, or locally advanced disease. In patients who are not suitable for liver transplant or tumor resection, local treatment alternatives such as radiofrequency ablation (RFA) and transarterial chemoembolization (TACE) are often considered, with favorable results in selected treatment populations [1]. Radiotherapy (RT) for the treatment of primary or secondary liver cancer has historically been used with caution, due to the documented risk of radiation-induced liver disease [2]. However, with recent advances in image guidance and treatment delivery, stereotactic body radiation therapy (SBRT) has the ability to spare functional liver while delivering high doses of highly focused radiation to tumor targets. It has, in recent times, emerged as an effective treatment option initially considered for patients who were not suitable for standard treatments but more recently as an alternative or an adjunct to other HCC treatments.

Pancreatic cancer carries a dismal prognosis, and a complete surgical resection with negative margins (R0) is currently the only curative treatment, with only 10–15% of patients presenting with resectable disease. In patients with borderline or locally advanced pancreatic cancer (LAPC), up to one-third die from locally advanced disease rather than distant metastasis, supporting the hypothesis that achieving local control or delaying local progression is fundamental in preventing tumor progression and improving overall survival. Historically, when combination chemoradiation treatment is considered, conventional fractionation (1.8−2 Gy per fraction) has been used. Nonetheless, outcomes remain poor with local control rates of 40–50% and median overall survival of 5–14 months [3]. SBRT brings many advantages to the treatment of pancreatic cancer: it can be administered as a hypofractionated (dose range, 30–45 Gy) regimen over 3–5 days, has the potential to provide adequate local control thus limiting the start of systemic therapy or surgical resection, and is shown to provide pain improvement while preserving quality of life [4]. SBRT has been used with more promising outcomes, although there is a lack of level one evidence and possibility for selection bias.

Despite overall encouraging outcomes with the use of SBRT for the treatment of liver and pancreatic malignancies, there continue to be several challenges that require further knowledge, including the presence of surrounding dose-limiting organs which pose a barrier to dose escalation, poor contrast with the use of kilovoltage (kV) images for image guidance in the treatment unit, and tumor motion.

The aim of this chapter is to review the current status of SBRT in the management of liver and pancreatic cancer, highlighting the planning and treatment challenges specific to its use in the treatment of these malignancies.

Site-Specific Considerations

Primary and Secondary Liver Cancer

The liver is a critically important organ that plays many vital roles within the body, including assisting the digestive process with the production of bile, facilitating the metabolism of ingested nutrients, and the elimination of many waste products. It is involved in glycogen storage, decomposition of red blood cells, plasma protein synthesis, and detoxification. It is described as a parallel-functioning organ and,

P. Munoz-Schuffenegger · A. S. Barry (✉) · L. A. Dawson
Princess Margaret Cancer Center, Radiation Medicine Program, Toronto, ON, Canada

University of Toronto, Department of Radiation Oncology, Toronto, ON, Canada
e-mail: Pablo.munoz@rmp.uhn.ca; Aisling.barry@rmp.uhn.ca; Laura.dawson@rmp.uhn.ca

D. M. Trifiletti et al. (eds.), *Stereotactic Radiosurgery and Stereotactic Body Radiation Therapy*,
https://doi.org/10.1007/978-3-030-16924-4_24

therefore, can receive high doses of radiation as long as a sufficient volume of healthy liver tissue is spared.

Liver motion is complex owing to organ deformation and rotation with respiration. Studies have shown that liver motion due to breathing is largest in the craniocaudal direction, ranging from 5–50 mm. This motion has adverse effects on RT planning and treatment including the introduction of artifacts on planning CT scans, altered dosimetry based on a static plan, increased volume of normal tissue radiation, increased toxicity, and limitations to the radiation dose that can safely be delivered to the target. Different strategies have been used to address liver motion during radiation treatment that include accounting for motion in the planning treatment volume and controlling motion through abdominal compression, breath-hold techniques, respiratory gating, and real-time tumor tracking [5].

Contouring for liver lesions should be performed on a multiphasic contrast-enhanced treatment planning CT scan with the aid of diagnostic imaging such as MRI to identify the gross tumor volume (GTV). Ideally, both a planning CT and MRI should be used for contouring, as there can be significant differences between CT- and MRI-based GTVs [6]. For most hepatic metastases, lesions are often best seen in the portal venous CT phase and appear hypodense in relation to the liver parenchyma as, on the other hand, primary liver cancer is best seen in the arterial or delayed phase CT, with vascular invasion of HCC best seen in venous phase imaging (Fig. 1). Given the proximity of luminal organs at risk

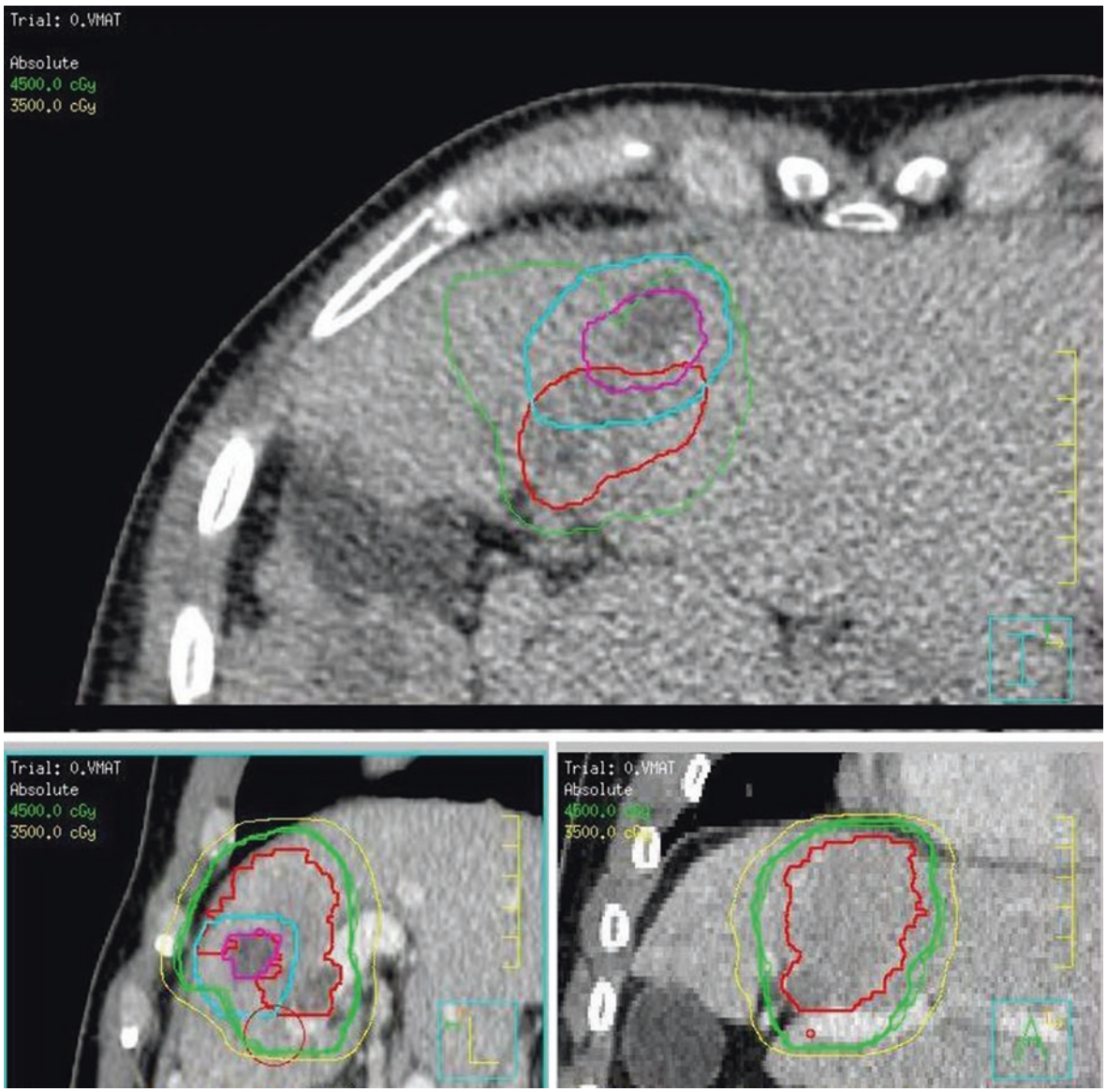

Fig. 1 HCC with vascular invasion. In the upper figure, the arterial phase helps in delineating the parenchymal tumor, although it does not show portal vein invasion as well as the venous phase does (below). Also note that a RFA cavity that looks similar to the parenchymal tumor on the arterial phase is better defined in the venous phase. Parenchymal GTV: red. RFA cavity: purple. Parenchymal PTV: dark green. RFA cavity PTV: cyan. Green: 45 Gy isodose. Yellow: 35 Gy isodose, in five fractions

(OAR), such as the stomach and duodenum, it is recommended to include oral water and/or contrast to aid in delineating these structures.

Daily image guidance is necessary for the treatment of liver cancer, as intra- and inter- fractional motion can be considerable. Ventilatory movement of the liver and liver tumors may be as high as 20 mm, and efforts to reduce or eliminate motion are needed, e.g., with breath-hold or abdominal compression. [7]. Image guidance using a soft tissue surrogate such as inserted fiducial markers, lipiodol following TACE, calcifications, surgical clips, the liver itself or portion of the liver adjacent to the tumor is needed. Cone-beam computed tomography (CBCT) liver matching has been suggested to be superior to orthogonal x-rays [8]. Breath-hold CBCT and respiratory correlated CBCT may have advantages to 3D CBCT.

Pancreatic Cancer

With current on-treatment image guidance strategies, pancreatic tumors are inadequately visualized due to poor soft tissue contrast. In addition, there are several sources of inter- and intrafraction pancreatic motion that need to be considered at the time of planning and treating with SBRT including breathing, bowel filling, and variation in patient positioning. Similar to that of liver, many methods to account for pancreatic motion exist [5]. Regardless of the motion management technique used, the approach should be customized to patient tolerance with a goal to reduce residual motion to as low as possible (e.g., <3–5 mm). At the time of simulation, intravenous and oral water/contrast is once again used to aid target and OAR contouring.

Fiducials are required to track tumor motion, as pancreatic motion can be highly variable, and tumor position does not correlate properly with abdominal wall or diaphragmatic motion [9]. Generally, three fiducial markers may be placed at the tumor periphery and within 1 cm of the tumor, either percutaneously with CT guidance or preferentially via endoscopic ultrasound guidance. Biliary stents do not remain in a stable configuration with intratumoral fiducials for pancreatic head tumors and can lead to potential over- and underestimation of respiratory-induced motion and thus should not be used as a surrogate for the tumor on their own [10].

Given that CT provides suboptimal soft tissue delineation for target delineation, MRI complementing CT has been shown to result in smaller target volumes and reduced interobserver variation [11]. Recommendations for MRI-based contouring of GTV and organs at risk for radiation treatment of pancreatic cancer have recently been published by Heerkens and associates [12].

Clinical Evidence

HCC

Several early-phase prospective trials on the role of SBRT for HCC have been reported and summarized on Table 1. Blomgren and coworkers published the first prospective trial in 1995 [13] in which a mixed patient population including primary and secondary liver tumors were treated. In this study, eight patients with biopsy-proven HCC received a treatment dose to the PTV of 15–45 Gy, delivered in one to three fractions. In four patients there was no tumor reduction on subsequent follow-up imaging, and in two patients there were volume reductions noted at 1.5 and 6 months, respectively. All patients developed fever and nausea after treatment; three patients developed classic RILD, and one patient died 2 days after treatment.

Mendez-Romero and coworkers published a prospective trial in 2006 [14], in which eight patients with 11 liver lesions measuring up to 7 cm, ineligible for other local therapies, were treated. The prescription dose ranged from 25 Gy in five fractions to 37.5 Gy in three fractions, based on the lesion size and the presence of cirrhosis. Local control and overall survival at 1 year were both 75%. Subsequently, there has been a plethora of primarily single-institution series showing similarly high rates of local control. Jang and coworkers reported outcomes on 82 patients that were unsuitable for surgery or local ablation and had incomplete response to TACE; these patients were treated with SBRT to a dose 33–60 Gy in three fractions (median dose, 51 Gy). With a median follow-up of 30 months, local control was 87% at 2 years [15]. Andolino and coworkers reported results from 60 patients with HCC treated with SBRT at Indiana University, to a median dose of 40 Gy in patients with Child-Pugh (CP)-A liver function and 44 Gy in those with CP-B liver function. With a median follow-up of 27 months, 2-year local control was 90%, and overall survival (OS) was 67%. Twenty percent of patients experienced a decline in their CP liver function within 3 months of treatment.

Bujold and coworkers published the largest prospective data series of HCC SBRT to date, in primarily locally advanced patients [16]. In sequential phase I/II trials conducted at the Princess Margaret Cancer Centre including 102 patients, all unsuitable for other local therapies, 55% with major portal vein invasion and 12% had extrahepatic disease. Local control and overall survival at 1 year after a treatment dose of 24–54 Gy in six fractions were 87% and 55%, respectively. Grade ≥ 3 toxicity occurred in 30% of patients, and seven deaths occurring 1.1–7.7 months after SBRT were probably related to treatment. Also, 29% of patients developed a decline in CP function class at 3 months after treatment.

Table 1 Selected series of prospective studies of SBRT for HCC

Study, type of data	Median follow-up	No. of patients	No. of lesions	Child-Pugh class B (%)	Portal vein thrombus (%)	Previous liver therapy (%)	Median GTV diameter (cm., range)	Total dose (Gy)/ no. of fractions	One-year local control (%)	One-year overall survival (%)	Grade 3+ toxicity (%)
Mendez-Romero et al. [14], phase II	12.9	8	11	25	25		3.5		75	75	12.5
Kang et al. [43], phase II	17	47	56	13 (all B7)	11	100	2.9	42–60/3	2-year: 95	2-year: 69	11 (GI ulcer), 4 (ascites), 11 (thrombocytopenia), 4 (hyperbilirrubinemia)
Bujold et al. [16], phase I/II	31.4	102	Multiple in 60.8%	0	55	52	7.2	Median = 36 (range, 24–54/6)	87	55	30
Culleton et al., on- and off-study [44]		29	Median of 2 lesions	97	76	14	Sum of all lesions: 8.6	Median = 30/6		32	63% had decline in CP score by 2 or more at 3 months
Lasley et al. [45], phase I/II	CPA, 33; CPB, 36	65	65	36	20	15	Volume: 33.6 mL	Median = 48	CPA: 91 CPB: 82	CPA: 94 CPB: 57	CPA: 11 CPB: 38
Scorsetti et al. [46], observational study	8	43	63	47	20	44	4.8 (1.0–12.5)	<3 cm: 48–75/3 3–6 cm: 36–60/6	86	78	16
Takeda et al. [17], phase II	41.7	90	90	32	3	64	2.3 (1.0–4.0)	35–40/5	3-year: 96.3%	3-year: 66.7%	16.7

Modified with permission of Elsevier from Murray and Dawson [47]
GTV gross tumor volume, *CP* Child-Pugh score.

Recently, Takeda and coworkers reported the results of a phase II study of SBRT and optional TACE for patients with solitary HCC measuring less than 4 cm, not amenable to resection or RFA [17]; the prescription dose was 35–40 Gy in five fractions. A total of 90 patients were evaluable, and 64% had TACE before SBRT; at a median follow-up of 41.7 months, 3-year primary local control rate was 96.3%, and the 3-year intrahepatic control rate was 33.9%. Three-year overall survival was 66.7%. Six patients developed grade 3 laboratory-related abnormalities, including elevated transaminases and decreased platelet counts. There was no treatment-related gastrointestinal side effects. The combination of TACE and SBRT is being investigated in randomized trials (NCT02507765).

Sorafenib, a small molecule tyrosine kinase inhibitor, has shown to increase overall survival in patients with major vascular involvement or extrahepatic disease in two randomized prospective studies [18, 19]. However, most patients treated eventually progressed within the liver and died of liver failure, providing the rationale to use SBRT in combination with sorafenib. Currently, this combination in patients with locally advanced HCC unsuitable for or refractory to TACE is the focus of the ongoing Radiation Therapy Oncology Group (RTOG) 1112 trial (NCT01730937), a phase 3 study comparing the combination of SBRT and sorafenib against sorafenib alone.

Several retrospective studies on the role of SBRT as a curative treatment in the management of early-stage HCC have been published. Recently, Wahl and coworkers compared radiofrequency ablation (RFA) and SBRT for small-sized HCC treated at the University of Michigan [20]. One-year freedom from local progression for tumors treated with RFA was 83.6%, compared to 97.4% in those treated with SBRT. Increasing tumor size predicted for freedom from local progression in lesions treated with RFA, but not with SBRT; for tumors larger than 2 cm, there was decreased freedom from local progression for RFA compared with SBRT. In a recent propensity score-matched analysis conducted in China comparing 82 patients treated with SBRT and 35 patients that underwent liver resection, 1-year progression-free survival was 84.4% in the SBRT group compared with 69% in the liver resection group; the SBRT group showed fewer complications, such as hepatic hemorrhage, hepatic pain, and weight loss [21]. Sapir and coworkers conducted a single-institution comparison of TACE and SBRT for patients with HCC with one or two tumors [22]. Patients treated with SBRT were older, had smaller tumors, and less frequently underwent liver transplantation. At 1 year, local control was 97% in patients treated with SBRT and 47% in those treated with TACE; patients needed more additional liver-directed therapies and systemic therapy after TACE compared to SBRT. Overall, most experience, primarily in patients with intact liver function (e.g., CP-A or early CP-B7), appears to suggest that HCC is a radiation-sensitive tumor, and SBRT is generally well tolerated in appropriately selected patients.

Liver transplantation remains the best treatment option for patients with selected HCC. Recently, Sapisochin and coworkers at the University of Toronto conducted a retrospective study comparing SBRT, TACE, and RFA as bridge to liver transplantation [23]. The drop-out rate was similar between groups, so were postoperative complications. One-year actuarial patient survival from the time of listing was 83% in the SBRT group, 86% in the TACE group, and 86% in the RFA group. These outcomes are encouraging and suggest that SBRT can be safely used as a bridge to liver transplantation in patients with HCC, as an alternative to conventional bridging therapies.

Liver Metastases

Many single- and multiple-institution series have been published on the role of SBRT for the treatment of liver metastases. However, to date, there are no published phase III randomized trials on the use of SBRT for liver metastases.

Blomgren and associates treated 14 patients with liver metastases as part of their initial SBRT experience at the Karolinska Institutet [13]. The total minimum dose to the PTV went from 7.7 to 45 Gy, delivered in one to four fractions. In five lesions there was local progression, six remained unchanged, and four resolved completely on subsequent imaging studies. Investigators from the Heidelberg University published the first report on prospective outcomes on single-fraction SBRT for liver metastases [24] in which 37 patients, with 55 liver lesions, were treated and a dose escalation approach starting from 14 Gy and escalating to 26 Gy was used. The 18-month local control was 67% for all patients, being significantly higher for those treated at 22–26 Gy compared to those treated at 14–20 Gy (82% vs. 0%); it was noted that local control improved in those patients who were enrolled later into the study.

Mendez-Romero and associates performed a phase I/II trial of three-fraction SBRT in patients with primary and metastatic liver lesions, in which 34 liver metastases were treated to a dose of 37.5 Gy in three fractions. A 2-year local control rate of 86% was reported; 1-year and 2-year overall survival was 85% and 62%, respectively. There were three grade 3 toxicities. Hoyer and associates reported outcomes of 44 liver metastases treated with SBRT to a dose of 45 Gy in three fractions, with a 2-year local control of 79%. Treatment-related toxicity included one patient who died of liver failure, one patient with colonic perforation that needed surgical management, and two patients with duodenal perforation managed conservatively.

In a multi-institutional phase I/II study led by the University of Colorado group, a 3-fraction SBRT regimen for patients with 3 or fewer metastases (measuring less than 6 cm) was evaluated in 47 patients with 63 metastases. Thirty-eight patients received the phase II dose of 60 Gy in three fractions. The 1-year and 2-year actuarial control rates were 95% and 92%, respectively; among lesions measuring less than 3 cm, the 2-year local control rate was 100%. Only one patient experienced grade 3 or higher toxicity.

The Princess Margaret Cancer Centre conducted a phase I trial on SBRT for liver metastases using a six-fraction regimen [25]. The radiation treatment dose was escalated in an individualized fashion, on the basis of each patient's expected risk of radiation-induced liver disease. The median prescribed dose was 41.4 Gy in six fractions (range, 27.7–60 Gy), and the median GTV per patient was 75.2 mL (range, 1.2–3090 mL), larger than most other series. Among 68 patients, there were only two grade-3 liver enzyme changes, with no RILD, or dose-limiting toxicities observed. With a median follow-up of 10.8 months, the 12-month local control rate was 71%, and the 18-month overall survival rate was 47% (Fig. 2).

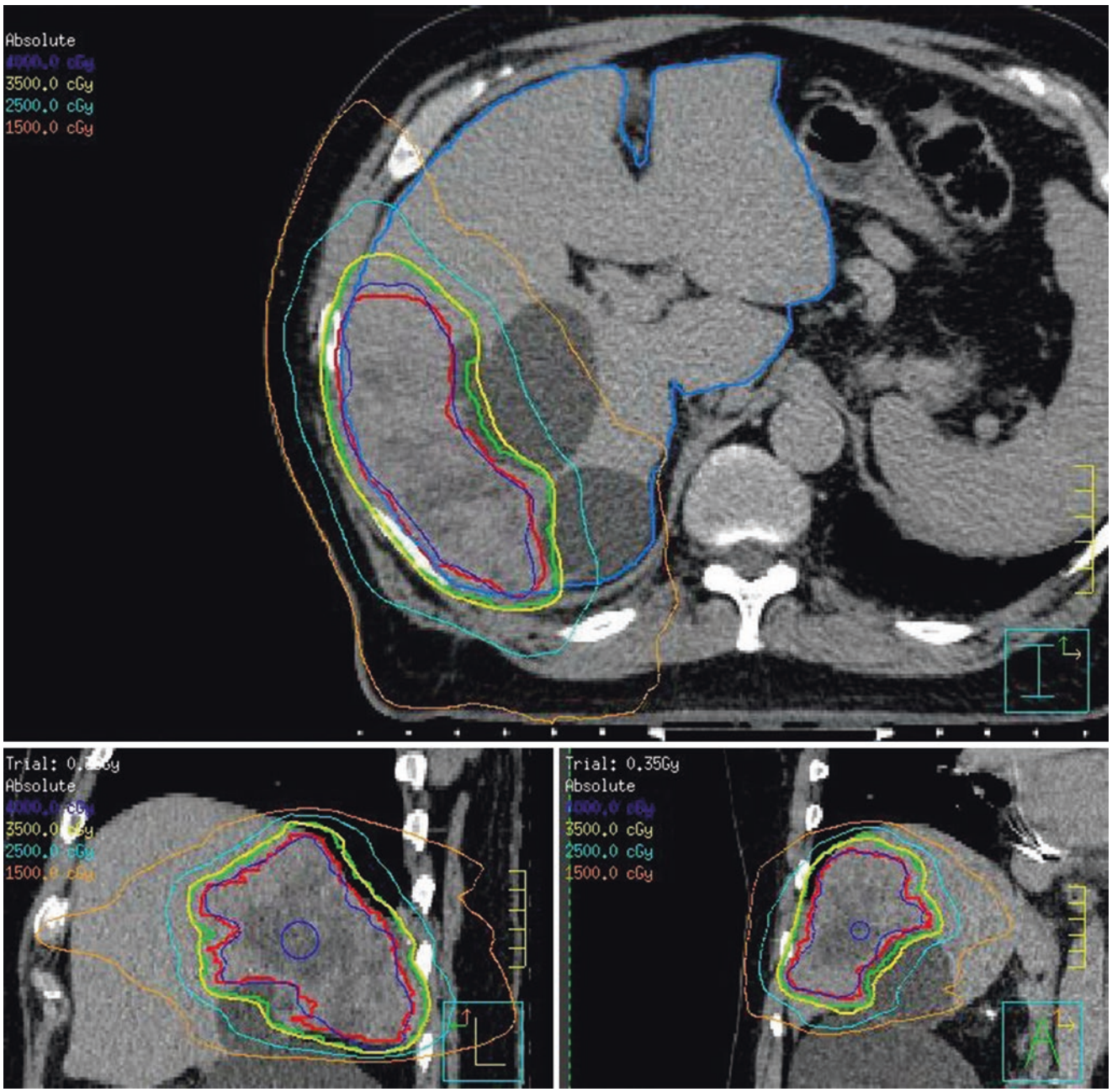

Fig. 2 A large-volume isolated liver metastases from colorectal cancer, treated to a dose of 35 Gy in five fractions. Note that this lesion is located next to a liver and a renal cyst. GTV: red. PTV: green. Yellow: 35 Gy isodose. Cyan: 25 Gy isodose. Orange: 15 Gy isodose

Many potential prognostic factors for local control after liver SBRT for liver metastases have been described, including tumor size [24, 25], treatment dose, and histology. In patients treated with SBRT for colorectal cancer liver metastases, a pooled analysis from three institutions revealed that total dose, dose per fraction, and BED were correlated with local control by lesion. Using different dose-response modeling methods, the estimated dose range needed for 1-year local control >90% was 46–52 Gy in three fractions [26]. Moreover, sustained local control was closely correlated with overall survival. A recent report on the long-term outcomes from the Princess Margaret Cancer Centre's phase I and II trials on SBRT for colorectal liver metastases confirmed the association between smaller tumor volumes, performance status 0 to 1, no extrahepatic disease at the time of treatment, and local control with overall survival [27].

Pancreatic Cancer

Despite not being recognized as a standard of care option in pancreatic cancer until recently, SBRT has been adopted in many institutions worldwide due primarily to advantages in shorter treatment time, allowing for local control while limiting the need for prolonged systemic treatment break. Improved pain control and preserved quality of life are also goals of SBRT in this setting.

Early phase I/II trials on the use of single-fraction SBRT (25 Gy in one fraction) for locally advanced pancreatic cancer demonstrated an excellent freedom from local progression and minimal acute toxicity but high rates of late 2–4 GI toxicity, primarily duodenal bleeding [28, 29].

A single-arm phase II multi-institutional study evaluated the use of fractionated SBRT, 33 Gy in five fractions, after gemcitabine in 49 patients. After SBRT, patients continued to receive gemcitabine until disease progression or toxicity [4]. Rates of acute and late grade ≥ 2 gastritis, enteritis, fistula, or ulcer toxicities were 2% and 11%, respectively. Freedom from local disease progression at 1 year was 78%. The median overall survival for this cohort was 13.9 months. Global quality-of-life score was not reduced at 4 months post-SBRT, and significant improvement in pancreatic pain was reported after treatment [30]. In a recent systematic review and meta-analysis of prospective and retrospective studies on SBRT for locally advanced pancreatic cancer comprising 19 studies and 1009 treated patients, the pooled percentage for locoregional control at 1 year was 72.3% and overall survival 51.6% [31].

The data on local recurrence after neoadjuvant chemotherapy and SBRT for upfront resectable or borderline resectable pancreatic cancer are limited to single-institution studies. A retrospective study from Moffitt Cancer Center include 159 patients (110 borderline resectable and 49 locally advanced) [32]. Among patients with borderline resectable pancreatic cancer, 51% underwent surgical resection with 97% achieving an R0 margin, and 7% had pathologic complete response. Median overall survival in the resected patients with borderline resectable disease was 34 months. Acute grade ≥ 3 toxicity was 2% and late grade ≥ 3 was 5%.

Johns Hopkins reported on 88 patients (74 with locally advanced and 14 with borderline resectable) who received induction systemic treatment (72% with gemcitabine) followed by SBRT to a dose of 25–33 Gy in five fractions. Nineteen patients (79% with locally advanced disease) underwent surgical resection, and 84% had margin-negative resections. Median overall survival in those patients who underwent surgical resection was 20.2 months versus 12.3 months in unresected patients.

More recently, treatment with combination systemic treatment with FOLFIRINOX has become the standard of care in patients with LAPC [33]. The combination of pancreatic SBRT and FOLFIRINOX is currently being studied as part of a multi-institutional phase III study comparing the addition of SBRT to systemic treatment alone (NCT01926197).

Toxicity

Patients with underlying chronic hepatic disease, such as viral hepatitis or cirrhosis, tend to develop hepatic toxicity that differs from classic radiation-induced liver disease, first described in patients without primary liver cancer (rapid weight gain, increased abdominal girth, anicteric ascites, isolated elevation of alkaline phosphatase), showing either a general decline in liver function, markedly elevated transaminases, or jaundice within 3 months of completing SBRT, termed "non-classic RILD." The CP scoring system has been used to describe the prognosis of RILD in patients treated with radiation therapy. This score comprises five variables: albumin, bilirubin, international normalized ratio (INR), ascites, and encephalopathy [2].

Many series have shown that liver toxicity is rarely seen after SBRT for liver metastases. In the University of Colorado trial, by sparing a volume of 700 cc of normal liver from receiving >15 Gy, no RILD or other severe toxicities were observed when these constraints were met [34]. In an update from the Princess Margaret Cancer Centre experience on two sequential prospective trials of six-fraction SBRT for liver metastases including 70 patients, low-grade, non-clinically relevant, transient liver enzyme toxicity up to 3 months post-SBRT occurred in 43 patients, mostly grade 1 or 2. The dose to 700 cc of spared liver was associated with this low-grade, transient, acute liver enzyme abnormality [35].

In contrast, patients treated for HCC are more likely to develop radiation-related toxicity, due in part to their underlying disease and comorbidities. A decline in CP score has

been seen following SBRT in 10–30% of early and locally advanced HCC patients within 3 months following SBRT [16]. In a recent prospective study analyzing clinical and dosimetric variables on 101 patients treated on sequential phase I/II trials of SBRT for HCC conducted at the Princess Margaret Cancer Centre, baseline CP score, platelet count, mean liver dose, and dose to 800 cc. of the liver were found to be the strongest variables associated with an increase in CP score 3 months after SBRT. In patients with CP B7 score, 54% experienced an increase in their CP score despite having similar liver volumes and smaller tumor volumes, emphasizing the role of baseline liver function in predicting its deterioration after SBRT [36].

Central biliary toxicity may occur following central hepatic irradiation and should be considered as a different entity from RILD. It presents with acute biliary edema and obstruction or late biliary stricture and/or secondary infection. Multiple dose-volume endpoints have been described as independent predictors of hepatobiliary toxicity after liver SBRT recently [37]. Challenges exist in distinguishing toxicity from potential disease progression, especially in patients with biliary malignancies.

Gastrointestinal, and particularly duodenal toxicity, remains a matter of concern when performing pancreatic SBRT, given the proximity of the pancreas to most organs at risk (Fig. 3a, b). Patients in whom tumors invade the duode-

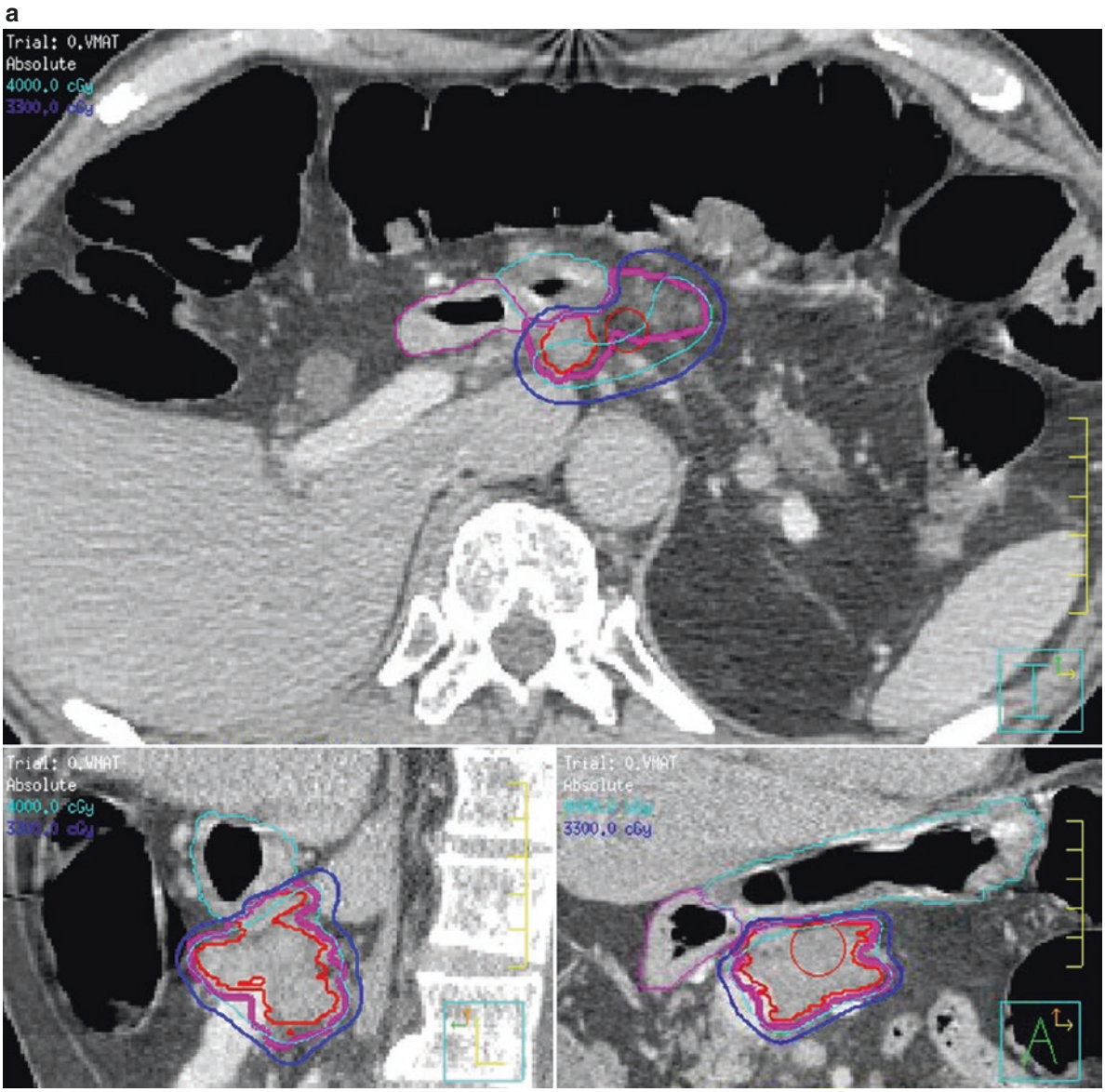

Fig. 3 (**a**) Planning CT scan for a pancreatic SBRT plan to deliver 40 Gy in five fractions to the modified PTV excluding the stomach and duodenum. (**b**) Cone-beam CT for the same patient at the time of the third treatment fraction, with considerable luminal organ distention. This fraction was canceled and treatment was resumed the day after. GTV: red. Modified PTV: purple. Yellow: colon. Stomach: cyan. Duodenum: pink. Blue: 33 Gy isodose, Cyan: 40 Gy isodose

b

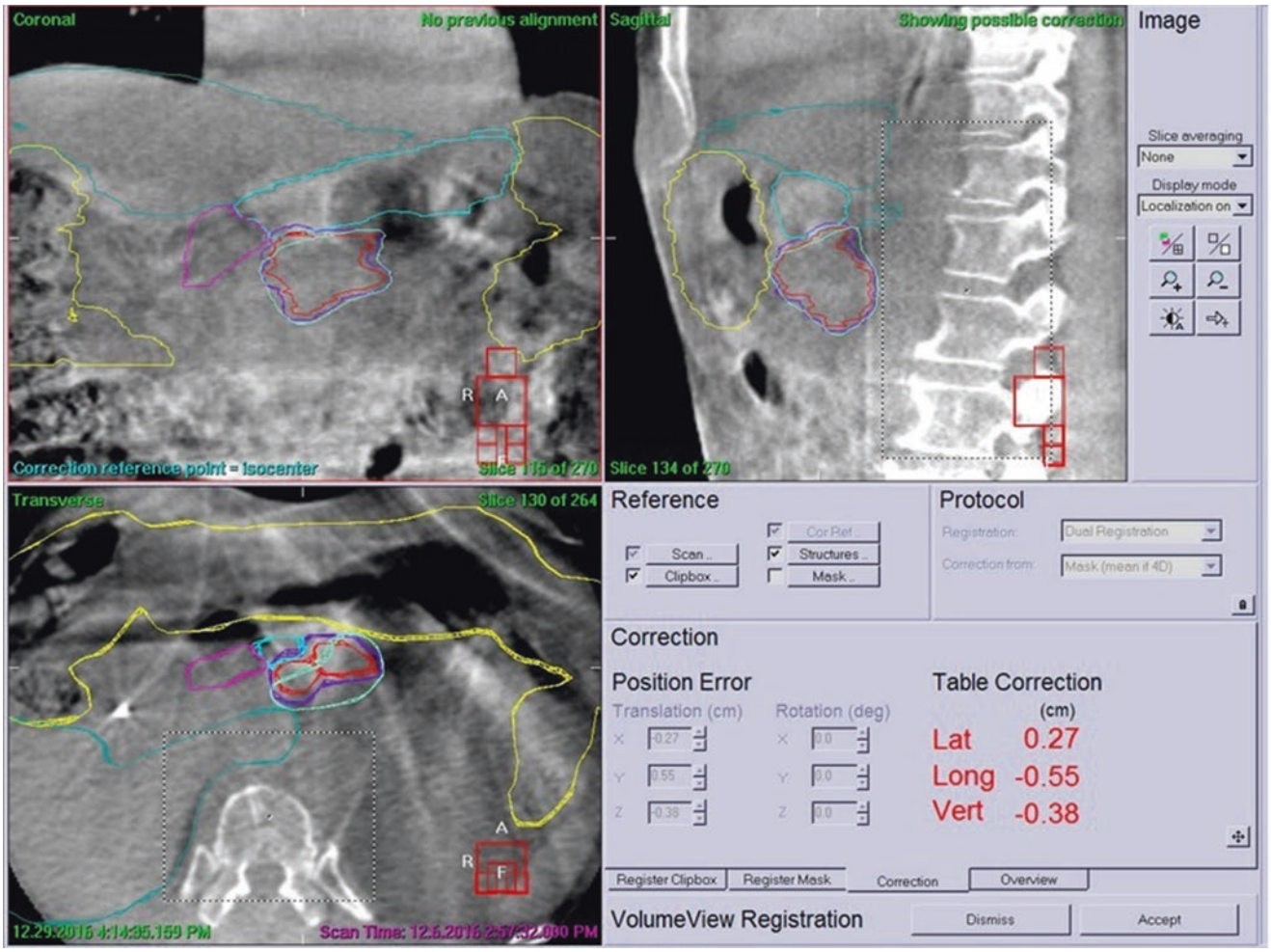

Fig. 3 (continued)

num are not suitable candidates for SBRT. Initial experience with single-fraction SBRT for locally advanced pancreatic cancer showed considerable gastrointestinal grade ≥ 2 late toxicities occurring in up to 47% of patients, mostly in the form of duodenal ulcer or stricture [28]. More recently, results from five- fraction SBRT have shown a considerable decrease in grade ≥ 2 late toxicities to 11%. A study comparing single- versus multi-fraction SBRT from the Stanford group showed that for gastrointestinal grade ≥ 3, the 6- and 12-month cumulative incidence of toxicity were 8.1% and 12.3%, respectively, in the single-fraction group, and both 5.6%, respectively, in the multi- fraction group [38].

Plan Quality

Liver SBRT

Dose objectives to tumor targets differ according to the primary tumor to be treated. When treating HCC, multiple targets, such as parenchymal tumors, RFA cavities, and vascular invasion, can be treated to differential doses to optimize normal liver sparing (Fig. 1). Also, when using SBRT for HCC as a bridging therapy, as the final objective is not complete ablation, doses no higher than 45 Gy in five fractions are recommended, and consideration should be given to reduce the doses in central lesions or in other locations in which fibrosis may lead to a potential increased risk of toxicity [23].

Dose prescription is based on the volume of normal tissues irradiated (correlated with the mean liver dose), as well as proximity to gastrointestinal luminal organs such as the stomach, duodenum, small and large bowel, to the target volumes. In the absence of adjacent GI luminal structures that may limit dose, the PTV dose prescription should be as high as possible based on the mean liver dose (MLD), e.g., as recommended in the RTOG 1112 study (Table 2). In CP B7 patients, strong efforts should be made to keep the MLD as low as possible; a MLD < 6Gy has been previously recommended [39]. Treatment every other day should also be considered particularly in this treatment population. A

Table 2 Mean liver dose constraints used when prescribing SBRT for HCC

Allowed mean liver dose (MLD) (Gy)	Planned prescription dose (Gy)	If maximum allowed MLD is exceeded at this planned dose
13.0	50	Reduce to 45 Gy and re-evaluate
15.0	45	Reduce to 40 Gy and re-evaluate
15.0	40	Reduce to 35 Gy and re-evaluate
15.5	35	Reduce to 30 Gy and re-evaluate
16.0	30	Reduce to 27.5 Gy and re-evaluate
17.0	27.5	Ineligible

Data from Ref. [48] (per the RTOG 1112 protocol (NCT01730937)

three-fraction SBRT regimen can be considered for patients with peripheral tumors and away from luminal structures.

When treating liver metastases, as higher SBRT doses have been associated with improved local control of liver metastases, there is a strong motivation to pursue dose escalation. In the updated Princess Margaret Cancer Centre experience, the delivered MLD was 16 Gy, and 20% of patients received doses >20 Gy in six fractions, without clinically significant toxicity, emphasizing that higher doses can be safely delivered to the same irradiated volume within the liver, compared to patients with HCC. Concomitance of systemic therapies, particularly cytotoxic chemotherapy and targeted therapies, must be avoided as this combination has proven to increase treatment-related toxicity.

Pancreatic Cancer

Several different dose-fractionation regimens and OAR constraints have been described previously [4, 28]. Up to a 30% dose heterogeneity within the PTV is generally permitted when planning, and coverage by the prescription dose should be 95% of at least a modified PTV excluding the luminal OARs (if needed to maintain OAR constraints), with 95% of a non modified PTV receiving 30–33 Gy in five fractions (Fig. 3a, b). In those areas of overlap or proximity to the OARs, less dose covering the PTV (e.g., 30 Gy in 5 fractions) might be advisable to meet dose constraints. An example of dose constraints published in the literature can be found in Table 3.

Future Directions

Dose accumulation and adaptive radiotherapy entails adapting a treatment plan in response to specific anatomic and biological changes that may occur during the course of treatment.

Table 3 Dose constraints for pancreas SBRT

Organ	V15	V20	1 cc	Others
Duodenum	<9 cc	<3 cc	<33Gy	
Stomach	<9 cc	<3 cc	<33Gy	
Spinal cord			<8Gy	Max point dose: 12 Gy
Liver				50% <12Gy
Kidneys				75% < 12Gy If one kidney >10Gy mean, the other should have a V10 < 10%

Used with permission of John Wiley and Sons from Herman et al. [4]

Upper abdominal tumors, such as pancreatic and liver cancer, are particularly suitable for performing adaptive radiation therapy because of their proximity to several critical organs such as the duodenum, stomach, and bowel. Multiple barriers including real time imaging, contouring, and quality assurance, while the patient is lying in bed waiting to be treated [40].

Magnetic Resonance Guided Radiation Therapy (MRgRT), by incorporating MR into the treatment process, provides superior soft tissue imaging with no radiation dose and it is expected to increase the accuracy and precision of treatment, facilitate the process of adaptive radiation treatment, and allow response assessment over the course of treatment. Given the insufficient soft tissue contrast provided by CBCT scans in upper abdominal tumors, it is expected that MRgRT will further improve target visualization and treatment adaptation.

Emerging data show promise for combining SBRT with immune therapy. The rationale is that tumor antigen release achieved by local radiation treatment promotes specific tumor targeting by the adaptive immune system, which can be further augmented by systemic-immune stimulating agents, such as checkpoint inhibitors. Immune-mediated abscopal effects have been seen after radiation treatment in HCC [41], and recently, a phase Ib/II trial of nivolumab (an antiPD-1 monoclonal antibody) in HCC in the second-line setting showed objective responses in 20% of patients; those occurred during the first 3 months and lasted for a median of 17 months [42]. The combination of SBRT and pembrolizumab (another antiPD-1 monoclonal antibody) is being explored as part of a phase 2 clinical trial (NCT03316872) led by our group.

Practical Considerations

Primary and Secondary Liver Cancer

- In HCC patients with CP A and B7 liver function, consider SBRT as a radical treatment or as a bridge to transplant in patients awaiting liver transplant who are not suitable for other bridging local therapies.

- Breathing motion should be minimized or eliminated during SBRT. Many possible strategies to address liver motion exist.
- Given that the risks of liver toxicity are higher in patients with HCC compared with liver metastases, strict observance to MLD constraints is advised.
- When treating liver metastases, in the absence of adjacent GI luminal structures that may limit dose, the PTV dose prescription should be as high as possible based on the mean liver dose (MLD). Otherwise, decreasing dose, or limited PTV under coverage, can be considered to meet dose to adjacent luminal structures.
- Consider treatment every other day in patients with decreased liver function or when dose to OARs is close to established dose constraints. Otherwise, treatment can be done on a daily basis.
- Closely follow-up liver function after SBRT for HCC, as up to 30% of patients with locally advanced HCC can experience a decrease in their CP score after treatment. Risks are higher in patients as baseline CP score worsens.

Pancreatic Cancer

- Given the risk of duodenal stricture and ulcer, patients in whom tumors are not invading the duodenum are potential candidates for SBRT.
- Motion should be minimized as much as possible. Consider several possible strategies to address liver motion according to reproducibility and patient tolerance. Active Breathing Control breath hold is highly recommended. Fiducials are highly recommended to address tumor motion and image guidance.
- Image guidance incorporating CBCT is highly recommended, given the complex relationship of the tumor target with the surrounding organs at risk.
- After SBRT for pancreatic cancer, patients should remain on follow-up with a high index of suspicion upon any new gastrointestinal symptoms.

References

1. Knox JJ, Cleary SP, Dawson LA. Localized and systemic approaches to treating hepatocellular carcinoma. J Clin Oncol. 2015;33(16):1835–44.
2. Munoz-Schuffenegger P, Ng S, Dawson LA. Radiation-induced liver toxicity. Semin Radiat Oncol. 2017;27(4):350–7.
3. Hammel P, Huguet F, van Laethem JL, Goldstein D, Glimelius B, Artru P, et al. Effect of chemoradiotherapy vs chemotherapy on survival in patients with locally advanced pancreatic cancer controlled after 4 months of gemcitabine with or without Erlotinib: the LAP07 randomized clinical trial. JAMA. 2016;315(17):1844–53.
4. Herman JM, Chang DT, Goodman KA, Dholakia AS, Raman SP, Hacker-Prietz A, et al. Phase 2 multi-institutional trial evaluating gemcitabine and stereotactic body radiotherapy for patients with locally advanced unresectable pancreatic adenocarcinoma. Cancer. 2015;121(7):1128–37.
5. Brandner ED, Chetty IJ, Giaddui TG, Xiao Y, Huq MS. Motion management strategies and technical issues associated with stereotactic body radiotherapy of thoracic and upper abdominal tumors: a review from NRG oncology. Med Phys. 2017;44(6):2595–612.
6. Voroney JP, Brock KK, Eccles C, Haider M, Dawson LA. Prospective comparison of computed tomography and magnetic resonance imaging for liver cancer delineation using deformable image registration. Int J Radiat Oncol Biol Phys. 2006;66(3):780–91.
7. Balter JM, Dawson LA, Kazanjian S, McGinn C, Brock KK, Lawrence T, et al. Determination of ventilatory liver movement via radiographic evaluation of diaphragm position. Int J Radiat Oncol Biol Phys. 2001;51(1):267–70.
8. Hawkins MA, Brock KK, Eccles C, Moseley D, Jaffray D, Dawson LA. Assessment of residual error in liver position using kV cone-beam computed tomography for liver cancer high-precision radiation therapy. Int J Radiat Oncol Biol Phys. 2006;66(2):610–9.
9. Feng M, Balter JM, Normolle D, Adusumilli S, Cao Y, Chenevert TL, et al. Characterization of pancreatic tumor motion using cine MRI: surrogates for tumor position should be used with caution. Int J Radiat Oncol Biol Phys. 2009;74(3):884–91.
10. van der Horst A, Lens E, Wognum S, de Jong R, van Hooft JE, van Tienhoven G, et al. Limited role for biliary stent as surrogate fiducial marker in pancreatic cancer: stent and intratumoral fiducials compared. Int J Radiat Oncol Biol Phys. 2014;89(3):641–8.
11. Hall WA, Heerkens HD, Paulson ES, Meijer GJ, Kotte AN, Knechtges P, et al. Pancreatic gross tumor volume contouring on computed tomography (CT) as compared with magnetic resonance imaging (MRI), results of an international contouring conference. Pract Radiat Oncol. 2018;8(2):107–15.
12. Heerkens HD, Hall WA, Li XA, Knechtges P, Dalah E, Paulson ES, et al. Recommendations for MRI-based contouring of gross tumor volume and organs at risk for radiation therapy of pancreatic cancer. Pract Radiat Oncol. 2017;7(2):126–36.
13. Blomgren H, Lax I, Naslund I, Svanstrom R. Stereotactic high dose fraction radiation therapy of extracranial tumors using an accelerator. Clinical experience of the first thirty-one patients. Acta Oncol. 1995;34(6):861–70.
14. Mendez Romero A, Wunderink W, Hussain SM, De Pooter JA, Heijmen BJ, Nowak PC, et al. Stereotactic body radiation therapy for primary and metastatic liver tumors: a single institution phase i-ii study. Acta Oncol. 2006;45(7):831–7.
15. Jang WI, Kim MS, Bae SH, Cho CK, Yoo HJ, Seo YS, et al. High-dose stereotactic body radiotherapy correlates increased local control and overall survival in patients with inoperable hepatocellular carcinoma. Radiat Oncol. 2013;8:250.
16. Bujold A, Massey CA, Kim JJ, Brierley J, Cho C, Wong RK, et al. Sequential phase I and II trials of stereotactic body radiotherapy for locally advanced hepatocellular carcinoma. J Clin Oncol. 2013;31(13):1631–9.
17. Takeda A, Sanuki N, Tsurugai Y, Iwabuchi S, Matsunaga K, Ebinuma H, et al. Phase 2 study of stereotactic body radiotherapy and optional transarterial chemoembolization for solitary hepatocellular carcinoma not amenable to resection and radiofrequency ablation. Cancer. 2016;122(13):2041–9.
18. Llovet JM, Ricci S, Mazzaferro V, Hilgard P, Gane E, Blanc JF, et al. Sorafenib in advanced hepatocellular carcinoma. N Engl J Med. 2008;359(4):378–90.
19. Cheng AL, Kang YK, Chen Z, Tsao CJ, Qin S, Kim JS, et al. Efficacy and safety of sorafenib in patients in the Asia-Pacific region with advanced hepatocellular carcinoma: a phase III randomised, double-blind, placebo-controlled trial. Lancet Oncol. 2009;10(1):25–34.
20. Wahl DR, Stenmark MH, Tao Y, Pollom EL, Caoili EM, Lawrence TS, et al. Outcomes after stereotactic body radiotherapy or radio-

frequency ablation for hepatocellular carcinoma. J Clin Oncol. 2016;34(5):452–9.
21. Su TS, Liang P, Liang J, Lu HZ, Jiang HY, Cheng T, et al. Long-term survival analysis of stereotactic ablative radiotherapy versus liver resection for small hepatocellular carcinoma. Int J Radiat Oncol Biol Phys. 2017;98(3):639–46.
22. Sapir E, Tao Y, Schipper MJ, Bazzi L, Novelli PM, Devlin P, et al. Stereotactic body radiation therapy as an alternative to transarterial chemoembolization for hepatocellular carcinoma. Int J Radiat Oncol Biol Phys. 2018;100(1):122–30.
23. Sapisochin G, Barry A, Doherty M, Fischer S, Goldaracena N, Rosales R, et al. Stereotactic body radiotherapy vs. TACE or RFA as a bridge to transplant in patients with hepatocellular carcinoma. An intention-to-treat analysis. J Hepatol. 2017;67(1):92–9.
24. Herfarth KK, Debus J, Lohr F, Bahner ML, Rhein B, Fritz P, et al. Stereotactic single-dose radiation therapy of liver tumors: results of a phase I/II trial. J Clin Oncol. 2001;19(1):164–70.
25. Lee MT, Kim JJ, Dinniwell R, Brierley J, Lockwood G, Wong R, et al. Phase I study of individualized stereotactic body radiotherapy of liver metastases. J Clin Oncol. 2009;27(10):1585–91.
26. Chang DT, Swaminath A, Kozak M, Weintraub J, Koong AC, Kim J, et al. Stereotactic body radiotherapy for colorectal liver metastases: a pooled analysis. Cancer. 2011;117(17):4060–9.
27. McPartlin A, Swaminath A, Wang R, Pintilie M, Brierley J, Kim J, et al. Long-term outcomes of phase 1 and 2 studies of SBRT for hepatic colorectal metastases. Int J Radiat Oncol Biol Phys. 2017;99(2):388–95.
28. Schellenberg D, Kim J, Christman-Skieller C, Chun CL, Columbo LA, Ford JM, et al. Single-fraction stereotactic body radiation therapy and sequential gemcitabine for the treatment of locally advanced pancreatic cancer. Int J Radiat Oncol Biol Phys. 2011;81(1):181–8.
29. Koong AC, Le QT, Ho A, Fong B, Fisher G, Cho C, et al. Phase I study of stereotactic radiosurgery in patients with locally advanced pancreatic cancer. Int J Radiat Oncol Biol Phys. 2004;58(4):1017–21.
30. Rao AD, Sugar EA, Chang DT, Goodman KA, Hacker-Prietz A, Rosati LM, et al. Patient-reported outcomes of a multicenter phase 2 study investigating gemcitabine and stereotactic body radiation therapy in locally advanced pancreatic cancer. Pract Radiat Oncol. 2016;6(6):417–24.
31. Petrelli F, Comito T, Ghidini A, Torri V, Scorsetti M, Barni S. Stereotactic body radiation therapy for locally advanced pancreatic cancer: a systematic review and pooled analysis of 19 trials. Int J Radiat Oncol Biol Phys. 2017;97(2):313–22.
32. Mellon EA, Hoffe SE, Springett GM, Frakes JM, Strom TJ, Hodul PJ, et al. Long-term outcomes of induction chemotherapy and neoadjuvant stereotactic body radiotherapy for borderline resectable and locally advanced pancreatic adenocarcinoma. Acta Oncol. 2015;54(7):979–85.
33. Suker M, Beumer BR, Sadot E, Marthey L, Faris JE, Mellon EA, et al. FOLFIRINOX for locally advanced pancreatic cancer: a systematic review and patient-level meta-analysis. Lancet Oncol. 2016;17(6):801–10.
34. Kavanagh BD, Schefter TE, Cardenes HR, Stieber VW, Raben D, Timmerman RD, et al. Interim analysis of a prospective phase I/II trial of SBRT for liver metastases. Acta Oncol. 2006;45(7):848–55.
35. Barry A, McPartlin A, Lindsay P, Wang L, Brierley J, Kim J, et al. Dosimetric analysis of liver toxicity after liver metastasis stereotactic body radiation therapy. Pract Radiat Oncol. 2017;7(5):e331–e7.
36. Velec M, Haddad CR, Craig T, Wang L, Lindsay P, Brierley J, et al. Predictors of liver toxicity following stereotactic body radiation therapy for hepatocellular carcinoma. Int J Radiat Oncol Biol Phys. 2017;97(5):939–46.
37. Toesca DA, Osmundson EC, Eyben RV, Shaffer JL, Lu P, Koong AC, et al. Central liver toxicity after SBRT: an expanded analysis and predictive nomogram. Radiother Oncol. 2017;122(1):130–6.
38. Pollom EL, Alagappan M, von Eyben R, Kunz PL, Fisher GA, Ford JA, et al. Single- versus multifraction stereotactic body radiation therapy for pancreatic adenocarcinoma: outcomes and toxicity. Int J Radiat Oncol Biol Phys. 2014;90(4):918–25.
39. Pan CC, Kavanagh BD, Dawson LA, Li XA, Das SK, Miften M, et al. Radiation-associated liver injury. Int J Radiat Oncol Biol Phys. 2010;76(3. Suppl):S94–100.
40. Lim-Reinders S, Keller BM, Al-Ward S, Sahgal A, Kim A. Online adaptive radiation therapy. Int J Radiat Oncol Biol Phys. 2017;99(4):994–1003.
41. Nakanishi M, Chuma M, Hige S, Asaka M. Abscopal effect on hepatocellular carcinoma. Am J Gastroenterol. 2008;103(5):1320–1.
42. El-Khoueiry AB, Sangro B, Yau T, Crocenzi TS, Kudo M, Hsu C, et al. Nivolumab in patients with advanced hepatocellular carcinoma (CheckMate 040): an open-label, non-comparative, phase 1/2 dose escalation and expansion trial. Lancet. 2017;389(10088):2492–502.
43. Kang JK, Kim MS, Cho CK, Yang KM, Yoo HJ, Kim JH, et al. Stereotactic body radiation therapy for inoperable hepatocellular carcinoma as a local salvage treatment after incomplete transarterial chemoembolization. Cancer. 2012;118(21):5424–31.
44. Culleton S, Jiang H, Haddad CR, Kim J, Brierley J, Brade A, et al. Outcomes following definitive stereotactic body radiotherapy for patients with Child-Pugh B or C hepatocellular carcinoma. Radiother Oncol. 2014;111(3):412–7.
45. Lasley FD, Mannina EM, Johnson CS, Perkins SM, Althouse S, Maluccio M, et al. Treatment variables related to liver toxicity in patients with hepatocellular carcinoma, Child-Pugh class A and B enrolled in a phase 1-2 trial of stereotactic body radiation therapy. Pract Radiat Oncol. 2015;5(5):e443–9.
46. Scorsetti M, Comito T, Cozzi L, Clerici E, Tozzi A, Franzese C, et al. The challenge of inoperable hepatocellular carcinoma (HCC): results of a single-institutional experience on stereotactic body radiation therapy (SBRT). J Cancer Res Clin Oncol. 2015;141(7):1301–9.
47. Murray LJ, Dawson LA. Advances in stereotactic body radiation therapy for hepatocellular carcinoma. Semin Radiat Oncol. 2017;27(3):247–55.
48. Protocol for Radiation Therapy Oncology Group (RTOG 1112) Trial: A randomized phase III study of sorafenib versus stereotactic body radiation therapy followed by sorafenib in hepatocellular carcinoma. Version Date: October 27, 2017.

SAbR for Primary Prostate Cancer

Michael R. Folkert, Raquibul Hannan, Neil B. Desai, and Robert D. Timmerman

Introduction

Large daily dose hypofractionated radiation treatment for prostate cancer has been used in clinical practice dating back to at least the 1960s. For example, Lloyd-Davis and colleagues published their experience treating 206 prostate cancer patients with 36Gy in 6 fractions between 1962–1984 [1]. A multitude of technological advances along with a better understanding of dose response, radiobiology, and critical tissue constraints made the modern stereotactic ablative body radiosurgery (SAbR), also known as stereotactic body radiation therapy (SBRT), for the treatment of primary prostate cancer not just feasible but a safe, effective, and convenient treatment option for a wide spectrum of patients. Although numbers of treated patients and long term follow-up data on safety and efficacy are much less comprehensive than that of brachytherapy or conventionally fractionated external beam approaches, SAbR approaches have benefited from a more formal clinical approach to testing in early clinical trials. Both dose-finding studies and some maturing clinical trials have been published, allowing patients and practitioners to thoughtfully consider SAbR as an option. Comparative cost-effectiveness analyses have found a superior cost-to-benefit ratio of SAbR compared to conventional fractionation [2, 3]. Because of the reduced fraction number, SAbR is also beneficial in terms of increased patient convenience and improved treatment access to patients. In this chapter, we will review the published literature and discuss the different techniques for the treatment of primary prostate cancer with SAbR.

Site Specific Considerations: Radiobiologic Rationale for Prostate SAbR

It has been suspected for a long time that prostate's α-β ratio is quite low and perhaps on the same level as that of the nearby late responding organs such as rectum and bladder [4]. A meta-analysis of seven international databases on the dose fraction sensitivity of prostate cancer revealed an α-β ratio of 1.4 Gy (0.9–2.2 Gy) with values of 0.6, 1.7, and 1.6 Gy for low-, intermediate-, and high-risk groups, respectively [5]. A repeat analysis of the same database, taking into account a more realistic number of clonogenic cells, showed α-β ratio of 0.10 ± 0.04 Gy, 0.11 ± 0.04 Gy, and 0.12 ± 0.04 Gy for low-, intermediate-, and high-risk groups, respectively [6]. Another meta-analysis that took into account the duration of therapy reported an overall α-β ratio of prostate cancer to be 0.58 Gy (95% CI -0.53–1.69) [7]. On the other hand, the α-β ratio of late rectal and bladder toxicity is estimated to be around 3–5 Gy [8, 9]. Therefore, with the prostate cancer's α-β ratio being significantly lower than that of the late toxicity of its surrounding tissues, there may be a gain in the therapeutic index in treating prostate cancer with fewer fractions and higher dose per fraction which may confer higher therapeutic response at the expense of lower rates of late toxicity. A low α-β ratio is consistent with greater capacity of repair by that tissue between fractions. Since prostate cancer has a lower α-β ratio compared to rectum and bladder, this would suggest that prostate cancer would benefit more from repair than its surrounding tissue by fractionation, and therefore, hypofractionation would

M. R. Folkert · N. B. Desai
University of Texas Southwestern Medical Center, Department of Radiation Oncology, Dallas, TX, USA

R. Hannan
University of Texas Southwestern Medical Center, Departments of Radiation Oncology and Immunology, Dallas, TX, USA

R. D. Timmerman (✉)
University of Texas Southwestern Medical Center, Departments of Radiation Oncology and Neurological Surgery, Dallas, TX, USA
e-mail: robert.timmerman@utsouthwestern.edu

D. M. Trifiletti et al. (eds.), *Stereotactic Radiosurgery and Stereotactic Body Radiation Therapy*,
https://doi.org/10.1007/978-3-030-16924-4_25

have a higher therapeutic index for the treatment of prostate cancer.

While justifying moderate hypofractionated regimens, the radiobiological arguments above may not directly justify the dose ranges used in SAbR. The α-β ratio is a tissue property of the "shoulder" of the in-vitro survival curve. Beyond the shoulder, most cell lines show purely linear, not curvilinear, survival with dose on a log-linear scale. So while the α-β ratio may be low for doses <6Gy per fraction [10] and the SAbR dose range that typically starts at >6 Gy/fraction for prostate, the purely linear shape of the curve does not effectively have an α-β ratio [11]. At doses >6 Gy/fraction, the cell survival curve is perhaps better estimated by the universal survival curve which is based on the multitarget model [11]. Indeed, the much written-about low α-β ratio of prostate cancer's response to radiation is irrelevant in characterizing tumor control from prostate SAbR treatments, although normal tissue dosing may still behave according to linear-quadratic principles. In this range, models to predict response are inadequate, and formal dose escalation patient treatment experiences are much more informative in determining radiobiological boundaries of therapy.

Traditionally, the primary mode of radiation effect has originated from creating DNA damage, both with regard to its benefit in controlling tumor and also its toxic effects on exposed normal tissues. Hypofractionation with SAbR would obviously cause considerable DNA damage. Ideally, the tumor deposits would be mortally wounded with irreparable DNA damage. Whether this DNA damage can be repaired, particularly in the normal tissues, creates the concern of many about late toxic effects related to hypofractionation. SAbR addresses this simply by trying to use technology to avoid normal tissue. For most SAbR treatments used in clinical trials for cancer, SAbR is treating gross tumor with minimal margin. Prostate cancer is unique in that most of the trials use the prostate, most of which is normal prostatic parenchyma and ducts, as the target. As an ablative treatment, the prostate might become "destroyed" and not perform its function of contributing to the seminal secretions during ejaculation. Indeed, patients have reported smaller ejaculate volumes which has been considered an acceptable side effect.

But more than just DNA damage may occur with SAbR-range hypofractionation. Some effects may follow a sigmoid dose-response relationship. Such responses, termed deterministic (having a threshold below which little effect is observed and then increasing frequency and severity with increasing dose), may be first exploited with large dose per fraction treatments. Such deterministic effects might never contribute to tumor control with low dose per fraction treatments because the treatment dose is below the threshold for initiating the effect. Such deterministic effects with greater than 2–3 Gy threshold might include vascular injury to blood vessels supplying tumor, stimulation of immune response, and others. Importantly and unlike DNA damage, only studies in vivo (e.g., in animal models) would likely reveal the potential tumor killing benefits of these larger dose threshold effects, since in vitro systems would unlikely have blood supply or immune reactions, etc. SAbR-range hypofractionation, then, could initiate several opportunities using various mechanisms to control tumor proliferation. Still, care must be exercised to avoid causing both heightened tumor eradication simultaneously with greater normal tissue injury as clinical benefits would be negated by collateral damage.

Clinical Evidence: Selected Clinical Data for Prostate SAbR

Dose escalation with conventional fractionation (1.8–2.0 Gy/fraction) and moderate hypofractionation (2.25–4 Gy/fraction) has been extensively reported; this section will focus on more "oligo" hypofractionated approaches (6–10 Gy per fraction), which we will now call oligofractionated. Mixed treatment schedules (e.g., conventional schedules with a SAbR "boost") will not be discussed/reviewed. Selected studies are summarized in Table 1. There has not yet been a direct comparison between oligofractionation schedules and conventionally or moderately hypofractionated schedules, but moderately hypofractionated schedules have been compared directly to conventional fractionation, with a general sense that the shorter schedules are as safe and effective as extended conventional courses [12–18].

As noted above, SAbR-like oligofractionation was established as a treatment technique for localized prostate cancer by Lloyd-Davies and colleagues at St. Thomas' Hospital in England using a six-fraction regimen of 36 Gy given twice weekly from 1966 to 1984 [1]. These treatments were performed in the pre-PSA era without modern technologies like image guidance and intensity modulation so are difficult to compare to modern outcomes data, but overall, patients did reasonably well with manageable toxicity. In terms of modern image-guided oligofractionated approaches at 6–10 Gy per fraction, the first experience reported was the Virginia Mason Medical Center phase I/II Stereotactic Hypofractionated Accurate Radiotherapy of the Prostate (SHARP) trial by Madsen and colleagues [19]. In this study, 40 men with low-risk disease (Gleason score $\leq$ 6, PSA < 10 ng/mL and clinical stage $\leq$ T2a) were treated to a total dose of 33.5 Gy in 5 fractions of 6.7 Gy per fraction using a conventional linear accelerator and multiple noncoplanar fields. The target was the prostate plus a 4–5 mm margin. Daily image guidance was used using implanted fiducial markers. There was one acute Grade 3 urinary toxicity (urinary retention requiring catheterization) and no acute Grade 4–5 toxicities. There were no $\geq$ Grade 3 toxicities; late Grade

Table 1 Summary of selected prostate SAbR studies

Study	Institution(s)	Trial type	Platform	Patients (N)	Eligibility	Dose regimens	Target/margin	Followup (years)	bRFS	RTOG/CTCAE toxicity
Madsen (PMID 17336216)	Virginia Mason Medical Center	Prospective, Phase I/II	LINAC	40	Low-risk	6.7 Gy × 5 fractions	Prostate +4–5 mm	3.4	90% at 4 y	Acute G3 GU 2.5% late G2 GU 20%, G2 GI 7.5%
King (PMID 21300474)	Stanford	Prospective, Phase II	CyberKnife	67	Low- and int-risk	7.25 Gy × 5 fractions	Prostate +3–5 mm	2.7	94% at 4y	Late G2 GU 5%, G3 GU 3.5%, late G2 GI 2%
Katz (PMID 25229051)	Winthrop	Prospective, Phase II	CyberKnife	304	Low-, int-, and high-risk	7 Gy × 5 fractions 7.25 Gy × 5 fractions	Prostate +5 mm (3 mm posterior)	2.5	97% at 5y, LR 90.7% at 5y, IR 74.1% at 5y, HR	Late G2 GU 14%, G2 GI 7%
Katz update (PMID 25229051)	Winthrop	Mixed Prospective/ retrospective	CyberKnife	477	Low- and int-risk	7 Gy × 5 fractions or 7.25 Gy × 5 fractions	Prostate +5 mm (3 mm posterior)	6.0	95.6% at 7y, LR 89.6% at 7y, IR	As above, plus late G3 GU 1.7%
Jackson (no PMID yet)	Michigan/ Multi-Institutional	Prospective, Phase II	LINAC	66	Low- and int-risk	7.4 Gy × 5 fractions	Prostate +3 mm	3.0	100% at 3y	Acute G2 GU 23%. GI 4% late G2 GU 9%, G2 GI 4
Mantz (PMID 25452933)	21st century oncology	Prospective, Phase II	LINAC	102	Low- and int-risk	8 Gy × 5 fractions	Prostate +2 mm	5.0	99% at 5y	Acute G3 GU 2%
Zelefsky (Now available as PMID: 30611838)	MSKCC	Prospective, Phase I	LINAC	136	Low- and int-risk	6.5 Gy × 5 fractions 7 Gy × 5 fractions 7.5 Gy × 5 fractions 8 Gy × 5 fractions	Prostate +5 mm (3 mm posterior)	5.9 5.4 4.1 3.5	85% at 5y 94% at 5y 100% at 5y 100% at 5y	32.5: Acute G2 GU 16.7%, G2 GI 0%; late G2 GU 23.3%, G2 GI 0% 35: Acute G2 GU 22.9%, G2 GI 2.9%; late G2 GU 25.7%, G2 GI 0% 37.5: Acute G2 GU 8.3%, G2 GI 2.8%; late G2 GU 27.8%, G2 GI 0% 40: Acute G2 GU 17.1%, G2 GI 11.4%; late G2 GU 31.4%, G2 GI 0%
King (PMID 24060175)	Consortium/ multi-institutional registry	Prospective registry	CyberKnife	1100	Low-, int-, and high-risk	7.25 Gy × 4–5 fractions (median)	Prostate +5 mm (3 mm posterior)	3.0	95% at 5y, LR 84% at 5y, IR 81% at 5y, HR	Not specifically reported
Freeman (PMID 25657929)	Multi-institutional registry	Prospective registry	CyberKnife	2000	Low-, int-, and high-risk	7–8 Gy × 4–5 fractions *6.5–7.25 Gy × 3 fractions as boost to conventional (8%)*	Not reported	2.0	99% at 2y, LR 97% at 2y, IR (favorable) 85% at 2y, IR (unfavorable) 87% at 2y, HR	Late G3 GI 0.05%
Hannan (PMID 27035363)	UTSW/ multi-institutional	Prospective, Phase I/II	LINAC/ Tomotherapy	91	Low- and int-risk	9 Gy × 5 fractions 9.5 Gy × 5 fractions 10 Gy × 5 fractions	Prostate +3 mm	4.5	100% at 5y, LR 98.6% at 5y, IR	Acute G2 GU 29.7%, G2 GI 20.9% Late G2 GU 20.9%, G3 GU 4.4%, G2 GI 13.2%, G3–4 GI 6.8% (G4 GI 1.6%)
Folkert (abstract, no PMID)	UTSW/MSKCC	Prospective, Phase II	LINAC/ CyberKnife	44	Low- and int-risk	9 Gy × 5 fx	Prostate +3 mm	1.0	100% at 1y	Acute G2 GU 36.4%, G3 GU 4.5%; G2 GI 22.7%

2 GU and GI toxicity rates were 20% and 7.5%, respectively. Median follow-up was 41 months; 4-year actuarial freedom from biochemical recurrence (FFBR) was 90%.

Increasing oligofractionated SAbR dose above 7 Gy was investigated by King and colleagues in a phase II trial at Stanford University [20]. Using a robotic radiation therapy delivery system (CyberKnife®, Accuray, Sunnyvale, CA, USA), 36.25 Gy in 5 fractions of 7.25 Gy was delivered to the prostate with the addition of a 3–5 mm planning margin. In 67 patients with low- to intermediate-risk features (Gleason score 6(3 + 3) or 7(3 + 4), PSA ≤ 10 ng/mL and clinical stage ≤ T2b), there were no Grade 4 or higher toxicities. Late Grade 2 and 3 GU toxicity rates were 5% and 3.5%, respectively. Late Grade 2 GI toxicity was 2% with no Grade 3 or higher toxicities seen. Patients who received QOD treatments were less likely to experience Grade 1–2 GI and GU toxicities than those who received QD treatments. At a median follow-up of 2.7 years, 4-year biochemical relapse-free survival was 94%.

The largest single institution report of prostate SAbR was reported by Katz and colleagues at the Winthrop University Hospital [21], also using a robotic radiation therapy delivery system. In their study incorporating all risk groups, 304 patients (69% low-risk, 27% intermediate risk, 4% high-risk) were treated. The first 50 patients received 35 Gy in 5 fractions of 7 Gy with the subsequent 254 patients receiving 36.25 Gy in 5 fractions of 7.25 Gy. Lower-dose patients had a median follow-up of 30 months and the higher-dose patients a median follow-up of 17 months. There were no Grade 3–4 acute complications. Late Grade 2 GU and GI toxicity were 14% and 7%, respectively. Five patients had late Grade 3 GU toxicity, with no late Grade ≥ 4 toxicities. Actuarial 5-year biochemical recurrence-free survival was 97% for low-risk, 90.7% for intermediate-risk, and 74.1% for high-risk patients. In a subsequent follow-up study reported by this group, a total of 477 men were treated [22]. All of the men had biopsy-proven, newly diagnosed, non-metastatic prostate cancer: 67.9% low-risk, Gleason score 6, and PSA < 10 ng/mL and 32.1% intermediate risk, Gleason score 7, or PSA 10–20 ng/ml. Fifteen of the men were treated prospectively to assess the feasibility of the approach; the rest of the participants were treated according to the approved protocol, but not in a prospective fashion, and their outcomes were incorporated as a retrospective study. There was no Grade ≥ 3 acute GU or GI toxicity; 9 (1.7%) participants had late Grade 3 genitourinary toxicity. With a median follow-up of 72 months, the biochemical disease-free survival rate was 93.7% for all participants; 95.9% for low risk and 89.3% for intermediate risk.

Further escalation was described in a recent trial published by Jackson and colleagues, in which 66 patients with low- (49%) or intermediate-risk (33% favorable, 18% unfavorable) prostate cancer were treated on a phase II trial at five centers [23]. Treatment was performed using conventional linear accelerator radiation delivery, electromagnetic transponders for motion management, and a 3 mm uniform PTV expansion. Patient received 37 Gy in 5 fractions of 7.4 Gy per fraction. No Grade ≥ 3 GU or GI toxicity was observed; acute Grade 2 GU toxicity was seen in 23% of treated patients, and 9% late Grade 2 GU toxicity was observed. Acute or late Grade ≥ 2 GI toxicity was noted in 4% and 5% of treated patients, respectively. At a median follow-up of 36 months, there have been no biochemical recurrences.

In a phase II trial reported by Mantz and colleagues using conventional linear-accelerator multifield or arc-based treatments and real-time target tracking with implanted transponders, 70 patients with Gleason score 6(3 + 3) and 32 patients with Gleason score 7(3 + 4) prostate cancer received a total of 40 Gy in 5 fractions QOD of 8 Gy per fraction [24]. The target was the prostate alone with a uniform 2 mm PTV expansion. Grade 3 acute GU toxicity was observed in 2% of patients, with no late Grade ≥ 3 GU or ≥ 2 GI toxicity. At a minimum follow-up of 5 years for the cohort, only one patient had experienced biochemical recurrence.

Bridging this range of doses from 32.5 Gy to 40 Gy in 5 fractions (6.5–8 Gy per fraction) is a comprehensive dose escalation study performed at Memorial Sloan Kettering Cancer Center and reported by Zelefsky and coworkers at the ASTRO 2017 Annual Meeting [25]. In their phase I study, 136 patients with low- and intermediate-risk prostate cancer received conventional linear-accelerator-based SAbR at escalating radiation dose levels starting at 32.5 Gy in 5 fractions delivered QOD and then escalated by 2.5 Gy increments after dose level accrual and the protocol-specified safety observation period was completed to a maximum dose of 40 Gy in 5 fractions QOD. Thirty patients received 32.5 Gy in 5 fractions, 35 patients received 35 Gy in 5 fractions, 36 patients received 37.5 Gy in 5 fractions, and 35 patients received 40 Gy in 5 fractions. The incidence of acute Grade 2 GI toxicities for dose levels 1–4 were 0%, 5.7%, 3.2%, and 3.2%, respectively. No Grade ≥ 3 acute GI toxicities were observed. The incidence of acute Grade 2 GU toxicities for dose levels 1–4 were 13.3%, 8.6%, 13.9%, and 6.5%, respectively. Only 1 patient at the 40 Gy dose level experienced a Grade 3 acute toxicity (urinary retention requiring Foley catheter placement). The incidence of late Grade 2 GI toxicities for dose levels 1–4 were 3.3%, 0%, 2.8%, and 0%, respectively. No Grade 3 or 4 late GI toxicities were observed. The incidence of late Grade 2 GU toxicities for dose levels 1–4 were 13.3%, 14.3%, 8.3%, and 9.7%, respectively. Only one late Grade 3 GU toxicity (urethral stricture) developed in the 32.5 Gy dose arm after treatment which was corrected with transurethral resection. No Grade ≥ 4 late GU toxicities were observed. At a median follow-up for the

increasing dose levels of 66, 54, 36, and 30 months, respectively, the 3-year biochemical recurrence free survival rates were 83%, 85%, 90%, and 98%, respectively. Patients underwent a posttreatment biopsy at 2 years. The incidence of a positive posttreatment biopsy was 45%, 12%, 17%, and 5%, respectively, for the 4 dose arms ($P < 0.001$). This posttreatment biopsy data support the use of larger dose per treatment oligofractionation.

Although not prospective, there are some large pooled, multi-institutional experiences being presented that may be hypothesis-generating. A pooled analysis of 1100 patients (11% high risk, 58% intermediate risk, 30% low risk) from prospective phase II trials using SAbR for the treatment of prostate cancer in which a median dose of 36.25 Gy was delivered in 4 to 5 fractions demonstrated a 93% 5-year biochemical relapse-free survival rate for all patients with favorable long-term patient reported outcomes with respect to urinary and bowel functions [26, 27]. Freeman and colleagues reported on the safety and efficacy of SAbR of the prostate in individuals with clinically localized prostate cancer [28]. In this registry data study, over 2000 men were enrolled and all received radiosurgery at least once in their treatment of prostate cancer. A total of 86% of the participants were treated with SAbR as monotherapy and 8% received radiotherapy as a boost following external beam radiation. For the entire study cohort, the 2-year biochemical disease-free survival rate was 92%, 99% for the low-risk group, 97% for the intermediate-risk group with Gleason 7(3 + 4), 85% for the intermediate-risk group with Gleason 7(4 + 3), and 87% for the high-risk group. There were no Grade 3 late urinary toxicities noted and there was 1 participant who reported a Grade 3 gastrointestinal toxicity (rectal bleeding).

Based on the consistent and reproducible date from SAbR studies, in May 2013, ASTRO updated its Model Policy for SAbR and stated "It is ASTRO's opinion that data supporting the use of SAbR for prostate cancer have matured to a point where SAbR could be considered an appropriate alternative for select patients with low to intermediate risk disease." Additionally, the 2017 National Comprehensive Cancer Network® Clinical Practice Guidelines (NCCN Guidelines®) for the treatment of prostate cancer note that SAbR is an emerging treatment modality and can be considered cautiously as an alternative to conventionally fractionated regimens.

Toxicity: The UT Southwestern Experience – Phase I and II Trials

At UT Southwestern (UTSW) we began investigating SAbR for prostate cancer in 2004 by examining prostate HDR dosimetry and generating dose response curves in animal models [29]. The results from the animal experiment showed an increasing dose-response relationship for a range of hypofractionated dose levels for prostate tumor grafts growing in nude mice with the 45 Gy in 5 fraction regimen achieving the best results [29]. Next we made a dosimetry comparison with HDR dose regimens to determine if SAbR could create HDR-like dose distributions. Using our animal experience, published HDR experience, and radiobiological modeling with the Universal Model previously mentioned, the 9 Gy × 5 fraction dose level was selected as the starting dose of a multicenter phase I/II dose escalation trial that enrolled 15 patients in each of the dose escalated cohort of prostate cancer patients from 9 Gy to 9.5 Gy to 10 Gy in each fraction (NCT00547339). As with the 3 + 3 design of phase I dose escalation, where dose-limiting toxicity is exceeded if a third or more of patients experience toxicity, the maximum tolerated dose was set as the dose at which 4 or fewer patients experience Grade ≥ 3 toxicity within 90 days of the treatment. More patients than a 3 + 3 design were enrolled at each dose level to allow better estimates of toxicity and begin to understand dose-response effects. For immobilization vacuum bag with stereotactic body frame along with a large (≥60 cc) rectal balloon was used. MRI co-registration was used when possible for volume delineation. Maximum tolerated dose (MTD) was not reached in the dose range tested up to 10 Gy × 5, and the collective outcome of the 45 patients in the phase I portion of the trial reported a GI Grade ≥ 2 and Grade ≥ 3 toxicity in 18% and 2%, respectively, and GU Grade ≥ 2 and Grade ≥ 3 toxicity in 31% and 4%, respectively [30]. In the initial experience, we noted higher rates of acute urinary toxicity similar to the prostate brachytherapy experience; this was prevented effectively by prophylactic treatment with α1-blocker. In the initial experience, we also noted an anterior rectal erosion or ulcer in 100% of assessed patients during the routine anoscopy performed at 6 weeks and beyond following treatment. Yet, most of these were totally asymptomatic and the vast majority of the patient's rectal erosions eventually healed except for one patient who was on immunosuppressive treatment for a previous renal transplant. This patient's rectal ulcer eventually healed after withholding immunosuppressive treatment. Prior to the start of the phase II portion of the trial, an amendment was added excluding patients on immunosuppressive treatment.

With no dose-limiting toxicity in the phase I portion of the trial, the study committee decided to use 10 Gy × 5 fractions for the phase II study dose. Another 46 patients were subsequently enrolled in the 10 Gy × 5 fraction phase II cohort. Given the concern of late effects with large dose per fraction radiation therapy, the institution imposed a 3-year moratorium on prostate SAbR treatments after

enrollment of the last phase II patient so that late effects could be observed without endangering more patients. While most again tolerated the treatment well, an unacceptable rate of late Grade ≥ 3 GI toxicity was encountered with 5 patients, ultimately requiring diverting colostomy. We have carefully analyzed the dosimetric data from these patients experiencing toxicity as compared to the majority who experienced no ill effects. This analysis proved to identify treatment factors most likely to predict treatment-related toxicity. Three constraints were derived from the analysis of these data: (1) patients that had >50% rectal circumference receiving 39 Gy or (2) 50 Gy to >3 cm^3 rectal wall experienced Grade 3+ delayed rectal toxicity; (3) Grade 2+ acute rectal toxicity correlated with treatment of >50% circumference of rectal wall to 24 Gy [31]. Importantly, meeting the newly-found constraints for "safe" treatment would have been achievable in all treated patients; however, as this was an exploratory experience, we had no insight motivating us to avoid the characteristics later found to condemn patients toward toxicity. This is the nature of a true phase I experience and a testament to the humanitarian and brave spirit of patients who agree to enroll on such trials.

Efficacy of our nearly 100 patient phase I/II trial was excellent. The 5-year outcome of this trial reported a biochemical recurrence free survival (bPFS) rate of 98.6%, with only one patient failing [32]. Similar to brachytherapy, PSA bounce was noted in 51% of patients undergoing SAbR, with some of them having multiple and late bounces [33]. The overall rate of late Grade ≥ 3 GI toxicity was 5% and GU toxicity was 4%. Interestingly, none of the late Grade ≥ 3 GI or GU toxicities happened in the 45Gy and 47.5 Gy cohorts, each of which enrolled 15 patients. With no dose response for efficacy and less toxicity, for the next clinical trial (NCT02353832), 45 Gy in 5 fractions was selected as the standard dose for low and low intermediate risk patients.

Rectal toxicity, although not frequent, was clearly the impediment to using higher SAbR doses for prostate cancer. Anatomically, the prostate and rectum are juxtaposed so that the prostate target with margin overlaps the anterior rectal wall. Toward the end of the phase I/II experience, reports of a new approach, in which a biodegradable rectal spacer could be interposed between the rectum and the prostate to separate the organs, emerged. The separation might allow the SAbR treatment to be carried out with less rectal toxicity. In an NCT02353832 phase II trial conducted at UTSW and Memorial Sloan Kettering Cancer Center (MSKCC) and reported by Folkert and coworkers at the 2017 ASTRO Annual Meeting [34], patients were treated with SAbR following placement of such a temporary hydrogel spacer instead of a rectal balloon; the impact of this intervention is shown in Fig. 1. Eligible patients included men with localized prostate cancer with Gleason score 6-7, PSA ≤ 15, and clinical/radiographic stage ≤ T2c. Prior to this trial, study institutions had no experience placing hydrogel spacers. Patients underwent hydrogel spacer placement followed by 45 Gy in 5 fractions to the prostate volume with a 3 mm planning margin; the seminal vesicles were not treated.

Recall that with even the initial dose levels of the previous phase I/II trial, all patients had an apparent rectal erosion on the anterior rectal wall after treatment as documented by anoscopy. The primary endpoints of the new study were reduction in rectal erosion/ulcer events and rates of space creation ≥7.5 mm. Potential rectal erosion/ulceration was assessed at 1.5, 3, 6, and 9 months posttreatment by direct anoscopy. Toxicity using Common Toxicity Criteria for Adverse Events v. 4.0, quality of life, dosimetric outcomes, and oncologic outcomes data were collected. The proposed study had >90% power to detect significant reduction in mucosal injury rate from the previously observed rate of 90% (alpha = 0.05, two-sided exact test) to <70%.

A total of 44 patients treated at 2 institutions (UTSW and MSKCC) were included: 7 patients (15.9%) had Gleason 6(3 + 3) disease, 25 (56.8%) had Gleason 7 (3 + 4) disease, and 12 (27.3%) had Gleason 7(4 + 3) disease. Median PSA at treatment was 6.5 (range 1.7–13.5). All patients received protocol treatment; overall rate of dosimetry noncompliance was 1.8%. A total of 6 rectal erosions/ulcers (five Grade 1, one Grade 2) were observed (13.6%), meeting the trial's primary objective. All were minimally symptomatic and resolved on repeat anoscopy within 6 months. Median space creation was 11.5 mm; only 1 spacer (2.3%) did not meet the protocol goal of > = 7.5 mm of space created, but overall trial endpoint was met with >95% of patients with spacer distance of > = 7.5 mm. At a median follow-up of 12 months, freedom from biochemical failure was 100%. There were no ≥ Grade 3 acute or chronic gastrointestinal toxicities. Acute and late urinary Grade 3 occurred in 2 (4.5%) of patients; one spacer site infection and one urinary tract pain, both resolved. No > Grade 3 toxicities occurred. Without a rectal spacer (as shown in Fig. 1), all patients treated with SAbR at these dose levels experienced rectal erosion, a small minority of which failed to heal leading to colostomy. This experience showed that with placement of a spacer, anterior rectal wall consequences of treatment are dramatically diminished, potentially facilitating high dose treatment.

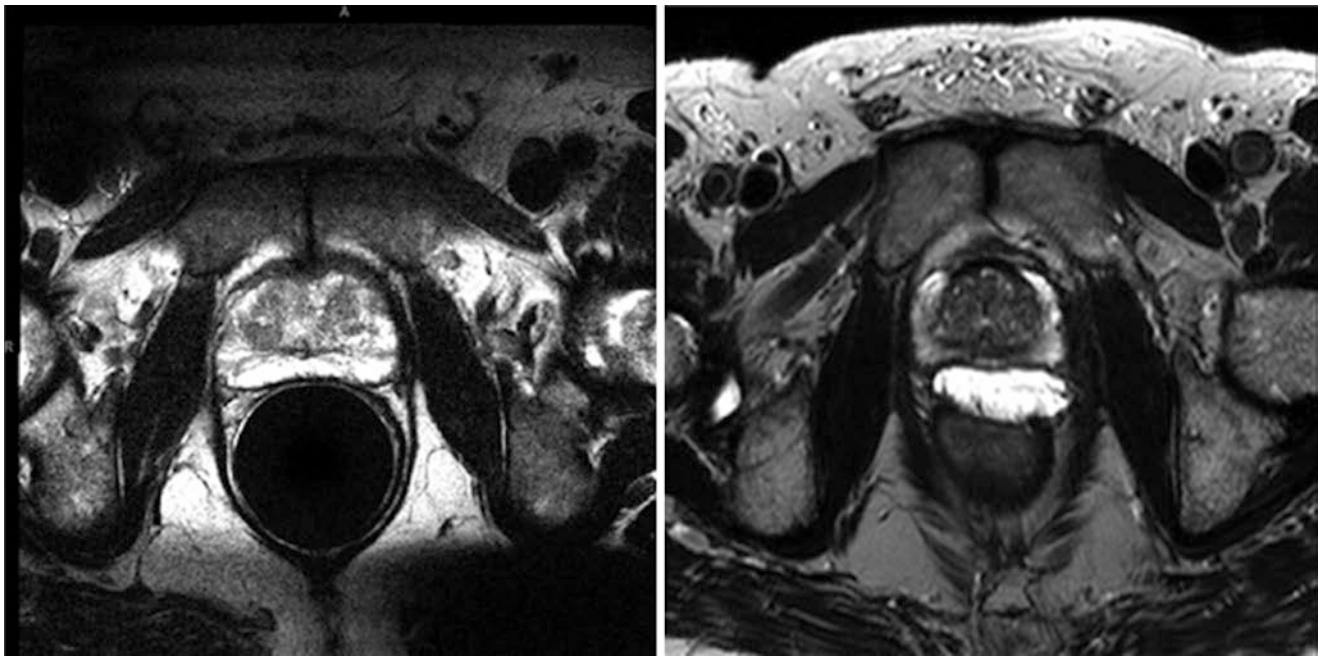

Fig. 1 Visual comparison of the rectal balloon vs the spacer gel in 2 similar patients. Left: Representative T2-weighted axial MRI obtained using a 3 T magnet in a patient with a radiation therapy endorectal balloon in place. Right: Representative T2-weighted axial MRI obtained using a 3 T magnet in a patient with the rectal spacer gel, seen in bright white, placed between the prostate and the rectum. (Reprinted with permission of Elsevier from Jones et al. [37])

Prostate SAbR Simulation, Planning, and Treatment Delivery Techniques

While SAbR is a powerful tool for managing prostate cancer, delivery of these high ablative doses requires experience and careful technique to ensure optimal and reproducible coverage of the prostate target and limit the risk of injury to nearby organs.

Pre-treatment Preparation

Patients who choose to pursue definitive radiation treatment for the management of their prostate cancer at our institution undergo a comprehensive diagnostic workup, assessment of comorbid conditions and baseline genitourinary, gastrointestinal, and sexual factors, and a discussion of available radiation therapy treatment options, including conventional radiation therapy, brachytherapy, and hypofractionated radiation therapy techniques. Patients who are eligible for and choose SAbR for the management of their prostate cancer are those with Gleason 6-7 disease (including high volume Gleason 7(4 + 3)) with PSA $\leq$ 15 ng/ml, clinical and radiographic T stage T1a-T2c, no significant obstructive urinary symptoms with AUA score $\leq$ 18, prostate gland sizes <100 cm^3 (for patients with prostate size >60 cm^3, we do recommend consideration of cytoreductive androgen deprivation therapy prior to treatment). We generally do not recommend SAbR for patients who have had prior pelvic radiation therapy, prior transurethral resection of the prostate (TURP) and/or cryotherapy, or patients who cannot undergo placement of fiducials and/or temporary hydrogel spacers for rectal protection. Patients unable to undergo MRI or with prosthetic hips are generally not considered for SAbR due to reduced ability to visualize and delineate the prostate, as well as limitations on beam angles through hardware. We also do not offer SAbR monotherapy as standard treatment for high-risk prostate cancer, but do have an active dose-escalation protocol (NCT02353819) for patients with high-risk prostate cancer in which patients received 2 years of androgen deprivation therapy as well as hypofractionated radiation therapy to the prostate, seminal vesicles, and pelvic lymph nodes in 5 fractions.

Nearly all patients who received SAbR at our institution currently undergo pre-simulation placement of a temporary hydrogel spacer (SpaceOAR®, Augmenix, Inc., Bedford, MA, USA), as well as intraparenchymal placement of gold fiducials into the prostate. This technique has been shown in a randomized prospective trial to reduce rectal toxicity severity and provide improved quality of life outcomes in patients receiving conventionally fractionated external beam radiation therapy to the prostate [35, 36]. We have evaluated the relative benefit of the rectal balloon versus the temporary hydrogel spacer and have found that the spacer provides

superior dosimetry (Fig. 1) [37] and have demonstrated a reduction in rectal erosion/ulcer events in a phase II trial of SAbR following rectal spacer placement [34]. Patients undergo transrectal ultrasound-guided transperineal injection of the spacer hydrogel into the potential space between the rectum and the prostate approximately 10–14 days prior to simulation; this can be performed in the clinic under local/moderate sedation or in the operating room under general anesthesia. Care must be taken at the time of rectal hydrogel spacer placement to ensure adequate distribution laterally and from apex to base for optimal dosimetry (Fig. 2a). We generally place 3 fiducials in the prostate at posterior base

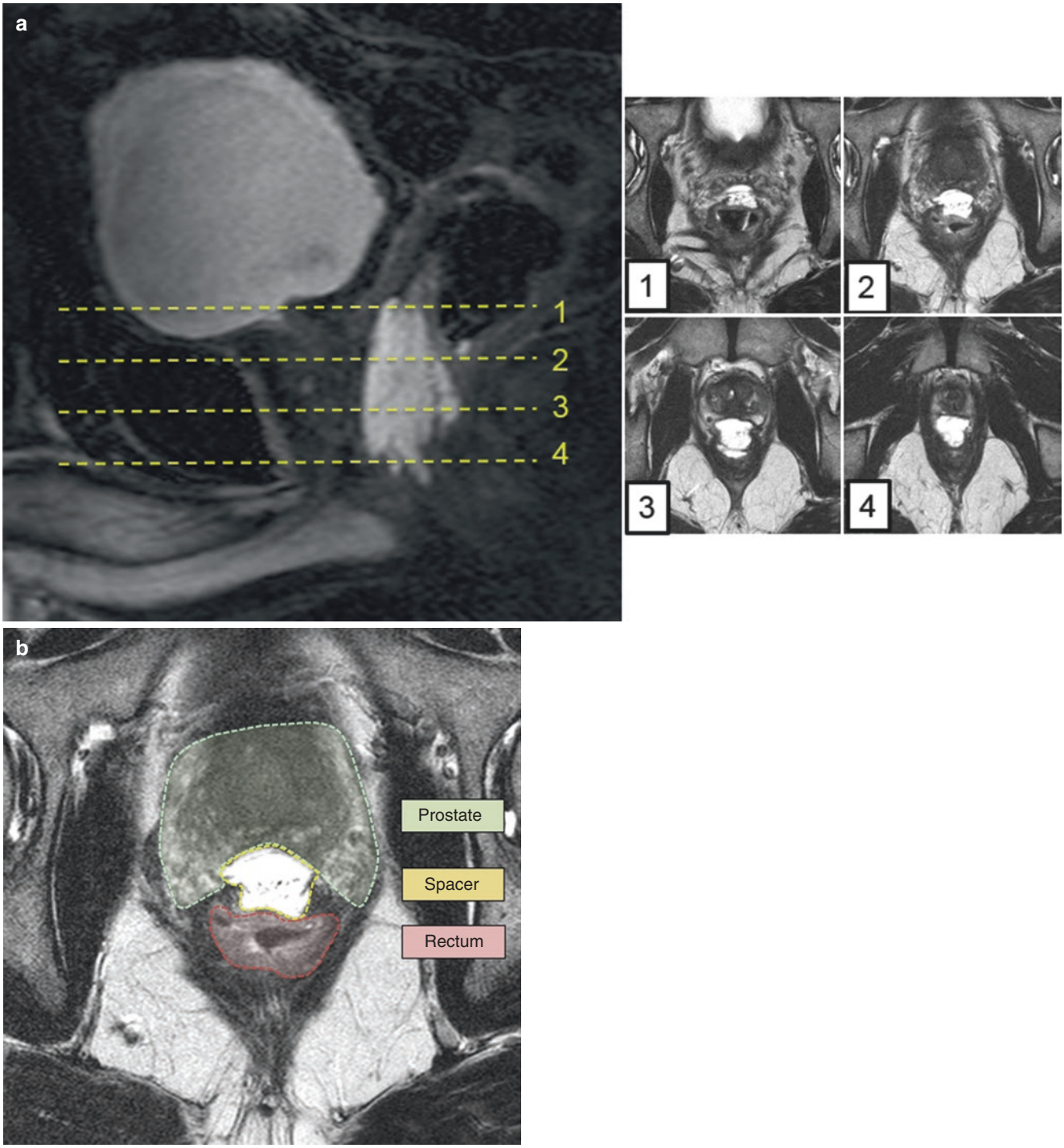

Fig. 2 (**a**–**c**) MRI imaging of rectal hydrogel spacer and treatment planning images. (**a**) Sagittal image and planes corresponding to the 4 axial images show good distribution of the rectal hydrogel spacer with separation of the prostate and rectum. (**b**) Axial prostate anatomy and temporary hydrogel spacer depiction with T2-weighted imaging. (**c**) Fiducial demarcation with T1-weighted imaging on left; yellow arrow notes location of implanted gold fiducial (hypointense area). On right, T2-weighted image, where the fiducial is not evident

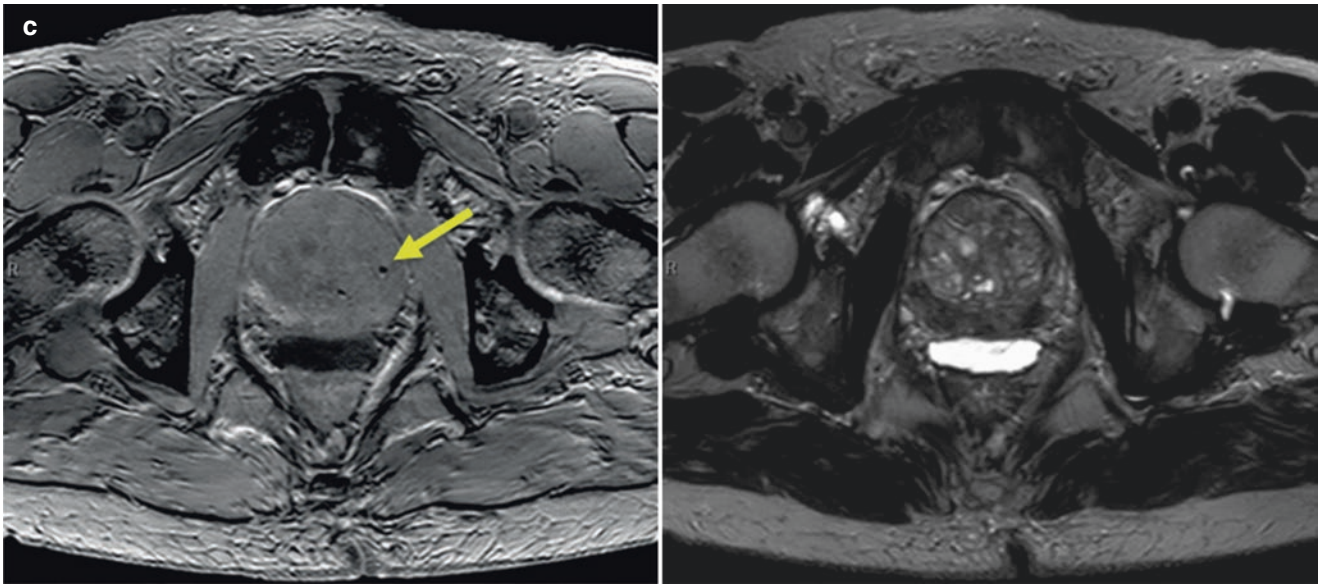

Fig. 2 (continued)

and apex on one side of the gland, and anterior mid-gland on the opposite lobe. While transperineal implantation carries low risk for infection, generally prophylactic intravenous cefazolin is used or clindamycin if penicillin/cephalosporin contraindication exists.

Simulation

In the case of prostate SAbR, there are significant concerns for daily positioning, due to the variability of the volume and position of the rectum, urethra, and bladder. In the case of the rectum, this may be alleviated through the use of daily enemas, and in some institutions a rectal balloon may be used, although potentially at the cost of increased exposure of rectal tissue to high radiation dose [37]. Bladder variability can be accommodated through the use of standardized bladder-filling protocols; at our institution, for example, the patient is instructed to stay well-hydrated through treatment. On treatment days, the patient is instructed to void and then drink ~24 ounces of water 30 minutes prior to simulation and treatment procedures.

Intra-fraction prostate motion is mostly a consequence of stool and gas colliding with the prostate as a consequence of peristalsis. This can be avoided with near complete rectal evacuation afforded by enemas (2 Fleets enemas or equivalent the morning of and 30–60 minutes before simulation/treatment). At our institution, we immobilize the patient within a stereotactic frame that surrounds them on three sides, with markers or rods placed at known locations within the frame to provide a fixed 3-D coordinate system. The frame is supplemented by a rigid pillow (vacuum bag) that conforms to the patient's external contours. The patient is registered to the frame with sternal, pelvis, and anterior tibial tattoos, and the frame is registered to the simulation/treatment coordinate system.

Carefully timed intravenous iodinated contrast administration during CT simulation is recommended to define the bladder/prostate interface and, if delineation of the neurovascular bundle is desired, to produce a pelvic CT angiogram (CTA) for delineation of relevant vasculature, provided there is no contraindication to the use of iodinated contrast by allergy or renal insufficiency. Our institutional CTA protocol for neurovascular bundle delineation is based upon a radiologic study of male pelvic anatomy [21] and will be used in our institutional Prostate Oncologic Therapy while Ensuring Neurovascular Conservation (POTEN-C) trial to evaluate the ability of dose-sparing of the neurovascular bundle and internal pudendal arteries. Use of vasodilator before scan (0.5 mg sublingual nitroglycerin) is optional. A "split bolus" technique with ~100 cc total iodinated contrast is suggested, wherein a small amount of contrast (i.e., 20 cc) is injected 5 minutes before the scan at 2 cc/second and a second larger bolus is injected during the scan (i.e., 80 cc) via power injector ideally at 3–5 cc/second (faster is preferred). Bolus triggering [22] at the abdominal aorta above the renal arteries is optional; otherwise, an empiric delay of 16–20 seconds before scanning after the high rate bolus is to be used. A 30 mL saline flush before and after the contrast injection is also used. The purpose of this "split bolus" technique is to allow visualization of both the bladder/prostate base interface (from delayed excretion of contrast into bladder) and pudendal/cavernosal arteries (using the arterial filling) in the same scan.

MRI fusion to the simulation/treatment planning CT is preferred at our institution. No Foley or indwelling urinary catheter is used that might deform the prostate or predispose to genitourinary infection. No contrast or endorectal coil is used for the treatment planning MRI; the patient is expected to perform 2 Fleets enemas and complete the same bladder fill for the treatment planning MRI as they would do for simulation and treatment. Optimally, the same immobilization used in the CT simulation would be used for the treatment planning MRI. A T1-weighted MRI sequence optimized for seed localization serves as the image registered to the treatment planning CT scan, and a co-registered T2-weighted MRI imaging sequence is used for anatomic delineation. Information on the pulse sequences used at our institution is provided in Table 2, with examples shown in Fig. 2b, c. Note, this MRI for radiation planning and fusion occurs after fiducial/rectal spacer placement and is separate from the requisite preregistration MRI of the prostate (preferably with endorectal coil and high Tesla strength magnet) which is used for staging.

Table 2 Pulse sequences used in MRI-based SAbR treatment planning for prostate cancer

Pulse sequence	Plane	Slice thickness; FOV	Duration	Comments
Localizer	Axial and sagittal	10 mm; 400 mm	30 seconds	Low spatial resolution images covering the entire pelvis in a short duration allows for planning the subsequent imaging focused on the areas of interest
T2WI FSE	Axial	3 mm; 180 mm	6–7 minutes	Best contrast resolution, depicts well the anatomy of the prostate and the surrounding structures, as well as the distribution of the spacer material, which appears hyperintense (bright) on this pulse sequence
T1WI SPGR	Axial	3 mm; 180 mm	3–4 minutes	This pulse sequence is vulnerable to artifacts caused by metallic foreign bodies, which helps precisely locate the fiducial markers; dense, punctate calcifications may have similar appearance and correlation with concurrent planning CT images is usually helpful

Plan Quality: Planning and Constraints

At UTSW, for the treatment of low- and intermediate-risk prostate cancer, the clinical target volume (CTV) generally includes the entire prostate gland without the seminal vesicles; CTV delineation is assisted by the fused T2-weighted magnetic resonance imaging (MRI) performed for simulation. In some cases, the proximal 1 cm or the entirety of the seminal vesicles may be included, although a reduced-dose PTV may be considered. Our institutional PTV expansion is a uniform 3 mm margin around the CTV based on analysis of our own pre- and posttreatment imaging analyzed for population error.

When static beams are used, a minimum of 10 (typically 13) non-opposing beams are used. For arc rotation techniques, a minimum of 300 degrees (cumulative for all beams) should be utilized, although we frequently do several 360 degree arcs for intensity-modulated arc therapy. For treatment with robotic linear accelerator techniques, care should be taken to avoid using beams that enter or exit through the scrotal sac and testicles. In all cases, the dose is generally prescribed such that 95% of the planning target volume (PTV) will receive the prescription dose. To avoid underdosing areas, we require that 99% of the PTV gets 90% of the prescription dose. For SAbR prostate cancer treatment, PTV coverage is prioritized over meeting normal tissue constraints described below. Examples of CyberKnife, multifield coplanar, and coplanar volumetric modulated arc (VMAT) plans are provided in Fig. 3a–c.

While each treating institution should use planning constraints that are consistent with their experience and planning priorities, Table 3 summarizes constraints used at our institution; these constraints were defined for the use of the most recent phase II protocol for low- and intermediate-risk prostate cancer with a rectal spacer and are now in regular use for off-protocol patient treatment. For the most part, these constraints were also used in the prior phase I/II study, although once the correlation between incidental dose to various volumes of rectal wall was noted [31], constraints were modified based on the more recent phase II study.

Treatment Delivery

In general, the delivery of SAbR fractional doses is similar to that performed for other sites. At our institution, a minimum of 36 hours and a maximum of 8 days should separate each treatment, and no more than 3 fractions will be delivered per week (7 consecutive days). All patients are expected to perform enemas and complete a bladder filling protocol prior to each treatment. Patients are generally prescribed 4 mg of oral dexamethasone prior to each of their treatments. They are also prescribed a starting dose of alpha-1 blocker

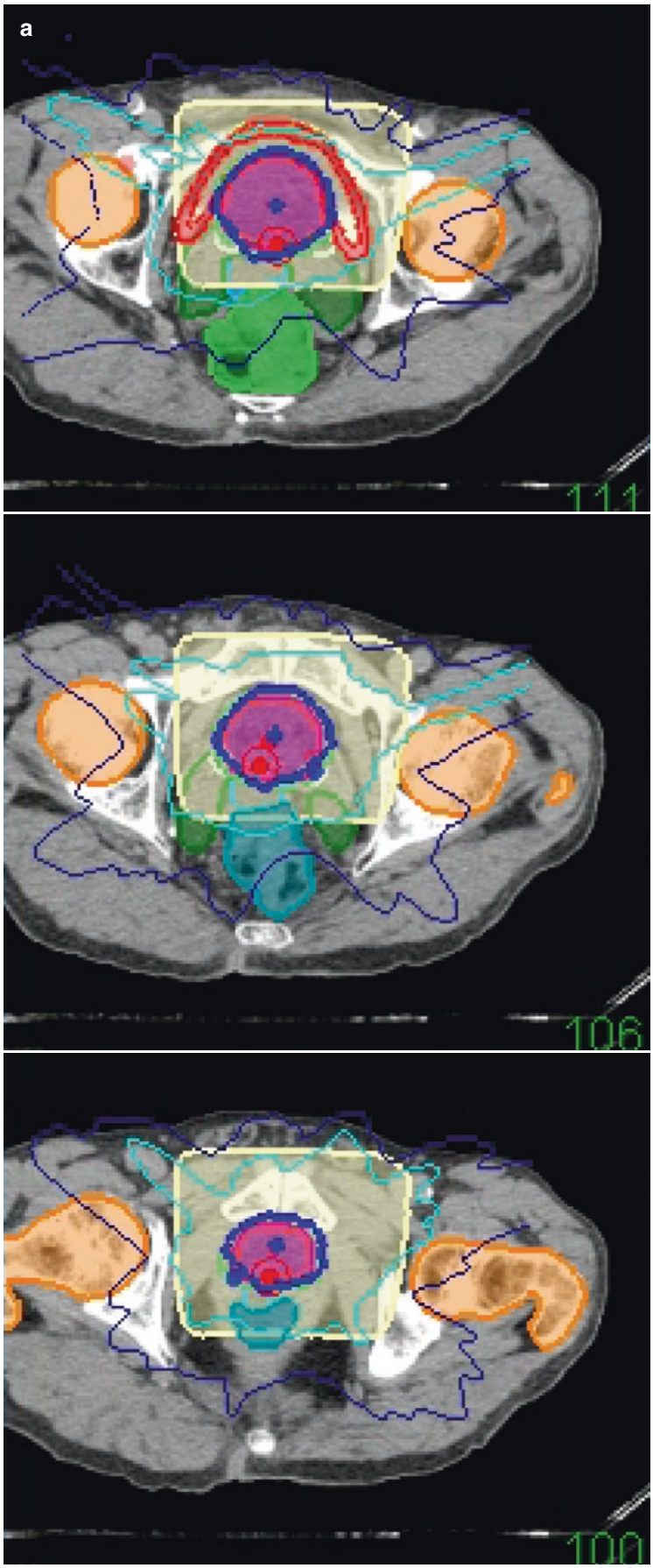

Fig. 3 (**a**–**c**) Representative prostate SAbR planning images. (**a**) CyberKnife plan to 45 Gy in 5 fractions, prescribed to 85% isodose line; 351 total beams, 199 nonzero beams, 115 imaging beams, 152 zero-dose beams. Multiple axial slices at base, mid, and apex; of note, patient had very enlarged median lobe indenting bladder. (**b**) 13-field coplanar SAbR plan to 45 Gy in 5 fractions, rectal balloon fixation; top image shows the beam arrangement, lower image an axial/sagittal/coronal dose distribution. (**c**) Volumetric modulated arc (VMAT) plan to 45 Gy in 5 fractions with temporary hydrogel spacer; 4 arcs used; axial, sagittal, and coronal planes shown

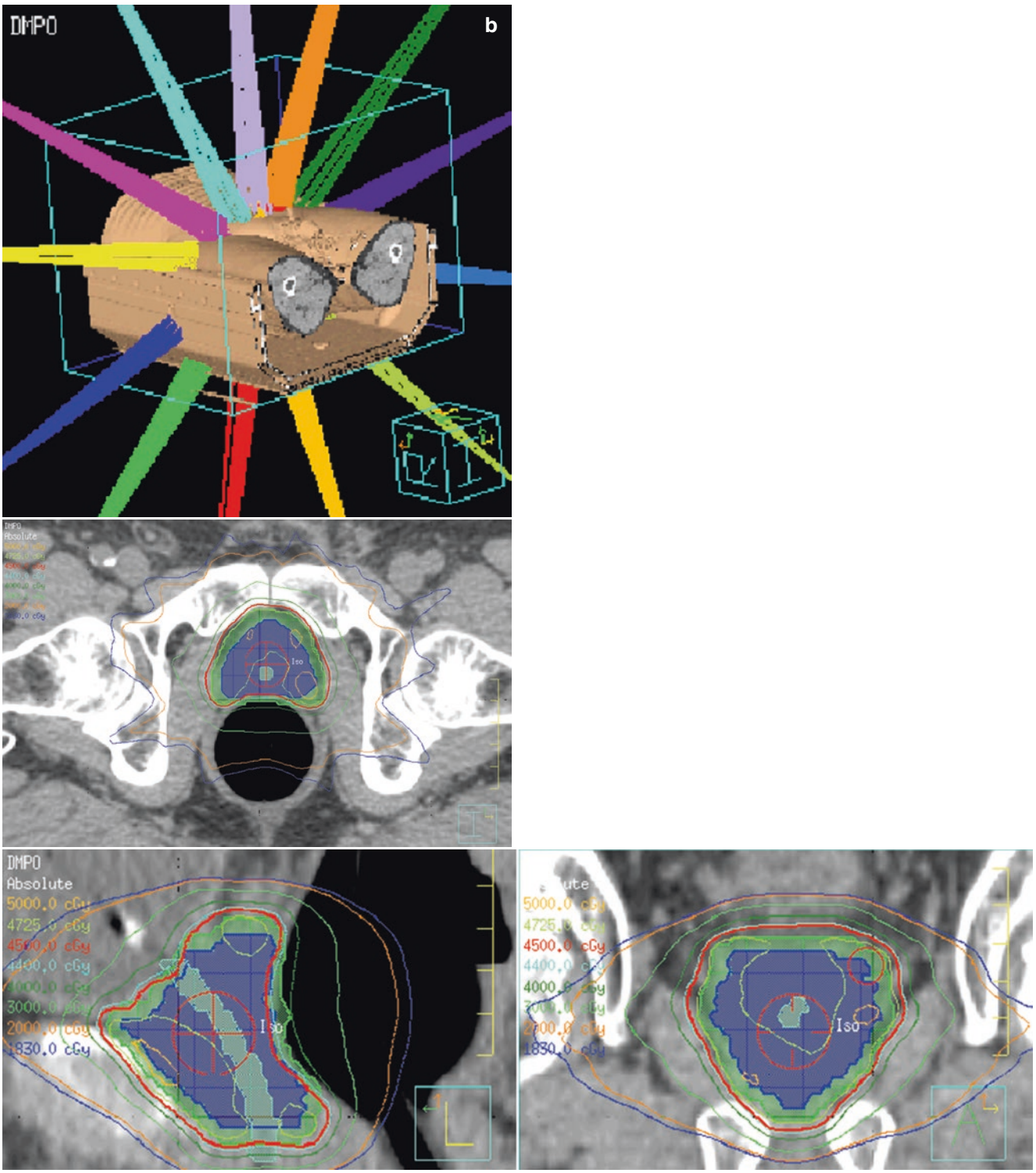

Fig. 3 (continued)

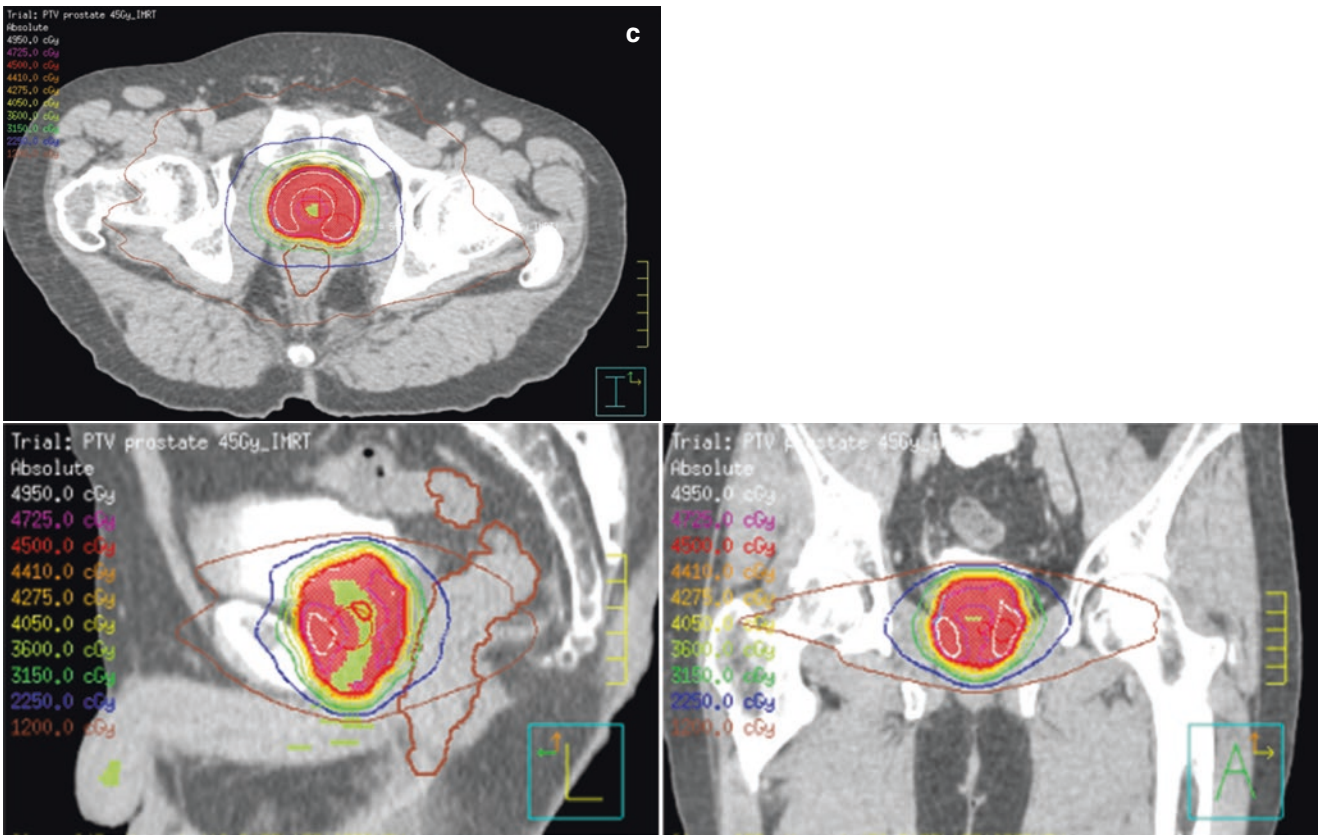

Fig. 3 (continued)

Table 3 Prostate SAbR Normal Tissue Constraints used at UT Southwestern

Organ	Evaluation	Goal		Unit
PTV	Rx Isodose	(60% ~ 90%)		%
	%VRx	>=	95%	%V
	D99%V	>=	0.00	GY
	V105%Out / V105%In	<=	15%	%V
Spinal cord	V20	<=	8.00	cc
	Dmax	<=	22.0	GY
Cauda equina	V25	<=	10.0	cc
	Dmax	<=	27.5	GY
Sacral plexus	V27.5	<=	10.0	cc
	Dmax	<=	30.0	GY
Rectum[a]	V50	<=	3.0	cc
	D50% circumference	<=	24.0	Gy
	D33 circumference	<=	39.0	Gy
Rectum superior to prostate	V25	<=	10.0	cc
	Dmax	<=	30.0	GY
Small intestine	V19.5	<=	10.0	cc
	Dmax	<=	29.0	GY
Prostatic urethra	Dmax	<=	0.00	GY
Bladder wall	V18.3	<=	18.0	cc
	Dmax	<=	0.00	GY
Penile bulb	V30.0	<=	3.00	cc
	Dmax	<=	0.0	GY
Femoral heads	V30	<=	10.0	cc
Skin within fold	Dmax	<=	20.0	GY
Skin not within fold	Dmax	<=	27.3	GY
Neurovascular bundle (right and left)	Dmax	<=	47.25	GY
Seminal vesicles	n/a			

Dmax "point" is defined as 0.035 cc or less
Note: The seminal vesicle dose is simply tracked- (there is not an objective to meet)
[a]Planning efforts should be made to keep the percent rectal circumference receiving 39 Gy < 20% and < 24 Gy under 25% in the post-spacer plan

(i.e., 0.4 mg of tamsulosin) that is continued for 3 months post treatment to prevent acute urinary symptoms. For frame-based SAbR, patients are registered to the stereotactic frame using the marks/tattoos placed at simulation, and then the frame is registered to the treatment machine isocenter. A cone-beam CT (CBCT) scan is then performed for final patient alignment, reviewed by the physician, and once confirmed, treatment is delivered.

The daily CBCT used to perform final patient alignment is also used to assess rectal and bladder filling. If a significant amount of fecal content is noted, the patient will be taken off the table and an enema will be performed, and then the procedure will be attempted again. If the bladder volume significantly deviates from the planned/simulated volume (+/− 20%), the patient will be given more time to fill or will be asked to void a small amount to reach the desired volume.

The physician assessing the final alignment CBCT will be expected to make sure that the implanted fiducials match the planning scan, but assessment of other structures is also necessary; if the physician is planning to cover the seminal vesicles (in whole or in part), they will need to assess whether the bladder fill that day has deformed or displaced the seminal vesicles out of the planned target volume. Even if the fiducials match perfectly, there can be significant deviation due to rotational error caused by the bladder.

Future Directions in SAbR for Prostate Cancer

This chapter has outlined the rapid development and early promising clinical results of SAbR for localized primary prostate cancer. Given the long natural history of prostate cancer, numerous existing good treatment options (particularly for low-risk disease), technological and training entry costs to starting SAbR programs, and current reimbursement models incentivizing more protracted fractionation, however, acceptance of the innovation and opinions on its future course have varied widely. Indeed, one study contrasted a 44% rate of intensity-modulated radiotherapy (IMRT) adoption 5 years after its introduction, compared to a meager 4% of patients receiving SAbR 5 years after its introduction [38], reflecting a fundamentally different development climate. Current studies accordingly appear to be directed to two distinct audiences: (a) those who require more mature data to compare to traditional therapy and (b) those early adopters who wish to see expanded and disease/toxicity-tailored customization of SAbR.

Admittedly, with many good treatment options available for low-risk disease, the biggest advantage of SAbR is simply convenience rather than improved cancer outcomes. To that end, some centers have reduced the number of treatments to a single fraction [39]. While brachytherapy is also convenient, brachytherapy has considerable issues related to unequal quality related to the competency and experience of the brachytherapist. It will be a future challenge for SAbR to find ways to train practitioners to deliver an impressive yet potentially dangerous therapy with standards of high quality and safety. For higher risk patients, the issues are distinctly different. Better treatments are desperately needed to improve control and cure. Future SAbR experiences would need to show better performance compared to conventional techniques, ideally by performing quality, prospective clinical trials.

Following the recent publication of several randomized trials of moderately hypofractionated versus conventionally fractionated radiotherapy, the SAbR community should be encouraged to note that several groups have now initiated trials comparing varying radiotherapy regimens against SAbR regimens. These trials not only will provide critical comparative data but also signify the acceptance of SAbR as a potentially effective and convenient treatment which can become the treatment of choice for many if not most men electing definitive radiotherapy. Further, they may provide the large quality of life questionnaire datasets needed to help guide selection of patients for varying regimens and refine dosimetric constraints. Selected active or recently completed trials are noted below:

- Prostate Advances in Comparative Evidence (PACE, NCT01584258): PACE-A (laparoscopic prostatectomy vs 36.25 Gy in 5 fractions) and PACE-B (78Gy in 39 fractions or 62 Gy in 20 fractions vs 36.25 Gy in 5 fractions) evaluates whether SAbR 36.25 Gy is superior in 5-year bPFS to surgery or conventionally/moderately hypofractionated radiotherapy.
- Swedish Hypofractionated radiotherapy of intermediate risk-localized prostate cancer (HYPO-RT-PC, ISRCTN): 42.7 Gy in 7 fractions versus 78 Gy in 39 fractions; 5-year PFS endpoint.
- Hypofractionation Extended Versus Accelerated Therapy (HEAT, NCT01794403): 36.25 Gy in 5 fractions versus 70.2 Gy in 26 fractions; non-inferiority 2-year PFS (biochemical or + biopsyPFS).
- NRG-GU 005 (NCT03367702): 36.25 Gy in 5 fractions versus 70 Gy in 28 fractions (RTOG 0415 moderate hypofractionation arm “winner” by virtue of noninferiority); EPIC quality of life based toxicity endpoint.

Still, for many already offering SAbR, the promise of a convenient, cost-effective therapy with ability to uniquely tailor dose distributions with high precision can be leveraged to expand its use in higher risk disease and to customize treatment according to patient-specific features. In particular, the ability to boost specific lesions or de-intensify dose to critical structures, based upon advances in multi-parametric MRI, is central to unique investigations focused on balanc-

ing quality of life with disease control. At Memorial Sloan Kettering Cancer Center (MSKCC), for instance, following the recent presentation of results from a dose-escalation SAbR trial showing higher positive biopsy rates in lower dose cohorts [25], a follow-up trial (NCT03269422) is exploring dose-escalation of MRI-targeted lesions to 45 Gy, in an effort to increase disease control. Further, on the heels of randomized data demonstrating a substantial bPFS benefit of combination brachytherapy with conventionally fractionated IMRT [40], the MSKCC group is exploring the safety of a combination of brachytherapy with SAbR to further escalate prostatic tumor dose, while improving the convenience of therapy (NCT02280356).

Reduction in toxicity through aggressive sparing approaches of critical structures also is being prospectively studied. As noted previously in this chapter, a UTSW/MSKCC trial of rectal spacer gel during SAbR demonstrated significant reduction of acute rectal ulceration [34]. Sexual function remains an under-addressed toxicity of all radiation therapies, and similarly is receiving attention in SAbR studies. While previously, the impact of treatment on sexual function has been seen as unavoidable in light of the proximity of several potential critical structures to the prostate, the introduction of MR-based target/OAR delineation, spacer gel to create extra degrees of freedom for treatment planning, and precise dose-delivery and conformability have opened up the possibility of sparing neurovascular structures supplying the penile structures. In an upcoming trial, for instance, a UTSW-led multi-institution randomized phase II investigation called the Prostate Oncologic Therapy while Ensuring Neurovascular Conservation (POTEN-C) trial will evaluate the ability of dose-sparing of the neurovascular bundle and internal pudendal arteries to decrease the incidence of erectile dysfunction in initially potent men undergoing SAbR (NCT03525262).

Together, the existing data noted in this chapter and these ongoing and future studies of SAbR offer the promise of truly disruptive innovations in localized prostate cancer, as measured by cost, toxicity, and efficacy.

Practical Considerations in SAbR for Prostate Cancer

- ASTRO Model Policy for SAbR supports the use of SAbR as an appropriate alternative for select patients with low to intermediate risk disease; support for use in high risk disease is under investigation.
- Patients eligible for prostate SAbR include those with Gleason 6–7 disease, including Gleason 7(4 + 3), with PSA $\leq$ 15 ng/ml, clinical and radiographic T stage T1a-T2c, no significant obstructive urinary symptoms with AUA score $\leq$ 18, and prostate gland sizes <100 cm^3.
- Patients with prior pelvic radiation therapy, prior transurethral resection of the prostate (TURP) and/or cryotherapy, or patients who cannot undergo placement of fiducials and/or temporary hydrogel spacers for rectal protection are poor candidates for prostate SAbR.
- The use of hypofractionated regimens may result in superior outcomes due to the underlying radiobiology of prostate cancer. Doses of 45 Gy in 5 fractions delivered every other day have been shown to be safe in the treatment of prostate cancer with SAbR techniques; the use of a temporary hydrogel spacer may help further reduce rectal toxicity.
- MRI-based treatment planning should be used to best define the prostate target. Special sequences allow for optimal visualization of implanted fiducials and rectal spacer (if used).
- To minimize daily variations in internal anatomy, a standardized bladder-filling protocol and daily enemas should be used. Daily cone-beam CT scans should be used for patient alignment as well as to assess rectum and bladder for anatomic variability. Any significant changes should be addressed before the patient receives treatment.
- Acute urinary symptoms are common; patients should be counseled on the use of NSAIDs and other medications to reduce urinary bother, and may require premedication with alpha blockers.
- Patients are generally followed after SAbR treatment every 3 months for the first year, every 6 months for years 2 and 3, and yearly thereafter with PSA testing.
- As with other radiation-based prostate cancer treatments, it is not recommended for patients to undergo biopsy in the area of the rectum abutting the prostate after treatment unless there is a clear clinical need; as such, colonoscopy should be performed prior to treatment if indicated.

References

1. Lloyd-Davies RW, Collins CD, Swan AV. Carcinoma of prostate treated by radical external beam radiotherapy using hypofractionation. Twenty-two years' experience (1962-1984). Urology. 1990;36(2):107–11.
2. Hodges JC, Lotan Y, Boike TP, Benton R, Barrier A, Timmerman RD. Cost-effectiveness analysis of stereotactic body radiation therapy versus intensity-modulated radiation therapy: an emerging initial radiation treatment option for organ-confined prostate cancer. J Oncol Pract. 2012;8(3 Suppl):e31s–7s.
3. Parthan A, Pruttivarasin N, Davies D, Taylor DC, Pawar V, Bijlani A, et al. Comparative cost-effectiveness of stereotactic body radiation therapy versus intensity-modulated and proton radiation therapy for localized prostate cancer. Front Oncol. 2012;2:81.
4. Brenner DJ, Martinez AA, Edmundson GK, Mitchell C, Thames HD, Armour EP. Direct evidence that prostate tumors show high sensitivity to fractionation (low alpha/beta ratio), similar to late-responding normal tissue. Int J Radiat Oncol Biol Phys. 2002;52(1):6–13.

5. Miralbell R, Roberts SA, Zubizarreta E, Hendry JH. Dose-fractionation sensitivity of prostate cancer deduced from radiotherapy outcomes of 5,969 patients in seven international institutional datasets: alpha/beta = 1.4 (0.9-2.2) Gy. Int J Radiat Oncol Biol Phys. 2012;82(1):e17–24.
6. Pedicini P, Caivano R, Strigari L, Benassi M, Fiorentino A, Fusco V. In regard to Miralbell, et al. Re: Dose-fractionation sensitivity of prostate cancer deduced from radiotherapy outcomes of 5969 patients in seven international institutional datasets: alpha/beta=1.4 (0.9-2.2) Gy. Int J Radiat Oncol Biol Phys. 2013;85(1):10–1.
7. Vogelius IR, Bentzen SM. Meta-analysis of the alpha/beta ratio for prostate cancer in the presence of an overall time factor: bad news, good news, or no news? Int J Radiat Oncol Biol Phys. 2013;85(1):89–94.
8. Marzi S, Saracino B, Petrongari MG, Arcangeli S, Gomellini S, Arcangeli G, et al. Modeling of alpha/beta for late rectal toxicity from a randomized phase II study: conventional versus hypofractionated scheme for localized prostate cancer. J Exp Clin Cancer Res. 2009;28:117.
9. Thames HD, Bentzen SM, Turesson I, Overgaard M, Van den Bogaert W. Time-dose factors in radiotherapy: a review of the human data. Radiother Oncol. 1990;19(3):219–35.
10. Douglas BG, Fowler JF. The effect of multiple small doses of x rays on skin reactions in the mouse and a basic interpretation. Radiat Res. 1976;66(2):401–26.
11. Park C, Papiez L, Zhang S, Story M, Timmerman RD. Universal survival curve and single fraction equivalent dose: useful tools in understanding potency of ablative radiotherapy. Int J Radiat Oncol Biol Phys. 2008;70(3):847–52.
12. Arcangeli G, Saracino B, Arcangeli S, Gomellini S, Petrongari MG, Sanguineti G, et al. Moderate hypofractionation in high-risk, organ-confined prostate cancer: final results of a phase III randomized trial. J Clin Oncol. 2017;35(17):1891–7.
13. Dearnaley D, Syndikus I, Mossop H, Khoo V, Birtle A, Bloomfield D, et al. Conventional versus hypofractionated high-dose intensity-modulated radiotherapy for prostate cancer: 5-year outcomes of the randomised, non-inferiority, phase 3 CHHiP trial. Lancet Oncol. 2016;17(8):1047–60.
14. Lee WR, Dignam JJ, Amin MB, Bruner DW, Low D, Swanson GP, et al. Randomized phase III noninferiority study comparing two radiotherapy fractionation schedules in patients with low-risk prostate cancer. J Clin Oncol. 2016;34(20):2325–32.
15. Catton CN, Lukka H, Gu CS, Martin JM, Supiot S, Chung PWM, et al. Randomized trial of a hypofractionated radiation regimen for the treatment of localized prostate cancer. J Clin Oncol. 2017;35(17):1884–90.
16. Incrocci L, Wortel RC, Alemayehu WG, Aluwini S, Schimmel E, Krol S, et al. Hypofractionated versus conventionally fractionated radiotherapy for patients with localised prostate cancer (HYPRO): final efficacy results from a randomised, multicentre, open-label, phase 3 trial. Lancet Oncol. 2016;17(8):1061–9.
17. Aluwini S, Pos F, Schimmel E, Krol S, van der Toorn PP, de Jager H, et al. Hypofractionated versus conventionally fractionated radiotherapy for patients with prostate cancer (HYPRO): late toxicity results from a randomised, non-inferiority, phase 3 trial. Lancet Oncol. 2016;17(4):464–74.
18. Pollack A, Walker G, Horwitz EM, Price R, Feigenberg S, Konski AA, et al. Randomized trial of hypofractionated external-beam radiotherapy for prostate cancer. J Clin Oncol. 2013;31(31):3860–8.
19. Madsen BL, Hsi RA, Pham HT, Fowler JF, Esagui L, Corman J. Stereotactic hypofractionated accurate radiotherapy of the prostate (SHARP), 33.5 Gy in five fractions for localized disease: first clinical trial results. Int J Radiat Oncol Biol Phys. 2007;67(4):1099–105.
20. King CR, Brooks JD, Gill H, Presti JC Jr. Long-term outcomes from a prospective trial of stereotactic body radiotherapy for low-risk prostate cancer. Int J Radiat Oncol Biol Phys. 2012;82(2):877–82.
21. Katz AJ, Santoro M, Diblasio F, Ashley R. Stereotactic body radiotherapy for localized prostate cancer: disease control and quality of life at 6 years. Radiat Oncol. 2013;8:118.
22. Katz AJ, Kang J. Stereotactic body radiotherapy as treatment for organ confined low- and intermediate-risk prostate carcinoma, a 7-year study. Front Oncol. 2014;4:240.
23. Jackson WC, Dess RT, Litzenberg DW, Li P, Schipper M, Rosenthal SA, et al. A multi-institutional phase II trial of prostate stereotactic body radiation therapy (SBRT) utilizing continuous real-time evaluation of prostate motion with patient reported quality of life. Practical Radiation Oncology. 2018;8(1):40–7.
24. Mantz C. A phase II trial of stereotactic ablative body radiotherapy for low-risk prostate cancer using a non-robotic linear accelerator and real-time target tracking: report of toxicity, quality of life, and disease control outcomes with 5-year minimum follow-up. Front Oncol. 2014;4:279.
25. Zelefsky MJ, Kollmeier MA, McBride S, Pei X, Happersett L, Lin M, et al. 5-year outcomes of a phase 1 dose escalation study using stereotactic body radiosurgery for patients with clinically localized prostate cancer. Int J Radiat Oncol Biol Phys. 2017;99(2):S156–S7.
26. King CR, Collins S, Fuller D, Wang PC, Kupelian P, Steinberg M, et al. Health-related quality of life after stereotactic body radiation therapy for localized prostate cancer: results from a multi-institutional consortium of prospective trials. Int J Radiat Oncol Biol Phys. 2013;87(5):939–45.
27. King CR, Freeman D, Kaplan I, Fuller D, Bolzicco G, Collins S, et al. Stereotactic body radiotherapy for localized prostate cancer: pooled analysis from a multi-institutional consortium of prospective phase II trials. Radiother Oncol. 2013;109(2):217–21.
28. Freeman D, Dickerson G, Perman M. Multi-institutional registry for prostate cancer radiosurgery: a prospective observational clinical trial. Front Oncol. 2014;4:369.
29. Lotan Y, Stanfield J, Cho LC, Sherwood JB, Abdel-Aziz KF, Chang CH, et al. Efficacy of high dose per fraction radiation for implanted human prostate cancer in a nude mouse model. J Urol. 2006;175(5):1932–6.
30. Boike TP, Lotan Y, Cho LC, Brindle J, DeRose P, Xie XJ, et al. Phase I dose-escalation study of stereotactic body radiation therapy for low- and intermediate-risk prostate cancer. J Clin Oncol. 2011;29(15):2020–6.
31. Kim DW, Cho LC, Straka C, Christie A, Lotan Y, Pistenmaa D, et al. Predictors of rectal tolerance observed in a dose-escalated phase 1-2 trial of stereotactic body radiation therapy for prostate cancer. Int J Radiat Oncol Biol Phys. 2014;89(3):509–17.
32. Hannan R, Tumati V, Xie XJ, Cho LC, Kavanagh BD, Brindle J, et al. Stereotactic body radiation therapy for low and intermediate risk prostate cancer-results from a multi-institutional clinical trial. Eur J Cancer. 2016;59:142–51.
33. Kim DN, Straka C, Cho LC, Lotan Y, Yan J, Kavanagh B, et al. Early and multiple PSA bounces can occur following high-dose prostate stereotactic body radiation therapy: subset analysis of a phase 1/2 trial. Pract Radiat Oncol. 2017;7(1):e43–e9.
34. Folkert MR, Zelefsky MJ, Hannan R, Desai NB, Lotan Y, Laine AM, et al. Multi-institutional phase 2 trial of high-dose stereotactic body radiation therapy with temporary hydrogel spacer for low- and intermediate-risk prostate cancer. Int J Radiat Oncol Biol Phys. 2017;99(5):1319–20.
35. Hamstra DA, Mariados N, Sylvester J, Shah D, Karsh L, Hudes R, et al. Continued benefit to rectal separation for prostate radiation therapy: final results of a phase III trial. Int J Radiat Oncol Biol Phys. 2017;97(5):976–85.

36. Mariados N, Sylvester J, Shah D, Karsh L, Hudes R, Beyer D, et al. Hydrogel spacer prospective multicenter randomized controlled pivotal trial: dosimetric and clinical effects of perirectal spacer application in men undergoing prostate image guided intensity modulated radiation therapy. Int J Radiat Oncol Biol Phys. 2015;92(5):971–7.
37. Jones RT, Hassan Rezaeian N, Desai NB, Lotan Y, Jia X, Hannan R, et al. Dosimetric comparison of rectal-sparing capabilities of rectal balloon vs injectable spacer gel in stereotactic body radiation therapy for prostate cancer: lessons learned from prospective trials. Med Dosim. 2017;42(4):341–7.
38. Jacobs BL, Yabes JG, Lopa SH, Heron DE, Chang CH, Schroeck FR, et al. The early adoption of intensity-modulated radiotherapy and stereotactic body radiation treatment among older Medicare beneficiaries with prostate cancer. Cancer. 2017;123(15):2945–54.
39. Arcangeli S, Greco C. Hypofractionated radiotherapy for organ-confined prostate cancer: is less more? Nat Rev Urol. 2016;13(7):400–8.
40. Morris WJ, Tyldesley S, Rodda S, Halperin R, Pai H, McKenzie M, et al. Androgen Suppression Combined with Elective Nodal and Dose Escalated Radiation Therapy (the ASCENDE-RT Trial): an analysis of survival endpoints for a randomized trial comparing a low-dose-rate brachytherapy boost to a dose-escalated external beam boost for high- and intermediate-risk prostate cancer. Int J Radiat Oncol Biol Phys. 2017;98(2):275–85.

Stereotactic Ablative Radiotherapy (SAbR) for Primary Renal Cell Carcinoma

Osama Mohamad, Robert D. Timmerman, and Raquibul Hannan

Abbreviations

4D CT	4-dimensional computer tomography
AUA	American Urologic Association
CBCT	Cone-beam computed tomography
CNS	Central nervous system
CSS	Cancer-specific survival
CT	Computed tomography
CTV	Clinical target volume
eGFR	Estimated glomerular filtration rate
GTV	Gross target volume
IMRT	Intensity-modulated radiation therapy
IORT	Intraoperative radiation therapy
ITV	Internal target volume
LC	Local control
MRI	Magnetic resonance imaging
NCCN	National Comprehensive Cancer Network
OS	Overall survival
PFS	Progression-free survival
PTV	Planning target volume
RCC	Renal cell cancer
RFA	Radiofrequency ablation
RT	Radiation therapy
SAbR	Stereotactic ablative radiation therapy
SBRT	Stereotactic body radiation therapy
VMAT	Volumetric modulated arc therapy

O. Mohamad
University of Texas Southwestern Medical Center, Radiation Oncology, Dallas, TX, USA

R. D. Timmerman
University of Texas Southwestern Medical Center, Radiation Oncology and Neurological Surgery, Dallas, TX, USA

R. Hannan (✉)
University of Texas Southwestern Medical Center, Radiation Oncology and Immunology, Dallas, TX, USA
e-mail: raquibul.hannan@utsouthwestern.edu

Introduction

The incidence of kidney cancers, most of which are renal cell carcinomas (RCCs), has steadily increased in the late 1990s and early 2000s [1]. In 2019, an estimated 73,820 cases will be diagnosed, and about 14,770 people will die of the disease [2]. These considerable numbers make kidney cancer the eighth most common cancer in the United States. Most RCCs are diagnosed at an early stage because of the increased use of diagnostic imaging [3, 4]. Surgery remains the standard curative treatment for RCCs. Partial nephrectomy achieves results similar to radical nephrectomy in properly selected patients with small renal tumors [5–12] and is valuable in patients with a solitary kidney, reduced renal function, and other medical conditions with future risk for reduced renal function. Laparoscopic and robotic partial nephrectomy approaches have reduced hospital stays [13–15]. However, depending on the patient's overall health status and tumor size, observation and in situ tumor ablation are alternative options to surgical resection [16].

Active surveillance is recommended for renal masses less than 3 cm in size, per the American Urologic Association (AUA), and for patients with T1a tumors or tumors less than 4 cm, per the National Comprehensive Cancer Network (NCCN) guidelines. The natural history of small renal masses is well described [17–22]. One meta-analysis followed 234 lesions for a median of 30 months and reported an average growth rate of 0.28 cm per year for all tumors and 0.4 cm per year in the subset of patients with biopsy-confirmed RCC. About one-third of all lesions did not grow [17]. Stable lesions such as these warrant observation. For growing lesions, however, various interventions can be offered, depending on tumor stage and other patient-related characteristics. Many patients are ineligible for surgery because of simultaneous comorbidities, particularly kidney disease, which is prevalent in patients with RCC. Ablative minimally invasive treatments, including cryoablation and radiofrequency ablation (RFA), are commonly used minimally invasive approaches

D. M. Trifiletti et al. (eds.), *Stereotactic Radiosurgery and Stereotactic Body Radiation Therapy*,
https://doi.org/10.1007/978-3-030-16924-4_26

in patients with RCC who need but cannot undergo surgical resection [9, 23–29]. These ablative therapies show good local control (LC) at an acceptable complication rate [30–33], but long-term outcomes are not available yet. Additional shortcomings of ablative techniques include their limited application (for example, hilar tumors are not good candidates due to the heat sink effect near large blood vessels and renal pelvis), a lack of good surrogate outcome measures (i.e., contrast enhancement loss on CT scan), suboptimal LC when compared to surgical excision, and difficult surgical salvage [32–34].

Traditionally, RCC has been considered a radioresistant tumor, and conventional radiotherapy (RT) has not been used to treat primary renal tumors [35]. In addition to the radiobiology, technical challenges associated with treating kidney tumors with RT include limited radiation tolerance of normal kidneys and nearby tissues and difficulty targeting a moving tumor. However, the emergence of completely noninvasive, image-guided stereotactic technologies has made feasible what was once considered technically challenging.

In this chapter, we will focus on the use of stereotactic ablative radiotherapy (SAbR) (also known as stereotactic body radiation therapy, SBRT) for patients with primary RCC. We will review the available literature and focus on patient selection and technical considerations.

Radiobiological Rationale

Historically, RCC was considered radioresistant. Much of this opinion was based on a single study that examined the radiosensitivity of multiple human cancer cell lines in vitro [36]. Since then, however, multiple in vitro and in vivo studies have demonstrated that RCC can be radiosensitive, especially at higher doses per fraction, such as those used for SAbR [37, 38]. In an in vitro cell model, for example, cell survival curves suggested a larger shoulder in the low-dose region followed by an exponential decrease in survival at doses greater than 6 Gy [37]. In an ex vivo model, high dose-per-fraction regimens effectively controlled implanted human RCC in nude mice [38]. Clinical experience corroborates this conclusion, as SAbR shows high LC for CNS and extracranial metastases [39–43]. In fact, at hypofractionated dose levels, RCC may even be more radiosensitive than other primary sites. Lung, for example, requires 54 Gy in three fractions for LC compared to RCC, where 36 Gy in three fractions appears to provide adequate control [42–45]. However, application of SAbR to primary RCC has been limited to a few retrospective and only a handful of prospective studies with limited follow-up [46].

Outcomes and Adverse Events of SAbR for Primary RCC

Conventionally fractionated (i.e., 1.8–2 Gy daily) preoperative (neoadjuvant) and postoperative (adjuvant) RTs have been investigated in patients with RCC without promising results [47–50]. In two randomized clinical trials delivering neoadjuvant conventional RT (30 or 33 Gy over 3 weeks) in more than 200 patients with primary RCC, overall survival (OS) was similar between the RT plus nephrectomy and nephrectomy only groups [47, 48]. Similarly, adjuvant conventional RT trials failed to show any difference in OS or local recurrence even in high-risk patients, such as those with venous involvement [49, 50]. Radiotherapy-related toxicities were higher in the RT group in both studies. A meta-analysis of adjuvant RT for RCC showed that, while most studies were retrospective and used older techniques, adjuvant RT reduced local recurrence but did not improve OS [51].

Very limited data are available for the use of intraoperative RT (IORT) for primary RCC, with no randomized trials. In one of the largest studies, a multi-institutional cohort of patients with advanced or recurrent RCC received preoperative or postoperative IORT with favorable outcomes compared to historical controls [52].

While the application of SAbR to primary RCC is newer, the results are promising. The first retrospective study reported the results of nine patients who refused surgery and were treated with SAbR to primary kidney tumors 1.5–10 cm in size, with a median follow-up of 26.7 months [53]. Most patients received 40 Gy in five fractions. No local failures were reported and adverse events were limited to nausea, vomiting, and weight loss. In another study, 33 primary renal lesions in 14 patients were treated with SAbR, resulting in LC of 94% at a median follow-up of 17 months [54]. The Karolinska Institute reported their experience with eight patients who received SAbR to inoperable primary RCC, among other patients who received SAbR to metastatic RCC lesions [43]. With more than 3 years of follow-up, LC exceeded 90% with acceptable toxicity. Another retrospective study by the same group analyzed 50 patients with primary and metastatic RCC which achieved high rates of LC with 40 Gy in five fractions and 45 Gy in three fractions [55].

The International Radiosurgery Oncology Consortium for Kidney published a pooled analysis of 223 patients with RCC from nine institutions with a median follow-up of 2.6 years. Patients received either a single fraction (median 25 Gy) or multiple fractions (median 4 fractions, median 40 Gy). When taken together, LC, progression-free survival (PFS), and OS at 4 years were 97.8%, 65.4%, and 70.7%, respectively. There were only three patients with grade 3/4

bowel toxicity. The mean reduction in eGFR (glomerular filtration rate) was 5.5 ml/min at last follow-up. Larger tumor size predicted worse PFS, and cancer-specific survival (CSS). Interestingly, multiple-fraction SAbR had worse distant control, PFS, and CSS than single-fraction, but no difference in LC [56, 57].

Evidence from Prospective Clinical Trials

In a prospective phase I dose-escalation study, 19 patients with medically inoperable primary RCC were treated with SAbR. They received 24–48 Gy, all in four fractions. With a median follow-up of 13.7 months, late grade 3/4 toxicity was reported in four patients (two patients with grade 3 renal toxicity and one with a grade 4 duodenal ulcer). All 15 evaluable patients had either partial response or stable disease [58].

In another prospective phase I dose-escalation study of inoperable RCC cases, tumors were treated using SAbR to 21, 27, 33, 39, and 48 Gy, all in three fractions (median of 33 Gy in three fractions). Two failures were reported at the lowest 7 and 9 Gy dose levels only with an LC of 87% at a median follow-up of 36.7 months. Only one late grade 3 toxicity (renal dysfunction) was reported [59]. In an update of this study, an analysis of a total of 41 renal tumors from 40 patients over a 5-year period found that the mean pretreatment tumor growth rate of 0.68 cm/y decreased to −0.37 cm/year posttreatment ($P < 0.0001$) and the mean tumor volume growth rate of 21.2 cm^3/per year before treatment decreased to −5.35 cm^3/y after treatment ($P = 0.002$). Local control, defined as less than 5 mm of growth, was achieved in 38 of 41 tumors [60]. Interestingly, the authors noticed that even in the setting of good local control, SAbR did not have an impact on the enhancement of the residual mass. Physicians treating renal tumors with thermal ablative technique are reassured when enhancement is lost since the technique inherently disrupts the treated tissue leading to loss of tumor vasculature and lack of contrast dye uptake. However, SAbR primarily kills tumor cells by DNA damage with minimal damage to the vasculature. As a result, it is not surprising that local control is seen in the setting of continued contrast enhancement.

In another prospective phase I study, 20 patients with primary RCC were treated with SAbR to 26 Gy in one fraction (tumors smaller than 5 cm) or 42 Gy in three fractions (tumors at least 5 cm). With a median follow-up of 6 months, grade 1/2 toxicity (nausea, chest wall pain, and fatigue) was observed in 60% of patients, and there was no grade 3 or higher toxicity [61].

Siva and colleagues reported a prospective study of 37 patients with primary RCC treated with SAbR to 26 Gy in one fraction (tumors smaller than 5 cm) or 42 Gy in three fractions (tumors at least 5 cm). With a median follow-up of 24 months, 2-year LC and OS were 100% and 92%, respectively, with grade 3 adverse events observed in only one patient (3%) [62, 63].

Staehler and colleagues reported a prospective study of 40 patients with renal tumors (mix of transitional cell and renal cell cancers) treated with CyberKnife® (Accuray, Sunnyvale, CA, USA) to deliver stereotactic RT to 25 Gy in one fraction. With a follow-up of 28.1 months, LC was 98% after 9 months. Nineteen patients had complete remissions [64]. The same group updated their results for 52 patients with RCC in an abstract in 2016. CyberKnife was used again to deliver the same dose. With a follow-up of 26.9 months, LC was 98% after 9 months. Six patients had complete remission, and 33 had partial remission. In both studies, adverse events were limited to grade 1/2 toxicities (dermatitis, fatigue, and nausea) [65].

In a prospective phase II study, SAbR was used to treat metastatic or inoperable primary RCC to 5–15 Gy in two to five fractions. After a follow-up of 52 months, median survival was 32 months, and LC was 79%. Ninety percent of toxicities were grade 1/2 [66].

Finally, a meta-analysis of seven retrospective and three prospective trials investigating one to six fractions of SAbR for 126 patients with primary RCC reported LC of 94% with 4% grade 3 or higher and 21% grade 1/2 toxicity [67].

Multiple studies of SAbR are currently accruing patients with primary RCC, including a phase II clinical trial at the University of Texas Southwestern Medical Center in Dallas, Texas, that is testing SAbR for small primary RCC (less than 5 cm) that is growing at a rate of more than 0.4 cm per year with the primary endpoint of biopsy confirmation of tumor no-viability at 1-year posttreatment (NCT02141919).

In all the above studies (Table 1), adverse events were not common, and when they happened, they were usually mild. Nausea, fatigue, and dermatitis were the most common in the acute setting, whereas renal dysfunction and duodenal ulcers were the most common late adverse events. SAbR is generally considered safe in patients with only one functioning kidney [55], but caution should be applied in patients with baseline chronic kidney disease, as SAbR may worsen renal function and some patients may potentially progress to dialysis [68]. An analysis of renal dysfunction after SAbR revealed that eGFR declined by 39% and 25% for every 10 Gy physical dose delivered in patients who received 26 Gy in one fraction or 42 Gy in three fractions, respectively [69]. As expected, the extent of SAbR-induced kidney damage is related to the volume of kidney parenchyma receiving RT, total dose, dose per treatment, and patient-related comorbidities, such as diabetes and hypertension. Thus, it is essential to limit dose to normal kidney tissue and to be hypervigilant with patients at the highest risk of developing kidney failure.

Table 1 Summary of reported studies treating primary RCC with radiation therapy

Study, publication year, number of patients	Participants	Fractionation	Outcomes/adverse events	Notes
Neoadjuvant				
[47], 1973, 141	Surgery vs. RT followed by surgery	Conventional, 30 Gy in 3 weeks	Preoperative irradiation did not improve outcomes	Prospective
[46], 1977, 88	Surgery vs. RT followed by surgery	Conventional, 33 Gy in 3 weeks	5-year OS 47% in the RT arm vs. 63% in the surgery arm; not statistically significant	Prospective
[74], 2017, 14	Metastatic RCC: SAbR followed by cytoreductive surgery	15 Gy in 1 fraction	Treatment well tolerated; SAbR increased expression of calreticulin and TAA, as well as the percentage of proliferating T cells compared with archived RCC tumors	Single-arm feasibility study
Adjuvant				
[48], 1973, 100	Surgery vs. surgery followed by RT	Conventional RT	Postoperative irradiation did not improve outcomes	Prospective
[49], 1987, 72	Stages II and III renal adenocarcinoma; surgery vs. surgery followed by RT	50 Gy in 20 fractions	Postoperative irradiation worsened complications and did not improve outcomes	Prospective
Definitive (SAbR)				
[52], 2004, 9	Nonmetastatic RCC	40 Gy in 5 fractions	With a median follow-up of 26.7 months, 4 of the 9 patients have survived with a median follow-up of 57.8 months. Adverse events were limited	Retrospective
[53], 2006, 14	Primary RCC	12–60 Gy (median 40) in 2–10 (median 5) fractions	LC of 94% with median follow-up of 17 months	Retrospective
[42], 2005, 8	Inoperable primary RCC	8 Gy × 4, 10 Gy × 4 and 15 Gy × 3	LC >90% with minimal toxicity	Retrospective
[57], 2015, 19	Inoperable primary RCC	24 to (48 Gy, all in 4 fractions	Dose escalation successfully achieved without dose-limiting toxicities with a median follow-up of 13.7 months	Prospective phase I dose-escalation study
[58], 2013, 15	Inoperable primary RCC	21, 27, 33, 39, and 48 Gy, all in 3 fractions	Only two failures at the lowest dose groups	Prospective phase I dose-escalation study
[60], 2014, 20	Inoperable primary RCC	3D conformal RT; 26 Gy in 1 fraction (tumor < 5 cm) or 42 Gy in 3 fractions (tumors > 5 cm)	Treatment well tolerated with no grade 3 toxicity	Prospective phase I study
[62], 2017, 37	Inoperable primary RCC	3D conformal RT; 26 Gy in 1 fraction (tumors < 5 cm) or 42 Gy in 3 fractions (tumors > 5 cm)	2-year OS and LC were 100% and 92%, respectively, with grade 3 adverse events observed in only 1 patient	Prospective
[64], 2016, 52	Primary RCC	CyberKnife; 25 Gy in 1 fraction	LC was 98% and adverse events were limited to grade 1/2 toxicities	Prospective
[65], 2006, 5	Inoperable primary RCC (plus 25 patients with metastatic RCC)	5–15 Gy in 2–5 fractions	Median survival was 32 months, and LC was 79%. Ninety percent of toxicities were grade 1/2	Prospective phase II study
[66], 2012, 126	Primary RCC	1–6 fractions (most common 40 Gy in 5 fractions)	LC of 94% with 4% grade 3 or higher and 21% grade 1/2 toxicity	Systematic review
[56], 2017, 223	Primary RCC	Single fraction (median 25 Gy) or multiple fractions (median 4 fractions, median 40 Gy)	LC, PFS, and OS at 4 years were 97.8%, 65.4%, and 70.7%, respectively. There were only 3 patients with grade 3/4 bowel toxicity	Retrospective

Abbreviations: *RT* radiotherapy, *Gy* Gray, *OS* overall survival, *RCC* renal cell carcinoma, *SAbR* stereotactic ablative radiotherapy, *LC* local control, *PFS* progression-free survival

Stereotactic Ablative Radiotherapy for Kidney Tumors: Technical Considerations

Kidney tumors exhibit significant inter- and intra-fractional motion. Thus, the successful application of SAbR requires additional technical considerations. These critical issues include robust immobilization for accurate tumor targeting, dynamic target motion management, dose distribution maps with rapid dose falloff, and image guidance with cone-beam computed tomography scanning (CBCT). Given the increased dose per fraction and the significance of immobilization and motion management, SAbR sessions are typically longer than conventional RT sessions, and, thus, patient comfort is of utmost importance for high-quality reproducible treatments. Positions that are uncomfortable for the patient should be avoided to prevent uncontrolled movement during treatments. An unstable patient setup jeopardizes LC and increases the risk of unwarranted adverse events.

Secure Immobilization

For accurate delivery of radiation beams, patients should be placed in a stable setup that allows accurate interfractional reproducibility of target positioning. To achieve this, modern stereotactic RT utilizes molded cushions, stereotactic body frames, and a rigorous setup process to ensure accurate patient immobilization prior to treatment delivery (Fig. 1a, b). Practically, the stereotactic system is defined by reliable fiducials within a three-dimensional coordinate system. External fiducials relate to the treatment frame, whereas internal fiducials may be implanted markers or reliably identified anatomic landmarks near the target volume. With modern image guidance, the tumor itself may serve as the fiducial. The fiducials and the coordinate system should be directly related to the radiation-producing device (e.g., couch and gantry) in a reproducible and secure fashion. In turn, targets should be well-defined according to this same 3D coordinate system. As such, the patient is set up for each treatment so the radiation can be directed toward an isocenter or target according to the known 3D coordinates, as determined in the treatment planning process. Excellent SAbR outcomes cannot be achieved without a well-designed, rigorous, and stable setup. Given the complexity of the process, a well-trained team of therapists is indispensable during simulation and radiation delivery to achieve the best outcomes.

Motion Assessment and Management

Respiratory motion causes significant geometric and dosimetric uncertainties in thoracic and upper abdominal RT [70, 71]. A large motion in a renal tumor may lead to significant uncertainties and enlargement in the target volume. The impact of such uncertainties is amplified in hypofractionated regimens such as SAbR. Multiple studies have investigated kidney displacement with breathing. Displacement was estimated to be less than 1 cm for both left and right kidneys, and it could not be predicted from the displacement of the diaphragm, liver dome, or abdominal wall surrogates, especially for the left kidney [72]. Such motion, in addition to the kidneys' close proximity to radiosensitive critical organs such as the liver and small and large intestines, can significantly increase the risk of adverse events in renal SAbR. Equally important is that a moving target will expose more of the normal kidney parenchyma to radiation and may

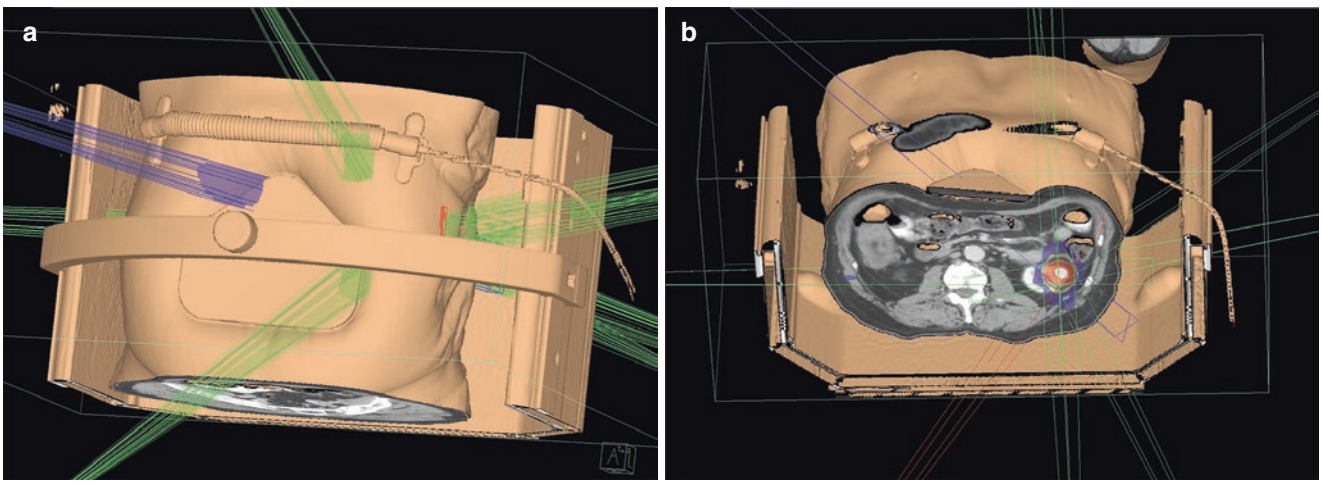

Fig. 1 (**a**, **b**) SAbR setup for the treatment of primary RCC. Stereotactic body frame (Elekta, Stockholm, Sweden) along with vacuum bag is used for reproducible setup. Abdominal compression is used for target motion control of primary kidney tumor. Multiple noncoplanar beam arrangement is shown

therefore cause significant kidney damage. Therefore, it is critical to account for target motion in patients receiving SAbR for primary RCC.

Typically, using diaphragmatic motion as a surrogate for tumor motion cannot replace a thorough understanding of the motion of the tumor itself, mostly because of the anatomic complexity and the differences in breathing patterns among different patients. Dynamic imaging, such as fluoroscopy, ultrasound, or 4D CT scans with the patient in the free-breathing state, would quantify the specific motion of a target and inform appropriate expansions of targets to encompass this movement or trigger the use of motion control in cases where motion was considered excessive. In our institution, if the initial assessment of tumor motion confirms that the tumor motion is greater than 0.5 cm in the axial plane and/or greater than 1.0 cm in the cranio-caudal plane, motion management protocols are activated [73]. Motion management is achieved by means that reduce that motion (e.g., active breath-hold or abdominal compression) or beam gating with the respiratory cycle. As a practical example in an RCC case in our institution, first a motion study is performed (typically using fluoroscopy or 4D CT) to determine if the gross tumor volume (GTV) is moving more than 1.0 cm in the longitudinal direction. If it is, abdominal compression (Fig. 1a, b) is applied with coaching (e.g., urging the patient not to "push back" against the abdominal plate) until the GTV moves less than 1.0 cm (verified again on fluoroscopy or 4D CT). Then, with compression/coaching applied when necessary, a 4D CT is performed. On the other hand, if motion is less than 1.0 cm in the longitudinal direction, a 4D CT is performed, bypassing motion management techniques. Since it is well established that both kidneys move with respiration, the initial motion assessment steps can be omitted and abdominal compression can be used upfront to reduce kidney motion, followed by 4D CT for target margin delineation.

Target Delineation

Any imaging modality can be used to define target volumes in RCC SAbR, as long as these images create sufficient contrast between the tumor and normal kidney tissue and can be reliably "fused" with the planning CT scan (1–3 mm sections), which should be done with IV contrast (arterial phase for better enhancement), if possible. The targeted lesion, the GTV, is outlined in all three planes using appropriate CT windowing, contrast images, and information from other diagnostic scans, such as MRI, fused to the planning CT scan. Typically, a 4D CT scan generates an internal target volume (ITV) after carefully considering the regularity of the breathing pattern. In patients with irregular breathing, ITV expansions can be erroneous. No clinical target volume (CTV) expansion is needed. We typically add an additional 0.5 cm isotropic margin to the GTV (or ITV) to constitute the planning target volume (PTV).

Contouring Critical Structures

Critical structure contours are drawn in primary planning 4D CT (average scan). In general, critical structures should be contoured if they are found within an axial slice within 10 cm in the cranio-caudal direction of any PTV slice. The spinal cord, for example, will be contoured along the extent of the tumor as well as 10 cm above and below the PTV. Normal kidney parenchyma should be carefully contoured subtracting the primary tumor, renal pelvis, and hilum from the total kidney. The serially functioning renal pelvis and ureters are contoured separately.

Dosimetry and Target Prescription Dose

SAbR to RCC tumors is prescribed to the PTV with ideally 95% target volume coverage. The common prescriptions used for SAbR of primary RCC include 25 Gy in one fraction, 36 Gy in three fractions every other day, or 40 Gy in five fractions every other day. At UTSW, we typically deliver two fractions per week. The dose fractionations should be chosen based on tumor size and proximity to the critical structures, allowing adherence to published dose constraints [74]. SAbR plans should prioritize adequate minimum target coverage and rapid dose fall-off gradients outside of the target without much consideration for target dose homogeneity. This rapid dose falloff outside the target avoids toxicity, especially in cases of oligo-hypofractionation. Accordingly, hotspots must be manipulated to occur within the target and not in adjacent normal tissue. This is especially important next to critical, serially functioning normal structures (e.g., the ureters, spinal cord, or intestines). For SAbR, 3D conformal treatment planning is preferred using at least seven non-opposing and noncoplanar beams with roughly equal weighting (Fig. 2a–c). Conformal or volumetric modulated arc therapy (VMAT) can also be used if noncoplanar arcs are utilized. IMRT may result in dosimetric inaccuracies, especially where tumor motion is either unknown or not properly controlled. IMRT, thus, should only be utilized if tumor motion is less than 5 mm.

Treatment Delivery and Image Guidance

Given this compact dosimetry and the delivery of potent ablative doses to targets in close association with critical normal structures, errors in beam or target positioning could be

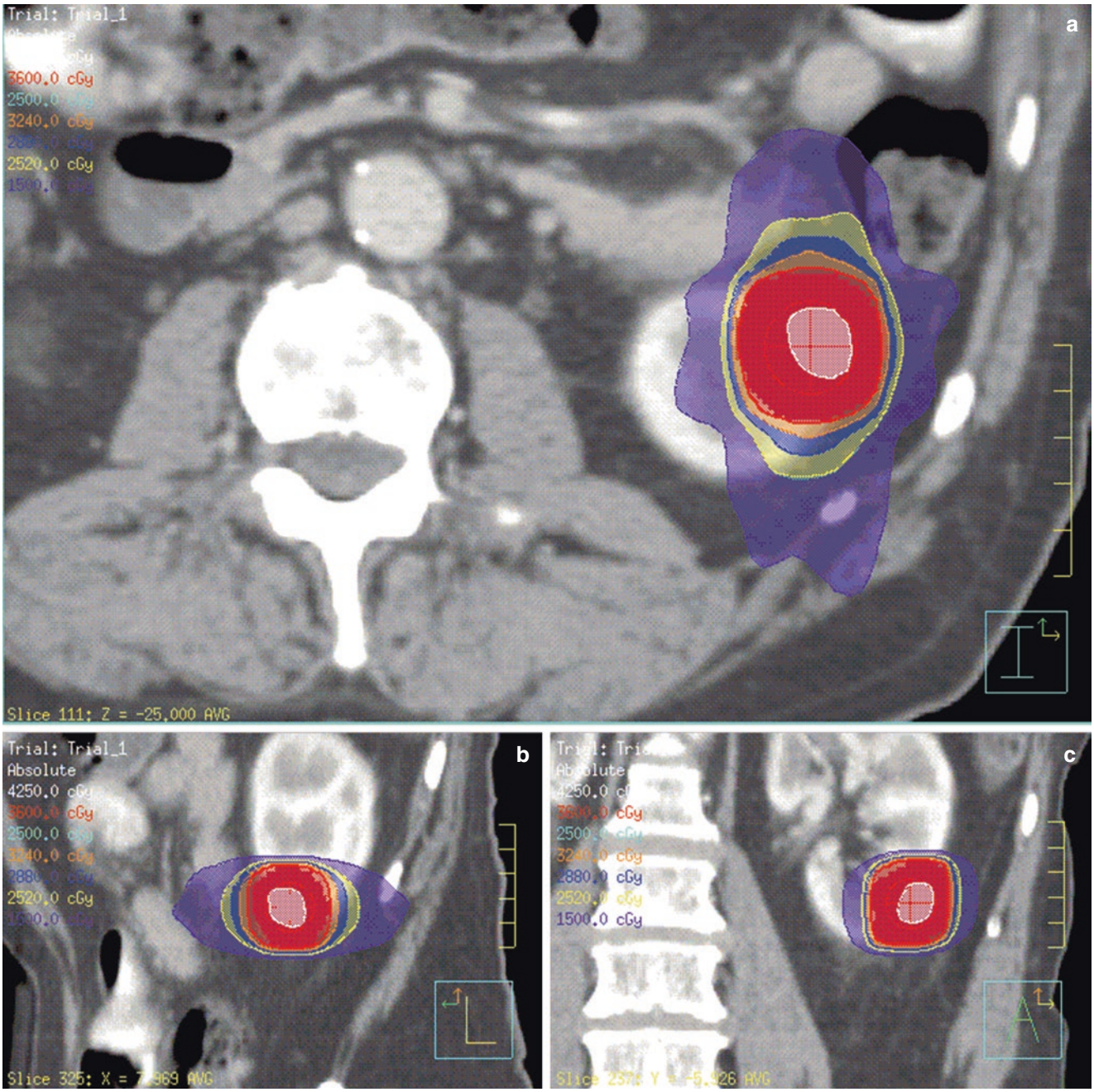

Fig. 2 SAbR plan for the treatment of primary RCC. Optimized SAbR plan isodose distribution for a left kidney tumor in axial (**a**), sagittal (**b**), and coronal (**c**) planes is shown with adequate PTV coverage and a sharp dose falloff to minimize dose to the nearby bowel and adjacent normal kidney

catastrophic with regard to both tumor control and toxicity. Image guidance increases the confidence in setup and reduces setup uncertainty margins. In our institution, we use CBCT prior to every fraction and also intrafractionally. Aligning setup CBCT to treatment CT scanning using the stereotactic fiducials (e.g., implanted markers, entire ipsilateral kidney, or even the tumor itself) before and during treatment mostly eliminates interfraction error and reduces intrafraction error, allowing the smaller margins critical to the overall SAbR approach. If tumor is not visible on CBCT, as often is the case for nonexophytic lesions, alignment with the entire kidney is performed. Six-degree couch with rotational correction is helpful in this setting. Sophisticated image guidance reduces uncertainties and allows smaller treatment margins. In our experience, SAbR sessions are usually separated by a minimum of 48 hours.

Successful Treatment Planning: Characteristics of a Good Treatment Plan

Successful SAbR treatment planning for RCC requires meeting the following criteria:

1. Normalization: Treatment plans should be normalized such that 100% corresponds to the center of mass of the PTV receiving the highest dose. As such, prescription dose is prescribed to a lower isodose compared to conventional planning (e.g., 70–80% isodose).
2. Prescription isodose surface coverage: Ninety-five of the PTV should be covered by the prescription isodose surface, and 99% of the PTV should receive at least 90% of the prescription dose.
3. Target dose heterogeneity: The prescription isodose surface must be at least 60% and no more than 90% of the maximum dose at the center of the PTV, which is the normalization point noted in number 1.
4. High-dose spillage: Any dose greater than 105% of the prescription dose should occur primarily within the PTV itself and not within the normal tissues outside the PTV. Conformality (defined as the ratio of the volume receiving the prescription dose to the volume of the PTV) is ideally less than 1.2, acknowledging that this is difficult to meet when targeting small lesions.
5. Dose fall-off gradient criteria (intermediate-dose spillage): The falloff gradient must be rapid in all directions.
6. Organs at risk (OAR) constraints: The normal tissue constraints, as previously published, should be met, if not improved upon [74]. However, we typically prioritize tumor coverage over OAR constraints (except spinal cord) in planning. For example, although a constraint is listed for renal pelvis, tumors in the renal pelvis have been treated safely without interrupting kidney drainage. Ideally, the critical volume for the uninvolved kidney will be preserved.

Future Directions

With the growing interest in SAbR, the advent of immune therapies, and the accumulating evidence that SAbR can initiate tumor antigen presentation and enhance the immune response against tumors, neoadjuvant SAbR followed by nephrectomy has been evaluated in a phase I pilot study where 14 patients with metastatic RCC received SAbR (15 Gy in one fraction) to the primary tumor followed by cytoreductive nephrectomy [75, 76]. The treatment was well-tolerated, and SAbR-treated tumors showed increased expression of tumor-associated antigens, indicating an immune-modulatory effect for SAbR. Neoadjuvant SAbR is also being investigated currently in patients with advanced RCC with inferior vena cava tumor thrombus with the intent of decreasing the high rates of systemic recurrence that is seen in this patient population (NCT02473536) [77]. Another potential application of SAbR for the treatment of primary tumor site in RCC may be in the metastatic setting where cytoreductive nephrectomy has been shown to improve OS [78, 79]. Noninvasive cytoreduction with SAbR has been evaluated as an alternative to cytoreductive nephrectomy in metastatic RCC [80], and this may be an opportune setting to bring in adjuvant immunotherapy to harness the immunogenic properties and in situ vaccination effect of SAbR and further reduce systemic recurrence.

Conclusions

Successful implementation of stereotactic radiosurgery of renal tumors is an effective approach that shows a very high rate of local control and the least invasive treatment modality available for primary RCC. Currently, the reported high rates of LC and the favorable toxicity profile of SAbR for the treatment of primary RCC make it a reasonable treatment choice for primary RCC patients. Even in the setting of surgical candidacy, it makes sense to consider SAbR because in the rare event that the tumor progresses after SAbR, partial or radical nephrectomy may still be a possibility. Formation of scar tissue in the radiated field has been a concern for surgeons performing surgery after radiation. However, with SAbR delivering extremely focused doses of radiation, the extent of scar tissue will be limited to regions immediately surrounding the tumor which may keep even the partial nephrectomy options open. More studies investigating SAbR for primary RCC are needed to establish it as a standard approach for treating these cancers.

Practical Considerations

- Indications/patient selection: Growing, biopsy-proven RCC with growth rate greater than 0.4 cm per year. Surgical candidacy should be considered as it is still considered the standard.
- Dose: Equivalent to or greater than 12 Gy in three fractions (other options include 25 Gy in one fraction, and 8 Gy in five fractions).
- Immobilization, motion management, and image guidance are key to successful treatments. Since both kidneys move with respiration, motion assessment and management techniques need to be in place.
- Follow the six points discussed earlier for acceptable treatment planning.
- Strictly respect spinal cord, and, ideally, normal kidney critical volume-dose constraints [74]. Patients should be

warned and consented if other OAR constraints are approached or exceeded.

- LC is defined using MRI or contrast CT. Close imaging follow-up is important to monitor response to SAbR treatments. LC in well-designed and delivered SAbR is expected to exceed 90%. Most tumors are expected to show stable disease or partial response, but tumor enhancement is not expected to change [60].
- Kidney function should be closely monitored to evaluate radiation-induced kidney toxicity, especially in patients with a solitary kidney or those who have baseline chronic kidney disease.

References

1. American Cancer Society. Cancer facts and figures 2012. 2012.
2. American Cancer Society. Key Statistics About Kidney Cancer. 2018; Available from: https://www.cancer.org/cancer/kidney-cancer/about/keystatistics.html.
3. Jayson M, Sanders H. Increased incidence of serendipitously discovered renal cell carcinoma. Urology. 1998;51(2):203–5.
4. Smith SJ, Bosniak MA, Megibow AJ, Hulnick DH, Horii SC, Raghavendra BN. Renal cell carcinoma: earlier discovery and increased detection. Radiology. 1989;170(3. Pt 1):699–703.
5. Belldegrun A, Tsui KH, deKernion JB, Smith RB. Efficacy of nephron-sparing surgery for renal cell carcinoma: analysis based on the new 1997 tumor-node-metastasis staging system. J Clin Oncol. 1999;17(9):2868–75.
6. Fergany AF, Hafez KS, Novick AC. Long-term results of nephron sparing surgery for localized renal cell carcinoma: 10-year followup. J Urol. 2000;163(2):442–5.
7. Herr HW. Partial nephrectomy for unilateral renal carcinoma and a normal contralateral kidney: 10-year followup. J Urol. 1999;161(1):33–4; discussion 34–5.
8. Lee CT, Katz J, Shi W, Thaler HT, Reuter VE, Russo P. Surgical management of renal tumors 4 cm. or less in a contemporary cohort. J Urol. 2000;163(3):730–6.
9. Lee DI, McGinnis DE, Feld R, Strup SE. Retroperitoneal laparoscopic cryoablation of small renal tumors: intermediate results. Urology. 2003;61(1):83–8.
10. Lerner SE, Hawkins CA, Blute ML, Grabner A, Wollan PC, Eickholt JT, et al. Disease outcome in patients with low stage renal cell carcinoma treated with nephron sparing or radical surgery. J Urol. 1996;155(6):1868–73.
11. Lerner SE, Hawkins CA, Blute ML, Grabner A, Wollan PC, Eickholt JT, et al. Disease outcome in patients with low stage renal cell carcinoma treated with nephron sparing or radical surgery. J Urol, 2002. 1996;167(2 Pt 2):884–9; discussion 889–90.
12. Morgan WR, Zincke H. Progression and survival after renal-conserving surgery for renal cell carcinoma: experience in 104 patients and extended followup. J Urol. 1990;144(4):852–7; discussion 857–8.
13. Gill IS, Desai MM, Kaouk JH, Meraney AM, Murphy DP, Sung GT, et al. Laparoscopic partial nephrectomy for renal tumor: duplicating open surgical techniques. J Urol. 2002;167(2 Pt 1):469–7; discussion 475–6.
14. Wolf JS Jr, Seifman BD, Montie JE. Nephron sparing surgery for suspected malignancy: open surgery compared to laparoscopy with selective use of hand assistance. J Urol. 2000;163(6):1659–64.
15. Wu Z, Li M, Liu B, Cai C, Ye H, Lv C, et al. Robotic versus open partial nephrectomy: a systematic review and meta-analysis. PLoS One. 2014;9(4):e94878.
16. Pierorazio PM, Hyams ES, Mullins JK, Allaf ME. Active surveillance for small renal masses. Rev Urol. 2012;14(1–2):13–9.
17. Chawla SN, Crispen PL, Hanlon AL, Greenberg RE, Chen DY, Uzzo RG. The natural history of observed enhancing renal masses: meta-analysis and review of the world literature. J Urol. 2006;175(2):425–31.
18. Volpe A, Jewett MA. The natural history of small renal masses. Nat Clin Pract Urol. 2005;2(8):384–90.
19. Oda T, Miyao N, Takahashi A, Yanase M, Masumori N, Itoh N, et al. Growth rates of primary and metastatic lesions of renal cell carcinoma. Int J Urol. 2001;8(9):473–7.
20. Rendon RA, Stanietzky N, Panzarella T, Robinette M, Klotz L, Thurston W, et al. The natural history of small renal masses. J Urol. 2000;164(4):1143–7.
21. Wehle MJ, Thiel DD, Petrou SP, Young PR, Frank I, Karsteadt N. Conservative management of incidental contrast-enhancing renal masses as safe alternative to invasive therapy. Urology. 2004;64(1):49–52.
22. Jewett MA, Mattar K, Basiuk J, Morash CG, Pautler SE, Siemens DR, et al. Active surveillance of small renal masses: progression patterns of early stage kidney cancer. Eur Urol. 2011;60(1):39–44.
23. Gervais DA, McGovern FJ, Arellano RS, McDougal WS, Mueller PR. Renal cell carcinoma: clinical experience and technical success with radio-frequency ablation of 42 tumors. Radiology. 2003;226(2):417–24.
24. Gill IS, Novick AC, Meraney AM, Chen RN, Hobart MG, Sung GT, et al. Laparoscopic renal cryoablation in 32 patients. Urology. 2000;56(5):748–53.
25. Gill IS, Remer EM, Hasan WA, Strzempkowski B, Spaliviero M, Steinberg AP, et al. Renal cryoablation: outcome at 3 years. J Urol. 2005;173(6):1903–7.
26. Jacomides L, Ogan K, Watumull L, Cadeddu JA. Laparoscopic application of radio frequency energy enables in situ renal tumor ablation and partial nephrectomy. J Urol. 2003;169(1):49–53. discussion 53.
27. Ogan K, Jacomides L, Dolmatch BL, Rivera FJ, Dellaria MF, Josephs SC, et al. Percutaneous radiofrequency ablation of renal tumors: technique, limitations, and morbidity. Urology. 2002;60(6):954–8.
28. Pavlovich CP, Walther M, Choyke PL, Pautler SE, Chang R, Linehan WM, et al. Percutaneous radio frequency ablation of small renal tumors: initial results. J Urol. 2002;167(1):10–5.
29. Shingleton WB, Sewell PE Jr. Percutaneous renal tumor cryoablation with magnetic resonance imaging guidance. J Urol. 2001;165(3):773–6.
30. Kunkle DA, Uzzo RG. Cryoablation or radiofrequency ablation of the small renal mass: a meta-analysis. Cancer. 2008;113(10):2671–80.
31. Tracy CR, Raman JD, Donnally C, Trimmer CK, Cadeddu JA. Durable oncologic outcomes after radiofrequency ablation: experience from treating 243 small renal masses over 7.5 years. Cancer. 2010;116(13):3135–42.
32. Campbell SC, Novick AC, Belldegrun A, Blute ML, Chow GK, Derweesh IH, et al. Guideline for management of the clinical T1 renal mass. J Urol. 2009;182(4):1271–9.
33. Gill IS, Aron M, Gervais DA, Jewett MA. Clinical practice. Small renal mass. N Engl J Med. 2010;362(7):624–34.
34. Goldberg SN, Grassi C, Cardella JF, Charboneau JW, Dodd GD 3rd, Dupuy DE, et al. Image-guided tumor ablation: standardization of terminology and reporting criteria. J Vasc Interv Radiol. 2009;20(7 Suppl):S377–90.

35. Blanco AI, Teh BS, Amato RJ. Role of radiation therapy in the management of renal cell cancer. Cancers (Basel). 2011;3(4):4010–23.
36. Deschavanne PJ, Fertil B. A review of human cell radiosensitivity in vitro. Int J Radiat Oncol Biol Phys. 1996;34(1):251–66.
37. Ning S, Trisler K, Wessels BW, Knox SJ. Radiobiologic studies of radioimmunotherapy and external beam radiotherapy in vitro and in vivo in human renal cell carcinoma xenografts. Cancer. 1997;80(12 Suppl):2519–28.
38. Walsh L, Stanfield JL, Cho LC, Chang CH, Forster K, Kabbani W, et al. Efficacy of ablative high-dose-per-fraction radiation for implanted human renal cell cancer in a nude mouse model. Eur Urol. 2006;50(4):795–800. discussion 800.
39. Shuto T, Matsunaga S, Suenaga J, Inomori S, Fujino H. Treatment strategy for metastatic brain tumors from renal cell carcinoma: selection of gamma knife surgery or craniotomy for control of growth and peritumoral edema. J Neuro-Oncol. 2010;98(2):169–75.
40. Gerszten PC, Burton SA, Ozhasoglu C, Vogel WJ, Welch WC, Baar J, et al. Stereotactic radiosurgery for spinal metastases from renal cell carcinoma. J Neurosurg Spine. 2005;3(4):288–95.
41. Nguyen QN, Shiu AS, Rhines LD, Wang H, Allen PK, Wang XS, et al. Management of spinal metastases from renal cell carcinoma using stereotactic body radiotherapy. Int J Radiat Oncol Biol Phys. 2010;76(4):1185–92.
42. Ranck MC, Golden DW, Corbin KS, Hasselle MD, Liauw SL, Stadler WM, et al. Stereotactic body radiotherapy for the treatment of oligometastatic renal cell carcinoma. Am J Clin Oncol. 2013;36(6):589–95.
43. Wersall PJ, Blomgren H, Lax I, Kalkner KM, Linder C, Lundell G, et al. Extracranial stereotactic radiotherapy for primary and metastatic renal cell carcinoma. Radiother Oncol. 2005;77(1):88–95.
44. Timmerman R, Paulus R, Galvin J, Michalski J, Straube W, Bradley J, et al. Stereotactic body radiation therapy for inoperable early stage lung cancer. JAMA. 2010;303(11):1070–6.
45. Wang CJ, Christie A, Lin MH, Jung M, Weix D, Huelsmann L, et al. Safety and efficacy of stereotactic ablative radiation therapy for renal cell carcinoma extracranial metastases. Int J Radiat Oncol Biol Phys. 2017;98(1):91–100.
46. Siva S, Kothari G, Muacevic A, Louie AV, Slotman BJ, Teh BS, et al. Radiotherapy for renal cell carcinoma: renaissance of an overlooked approach. Nat Rev Urol. 2017;14(9):549–63.
47. Juusela H, Malmio K, Alfthan O, Oravisto KJ. Preoperative irradiation in the treatment of renal adenocarcinoma. Scand J Urol Nephrol. 1977;11(3):277–81.
48. van der Werf-Messing B. Proceedings: carcinoma of the kidney. Cancer. 1973;32(5):1056–61.
49. Finney R. The value of radiotherapy in the treatment of hypernephroma – a clinical trial. Br J Urol. 1973;45(3):258–69.
50. Kjaer M, Iversen P, Hvidt V, Bruun E, Skaarup P, Bech J, et al. A randomized trial of postoperative radiotherapy versus observation in stage II and III renal adenocarcinoma. A study by the Copenhagen Renal Cancer Study Group. Scand J Urol Nephrol. 1987;21(4):285–9.
51. Tunio MA, Hashmi A, Rafi M. Need for a new trial to evaluate postoperative radiotherapy in renal cell carcinoma: a meta-analysis of randomized controlled trials. Ann Oncol. 2010;21(9):1839–45.
52. Paly JJ, Hallemeier CL, Biggs PJ, Niemierko A, Roeder F, Martinez-Monge R, et al. Outcomes in a multi-institutional cohort of patients treated with intraoperative radiation therapy for advanced or recurrent renal cell carcinoma. Int J Radiat Oncol Biol Phys. 2014;88(3):618–23.
53. Beitler JJ, Makara D, Silverman P, Lederman G. Definitive, high-dose-per-fraction, conformal, stereotactic external radiation for renal cell carcinoma. Am J Clin Oncol. 2004;27(6):646–8.
54. Gilson B, Lederman G, Qian G, Fastaia M, Cangiane L. Hypofractionated stereotactic extra-cranial radiosurgery (HFSR) for primary and metastatic renal cell carcinoma. Int J Radiat Oncol Biol Phys. 2006;66:S349.
55. Svedman C, Karlsson K, Rutkowska E, Sandstrom P, Blomgren H, Lax I, et al. Stereotactic body radiotherapy of primary and metastatic renal lesions for patients with only one functioning kidney. Acta Oncol. 2008;47(8):1578–83.
56. Siva S, Muacevic A, Staehler M, Warner A, Gandhidasan A, Ponsky L, et al. Individual patient data meta-analysis of SBRT kidney: a report from the International Radiosurgery Oncology Consortium for Kidney (IROCK). Int J Radiat Oncol Biol Phys. 2017;99(Supplement (2S)):S153.
57. Siva S, Louie AV, Warner A, Muacevic A, Gandhidasan A, Ponsky L, et al. Pooled analysis of stereotactic ablative radiotherapy for primary renal cell carcinoma: a report from the International Radiosurgery Oncology Consortium for Kidney (IROCK). Cancer. 2018;124(5):934–42.
58. Ponsky L, Lo SS, Zhang Y, Schluchter M, Liu Y, Patel R, et al. Phase I dose-escalation study of stereotactic body radiotherapy (SBRT) for poor surgical candidates with localized renal cell carcinoma. Radiother Oncol. 2015;117(1):183–7.
59. McBride SM, Wagner AA, Kaplan ID. A phase 1 dose-escalation study of robotic radiosurgery in inoperable primary renal cell carcinoma. Int J Radiat Oncol Biol Phys. 2013;87:S84.
60. Sun MR, Brook A, Powell MF, Kaliannan K, Wagner AA, Kaplan ID, et al. Effect of stereotactic body radiotherapy on the growth kinetics and enhancement pattern of primary renal tumors. AJR Am J Roentgenol. 2016;206(3):544–53.
61. Pham D, Thompson A, Kron T, Foroudi F, Kolsky MS, Devereux T, et al. Stereotactic ablative body radiation therapy for primary kidney cancer: a 3-dimensional conformal technique associated with low rates of early toxicity. Int J Radiat Oncol Biol Phys. 2014;90(5):1061–8.
62. Siva S, Pham DJ, Tan TH, Lam J, Bressel M, Price J, et al. Principal analysis of a phase Ib trial of stereotactic body radiation therapy (SBRT) for primary kidney cancer. Int J Radiat Oncol Biol Phys. 2016;96(2):S96.
63. Siva S, Pham D, Kron T, Bressel M, Lam J, Tan TH, et al. Stereotactic ablative body radiotherapy for inoperable primary kidney cancer: a prospective clinical trial. BJU Int. 2017;120(5):623–30.
64. Staehler M, Bader M, Schlenker B, Casuscelli J, Karl A, Roosen A, et al. Single fraction radiosurgery for the treatment of renal tumors. J Urol. 2015;193(3):771–5.
65. Staehler MD, Schlenker B, Karl A, Spek A, Muacevic A. Single-fraction radiosurgery for the treatment of renal cell carcinoma. J Clin Oncol. 2016;34(2 Suppl):590.
66. Svedman C, Sandstrom P, Pisa P, Blomgren J, Lax I, Kalkner KM, et al. A prospective Phase II trial of using extracranial stereotactic radiotherapy in primary and metastatic renal cell carcinoma. Acta Oncol. 2006;45(7):870–5.
67. Siva S, Pham D, Gill S, Corcoran NM, Foroudi F. A systematic review of stereotactic radiotherapy ablation for primary renal cell carcinoma. BJU Int. 2012;110(11 Pt B):E737–43.
68. Chang JH, Cheung P, Erler D, Sonier M, Korol R, Chu W. Stereotactic ablative body radiotherapy for primary renal cell carcinoma in non-surgical candidates: initial clinical experience. Clin Oncol (R Coll Radiol). 2016;28(9):e109–14.
69. Siva S, Jackson P, Kron T, Bressel M, Lau E, Hofman M, et al. Impact of stereotactic radiotherapy on kidney function in primary renal cell carcinoma: establishing a dose-response relationship. Radiother Oncol. 2016;118(3):540–6.
70. George R, Keall PJ, Kini VR, Vedam SS, Siebers JV, Wu Q, et al. Quantifying the effect of intrafraction motion during breast IMRT planning and dose delivery. Med Phys. 2003;30(4):552–62.
71. Hugo G, Tenn S, Agazaryan N. An evaluation of intrafraction motion-induced error for fractionated IMRT delivery. Med Phys. 2003;30(6):1470–0.

72. Siva S, Pham D, Gill S, Bressel M, Dang K, Devereux T, et al. An analysis of respiratory induced kidney motion on four-dimensional computed tomography and its implications for stereotactic kidney radiotherapy. Radiat Oncol. 2013;8:248.
73. Heinzerling JH, Anderson JF, Papiez L, Boike T, Chien S, Zhang G, et al. Four-dimensional computed tomography scan analysis of tumor and organ motion at varying levels of abdominal compression during stereotactic treatment of lung and liver. Int J Radiat Oncol Biol Phys. 2008;70(5):1571–8.
74. Kim DWN, Medin PM, Timmerman RD. Emphasis on repair, not just avoidance of injury, facilitates prudent stereotactic ablative radiotherapy. Semin Radiat Oncol. 2017;27(4):378–92.
75. Singh AK, Winslow TB, Kermany MH, Goritz V, Heit L, Miller A, et al. A pilot study of stereotactic body radiation therapy combined with cytoreductive nephrectomy for metastatic renal cell carcinoma. Clin Cancer Res. 2017;23(17):5055–65.
76. Weichselbaum RR, Liang H, Deng L, Fu YX. Radiotherapy and immunotherapy: a beneficial liaison? Nat Rev Clin Oncol. 2017;14(6):365–79.
77. Hannan R, Margulis V, Chun SG, Cannon N, Kim D, Abdulrahman RE, et al. Stereotactic radiation therapy of renal cancer inferior vena cava tumor thrombus. Cancer Biol Ther. 2015;16(5):657–61.
78. Mickisch GH, Garin A, van Poppel H, de Prijck L, Sylvester R, et al. Radical nephrectomy plus interferon-alfa-based immunotherapy compared with interferon alfa alone in metastatic renal-cell carcinoma: a randomised trial. Lancet. 2001;358(9286):966–70.
79. Flanigan RC, Salmon SE, Blumenstein BA, Bearman SI, Roy V, McGrath PC, et al. Nephrectomy followed by interferon alfa-2b compared with interferon alfa-2b alone for metastatic renal-cell cancer. N Engl J Med. 2001;345(23):1655–9.
80. Correa RJ, Rodrigues GB, Chen H, Warner A, Ahmad B, Louie AV. Stereotactic ablative radiotherapy (SABR) for large renal tumors: a retrospective case series evaluating clinical outcomes, toxicity, and technical considerations. Am J Clin Oncol. 2018;41(6):568–75.

Head and Neck Stereotactic Body Radiation Therapy

Pencilla Lang, Ian Poon, Lee Chin, and Irene Karam

Introduction

Multimodality management with a combination of surgery, radiation therapy and chemotherapy remains the standard of care for locally advanced head and neck cancers [1]. However, some patients are felt to be unsuited for aggressive curative treatment, and local recurrence remains a significant problem in 20–35% of patients [2, 3]. Improvements in immobilization, image guidance and treatment planning techniques have allowed SBRT to emerge as a potential therapy for head and neck malignancies. It has been proposed that SBRT may have the potential to limit toxicity with improved conformality around the target and steep dose gradients, as well as allowing for dose escalation delivered within a short period of time with fewer hospital visits [4–7]. Over the past decade, more than 2000 patients have been treated with head and neck SBRT worldwide [7]. There is an increasing body of evidence supporting the use of SBRT in head and neck cancer as a primary treatment strategy for de novo tumours and as retreatment in patients with recurrent unresectable disease or a secondary primary malignancy within a previously irradiated field [4–6]. This chapter will outline the indications, treatment planning techniques, efficacy and toxicity of head and neck SBRT and review the available clinical evidence.

Multiple indications for head and neck SBRT have emerged, including [7]:

1. Primary treatment for patients with newly diagnosed head and neck cancer with radical palliative intent
2. Boost following standard fractionation for primary or nodal disease
3. Salvage treatment for in-field recurrences
4. Post-operative treatment for close/positive margins, residual disease or evidence of nodal extracapsular extension

A recent survey of 15 international institutions with significant experience in head and neck SBRT demonstrated significant heterogeneity in patient selection and techniques used amongst the different centres. SBRT was used 0–10% of the time for newly diagnosed head and neck cancers, 0–15% of the time as a boost for primary disease and 10–100% of the time for recurrent disease. Common subsites treated included the nasopharynx, oropharynx, skin, parotid, sinonasal area and regional nodes [7].

Site-Specific Considerations

Tumours of the head and neck present unique challenges due to the large number of subsites with variations in anatomy, pathophysiology and natural disease history. In addition, there are a large number of organs at risk within a small area in the head and neck, often with tumour abutting or invading these structures adding another level of complexity to the radiation treatment.

Patient Eligibility

Based on the experience of major centres to date, most employ the following selection criteria for consideration of head and neck SBRT treatment [7–10]:

- ECOG 0–2 or KPS ≥60 (majority of centres will treat even if asymptomatic)

P. Lang · I. Poon · I. Karam (✉)
Sunnybrook Health Sciences Centre, Radiation Oncology, Toronto, ON, Canada
e-mail: irene.karam@sunnybrook.ca

L. Chin
Sunnybrook Health Sciences Centre, Medical Physics, Toronto, ON, Canada

D. M. Trifiletti et al. (eds.), *Stereotactic Radiosurgery and Stereotactic Body Radiation Therapy*,
https://doi.org/10.1007/978-3-030-16924-4_27

- No upper age limit
- Size/volume constraint of 3–5 cm or 25–50 cc
- Subsites of the nasopharynx, oropharynx, skin, parotid, sinonasal, skull base and lymph nodes (the larynx and hypopharynx are treated with caution due to a possible elevated risk of toxicity)
- Primary, recurrent or oligometastatic disease

Relative contraindications to SBRT treatment include [7, 10, 11]:

- Skin ulcer overlying a blood vessel
- Disease encasing the carotid artery with ≥180 degrees of contact
- Disease in contact with the brachial plexus
- Disease in proximity to optic pathways, brain and cavernous sinus
- Connective tissue disorder (e.g. scleroderma)

Staging and Workup Considerations

Pretreatment staging investigations should include diagnostic CT and MRI of the head and neck to help define the local extent of disease and invasion into surrounding structures and CT of the chest, abdomen and pelvis or PET-CT to evaluate for distant metastases. A biopsy should be required prior to SBRT. It is important to confirm histology, as many institutions may consider approaching squamous cell carcinoma differently than other histologies with differing dose and fractionation, margins and use of systemic therapies [7].

Clinical Evidence

SBRT as Primary Treatment

The incidence of elderly patients with head and neck malignancies is increasing with the growing aging population [12, 13]. Advanced age and underlying comorbidities can have a significant impact on quality of life both during and after treatment and can increase the risk of treatment-related complications. The complex interplay between cancer-related morbidity and mortality, underlying comorbidities, advanced age and functional status presents unique challenges [4]. Previous studies have shown that conventional radiation therapy can be delivered safely to the elderly population in well-selected patients; however, elderly patients are more likely to receive palliative management at the time of diagnosis [14].

Hypofractionation used with curative or palliative intent in head and neck cancers has demonstrated a good response with a median survival of 5–6 months and progression-free survival of 3–4 months [15–19]. Fractionation schemes have varied widely, including the "QUAD SHOT" regimen with 14 Gy in 4 fractions given twice daily and repeated once a month for three cycles [17], 40 Gy in 16 daily fractions [16], the Irradiation HypoFractionnée 2 Séances Quotidiennes (IHF2SQ) regimen with 3 Gy given twice daily on days one and three of weeks 1, 3, 5 and 7 [15] and 18–48 Gy delivered in 1–6 fractions [18].

SBRT has several characteristics making it favourable to elderly patients, including a short treatment time with fewer hospital visits, and the potential for less acute toxicity than standard definitive radiotherapy but better local control than palliative regimens. A small body of literature has developed over the past decade studying primary SBRT in the medically inoperable or unfit head and neck cancer patients, summarized in Table 1 [20–24]. All of the reported studies are retrospective and comprised very small numbers of patients, limiting the conclusions that can be drawn from the literature. In addition, most of the studies report very short follow-up of up to a year, making it difficult to assess late complications and quality of life outcomes. In total, 64 patients were included in five studies, with local control ranging from 70% to 85%, overall survival of 60–85% and a complete response rate of 40–80%. The delivered doses ranged from 35 to 48 Gy in 3–8 fractions. The main pattern of failure was locoregional [20–24].

The largest series by Khan et al. [24] included 17 malignancies treated with primary SBRT because the patients were medically unfit or frail. Quality of life scores with

Table 1 Summary of data for primary stereotactic body radiation therapy in the head and neck

Study (year)	*n*	Dose	LC	OS	Late toxicity G3+	References
Siddiqui et al. (2009) [20]	10	18–48 Gy in 1–8 fx	1 year – 83%	1 year – 70%	Cataract (1), pain (1)	[20]
Kodani et al. (2011) [21]	13	19.5–42 Gy in 3–8 fx	38% (CR rate)	1 year – 85%	None	[21]
Kawaguchi et al. (2012) [22]	14	35–42 Gy in 3–5 fx	71% crude rate	79% crude	Osteoradionecrosis (1)	[22]
Vargo et al. (2014) [23]	10	20–44 Gy in 1–5 fx	1 year – 69%	1 year – 64%	Dysphagia (1), mucositis (1)	[23]
Khan et al. (2015) [24]	17	35–48 Gy in 5–6 fx	1 year – 87%	1 year – 60% (recurrent + de novo cases)	None	[24]

Adapted with permission of Future Medicine LTD from Karam et al. [6]

symptom-related items such as pain, swallowing, taste and coughing were assessed prior to and after radiation treatment. Local control rates were excellent at 87% at 1 year. There was an improvement in quality of life scores from baseline to follow-up, suggesting a decreased symptom burden.

One series by Vargo et al. [23] added cetuximab to primary SBRT in some patients. The study included ten patients with medically inoperable head and neck cancer treated with primary SBRT, but only three received concurrent cetuximab. The 1-year actuarial local progression-free survival and overall survival were 100% and 64%, respectively. In the patients that received cetuximab, it was well-tolerated. The study was too small to draw any conclusions about potential benefit or toxicity but encourages further investigation.

Overall, the published literature on primary head and neck SBRT suggests good local control with acceptable severe toxicity rates. SBRT treatment was well-tolerated with two series having no ≥ grade 3 late toxicities [21, 24], and only a few patients develop pain, dysphagia, mucositis and osteoradionecrosis in the remaining studies [20, 22, 23]. The small sample sizes and large inhomogeneities in the patient and tumour factors as well as differences in reported outcomes make it difficult to compare SBRT, hypofractionated and palliative techniques in elderly patients not suitable for conventional treatment. Further studies comparing the different options are required to better assess disease control, toxicity and quality of life.

Hypofractionation as a Boost

Dose escalation in external beam radiotherapy (EBRT) is limited by the tolerance of adjacent critical structures. It is hypothesized that a hypofractionated SBRT boost following conventional treatment could improve local control rates in unfavourable, locally advanced disease or persistent local disease. Clinical data on this approach remain limited and are summarized in Table 2 [10, 25–28]. A Phase I/II clinical trial using a dose-escalated SRS boost on unfavourable locally advanced oropharyngeal HPV-negative cancer patients with high nodal stage is currently ongoing [29]. Two large retrospective series looked at nasopharynx cancer [25, 26], while one series looked at oropharynx cancer [27]. Several other case series have included a mix of head and neck subsites [10, 28].

Hara et al. [26] and Chen et al. [25] have published institutional results of patients treated with an SBRT boost for locally advanced nasopharynx cancer. In both series, patients were treated with conventional radiotherapy to 64.8–70 Gy using a 3D conformal (3DCRT) or IMRT technique prior to SBRT boost. In Hara et al. [26], a frame-based SBRT approach was used to treat 82 patients, whereas in Chen et al. [25], the CyberKnife system was used to treat 64 patients. Both studies demonstrated excellent local control of greater than 90%. Hara et al. reported ten patients with temporal lobe necrosis, of which two were symptomatic with seizures, as well as retinopathy in three patients and transient cranial

Table 2 Summary of data for SBRT as boost in head and neck cancer

Study (year)	Treatment site	*n*	Initial conventional dose (Gy)	Boost dose	LC	OS	Late toxicity (≥ grade 3)	References
Chen et al. (2006) [25]	Nasopharynx	64	64.8–68.4	12–15 Gy in 3 fx	3 years – 93%	3 years – 85%	Nasal bleeding (3)	[25]
Hara et al. (2008) [26]	Nasopharynx	82	64.8–70	7–15 Gy in 1 fx	5 years – 98%	5 years – 69%	Retinopathy (3), carotid aneurysm (1), temporal lobe necrosis (10), transient cranial nerve weakness (4)	[26] Update of Le et al. study (2003)
Al-Mamgani (2012) [27]	Oropharynx	51	46	16.5 in 3 fx	2 years – 86%	2 years – 82%	Dysphagia (2) Xerostomia (2)	[27]
Lee et al. (2012) [28]	Nasopharynx (10) Nasal cavity/ paranasal sinus (8) Periorbit (4) Tongue (3) Oropharynx (1)	26	39.6–70.2	10–25 Gy in 2–5fx	2 years – 86%	2 years – 46%	Temporal lobe/pontine necrosis (4) Base of skull/soft tissue necrosis (3) Bleeding (1) Retinopathy (2) Neurovascular glaucoma (2) Optic neuropathy (1)	[28]
Yamazaki et al. (2014) [11]	Nasopharynx (11) Oropharynx (7) Hypopharynx (1) Nasal cavity (3) Oral cavity (3)	25	35–72	12–35 Gy in 1–5 fx	2 years – 89%	2 years – 89%	None	[10]

Adapted with permission of Future Medicine LTD from Karam et al. [6]

nerve weakness. Chen et al. reported three cases of fatal nasal bleeding.

In one series by Lee et al. [28], the rate of late toxicities was unacceptably high with 9 of 26 (34%) patients developing severe grade 3 toxicity. Radiation doses to 64.8–70 Gy using a 3D conformal (3DCRT) or IMRT technique, associated with a large treatment volume and large fractional doses were predictive of late toxcities. Ten patients were treated to the nasopharynx, including the base of the skull with a median fractional dose of 6.5 Gy (5–7 Gy) and a cumulative dose (BED_{10}) of 103.7 Gy (92–118.5 Gy). The remainder included a mix of sites, including the nasal cavity and paranasal sinuses, periorbit and tongue with a median fractional dose of 5 Gy (3–8 Gy). Of the nine cases with severe late toxicities, seven were treated to the skull base, orbit or lacrimal gland, and these patients received a cumulative BED of 87.5–118.5 Gy. The median GTV volume of patients with severe late toxicities was 47.7 cc (20.9–66.8 cc), and GTV volume and SBRT fractional dose were both significantly associated with a risk of severe toxicity.

Although radiation dose escalation with SBRT boost demonstrates excellent local control and may be a viable option for patients with locally advanced unfavourable disease, the risk of severe late complications is significant in the early series [10, 25–28]. This technique should be reserved for highly selected patients, and care should be taken to limit the boost volume, as well as dose to the critical structures, such as the temporal lobe and optic structures. Recent interest in image-guided dose painting with subvolume boosts based on PET may present a way to reduce treatment-related toxicity.

Re-irradiation for Disease Recurrence or Second Primary Malignancy

Local recurrence remains a significant problem in head and neck cancer, occurring in 20–35% of patients [3, 30]. These patients have a poor prognosis and limited treatment options. Surgical salvage remains the preferred option for patients with resectable tumours, with an estimated survival rate of 39% at 5 years [2]. However, many patients remain unresectable due to technical infeasibility or medical comorbidities, and definitive re-irradiation, with or without chemotherapy, has become an established approach for these patients [31].

Two randomized trials comparing re-irradiation with concurrent chemotherapy to systemic therapy were attempted, but both closed early due to poor accrual [32, 33]. Two phase II trials looked at re-irradiation for unresectable recurrent head and neck cancer. RTOG 96-10 was a multi-institutional trial with 79 patients and evaluated fluorouracil and hydroxyurea with radiotherapy given 1.5 Gy twice daily (bid) for four weekly cycles each separated by a week of rest. The 2-year OS was 15%, and there was a 19% ≥ grade 3 late toxicity. This was followed by RTOG 99-11, another multi-institutional trial looking at the same radiation fractionation given with cisplatin and paclitaxel in 99 patients. The 2-year overall survival rate was 25.9% with 17% of patients ≥ grade 3 late toxicity with a treatment-related death rate of 8% [34]. These findings are supported by several other large retrospective institutional series using several [33] different fractionation schemes, including both bid and daily treatments. Higher doses are associated with improved locoregional control and overall survival [33].

With the increased use of IMRT, the proportion of patients treated with salvage re-irradiation has increased as it allows larger treatment volumes while minimizing dose to adjacent structures. Hyper-fractionation can be used to attempt to minimize late toxicity, but this can be time-intensive and tiring for patients [34, 35].

SBRT has emerged as an attractive option with steep dose fall-off outside the tumour volume and reduced demands on patients with hospital visits. In the following decade, an emerging body of evidence has developed to support this technique with generally promising results [14, 30, 31]. A summary of recently published outcomes is shown in Table 3 [8, 20, 21, 33, 36–45]. Early retrospective data published in 2006 from the University of Pittsburgh Cancer Institute demonstrated the feasibility of this technique on 22 patients with previously irradiated head and neck cancer treated with 20 Gy in 4 fractions or 30 Gy in 6 fractions [36]. This was followed by a number of other retrospective institutional series [20, 37] and several phase I/II trials [38] looking at dose selection and safety and efficacy of SBRT. In general, the number of patients reported in individual series is low, and there is a significant heterogeneity with respect to patient selection and radiation dose and fractionation. Overall, the local control varied significantly from 30% to 80% at 1–2 years. Predictors for better overall survival include a nasopharynx primary site, treatment interval greater than 12 months, tumour volume ≤25 cc and prescribed dose ≥35 Gy [10, 32–35].

The largest published series is a multi-institutional review by Vargo et al. [8] which compared IMRT and SBRT re-irradiation in patients with recurrent or second primary squamous cell carcinoma of the head and neck. This study included 217 patients treated with IMRT and 197 with SBRT. The median retreatment dose was 60 Gy in 33 fractions for IMRT and 40 Gy in 5 fractions for SBRT. Survival was significantly better with conventional fractionation, with a 2-year OS of 35.4% with IMRT and 16.3% with SBRT. However, there were significant differences in the patient populations, with the SBRT cohort being older and more likely to be treated for a recurrence rather than a second primary malignancy and at a shorter time interval from pre-

Table 3 Summary of data for SBRT for re-irradiation in head and neck cancer

Article	No. of patients	Median time to re-RT (months)	Tumour volume, median range (cc)	LC	OS	Late toxicity (≥ grade 3)	Citation
Voynov et al. (2006) [36]	22		19.1 (2.5–140.3)	2 years – 26%	2 years – 22%	None	[36]
Roh et al. (2009) [37]	36	24	22.6 (0.2–114.9)	2 years – 52%	2 years – 31%	Bone necrosis (1), soft tissue necrosis (2), trismus (2)	[37]
Heron et al. (2009) [38]	25	13	44.8 (4.2–216.6)	17% response rate	Median – 6 months	None	[38]
Siddiqui et al. (2009) [20]	21	19	15.5 (1.7–155)	2 years – 40%	2 years – 14%	Dysphagia (1), fistula (3), mandibular necrosis (1), ulceration (1)	[20]
Unger et al. (2010) [40]	65	26	75 (7–276)	2 years – 30%	2 years – 41%	Arterial bleeding (2), dysphagia (2), soft tissue necrosis (1), fistula formation (1), death (1)	[40]
Rwigema et al. (2011) [39]	96	19.4	24.3 (2.5–162)	2 years – 31%	2 years – 28%	Dysphagia (2), fibrosis (1)	[39]
Kodani et al. (2011) [21]	21		11.6 (0.7–78.1)	29% CR rate	2 years – 58%	Pharynx haemorrhage (2), severe mucositis (2), dysphagia (2), skin necrosis (1), deaths (2)	[21]
Cengiz et al. (2011) [41]	46	38	45 (3–206)	1 year – 84%	1 year – 47%	Soft tissue necrosis (1), mandibular necrosis (1), dysphagia (3), carotid blowout (8), deaths (7)	[41]
Ozyigit et al. (2011) [42]		38	63.4 (26.3–170.4)	2 years – 82%	2 years – 64% (CSS)	Cranial neuropathy (1), carotid blowout (4), brain necrosis (1)	[42]
Vargo et al. (2012) [43]		53	19.6 (4.5–103.9)	1 year – 59%	1 year – 59%	Osteoradionecrosis (1), pain (1)	[43]
Lartigauet al. (2013) [33]	60	38		3 months – 92%	1 year – 47%	Fibrosis (1), xerostomia (2), fistula (1), death (1)	[33]
Comet et al. (2012) [44]	40 (15 with cetuximab)	31.6	64.1 (4.7–295.6)		1 year – 58% 2 years – 24%	Dysphagia (1), induration (1), fibrosis (1)	[44]
Vargo et al. (2015) [45]	50	18	36.5 (3.6–209.2)	1 year – 60%	1 year – 40%	Dysphagia (1), fistula (1)	[45]
Vargo et al. (2018) [8]	197	14.4	30 (1–427)	2 years – 45.5%	2 years – 16.3%	11.6%	[8]

Adapted with permission of Future Medicine LTD from Karam et al. [6]

vious therapy. IMRT patients were also more likely to receive chemotherapy. After controlling for baseline characteristics, there were no significant differences in OS or LF between the IMRT and SBRT groups. This study also found that for small tumours, there was worse overall survival for patients treated with SBRT to a dose of <35 Gy, with no difference between IMRT and SBRT to doses ≥35 Gy. For large tumours, treatment with IMRT was associated with improved overall survival. This supports findings from previous studies that dose and volume are significant predictors of outcome. Rwigema et al. [39] did a volumetric-dose analysis of treatment response and locoregional control in 96 previously irradiated head and neck patients treated with SBRT. High SBRT dose and small volume disease were significant predictors of locoregional control, with a 2-year control rate of 58% for patients receiving 40–50 Gy compared to 32% for those receiving 15–36 Gy. Furthermore, patients with a GTV of ≤25 cc had a locoregional control rate of 67% compared to 19% for patients with a GTV > 25 cc. Larger tumour volumes require higher doses to achieve optimal response rates.

Previously published randomized data have demonstrated that for primary head and neck cancer radiation therapy with concurrent cetuximab significantly improves local control and survival without significantly increasing toxicity [46].

Table 4 Comparative analysis of salvage treatments for recurrent head and neck cancer including systemic therapy

	Median survival (months)	Toxicity (≧ grade 3)	
		Acute (%)	Late (%)
EXTREME: platinum +5FU	7.4	82	
EXTREME: platinum +5FU + cetuximab	10.1	76	
RTOG 9911 60 Gy + cisplatin/paclitaxel	12.1	77.8	37.4
UPCI 06–093: SBRT + cetuximab	10	8	4
French SBRT + cetuximab	13.6	7.5	2.5

Data from Refs. [35, 40, 41, 45, 47]

This has driven increasing interest in using cetuximab as a radiosensitizer with SBRT to improve disease outcome. Two phase II trials have looked at re-irradiation with SBRT with concomitant cetuximab. Lartigau et al. [33] performed a phase II trial of 56 patients with inoperable recurrent or new primary tumour in a previously irradiated area to a dose of 36 Gy in 6 fractions with concomitant cetuximab. The 1-year OS rate was 47.5% with a complete response (CR) in 49% of patients. Another phase II study by Vargo et al. [45] looked at 50 patients who were treated with SBRT with 40–45 Gy in 5 fractions with concurrent cetuximab for previously irradiated head and neck squamous cell carcinoma and reported a 1-year overall survival of 40% and progression-free survival of 60%. These results suggest that SBRT with concurrent cetuximab is a feasible option with an acceptable toxicity profile and warrants further investigation.

There have been no randomized trials comparing head and neck SBRT in the retreatment setting to other salvage modalities, but prospective trials with other modalities have reported comparable survival results with higher rates of toxicity (Table 4) [35, 40, 41, 46, 47]. The data suggest that SBRT may have acceptable local control, overall survival and toxicity outcomes compared to IMRT for small volume tumours treated to at least 35 in 5 fractions.

Recently, several studies on using proton therapy or other heavy particles have been reported [48–50]. However, due to paucity of data, it is unclear how efficacy and toxicity results compare to re-irradiation with SBRT or IMRT.

Toxicity

Toxicities for Primary Treatment

In published series, SBRT treatment of de novo tumours was well-tolerated with two series having no ≥ grade 3 late toxicities [10, 13], and only a few patients develop pain, dysphagia, mucositis and osteoradionecrosis in the remaining studies [9, 11, 12]. In contrast, when SBRT is used as a boost for locally advanced disease after conventional radiotherapy, significant toxicities have been reported including temporal lobe necrosis, fatal bleeding and radiation retinopathy [25, 26]. In the series by Lee et al. [28], the rate of late toxicities was unacceptably high with 9 of 26 (34%) patients developing severe (≥ grade 3) toxicities including pontine, temporal lobe and base of skull necrosis, radiation retinopathy and two radiation-related deaths. The late toxicities were associated with a large treatment volume and large fractional doses.

Toxicities for Re-irradiation

High cumulative doses used in the retreatment setting have resulted in a significant risk of severe, acute and late toxicities with series in the literature reporting of skull necrosis and radiation retinopathy of 10–20% [8]. Of particular concern, is the risk of carotid blowout syndrome (CBS), which is a significant cause of treatment-related mortality [11]. Acute toxicities (<90 days) reported include hospital admissions for aspiration pneumonia/other infection, new tracheostomy use, new feeding tube placement, oesophageal stricture and soft tissue necrosis. In addition to CBS, late (>90 days) radiation-induced complications that have been reported in the literature include mandible necrosis, trismus, chronic ulcer, skull-base or soft tissue necrosis, dysphagia requiring long-term G-tube and oesophago-/oro-/pharyngocutaneous fistula [4, 6, 41].

In the multi-institutional review by Vargo et al. [8], the toxicities of 217 and 197 patients treated with IMRT and SBRT, respectively, were reported. The cumulative incidence of ≥ grade 3 late toxicity was approximately 12% at 2 years, and there was no significant difference between the IMRT and SBRT cohorts. Acute deaths unrelated to tumour progression was 2% and 0.5% for IMRT and SBRT patients and were not statistically different between the two cohorts [8].

Similar results were reported in a systematic statistical analysis by Baliga et al. of five institutional series with 233 patients. The overall rate of ≥ grade 3 acute and late toxicities were 20.2% and 8.2%, respectively [4].

In an institutional toxicity review by Ling et al. [51] looking at 291 patients, 11% experienced grade ≥ grade 3 acute toxicity and 19% experienced ≥ grade 3 late toxicity. Patients treated for a recurrence in the larynx/hypopharynx had a 50% risk of severe toxicity, which was significantly more than the other sites. The oropharyngeal and oral cavity, base of the skull/paranasal sinus, salivary gland or nodal sites of recurrence had a 6–20% risk of severe toxicity.

Figures 1a, b and 2 illustrate some of the complexities surrounding decision-making when attempting to balance

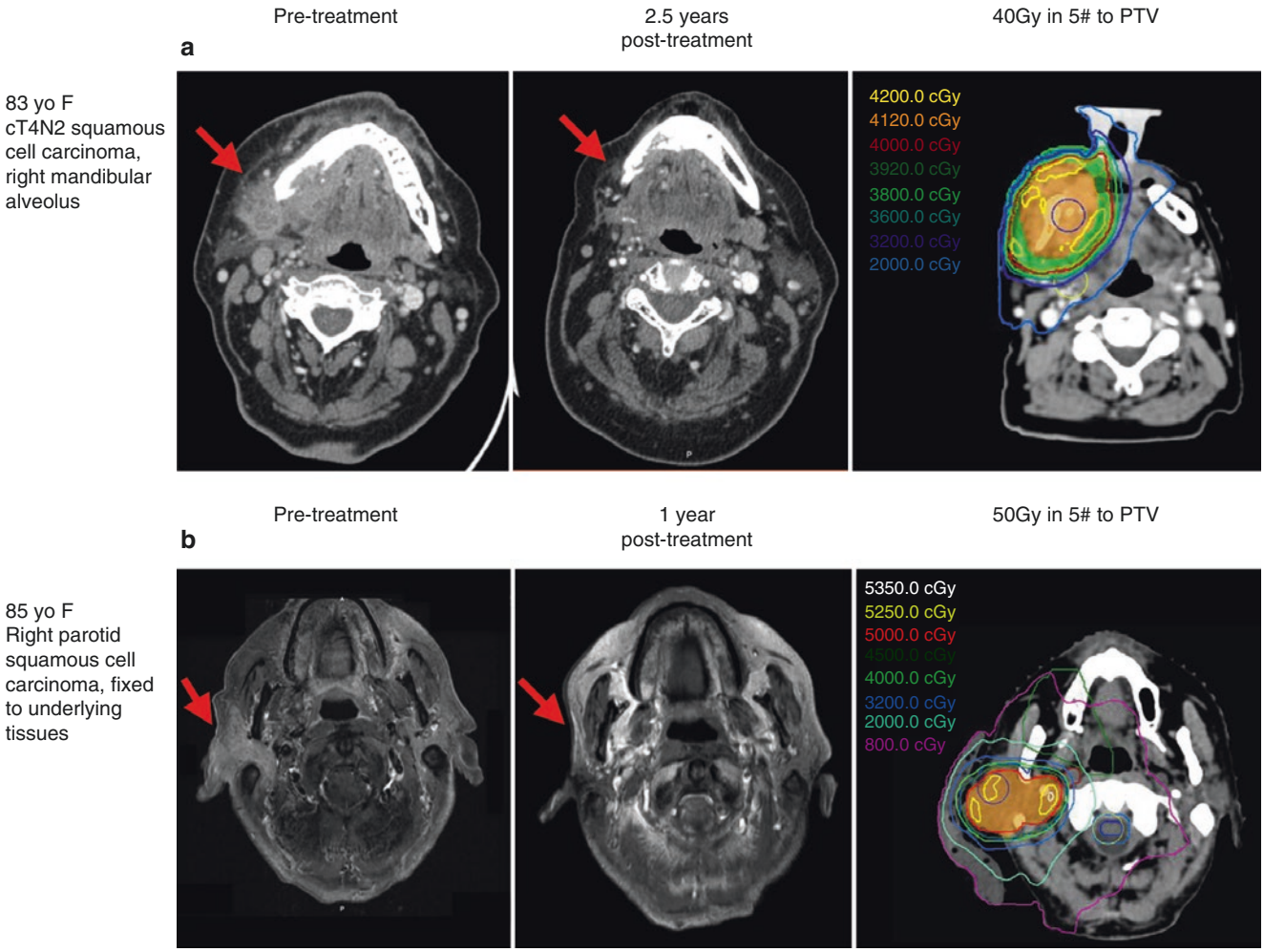

Fig. 1 (**a**) An 83-year-old female with cT4N2 scc of the right mandibular alveolus, not a candidate for surgery or chemotherapy. Treated with primary SBRT with 40 Gy in 5 fractions delivered to the PTV every other day. More than 2 years after completion of treatment, she remains well with no evidence of recurrent disease or severe treatment toxicity. (**b**) An 85-year-old female with a right parotid squamous cell carcinoma involving skin and fixed to underlying tissues, not a candidate for surgery or chemotherapy. Treated with primary SBRT with 50 Gy in 5 fractions delivered to the PTV every other day with excellent response 1 year following completion of treatment

disease control and treatment-related toxicity. In Fig. 2, a 91-year-old gentleman from a nursing home with multiple comorbidities, including coronary artery disease, congestive heart failure and chronic kidney disease, presented with a 2 cm squamous cell carcinoma (SCC) of the left pinna, resected with persistent positive margins. He was given adjuvant radiotherapy, initially planned for 45 Gy in 15 fractions using a direct appositional electron field technique. However, rapid disease progression was noted with an enlarging 3 cm mass after 3 fractions, and a bid boost of 15 Gy in 6 fractions was added. Six months later disease recurrence was noted, and he was treated with an auriculectomy and flap closure with negative margins. However, after 8 months, he was noted to have another recurrence in the centre of the surgical bed. He declined a lateral temporal bone resection and was treated with SBRT with 50 Gy in 5 fractions. He remains disease-free 3.5 years later but developed a chronic non-healing grade 3 ulcer approximately 1 year after completing treatment. Overall, he continues to enjoy an excellent quality of life with minimal discomfort. In this case, SBRT could provide good control of aggressive disease persistence after conventional radiotherapy and multiple surgical resections. While the patient developed a chronic non-healing ulcer, this was symptomatically less severe than the pain he was experiencing from progressive disease. The 5-fraction treatment also minimized the number of visits to hospital required, significantly influenced quality of life for this gentleman with limited mobility and several comorbidities.

Carotid Blowout Syndrome

Early series reported carotid blowout syndrome (CBS) rates as high as 10–20% [11, 21, 38]. CBS can be treated with coil embolization, endovascular stent-graft placement, balloon occlusion or surgical repair but remains fatal in 75% of

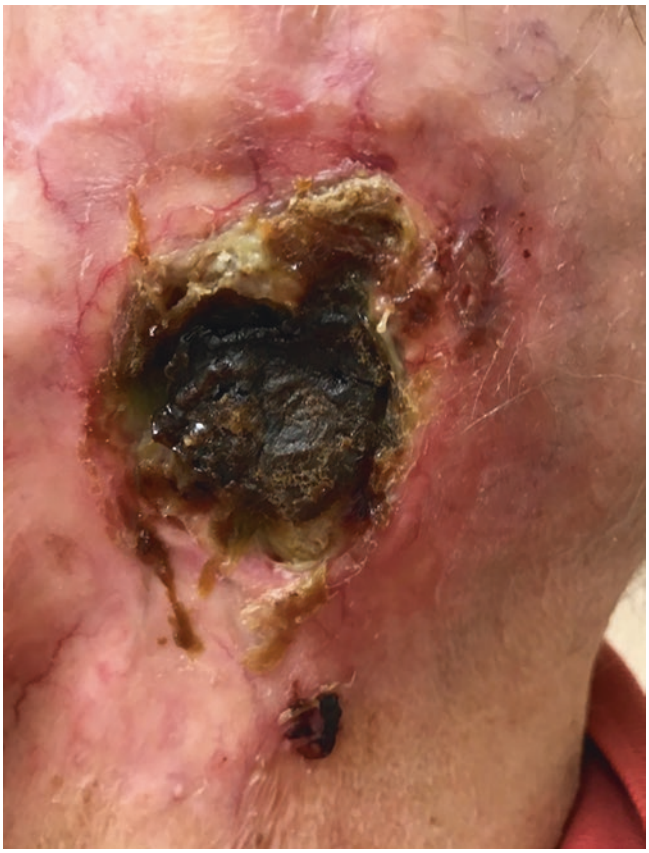

Fig. 2 Non-healing ulcer after repeat irradiation for recurrent squamous cell carcinoma of the ear following multiple surgical resections and conventionally fractionated radiotherapy

patients and can result in significant neurological morbidity even if successfully treated [52].

Retrospective studies have identified daily SBRT fractionation [53], carotid encasement of >180° [11, 41], presence of ulceration [11] and lymph node irradiation [11, 21] as significant risk factors for CBS.

Yamazaki et al. [11] performed a multi-institutional matched-pair analysis of CBS in pharyngeal cancer patients treated with re-irradiation in four institutes, comparing 12 cases of CBS compared to 60 patients without CBS. Patients were retreated to a median dose of 30 Gy in 5 fractions with CyberKnife SBRT after 60 Gy in 30 fractions of previous radiotherapy. The median duration of CBS onset was 5 months, and CBS cases had a median survival time of 5.5 months compared to 22.8 months for non-CBS cases. Twenty-four percent of patients with carotid invasion of >180° developed CBS, whereas no patients with less than 90° involvement developed CBS. Other risk factors for CBS identified on multivariate analysis included the presence of ulceration and irradiation to lymph nodes.

Larger series have demonstrated more favourable results, suggesting a rate of carotid blowout of approximately 1%. Vargo et al. [8] looked at 217 patients treated with IMRT and 197 with SBRT and reported a crude CBS rate of 1%, with no difference between the groups. Similarly, in a review by Baliga et al. [2] looking at five institutional series with 233 patients, the rate of carotid blowout was 1%.

In a more recent study by the Pittsburgh group [47], a low risk of bleeding following re-irradiation with SBRT was reported even when tumour is completely encasing the carotid artery. They reported on 186 patients with recurrent, previously irradiated head and neck cancer treated to a median dose up to 44 Gy (range, 40–50 Gy) in 5 fractions delivered on a twice-weekly basis. The overall median D0.1cc and mean carotid doses were 40.8 Gy and 15 Gy. A total of four bleeding events were reported, including two patients suffering from CBS with D0.1cc of 48.4 Gy and 47.6 Gy. No CBS events were noted when D0.1cc was <47.6 Gy.

Plan Quality

Simulation and Treatment Technique

CT and/or MRI simulation using 1–3 mm slice thickness in a thermoplastic mask is recommended to allow for the accurate contouring required to create a highly conformal plan. Organ motion control using 4DCT or robotic tracking is also commonly used in practice. A variety of treatment techniques have been used, including intensity-modulated radiation therapy (IMRT), volumetric arc therapy (VMAT), robotic radiosurgery systems and Co-60 stereotactic radiosurgery [7].

Planning

Using IMRT or VMAT, a target coverage of V100 > 95% can be achieved but may be compromised in order to maintain organ-at-risk constraints. Hotspots of up to 115% are acceptable but are limited within the PTV. In addition, to minimize dose to normal tissues, a tight, conformal distribution should be sculpted around the high-dose target. Conformity indices less than 1.1 are attainable for the high-dose volumes (GTV, PTV40) due to their often simple, spherical shape. The distributions are larger; more complex low-dose volumes (PTV25, PTV35) are slightly less conformal with a typical CI in the range of 1.3 to 1.5.

Contouring

Gross disease as determined by physical examination and pretreatment imaging using MRI, CT with IV contrast and PET/CT is contoured as gross tumour volume (GTV). Planning

Table 5 Recommended dose-volume constraints for organs at risk

	Dose-volume constraint (5 fractions)	
Organ	Primary disease	Re-RT
Spinal canal	D_{max} 20–30 Gy V22.5 < 0.25 cc	D_{max} 10–20 Gy
Spinal canal +5 mm	D_{max} < 25.3 Gy	
Brainstem	V24.5 Gy < 0.25 cc V15.5 < 1.2 cc	D_{max} 9–15 Gy
Brainstem +5 mm	D_{max} < 30 Gy	
Brain	D_{max} ≤ 30 Gy	D_{max} 10–25 Gy
Brachial plexus	D_{max} 30–40 Gy	D_{max} 20–32 Gy V30 < 3 cc
Optic chiasm	D_{max}≤25 Gy	D_{max} 10 Gy
Retina	D_{max} 27 Gy	D_{max} 10 Gy
Optic nerves	D_{max} ≤ 25 Gy	D_{max} 10–12 Gy
Cochlea	D_{max} < 27.5 Gy	D_{max} 20–27.5 Gy
Skin	D_{max} < 39.5 Gy V36.5 Gy < 10 cc	
Mandible	D_{max} < 40 Gy	
Parotids	As low as reasonably achievable	
Larynx	D_{max} 20 Gy	D_{max} 20 Gy
Carotid artery	D_{max} 25–47 Gy	D_{max} 15–34 Gy <50% gets PTV dose

Data from Ref. [7]

tumour volumes (PTV) is typically a 0.3–0.5 cm expansion around GTV to encompass potential day-to-day variation in target position. A microscopic margin (CTV) is typically not defined, to reduce the size of the treated volume.

Due to the highly conformal nature of SBRT radiation plans, high-quality pretreatment imaging verification is required. Different centres have used a variety of techniques including cone-beam CT (CBCT), optical-based surface alignment and CT-on-rail. The action level for correction of setup errors is generally 1–3 mm, and pre- and post-shift imaging is recommended. It is important for each treating institution to measure setup accuracy in quality assurance (QA) processes and use this to inform PTV and plan design [7].

Recommended Dose-Volume Constraints

See Table 5 [7] for suggested dose-volume constraints for organs at risk.

Future Directions

There is a growing interest in the use of immune checkpoint inhibitors in recurrent head and neck cancer. RTOG 3507 is a clinical trial examining the integration of novel immune checkpoint inhibitors (PD-1 antibody pembrolizumab) or CTLA-4 antibody (ipilimumab) delivered concurrently with HN SBRT to promote tumour control.

MRI-guided radiotherapy is another growing area of interest, as it may facilitate tighter treatment margins and smaller volumes, further limiting dose to normal tissues.

Practical Considerations

Approaches to patient selection and treatment planning vary significantly between different centres [6]. Below, we provide a brief overview of the Sunnybrook approach to treatment.

Patient Selection

Indications

- Newly diagnosed head and neck cancer in patients unsuitable for conventional radical treatment due to comorbidities
- Salvage treatment for in-field recurrence
- Boost technique for primary disease following conventional fractionation

Relative Contraindications

- Tumour circumscribing carotid artery walls ≥180°
- Overlying blood vessel
- Tumour in close proximity to brachial plexus, optic structures, brain or cavernous sinus
- Skin infiltration
- ECOG performance status ≥3
- Connective tissue disorder

Contouring

- *GTV* – gross disease
- *CTV* – non-applicable
- *PTV* – 0.3–0.5 cm expansion around GTV to encompass potential day-to-day variation in target position
- *Dose/Fractionation*
  - Option 1: SIB 45 Gy to GTV and 40 Gy to PTV in 5 fractions
  - Option 2: 40 Gy/5 to PTV
  - Option 3: 45 Gy/5 to PTV
- Use alternate-day treatment schedule.
- Patients are to be planned and treated using a Synergy Beam Modulator (4 mm MLC leaf width) or Agility (5 mm MLC) using IMRT or VMAT planning.
- *Evaluate HN SBRT DVH*
  - Hotspots up to 115% acceptable within PTV
  - Avoid prescription dose outside of target
  - Aim to achieve a conformality index, CI < 1.1

- *Target Coverage*
  - *Option 1: SIB 45 Gy to GTV ± 40 Gy to PTV in 5 fractions*
  - GTV V45 Gy > 99%, V47.25 < 35%
  - PTV V40 > 95%
  - *Option 2: 40 Gy/5 to PTV*
  - PTV V40 Gy > 95%
  - *Option 3: 45 Gy/5 to PTV*
  - PTV V45 Gy > 95%
  - For all cases: V115% <1% (must be within PTV)
- *Verification Imaging*
  - Daily cone-beam CT (CBCT) imaging, pre- and post-shift
    - Match to bone, and visually inspect the tumour alignment between the CT and CBCT (GTV, PTV, and all vital organs at risk).
    - Use of 6-DOF, high accuracy hexapod couch for positioning.
  - Day 1 registration – physician approval required
- *IMRT QA*
  - All plans measured using ArcCheck and analysed with a gamma threshold of 3%/3 mm and 10% threshold
    - Gamma pass rate = 95%
    - If it fails VMAT replanned with IMRT using fewer and larger segments

Follow-Up

- Follow-up imaging with CT/MRI and clinic visit with history and physical every 3 months for the first 2 years and then every 3–6 months until 5 years

References

1. Argiris A, Karamouzis MV, Raben D, Ferris RL. Head and neck cancer. Lancet. 2008;371(9625):1695–709.
2. Goodwin WJ Jr. Salvage surgery for patients with recurrent squamous cell carcinoma of the upper aerodigestive tract: when do the ends justify the means? Laryngoscope. 2000;110(3 II):1–18.
3. O'Sullivan B, Huang SH, Siu LL, Waldron J, Zhao H, Perez-Ordonez B, et al. Deintensification candidate subgroups in human papillomavirus-related oropharyngeal cancer according to minimal risk of distant metastasis. J Clin Oncol. 2013;31(5):543–50.
4. Baliga S, Kabarriti R, Ohri N, Haynes-Lewis H, Yaparpalvi R, Kalnicki S, et al. Stereotactic body radiotherapy for recurrent head and neck cancer: a critical review. Head Neck. 2017 Mar;39(3):595–601.
5. Ling DC, Vargo JA, Heron DE. Stereotactic body radiation therapy for recurrent head and neck cancer. Cancer J. 2016;22(4):302–6.
6. Karam I, Poon I, Lee J, Liu S, Higgins K, Enepekides D, et al. Stereotactic body radiotherapy for head and neck cancer: an addition to the armamentarium against head and neck cancer. Future Oncol. 2015;11(21):2937–47.
7. Karam I, Yao M, Heron DE, Poon I, Koyfman SA, Yom SS, et al. Survey of current practices from the International Stereotactic Body Radiotherapy Consortium (ISBRTC) for head and neck cancers. Future Oncol. 2017;13(7):603–13.
8. Vargo JA, Ward MC, Caudell JJ, Riaz N, Dunlap NE, Isrow D, et al. A multi-institutional comparison of SBRT and IMRT for definitive reirradiation of recurrent or second primary head and neck cancer. Int J Radiat Oncol Biol Phys. 2018;100(3):595–605.
9. Rwigema JC, Heron DE, Ferris RL, Gibson M, Quinn A, Yang Y, et al. Fractionated stereotactic body radiation therapy in the treatment of previously-irradiated recurrent head and neck carcinoma: updated report of the University of Pittsburgh experience. Am J Clin Oncol. 2010;33(3):286–93.
10. Yamazaki H, Ogita M, Himei K, Nakamura S, Yoshida K, Kotsuma T, et al. Hypofractionated stereotactic radiotherapy using CyberKnife as a boost treatment for head and neck cancer, a multi-institutional survey: impact of planning target volume. Anticancer Res. 2014;34(10):5755.
11. Yamazaki H, Ogita M, Himei K, Nakamura S, Kotsuma T, Yoshida K, et al. Carotid blowout syndrome in pharyngeal cancer patients treated by hypofractionated stereotactic re-irradiation using CyberKnife: a multi-institutional matched-cohort analysis. Radiother Oncol. 2015;115(1):67–71.
12. Syrigos KN, Karachalios D, Karapanagiotou EM, Nutting CM, Manolopoulos L, Harrington KJ. Head and neck cancer in the elderly: an overview on the treatment modalities. Cancer Treat Rev. 2009;35(3):237–45.
13. Chaturvedi AK, Anderson WF, Lortet-Tieulent J, Paula Curado M, Ferlay J, Franceschi S, et al. Worldwide trends in incidence rates for oral cavity and oropharyngeal cancers. J Clin Oncol. 2013;31(36):4550–9.
14. Huang SH, O'Sullivan B, Waldron J, Lockwood G, Bayley A, Kim J, et al. Patterns of care in elderly head-and-neck cancer radiation oncology patients: a single-center cohort study. Int J Radiat Oncol Biol Phys. 2011;79(1):46–51.
15. Monnier L, Touboul E, Durdux C, Lang P, St Guily JL, Huguet F. Hypofractionated palliative radiotherapy for advanced head and neck cancer: the IHF2SQ regimen. Head Neck. 2013;35(12):1683–8.
16. Bonomo P, Desideri I, Loi M, Lo Russo M, Olmetto E, Maragna V, et al. Elderly patients affected by head and neck squamous cell carcinoma unfit for standard curative treatment: is de-intensified, hypofractionated radiotherapy a feasible strategy? Oral Oncol. 2017;74:142–7.
17. Corry J, Peters LJ, Costa ID, Milner AD, Fawns H, Rischin D, et al. The 'QUAD SHOT'—a phase II study of palliative radiotherapy for incurable head and neck cancer. Radiother Oncol. 2005;77(2):137–42.
18. Teckie S, Lok BH, Rao S, Gutiontov SI, Yamada Y, Berry SL, et al. High-dose hypofractionated radiotherapy is effective and safe for tumors in the head-and-neck. Oral Oncol. 2016;60:74–80.
19. Stevens CM, Huang SH, Fung S, Bayley AJ, Cho JB, Cummings BJ, et al. Retrospective study of palliative radiotherapy in newly diagnosed head and neck carcinoma. Int J Radiat Oncol Biol Phys. 2011;81(4):958–63.
20. Siddiqui F, Patel M, Khan M, McLean S, Dragovic J, Jin J, et al. Stereotactic body radiation therapy for primary, recurrent, and metastatic tumors in the head-and-neck region. Int J Radiat Oncol Biol Phys. 2009;74(4):1047–53.
21. Kodani N, Yamazaki H, Tsubokura T, Shiomi H, Kobayashi K, Nishimura T, et al. Stereotactic body radiation therapy for head and neck tumor: disease control and morbidity outcomes. J Radiat Res. 2011;52(1):24–31.
22. Kawaguchi K, Sato K, Yamada H, Horie A, Nomura T, Iketani S, et al. Stereotactic radiosurgery in combination with chemotherapy as primary treatment for head and neck cancer. J Oral Maxillofac Surg. 2012;70(2):461–72.
23. Vargo JA, Ferris RL, Clump DA, Heron DE. Stereotactic body radiotherapy as primary treatment for elderly patients with medically inoperable head and neck cancer. Front Oncol. 2014;4:214.

24. Khan L, Tjong M, Raziee H, Lee J, Erler D, Chin L, et al. Role of stereotactic body radiotherapy for symptom control in head and neck cancer patients. Support Care Cancer. 2015;23(4):1099.
25. Chen HHW, Tsai S, Wang M, Wu Y, Hsueh W, Yang M, et al. Experience in fractionated stereotactic body radiation therapy boost for newly diagnosed nasopharyngeal carcinoma. Int J Radiat Oncol Biol Phys. 2006;66(5):1408–14.
26. Hara W, Loo BW, Goffinet DR, Chang SD, Adler JR, Pinto HA, et al. Excellent local control with stereotactic radiotherapy boost after external beam radiotherapy in patients with nasopharyngeal carcinoma. Int J Radiat Oncol Biol Phys. 2008;71(2):393–400.
27. Al-Mamgani A, Tans L, Teguh DN, van Rooij P, Zwijnenburg EM, Levendag PC. Stereotactic body radiotherapy: a promising treatment option for the boost of oropharyngeal cancers not suitable for brachytherapy: a single-institutional experience. Int J Radiat Oncol Biol Phys. 2012;82(4):1494–500.
28. Lee DS, Kim YS, Cheon JS, Song JH, Son SH, Jang JS, et al. Long-term outcome and toxicity of hypofractionated stereotactic body radiotherapy as a boost treatment for head and neck cancer: the importance of boost volume assessment. Radiat Oncol. 2012;7(1):85.
29. Ghaly M, Halthore A, Antone J, Zhang H, Cohen J, Sachs H, et al. Dose-escalated stereotactic radiosurgery (SRS) boost for unfavorable locally advanced oropharyngeal cancer: phase I/II trial. Int J Radiat Oncol Biol Phys. 90(1):S122.
30. Patel PR, Salama JK. Reirradiation for recurrent head and neck cancer. Expert Rev Anticancer Ther. 2012;12(9):1177–89.
31. McDonald MW, Lawson J, Garg MK, Quon H, Ridge JA, Saba N, et al. ACR appropriateness criteria retreatment of recurrent head and neck cancer after prior definitive radiation: Expert panel on radiation oncology-head and neck cancer. Int J Radiat Oncol Biol Phys. 2011;80(5):1292–8.
32. Tortochaux J, Tao Y, Tournay E, Lapeyre M, Lesaunier F, Bardet E, et al. Randomized phase III trial (GORTEC 98-03) comparing re-irradiation plus chemotherapy versus methotrexate in patients with recurrent or a second primary head and neck squamous cell carcinoma, treated with a palliative intent. Radiother Oncol. 2011;100(1):70–5.
33. Lartigau EF, Tresch E, Thariat J, Graff P, Coche-Dequeant B, Benezery K, et al. Multi institutional phase II study of concomitant stereotactic reirradiation and cetuximab for recurrent head and neck cancer. Radiother Oncol. 2013;109(2):281–5.
34. Langer CJ, Harris J, Horwitz EM, Nicolaou N, Kies M, Curran W, et al. Phase II study of low-dose paclitaxel and cisplatin in combination with split-course concomitant twice-daily reirradiation in recurrent squamous cell carcinoma of the head and neck: results of radiation therapy oncology group protocol 9911. J Clin Oncol. 2007;25(30):4800–5.
35. Spencer SA, Harris J, Wheeler RH, Machtay M, Schultz C, Spanos W, et al. Final report of RTOG 9610, a multi-institutional trial of reirradiation and chemotherapy for unresectable recurrent squamous cell carcinoma of the head and neck. Head Neck. 2008;30(3):281–8.
36. Voynov G, Heron DE, Burton S, Grandis J, Quinn A, Ferris R, et al. Frameless stereotactic radiosurgery for recurrent head and neck carcinoma. Technol Cancer Res Treat. 2006;5(5):529–35.
37. Roh K, Jang J, Jang H, Kim M, Kim B, Kim Y, et al. Fractionated stereotactic radiotherapy as reirradiation for locally recurrent head and neck cancer. Int J Radiat Oncol Biol Phys. 2009;74(5):1348–55.
38. Heron DE, Ferris RL, Karamouzis M, Andrade RS, Deeb EL, Burton S, et al. Stereotactic body radiotherapy for recurrent squamous cell carcinoma of the head and neck: results of a phase I dose-escalation trial. Int J Radiat Oncol Biol Phys. 2009;75(5):1493–500.
39. Rwigema JCM, Heron DE, Ferris RL, Andrade RS, Gibson MK, Yang Y, et al. The impact of tumor volume and radiotherapy dose on outcome in previously irradiated recurrent squamous cell carcinoma of the head and neck treated with stereotactic body radiation therapy. Am J Clin Oncol. 2011;34(4):372–9.
40. Unger KR, Lominska CE, Deeken JF, Davidson BJ, Newkirk KA, Gagnon GJ, et al. Fractionated stereotactic radiosurgery for reirradiation of head-and-neck cancer. Int J Radiat Oncol Biol Phys. 2010;77(5):1411–9.
41. Cengiz M, Özyiğit G, Yazici G, Doğan A, Yildiz F, Zorlu F, et al. Salvage reirradiation with stereotactic body radiotherapy for locally recurrent head-and-neck tumors. Int J Radiat Oncol Biol Phys. 2011;81(1):104–9.
42. Ozyigit G, Cengiz M, Yazici G, Yildiz D, Yildiz F, Gurkaynak M, et al. A retrospective comparison of robotic stereotactic body radiotherapy and three-dimensional conformal radiotherapy for the reirradiation of locally recurrent nasopharyngeal carcinoma. Int J Radiat Oncol Biol Phys. 2011;81(4):e268.
43. Vargo JA, Wegner RE, Heron DE, Ferris RL, Rwigema JM, Quinn A, et al. Stereotactic body radiation therapy for locally recurrent, previously irradiated nonsquamous cell cancers of the head and neck. Head Neck. 2012;34(8):1153–61.
44. Comet B, Kramar A, Faivre-Pierret M, Dewas S, Coche-Dequeant B, Degardin M, et al. Salvage stereotactic reirradiation with or without cetuximab for locally recurrent head-and-neck cancer: a feasibility study. Int J Radiat Oncol Biol Phys. 2012;84(1):203–9.
45. Vargo JA, Ferris RL, Ohr J, Clump DA, Davis KS, Duvvuri U, et al. A prospective phase 2 trial of reirradiation with stereotactic body radiation therapy plus cetuximab in patients with previously irradiated recurrent squamous cell carcinoma of the head and neck. Int J Radiat Oncol Biol Phys. 2015;91(3):480–8.
46. Bonner JA, Harari PM, Giralt J. Radiotherapy plus cetuximab for squamous-cell carcinoma of the head and neck. N Engl J Med. 2006;354:567.
47. Gebhardt BJ, Vargo JA, Ling D, Jones B, Mohney M, Clump DA, et al. Carotid dosimetry and the risk of carotid blowout syndrome following re-irradiation with head and neck stereotactic body radiation therapy. Int J Radiat Oncol Biol Phys. 2018;101(1):195–200.
48. Kong L, Hu J, Guan X, Gao J, Lu R, Lu JJ. Phase I/II trial evaluating carbon ion radiotherapy for salvaging treatment of locally recurrent nasopharyngeal carcinoma. J Cancer. 2016;7(7):774–83.
49. Romesser PB, Cahlon O, Scher ED, Hug EB, Sine K, Deselm C, et al. Proton beam reirradiation for recurrent head and neck cancer: multi-institutional report on feasibility and early outcomes. Int J Radiat Oncol Biol Phys. 2016;95(1):386–95.
50. McDonald MW, Zolali-Meybodi O, Lehnert SJ, Estabrook NC, Liu Y, Cohen-Gadol AA, et al. Reirradiation of recurrent and second primary head and neck cancer with proton therapy. Int J Radiat Oncol Biol Phys. 2016;96(4):808–19.
51. Ling DC, Vargo JA, Ferris RL, Ohr J, Clump DA, Yau W-W, et al. Risk of severe toxicity according to site of recurrence in patients treated with stereotactic body radiation therapy for recurrent head and neck cancer. Int J Radiat Oncol Biol Phys. 2016;95(3):973–80.
52. Liang NL, Guedes BD, Duvvuri U, Singh MJ, Chaer RA, Makaroun MS, et al. Outcomes of interventions for carotid blowout syndrome in patients with head and neck cancer. J Vasc Surg. 2016;63(6):1525–30.
53. Yazici G, Sanlı TY, Cengiz M, Yuce D, Gultekin M, Hurmuz P, et al. A simple strategy to decrease fatal carotid blowout syndrome after stereotactic body reirradiation for recurrent head and neck cancers. Radiat Oncol. 2013;8(1):242.

Pediatric Radiosurgery

Aditya Juloori and Erin S. Murphy

Introduction

Stereotactic radiosurgery (SRS) has a well-established role in the treatment of benign and malignant tumors in the adult population. There is an increasing role for the use of this modality in the pediatric population, though this remains an area of evolving study. Given the high conformality that radiosurgery provides, SRS and SBRT offer a theoretical advantage of sparing normal tissue in a population for whom late toxicity is an important concern. Radiosurgery has been used in children in three main fashions – as primary treatment for benign conditions, as an adjunct to standard therapy in malignant tumors, and, more recently, for treatment of oligometastatic disease. For pediatric tumors such as medulloblastoma and ependymoma, there is a known dose-response relationship for improved local control [1–3]. Due to immobilization techniques, utilization of high-definition imaging, daily image guidance, and beam arrangements, such as VMAT, stereotactic radiosurgery can be used to dose escalate with a rapid gradient, making it a useful tool for local control in patients with recurrent, residual, or metastatic disease. The most important part of initial management for most pediatric brain tumors involves maximally safe resection, and the extent of resection has been identified as a key prognostic factor in patients with medulloblastoma [4], high-grade glioma [5], low-grade glioma [6], and ependymoma [7]. Conventionally fractionated radiation therapy is often utilized to treat either the resection cavity or areas of residual disease after resection in order to improve outcomes but can be associated with an increased risk of neurocognitive decline [8, 9], radiation necrosis [10, 11], endocrine dysfunction [12], and secondary malignancies [13, 14]. Radiosurgery can potentially reduce the risk of some of these late effects. Radiosurgery has also been used in the management of patients with arteriovenous malformations that may not otherwise be appropriate candidates for surgery. Perhaps the most novel use of radiosurgery has been for patients with oligometastatic pediatric sarcomas, though there has been limited prospective evidence on clinical benefit to this point [15]. In this chapter, we discuss indications for radiosurgery in the pediatric population and review the corresponding data on outcomes and toxicity.

AVM

The role for radiosurgery in the pediatric population is perhaps most well-established for treatment of cerebral arteriovenous malformations (AVMs). AVMs are vascular malformations formed at birth that carry a lifetime risk of spontaneous hemorrhage. Cerebral AVMs are the most common cause of brain hemorrhage in the pediatric population [16, 17], making up the cause of 50% of pediatric hemorrhagic strokes [18]. In fact, pediatric patients with cerebral AVMs are more likely to present with intracranial hemorrhage than their adult counterparts [19]. The 30-day mortality of intracranial hemorrhage in the pediatric population has been reported to be 22% [20]. Due to the potential lifetime risk for morbidity and mortality associated with AVM hemorrhage in children, preventative treatment is often warranted. Primary treatment options include surgical resection as well as embolization. Stereotactic radiosurgery is an

A. Juloori
Department of Radiation Oncology, Cleveland Clinic, Cleveland, OH, USA

E. S. Murphy (✉)
Department of Radiation Oncology, Cleveland Clinic, Cleveland, OH, USA

Cleveland Clinic Lerner College of Medicine, Cleveland, OH, USA

Rose Ella Burkhardt Brain Tumor and Neuro-Oncology Center, Cleveland Clinic, Cleveland, OH, USA
e-mail: murphye3@ccf.org

D. M. Trifiletti et al. (eds.), *Stereotactic Radiosurgery and Stereotactic Body Radiation Therapy*,
https://doi.org/10.1007/978-3-030-16924-4_28

established alternative for those in whom the risk for surgery is deemed prohibitively high. This is the case, for example, when AVMs are located in deep or eloquent areas of the brain, which has been reported to be the case in up to 70–90% of patients [21–26].

The strongest compilation of data for the use of radiosurgery in this population comes from a pooled analysis of seven institutions which make up the International Gamma Knife Research Foundation (IGKRF) [27, 28]. The analysis included 357 patients aged 18 years and younger who were treated with radiosurgery for AVMs. The cohort had a mean age of 12.6 years, 69% of whom initially had a hemorrhagic presentation, and 77% of lesions were located in eloquent regions of the brain. All patients had at least 12 months of follow-up, and favorable outcome was defined as AVM obliteration without post-radiosurgical hemorrhage or permanent radiation-related side effects. With a mean follow-up after treatment of 92 months, AVM obliteration was observed in 63% of patients with a postradiosurgery hemorrhage rate of 1.4% a year (0.8%/year for unruptured versus 1.6%/year for ruptured prior to treatment). Only 3% of treated patients had permanent radiation-induced changes. Favorable outcomes as defined by the study group were observed in 59% of cases, with a mean time to obliteration after radiosurgery of 49 months. A dose-response relationship was observed in this series with a marginal radiosurgery dose of 22 Gy or higher being associated with a significantly higher probability of favorable outcome (78% versus 47%) and AVM obliteration (81.6% versus 51.4%). A similar observation has been seen in multiple other reports with improved obliteration rates with increased dose [25, 29]. Based on this collective data, we recommend a dose of 22 Gy in order to maximize response with an acceptably low toxicity rate; the toxicity profiles reported in the IGKRF series were favorable with a mean dose of 21 Gy. We must note that there was one study – a large UK series of 363 pediatric patients – that showed no observed difference in obliteration rates between patients treated with 20 Gy and those treated with 25 Gy [30]. The authors noted that this finding was surprising and in contrast to the remainder of the literature. They qualified their findings by noting that the vast majority of the patients had a small range of dosing, which perhaps obscured the ability to statistically detect a dose-response effect.

The IGKRF analysis identified factors that were predictive for hemorrhagic presentation, including deep venous drainage, female gender, and smaller AVM volume [27]. These may be criteria in which to consider a more proactive treatment approach in patients with unruptured AVMs. There have also been data previously published that suggest that pediatric patients have a quicker response rate to radiosurgery than the adult population [31]. The preponderance of the existing literature suggests that radiosurgery is a safe and effective treatment for AVMs in pediatric patients, the UK cohort showed 71% obliteration rates with only a 1.1% risk of radiation necrosis [30], while the Italian experience reported by Nicolato and colleagues [29] showed 88% obliteration rate at 5 years with 11% permanent complication rates (radiation necrosis, edema, and delayed cyst formation). The authors identified AVM volume ≤10 ml and prescription dose >16 Gy as factors that were significantly associated with both higher obliteration rate and lower rates of permanent complications. Thus, in order to maximize the therapeutic window, staged treatment is recommended if the AVM nidus is greater than 10 ml in volume or if a dose higher than 16 Gy is prohibited due to proximity to a critical location or nidus size.

Following radiosurgery for AVMs, there is a latency period during which patients remain at risk for developing hemorrhage while the obliteration process occurs. Nine percent of patients in the Italian series developed bleeding during the latency period (one leading to death, one leading to permanent neurologic dysfunction). The latency period bleeding rate was similar, 8.4%, in the IGKRF series, and patients should be counseled about the risks during this time period following treatment. A large analysis examining predictors for latency period hemorrhage in the adults identified only low marginal radiosurgery dose as predictive [32].

Craniopharyngioma

Craniopharyngiomas are rare pediatric tumors derived from Rathke's pouch with an annual incidence of roughly 350 cases a year in the United States [33]. There is a bimodal age distribution of incidence, with one peak in children aged between 5 and 14 years and another in adults between 50 and 75 years [33]. The primary modality of treatment is surgical resection. Even in patients in whom a gross total resection is achievable, the rates of local recurrence have been reported to be 20–27% [34, 35]. Therefore, these patients need to be followed closely. For patients with less than a gross total resection upfront, the typical treatment paradigm involves adjuvant conventionally fractionated radiotherapy to treat residual disease. Given the proximity of these tumors to the optic apparatus and the pituitary stalk, surgery and radiation therapy are associated with potential for pituitary deficiency, visual deficits, cognitive deficiencies, and secondary malignancies [36–39]. Furthermore, the impact of these may be magnified in younger patients. An approach with limited surgical resection followed by radiation has been adopted at St. Jude Children's Research Hospital with lower rates of reported cognitive, neurologic, ophthalmic, and endocrine dysfunction compared to those with more extensive initial resection [40].

Radiosurgery can be used for treatment of residual or recurrent disease, though reports are limited. Craniopharyngiomas may be favorable targets for radiosurgery given that they are often well-defined radiographically

with low concern for spread along the craniospinal axis compared to other pediatric tumors. In addition, there can be significant change in size of the tumor during fractionated radiotherapy requiring mid-treatment imaging and possible alteration in treatment plans, which is avoided with single treatment radiosurgery. However, the proximity to the optic chiasm is a potentially limiting factor to SRS.

The largest published experience comes from a Japanese cohort of 98 patients treated with Gamma Knife radiosurgery with at least 6 months of posttreatment follow-up and a median follow-up of 63 months [41]. Thirty-eight pediatric patients aged 15 or younger were included in the study. The mean margin dose used for the entire population was 11.5 Gy; progression-free survival was not reported separately for adults and children – the 5- and 10-year progression-free survival were 60.8% and 53.8%, respectively. Of treated patients, 6.1% had a deterioration in either vision or endocrine function. The authors discussed that over time they utilized a dose reduction strategy to the optic nerve because of some visual deterioration and loss they observed in some early cases. The mean marginal dose was lowered from 12.7 Gy to 11.5 Gy over the period of the study, with the goal of keeping maximum dose to the optic nerve to less than 10.7 Gy. The authors reported that though this led to a lower response and higher rates of progression, the goal of reducing incidence of visual deterioration was achieved (reduction of 6% to 3%). The control rates in other published series of radiosurgery patients with at least 4 years of follow-up range from 67% to 100% [42–47], though various institutions use different definitions for control. Multiple series have suggested that local control after radiosurgery is highest for solid tumors as opposed to those with cystic or mixed makeup [44–46]. Radiosurgical dosing should be based on what is achievable for a given optic nerve tolerance.

The optic pathways represent the primary dose-limiting structure during radiosurgical planning for craniopharyngioma patients. The rate of long-term visual complications after single fraction radiosurgery for patients with craniopharyngioma has been reported to be between 0% and 8% [42–47]. A recent large analysis of 1578 patients undergoing single- or multi-fraction radiosurgery for skull base tumors (including pituitary adenomas, cavernous sinus meningiomas, and craniopharyngioma among others) examined the risks for radiation-induced optic neuropathy (RION) [48]. While prior resection was not associated with a higher risk for RION, patients who had prior radiation therapy had a ten times higher crude rate of optic neuropathy. The authors provided dose constraints (maximum dose to the optic nerves or chiasm) in order to keep the risk for RION development to less than 1% in patients without previous radiation – 12 Gy in one fraction, 20 Gy in three fractions, and 25 Gy in five fractions [48]. The single fraction dose constraint of 12 Gy is higher than the historical 8 Gy or 10 Gy constraints that are commonly used, and has also been corroborated in other studies [49]. In the absence of prospective data, it may be reasonable to use 12 Gy as a maximum acceptable dose, with a lower constraint in the setting of recurrence after prior radiation. Some practitioners may choose to be more conservative in the pediatric population; however, the concern for RT-related toxicity must be balanced by the need for tumor control.

The other significant toxicity after radiation for craniopharyngiomas is hypothalamic-pituitary dysfunction. Endocrine function is likely to be altered in craniopharyngioma patients prior to any radiation, due to the compressive nature of the tumor or the surgical resection [45]. Both conventionally fractionated radiotherapy and radiosurgery can worsen pre-existing hypothalamic-pituitary function. The rates of reported endocrine deficiency after radiosurgery ranges from 2% to 8% in published series [43–47].

The existing literature for pediatric patients is limited by small patient cohorts with heterogeneous treatment histories. Prospective data are needed in pediatric patients in order to better counsel patients in terms of the impact on disease control as well as long-term toxicity. Radiosurgery should be a treatment option to discuss with patients and their families in those with limited recurrent disease or limited residual disease after surgery.

Vestibular Schwannoma

Vestibular schwannomas are benign tumors of the myelin-forming cells of the eighth cranial nerve, characterized by slow growth. The use of radiosurgery for definitive management of vestibular schwannomas is common in the adult population. Multiple large-scale retrospective reports have shown excellent long-term control with minimal morbidity [50, 51] with preservation of facial sensation and motor function of greater than 95% [52]. Radiosurgery has been shown to be associated with improved functional outcomes and quality of life compared to patients treated with microsurgical resection [53, 54]. Given the excellent outcomes in the adult population, SRS has also been used for pediatric vestibular schwannoma patients. The largest published experience examined outcomes in children with NF2-related vestibular schwannomas treated in Korea [50]. Twenty-four patients were treated with Gamma Knife radiosurgery with a mean marginal dose of 12.4 Gy. With a mean follow-up after treatment of 89.3 months, the 3-year tumor control rate was reported to be 35% with a 5-year hearing preservation rate of 53%. These reported outcomes are certainly not as favorable as those seen in adult radiosurgery series, though data suggest that patients with NF2-related vestibular schwannoma may not respond as favorably as patients with sporadic origin [55]. Given the relatively lower control rates observed in this

series as well as the reported incidence of hearing loss after treatment, it may be reasonable to have a higher threshold before offering radiosurgery in this population. There is also evidence that those with NF2 may have a higher likelihood of malignant transformation after receiving radiotherapy [56], although this outcome would be less likely with radiosurgery. Considering the slow rate of growth, treatment may be better reserved for those who develop clinical symptoms, or who are not good surgical candidates. The outcomes of radiosurgery for pediatric patients with sporadic vestibular schwannoma have not been clearly delineated in the literature as this finding would be rare.

Ependymoma

Ependymomas are rare malignant brain and spine tumors with an annual incidence of roughly 200 cases in the United States [57]. Despite their relative rarity, these tumors still represent the third most common brain tumor in children [1]. The most common location in pediatric patients is in the fourth ventricle [57], with 90% occurring intracranially overall [58]. The treatment paradigm for ependymoma typically involves maximally safe resection with adjuvant conventionally fractionated radiotherapy. It has been clearly established in the surgical literature that the most important prognostic factor in this patient population is the extent of surgical resection [7, 59–63], with improved disease-free and overall survival observed in those who have a gross total resection. In those who have a recurrence, the most common site is locally in the treatment field [11]. Radiosurgery has been utilized in the treatment of residual or recurrent disease. The two largest series discussing outcomes in the setting of recurrence come from Mayo Clinic [64] and The University of Pittsburgh [65]. The Mayo series included 26 patients, 12 of whom were aged 18 and younger, treated with a median SRS dose of 18 Gy. Local control at 3 years was noted to be 72% with a median overall survival of 5.5 years, and two patients were reported to develop radiation necrosis [64]. The Pittsburgh series [65] looked at 21 patients, all of whom were children, who had undergone initial surgery and adjuvant conventional radiation. The median radiosurgical volume was 2.2 cc with a median margin dose of 15 Gy. Three-year progression-free survival was noted to be 42% at 3 years after treatment, with only three patients developing radiation necrosis. This relatively low PFS at 3 years was driven largely by distant metastases, with a 3-year distant relapse rate of 80.3%. Taken together these two studies suggest that radiosurgery provides effective local control with an acceptable side effect profile, though due to distant failure the prognosis remains poor with a 3-year overall survival of 23% in the Pittsburgh series. Factors predictive for higher rates of distant failure included fourth ventricle location, spine metastases at diagnosis, as well as time period of less than 18 months from initial radiation course to radiosurgery [65]. Given the small numbers of patients for whom outcomes have been reported in the recurrent setting, larger patient cohorts with longer follow-up are needed in order to better understand the patterns of failure after treatment which may help guide patient selection for salvage radiosurgery.

Radiosurgery has also been utilized in the upfront setting as a boost in addition to conventional radiation treatment, though the published literature is very limited. St. Jude Children's Research Hospital reported on five children who received radiosurgery as part of their initial therapy after conventional adjuvant radiation and had radiographically well-defined tumors which measured 3 cm or less after initial treatment [66]. Four of the five patients were treated within 30 days of initial RT and one patient was treated within 6 months. With a median follow-up of 24 months, all four patients who had received immediate SRS remained alive and free of disease without any significant toxicities. The patient who had been treated in a delayed manner developed an infield recurrence 16 months after SRS and died due to progression.

Reported outcomes have not always been so promising. In a series of 90 pediatric patients from Boston treated with radiosurgery for various diagnoses, 28 were treated for ependymoma, either for recurrence (25 cases) or in the upfront setting (3 cases) with a median dose of 12.5 Gy [67]. The reported median PFS was 8.5 months and 3-year local control was only 29%. In addition to the relatively poor control outcomes, the authors reported significant toxicity related to SRS, with 20% of the patients in the overall cohort requiring surgery for radiation necrosis.

Radiosurgery for focally recurrent ependymoma has been associated with durable local control, so it should be a treatment consideration for select patients. However, rates of toxicity can potentially be prohibitive, and other options – including pulsed reduced dose rate conventionally fractionated radiation [68] and proton radiotherapy [69] – have been used with good efficacy and reasonable toxicity and may be preferred.

Gliomas

The standard treatment paradigm for high-grade gliomas includes maximal safe resection followed by adjuvant radiation and chemotherapy. These are aggressive malignancies with high rates of clinical progression even with extensive upfront therapy, and in some cases radiosurgery has been utilized for treatment of focal recurrences. In a large series of pediatric radiosurgery patients treated in Boston, 18 were treated for either glioblastoma or anaplastic astrocytomas with reported 3-year local control of 50% [67]. The authors did not outline toxicities for this specific cohort of patients.

There have been more reports of pediatric patients treated with SRS for low-grade gliomas. The standard of care treatment for children with these tumors includes upfront gross total resection followed by observation with generally good outcomes, with 4-year PFS ranging from 77% to 89% depending on extent of resection [70]. Radiosurgery has been used in both the adjuvant and recurrent settings. The largest series of pediatric patients comes from The University of Pittsburgh [71] and describes 50 patients with juvenile pilocytic astrocytoma (JPA) who underwent radiosurgery with a median dose of 14.5 Gy. Thirty-four patients were treated at recurrence and 16 were treated for residual disease. Five-year progression-free survival was noted to be 71%. Ten percent of treated patients developed adverse radiation effects. A longer progression-free survival was seen for those with solid (as opposed to cystic) tumors, with smaller treatment volume (less than 8 cc), and without brainstem involvement. The authors concluded that SRS is most effective for JPA in patients with small residual tumors. In the recurrent setting, they recommended consideration of SRS if reresection is not possible or if a patient has an early recurrence after initial treatment. There have been multiple other reports of radiosurgery for children with low-grade glioma – with reports of excellent local control from 70.8% to 100% with follow-up ranging from 19 to 144 months [71–77]. The series with the longest follow-up reported on 24 patients treated at University of Virginia (UVA) [77]. Progression-free survival at last follow-up was noted in 83% of patients. The median time to decrease in tumor size was 12.5 months. It is notable, however, that some patients did not have a response until 40 months after SRS and were still able to eventually have a complete response. Larger target volume was significantly associated with disease progression in this series. The most common radiation-related side effect was peritumoral edema, which occurred in three patients. This edema was noted to resolve in all three cases. Prospective trials are warranted to help identify which pediatric patients most benefit from the addition of radiosurgery to their treatment paradigm, but it appears that radiosurgery is most suitable for those with small-volume recurrences or residual disease after initial treatment.

Medulloblastoma

The most common intracranial tumor in children is medulloblastoma, with an annual incidence in the United States of 500 cases per year [78]. Typical treatment for patients includes maximal safe resection followed by craniospinal irradiation and chemotherapy with 5-year event-free survival of 80% for average-risk patients [79] and 70% for high-risk disease [80]. Radiosurgery has been used for patients with recurrent disease or as an upfront boost. The Brigham experience reported on 11 patients who were treated for recurrence and 3 treated with a boost for residual disease [81]. The median peripheral dose used was 12 Gy and with a median follow-up of 27 months, all patients treated with radiosurgery with intent to boost sites of residual disease were still alive and free of disease. On the other hand, over half of the patients treated with SRS for recurrence were dead due to progressive disease. Of all patients treated, the most common site of failure was distally within the CNS, and there were no failures noted within the SRS target. Multiple other series have reported on radiosurgery in this population [67, 80, 82, 83]. Local control in these series is generally quite good and the pattern of failure is predominantly outside of the SRS volume. In the largest of these series, in which 16 patients were treated [67], 3-year progression-free survival was noted to be only 15%, underlining the importance of optimizing systemic therapy in this population in order to reduce the incidence of distant metastases and perhaps alter overall survival. Reports of toxicity varied across the multiple published series – in the series with the longest reported follow-up (3 patients with follow-up of 30, 39, and 48 months) [82], there was no reported toxicity. However, toxicity, when it did occur, could be quite significant, with one series reporting an occurrence of brainstem edema causing long-term quadriparesis [67].

Treatment of Oligometastatic Disease

An emerging role for radiosurgery in the pediatric population is in the treatment of oligometastatic sarcoma, specifically Ewing's sarcoma and osteosarcoma. Definitive treatment for localized Ewing's sarcoma has evolved to include both systemic chemotherapy as well as local therapy with surgery, radiation therapy, or both. With definitive treatment, prognosis is generally quite good with 5-year overall survival of 70–80% [84, 85]. Twenty-five percent of patients with Ewing's sarcoma present with metastatic disease at diagnosis [86], and unfortunately, this subset of patients has relatively poorer outcomes with multiple series demonstrating an average 5-year event-free survival and overall survival of 25% and 33%, respectively [87–99]. Among patients with metastatic Ewing's sarcoma, prognosis is better for those with pulmonary metastatic disease as opposed to those with osseous and soft tissue metastases. Five-year survival for patients with limited pulmonary metastases who undergo systemic chemotherapy and metastasectomy has been reported to be between 20% and 40% [97, 100, 101]. Whole lung irradiation is also a standard treatment option for those with pulmonary involvement. On the other hand, 4-year event-free survival has been reported to be 28% for those with osseous or bone marrow metastases or as low as 14% for those with both lung and bone/bone marrow metastases

[93]. Select patients with metastatic disease are able to have extended survival with local therapy to these sites of distant disease. In addition, 20% of patients who initially have localized disease will then go on to develop metastatic disease [102], perhaps representing a population in which metastatic deposits can be eradicated to possibly alter the natural history of disease progression.

A similar thought process has been proposed for patients with metastatic osteosarcoma. Distant metastases are present at diagnosis in roughly 10–20% [103] of patients with osteosarcoma and will eventually develop in 30–50% of patients who initially have localized disease [104]. Historically, patients received only local treatment with relatively poor long-term survival of only 16% due to the high rates of distant failure [105]. With the addition of multiagent chemotherapy to surgery as part of definitive treatment, 5-year overall survival has improved to 70% [105], similar to outcomes in patients with Ewing's sarcoma. Patients with a limited number of distant metastasis can potentially have extended survival with an aggressive approach to local treatment. The reported 10-year overall survival of patients with metastatic disease who underwent surgery of all resectable metastatic sites is 24% [103]. Without randomized evidence, it is difficult to know what the long-term survival rates would be in this subset with chemotherapy alone. However, this paradigm of limited surgery for patients with oligometastases at diagnoses or those with oligoprogression has been accepted. Given the relative radioresistance of osteosarcoma, historically there has been a limited role for local radiation therapy for metastases other than in the setting of palliation. More recently, with improvements in technology and the ability to safely escalate dose to focal targets with SBRT, there has been a renewed interest in using radiosurgery to eradicate osteosarcoma metastases.

To date, the published evidence for radiotherapy to metastases in Ewing's and osteosarcoma patients is very limited. The best data available for the Ewing's population come from patients included in the EURO-EWING 99 trial [106]. This multi-institutional trial included 281 patients with a new diagnosis of Ewing's sarcoma with multiple extrapulmonary metastases, and its purpose was to determine the efficacy and feasibility of treatment intensification in patients with primary disseminated disease. Patients were treated with six courses of induction VIDE chemotherapy (vincristine, ifosfamide, doxorubicin, etoposide) followed by local treatment to the primary tumor and further adjuvant chemotherapy and stem cell transplant. If feasible, local therapy to sites of metastasis was done either concurrently or after adjuvant systemic therapy. The most common sites of metastatic involvement in this patient cohort were osseous (78.3%) and the bone marrow (38.3%). A secondary analysis of this trial [86] as presented by Haeusler and colleagues examined outcomes in 120 patients in the study who were enrolled at a single institution [86]. The authors found that 3-year event-free survival was 39% in those who received local therapy to both the primary and metastatic sites, 17% in those who received treatment to either the primary or distant sites of disease, and 14% in those who received no local therapy at all. Local therapy to all sites of disease significantly extended event-free survival and the authors concluded that this should be an important addition to systemic treatment in patients with disseminated disease. It is important to note that metastatic treatment in this study was done with either surgery or radiation therapy, with 7.5% of this cohort having both surgery and RT, 5% having surgery alone, 27% receiving RT alone, and 60% not undergoing any local therapy. The authors did not include details of the radiation treatments, though given the treatment era, conventional radiation would be expected rather than radiosurgery. The analysis also suggested that those with limited number of metastases may have a greater magnitude of benefit from an aggressive approach – 3-year EFS was 61% in those with one osseous metastasis vs. 19% in those with greater than five osseous metastases treated. This is perhaps reflective of differing biology of disease in those with multiple metastases – patients with multiple sites of distant spread may have a higher burden of circulating tumor cells or a cancer cell architecture with greater ability to access channels for distant spread. Thus, there may be less potential for radiosurgery to alter the natural history of disease in this cohort.

There has been one published report on the use of radiosurgery for oligometastatic Ewing's sarcoma and osteosarcoma. Brown and colleagues reported on 14 patients with recurrent or metastatic Ewing's sarcoma or osteosarcoma treated at Mayo Clinic with radiosurgery to 27 lesions [15]. The median dose used was 40 Gy in 5 fractions. Two grade 2 late toxicities (myonecrosis and avascular necrosis) and one grade 3 late toxicity (sacral plexopathy) were noted. The patient who developed grade 2 myonecrosis received concurrent gemcitabine, which is a known potent radiosensitizer. The patient who developed grade 3 sacral plexopathy underwent 60 Gy in 10 to the sacrum and had received previous radiation to that site at initial diagnosis (59.4 Gy in 33 fx, 1.75 years prior). The authors noted that the sacral plexus had received 105% of prescription dose on initial treatment and 100% of prescription dose during the second course. In the case of the avascular necrosis, the entirety of the femoral head was clinically involved and received 60 Gy in 10 fx, certainly higher than the 10 fx dose constraints recommended by Timmerman for the femoral head (max point dose of 43.5 Gy and 10 cc volume constraint of 38 Gy). However, the patient required only conservative management of this toxicity and remained free of disease for 1.6 years at the time of publication. The authors of the study did not report the oncologic outcomes, but the results suggest feasibility and safety of such an approach, though special

caution should be given in the setting of concurrent chemotherapy or reirradiation. In these clinical situations, it may be prudent to consider more conservative normal tissue constraints or to increase the interval from prior treatment.

There are currently two ongoing trials for patients with oligometastatic pediatric sarcomas. AEWS 1221 is a randomized phase III study sponsored by the Children's Oncology Group (COG) examining the addition of an IGF-1R monoclonal antibody Ganitumab to standard multiagent chemotherapy in patients with metastatic Ewing's sarcoma (NCT02306161). Irrespective of whether patients are randomized to the Ganitumab arm or not, patients receive induction chemotherapy and go on to have local treatment to the primary tumor (with surgery and/or conventionally fractionated radiation), consolidation chemotherapy, and finally treatment of *all* metastatic sites with radiation, as long as they do not have progressive disease. The rationale for treatment of metastatic sites after chemotherapy has been completed is due to the potential volume of bone marrow in the radiation field and associated toxicities; an interval of at least 3 weeks after chemotherapy is mandated by the protocol. Patients with lung involvement undergo whole lung irradiation (1.5 Gy daily fractionation), while all bone metastases less than 5 cm in maximal dimension at diagnosis are to be treated with radiosurgery (40 Gy in five fractions). Osseous metastases greater than 5 cm in greatest dimension and nonosseous metastases are treated with conventional radiation therapy. For patients undergoing radiosurgery, a 1 cm CTV margin is given to the area of residual disease on imaging to account for microscopic disease; a 2 mm PTV margin is recommended.

While AEWS 1221 is limited to patients with Ewing's sarcoma, there is also an ongoing multi-institutional trial (St. Jude, Mayo Clinic, Johns Hopkins Hospital, Stanford) examining the use of SBRT for up to five bony metastases for patients with any pediatric sarcoma other than rhabdomyosarcoma. Patients are eligible for inclusion in the study if greater than 3 years of age with at least one osseous metastatic site $\geq$2 cm in size on conventional CT, MRI, or PET/CT or $\geq$1 cm in size as measured on spiral CT scan. Patients are excluded if any osseous metastases are greater than 5 cm in size in greatest dimension. For nonspine bony sites, the GTV is expanded by 2 mm to form the PTV, which is given 40 Gy in five fractions. For vertebral body metastases, the GTV is given 40 Gy in five fractions; the CTV is the entire vertebral body and is expanded by 2 mm to form a PTV that is given 30 Gy in five fractions. The protocol calls for five daily fractions, but does allow for up to 2 weeks for delivery. It is also important to note that the protocol does allow for a dose reduction to 35 Gy in five fractions to the GTV for young children under the age of 10, if the clinician is concerned about dose to the surrounding normal tissues.

Both of these ongoing trials will help clinicians better understand which patient subsets most benefit from the addition of local therapy for metastatic disease and will also provide a framework for understanding acute and long-term toxicities. Neither of these trials include the use of radiosurgery for pulmonary metastases, which is an area of fertile interest as well. Off trial, in the absence of prospective evidence to this point, we would recommend following the dose and fractionation used in these protocols for well-selected patients with favorable prognostic factors. The Mayo series [15] did report incidence of grade 3 toxicity when 40 Gy in five fractions was used. Our practice has been to consider using lower doses for some patients in whom poorer long-term prognosis is suspected, with the thought being to minimize chance of toxicity when clinical benefit is uncertain.

In our own clinical experience of using radiosurgery for pediatric patients with oligometastatic disease, we have noted some toxicities. Patient A is a 15-year-old patient with a history of osteosarcoma of the femur who had metastasis to the lung at diagnosis. She was treated with standard chemotherapy (methotrexate, doxorubicin, cisplatin) and underwent limb salvage therapy. One year after diagnosis she had a recurrence of the lung metastasis and then received systemic treatment with ifosfamide and etoposide with good response. Two years later, 3 years after initial diagnosis, she developed an isolated sacral mass causing bowel and bladder retention. The patient then received and had response to high dose methotrexate and doxorubicin. Given the isolated relapse, the case was deemed appropriate for radiosurgery. Figure 1a shows the PET/CT prior to SBRT. She received 35 Gy in five fractions, delivered daily over 1 week. Figures 2 shows a representative image of the treatment plan. Figure 1b shows a representative PET image after radiosurgery, with good imaging and clinical response as her neurologic symptoms resolved. She did well during treatment but did develop grade 2 radiation dermatitis in the treatment field 2 weeks after treatment was completed, as displayed in Fig. 3. This was self-limiting and resolved, and the patient remained disease-free for 9 months before developing new metastatic disease in the chest. She has received further systemic chemotherapy and conventional palliative RT treatments, and remains alive with continuing progressive disease 15 months after treatment. Patient B is a patient with osteosarcoma of the R proximal tibia with previous above knee amputation who underwent standard adjuvant systemic therapy and then developed left leg cramping and numbness and was found on imaging to have a 6 cm sacral mass with a soft tissue component consistent with metastasis, as shown in Fig. 4. The patient had three cycles of ifosfamide and etoposide with minimal response on imaging. There was no other metastatic disease, and the patient was referred for consideration of SBRT. He received 40 Gy in five fractions in daily fractions over 1 week with no acute toxicity. Following treatment, the

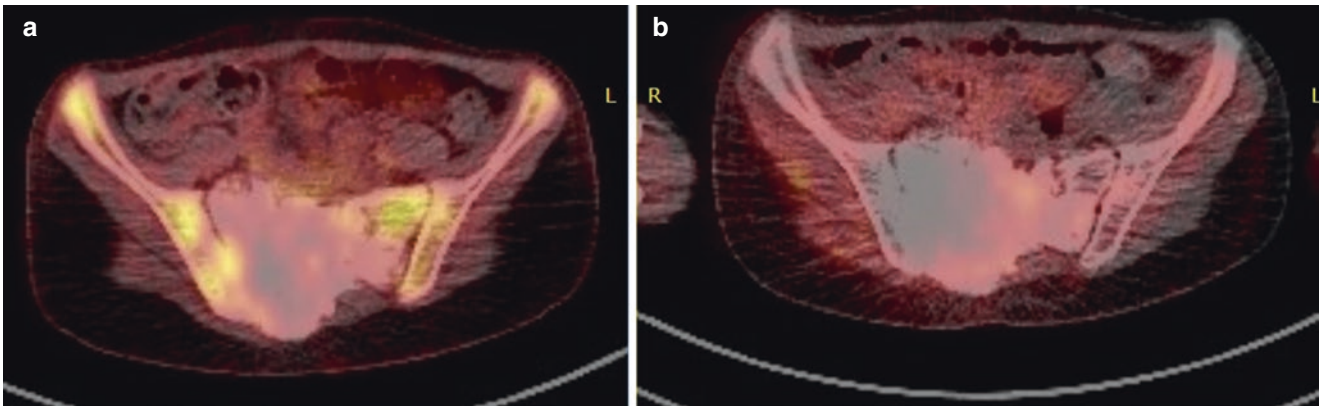

Fig. 1 (**a**, **b**) Representative axial slices from PET/CT before and after radiosurgery for metastatic osteosarcoma of the femur for a pediatric Patient A

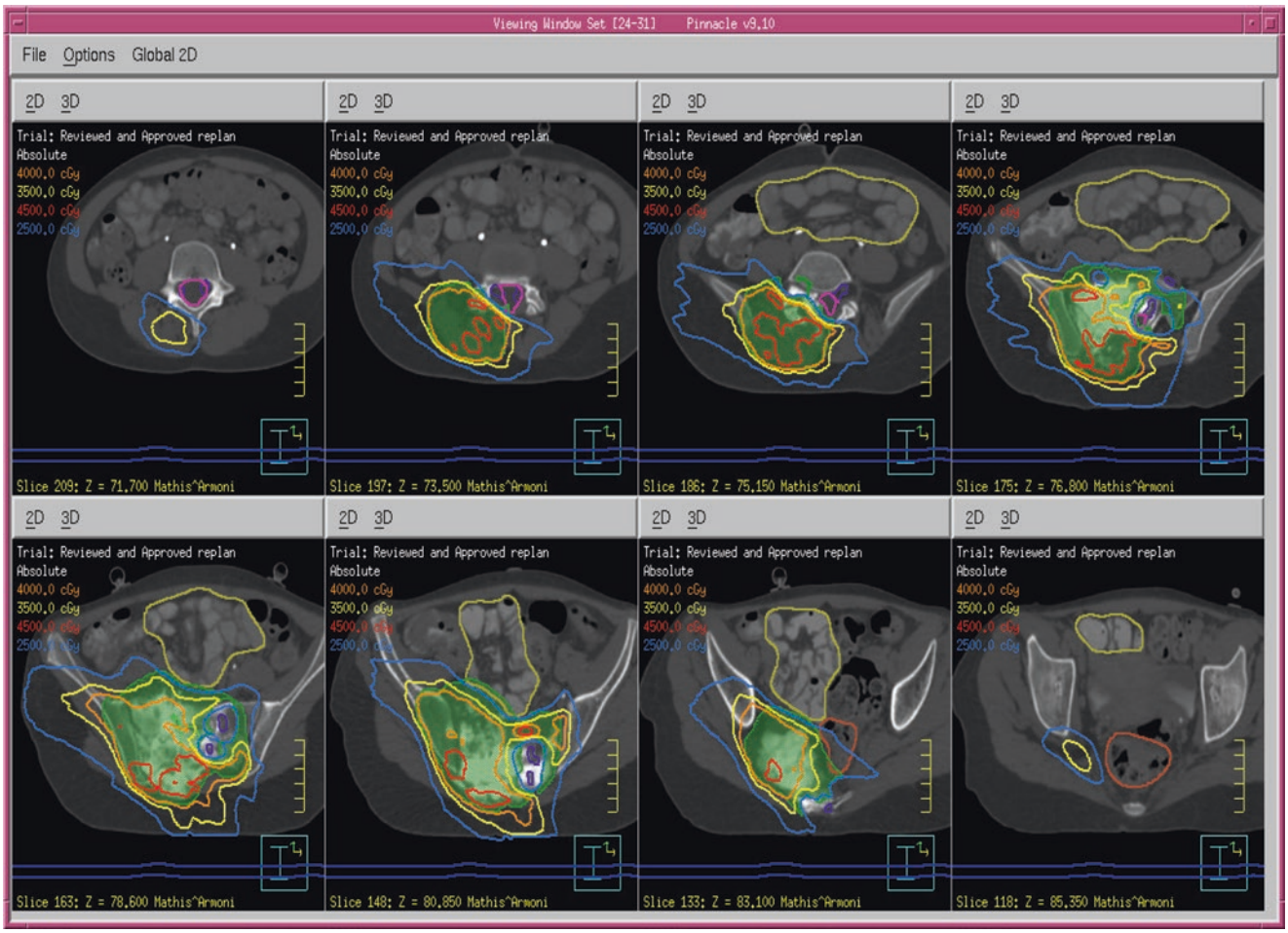

Fig. 2 Representative axial slice from Patient A's treatment plan

patient has had good local control and 18 months of stable disease on imaging. He did develop persistent pain in the L hip with clinical concern for sacral insufficiency fracture, with negative diagnostic imaging. He did have a sacroplasty with cement injection with good clinical response.

We have also had patients who have been treated with multiple sessions of radiosurgery with no toxicity to date. Patient C is a patient with osteosarcoma of the humerus with metastatic disease (osseous, lung) at diagnosis who was treated on the AEWS 1221 protocol discussed above. She

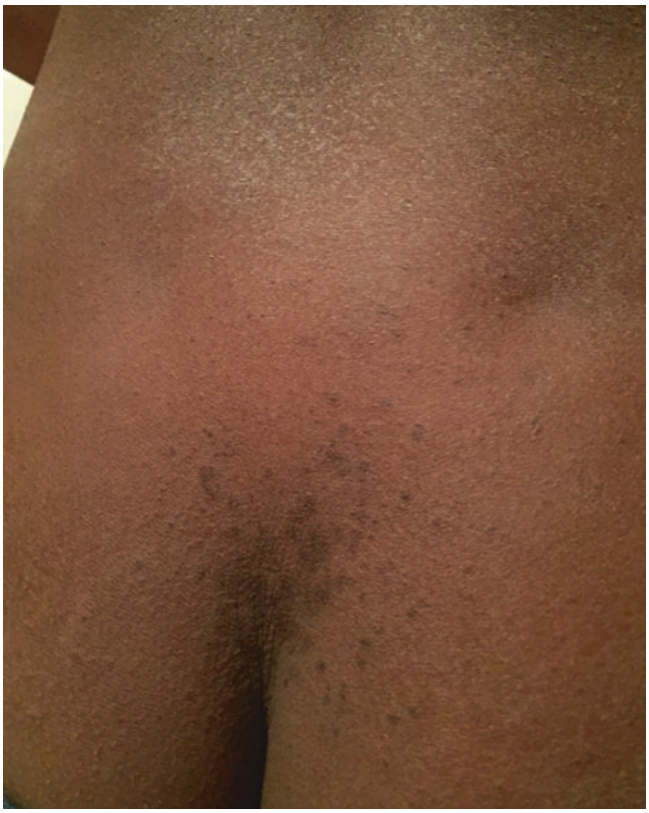

Fig. 3 Radiation dermatitis (grade 2) after radiosurgery to metastatic sacral lesion for Patient A

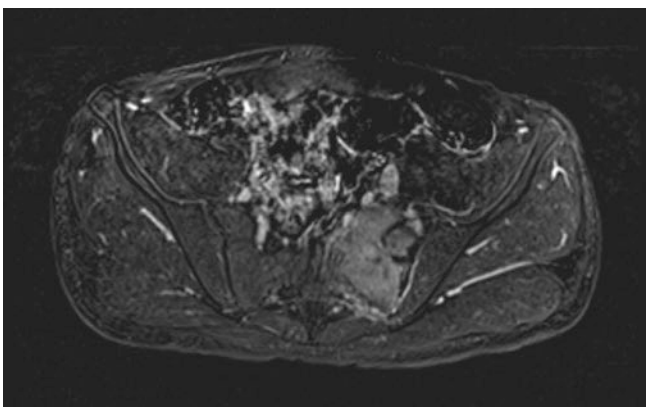

Fig. 4 Metastatic osteosarcoma to the L sacral ala

received standard chemotherapy and definitive radiation to the humerus, 55.8 Gy in 33 fractions. Patient C then had concurrent treatment to four sites with residual metastatic disease on imaging after primary therapy – T11, T12, R femur, and sacrum. The treatments were delivered in consecutive treatment days; treatment was 35 Gy in five fractions to the thoracic spine vertebral bodies and the R femur. However, because the sacral mass was larger than 5 cm, 30 Gy in five fractions was used. Patient C tolerated the treatments well with no pain flare or other acute toxicity noted. Given the fact that this initial treatment went well, we proceeded to treat other metastatic sites that were initially involved at the time of diagnosis – T4/T5, L3, T9/10, treated to 35 Gy in five fractions. This was followed by whole lung irradiation, 15 Gy in ten fractions. There has not been enough follow-up time to date to comment on local control and the overall impact on Patient C's natural disease history, but Patient C's case is demonstrative of the tolerance of multiple radiosurgery sessions, some of which are concurrent.

Practical Considerations

In addition to the associated technical challenges of treatment planning and delivery, stereotactic radiosurgery in adults is accomplished through a host of physical requirements of the patient, often including rigid immobilization which may be invasive or noninvasive depending on clinical indications and physician preference. Skull fixation allows for precision of radiation delivery to the tumor, a matter which is of critical importance given the high doses being used. Cranial radiosurgery is often completed with the use of a stereotactic head frame if the Gamma Knife is used, whereas a noninvasive thermoplastic mask is more often used with LINAC-based radiosurgery. For radiosurgery of body sites, immobilization with a BodyFix (Elekta, Stockholm, Sweden) or motion management may be needed. These requirements can raise practical challenges when used in the pediatric population. In adults, Gamma Knife radiosurgery is usually done with local anesthesia and under light sedation for adults; however, pediatric patients may have difficulty tolerating an extended time on the treatment machine or the placement of the head frame. Thus, general anesthesia can be necessary which carries its own potential risk for complications. Newer models of the Gamma Knife allow for mask-based immobilization, but pediatric patients may need sedation to tolerate a mask, whether on the Gamma Knife or traditional linear accelerator. In addition, use of a mask can make it difficult to ensure airway access in a patient who needs general anesthesia. In patients who do have a classic head frame placed for Gamma Knife radiosurgery, another challenge is the thinner skull thickness of the pediatric patient in comparison to adults, which can make fixation of the frame more difficult because of concern for skull penetration by the pins.

Toxicity

There are important toxicity considerations specific to the pediatric population. Radiosurgery often involves the delivery of radiation in arcs, which may raise the integral dose

distribution to the patient compared to traditional limited fields. This is an important concern in pediatric patients given the potential for an increased risk for secondary malignancy in a population that may be expected to have a longer period over which malignancy can develop. There is also a well-understood differential response of normal tissue to radiation in pediatric patients. Among patients who receive cranial radiotherapy for pediatric brain tumors, younger age at the time of treatment has been identified as a risk factor for increase in IQ decline [107]. Traditional dose constraints for radiosurgery are largely lacking in prospective validation in the adult population, and there certainly is an absence of such data for pediatric patients as well. Some have suggested a reduction of 10–20% in the allowances set forth by the Timmerman tables or TG101, though this should be balanced by the requirements of the clinical picture as not to compromise local control. Prospective data are needed, and current ongoing protocols for treatment of oligometastatic disease provide appropriate dose constraints.

Future Directions

Prospective randomized trials for the role of CNS radiosurgery for pediatric patients are unlikely given the small numbers and the fact that the utility of radiosurgery is often not in the upfront setting. However, expanding our understanding of the utility and toxicity of CNS radiosurgery in this sensitive population is imperative, and perhaps combining multi-institutional experiences may be beneficial.

In the era of improved systemic therapy with biologically targeted agents and immunotherapy, we anticipate that aggressive local management of oligometastatic disease will find an increasingly important role. This will also translate to the pediatric population in which we already have an aggressive approach for many patients who present with metastatic disease at diagnosis. We need to be thoughtful early in this process to gain a better understanding of appropriate dosing schemes, and potential toxicities of these newer radiotherapy applications. The role of SBRT for metastases can be particularly challenging for diseases in which we have historically applied definitive radiotherapy dosing for all initial metastatic sites. This introduces a paradigm of potential multiple SBRT sessions for these young patients.

References

1. Goldwein JW, Leahy JM, Packer RJ, Sutton LN, Curran WJ, Rorke LB, et al. Intracranial ependymomas in children. Int J Radiat Oncol Biol Phys. 1990;19(6):1497–502.
2. Merchant TE, Haida T, Wang MH, Finlay JL, Leibel SA. Anaplastic ependymoma: treatment of pediatric patients with or without craniospinal radiation therapy. J Neurosurg. 1997;86(6):943–9.
3. Tarbell NJ, Loeffler JS, Silver B, Lynch E, Lavally BL, Kupsky WJ, et al. The change in patterns of relapse in medulloblastoma. Cancer. 1991;68(7):1600–4.
4. Massimino M, Giangaspero F, Garre ML, Gandola L, Poggi G, Biassoni V, et al. Childhood medulloblastoma. Crit Rev Oncol Hematol. 2011;79(1):65–83.
5. Wisoff JH, Boyett JM, Berger MS, Brant C, Li H, Yates AJ, et al. Current neurosurgical management and the impact of the extent of resection in the treatment of malignant gliomas of childhood: a report of the Children's Cancer Group trial no. CCG-945. J Neurosurg. 1998;89(1):52–9.
6. Wisoff JH, Sanford RA, Heier LA, Sposto R, Burger PC, Yates AJ, et al. Primary neurosurgery for pediatric low-grade gliomas: a prospective multi-institutional study from the Children's Oncology Group. Neurosurgery. 2011;68(6):1548–54; discussion 1554–1545.
7. Rousseau P, Habrand JL, Sarrazin D, Kalifa C, Terrier-Lacombe MJ, Rekacewicz C, et al. Treatment of intracranial ependymomas of children: review of a 15-year experience. Int J Radiat Oncol Biol Phys. 1994;28(2):381–6.
8. Mulhern RK, Palmer SL, Merchant TE, Wallace D, Kocak M, Brouwers P, et al. Neurocognitive consequences of risk-adapted therapy for childhood medulloblastoma. J Clin Oncol Off J Am Soc Clin Oncol. 2005;23(24):5511–9.
9. Ris MD, Packer R, Goldwein J, Jones-Wallace D, Boyett JM. Intellectual outcome after reduced-dose radiation therapy plus adjuvant chemotherapy for medulloblastoma: a Children's Cancer Group study. J Clin Oncol Off J Am Soc Clin Oncol. 2001;19(15):3470–6.
10. Murphy ES, Merchant TE, Wu S, Xiong X, Lukose R, Wright KD, et al. Necrosis after craniospinal irradiation: results from a prospective series of children with central nervous system embryonal tumors. Int J Radiat Oncol Biol Phys. 2012;83(5):e655–60.
11. Merchant TE, Li C, Xiong X, Kun LE, Boop FA, Sanford RA. Conformal radiotherapy after surgery for paediatric ependymoma: a prospective study. Lancet Oncol. 2009;10(3):258–66.
12. Laughton SJ, Merchant TE, Sklar CA, Kun LE, Fouladi M, Broniscer A, et al. Endocrine outcomes for children with embryonal brain tumors after risk-adapted craniospinal and conformal primary-site irradiation and high-dose chemotherapy with stem-cell rescue on the SJMB-96 trial. J Clin Oncol Off J Am Soc Clin Oncol. 2008;26(7):1112–8.
13. Neglia JP, Robison LL, Stovall M, Liu Y, Packer RJ, Hammond S, et al. New primary neoplasms of the central nervous system in survivors of childhood cancer: a report from the Childhood Cancer Survivor Study. J Natl Cancer Inst. 2006;98(21):1528–37.
14. Mike V, Meadows AT, D'Angio GJ. Incidence of second malignant neoplasms in children: results of an international study. Lancet (London, England). 1982;2(8311):1326–31.
15. Brown LC, Lester RA, Grams MP, Haddock MG, Olivier KR, Arndt CAS, et al. Stereotactic body radiotherapy for metastatic and recurrent ewing sarcoma and osteosarcoma. Sarcoma. 2014;2014:418270.
16. Hladky JP, Lejeune JP, Blond S, Pruvo JP, Dhellemmes P. Cerebral arteriovenous malformations in children: report on 62 cases. Childs Nerv Syst. 1994;10(5):328–33.
17. Kondziolka D, Kano H, Yang HC, Flickinger JC, Lunsford L. Radiosurgical management of pediatric arteriovenous malformations. Childs Nerv Syst. 2010;26(10):1359–66.
18. Meyer-Heim AD, Boltshauser E. Spontaneous intracranial haemorrhage in children: aetiology, presentation and outcome. Brain Dev. 2003;25(6):416–21.
19. Di Rocco C, Tamburrini G, Rollo M. Cerebral arteriovenous malformations in children. Acta Neurochir. 2000;142(2):145–56; discussion 156-148.
20. Broderick J, Talbot GT, Prenger E, Leach A, Brott T. Stroke in children within a major metropolitan area: the surprising importance of intracerebral hemorrhage. J Child Neurol. 1993;8(3):250–5.

21. Kano H, Kondziolka D, Flickinger JC, Yang HC, Flannery TJ, Awan NR, et al. Stereotactic radiosurgery for arteriovenous malformations, part 2: management of pediatric patients. J Neurosurg Pediatr. 2012;9(1):1–10.
22. Nicolato A, Foroni R, Crocco A, Zampieri PG, Alessandrini F, Bricolo A, et al. Gamma knife radiosurgery in the management of arteriovenous malformations of the Basal Ganglia region of the brain. Minim Invasive Neurosurg. 2002;45(4):211–23.
23. Nicolato A, Foroni R, Seghedoni A, Martines V, Lupidi F, Zampieri P, et al. Leksell gamma knife radiosurgery for cerebral arteriovenous malformations in pediatric patients. Childs Nerv Syst. 2005;21(4):301–7; discussion 308.
24. Nicolato A, Lupidi F, Sandri MF, Foroni R, Zampieri P, Mazza C, et al. Gamma knife radiosurgery for cerebral arteriovenous malformations in children/adolescents and adults. Part I: Differences in epidemiologic, morphologic, and clinical characteristics, permanent complications, and bleeding in the latency period. Int J Radiat Oncol Biol Phys. 2006;64(3):904–13.
25. Yen CP, Monteith SJ, Nguyen JH, Rainey J, Schlesinger DJ, Sheehan JP. Gamma Knife surgery for arteriovenous malformations in children. J Neurosurg Pediatr. 2010;6(5):426–34.
26. Zabel-du Bois A, Milker-Zabel S, Huber P, Schlegel W, Debus J. Pediatric cerebral arteriovenous malformations: the role of stereotactic linac-based radiosurgery. Int J Radiat Oncol Biol Phys. 2006;65(4):1206–11.
27. Ding D, Starke RM, Kano H, Mathieu D, Huang PP, Feliciano C, et al. International multicenter cohort study of pediatric brain arteriovenous malformations. Part 1: Predictors of hemorrhagic presentation. Journal of neurosurgery. Pediatrics. 2017;19(2):127–35.
28. Starke RM, Ding D, Kano H, Mathieu D, Huang PP, Feliciano C, et al. International multicenter cohort study of pediatric brain arteriovenous malformations. Part 2: Outcomes after stereotactic radiosurgery. J Neurosurg Pediatr. 2017;19(2):136–48.
29. Nicolato A, Longhi M, Tommasi N, Ricciardi GK, Spinelli R, Foroni RI, et al. Leksell Gamma Knife for pediatric and adolescent cerebral arteriovenous malformations: results of 100 cases followed up for at least 36 months. J Neurosurg Pediatr. 2015;16(6):736–47.
30. Dinca EB, de Lacy P, Yianni J, Rowe J, Radatz MW, Preotiuc-Pietro D, et al. Gamma knife surgery for pediatric arteriovenous malformations: a 25-year retrospective study. J Neurosurg Pediatr. 2012;10(5):445–50.
31. Nicolato A, Lupidi F, Sandri MF, Foroni R, Zampieri P, Mazza C, et al. Gamma Knife radiosurgery for cerebral arteriovenous malformations in children/adolescents and adults. Part II: Differences in obliteration rates, treatment-obliteration intervals, and prognostic factors. Int J Radiat Oncol Biol Phys. 2006;64(3):914–21.
32. Yen CP, Sheehan JP, Schwyzer L, Schlesinger D. Hemorrhage risk of cerebral arteriovenous malformations before and during the latency period after GAMMA knife radiosurgery. Stroke. 2011;42(6):1691–6.
33. Bunin GR, Surawicz TS, Witman PA, Preston-Martin S, Davis F, Bruner JM. The descriptive epidemiology of craniopharyngioma. J Neurosurg. 1998;89(4):547–51.
34. Elliott RE, Hsieh K, Hochm T, Belitskaya-Levy I, Wisoff J, Wisoff JH. Efficacy and safety of radical resection of primary and recurrent craniopharyngiomas in 86 children. J Neurosurg Pediatr. 2010;5(1):30–48.
35. Hoffman HJ, De Silva M, Humphreys RP, Drake JM, Smith ML, Blaser SI. Aggressive surgical management of craniopharyngiomas in children. J Neurosurg. 1992;76(1):47–52.
36. Kiehna EN, Merchant TE. Radiation therapy for pediatric craniopharyngioma. Neurosurg Focus. 2010;28(4):E10.
37. Aquilina K, Merchant TE, Rodriguez-Galindo C, Ellison DW, Sanford RA, Boop FA. Malignant transformation of irradiated craniopharyngioma in children: report of 2 cases. J Neurosurg Pediatr. 2010;5(2):155–61.
38. Dolson EP, Conklin HM, Li C, Xiong X, Merchant TE. Predicting behavioral problems in craniopharyngioma survivors after conformal radiation therapy. Pediatr Blood Cancer. 2009;52(7):860–4.
39. Merchant TE. Craniopharyngioma radiotherapy: endocrine and cognitive effects. J Pediatr Endocrinol Metab. 2006;19(Suppl 1):439–46.
40. Merchant TE, Kiehna EN, Sanford RA, Mulhern RK, Thompson SJ, Wilson MW, et al. Craniopharyngioma: the St. Jude Children's Research Hospital experience 1984–2001. Int J Radiat Oncol Biol Phys. 2002;53(3):533–42.
41. Kobayashi T, Kida Y, Mori Y, Hasegawa T. Long-term results of gamma knife surgery for the treatment of craniopharyngioma in 98 consecutive cases. J Neurosurg. 2005;103(6 Suppl):482–8.
42. Barua KK, Ehara K, Kohmura E, Tamaki N. Treatment of recurrent craniopharyngiomas. Kobe J Med Sci. 2003;49(5–6):123–32.
43. Jeon C, Kim S, Shin HJ, Nam DH, Lee JI, Park K, et al. The therapeutic efficacy of fractionated radiotherapy and gamma-knife radiosurgery for craniopharyngiomas. J Clin Neurosci. 2011;18(12):1621–5.
44. Kobayashi T. Long-term results of gamma knife radiosurgery for 100 consecutive cases of craniopharyngioma and a treatment strategy. Prog Neurol Surg. 2009;22:63–76.
45. Lee CC, Yang HC, Chen CJ, Hung YC, Wu HM, Shiau CY, et al. Gamma Knife surgery for craniopharyngioma: report on a 20-year experience. J Neurosurg. 2014;121 Suppl:167–78.
46. Niranjan A, Kano H, Mathieu D, Kondziolka D, Flickinger JC, Lunsford LD. Radiosurgery for craniopharyngioma. Int J Radiat Oncol Biol Phys. 2010;78(1):64–71.
47. Xu Z, Yen CP, Schlesinger D, Sheehan J. Outcomes of Gamma Knife surgery for craniopharyngiomas. J Neuro-Oncol. 2011;104(1):305–13.
48. Milano MT, Grimm J, Soltys SG, Yorke E, Moiseenko V, Tomé WA, et al. Single- and multi-fraction stereotactic radiosurgery dose tolerances of the optic pathways. Int J Radiat Oncol Biol Phys. 2018. pii: S0360–3016(18)30125–1. https://doi.org/10.1016/j.ijrobp.2018.01.053. [Epub ahead of print].
49. Pollock BE, Link MJ, Leavitt JA, Stafford SL. Dose-volume analysis of radiation-induced optic neuropathy after single-fraction stereotactic radiosurgery. Neurosurgery. 2014;75(4):456–60; discussion 460.
50. Boari N, Bailo M, Gagliardi F, Franzin A, Gemma M, del Vecchio A, et al. Gamma Knife radiosurgery for vestibular schwannoma: clinical results at long-term follow-up in a series of 379 patients. J Neurosurg. 2014;121 Suppl:123–42.
51. Chung WY, Liu KD, Shiau CY, Wu HM, Wang LW, Guo WY, et al. Gamma knife surgery for vestibular schwannoma: 10-year experience of 195 cases. J Neurosurg. 2013;119(Suppl):87–97.
52. Murphy ES, Suh JH. Radiotherapy for vestibular schwannomas: a critical review. Int J Radiat Oncol Biol Phys. 2011;79(4):985–97.
53. Pollock BE, Driscoll CL, Foote RL, Link MJ, Gorman DA, Bauch CD, et al. Patient outcomes after vestibular schwannoma management: a prospective comparison of microsurgical resection and stereotactic radiosurgery. Neurosurgery. 2006;59(1):77–85; discussion 77–85.
54. Regis J, Pellet W, Delsanti C, Dufour H, Roche PH, Thomassin JM, et al. Functional outcome after gamma knife surgery or microsurgery for vestibular schwannomas. J Neurosurg. 2013;119(Suppl):1091–100.
55. Brackmann DE, Fayad JN, Slattery WH 3rd, Friedman RA, Day JD, Hitselberger WE, et al. Early proactive management of vestibular schwannomas in neurofibromatosis type 2. Neurosurgery. 2001;49(2):274–80; discussion 280-273.
56. Baser ME, Evans DG, Jackler RK, Sujansky E, Rubenstein A. Neurofibromatosis 2, radiosurgery and malignant nervous system tumours. Br J Cancer. 2000;82(4):998.

57. Childhood Ependymoma Treatment (PDQ(R)): Health Professional Version. PDQ Cancer Information Summaries. Bethesda; 2002.
58. Paulino AC, Wen BC, Buatti JM, Hussey DH, Zhen WK, Mayr NA, et al. Intracranial ependymomas: an analysis of prognostic factors and patterns of failure. Am J Clin Oncol. 2002;25(2):117–22.
59. Merchant TE, Jenkins JJ, Burger PC, Sanford RA, Sherwood SH, Jones-Wallace D, et al. Influence of tumor grade on time to progression after irradiation for localized ependymoma in children. Int J Radiat Oncol Biol Phys. 2002;53(1):52–7.
60. Nazar GB, Hoffman HJ, Becker LE, Jenkin D, Humphreys RP, Hendrick EB. Infratentorial ependymomas in childhood: prognostic factors and treatment. J Neurosurg. 1990;72(3):408–17.
61. Pollack IF, Gerszten PC, Martinez AJ, Lo KH, Shultz B, Albright AL, et al. Intracranial ependymomas of childhood: long-term outcome and prognostic factors. Neurosurgery. 1995;37(4):655–66; discussion 666–667.
62. van Veelen-Vincent ML, Pierre-Kahn A, Kalifa C, Sainte-Rose C, Zerah M, Thorne J, et al. Ependymoma in childhood: prognostic factors, extent of surgery, and adjuvant therapy. J Neurosurg. 2002;97(4):827–35.
63. Robertson PL, Zeltzer PM, Boyett JM, Rorke LB, Allen JC, Geyer JR, et al. Survival and prognostic factors following radiation therapy and chemotherapy for ependymomas in children: a report of the Children's Cancer Group. J Neurosurg. 1998;88(4):695–703.
64. Stauder MC, Ni Laack N, Ahmed KA, Link MJ, Schomberg PJ, Pollock BE. Stereotactic radiosurgery for patients with recurrent intracranial ependymomas. J Neuro-Oncol. 2012;108(3):507–12.
65. Kano H, Yang HC, Kondziolka D, Niranjan A, Arai Y, Flickinger JC, et al. Stereotactic radiosurgery for pediatric recurrent intracranial ependymomas. J Neurosurg Pediatr. 2010;6(5):417–23.
66. Aggarwal R, Yeung D, Kumar P, Muhlbauer M, Kun LE. Efficacy and feasibility of stereotactic radiosurgery in the primary management of unfavorable pediatric ependymoma. Radiother Oncol. 1997;43(3):269–73.
67. Hodgson DC, Goumnerova LC, Loeffler JS, Dutton S, Black PM, Alexander E 3rd, et al. Radiosurgery in the management of pediatric brain tumors. Int J Radiat Oncol Biol Phys. 2001;50(4):929–35.
68. Mohindra P, Robins HI, Tome WA, Hayes L, Howard SP. Wide-field pulsed reduced dose rate radiotherapy (PRDR) for recurrent ependymoma in pediatric and young adult patients. Anticancer Res. 2013;33(6):2611–8.
69. Eaton BR, Chowdhry V, Weaver K, Liu L, Ebb D, MacDonald SM, et al. Use of proton therapy for re-irradiation in pediatric intracranial ependymoma. Radiother Oncol. 2015;116(2):301–8.
70. Gajjar A, Sanford RA, Heideman R, Jenkins JJ, Walter A, Li Y, et al. Low-grade astrocytoma: a decade of experience at St. Jude Children's Research Hospital. J Clin Oncol Off J Am Soc Clin Oncol. 1997;15(8):2792–9.
71. Kano H, Niranjan A, Kondziolka D, Flickinger JC, Pollack IF, Jakacki RI, et al. Stereotactic radiosurgery for pilocytic astrocytomas part 2: outcomes in pediatric patients. J Neuro-Oncol. 2009;95(2):219–29.
72. Barcia JA, Barcia-Salorio JL, Ferrer C, Ferrer E, Algas R, Hernandez G. Stereotactic radiosurgery of deeply seated low grade gliomas. Acta Neurochir Suppl. 1994;62:58–61.
73. Boethius J, Ulfarsson E, Rahn T, Lippittz B. Gamma knife radiosurgery for pilocytic astrocytomas. J Neurosurg. 2002;97(5 Suppl):677–80.
74. Hadjipanayis CG, Kondziolka D, Gardner P, Niranjan A, Dagam S, Flickinger JC, et al. Stereotactic radiosurgery for pilocytic astrocytomas when multimodal therapy is necessary. J Neurosurg. 2002;97(1):56–64.
75. Kida Y, Kobayashi T, Mori Y. Gamma knife radiosurgery for low-grade astrocytomas: results of long-term follow up. J Neurosurg. 2000;93(Suppl 3):42–6.
76. Somaza SC, Kondziolka D, Lunsford LD, Flickinger JC, Bissonette DJ, Albright AL. Early outcomes after stereotactic radiosurgery for growing pilocytic astrocytomas in children. Pediatr Neurosurg. 1996;25(3):109–15.
77. Weintraub D, Yen CP, Xu Z, Savage J, Williams B, Sheehan J. Gamma knife surgery of pediatric gliomas. J Neurosurg Pediatr. 2012;10(6):471–7.
78. McNeil DE, Cote TR, Clegg L, Rorke LB. Incidence and trends in pediatric malignancies medulloblastoma/primitive neuroectodermal tumor: a SEER update. Surveillance Epidemiology and End Results. Med Pediatr Oncol. 2002;39(3):190–4.
79. Packer RJ, Gajjar A, Vezina G, Rorke-Adams L, Burger PC, Robertson PL, et al. Phase III study of craniospinal radiation therapy followed by adjuvant chemotherapy for newly diagnosed average-risk medulloblastoma. J Clin Oncol Off J Am Soc Clin Oncol. 2006;24(25):4202–8.
80. Patrice SJ, Tarbell NJ, Goumnerova LC, Shrieve DC, Black PM, Loeffler JS. Results of radiosurgery in the management of recurrent and residual medulloblastoma. Pediatr Neurosurg. 1995;22(4):197–203.
81. Abe M, Tokumaru S, Tabuchi K, Kida Y, Takagi M, Imamura J. Stereotactic radiation therapy with chemotherapy in the management of recurrent medulloblastomas. Pediatr Neurosurg. 2006;42(2):81–8.
82. King D, Connolly D, Zaki H, Lee V, Yeomanson D. Successful treatment of metastatic relapse of medulloblastoma in childhood with single session stereotactic radiosurgery: a report of 3 cases. J Pediatr Hematol Oncol. 2014;36(4):301–4.
83. Woo C, Stea B, Lulu B, Hamilton A, Cassady JR. The use of stereotactic radiosurgical boost in the treatment of medulloblastomas. Int J Radiat Oncol Biol Phys. 1997;37(4):761–4.
84. Jürgens H, Exner U, Gadner H, Harms D, Michaelis J, Sauer R, et al. Multidisciplinary treatment of primary Ewing's sarcoma of bone. A 6-year experience of a European Cooperative Trial. Cancer. 1988;61(1):23–32.
85. Granowetter L, Womer R, Devidas M, Krailo M, Wang C, Bernstein M, et al. Dose-intensified compared with standard chemotherapy for nonmetastatic Ewing sarcoma family of tumors: a Children's Oncology Group Study. J Clin Oncol Off J Am Soc Clin Oncol. 2009;27(15):2536–41.
86. Haeusler J, Ranft A, Boelling T, Gosheger G, Braun-Munzinger G, Vieth V, et al. The value of local treatment in patients with primary, disseminated, multifocal Ewing sarcoma (PDMES). Cancer. 2010;116(2):443–50.
87. Craft A, Cotterill S, Malcolm A, Spooner D, Grimer R, Souhami R, et al. Ifosfamide-containing chemotherapy in Ewing's sarcoma: The Second United Kingdom Children's Cancer Study Group and the Medical Research Council Ewing's Tumor Study. J Clin Oncol Off J Am Soc Clin Oncol. 1998;16(11):3628–33.
88. Donaldson SS, Torrey M, Link MP, Glicksman A, Gilula L, Laurie F, et al. A multidisciplinary study investigating radiotherapy in Ewing's sarcoma: end results of POG #8346. Pediatric Oncology Group. Int J Radiat Oncol Biol Phys. 1998;42(1):125–35.
89. Kushner BH, Meyers PA, Gerald WL, Healey JH, La Quaglia MP, Boland P, et al. Very-high-dose short-term chemotherapy for poor-risk peripheral primitive neuroectodermal tumors, including Ewing's sarcoma, in children and young adults. J Clin Oncol Off J Am Soc Clin Oncol. 1995;13(11):2796–804.
90. Pinkerton CR, Bataillard A, Guillo S, Oberlin O, Fervers B, Philip T. Treatment strategies for metastatic Ewing's sarcoma. Eur J Cancer. 2001;37(11):1338–44.
91. Hayes FA, Thompson EI, Parvey L, Rao B, Kun L, Parham D, et al. Metastatic Ewing's sarcoma: remission induction and survival. J Clin Oncol Off J Am Soc Clin Oncol. 1987;5(8):1199–204.
92. Sandoval C, Meyer WH, Parham DM, Kun LE, Hustu HO, Luo X, et al. Outcome in 43 children presenting with metastatic Ewing sar-

coma: the St. Jude Children's Research Hospital experience, 1962 to 1992. Med Pediatr Oncol. 1996;26(3):180–5.
93. Paulussen M, Ahrens S, Burdach S, Craft A, Dockhorn-Dworniczak B, Dunst J, et al. Primary metastatic (stage IV) Ewing tumor: survival analysis of 171 patients from the EICESS studies. European Intergroup Cooperative Ewing Sarcoma Studies. Ann Oncol. 1998;9(3):275–81.
94. Craft AW, Cotterill SJ, Bullimore JA, Pearson D. Long-term results from the first UKCCSG Ewing's Tumour Study (ET-1). United Kingdom Children's Cancer Study Group (UKCCSG) and the Medical Research Council Bone Sarcoma Working Party. Eur J Cancer. 1997;33(7):1061–9.
95. Demeocq F, Oberlin O, Benz-Lemoine E, Boilletot A, Gentet JC, Zucker JM, et al. Initial chemotherapy including ifosfamide in the management of Ewing's sarcoma: preliminary results. A protocol of the French Pediatric Oncology Society (SFOP). Cancer Chemother Pharmacol. 1989;(24 Suppl 1):S45–7.
96. Marina NM, Pappo AS, Parham DM, Cain AM, Rao BN, Poquette CA, et al. Chemotherapy dose-intensification for pediatric patients with Ewing's family of tumors and desmoplastic small round-cell tumors: a feasibility study at St. Jude Children's Research Hospital. J Clin Oncol Off J Am Soc Clin Oncol. 1999;17(1):180–90.
97. Paulussen M, Ahrens S, Craft AW, Dunst J, Fröhlich B, Jabar S, et al. Ewing's tumors with primary lung metastases: survival analysis of 114 (European Intergroup) Cooperative Ewing's Sarcoma Studies patients. J Clin Oncol Off J Am Soc Clin Oncol. 1998;16(9):3044–52.
98. Cangir A, Vietti TJ, Gehan EA, Burgert EO Jr, Thomas P, Tefft M, et al. Ewing's sarcoma metastatic at diagnosis. Results and comparisons of two intergroup Ewing's sarcoma studies. Cancer. 1990;66(5):887–93.
99. Brunetto AL, Castillo LA, Petrilli AS, Macedo CD, Boldrini E, Costa C, et al. Carboplatin in the treatment of Ewing sarcoma: results of the first Brazilian collaborative study group for Ewing sarcoma family tumors-EWING1. Pediatr Blood Cancer. 2015;62(10):1747–53.
100. Bacci G, Briccoli A, Picci P, Ferrari S. Metachronous pulmonary metastases resection in patients with Ewing's sarcoma initially treated with adjuvant or neoadjuvant chemotherapy. Eur J Cancer. 1995;31A(6):999–1001.
101. Dunst J, Paulussen M, Jurgens H. Lung irradiation for Ewing's sarcoma with pulmonary metastases at diagnosis: results of the CESS-studies. Strahlentherapie und Onkologie: Organ der Deutschen Rontgengesellschaft [et al]. 1993;169(10):621–3.
102. Womer RB, West DC, Krailo MD, Dickman PS, Pawel BR, Grier HE, et al. Randomized controlled trial of interval-compressed chemotherapy for the treatment of localized Ewing sarcoma: a report from the Children's Oncology Group. J Clin Oncol Off J Am Soc Clin Oncol. 2012;30(33):4148–54.
103. Kager L, Zoubek A, Potschger U, Kastner U, Flege S, Kempf-Bielack B, et al. Primary metastatic osteosarcoma: presentation and outcome of patients treated on neoadjuvant Cooperative Osteosarcoma Study Group protocols. J Clin Oncol Off J Am Soc Clin Oncol. 2003;21(10):2011–8.
104. Whelan JS, Jinks RC, McTiernan A, Sydes MR, Hook JM, Trani L, et al. Survival from high-grade localised extremity osteosarcoma: combined results and prognostic factors from three European Osteosarcoma Intergroup randomised controlled trials. Ann Oncol. 2012;23(6):1607–16.
105. Anninga JK, Gelderblom H, Fiocco M, Kroep JR, Taminiau AH, Hogendoorn PC, et al. Chemotherapeutic adjuvant treatment for osteosarcoma: where do we stand? Eur J Cancer. 2011;47(16):2431–45.
106. Ladenstein R, Potschger U, Le Deley MC, Whelan J, Paulussen M, Oberlin O, et al. Primary disseminated multifocal Ewing sarcoma: results of the Euro-EWING 99 trial. J Clin Oncol Off J Am Soc Clin Oncol. 2010;28(20):3284–91.
107. Mulhern RK, Merchant TE, Gajjar A, Reddick WE, Kun LE. Late neurocognitive sequelae in survivors of brain tumours in childhood. Lancet Oncol. 2004;5(7):399–408.

Part VI

The Future of Radiosurgery and SBRT

Patient Selection in SBRT and SRS

Christopher Wilke, L. Chinsoo Cho, and Paul W. Sperduto

Introduction

The use of stereotactic body radiotherapy (SBRT) and stereotactic radiosurgery (SRS) has grown exponentially over the previous decade [1]. Once predominantly confined to the treatment of small central nervous system (CNS) lesions, SBRT/SRS techniques are now widely applied to a plethora of tumor histologies spanning a range of anatomic disease sites. A rationale for this observed trend is the ability of SBRT/SRS techniques to deliver high dose ablative radiotherapy to small conformal target volumes with relative sparing of the surrounding organs at risk (OARs), thus providing robust local disease control while minimizing excessive radiation-induced toxicity.

With the growth of SBRT and SRS utilization, the selection of patients who are appropriate candidates for these therapies has similarly continued to evolve. Data on treatment safety and efficacy have helped further refine the role of ablative radiotherapy for many disease sites as well as the patients who would derive the maximal benefit from them. The purpose of this chapter is to review criteria for patient selection and associated radiotherapy techniques for some of the most commonly encountered tumors amenable to SBRT/SRS.

C. Wilke · L. C. Cho
University of Minnesota, Department of Radiation Oncology, Minneapolis, MN, USA

P. W. Sperduto (✉)
Gamma Knife Center, University of Minnesota Medical Center, Department of Radiation Oncology, Minneapolis, MN, USA

Minneapolis Radiation Oncology, Waconia, MN, USA
e-mail: psperduto@mropa.com

Patient Selection for Intracranial Radiosurgery

Malignant CNS Tumors

Metastases

Brain metastases are a common and complex conundrum for cancer care. An estimated 300,000 patients are diagnosed each year with brain metastases in the United States [1] and that incidence is growing due to advances in treatment that result in patients living longer and thus at risk for brain metastases [2]. It is a complex problem because of the marked heterogeneity of this patient population: brain metastases may arise from a wide variety of tumor types and subtypes. Furthermore, these patients may have already received a plethora of different treatments for their cancer or may present with brain metastases at the time of initial diagnosis. This heterogeneity has long plagued interpretation of clinical trials involving this patient population because it was essentially impossible to sufficiently stratify studies to verify similar groups of patients were being compared [3]. Interpretation of clinical trials and efforts to estimate prognosis are further complicated by the plethora of possible combinations of currently available treatment options: surgery, stereotactic radiosurgery (SRS), whole brain radiation therapy (WBRT), chemotherapy, targeted drug therapies, and immunotherapies. Furthermore, four prospective randomized trials have shown WBRT adds no survival benefit over SRS alone in SRS-eligible patients [4–7] and, on the other end of the prognostic spectrum, there is evidence that supportive care may be as effective as WBRT [8]. Accordingly, WBRT is used less commonly than in the past.

These concerns have led to efforts to better understand prognosis. The purpose of a prognostic index is to predict outcome prior to treatment and is important to distinguish from predictive factors. A prognostic factor stratifies outcome independent of the employed treatment method, while a predictive factor stratifies outcomes for a specific

D. M. Trifiletti et al. (eds.), *Stereotactic Radiosurgery and Stereotactic Body Radiation Therapy*,
https://doi.org/10.1007/978-3-030-16924-4_29

Table 1 Median survival time for patients with brain metastases by diagnosis-specific Graded Prognostic Assessment score

	DS-GPA					
Diagnosis	Overall MST (95% CI) *n*	0–1.0 MST (95% CI) *n* (%)	1.5–2.0 MST (95% CI) *n* (%)	2.5–3.0 MST (95% CI) *n* (%)	3.5–4.0 MST (95% CI) *n* (%)	*p* (log-rank)
NSCLC	15.23 (14.17–16.53) 1521	6.90 (5.73–8.70) 337 (22%)	13.67 (11.97–15.33) 664 (44%)	26.47 (23.40–30.63) 455 (30%)	46.77 (36.87–NE) 65 (4%)	<0.001
SCLC	4.90 (4.30–6.20) 281	2.79 (1.83–3.12) 65 (23%)	4.90 (4.04–6.51) 119 (42%)	7.67 (6.27–9.13) 84 (30%)	17.05 (4.70–27.43) 13 (5%)	<0.001
Melanoma	9.80 (9.08–10.59) 823	4.92 (3.67–6.92) 136 (17%)	8.30 (7.34–9.28) 386 (47%)	15.77 (13.12–18.82) 256 (31%)	34.07 (23.61–50.46) 45 (5%)	<0.001
RCC	9.63 (7.66–10.91) 286	3.27 (2.04–5.10) 43 (15%)	7.29 (3.73–10.91) 76 (27%)	11.27 (8.80–14.80) 104 (36%)	14.77 (9.73–19.79) 63 (22%)	<0.001
Breast cancer	13.80 (11.53–15.87) 400	3.35 (3.13–3.78) 23 (6%)	7.70 (5.62–8.74) 104 (26%)	15.07 (12.94–15.87) 140 (35%)	25.30 (23.10–26.51) 133 (33%)	<0.001
GI cancer	5.36 (4.30–6.30) 209	3.13 (2.37–4.57) 76 (36%)	4.40 (3.37–6.53) 65 (31%)	6.87 (4.86–11.63) 50 (24%)	13.54 (9.76–27.12) 18 (9%)	<0.001
Other	6.37 (5.22–7.49) 450	–	–	–	–	–

The top row in each cell is the median survival time (MST) in months and its associated 95% CI. The bottom row is the frequency and percentage of patients with the corresponding DS-GPA category for a given diagnosis

Based on data from Refs. [13, 15, 17]

Abbreviations: *DS-GPA* diagnosis-specific Graded Prognostic Assessment, *NSCLC* non-small cell lung cancer (adenocarcinoma), *SCLC* small cell lung cancer, *RCC* renal cell carcinoma, *GI* gastrointestinal, *NE* not estimable

intervention. Gaspar and colleagues published the Radiation Therapy Oncology Group (RTOG) Recursive Partitioning Analysis for brain metastases (Table 1) in 1997 [9]. This prognostic index consisted of three classes, I (age < 65, Karnofsky Performance Score (KPS) > 70, controlled primary tumor, no extracranial metastases), II (all patients not in class I or III), and III (KPS < 70), which correlated with median survival of 7.7, 4.5, and 2.3 months, respectively.

Sperduto and colleagues published the Graded Prognostic Assessment (GPA) in 2008 [10] based on 1960 patients from 5 randomized Radiation Therapy Oncology Group (RTOG) trials (7916, 8528, 8905, 9104, and 9508). Analysis showed four prognostic factors (age, KPS, extracranial metastases, and number of brain metastases) were significant for survival. Those prognostic factors were weighted in proportion to their regression coefficients and scaled such that patients with the best/worst prognosis would have a GPA of 4.0/0.0, respectively. In 2010, the GPA was refined based on an analysis of a retrospective multi-institutional database of 4259 patients. That study found survival varies by diagnosis and diagnosis-specific prognostic factors [11]. The GPA was further refined with the addition of tumor subtype to the Breast-GPA [12] with a summary report published in 2012 [13]. More recently, the GPA indices for lung cancer and melanoma have been updated using new data from patients (2186 lung cancer and 823 melanoma patients) diagnosed since 2005 with the inclusion of molecular factors. The Lung-molGPA incorporates EGFR and ALK gene status [14, 15] and similarly the Melanoma-molGPA incorporates *BRAF* status [16, 17]. The original Melanoma-GPA found only two factors were significant (KPS and the number of brain metastases) whereas in the updated Melanoma-molGPA, other clinical factors (age and extracranial metastases) were found to be significant, in addition to *BRAF* status.

The median survival time for patients with brain metastases by diagnosis-specific GPA is highlighted in Table 1. Table 2 displays a user-friendly worksheet to facilitate calculation of the Graded Prognostic Assessment by diagnosis and estimate survival for patients with brain metastases. A free online/smartphone application is available at brainmetgpa.com which further simplifies calculation of the GPA. Table 3 shows a multivariate analysis of risk of death and median survival by treatment (excluding drug therapies) and diagnosis. It is important to reinforce that these data are retrospective in nature with the inherent selection bias as in all retrospective studies and thus should not be used to draw definitive conclusions on comparative treatment efficacy.

The diagnosis-specific GPA indices presented here hold several implications for clinical management and research involving patients with brain metastases:

1. There is marked heterogeneity in outcomes for patients with brain metastases and these outcomes vary not only by diagnosis but also by diagnosis-specific prognostic factors, as detailed herein. Because of this heterogeneity, we should not treat all patients with brain metastases the same way; treatment should be individualized and the past philosophy of fatalistic futility should be abandoned.

Table 2 GPA worksheet to estimate survival from brain metastases by diagnosis

Non-small cell/small cell lung cancer	GPA scoring criteria			Patient
	0	0.5	1.0	Score
Age	≥70	<70	n/a	_____
KPS	≤70	80	90–100	_____
ECM	Present		Absent	_____
#BM	> 4	1–4	n/a	_____
Gene status	EGFR neg/unk	n/a	EGFR pos	
	ALK neg/unk		or ALK pos	_____
			Sum total	_____
Adenocarcinoma MS by GPA: GPA 0–1.0 = 6.9; 1.5–2.0 = 13.7; 2.5–3.0 = 26.5; 3.5–4.0 = 46.8				
Non-adenocarcinoma MS by GPA: GPA 0–1.0 = 5.3; 1.5–2.0 = 9.8; 2.5–3.0 = 12.8				

Melanoma	0	0.5	1.0	Score
Age	70	<70	n/a	____
KPS	<70	80	90–100	____
ECM	Present	n/a	Absent	____
#BM	>4	2–4	1	____
Gene status	BRAF neg/unk	BRAF pos	n/a	____
			Sum total =	_____
MS (mo) by GPA: 0–1.0 = 4.9, 1.5–2.0 = 8.3, 2.5–3.0 = 15.8, 3.5–4.0 = 34.1_____				

Breast cancer	0	0.5	1.0	1.5	2.0	Score
KPS	≤50	60	70–80	90–100	n/a	____
Subtype	basal	n/a	LumA	HER2	LumB	____
Age	≥60	<60	n/a	n/a	n/a	____
					Sum total =	_____
Subtype:	Basal = Triple negative (ER/PR/HER2-neg),					
	LumA = Luminal A (ER/PR-pos, HER2-neg)					
	LumB = Luminal B (triple positive, ER/PR/HER2-pos)					
	HER2 = HER2-pos, ER/PR-neg					
MS (mo) by GPA: 0–1.0 = 3.4, 1.5–2.0 = 7.7, 2.5–3.0 = 15.1, 3.5–4.0 = 25.3_____						

Renal cell carcinoma		0	1.0	2.0	Score
	KPS	<70	70–80	90–100	____
	#BM	>3	2–3	1	____
				Sum total =	_____
MS (mo) by GPA: 0–1.0 = 3.3, 1.5–2.0 = 7.3, 2.5–3.0 = 11.3, 3.5–4.0 = 14.8_____					

GI cancers	0	1	2	3	4	Score
KPS	<70	70	80	90	100	____
MS (mo) by GPA: 0–1.0 = 3.1, 2.0 = 4.4, 3.0 = 6.9, 4.0 = 13.5_____						

Based on data from Refs. [13, 15, 17]

Abbreviations: *GPA* Graded Prognostic Assessment, *KPS* Karnofsky Performance Score, *ECM* extracranial metastases, *#BM* number of brain metastases, *ER* estrogen receptor, *PR* progesterone receptor, *HER2* human epidermal growth factor receptor 2, *MS* median survival in months, *neg/unk* negative or unknown

2. On the other hand, as shown in Table 1, if a patient has a GPA of 0–1.0, regardless of diagnosis, their expected survival is poor. For these patients, supportive care, as suggested by the QUARTZ Trial [8], may be the best option.
3. For patients with GPA scores above 1.0, the median survival time (Table 1) is more variable dependent upon diagnosis and aggressive treatment strategies may be appropriate, but these retrospective data do not provide a basis for assuming that longer survival is a consequence of more aggressive treatment. Indeed, the survival by treatment data shown in Table 3 is certainly fraught with selection bias and should not be blindly applied or expected. Nonetheless, these data reflect patterns of care for patients with brain metastases.
4. Performance status is prognostic in every diagnosis. Clinicians should take the time to accurately assess and document their patients' performance status.
5. Table 2 shows the number of brain metastases is a significant prognostic factor for lung cancer, melanoma, and renal cell carcinoma, but not for breast or gastrointestinal cancers. Patients should not be categorically denied treatment because of the number of brain metastases.
6. Extracranial metastases are only prognostic in lung cancer and melanoma but not in breast cancer, renal cell carcinoma, or gastrointestinal cancers. The implication here is that those patients with non-lung, non-melanoma malignancies should not be denied aggressive treatment for their brain metastases because they have extracranial metastases.
7. Age is strongly prognostic in lung cancer and weakly prognostic in breast cancer and melanoma but not prognostic in renal cell carcinoma or gastrointestinal cancers. Thus, age should not be used as a rationale to withhold aggressive treatment for non-lung malignancies.
8. Because lung cancer and brain metastases from lung cancer are so common, those patients have masked our understanding of the distinct course for patients with non-lung malignancies and brain metastases, as demonstrated by points 5, 6, and 7 above.
9. Tumor subtype, particularly in breast cancer, is critically important, but tumor subtype alone is not as prognostic as the Breast-GPA index.
10. A disproportionate number of patients with gastrointestinal cancers present with GPA of 0–1.0. Whether this is due to lack of screening magnetic resonance imaging (MRI) in these patients versus other biological reasons remains unclear, but the finding should serve as a

Table 3 Multivariable analysis of risk of death and median survival[b] by treatment and diagnosis

		Treatment					
		WBRT	SRS	WBRT + SRS	S + SRS	S + WBRT	S + WBRT+SRS
Diagnosis	Statistics						
NSCLC $n = 1521$	Risk of death (HR)	1.0	1.08	1.20	0.66[a]	0.78	0.79
	95% CI		0.92–1.27	0.94–1.54	0.50–0.88	0.58–1.06	0.40–1.58
	p-value		0.35	0.15	< 0.01	0.11	0.51
	Median survival[b] *n* (%)	13 342 (22%)	14 767 (50%)	10 139 (9%)	32 114 (7%)	20 76 (5%)	20 13 (1%)
SCLC $n = 281$	Risk of death (HR)	1.0	0.97	0.24[a]	0.00	0.42[a]	0.00
	95% CI		0.41–2.26	0.10–0.59	NA	0.25–0.73	NA
	p-value		0.94	0.002	0.99	0.002	0.98
	median survival[b]	4	7	15	12	15	15
	n (%)	229 (81%)	13 (5%)	21 (7%)	1 (0.4%)	16 (6%)	1 (0.4%)
Melanoma $n = 823$	Risk of death (HR)	1.0	0.69[a]	0.62[a]	0.50[a]	0.54[a]	0.70
	95% CI		0.54–0.89	0.45–0.86	0.36–0.69	0.35–0.84	0.36–1.36
	p-value		< 0.01	< 0.01	< 0.01	< 0.01	0.29
	median survival[b]	6	10	9	13	11	11
	n (%)	91 (11%)	464 (56%)	73 (9%)	95 (12%)	34 (4%)	12 (1%)
Renal cell $n = 286$	Risk of death (HR)	1.0	0.83	0.70	0.87	0.66	0.68
	95% CI		0.56–1.21	0.43–1.14	0.42–1.83	0.37–1.17	0.09–5.01
	p-value		0.33	0.15	0.71	0.16	0.70
	median survival[b]	5	11	12	13	16	9
	n (%)	78 (27%)	131 (46%)	46 (16%)	11 (4%)	18 (6%)	2 (1%)
Breast cancer $n = 400$	Risk of death (HR)	1.0	1.07	0.74	0.59	0.72	0.47[a]
	95% CI		0.66–1.73	0.47–1.16	0.28–1.23	0.43–1.21	0.23–0.96
	p-value		0.80	0.18	0.16	0.72	0.04
	median survival[b]	7	13	15	24	18	30
	n (%)	131 (33%)	115 (29%)	86 (22%)	19 (5%)	28 (7%)	20 (5%)
GI cancer $n = 209$	Risk of death (HR)	1.0	0.72	0.69	2.30	0.33[a]	0.39[a]
	95% CI		0.40–1.28	0.39–1.22	0.43–12.4	0.19–0.56	0.17–0.90
	p-value		0.26	0.21	0.33	< 0.001	0.03
	median survival[b]	3	7	7	9	10	8
	n (%)	95 (45%)	35 (17%)	35 (17%)	2 (1%)	34 (16%)	8 (4%)

Based on data from Ref. [13, 15, 17]
Diagnoses: *NSCLC* non-small cell lung cancer (adenocarcinoma), *SCLC* small cell lung cancer, *GI* gastrointestinal
Treatments: *S* surgery, *WBRT* whole brain radiation therapy, *SRS* stereotactic radiosurgery
Statistics: Risk of death: hazard ratio (HR) normalized to patients treated with whole brain radiation therapy alone (HR = 1.0) and calculated by multivariable Cox regression, adjusted for DS-GPA and stratified by institution
[a]Statistically significantly better than WBRT alone; 95% confidence interval
[b]Median survival in months based on one-sample Kaplan-Meier method

reminder that brain metastases are not uncommon in gastrointestinal (GI) cancer patients.

11. Clinicians may use the worksheet in Table 2 to calculate their patients' GPA score and estimate survival to guide therapeutic decisions.
12. Due to the inherent heterogeneity of the population of patients who present with brain tumors, the GPA is a useful tool for stratification in clinical trials.

Glioblastoma

Because RTOG 9305, a randomized trial of radiation therapy with and without a SRS boost showed no benefit with the addition of SRS [18], SRS is not routinely used for newly diagnosed patients with glioblastoma. There remain no randomized data showing SRS or fractionated stereotactic radiation therapy (FSRT) is of benefit as a boost to conventional radiation therapy (60 Gy in 30 fractions) which remains the current standard of care. For elderly patients or those with borderline performance status, hypofractionated radiotherapy has been shown to be efficacious and well-tolerated in this population [19].

In patients with recurrent glioblastoma, clinical trials of various radiation schedules have shown insufficient evidence to support one scheme over another [20]. SRS can be used as salvage therapy for small lesions with FSRT or hypofractionated (HF)-SRS for treatment of larger lesions.

Benign CNS Tumors

Vestibular Schwannomas

Patients with a vestibular schwannoma and significant mass effect should be referred for surgical resection. If the tumor is less than 3 cm in maximum dimension without significant mass effect, SRS with 13 Gy is the standard of care [21]. For larger lesions, FSRT (7 Gy × 3, 5 Gy × 5, or 2 Gy × 27) is routinely used. These schemes have demonstrated similar local control and preservation rates for hearing, facial, and trigeminal nerve function [20].

Meningiomas

Among patients with meningiomas involving the skull base, cavernous sinus, or petroclival region, SRS treatment with doses of 13 Gy results in local control rates of >90% at 10 years with a 7–8% complication rate [22, 23]. For meningiomas >10 cc or in close proximity to the optic apparatus, HF-SRS (7 Gy × 3 or 5 Gy × 5) and FSRT (2 Gy × 27) are excellent options [24].

Pituitary Adenomas

Surgery remains the standard of care for treatment of pituitary adenomas. For residual or recurrent non-secretory pituitary adenomas that are ≥5 mm from the optic nerves or chiasm, SRS (13 Gy) provides improved disease control with a favorable side-effect profile. For secretory adenomas, higher doses (24 Gy) are required but the plan must still comply with the dose constraints of the surrounding normal tissues as above. For residual or recurrent adenomas <5 mm from the optic nerves or chiasm, FSRT (1.8–2.0 Gy × 25) is more appropriate.

Patient Selection for Extracranial Stereotactic Body Radiotherapy

Lung SBRT

Primary Lung Cancer

Outside of clinical studies, surgery remains the current recommendation for medically operable early stage (T1-T2 N0 M0) non-small cell lung cancer (NSCLC) patients. In patients with early stage NSCLC, SBRT offers highly effective treatment that may be comparable to surgery [25]. Although small series of patients have been treated with SBRT in the past, it was not until the report of the prospective study at Indiana University by Timmerman and colleagues that promoted a rapid adoption of the technology [26]. There have been subsequent confirmations of the efficacy of SBRT by the RTOG and other investigators around the world [27–31]. As a result, SBRT has become the standard treatment for medically inoperable, stage I NSCLC mainly located in the periphery of the lung.

The three-fraction SBRT regimen as reported on RTOG 0236 remains the standard therapy for medically inoperable peripherally located stage I NSCLC measuring up to 5 cm in greatest diameter [27]. This treatment course consists of three 18 Gy fractions delivered over 1.5–2 weeks. This regimen has demonstrated excellent local disease control with a relatively favorable side effect profile with the treatment of small peripheral tumors [27]. In select cases, tumors >5 cm may be treated with SBRT provided the various normal tissue constraints can be satisfied [30]. A subset of patients will present with multiple primary lung tumors as primary tumors which can be addressed by SBRT, typically in a sequential fashion, after a careful consideration of the histology, staging, and potential toxicities [32].

Although effective in ablation of the peripheral lung tumors, SBRT delivered to central tumors has demonstrated significant toxicity [33]. The central tumors as defined in the Indiana University study include tumors within 2 cm of the proximal tracheobronchial tree. Toxicity concerns related to the delivery of ablative radiotherapy doses to the central structures include concern for damage to the esophagus, heart, bronchial tree, and the spinal cord. In this location, the three-fraction regimen should be avoided in favor of greater fractionation schemes.

Lung Metastases

Radiotherapy has also been utilized to treat metastatic lung cancers of varying histology. Although traditional radiotherapy for metastatic lung cancer has been reported in the past, it typically provides suboptimal control of many lung metastases [34]. Aggressive local therapy has shown promising outcomes in good performance status patients with a limited number of metastatic pulmonary lesions [35]. While surgery is typically the preferred modality for treatment of de novo early stage primary lung cancer, SBRT may be preferred over pulmonary metastasectomy due to the non-invasive nature and relatively favorable side effect profile of the former. When addressing multiple metastatic lesions, however, SBRT may severely compromise lung capacity and similar normal tissue constraints as used in primary lung cancer SBRT must be carefully considered. The quality of life of a patient following multiple SBRT treatments for metastatic lung cancer must be balanced against the desire to eradicate all visible disease.

SBRT has been successfully used in combination with targeted agents for patients with EGFR- or ALK-mutated NSCLC [36, 37]. Ablative doses of radiotherapy have additionally received heightened interest in many other solid tumors with respect to immune system activation and the abscopal effect [38–40]. It is likely that the use of SBRT in combination with targeted immunotherapy agents for patients with metastatic disease will continue to increase in prevalence.

GU Malignancies

Prostate

The rationale for SBRT in the treatment of low- to intermediate-risk prostate cancer comes from limited numbers of prospective studies and consortium data that took advantage of the perceived low α/β ratio in prostate cancer [41–45]. Prostate SBRT involves an abbreviated regimen of five or fewer fractions administered using image guidance and precise radiotherapy delivery techniques and can be delivered safely using any of several commercially available treatment systems. Treatment delivery may consist of multiple non-coplanar beams aimed at the target (prostate) or intensity-modulated radiation therapy (IMRT) delivery with static intensity-modulated beams or rotating modulated arcs.

The first prospective trial of SBRT for prostate cancer was reported by Madsen and colleagues [41], who treated 40 patients with SBRT using a daily dose of 6.7 Gy to a total dose of 33.5 Gy. The fractionation schedule was calculated to be equivalent to 78 Gy in 2 Gy fractions using an estimated α/β ratio of 1.5. A prospective SBRT study by King and colleagues administered slightly higher dose of 36.25 Gy in five daily fractions although with a change from daily fractionation to every-other-day treatment with a corresponding reduction in rates of severe rectal toxicities [42]. A multi-institutional prospective phase I–II study sponsored by the University of Texas Southwestern Medical Center (UTSW) administered up to 45–50 Gy in five fractions with a minimum interval of 36 hours between fractions [44]. A subsequent analysis of this trial revealed a correlation between rectal wall dosimetry and late grade 3+ rectal toxicity. The predictive factors for late rectal toxicity included 50 Gy delivered to >3 cc of the rectal wall and treatment of >35% circumference to 39 Gy, while acute grade 2+ rectal toxicity was correlated with treatment of >50% circumference of the rectal wall to 24 Gy [46]. Rectal balloons and injectable spacer gel can aid in reducing excess radiotherapy dose to the rectum and should be considered in patients undergoing prostate SBRT [47].

The results of the prospective trials have shown biochemical relapse-free survival rates of 84–100% for low- to intermediate-risk prostate cancer. In recognition of the accumulating evidence for SBRT in the management of localized prostate cancer, the National Comprehensive Cancer Network guidelines have listed prostate SBRT as an emerging alternative to conventionally fractionated regimens at clinics with appropriate expertise. Thus, patients eligible for SBRT include those with organ-confined, low- to intermediate-risk disease.

For patients with high-risk disease, there are currently not enough long-term data to justify the routine use of SBRT outside of the clinical trial setting. However, in light of the results from the ASCENDE-RT trial, which demonstrated a prostate-specific antigen (PSA) control benefit with low dose rate prostate brachytherapy following pelvic external beam radiotherapy (EBRT) [48], SBRT could potentially be similarly used as a focal boost in conjunction with EBRT. Ongoing clinical trials will help to further refine the role of prostate SBRT in this patient population. It is likely, though, that the use of prostate SBRT will increase in clinical practice as this regimen is convenient for patients, has a radiobiological rationale, and it is less costly than conventionally fractionated EBRT.

Renal Cell Carcinoma

Surgery remains the standard treatment of choice for operable patients with primary renal cell cancer (RCC). For patients with an anticipated high surgical morbidity, alternative therapies including SBRT can be considered. Beitler and colleagues first reported SBRT for primary renal cell cancer with a dose of 40 Gy in five fractions and noticed no local relapse with a median follow-up of 26.7 months [49]. Others have examined the efficacy of SBRT for both primary tumors and metastatic renal cell carcinomas [50–52] with some reporting successful treatment of large (>4 cm) primary tumors using SBRT [53–55]. Currently, there is no published prospective trial comparing SBRT to other minimally invasive forms of ablation including cryotherapy, microwave ablation, and radiofrequency ablation.

In the oligometastatic setting, SBRT can be utilized with potentially curative intent. In non-curative patients, SBRT has been shown to provide excellent local control as well as potentially induce an abscopal effect [39, 40]. Although anti-CTLA-4 and anti-PD-1 antibody have been shown to be effective with less toxicity than IL-2, the rate of the abscopal effect when combined with SBRT remains unclear and is the focus of active investigation.

There is a wide range of doses and fractionations that are used for SBRT in the treatment of renal cell carcinoma. The most commonly used regimen consists of 40 Gy delivered in 4–5 fractions with other regimens ranging from 25 Gy delivered in single fraction to 51 Gy in multiple fractions [51, 52, 54, 56]. The overall local control of the published results are >90% with approximately 4% grade ≥ 3 toxicity [57]. The most commonly observed acute toxicities after SBRT for primary renal cell carcinoma include nausea, fatigue, and bowel related discomfort. The rate of radiotherapy-induced renal failure requiring dialysis, however, is low [54].

Head and Neck Malignancies

Reirradiation

The treatment of locally recurrent disease or second primary malignancies poses a significant challenge in patients who have previously received full dose radiotherapy for head and neck cancers. Prior trials have shown that retreatment with conventionally fractionated chemoradiotherapy in this group of patients is feasible with encouraging rates of locoregional disease control [58, 59]. This therapy, though, is not without cost with many studies demonstrating high rates of associated toxicities. A

phase III multi-institutional trial from Institut Gustave-Roussy in which patients were randomized to observation versus chemoradiotherapy following salvage surgery revealed an approximately 30% rate of acute grade 3–4 mucositis/pharyngitis with 40% experiencing late grade 3–4 toxicities. Additionally, 5 of the 65 patients randomized to adjuvant chemoradiotherapy died from treatment-related complications (sepsis, 2; hemorrhage, 1; mucosal necrosis, 1; laryngeal edema, 1) [60].

Due to the concern for enhanced toxicity of head and neck structures following reirradiation with conventional doses and/or volumes, SBRT has emerged as a viable retreatment modality in select patients. There are several appealing aspects of SBRT for localized disease including the ability to deliver highly conformal ablative doses for enhanced tumor cell kill, a relatively compact treatment duration and, potentially, enhancement of the host immune response through combination of radiotherapy with immunotherapy agents [61]. Despite this, the routine use of SBRT for head and neck reirradiation remains largely limited to a small number of high-volume centers.

Ideal patients for head and neck SBRT are those with a small disease burden with either no or limited nodal metastases. Rwigema and colleagues demonstrated a strong correlation between tumor volume and local disease control following SBRT with 2-year locoregional control rates of 67% and 19% for tumor volumes $\leq$25 cm^3 and > 25 cm^3, respectively [62]. Tumor location is also a critical consideration in the selection of patients for head and neck SBRT. Several institutional trials have demonstrated generally acceptable toxicity profiles with the use of head and neck SBRT with low rates of grade 3+ toxicity [63–65]. A retrospective study by Ling and associates, though, revealed significantly increased severe late-term toxicity among patients receiving SBRT to the larynx or hypopharyngeal structures compared with other head and neck sites with 50% of these patients experiencing grade 3+ late toxicity [66]. Carotid blowout syndrome is an additional potentially fatal complication observed infrequently among patients receiving reirradiation with SBRT. Risk factors for carotid blowout have been shown to include >180° carotid invasion and irradiation of nodal regions [67]. For these patients, reirradiation with intensity-modulated radiation therapy (IMRT) using more protracted fractionation schemes may be a better option [68].

Primary Treatment

SBRT is infrequently utilized in the curative setting for treatment of de novo head and neck malignancies. Several small single-institutional trials have examined the efficacy of definitive SBRT in the treatment of early stage laryngeal cancer [69], as primary therapy in elderly patients with unresectable disease [70], and as a boost following conventional radiotherapy [71]. While these have demonstrated encouraging preliminary results, there is currently a lack of prospective data to justify the routine use of SBRT as primary treatment outside of the setting of a clinical trial.

GI Malignancies

Liver

Radiotherapy is an effective treatment for both primary and metastatic hepatic tumors. In the treatment of metastatic disease, patients felt to have the greatest potential benefit from liver-directed focal radiation are those with well-controlled systemic disease, three or fewer hepatic lesions, a tumor burden <6 cm in size, and a minimum distance of at least 1.5 cm to the luminal gastrointestinal organs [72]. In a cohort of heavily pretreated patient with primary and metastatic hepatic tumors, SBRT was shown to be generally effective and well-tolerated with caution advised for patients with Child-Pugh Class B with previous liver-directed therapy due to a potential increased risk of radiation-induced liver disease in this population [73]. For patients with large tumors that are otherwise not eligible for other local therapies, treatment with hypofractionated radiotherapy to high biological equivalent doses (BEDs) using SBRT techniques can be considered [74].

Pancreas

The routine use of conventional radiotherapy in the treatment of pancreatic cancer is controversial without a demonstrated survival benefit compared with modern chemotherapy regimens alone [75]. Local disease control, though, remains important with up to 30% of patients dying from locally destructive disease on an autopsy series from Johns Hopkins [76]. Given the lack of significant improvement with conventional doses/fractionation, interest has grown in the use of SBRT due to the ability to provide dose escalation with ablative regimens to small target volumes.

SBRT for treatment of locally advanced and recurrent pancreatic cancer has been shown to be safe and effective with low rates of severe toxicity [77–79]. Despite encouraging safety data, many commonly used regimens consisting of approximately 25–30 Gy delivered in five fractions have not resulted in substantially improved rates of disease control. Efforts to improve the efficacy of treatment include both the delivery of a large single fractions [80] and hypofractionated radiotherapy using SBRT techniques [81] in order to achieve ablative radiotherapy doses. The dose limiting structures for delivery of ablative therapy are predominantly the surrounding luminal organs, most notably the duodenum. The advent of novel devices, such as injectable hydrogel spacers [82], will likely enable the future treatment of those tumors previously not amenable to SBRT due to proximity of the surrounding organs.

Spine Metastases

It is hypothesized that the prevalence of spinal metastases will continue to rise with improvements in chemotherapy and targeted agents resulting in better systemic disease con-

trol. Conventional radiotherapy is commonly used in patients who present with spinal disease and has been shown to be efficacious in alleviating pain and preventing complications from local disease progression [83]. A drawback, though, with conventional radiotherapy approaches lies in the limited dose that can be delivered to the tumor due to spinal cord constraints. This further limits subsequent treatment options with standard fractionation therapy in the event of a local treatment failure. Recent advances in image-guided therapy, patient immobilization, and treatment delivery have enabled the use of SBRT to provide a mechanism by which high ablative doses are delivered to the tumor with a steep dose gradients to minimize radiation-induced toxicity to the surrounding organs at risk, namely the spinal cord [84].

The best candidates for spine SBRT/SRS are those with oligometastatic disease in which durable local control would provide maximal benefit. Conversely, those with tumors causing acute neurologic compromise should be treated with upfront surgery, while those with poorly controlled systemic disease burden or limited life expectancy may be better served with short-course conventional palliative radiotherapy treatment. The neurologic, oncologic, mechanical, and systemic (NOMS) framework has been designed by Memorial Sloan Kettering Cancer Center to aide in decision-making regarding optimal treatment modality for patients with spine metastases [85]. Using this paradigm, patients felt to be most appropriate for ablative radiotherapy regimens are those with limited spinal cord compromise, radioresistant tumors, no evidence of spinal instability, good performance status, and limited systemic disease burden [84]. For patients without prior radiotherapy who are candidates for SRS/SBRT, single-fraction regimens have demonstrated excellent responses in pain improvement and local disease control. For patients with prior radiotherapy to the spine or tumors near critical structures, such as the cord, three- to five-fraction SBRT regimens have been shown to be safe and effective [84].

Conclusions

Advances in imaging, patient immobilization and treatment planning systems have helped to produce a dramatic growth in the adoption of SBRT and SRS techniques over the past decade. Today, many of these modalities are widely considered part of the routine clinical practice in numerous radiation therapy centers across the country and it is anticipated that their use will continue to increase in prevalence in the foreseeable future. The veritable explosion in the utilization of SBRT/SRS has made patient selection of paramount importance, namely in identifying those individuals who would derive the maximal benefit from focal ablative therapies. This chapter has described current considerations in the patient selection process based upon the best available evidence with further refinements to be guided by ongoing and future clinical trials.

Practical Considerations

Metastatic CNS Disease

- The GPA is a useful prognostic tool to estimate survival for patients with brain metastases. This can guide clinical decision-making as patients and their physicians contemplate aggressive versus less aggressive treatment versus supportive care.
- The GPA can be used to stratify future clinical trials and to better interpret past trials.
- Patient eligibility for treatment with SRS is rapidly expanding and patients with more than three metastases or those with extracranial disease should not be routinely denied therapy.

Primary and Benign CNS Tumors

- There is currently no evidence to support the routine use of upfront SRS in the treatment of primary gliomas although SRS may be considered for salvage therapy for small recurrent lesions.
- For benign CNS tumors not amenable to surgical resection, SRS remains an attractive treatment option with a favorable toxicity profile and excellent rates of disease control.

Primary and Metastatic Lung Cancer

- The three-fraction SBRT regimen as reported on RTOG 0236 remains the standard therapy for medically inoperable peripherally located stage I NSCLC measuring up to 5 cm in greatest diameter.
- In central location, the three-fraction regimen should be avoided in favor of greater fractionation schemes.
- SBRT may be preferred over pulmonary metastasectomy due to the non-invasive nature and relatively favorable side effect profile.

GU (Prostate and Renal)

- Patients eligible for prostate SBRT alone include those with organ-confined, low- to intermediate-risk disease. For those with high-risk disease, SBRT could potentially be used as a focal boost in conjunction with EBRT.
- Surgery remains the standard of care for operable patients with renal cell carcinoma although SBRT has been shown

to provide acceptable rates of local control for both primary and metastatic tumors.

Head and Neck

- There is currently a lack of prospective data to justify the use of SBRT/SRS for upfront treatment of head and neck malignancies outside the clinical trial setting. In the salvage setting, SBRT has been shown to be efficacious with a relatively favorable side effect profile in patients with localized, unresectable disease.

GI (Pancreas and Liver)

- Patients with hepatic tumors most likely to benefit from SBRT regimens are those with well-controlled systemic disease, limited intrahepatic tumor burden located adequate distances from the luminal gastrointestinal organs.
- Commonly used low-dose (25–30 Gy/5 fx) SBRT regimens for treatment of localized pancreatic cancer are well-tolerated with low rates of toxicity although the optimal dose/fractionation regimen for more robust local disease control remains under active investigation.

Spine Metastases

- Spine SRS/SBRT can provide excellent rates of local disease control while maintaining a low incidence of severe toxicity to the spinal cord in both the de novo and reirradiation setting.
- Use of a standardized decision-making template, such as the MSKCC NOMS framework, provides a useful tool in the selection of those patients who would most likely benefit from spine SRS/SBRT.

References

1. Pan HY, Jiang J, Shih Y-CT, Smith BD. Adoption of radiation technology among privately insured nonelderly patients with cancer in the United States, 2008 to 2014: a claims-based analysis. J Am Coll Radiol. 2017;14(8):1027–1033.e2.
2. Gavrilovic IT, Posner JB. Brain metastases: epidemiology and pathophysiology. J Neurooncol. 2005;75(1):5–14.
3. Park DM, Posner JB. Management of intracranial metastases: history. In: Sawaya R, editor. Intracranial metastases: current management strategies. Oxford, England: Blackwell Publishing Ltd; 2004. p. 3–19.
4. Aoyama H, Shirato H, Tago M, Nakagawa K, Toyoda T, Hatano K, et al. Stereotactic radiosurgery plus whole-brain radiation therapy vs stereotactic radiosurgery alone for treatment of brain metastases. JAMA. 2006;295(21):2483.
5. Chang EL, Wefel JS, Hess KR, Allen PK, Lang FF, Kornguth DG, et al. Neurocognition in patients with brain metastases treated with radiosurgery or radiosurgery plus whole-brain irradiation: a randomised controlled trial. Lancet Oncol. 2009;10(11):1037–44.
6. Kocher M, Soffietti R, Abacioglu U, Villà S, Fauchon F, Baumert BG, et al. Adjuvant whole-brain radiotherapy versus observation after radiosurgery or surgical resection of one to three cerebral metastases: results of the EORTC 22952–26001 study. J Clin Oncol. 2011;29(2):134–41.
7. Brown PD, Jaeckle K, Ballman KV, Farace E, Cerhan JH, Anderson SK, et al. Effect of radiosurgery alone vs radiosurgery with whole brain radiation therapy on cognitive function in patients with 1 to 3 brain metastases. JAMA. 2016;316(4):401.
8. Mulvenna P, Nankivell M, Barton R, Faivre-Finn C, Wilson P, McColl E, et al. Dexamethasone and supportive care with or without whole brain radiotherapy in treating patients with non-small cell lung cancer with brain metastases unsuitable for resection or stereotactic radiotherapy (QUARTZ): results from a phase 3, non-inferiority. Lancet. 2016;388(10055):2004–14.
9. Gaspar L, Scott C, Rotman M, Asbell S, Phillips T, Wasserman T, et al. Recursive partitioning analysis (RPA) of prognostic factors in three radiation therapy oncology group (RTOG) brain metastases trials. Int J Radiat Oncol. 1997;37(4):745–51.
10. Sperduto PW, Berkey B, Gaspar LE, Mehta M, Curran W. A new prognostic index and comparison to three other indices for patients with brain metastases: an analysis of 1,960 patients in the RTOG database. Int J Radiat Oncol. 2008;70(2):510–4.
11. Sperduto PW, Chao ST, Sneed PK, Luo X, Suh J, Roberge D, et al. Diagnosis-specific prognostic factors, indexes, and treatment outcomes for patients with newly diagnosed brain metastases: a multi-institutional analysis of 4,259 patients. Int J Radiat Oncol. 2010;77(3):655–61.
12. Sperduto PW, Kased N, Roberge D, Xu Z, Shanley R, Luo X, et al. Effect of tumor subtype on survival and the graded prognostic assessment for patients with breast cancer and brain metastases. Int J Radiat Oncol. 2012;82(5):2111–7.
13. Sperduto PW, Kased N, Roberge D, Xu Z, Shanley R, Luo X, et al. Summary report on the graded prognostic assessment: an accurate and facile diagnosis-specific tool to estimate survival for patients with brain metastases. J Clin Oncol. 2012;30(4):419–25.
14. Sperduto PW, Yang TJ, Beal K, Pan H, Brown PD, Bangdiwala A, et al. The effect of gene alterations and tyrosine kinase inhibition on survival and cause of death in patients with adenocarcinoma of the lung and brain metastases. Int J Radiat Oncol. 2016;96(2):406–13.
15. Sperduto PW, Yang TJ, Beal K, Pan H, Brown PD, Bangdiwala A, et al. Estimating survival in patients with lung cancer and brain metastases. JAMA Oncol. 2017;3(6):827.
16. Sperduto PW, Jiang W, Brown PD, Braunstein S, Sneed P, Wattson DA, et al. The prognostic value of BRAF, C-KIT, and NRAS mutations in melanoma patients with brain metastases. Int J Radiat Oncol. 2017;98(5):1069–77.
17. Sperduto PW, Jiang W, Brown PD, Braunstein S, Sneed P, Wattson DA, et al. Estimating survival in melanoma patients with brain metastases: an update of the graded prognostic assessment for melanoma using molecular markers (melanoma-molGPA). Int J Radiat Oncol. 2017;99(4):812–6.
18. Souhami L, Seiferheld W, Brachman D, Podgorsak EB, Werner-Wasik M, Lustig R, et al. Randomized comparison of stereotactic radiosurgery followed by conventional radiotherapy with carmustine to conventional radiotherapy with carmustine for patients with glioblastoma multiforme: Report of Radiation Therapy Oncology Group 93–05 protocol. Int J Radiat Oncol. 2004;60(3):853–60.
19. Minniti G, Lanzetta G, Scaringi C, Caporello P, Salvati M, Arcella A, et al. Phase II study of short-course radiotherapy plus concomi-

tant and adjuvant temozolomide in elderly patients with glioblastoma. Int J Radiat Oncol. 2012;83(1):93–9.
20. Kirkpatrick JP, Soltys SG, Lo SS, Beal K, Shrieve DC, Brown PD. The radiosurgery fractionation quandary: single fraction or hypofractionation? Neuro Oncol. 2017;19(suppl_2):ii38–49.
21. Kondziolka D, Lunsford LD, McLaughlin MR, Flickinger JC. Long-term outcomes after radiosurgery for acoustic neuromas. N Engl J Med. 1998;339(20):1426–33.
22. Flannery TJ, Kano H, Lunsford LD, Sirin S, Tormenti M, Niranjan A, et al. Long-term control of petroclival meningiomas through radiosurgery. J Neurosurg. 2010;112(5):957–64.
23. Lee JYK, Niranjan A, McInerney J, Kondziolka D, Flickinger JC, Lunsford LD. Stereotactic radiosurgery providing long-term tumor control of cavernous sinus meningiomas. J Neurosurg. 2002;97(1):65–72.
24. Heron D, Burton S, Bria C, Wegner R, Clump D, Vargo J, et al. Fractionated stereotactic radiosurgery for the treatment of meningiomas. J Cancer Res Ther. 2011;7(1):52.
25. Chang JY, Senan S, Paul MA, Mehran RJ, Louie AV, Balter P, et al. Stereotactic ablative radiotherapy versus lobectomy for operable stage I non-small-cell lung cancer: a pooled analysis of two randomised trials. Lancet Oncol. 2015;16(6):630–7.
26. Timmerman R, Papiez L, McGarry R, Likes L, DesRosiers C, Frost S, et al. Extracranial stereotactic radioablation: results of a phase I study in medically inoperable stage I non-small cell lung cancer. Chest. 2003;124(5):1946–55.
27. Timmerman R, Paulus R, Galvin J, Michalski J, Straube W, Bradley J, et al. Stereotactic body radiation therapy for inoperable early stage lung cancer. JAMA. 2010;303(11):1070.
28. Baumann P, Nyman J, Hoyer M, Wennberg B, Gagliardi G, Lax I, et al. Outcome in a prospective phase II trial of medically inoperable stage i non–small-cell lung cancer patients treated with stereotactic body radiotherapy. J Clin Oncol. 2009;27(20):3290–6.
29. Nagata Y, Hiraoka M, Shibata T, Onishi H, Kokubo M, Karasawa K, et al. Prospective trial of stereotactic body radiation therapy for both operable and inoperable T1N0M0 non-small cell lung cancer: japan clinical oncology group study JCOG0403. Int J Radiat Oncol. 2015;93(5):989–96.
30. Woody NM, Stephans KL, Marwaha G, Djemil T, Videtic GMM. Stereotactic body radiation therapy for non-small cell lung cancer tumors greater than 5 cm: safety and efficacy. Int J Radiat Oncol. 2015;92(2):325–31.
31. Nyman J, Hallqvist A, Lund J-Å, Brustugun O-T, Bergman B, Bergström P, et al. SPACE – a randomized study of SBRT vs conventional fractionated radiotherapy in medically inoperable stage I NSCLC. Radiother Oncol. 2016;121(1):1–8.
32. Videtic GMM, Donington J, Giuliani M, Heinzerling J, Karas TZ, Kelsey CR, et al. Stereotactic body radiation therapy for early-stage non-small cell lung cancer: Executive Summary of an ASTRO Evidence-Based Guideline. Pract Radiat Oncol. 2017;7(5):295–301.
33. Timmerman R, McGarry R, Yiannoutsos C, Papiez L, Tudor K, DeLuca J, et al. Excessive toxicity when treating central tumors in a phase II study of stereotactic body radiation therapy for medically inoperable early-stage lung cancer. J Clin Oncol. 2006;24(30):4833–9.
34. Turnbull AD, Pool JL, Arthur K, Golbey RB. The role of radiotherapy and chemotherapy in the surgical management of pulmonary metastases. Am J Roentgenol Radium Ther Nucl Med. 1972;114(1):99–105.
35. Pastorino U, Buyse M, Friedel G, Ginsberg RJ, Girard P, Goldstraw P, et al. Long-term results of lung metastasectomy: prognostic analyses based on 5206 cases. J Thorac Cardiovasc Surg. 1997;113(1):37–49.
36. Iyengar P, Kavanagh BD, Wardak Z, Smith I, Ahn C, Gerber DE, et al. Phase II trial of stereotactic body radiation therapy combined with erlotinib for patients with limited but progressive metastatic non–small-cell lung cancer. J Clin Oncol. 2014;32(34):3824–30.
37. Gan GN, Weickhardt AJ, Scheier B, Doebele RC, Gaspar LE, Kavanagh BD, et al. Stereotactic radiation therapy can safely and durably control sites of extra-central nervous system oligoprogressive disease in anaplastic lymphoma kinase-positive lung cancer patients receiving crizotinib. Int J Radiat Oncol. 2014;88(4):892–8.
38. Golden EB, Chhabra A, Chachoua A, Adams S, Donach M, Fenton-Kerimian M, et al. Local radiotherapy and granulocyte-macrophage colony-stimulating factor to generate abscopal responses in patients with metastatic solid tumours: a proof-of-principle trial. Lancet Oncol. 2015;16(7):795–803.
39. Wersäll PJ, Blomgren H, Pisa P, Lax I, Kälkner K-M, Svedman C. Regression of non-irradiated metastases after extracranial stereotactic radiotherapy in metastatic renal cell carcinoma. Acta Oncol (Madr). 2006;45(4):493–7.
40. Ishiyama H, Teh BS, Ren H, Chiang S, Tann A, Blanco AI, et al. Spontaneous regression of thoracic metastases while progression of brain metastases after stereotactic radiosurgery and stereotactic body radiotherapy for metastatic renal cell carcinoma: abscopal effect prevented by the blood-brain barrier? Clin Genitourin Cancer. 2012;10(3):196–8.
41. Madsen BL, Hsi RA, Pham HT, Fowler JF, Esagui L, Corman J. Stereotactic hypofractionated accurate radiotherapy of the prostate (SHARP), 33.5 Gy in five fractions for localized disease: First clinical trial results. Int J Radiat Oncol. 2007;67(4):1099–105.
42. King CR, Brooks JD, Gill H, Pawlicki T, Cotrutz C, Presti JC. Stereotactic body radiotherapy for localized prostate cancer: interim results of a prospective phase II clinical trial. Int J Radiat Oncol. 2009;73(4):1043–8.
43. King CR, Brooks JD, Gill H, Presti JC. long-term outcomes from a prospective trial of stereotactic body radiotherapy for low-risk prostate cancer. Int J Radiat Oncol. 2012;82(2):877–82.
44. Boike TP, Lotan Y, Cho LC, Brindle J, DeRose P, Xie X-J, et al. Phase I dose-escalation study of stereotactic body radiation therapy for low- and intermediate-risk prostate cancer. J Clin Oncol. 2011;29(15):2020–6.
45. King CR, Freeman D, Kaplan I, Fuller D, Bolzicco G, Collins S, et al. Stereotactic body radiotherapy for localized prostate cancer: pooled analysis from a multi-institutional consortium of prospective phase II trials. Radiother Oncol. 2013;109(2):217–21.
46. Kim DWN, Cho LC, Straka C, Christie A, Lotan Y, Pistenmaa D, et al. Predictors of rectal tolerance observed in a dose-escalated phase 1–2 trial of stereotactic body radiation therapy for prostate cancer. Int J Radiat Oncol. 2014;89(3):509–17.
47. Jones RT, Hassan Rezaeian N, Desai NB, Lotan Y, Jia X, Hannan R, et al. Dosimetric comparison of rectal-sparing capabilities of rectal balloon vs injectable spacer gel in stereotactic body radiation therapy for prostate cancer: lessons learned from prospective trials. Med Dosim. 2017;42(4):341–7.
48. Rodda S, Tyldesley S, Morris WJ, Keyes M, Halperin R, Pai H, et al. ASCENDE-RT: an analysis of treatment-related morbidity for a randomized trial comparing a low-dose-rate brachytherapy boost with a dose-escalated external beam boost for high- and intermediate-risk prostate cancer. Int J Radiat Oncol. 2017;98(2):286–95.
49. Beitler JJ, Makara D, Silverman P, Lederman G. Definitive, high-dose-per-fraction, conformal, stereotactic external radiation for renal cell carcinoma. Am J Clin Oncol. 2004;27(6):646–8.
50. Teh B, Bloch C, Galli-Guevara M, Doh L, Richardson S, Chiang S, et al. The treatment of primary and metastatic renal cell carcinoma (RCC) with image-guided stereotactic body radiation therapy (SBRT). Biomed Imaging Interv J. 2007;3(1):e6.
51. Svedman C, Sandström P, Pisa P, Blomgren H, Lax I, Kälkner K-M, et al. A prospective Phase II trial of using extracranial stereotactic radiotherapy in primary and metastatic renal cell carcinoma. Acta Oncol (Madr). 2006;45(7):870–5.
52. Wersäll PJ, Blomgren H, Lax I, Kälkner K-M, Linder C, Lundell G, et al. Extracranial stereotactic radiotherapy for primary and metastatic renal cell carcinoma. Radiother Oncol. 2005;77(1):88–95.

53. Siva S, Ellis RJ, Ponsky L, Teh BS, Mahadevan A, Muacevic A, et al. Consensus statement from the International Radiosurgery Oncology Consortium for Kidney for primary renal cell carcinoma. Future Oncol. 2016;12(5):637–45.
54. Siva S, Pham D, Kron T, Bressel M, Lam J, Tan TH, et al. Stereotactic ablative body radiotherapy for inoperable primary kidney cancer: a prospective clinical trial. BJU Int. 2017;120(5):623–30.
55. Kaidar-Person O, Price A, Schreiber E, Zagar TM, Chen RC. Stereotactic body radiotherapy for large primary renal cell carcinoma. Clin Genitourin Cancer. 2017;15(5):e851–4.
56. Staehler M, Bader M, Schlenker B, Casuscelli J, Karl A, Roosen A, et al. Single fraction radiosurgery for the treatment of renal tumors. J Urol. 2015;193(3):771–5.
57. Siva S, Pham D, Gill S, Corcoran NM, Foroudi F. A systematic review of stereotactic radiotherapy ablation for primary renal cell carcinoma. BJU Int. 2012;110(11b):E737–43.
58. Spencer SA, Harris J, Wheeler RH, Machtay M, Schultz C, Spanos W, et al. RTOG 96–10: Reirradiation with concurrent hydroxyurea and 5-fluorouracil in patients with squamous cell cancer of the head and neck. Int J Radiat Oncol Biol Phys. 2001;51(5):1299–304.
59. Langer CJ, Harris J, Horwitz EM, Nicolaou N, Kies M, Curran W, et al. Phase II study of low-dose paclitaxel and cisplatin in combination with split-course concomitant twice-daily reirradiation in recurrent squamous cell carcinoma of the head and neck: Results of Radiation Therapy Oncology Group protocol 9911. J Clin Oncol. 2007;25(30):4800–5.
60. Janot F, De Raucourt D, Benhamou E, Ferron C, Dolivet G, Bensadoun RJ, et al. Randomized trial of postoperative reirradiation combined with chemotherapy after salvage surgery compared with salvage surgery alone in head and neck carcinoma. J Clin Oncol. 2008;26(34):5518–23.
61. Baliga S, Kabarriti R, Ohri N, Haynes-Lewis H, Yaparpalvi R, Kalnicki S, et al. Stereotactic body radiotherapy for recurrent head and neck cancer: a critical review. Eisele DW, editor. Head Neck. 2017;39(3):595–601.
62. Rwigema J-CM, Heron DE, Ferris RL, Andrade RS, Gibson MK, Yang Y, et al. The impact of tumor volume and radiotherapy dose on outcome in previously irradiated recurrent squamous cell carcinoma of the head and neck treated with stereotactic body radiation therapy. Am J Clin Oncol. 2011;34(4):372–9.
63. Kress M-AS, Sen N, Unger KR, Lominska CE, Deeken JF, Davidson BJ, et al. Safety and efficacy of hypofractionated stereotactic body reirradiation in head and neck cancer: Long-term follow-up of a large series. Head Neck. 2015;37(10):1403–9.
64. Vargo JA, Kubicek GJ, Ferris RL, Duvvuri U, Johnson JT, Ohr J, et al. Adjuvant stereotactic body radiotherapy +/− cetuximab following salvage surgery in previously irradiated head and neck cancer. Laryngoscope. 2014;124(7):1579–84.
65. Vargo JA, Ferris RL, Ohr J, Clump DA, Davis KS, Duvvuri U, et al. A prospective phase 2 trial of reirradiation with stereotactic body radiation therapy plus cetuximab in patients with previously irradiated recurrent squamous cell carcinoma of the head and neck. Int J Radiat Oncol Biol Phys. 2015;91(3):480–8.
66. Ling DC, Vargo JA, Ferris RL, Ohr J, Clump DA, Yau WYW, et al. Risk of severe toxicity according to site of recurrence in patients treated with stereotactic body radiation therapy for recurrent head and neck cancer. Int J Radiat Oncol Biol Phys. 2016;95(3):973–80.
67. Yamazaki H, Ogita M, Himei K, Nakamura S, Kotsuma T, Yoshida K, et al. Carotid blowout syndrome in pharyngeal cancer patients treated by hypofractionated stereotactic re-irradiation using CyberKnife: a multi-institutional matched-cohort analysis. Radiother Oncol. 2015;115(1):67–71.
68. Vargo JA, Ward MC, Caudell JJ, Riaz N, Dunlap NE, Isrow D, et al. A multi-institutional comparison of SBRT and IMRT for definitive reirradiation of recurrent or second primary head and neck cancer. Int J Radiat Oncol Biol Phys. 2018;100(3):595–605.
69. Schwartz DL, Sosa A, Chun SG, Ding C, Xie XJ, Nedzi LA, et al. SBRT for early-stage glottic larynx cancer-Initial clinical outcomes from a phase i clinical trial. PLoS One. 2017;12(3):1–10.
70. Vargo JA, Ferris RL, Clump DA, Heron DE. Stereotactic body radiotherapy as primary treatment for elderly patients with medically inoperable head and neck cancer. Front Oncol. 2014;4(August):214.
71. Lee D, Kim Y, Cheon J, Song J, Son S, Jang J, et al. Long-term outcome and toxicity of hypofractionated stereotactic body radiotherapy as a boost treatment for head and neck cancer: the importance of boost volume assessment. Radiat Oncol. 2012;7(1):85.
72. Schefter TE, Kavanagh BD. Radiation therapy for liver metastases. Semin Radiat Oncol. 2011;21(4):264–70.
73. Liu E, Stenmark MH, Schipper MJ, Balter JM, Kessler ML, Caoili EM, et al. Stereotactic body radiation therapy for primary and metastatic liver tumors. Transl Oncol. 2013;6(4):442–6.
74. Crane CH, Koay EJ. Solutions that enable ablative radiotherapy for large liver tumors: Fractionated dose painting, simultaneous integrated protection, motion management, and computed tomography image guidance. Cancer. 2016;122(13):1974–86.
75. Hammel P, Huguet F, van Laethem J-L, Goldstein D, Glimelius B, Artru P, et al. Effect of chemoradiotherapy vs chemotherapy on survival in patients with locally advanced pancreatic cancer controlled after 4 months of gemcitabine with or without erlotinib. JAMA. 2016;315(17):1844.
76. Iacobuzio-Donahue CA, Fu B, Yachida S, Luo M, Abe H, Henderson CM, et al. DPC4 gene status of the primary carcinoma correlates with patterns of failure in patients with pancreatic cancer. J Clin Oncol. 2009;27(11):1806–13.
77. Ryan JF, Groot VP, Rosati LM, Hacker-Prietz A, Narang AK, McNutt TR, et al. Stereotactic body radiation therapy for isolated local recurrence after surgical resection of pancreatic ductal adenocarcinoma appears to be safe and effective. Ann Surg Oncol. 2018;25(1):280–9.
78. Rao AD, Sugar EA, Chang DT, Goodman KA, Hacker-Prietz A, Rosati LM, et al. Patient-reported outcomes of a multicenter phase 2 study investigating gemcitabine and stereotactic body radiation therapy in locally advanced pancreatic cancer. Pract Radiat Oncol. 2016;6(6):417–24.
79. Zhong J, Patel K, Switchenko J, Cassidy RJ, Hall WA, Gillespie T, et al. Outcomes for patients with locally advanced pancreatic adenocarcinoma treated with stereotactic body radiation therapy versus conventionally fractionated radiation. Cancer. 2017;123(18):3486–93.
80. Chang DT, Schellenberg D, Shen J, Kim J, Goodman KA, Fisher GA, et al. Stereotactic radiotherapy for unresectable adenocarcinoma of the pancreas. Cancer. 2009;115(3):665–72.
81. Krishnan S, Chadha AS, Suh Y, Chen H-C, Rao A, Das P, et al. Focal radiation therapy dose escalation improves overall survival in locally advanced pancreatic cancer patients receiving induction chemotherapy and consolidative chemoradiation. Int J Radiat Oncol. 2016;94(4):755–65.
82. Rao AD, Feng Z, Shin EJ, He J, Waters KM, Coquia S, et al. A novel absorbable radiopaque hydrogel spacer to separate the head of the pancreas and duodenum in radiation therapy for pancreatic cancer. Int J Radiat Oncol. 2017;99(5):1111–20.
83. Bates T. A review of local radiotherapy in the treatment of bone metastases and cord compression. Int J Radiat Oncol. 1992;23(1):217–21.
84. Katsoulakis E, Kumar K, Laufer I, Yamada Y. Stereotactic body radiotherapy in the treatment of spinal metastases. Semin Radiat Oncol. 2017;27(3):209–17.
85. Laufer I, Rubin DG, Lis E, Cox BW, Stubblefield MD, Yamada Y, et al. The NOMS framework: approach to the treatment of spinal metastatic tumors. Oncologist. 2013;18(6):744–51.

SRS and SBRT Complications and Management

Samuel T. Chao, Erin S. Murphy, Simon S. Lo, and John H. Suh

Introduction

By definition, stereotactic radiosurgery (SRS) and stereotactic body radiation therapy (SBRT) or stereotactic ablative radiotherapy (SABR) deliver relatively high-dose radiation in five fractions or less using a conformal approach that best minimizes dose to the surrounding normal tissue. This technique has shown to be efficacious in the management of both malignant and benign tumors, and has been used to treat benign diseases such as trigeminal neuralgia, arteriovenous malformations, and tremors. The success of this technique is thought to be due to the radiobiology of the high doses and limited fractions/sessions used which was reviewed earlier in this book. As technologies have improved, the simplification of the delivery process and the improvement in accuracy and precision have made it safer for more practitioners to deliver SRS and SBRT.

Minimizing dose to the normal tissue is critical in reducing the risk for complications. Despite this, our understanding of tolerance doses to various organs-at-risk (OAR) is rather limited, particularly with higher dose per fraction which makes management of complications important. This chapter reviews the general and more concerning complications seen with SRS and SBRT/SABR, and its management. The more nuanced toxicities were reviewed under each indication in this textbook.

S. T. Chao (✉) · E. S. Murphy · J. H. Suh
Department of Radiation Oncology, Cleveland Clinic, Cleveland, OH, USA

Rose Ella Burkhardt Brain Tumor and Neuro-Oncology Center, Cleveland Clinic, Cleveland, OH, USA
e-mail: chaos@ccf.org

S. S. Lo
University of Washington Medical Center, Department of Radiation Oncology, Seattle, WA, USA

University of Washington School of Medicine, Department of Radiation Oncology, Seattle, WA, USA

Site-specific Considerations/Clinical Evidence

Stereotactic Radiosurgery

Radiation Necrosis

Radiation necrosis is a late complication in the brain from SRS. With greater use of SRS, the incidence of radiation necrosis is increasing. Radiation necrosis develops in 7–24% of patients undergoing SRS, depending on the diagnostic criteria used [1, 2]. Vascular injury appears to be the biggest driver for radiation necrosis. This appears to result in an increase in VEGF expression, generated by surrounding astrocytes in the perinecrotic tissue [3, 4]. Uncontrolled VEGF results in leaky blood vessels and edema which is thought to drive the pathophysiology of radiation necrosis.

Risk factors include dose, fraction size, treatment duration, and volume treated [5]. The Radiation Therapy Oncology Group 90-05 study provided the maximum tolerated dose (MTD) to limit Grade 3-5 toxicity to less than 20%, with dose limitations based on maximum tumor diameter for recurrent brain metastases and gliomas [6]. Although the MTD was not reached for the 2 cm or less cohort, 24 Gy was the recommended dose for these patients. For a tumor diameter of 2.1–3 cm, 18 Gy was the MTD, and for a tumor diameter of 3.1–4 cm, 15 Gy was the MTD. The ratio of the maximum dose and the prescribed dose, known as dose homogeneity, and the ratio of the prescription isodose volume and the tumor volume, known as conformity index, also predicted for toxicity. These ratios should ideally be kept to two or less, unless the tumor volume is small.

Since the diagnosis of radiation necrosis is difficult, arteriovenous malformation is an easy model to use as any increase in enhancement and/or edema is likely radiation necrosis. Using this model, Flickinger and colleagues showed that the 12 Gy volume and location predicted for radiation necrosis [7]. Subsequently, other studies have consistently demonstrated that 10 cc or more receiving at least

D. M. Trifiletti et al. (eds.), *Stereotactic Radiosurgery and Stereotactic Body Radiation Therapy*,
https://doi.org/10.1007/978-3-030-16924-4_30

10–12 Gy increased the risk up to 50% [2, 8, 9]. It appears that other risk factors include tumor biomarkers, particularly Her2 amplified breast cancer, BRAF wild-type melanoma, and adenocarcinoma non-small cell lung cancer, specifically ALK positive non-small cell lung cancer [10]. Concurrent therapy had historically been avoided because of its concern about increasing the risk of neurological toxicity and radiation necrosis. However, a couple of studies have debunked this. Shen and coworkers evaluated 291 patients and found there was no difference in the risk of radiation necrosis when concurrent systemic therapy was given [11]. In fact, there was better survival in those receiving early systemic therapy along with their SRS versus SRS alone (41.6 months compared to 21.5 months, $p < 0.05$). Similarly, Kim and coworkers evaluated 445 patients who received concurrent systemic therapy along with their SRS. Like Shen and coworkers, there was no difference in the risk of radiation necrosis in those receiving concurrent systemic therapy versus those who did not (6.6 versus 5.3%, $p = 0.14$) [12]. However, there did appear to be an increased risk of radiation necrosis in patients who received whole-brain radiation therapy (WBRT) along with their upfront SRS. Particularly in those receiving WBRT, concurrent vascular endothelial growth factor (VEGF) tyrosine kinase inhibitors (TKIs) and epidermal growth factor receptor (EGFR) TKIs appear to increase the risk of radiation necrosis. Immunotherapy appears to increase the risk of radiation necrosis as well to almost 40% [13–15].

Diagnosis can be complicated as radiation necrosis is typically characterized by increasing contrast enhancement and edema, which is also seen with tumor progression [5]. This makes standard CT and MRI sequences insufficient in distinguishing between the two. Figure 1a–c is MRI of radiation necrosis that was later treated with laser interstitial thermal therapy. While efforts have been made to use standard MRI sequences to diagnose radiation necrosis, such as lesion quotient [16–18], special MRI sequences, such as perfusion or cerebral blood volume (CBV), appear to be more accurate. CBV has sensitivity of 100% and specificity of 95.2%, making it a useful tool to diagnose radiation necrosis [19].

Another common and ubiquitous imaging modality is fluorodeoxyglucose (FDG) positron emission tomography (PET). As would be expected, there would be more FDG uptake in tumor given its increased metabolism, but decreased uptake in necrosis given lack of viable cells. One issue with FDG PET is the fact that there is no standard way to report PET. Also, some benign tumors and other targets of radiosurgery may not take up FDG. Furthermore, inflammatory cells that may be seen with necrosis may take up FDG. As such, although some studies report reasonable sensitivity and specificity in the 80% range [20], other studies show this modality to have poor sensitivity or poor specificity [5]. Since PET is available at most institutions, it is often used as the primary modality outside of MRI. Amino acid PET shows promise with good accuracy, but remains investigational [21].

Magnetic resonance spectroscopy (MRS) is a promising technique, but requires increased imaging time to obtain. Some studies show this technique to be highly sensitive and specific, and in one study using multivoxel MRS, the sensitivity and specificity were both 100% [22]. A meta-analysis shows fairly good sensitivity and specificity, but perhaps not much better than CBV [23]. In general, MRS is still considered investigational, but can be considered if other imaging modalities are equivocal in diagnosing or ruling out radiation necrosis.

Treatment can include observation for asymptomatic radiation necrosis and steroids for symptomatic radiation necrosis. Surgery is typically reserved for steroid refractory radiation necrosis. Pentoxifylline and vitamin E are non-invasive, medical options. Williamson and coworkers performed a pilot study of 11 patients using this drug combination, with all patients but 1 demonstrating improvement [24]. The one patient that did not improve was later found to have tumor recurrence. Two patients had nausea and abdominal discomfort that resulted in discontinuation of the medications. That said, given its tolerability, at the Cleveland Clinic, this is being used more frequently for radiographically progressive, asymptomatic radiation necrosis.

Hyperbaric oxygen historically had been used to force oxygen into necrotic tissues and encourage new vessels to grow to reverse the necrosis [5]. Despite its historical and current use, there is no prospective study specifically for radiation necrosis of the brain, which has limited its adoption. Data are provided by case reports only [25]. Also, it is relatively cumbersome to give since it may require 30–40 dives to see an effect.

Bevacizumab has emerged as the best supported agent in the management of radiation necrosis. Since VEGF is dysregulated with radiation necrosis, using a VEGF inhibitor presumably can reverse its effects. MD Anderson conducted a double-blind, placebo-controlled study of placebo versus bevacizumab for patients with presumed radiation necrosis [26]. Bevacizumab was given at a dose of 7.5 mg/m^2 at 3 week intervals for 2 cycles. If there was improvement, treatment would continue for another 2 cycles. Patients who did not respond crossed over to the other arm. Fourteen patients were randomized. None of those receiving placebo responded. All patients who were randomized to the treatment arm and those who crossed over from the placebo arm responded. All patients had decrease in the T2-weighted FLAIR and T1-weighted gadolinium-enhanced volumes. Neurological signs and symptoms also improved. Other studies have supported its use [27, 28]. Despite this, payers have not universally accepted the use of bevacizumab for radiation necrosis; thus an ongoing ALLIANCE study is randomizing patients to bevacizumab versus supportive care,

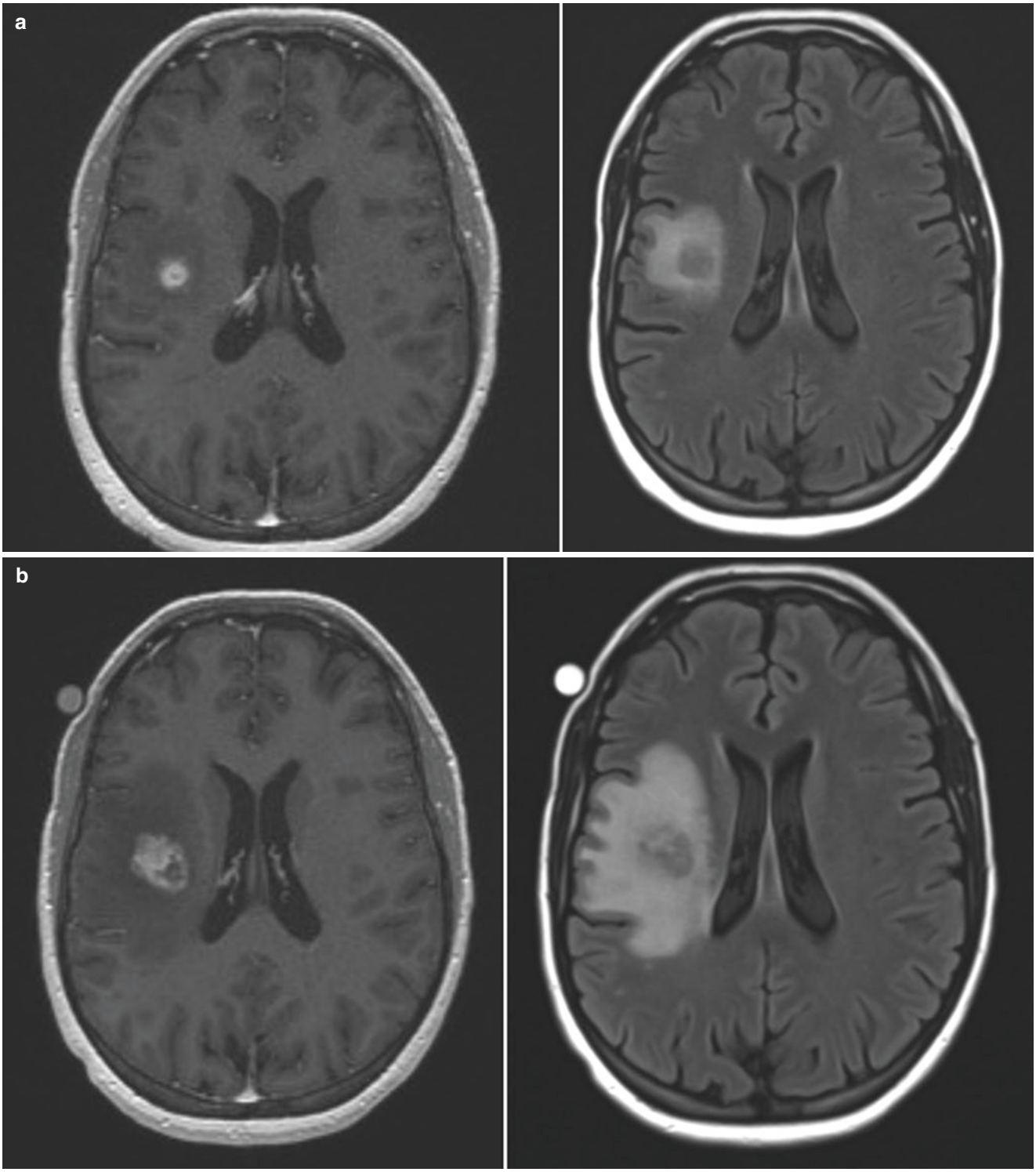

Fig. 1 (**a**) 36-year-old with ER-/PR-/Her2+ breast CA with brain metastasis s/p stereotactic radiosurgery to right frontal lesion. MRI 1 month post-SRS showed partial response. (**b**) Over 8 months, there was progressive enlargement with edema. (**c**) Patient underwent laser interstitial thermal therapy (LITT). Biopsy prior to LITT showed radiation necrosis. Follow-up MRI 3 months post-LITT shows no evidence of recurrence

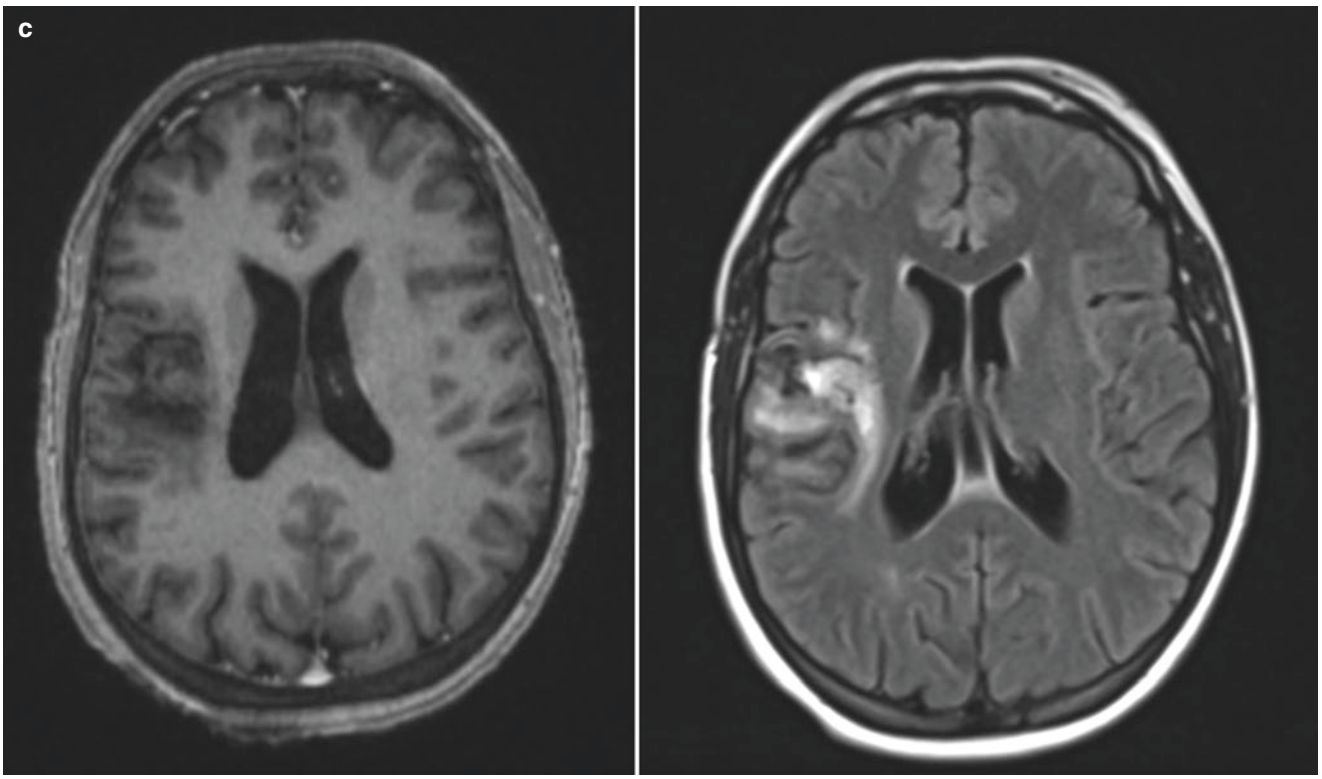

Fig. 1 (continued)

with larger patient numbers (n = 130) [29]. Caution should be used for patients with squamous cell lung cancer and with cerebral hemorrhage undergoing bevacizumab treatment [5].

As an alternative to resection, laser interstitial thermal therapy (LITT) has emerged as a modality to treat either tumor progression or radiation necrosis. The exact mechanism of action is unclear, but it likely replaces the radiation necrosis with coagulative necrosis, which has a different pathophysiology. Typically prior to LITT, a biopsy is obtained to determine histology. A prospective, phase II study, Laser Ablation After Stereotactic Radiosurgery (LAASR), was conducted to further determine its role in the management of radiation necrosis or tumor recurrence after radiosurgery. Improved survival was seen when a diagnosis of radiation necrosis was made as opposed to tumor recurrence on biopsy (100% with radiation necrosis versus 71% for tumor at 12 weeks, p=0.02) [30]. All of the patients with radiation necrosis regardless of ablation coverage and tumor that was totally ablated did not have recurrence, while 62.5% of the patients with subtotal ablation of tumor eventually developed progression. Accumulated data also support its use [31].

Although radiation necrosis is a feared complication of brain radiosurgery, there are now numerous treatment options that may make it less feared, paving the way for radiosurgery combined with systemic therapies and dose escalation, either in a single or multiple sessions.

Radiation Optic Neuropathy

Another late complication of radiosurgery around the optic pathway is radiation optic neuropathy (RON). As with radiation necrosis, this can be symptomatic, potentially resulting in permanent visual field deficits or blindness. As such, reducing the risk of RON is critical.

RON can develop as early as 3 months post radiation, but can take years to develop. The peak incidence is 1–1.5 years [32]. Some may have complete loss of light perception, while others may decline in visual acuity, below 20/200 or worse. Differential diagnosis includes tumor progression, radiation retinopathy, secondary malignancy from radiation, and adhesions. Giant cell arteritis should be considered in patients over the age of 60 years old. CT scans are typically normal, but on MRI, enhancement is seen usually with administration of gadolinium, which is non-specific and is seen with other pathologies. This resolves after several months.

The pathophysiology is not known, but may be similar to radiation necrosis [32]. Damage to the vascular endothelium and subsequent disruption of the blood brain barrier may be responsible. MRS imaging may show a pattern seen with radiation necrosis. Demyelination may also be responsible.

This risk of RON is dependent on the dose. Typically, a single session dose of 10 Gy to the optic nerves or chiasm appears to have a very low risk of RON. A slightly higher dose of 12 Gy has a higher risk, but relatively small. Leavitt

and coworkers published their results from 222 patients who received radiosurgery adjacent to the anterior visual pathway [33]. Tumors included meningiomas, pituitary adenomas, and craniopharyngiomas. Patients receiving maximum doses up to 12 Gy to the optic nerves or chiasm had a 0% chance of RON, but those receiving greater than 12 Gy had a 10% risk. The risk of tumor recurrence, which can also lead to blindness, needs to be carefully balanced against the risk of RON at the time of treatment. In some cases, fractionating SRS can reduce the risk of RON, yet still provide a good dose for tumor control. Using pooled data from 34 studies, Milano and coworkers recommended a maximum dose to the optic nerve or chiasm of 25 Gy for five fraction SRS and 20 Gy for three fraction SRS to limit the risk of RON to 1% [34].

Treatment options include hyperbaric oxygen, especially if initiated within 72 hours of initial symptoms. After 2 weeks, significant recovery may not be seen [35–37]. Unlike in radiation necrosis, corticosteroids may have less of a benefit [38]. One case study demonstrated reversal of RON following steroids, warfarin, pentoxifylline, and vitamin E, despite therapy being started 2 weeks after onset of symptoms [39]. One other case report showed successful reversal of RON following eye plaque brachytherapy with intravitreal injection of bevacizumab [40]. A study of 14 patients demonstrated stability or improvement in 9 patients when treated with this technique [41]. Another case report showed resolution of RON following intravenous bevacizumab, along with dexamethasone and pentoxifylline [42].

Radiation Myelopathy

Radiation myelopathy has always been one of the most feared complications for radiation oncologists when delivering radiation around the spinal cord. With the advent of spine stereotactic radiosurgery/body radiation therapy, there were concerns regarding patient setup, cord contouring, and cord dosing in order to minimize this complication which can dramatically affect quality of life due to its potential for paralysis. However, with experience, many of those concerns have been mitigated, but one should still remain mindful of this toxicity.

As with radiation necrosis, the categorization of early injury, early delayed injury, and late injury applies [43]. Acute early injury is not typically seen as acute symptoms are related to tumor edema. Early delayed injury is seen as Lhermitte's syndrome, which is characterized by paresthesia in the back and extremities following flexion of the neck. It is typically seen 2–4 months post treatment and occurs with doses less than what is seen for myelopathy. It is not associated with permanent myelopathy. On the other hand, late injury of the spinal cord refers to radiation myelopathy [43]. This is typically irreversible. Symptoms can range from minor motor or sensory deficits to Brown-Sequard syndrome. Latency time is typically 1–1.5 years. As a diagnosis of exclusion, like RON, tumor progression, metastasis to the spinal cord, secondary tumor of the spinal cord, and other causes needs to be ruled out.

On MRI, T2 changes and enhancement is seen, secondary to the disruption of the blood brain barrier [43]. Biologically, there is reactive gliosis, demyelination and necrosis in the white matter, and vascular changes in the white and gray matter. Figure 2a, b is an MRI of a patient with radiation myelopathy post spine SRS.

A multi-institutional study provides guidelines for the safe practice of spine SBRT [44]. By using data from multiple academic institutions, they assessed five patients with radiation myelopathy compared against a large cohort and looked at the thecal sac dosing as a correlate for spine cord contours. Using this data, they developed probabilities for radiation myelitis based on dose to the thecal sac. These guidelines are summarized in Table 1. Alternatively, some may use the RTOG spinal cord constraint which is no more than 10% of the spinal cord receiving 10 Gy or more with a maximum dose of 14 Gy. For the cauda equina, the constraints are more relaxed with less than 10% of the thecal sac encompassing the cauda equina limited to 12 Gy or more with a maximum dose of 16 Gy. Katsoulakis and coworkers have shown that a max dose of 14 Gy to the spinal cord results in a less than 1% risk of myelopathy [45].

Treatment of radiation myelopathy mimics the treatment of RON given limited evidence. This includes corticosteroids and bevacizumab as upregulation of VEGF is seen in radiation myelopathy [46, 47]. Although radiographic improvement may be seen, clinical improvement may only be modest [47].

Stereotactic Body Radiation Therapy

Vertebral Compression Fractures

Spine SRS or SBRT, as well as SBRT to sites adjacent to the spine, may have implications on the integrity of the bony spine. In fact, the most frequent late toxicity of spine SRS/SBRT is vertebral compression fractures (VCF) [48]. Depending on the series, and consequentially the doses used, the risk of VCF ranges from 10 to almost 40% [49]. While not all cases are symptomatic, VCF has the potential to result in pain and neurological symptoms if severe enough.

Collagen is essential in maintaining vertebral body health. When high doses of radiation are used, collagen is damaged and degraded due to damaged peptide bonds from radiation, decreasing its strength. This, coupled with intrinsically damaged bone from either osteolytic disease or osteoblastic disease, results in further weakened bone, resulting in collapse and compression. This can result in kyphosis of the spine with anterior compression, but there can be retropulsion of bone that intrudes into the spinal canal and compresses the spinal cord, resulting in neurological symptoms [48].

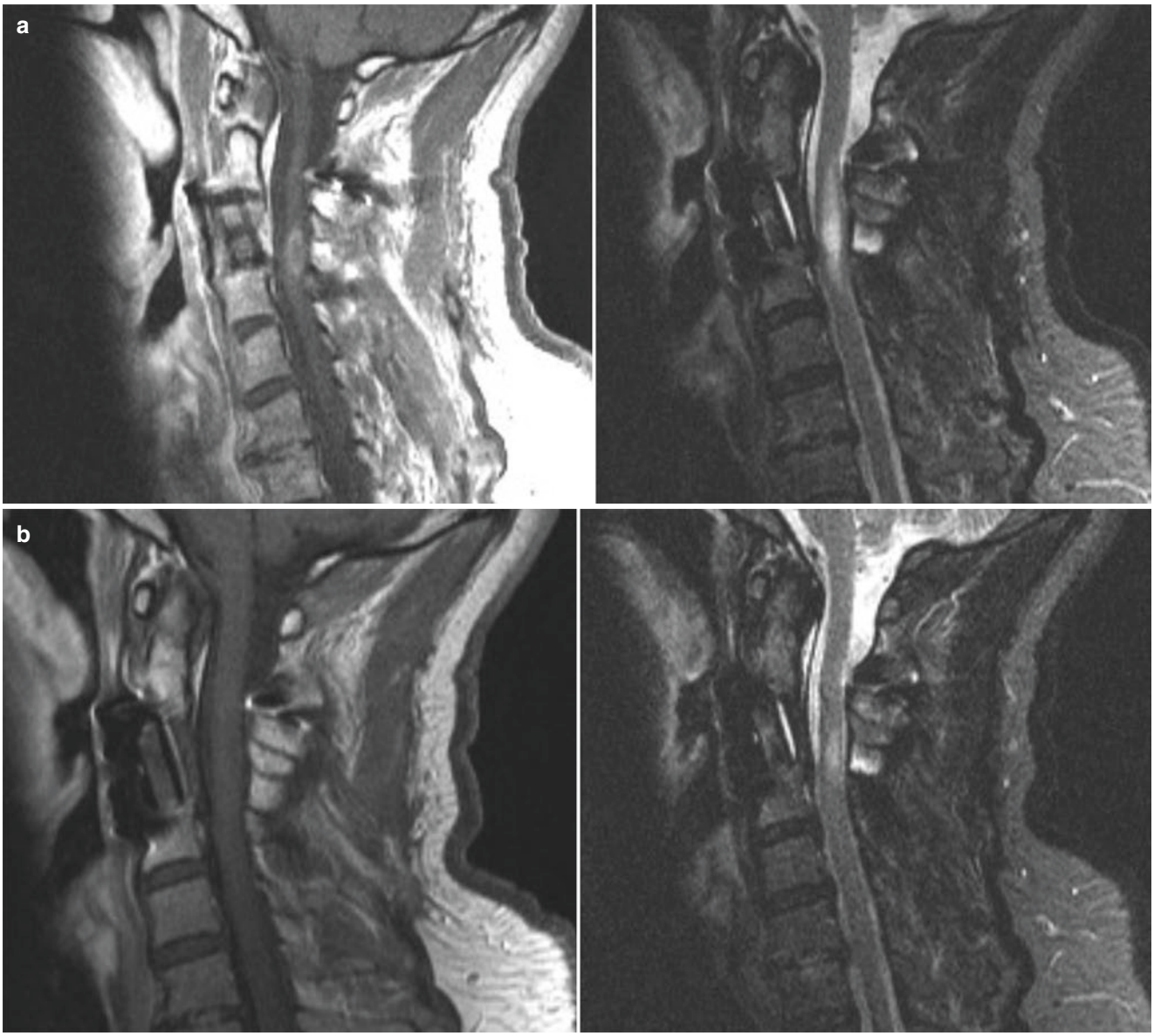

Fig. 2 (**a**, **b**) 53-year-old with a chordoma s/p C3 corpectomy, followed by adjuvant SRS to 16 Gy. (**a**) MRI 3 months later showed enhancement and edema in the cord consistent with spinal cord myelopathy. He had arm weakness and was treated with steroids. (**b**) MRI 5 months later shows resolution of enhancement (contrast enhanced T1) and improvement of edema (STIR). His arm weakness improved

Table 1 Probability of radiation myelopathy based on P_{max} for 1–5 fraction SBRT

	1 fraction P_{max} limit (Gy)	2 fraction P_{max} limit (Gy)	3 fraction P_{max} limit (Gy)	4 fraction P_{max} limit (Gy)	5 fraction P_{max} limit (Gy)
1% probability	9.2	12.5	14.6	16.7	18.2
2% probability	10.7	14.6	17.4	19.6	21.5
3% probability	11.5	15.7	18.8	21.2	23.1
4% probability	12.0	16.4	19.6	22.2	24.4
5% probability	12.4	17.0	20.3	23.0	25.3

Used with permission of Elsevier from Sahgal et al. [44]

Risk factors for VCF include osteolytic disease [50–53], greater vertebral body involvement [51], pre-existing VCF [50, 52], kyphosis/scoliosis [53], lung histology [53], and liver histology [53]. Pre-existing spine instability increases the risk [48, 50]. The Spinal Instability Neoplastic Score (SINS) is used to guide the need for spine stabilization and is also used to predict the risk of VCF post-SBRT [53]. The SINS score is shown in Table 2 [54].

Another risk factor is dose per fraction. A multi-institutional study demonstrated that fractional doses

Table 2 Spine Instability Neoplastic Score (SINS)

Location	
3 points	Junctional (C0–2, C7-T2, T11-L1, L5-S1)
2 points	Mobile spine (C3-C6, L2–4)
1 point	Semi-rigid (T3–10)
0 points	Rigid (S2–5)
Pain relief with recumbancy and/or pain with movement/loading of spine	
3 points	Yes
1 point	No (occasional pain, but not mechanical)
0 points	Pain free lesion
Bone lesion	
2 points	Lytic
1 point	Mixed (lytic/blastic)
0 points	Pain free lesion
Radiographic spinal alignment	
4 points	Subluxation/translation present
2 points	De novo deformity (kyphosis/scoliosis)
0 points	Normal alignment
Vertebral body collapse	
3 points	>50% collapse
2 points	<50% collapse
1 point	No collapse with >50% vertebral body involvement
0 points	None of the above
Posterolateral involvement of the spinal elements	
3 points	Bilateral
1 point	Unilateral
0 points	None of the above

Total score: 0–6 is stable, 7–12 is indeterminate stability, 13–18 is instability (7–18 should be considered for surgery)
Used with permission of Wolters Kluwer Health, Inc., from Fisher et al. [54]

20 Gy or more result in a higher risk of compression fracture, more so than total dose [50]. For doses 19 Gy or less, the rate of VCF is 10% at 1 year versus 39% for 24 Gy or more. This should be balanced against the fact that higher doses may result in a higher rate of control. Thus, a hypofractionated regimen over a single fraction regimen is advocated by some to result in a high rate of control, but lower rate of VCF [55]. Another large study, however, suggests a higher prescription dose, greater than EQD2 of 41.8 Gy, and is responsible, irrespective of the number of fractions [56].

Vertebral fractures can occur outside of spine SBRT. One case report demonstrated a vertebral body fracture following SBRT for a metastatic lung nodule [57].

Approximately a third of patients with VCF may need surgical intervention to manage their symptoms [48]. This may include percutaneous vertebral augmentation and open surgical reconstruction. Prophylactic vertebral augmentation, as opposed to vertebral augmentation for symptomatic instability, has been suggested by some to prevent VCF, especially in those with more vertebral body involvement, pre-existing VCF, or other risk factors. However, the benefit of this approach is unclear and it will delay SRS/SBRT, and likely, systemic treatment.

Radiation Pneumonitis/Pulmonary Fibrosis

Radiation pneumonitis (RP) is one of the most common toxicities after SBRT to the lung [58]. The rates of symptomatic RP range from 9 to 28% [58–61]. In RTOG 0236, Grade 3 RP was seen in 3.6% of the patients [62]. Symptoms include shortness of breath, cough, low-grade fevers, and pleuritic chest pain [63]. Malaise and weight loss may also be associated with RP. In progressive cases, patients can have chronic damage 3–6 months afterward. Acute respiratory distress may be seen in extreme case and can be life threatening.

RP needs to be distinguished from other causes of dyspnea, including tumor progression, pneumonia, chronic obstructive pulmonary disease exacerbation, or airway obstruction [63]. On CT imaging, non-specific infiltrates, ground-glass opacities, or both are seen in areas that have received radiation.

Predictors of RP include mean lung dose (MLD), V5, V20, V25, and conformity index (CI) [58]. Of these, the most consistent predictors appear to be MLD and V20 [64–66]. Barriger and associates looked at 251 patients treated with 3–5 fractions of stereotactic body radiation therapy. Grade 2–4 RP occurred in 4.3% of the patients with MLD of 4 Gy or less versus 17.6% for those greater than 4 Gy. Also, Grade 2–4 RP developed in 4.3% of the patients with V20 of 4% or less versus 16.4% in patients with V20 of greater than 4%. These dosimetric factors should be considered when planning for lung SBRT.

Steroids are used to manage RP. Prednisone is typically given at a dose of 40–60 mg daily and tapered over 8–12 weeks while monitoring the patient's symptoms [67]. Steroids should be considered early in the course, before the onset of pulmonary fibrosis, when steroids will have little effect [68]. Supplemental oxygen may be used as well.

Pulmonary fibrosis, on the other hand, is a late effect of SBRT of the lung as a cascade of events from RP [63]. It needs to be differentiated from tumor recurrence, which is not necessarily straightforward as imaging characteristics may be similar. Inhalers and corticosteroids remain the treatment of choice, although pentoxifylline, vitamin E, and hyperbaric oxygen have been investigated with moderate success [63, 69].

Esophageal Toxicities

While acute esophagitis can be common with SBRT, late esophageal toxicity, specifically stricture and perforation, is less common but may occur. Both can be morbid and difficult to manage. Avoiding this late toxicity is crucial.

Although much has been published regarding esophageal limits with SBRT, the published dose constraints from these studies are inconsistent. Nuyttens and associates compiled recommend dose constraints from various studies of D_{max} EQD_2 varying from 48 to 108 Gy [70–72]. EQD_2 D_{5cc} can range from 35 to 47 Gy [70, 73]. Looking specifically at patients who developed toxicity, Nuyttens and associates calculated BED for those with Grade 3–5 toxicity which occurred at a median D_{max} dose of 141 Gy, D_{1cc} of 133 Gy, and D_{5cc} of 67 Gy.

Cox and associates looked specifically at esophageal toxicity from spine radiosurgery given the proximity of the esophagus to the thoracic spine [74]. In their series of 204 spine metastases abutting the esophagus, they noted at 5% Grade 3 or higher late esophageal toxicity rate. Of these, four patients had Grade 4 late toxicity including fistula and stenosis, and one patient had a Grade 5 late toxicity due to fistula. A couple of these patients had radiation recall with gemcitabine and doxorubicin. By modeling the doses, in order to keep the Grade 3 or more toxicity to less than 5%, they recommended a dose of 14 Gy or less to the hottest 2.5 cc of esophagus. They also recommended a maximum dose less than 22 Gy. The authors also cautioned against iatrogenic manipulation of the esophagus as they described a case of a patient who had esophagogastroduodenoscopy with biopsy that consequentially developed into a fistula.

Similarly, Abelson and associates looked at 31 patients with disease less than 1 cm from the esophagus. They identified three patients with toxicity of the esophagus, one with Grade 2 esophagitis and two with Grade 4–5 esophageal perforation. As in the case with Cox and associates, the two patients with Grade 4–5 toxicities had chemotherapy that may have resulted in their toxicity. One patient had gemcitabine chemotherapy that resulted in a tracheoesophageal fistula 6 months after SBRT. Another patient had chemoradiation that was followed by SBRT. After SBRT, the patient resumed chemotherapy with ifosfamide and etoposide that resulted in perforation and mediastinitis. These toxicities developed at a lower dose than published constraints. The authors recommended for single-fraction SBRT an esophageal D_{max} to 15.4 Gy and D_{5cc} to 11.9 Gy, which is lower than the recommended constraint from Cox and associates. The authors also recommended avoiding circumferential irradiation of the esophagus.

The management of esophageal strictures involves balloon dilatation [75]. Earlier onset of esophageal strictures may predict for decreased response to balloon dilatation. Temporary stents can also be used to manage strictures, but may also result in a foreign-body sensation, severe pain, fistula formation, or perforation [76].

Esophageal stents may be used to treat esophageal perforation, in lieu of operative repair, especially in those who failed prior surgery or are poor surgical candidates. Risk factors for stent failure include esophageal leak of the proximal cervical esophagus, one that traversed the gastroesophageal junction, injury longer than 6 cm, or a leak associated with a more distal conduit leak [77].

Radiation Plexopathy

Although reported, it is often difficult to distinguish plexopathy and radiculopathy given that tumor progression or radiation injury to the spinal nerves may result in similar symptoms. In a phase I/II study looking at single fraction spine SRS (16–24 Gy) at MD Anderson, 10 out of 61 patients experienced mild Grade 1 or 2 numbness and tingling and 1 developed Grade 3 radiculopathy [78]. Another study from the same institution looked at reirradiation with spine SRS in 59 patients and found 2 patients with Grade 3 lumbar plexopathy [79].

Brachial plexopathy may have a higher incidence in apical lung cancers treated with SBRT. Forquer and associates looked at 36 patients with 37 primary apical lung cancers treated to a dose of 30–72 Gy in 3–4 fractions [80]. They found seven cases of Grade 2–4 brachial plexopathy and determined a threshold dose of 26 Gy in 3–4 fractions increased this risk. Beyond 26 Gy, the risk of plexopathy was 46% versus 8% when the dose is kept to 26 Gy or less. This corresponds to the dose constraint of 24 Gy in three fractions used by RTOG trials. Table 3 summarizes the RTOG constraints for brachial plexus.

Bowel Toxicities

Similar to the esophagus, the data for small bowel tolerance to SBRT are inconsistent. To further complicate the inconsistencies, it is difficult to compare various studies given different fractionation schemes. These toxicities include mucositis, ulceration, gastroparesis, and perforation. LaCouture and associates reviewed and compiled data from multiple studies

Table 3 Plexus constraints per RTOG trials

Fractions	RTOG study	Constraint
1	0631/0915	Brachial: 17.5 Gy (<0.03 cc) and 14 Gy (<3 cc) Sacral: 18 Gy (<0.03 cc) and 14.4 Gy (<5 cc)
2	0236/0618	Brachial: 24 Gy maximum and 20.4 Gy (<3 cc)
4	0915	Brachial: 27.2 Gy maximum and 23.2 Gy (<3 cc)
5	0813	Brachial: 32 Gy maximum and 30 Gy (<3 cc)

Table 4 Dose constraints for Grade 3 or higher ulcer/bleeding/perforation for small bowel

	3 fractions	5 fractions
D2cc	<24.5 Gy	<30 Gy
D5cc	<21 Gy	<25 Gy

Data from Pollom et al. [82]

to determine a dose limit for "low risk," defined as a 4% or less risk, and "high risk," defined as 8.2% or less, of developing small bowel toxicity [81]. For low risk, D_{5cc} is 9.8 Gy, 13.5 Gy, 16.2 Gy, 17.9 Gy, and 19.5 Gy for one, two, three, four, and five fractions, respectively. Max dose is 12 Gy, 18.6 Gy, 25.2 Gy, 28.5 Gy, and 29 Gy for one, two, three, four, and five fractions, respectively. For high risk, D_{5cc} is 11.9 Gy, 17 Gy, 21 Gy, 23 Gy, and 25 Gy for one, two, three, four, and five fractions, respectively. Max dose is 19 Gy, 24.5 Gy, 30 Gy, 33.2 Gy, and 35 Gy for one, two, three, four, and five fractions, respectively.

Pollom and associates attempted to summarize the data and developed dose constraints for various structures, including the duodenum and small bowel [82]. Table 4 shows updated constraints to these structures.

Other factors may increase the risk of small bowel toxicity. Barney and associates looked at 71 patients who received SBRT. Bowel toxicity developed in 9%, but increased to 38% if VEGF inhibitor, inclusive of bevacizumab or VEGF TKI, was given within 3 months of completing SBRT [83]. Some institutions consider withholding VEGF inhibitors 2 weeks before and 2 weeks after SBRT [81]. As with other sites, the risk of concurrent therapies in increasing the risk of toxicity needs to be considered and further studied.

Probiotics may be considered as a preventative for someone at high risk of bowel toxicity from radiation [84]. The management of bowel toxicity is unfortunately limited [85]. For those with diarrhea, anti-diarrheals may be considered [84]. This includes octreotide, which modulates pancreatic secretions [86].

Non-spine Bone SBRT and Musculoskeletal Toxicity

SBRT for oligometastatic bone disease outside of the spinal column is a newer application of these techniques and has been considered for both radiation resistant and sensitive histologies. The potential toxicities are related to the surrounding normal and involved tissues. Dose and fractionation schemes are not standard and there are currently limited data available. Brown and associates reported on 14 patients with recurrent or metastatic Ewing's sarcoma or osteosarcoma treated at Mayo Clinic [87]. The median dose used was 40 Gy in five fractions, but ranged 30–60 Gy in 3–10 fractions. Two Grade 2 late toxicities (myonecrosis and avascular necrosis) and one Grade 3 late toxicity (sacral plexopathy) were noted. The patient that developed Grade 2 myonecrosis received concurrent gemcitabine. The patient who developed Grade 3 sacral plexopathy was treated with 60 Gy in ten fractions SBRT to the sacrum and had received previous radiation to that site at initial diagnosis (59.4 Gy in 33 fractions, 1.75 years prior). The sacral plexus received 105% of the prescription dose on initial treatment and 100% of the prescription dose during the second course. In the case of the avascular necrosis, the entirety of the femoral head was clinically involved and received 60 Gy in ten fractions SBRT. However, the patient required only conservative management of this toxicity and remained free of disease for 1.6 years at the time of publication. The authors describe a 2-year local control of 85% for the patients that were treated with a definitive intent. The results suggest feasibility of non-spine bone SBRT and that caution should be given in the setting of concurrent chemotherapy or reirradiation.

Vascular Toxicity

Vascular injury with SBRT is a potentially fatal complication, particularly in patients being retreated with SBRT. This is particularly concerning for patients with disease in close proximity or invading the carotid artery. Yamazaki and associates did a matched pair analysis using patients from four institutions undergoing reirradiation for pharyngeal cancer [88]. There were 12 cases of carotid blowout syndrome (CBOS) and 60 cases without. Median retreatment dose was 30 Gy in 5 fractions after an initial treatment dose of 60 Gy in 30 fractions. Median time to CBOS was 5 months (range, 0–69 months). Those with carotid involvement of >180 degrees developed CBOS, but those with less than half of circumferential involvement did not develop CBOS. On multivariate analysis, the area of lymph node involvement and skin ulceration were predisposing factors. Cengiz and associates, looking at similar retreatment doses, also found that >180 degree involvement increased the risk of CBOS in their group of 46 patients [89].

Concomitant Systemic Therapy

As discussed previously, concomitant or concurrent systemic therapy may or may not increase the risk of toxicity. For cranial radiation necrosis, there appears to be a higher risk with concurrent VEGF TKIs or EGFR TKIs, in particular for those receiving WBRT (in addition to SRS), but not with cytotoxic, cytokine, or hormonal therapy [12]. Another study confirmed these results for the most part, showing that concurrent systemic therapy may be given with cranial SRS without additive myelotoxicity or neurotoxicity [11]. A phase I study of sorafenib did not appear to increase toxicity associated with SRS of the brain [90]. A very complete review by Kroeze and coworkers did a literature search of targeted therapy and immunotherapy and stereotactic radiotherapy [91]. They found an increased risk of toxicity with

EGFR TKIs and bevacizumab, but in this case with extracranial stereotactic radiotherapy. They also found an increased risk with BRAF-inhibitors with cranial SRS.

Miller and colleagues looked at concurrent VEGF TKIs and spine SRS [92]. Unlike in the brain, concurrent VEGF TKIs seemed to improve local control without increased toxicity, including vertebral compression fractures and pain flare. Local relapse was only 4% in those receiving concurrent VEGF TKIs and was statistically significantly less than those who were systemic therapy naïve, and those who have previously failed first line therapy. It was also improved compared to those receiving VEGF TKI alone. Importantly, there were no Grade 3 or more toxicities in the group receiving concurrent therapy, and it is felt safe to be given concurrently.

As previously reviewed, there is a risk of severe toxicity when VEGF inhibitors like bevacizumab is given concurrently when SBRT is given adjacent to a luminal/mucosal structure such as with the bowel [83] or the proximal bronchial tree as seen with central lung tumors [93]. Further studies are needed as concurrent therapy may or may not increase toxicity based upon location.

Plan Quality: Compiled Published Dose Constraints for SRS/SBRT

Compiling these data is very difficult work given the breadth of published recommendations, but necessary for those practicing SRS and SBRT in order to ensure safe delivery and minimizing toxicities. The Emami table [94] had been the historic standard, but was compiled using older data and only applied to conventionally fractionated radiation.

There are two contemporary complied sources for this data. One is known euphoniously as the "Timmerman tables" and the other is Quantitative Analysis of Normal Tissue Effects in the Clinic (QUANTEC). The "Timmerman tables" published admittedly unvalidated dose constraints used at the University of Texas, Southwestern [95]. These were derived mainly from observations and mathematical modeling. That said, it is a very quick and easy single-source reference.

QUANTEC pools published data of what is known and attempts to provide consensus for various structures [96]. Whereas the Timmerman tables provide breadth, QUANTEC provide depth, but cannot provide data when data do not exist. For instance, QUANTEC is unable to provide brainstem constraints, although this was attempted [97]. However, in the same manuscript, QUANTEC is able to summarize the data for RON and suggests that the incidence of RON is rare with D_{max} less than 8 Gy, increases in the range of 8–12 Gy, and is greater than 10% when D_{max} is greater than 12 Gy.

Since 2008 when the well-used Timmerman tables were published and given limitations of QUANTEC specifically for SBRT outside of the brain and spine, Pollom and coworkers compiled published data for thoracic and abdominal SBRT and subsequently proposed modified dose constraints for various organs in the chest and abdomen compared to the Timmerman tables [82]. Table 5 lists selected dose constraints suggested aside from what is already listed in Table 4.

Future Directions/Conclusion

SRS and SBRT is a burgeoning field and much remains to be learned about balancing the risk of complications and tumor control. Complications, when they do occur, need to be managed and treated. However, in many cases, the options are limited, resulting in permanent morbidity and diminished quality of life. Consequentially, it is critical to adhere with known dose tolerances of various structures to avoid toxicity. Pooling clinical data and ongoing research will help establish better dose constraints to be used in SRS and SBRT. The impact of concurrent systemic therapy, targeted agents, and immunotherapy on complications needs further investigation.

Table 5 Dose constraints for Grade 3 or higher for selected organs

Organ	Toxicity	Fractions	Constraint	Dose
Duodenum	Ulcer, bleeding, perforation	3	D_{1cc}	<30 Gy
		5	D_{1cc}	<35 Gy
Lung	Pneumonitis	4	V20	10%
			Ipsilateral V30	15%
			MLD	6 Gy
Trachea/mainstem bronchi	Stenosis/fistula	4–5	D_{max}	<52.5 Gy
			V33.5	<4 cc
Great vessels	Aneurysm	4–5	D_{max} (pulmonary artery)	<52.5 Gy
			D_{max} (aorta)	<60 Gy
Esophagus	Esophagitis	1	D_{2cc}	<14 Gy
		5	D_{max}	<50 Gy

Data from Pollom et al. [82]

Practical Considerations

- Larger treatment volume and higher dose can increase the risk of radiation necrosis. Management options for radiation necrosis include steroids, bevacizumab, hyperbaric oxygen, pentoxifylline resection, and laser interstitial thermal therapy.
- Radiation optic neuropathy is very low for 10 Gy or less to the optic pathways. Treatment options are limited, although bevacizumab may help.
- Radiation myelopathy is rare when dose limits are applied to the spinal cord. Again, steroids and bevacizumab may offer modest help in patients with radiation myelopathy.
- Risk factors for vertebral compression fractures include osteolytic disease, greater involvement, pre-existing compression fracture, and spinal instability. Dose per fraction greater than 20 Gy may increase the risk. Only symptomatic compression fractures may need intervention which may include vertebral augmentation and surgical reconstruction.
- Radiation pneumonitis may occur with lung SBRT. Mean lung dose less than 4 Gy and V20 less than 4% decreases risk. Steroids are used to manage symptomatic radiation pneumonitis.
- Esophageal toxicity may be seen with spine SBRT. Iatrogenic manipulation or chemotherapy may cause fistulas when esophageal dose constraints are exceeded.
- VEGF inhibitors may increase the risk of bowel and proximal bronchial tree toxicities from SBRT.
- Some, but not all systemic therapeutics may increase the risk of normal tissue toxicity when given concurrently with SRS or SBRT. Further studies are needed.
- Pooling of data may help standardize dose constraints used in SRS and SBRT.

References

1. Chin LS, Ma L, DiBiase S. Radiation necrosis following gamma knife surgery: a case-controlled comparison of treatment parameters and long-term clinical follow up. J Neurosurg. 2001;94:899–904.
2. Minniti G, Clarke E, Lanzetta G, Osti MF, Trasimeni G, Bozzao A, et al. Stereotactic radiosurgery for brain metastases: analysis of outcome and risk of brain radionecrosis. Radiat Oncol. 2011;6:48.
3. Nordal RA, Nagy A, Pintilie M, Wong CS. Hypoxia and hypoxia-inducible factor-1 target genes in central nervous system radiation injury: a role for vascular endothelial growth factor. Clin Cancer Res. 2004;10:3342–53.
4. Nonoguchi N, Miyatake S, Fukumoto M, Furuse M, Hiramatsu R, Kawabata S, et al. The distribution of vascular endothelial growth factor-producing cells in clinical radiation necrosis of the brain: pathological consideration of their potential roles. J Neurooncol. 2011;105:423–31.
5. Chao ST, Ahluwalia MS, Barnett GH, Stevens GH, Murphy ES, Stockham AL, et al. Challenges with the diagnosis and treatment of cerebral radiation necrosis. Int J Radiat Oncol Biol Phys. 2013;87:449–57.
6. Shaw E, Scott C, Souhami L, Dinapoli R, Bahary JP, Kline R, et al. Radiosurgery for the treatment of previously irradiated recurrent primary brain tumors and brain metastases: initial report of radiation therapy oncology group protocol (90-05). Int J Radiat Oncol Biol Phys. 1996;34:647–54.
7. Flickinger JC, Kondziolka D, Lunsford LD, Kassam A, Phuong LK, Liscak R, et al. Development of a model to predict permanent symptomatic postradiosurgery injury for arteriovenous malformation patients. Arteriovenous Malformation Radiosurgery Study Group. Int J Radiat Oncol Biol Phys. 2000;46:1143–8.
8. Korytko T, Radivoyevitch T, Colussi V, Wessels BW, Pillai K, Maciunas RJ, et al. 12 Gy gamma knife radiosurgical volume is a predictor for radiation necrosis in non-AVM intracranial tumors. Int J Radiat Oncol Biol Phys. 2006;64:419–24.
9. Blonigen BJ, Steinmetz RD, Levin L, Lamba MA, Warnick RE, Breneman JC. Irradiated volume as a predictor of brain radionecrosis after linear accelerator stereotactic radiosurgery. Int J Radiat Oncol Biol Phys. 2010;77:996–1001.
10. Miller JA, Bennett EE, Xiao R, Kotecha R, Chao ST, Vogelbaum MA, et al. Association between radiation necrosis and tumor biology after stereotactic radiosurgery for brain metastasis. Int J Radiat Oncol Biol Phys. 2016;96:1060–9.
11. Shen CJ, Kummerlowe MN, Redmond KJ, Rigamonti D, Lim MK, Kleinberg LR. Stereotactic radiosurgery: treatment of brain metastasis without interruption of systemic therapy. Int J Radiat Oncol Biol Phys. 2016;95:735–42.
12. Kim JM, Miller JA, Kotecha R, Xiao R, Juloori A, Ward MC, et al. The risk of radiation necrosis following stereotactic radiosurgery with concurrent systemic therapies. J Neurooncol. 2017;133:357–68.
13. Martin AM, Cagney DN, Catalano PJ, Alexander BM, Redig AJ, Schoenfeld JD, Aizer AA. Immunotherapy and symptomatic radiation necrosis in patients with brain metastases treated with stereotactic radiation. JAMA Oncol. 2018;4(8):1123.
14. Fang P, Jiang W, Allen P, Glitza I, Guha N, Hwu P, Ghia A, Phan J, Mahajan A, Tawbi H, Li J. Radiation necrosis with stereotactic radiosurgery combined with CTLA-4 blockade and PD-1 inhibition for treatment of intracranial disease in metastatic melanoma. J Neuro-Oncol. 2017;133(3):595–602.
15. Colaco RJ, Martin P, Kluger HM, Yu JB, Chiang VL. Does immunotherapy increase the rate of radiation necrosis after radiosurgical treatment of brain metastases? J Neurosurg. 2016;125(1):17–23.
16. Dequesada IM, Quisling RG, Yachnis A, Friedman WA. Can standard magnetic resonance imaging reliably distinguish recurrent tumor from radiation necrosis after radiosurgery for brain metastases? A radiographic-pathological study. Neurosurgery. 2008;63:898–903; discussion 4
17. Kano H, Kondziolka D, Lobato-Polo J, Zorro O, Flickinger JC, Lunsford LD. T1/T2 matching to differentiate tumor growth from radiation effects after stereotactic radiosurgery. Neurosurgery. 2010;66:486–91; discussion 91–2
18. Stockham AL, Tievsky AL, Koyfman SA, Reddy CA, Suh JH, Vogelbaum MA, et al. Conventional MRI does not reliably distinguish radiation necrosis from tumor recurrence after stereotactic radiosurgery. J Neurooncol. 2012;109:149–58.
19. Mitsuya K, Nakasu Y, Horiguchi S, Harada H, Nishimura T, Bando E, et al. Perfusion weighted magnetic resonance imaging to distinguish the recurrence of metastatic brain tumors from radiation necrosis after stereotactic radiosurgery. J Neurooncol. 2010;99:81–8.

20. Chao ST, Suh JH, Raja S, Lee SY, Barnett G. The sensitivity and specificity of FDG PET in distinguishing recurrent brain tumor from radionecrosis in patients treated with stereotactic radiosurgery. Int J Cancer. 2001;96:191–7.
21. Li H, Deng L, Bai HX, Sun J, Cao Y, Tao Y, States LJ, Farwell MD, Zhang P, Xiao B, Yang L. Diagnostic accuracy of amino acid and FDG-PET in differentiating brain metastasis recurrence from radionecrosis after radiotherapy: a systematic review and meta-analysis. Am J Neuroradiol. 2018;39(2):280–8.
22. Chernov M, Hayashi M, Izawa M, Ochiai T, Usukura M, Abe K, et al. Differentiation of the radiation-induced necrosis and tumor recurrence after gamma knife radiosurgery for brain metastases: importance of multi-voxel proton MRS. Minim Invasive Neurosurg. 2005;48:228–34.
23. Zhang H, Ma L, Wang Q, Zheng X, Wu C, Xu BN. Role of magnetic resonance spectroscopy for the differentiation of recurrent glioma from radiation necrosis: a systematic review and meta-analysis. Eur J Radiol. 2014;83:2181–9.
24. Williamson R, Kondziolka D, Kanaan H, Lunsford LD, Flickinger JC. Adverse radiation effects after radiosurgery may benefit from oral vitamin E and pentoxifylline therapy: a pilot study. Stereotact Funct Neurosurg. 2008;86:359–66.
25. Leber KA, Eder HG, Kovac H, Anegg U, Pendl G. Treatment of cerebral radionecrosis by hyperbaric oxygen therapy. Stereotact Funct Neurosurg. 1998;70(Suppl 1):229–36.
26. Levin VA, Bidaut L, Hou P, Kumar AJ, Wefel JS, Bekele BN, et al. Randomized double-blind placebo-controlled trial of bevacizumab therapy for radiation necrosis of the central nervous system. Int J Radiat Oncol Biol Phys. 2011;79:1487–95.
27. Sadraei NH, Dahiya S, Chao ST, Murphy ES, Osei-Boateng K, Xie H, et al. Treatment of cerebral radiation necrosis with bevacizumab: the Cleveland clinic experience. Am J Clin Oncol. 2015;38:304–10.
28. Tye K, Engelhard HH, Slavin KV, Nicholas MK, Chmura SJ, Kwok Y, et al. An analysis of radiation necrosis of the central nervous system treated with bevacizumab. J Neurooncol. 2014;117:321–7.
29. https://www.allianceforclinicaltrialsinoncology.org/main/cmsfile?cmsPath=/Public/Annual%20Meeting/files/CommunityOncology-A221208.pdf.
30. Ahluwalia M, Barnett GH, Deng D, Tatter SB, Laxton AW, Mohammadi AM, Leuthardt E, Chamoun R, Judy K, Asher A, Essig M, Dietrich J, Chiang VL. Laser ablation after stereotactic radiosurgery: a multicenter prospective study in patients with metastatic brain tumors and radiation necrosis. J Neurosurg:1–8.
31. Chaunzwa TL, Deng D, Leuthardt EC, Tatter SB, Mohammadi AM, Barnett GH, et al. Laser thermal ablation for metastases failing radiosurgery: a multicentered retrospective study. Neurosurgery. 2018;82:56–63.
32. Danesh-Meyer HV. Radiation-induced optic neuropathy. J Clin Neurosci. 2008;15:95–100.
33. Leavitt JA, Stafford SL, Link MJ, Pollock BE. Long-term evaluation of radiation-induced optic neuropathy after single-fraction stereotactic radiosurgery. Int J Radiat Oncol Biol Phys. 2013;87:524–7.
34. Milano MT, Grimm J, Soltys SG, Yorke E, Moiseenko V, Tomé WA, et al. Single- and multi-fraction stereotactic radiosurgery dose tolerances of the optic pathways. Int J Radiat Oncol Biol Phys. 2018. pii: S0360-3016(18)30125-1. doi: https://doi.org/10.1016/j.ijrobp.2018.01.053. [Epub ahead of print].
35. Lee MS, Borruat FX. Should patients with radiation-induced optic neuropathy receive any treatment? J Neuroophthalmol. 2011;31:83–8.
36. Guy J, Schatz NJ. Hyperbaric oxygen in the treatment of radiation-induced optic neuropathy. Ophthalmology. 1986;93:1083–8.
37. Levy RL, Miller NR. Hyperbaric oxygen therapy for radiation-induced optic neuropathy. Ann Acad Med Singapore. 2006;35:151–7.
38. Indaram M, Ali FS, Levin MH. In search of a treatment for radiation-induced optic neuropathy. Curr Treat Options Neurol. 2015;17:325.
39. Weintraub JA, Bennett J, Gaspar LE. Successful treatment of radiation-induced optic neuropathy. Pract Radiat Oncol. 2011;1:40–4.
40. Finger PT. Anti-VEGF bevacizumab (Avastin) for radiation optic neuropathy. Am J Ophthalmol. 2007;143:335–8.
41. Finger PT, Chin KJ. Antivascular endothelial growth factor bevacizumab for radiation optic neuropathy: secondary to plaque radiotherapy. Int J Radiat Oncol Biol Phys. 2012;82:789–98.
42. Farooq O, Lincoff NS, Saikali N, Prasad D, Miletich RS, Mechtler LL. Novel treatment for radiation optic neuropathy with intravenous bevacizumab. J Neuroophthalmol. 2012;32:321–4.
43. Wong CS, Fehlings MG, Sahgal A. Pathobiology of radiation myelopathy and strategies to mitigate injury. Spinal Cord. 2015;53:574–80.
44. Sahgal A, Weinberg V, Ma L, Chang E, Chao S, Muacevic A, et al. Probabilities of radiation myelopathy specific to stereotactic body radiation therapy to guide safe practice. Int J Radiat Oncol Biol Phys. 2013;85:341–7.
45. Katsoulakis E, Jackson A, Cox B, Lovelock M, Yamada Y. A detailed dosimetric analysis of spinal cord tolerance in high-dose spine radiosurgery. Int J Radiat Oncol Biol Phys. 2017;99:598–607.
46. Chamberlain MC, Eaton KD, Fink J. Radiation-induced myelopathy: treatment with bevacizumab. Arch Neurol. 2011;68:1608–9.
47. Psimaras D, Tafani C, Ducray F, Leclercq D, Feuvret L, Delattre JY, et al. Bevacizumab in late-onset radiation-induced myelopathy. Neurology. 2016;86:454–7.
48. Sahgal A, Whyne CM, Ma L, Larson DA, Fehlings MG. Vertebral compression fracture after stereotactic body radiotherapy for spinal metastases. Lancet Oncol. 2013;14:e310–20.
49. Faruqi S, Tseng CL, Whyne C, Alghamdi M, Wilson J, Myrehaug S, et al. Vertebral compression fracture after spine stereotactic body radiation therapy: a review of the pathophysiology and risk factors. Neurosurgery. 2018;83(3):314–22.
50. Sahgal A, Atenafu EG, Chao S, Al-Omair A, Boehling N, Balagamwala EH, et al. Vertebral compression fracture after spine stereotactic body radiotherapy: a multi-institutional analysis with a focus on radiation dose and the spinal instability neoplastic score. J Clin Oncol. 2013;31:3426–31.
51. Rose PS, Laufer I, Boland PJ, Hanover A, Bilsky MH, Yamada J, et al. Risk of fracture after single fraction image-guided intensity-modulated radiation therapy to spinal metastases. J Clin Oncol. 2009;27:5075–9.
52. Boehling NS, Grosshans DR, Allen PK, McAleer MF, Burton AW, Azeem S, et al. Vertebral compression fracture risk after stereotactic body radiotherapy for spinal metastases. J Neurosurg Spine. 2012;16:379–86.
53. Cunha MV, Al-Omair A, Atenafu EG, Masucci GL, Letourneau D, Korol R, et al. Vertebral compression fracture (VCF) after spine stereotactic body radiation therapy (SBRT): analysis of predictive factors. Int J Radiat Oncol Biol Phys. 2012;84:e343–9.
54. Fisher CG, DiPaola CP, Ryken TC, Bilsky MH, Shaffrey CI, Berven SH, et al. A novel classification system for spinal instability in neoplastic disease: an evidence-based approach and expert consensus from the Spine Oncology Study Group. Spine (Phila Pa 1976). 2010;35:E1221–9.
55. Redmond KJ, Sahgal A, Foote M, Knisely J, Gerszten PC, Chao ST, et al. Single versus multiple session stereotactic body radiotherapy for spinal metastasis: the risk-benefit ratio. Future Oncol. 2015;11:2405–15.
56. Jawad MS, Fahim DK, Gerszten PC, Flickinger JC, Sahgal A, Grills IS, et al. Vertebral compression fractures after stereotactic body radiation therapy: a large, multi-institutional, multinational evaluation. J Neurosurg Spine. 2016;24:928–36.

57. Rodriguez-Ruiz ME, San Miguel I, Gil-Bazo I, Perez-Gracia JL, Arbea L, Moreno-Jimenez M, et al. Pathological vertebral fracture after stereotactic body radiation therapy for lung metastases. Case report and literature review. Radiat Oncol. 2012;7:50.
58. Yamashita H, Takahashi W, Haga A, Nakagawa K. Radiation pneumonitis after stereotactic radiation therapy for lung cancer. World J Radiol. 2014;6:708–15.
59. Yamashita H, Nakagawa K, Nakamura N, Koyanagi H, Tago M, Igaki H, et al. Exceptionally high incidence of symptomatic grade 2-5 radiation pneumonitis after stereotactic radiation therapy for lung tumors. Radiat Oncol. 2007;2:21.
60. Guckenberger M, Baier K, Polat B, Richter A, Krieger T, Wilbert J, et al. Dose-response relationship for radiation-induced pneumonitis after pulmonary stereotactic body radiotherapy. Radiother Oncol. 2010;97:65–70.
61. Borst GR, Ishikawa M, Nijkamp J, Hauptmann M, Shirato H, Onimaru R, et al. Radiation pneumonitis in patients treated for malignant pulmonary lesions with hypofractionated radiation therapy. Radiother Oncol. 2009;91:307–13.
62. Timmerman R, Paulus R, Galvin J, Michalski J, Straube W, Bradley J, et al. Stereotactic body radiation therapy for inoperable early stage lung cancer. JAMA. 2010;303:1070–6.
63. Simone CB 2nd. Thoracic radiation normal tissue injury. Semin Radiat Oncol. 2017;27:370–7.
64. Lo SS, Sahgal A, Chang EL, Mayr NA, Teh BS, Huang Z, et al. Serious complications associated with stereotactic ablative radiotherapy and strategies to mitigate the risk. Clin Oncol. 2013;25:378–87.
65. Barriger RB, Forquer JA, Brabham JG, Andolino DL, Shapiro RH, Henderson MA, et al. A dose-volume analysis of radiation pneumonitis in non-small cell lung cancer patients treated with stereotactic body radiation therapy. Int J Radiat Oncol Biol Phys. 2012;82:457–62.
66. Harder EM, Park HS, Chen ZJ, Decker RH. Pulmonary dose-volume predictors of radiation pneumonitis following stereotactic body radiation therapy. Pract Radiat Oncol. 2016;6:e353–e9.
67. Bledsoe TJ, Nath SK, Decker RH. Radiation pneumonitis. Clin Chest Med. 2017;38:201–8.
68. Abratt RP, Morgan GW, Silvestri G, Willcox P. Pulmonary complications of radiation therapy. Clin Chest Med. 2004;25:167–77.
69. Delanian S, Porcher R, Rudant J, Lefaix JL. Kinetics of response to long-term treatment combining pentoxifylline and tocopherol in patients with superficial radiation-induced fibrosis. J Clin Oncol. 2005;23:8570–9.
70. Nuyttens JJ, Moiseenko V, McLaughlin M, Jain S, Herbert S, Grimm J. Esophageal dose tolerance in patients treated with stereotactic body radiation therapy. Semin Radiat Oncol. 2016;26:120–8.
71. Herfarth KK, Debus J, Lohr F, Bahner ML, Rhein B, Fritz P, et al. Stereotactic single-dose radiation therapy of liver tumors: results of a phase I/II trial. J Clin Oncol. 2001;19:164–70.
72. Tse RV, Hawkins M, Lockwood G, Kim JJ, Cummings B, Knox J, et al. Phase I study of individualized stereotactic body radiotherapy for hepatocellular carcinoma and intrahepatic cholangiocarcinoma. J Clin Oncol. 2008;26:657–64.
73. Videtic GM, Hu C, Singh AK, Chang JY, Parker W, Olivier KR, et al. A randomized phase 2 study comparing 2 stereotactic body radiation therapy schedules for medically inoperable patients with stage I peripheral non-small cell lung cancer: NRG Oncology RTOG 0915 (NCCTG N0927). Int J Radiat Oncol Biol Phys. 2015;93:757–64.
74. Cox BW, Jackson A, Hunt M, Bilsky M, Yamada Y. Esophageal toxicity from high-dose, single-fraction paraspinal stereotactic radiosurgery. Int J Radiat Oncol Biol Phys. 2012;83:e661–7.
75. Tuna Y, Kocak E, Dincer D, Koklu S. Factors affecting the success of endoscopic bougia dilatation of radiation-induced esophageal stricture. Dig Dis Sci. 2012;57:424–8.
76. Hourneaux de Moura EG, Toma K, Goh KL, Romero R, Dua KS, Felix VN, et al. Stents for benign and malignant esophageal strictures. Ann N Y Acad Sci. 2013;1300:119–43.
77. Freeman RK, Ascioti AJ, Giannini T, Mahidhara RJ. Analysis of unsuccessful esophageal stent placements for esophageal perforation, fistula, or anastomotic leak. Ann Thorac Surg. 2012;94:959–64; discussion 64–5
78. Garg AK, Shiu AS, Yang J, Wang XS, Allen P, Brown BW, et al. Phase 1/2 trial of single-session stereotactic body radiotherapy for previously unirradiated spinal metastases. Cancer. 2012;118:5069–77.
79. Garg AK, Wang XS, Shiu AS, Allen P, Yang J, McAleer MF, et al. Prospective evaluation of spinal reirradiation by using stereotactic body radiation therapy: The University of Texas MD Anderson Cancer Center experience. Cancer. 2011;117:3509–16.
80. Forquer JA, Fakiris AJ, Timmerman RD, Lo SS, Perkins SM, McGarry RC, et al. Brachial plexopathy from stereotactic body radiotherapy in early-stage NSCLC: dose-limiting toxicity in apical tumor sites. Radiother Oncol. 2009;93:408–13.
81. LaCouture TA, Xue J, Subedi G, Xu Q, Lee JT, Kubicek G, et al. Small bowel dose tolerance for stereotactic body radiation therapy. Semin Radiat Oncol. 2016;26:157–64.
82. Pollom EL, Chin AL, Diehn M, Loo BW, Chang DT. Normal tissue constraints for abdominal and thoracic stereotactic body radiotherapy. Semin Radiat Oncol. 2017;27:197–208.
83. Barney BM, Markovic SN, Laack NN, Miller RC, Sarkaria JN, Macdonald OK, et al. Increased bowel toxicity in patients treated with a vascular endothelial growth factor inhibitor (VEGFI) after stereotactic body radiation therapy (SBRT). Int J Radiat Oncol Biol Phys. 2013;87:73–80.
84. Hauer-Jensen M, Denham JW, Andreyev HJ. Radiation enteropathy – pathogenesis, treatment and prevention. Nat Rev Gastroenterol Hepatol. 2014;11:470–9.
85. Teo MT, Sebag-Montefiore D, Donnellan CF. Prevention and management of radiation-induced late gastrointestinal toxicity. Clin Oncol. 2015;27:656–67.
86. Hauer-Jensen M, Wang J, Denham JW. Bowel injury: current and evolving management strategies. Semin Radiat Oncol. 2003;13:357–71.
87. Brown LC, Lester RA, Grams MP, Haddock MG, Olivier KR, Arndt CAS, et al. Stereotactic body radiotherapy for metastatic and recurrent Ewing sarcoma and osteosarcoma. Sarcoma. 2014;2014:418270.
88. Yamazaki H, Ogita M, Himei K, Nakamura S, Kotsuma T, Yoshida K, et al. Carotid blowout syndrome in pharyngeal cancer patients treated by hypofractionated stereotactic re-irradiation using CyberKnife: a multi-institutional matched-cohort analysis. Radiother Oncol. 2015;115:67–71.
89. Cengiz M, Ozyigit G, Yazici G, Doğan A, Yildiz F, Zorlu F, et al. Salvage reirradiaton with stereotactic body radiotherapy for locally recurrent head-and-neck tumors. Int J Radiat Oncol Biol Phys. 2011;81:104–9.
90. Arneson K, Mondschein J, Stavas M, Cmelak AJ, Attia A, Horn L, et al. A phase I trial of concurrent sorafenib and stereotactic radiosurgery for patients with brain metastases. J Neurooncol. 2017;133:435–42.
91. Kroeze SG, Fritz C, Hoyer M, Lo SS, Ricardi U, Sahgal A, et al. Toxicity of concurrent stereotactic radiotherapy and targeted therapy or immunotherapy: a systematic review. Cancer Treat Rev. 2017;53:25–37.
92. Miller JA, Balagamwala EH, Angelov L, Suh JH, Rini B, Garcia JA, et al. Spine stereotactic radiosurgery with concurrent tyrosine kinase inhibitors for metastatic renal cell carcinoma. J Neurosurg Spine. 2016;25:766–74.
93. Haseltine JM, Rimner A, Gelblum DY, Modh A, Rosenzweig KE, Jackson A, Yorke ED, Wu AJ. Fatal complications after stereotactic

body radiation therapy for central lung tumors abutting the proximal bronchial tree. Pract Radiat Oncol. 2016;6(2):e27–33.
94. Emami B, Lyman J, Brown A, Coia L, Goitein M, Munzenrider JE, et al. Tolerance of normal tissue to therapeutic irradiation. Int J Radiat Oncol Biol Phys. 1991;21:109–22.
95. Timmerman RD. An overview of hypofractionation and introduction to this issue of seminars in radiation oncology. Semin Radiat Oncol. 2008;18:215–22.
96. Bentzen SM, Constine LS, Deasy JO, Eisbruch A, Jackson A, Marks LB, et al. Quantitative Analyses of Normal Tissue Effects in the Clinic (QUANTEC): an introduction to the scientific issues. Int J Radiat Oncol Biol Phys. 2010;76:S3–9.
97. Kirkpatrick JP, Marks LB, Mayo CS, Lawrence YR, Bhandare N, Ryu S. Estimating normal tissue toxicity in radiosurgery of the CNS: application and limitations of QUANTEC. J Radiosurg SBRT. 2011;1:95–107.

SRS and SBRT Integration with Supportive Care

Daniel N. Cagney and Tracy A. Balboni

Introduction

The burden of cancer is increasing globally [1]. Thus, the need for integrated oncological care including optimal palliation and supportive care is also increasing. Palliative care is defined as "patient and family-centered care that optimizes quality of life by anticipating, preventing, and treating suffering. Palliative care throughout the continuum of illness involves addressing physical, intellectual, emotional, social, and spiritual needs and to facilitate patient autonomy, access to information, and choice" [2]. Palliative radiation therapy aims to achieve meaningful relief of symptoms and promote quality of life in patients with advanced cancer. Palliative care delivered in definitive cancer care settings is at times separately referred to as "supportive care" [2].

Due to the frequently poor physical condition of patients with terminal cancers, and the need to achieve a fast relief response, the ideal would be to use a radiation modality that is delivered in a short time with minimal acute toxicity to attain durable palliation. This defines stereotactic radiation, a radiation therapy technique which prescribes fewer, larger-dose-per fraction treatments given over a shorter time than the usually protracted conventional radiation scheme. The goal of stereotactic radiation, stereotactic radiosurgery (SRS), and stereotactic body radiotherapy (SBRT) is to deliver ablative doses of radiation to tumors without damaging the surrounding healthy tissue. Their unique physical characteristics are high precision, high dose gradient outside of target volume, and high dose. Much of early and present mainstream clinical applications of SRS/SBRT are with curative intent or patients with a favorable prognosis.

D. N. Cagney (✉) · T. A. Balboni
Dana-Farber/Brigham and Women's Cancer Center, Boston, MA, USA

Harvard University, Department of Radiation Oncology, Boston, MA, USA
e-mail: dcagney@bwh.harvard.edu

Supportive care is a multi- and interdisciplinary effort. The function of supportive care is to reduce pain and suffering, allow discussions of goals of care, facilitate death with dignity, promote quality of life, and support patients, their families, and their caregivers. After a comprehensive clinical assessment, prognostication about the illness trajectory, the expected timelines, and maximizing the goals that are important to the patient come into play. Radiation oncologists play a crucial role in the delivery of supportive care in their role in administering radiation. This chapter highlights the current position of SRS/SBRT and its essential integration with supportive care.

Site-Specific Considerations

Importance of Estimating Life Expectancy

Life expectancy and the quality of remaining life are among the most important issues patients with metastatic cancer face. Physicians and other care providers often overestimate life expectancy, by as much as 3 months or more [3]. Accurate estimates of life expectancy are important to patients and physicians to set goals so that treatments that will have little or no benefit will be avoided, and treatments that will be effective or supportive care are implemented. Numerous prognostication models exist in radiation oncology which allows for the timely delivery of palliative radiation [4, 5]. Similarly, some site-specific models exist which allow for prognostication of patients; examples include with brain metastases [6, 7] or spinal metastases [8, 9]. Administration of chemotherapy and radiation therapy within the last month of life is cited as an indicator of poor quality of care [10]. Similarly, longer-courses of radiation are inappropriate during the last days or weeks of life. Without accurate estimates of life expectancy, avoiding overly aggressive therapy can be difficult. Though longer life expectancy has been used as an argument for longer,

D. M. Trifiletti et al. (eds.), *Stereotactic Radiosurgery and Stereotactic Body Radiation Therapy*,
https://doi.org/10.1007/978-3-030-16924-4_31

multifraction palliative regimens for the treatment of bone and brain metastasis, there are limited data to support this approach. Shorter life expectancy argues for a hypofractionated shorter course of radiation in all settings, given the equivalence of different fractionation regimens. If a person's survival is shorter than the time required for the onset of maximal palliative benefit from radiation, palliative care alone is appropriate.

Evolving Role of SRS/SBRT

Stereotactic radiation has become mainstream in oncology practice due to technical innovations including improvement in radiation treatment units with faster delivery of higher dose, intensity modulation, and improved radiation planning systems, use of image-guided techniques, and the acquisition of new radiobiological data. This innovative technology is usually called SRS when used in the brain and SBRT when used in the body. As defined by the American Society of Therapeutic Radiation Oncology (ASTRO), "Stereotactic Radiosurgery (SRS) is a distinct discipline that utilizes externally generated ionizing radiation in some instances to inactivate or eradicate (a) defined target(s) in the head and spine without the need to make an incision. The target is determined by high-resolution stereotactic imaging" [11]. These advances enabled the extension of radiosurgery to other body sites outside of intracranial region making it practical to deliver ablative radiation dose in 1 to 5 fractions. Stereotactic body radiotherapy (SBRT) is an external beam radiation therapy method used to very precisely give a high dose of radiation to an extracranial target within the body, using either a single dose or a limited number of fractions [12]. SBRT can be applied using noninvasive or minimally invasive stereotactic localization and radiation delivery techniques. It requires significantly improved delivery precision over that needed for conventional radiotherapy.

The justification for utilizing SRS/SBRT in all patients, particularly in patients with complicated palliative needs, is sound and straightforward; the higher fractional dose leads to quicker treatment delivery with resultant faster return to other therapies, e.g., systemic therapies or home hospice care, speedier relief, and/or prevention of symptoms and/or loss of function, and the high dose gradient minimizes radiation toxicity of normal tissues and thus better preserves patients' quality of life. Hypofractionated courses of radiation therapy are an ideal approach for palliation in advanced cancer patients including for symptoms such as pain, neurological symptoms, bleeding, and obstruction of the upper airway or urinary or gastrointestinal tracts making it possible to obtain excellent prompt results in a short treatment course.

Evidence for Supportive Care in Advanced Cancer

The provision of supportive and palliative care has undergone recent transformation mirroring the evolution in the precise delivery of stereotactic radiation. Several randomized controlled trials have provided level I evidence that supports the early integration of palliative care for patients with advanced-stage cancer [13–16]. For example, Temel and colleagues [14] published a landmark trial that enrolled 151 patients within 8 weeks of diagnosis of metastatic non-small-cell lung cancer (NSCLC) and randomly assigned them to receive routine oncological care either alone or combined with early specialist palliative care. The early provision of palliative care was associated with better quality of life, fewer depressive symptoms, less aggressive care at the end of life, improved longitudinal prognostic awareness, and longer survival (median 11.6 months versus 8.9 months; $P = 0.02$). More recently, a large cluster randomization trial compared specialist palliative care to routine oncological follow up in 461 patients with metastatic solid tumor, use of palliative care was associated with improved QoL, symptom burden, and patient satisfaction over time, whereas the group assigned to standard oncological care experienced a deterioration in these domains [15]. Bakitas and colleagues [16] examined the effect of combining nurse-led palliative care intervention and standard care in the Project ENABLE II trial. QoL and mood were found to be significantly better in the palliative care arm of this trial, although symptom burden, quality of end-of-life care, and survival were similar. Given these findings, the American Society of Clinical Oncology recently published recommendations for the early integration of concurrent palliative care in the care of advanced cancer patients [13].

SRS/SBRT and its integration with the incremental improvements in the provision of supportive care is likely to be a significant research topic in the future. There is the opportunity for patients who currently cannot be considered for treatment to have the possibility of a relatively nontoxic and short course of radiotherapy. This may improve their outcomes regarding either survival, palliation, or quality of life. It may well be that SBRT has the greatest role to play in these situations, for example, enabling patients currently considered to be without treatment options to be treated and cancer-related symptoms palliated.

Clinical Evidence

Brain Metastases

Brain metastases represent a common oncologic problem, most frequently from lung, breast, and melanoma

primary malignancies [17, 18]. Brain metastases are a frequent manifestation of advanced malignancy and may present with a variety of distressing symptoms, including headache, nausea, vomiting, unsteadiness, decreased memory, altered speech, and focal motor or sensory deficit. Moreover, the proper management of brain metastases also requires that the aggressiveness of treatment be tailored to factors related to the patient, the tumor, and the technologies available to the treating radiation oncologist. Several prognostic classification schemas form the basis for treatment recommendations, survival prediction, and for comparing treatment results [6, 7]. Prognostic scoring systems help guide these treatment decisions, with therapy ranging from whole brain treatment to surgical resection or SRS.

Data indicate that SRS without WBRT is the best initial treatment for patients with 1–4 brain metastases (assuming SRS is suitable based upon metastasis size, good patient performance status, and a controlled/controllable extracranial disease status), because WBRT does not improve survival and degrades cognitive performance [19–21]. The level 1 evidence in aggregate has been considered by radiation oncology professional societies resulting in increasing support for SRS alone for patients with limited brain metastases. WBRT can be reserved for salvage therapy in the event of relapse [22].

One resounding advantage to SRS for brain metastases, especially for frail and near-terminal patients, is the potential for completion of radiation treatment in a single day. The inconvenience of journeying back-and-forth for treatment is eliminated. This is particularly attractive in a national healthcare system setting where patients frequently travel long distances for their cancer treatments. Also, the probability of durable lesion control with SRS is far superior to that achieved with WBRT alone, conservatively estimated at ~70–80% after 1 year, with improvements from this baseline for smaller tumors, specific histologies, and the use of systemic therapy [19, 20]. Although further SRS treatment may be required in ~50% of patients due to distant brain metastases, the ease of repeating SRS for intracranial recurrence will ensure that WBRT continues to be a less commonly used palliative intervention reserved for leptomeningeal disease. The use of SRS alone in patients with more than four metastases has been reported. This study enrolled over a thousand patients. They concluded that there were no differences in survival for patients managed with definitive SRS for 2–4 brain metastases or 5–10 brain metastases [23]. At present, these are the best data to support the sole use of SRS for between five and ten brain metastases or indeed for patients with more than ten brain metastases.

Bone Metastases

Bone is a prevalent site of metastatic disease, affecting up to 70% of patients with advanced breast or prostate cancer and 15–30% of patients with carcinoma of other sites [24]. Bone metastases can be a significant source of morbidity, with symptoms including pain, fracture, hypercalcemia, and spinal cord or nerve root compression [25]. Treatment for bone metastases is often a collaborative effort between multiple practitioners including surgeons, radiation oncologists, medical oncologists, pain medicine specialists, and palliative medicine clinicians.

External beam radiation (EBRT) is often used for management of bone metastases and has been shown in multiple trials to offer symptom relief and local control [26–29]. However, with standard palliative fractionation, either single fraction or numerous fractions, for metastatic disease, there are moderate rates of toxicity, mainly fatigue and nausea/vomiting. In patients with longer anticipated life expectancies as indicated by (1) oligometastatic disease and/or (2) a prognostic algorithm estimating a median life expectancy greater than 12 months, SBRT enabling high target doses and minimizing dose to normal surrounding tissue can be a useful tool. Multiple publications examining SBRT in oligometastatic disease have shown promising outcomes. These studies have treated oligometastatic sites throughout the body including lung, liver, lymph node, and bone metastases [30, 31]. Among these patients with extended overall survival (median survival of approximately 24 months), excellent local control (about 75% at 2 years) and low rates of toxicity (<10% risk of grade 3 toxicity) have been reported.

Many anatomic structures have maximum cumulative tolerable doses; higher doses can cause severe toxicity. Reirradiation, particularly in the spine, presents technical challenges due to safety concerns in reirradiating normal tissues. The spinal cord has a tolerance that, if exceeded, can lead to cord myelopathy and/or spinal nerve radiculopathy causing significant morbidity [32]. SBRT allows high doses to be delivered in a highly conformal nature, minimizing dose to the spinal cord while still allowing the tumor to receive a high dose of radiation. A publication from Beth Israel Deaconess Medical Center reported their use of SBRT for reirradiation of epidural spinal metastases [33]. In patients with a local recurrence who were previously treated with EBRT (3 Gy × 10), SBRT was given (either 8 Gy × 3 if the tumor did not touch spinal cord or 5–6 Gy × 5 when tumor abutted the spinal cord). They reported very low toxicity (40% grade 1 fatigue and 20% grade 2 nausea), adequate pain relief (65%), and good local control (93% of the patients had stable or improved disease) at 1 year.

A series from MD Anderson Cancer Center [34] which treated 63 patients with spinal metastasis with fractionated SBRT (either 6 Gy 5 or 9 Gy × 3) showed no grade 3 or higher neurologic toxicity, low rates of overall toxicity (4 patients with grade 3 toxicity), and a 1-year freedom from tumor progression of 84%. A series from Memorial Sloan Kettering Cancer Center that treated 93 patients with spinal metastasis using single-fraction SBRT (18–24 Gy) showed a local failure rate of 7.5% at 2 years [35]. The Mayo Clinic published their series of SBRT for nonspine oligometastatic disease showing excellent local control (92% at 1 year and 86% at 2 years) and no grade 3 or higher toxicities [36]. Of the toxicities, fatigue and pain flare were the most common. SBRT for nonspine bone metastasis is also increasingly offered to patients. In most cases of nonspine bone metastases, critical structures are remote from the treated areas, and, therefore, highly conformal techniques delivering high dose or ablative radiotherapy are less frequently necessary. However, the most current ACR Appropriateness Criteria document does not recommend offering SBRT for painful nonspine bone metastases routinely [37]. Furthermore, the safety of bone SBRT in critical areas such as articular surfaces, long bones, and digits is unknown.

Given the good local control and low rates of toxicity, there are two clinical situations where SBRT can be a useful tool in patients with metastatic disease: (1) patients with excellent life expectancies, such as for those with an oligometastatic disease state or (2) those who need adequate reirradiation dose delivery to a previously treated bony site. These clinical applications are based on the goals of providing an adequate dose to (a) control the lesion for the patient's long life expectancy and (b) ensure normal tissue sparing to minimize treatment risks, particularly in the reirradiation setting.

Lung Cancer and Lung Metastases

The signature indication for SBRT is a patient with medically inoperable early-stage lung non-small-cell lung cancer. This population of patients frequently died of cancer if left untreated. Studies from the Nordic Group and the Radiation Therapy Oncology Group (RTOG) have shown over 90% local lesion control and 3-year overall survival of approximately 60% [38, 39]. The survival is roughly twice what was typically achieved historically.

In patients with a limited number of lung metastasis, SBRT may be used if surgical resection is not possible [40, 41]. Like cranial SRS, SBRT across all tumor sites may be interdigitated between chemotherapy cycles thus ensuring no compromise in systemic disease control. The usefulness of stereotactic radiotherapy in this setting is not only to prolong survival but also to limit the development of significant tumor-specific complications. Neoplasms involving the lung and mediastinum can cause problematic symptoms such as shortness of breath, cough, chest pain, hemoptysis, postobstructive pneumonia, and brachial plexopathy.

Liver Metastases

Liver metastases are a common clinical scenario in advanced malignancy that was rarely treated with palliative radiotherapy [42]. Still, the prevalence of liver metastases is high, and the resulting symptoms may be debilitating, including fatigue, abdominal pain, urticaria, nausea, vomiting, and altered mental status. While whole liver external beam radiotherapy was historically used as a treatment for painful liver metastases, the relatively low normal tissue tolerance of the entire liver has limited both the dose and the efficacy of this approach. Recent advances in the radiographic delineation of liver metastases, the delivery of SBRT, and the potential for image-guided radiation therapy have allowed for a more conformal dose delivery to liver lesions with a more favorable risk of side effects [43, 44]. Though further studies are required, the primary role of SBRT for liver metastases may mostly be in the prevention of tumor-related symptoms in the liver due to organ-replacing, progressive disease. Once the liver tumor burden has reached the point of causing symptoms, often the tumor extent is beyond what SBRT can safely manage, leaving only low-dose whole liver radiotherapy as a safe, palliative option. By managing metastatic liver disease early with highly ablative procedures, while sparing healthy liver, the progression of tumor to the aforementioned symptoms may be prevented.

Adrenal Metastases

Most adrenal metastases are asymptomatic and are detected during the process of imaging staging. However, some patients with extensive adrenal metastases experience significant pain for which palliative radiotherapy may be used. SBRT has been used to treat adrenal metastasis either as focal therapy for oligometastatic disease or pain palliation.

Toxicity and Rationale to Adopt SRS/SBRT

Brain Metastases

The prognosis of patients with brain metastases is often poor, and in patients with multiple intracranial lesions, the paradigm for treatment relies on the maximization of quality of life. Nearly all patients with brain metastases receive radiation therapy. This can be given as either whole-brain

radiation (WBRT) or as stereotactic radiation, which is distinguished by delivery of a higher dose to a highly focused area in either a single session (fraction) or multiple fractions. An increasing body of literature suggests that WBRT, relative to stereotactic radiation, can adversely impact quality of life among patients with a limited number of brain metastases. For patients with >4 brain metastases, however, no randomized trials comparing WBRT with stereotactic radiation exist, and it remains unknown whether stereotactic radiation or WBRT yields superior quality of life. There are several ongoing randomized studies currently evaluating this specific question.

Bone Metastases

Toxicities of spine RT have been reported as mild though often with substandard assessment (e.g., without patient-reported outcomes). GI toxicities have been assessed more rigorously among some bone metastases trials comparing 8 Gy × 1 to multifraction regimens for uncomplicated bone metastases, with GI toxicity rates as high as 17%. These reports are among all bone metastases (including nonspine) patients, however, so likely underestimate GI toxicities in the spine metastases population. Advances in modes of radiation delivery over the past few decades have produced novel methods of RT delivery that improve conformality to the target while minimizing dose to normal structures, and therefore RT-related toxicities. Among patients treated with spine SBRT, excellent local control (approximately 91% at 1 year) and low rates of toxicity (3% risk of grade 3 toxicity) have been reported.

Future Directions

Radiation therapy represents an essential tool for palliation in advanced cancer patients. With the advances in contemporary radiation therapy technologies, SRS/SBRT has become more readily accessible. Patients can benefit from its use to achieve higher dose delivery to tumor, better sparing of normal tissues and short treatment times. Because SRS/SBRT can produce rapid and efficacious palliation while minimizing toxicities, it is a valuable tool to optimize palliative care in advanced cancer for patients and their families. SRS and SBRT have become increasingly important in the palliative treatment of cancer patients over the past decade, and ongoing clinical experience and studies will shape what is likely to be a growing role in palliative and supportive cancer care.

SRS for brain metastases, admittedly nearly always a palliative intervention, has based on level 1 evidence recently been demonstrated to be the best treatment for most patients with brain metastases. Technological advances, including single isocenter linear accelerator-based therapy that permits more ready adoption of focused treatment of intracranial tumors, will also hasten the acceptance of this form of treatment, while WBRT becomes more selectively used for patients with leptomeningeal carcinomatosis or other clinical indications where focal therapies are not superior.

Just as for SRS, SBRT is a particularly attractive treatment modality where palliative patients with problematic symptoms frequently travel for long distances to get to a tertiary center for their cancer treatments. SBRT has developed into one of the standard therapies for spinal metastases; some may argue that it has not been compared with conventional radiotherapy concerning efficacy and toxicity in phase 3 randomized trials. Radiation Therapy Oncology Group (RTOG) study 0631 is an ongoing randomized controlled trial comparing traditional radiotherapy (8 Gy in 1 fraction) and SBRT (16 or 18 Gy in 1 fraction) in patients with 1–3 spinal metastases. Canadian researchers have opened a randomized phase 2 trial comparing 20 Gy in 5 fractions delivered conventionally to 24 Gy in 2 fractions given with SBRT.

Many centers are conducting various SBRT trials for numerous indications such as primary and metastatic lung tumors, primary and metastatic liver tumors, primary and recurrent pancreatic cancer, metastatic renal cell carcinoma, as a boost treatment for or salvage treatment for head and neck cancers. As more significant experience develops, there will be more apparent clinical data to guide indications for SBRT in the palliative (or curative) setting to prolong disease-free survivals, to potentiate impactful immunologic therapies, and to improve quality of life and overall survival.

Ongoing trials are needed to demonstrate the efficacy of these therapies in disease and quality of life outcomes for patients and their families. Future directions for palliative SRS/SBRT are anticipated to include simplification, through greater automation, of the detailed steps that are required for safe treatment delivery, thereby easing the costs of treatment delivery and the need for travel to tertiary cancer centers to receive these advanced palliative interventions. It is an exciting time to participate in the transformation currently ongoing in palliative radiotherapy that SRS and SBRT have ushered in.

Practical Considerations

- Ensure early provision of palliative care in patients with advanced malignancy.
- Radiation oncologists play a vital role in the delivery of supportive care and refer to a palliative care specialist for complex situations.
- Use a tool to screen for symptoms and other quality of life concerns routinely.

- Integrate life expectancy, QoL, and functional outcomes into prognostication.
- Discuss and document specific goals of care, mainly when there is a significant change in the patient's illness trajectory.
- The role of SRS/SBRT in patients with advanced cancer remains an active clinical question, particularly for patients with short anticipated life expectancy.
- As SRS/SBRT use continues to increase, it will be incumbent upon radiation oncologists to demonstrate the value of these techniques, particularly in patients with limited life expectancy.
- Ongoing studies must continue to evaluate questions of efficacy, toxicity, and long-term outcomes in comparison with both conventional palliative radiotherapy and best supportive care.

References

1. Ferlay J, Soerjomataram I, Dikshit R, Eser S, Mathers C, Rebelo M, et al. Cancer incidence and mortality worldwide: sources, methods and major patterns in GLOBOCAN 2012. Int J Cancer. 2015;136:359–86.
2. Clinical practice guidelines for quality palliative care. 3rd ed. National Consensus Project for Quality Palliative Care; 2013.
3. Glare P, Virik K, Jones M, Hudson M, Eychmuller S, Simes J, et al. A systematic review of physicians' survival predictions in terminally ill cancer patients. BMJ. 2003;327:195.
4. Chow E, Abdolell M, Panzarella T, Harris K, Bezjak A, Warde P, et al. Predictive model for survival in patients with advanced cancer. J Clin Oncol. 2008;26:5863–9.
5. Krishnan MS, Epstein-Peterson Z, Chen YH, Tseng YD, Wright AA, Temel JS, et al. Predicting life expectancy in patients with metastatic cancer receiving palliative radiotherapy: the TEACHH model. Cancer. 2014;120:134–14.
6. Sperduto PW, Berkey B, Gaspar LE, Mehta M, Curran W. A new prognostic index and comparison to three other indices for patients with brain metastases: an analysis of 1,960 patients in the RTOG database. Int J Radiat Oncol Biol Phys. 2008;70:510–4.
7. Gaspar L, Scott C, Rotman M, Asbell S, Phillips T, Wasserman T, et al. Recursive partitioning analysis (RPA) of prognostic factors in three Radiation Therapy Oncology Group (RTOG) brain metastases trials. Int J Radiat Oncol Biol Phys. 1997;37:745–51.
8. Rades D, Stalpers LJ, Veninga T, Schulte R, Hoskin PJ, Obralic N, et al. Evaluation of five radiation schedules and prognostic factors for metastatic spinal cord compression. J Clin Oncol. 2005;23:3366–37.
9. Shi DD, Chen YH, Lam TC, Leonard D, Balboni TA, Schoenfeld A, et al. Assessing the utility of a prognostication model to predict 1-year mortality in patients undergoing radiation therapy for spinal metastases. Spine J. 2018;18(6):935–40.
10. Earle CC, Landrum MB, Souza JM, Neville BA, Weeks JC, Ayanian JZ. Aggressiveness of cancer care near the end of life: is it a quality-of-care issue? J Clin Oncol. 2008;26:3860–6.
11. Seung SK, Larson DA, Galvin JM, Mehta MP, Potters L, Schultz CJ, et al. American College of Radiology (ACR) and American Society for Radiation Oncology (ASTRO) practice guideline for the performance of stereotactic radiosurgery (SRS). Am J Clin Oncol. 2013;36:310.
12. Potters L, Kavanagh B, Galvin JM, Hevezi JM, Janjan NA, Larson DA, et al. American Society for Therapeutic Radiology and Oncology (ASTRO) and American College of Radiology (ACR) practice guideline for the performance of stereotactic body radiation therapy. Int J Radiat Oncol Biol Phys. 2010;76:326–32.
13. Ferrell BR, Temel JS, Temin S, Alesi ER, Balboni TA, Basch EM, et al. Integration of palliative care into standard oncology care: American Society of Clinical Oncology Clinical Practice Guideline update. J Clin Oncol. 2017;35:96–112.
14. Temel JS, Greer JA, Muzikansky A, Gallagher ER, Admane S, Jackson VA, et al. Early palliative care for patients with metastatic non-small-cell lung cancer. N Engl J Med. 2010;363:733–42.
15. Zimmermann C, Swami N, Krzyzanowska M, Hannon B, Leighl N, Oza A, et al. Early palliative care for patients with advanced cancer: a cluster-randomised controlled trial. Lancet. 2014;383:1721–30.
16. Bakitas MA, Tosteson TD, Li Z, Lyons KD, Hull JG, Li Z, et al. Early versus delayed initiation of concurrent palliative oncology care: patient outcomes in the ENABLE III randomized controlled trial. J Clin Oncol. 2015;33:1438–45.
17. Nayak L, Lee EQ, Wen PY. Epidemiology of brain metastases. Curr Oncol Rep. 2012;14:48–54.
18. Cagney DN, Martin AM, Catalano PJ, Redig AJ, Lin NU, Lee EQ, et al. Incidence and prognosis of patients with brain metastases at diagnosis of systemic malignancy: a population-based study. Neuro-Oncology. 2017;19(11):1511–21.
19. Brown PD, Jaeckle K, Ballman KV, Farace E, Cerhan JH, Anderson SK, et al. Effect of radiosurgery alone vs radiosurgery with whole brain radiation therapy on cognitive function in patients with 1 to 3 brain metastases: a randomized clinical trial. JAMA. 2016;316:401–9.
20. Aoyama H, Shirato H, Tago M, Nakagawa K, Toyoda T, Hatano K, et al. Stereotactic radiosurgery plus whole-brain radiation therapy vs stereotactic radiosurgery alone for treatment of brain metastases: a randomized controlled trial. JAMA. 2006;295:2483–91.
21. Chang EL, Wefel JS, Hess KR, Allen PK, Lang FF, Kornguth DG, et al. Neurocognition in patients with brain metastases treated with radiosurgery or radiosurgery plus whole-brain irradiation: a randomised controlled trial. Lancet Oncol. 2009;10:1037–44.
22. Soltys SG, Kirkpatrick JP, Laack NN, Kavanagh BD, Breneman JC, Shih HA. Is less, more? The evolving role of radiation therapy for brain metastases. Int J Radiat Oncol Biol Phys. 2015;92:963–6.
23. Yamamoto M, Serizawa T, Shuto T, Akabane A, Higuchi Y, Kawagishi J, et al. Stereotactic radiosurgery for patients with multiple brain metastases (JLGK0901): a multi-institutional prospective observational study. Lancet Oncol. 2014;15:387–95.
24. Gavrilovic IT, Posner JB. Brain metastases: epidemiology and pathophysiology. J Neuro-Oncol. 2005;75:5–14.
25. Coleman R. Metastatic bone disease: clinical features, pathophysiology and treatment strategies. Cancer Treat Rev. 2001;27:165–176, 2001.
26. Chow E, Harris K, Fan G, Tsao M, Sze WM. Palliative radiotherapy trials for bone metastases: a systematic review. J Clin Oncol. 2007;25:1423–36.
27. Cole D. A randomized trial of a single treatment versus conventional fractionation in the palliative radiotherapy of painful bone metastases. Clin Oncol. 1989;1:59–62.
28. Wu JSY, Wong R, Johnston M, Bezjak A, Whelan T, Cancer Care Ontario Practice Guidelines Initiative Supportive Care Group. Meta-analysis of dose-fractionation radiotherapy trials for the palliation of painful bone metastases. Int J Radiat Oncol Biol Phys. 2003;55:594–605.
29. van der Linden YM, Steenland E, van Houwelingen HC, Post WJ, Oei B, Marijnen CA, et al. Patients with a favourable prognosis are equally palliated with single and multiple fraction radiotherapy:

results on survival in the Dutch Bone Metastasis Study. Radiother Oncol. 2006;78:245–53.
30. Tree AC, Khoo VS, Eeles RA, Ahmed M, Dearnaley DP, Hawkins MA, et al. Stereotactic body radiotherapy for oligometastases. Lancet Oncol. 2013;14:e28–37.
31. Milano MT, Katz AW, Muhs AG, Philip A, Buchholz DJ, Schell MC, et al. A prospective pilot study of curative-intent stereotactic body radiation therapy in patients with 5 or fewer oligometastatic lesions. Cancer. 2008;112:650–8.
32. Nieder C, Grosu AL, Andratschke NH, Molls M. Update of human spinal cord reirradiation tolerance based on additional data from 38 patients. Int J Radiat Oncol Biol Phys. 2006;66:1446–9.
33. Mahadevan A, Floyd S, Wong E, Jeyapalan S, Groff M, Kasper E. Stereotactic body radiotherapy reirradiation for recurrent epidural spinal metastases. Int J Radiat Oncol Biol Phys. 2011;81:1500–5.
34. Chang EL, Shiu AS, Mendel E, Mathews LA, Mahajan A, Allen PK, et al. Phase I/II study of stereotactic body radiotherapy for spinal metastasis and its pattern of failure. J Neurosurg Spine. 2007;7(2):151–60.
35. Yamada Y, Bilsky MH, Lovelock DM, Venkatraman ES, Toner S, Johnson J, et al. High-dose, single-fraction image-guided intensity-modulated radiotherapy for metastatic spinal lesions. Int J Radiat Oncol Biol Phys. 2008;71:484–90.
36. Owen D, Laack NN, Mayo CS, Garces YI, Park SS, Bauer HJ, et al. Outcomes and toxicities of stereotactic body radiation therapy for non-spine bone oligometastases. Pract Radiat Oncol. 2014;4:e143–9.
37. Lutz ST, Lo SS, Chang EL, Galanopoulos N, Howell DD, Expert Panel On Radiation Oncology-Bone Metastases, et al. ACR Appropriateness Criteria® non-spine bone metastases. J Palliat Med. 2012;15:521–6.
38. Timmerman R, Paulus R, Galvin J, Michalski J, Straube W, Bradley J, et al. Stereotactic body radiation therapy for inoperable early stage lung cancer. JAMA. 2010;303:1070–6.
39. Baumann P, Nyman J, Hoyer M, Wennberg B, Gagliardi G, Lax I, et al. Outcome in a prospective phase II trial of medically inoperable stage I non–small-cell lung cancer patients treated with stereotactic body radiotherapy. J Clin Oncol. 2009;27:3290–6.
40. Rusthoven KE, Kavanagh BD, Burri SH, Chen C, Cardenes H, Chidel MA, et al. Multi-institutional phase I/II trial of stereotactic body radiation therapy for lung metastases. J Clin Oncol. 2009;27:1579–84.
41. Ricardi U, Filippi AR, Guarneri A, Ragona R, Mantovani C, Giglioli F, et al. Stereotactic body radiation therapy for lung metastases. Lung Cancer. 2012;75:77–81.
42. Manfredi S, Lepage C, Hatem C, Coatmeur O, Faivre J, Bouvier AM. Epidemiology and management of liver metastases from colorectal cancer. Ann Surg. 2006;244:254.
43. Tse RV, Hawkins M, Lockwood G, Kim JJ, Cummings B, Knox J, et al. Phase I study of individualized stereotactic body radiotherapy for hepatocellular carcinoma and intrahepatic cholangiocarcinoma. J Clin Oncol. 2008;26:657–64.
44. Tanguturi SK, Wo JY, Zhu AX, Dawson LA, Hong TS. Radiation therapy for liver tumors: ready for inclusion in guidelines? Oncologist. 2014;19:868–79.

Targeted Agents and Immunotherapy

Arrvind Raghunath, Vyshak Alva Venur,
and Manmeet S. Ahluwalia

Introduction

Brain metastases (BM) are the most common intracranial tumors in adults and are a devastating complication of advanced malignancies causing significant morbidity for patients. The most common malignancies resulting in BM are lung cancer, breast cancer, and melanoma. The estimated global incidence of BM was 9.6% for all primary sites combined, and highest for lung (19.9%), followed by melanoma (6.9%), renal (6.5%), and breast (5.1%) [1]. It is estimated that approximately 40% of patients with metastatic cancer will develop a symptomatic BM [2]. In the past, the cornerstone for treatment of BM was whole brain radiation therapy (WBRT), stereotactic radiosurgery (SRS), and surgery. Conventional chemotherapeutic agents had limited activity in BM due to poor blood-brain barrier penetration and the activity of efflux pumps. The discovery of driver mutations and agents targeting these mutations has dramatically changed the approach to treating these patients in the past decade. The most common actionable mutations are the epidermal growth factor receptor (EGFR) mutation and the anaplastic lymphoma kinase (ALK) translocations in non-small cell lung cancer, human epidermal growth factor receptor 2 (HER2) in breast cancer, and BRAF mutation in melanoma. Prognostic indices have been developed to predict treatment outcomes. Recently, disease-specific graded prognostic assessment identified prognostic factors for each of the major tumor types resulting in BM [3]. Further revised prognostic indices are incorporating various genetic alterations like EGFR and ALK mutation in lung cancer; estrogen receptor (ER), progesterone receptor (PR), and HER-2 in breast cancer; and BRAF mutation in melanoma, thereby reflecting the increased treatment sensitivity of tumors with these mutations.

Unique Challenges and Biology of Using Systemic Treatment for BM

The genetic makeup of BM can differ from the primary tumor. Several proteins belonging to the PI3/AKT pathway were overexpressed in the BM on parallel evaluation of copy number variations, hotspot mutations, global mRNA expression patterns, quantitative analysis of protein expression, and activation in pairs of melanoma BM and extracranial metastases [4]. Genomic study of BM patients compared somatic point mutations and copy number variations with primary tumors in 86 patients showed a branched evolutionary pattern. The study demonstrated that both primary tumor and BM share a number of common mutations, but BM also developed distinct mutations at times [5]. These results highlight the importance to individualize systemic therapeutic approaches in BM. In addition, efficacy of a systemic anticancer agent depends on its ability to reach the tumor microenvironment in high enough concentrations. The tight junctions of the blood-brain barrier (BBB) prevent the entry of large molecules (>150 kDa) across it. The barrier limits the hydrophilic, ionized, and protein-bound molecules from getting in the brain. In addition, the efflux pumps on blood vessels actively pump out drugs that are able to permeate the barrier [6, 7]. Some of the methods that have been tested so far include convection-enhanced delivery, disruption of barrier by ultrasound, and osmotic barrier disruption [8, 9]. Until recently, central nervous system (CNS) was believed to an immune-privileged organ. However, the use

A. Raghunath
Cleveland Clinic Akron General, Akron, OH, USA

Cleveland Clinic Lerner School of Medicine, Department of Internal Medicine, Cleveland, OH, USA

V. A. Venur
Dana-Farber Cancer Institute, Division of Neuro-Oncology, Boston, MA, USA

M. S. Ahluwalia (✉)
Cleveland Clinic, Burkhardt Brain Tumor and Neuro-Oncology Center, Cleveland, OH, USA
e-mail: ahluwam@ccf.org

D. M. Trifiletti et al. (eds.), *Stereotactic Radiosurgery and Stereotactic Body Radiation Therapy*,
https://doi.org/10.1007/978-3-030-16924-4_32

of immunotherapy has shown immune responses in BM [10]. Use of immunotherapy impacts the expression of microglial cells, myeloid-derived suppressor cells, macrophages, and tumor-infiltrating lymphocytes in the tumor microenvironment, and there are several ongoing studies to examine the role of immunotherapy in BM [11]. In this review, we will discuss the current state of the development of targeted and immunotherapy agents in BM.

Lung Cancer and Brain Metastases

Lung cancer is the leading cause of cancer-related mortality worldwide and has the highest incidence of BM [12]. Lung cancer is divided into two groups: non-small cell lung cancer (NSCLC) and small cell lung cancer. At presentation, approximately 7–8% of patients with NSCLC harbor BM, and up to half of the patients develop BM during the course of their disease [13, 14]. A number of patients with lung cancer develop leptomeningeal metastases that have dismal prognosis of 2–4 months on an average [15]. Several small molecule inhibitors that target EGFR and ALK tyrosine kinases are approved.

EGFR Tyrosine Kinase Inhibitors

EGFR of the HER/erbB family is a transmembrane protein receptor with tyrosine kinase activity along the inner cytoplasmic domain. The extracellular domain of EGFR interacts with specific ligands, and that leads to homodimerization, resulting in autophosphorylation and consequent transduction of growth signals from the extracellular portion into the cell [16]. Activating mutations in the tyrosine kinase domain of the EGFR receptor are reported in 35% of people of East Asian origin and in 10% of Caucasian population [17]. Of all known EGFR mutations, the two most common are the Exon 19 (in-frame) deletions and point mutations (L858R) at exon 21 that constitute 90% mutations [18]. There is evidence that patients with an EGFR mutation have a propensity to develop BM more commonly, tend to have more numerous however smaller lesions, and have a better overall survival compared with BM in lung cancer patients that lack oncogenic drivers [19]. There are three generations of EGFR inhibitors in clinical use. The first-generation EGFR targeting tyrosine kinase inhibitors (TKI) include erlotinib and gefitinib. They are both approved by the FDA for use in lung cancer [20]. Erlotinib does not penetrate the normal CNS in high concentrations; however, it demonstrates penetration when the BBB is broken such as in the presence of BM [21]. Its active metabolite—OSI-420—is a substrate of P-glycoprotein (P-gp) that results in efflux of this metabolite [22]. Gefitinib inhibits P-gp activity, and none of its known metabolites are substrates of P-gp activity [23]. However, both of these drugs have limited penetration through the barrier, and CSF concentrations of both of these drugs (erlotinib 5%, gefitinib 2.5%) are relatively low [24, 25]. A phase II study of 31 patients with EGFR-mutant NSCLC and asymptomatic BM treated with gefitinib or erlotinib showed 74% intracranial objective response rate. The treatment was associated with overall survival (OS) of 18.8 months and progression-free survival (PFS) of 7.1 months showing efficacy of the regimen [26]. Another study of 41 BM and EGFR-mutant NSCLC patients when treated with gefitinib resulted in response rate of 87.8%. Gefitinib use resulted in OS of 21.9 months and a PFS of 14.5 months [27]. Several preclinical studies with human cell lines have indicated that EGFR TKIs enhance radiation therapy [28]. In a prospective phase II study, 40 patients with BM received erlotinib for 1 week prior to WBRT, concurrently with WBRT followed by maintenance erlotinib [29]. Nine of the 40 patients carried an EGFR mutation, and an overall response rate of 89.9% with a median overall survival of 19.1 months was noted in that group. In a randomized phase II study, 80 patients with BM from NSCLC received either erlotinib or placebo with WBRT [30]. Thirty-five of 40 patients in the erlotinib arm had wild-type EGFR; no significant difference in progression-free survival and overall survival was noted between the two groups.

The second-generation EGFR-TKI, afatinib, is an irreversible inhibitor of EGFR [31]. It also inhibits HER2 and ErbB4 receptors and was initially developed to overcome the T790 M mutation [32]. Two phase III studies LUX-Lung 3, a randomized phase III study of afatinib or cisplatin plus pemetrexed in metastatic lung adenocarcinoma with EGFR mutation, and LUX-Lung 6, a randomized, open label phase III study of afatinib versus chemotherapy as first-line therapy for patients with stage IIIB or IV adenocarcinoma of lung harboring an EGFR activating mutation, included patients with asymptomatic BM [31, 32]. Although intracranial response rates were not assessed, the afatinib group had a significantly higher median progression-free survival to the chemotherapy group in both the trials [Lux-Lung 3, 11.14 versus 5.39 months, HR = 0.54 (95% CI = 0.23–1.25); and Lux-Lung 6, 8.21 versus 4.62 months, HR = 0.47 (95% CI = 0.18–1.21)]. There was no significant difference in OS in either trial [33].

Several third-generation EGFR TKIs, including osimertinib, rociletinib, ASP-8273, and HM-61713, are in clinical investigations [30, 31, 34]. These agents spare wild-type EGFRs and target mutant EGFRs, including T790M [35]. There have been case reports of osimertinib having CNS activity, and the initial trials (AURA and AURA 2) enrolled 162 patients with BM, showing impressive response rates of

approximately 54% [36]. AZD-3759 is a novel EGFR TKI designed to cross the BBB; however, it lacks activity against T790 M mutation [37]. Preclinical studies have shown that AZD-3759 is not a substrate of P-gp efflux pumps and has significantly higher penetration across the BBB. Preliminary results of the ongoing phase I trial of AZD-3759 demonstrated that the drug was well tolerated, with early evidence of intracranial activity [38].

ALK Tyrosine Kinase Inhibitors

In 2–7% of lung adenocarcinomas, an inversion of chromosome 2p is noted resulting in the fusion of the intracellular signaling portion of the ALK receptor tyrosine kinase with a protein encoded by the echinoderm microtubule-associated protein-like 4 (EML-4). This fusion protein constitutively activates the tyrosine kinase and downstream pathway including the PI3-kinase and RAS pathways [39]. The first approved anti-ALK tyrosine kinase inhibitor was crizotinib has limited CNS penetration, evidenced by CSF-serum ratio of <0.1–0.26% in two separate studies [40]. Nevertheless, CNS activity has been seen in several case reports and retrospective sub-analyses of clinical trials. In a retrospective pooled analysis of 388 patients enrolled in the PROFILE 1005–1007 clinical trial of crizotinib, 275 patients had asymptomatic BM [41]. Of the 275 patients with BM, 166 had received prior treatment. Among the patients who received prior treatment compared with treatment-naïve patients, the intracranial disease control rate was similar. However, the median intracranial time to tumor progression was 7 months for patients with previously untreated BM compared with 13.2 months for patients with previously treated BM. In addition, the patients who continue crizotinib beyond progression had better overall survival compared with those who discontinued treatment at progression. Ceritinib and alectinib are second-generation ALK inhibitors that can be used to overcome drug resistance to crizotinib [42, 43]. The phase I trial of ceritinib (ASCEND-1) accrued 246 patients, 124 of which had BM at baseline [44]. Of these, 98 patients had received ALK inhibitors in the past, whereas 26 patients were ALK inhibitor-naïve. Seven out of the 14 patients with measurable BM showed an intracranial response, and 3 patients had stable disease. Brigatinib is another ALK inhibitor that has shown intracranial activity in an early phase I/II trial [45]. A phase I trial of brigatinib included 46 patients with BM. Thirteen patients had evaluable BM; nine patients (69%) had regression of the intracranial lesions, including four patients with a complete response and two with a partial response [45]. The median intracranial PFS was 97 weeks. The phase II trial of this agent is currently accruing patients and includes a cohort of patients with BM [45].

Vascular Endothelial Growth Factor (VEGF) Inhibitors

VEGF targeting agents have been used with some success in primary brain tumors, but have only shown modest activity in BM patients. A non-randomized phase II study investigating the efficacy and safety of bevacizumab in chemotherapy-naïve or pretreated patients with NSCLC and asymptomatic untreated BM was done. Patients with untreated, symptomatic BM received first-line bevacizumab (B) plus carboplatin and paclitaxel (CP) or second-line bevacizumab plus erlotinib (E). The B + CP group had median progression-free survival and median overall survival of 6.7 and 16.0 months, respectively. Overall response rate with B + CP was 62.7%. The B + E group had median progression-free survival and median overall survival of 6.3 and 12 months, respectively, with objective response rate of 12.5%. The trial used Response Evaluation Criteria in Solid Tumors (RECIST 1.0) criteria to assess response and bevacizumab was used in both the groups, therefore it is difficult to predict the effect of bevacizumab in either arm. Moreover, from glioma trials it is clear that bevacizumab can improve progression-free survival, without affecting overall survival [46].

Small Cell Lung Cancer (SCLC) and Brain Metastases

SCLC accounts for 20% of all lung cancers [47]. Approximately, 10% of patients present with BM at the time of initial diagnosis, and an additional 40–50% will develop BM during the disease [48, 49]. SCLC is generally chemosensitive. Prophylactic cranial irradiation is recommended for limited-stage SCLC as BM from SCLC has a poor prognosis. Traditionally, BM from SCLC has been treated with WBRT. Current standard of care for SCLC BM is individualized based on the presence of symptoms. For asymptomatic BM, upfront systemic therapy can be considered followed by WBRT, while for symptomatic BM, WBRT is given first followed by systemic therapy.

Breast Cancer and Brain Metastases

Breast cancer is the second most common malignancy that results in BM. It is further classified by estrogen, progesterone, and HER2 receptor status (ER/PR/HER2) into four intrinsic molecular subtypes: luminal A (ER, PR positive, HER2 negative), luminal B (ER/PR positive, HER2 positive), HER2 (HER2 positive, ER/PR negative), and basal subtype (ER/PR and HER2 negative). The incidence of BM

varies by these subtypes, with HER2 being the most common accounting for approximately 30–55% of BM from breast cancer [50, 51]. The anti-HER2 agents like trastuzumab have been effective in controlling the extracranial disease hence prolonging the overall survival. However, most of these anti-HER2 monoclonal antibodies do not cross the BBB leading to increased incidence of BM with controlled extracranial disease [52]. The time from primary diagnosis to the development of BM and prognosis once BM have occurred both correlate with subtype, with the basal subtype having the worst median survival of 3–4 months and luminal B having the best median survival of 19–20.7 months [53, 54].

The HER2 receptor belongs to the EGFR family of transmembrane tyrosine kinase receptors. Trastuzumab is a monoclonal antibody which attaches to the extracellular domain of the HER2 receptor, and blocks its homodimerization, preventing phosphorylation and downstream activity [55]. The CSF concentration of trastuzumab is dependent on the integrity of the blood-brain barrier. The plasma to CSF ratio ranges from 300:1 in patients without BM to 79:1 after receiving radiation therapy for the treatment of BM [56, 57]. Despite this increase in CSF concentration, trastuzumab has limited intracranial efficacy. Several studies have shown survival benefit with continuing trastuzumab beyond the development of BM as it provides excellent extracranial disease control [51, 58, 59].

The HER2 receptors can be activated by heterodimerization with EGFR receptors, and occasionally even when HER2 is downregulated, EGFR receptors can cause activation of downstream pathway [60, 61]. Therefore, dual inhibitors of HER2 and EGFR receptors were developed [62]. One such small molecule tyrosine kinase inhibitor, lapatinib, is approved in combination with capecitabine for metastatic breast cancer [63]. Although, lapatinib as a single agent had modest intracranial activity with a response rate of 3–6%, in a phase II study of treatment-naïve HER2-positive breast cancer patients with BM, the combination of lapatinib and capecitabine improved the intracranial response rate to 66% [64–67]. Three other small molecule anti-HER2 inhibitors, namely, neratinib, tesevatinib, and ONT-380, are being studied in advanced breast cancer patients with BM [68]. A phase II multicenter study showed modest intracranial activity with neratinib, an irreversible inhibitor of erbB1, HER2, and erbB4. The intracranial response rate was 8% with a median progression-free survival of 1.9 months and overall survival of 8.7 months among 40 patients enrolled in the study [69]. The drug-antibody conjugate T-DM1 (trastuzumab plus emtansine) is approved by the FDA for HER2-positive breast cancer after progression on trastuzumab. In a retrospective report involving ten patients with asymptomatic or progressive BM, an intracranial response rate of 20% was seen [70].

Melanoma and Brain Metastases

Melanoma has generally been resistant to chemotherapy. Approximately 50% of the advanced melanoma patients harbor *BRAF* mutation, and the discovery of BRAF and MEK inhibitors has led to improved survival in this subgroup of patients. 40–60% of melanoma patients develop BM during the course of the disease [71]. The BRAF kinase is an integral part of the mitogen-activated protein kinase (MAP) pathway that transmits mitogenic signals from activated cell surface growth factor receptors. Dabrafenib and vemurafenib are two FDA-approved BRAF inhibitors [72]. The combination of BRAF inhibitors and MEK inhibitors (trametinib and cobimetinib) has improved outcomes compared to single agent BRAF inhibitors. Promising intracranial activity was reported in an interim analysis of a phase II study of dabrafenib and trametinib (COMBI-MB) in patients with BM from BRAF mutant melanoma[74]. This trial has four cohorts. Cohort A and cohort B enrolled patients with BRAF V600E mutation and asymptomatic BM; however, cohort A included treatment-naïve patients, whereas cohort B included patients with progressive BM. The cohort C enrolled BRAF V600 D/K/R with asymptomatic BM and cohort D enrolled V600 E/K/R with symptomatic BM. The patients in all the cohorts were treated with dabrafenib 150 mg twice daily and trametinib 2 mg once daily. The interim results reported the intracranial activity in 76 patients enrolled in cohort A, 16 each in cohorts B and C, and 17 in cohort D. The intracranial disease control rates were 78, 75, 88, and 82% in cohorts A, B, C, and D, respectively. Complete responses were reported in three patients in cohort A and one each in cohorts B and C. Cohort B had the longest median progression-free survival with 7.2 months, while cohort C had the shortest median progression-free survival with 4.2 months. Cohorts A and D had median progression-free survival of 5.6 and 5.5 months, respectively. The median duration of response was 6.5, 7.3, 8.3, and 4.5 months in cohorts A, B, C, and D, respectively [73]. Although, the mature results of this study are awaited, the reported response rates and disease control rates are striking.

Checkpoint inhibition, with either anti-CTLA4 antibody or anti-PD1 antibodies, is being employed as another key treatment option for metastatic melanoma, irrespective of the *BRAF* mutation status. These antibodies potentiate the immune response to cancer antigens by blocking the downregulating interaction between the T-cells or tumor cells and T-cells. A phase II study reported intracranial activity of ipilimumab, an anti-CTLA4 antibody [74]. It included 72 patients; a 12-week intracranial disease control rate of 18% was reported for patients not on steroids, compared to 5% in those on steroids. Pembrolizumab

and nivolumab are two checkpoint inhibitors that target the programmed death-1 (PD-1) axis and are approved for metastatic melanoma. A phase II Australian study of nivolumab or nivolumab plus ipilimumab in patients with active BM from melanoma was recently published [74]. The treatment-naïve patients were randomized to two arms: 33 patients in arm A who received nivolumab 1 mg/kg plus ipilimumab 3 mg/kg every 3 weeks for 4 doses, followed by nivolumab 3 mg/kg once every 2 weeks, and 27 patients in arm B who received nivolumab 3 mg/kg every 2 weeks. Patients on steroids were excluded from both the arms; however, 16 patients with previously treated brain metastases were enrolled in arm C who could be on prednisone <10 mg. Intracranial response rate at 12 weeks, by RECIST v1.1 criteria, was the primary endpoint. With a median follow-up of 16.4 months, intracranial response was noted in 42, 20, and 6% of patients in arms A, B, and C, respectively. The median intracranial PFS was 4.8 months in arm A, 2.7 months in arm B, and 2.5 months in arm C. The neurologic adverse events were seen in four patients only (one radionecrosis, one seizure, and two headaches).

Conclusions/Future Directions

The newer targeted and immunotherapy agents have shown promising results in our war against BM. New agents are being developed with better CNS penetration. Several organizations, including the FDA and the American Society of Clinical Oncology, are emphasizing the inclusion of patients with BM in all phases of clinical drug development [75]. Improved understanding of biology and innovative drug development can help lead to improvement in the management of BM. Increasingly targeted therapies will have a significant role in the treatment of patients with BM with actionable mutations.

A new area of research is the integration of radiation therapy, both SRS and WBRT with immunotherapy. The rationale of combining the two as an effective modality has been due to the abscopal effect where radiation at one site leads to regression of metastases at a different site that has not been exposed to radiation. There have been studies validating this phenomenon which have shown better overall survival and less regional recurrence [76–78]. There are at least two ongoing trials (NCT03340129, NCT02696993) investigating this effect. This phenomenon could be explored further to prove the benefit of concurrent immunotherapy and SRS for BM. There have been studies to prove that concurrent use of immune checkpoint inhibitors and SRS for BM is associated with a decreased incidence of new BM [79]. More studies are needed to look at outcomes of targeted therapies as salvage therapy for recurrences post-SRS.

Practical Considerations

- Brain metastases are the most common intracranial tumors in adults. The most common malignancies that metastasize to the brain include lung, breast, melanoma, and renal.
- The traditional cornerstone for treatment of BM included WBRT, SRS, and surgery due to limited activity of conventional chemotherapeutic agents secondary to multiple factors.
- The most common actionable mutations are the EGFR and ALK mutations in NSCLC, HER2 in breast cancer, and BRAF mutations in melanoma.
- It is important to individualize systemic approaches in BM as the genetic makeup of BM differs from the primary tumor.
- Immunotherapy has shown to have a response rates in BM comparable to systemic treatment.
- The first-generation EGFR agents, erlotinib and gefitinib, have been approved by the FDA and have shown efficacy. Studies have also shown that radiation therapy is enhanced by EGFR agents. Although with WBRT and erlotinib studies failed to show any survival benefit in prospective manner in unenriched patient population.
- Afatinib is an irreversible EGFR inhibitor developed to overcome the T790 M mutation and has shown to have a higher median progression-free survival.
- The third-generation agents, osimertinib and rociletinib, were developed to spare wild-type EGFRs and target mutant EGFRs. They have been shown to have impressive response rates.
- The first approved anti-ALK agent was crizotinib and has limited CNS penetration, but has shown intracranial disease control.
- The drug resistance to crizotinib can be overcome by second-generation ALK agents such as ceritinib and alectinib.
- Anti-VEGF agents have shown limited activity in BM, as compared to their activity against primary brain tumors. They have been shown to increase progression-free survival without affecting overall survival.
- Trastuzumab is a monoclonal antibody against HER2 receptor. It has limited intracranial efficacy in BM from breast cancer but has excellent extracranial activity.
- Lapatinib with capecitabine is approved for metastatic breast cancer and improved the intracranial response rate to 66% in radiation-naïve patients. The durability of response was limited in with such combination of approximately 6 months.
- The drug-antibody conjugate T-DM1 is FDA approved for HER2-positive breast cancer after progression on trastuzumab. It has shown intracranial activity in case reports.

- Melanoma is generally chemoresistant. The discovery of BRAF and MEK inhibitors has led to improved survival. Dabrafenib and vemurafenib are drugs that target BRAF.
- The combination of BRAF and MEK inhibitors has improved outcomes with intracranial disease control compared to single-agent BRAF inhibitors.
- Immune checkpoint inhibitors with either anti-CTLA-4 or anti-PD1 antibodies are being used in melanoma have demonstrated preliminary efficacy in brain metastases in asymptomatic patients.

References

1. Barnholtz-Sloan JS, Sloan AE, Davis FG, Vigneau FD, Lai P, Sawaya RE. Incidence proportions of brain metastases in patients diagnosed (1973 to 2001) in the metropolitan detroit cancer surveillance system. J Clin Oncol. 2004;22(14):2865–72.
2. Tabouret E, Chinot O, Metellus P, Tallet A, Viens P, Gonçalves A. Recent trends in epidemiology of brain metastases: an overview. Anticancer Res. 2012 Nov;32(11):4655–62.
3. Sperduto PW, Chao ST, Sneed PK, Luo X, Suh J, Roberge D, et al. Diagnosis-specific prognostic factors, indexes, and treatment outcomes for patients with newly diagnosed brain metastases: a multi-institutional analysis of 4,259 patients. Int J Radiat Oncol. 2010;77(3):655–61.
4. Chen G, Chakravarti N, Aardalen K, Lazar AJ, Tetzlaff MT, Wubbenhorst B, et al. Molecular profiling of patient-matched brain and extracranial melanoma metastases implicates the PI3K pathway as a therapeutic target. Clin Cancer Res. NIH Public Access. 2014;20(21):5537–46.
5. Brastianos PK, Carter SL, Santagata S, Cahill DP, Taylor-Weiner A, Jones RT, et al. Genomic characterization of brain metastases reveals branched evolution and potential therapeutic targets. Cancer Discov. American Association for Cancer Research. 2015;5(11):1164–77.
6. Eichler AF, Chung E, Kodack DP, Loeffler JS, Fukumura D, Jain RK. The biology of brain metastases—translation to new therapies. Nat Rev Clin Oncol. 2011;8(6):344–56.
7. Fortin D. The blood-brain barrier: its influence in the treatment of brain tumors metastases. Curr Cancer Drug Targets. 2012;12(3):247–59.
8. Muldoon LL, Soussain C, Jahnke K, Johanson C, Siegal T, Smith QR, et al. Chemotherapy delivery issues in central nervous system malignancy: a reality check. J Clin Oncol. 2007;25(16):2295–305.
9. Chen J, Xiao L, Rao JN, Zou T, Liu L, Bellavance E, et al. JunD represses transcription and translation of the tight junction protein zona occludens-1 modulating intestinal epithelial barrier function. Mol Biol Cell. American Society for Cell Biology. 2008;19(9):3701–12.
10. Berghoff AS, Fuchs E, Ricken G, Mlecnik B, Bindea G, Spanberger T, et al. Density of tumor-infiltrating lymphocytes correlates with extent of brain edema and overall survival time in patients with brain metastases. Oncoimmunology. 2016;5(1):e1057388.
11. Berghoff AS, Preusser M. In search of a target: PD-1 and PD-L1 profiling across glioma types. Neuro-Oncology. 2016;18(10):1331–2.
12. Hubbs JL, Boyd JA, Hollis D, Chino JP, Saynak M, Kelsey CR. Factors associated with the development of brain metastases. Cancer. 2010;116(21):5038–46.
13. Peters S, Bexelius C, Munk V, Leighl N. The impact of brain metastasis on quality of life, resource utilization and survival in patients with non-small-cell lung cancer. Cancer Treat Rev. 2016;45:139–62.
14. D'Antonio C, Passaro A, Gori B, Del Signore E, Migliorino MR, Ricciardi S, et al. Bone and brain metastasis in lung cancer: recent advances in therapeutic strategies. Ther Adv Med Oncol. 2014;6(3):101–14.
15. Herrlinger U, Förschler H, Küker W, Meyermann R, Bamberg M, Dichgans J, et al. Leptomeningeal metastasis: survival and prognostic factors in 155 patients. J Neurol Sci. 2004;223(2):167–78.
16. Bronte G, Rolfo C, Giovannetti E, Cicero G, Pauwels P, Passiglia F, et al. Are erlotinib and gefitinib interchangeable, opposite or complementary for non-small cell lung cancer treatment? Biological, pharmacological and clinical aspects. Crit Rev Oncol Hematol. 2014;89(2):300–13.
17. Pao W, Miller VA. Epidermal growth factor receptor mutations, small-molecule kinase inhibitors, and non-small-cell lung cancer: current knowledge and future directions. J Clin Oncol. 2005;23(11):2556–68.
18. Lynch TJ, Bell DW, Sordella R, Gurubhagavatula S, Okimoto RA, Brannigan BW, et al. Activating mutations in the epidermal growth factor receptor underlying responsiveness of non–small-cell lung cancer to gefitinib. N Engl J Med. 2004;350(21):2129–39.
19. Eichler AF, Kahle KT, Wang DL, Joshi VA, Willers H, Engelman JA, et al. EGFR mutation status and survival after diagnosis of brain metastasis in nonsmall cell lung cancer. Neuro-Oncology. 2010;12(11):1193–9.
20. Cross DAE, Ashton SE, Ghiorghiu S, Eberlein C, Nebhan CA, Spitzler PJ, et al. AZD9291, an irreversible EGFR TKI, overcomes T790M-mediated resistance to EGFR inhibitors in lung cancer. Cancer Discov. 2014;4(9):1046–61.
21. Weber B, Winterdahl M, Memon A, Sorensen BS, Keiding S, Sorensen L, et al. Erlotinib accumulation in brain metastases from non-small cell lung cancer: visualization by positron emission tomography in a patient harboring a mutation in the epidermal growth factor receptor. J Thorac Oncol. 2011;6(7):1287–9.
22. Elmeliegy MA, Carcaboso AM, Tagen M, Bai F, Stewart CF. Role of ATP-binding cassette and solute carrier transporters in erlotinib CNS penetration and intracellular accumulation. Clin Cancer Res. 2011;17(1):89–99.
23. Kitazaki T, Oka M, Nakamura Y, Tsurutani J, Doi S, Yasunaga M, et al. Gefitinib, an EGFR tyrosine kinase inhibitor, directly inhibits the function of P-glycoprotein in multidrug resistant cancer cells. Lung Cancer. 2005;49(3):337–43.
24. Togashi Y, Masago K, Fukudo M, Terada T, Fujita S, Irisa K, et al. Cerebrospinal fluid concentration of erlotinib and its active metabolite OSI-420 in patients with central nervous system metastases of non-small cell lung cancer. J Thorac Oncol. 2010;5(7):950–5.
25. Wakeling AE, Guy SP, Woodburn JR, Ashton SE, Curry BJ, Barker AJ, et al. ZD1839 (Iressa): an orally active inhibitor of epidermal growth factor signaling with potential for cancer therapy. Cancer Res. 2002;62(20):5749–54.
26. Kim J-E, Lee DH, Choi Y, Yoon DH, Kim S-W, Suh C, et al. Epidermal growth factor receptor tyrosine kinase inhibitors as a first-line therapy for never-smokers with adenocarcinoma of the lung having asymptomatic synchronous brain metastasis. Lung Cancer. 2009;65(3):351–4.
27. Iuchi T, Shingyoji M, Sakaida T, Hatano K, Nagano O, Itakura M, et al. Phase II trial of gefitinib alone without radiation therapy for Japanese patients with brain metastases from EGFR-mutant lung adenocarcinoma. Lung Cancer. 2013;82(2):282–7.
28. Dempke WCM, Edvardsen K, Lu S, Reinmuth N, Reck M, Inoue A. Brain metastases in NSCLC - are TKIs changing the treatment strategy? Anticancer Res. 2015;35(11):5797–806.
29. Welsh JW, Komaki R, Amini A, Munsell MF, Unger W, Allen PK, et al. Phase II trial of erlotinib plus concurrent whole-brain radiation therapy for patients with brain metastases from non–small-cell lung cancer. J Clin Oncol. 2013;31(7):895–902.

30. Lee SM, Lewanski CR, Counsell N, Ottensmeier C, Bates A, Patel N, et al. Randomized trial of erlotinib plus whole-brain radiotherapy for NSCLC patients with multiple brain metastases. JNCI J Natl Cancer Inst. 2014;106(7)
31. Sequist LV, Yang JC-H, Yamamoto N, O'Byrne K, Hirsh V, Mok T, et al. Phase III study of Afatinib or cisplatin plus pemetrexed in patients with metastatic lung adenocarcinoma with *EGFR* mutations. J Clin Onco. 2013;31(27):3327–34.
32. Wu Y-L, Zhou C, Hu C-P, Feng J, Lu S, Huang Y, et al. Afatinib versus cisplatin plus gemcitabine for first-line treatment of Asian patients with advanced non-small-cell lung cancer harbouring EGFR mutations (LUX-Lung 6): an open-label, randomised phase 3 trial. Lancet Oncol Elsevier. 2014;15(2):213–22.
33. Schuler M, Wu Y-L, Hirsh V, O'Byrne K, Yamamoto N, Mok T, et al. First-line afatinib versus chemotherapy in patients with non–small cell lung cancer and common epidermal growth factor receptor gene mutations and brain metastases. J Thorac Oncol. 2016;11(3):380–90.
34. Wang S, Cang S, Liu D. Third-generation inhibitors targeting EGFR T790M mutation in advanced non-small cell lung cancer. J Hematol Oncol. BioMed Central. 2016;9:34.
35. Jänne PA, Yang JC-H, Kim D-W, Planchard D, Ohe Y, Ramalingam SS, et al. AZD9291 in EGFR inhibitor–resistant non–small-cell lung cancer. N Engl J Med. 2015;372(18):1689–99.
36. Ricciuti B, Baglivo S, Paglialunga L, De Giglio A, Bellezza G, Chiari R, et al. Osimertinib in patients with advanced epidermal growth factor receptor T790M mutation-positive non-small cell lung cancer: rationale, evidence and place in therapy. Ther Adv Med Oncol. 2017;9(6):387–404.
37. Yang JC-H, Ahn M-J, Kim D-W, Ramalingam SS, Sequist LV, Su W-C, et al. Osimertinib in pretreated T790M-positive advanced non–small-cell lung cancer: AURA study phase II extension component. J Clin Oncol. 2017;35(12):1288–96.
38. Zeng Q, Wang J, Cheng Z, Chen K, Johnström P, Varnäs K, et al. Discovery and evaluation of clinical candidate AZD3759, a potent, oral active, central nervous system-penetrant, epidermal growth factor receptor tyrosine kinase inhibitor. J Med Chem. 2015;58(20):8200–15.
39. Zhang I, Zaorsky NG, Palmer JD, Mehra R, Lu B. Targeting brain metastases in ALK-rearranged non-small-cell lung cancer. Lancet Oncol. 2015;16(13):e510–21.
40. Metro G, Lunardi G, Floridi P, Pascali JP, Marcomigni L, Chiari R, et al. CSF concentration of crizotinib in two ALK-positive non-small-cell lung cancer patients with CNS metastases deriving clinical benefit from treatment. J Thorac Oncol. 2015;10(5):e26–7.
41. Costa DB, Kobayashi S, Pandya SS, Yeo W-L, Shen Z, Tan W, et al. CSF concentration of the anaplastic lymphoma kinase inhibitor crizotinib. J Clin Oncol. 2011;29(15):e443–5.
42. Shaw AT, Kim D-W, Mehra R, Tan DSW, Felip E, Chow LQM, et al. Ceritinib in *ALK* -rearranged non–small-cell lung cancer. N Engl J Med. 2014;370(13):1189–97.
43. Seto T, Kiura K, Nishio M, Nakagawa K, Maemondo M, Inoue A, et al. CH5424802 (RO5424802) for patients with ALK-rearranged advanced non-small-cell lung cancer (AF-001JP study): a single-arm, open-label, phase 1–2 study. Lancet Oncol. 2013;14(7):590–8.
44. Shaw A, Mehra R, Tan DSW, Felip E, Chow LQM, Ross Camidge D, et al. BM-32 ∗ ceritinib (LDK378) for treatment of patients with ALK-rearranged (ALK+) Non-Small Cell Lung Cancer (NSCLC) and Brain Metastases (BM) in the ascend-1 trial. Neuro-Oncology. 2014;16(suppl 5):v39–v39.
45. Kim D-W, Tiseo M, Ahn M-J, Reckamp KL, Hansen KH, Kim S-W, et al. Brigatinib in patients with crizotinib-refractory anaplastic lymphoma kinase–positive non–small-cell lung cancer: a randomized, multicenter phase II trial. J Clin Oncol. 2017;35(22):2490–8.
46. Besse B, Le Moulec S, Mazieres J, Senellart H, Barlesi F, Chouaid C, et al. Bevacizumab in patients with nonsquamous non-small cell lung cancer and asymptomatic, untreated BRAIN metastases (BRAIN): a nonrandomized, phase II study. Clin Cancer Res. 2015;21(8):1896–903.
47. Jemal A, Tiwari RC, Murray T, Ghafoor A, Samuels A, Ward E, et al. Cancer statistics, 2004. CA Cancer J Clin. 2004;54(1):8–29.
48. Lee JS, Murphy WK, Glisson BS, Dhingra HM, Holoye PY, Hong WK. Primary chemotherapy of brain metastasis in small-cell lung cancer. J Clin Oncol. 1989;7(7):916–22.
49. Lassen U, Kristjansen PEG, Hansen HH. Brain metastases in small-cell lung cancer. Ann Oncol. 1995;6(9):941–4.
50. Brufsky AM, Mayer M, Rugo HS, Kaufman PA, Tan-Chiu E, Tripathy D, et al. Central nervous system metastases in patients with HER2-positive metastatic breast cancer: incidence, treatment, and survival in patients from registHER. Clin Cancer Res. 2011;17(14):4834–43.
51. Olson EM, Abdel-Rasoul M, Maly J, Wu CS, Lin NU, Shapiro CL. Incidence and risk of central nervous system metastases as site of first recurrence in patients with HER2-positive breast cancer treated with adjuvant trastuzumab. Ann Oncol. 2013;24(6):1526–33.
52. Pestalozzi BC, Holmes E, de Azambuja E, Metzger-Filho O, Hogge L, Scullion M, et al. CNS relapses in patients with HER2-positive early breast cancer who have and have not received adjuvant trastuzumab: a retrospective substudy of the HERA trial (BIG 1-01). Lancet Oncol. 2013;14(3):244–8.
53. Aversa C, Rossi V, Geuna E, Martinello R, Milani A, Redana S, et al. Metastatic breast cancer subtypes and central nervous system metastases. Breast. 2014;23(5):623–8.
54. Sperduto PW, Kased N, Roberge D, Chao ST, Shanley R, Luo X, et al. The effect of tumor subtype on the time from primary diagnosis to development of brain metastases and survival in patients with breast cancer. J Neuro-Oncol. 2013;112(3):467–72.
55. Vu T, Claret FX. Trastuzumab: updated mechanisms of action and resistance in breast cancer. Front Oncol. Frontiers. 2012;2:62.
56. Stemmler HJ, Kahlert S, Siekiera W, Untch M, Heinrich B, Heinemann V. Characteristics of patients with brain metastases receiving trastuzumab for HER2 overexpressing metastatic breast cancer. Breast. 2006;15(2):219–25.
57. Scott BJ, Kesari S. Leptomeningeal metastases in breast cancer. Am J Cancer Res. 2013;3(2):117–26.
58. Bartsch R, Rottenfusser A, Wenzel C, Dieckmann K, Pluschnig U, Altorjai G, et al. Trastuzumab prolongs overall survival in patients with brain metastases from Her2 positive breast cancer. J Neuro-Oncol. 2007;85(3):311–7.
59. Yap YS, Cornelio GH, Devi BCR, Khorprasert C, Kim SB, Kim TY, et al. Brain metastases in Asian HER2-positive breast cancer patients: anti-HER2 treatments and their impact on survival. Br J Cancer. 2012;107(7):1075–82.
60. Graus-Porta D, Beerli RR, Daly JM, Hynes NE. ErbB-2, the preferred heterodimerization partner of all ErbB receptors, is a mediator of lateral signaling. EMBO J. 1997;16(7):1647–55.
61. Worthylake R, Opresko LK, Wiley HS. ErbB-2 amplification inhibits down-regulation and induces constitutive activation of both ErbB-2 and epidermal growth factor receptors. J Biol Chem. 1999;274(13):8865–74.
62. Rusnak DW, Affleck K, Cockerill SG, Stubberfield C, Harris R, Page M, et al. The characterization of novel, dual ErbB-2/EGFR, tyrosine kinase inhibitors: potential therapy for cancer. Cancer Res. 2001;61(19):7196–203.
63. Rusnak D, Gilmer TM. The discovery of lapatinib (GW572016). Mol Cancer Ther. 2011;10(11):2019.
64. Taskar KS, Rudraraju V, Mittapalli RK, Samala R, Thorsheim HR, Lockman J, et al. Lapatinib distribution in HER2 overexpressing experimental brain metastases of breast cancer. Pharm Res. 2012;29(3):770–81.
65. Bachelot T, Romieu G, Campone M, Diéras V, Cropet C, Dalenc F, et al. Lapatinib plus capecitabine in patients with previously

untreated brain metastases from HER2-positive metastatic breast cancer (LANDSCAPE): a single-group phase 2 study. Lancet Oncol. 2013;14(1):64–71.
66. Lin NU, Carey LA, Liu MC, Younger J, Come SE, Ewend M, et al. Phase II trial of lapatinib for brain metastases in patients with human epidermal growth factor receptor 2-positive breast cancer. J Clin Oncol. 2008;26(12):1993–9.
67. Lin NU, Diéras V, Paul D, Lossignol D, Christodoulou C, Stemmler H-J, et al. Multicenter phase II study of lapatinib in patients with brain metastases from HER2-positive breast cancer. Clin Cancer Res. 2009;15(4):1452–9.
68. Venur V, Leone J. Targeted therapies for brain metastases from breast cancer. Int J Mol Sci. 2016;17(9):1543.
69. Freedman RA, Gelman RS, Wefel JS, Melisko ME, Hess KR, Connolly RM, et al. Translational breast cancer research consortium (TBCRC) 022: a phase II trial of neratinib for patients with human epidermal growth factor receptor 2-positive breast cancer and brain metastases. J Clin Oncol. 2016;34(9):945–52.
70. Bartsch R, Berghoff AS, Vogl U, Rudas M, Bergen E, Dubsky P, et al. Activity of T-DM1 in Her2-positive breast cancer brain metastases. Clin Exp Metastasis. 2015;32(7):729–37.
71. Davies MA, Liu P, McIntyre S, Kim KB, Papadopoulos N, Hwu W-J, et al. Prognostic factors for survival in melanoma patients with brain metastases. Cancer. 2011;117(8):1687–96.
72. Flaherty KT, McArthur G. BRAF, a target in melanoma. Cancer. 2010;116(21):4902–13.
73. Davies MA, Saiag P, Robert C, Grob J-J, Flaherty KT, Arance A, et al. Dabrafenib plus trametinib in patients with BRAFV600-mutant melanoma brain metastases (COMBI-MB): a multicentre, multicohort, open-label, phase 2 trial. Lancet Oncol. 2017;18(7):863–73.
74. Margolin K, Ernstoff MS, Hamid O, Lawrence D, McDermott D, Puzanov I, et al. Ipilimumab in patients with melanoma and brain metastases: an open-label, phase 2 trial. Lancet Oncol. 2012;13(5):459–65.
75. Kim ES, Bruinooge SS, Roberts S, Ison G, Lin NU, Gore L, et al. Journal of clinical oncology broadening eligibility criteria to make clinical trials more representative: American Society of Clinical Oncology and Friends of Cancer Research Joint Research Statement. J Clin Oncol. 2017;35:3737–44.
76. Williams NL, Wuthrick EJ, Kim H, Palmer JD, Garg S, Eldredge-Hindy H, et al. Phase 1 study of ipilimumab combined with whole brain radiation therapy or radiosurgery for melanoma patients with brain metastases. Int J Radiat Oncol Biol Phys. 2017;99(1):22–30.
77. Kiess AP, Wolchok JD, Barker CA, Postow MA, Tabar V, Huse JT, et al. Stereotactic radiosurgery for melanoma brain metastases in patients receiving ipilimumab: safety profile and efficacy of combined treatment. Int J Radiat Oncol Biol Phys. 2015;92(2):368–75.
78. Skrepnik T, Sundararajan S, Cui H, Stea B. Improved time to disease progression in the brain in patients with melanoma brain metastases treated with concurrent delivery of radiosurgery and ipilimumab. Oncoimmunology. 2017;6(3):e1283461.
79. Chen L, Douglass J, Kleinberg L, Ye X, Marciscano AE, Forde PM, et al. Concurrent immune checkpoint inhibitors and stereotactic radiosurgery for brain metastases in non-small cell lung cancer, melanoma, and renal cell carcinoma. Int J Radiat Oncol. 2018;100(4):916–25.

Diagnostic Imaging Advances

Joseph H. Donahue, Juliana Bueno, and Jason N. Itri

Abbreviations

ADC	Apparent diffusion coefficient
CT	Computed tomography
DTI	Diffusion tensor imaging
DWI	Diffusion-weighted imaging
FLAIR	Fluid attenuated inversion recovery
GRE	Gradient echo
mpMRI	Multiparametric magnetic resonance imaging
MRA	Magnetic resonance angiography
MRI	Magnetic resonance imaging
MRS	Magnetic resonance spectroscopy
NSCLC	Non-small cell lung cancer
PET	Positron emission tomography
SABR	Stereotactic ablative radiotherapy
SBRT	Stereotactic body radiation therapy
SI	Signal intensity
SWI	Susceptibility-weighted imaging

Part I. Stereotactic Radiosurgery: Intracranial Applications

Vestibular Schwannoma

Vestibular schwannomas are typified by an enhancing cisternal and/or canalicular extra-axial cerebellopontine angle mass causing smoothly expansile remodeling of the internal auditory canal, variable degrees of mass effect, and occasionally demonstrating areas of intralesional microhemorrhage or accompanying increased cochlear FLAIR signal [1, 2]. Less commonly schwannomas may be confined to or primarily involve the bony labyrinth, termed intralabyrinthine schwannomas [3]. Most lesions are sporadic and small to moderate size at presentation (<30 mm) and demonstrate slow growth on serial examination (70% within 5-year follow-up) [4].

Preoperative MR imaging protocols generally include a high-resolution heavily T2-weighted series and pre-/post-contrast T1-weighted series. Isotropic data sets, particularly post-contrast series, are valuable for providing precise volumetric measurements on preoperative and follow-up imaging, as well as detailing the lateral tumor margin and delineating labyrinthine involvement. Tumors may be morphologically classified as homogeneous, microcystic, or macrocystic based on contrast enhancement patterns [5]. While controversy regarding the radiosurgical treatment of predominantly cystic (>50% total tumor diameter) or macrocystic schwannomas has historically related to concern for rapid cyst enlargement and higher rates of treatment failure [6–8], several recent publications have found no difference or even improved tumor volume reduction of cystic schwannomas compared to solid tumors [5, 9–11].

Several patterns of treatment response are recognized, including serial volumetric regression, minimal posttreatment enlargement with subsequent stability, and pseudoprogression (Fig. 1a–c). Pseudoprogression is a well-recognized phenomenon of transient posttreatment tumor enlargement that peaks at 6–18 months following radiosurgery, with some investigators noting pseudoprogression as late as 3–4 years [12, 13]. While multiple metrics for defining treatment failure exist (serial growth >20%, need for second procedure, etc.), most authors agree that treatment failure should not be declared on imaging basis alone within the first 2 years. The overall growth observed during pseudoprogression may be attributable to solid and/or cystic component enlargement. Decreased central contrast enhancement is a common treatment-related finding (Fig. 1b, c), reported in up to 84% of cases, though significant correlation with subsequent tumor growth control is not definitive [10, 14].

J. H. Donahue (✉) · J. Bueno · J. N. Itri
University of Virginia Health System, Department of Radiology and Medical Imaging, Charlottesville, VA, USA
e-mail: Jd2uc@hscmail.mcc.virginia.edu

D. M. Trifiletti et al. (eds.), *Stereotactic Radiosurgery and Stereotactic Body Radiation Therapy*,
https://doi.org/10.1007/978-3-030-16924-4_33

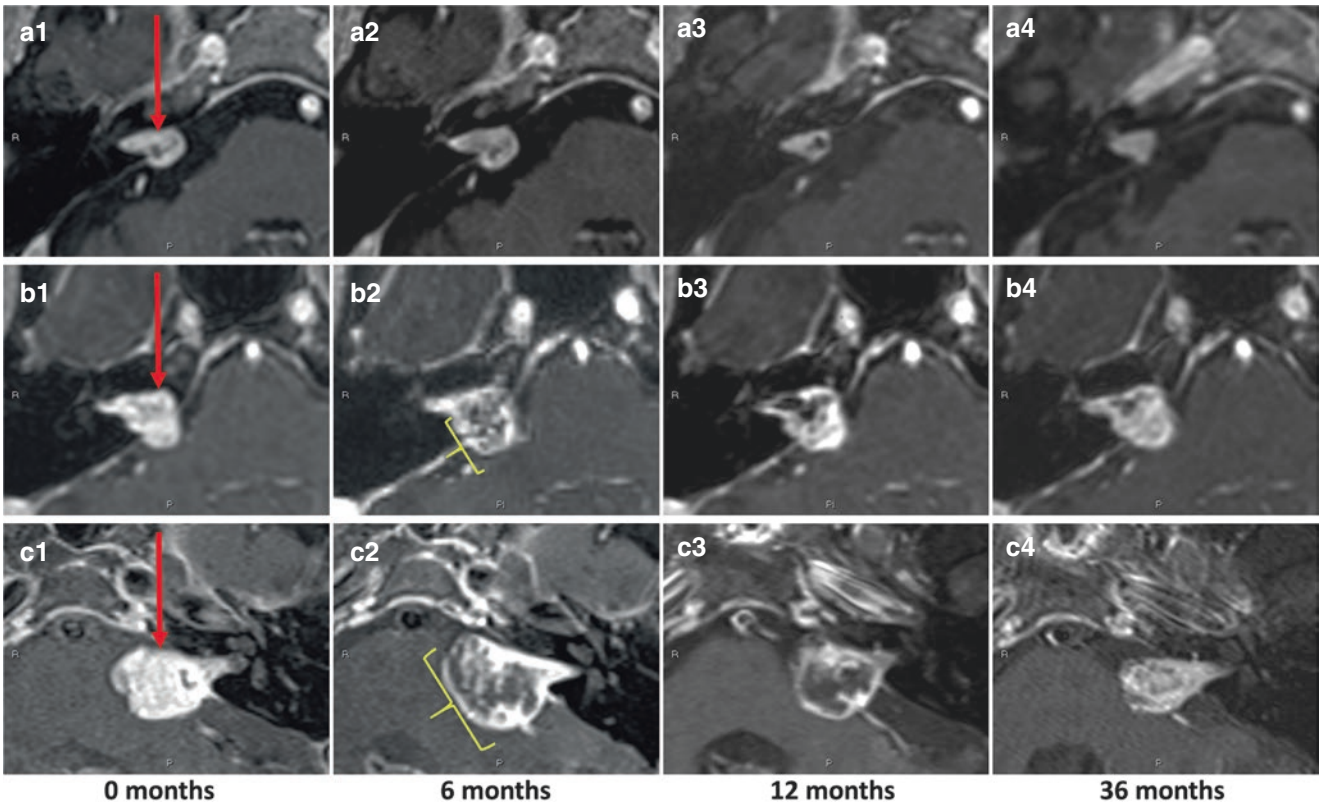

Fig. 1 Vestibular schwannoma. Continuum of images illustrates various patterns of treatment response. Serial axial T1-weighted images in three patients obtained at time points 0 month pretreatment baseline (column 1), 6 months (column 2), 12 months (column 3), and 36 months (column 4). (**a**) Top row: Uncomplicated treatment response. Baseline pretreatment examination (**a1**) demonstrates a right cisternal and canalicular vestibular schwannoma (red arrow). Size stability of the right vestibular schwannoma is noted on 6-month posttreatment examination (**a2**), with serial size regression appreciable at 12 months (**a3**) and 36 months (**a4**). (**b**) Middle row: Posttreatment enlargement followed by size stability. Baseline pretreatment examination (**b1**) demonstrates a right cisternal and canalicular vestibular schwannoma (red arrow). Minimal enlargement of the cisternal portion of the right vestibular schwannoma (yellow bracket) is noted at 6 months (**b2**) and is associated with new central hypoenhancement. The schwannoma subsequently demonstrates long-term size stability at 12 months (**b3**) and 36 months (**b4**). (**c**) Bottom row: Pseudoprogression. Baseline pretreatment examination (**c1**) demonstrates a left cisternal and canalicular vestibular schwannoma (red arrow). The left vestibular schwannoma demonstrates enlargement of the cisternal portion (yellow bracket) and marked central hypoenhancement at 6 months (**c2**). Size regression begins at 12 months (**c3**), with the lesion measuring smaller than baseline pretreatment volume at 36 months (**c4**)

Complications and Toxicity

Hydrocephalus is an uncommon complication following vestibular schwannoma radiosurgery (1–5%). Rarely, mass-effect-related obstructive hydrocephalus is encountered as a result of cyst formation or pseudoprogression. Communicating hydrocephalus, a relatively more frequent occurrence, may present in absence of tumor growth and likely relates to sloughing of tumor debris into the CSF with resultant hyperproteinorrhachia [15–17].

Future Directions

The utility of preoperative diffusion-weighted imaging (DWI) and apparent diffusion coefficient (ADC) in predicting tumor response remains somewhat ambiguous at present. Yousem and colleagues proposed that pretreatment ADC_{min} value of less than 800×10^{-6} mm^2/s portends favorable treatment response, while Yang and colleagues found relatively higher pretreatment ADC_{max} values to be predictive of treatment response [10, 18]. In the early posttreatment setting, changes in diffusion tensor metrics, particularly fractional anisotropy, have been proposed as an early indicator (8 weeks) of irreversible cytoarchitectural disruption [19].

Meningioma

Although the majority of meningiomas are histologically designated as WHO grade I (65–80%), significant overlap in imaging features exists between these benign lesions and atypical (WHO grade II) and malignant lesions (WHO grade III), with reliable radiologic distinction difficult or impossible in many cases. However, some imaging features are suggestive of more aggressive lesion character and may prognosticate shorter recurrence-free survival (Table 1) [20, 21].

As with other intracranial mass lesions, preoperative isotropic post-contrast T1-weighted MRI series afford the

most accurate baseline volumetric tumor measurements. Apparent diffusion coefficient (ADC) values, a sequence typically included in preoperative imaging, is known to correlate inversely with Ki-67 proliferation indices in meningiomas, with various proposed ADC_{mean} cutoff values of 700–850 × 10^{-6} mm^2/s for distinguishing WHO grade I from grade II/III lesions [22, 23].

Table 1 Imaging features predictive of histologic grade in meningioma

Histology	Enhancement pattern	Others
Benign (WHO I)	Homogeneous enhancement. Distinct tumor margins with enhancing capsule. CSF cleft at brain-tumor interface	Dense tumoral calcification. Profoundly low T2 signal intensity
High grade (WHO II and III)	Heterogeneous enhancement. Poorly marginated lesion with indistinct brain-tumor interface	Non-skull base location. Male gender. Scalp or foraminal invasion. FDG uptake > cortex. Increased CBV in peritumoral edema. Low alanine on MRS. ADC mean <700–850 × 10^{-6} mm^2/s

Data from: References [20, 21, 136–138]

A smooth dural tail is a common but not pathognomonic feature of meningioma and typically represents non-tumoral reactive thickening and vascular congestion with few neoplastic cells present more that 1–2 cm from the tumor mass base. Varying degrees of peritumoral parenchymal edema are another common finding and are thought to reflect the presence of tumor-derived vascular growth factors or other signaling agents. While the presence of peritumoral edema does increase seizure risk and may even portend future tumor growth, it does not typically represent direct parenchymal tumor infiltration [24, 25]. The presence of calcification and profound low T2 signal is suggestive of a lower-grade lesion with less future growth potential [21].

A variety of radiographic changes within treated meningiomas have been reported following stereotactic radiosurgery. Coagulative necrosis (central or peripheral tumor non-enhancement), radiation-induced inflammatory leukoencephalopathy (peritumoral parenchymal enhancement), worsening peritumoral parenchymal edema, and resorption of tumoral calcification have all been reported (Figs. 2 and 3a–d) [26, 27].

Although tumor response and progression are variably defined and reported, several series demonstrate that careful MRI analysis may capture prognostic volumetric changes

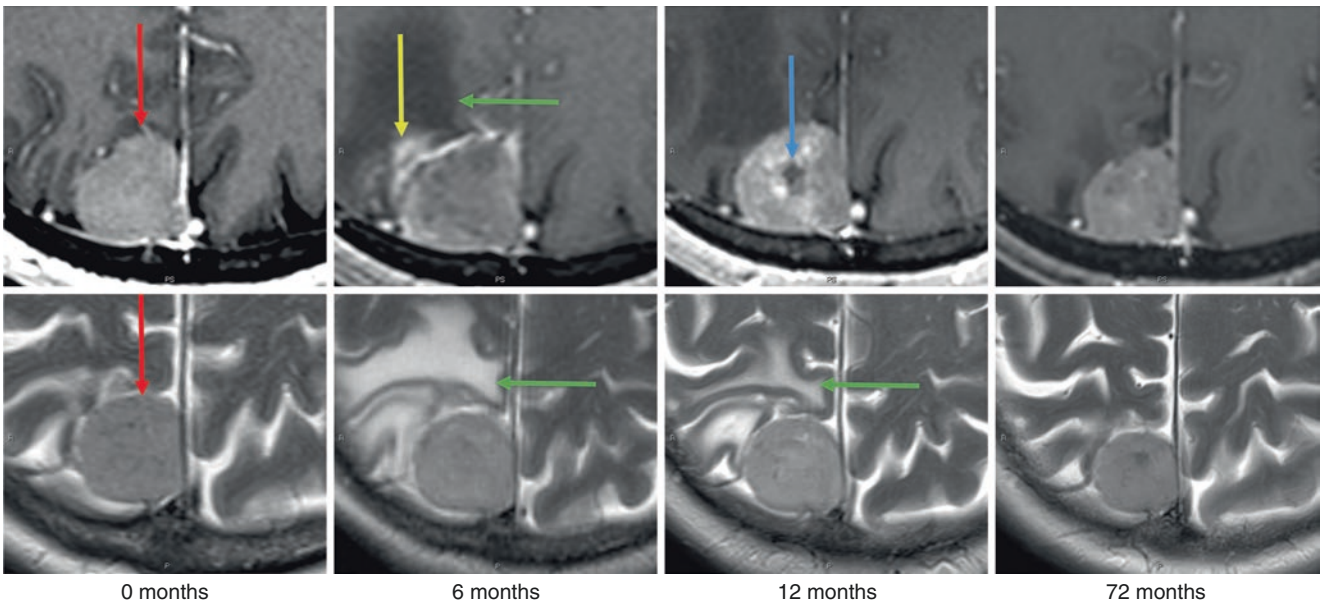

Fig. 2 Meningioma. Axial post-contrast T1-weighted (top row) and axial T2-weighted (bottom row) MR imaging obtained at 0, 6, 12, and 72 months. Baseline pretreatment examination at 0 months demonstrates features typical of a meningioma (red arrows), with homogeneous enhancement and broad dural attachment; note the lack of perilesional edema present on T2-weighted images at 0 months. At 6 months, there is new perilesional edema shown as low signal on T1 and high signal on T2-weighted images (green arrows). Radiation-induced inflammatory leukoencephalopathy is seen as peritumoral parenchymal enhancement (yellow arrows) at 6 months, which resolves at 12 months. At 12 months, central coagulative necrosis is appreciated as a small area of central hypoenhancement on post-contrast T1-weighted image (blue arrow), with decreased but persistent perilesional edema (green arrow). Volumetric tumor regression is appreciated at 72 months when the lesion measured 7.1 cubic cm, reduced from 11.5 cubic cm at baseline pretreatment examination (measurements not shown). Perilesional edema has resolved at 72 months

in the early posttreatment period (6–12 months). While the majority of treated lesions display size stability or regression, a small percentage of lesions may demonstrate dynamic volumetric changes in the early posttreatment period with both pseudoprogression (1.6–6%) and pseudoresponse (2–3.7%) possible [28–30].

Complications and Toxicity

New or worsening peritumoral parenchymal vasogenic edema is one of the most common complications following radiotherapy. Vasogenic edema is recognized as increased T2/FLAIR signal abnormality within the juxta-/subcortical white matter, possibly with associated mass effect (Fig. 2). Post-contrast enhancement is absent, and no diffusion restriction is present (differentiating vasogenic edema from irreversible cytotoxic edema). While the underlying mechanism is debated (release of tumoral vasogenic mediators or direct parenchymal radiation effect), the development of vasogenic edema closely relates to the surface area of the brain-tumor interface, explaining why this complication occurs more frequently in supratentorial interhemispheric lesions.

Peritumoral or parenchymal cyst formation is a rare complication, occasionally producing mass effect symptoms and requiring shunt diversion (Fig. 3a–d). Communicating or obstructive hydrocephalus is similarly infrequent, more commonly occurring with skull base or petroclival lesions [31].

Future Directions

Noninvasive determination of tumor grade and prognostication of radiosurgical response through advanced imaging biomarkers may be possible [32]. For instance in one study,

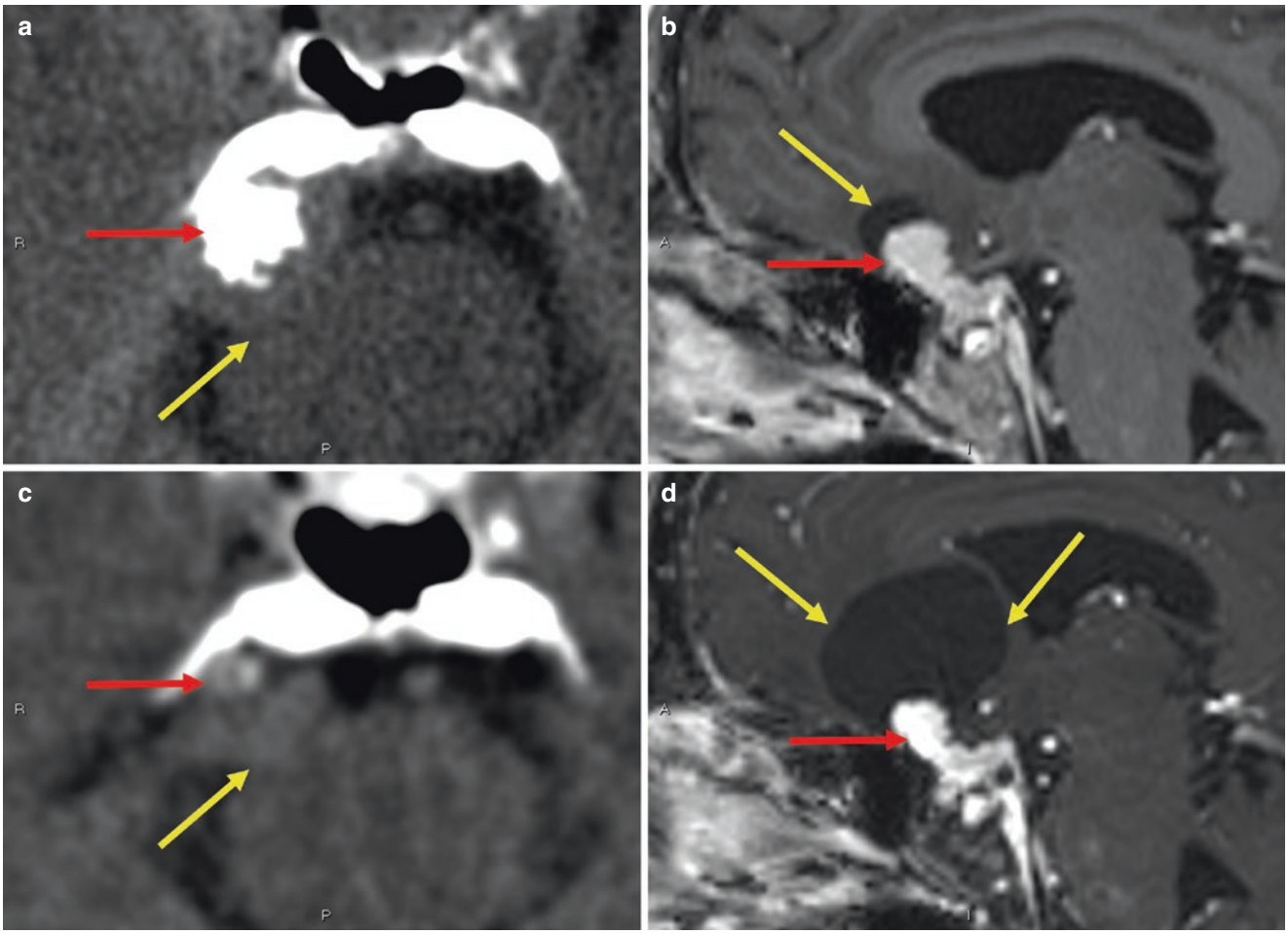

Fig. 3 Meningioma. Tumoral calcification resorption (**a**, **b**). Axial non-contrast CT examinations at 0 months (**a**) and 55 months (**b**) show the presence of dense central calcification within a right petroclival meningioma (red arrow in **a**), which is only faintly present at 55-month follow-up (red arrow in **b**). Note volumetric regression is evident at 55 months (**b**) with less nearly resolved mass effect on the ventral pons (yellow arrows). Peritumoral cyst formation (**c**, **d**). Sagittal post-contrast T1-weighted MRI examinations at 0 months (**c**) and 60 months (**d**) demonstrate posttreatment peritumoral cyst enlargement. A homogeneously enhancing planum sphenoidale meningioma (red arrows in **c** and **d**) demonstrates volumetric regression at 55 months (**d**), though there is marked interval enlargement of a non-enhancing peritumoral cyst cephalad to the meningioma (yellow arrows). The cyst required shunt diversion due to mass effect symptoms

diffusion tensor metrics, particularly high fractional anisotropy (FA) values, correlated with a diminished response rate to radiotherapy, and were proposed to indicate the presence of more fiber-rich, less radiosensitive tissues such as in fibroblastic meningioma [33].

Trigeminal Neuralgia

Trigeminal neurovascular contact noted on imaging most closely correlates with symptoms when compression occurs at or near the transitional zone from central to peripheral myelination, typically involving the superior cerebellar artery or less commonly a loop of the anterior inferior cerebellar artery. Specificity for symptomatic vascular compression is heightened when nerve root displacement or atrophy is observed (Fig. 4a–d). In patients where clear neurovascular conflict is demonstrated, pain relief following radiosurgery may correlate with higher dose delivery to the point of vessel impingement [34].

In addition to detailing the presence and site of neurovascular conflict, preoperative imaging protocols should effectively exclude alternate causes of trigeminal neuralgia, including perineural tumor spread or other skull base mass lesions, vascular malformations, and multiple sclerosis (Fig. 5a–e). Typical MRI protocols include at least a high-resolution heavily T2-weighted series, thin section or isotropic post-contrast T1-weighted images, and often a time-of-flight magnetic resonance angiography (TOF MRA) [35]. In patients with an implanted MR-incompatible device or other contraindication to MRI, CT cisternogram may afford excellent anatomic resolution (Fig. 6a, b).

Focal post-contrast enhancement of the trigeminal nerve root following radiotherapy is commonly reported (83%), with studies noting occurrence at 1–6 months posttreatment (Fig. 4a–d) [36, 37]. Such a finding, while not predictive of clinical outcomes, does confirm dose delivery site, correlating with a median minimum dose of 77 Gy to the enhancing area [37]. Variable degrees of nerve root volume loss have been reported in the late posttreatment period.

Complications and Toxicity

Radiographically appreciable complications following trigeminal neuralgia radiosurgery are extraordinarily low.

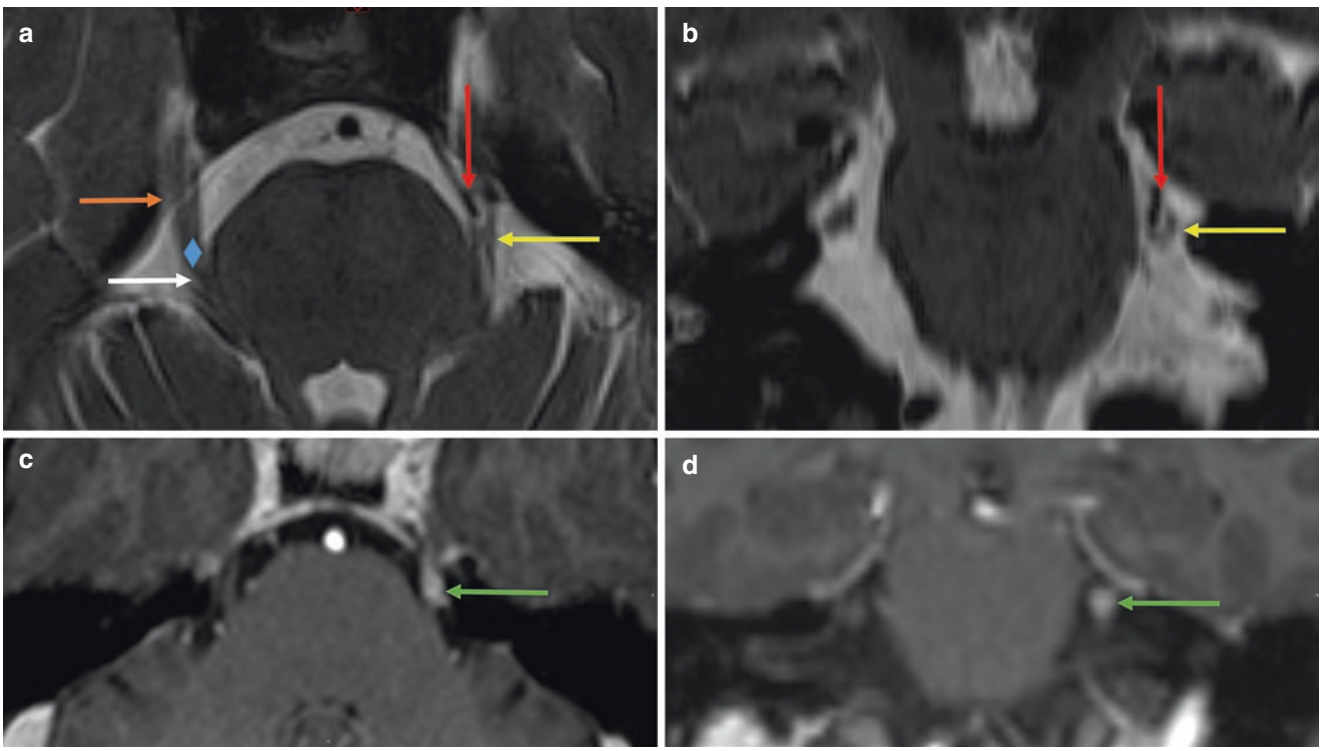

Fig. 4 Trigeminal neuralgia. High-grade neurovascular conflict (**a**, **b**). Axial (**a**) and coronal (**b**) high-resolution T2-weighted MR images show the left superior cerebellar artery (red arrows) causing displacement and deformity of the mid cisternal segment of the left trigeminal nerve (yellow arrows). Note mild atrophy of the affected nerve at the site of vascular impingement. Normal right trigeminal nerve anatomy is illustrated: The cisternal segment of the trigeminal nerve is bounded posteriorly by the apparent nerve root origin (white arrow) and ventrally by the porus trigeminus (orange arrow). The approximate site of the central to peripheral myelination transitional zone is indicated (blue diamond). Posttreatment Enhancement (**c**, **d**). Axial (**c**) and coronal (**d**) post-contrast T1-weighted MR images obtained at 12 months following radiosurgery demonstrate expected focal enhancement of the left trigeminal nerve root corresponding to site of radiosurgical dose delivery (green arrows)

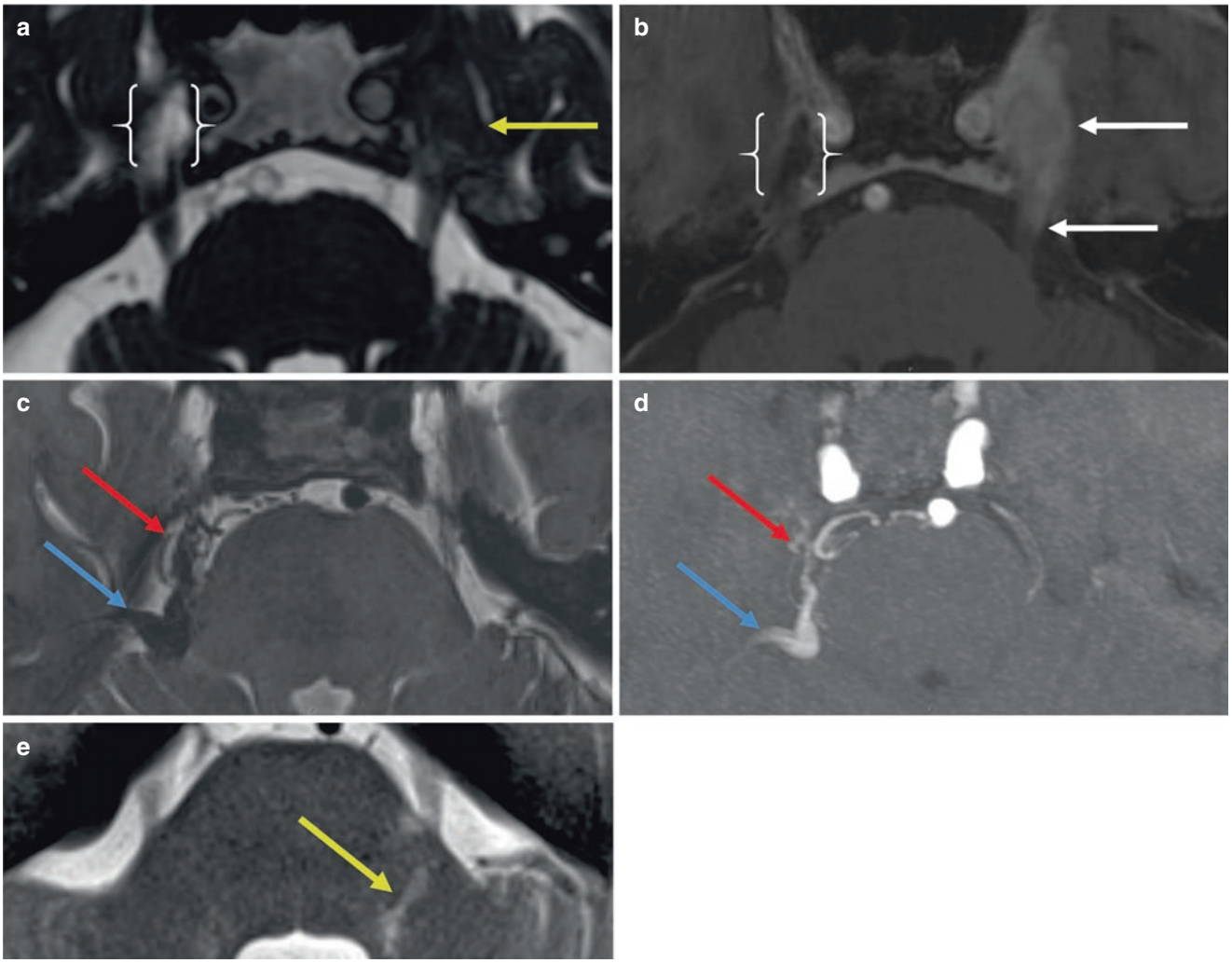

Fig. 5 Less common causes of trigeminal neuralgia. Perineural tumor spread (**a**, **b**). Axial high-resolution T2-weighted (**a**) and axial post-contrast T1-weighted (**b**) MR images demonstrating replacement of normal fluid signal in the left Meckel's cave (yellow arrow) with abnormal enhancing soft tissue that tracks proximally along the ventral cisternal trigeminal nerve (white arrows). The normal appearance of right Meckel's cave is illustrated (white brackets). Arteriovenous malformation (AVM) (**c**, **d**). Axial high-resolution T2-weighted (**c**) MR image and axial time-of-flight magnetic resonance angiogram (TOF MRA) (**d**) in maximum intensity projection demonstrates abnormal right prepontine cistern vascular structures closely associated with the right cisternal trigeminal nerve. The compact AVM nidus (red arrows) demonstrates flow-related signal on TOF MRA with arterialized flow appreciable within the dilated draining vein (blue arrows). Multiple sclerosis (**e**). Axial T2-weighted spin echo (**e**) MR image demonstrates a linear chronic demyelinating plaque within the left brachium pontis (yellow arrow) in the region of the trigeminal nerve nuclei

Future Directions

Though diffusion tensor metrics are not typically assessed on preoperative imaging, several small proof-of-concept series have investigated the utility of diffusion tensor imaging (DTI) in the evaluation of trigeminal neuralgia. Differences in baseline DTI metrics of the affected nerve may be appreciable independent of the presence of neurovascular conflict [38]. Focal changes in DTI metrics following radiosurgery may be noted, even in absence of corresponding post-contrast enhancement, and may even be predictive of pain recurrence [39]. Additionally, DTI could hold future promise in discriminating treatment responders from non-responders and classifying cases based on the underlying pathophysiologic mechanisms [40, 41].

Arteriovenous Malformation

An arteriovenous malformation is composed of a nidus, a tangled network of dysplastic vasculature, which is the site of arteriovenous shunting from the supplying arteries and draining veins. Gliotic parenchyma is often interspersed within the nidus and surrounding tissues [42].

Digital subtraction catheter angiography (DSA) remains the reference standard for imaging evaluation of arteriove-

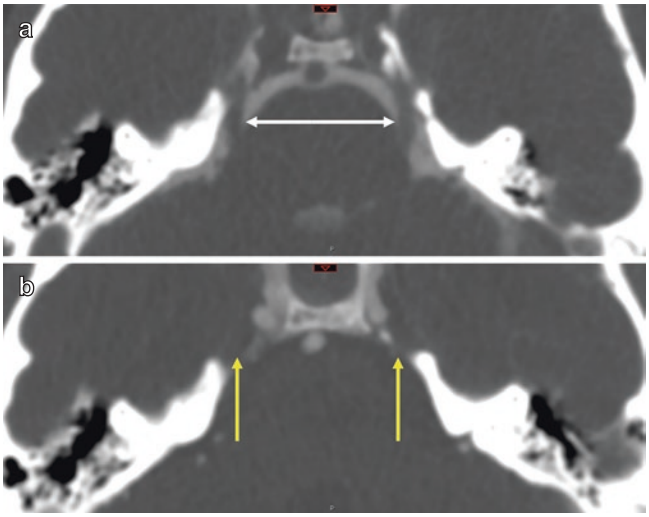

Fig. 6 CT landmarks of trigeminal nerve. CT cisternogram (**a**) and contrast-enhanced CT (**b**) demonstrating the trigeminal impression on the petrous ridge (yellow arrow) and the pars triangularis of the cisternal segment CN V several millimeters proximally (white arrow)

nous malformations, affording unsurpassed temporal resolution, depiction of the site and magnitude of arteriovenous shunting, and clear delineation of arterial supply and venous drainage. Moreover, to confidently assert cure of an AVM, most clinicians regard DSA as a necessary imaging examination [42].

MRI and CT offer noninvasive means of detection and monitoring, often providing complimentary information with respect to hemorrhage, nidus location, and treatment-related changes. On conventional MRI, the nidus is best depicted as hypointense flow voids on T2-weighted images. The T2 and FLAIR sequences also depict intranidal/perinidal gliosis, as well as radiation-induced parenchymal changes (Figs. 7a–g and 8).

The presence of prior or interval hemorrhage is best evaluated with hemosiderin-sensitive sequences (GRE and SWI), where chronic blood products will appear as hypointense signal. SWI also demonstrates the presence of arterialized flow within draining veins as hyperintense intravascular signal, as opposed to the normal hypointensity of veins owing to

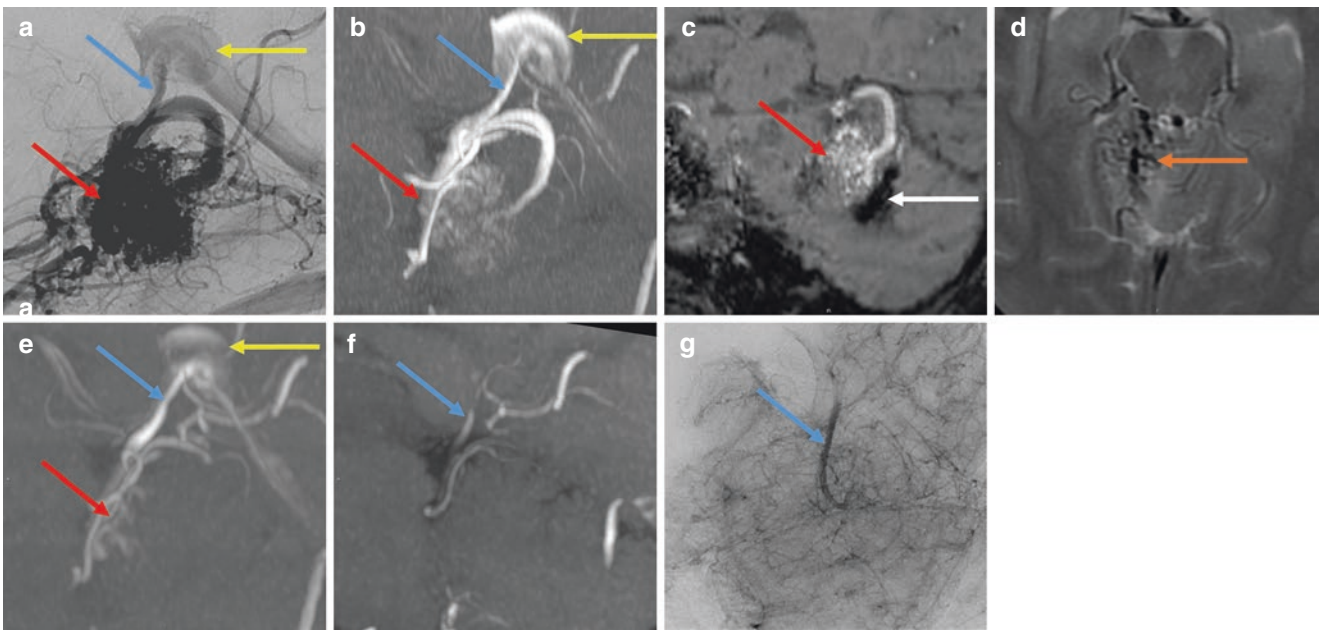

Fig. 7 Subtotal arteriovenous malformation obliteration. Preprocedural imaging (top row) (**a**–**d**). Sagittal vertebral artery injection digital subtraction angiogram (DSA) (**a**) demonstrating a superior cerebellar AVM with compact nidus (red arrows). Arteriovenous shunting is demonstrated with deep venous drainage in part via the precentral cerebellar vein (blue arrow) to the vein of Galen (yellow arrow). Sagittal maximum intensity projection of a time-of-flight MRA (**b**) demonstrates flow-related signal within the nidus and the draining veins, closely mirroring the DSA findings. Sagittal susceptibility-weighted MR image (SWI) (**c**) shows evidence of prior hemorrhage as low parenchymal signal intensity inferior to the nidus (white arrow). Note the SWI displays the arterialized flow within the nidus and draining veins as high signal intensity (red arrow). Axial T2-weighted MR image (**d**) demonstrates low signal intensity of arterialized flow voids (orange arrow). Post-procedural imaging (bottom row) (**e**–**g**). Sagittal maximum intensity projection of a time-of-flight MRA at 1.5 years posttreatment (**e**) shows partial nidus regression (red arrow) with persistent flow-related signal within the precentral cerebellar vein (blue arrow). Sagittal maximum intensity projection of a time-of-flight MRA at 3 years posttreatment (**f**) shows radiographic resolution of the nidus with decreased but persistent flow-related signal within the precentral cerebellar vein (blue arrow). Sagittal vertebral artery injection digital subtraction angiogram (DSA) at 3 years posttreatment (**g**) shows angiographic nidus obliteration with persistent late arterial phase and early capillary phase (pictured) opacification of the precentral cerebellar vein (blue arrow), indicating subtotal obliteration

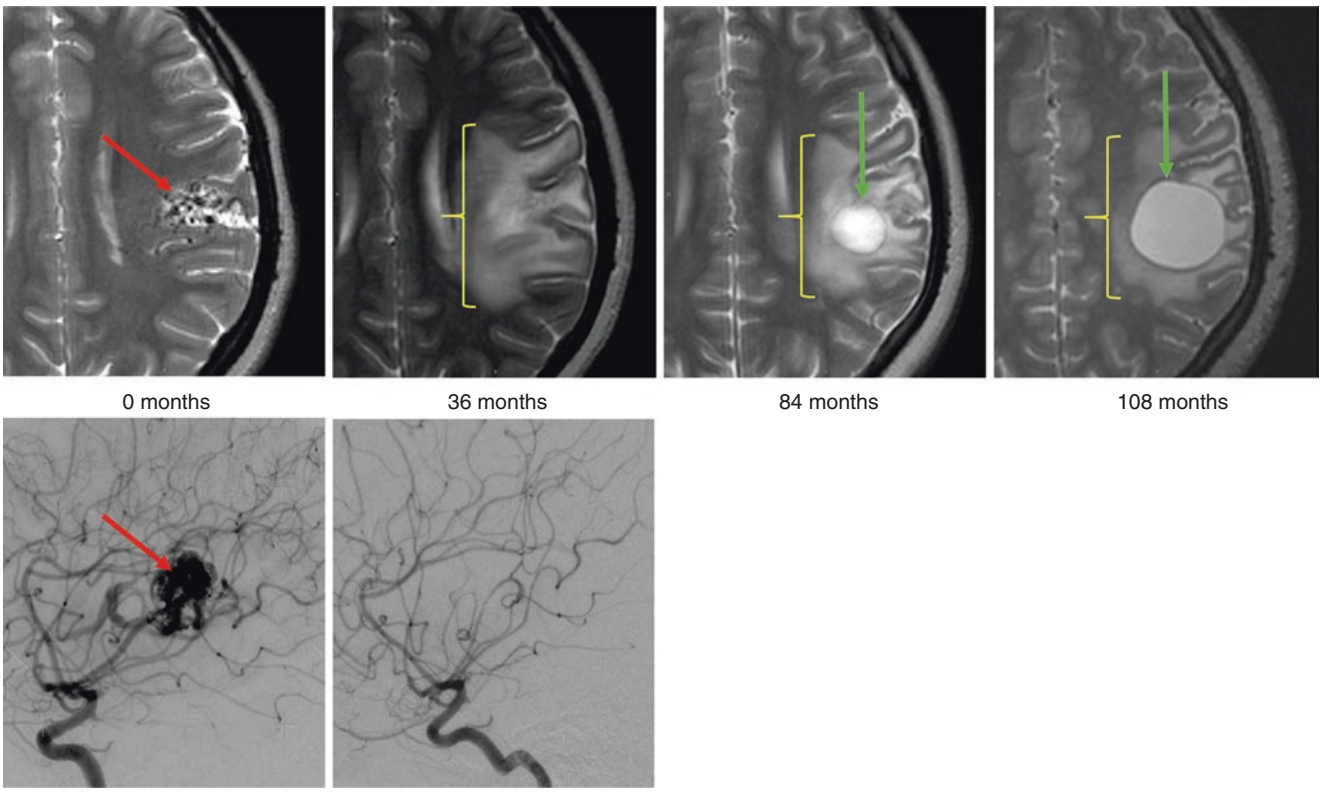

Fig. 8 Arteriovenous malformation with intraparenchymal cyst formation. Axial T2-weighted MR images (top row) obtained at 0, 36, 84, and 108 months with corresponding left middle cerebral artery catheter angiogram (bottom row) at 0 and 36 months. At baseline pretreatment examination, the AVM nidus is seen as hypointense flow voids on the T2-weighted image within the lateral left frontal lobe and as a compact nidus on the catheter angiogram (red arrow). Note the absence of perinidal gliosis or edema at baseline examination. At 36 months, nidus obliteration is appreciated by MRI and catheter angiogram, though new perinidal parenchymal T2 hyperintensity is present (yellow bracket) indicating development of radiation-induced imaging change. At 84 months, a discrete intraparenchymal cyst (green arrow) has developed within the area radiation-induced imaging change (yellow bracket). The intraparenchymal cyst continued to enlarge at 108 months (green arrow) and eventually required shunt diversion, while the radiation-induced imaging changes (yellow bracket) remained stable

deoxyhemoglobin content (Fig. 7a–g). The ability of SWI to depict arteriovenous shunting by identifying abnormal venous flow may be superior to time-of-flight magnetic resonance angiography (TOF MRA), with this effect potentially enhanced by gadolinium post-contrast SWI series [42–44].

Time-of-flight magnetic resonance angiography (TOF MRA) is a non-contrast noninvasive technique in which stationary tissues are suppressed by magnetic saturation, while the unsaturated signal of the incoming arterialized blood flow produces high-resolution arterial images. Note that some phases of hemorrhage or vascular thrombus may appear as hyperintense on TOF MRA ("T1 shine through") and confound assessment; additionally, slow or turbulent vascular flow may not be captured by TOF MRA technique. While this technique provides high resolution of most arterial AVM components, small feeding arteries may be missed and venous components are not reliably imaged [45]. Following radiosurgery, TOF MRA has variable accuracy in determining nidus obliteration, particularly when the nidus is less than 10 mm diameter, with reported sensitivities of 50–85% and specificities of 89–95% [46–48]. Computed tomography angiography (CTA) may offer superior assessment of small nidi, aneurysms, and venous drainage [49, 50].

A variety of dynamic contrast-enhanced MRA or CTA techniques (4D techniques) may be utilized to noninvasively overcome the limitations in temporal resolution inherent to the aforementioned single-phase angiographic studies. Following contrast agent bolus administration, images are acquired at close intervals to capture multiple time points in arterial and venous phases of enhancement. While generally achieving good agreement with DSA regarding nidus size and identifying involved vessels, some angio-architectural features including small vessels and aneurysms may not be identified or are mischaracterized [51–53].

Following radiosurgery, MRI examinations are typically performed at 6- to 12-month intervals to track nidus regression. AVM nidus obliteration usually occurs over a 2- to 5-year period, with favorable outcomes ranging from approximately 80% in grade 0–40% in grade IV Virginia Radiosurgical AVM Scale lesions [54]. Imaging changes preceding nidus obliteration include decreasing diameter of the nidus and feeding arteries with variable reduction in draining vein caliber (Fig. 7a–g). Radiologic response to treatment may be categorized as no change in the AVM, partial obliteration (decreased but persistent nidus), subtotal obliteration (no appreciable residual nidus but continued early venous drainage indicat-

ing persistent shunting) (Fig. 7a–g), and total obliteration of the nidus. Subtotal obliteration carries a markedly reduced risk of future hemorrhage as compared with untreated or partially obliterated lesions [55, 56]. Overall, lower rates of nidus obliteration are known to occur in patients with history of prior endovascular embolization [54].

Complications and Toxicity

The most commonly reported complication following radiosurgery is radiation-induced imaging changes within brain parenchymal surrounding the treated nidus (approx. 30–35% at 12–13 months), characterized as transient or permanent perinidal T2 hyperintensity with or without attendant mass effect (Fig. 8). While the majority of these imaging changes are clinically asymptomatic, symptoms occur in approximately 9% of cases, with 3.8% of patients endorsing permanent deficits [54, 57, 58].

Intraparenchymal cyst formation, an uncommon delayed complication following radiosurgery (3% at 6.5 years), may produce mass-effect symptoms (32.8%) and require surgical intervention. Cyst formation is statistically more likely to occur in patients with prior radiation-induced imaging changes and is appreciated as a discrete fluid-signal nonenhancing intra-axial structure in the region of prior radiosurgery (Fig. 8). Due to the prolonged latency period of this complication, nidal obliteration is typically achieved (77%) prior to the development of parenchymal cysts [59, 60].

Latency period hemorrhage (i.e., hemorrhage occurring after radiosurgery but prior to nidus obliteration) is uncommon (1.1% annual risk) though is somewhat more likely in patients with history of prior hemorrhage [54].

Future Directions

Ferumoxytol (Feraheme, AMAG Pharmaceuticals Waltham, MA, USA) is an ultra-small iron oxide particle that is approved for use by the U.S. Food and Drug Administration in the treatment of iron deficiency anemia in the setting of chronic kidney disease, though has off-label use as an MRI contrast agent [42]. Ferumoxytol behaves as a blood pool contrast agent for approximately the first 24 hours following intravenous administration, potentially allowing differentiation of residual nidus vascular enhancement from parenchymal enhancement related to increased blood-brain barrier permeability following radiation therapy. After 1–5 days following ferumoxytol administration, iron oxide particle macrophage-mediated active cellular transport occurs. If a link between intranidal inflammation and hemorrhage can be established, this may serve as a biomarker for risk stratification [61, 62].

Intracranial Metastasis

Local control of cerebral metastasis is one of the commonest indications for radiosurgery, whether as a stand-alone treatment or as an adjuvant to whole brain radiation therapy or surgical resection. Preoperative and follow-up imaging is tasked with rigorous lesion detection and characterization of radiosurgical response, including differentiating treatment-related changes from tumor progression.

Volumetric post-contrast T1-weighted MRI is invaluable in the detection of cerebral metastasis, with some more recently developed black blood techniques allowing signal suppression of sulcal arteries and thereby improving conspicuity of small juxtacortical lesions [63, 64]. Utilizing 3 Tesla MRI units and introducing a delay of 10–15 minutes between intravenous contrast agent administration and acquisition of post-contrast T1-weighted series has also been shown to improve small lesion detection [65]. While 3 Tesla units typically achieve higher signal-to-noise and improved image quality, the higher field strength may exacerbate geometric distortion and requires careful attention to distortion correction [66, 67].

Radiosurgery generally achieves a high degree of local tumor control, though a substantial minority of lesions (32%) demonstrates posttreatment volumetric increases that do not represent treatment failure, so-called pseudoprogression [68]. While conventional MRI at a single time point is not wholly reliable in distinguishing pseudoprogression/radiation necrosis from tumor progression, some imaging features may be helpful. A clearly marginated nodular area of intermediate or low T2 signal that closely matches the borders of the enhancing lesion (T1/T2 match) has been proposed as indicative of recurrent tumor (Fig. 9a–f) [69, 70], though other studies have failed to support this metric [71, 72]. Leeman and colleagues [71] noted that the enhancement of radiation necrosis is typically surrounded by a greater volume of parenchymal edema than were the enhancing portions of true tumor progression. Moreover, in their series of 52 surgically resected lesions, Leeman and colleagues [71] found no cases of tumor progression after 12 months following radiosurgery, results supported by Patel and colleagues [68] who demonstrated the volumetric changes of pseudoprogression to peak in the 12–15-month posttreatment period.

DWI and ADC series are routinely acquired MRI sequences that allow characterization of free water movement. Radionecrosis has been demonstrated to show both facilitated (increased ADC value) and restricted (decreased ADV value) diffusion, often with a core of facilitated diffusion surrounded by a ring of restricted diffusion, which in turn may be surrounded by an outer rim of enhancement and low-grade hyperperfusion, producing a three-layered appearance (Fig. 10a–h) [73]. A highly cellular solid tumor environment, whether untreated or recurrent disease, often allows for less free water movement (lower ADC values) compared to normal brain and perilesional edema, though the ADC measurements of recurrent tumor should be higher than the “infarct-like” changes seen in radiation necrosis; importantly, the areas of suspicious ADC signal should correlate with post-contrast enhancement in viable

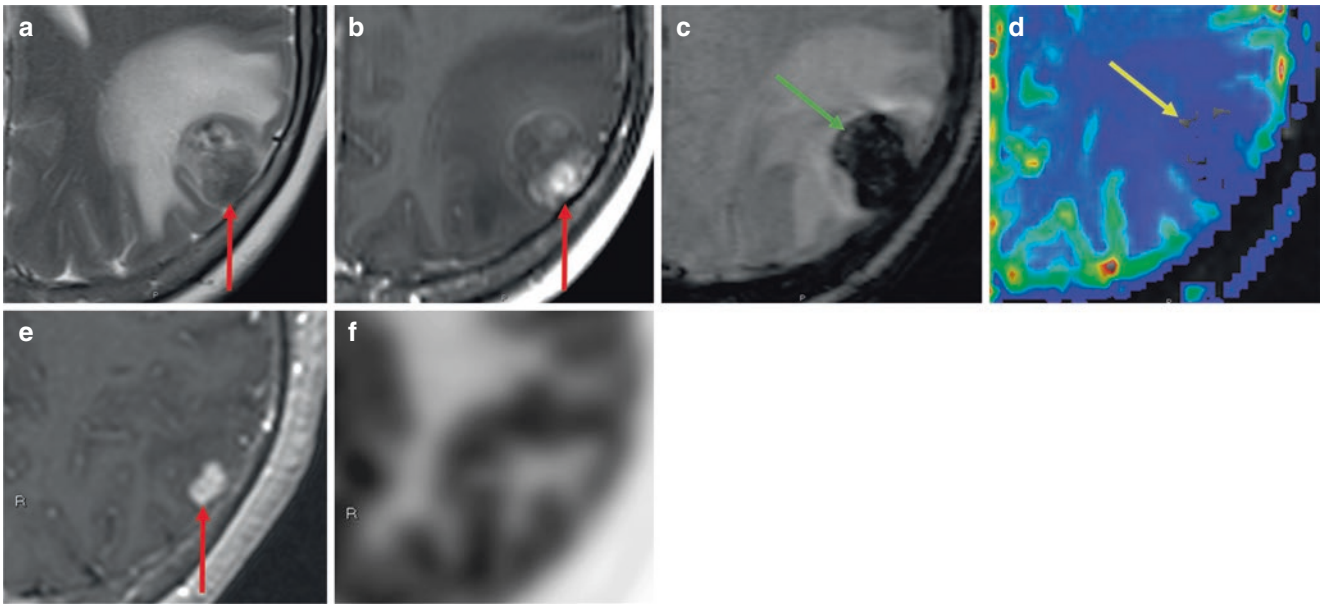

Fig. 9 Cerebral Metastasis. Tumor Progression. Melanoma metastasis of the left parietal lobe. Axial T2-weighted MRI (**a**), axial post-contrast T1-weighted MRI (**b**), axial susceptibility-weighted MRI (**c**), and axial DSC perfusion-weighted MRI corrected cerebral blood volume map (**d**) obtained at 10 months following radiosurgery. A discrete nodular focus of intermediate T2 signal (red arrow in **a**) very closely matches the area of post-contrast enhancement (red arrows in **b**), the T1/T2 match sign of recurrent tumor. Magnetic susceptibility from tumor-related hemorrhage (low intralesional signal in G; green arrow) is responsible for a spuriously decreased CBV (hypointense region in H; yellow arrow). Subsequent biopsy proven local melanoma recurrence. Axial post-contrast T1-weighted MRI (**e**) shows the same metastasis at 8 months following radiosurgery (red arrow in **e**) with the corresponding section of a concurrent axial FDG PET attenuation-corrected source image (**f**), illustrating a false-negative PET examination (no appreciable focal radiotracer accumulation in **f**) owing to the small metastasis size and proximity to high physiologic levels of cortical radiotracer uptake

tumor [73]. Increasing ADC values following radiosurgery of cerebral metastases are predictive of good tumor control, and may even be appreciated prior to changes in enhancing lesion volume [74–76]. Note that pus, hemorrhage, or other highly proteinaceous material may also result in low ADC values.

Perfusion-weighted imaging is a commonly available adjunct to conventional MRI sequences, typically adding 2–5 minutes to overall scan time. A variety of MR perfusion techniques are available, with dynamic susceptibility contrast-enhanced (DSC) more so than dynamic contrast-enhanced (DCE) protocols utilized most commonly in clinical neuro-oncology practices [77]. Changes in tumoral vascular density following radiosurgery are best captured in the cerebral blood volume (CBV), which is often compared with white matter, corrected for leakage, and reported as a unit-less normalized relative cerebral blood volume (rCBV). Multiple studies have shown increased normalized rCBV to be a useful marker of radiosurgical treatment failure in cerebral metastasis, with optimized threshold values ranging from 1.54 to 2.1 [78–82]. Major artifacts of DSC perfusion imaging that may result in erroneous perfusion maps include significant intralesional blood products or heavy calcification (best appreciable on GRE or SWI series) (Fig. 9a–f) and substantial first-pass contrast agent leakage (this should be mitigated with contrast agent preload bolus and/or model-based leakage correction software algorithms) [83].

Hydrogen-1 (^{1}H) MR spectroscopy provides in vivo information regarding the proportional abundance of metabolite species. Briefly, N-acetylaspartate (NAA) is a mitochondrial marker that indicates neuronal viability, choline (Cho) is a cell membrane derivative that indicates cellular proliferation or membrane turnover, creatine (Cr) is a relatively constant marker of cellular metabolism which may serve as an internal reference peak, lipid (Lip) is an indicator of cell degradation and necrosis, and lactate (Lac) is a non-specific marker of cellular stress as found in anaerobic metabolism and inflammation [84]. As such, recurrent metastases typically display reduced NAA and increased choline peaks, often with reduced Cr peaks and sometimes with Lip/Lac peaks. Radiation necrosis typically displays an elevated Lip/Lac peak with a generalized decrease in other metabolites [85, 86]. Several metabolite ratio thresholds have been proposed to identify recurrent metastatic disease, including Cho/Cr >2.5 [87], Cho/Lip >0.3 [88], and Cho/nCho >1.2 [81]. Similarly to perfusion MR, MR spectroscopy may render non-diagnostic by the presence of blood products, close proximity to the skull base/calvarium or ventricles, and small lesion size.

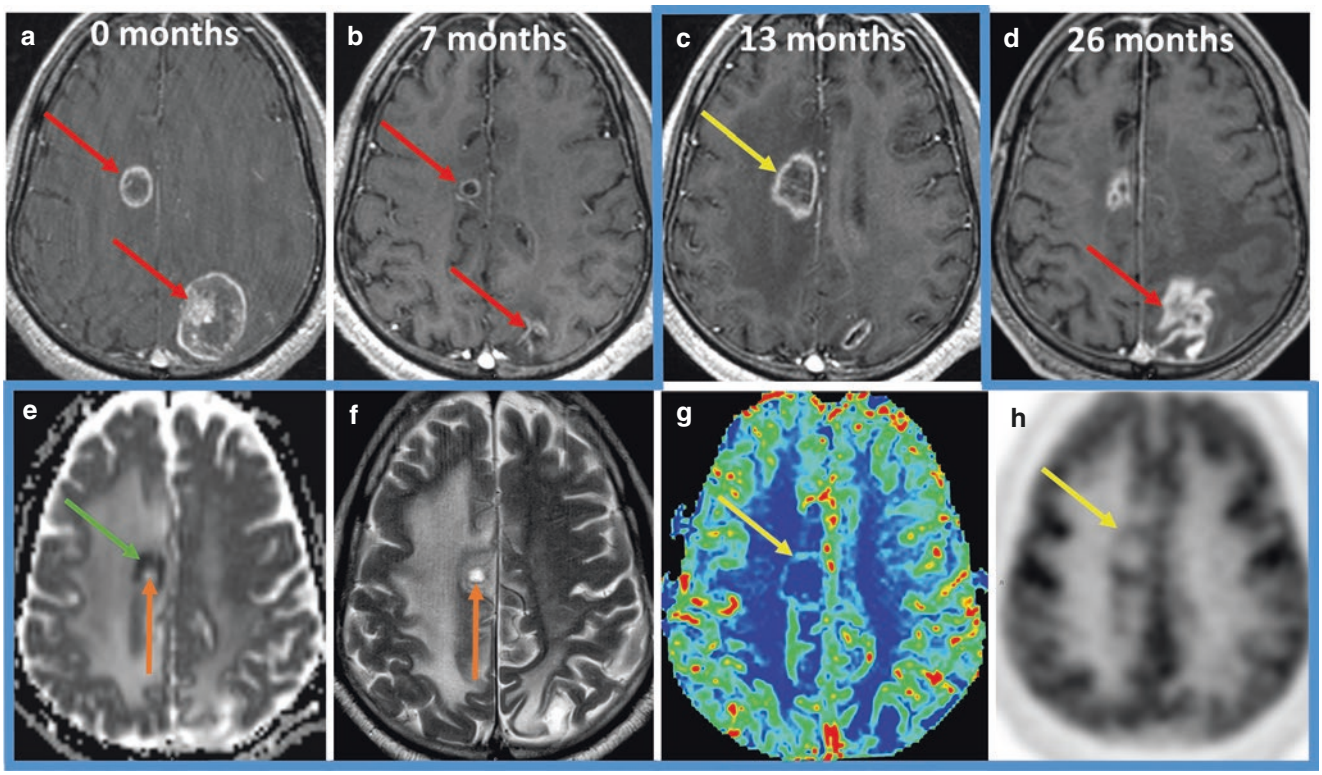

Fig. 10 Cerebral metastasis. Pseudoprogression. Axial post-contrast T1-weighted MR images obtained at baseline pretreatment 0 months (**a**), 7 months (**b**), 13 months (**c**), and 26 months (**d**). Additional images obtained at 13 months (blue border inlay) include axial ADC map MRI (**e**), axial T2-weighted MRI, axial DSC perfusion-weighted MRI corrected cerebral blood volume map (**g**), and axial FDG PET attenuation corrected source images (**h**). Baseline pretreatment exam (**a**) demonstrates parasagittal right frontal and left parietal non-small cell lung cancer metastasis (red arrows). At 7 months following radiosurgery (**b**) there is marked treatment response with small residual areas of enhancement present (red arrows). At 13 months (**c**, **e**–**h**) pseudoprogression of the right frontal metastasis is noted as an enlarging area of predominantly peripheral ring-like enhancement (yellow arrow in **c**). Corresponding to the peripheral ring of enhancement are low-level hyperperfusion (yellow arrow in **g**) and mild FDG uptake (yellow arrow in **h**). Just deep to this outer peripheral ring of signal abnormality is a middle ring of diffusion restriction seen as hypointense ADC signal (green arrow in **e**) which in turn surrounds a core of facilitated diffusion that is seen as hyperintense ADC signal (orange arrow in **e**) and hyperintense T2 signal (orange arrow in **f**). At 13 months, the right frontal metastasis was biopsied and revealed pure radiation necrosis without viable tumor cells. At 26 months, the left parietal metastasis also demonstrates pseudoprogression (red arrow in **d**), which subsequently followed a similar imaging course as the right frontal metastasis (not shown)

Positron emission tomography (PET) with 2-deoxy-[18F]fluoro-D-glucose (FDG) is commonly used to differentiate radiation necrosis from local metastasis recurrence, with reported sensitivity and specificity of 50–82% and 80–100%, respectively. Positive FDG PET/CT findings are variably defined as any radiotracer uptake or >1.4 times the radiotracer uptake of normal white matter [82, 85, 89–91]. FDG PET/CT sensitivity for recurrent metastasis may suffer due to the inherent limitations in spatial resolution and the normally high physiologic radiotracer accumulation in brain cortex that may obscure lesion uptake (Fig. 9a–f).

Complications and Toxicity

Adverse radiation effects, including symptomatic edema and radiation necrosis, though still infrequent (13–14%), are more commonly identified following treatment of larger lesions (2–5 cm) and lesions previously treated with radiation therapy [92].

Future Directions

Amino acid PET radiotracers such as 11C-methionine (MET) are proving useful in neuro-oncology applications as high neoplasm radiotracer uptake compared to relatively lower physiologic brain uptake improves lesion conspicuity [93, 94].

Practical Considerations

- Transient posttreatment enlargement, pseudoprogression, of vestibular schwannomas and cerebral metastases is a common occurrence and does not necessarily imply treatment failure.

- Isotropic post-contrast T1-weighted images are essential for small metastasis detection and accurate volumetric measurements following solid tumor radiosurgery.
- Digital Subtraction Angiography remains the reference standard in evaluation of arteriovenous malformations, and is generally performed during treatment planning and to document nidus obliteration.
- Dynamic susceptibility contrast-enhanced (DSC) perfusion is commonly available with most MRI scanners, adds only a few minutes to scan time, and has proven utility in the differentiation of tumor recurrence from treatment-related changes.

Part II. Stereotactic Ablative Radiotherapy: Applications in the Lung

The use of local radiotherapy for the treatment of pulmonary neoplasms has undergone significant advancements after the development of lung stereotactic ablative radiotherapy (SABR) in the early 1990s [95]. Technical developments in the past decade have optimized the precision of radiotherapy delivery methods and image-guided techniques, which have increased the applicability, efficiency, and safety of local radiation in the treatment of pulmonary neoplasms.

Surgery remains the standard of care for early stage non-small cell lung cancer (NSCLC), with loco-regional control rates ranging between 78% and 90% according to different series [96, 97]. Despite the acceptable results obtained with surgical resection at early stages, the impact of lobectomy in the functional pulmonary reserve and its inevitable morbidity and mortality are important considerations for management decisions [98, 99]. The use of local radiation as an alternative treatment strategy in patients with surgical contraindications has rapidly evolved. Until recently, conventionally fractionated radiotherapy (CFR) has traditionally been the standard alternative to surgery for non-operable patients with early lung cancer [97], with 5-year survival rates after CFR for stage I NSCLC ranging around 15–30%. The limitations to the use of CFR mainly derive from total dose tolerance by the lung parenchyma in peripheral tumors and by mediastinal organs in central tumors [97].

With the development of SABR, high doses per fraction allow an ablative tumor effect and safer treatment with a higher biological effective dose (BED) than is possible with CFR [97]. The exact comparison between survival rates in patients treated with surgery or radiation therapy is limited by the difficulty in obtaining an accurate pathological staging in patients who do not undergo surgical resection, but both treatment options have resulted in comparable local control rates [100–102]. Owing to the conformity of treatment dose delivery and appropriate dose fractionation, the side effects to surrounding tissues with SABR are minimal [95, 103], an important advantage over CFR. SABR is now a standard treatment option for early stage, node-negative NSCLC in patients with contraindications to surgical resection [102, 104]. It has also been introduced as an option for the treatment of oligometastatic disease to the lung, delivered alone or in combination with systemic therapy [105–107].

Despite the proved efficiency of SABR for the treatment of early stage NSCLC and its promising applications in oligometastatic disease, the safe delivery of high doses of radiation per fraction to the lung poses specific challenges. As a moving organ along the respiratory cycle, the lungs represent a special challenge to the precise and safe delivery of local radiation. The use of ablative doses requires a highly accurate technique, not only to optimize the delivery of treatment-appropriate doses to the neoplastic tissue but, almost as importantly, to avoid unnecessary exposure and potential damage of non-target organs [95]. The accuracy and precision should be ensured repetitively during daily treatment sessions, which require the implementation of specific strategies to deal with the inherent motion of the lungs.

Patient positioning should be comfortable and stable, in order to ensure reproducibility. Supine decubitus with arms above the head is most frequently used, although modifications may be required for individual patients. Immobilization of an organ such as the lung is not entirely possible. Although breath holding and abdominal compression can temporarily decrease motion, these techniques alone fall short for the precision needed for an ablative treatment such as SABR. Computed tomography (CT)-based techniques have been playing an increasingly important role in the planning of SABR, not only to estimate the planning target volume, but specifically to calculate and correct for motion of the tumor during the breathing cycle [103, 108]. Four-dimensional CT is the preferred method in most institutions to resolve respiratory motion and calculate the internal target volume (ITV). Sequential imaging is acquired during the entire breathing cycle, which allows accurate contouring of the lesions along the different phases of respiration [109].

Delivering the highest required dose to the target lesion (as high as 100 Gy) while carefully avoiding increasing the dose to normal critical organs is the main objective while planning treatment. Dose-limiting structures that are considered while treating central lung tumors (within 2 cm from the proximal bronchi or mediastinum) include the normal lung, trachea, bronchi, major vessels, and esophagus [110]. For peripheral tumors, the chest wall, brachial plexus, spinal cord, and skin are the main organs at risk and regulate both the dose and fractionation [103, 110]. A scheme of dose fractionation selection as detailed in the UK SABR Consortium Guidelines is presented in Fig. 11.

Fractionation	*Dose*	*Scheme*
Standard Fractionation PTV is not in proximity with chest wall or mediastinum	54 Gy 3 Fraction	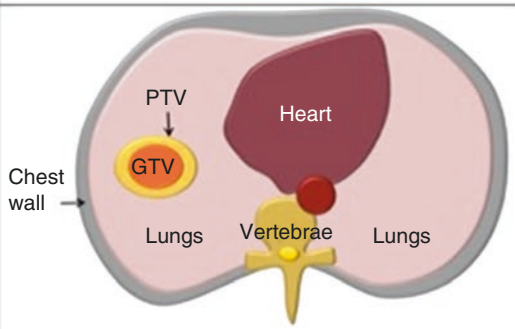
Conservative Fractionation PTV is in proximity or touches the chest wall	55 – 60 Gy 5 Fractions	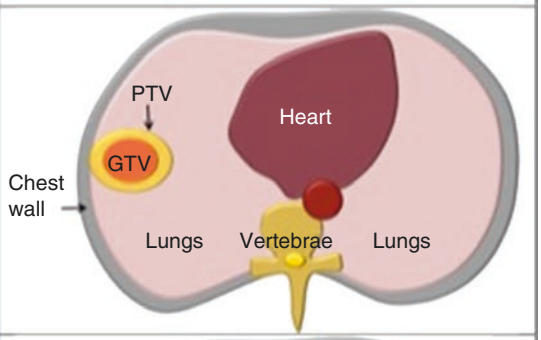
Very Conservative Fractionation The dose constrains for an organ at risk cannot be met by 3 or 5 fractions scheme	60 Gy 8 Fractions	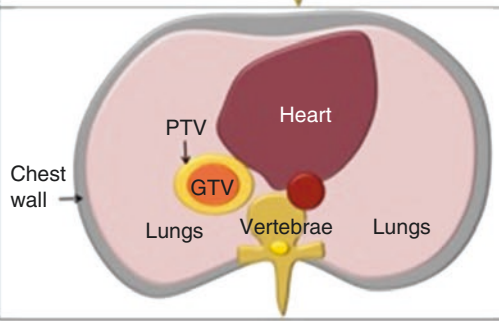

Fig. 11 Scheme of dose fractionation selection as detailed in the UK SABR Consortium Guidelines

Complications and Toxicity

The doses used in lung SABR are empirically based on existing literature and are constantly revaluated. Many different fractionation schemes have been used and reported, with widely variable results that suggest that multiple factors (patient-, tumor-, and dose-related) influence the incidence of toxicity in organs at risk [110, 111].

Lung Parenchyma

Pulmonary toxicity is uncommon with SABR and more frequently seen with CFR, where larger volumes of lung tissue are exposed to radiation. Due to the limited tissue volume that receives the ablative doses in SABR, pulmonary toxicity (with ablative effect) is limited to the planning target volume (PTV) region, which is created by a 5 mm universal expansion margin from the internal target volume (ITV) [95, 110]. Excessive radiation dose can cause pulmonary toxicity, usually seen with median prescription doses >60 Gy in 3 fractions [110].

Many variables participate in the development of toxicity to the lungs after radiation, most of which are more relevant with therapeutic strategies that imply radiation to a larger volume of tissue such as CRT. Toxic effects of SABR are uncommon, although similar factors should be kept in mind and assessed during the patient selection process. Patient-specific factors such as lung performance status, coexisting lung diseases, and functional impairment play a role in the development of toxicity [112]. Similarly, concomitant chemotherapeutic agents (such as bleomycin and busulfan, among others) may increase the likelihood of pulmonary toxicity.

The pathophysiology of radiation pneumonitis is similar to any other type of acute alveolar damage, in which three phases of lung injury are well recognized: exudative, proliferative (or organizing), and fibrotic phases [113]. Radiation pneumonitis is usually evident 4–12 weeks after completion of radiation therapy, but lung tissue fibrosis may take up to 12–24 months to evolve and establish [114]. Preexisting lung disease (such as interstitial lung disease or smoking-related lung disease), concomitant chemotherapy, and underlying functional capacity take part in the development and severity of tissue damage after radiation [110, 114]. As an active inflammatory process, the initial stages of radiation pneumonitis are characterized by acute inflammatory exudate within the alveolar spaces, followed by proliferation of fibroblasts. These two phases manifest as ground-glass and consolidative opacities on CT images, confined to the area of radiation. Figure 12 demonstrates the normal evolution of radiation-induced changes in the lung after CFR, where the volume of normal lung that is exposed to therapeutic doses of radiation is larger, and thus, morphologic changes are more frequent. Figures 13a–c and 14a, b illustrate the normal evolution of a lesions treated with SABR, where a smaller volume of normal lung tissue is radiated; thus, the changes in the parenchyma are limited to the lesion; minimal surrounding pneumonitis and fibrosis develop.

The active inflammatory response of the lung during the exudative and proliferative phases evolves into deposition of fibroblasts, which are responsible for the latest stage of tissue damage and result in fibrosis of the radiated lung. This active inflammatory phase can take up to 6 months to evolve, and thus, it is actively changing over the first period after radiation [112]. The areas of fibrosis start to appear after approximately 6 months of the final treatment session and are characterized by cicatricial atelectasis, volume loss, and traction bronchiectasis, again limited to the field of irradiation [113, 114].

The appropriate timing for the imaging follow-up of patients treated with SABR is determined by the dose fractionation and date of completion of treatment. Due to the initial inflammatory phase induced by radiation, recognized as radiation pneumonitis during the first 6 months of treatment, the radiated tissue will demonstrate continuous changes. Interpretation of diagnostic images is limited during this initial stage, and the differentiation between expected pneumonitis from complications such as infection and early tumor recurrence is very challenging.

Routinely, imaging follow-up with Chest CT is not indicated during the first 6 months after completion of

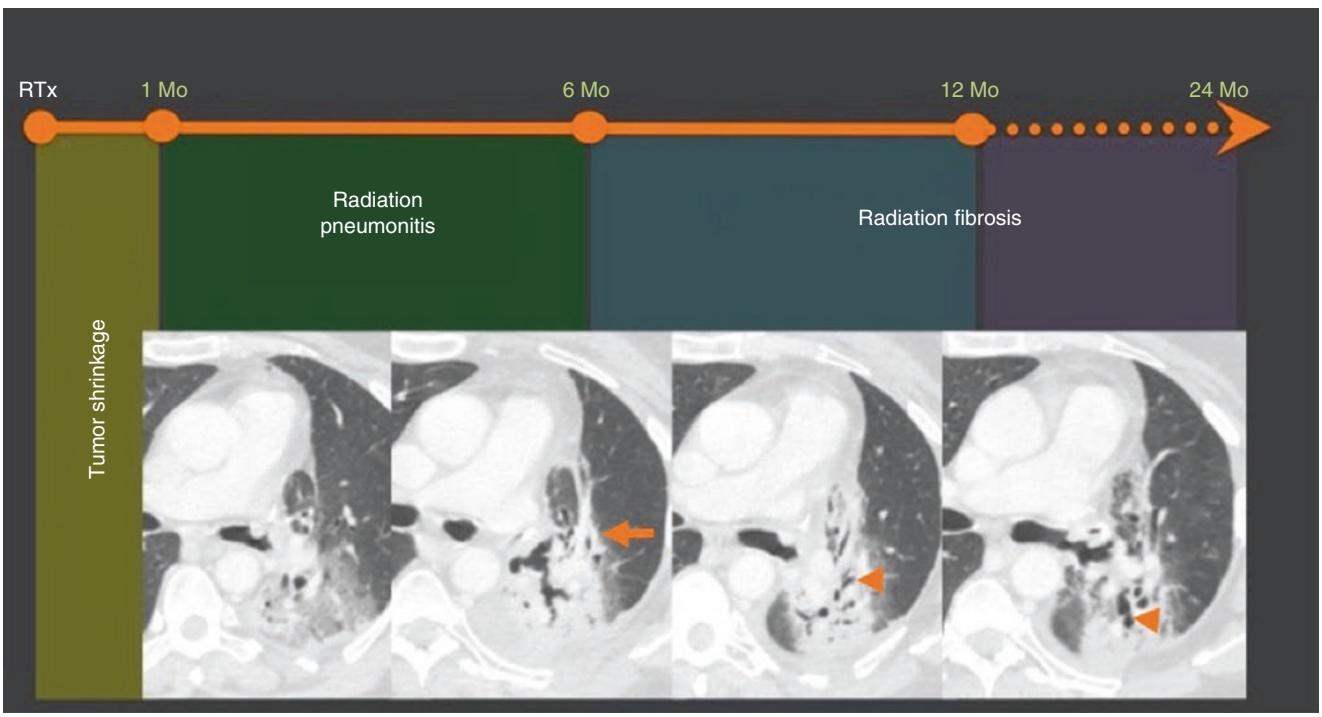

Fig. 12 Timeline of the imaging findings after CRT to the lung. Ground-glass and consolidative opacities appear in the radiation field and evolve during the first 6 months after completion of therapy, characterizing the acute phase of pneumonitis. There is a characteristic straight and clear boundary between these opacities and the normal lung (arrow), which conforms to the radiation beam. After 6 months, the radiation fibrosis starts to appear as contraction of the radiated lung parenchyma and appearance of traction bronchiectasis (arrowheads)

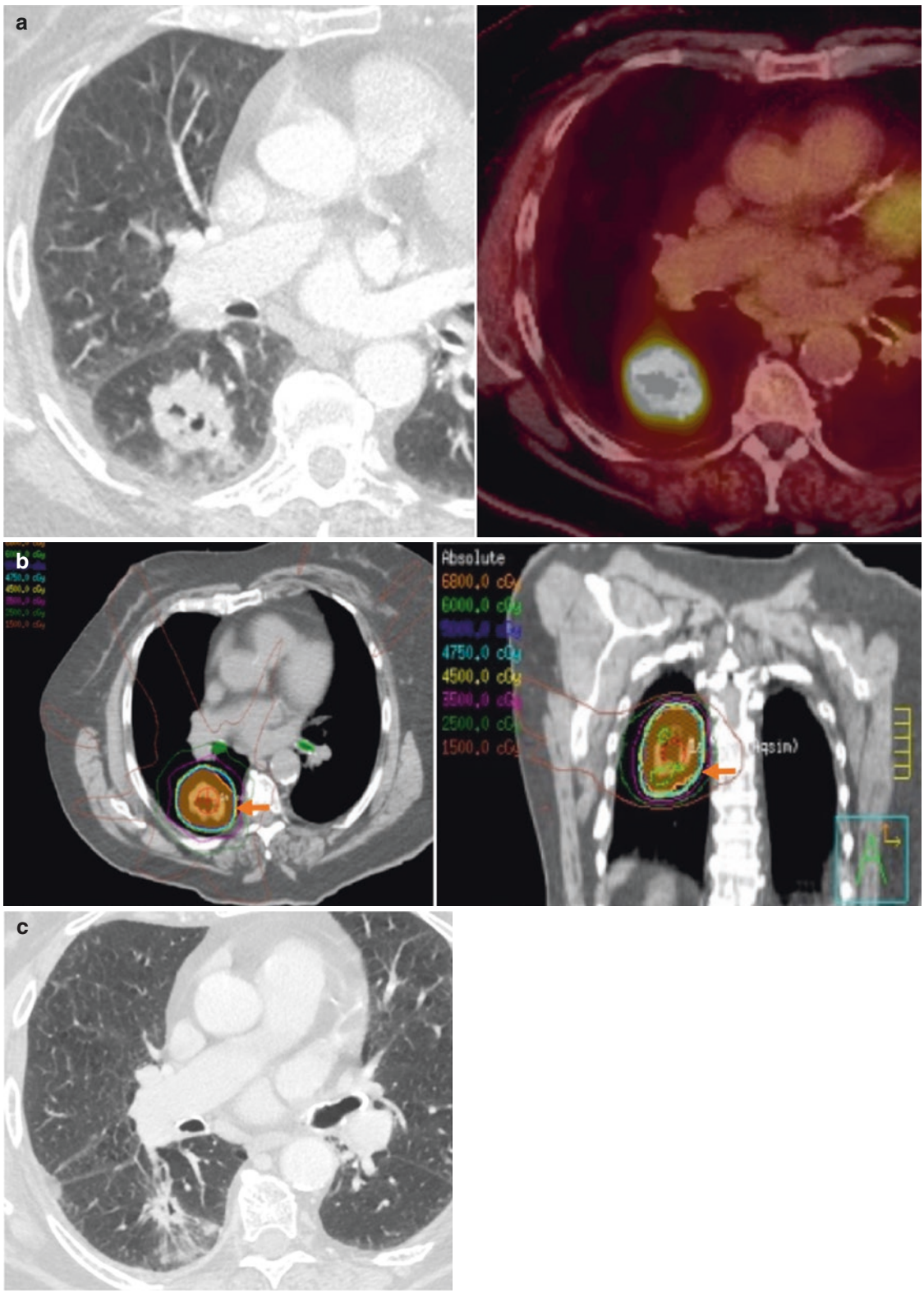

Fig. 13 Normal evolution of lesions treated with SABR as seen by CT. (**a**) Cavitary neoplastic mass in the right lower lobe demonstrates high abnormal FDG uptake and represents a primary non-small cell neoplasm (squamous cell carcinoma in this case). (**b**) Illustration of the radiation planning and resultant radiation dose distribution. The light green line (arrow) delineated the PTV, receiving the highest therapeutic dose. (**c**) Imaging appearance of the residual lesion 6 months after completion of therapy. The primary lesion has decreased in size and now demonstrates spiculated contours, representing cicatricial atelectasis and established radiation fibrosis

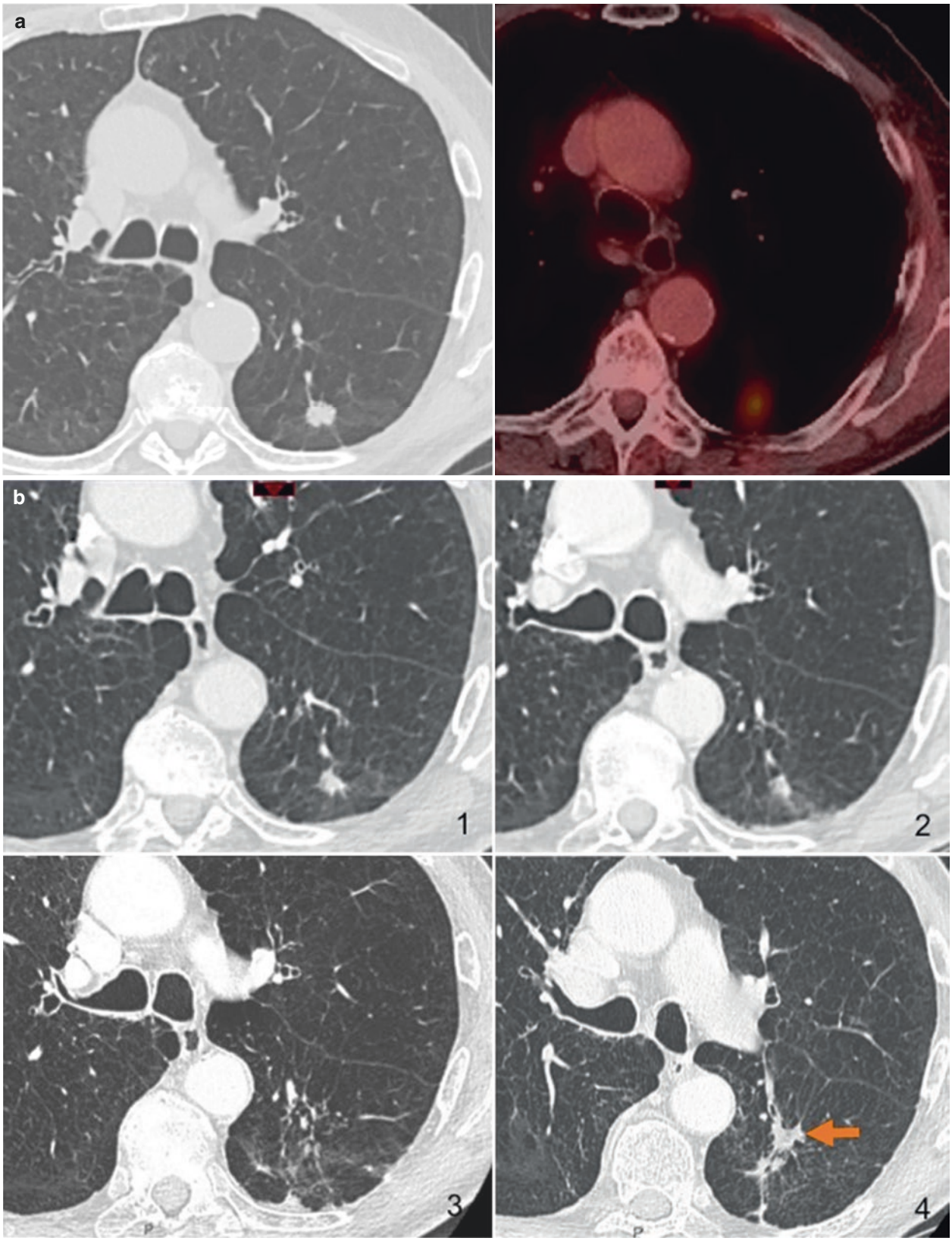

Fig. 14 (**a**) Axial CT and PET CT images demonstrate solid nodule in the left lower lobe with abnormal increased FDG uptake, known to represent a stage IA adenocarcinoma. (**b**) Continuum of images illustrates the morphologic changes of the nodule after SABR. Only minimal decrease in size is noted at 3 months (1) and 14 months (2), with surrounding ground glass representing radiation fibrosis limited to the PTV. At 1.4 years after treatment (3), the nodule resolves and cicatricial atelectasis characterizes the focal radiation fibrosis. A new solid component appears at the site of radiation after 2 years (4) of therapy completion (arrow), representing subsequently biopsy-proven local recurrence

treatment, unless an early complication (most commonly infection) is suspected [112]. Commonly, imaging follow-up is scheduled at 6 and 12 months after completion of treatment; comparison with prior imaging is essential for the assessment of the radiation bed and detection of early recurrence and non-neoplastic complications. CT and PET CT are the imaging methods of choice for follow-up of these patients [113].

Trachea and Mainstem Bronchi

Various organs are at risk of radiation injury, depending on the location of the tumor. The central airways are one of the most sensitive of these organs and are specifically important in centrally localized lesions, with potential lethal toxicities [103, 110]. Radiation to proximal bronchi (lobar and mainstem bronchi) and trachea, known as the "no-fly zone" (Fig. 15), may result in radiation-induced injuries that significantly increase morbidity of patients [115]. Strictures, high-grade stenosis, occlusion, and fistula formation are some of the most frequently reported [110, 116].

Esophagus and Great Vessels

The incidence of toxicity to mediastinal organs with SABR is low given the limited field of radiation that receives ablative doses. Complications associated with injury of the great vessels such as bronchovascular fistulas, venous stenosis, and radiation vasculitis were described with prior therapeutic regimens that involve larger volumes of tissue receiving high doses of radiation, such as conventional radiotherapy and CFR [110]. The esophagus is at risk of radiation injury during treatment of central and posterior lesions. Esophagitis, strictures, and fistulas are the most commonly described complications [110, 115].

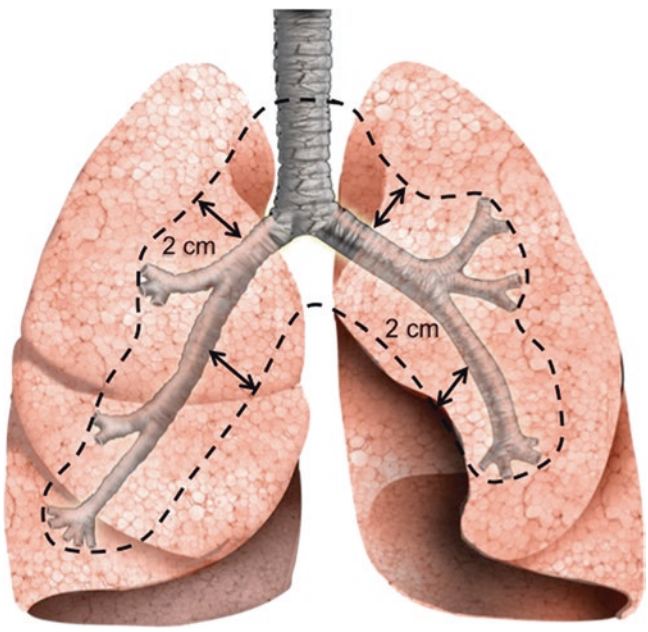

Fig. 15 Illustration of the "no fly zone." A 2-cm perimeter around the proximal bronchial tree in which high-dose fractions are not recommended due to excessive toxicity

Chest Wall

Structures of the chest wall are specifically at risk when the tumor is in the periphery of the lung. Ribs and cartilaginous components of the costosternal junctions are more commonly the cause of pain after treatment, usually secondary to osteitis, chondritis, or fractures (Fig. 16a–d).

Future Directions

Extensive literature currently supports the use of SBAR as the treatment strategy of choice in patients with early, node-negative NSCLC, with results similar to those obtained by surgical resection [98, 104, 117]. As a technique that allows highly efficient and overall safe local delivery of high doses of radiation, it has been proposed and recently used for the local treatment of other neoplastic processes, specifically oligometastatic disease to the lungs, with promissory results.

The lungs are the most common site of metastasis of solid tumors, and metastasis, in general, remains the first cause of cancer death [118]. Surgical metastasectomy has been implemented over the last decade for the treatment of solid tumors such as colorectal carcinoma, breast cancer, and melanoma with limited pulmonary metastatic disease, with reported better long-term disease control [118, 119] by single institutions; high-level data on the impact of these type of treatments remain limited. As a noninvasive alternative with proven high capacity for local control, SBAR has been proposed and implemented as a reasonable alternative to surgical metastasectomy.

The definition of oligometastatic disease is not unanimous, but generally accepted as limited distant hematogenous spread involving 1–5 metastatic sites. It has been demonstrated that patients with oligometastatic disease have better outcomes than patients with polymetastases [118] and that their disease tends to progress in limited organs. The possibility to pursue curative treatment through local ablation of metastatic deposits has revolutionized the approach to metastatic disease and represents an excellent alternative for selected patients.

The benefits of the use of SABR in conjunction with systemic therapy have yet to be proven and are a source of investigation [118]. Similarly, patient selection, definition of specific prognostic factors, and defining the impact of the addition of SABR to standard regimens still require further research [120].

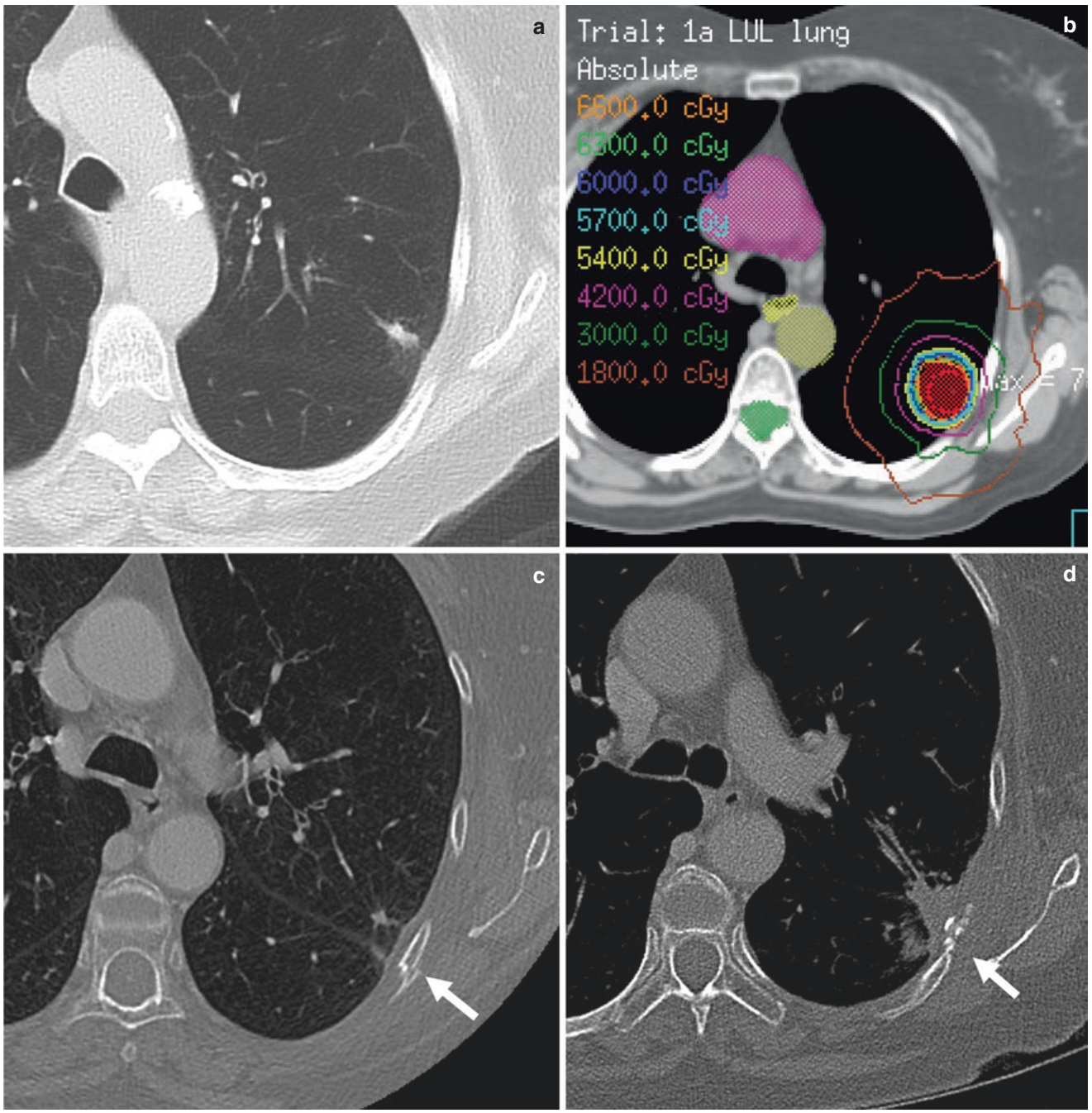

Fig. 16 Radiation osteitis and pathologic rib fracture. The radiation planning for a peripheral LUL neoplastic nodule (**a**, **b**) includes the adjacent chest wall in the irradiated volume (orange outer line on **b**). Nine months after completion of treatment (**c**), there is a new pathologic fracture in the adjacent rib (arrow in **c**). Osseous fragmentation, sclerosis, and soft tissue surrounding the fracture foci characterize radiation osteitis, 2 years after completion of therapy (arrow in **d**)

Practical Considerations

Potential toxicities In SABR, the location and size of the lesion determine the organs at risk of toxicity, which will thus modify the dose and fractionation (Fig. 15).

- *Central lung tumors* (within 2 cm from the proximal bronchi or mediastinum): organs at risk include the normal lung, trachea, bronchi, major vessels, and esophagus.
- *Peripheral tumors*: the chest wall, brachial plexus, spinal cord, and skin.

Assessment of treatment response Assessment of treatment response is performed by a combination of clinical and imaging assessment methods, with imaging playing an important role in the detection of early complications.

- Chest CT and PET CT are the main imaging methods of choice for the assessment of the radiation field [112, 113].
- Imaging follow-up is not routinely indicated during the first 6 months after completion of treatment given the constant change in the appearance of the radiation bed induced by active inflammatory response in the lung tissue (radiation pneumonitis).
- Radiation pneumonitis evolves into radiation fibrosis around 6–12 months after completion of therapy, although changes may be seen up to 2 years in some cases of SBAR [113].
- Radiation fibrosis is characterized by cicatricial atelectasis, traction bronchiectasis, and volume loss of the treated parenchyma, limited to the port of radiation.
- Imaging findings such as new consolidation or new ground-glass opacities in the area of radiation after 6 months should prompt closer imaging follow-up and raise suspicion for complications such as infection and local recurrence. Correlation with clinical symptoms is paramount.
- PET/CT plays an essential role in the suspicion of local recurrence after 12 months of treatment completion, although it has a limited role in earlier stages after treatment, given expected increased metabolic activity of the parenchyma in the radiation pneumonitis phase [113].

Part III. Stereotactic Ablative Radiotherapy: Applications in the Prostate

Multiparametric Magnetic Resonance Imaging (mpMRI) of the prostate gland is the imaging modality of choice for the detection, staging, and localization of clinically significant prostate cancer, as well as surveillance and detection of recurrence after prostatectomy and radiation therapy [121, 122]. Computed tomography (CT) and bone scintigraphy are typically performed for the detection of nodal disease and distant bone metastases, whereas positron emission tomography (PET) is reserved for biochemical relapse [123]. Advantages of mpMRI over other imaging modalities include high spatial resolution providing superior anatomic detail combined with functional tissue information obtained using dynamic contrast agent-enhanced imaging, diffusion-weighted imaging (DWI), and hydrogen 1 MR spectroscopic (MRS) imaging techniques. MpMRI can reliably differentiate the normal intermediate- to high-signal-intensity peripheral zone from the low-signal-intensity central and transition zones. More importantly, mpMRI can accurately identify clinically significant (Gleason 7 and higher) prostate cancer based on focal low signal intensity on T2-weighted imaging with restricted diffusion and early enhancement on dynamic contrast-enhanced imaging (Fig. 17a–d).

Predictable changes occur in the prostate gland after various types of therapy. The main effects of stereotactic body radiation therapy (SBRT) on the MRI appearance of the prostate gland include a decrease in size and diffusely decreased signal intensity (SI) on T2-weighted imaging due to glandular loss and fibrosis (Fig. 18a–d) [121]. This decrease in SI typically reduces the conspicuity of prostate cancer, particularly in the peripheral zone where the intermediate to high SI of the normal peripheral zone outlines low SI prostate cancer. When interpreting mpMRI after radiation therapy to evaluate for recurrence, the first important factor to consider is that recurrence usually occurs at the site of primary cancer, highlighting the importance of reviewing pretherapy imaging. Despite the diffusely decreased SI of the prostate gland, recurrent prostate cancer tends to remain lower in SI compared to surrounding gland. Moreover, recurrence tends to demonstrate early arterial enhancement on dynamic contrast-enhanced MRI with washout, restricted diffusion, and characteristic changes on MRS that can be used to differentiate treated prostate cancer from recurrence [124–128].

Complications and Toxicity

Radiographically appreciable complications following prostate SBRT radiosurgery are low.

Future Directions

There are several new PET radiotracers in clinical use that show promise in the detection of prostate cancer recurrence after SBRT and other forms of therapy. Fluorodeoxyglucose is the most widely used PET tracer but is limited in the evaluation of prostate cancer due to the relatively low glucose metabolism of most prostate tumors [123]. ^{11}C-Choline and ^{18}F-Choline target cell membrane metabolism and are more accurate in the detection of lymph node recurrence compared to mpMRI, with mpMRI demonstrating better accuracy in the detection and localization of prostate/prostatic fossa recurrence [129–131]. ^{68}Ga-PSMA targets prostate-specific membrane antigen and is highly sensitive for biochemical relapse in patients with lower prostate-specific antigen (PSA) levels compared to choline PET/CT [132, 133]. A promising area of research is the possibility of using ^{177}Lu- or ^{90}Y-labeled PSMA ligands for targeted radionuclide therapy [123]. ^{18}F-Fluciclovine is an amino acid analog that has been shown to allow detection of local and distant recurrence

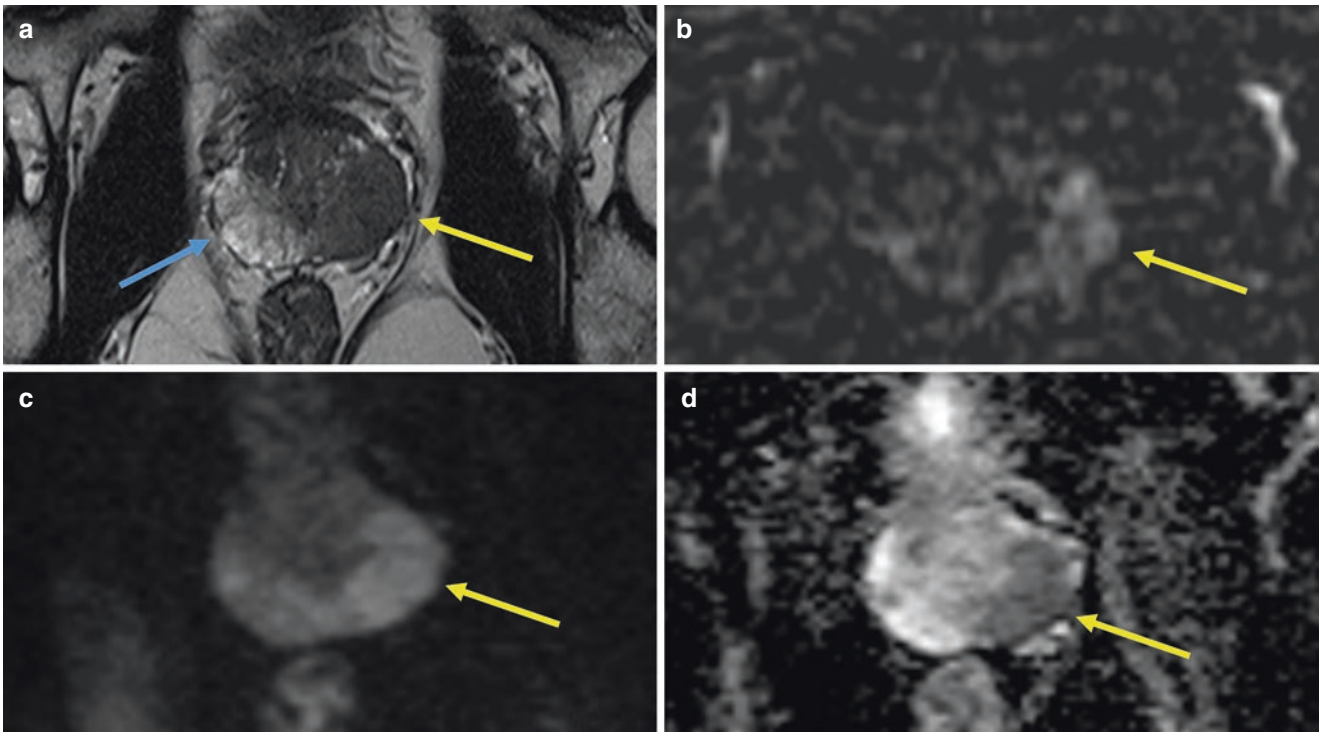

Fig. 17 Prostate adenocarcinoma prior to treatment. A 72-year-old male with suspicious prostate nodule, PSA at 27. No prior biopsy. Small field of view mpMRI demonstrates a suspicious lesion (yellow arrows) in the left peripheral gland with focal low T2 SI (**a**), early enhancement on dynamic contrast-enhanced images (**b**), and restricted diffusion on high b-value (**c**) and ADC (**d**) images. Compare with the high SI in the normal peripheral zone on T2-weighted images (blue arrow in **a**)

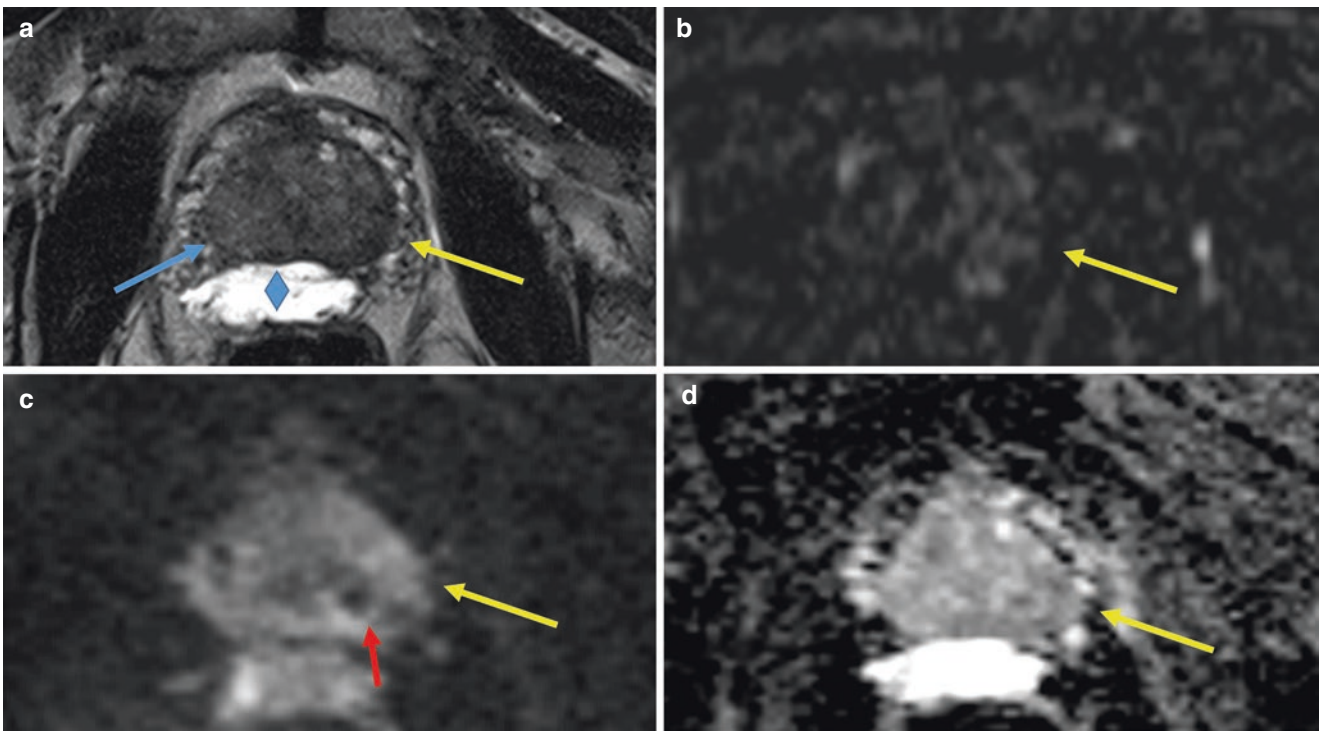

Fig. 18 Prostate adenocarcinoma after radiation therapy. Small field of view mpMRI demonstrates decreased SI diffusely throughout the prostate gland (blue arrow), which reduces the conspicuity of the left peripheral zone prostate adenocarcinoma (yellow arrow) on T2-weighted imaging (**a**). There is loss of early enhancement on (**b**) dynamic contrast-enhanced images (**b**), as well as reduction in diffusion restriction previously seen on high b-value DWI (**c**) and ADC (**d**) images, reflecting interval radiation treatment. Note susceptibility from fiducial markers (red arrow in **c**). Hydrogel spacer (blue diamond in **a**) increases distance between the prostate gland and rectum, which reduces radiation effects on the rectum

of prostate cancer across a wide range of PSA values and is superior to choline PET, but has not been directly compared with ^{68}Ga-PSMA [123, 134, 135]. ^{18}F-Sodium Fluoride is an analog of the hydroxyl group in hydroxyapatite bone crystals that is a sensitive imaging technique for the detection of bone metastases but does not assess soft tissue and has no utility in the detection of local or nodal recurrence.

Practical Considerations

- Recurrence most often occurs at the site of primary prostate cancer, highlighting the importance of reviewing pretherapy imaging in the setting of suspected recurrence.
- Focal lesions demonstrating low T2 SI may represent treated tumor rather than recurrence.
- Recurrent tumors may not be apparent on T2-weighted images after SBRT due to the diffuse decrease in T2 SI of the prostate gland.
- Growth of a focal lesion, progressive bulging of the prostatic capsule, restricted diffusion, and early enhancement with washout on dynamic contrast-enhanced imaging are features of recurrence.
- Radiation-induced capsular irregularity may impede assessment of extracapsular extension.

References

1. Bonneville F, Savatovsky J, Chiras J. Imaging of cerebellopontine angle lesions: an update. Part 1: enhancing extra-axial lesions. Eur Radiol. 2007;17(10):2472–82.
2. Kim DY, Lee JH, Goh MJ, Sung YS, Choi YJ, Yoon RG, et al. Clinical significance of an increased cochlear 3D fluid-attenuated inversion recovery signal intensity on an MR imaging examination in patients with acoustic neuroma. AJNR Am J Neuroradiol. 2014;35(9):1825–9.
3. Salzman KL, Childs AM, Davidson HC, Kennedy RJ, Shelton C, Harnsberger HR. Intralabyrinthine schwannomas: imaging diagnosis and classification. AJNR Am J Neuroradiol. 2012;33(1):104–9.
4. Kondziolka D, Mousavi SH, Kano H, Flickinger JC, Lunsford LD. The newly diagnosed vestibular schwannoma: radiosurgery, resection, or observation? Neurosurg Focus. 2012;33(3):E8.
5. Bowden G, Cavaleri J, Iii EM, Niranjan A, Flickinger J, Lunsford LD. Cystic vestibular schwannomas respond best to radiosurgery. Neurosurgery. 2017;81(3):490–7.
6. Link MJ, Driscoll CL, Foote RL, Pollock BE. Radiation therapy and radiosurgery for vestibular schwannomas: indications, techniques, and results. Otolaryngol Clin N Am. 2012;45(2):353–66, viii–ix.
7. Pendl G, Ganz JC, Kitz K, Eustacchio S. Acoustic neurinomas with macrocysts treated with Gamma Knife radiosurgery. Stereotact Funct Neurosurg. 1996;66(Suppl 1):103–11.
8. Delsanti C, Regis J. Cystic vestibular schwannomas. Neurochirurgie. 2004;50(2–3 Pt 2):401–6.
9. Frisch CD, Jacob JT, Carlson ML, Foote RL, Driscoll CL, Neff BA, et al. Stereotactic radiosurgery for cystic vestibular schwannomas. Neurosurgery. 2017;80(1):112–8.
10. Wu CC, Guo WY, Chung WY, Wu HM, Lin CJ, Lee CC, et al. Magnetic resonance imaging characteristics and the prediction of outcome of vestibular schwannomas following Gamma Knife radiosurgery. J Neurosurg. 2017;127:1–8.
11. Nagano O, Serizawa T, Higuchi Y, Matsuda S, Sato M, Yamakami I, et al. Tumor shrinkage of vestibular schwannomas after Gamma Knife surgery: results after more than 5 years of follow-up. J Neurosurg. 2010;113(Suppl):122–7.
12. Regis J, Delsanti C, Roche PH. Editorial: vestibular schwannoma radiosurgery: progression or pseudoprogression? J Neurosurg. 2017;127(2):374–9.
13. Hayhurst C, Zadeh G. Tumor pseudoprogression following radiosurgery for vestibular schwannoma. Neuro-Oncology. 2012;14(1):87–92.
14. Nakamura H, Jokura H, Takahashi K, Boku N, Akabane A, Yoshimoto T. Serial follow-up MR imaging after gamma knife radiosurgery for vestibular schwannoma. AJNR Am J Neuroradiol. 2000;21(8):1540–6.
15. Fukuoka S, Takanashi M, Hojyo A, Konishi M, Tanaka C, Nakamura H. Gamma knife radiosurgery for vestibular schwannomas. Prog Neurol Surg. 2009;22:45–62.
16. Bloch J, Vernet O, Aube M, Villemure JG. Non-obstructive hydrocephalus associated with intracranial schwannomas: hyperproteinorrhachia as an etiopathological factor? Acta Neurochir. 2003;145(1):73–8.
17. Jeon CJ, Kong DS, Nam DH, Lee JI, Park K, Kim JH. Communicating hydrocephalus associated with surgery or radiosurgery for vestibular schwannoma. J Clin Neurosci. 2010;17(7):862–4.
18. Camargo A, Schneider T, Liu L, Pakpoor J, Kleinberg L, Yousem DM. Pretreatment ADC values predict response to radiosurgery in vestibular schwannomas. AJNR Am J Neuroradiol. 2017;38(6):1200–5.
19. Lin YC, Wang CC, Wai YY, Wan YL, Ng SH, Chen YL, et al. Significant temporal evolution of diffusion anisotropy for evaluating early response to radiosurgery in patients with vestibular schwannoma: findings from functional diffusion maps. AJNR Am J Neuroradiol. 2010;31(2):269–74.
20. Nanda A, Bir SC, Konar S, Maiti T, Kalakoti P, Jacobsohn JA, et al. Outcome of resection of WHO Grade II meningioma and correlation of pathological and radiological predictive factors for recurrence. J Clin Neurosci. 2016;31:112–21.
21. Lee EJ, Kim JH, Park ES, Kim YH, Lee JK, Hong SH, et al. A novel weighted scoring system for estimating the risk of rapid growth in untreated intracranial meningiomas. J Neurosurg. 2017;127:1–10.
22. Tang Y, Dundamadappa SK, Thangasamy S, Flood T, Moser R, Smith T, et al. Correlation of apparent diffusion coefficient with Ki-67 proliferation index in grading meningioma. AJR Am J Roentgenol. 2014;202(6):1303–8.
23. Surov A, Ginat DT, Sanverdi E, Lim CC, Hakyemez B, Yogi A, et al. Use of diffusion weighted imaging in differentiating between maligant and benign meningiomas. A multicenter analysis. World Neurosurg. 2016;88:598–602.
24. Chen WC, Magill ST, Englot DJ, Baal JD, Wagle S, Rick JW, et al. Factors associated with pre- and postoperative seizures in 1033 patients undergoing supratentorial meningioma resection. Neurosurgery. 2017;81(2):297–306.
25. Berhouma M, Jacquesson T, Jouanneau E, Cotton F. Pathogenesis of peri-tumoral edema in intracranial meningiomas. Neurosurg Rev. 2017. https://doi.org/10.1007/s10143-017-0897-x. [Epub ahead of print].
26. Alomari A, Rauch PJ, Orsaria M, Minja FJ, Chiang VL, Vortmeyer AO. Radiologic and histologic consequences of radiosurgery for brain tumors. J Neuro-Oncol. 2014;117(1):33–42.
27. Raper D, Yen CP, Mukherjee S, Sheehan J. Decreased calcification of a petroclival meningioma after gamma knife radiosurgery.

BMJ Case Rep. 2014;pii:bcr2014204272. https://doi.org/10.1136/bcr-2014-204272.
28. Harrison G, Kano H, Lunsford LD, Flickinger JC, Kondziolka D. Quantitative tumor volumetric responses after Gamma Knife radiosurgery for meningiomas. J Neurosurg. 2016;124(1):146–54.
29. Feigl GC, Samii M, Horstmann GA. Volumetric follow-up of meningiomas: a quantitative method to evaluate treatment outcome of gamma knife radiosurgery. Neurosurgery. 2007;61(2):281–6; discussion 6–7.
30. Kollova A, Liscak R, Novotny J Jr, Vladyka V, Simonova G, Janouskova L. Gamma Knife surgery for benign meningioma. J Neurosurg. 2007;107(2):325–36.
31. Sheehan JP, Starke RM, Kano H, Barnett GH, Mathieu D, Chiang V, et al. Gamma Knife radiosurgery for posterior fossa meningiomas: a multicenter study. J Neurosurg. 2015;122(6):1479–89.
32. Wang S, Kim S, Zhang Y, Wang L, Lee EB, Syre P, et al. Determination of grade and subtype of meningiomas by using histogram analysis of diffusion-tensor imaging metrics. Radiology. 2012;262(2):584–92.
33. Speckter H, Bido J, Hernandez G, Mejia DR, Suazo L, Valenzuela S, et al. Prognostic value of diffusion tensor imaging parameters for Gamma Knife radiosurgery in meningiomas. J Neurosurg. 2016;125(Suppl 1):83–8.
34. Sheehan JP, Ray DK, Monteith S, Yen CP, Lesnick J, Kersh R, et al. Gamma Knife radiosurgery for trigeminal neuralgia: the impact of magnetic resonance imaging-detected vascular impingement of the affected nerve. J Neurosurg. 2010;113(1):53–8.
35. Hughes MA, Frederickson AM, Branstetter BF, Zhu X, Sekula RF Jr. MRI of the trigeminal nerve in patients with trigeminal neuralgia secondary to vascular compression. AJR Am J Roentgenol. 2016;206(3):595–600.
36. Alberico RA, Fenstermaker RA, Lobel J. Focal enhancement of cranial nerve V after radiosurgery with the Leksell Gamma Knife: experience in 15 patients with medically refractory trigeminal neuralgia. AJNR Am J Neuroradiol. 2001;22(10):1944–8.
37. Massager N, Abeloos L, Devriendt D, Op de Beeck M, Levivier M. Clinical evaluation of targeting accuracy of Gamma Knife radiosurgery in trigeminal neuralgia. Int J Radiat Oncol Biol Phys. 2007;69(5):1514–20.
38. Lutz J, Thon N, Stahl R, Lummel N, Tonn JC, Linn J, et al. Microstructural alterations in trigeminal neuralgia determined by diffusion tensor imaging are independent of symptom duration, severity, and type of neurovascular conflict. J Neurosurg. 2016;124(3):823–30.
39. Hodaie M, Chen DQ, Quan J, Laperriere N. Tractography delineates microstructural changes in the trigeminal nerve after focal radiosurgery for trigeminal neuralgia. PLoS One. 2012;7(3):e32745.
40. Hung PS, Chen DQ, Davis KD, Zhong J, Hodaie M. Predicting pain relief: use of pre-surgical trigeminal nerve diffusion metrics in trigeminal neuralgia. Neuroimage Clin. 2017;15:710–8.
41. Chen DQ, DeSouza DD, Hayes DJ, Davis KD, O'Connor P, Hodaie M. Diffusivity signatures characterize trigeminal neuralgia associated with multiple sclerosis. Mult Scler. 2016;22(1):51–63.
42. Tranvinh E, Heit JJ, Hacein-Bey L, Provenzale J, Wintermark M. Contemporary imaging of cerebral arteriovenous malformations. AJR Am J Roentgenol. 2017;208(6):1320–30.
43. Jagadeesan BD, Delgado Almandoz JE, Benzinger TL, Moran CJ. Postcontrast susceptibility-weighted imaging: a novel technique for the detection of arteriovenous shunting in vascular malformations of the brain. Stroke. 2011;42(11):3127–31.
44. Jagadeesan BD, Delgado Almandoz JE, Moran CJ, Benzinger TL. Accuracy of susceptibility-weighted imaging for the detection of arteriovenous shunting in vascular malformations of the brain. Stroke. 2011;42(1):87–92.
45. Chang W, Wu Y, Johnson K, Loecher M, Wieben O, Edjlali M, et al. Fast contrast-enhanced 4D MRA and 4D flow MRI using constrained reconstruction (HYPRFlow): potential applications for brain arteriovenous malformations. AJNR Am J Neuroradiol. 2015;36(6):1049–55.
46. Lee CC, Reardon MA, Ball BZ, Chen CJ, Yen CP, Xu Z, et al. The predictive value of magnetic resonance imaging in evaluating intracranial arteriovenous malformation obliteration after stereotactic radiosurgery. J Neurosurg. 2015;123(1):136–44.
47. Mukherji SK, Quisling RG, Kubilis PS, Finn JP, Friedman WA. Intracranial arteriovenous malformations: quantitative analysis of magnitude contrast MR angiography versus gradient-echo MR imaging versus conventional angiography. Radiology. 1995;196(1):187–93.
48. Buis DR, Bot JC, Barkhof F, Knol DL, Lagerwaard FJ, Slotman BJ, et al. The predictive value of 3D time-of-flight MR angiography in assessment of brain arteriovenous malformation obliteration after radiosurgery. AJNR Am J Neuroradiol. 2012;33(2):232–8.
49. Giesel FL, Essig M, Zabel-Du-Bois A, Bock M, von Tengg-Kobligk H, Afshar-Omarei A, et al. High-contrast computed tomographic angiography better detects residual intracranial arteriovenous malformations in long-term follow-up after radiotherapy than 1.5-Tesla time-of-flight magnetic resonance angiography. Acta Radiol. 2010;51(1):64–70.
50. Gross BA, Frerichs KU, Du R. Sensitivity of CT angiography, T2-weighted MRI, and magnetic resonance angiography in detecting cerebral arteriovenous malformations and associated aneurysms. J Clin Neurosci. 2012;19(8):1093–5.
51. Hadizadeh DR, Kukuk GM, Steck DT, Gieseke J, Urbach H, Tschampa HJ, et al. Noninvasive evaluation of cerebral arteriovenous malformations by 4D-MRA for preoperative planning and postoperative follow-up in 56 patients: comparison with DSA and intraoperative findings. AJNR Am J Neuroradiol. 2012;33(6):1095–101.
52. Haridass A, Maclean J, Chakraborty S, Sinclair J, Szanto J, Iancu D, et al. Dynamic CT angiography for cyberknife radiosurgery planning of intracranial arteriovenous malformations: a technical/feasibility report. Radiol Oncol. 2015;49(2):192–9.
53. Turner RC, Lucke-Wold BP, Josiah D, Gonzalez J, Schmidt M, Tarabishy AR, et al. Stereotactic radiosurgery planning based on time-resolved CTA for arteriovenous malformation: a case report and review of the literature. Acta Neurochir. 2016;158(8):1555–62.
54. Starke RM, Kano H, Ding D, Lee JY, Mathieu D, Whitesell J, et al. Stereotactic radiosurgery for cerebral arteriovenous malformations: evaluation of long-term outcomes in a multicenter cohort. J Neurosurg. 2017;126(1):36–44.
55. Yen CP, Varady P, Sheehan J, Steiner M, Steiner L. Subtotal obliteration of cerebral arteriovenous malformations after gamma knife surgery. J Neurosurg. 2007;106(3):361–9.
56. Abu-Salma Z, Nataf F, Ghossoub M, Schlienger M, Meder JF, Houdart E, et al. The protective status of subtotal obliteration of arteriovenous malformations after radiosurgery: significance and risk of hemorrhage. Neurosurgery. 2009;65(4):709–17; discussion 17–8.
57. Yen CP, Matsumoto JA, Wintermark M, Schwyzer L, Evans AJ, Jensen ME, et al. Radiation-induced imaging changes following Gamma Knife surgery for cerebral arteriovenous malformations. J Neurosurg. 2013;118(1):63–73.
58. Ilyas A, Chen CJ, Ding D, Buell TJ, Raper DMS, Lee CC, et al. Radiation-induced changes after stereotactic radiosurgery for brain arteriovenous malformations: a systematic review and meta-analysis. Neurosurgery. 2018;83(3):365–76.
59. Ilyas A, Chen CJ, Ding D, Mastorakos P, Taylor DG, Pomeraniec IJ, et al. Cyst formation after stereotactic radiosurgery for brain arteriovenous malformations: a systematic review. J Neurosurg. 2017;128:1–10.

60. Pollock BE, Link MJ, Branda ME, Storlie CB. Incidence and management of late adverse radiation effects after arteriovenous malformation radiosurgery. Neurosurgery. 2017;81(6):928–34.
61. Hasan DM, Amans M, Tihan T, Hess C, Guo Y, Cha S, et al. Ferumoxytol-enhanced MRI to image inflammation within human brain arteriovenous malformations: a pilot investigation. Transl Stroke Res. 2012;3(Suppl 1):166–73.
62. Gkagkanasiou M, Ploussi A, Gazouli M, Efstathopoulos EP. USPIO-enhanced MRI neuroimaging: a review. J Neuroimaging. 2016;26(2):161–8.
63. Park J, Kim J, Yoo E, Lee H, Chang JH, Kim EY. Detection of small metastatic brain tumors: comparison of 3D contrast-enhanced whole-brain black-blood imaging and MP-RAGE imaging. Investig Radiol. 2012;47(2):136–41.
64. Lee S, Park DW, Lee JY, Lee YJ, Kim T. Improved motion-sensitized driven-equilibrium preparation for 3D turbo spin echo T1 weighted imaging after gadolinium administration for the detection of brain metastases on 3T MRI. Br J Radiol. 2016;89(1063):20150176.
65. Kushnirsky M, Nguyen V, Katz JS, Steinklein J, Rosen L, Warshall C, et al. Time-delayed contrast-enhanced MRI improves detection of brain metastases and apparent treatment volumes. J Neurosurg. 2016;124(2):489–95.
66. Seibert TM, White NS, Kim GY, Moiseenko V, McDonald CR, Farid N, et al. Distortion inherent to magnetic resonance imaging can lead to geometric miss in radiosurgery planning. Pract Radiat Oncol. 2016;6(6):e319–e28.
67. Karaiskos P, Moutsatsos A, Pappas E, Georgiou E, Roussakis A, Torrens M, et al. A simple and efficient methodology to improve geometric accuracy in gamma knife radiation surgery: implementation in multiple brain metastases. Int J Radiat Oncol Biol Phys. 2014;90(5):1234–41.
68. Patel TR, McHugh BJ, Bi WL, Minja FJ, Knisely JP, Chiang VL. A comprehensive review of MR imaging changes following radiosurgery to 500 brain metastases. AJNR Am J Neuroradiol. 2011;32(10):1885–92.
69. Kano H, Kondziolka D, Lobato-Polo J, Zorro O, Flickinger JC, Lunsford LD. T1/T2 matching to differentiate tumor growth from radiation effects after stereotactic radiosurgery. Neurosurgery. 2010;66(3):486–91; discussion 91–2.
70. Dequesada IM, Quisling RG, Yachnis A, Friedman WA. Can standard magnetic resonance imaging reliably distinguish recurrent tumor from radiation necrosis after radiosurgery for brain metastases? A radiographic-pathological study. Neurosurgery. 2008;63(5):898–903; discussion 4.
71. Leeman JE, Clump DA, Flickinger JC, Mintz AH, Burton SA, Heron DE. Extent of perilesional edema differentiates radionecrosis from tumor recurrence following stereotactic radiosurgery for brain metastases. Neuro-Oncology. 2013;15(12):1732–8.
72. Stockham AL, Tievsky AL, Koyfman SA, Reddy CA, Suh JH, Vogelbaum MA, et al. Conventional MRI does not reliably distinguish radiation necrosis from tumor recurrence after stereotactic radiosurgery. J Neuro-Oncol. 2012;109(1):149–58.
73. Cha J, Kim ST, Kim HJ, Kim BJ, Jeon P, Kim KH, et al. Analysis of the layering pattern of the apparent diffusion coefficient (ADC) for differentiation of radiation necrosis from tumour progression. Eur Radiol. 2013;23(3):879–86.
74. Lee CC, Wintermark M, Xu Z, Yen CP, Schlesinger D, Sheehan JP. Application of diffusion-weighted magnetic resonance imaging to predict the intracranial metastatic tumor response to gamma knife radiosurgery. J Neuro-Oncol. 2014;118(2):351–61.
75. Goldman M, Boxerman JL, Rogg JM, Noren G. Utility of apparent diffusion coefficient in predicting the outcome of Gamma Knife-treated brain metastases prior to changes in tumor volume: a preliminary study. J Neurosurg. 2006;105(Suppl):175–82.
76. Huang CF, Chou HH, Tu HT, Yang MS, Lee JK, Lin LY. Diffusion magnetic resonance imaging as an evaluation of the response of brain metastases treated by stereotactic radiosurgery. Surg Neurol. 2008;69(1):62–8; discussion 8.
77. Essig M, Shiroishi MS, Nguyen TB, Saake M, Provenzale JM, Enterline D, et al. Perfusion MRI: the five most frequently asked technical questions. AJR Am J Roentgenol. 2013;200(1):24–34.
78. Hoefnagels FW, Lagerwaard FJ, Sanchez E, Haasbeek CJ, Knol DL, Slotman BJ, et al. Radiological progression of cerebral metastases after radiosurgery: assessment of perfusion MRI for differentiating between necrosis and recurrence. J Neurol. 2009;256(6):878–87.
79. Barajas RF, Chang JS, Sneed PK, Segal MR, McDermott MW, Cha S. Distinguishing recurrent intra-axial metastatic tumor from radiation necrosis following gamma knife radiosurgery using dynamic susceptibility-weighted contrast-enhanced perfusion MR imaging. AJNR Am J Neuroradiol. 2009;30(2):367–72.
80. Mitsuya K, Nakasu Y, Horiguchi S, Harada H, Nishimura T, Bando E, et al. Perfusion weighted magnetic resonance imaging to distinguish the recurrence of metastatic brain tumors from radiation necrosis after stereotactic radiosurgery. J Neuro-Oncol. 2010;99(1):81–8.
81. Huang J, Wang AM, Shetty A, Maitz AH, Yan D, Doyle D, et al. Differentiation between intra-axial metastatic tumor progression and radiation injury following fractionated radiation therapy or stereotactic radiosurgery using MR spectroscopy, perfusion MR imaging or volume progression modeling. Magn Reson Imaging. 2011;29(7):993–1001.
82. Hatzoglou V, Ulaner GA, Zhang Z, Beal K, Holodny AI, Young RJ. Comparison of the effectiveness of MRI perfusion and fluorine-18 FDG PET-CT for differentiating radiation injury from viable brain tumor: a preliminary retrospective analysis with pathologic correlation in all patients. Clin Imaging. 2013;37(3):451–7.
83. Welker K, Boxerman J, Kalnin A, Kaufmann T, Shiroishi M, Wintermark M. ASFNR recommendations for clinical performance of MR dynamic susceptibility contrast perfusion imaging of the brain. AJNR Am J Neuroradiol. 2015;36(6):E41–51.
84. Rapalino O, Ratai EM. Multiparametric imaging analysis: magnetic resonance spectroscopy. Magn Reson Imaging Clin N Am. 2016;24(4):671–86.
85. Chernov M, Hayashi M, Izawa M, Ochiai T, Usukura M, Abe K, et al. Differentiation of the radiation-induced necrosis and tumor recurrence after gamma knife radiosurgery for brain metastases: importance of multi-voxel proton MRS. Minim Invasive Neurosurg. 2005;48(4):228–34.
86. Chernov MF, Hayashi M, Izawa M, Usukura M, Yoshida S, Ono Y, et al. Multivoxel proton MRS for differentiation of radiation-induced necrosis and tumor recurrence after gamma knife radiosurgery for brain metastases. Brain Tumor Pathol. 2006;23(1):19–27.
87. Kimura T, Sako K, Tanaka K, Gotoh T, Yoshida H, Aburano T, et al. Evaluation of the response of metastatic brain tumors to stereotactic radiosurgery by proton magnetic resonance spectroscopy, 201TlCl single-photon emission computerized tomography, and gadolinium-enhanced magnetic resonance imaging. J Neurosurg. 2004;100(5):835–41.
88. Kimura T, Sako K, Tohyama Y, Aizawa S, Yoshida H, Aburano T, et al. Diagnosis and treatment of progressive space-occupying radiation necrosis following stereotactic radiosurgery for brain metastasis: value of proton magnetic resonance spectroscopy. Acta Neurochir. 2003;145(7):557–64; discussion 64.
89. Chao ST, Suh JH, Raja S, Lee SY, Barnett G. The sensitivity and specificity of FDG PET in distinguishing recurrent brain tumor from radionecrosis in patients treated with stereotactic radiosurgery. Int J Cancer. 2001;96(3):191–7.
90. Hatzoglou V, Yang TJ, Omuro A, Gavrilovic I, Ulaner G, Rubel J, et al. A prospective trial of dynamic contrast-enhanced MRI per-

fusion and fluorine-18 FDG PET-CT in differentiating brain tumor progression from radiation injury after cranial irradiation. Neuro-Oncology. 2016;18(6):873–80.
91. Belohlavek O, Simonova G, Kantorova I, Novotny J Jr, Liscak R. Brain metastases after stereotactic radiosurgery using the Leksell gamma knife: can FDG PET help to differentiate radionecrosis from tumour progression? Eur J Nucl Med Mol Imaging. 2003;30(1):96–100.
92. Sneed PK, Mendez J, Vemer-van den Hoek JG, Seymour ZA, Ma L, Molinaro AM, et al. Adverse radiation effect after stereotactic radiosurgery for brain metastases: incidence, time course, and risk factors. J Neurosurg. 2015;123(2):373–86.
93. Kickingereder P, Dorn F, Blau T, Schmidt M, Kocher M, Galldiks N, et al. Differentiation of local tumor recurrence from radiation-induced changes after stereotactic radiosurgery for treatment of brain metastasis: case report and review of the literature. Radiat Oncol. 2013;8:52.
94. Tomura N, Kokubun M, Saginoya T, Mizuno Y, Kikuchi Y. Differentiation between treatment-induced necrosis and recurrent tumors in patients with metastatic brain tumors: comparison among (11)C-methionine-PET, FDG-PET, MR permeability imaging, and MRI-ADC-preliminary results. AJNR Am J Neuroradiol. 2017;38(8):1520–7.
95. Franks KN, Jain P, Snee MP. Stereotactic ablative body radiotherapy for lung cancer. Clin Oncol (R Coll Radiol). 2015;27(5):280–9.
96. Palma D, Lagerwaard F, Rodrigues G, Haasbeek C, Senan S. Curative treatment of stage I non-small-cell lung cancer in patients with severe COPD: stereotactic radiotherapy outcomes and systematic review. Int J Radiat Oncol Biol Phys. 2012;82(3):1149–56.
97. Martin A, Gaya A. Stereotactic body radiotherapy: a review. Clin Oncol (R Coll Radiol). 2010;22(3):157–72.
98. Boffa DJ, Allen MS, Grab JD, Gaissert HA, Harpole DH, Wright CD. Data from The Society of Thoracic Surgeons General Thoracic Surgery database: the surgical management of primary lung tumors. J Thorac Cardiovasc Surg. 2008;135(2):247–54.
99. Smith CB, Swanson SJ, Mhango G, Wisnivesky JP. Survival after segmentectomy and wedge resection in stage I non-small-cell lung cancer. J Thorac Oncol. 2013;8(1):73–8.
100. Agolli L, Valeriani M, Nicosia L, Bracci S, De Sanctis V, Minniti G, et al. Stereotactic ablative body radiotherapy (SABR) in pulmonary oligometastatic/oligorecurrent non-small cell lung cancer patients: a new therapeutic approach. Anticancer Res. 2015;35(11):6239–45.
101. Ceniceros L, Aristu J, Castanon E, Rolfo C, Legaspi J, Olarte A, et al. Stereotactic body radiotherapy (SBRT) for the treatment of inoperable stage I non-small cell lung cancer patients. Clin Transl Oncol. 2016;18(3):259–68.
102. Aridgides P, Bogart J. Stereotactic body radiation therapy for stage I non-small cell lung cancer. Thorac Surg Clin. 2016;26(3):261–9.
103. De Rose F, Franceschini D, Reggiori G, Stravato A, Navarria P, Ascolese AM, et al. Organs at risk in lung SBRT. Phys Med. 2017;44:131–8.
104. Alongi F, Arcangeli S, De Bari B, Giaj-Levra N, Fiorentino A, Mazzola R, et al. Stage-I small cell lung cancer: a new potential option for stereotactic ablative radiation therapy? A review of literature. Crit Rev Oncol Hematol. 2017;112:67–71.
105. Milano MT, Katz AW, Zhang H, Okunieff P. Oligometastases treated with stereotactic body radiotherapy: long-term follow-up of prospective study. Int J Radiat Oncol Biol Phys. 2012;83(3):878–86.
106. Scorsetti M, Clerici E, Navarria P, D'Agostino G, Piergallini L, De Rose F, et al. The role of stereotactic body radiation therapy (SBRT) in the treatment of oligometastatic disease in the elderly. Br J Radiol. 2015;88(1053):20150111.
107. Wild AT, Yamada Y. Treatment options in oligometastatic disease: stereotactic body radiation therapy – focus on colorectal cancer. Visc Med. 2017;33(1):54–61.
108. Giglioli FR, Clemente S, Esposito M, Fiandra C, Marino C, Russo S, et al. Frontiers in planning optimization for lung SBRT. Phys Med. 2017;44:163–70.
109. Smith DW, Dean C, Lilley J. A practical method of identifying data loss in 4DCT. Radiother Oncol. 2012;102(3):393–8.
110. Pollom EL, Chin AL, Diehn M, Loo BW, Chang DT. Normal tissue constraints for abdominal and thoracic stereotactic body radiotherapy. Semin Radiat Oncol. 2017;27(3):197–208.
111. Ruggieri R, Stavrev P, Naccarato S, Stavreva N, Alongi F, Nahum AE. Optimal dose and fraction number in SBRT of lung tumours: a radiobiological analysis. Phys Med. 2017;44:188–95.
112. Larici AR, del Ciello A, Maggi F, Santoro SI, Meduri B, Valentini V, et al. Lung abnormalities at multimodality imaging after radiation therapy for non-small cell lung cancer. Radiographics. 2011;31(3):771–89.
113. Choi YW, Munden RF, Erasmus JJ, Park KJ, Chung WK, Jeon SC, et al. Effects of radiation therapy on the lung: radiologic appearances and differential diagnosis. Radiographics. 2004;24(4):985–97; discussion 98.
114. Park KJ, Chung JY, Chun MS, Suh JH. Radiation-induced lung disease and the impact of radiation methods on imaging features. Radiographics. 2000;20(1):83–98.
115. Timmerman R, McGarry R, Yiannoutsos C, Papiez L, Tudor K, DeLuca J, et al. Excessive toxicity when treating central tumors in a phase II study of stereotactic body radiation therapy for medically inoperable early-stage lung cancer. J Clin Oncol. 2006;24(30):4833–9.
116. Kang KH, Okoye CC, Patel RB, Siva S, Biswas T, Ellis RJ, et al. Complications from stereotactic body radiotherapy for lung cancer. Cancers (Basel). 2015;7(2):981–1004.
117. Chang JY, Roth JA. Stereotactic body radiation therapy for stage I non-small cell lung cancer. Thorac Surg Clin. 2007;17(2):251–9.
118. Hong JC, Salama JK. The expanding role of stereotactic body radiation therapy in oligometastatic solid tumors: what do we know and where are we going? Cancer Treat Rev. 2017;52:22–32.
119. Pastorino U, Buyse M, Friedel G, Ginsberg RJ, Girard P, Goldstraw P, et al. Long-term results of lung metastasectomy: prognostic analyses based on 5206 cases. J Thorac Cardiovasc Surg. 1997;113(1):37–49.
120. Navarria P, De Rose F, Ascolese AM. SBRT for lung oligometastases: who is the perfect candidate? Rep Pract Oncol Radiother. 2015;20(6):446–53.
121. Vargas HA, Wassberg C, Akin O, Hricak H. MR imaging of treated prostate cancer. Radiology. 2012;262(1):26–42.
122. Hoeks CM, Barentsz JO, Hambrock T, Yakar D, Somford DM, Heijmink SW, et al. Prostate cancer: multiparametric MR imaging for detection, localization, and staging. Radiology. 2011;261(1):46–66.
123. Wallitt KL, Khan SR, Dubash S, Tam HH, Khan S, Barwick TD. Clinical PET imaging in prostate cancer. Radiographics. 2017;37(5):1512–36.
124. Westphalen AC, Coakley FV, Roach M 3rd, McCulloch CE, Kurhanewicz J. Locally recurrent prostate cancer after external beam radiation therapy: diagnostic performance of 1.5-T endorectal MR imaging and MR spectroscopic imaging for detection. Radiology. 2010;256(2):485–92.
125. Rouviere O, Valette O, Grivolat S, Colin-Pangaud C, Bouvier R, Chapelon JY, et al. Recurrent prostate cancer after external beam radiotherapy: value of contrast-enhanced dynamic MRI in localizing intraprostatic tumor – correlation with biopsy findings. Urology. 2004;63(5):922–7.
126. Haider MA, Chung P, Sweet J, Toi A, Jhaveri K, Menard C, et al. Dynamic contrast-enhanced magnetic resonance imaging for

localization of recurrent prostate cancer after external beam radiotherapy. Int J Radiat Oncol Biol Phys. 2008;70(2):425–30.
127. Kim CK, Park BK, Lee HM. Prediction of locally recurrent prostate cancer after radiation therapy: incremental value of 3T diffusion-weighted MRI. J Magn Reson Imaging. 2009;29(2):391–7.
128. Akin O, Gultekin DH, Vargas HA, Zheng J, Moskowitz C, Pei X, et al. Incremental value of diffusion weighted and dynamic contrast enhanced MRI in the detection of locally recurrent prostate cancer after radiation treatment: preliminary results. Eur Radiol. 2011;21(9):1970–8.
129. Fanti S, Minozzi S, Castellucci P, Balduzzi S, Herrmann K, Krause BJ, et al. PET/CT with (11)C-choline for evaluation of prostate cancer patients with biochemical recurrence: meta-analysis and critical review of available data. Eur J Nucl Med Mol Imaging. 2016;43(1):55–69.
130. Evangelista L, Zattoni F, Guttilla A, Saladini G, Zattoni F, Colletti PM, et al. Choline PET or PET/CT and biochemical relapse of prostate cancer: a systematic review and meta-analysis. Clin Nucl Med. 2013;38(5):305–14.
131. Vees H, Buchegger F, Albrecht S, Khan H, Husarik D, Zaidi H, et al. 18F-choline and/or 11C-acetate positron emission tomography: detection of residual or progressive subclinical disease at very low prostate-specific antigen values (<1 ng/mL) after radical prostatectomy. BJU Int. 2007;99(6):1415–20.
132. Treglia G, Ceriani L, Sadeghi R, Giovacchini G, Giovanella L. Relationship between prostate-specific antigen kinetics and detection rate of radiolabelled choline PET/CT in restaging prostate cancer patients: a meta-analysis. Clin Chem Lab Med. 2014;52(5):725–33.
133. Perera M, Papa N, Christidis D, Wetherell D, Hofman MS, Murphy DG, et al. Sensitivity, specificity, and predictors of positive (68)Ga-prostate-specific membrane antigen positron emission tomography in advanced prostate cancer: a systematic review and meta-analysis. Eur Urol. 2016;70(6):926–37.
134. Nanni C, Zanoni L, Pultrone C, Schiavina R, Brunocilla E, Lodi F, et al. (18)F-FACBC (anti1-amino-3-(18)F-fluorocyclobutane-1-carboxylic acid) versus (11)C-choline PET/CT in prostate cancer relapse: results of a prospective trial. Eur J Nucl Med Mol Imaging. 2016;43(9):1601–10.
135. Bach-Gansmo T, Nanni C, Nieh PT, Zanoni L, Bogsrud TV, Sletten H, et al. Multisite experience of the safety, detection rate and diagnostic performance of fluciclovine ((18)F) positron emission tomography/computerized tomography imaging in the staging of biochemically recurrent prostate cancer. J Urol. 2017;197(3 Pt 1):676–83.
136. Kawahara Y, Nakada M, Hayashi Y, Kai Y, Uchiyama N, Nakamura H, et al. Prediction of high-grade meningioma by preoperative MRI assessment. J Neuro-Oncol. 2012;108(1):147–52.
137. Lin BJ, Chou KN, Kao HW, Lin C, Tsai WC, Feng SW, et al. Correlation between magnetic resonance imaging grading and pathological grading in meningioma. J Neurosurg. 2014;121(5):1201–8.
138. Yin B, Liu L, Zhang BY, Li YX, Li Y, Geng DY. Correlating apparent diffusion coefficients with histopathologic findings on meningiomas. Eur J Radiol. 2012;81(12):4050–6.

Comparative Effectiveness of SBRT

Sanjay Aneja, Rahul J. Kumar, and James B. Yu

Introduction

As the use of stereotactic body radiation therapy (SBRT) across multiple disease sites increases over time, there has been a growing area of research comparing the effectiveness of SBRT to alternative treatment modalities. Comparative effectiveness studies within SBRT come from a variety of different data sources including prospective and retrospective series, large database analyses, and cost-effectiveness studies. In this chapter, we will discuss comparative effectiveness studies within SBRT. We will limit our discussion to comparative effectiveness studies evaluating stereotactic treatment to the brain, prostate, lung, and liver. For each disease site, we will include a brief overview of prospective and retrospective series, followed by a discussion of comparative effectiveness studies using large databases, and finally cost-effectiveness studies. Summaries of the selected studies for each disease site are located in the tables throughout the chapter as references.

S. Aneja
Yale New Haven Hospital, Department of Therapeutic Radiology, New Haven, CT, USA

Yale School of Medicine, Department of Therapeutic Radiology, New Haven, CT, USA

R. J. Kumar
California Pacific Medical Center, Department of Radiation Oncology, San Francisco, CA, USA

J. B. Yu (✉)
Yale New Haven Hospital, Department of Therapeutic Radiology, New Haven, CT, USA

Yale School of Medicine, Department of Therapeutic Radiology, New Haven, CT, USA
e-mail: James.b.yu@yale.edu

Brain

Prospective and Retrospective Series

Several prospective clinical trials have been conducted to compare treatment strategies for brain metastases [1, 2]. Initially, whole brain radiotherapy and radiosurgery were combined in several trails. In a phase III trial by Muacevic and colleagues, patients with a solitary brain metastasis were randomized to surgery followed by whole brain radiotherapy or Gamma Knife radiosurgery alone. Local recurrence was similar between both groups, but distant recurrence was experienced more often in the radiosurgery group. This difference was lost after adjusting for the effects of salvage radiosurgery [3]. RTOG 9508 randomized patients to whole brain radiation therapy (WBRT) versus WBRT plus a stereotactic radiosurgery (SRS) boost. On univariate analysis, there was improved median survival in the WBRT + SRS group compared to the WBRT-alone group (MS 6.5 vs. 4.9 months). Multivariate analysis showed improved survival in patients with RPA class I or favorable histology [4]. Gantery and colleagues randomized a total of 60 patients with 1–3 brain metastases to SRS and WBRT, SRS alone, or WBRT alone. Local control was improved in the group who received combined therapy compared to SRS alone or WBRT alone (median local control of 10 vs. 5 vs. 5 months, respectively) [5].

Given the increased cognitive side effects of whole brain radiotherapy, comparative trials were also conducted to eliminate WBRT from treatment of metastatic brain disease. In EORTC 22952–26,001, patients with 1–3 brain metastases who underwent surgery or SRS were randomized to WBRT or observation. The 2-year relapse rate at initial sites and new sites was decreased in the WBRT group compared to the observation group, but overall survival (OS) was similar in both groups (10.9 vs. 10.7 months) [6]. A later publication revealed that health-related quality of life scores were higher in the observation group, including cognitive function at 8 weeks and 12 months [7]. JROSG

D. M. Trifiletti et al. (eds.), *Stereotactic Radiosurgery and Stereotactic Body Radiation Therapy*,
https://doi.org/10.1007/978-3-030-16924-4_34

99–1 randomized 132 patients with 1–4 brain metastases to SRS and WBRT or SRS alone. Overall survival was similar in both groups, but 12-month brain tumor recurrence was improved in the patients who received WBRT in addition to SRS (46.8% vs. 76.4%). Local tumor control at 12 months was also improved in the patients who received combined therapy (88.7% vs. 72.5%) [8]. Chang and colleagues conducted a trial with similar randomization, but the main outcome was neurocognitive effects. In this study, 58 patients with 1–3 brain metastases were randomized to SRS and WBRT versus SRS alone. However, the trial was stopped early by the data monitoring committee because there was a high probability that patients receiving combined therapy were more likely to show a decline in learning and memory function at 4 months compared to patients who received SRS alone [9].

Sahgal and colleagues conducted an individual patient meta-analysis of phase III trials that evaluated patients with 1–4 brain metastases who were randomized to SRS alone or SRS plus WBRT. A total of 364 patients were included in the analysis from three randomized trials. SRS alone was found to improve survival in patients ≤50 years of age, but local control was improved with the addition of WBRT in all age groups [10].

Surgery and radiosurgery alone have never been directly compared in a randomized trial, as surgery is rarely used alone in the treatment of brain metastases in the modern era. Patchell and colleagues randomized patients with a single brain metastasis who underwent complete surgical resection to whole brain radiation therapy or observation. Local recurrence at the site of metastasis was 46% in the patients who received surgery alone [11]. This does not compare favorably to historical data of SRS alone (12-month local tumor recurrence rate of 27.5% in JROSG 99-1) [8].

A retrospective series by O'Neill and colleagues directly compared surgery and radiosurgery alone. In this study, 74 patients underwent surgical resection, and 23 patients underwent radiosurgery. After a median follow-up of 20 months for living patients, no SRS patients had local recurrence compared to 58% of patients in the surgical group [12].

Given the poor local control of surgery alone, surgery followed by postoperative radiosurgery has been evaluated in prospective single-arm series as well as retrospective studies. Brennan and coworkers conducted a prospective phase II trial that included 39 patients with 40 lesions who received adjuvant SRS to the surgical bed with a median dose of 1800 cGy. At 12 months, local failure was 22% and regional failure outside the treated metastasis was 44% [13]. A retrospective series by Soltys and coworkers examined 72 patients with 76 cavities who received postoperative SRS. Local control was 88% and 70% at 6 and 12 months, respectively [12, 14].

The question of radiosurgery alone versus surgery combined with radiosurgery was addressed in a retrospective series by Prabhu and coworkers that examined patients with large brain metastases ≥4 cm^3 (2 cm diameter). In this study, 213 patients with 223 brain metastases were included, and 30% were treated with SRS alone, while the remaining 70% received surgery and SRS, which was either preoperative or postoperative. The 1-year local recurrence rate was higher in the patients who received surgery alone compared to those who received surgery and SRS (36.7% vs. 20.5%) [15]. A summary of select SRS series is found in Table 1.

Large Database Studies

There are limited comparative effectiveness data from large national databases, but this may change in the near future. In 2014, the American Association of Neurological Surgeons (AANS) and the American Society for Radiation Oncology (ASTRO) launched a national registry for SRS treatments [16]. Regarding other national database publications, Kann and coworkers conducted a National Cancer Database (NCDB) study that examined patients with metastatic NSCLC, breast cancer, colorectal cancer, and melanoma who received radiation therapy to the brain. A total of 75,953 patients were included in the study, and of these,

Table 1 Select brain series: local control

Authors	Year	Comparison	Total dose	Lesions	N	Median survival (years)	Local control
Muacevic et al. [3]	2008	Surgery + WBRT vs. SRS	14–27 Gy	1	64	10.3	1 yr: 82% vs. 96.8%
Andrews et al. (RTOG 9508) [4]	2004	WBRT vs. WBRT + SRS	15–24 Gy	1–3	331	6.5	1 yr: 71% vs. 82%
El Gantery et al. [5]	2014	SRS + WBRT vs. SRS vs. WBRT	14–20 Gy	1–3	60	12	1 yr: 43% vs. 22% vs. 19%
Kocher et al. (EORTC 22952–26,001) [6]	2011	SRS + WBRT vs. SRS vs. surgery + SRS vs. surgery	20 Gy	1–3	359	10.9	2 yr: 81% vs. 69% vs. 73% vs. 41%
Aoyama et al. (JROSG 99-1) [8]	2006	SRS + WBRT vs. SRS	18–25 Gy	1–4	132	8	1 yr: 88.7% vs. 72.5%
Chang et al. [9]	2009	SRS+ WBRT vs. SRS	15–20 Gy	1–3	58	15.2	1 yr: 100% vs. 67%

Table 2 Large database and cost-effectiveness studies in SRS

Authors	Year	Analysis	Comparison	Evaluated costs	Findings
Lal et al. [19]	2012	Decision Tree	SRS + WBRT	Yes	SRS with salvage is most costly than SRS + WBRT, but also more effective
Kimmel et al. [20]	2015	Decision Tree	Surgery WBRT	Yes	SRS + WBRT and SRS alone are more cost-effective than WBRT
Lester-Coll et al. [21]	2016	Markov Analysis	WBRT SRS + WBRT	Yes	For patients with up to 10 brain metastases, SRS alone is more cost-effective than SRS + WBRT
Hall et al. [53]	2014	Retrospective	SRS + WBRT Surgery + SRS	Yes	SRS alone is more cost-effective than SRS + WBRT, but increased salvage
Savitz et al. [54]	2015	Markov Analysis	WBRT+/− Hippocampal Avoidance	Yes	SRS is cost-effective for patients with life expectancy <1 yr, otherwise HA-WBRT cost-effective
Wernicke et al. [55]	2016	Retrospective	Surgery+ CS-131 Surgery+ SRS	Yes	Surgery + Cs-131 is more cost-effective than Surgery + SRS
Kann et al. [17]	2017	NCDB	Non-SRS	No	1 yr OS favoring SRS

16.1% received SRS and the remaining 83.9% received non-SRS. The proportion of patients receiving SRS compared to non-SRS increased over time from 2004 to 2014 (9.8% to 25.6%). 1-year survival was higher in the patients who received SRS compared to those who received non-SRS (40.9% vs. 24.1%) [17].

Cost-Effectiveness Studies

Several studies have examined the cost-effectiveness of local therapies for brain metastases [18]. Lal and coworkers conducted a cost-effectiveness study using data from patients with brain metastases in a randomized trial, in which patients received either SRS and observation or SRS and WBRT. Despite SRS with salvage therapy having a higher cost compared to SRS and following WBRT, it was found to be more cost-effective [19]. Kimmel and coworkers conducted a cost-effectiveness analysis for various combinations of treatments for brain metastases. SRS and WBRT combination was cost-effective compared to WBRT alone, and SRS alone was more cost-effective than WBRT [20]. In the setting of multiple brain metastases, Lester-Coll and coworkers found SRS to be more cost-effective than SRS + WBRT in patients with up to 10 brain metastases [21]. A summary of selected large database and cost-effectiveness studies of SRS is found in Table 2.

Prostate Cancer

Prospective and Retrospective Series

Prostate cancer is one of the most commonly treated primary tumors with stereotactic body radiation therapy (SBRT) increasing in utilization across the country [22]. Although conventionally fractionated radiation therapy has shown to be quite effective in the treatment of prostate cancer, it is associated with as many as 45 treatment sessions over the course of 9 weeks. With increasing research studying the effectiveness of shortened hypofractionated dose regiments, SBRT was a natural progression in advances in treatment. Moreover, many argue that given the low alpha-beta ratio of prostate cancer, SBRT would have a radiobiological advantage to doses delivered at a larger fraction size [23].

The major limitation comparing SBRT to conventionally fractionated radiation therapy for prostate cancer is the lack of long-term SBRT follow-up and randomized data. Much of the growing evidence supporting SBRT for prostate cancer is founded upon comparisons to historical outcomes of dose-escalated conventionally fractionated radiation therapy using 3D/IMRT techniques. Among the first studies to look at prostate SBRT was from Madsen and associates in 2007 [24]. This phase I/II clinical trial evaluated the effectiveness of 33.5 Gy in 5 fractions to 40 patients with low-risk prostate cancer. With a median follow-up of 3.4 years, authors reported biochemical control of 90% by Phoenix criteria and 70% by ASTRO definition. The toxicity was acceptable with only 1 acute Grade 3 GU toxicity and no late Grade 3 or higher toxicity. In 2011, King and associates from Stanford published a prospective phase II trial of 67 patients with low to intermediate risk prostate cancer treated to a higher dose of 36.25 Gy in 5 fractions using Cyberknife SBRT [25]. With a median follow-up of 2.7 years, the authors reported a 4-year biochemical relapse-free survival was 94%. The toxicity profile remained relatively favorable with only 3.5% late grade 3 GU toxicity. More importantly, the authors found every other day treatment to be associated with a more favorable toxicity profile than daily treatment. The criticism of the initial prostate SBRT experiences was a lack of long-term follow-up data. The longest follow-up experience published to date is a retrospective series published by Katz and associates in 2016 [26]. Among 515 patients treated with organ defined low-, intermediate-, and high-risk prostate cancer treated with

35–36.25 Gy in 5 fractions, the authors found an 8-year biochemical disease-free survival of 93.6% (low risk), 84.3% (intermediate risk), and 65.0% (high risk). The authors similarly noted a late grade GU toxicity of 2% at 7 years.

Unfortunately, there is a paucity of published randomized controlled trials for which SBRT is compared to conventional radiation therapy or surgery. RTOG 0938 compared the effectiveness of 36.25 Gy in 5 fractions versus 51.6 Gy in 12 fractions for patients with favorable risk prostate cancer [27, 28] and reported initial quality of life analysis in 2016. Both fractionation schema were well tolerated [29]. The HYPO-RT-PC study compared 6.1 Gy × 7 fractions to 2 Gy × 39 fractions, enrolling 1200 patients. The study, also reported at ASTRO in 2016, reported increased urinary side effects for the more extreme fractionation arm at 1 year, but no differences at 2 years. Bowel symptoms were also greater after radiation treatment, but no differences were seen at later endpoints [30].

Ongoing trials include the UK-based phase 3 PACE trial in which low- and favorable intermediate-risk prostate cancer patients who are surgical candidates are randomized to SBRT versus surgery and those who are not surgical candidates are randomized to SBRT versus conventional radiotherapy. The NRG Oncology GU-005 study is comparing 5 fractions of 7.25 Gy to 28 fractions of 2.5 Gy and has both biochemical and quality of life endpoints.

A summary of select prostate SBRT series is found in Table 3.

Large Database Studies

Some of the most significant work comparing SBRT to alternative treatment modalities has been using large national databases. In 2014, Yu and associates published an analysis of patients from the CMS Chronic Conditions Data Warehouse who received SBRT or IMRT as a primary treatment for prostate cancer [28]. Using Medicare claims to assess for GI and GU toxicity, the authors found SBRT to be associated with worse GU toxicity at 6 months (15.6% vs. 12.6%) and 24 months (43% vs. 36%). The differences were largely driven by claims indicative of urethritis, urinary incontinence, and obstruction. Similarly, there was worse GI toxicity associated with SBRT at 6 months (5.8% vs. 4.1%). There is no large national database analysis of biochemical control for prostate SBRT versus conventionally fractionated radiation therapy; however, a recent analysis of the National Cancer Database from Ricco and associates published in 2017 found no difference in 8-year overall survival when comparing prostate cancer patients treated with SBRT versus IMRT [31].

Cost-Effectiveness Studies

There has been substantial work studying cost-effectiveness of prostate SBRT. In the previously described study by Yu and associates, the authors also examined the costs of prostate SBRT versus IMRT among Medicare beneficiaries [28]. The authors found SBRT was cheaper than IMRT ($13,645 vs. $21,023) but most expensive with respect to non-radiation-related cancer care ($2963 vs. $1978). Halpern and associates published a cost analysis in 2016 of prostate cancer patients treated with SBRT, IMRT, proton beam therapy, or brachytherapy. Brachytherapy ($17,183) was found to be the least expensive treatment modality followed by SBRT ($27,145), IMRT ($37,090), and proton therapy ($54,706) [22]. Cost-effectiveness studies by Parthan and associates which analyzed costs and toxicity using Markov modeling found prostate SBRT to be more cost-effective than proton therapy and IMRT [32]. One criticism of this study is that authors used a singular institutional source to estimate estimated rates of toxicity [18]. Sher and associates published a similar updated Markov analysis in 2014 assuming worse toxicity for SBRT and with a larger variety of sources to estimate rates of toxicity. The authors found SBRT to most likely to be cost-effective compared to IMRT [33]. A summary of select large database analysis and cost-effectiveness studies of prostate SBRT can be found in Table 4.

Table 3 Select Prostate Series: Biochemical Control and Toxicity

Authors	Year	Total dose	Fractions	N	Median follow-up	Biochemical control	Late GI toxicity	Late GU toxicity
Madsen et al. [24]	2007	33.5 Gy	5	40	3.4 years	90% (low risk)	G1–2 (37%) G3 (0%)	G1–2 (45%) G3 (3%)
Freeman et al. [56]	2011	35–36.25 Gy	5	41	5 years	93% (low risk)	G1–2 (16%) G3 (0%)	G1–2 (32%) G3 (3%)
King et al. [25]	2012	36.25 Gy	5	45	2.7 years	94% (low + int risk)	G1–2 (16%) G3 (0%)	G1–2 (28%) G3 (3%)
Katz et al. [26]	2016	35–36.25 Gy	5	515	7 years	93% (low risk) 84% (int risk) 65% (high risk)	G2 (4%) G3 (0%)	G2 (9%) G3 (3%)
Meier et al. [57]	2016	36.25 Gy	5	309	5.1 years	97% (low/int risk)	G2 (2%) G3 (0%)	G2 (12%) G3 (0%)

Table 4 Large database and cost-effectiveness studies in prostate SBRT

Authors	Year	Analysis	Comparison	Evaluated costs	Findings
Yu et al. [28]	2014	CCW Medicare	IMRT	Yes	Compared to IMRT, SBRT associated with lower costs, but higher GU toxicity.
Ricco et al. [31]	2017	NCDB	IMRT	No	No 8-year OS difference between SBRT and IMRT
Parthan et al. [32]	2012	Markov Model	3D/IMRT	Yes	SBRT is likely more cost-effective than IMRT
Sher et al. [33]	2014	Markov Model	IMRT	Yes	SBRT is likely more cost-effective than IMRT
Halpern et al. [22]	2016	SEER-Medicare	Proton, IMRT, Brachytherapy	Yes	SBRT associated with greater toxicity but lower costs compared to IMRT. Brachytherapy less costly than SBRT, but associated with greater toxicity
Hodges et al. [58]	2012	Markov Model	IMRT	Yes	SBRT cost-effective compared to IMRT, but highly sensitive to quality-of-life outcomes

Lung

Prospective and Retrospective Series

Relative to other disease sites, lung SBRT has been an area of significant comparative effectiveness research. Similar to prostate SBRT, initial trials studying the effectiveness of lung SBRT were single-arm studies compared to historical controls. Uematsu and associates published one of the first experiences of SBRT in inoperable lung cancer in 1998. With a median follow-up of 36 months, the authors found SBRT to be associated with a 2-year local control of 94% [34]. The landmark study which solidified SBRT for inoperable NSCLC was published in 2010 by Timmerman and associates. RTOG 0236 was a prospective multicenter single-arm study of 55 patients with inoperable early-stage NSCLC treated to 60 Gy in 3 fractions [35]. The authors found a promising 3-year tumor control rate of 97% with a favorable toxicity profile.

Studies comparing surgery to SBRT for lung cancer have been difficult given SBRT has often been reserved for patients who are not candidates for surgical resection. Crabtree and associates published one of the largest single institutional series of matched patients comparing surgery and SBRT [36]. The authors found no differences in 4-year local, regional, or cancer-specific survival when comparing SBRT to surgical resection. Mokhles and associates have published the comparative series with the longest follow-up [37]. With a median follow-up of 49 months, the authors studied 146 patients treated with SBRT or surgery. After propensity score matching, there was no difference in 1-year or 5-year overall survival between surgery and SBRT.

Patient accrual has halted many efforts at randomized clinical trials comparing SBRT to surgery. Both the STARS and ROSEL clinical trials which randomized SBRT to surgery for early-stage NSCLC failed to meet accrual goals. A pooled analysis of both studies was published by Chang and associates in 2016 and found SBRT to be associated with a 3-year overall survival benefit [38]. Thus, there is mounting evidence to suggesting equipoise between both surgery and SBRT for early-stage NSCLC. A summary of select lung SBRT series is found in Table 5.

Large Database Studies

Given the paucity of randomized clinical trials studying the efficacy of SBRT versus surgery for early-stage lung cancer, much of the comparative effectiveness research has risen from large database studies. Yu and colleagues, Shirvani and colleagues, and Ezer and colleagues have all conducted analysis of the SEER-Medicare database comparing surgery to SBRT for early-stage NSCLC [39–41]. Both studies from Yu and Shirvani found SBRT to be an effective treatment option compared to surgery for patients with short life expectancy and/or multiple comorbidities. Ezer and colleagues found no differences in overall survival when comparing SBRT to wedge resection, but did find segmentectomy to be associated with improved overall survival compared to SBRT. When comparing radiofrequency ablation (RFA) to SBRT for lung cancer, a meta-analysis from Bi and colleagues found SBRT to be associated with improved local control at both 1 and 5 years [42].

Cost-Effectiveness Studies

There have been a number of cost-effectiveness studies evaluating the utility of SBRT for lung cancer. Sher and colleagues published one of the first Markov analysis comparing SBRT, 3DCRT, and RFA for inoperable early-stage lung cancer [43]. SBRT was the most cost-effective under a variety of different clinical scenarios. When studying operable early-stage lung cancer, Shah and colleagues

Table 5 Select lung series

Authors	Year	Total dose	Fractions	Trial notes	N	Median follow-up	Outcome
Uematsu et al. [34]	1998	50–60 Gy	5–10	Single Arm Inoperable	50	36 months	2 yr LC: 94%, CSS: 88%
Onishi et al. [59]	2004	18–75 Gy	1–22	Single Arm Inoperable	245	24 months	2 yr LC: 85%
Timmerman et al. (RTOG 0236) [35]	2010	60 Gy	3	Single Arm Inoperable	55	34 months	3 yr tumor control: 97%
Grills et al. [60]	2010	48–60 Gy	4–5	Retrospective Compared to Wedge Resection	124	30 months	2.5 yr: No differences in local, regional, distant recurrences, or OS
Crabtree et al. [36]	2010	54 Gy	3	Propensity Matched Compared to Surgical Resection	538	31 months	4 yr: No differences in local, regional, or CSS
Onishi et al. [61]	2011	45–72.5 Gy	3–10	Single Arm Operable	87	55 months	5 yr LC: 92% (T1), 73% (T2), OS: 72% (IA), 62% (IB)
Mokhles et al. [37]	2015	54–60 Gy	3–8	Propensity Matched Compared to Surgical Resection	146	49 months	1 yr: No differences in OS, 5 yr: No differences in OS
Timmerman et al. [62]	2014 (abstract)	54 Gy	3	Single Arm Operable	26	25 months	2 yr: LC 81%, PFS 65%, OS 84%
Chang et al. [38]	2015	50–54 Gy	3–5	Pooled Trial Compared to Surgery	58	35 months	3 yr: OS Favored SBRT over Surgery

Table 6 Large database and cost-effectiveness studies in lung SBRT

Authors	Year	Analysis	Comparison	Patients	Evaluated costs	Findings
Bi et al. [42]	2016	Meta-analysis	RFA	3095 (43 studies)	No	1–5 yr.: LC Favored SBRT over RFA
Ezer et al. [41]	2015	SEER Medicare Analysis	Limited surgery	2243	No	No OS difference between SBRT and Wedge, but OS favored Segmentectomy over SBRT
Nanda et al. [63]	2015	NCDB Analysis	No Treatment	3147	No	Improved OS with SBRT despite significant comorbidity
Yu et al. [39]	2015	SEER Medicare Analysis	Surgery	1077	No	Short life expectancy: OS SBRT favored long life expectancy: Surgery favored
Smith et al. [64]	2015	SEER Medicare Analysis	Surgery	9093	Yes	SBRT less costly, but with inferior survival
Shirvani et al. [40]	2014	SEER Medicare Analysis	Surgery	9093	No	SBRT effective for patients with advanced age and multiple comorbidities
Louie et al. [65]	2011	Markov Analysis	Lobectomy	NA	No	OS favors Surgery for operable patients
Sher et al. [43]	2011	Markov Analysis	3D CRT RFA	NA	Yes	SBRT most cost-effective in inoperable stage I patients
Lanni et al. [45]	2011	Markov analysis	3D CRT	NA	Yes	SBRT more cost-effective than 3DCRT
Shah et al. [44]	2013	Markov Analysis	Surgery	NA	Yes	SBRT most cost-effective in operable stage I patients

found SBRT to be more cost-effective than surgery unless the patient was "clearly operable" and willing to undergo lobectomy [44]. The cost-effectiveness of lung SBRT is affected somewhat by the health system in which one practices. Lanni and colleagues found SBRT to be more cost-effective than 3DCRT in a US-based healthcare system in which reimbursements are based on the number of fractions [45]. However, from the Canadian payer perspective, SBRT was less cost-effective than 3DCRT because in Canada activity-related reimbursements based on the total course of treatment are used to calculate costs rather than the number of fractions received. A summary of select large database analysis and cost-effectiveness studies of lung SBRT can be found in Table 6.

Liver

Prospective and Retrospective Series

In patients with hepatic metastatic disease, options for local therapy include surgery, SBRT, Y-90 microspheres, chemo-

Table 7 Select liver series: local control

Authors	Year	Total dose	Fractions	N	Median follow-up	Outcome
Rusthoven et al. [47]	2009	36–60 Gy	3	47	16 months	2 yr LC: 92%
Milano et al. [66]	2008	50 Gy	10	121	41 months	2 yr LC: 67%
Hoyer et al. [67]	2006	45 Gy	3	44	4.3 years	2 yr LC: 79%
Mendez-Romero et al. [68]	2006	30–37.5 Gy	3	17	12.9 months	2 yr LC: 86%

embolization, and radiofrequency ablation. To our knowledge, there are no randomized trials directly comparing these modalities with SBRT. Table 1 displays the results of liver SBRT outcomes in the setting of hepatic metastases from various prospective Phase I/II trials. Actuarial local control ranges from 67% to 92% at 2 years. In terms of microsphere treatment, SIRFLOX was a phase III trial in which patients with metastatic colorectal cancer with hepatic metastases were randomized to modified FOLFOX plus or minus Y-90 microspheres. Median PFS in the liver was better in the Y-90 group (20.5 months vs. 12.6 months, $P = 0.002$) [46]. For SBRT, the median progression-free survival in the phase II trial of SBRT by Rusthoven and colleagues was 6.1 months [47].

There are also limited data regarding comparison of treatment options for hepatocellular carcinoma. RTOG 1112 is currently accruing, and it randomizes patients with unresectable HCC to sorafenib or SBRT followed by sorafenib. Su and colleagues conducted a retrospective analysis of 117 patients with hepatocellular carcinoma, 82 of which received SBRT. The remaining 35 patients underwent liver resection. After propensity score matching, overall survival and progression-free survival were similar between both groups. The 3-year OS was 91.8% in the SBRT group and 89.3% in the resection group, and the 3-year PFS was 59.2% and 62.4%, respectively [48].

Wahl and colleagues conducted a retrospective study that compared radiofrequency ablation (RFA) to SBRT of the liver for patients with hepatocellular carcinoma. A total of 224 patients with inoperable hepatocellular carcinoma were included in the study, with 161 patients undergoing RFA and 63 patients receiving SBRT. 2-year freedom from local progression was 80.2% in patients who received RFA and 83.8% in patients who received SBRT ($P = 0.016$). Overall survival at 2 years was not statistically different between groups [49]. A summary of select liver SBRT series is found in Table 7.

Large Database Studies

Given the use of SBRT to treat liver disease has only recently become more popularized, there are limited large database studies studying liver SBRT. Berber and colleagues conducted a study of 153 patients from a combined multicenter database who received SBRT for metastatic disease to the liver. A total of 363 metastatic liver lesions were included, and mean dose was 37.5 Gy. After a mean follow-up of 25 months, local control was 62% with a 1-year OS of 51% [50]. Oladeru and colleagues conducted a SEER analysis of 189 patients with unresectable HCC treated with either SBRT to selective internal radiation therapy [51]. With a median survival of 14 months, the authors found no differences in statistical significance in overall survival or disease-specific survival.

Table 8 Large database and cost-effectiveness studies in liver SBRT

Authors	Year	Analysis	Comparison	Evaluated costs	Findings
Leung et al. [69]	2016	Markov Analysis	Sorafenib	Yes	SBRT more cost-effective than Sorafenib
Kim et al. [52]	2016	Markov Analysis	RFA	Yes	SBRT less cost-effective inoperable for liver metastases
Oladeru et al. [51]	2016	SEER Analysis	SIRT	No	No differences in OS or DSS between SBRT and SIRT

Cost-Effectiveness Studies

Compared to SRS and SBRT of other body sites, relatively few cost-effectiveness studies have been conducted for SBRT of the liver. Leung and colleagues conducted a cost-effectiveness analysis of Sorafenib compared to SBRT for unresectable hepatocellular carcinoma and found SBRT to be more cost-effective in all clinical scenarios. In a study by Kim and colleagues, cost-effectiveness of SBRT was compared to radiofrequency ablation (RFA) in patients with unresectable liver metastases. The authors found that SBRT was less cost-effective than RFA for inoperable liver metastasis [52]. A summary of select large database analysis and cost-effectiveness studies of liver SBRT can be found in Table 8.

Conclusion

In this chapter, we have briefly introduced the growing comparative effectiveness research surrounding stereotactic body radiation therapy. As the use of SBRT increases, there will continue to be advances in this emerging area of research.

Moreover, as we begin to generate long-term follow-up on patients who have undergone SBRT, the utility of comparative effectiveness studies will become more important.

References

1. Badiyan SN, Regine WF, Mehta M. Stereotactic radiosurgery for treatment of brain metastases. J Oncol Pract. 2016;12(8):703–12.
2. Sheehan JP, Yen CP, Lee CC, Loeffler JS. Cranial stereotactic radiosurgery: current status of the initial paradigm shifter. J Clin Oncol. 2014;32(26):2836–46.
3. Muacevic A, Wowra B, Siefert A, Tonn JC, Steiger HJ, Kreth FW. Microsurgery plus whole brain irradiation versus Gamma Knife surgery alone for treatment of single metastases to the brain: a randomized controlled multicentre phase III trial. J Neuro-Oncol. 2008;87(3):299–307.
4. Andrews DW, Scott CB, Sperduto PW, Flanders AE, Gaspar LE, Schell MC, et al. Whole brain radiation therapy with or without stereotactic radiosurgery boost for patients with one to three brain metastases: phase III results of the RTOG 9508 randomised trial. Lancet. 2004;363(9422):1665–72.
5. El Gantery MM, Abd El Baky HM, El Hossieny HA, Mahmoud M, Youssef O. Management of brain metastases with stereotactic radiosurgery alone versus whole brain irradiation alone versus both. Radiat Oncol. 2014;9:116.
6. Kocher M, Soffietti R, Abacioglu U, Villa S, Fauchon F, Baumert BG, et al. Adjuvant whole-brain radiotherapy versus observation after radiosurgery or surgical resection of one to three cerebral metastases: results of the EORTC 22952-26001 study. J Clin Oncol. 2011;29(2):134–41.
7. Soffietti R, Kocher M, Abacioglu UM, Villa S, Fauchon F, Baumert BG, et al. A European Organisation for Research and Treatment of Cancer phase III trial of adjuvant whole-brain radiotherapy versus observation in patients with one to three brain metastases from solid tumors after surgical resection or radiosurgery: quality-of-life results. J Clin Oncol. 2013;31(1):65–72.
8. Aoyama H, Shirato H, Tago M, Nakagawa K, Toyoda T, Hatano K, et al. Stereotactic radiosurgery plus whole-brain radiation therapy vs stereotactic radiosurgery alone for treatment of brain metastases: a randomized controlled trial. JAMA. 2006;295(21):2483–91.
9. Chang EL, Wefel JS, Hess KR, Allen PK, Lang FF, Kornguth DG, et al. Neurocognition in patients with brain metastases treated with radiosurgery or radiosurgery plus whole-brain irradiation: a randomised controlled trial. Lancet Oncol. 2009;10(11):1037–44.
10. Sahgal A, Aoyama H, Kocher M, Neupane B, Collette S, Tago M, et al. Phase 3 trials of stereotactic radiosurgery with or without whole-brain radiation therapy for 1 to 4 brain metastases: individual patient data meta-analysis. Int J Radiat Oncol Biol Phys. 2015;91(4):710–7.
11. Patchell RA, Tibbs PA, Regine WF, Dempsey RJ, Mohiuddin M, Kryscio RJ, et al. Postoperative radiotherapy in the treatment of single metastases to the brain: a randomized trial. JAMA. 1998;280(17):1485–9.
12. O'Neill BP, Iturria NJ, Link MJ, Pollock BE, Ballman KV, O'Fallon JR. A comparison of surgical resection and stereotactic radiosurgery in the treatment of solitary brain metastases. Int J Radiat Oncol Biol Phys. 2003;55(5):1169–76.
13. Brennan C, Yang TJ, Hilden P, Zhang Z, Chan K, Yamada Y, et al. A phase 2 trial of stereotactic radiosurgery boost after surgical resection for brain metastases. Int J Radiat Oncol Biol Phys. 2014;88(1):130–6.
14. Soltys SG, Adler JR, Lipani JD, Jackson PS, Choi CY, Puataweepong P, et al. Stereotactic radiosurgery of the postoperative resection cavity for brain metastases. Int J Radiat Oncol Biol Phys. 2008;70(1):187–93.
15. Prabhu RS, Press RH, Patel KR, Boselli DM, Symanowski JT, Lankford SP, et al. Single-fraction stereotactic radiosurgery (SRS) alone versus surgical resection and SRS for large brain metastases: a multi-institutional analysis. Int J Radiat Oncol Biol Phys. 2017;99(2):459–67.
16. Sheehan JP, Kavanagh BD, Asher A, Harbaugh RE. Inception of a national multidisciplinary registry for stereotactic radiosurgery. J Neurosurg. 2016;124(1):155–62.
17. Kann BH, Park HS, Johnson SB, Chiang VL, Yu JB. Radiosurgery for brain metastases: changing practice patterns and disparities in the United States. J Natl Compr Cancer Netw. 2017;15(12):1494–502.
18. Lester-Coll NH, Sher DJ. Cost-effectiveness of stereotactic radiosurgery and stereotactic body radiation therapy: a critical review. Curr Oncol Rep. 2017;19(6):41.
19. Lal LS, Byfield SD, Chang EL, Franzini L, Miller LA, Arbuckle R, et al. Cost-effectiveness analysis of a randomized study comparing radiosurgery with radiosurgery and whole brain radiation therapy in patients with 1 to 3 brain metastases. Am J Clin Oncol. 2012;35(1):45–50.
20. Kimmell KT, LaSota E, Weil RJ, Marko NF. Comparative effectiveness analysis of treatment options for single brain metastasis. World Neurosurg. 2015;84(5):1316–32.
21. Lester-Coll NH, Dosoretz AP, Magnuson WJ, Laurans MS, Chiang VL, Yu JB. Cost-effectiveness of stereotactic radiosurgery versus whole-brain radiation therapy for up to 10 brain metastases. J Neurosurg. 2016;125(Suppl 1):18–25.
22. Halpern JA, Sedrakyan A, Hsu WC, Mao J, Daskivich TJ, Nguyen PL, et al. Use, complications, and costs of stereotactic body radiotherapy for localized prostate cancer. Cancer. 2016;122(16):2496–504.
23. Fowler J, Chappell R, Ritter M. Is alpha/beta for prostate tumors really low? Int J Radiat Oncol Biol Phys. 2001;50(4):1021–31.
24. Madsen BL, Hsi RA, Pham HT, Fowler JF, Esagui L, Corman J. Stereotactic hypofractionated accurate radiotherapy of the prostate (SHARP), 33.5 Gy in five fractions for localized disease: first clinical trial results. Int J Radiat Oncol Biol Phys. 2007;67(4):1099–105.
25. King CR, Brooks JD, Gill H, Presti JC Jr. Long-term outcomes from a prospective trial of stereotactic body radiotherapy for low-risk prostate cancer. Int J Radiat Oncol Biol Phys. 2012;82(2):877–82.
26. Katz A, Formenti SC, Kang J. Predicting biochemical disease-free survival after prostate stereotactic body radiotherapy: risk-stratification and patterns of failure. Front Oncol. 2016;6:168.
27. Zaorsky NG, Studenski MT, Dicker AP, Gomella L, Den RB. Stereotactic body radiation therapy for prostate cancer: is the technology ready to be the standard of care? Cancer Treat Rev. 2013;39(3):212–8.
28. Yu JB, Cramer LD, Herrin J, Soulos PR, Potosky AL, Gross CP. Stereotactic body radiation therapy versus intensity-modulated radiation therapy for prostate cancer: comparison of toxicity. J Clin Oncol. 2014;32(12):1195–201.
29. Lukka H, Stephanie P, Bruner D, Bahary JP, Lawton CAF, Efstathiou JA, et al. Patient-reported outcomes in NRG oncology/RTOG 0938, a randomized phase 2 study evaluating 2 Ultrahypofractionated Regimens (UHRs) for prostate cancer. Int J Radiat Oncol Biol Phys. 2016;94(1):2.
30. Widmark A, Gunnlaugsson A, Beckman L, Thellenberg-Karlsson C, Hoyer M, Lagerlund M, et al. Extreme hypofractionation versus conventionally fractionated radiotherapy for intermediate risk prostate cancer: early toxicity results from the Scandinavian Randomized Phase III Trial "HYPO-RT-PC". Int J Radiat Oncol Biol Phys. 2016;96(5):938–9.
31. Ricco A, Hanlon A, Lanciano R. Propensity score matched comparison of intensity modulated radiation therapy vs stereotactic body

radiation therapy for localized prostate cancer: a survival analysis from the National Cancer Database. Front Oncol. 2017;7:185.
32. Parthan A, Pruttivarasin N, Davies D, Taylor DC, Pawar V, Bijlani A, et al. Comparative cost-effectiveness of stereotactic body radiation therapy versus intensity-modulated and proton radiation therapy for localized prostate cancer. Front Oncol. 2012;2:81.
33. Sher DJ, Parikh RB, Mays-Jackson S, Punglia RS. Cost-effectiveness analysis of SBRT versus IMRT for low-risk prostate cancer. Am J Clin Oncol. 2014;37(3):215–21.
34. Uematsu M, Shioda A, Tahara K, Fukui T, Yamamoto F, Tsumatori G, et al. Focal, high dose, and fractionated modified stereotactic radiation therapy for lung carcinoma patients: a preliminary experience. Cancer. 1998;82(6):1062–70.
35. Timmerman R, Paulus R, Galvin J, Michalski J, Straube W, Bradley J, et al. Stereotactic body radiation therapy for inoperable early stage lung cancer. JAMA. 2010;303(11):1070–6.
36. Crabtree TD, Denlinger CE, Meyers BF, El Naqa I, Zoole J, Krupnick AS, et al. Stereotactic body radiation therapy versus surgical resection for stage I non-small cell lung cancer. J Thorac Cardiovasc Surg. 2010;140(2):377–86.
37. Mokhles S, Nuyttens JJ, Maat AP, Birim O, Aerts JG, Bogers AJ, et al. Survival and treatment of non-small cell lung cancer stage I-II treated surgically or with stereotactic body radiotherapy: patient and tumor-specific factors affect the prognosis. Ann Surg Oncol. 2015;22(1):316–23.
38. Chang JY, Senan S, Paul MA, Mehran RJ, Louie AV, Balter P, et al. Stereotactic ablative radiotherapy versus lobectomy for operable stage I non-small-cell lung cancer: a pooled analysis of two randomised trials. Lancet Oncol. 2015;16(6):630–7.
39. Yu JB, Soulos PR, Cramer LD, Decker RH, Kim AW, Gross CP. Comparative effectiveness of surgery and radiosurgery for stage I non-small cell lung cancer. Cancer. 2015;121(14):2341–9.
40. Shirvani SM, Jiang J, Chang JY, Welsh J, Likhacheva A, Buchholz TA, et al. Lobectomy, sublobar resection, and stereotactic ablative radiotherapy for early-stage non-small cell lung cancers in the elderly. JAMA Surg. 2014;149(12):1244–53.
41. Ezer N, Veluswamy RR, Mhango G, Rosenzweig KE, Powell CA, Wisnivesky JP. Outcomes after stereotactic body radiotherapy versus limited resection in older patients with early-stage lung cancer. J Thorac Oncol. 2015;10(8):1201–6.
42. Bi N, Shedden K, Zheng X, Kong FS. Comparison of the effectiveness of radiofrequency ablation with stereotactic body radiation therapy in inoperable stage I non-small cell lung cancer: a systemic review and pooled analysis. Int J Radiat Oncol Biol Phys. 2016;95(5):1378–90.
43. Sher DJ, Wee JO, Punglia RS. Cost-effectiveness analysis of stereotactic body radiotherapy and radiofrequency ablation for medically inoperable, early-stage non-small cell lung cancer. Int J Radiat Oncol Biol Phys. 2011;81(5):e767–74.
44. Shah A, Hahn SM, Stetson RL, Friedberg JS, Pechet TT, Sher DJ. Cost-effectiveness of stereotactic body radiation therapy versus surgical resection for stage I non-small cell lung cancer. Cancer. 2013;119(17):3123–32.
45. Lanni TB Jr, Grills IS, Kestin LL, Robertson JM. Stereotactic radiotherapy reduces treatment cost while improving overall survival and local control over standard fractionated radiation therapy for medically inoperable non-small-cell lung cancer. Am J Clin Oncol. 2011;34(5):494–8.
46. van Hazel GA, Heinemann V, Sharma NK, Findlay MP, Ricke J, Peeters M, et al. SIRFLOX: randomized phase III trial comparing first-line mFOLFOX6 (plus or minus bevacizumab) versus mFOLFOX6 (plus or minus bevacizumab) plus selective internal radiation therapy in patients with metastatic colorectal cancer. J Clin Oncol. 2016;34(15):1723–31.
47. Rusthoven KE, Kavanagh BD, Cardenes H, Stieber VW, Burri SH, Feigenberg SJ, et al. Multi-institutional phase I/II trial of stereotactic body radiation therapy for liver metastases. J Clin Oncol. 2009;27(10):1572–8.
48. Su TS, Liang P, Liang J, Lu HZ, Jiang HY, Cheng T, et al. Long-term survival analysis of stereotactic ablative radiotherapy versus liver resection for small hepatocellular carcinoma. Int J Radiat Oncol Biol Phys. 2017;98(3):639–46.
49. Wahl DR, Stenmark MH, Tao Y, Pollom EL, Caoili EM, Lawrence TS, et al. Outcomes after stereotactic body radiotherapy or radiofrequency ablation for hepatocellular carcinoma. J Clin Oncol. 2016;34(5):452–9.
50. Berber B, Ibarra R, Snyder L, Yao M, Fabien J, Milano MT, et al. Multicentre results of stereotactic body radiotherapy for secondary liver tumours. HPB (Oxford). 2013;15(11):851–7.
51. Oladeru OT, Miccio JA, Yang J, Xue Y, Ryu S, Stessin AM. Conformal external beam radiation or selective internal radiation therapy-a comparison of treatment outcomes for hepatocellular carcinoma. J Gastrointest Oncol. 2016;7(3):433–40.
52. Kim H, Gill B, Beriwal S, Huq MS, Roberts MS, Smith KJ. Cost-effectiveness analysis of stereotactic body radiation therapy compared with radiofrequency ablation for inoperable colorectal liver metastases. Int J Radiat Oncol Biol Phys. 2016;95(4):1175–83.
53. Hall MD, McGee JL, McGee MC, Hall KA, Neils DM, Klopfenstein JD, et al. Cost-effectiveness of stereotactic radiosurgery with and without whole-brain radiotherapy for the treatment of newly diagnosed brain metastases. J Neurosurg. 2014;121 Suppl:84–90.
54. Savitz ST, Chen RC, Sher DJ. Cost-effectiveness analysis of neurocognitive-sparing treatments for brain metastases. Cancer. 2015;121(23):4231–9.
55. Wernicke AG, Yondorf MZ, Parashar B, Nori D, Clifford Chao KS, Boockvar JA, et al. The cost-effectiveness of surgical resection and cesium-131 intraoperative brachytherapy versus surgical resection and stereotactic radiosurgery in the treatment of metastatic brain tumors. J Neuro-Oncol. 2016;127(1):145–53.
56. Freeman DE, King CR. Stereotactic body radiotherapy for low-risk prostate cancer: five-year outcomes. Radiat Oncol. 2011;6:3.
57. Meier R, Beckman A, Henning G, Mohideen N, Woodhouse SA, Cotrutz C, et al. Five-year outcomes from a multicenter trial of stereotactic body radiation therapy for low- and intermediate-risk prostate cancer. Int J Radiat Oncol Biol Phys. 2016;96(2):S33–S4.
58. Hodges JC, Lotan Y, Boike TP, Benton R, Barrier A, Timmerman RD. Cost-effectiveness analysis of stereotactic body radiation therapy versus intensity-modulated radiation therapy: an emerging initial radiation treatment option for organ-confined prostate cancer. J Oncol Pract. 2012;8(3 Suppl):e31s–7s.
59. Onishi H, Araki T, Shirato H, Nagata Y, Hiraoka M, Gomi K, et al. Stereotactic hypofractionated high-dose irradiation for stage I non-small cell lung carcinoma: clinical outcomes in 245 subjects in a Japanese multiinstitutional study. Cancer. 2004;101(7):1623–31.
60. Grills IS, Mangona VS, Welsh R, Chmielewski G, McInerney E, Martin S, et al. Outcomes after stereotactic lung radiotherapy or wedge resection for stage I non-small-cell lung cancer. J Clin Oncol. 2010;28(6):928–35.
61. Onishi H, Shirato H, Nagata Y, Hiraoka M, Fujino M, Gomi K, et al. Stereotactic body radiotherapy (SBRT) for operable stage I non-small-cell lung cancer: can SBRT be comparable to surgery? Int J Radiat Oncol Biol Phys. 2011;81(5):1352–8.
62. Timmerman RD, Hu C, Michalski J, Straube W, Galvin J, Johnstone D, et al. Long-term results of RTOG 0236: a phase II trial of stereotactic body radiation therapy (SBRT) in the treatment of patients with medically inoperable stage I non-small cell lung cancer. Int J Radiat Oncol Biol Phys. 2014;90(1):S30.
63. Nanda RH, Liu Y, Gillespie TW, Mikell JL, Ramalingam SS, Fernandez FG, et al. Stereotactic body radiation therapy versus no treatment for early stage non-small cell lung cancer in medically inoperable elderly patients: a National Cancer Data Base analysis. Cancer. 2015;121(23):4222–30.

64. Smith BD, Jiang J, Chang JY, Welsh J, Likhacheva A, Buchholz TA, et al. Cost-effectiveness of stereotactic radiation, sublobar resection, and lobectomy for early non-small cell lung cancers in older adults. J Geriatr Oncol. 2015;6(4):324–31.
65. Louie AV, Rodrigues G, Hannouf M, Zaric GS, Palma DA, Cao JQ, et al. Stereotactic body radiotherapy versus surgery for medically operable Stage I non-small-cell lung cancer: a Markov model-based decision analysis. Int J Radiat Oncol Biol Phys. 2011;81(4):964–73.
66. Milano MT, Katz AW, Muhs AG, Philip A, Buchholz DJ, Schell MC, et al. A prospective pilot study of curative-intent stereotactic body radiation therapy in patients with 5 or fewer oligometastatic lesions. Cancer. 2008;112(3):650–8.
67. Hoyer M, Roed H, Traberg Hansen A, Ohlhuis L, Petersen J, Nellemann H, et al. Phase II study on stereotactic body radiotherapy of colorectal metastases. Acta Oncol. 2006;45(7):823–30.
68. Mendez Romero A, Wunderink W, Hussain SM, De Pooter JA, Heijmen BJ, Nowak PC, et al. Stereotactic body radiation therapy for primary and metastatic liver tumors: a single institution phase i-ii study. Acta Oncol. 2006;45(7):831–7.
69. Leung HW, Liu CF, Chan AL. Cost-effectiveness of sorafenib versus SBRT for unresectable advanced hepatocellular carcinoma. Radiat Oncol. 2016;11:69.

Index

D. M. Trifiletti et al. (eds.), *Stereotactic Radiosurgery and Stereotactic Body Radiation Therapy*,
https://doi.org/10.1007/978-3-030-16924-4